

LIBRARY COPY

FINAL REPORT

Analysis of Exposure and Risks to the Public from Radionuclides and Chemicals Released by the Cerro Grande Fire at Los Alamos

Task 2.7: Estimated Risks from Releases to Surface Water

**Revision 1
June 12, 2002**

***Submitted to the New Mexico Environment Department
in Partial Fulfillment of Contract No. 01 667 5500 0001***



FINAL REPORT

Analysis of Exposure and Risks to the Public from Radionuclides and Chemicals Released by the Cerro Grande Fire at Los Alamos

Task 2.7: Estimated Risks from Releases to Surface Water

**Revision 1
June 12, 2002**

***Submitted to the New Mexico Environment Department
in Partial Fulfillment of Contract No. 01 667 5500 0001***

"Setting the standard in environmental health"



Risk Assessment Corporation

417 Till Road, Neeses, SC 29107
Phone 803.536.4883 Fax 803.534.1995

FINAL REPORT

Analysis of Exposure and Risks to the Public from Radionuclides and Chemicals Released by the Cerro Grande Fire at Los Alamos

Task 2.7: Estimated Risks from Releases to Surface Water

**Revision 1
June 12, 2002**

Contributing Authors

**James R. Rocco, Sage Risk Solutions LLC
Kathleen R. Meyer, Ph.D., Keystone Scientific, Inc.
H. Justin Mohler, Bridger Scientific, Inc.
Jill W. Aanenson, Scientific Consulting, Inc.
Lesley Hay Wilson, Ph.D., Sage Risk Solutions LLC
Arthur S. Rood, K-Spar, Inc.
Patricia D. McGavran, Environmental Risk Assessment, Inc.**

Principal Investigator

John E. Till, Ph.D., *Risk Assessment Corporation*

***Submitted to the New Mexico Environment Department
in Partial Fulfillment of Contract No. 01 667 5500 0001***

EXECUTIVE SUMMARY

The Cerro Grande Fire, which burned about 45,000 acres ($\sim 180 \text{ km}^2$) in northern New Mexico, originated in the Bandelier National Monument on the evening of May 4, 2000, and spread east-northeast over the next 16 days consuming residential structures within the County of Los Alamos and approximately 7500 acres ($\sim 30 \text{ km}^2$) within the Los Alamos National Laboratory (LANL) boundary. Some of the areas that burned were known or suspected to be contaminated with radionuclides and chemicals. The public expressed concern with regard to:

- Radionuclides and chemicals associated with soil and vegetation burned by the fire and subsequently suspended and transported via air
- Radionuclides and chemicals associated with soil, sediments, and ash mobilized and transported via surface water following the fire
- Potential exposures and health risks to people related to the transport of radionuclides and chemicals via both air and surface water.

In response to these concerns, the New Mexico Environment Department (NMED) contracted with *Risk Assessment Corporation (RAC)* to make an independent assessment of the potential incremental health risks to the communities of northern New Mexico from these radionuclides and chemicals. This report evaluates the risks to people exposed to radionuclides and chemicals in surface water from the Cerro Grande Fire.

Objectives of this Report

The original objective was to analyze the immediate consequences and the longer-term impacts of the Cerro Grande Fire in terms of increased public exposures and potential risks from radionuclides and chemicals associated with the LANL facility. Specifically, this report focuses on the magnitude of incremental exposure and associated risks to the public, and fire cleanup personnel from transport of radionuclides and chemicals associated with the LANL facility released as a result of the fire through the surface water transport pathway. The scope was subsequently changed to include an assessment of the risks from the burned areas around the LANL site. The report does not address the risk associated with the burning of buildings and home sites in Los Alamos.

Methodology and Approach

We followed a number of defined steps to develop a surface water model domain, evaluate the available surface and storm water monitoring data, identify the sources and magnitude of chemical and radionuclide releases, model the release and transport of radionuclides and chemicals in surface and storm water, define representative exposure scenarios and parameter values, and estimate the associated health risks. An important part of the overall project was to identify and discuss the potential impact of uncertainties and limitations associated with each of these steps.

The surface water model domain encompassed an area of approximately 285 mi^2 (738 km^2) that extended from the LANL facility to the west to include the upper watersheds for the canyons

that cross the LANL facility, to the north to include the extent of the burned area in Santa Clara Canyon, to the east to include the Rio Grande, and to the south along the Rio Grande and downstream of Cochiti Dam.

Monitoring Data Evaluation

Before we developed the model and performed risk calculations for the project, we reviewed water and sediment monitoring data from Environmental Safety and Health (ESH)-18 and Environmental Restoration (ER) Divisions at LANL and from the New Mexico Environment Department (NMED). Because of the large number of measured chemicals and radionuclides, it was necessary to develop a two-stage screening procedure to focus the analysis on the chemical and radionuclides with the highest potential to contribute to the health risk of those exposed directly or indirectly to surface water runoff from LANL. In essence, our screening process used the available monitoring data for radionuclides and chemicals collected after the fire along with readily available risk coefficients for radionuclides, and slope factors and reference doses for chemicals to calculate a screening index. Of the more than 250 chemicals and 75 radioactive materials evaluated during this screening process, we identified 45 chemicals and radionuclides as most important in terms of human health, and we focused our monitoring data evaluation on the human-made radionuclides in this list.

Our monitoring data analysis of water and sediments identified readily apparent trends suggesting the presence or lack of an impact by either LANL or the fire on environmental media. We could draw few definitive conclusions about chemicals because of a lack of post-fire monitoring data and results that were below detection limits. As a result, the monitoring data evaluation focused primarily on the analysis of the radionuclides, ^{241}Am , ^{137}Cs , $^{239,240}\text{Pu}$, ^{238}Pu , and ^{90}Sr in surface water, storm water, and sediment. The monitoring data were useful for identifying apparent increases in concentration for some radionuclides and chemicals following the fire and also for identifying the possibility of LANL impact on measured concentrations.

Source Term Development

The most critical step in the risk estimation process is calculating the quantity, or source term, of material available for potential release. We selected a modeling approach for estimating concentrations of chemicals and radionuclides in source areas that used measured concentrations of chemicals and radionuclides in soil or sediment across defined source areas, in conjunction with water runoff and sediment erosion yields. We then calculated downstream concentrations of chemicals and radionuclides at defined points of exposure. During this process, we identified four distinct source areas at LANL with the potential for the release of chemicals and radionuclides that may move by erosion and storm water flow. These four categories were (1) potential release sites (PRS), (2) canyon sediments (geomorphic units), (3) canyon sediments characterized by inventory estimates for ^{137}Cs and $^{239,240}\text{Pu}$ only (unsampled reaches), and (4) burned area ash (burned areas). We used available sampling data to identify the chemicals and radionuclides detected in each of these four source areas to estimate average, representative concentrations of chemicals and radionuclides in each source area.

From 198 analytes with detected concentrations of chemicals and radionuclides in these source areas, we focused on those that were most important in terms of potential health risk. To complete this procedure, we:

- Calculated average concentrations of chemicals and radionuclides across each source area and compared the highest average concentration to the residential combined preliminary remediation goals (PRGs) for soil.
- Eliminated general water quality parameter analytes for which associated risks are not expected and some other general categories of materials like total petroleum hydrocarbons and lubricant range organics for which specific risk coefficients are not available.
- Selected the chemicals and radionuclides that were identified through the screening process used to evaluate the environmental monitoring data, and if not already included, added chemicals or radionuclides that had significantly elevated concentrations in burned area ash.
- Added chromium, mercury, RDX (hexahydro-1,3,5-trinitro-1,3,5-triazine), and uranium because of either known public concern or high source area concentrations.

This process resulted in a final list of 37 chemicals and radionuclides for which we developed source term estimates. Because of time and resource constraints, we relied on the characterization data that were provided to us. We were not able to investigate the rationale behind the collection of those data in detail. We then calculated downstream concentrations of chemicals and radionuclides at defined points of exposure.

Development of Scenarios and Points of Exposure

We designed four scenarios to account for the different types of individuals and activities that may have resulted in exposure to radionuclides and chemicals released to surface water during and after the Cerro Grande Fire. We developed the scenarios with caution so that a potentially exposed person or an exposure pathway would not be missed and that risks estimated for the hypothetical individuals in the scenarios would be greater than risks of other individuals who might be in the area for less time or under less exposed conditions. The hypothetical individuals described in the scenarios do not represent known individuals with these characteristics at these locations.

1. Local hunter from White Rock with exposure to deposited sediments near the Rio Grande and near the lower Los Alamos Canyon stream.
2. Family (adult and child) living near the Rio Grande just below the Cochiti Lake, participating in recreational activities on the lake.
3. Resident living near the Rio Grande below the confluence of the Water Canyon.
4. Local fire cleanup worker at the LANL site during and after the fire.

The exposure pathways we considered were:

- Drinking untreated water from the Rio Grande or Cochiti Lake (Scenarios 1, 2, and 3).
- Sediment exposure (ingestion, external exposure, and dermal contact) (All scenarios)

- Swimming or contact with water in Cochiti Lake and the Rio Grande (immersion and inadvertent ingestion) (Scenario 2).
- Eating fish from Rio Grande and Cochiti Lake (Scenarios 1, 2, and 3).
- Eating garden produce irrigated with river water (Scenarios 2 and 3)
- Eating beef from cattle using water from the river and Cochiti Lake (Scenarios 2 and 3)

We identified likely points of exposure for each scenario to represent locations where an individual would likely come in contact with surface water, suspended sediments, or deposited sediments containing concentrations of chemicals or radionuclides. We further assumed these points of exposure were immediately downgradient of source areas or at the outlet points of a watershed and that the points of exposure would be within a stream segment where the highest storm water flow and sediment concentration would be expected.

Transport Modeling

We developed the concentration estimates at the points of exposure for chemicals and radionuclides in storm water and surface water, in the dissolved phase of storm water and surface water, in suspended sediments, and in deposited sediments. To accomplish this, we:

- Developed conservative estimates of the surface water flow within the watersheds and at outlets to the Rio Grande for 2-, 5-, 10-, 25-, 50-, 100-, and 500-year design storm events of 6-hour duration
- Developed pre-fire and post-fire estimates of suspended sediment concentrations based on an analysis of pre-fire and post-fire empirical total suspended solids (TSS) data
- Identified the watershed contributing storm water flow to each point of exposure and the important source areas
- Estimated the maximum potential chemical mass and radionuclide activity that could result from storm water flow across a source area and that could be present at each point of exposure
- Identified background storm water flow and suspended sediment concentration in the Rio Grande and in Cochiti Lake
- Distributed the chemical mass and radionuclide activity in environmental media to estimate concentrations of chemicals and radionuclides at each point of exposure.

We used readily available data from LANL and from publicly available sources such as the U.S. Geological Survey. We calculated storm water flow in several steps using the spatial and raster capabilities of ArcView 3.1 Geographical Information System (GIS) and existing spatial data collected from a number of sources. To develop upper bound conservative estimates, we assumed

- Non-depleting sources. That is, we attributed no losses of chemical mass or radionuclide activity to natural processes of deposition and resuspension as the storm water flowed away from the source areas to the point of exposure
- Each 6-hour rain event occurred throughout the watershed contributing to the point of exposure.
- Each rain event resulted in the same concentrations of chemicals and radionuclides.

- Soil to water partitioning coefficient (K_d) values that were biased low and tended to predict higher water concentrations and lower suspended sediment concentrations.
- Infinite source areas. That is, we assumed sufficient chemical mass or radionuclide activity at the source areas to be in equilibrium with the storm water that flowed over the source area for each storm event.

The results of the transport modeling suggest that while the fire did impact the potential transport of chemicals and radionuclides, there was no consistent change in the resulting concentrations from pre-fire to post-fire concentrations. In other words, there was no more than a ten-fold difference between pre-fire and post-fire concentrations. Concentrations of chemicals and radionuclides decreased as the point of exposure was moved further away from the source areas, resulting in higher concentrations within the canyons immediately below the LANL facility than along the Rio Grande and Cochiti Lake.

Comparison to Measured Values

We compared predicted and measured concentrations at each point of exposure to understand how our predicted concentrations compared to measured concentrations in surface water and sediment. The comparisons suggest that our predicted concentrations are consistently greater than measured values by 10 to 100 times for ^{241}Am , ^{137}Cs , ^{238}Pu , and $^{239,240}\text{Pu}$ in sediments, which also have predicted sediment concentrations much higher than background for points of exposure impacted by the geomorphic unit and unsampled reach source areas. Predicted concentrations for RDX and polycyclic aromatic hydrocarbons are generally ten to 1000 times greater than measured concentrations. This over-prediction supports the noted conservatism that has been incorporated into both our source term development and transport calculations. The over-prediction was generally greater for water (with no apparent difference between filtered and unfiltered water) than for sediment, likely because we used low-biased K_d values, which translated into higher predicted water concentrations.

Risk Estimates

We presented risk estimates as cancer morbidity risks for carcinogenic chemicals and radionuclides or as hazard quotients for noncarcinogens. We estimated the potential annual cancer risk from the Cerro Grande Fire burning on the LANL site to be less than 3 in 1 million from exposure to any LANL-derived chemical or radionuclide that may have been carried in the surface water and sediments to the Rio Grande and Cochiti Lake. If exposure to the same concentrations of LANL-derived chemicals or radioactive materials was assumed to continue for 7 years (the time it may take to return to pre-fire vegetation conditions in the area), then the potential cancer risk was greater at about 20 in 1 million. For potential exposure to noncarcinogenic chemicals, intakes of all chemicals were less than acceptable intakes (a hazard quotient <1) established by the U.S. Environmental Protection Agency (EPA).

Of the different individuals considered in the hypothetical exposure scenarios, the health risks were highest to the resident living year-round on the bank of the Rio Grande near the confluence of Water Canyon. The type of exposure contributing most to the potential risk was eating fish.

However, the risks should be viewed as upper bound values because of the conservatism we assumed in estimating concentrations and in selecting lifestyle activities and values for the hypothetical individuals. For all other exposure pathways, the risks for chemicals and radionuclides are lower than for the fish ingestion pathway.

The hunter and fire cleanup worker, who were potentially exposed to higher concentrations in water and sediments, spent less time at those locations and were exposed through fewer exposure pathways. Exposure through other pathways was less important. Risk estimates and hazard quotients for the child and the adult at Cochiti Lake were generally similar. Risks for all pathways associated with the 500-year storm event were generally higher by less than ten times the risks from the 2-year storm event, and the differences between the two are likely within the uncertainties of the calculations.

Being able to look at the impact of individual PRSs or other source areas for chemicals (like for PAH and RDX) is an important tool from this work. A key message from the surface water pathway risk results is that an individual PRS can have a significant impact on the concentrations at a point of exposure and that there is a need for further and continuing investigations into the magnitude and extent of chemicals and radionuclides at these PRSs. In addition, concentrations of chemicals and radionuclides in stream segments and reaches below the LANL facility can also have a significant impact at the point of exposure and there is a need to characterize additional stream segments and reaches.

We estimated upper bound risks and identified potential areas of concern to guide future actions through our risk estimation process. We used simple models and conservative assumptions and source term concentration estimates to predict concentrations of chemicals and radionuclides at points of exposure within the surface water domain. We estimated post-fire risk and pre-fire and post-fire incremental risks using these predicted concentrations and exposures. The resulting risk estimates provide a conservative representation of potential impacts of the fire within the surface water domain. The limited monitoring data available for comparison to the model predictions support the notion that the predicted values tend to be high.

CONTENTS

EXECUTIVE SUMMARY	iii
CONTENTS	ix
FIGURES	xiii
TABLES	xv
ACRONYMS	xviii
1 INTRODUCTION	1-1
1.1 Background	1-1
1.2 Objectives	1-1
1.3 Approach	1-2
1.4 Surface Water Model Domain	1-4
1.5 Summary of Collected Data	1-6
1.6 References for Chapter 1	1-8
2 MONITORING DATA ANALYSIS	2-1
2.1 Data Sources and Limitations	2-1
2.1.1 Agencies Monitoring Water And Sediment	2-2
2.1.2 Screening Process to Prioritize Radionuclides and Chemicals	2-7
2.1.3 Data Compilation Process: Difficulties and Challenges	2-8
2.2 Surface Water And Storm Water Monitoring Data: Radionuclides	2-16
2.2.1 Completeness of the Data	2-16
2.2.2 Background Concentrations	2-18
2.2.3 Temporal Trends in Water Data	2-20
2.2.4 Spatial Trends in Surface and Storm Water Data	2-25
2.3 Sediment and Ash Monitoring Data	2-28
2.3.1 Background Concentrations	2-28
2.3.2 Data Trends	2-33
2.4 Chemical Concentrations in Water and Sediments	2-47
2.5 Surface Water Flow and Total Suspended Solids Data	2-47
2.6 Recommendations for Monitoring	2-47
2.8 Uses for the Environmental Monitoring Data	2-49
2.7 Conclusions	2-50
3 SURFACE WATER SOURCE TERM DEVELOPMENT	3-1
3.1 Ranking the Watersheds	3-1
3.2 Identifying and Defining Source Areas	3-4
3.2.1 Potential Release Site Source Areas	3-5
3.2.2 Geomorphic Unit Source Areas	3-6
3.2.3 Unsampled Reach Source Areas	3-8
3.2.4 Burned Area Source Areas	3-10
3.3 Screening Calculations to Prioritize Analysis of Radionuclides and Chemicals	3-11
3.3.1 Setting a Risk-based Decision Criterion	3-11

3.3.2 Screening of Contaminants Measured in Water Samples.....	3-13
3.3.3 Screening of Contaminants Measured in Sediments	3-24
3.4 Selecting Chemicals and Radionuclides for Surface Water Modeling Assessment.....	3-25
3.5 Estimating Concentrations of Chemicals and Radionuclides in Source Areas	3-26
3.5.1 Soil and Sediment Concentrations.....	3-26
3.5.2 Potential Release Site Source Area Characterization	3-27
3.5.3 Geomorphic Unit Source Area Characterization	3-27
3.5.4 Unsampled Reach Source Area Characterization	3-29
3.5.5 Burned Area Source Area Characterization.....	3-29
3.5.6 Adjusting Concentrations for Polygons Established for Modeling	3-29
3.5.7 Chemical and Radionuclide Levels from LANL Operations or Cerro Grande Fire..	3-30
3.5.8 Limitations and Uncertainties Associated with Source Area Concentrations	3-32
4 ESTIMATING CONCENTRATIONS AT POINTS OF EXPOSURE	4-1
4.1 Storm Water Flow Estimates.....	4-2
4.1.1 Hydrologic Model.....	4-2
4.1.2 Precipitation.....	4-5
4.1.3 Storm Water Flow	4-7
4.1.4 Hydrologic Flow Model	4-12
4.1.5 Grid-based Storm Water Flow Estimate Results	4-18
4.1.6 HEC-HMS-based Storm Water Flow Results	4-22
4.1.7 Storm Water Flow Estimate Results and Discussion.....	4-24
4.2 Suspended Sediment Evaluation	4-29
4.2.1 Methodology.....	4-30
4.2.2 Erosion Estimate Results and Discussion.....	4-32
4.3 Points of Exposure.....	4-37
4.4 Chemical and Radionuclide Concentration Estimates at Points of Exposure	4-47
4.4.1 Chemical Mass and Radionuclide Activity at the Source Areas	4-48
4.4.2 Soil to Water Partition Coefficients (Kd)	4-50
4.4.3 Background Surface Water Flow in the Rio Grande	4-53
4.4.4 Background Suspended Sediment Concentration in the Rio Grande	4-55
4.4.5 Water Volume and Suspended Sediment Concentration in the Cochiti Lake	4-56
4.4.6 Storm Water Flow across the Source Areas	4-57
4.4.7 Suspended Sediment in Storm Water	4-57
4.4.8 Suspended and Deposited Sediment Characteristics	4-58
4.4.9 Total Volume of Storm Water	4-58
4.4.10 Concentrations of Chemicals and Radionuclides at the Point of Exposure.....	4-59
4.4.11 Point of Exposure Concentration Estimate Results and Discussion	4-63
4.5 Sensitivity of Point of Exposure Concentrations.....	4-69
4.5.1 Source Areas.....	4-69
4.5.2 TSS Concentration.....	4-72
4.5.3 Storm Water Flow across the Source Areas	4-73
4.5.4 Soil to Water Partitioning Coefficients (Kd)	4-73
4.6 Limitations and Uncertainties of Surface Water Pathway Calculations.....	4-76
4.7 Comparison of Predicted to Measured Concentrations	4-79

4.7.1 Selecting Sampling Locations for Comparison	4-79
4.7.2 Limitations of Comparing Predicted and Measured Concentrations	4-80
4.7.3 Comparisons of Predicted and Measured Concentrations	4-82
4.7.4 Comparison of Predicted Sediment Concentrations with Background.....	4-91
4.7.5 Conclusions	4-92
5 RISK ESTIMATES.....	5-1
5.1 Exposure Scenarios	5-1
5.2 Methods of Risk Calculation	5-8
5.2.1 Drinking Water Ingestion	5-8
5.2.2 Deposited Sediment Exposure Pathways.....	5-9
5.2.3 Fish Consumption.....	5-15
5.2.4 Produce Consumption.....	5-16
5.2.5 Meat Consumption	5-17
5.2.6 Swimming.....	5-20
5.3 Risk Results.....	5-24
5.3.1 Annual Potential Risks by Individual Analyte	5-25
5.3.2 Potential Risks for 7-year Exposure Duration by Pathway	5-32
5.4 Limitations.....	5-35
6 CONCLUSIONS	6-1
7 REFERENCES	7-1

APPENDIX LISTING

Appendices for Chapter 1

None

Appendices for Chapter 2

APPENDIX A. Radionuclides and chemicals in water samples measured by LANL after the Cerro Grande FireA-1

Appendices for Chapter 3

APPENDIX B. Data for watershed rankingB-1
APPENDIX C. Screening calculations for radionuclides and chemicals in waterC-1
APPENDIX D. Screening calculations for radionuclides and chemicals in sediment.....D-1
APPENDIX E. Selection of radionuclides and chemicals based on source area and monitoring dataE-1
APPENDIX F. PRS and Geomorphic Unit area adjustment factors, and PRS erosion matrix adjustment factors (included only as electronic Excel file).....F-1
APPENDIX G. Assumed source area concentrations (included only as electronic Excel file)..G-1

Appendices for Chapter 4

APPENDIX H. Pre- and post-fire storm water flow (included only as electronic Excel file)....	H-1
APPENDIX I. Estimated POE concentrations, including relevant PRS erosion matrix scores (baseline case) (included only as electronic Excel file)	I-1
APPENDIX J. Estimated POE concentrations excluding burn area, compared to baseline case (included only as electronic Excel file).....	J-1
APPENDIX K. Estimated POE concentrations excluding Geomorphic Unit and Unsourced Reach source areas, compared to baseline case (included only as electronic Excel file)	K-1
APPENDIX L. Estimated POE concentrations excluding PRS source areas, compared to baseline case (included only as electronic Excel file)	L-1
APPENDIX M. Estimated POE concentrations excluding all erosion matrix scores, compared to baseline case (included only as electronic Excel file).....	M-1
APPENDIX N. Estimated POE concentrations, using maximum PRS, Geomorphic Unit, and burn area concentrations, compared to baseline case (included only as electronic Excel file)	N-1
APPENDIX O. Estimated POE concentrations using TSS of 5000, compared to baseline case (included only as electronic Excel file).....	O-1
APPENDIX P. Estimated POE concentrations using TSS of 15000, compared to baseline case (included only as electronic Excel file).....	P-1
APPENDIX Q. Estimated POE concentrations using TSS of 20000, compared to baseline case (included only as electronic Excel file).....	Q-1
APPENDIX R. Comparison of estimated baseline case POE concentration to relevant empirical data (numbers provided as electronic Excel file)	R-1

Appendices for Chapter 5

APPENDIX S. Risk coefficients and dose conversion factors for radionuclide calculations (table in Appendix).....	S-1
APPENDIX T. Slope factors and reference doses for chemical risk calculations (table in Appendix).....	T-1
APPENDIX U. Risk Calculations and Results (included only as electronic Excel file)	U-1

Example calculation (from Chapters 3, 4, and 5)

APPENDIX V. Example calculation (for $^{239,240}\text{Pu}$ only)	
V-1. Chapter 3—Source area concentration for PRS-10.....	V-1
V-2. Chapter 4—POE 1.2 concentration from source areas PRS-10 and burn area.....	V-2
V-3. Chapter 5—Risk based on total POE concentrations	V-3

Other Supporting Appendices

APPENDIX W. Information on PRS source areas for this assessment.....	W-1
--	-----

FIGURES

Figure 1-1. Overview of the surface water pathway risk analysis process.....	1-3
Figure 1-2. Surface water model domain for analysis of the Cerro Grande Fire.	1-5
Figure 2-1. ESH-18 surface water and storm water sampling locations during 2000..	2-3
Figure 2-2. ER sediment, storm water, and surface water sampling locations in 2000.....	2-5
Figure 2-3. New Mexico Environment Department storm water sampling locations during 2000.....	2-6
Figure 2-4. Concentrations of ^{137}Cs in surface water from background locations.	2-22
Figure 2-5. Concentrations of $^{239,240}\text{Pu}$ in surface water from background locations.....	2-23
Figure 2-6. Relative magnitude of measured concentrations of ^{137}Cs in surface following fire.....	2-26
Figure 2-7. Relative magnitude of measured concentrations of ^{137}Cs in storm water following fire.....	2-27
Figure 2-8. ESH-18 background sediment sampling locations..	2-29
Figure 2-9. ER background sediment sampling locations (129, 115, 109, and 110).....	2-30
Figure 2-10. NMED background sediment/ash and soil sampling locations.	2-31
Figure 2-11. ESH-18 sediment sampling locations during 2000.....	2-35
Figure 2-12. NMED sediment sampling locations during 2000.....	2-36
Figure 2-13. ESH-18 sediment sampling locations above, below LANL, and downriver.....	2-38
Figure 2-14. Cesium-137 concentrations measured in sediment	2-39
Figure 2-15. Americium-241 concentrations measured in sediment	2-39
Figure 2-16. Strontium-90 concentrations measured in sediment.....	2-40
Figure 2-17. Plutonium-238 concentrations measured in sediment	2-40
Figure 2-18. Plutonium-239,240 concentrations measured in sediment ..	2-41
Figure 2-19. Relative magnitude of average measured concentrations of ^{137}Cs f or sediment at locations sampled historically and after the fire during 2000	2-42
Figure 2-20. Relative magnitude of average measured concentrations of $^{239,240}\text{Pu}$ f or sediment at locations sampled historically and after the fire during 2000	2-43
Figure 2-21. Relative magnitude of measured concentrations of ^{137}Cs in sediment following fire.....	2-44
Figure 2-22. Relative magnitude of measured concentrations of $^{239,240}\text{Pu}$ in sediment following fire.....	2-45
Figure 2-23. Relative ratio of ^{238}U to ^{234}U in sample collected by ESH-18, ER, and NMED....	2-46
Figure 3-1. Outlet points on the Rio Grande River for the LANL watersheds.	3-3
Figure 3-2. PRS Source Area Locations.....	3-6
Figure 3-3. Geomorphic Unit Source Area Locations.....	3-8
Figure 3-4. Unsampld Reach Source Area Locations.....	3-9
Figure 3-5. Burned Area.....	3-10
Figure 3-6. Surface water screening process	3-14

Figure 4-1. Composite digital elevation model.	4-3
Figure 4-2. Delineated watersheds	4-4
Figure 4-3. Watershed outlets.....	4-5
Figure 4-4. Linear regression equation development for the 100-year 6-hour design storm.	4-6
Figure 4-5. Two-, 25-, 50-, and 100-year precipitation depth grids.	4-7
Figure 4-6. Comparison of uniformly distributed storm versus normally distributed storm.....	4-8
Figure 4-7. Pre-fire and post-fire soil curve number estimates..	4-10
Figure 4-8. Ratio of post-fire to pre fire soil curve numbers.	4-11
Figure 4-9. Geo-HMS stream/watershed characterization of Los Alamos basin	4-13
Figure 4-10. Geo-HMS stream/ watershed characterization of the Water basin	4-14
Figure 4-11. Storm water flow grids for pre-fire and post-fire 2- and 100-year storm events. ...	4-19
Figure 4-12. Comparison of grid pre-fire/post-fire storm flow ratio.....	4-22
Figure 4-13. Comparison of HMS pre-fire/post-fire storm water flow ratio.....	4-24
Figure 4-14. Storm flow gauging locations.	4-25
Figure 4-15. Gage station locations.....	4-26
Figure 4-16. Pre-fire convergence of the sample mean.....	4-34
Figure 4-17. Post-fire convergence of the sample mean.	4-34
Figure 4-18. TSS concentration as a function of drainage area (mi ²).....	4-35
Figure 4-19. TSS concentration as a function of drainage area (mi ²).....	4-36
Figure 4-20. TSS concentration as a function of stream flow.	4-37
Figure 4-21. Point of exposure locations for POE 1.1, 1.2, 3.1, 4.1a, and 4.1b	4-39
Figure 4-22. POE 1.1 watershed.....	4-41
Figure 4-23. POE 1.2 watershed.....	4-42
Figure 4-24. POE 2.1R, 2.1BD, and 3.1 watershed.....	4-44
Figure 4-25. POE 4.1a watershed.....	4-45
Figure 4-26. POE 4.1b watershed.....	4-46
 Figure 5-1. Point of exposure locations for POE 1.1, 1.2, 3.1, 4.1a, and 4.1b.	 5-2
Figure 5-2. Comparison of annual risk values for exposure to carcinogenic chemicals (top) and radionuclides (bottom) for the adult in Scenario 3 eating fish from the Rio Grande at the confluence of Water Canyon	5-27
Figure 5-3. Comparison of annual risk values for exposure to carcinogenic chemicals through the fish ingestion pathway for the adult (top) and (child) in Scenario 2	5-28
Figure 5-4. Comparison of annual incremental risk values for exposure to radionuclides through the fish ingestion pathway for the adult (top) and (child) in Scenario 2	5-29
Figure 5-5. Comparison of hazard quotient values for exposure to radionuclides through ingesting fish from the Rio Grande at confluence of Water Canyon (Scenario 3) and from Cochiti Lake (Scenario 2)	5-30
Figure 5-6. Comparison of annual risk values Scenario 2 for carcinogenic chemicals in drinking water for an adult (top) and child (bottom) living below Cochiti dam.....	5-31

TABLES

Table 2-1. ESH-18 Pre-fire and Post-fire Water Monitoring Data for Stage 2 Radionuclides ..	2-17
Table 2-2. Summary of Post-fire ER Water Monitoring Data	2-18
Table 2-3. ESH-18 Surface Water Data from Locations Designated as Background	2-20
Table 2-4. ESH-18 Storm Water Data from Locations Designated by RAC as Background	2-21
Table 2-5. Statistics on ¹³⁷ Cs Data Collected Historically through 2000	2-23
Table 2-6. Average Concentrations of Radionuclides in Storm Water	2-24
Table 2-7. Concentrations of Radionuclides in Areas Not Influenced by LANL Operations or Impacted by Recent Fires	2-32
Table 2-8. Concentrations of Radionuclides in Areas not Influenced by LANL Operations but Impacted by Recent Fires	2-33
Table 2-9. Range of Mean Background Radionuclide Concentrations in Areas not Impacted by Fire and in Areas Impacted by Fire	2-34
Table 2-10. Chemical Data from LANL for Water and Sediment	2-48
Table 3-1. Summary of Input Values to Total Ranking Factor	3-4
Table 3-2. Radionuclides Emerging from Stage 1 Screening Evaluation	3-16
Table 3-3. Radionuclides Emerging from Stage 2 Screening	3-16
Table 3-4a. Toxicity Equivalency Factors for Carcinogenic Polycyclic Aromatic Hydrocarbons	3-19
Table 3-4b. Toxicity Equivalency Factors for Chlorinated Dioxins	3-19
Table 3-4c. Toxicity Equivalency Factors for Chlorinated Furans	3-19
Table 3-5. Chemicals Emerging from Stage 1 Screening Evaluation	3-20
Table 3-6a. Chemicals Identified in Stage 2 Screening Based on Risk Index.....	3-23
Table 3-6b. Chemicals Emerging from Stage 2 Screening Based on Hazard Quotient	3-24
Table 3-7. Selected Chemicals and Radionuclides.....	3-26
Table 3-8. Comparison of Estimated Inventory Based on Different Binning Methods	3-28
Table 3-9. Analytes with Average Concentrations in Ash at Least a Factor of Five Higher than Average Background Concentrations.....	3-29
Table 3-10. Assumed Soil and Sediment Background Concentrations for Chemicals and Radionuclides Included in the Surface Water Pathway Source Term.....	3-31
Table 3-11. Descriptive Statistics for the Ratio of GIS-Based PRS Areas to PRS Areas that were Redefined Based on Existing Sample Locations.....	3-35
Table 4-1. Linear Regression Equations Relating Elevation to Precipitation Depths	4-6
Table 4-2. HEC-HMS Model Input Parameters for Los Alamos Basin Precipitation.....	4-17
Table 4-3. HEC-HMS Model Input Parameters for Water Basin Precipitation	4-17
Table 4-4. Precipitation Depth Distributions for Los Alamos Basin.....	4-18
Table 4-5. Precipitation Depth Distributions for Water Basin	4-18
Table 4-6. Estimated Pre-fire and Post-fire Storm Water Flow at Outlet Locations.....	4-20

Table 4-7. Ratio of Pre-fire to Post-fire for Grid Storm Water Flow Estimates.....	4-21
Table 4-8. HEC-HMS Storm Water Flow Estimates for Los Alamos and Water Basins	4-23
Table 4-9. Maximum Measured Precipitation Depth from 1/1/00 through 5/21/01 and Estimated Precipitation Depth for Gage Locations based on the 2-year and 5-year Design Storm Events	4-26
Table 4-10. Summary of Maximum Measured and Estimated Pre-fire Storm Water Flow	4-27
Table 4-11. Summary of Maximum Measured and Estimated Post-fire Storm Water Flow	4-28
Table 4-12. Estimated Annual Soil Erosion Rates	4-30
Table 4-13. Pre-fire TSS Concentration Descriptive Statistics	4-33
Table 4-14. Post-fire TSS Concentration Descriptive Statistics.....	4-33
Table 4-15. Regression Statistics for TSS	4-36
Table 4-16. Storm Water Flow at the Points of Exposure	4-40
Table 4-17. Source Areas Included in POE 1.1	4-41
Table 4-18. Source Areas Included in POE 1.2.....	4-42
Table 4-19. Source Areas Included in POE 4.1a.....	4-45
Table 4-20. Source Areas Included in POE 4.1b.....	4-46
Table 4-21. Soil-Water Distribution and Organic Carbon Partition Coefficients for Surface Water Source Term Chemicals and Radionuclides	4-51
Table 4-22. Statistics for Rio Grande Flow Data	4-54
Table 4-23. Statistics for the Rio Grande Flow Data below the Cochiti Dam	4-55
Table 4-24. Statistics for Rio Grande Suspended Sediment Concentrations Data	4-55
Table 4-25. Statistics for Suspended Sediments in Rio Grande Below Cochiti Dam	4-56
Table 4-26. Statistics for Volume in the Cochiti Lake	4-57
Table 4-27. Difference in Concentrations from Pre-Fire to Post-Fire for POE 4.1b.....	4-66
Table 4-28. Comparison of Mass and Activity Ratios to Volume Ratios	4-67
Table 4-29. Average Soil Erosion for PRSs (in meters).....	4-68
Table 4-30. Average Precipitation Depths in Inches by Storm Event and Point of Exposure ...	4-68
Table 4-31. Average Soil Erosion for Geomorphic Units and Unsampld Reaches (in meters)	4-69
Table 4-32. Change in Concentration from 2-Year to 500-Year Storm Event for POE 4.1b.....	4-74
Table 4-33. Kd Change Comparison for Benzo(a)anthracene at POE 4.1b	4-75
Table 4-34. Kd Change Comparison for Cesium-137 at POE 4.1b.....	4-76
Table 4-35. Point of Exposure Coordinates.....	4-79
Table 4-36. Monitoring Locations for Comparison to Predicted POE Concentrations.....	4-81
Table 4-37. P to O Ratios for Sediments with Background Values at POE 1.2	4-83
Table 4-38. P to O Ratios for Sediments with Background Values at POE 3.1	4-84
Table 4-39. P to O Ratios for Sediments with Background Values at POE 2.1R	4-85
Table 4-40. P to O Ratios for Sediments without Background Values at POE 3.1	4-86
Table 4-41. P to O Ratios for Sediments without Background Values at POE 2.1R	4-87
Table 4-42. P to O Ratios for Water with Background Values at POE 1.2.....	4-88
Table 4-43. P to O Ratios for Water with Background Values at POE 3.1	4-89
Table 4-44. P to O Ratios for Water without Background Values at POE 3.1	4-90
Table 4-45. P to O Ratios for Water without Background Values at POE 2.1BD	4-91
Table 4-46. Percent Contribution of Background added to Predicted Sediment Concentrations	4-92

Table 5-1. Scenarios and Selected Exposure Parameters for Surface Water Pathways	5-7
--	-----

Table 5-2. Transfer Coefficients for Chemicals of Concern	5-23
Table 5-3. Transfer Coefficients for Radionuclides of Concern	5-24
Table 5-4. Scenario Pathways that Result in Annual Risks Greater than Risk Criteria	5-26
Table 5-5. Radionuclide Incremental Risk Estimates for Exposure Scenarios	5-33
Table 5-6. Carcinogenic Chemical Incremental Risk Estimates for Exposure Scenarios	5-34
Table 5-7. Upper-bound Health Impacts by Pathway For Noncarcinogenic Chemicals	5-35
Table 5-8. Summary of Source Area with Maximum Mass Contribution to POE	5-36
Table 6-1. Highest Estimated Impacts by Scenario, Individual Chemical or Radionuclide, and Selected Pathways	6-2
Table 6-22. Conservatism and Uncertainty in Modeling Components of Exposure and Risk Calculations for Surface Water Pathways	6-5

ACRONYMS

BMP	best management practice
cfs	cubic feet per second
DEM	digital elevation models
EPA	U.S. Environmental Protection Agency
ER	Environmental Restoration Project
ESH	Environment, Safety, and Health (Division)
EMC	Event Mean Concentration
GIS	geographical information system
HMS	(Army Corps of Engineer's) Hydrologic Modeling System
IR	infrared
Kd	Soil to water partitioning coefficient
Koc	Organic Carbon Partition
LANL	Los Alamos National Laboratory
NCRP	National Council on Radiation Protection and Measurements
NMED	New Mexico Environment Department
NRC	U.S. Nuclear Regulatory Commission
PAH	polycyclic aromatic hydrocarbon
pCi	picocuries
POE	point of exposure
ppm	parts per million
PRG	preliminary remediation goals
PRS	potential release site
<i>RAC</i>	<i>Risk Assessment Corporation</i>
<i>RfD</i>	<i>Reference dose</i>
SCS	Soil Conservation Service
TSS	total suspended solids
USGS	United States Geological Survey
USLE	Universal Soil Loss Equation
UTM	Universal Transverse Mercator

1 INTRODUCTION

1.1. Background

The Cerro Grande Fire, which burned over 45,000 acres (~180 km²) in northern New Mexico, originated in the Bandelier National Monument on the evening of May 4, 2000, and spread east-northeast over the next 16 days consuming residential structures within the County of Los Alamos and over 7500 acres (~30 km²) within the Los Alamos National Laboratory (LANL) boundary (DOE 2000a). LANL encompasses about 27,500 acres (110 km²) and is situated on the Pajarito Plateau, described as a series of finger-like mesas separated by deep east-to-west oriented canyons cut by intermittent streams. The mesas range in elevation from approximately 7800 ft (2377 m) on the flanks of the Jemez Mountains to about 6200 ft (1890 m) above the Rio Grande Canyon.

The fire caused significant damage to structures and property on LANL land. Some of the areas that burned were known or suspected to be contaminated with radionuclides and chemicals. Concern was expressed by the public with regard to:

- Radionuclides and chemicals associated with soil and vegetation burned by the fire and subsequently suspended and transported via air
- Radionuclides and chemicals associated with soil, sediments, and ash mobilized and transported via surface water following the fire
- Potential exposures and health risks to people related to the transport of radionuclides and chemicals via both air and surface water.

In response to these concerns, the New Mexico Environment Department (NMED) recognized the need for an independent assessment of exposures and risks to the public from radionuclides and chemicals associated with the LANL facility released as a result of the fire. NMED contracted with *Risk Assessment Corporation (RAC)* to evaluate the potential incremental health risks to the communities of northern New Mexico from these radionuclides and chemicals.

1.2. Objectives

The primary objective was to analyze the immediate consequences and the longer-term impacts of the Cerro Grande Fire in terms of increased public exposures and potential risks from radionuclides and chemicals associated with the LANL facility released as a result of the fire in the vicinity of the LANL.

Specifically, the overall project focused on the

- Magnitude of incremental exposure and associated risks to the public, emergency response personnel, and firefighters from transport of radionuclides and chemicals associated with the LANL facility released as a result of the fire through the *air transport pathway*. The scope was subsequently changed to include an assessment of risks from naturally occurring radionuclides and metals released from the forests burning around the LANL site. This assessment is described in the air pathway report (Rood et al. 2002).

- Magnitude of incremental exposure and associated risks to the public from transport of radionuclides and chemicals associated with the LANL facility released as a result of the fire through *surface water pathways*. The scope was also subsequently changed to include risks from the fire from areas burned around the LANL site. This assessment is described in this report.
- Conclusions of the study and recommendations for similar events in the future. An important goal of the study was to actively, openly, and accurately convey information about the risks from the fire to the public, including the lessons learned from the fire analysis and the effectiveness of communication with the public during and following the fire. These conclusions are presented in a companion report (Mohler et al. 2002).

1.3. Approach

The risk analysis process for the surface water pathway included a number of defined steps that are described in the different chapters of this report and summarized in Figure 1-1. These steps were developing a surface water model domain, evaluating the available surface and storm water monitoring data, identifying the sources and magnitude of chemical and radionuclide releases, modeling the release and transport of radionuclides and chemicals in surface and storm water, defining representative exposure scenarios and parameter values, and estimating the associated health risks. An important part of the overall project is to identify and discuss the potential impact of uncertainties and limitations associated with each of these steps.

To characterize the risks from radionuclides and chemicals released to surface and storm water during the Cerro Grande Fire, we considered the following questions.

1. What is the geographic area of interest for which environmental transport calculations and risk assessments are performed? What data are available to support this effort? (Chapter 1)
2. What environmental data related to the surface water pathway were available for periods during and after the fire and how could they be used to evaluate risk? (Chapter 2)
3. What chemicals and radionuclides have the potential to be transported through the canyons to downstream locations? Where are these chemicals and radionuclides located and how much is present at those areas? (Chapter 3)
4. What are the changes in water flows in the major canyons that cross the LANL facility, given the changes in the watersheds as a result of the Cerro Grande Fire? What are the potential environmental concentrations of chemicals and radionuclides at selected exposure locations? (Chapter 4)
5. What are the main exposure pathways for chemicals and radionuclides released to surface water during and after the fire? What types of individuals are located in the vicinity of the fire during and after the fire? What activities are they engaged in and where are these individuals located? What are the potential risks to these individuals? (Chapter 5)

6. What are the limitations and uncertainties with this approach to estimating risks associated with the transport of chemicals and radionuclides in surface water? (Chapters 2, 3, 4, 5, and 6)

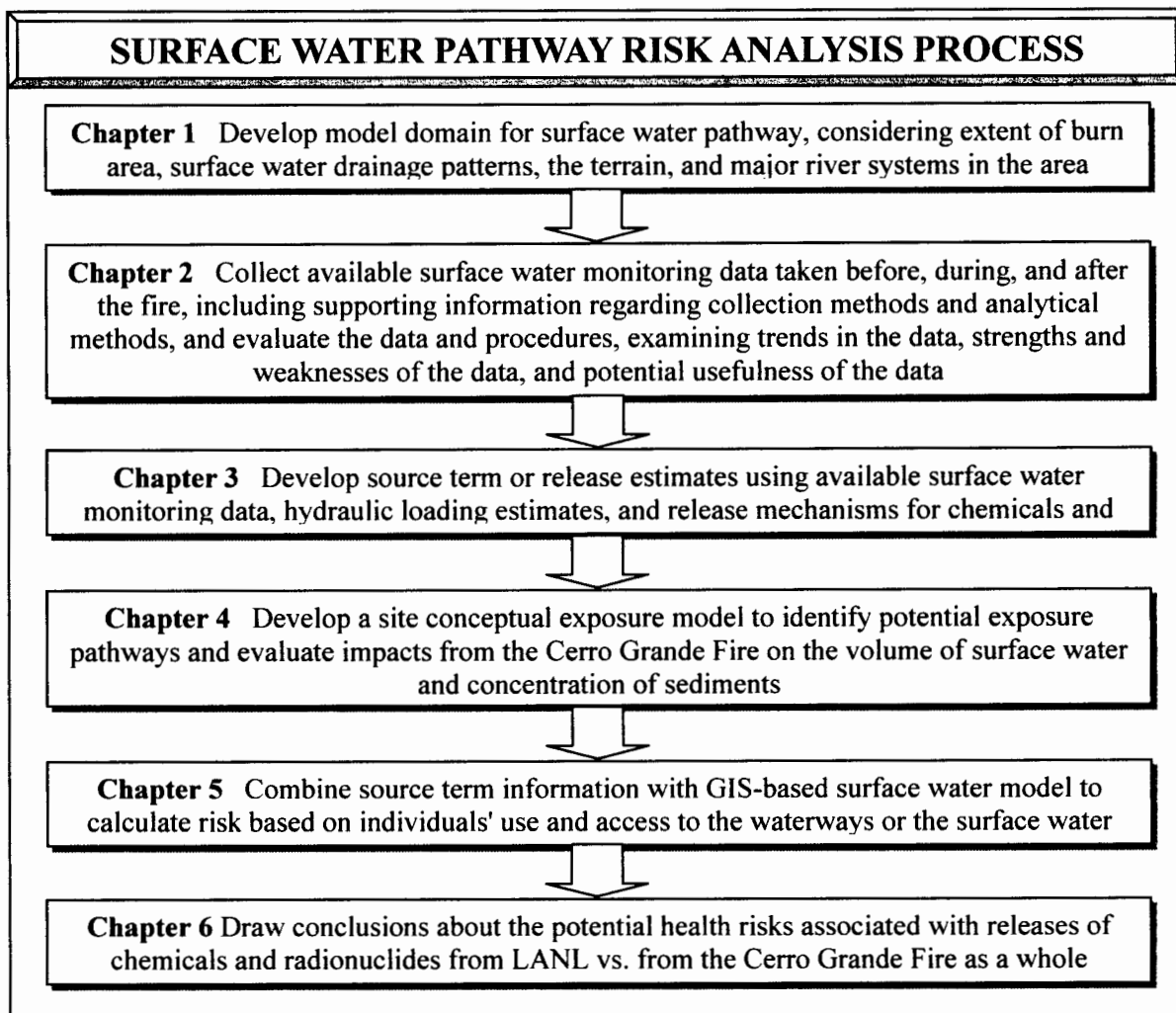


Figure 1-1. Overview of the surface water pathway risk analysis process.

The environmental data collected before, during, and after the fire pertaining to the surface water pathway were compiled and evaluated, as described in Chapter 2. Because a large number of radionuclides and chemicals were identified with the potential to be released following the fire, we developed a screening procedure and used available water monitoring data to identify those radionuclides and chemicals that were potentially most important in terms of health risk. Radionuclides and chemicals that fell below a predetermined level of health risk, when risk was calculated conservatively, were removed from further consideration as described in Chapter 3. Source term estimates were developed for the radionuclides and chemicals identified as possibly resulting from LANL operations. A final list of radionuclides and chemicals was developed based on the monitoring data screening results and the source term data (Chapter 3). The surface water

and sediment transport of these radionuclides and chemicals released during and after the fire was modeled, as described in Chapter 4. The exposure scenarios used to determine potential risks to representative individuals from the radionuclides and chemicals released during the fire are described in Chapter 5 together with the methods for the risk calculations and the estimated risks. Finally, conclusions and observations about the potential health risks associated with estimated releases of chemicals and radionuclides to surface water are presented in Chapter 6.

1.4. Surface Water Model Domain

An essential first step in assessing the importance of the surface water pathway was to establish the domain for the study. The model domain is the geographic area of interest for which environmental transport calculations and risk assessments are performed. While it is desirable that the model domain cover as large an area as possible, the resources needed to acquire and process spatial data limit its geographical extent. Figure 1-2 shows the surface water model domain. We defined the extent of the surface water model domain on the basis of six considerations: (1) the terrain, (2) the direction of surface water movement across the landscape, (3) the extent of the burn area west of LANL, (4) the location of potential chemical and radionuclide source areas, (5) the potential for rainfall and surface water runoff in canyons around the LANL facility that may mobilize radionuclides and chemicals in contaminated areas, and (6) the potential exposure locations. In addition, the primary surface water monitoring locations were identified and confirmed to be within the surface water model domain.

The surface water model domain has been defined as an area of approximately 285 mi² (738 km²) that extends to the west of the LANL facility to include the upper watersheds for the canyons that cross the LANL facility, to the north of LANL to include the extent of the burned area in Santa Clara Canyon, to the east of LANL to include the Rio Grande, and to the south of LANL along the Rio Grande and downstream of Cochiti Dam.

The movement of water across the landscape is generally modeled using digital elevation models (DEM) that depict the surface of the landscape (Maidment and Djokic 2000). The DEM is a square-cell grid of elevation measurements. The size of the electronic DEM file is directly proportional to its resolution. That means that small cell sizes with high resolution require larger file sizes. The direction of runoff water flow is calculated by the steepest descent from each terrain model cell considering the eight adjacent cells. To include an extensive area in a surface water model, very large computer files must be used to characterize the area with respect to the rainfall distribution, land surface conditions that determine the amount of runoff water that will be generated, and the DEM. Computing resources, data storage, and model complexity can be prohibitive if the model domain is too large. The size of the surface water domain, therefore, is a balance between the geographic extent of the watersheds of interest, the locations of potential exposures, the availability of high-resolution data, and the logistical constraints of computing resources and data storage.

The area that contributes runoff flow to a particular stream is defined as the watershed for that stream (Chow et al. 1988). Therefore, to determine the potential for chemicals of concern or radionuclides to be mobilized as the result of rainfall and surface water runoff, the surface water domain was developed to include all of the streams that cross the LANL facility and their associated watersheds (LANL 2000). In addition, the watersheds burned in the Cerro Grande Fire

were included in the surface water domain to help evaluate the impact of non-LANL related background sources of the chemicals of concern or radionuclides in soil, sediments, or surface water (LANL 2000).

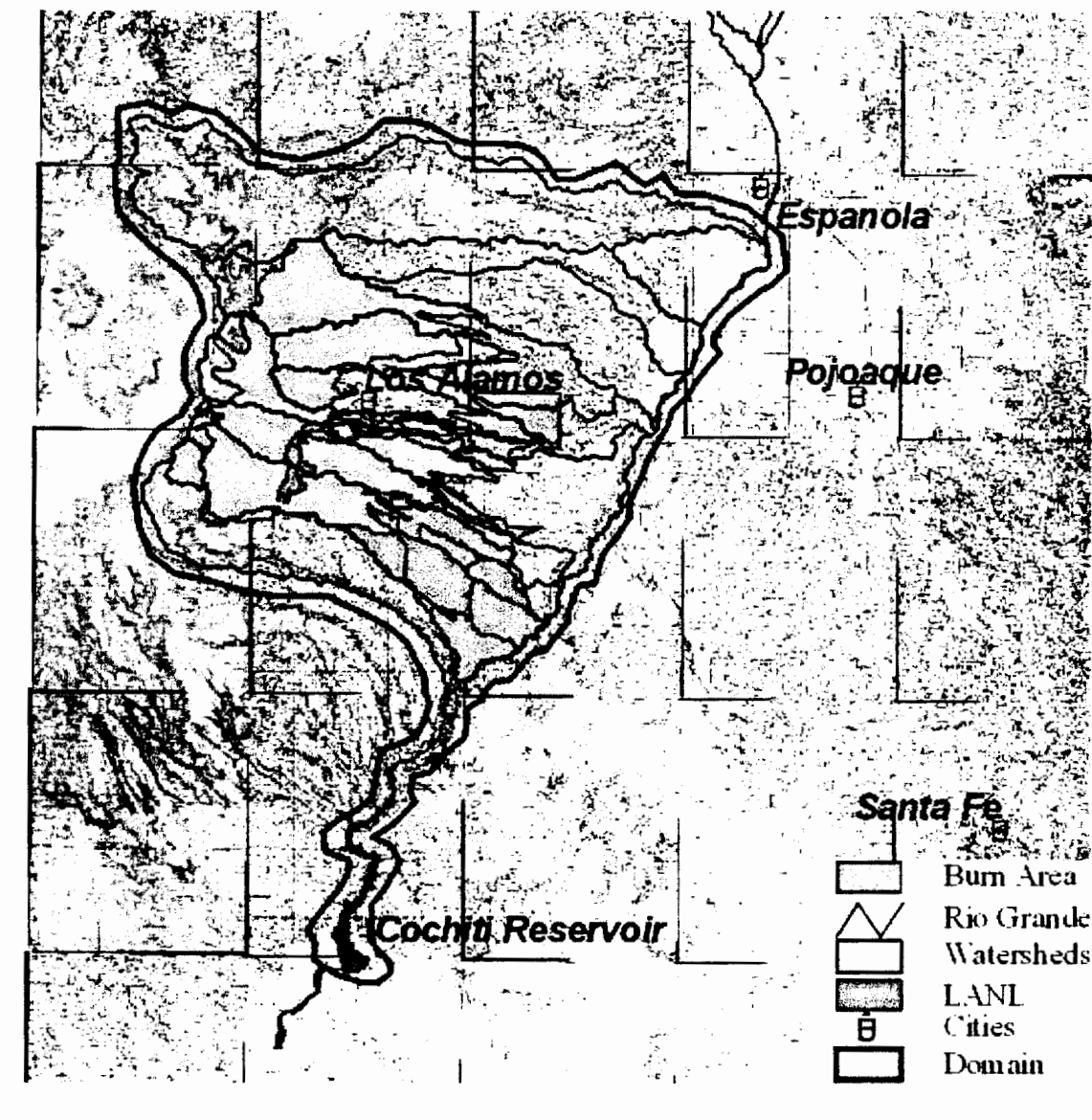


Figure 1-2. Surface water model domain for analysis of the Cerro Grande Fire. The figure also shows the watersheds in the vicinity of the LANL Facility, including watersheds that were burned during the fire.

1.5. Summary of Collected Data

An essential component of this project has been gathering all available information relevant to estimating the potential for increased health risks associated with the Cerro Grande Fire, to the extent possible. Because of the heightened awareness and concern about increased potential for chemical and radionuclide dispersal, both during and following the fire, and also as part of the routine environmental surveillance and characterization programs maintained by LANL and other organizations, large amounts of environmental monitoring data have been and continue to be collected. The fundamental purpose behind such data collection is to understand and quantify the offsite¹ movement and levels of chemicals and radionuclides, with the underlying goal of minimizing human exposure to those materials, particularly to members of the public. However, the importance of this environmental monitoring extends beyond the potential exposure and risks associated with the Cerro Grande fire. Establishing and maintaining a complete record of environmental monitoring is a critical aspect of understanding the impact of and minimizing exposure associated with operations of a nuclear facility - past, present, and future.

There are, however, a number of unique aspects of the current work that dictate the relative importance of available data. It is well understood that all forest fires, even in the absence of a nuclear weapons facility, release and mobilize radionuclides and other chemicals to the environment (Nance et al. 1993, Lambert et al. 1991, and LeCloarec et al. 1995), thereby creating the potential for increased exposure and risk to anyone in the vicinity of the fire. This project is focused on understanding if there was an increase in exposure and risk that may have occurred to members of the public specifically because the fire occurred at LANL. Therefore, in addition to the environmental measurements made during and shortly after the fire, it has been important to obtain datasets for time periods prior to the fire to gain an understanding of typical environmental concentrations of chemicals and radionuclides in the LANL environment. Beyond this, establishing appropriate background concentrations is essential to distinguish between chemicals and radionuclides present in the environment as a result of laboratory operations and chemicals and radionuclides present because of other activities, such as worldwide atmospheric weapons testing. In this context, an effort has also been made to identify and compile environmental monitoring data collected during similar forest fire events that did not involve a nuclear weapons facility. We have also collected information to help characterize background concentrations in LANL-area soils that would be expected without the existence of LANL or the occurrence of a fire.

This task has been challenging because many different groups and organizations collected and compiled data. These organizations used a variety of techniques and formats for data compilation and placed varying emphasis on the preparation of supporting information to document the collection methods and analytical procedures. In addition, the major focus of sampling was on determining whether there was the possibility of immediate acute health effects from released materials and not necessarily on following standard operating procedures or sampling protocols. This is understandable considering the situation, but in some cases it also complicates analysis of the data.

Two broad categories of information were used to complete this work:

¹ In this context, offsite refers to areas outside the LANL boundary or areas that are otherwise accessible to members of the public

- Data files representing compilations of environmental conditions and chemical and radionuclide inventories existing at a specific location and time (e.g., chemical and radionuclide concentrations in environmental media, surface water flow measurements, suspended sediment measurements, source area characterization data), and
- Geographic Information System (GIS) files that provide an electronic means of geographically representing conditions or features in the LANL environs (e.g., topography, burn extent and severity, watershed boundaries). In addition to facilitating a visual representation of existing conditions, these GIS files are used in combination with erosion and surface flow models to predict the magnitude and consequences of increased flooding and associated sediment transport resulting from potential rain events known to occur in the Los Alamos area during the monsoon season, which typically begins in June and lasts through September.

The data files and documents that have been gathered for this work have been divided generally into those that pertain to analysis of the air pathway (Rood et al 2002) and those that pertain to analysis of the surface water pathway. We organized our working files further according to the organization responsible for collecting the data. Finally, we sorted the data based on the purpose for which they have been acquired (e.g., monitoring data or source term data). Additional information related to such things as collection methodology, analytical procedures, and sample locations has often been received by way of various separate files.

The Geographic Information System (GIS) files that have been collected for this work are generally subdivided according to the coordinate projection in which they were provided to *RAC* and further separated under each projection by the original organization supplying the information. *RAC* also obtained GIS files as part of the Memorandum of Understanding (MOU) with the Environmental Restoration (ER) project at LANL. All GIS files for the project were converted to a common projection and separated by data content (e.g., hydrology of streams, the Rio Grande, and the Cochiti Lake).

Additional information related to the use of specific pieces of information or data is provided in the chapters where those data are discussed. Observations about the utility of the data, recommendations for improvement, and discussions of limitations and uncertainties are also included where appropriate in the chapters where the data are discussed.

2 MONITORING DATA ANALYSIS

2.1 Data Sources and Limitations

An important aspect of the project was analyzing monitoring data collected during normal flow situations and storm events both before and after the fire through the end of 2000. This helped to identify possible increases in concentrations of chemicals and radionuclides in surface and storm water and sediments resulting from the fire. In completing this task, we also evaluated the current monitoring program that was in place at the time of the fire and recommended additional data collection that may contribute to the fire risk analysis or a better understanding of potential risks in the future.

We considered several basic questions related to the monitoring data analysis:

1. What monitoring data are available and what organizations provided the data?
2. What are the limitations of the data?
3. Are there differences in concentrations of radionuclides or chemicals *above* (to the West of the site on the plateau) and *below* (to the east of the site below the operational area of the site) LANL—spatial differences as the result of location?
4. Are differences in concentration seen before and after the fire—temporal differences as the result of time?
5. How can the monitoring data be used to support an analysis of health risk?
6. Are there ways to improve the monitoring program in place at the time of the fire?

We completed the primary evaluation of available monitoring data relevant for understanding potential risks from the surface water pathway while we were still identifying and gathering information and updating data sets to ensure we were working with the most current and accurate information. The data we present and evaluations made in this chapter are based on data sets that have undergone some minor revisions since our evaluation. Therefore, in some cases it may be difficult to use updated data sets to exactly reconstruct the analyses presented in this chapter. However, we believe that these minor updates to some of the data sets would not change the general conclusions we made based on the monitoring data.

A number of issues also complicate this analysis. Some laboratory methods have changed over time, such as filtering water samples in the analytical laboratory and modified digestion methods. Historically, soil and sediments were dried and then sieved before analysis, but starting in 1998, samples were dried and then ball milled to achieve more complete homogenization. There also are issues related to high analytical biases for some radionuclides, such as ⁹⁰Sr results for 1999. Additionally, some radionuclides are analyzed by multiple methods (e.g., gamma and alpha spectroscopy), and the accuracy of the result is dependent on the analytical method. Many of these issues had not been identified when the monitoring data were evaluated. Because of the massive amount of data that have been collected, attempting to account for these issues goes beyond the scope of this work. Examining temporal trends becomes more difficult and less precise when these complicating issues are considered.

We have evaluated the data to the extent possible based on the data that were provided to us. The goal of our analyses was to identify readily apparent trends that suggested the presence or

lack of an impact by LANL or the Cerro Grande Fire on environmental media, focusing on water and sediment sampling data.

It is also important to understand the difficulty in comparing samples collected at different locations. These comparisons are complicated by things such as differences in media type, elevation, vegetation cover, sample collection time, seasonal variation, and differences in water flow and runoff. We used these data, however, because they were the only data available.

For the purposes of calculating average concentrations and plotting results for this analysis of environmental monitoring data, we generally considered only positive results reported as "detected" because the detected values represent an estimate of the true concentration as opposed to the upper bound value represented by a "nondetect" value. We recognize, however, that there are differing opinions about including nondetectable values. For the purpose of this analysis, we consider our approach sufficient for identifying possible post-fire impacts based on measured concentrations in water or sediment.

2.1.1 Agencies Monitoring Water and Sediment

The majority of the water and sediment monitoring data originated from two divisions at LANL (Environmental, Safety, and Health Division [ESH-18] and the ER Project) and from the NMED monitoring program. ESH-18 performs the most comprehensive routine surface water monitoring, surveillance, and compliance activities to confirm compliance with State and Federal environmental regulations such as the Clean Water Act, the National Pollutant Discharge Elimination System, and New Mexico Water Quality Control Commission Regulations. Sediment samples are collected to assist with understanding chemical and radionuclide movement from contaminated areas, although there are no specific compliance-related standards related to sediment monitoring.

Sources of information on historic and current site operations and disposal practices are readily available (Rogers 1977; Hakonson et al. 1973; LANL 1999a). LANL has disposed of radioactive waste at various locations within the LANL boundary since 1944, and, historically, some wastes were characterized in various canyons (Rogers 1977). Recent studies at LANL are focused on more thoroughly characterizing the contaminated areas, called potential release sites (PRSs), and this information will be used during the source term development task for the project.

Runoff samples have historically been collected as grab samples (both manual and automated) from usually dry portions of drainages during or shortly after storm events. While there are no perennial surface water flows that extend completely across LANL in any canyon, periodic natural surface runoff occurs. LANL reports two runoff modes: (1) spring snowmelt runoff that occurs over days to weeks and (2) summer runoff from thunderstorms that occurs over hours at a high discharge rate and sediment load (LANL 1999a). The surface water within LANL flows through a series of discrete canyons eastward and drains into the Rio Grande. Generally, surface water grab samples are collected annually from Pajarito Plateau stations located near LANL and from regional stations where effluent discharges or natural runoff maintain stream flow. Regional surface water samples, collected from stations on the Rio Grande and Rio Chama and Jemez Rivers, provided background data from areas beyond the Laboratory boundary (see Figure 2-8, surface water sampling locations 177, 174, and 98, respectively).

During the course of the project we received data files from ESH-18 of historic monitoring data from 1951 through 1999 and water and sediment data collected during and after the Cerro

Grande Fire in May 2000. The historic data set contained over 150,000 analytical results for over 200 analytes. Figure 2-1 shows the ESH-18 surface water and storm water sampling locations during 2000. It is evident that the locations for collecting surface water and water following storm events differ. In addition, the storm water sampling locations, all located within the boundaries of LANL, were more numerous than the surface water sampling locations. However, not all storm water sampling locations noted in Figure 2-1 were sampled after each storm event. There were seven surface water sampling locations along the Rio Grande and at the Cochiti Reservoir to the southwest.

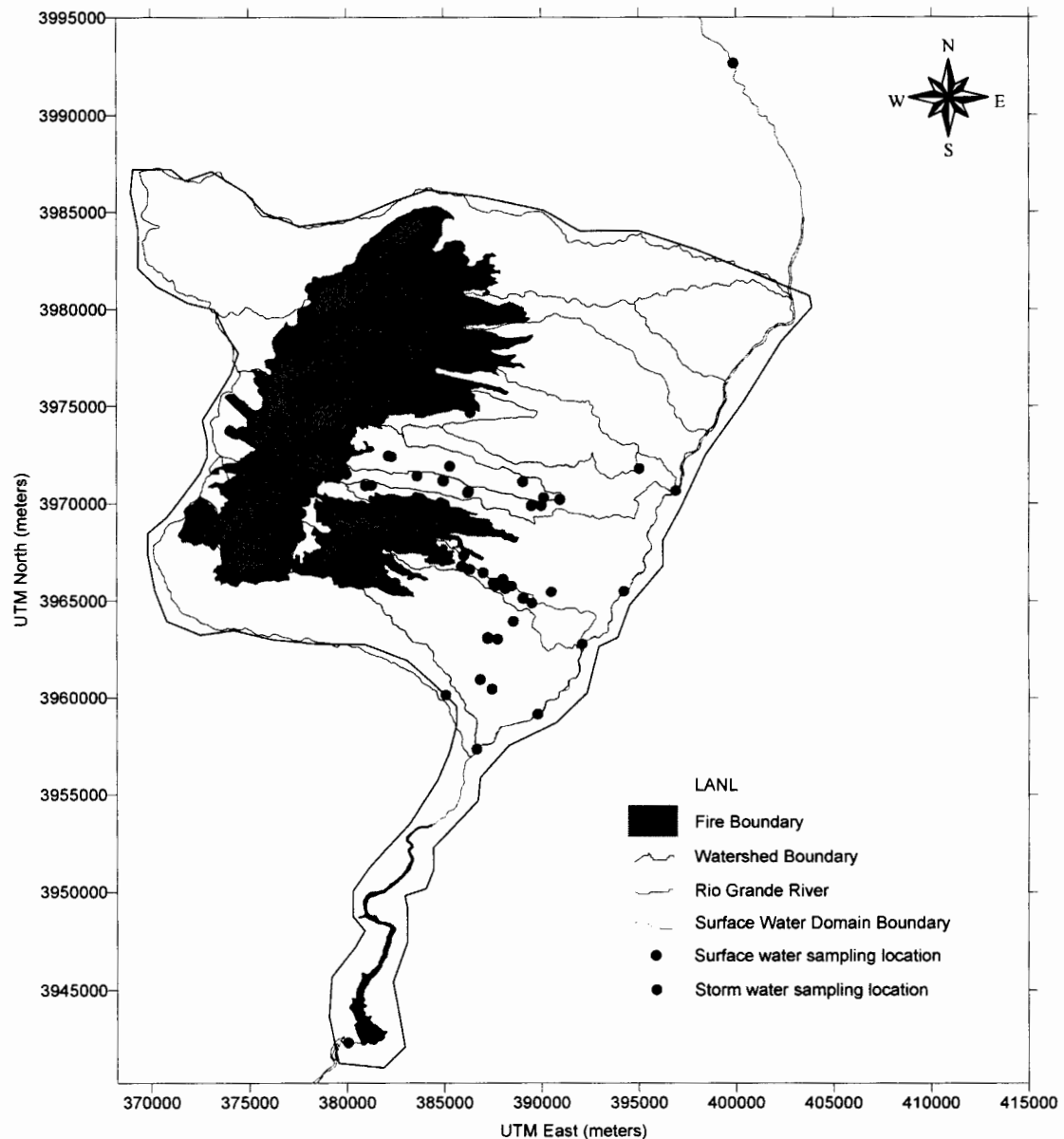


Figure 2-1. ESH-18 surface water and storm water sampling locations during 2000. The extent of the surface water domain is also shown.

ER also performs surface water, storm water, and sediment monitoring. ER identifies and characterizes potentially contaminated areas within the LANL boundaries from past operations, and, with that information, mitigates sources of contamination. Storm water samples have, for the most part, been collected manually. In recent years, automated sampling of runoff flows has been instigated in some locations. Storm water runoff events that occurred during 2000 following the fire at LANL have been described from stream gaging stations where storm water runoff samples were collected between June 2 and October 29, 2000. Automated runoff samplers were operational at some locations within DP, Los Alamos, Mortandad, Cañada del Buey, Pajarito, Water, and Ancho Canyons (Koch et al. 2001). The NMED also collects surface water, storm water, and sediment samples as part of the U.S. Department of Energy (DOE) Oversight program. The NMED was also involved with a significant amount of sampling conducted following the fire, which included additional media such as ash and area farm soils.

Figure 2-2 shows the ER surface water, storm water, and sediment sampling locations during 2000. All ER sampling locations for both surface and storm water are within LANL boundaries, with a greater number of surface water sampling locations than storm water sampling locations. ER also collected sediment and ash samples before and after the fire. Figure 2-3 shows storm water sampling locations maintained by NMED during 2000. We also considered results for samples collected from these locations in this evaluation.

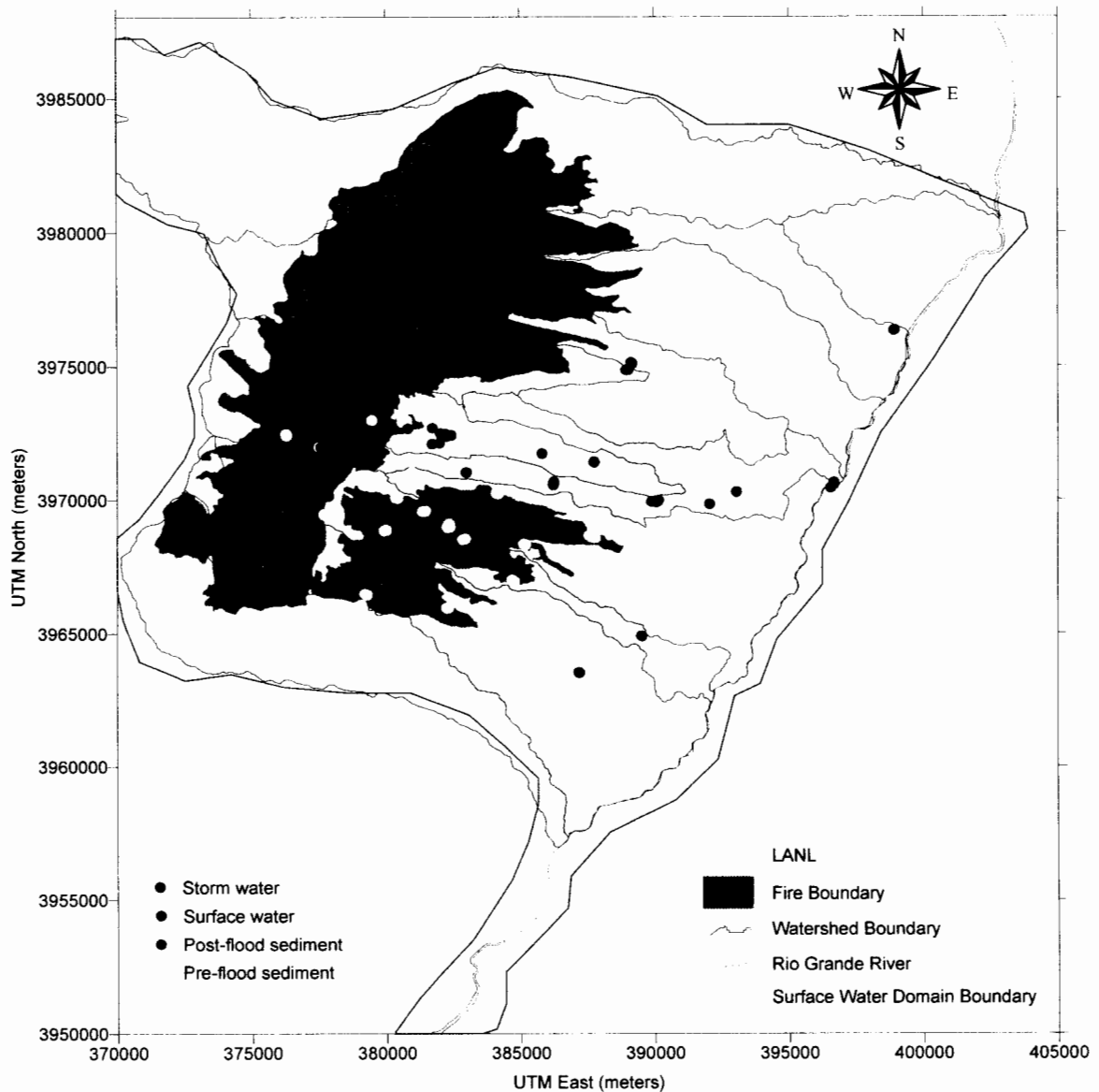


Figure 2-2. ER sediment, storm water, and surface water sampling locations during 2000. Pre-flood and post-flood designations indicate the time of the sampling. Pre-flood sediment samples were collected before the beginning of the monsoon season in June. All samples were collected following the fire.

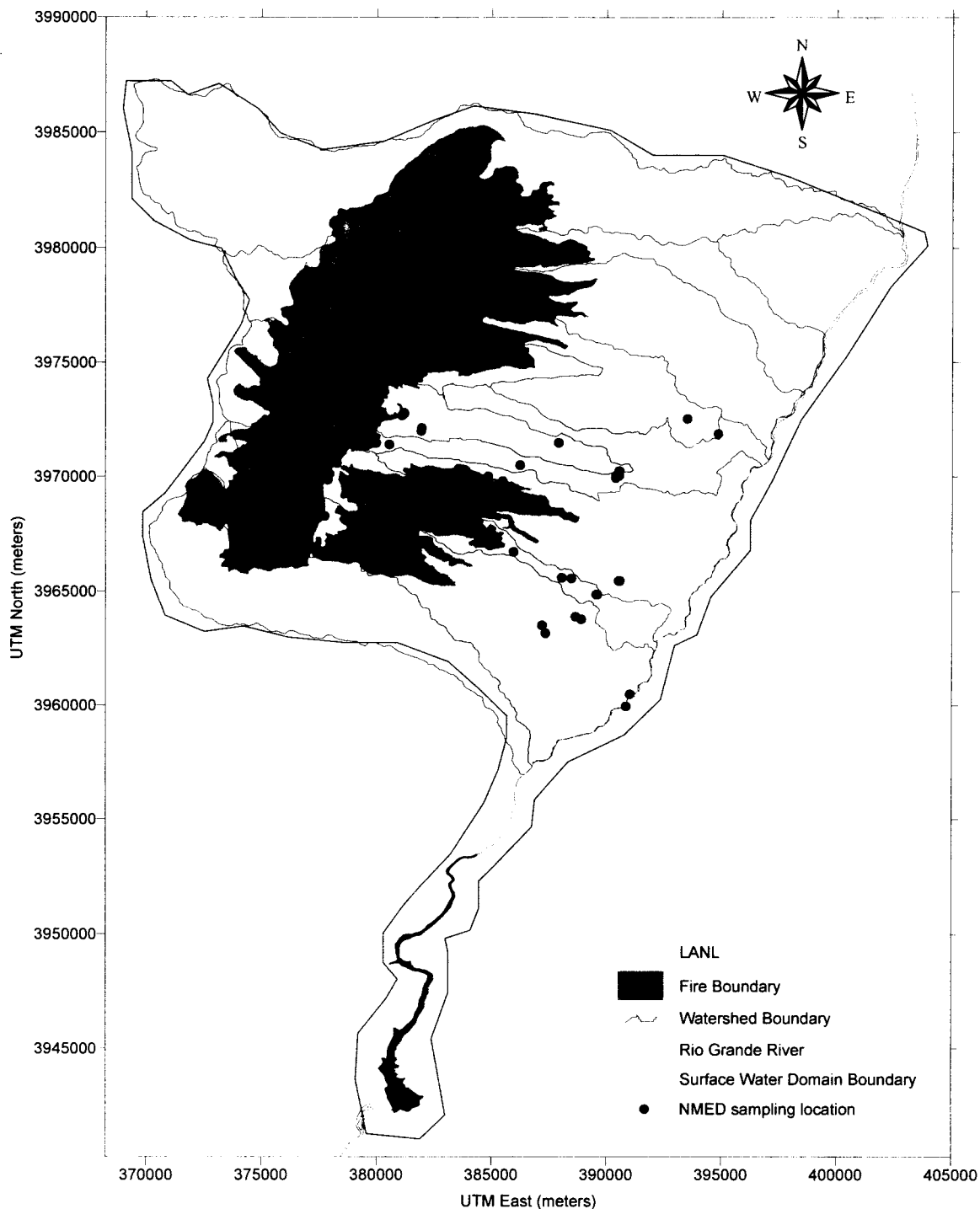


Figure 2-3. NMED storm water sampling locations during 2000.

Tables A-1 and A-2 (Appendix A) list the radionuclides and chemicals for which ESH-18 and ER monitored and reported data after the fire. Water samples were analyzed for about 75 specific radionuclides (Table A-1) and over 200 different chemicals (Table A-2). For both data sets, LANL categorized water samples by their origin as surface water (WS), storm water (WT),

or ground water (GW). The number of samples collected and analyzed for each analyte was quite variable (Tables A-1 and A-2).

The tables list the maximum and mean concentrations of each analyte measured in 2000, considering all water sources. We included the ground water sample results in this table because we used them in the screening to ensure chemicals or radionuclides were not overlooked that should be included in the risk analysis (Chapter 3). In the surface water exposure pathway evaluations for this project, we used the surface water and storm water data to compare to predicted concentrations based on the surface water modeling.

We recognize the current efforts and public concern surrounding groundwater issues at LANL and the need to understand the impact that the Cerro Grande Fire may have on groundwater in the future (LANL 2001a). While the groundwater pathway may be an important potential pathway of exposure to the public in the future, the objective of this project, funded by NMED, was on the air and surface water exposure pathways.

2.1.2 Screening Process to Prioritize Radionuclides and Chemicals

Because of the great number of samples collected and analyzed for chemicals and radionuclides in a short time period during and after the fire, we designed a screening procedure to focus our analysis on those analytes with the highest potential to contribute to the health risk of those exposed to surface water runoff from LANL. We calculated a screening index by using the available monitoring data for radionuclides and chemicals collected after the fire, readily available risk coefficients for radionuclides, and slope factors and reference doses for chemicals. Chapter 3 describes this two-stage screening process in more detail (see Figure 3-6). The reference dose is an estimate (with uncertainty spanning perhaps an order of magnitude) of a daily exposure to the human population (including sensitive subgroups) that is likely to be without an appreciable risk of deleterious effects.

For the screening process, we used measurement data from both ESH-18 and the ER. We did not incorporate the NMED data in the screening analysis because we were still in the process of compiling the necessary pieces of information into the complete data set. The Stage 1 screening conservatively assumed the maximum measured value for each analyte as reported by either organization at any onsite and offsite locations. The Stage 2 screening process was more realistic and used the highest average of all reported values by each organization for each analyte. Table 3-3 list the 17 radionuclides remaining after the Stage 2 screening. For the chemicals, two prioritized lists emerged from Stage 2 screening process: a list of 40 carcinogens where contaminants were compared by the risk index (Table 3-6a), and a list of 5 noncarcinogens where contaminants were compared by the hazard quotient (Table 3-6b).

We focused our evaluation of the monitoring data on the radionuclides and chemicals of concern that were ranked highest after the Stage 2 screening (Tables 3-3, 3-6a, and 3-6b). Our emphasis in the monitoring data analyses was to look at the data both spatially (i.e., to determine changes in concentrations at various locations on and around LANL) and temporally (i.e., to determine trends in concentrations at particular locations over time from before the Cerro Grande Fire through the year 2000). This was not intended to be an in-depth evaluation with detailed statistical analyses, but rather a broad overview of a massive amount of data to understand if and where impacts from either LANL or the fire may be suggested.

The first step in the surface water, storm water, and sediment data evaluation was to understand the times and locations that the pre-fire and post-fire monitoring data were gathered for the radionuclides and chemicals emerging from the Stage 2 screening. In an ideal situation, monitoring data for a particular analyte would have been collected regularly in the past and consistently at various locations around the LANL facility. To fully evaluate the potential for a particular analyte in water or sediment to have originated from LANL, the sampling locations would include (1) background locations (sampling locations distant from LANL that have not been affected by LANL activities), including locations upriver of LANL in the Rio Grande, and (2) various locations downstream in the Rio Grande or in Cochiti Reservoir. In addition to these locations, sampling locations within the site boundaries would be helpful to characterize onsite conditions and understand where the greatest potential for offsite migration may exist.

2.1.3 Data Compilation Process: Difficulties and Challenges

This section discusses some of the difficulties and specific challenges encountered as part of the data collection process (see Chapter 1), suggests some approaches for compiling data for future data analyses, and provides some recommendations related to actual sampling. Difficulties related to data files are addressed first, followed by those related to GIS files.

2.1.3.1 Data Files. At the outset of the project, we assumed that environmental monitoring data collected before, during, and following the fire would be readily available and in a format suitable for more or less immediate trend analysis. We also assumed that site-wide contaminant inventory estimates would be available to serve as a starting point for developing estimates of contaminant releases to air during the fire, as well as estimates of potential contaminant releases to surface water following the fire under a range of possible environmental conditions. This was not the case, however, and the data collection process proved to be much more complex than we anticipated.

We expended significant time and effort to modify the data into a readily interpretable format. This situation was the result of the widely varying methodologies and formats used by different organizations, and groups within organizations to compile and report analytical results. However, this additional effort also resulted from underestimating the sheer volume of data collected during the year 2000 as part of both the routine sampling program and the increased sampling efforts to understand the impacts of the fire. When the year 2000 data sets were combined with data collected in previous years to provide comparative measurements of contaminant concentrations in various media, it was clear that handling data volume would be a challenge. The key difficulties associated with the data collection process are summarized in more detail below; however, most of these difficulties were related to the absence of consistent data compilation methods, which applied to and existed across all organizations collecting data.

Lack of consistent collection and analytical methods—We assumed that most of the key pieces of information would be readily available with some clear and consistent method of organization because of the existing environmental monitoring programs in place at LANL and those conducted by other organizations, such as the NMED. This assumption was particularly important because of the massive amount of data collected and the additional sampling conducted by other organizations in response to the fire. Some of these organizations are the United States Geological Survey (USGS), U.S. Environmental Protection Agency (EPA), and the Department

of Energy (DOE). However, it quickly became evident that each organization had its own method for data compilation, and there appeared to be limited communication or sharing of data between the various organizations. This situation is unfortunate because it diminishes the effectiveness and utility of having multiple groups involved in sampling and data collection efforts, which is clearly an important resource during an event like the Cerro Grande Fire. Environmental monitoring data should be compiled by each organization using a common method, which would enable data to be contained and transferred, when necessary, as a single database file. Agreeing on a common format would be far preferable to the current practice, which results in the data being spread across a multitude of differently formatted files. This issue and recommendations for improvement are addressed in a later section of this report.

Incomplete data sets—Analytical results for samples collected during 2000 were not complete for some data sets almost a year after the fire. We made every effort to obtain all relevant data sets as soon as they became available, but because there was no centralized method for collecting the data, this effort required frequent and repeated communication with representatives from the various organizations that provided data. Further, some data sets were updated and/or appended with new data and provided to us with no mechanism to identify what values had changed, so any manipulation or analysis begun with the initial data sets had to be redone. In addition, some important data sets were under review and not publicly available as we began our analyses.

Large number of samples—Because of the immediate public concerns related to possible impacts of the fire, an accelerated and augmented sampling effort was put into place during the year 2000. Consequently, a very large number of samples were collected, and an even larger number of analyses were completed. Many different individuals suggested we analyze different data sets for various sampled media. We followed up on the potentially relevant data sets, regardless of their relative importance for understanding the movement of contaminants. In some cases, this effort shifted our focus to obtain information for a set of data that might not provide meaningful interpretation of potential fire impacts. In addition, it is critical to an independent analysis to obtain individual sampling results as opposed to data summaries. This need led our acquisition of several data sets containing tens of thousands of individual records. The large number of data records reinforces the need for all monitoring groups to report data using consistent methods so analytical results can be evaluated efficiently.

Lack of location coordinates—One of the most time-consuming challenges of the data collection effort was obtaining location coordinates for collected samples. To determine the important locations, it was necessary to view the sampling locations relative to major geographic features, such as watersheds or drainages, or potential areas of contamination. In addition, it was critical to readily identify and select all sample results that corresponded to a given location. To accomplish this, all analytical results for a given sample had to be linked to a specific location, identified by its coordinates. The ability to spatially visualize sampling locations is also extremely valuable for understanding where the highest concentrations of a given contaminant are occurring.

While organizations provided some maps with data sets, a map showing sampling locations was insufficient unless it specifically labeled each sampling location with a unique identifier that was linked to the analytical results. We did not receive any data sets meeting this requirement. Therefore, we had to request location coordinates, which were often provided once initially and then again following updates or revisions. In these cases, the coordinates were provided in

separate files (in another instance, sample collection dates were provided in a separate file), requiring our effort to link to the appropriate analytical results in a data set containing thousands of records.

Furthermore, we received location coordinates in various projections (e.g., Universal Transverse Mercator, State Plane, and latitude-longitude). To compare sampling results from different organizations, all coordinates must be in the same projection. We expended significant unanticipated effort to reproject many location coordinates. We were required to reproject and produce new maps multiple times when we received updated coordinates. The importance of a consistent projection for both sampling location coordinates and other GIS attribute files is discussed further in a later section of this report.

Data dictionary not readily available—Another unanticipated challenge was the receipt of large data sets with field names, codes, or notes whose meanings were unclear. Furthermore, these fields were often populated with code identifiers whose meanings were not readily apparent. For transmission of large data sets to anyone analyzing the data, it is imperative that a data dictionary be provided along with the data set to define field names, data types, and code identifiers. We received a number of data sets with unclear field names and code identifiers and spent significant effort to clarify this information.

We received some data sets that contained numerous fields that appeared to be clearly unimportant for analyzing data trends and fields containing duplicate information, which only complicated the process of identifying and separating the useful information. This additional information also unnecessarily increased the files size and made transmitting the data more difficult. The process of distinguishing between useful and not useful information was particularly tedious when a data dictionary that defined the various fields containing information did not accompany the data set. We began the project with the assumption that data sets containing the information useful for trend analysis would be readily available because the monitoring programs that collect information to enable these analyses have been in place for some time.

Lack of supporting information—It is important to clearly understand sample collection methodologies and analytical procedures to compare values from different organizations in a meaningful way. With few exceptions, this type of supporting documentation either did not accompany the various data sets or the lack of a data dictionary precluded our ability to decipher the meanings of various field codes. Furthermore, in a number of instances, the data providers gave us data that they knew to either be incorrect or have some sort of associated bias without indicating these issues. As a result, our process of understanding temporal trends was substantially complicated in some cases. Many of these data problems or other issues are discussed in various documents (e.g., annual LANL Environmental Surveillance Reports), but tracking this type of information down through sources separate from the actual data and attempting to understand and incorporate its significance is not efficient when rapid and independent analysis of data is desired.

Other difficulties—We obtained some smaller data sets that contained symbols or highlighted cells, whose meanings were not clearly defined. Other data sets were formatted to contain extra rows, which complicated trend analysis. Some analytical data were compiled so that results and uncertainty values were contained within a single cell, requiring us to separate the values to evaluate their meaning. These values had to be separated multiple times when we received updates to the data set.

2.1.3.2 Geographic Information System Files. The appropriate documentation for each GIS file is a complete meta data file. The meta data files should conform to the Federal Geography Data Committee (FGDC) content standard for digital geospatial meta data. This standard requires documentation of the base source of the information in the GIS file; the known accuracy of the data; the coordinate projection, dates, authors, and summaries of any changes or updates to the data; and a description of the attribute fields included in the GIS file.

The importance of maintaining meta data for GIS files cannot be overstated. We received GIS files from various sources at LANL and from other groups. Some form of meta data was provided in many but not all cases. In addition, the quality and completeness of the information provided in the meta data varied significantly. In some instances, the files that we received were based on files developed by other government agencies (e.g., digital line files from the USGS that were updated and modified for LANL). These are important improvements; however, without the appropriate meta data documentation, it was difficult to interpret the data and to make an independent judgment about the veracity of the data. As with the environmental data sets, we evaluated the GIS files for completeness and application to the current analysis. As a result, it was necessary to request clarification for various attributes for a number of the GIS files.

In addition to the meta data, each organization that keeps a GIS database should also keep an up-to-date data dictionary that summarizes all of the GIS files available in the database. The table or database describes each of the available files along with a list of the attributes of each file, the source of the data and a reference to the file name, and the meta data file name.

The coordinate projections used for GIS data files are mathematical representations that translate points and locations on the ellipsoidal, three-dimensional earth into mapped locations on a rectangular, two-dimensional map. A large number of projection systems are available. Because each is a mathematical representation, some are better than others for different sizes and orientations of study areas. To assist in the transfer and use of available data within an organization such as LANL as well as between LANL and other organizations, it is important to identify and adopt a consistent coordinate system. The GIS resources that we collected for this project were provided in several coordinate systems. In addition, the sampling locations for soil, groundwater, surface water, and sediment were also in several different coordinate systems. The USGS quadrangle maps and digital elevation model files that are publicly available across the country are in the UTM, North American Datum 1927 (UTM, NAD 27) coordinate projection. Many of the GIS files collected from LANL are in the New Mexico State Plane, North American Datum 1983 (State Plane, NAD 83) coordinate projection. Some files from the NMED were received with no documentation about their coordinate projections. Some of the sampling location coordinates, as mentioned previously, were in State Plane coordinates and some were in geographic coordinates (i.e., latitude and longitude). Proper meta data files, including all of the projection parameters for each GIS file, are important to maintain for each spatial file.

Because the air dispersion modeling used the CALPUFF model, which uses UTM coordinates for input data, we decided that the most appropriate projection for the current risk evaluation project was UTM, NAD 83. All of the files used for preparing maps and for implementing models or screening concentration data to develop source term values must be in a consistent coordinate projection to enable use and comparison of data. We expended considerable effort to reproject all of the GIS files and sampling location coordinates into the UTM, NAD 83 projection.

2.1.3.3 Recommendations for Data Compilation. The following sections describe the specific pieces of information required for data analysis and provide general recommendations for improving data compilation methods. We address recommendations related to data files first, followed by suggestions related to GIS files.

Data files—There are a number of reasons to maintain an environmental monitoring program. Quite often, the primary push behind environmental sampling is to satisfy regulatory compliance or permit requirements. In other cases, environmental sampling is used to characterize specific areas of known contamination. However, it is prudent to maintain an environmental monitoring program with the goal of understanding the presence, distribution, and historical trends of contaminants in environmental media associated with the operation of a facility onsite in the surrounding area. One significant advantage of consistent historical monitoring data is to provide a baseline for the evaluation of unique or unexpected events such as the Cerro Grande Fire.

Collecting environmental monitoring data to assess potential impacts of an event like a fire is critical in identifying the magnitude of contaminant concentrations and understanding the consequences of contaminant movement. To do this, it is critical to be able to evaluate historical trends at specific locations to identify apparent peaks or changes in contaminants that may be related to a specific event, such as a fire or flood. Furthermore, having multiple and different organizations collect data provides a mechanism for validating or confirming analytical results and an avenue for conducting additional sampling that may not be part of an existing program (e.g., EPA sampling for chemicals in air). The following recommendations apply to all environmental sampling, whether it is conducted to more fully understand the distribution and magnitude of contaminant levels in the environment, satisfy regulatory requirements, or characterize known areas of contamination.

A number of basic pieces of information are required to understand spatial (location) and temporal (time) trends. The following list provides a description of this information and its importance when compiling analytical results to evaluate data trends. This list should not be considered exhaustive, and adopting a suitable design requires input from a number of different organizations to identify special purposes for the data. For example, the ER Project at LANL has developed geomorphic unit identifiers for the various canyons that are useful for translating point concentrations into inventories.

Organizations responsible for sampling should be able to provide basic pieces of information related to each collected sample in a consistent format to enable efficient data analysis. All relevant information should be compiled as a single record or row for each separate analysis (e.g., all relevant data for a sediment sample analyzed for ^{137}Cs should be compiled as a single record or row). Most importantly, the design for data compilation must consider the eventual uses for the data.

- **Organization**—Who was responsible for collecting and analyzing the sample? If it is not clear based on the organization conducting the sampling, an additional field to describe the purpose of sampling may also be useful.
- **Unique sample ID**—This ID should uniquely identify a specific sample. If a sample is analyzed in duplicate or split between two or more organizations for separate analyses,

there should be some mechanism to readily identify the duplicate or split samples. All organizations should work together to adopt an identification convention that is suitable.

- **Sample collection date**—Documents when the sample was collected.
- **Sample analysis date**—Documents when the sample was analyzed. It is important to distinguish between collection and analysis dates because some radionuclides can decay appreciably or build up to higher levels, depending on the time interval. Similarly, many chemical contaminants can degrade or break down over time into various by-products.
- **Location name**—Provides a brief text description of where the sample was collected. This information is useful for selecting only those sampling results for a particular canyon or specific area.
- **Location ID**—Provides a unique identifier for the location where the sample was collected (e.g., a number or some other short series of characters) that can be readily plotted on a map designed to show the placement of sampling locations with respect to major geographical features, such as canyons, or areas of known contamination. If a longer location ID is required, a separate field should be used for a shorter map ID. Organizations conducting sampling at the same location should all use the same ID for that location.
- **x-coordinate**—In combination with a y-coordinate, this provides precise documentation for the sample collection location. At a minimum, all agencies should agree on a projection and use that exclusively. Alternatively, a better solution would be to compile coordinates for each location in a number of different projections (e.g., UTM, State Plan, latitude-longitude).
- **y-coordinate**—In combination with an x-coordinate, this provides precise documentation for the sample collection location. At a minimum, all agencies should agree on a projection and use that exclusively. Alternatively, a better solution would be to compile coordinates for each location in a number of different projections (e.g., UTM, State Plan, latitude-longitude).
- **Media**—Identifies what the sample was (e.g., sediment, soil, air, surface water, etc.). Defined codes are sufficient for this purpose, but all organizations should adopt a consistent naming convention.
- **Analyte**—Identifies the specific contaminant or other material for which analyses were conducted. Defined codes are sufficient, but all organizations should adopt the same naming convention.
- **Result**—Provides a numeric value of the analytical results. Units must be provided, and all organizations should attempt to report results using consistent units.

- **Units**—Units of measure must be provided, and all organizations should report results using consistent units.
- **Uncertainty**—Provides a numeric value describing the analytical uncertainty associated with the report result. This should always be reported in a field separate from the “Results” field.
- **Detection limit**—Specifies the minimum contaminant concentration or activity level capable of being detected by a specific analytical procedure.
- **Sampling methodology**—Describes the method used to collect the sample, which may be important for comparing results obtained by different organizations using various collection methodologies. Defined codes are suitable for this purpose, and all organizations should adopt a naming convention that includes all used sampling methods.
- **Analytical technique**—Provides documentation of the basic technique used to analyze the sample, which may be important for comparing results obtained by different organizations using various analytical techniques (e.g., gamma spectrometry, alpha spectroscopy, or liquid scintillation). Additional details, if necessary, would be through reference to a specific, documented procedure.
- **Analytical procedure**—Provides reference to a specific, documented analytical procedure (e.g., EPA), if necessary.
- **Known biases of procedure**—Identifies any known mechanisms by which the procedure used may create biases (negative or positive) in the analytical results or otherwise hinder interpretation of the results. For example, data providers have indicated this to be the case for some methods of strontium and americium analysis, and interpretation of uranium analyses has been reported to be complicated by the use of glass fibers vs. polypropylene filters.
- **Status of data**—Indicates whether the data should be considered final or preliminary. A final data set is one whose information is not expected to change, whereas a preliminary data set may change as a result of validation efforts or additional entries. A data set should not be considered final until all necessary quality assurance has been completed.

Some additional information may be important to record, depending on the particular sample that is collected or the analytical technique that is used. The following list provides examples of this type of information, but it is not intended to identify all data that may be important.

- **Sample depth**—Describes the vertical position of a sediment or soil sample. Separate fields should be used for start and end depths.
- **Sample weight**—Documents the weight of a given sample.

- **Flow rate**—Identifies the rate at which an air, or other integrated, sample is collected.
- **Sampling duration**—Indicates the time interval during which an integrated sample was collected. The flow rate and sampling duration can be used together to determine the total collected volume for a given sample.
- **Count time**—Documents the length of time for which a sample was counted for radionuclide analyses.
- **Moisture content**—Identifies the sample fraction composed of water.
- **Dry weight and wet weight**—For biotic samples that are dried before analysis, helps to compare data reported on a dry and wet weight bases.

If all agencies adopted a consistent data compilation protocol, it would greatly enhance the ability of an outside group or individual to evaluate the meaning of the data and significantly increase the efficiency, timeliness, and thoroughness with which the massive amount of currently collected data could be interpreted by the primary collecting agencies, including LANL and NMED. It would also allow the use of monitoring data to calibration atmospheric, surface water flow, and erosion models, as well as validate modeled concentrations and contaminant transport.

GIS Files— As mentioned previously, a meta data file that is updated each time the file is revised should accompany each GIS data file. This meta data file includes important information about coordinate projections, data precision and accuracy, underlying source of the data, and methods used to translate the underlying data into GIS data structures.

As with any database resource and because multiple users at LANL access the GIS files, it is important for the versions of the files to be tracked and for the integrity of the files to be monitored. All of the GIS data should be tracked using a spreadsheet or database data dictionary system. It is important for this information to be kept up to date according to data revisions, and it should define all of the attribute fields in each GIS file.

A single coordinate projection should be adopted for all LANL-related data collection and GIS applications. This consistent coordinate projection should be used by the LANL facility, the NMED, and any other agencies involved in data sharing.

Any GIS files of sampling locations, such as weather monitoring stations or groundwater monitoring wells, must have location ID and description fields that match sampling locations IDs used for the sample collection and analytical results. This will allow sampling data to be evaluated spatially. Finally, each data record in a GIS file should have a unique ID. These IDs should be consistent and unique across all GIS data sets in the spatial database for the facility.

Other recommendations—To assess the impacts of potential flooding, it would be prudent to focus on collecting representative surface and storm water samples immediately downstream from areas known to be highly contaminated or susceptible to erosion. To evaluate risks associated with LANL-derived contamination, it would be helpful to implement some additional sampling, particularly in the watersheds and drainages to the north of the Laboratory boundary, but still within the area impacted by the fire. For surface and storm water samples, an integrating sampler would also help quantify actual contaminant transport during and following a storm event. If resources are not available to support this type of sampling, collecting a larger

number of grab samples from a location during a storm event would be an improvement over a single sample.

One of the biggest limitations to conducting an analysis of risks associated with potential contaminant transport relates to the lack of information available to quantify the inventory of contaminants at existing locations identified by LANL as PRSs. Increased effort is needed to prioritize these PRSs with respect to their existing contamination levels. Documented inventories of contamination for many areas and canyons do not currently exist, and where they are available for Pueblo and Los Alamos Canyons, they are based on limited sampling conducted in 1996 and 1997. Sampling has continued in successive years to further characterize the extent of contamination, but it is not apparent that this subsequent sampling has contributed to inventory estimates for either Pueblo or Los Alamos Canyons. Including additional sampling data could lead to more defensible and refined inventory estimates. Accurate source term or inventory estimates are particularly important because of the greater potential for contaminant mobilization, transport, and relocation resulting from increased runoff following the Cerro Grande Fire.

2.2 Surface Water and Storm Water Monitoring Data: Radionuclides

2.2.1 Completeness of the Data

This section summarizes the available monitoring data and discusses trends in concentrations of radionuclides in surface and storm water. Background locations can be particularly important for identifying concentrations of analytes that are normally present in the region (such as naturally occurring radionuclides or radionuclides resulting from atmospheric weapons tests) or that appear as a result of LANL operations. In the case of the Cerro Grande Fire, it was also important to identify the chemicals and radionuclides that increased in concentrations as a direct result of the fire, regardless of the fire's proximity to LANL. With this information, it may be possible to observe changes in concentrations of key materials mobilized by a fire and related activities through spatial or temporal trend analysis. Table 2-1 provides information on the available pre-fire and post-fire surface and storm water monitoring data from ESH-18 at various locations around LANL. Surface water samples were collected under routine circumstances when water was flowing in site streams. Storm water samples were collected following heavy rainfall events, which usually occur from June through September. Storm water samples were generally from higher volume, faster moving stream locations. Similar information has been compiled for ER water samples in Table 2-2.

- For the ESH-18 surface water and storm water data (Table 2-1), historic data (from 1973–present) were gathered for ^{241}Am , ^{137}Cs , $^{239,240}\text{Pu}$, ^{90}Sr , and ^{40}K , as well as a number of other radionuclides and chemicals. Thus, it was possible to examine temporal trends for these analytes when the sampling locations remained the same over this time period.
- ESH-18 background data, that is data collected at locations not expected to be impacted by LANL operations, were collected for ^{241}Am , ^{137}Cs , $^{239,240}\text{Pu}$, and ^{90}Sr (as well as other contaminants) in both surface and storm water samples. These more distant locations provided data for spatial trend analysis to evaluate the impact of LANL on the offsite

environment. These locations were particularly helpful for determining the additional potential for releases from burned areas onsite following the Cerro Grande Fire.

- Sample results were below the detection limits for many of the naturally occurring radionuclides in surface water measured after the fire. For other radionuclides, like ^{137}Cs , about 50% were not detected (nondetects) in surface water samples and 70% (95 of 136) in storm water samples.
- For the ER sediment and water data, only post-fire data were evaluated.

Table 2-1. Summary of ESH-18 Water Monitoring Data Available Pre-fire and Post-fire for the Stage 2 Radionuclides

Radionuclides ^a	Number of samples			
	Surface water		Storm water	
	Pre-fire ^{b, c}	Post-fire ^{b, c}	Pre-fire ^{b, c}	Post-fire ^{b, c}
Pb-210	0	0	0	91 (52)
Ra-228	0	15 (0)	0	147 (45)
Ra-226	37 (37)	15 (3)	0	166 (74)
K-40	69 (69)	31 (20)	12 (10)	147 (70)
Pa-231	0	15 (0)	0	110 (4)
Ra-224	0	15 (0)	0	54 (0)
Ra-223	0	15 (0)	0	111 (5)
Th-234	0	15 (2)	0	147 (29)
Th-228	0	0		127 (104)
U-238	68 (68)	49 (34)	0	216 (116)
Cs-137	860 (859)	31 (16)	142 (142)	133 (41)
Th-230	0	0	0	164 (130)
Th-232	0	0	0	129 (101)
Pu-239	1030 (1030)	33 (29)	496 (496)	126 (92)
Sr-90	294 (293)	35 (28)	81 (81)	119 (116)
Am-241	373 (372)	64 (45)	64 (64)	263 (102)
Tritium		182		

^a These radionuclides contributed greater than 99% of the risk index (see Table 3-3).

^b Pre-fire refers to the time period before May 2000; post-fire refers to samples collected after the May 2000 Cerro Grande Fire.

^c Total number of samples; number in parentheses is the number of samples with detectable concentrations. Other concentrations were reported as below the detection limit based on the information received from LANL.

Of the 17 radionuclides ranked highest after the Stage 2 screening assessment (Table 3-3), 12 are naturally occurring radionuclides. ESH-18 has monitored some of these radionuclides in surface water since the fire (Table 2-1), in addition to the human-made radionuclides. ER has also monitored the human-made radionuclides (^{241}Am , ^{137}Cs , $^{239,240}\text{Pu}$, and ^{90}Sr), and the year 2000 monitoring data were available from ER (Table 2-2). All wildfires, regardless of origin, mobilize certain naturally occurring progeny of radon, specifically ^{210}Po , ^{210}Bi , and ^{210}Pb . Radon accumulates in forest litter and vegetation, and its natural decay processes produce these particulate decay products. Measured concentrations in soils from known contaminated areas at LANL (referred to as PRSs), also indicate several other naturally occurring radionuclides that would be detected in soils anywhere (Rood et al. 2002). For example, the decay series of ^{232}Th

and several of its progeny, including ^{228}Th , ^{224}Ra , and ^{212}Pb , were measured in soil at the PRSs but are not produced by LANL. Uranium is another naturally occurring radionuclide in soil. Uranium-238 and its progeny (^{234}U , ^{226}Ra , ^{230}Th , and ^{210}Pb) have been measured at the LANL PRS locations and are primarily from naturally occurring uranium. LANL does, however, use depleted uranium (^{238}U) in munitions and firing tests. For this analysis, we focused primarily on the human-made radionuclides.

Table 2-2. Summary of Post-fire ER Water Monitoring Data for the Stage 2 Radionuclides^a

Radionuclides	Number of samples	
	ER: Surface water	ER: Storm water
Pb-210	0	0
Ra-228	0	0
Ra-226	0	0
K-40	0	0
Pa-231	0	0
Ra-224	0	0
Ra-223	0	0
Th-234	0	0
Th-228	0	0
U-238	15	0
Cs-137	2 (1) ^b	70 (2) ^b
Th-230	0	0
Th-232	0	0
Pu-239	53 (18) ^b	48 (39) ^b
Sr-90	53 (53) ^b	52 (52) ^b
Am-241	28 (9) ^b	70 (9) ^b
Tritium		30

^a Pre-fire refers to the time period before May 2000; post-fire refers to samples collected after the May 2000 Cerro Grande Fire.

^b Total number of samples; number in parentheses is the number of samples with detectable concentrations. Other concentrations were reported as below the detection limit, based on the information received from LANL.

2.2.2 Background Concentrations

The term “background concentrations” refers to concentrations found at locations that are above the LANL boundary to the west, upriver, or more distant. The use of this term does not necessarily imply that airborne materials from LANL were not deposited at these locations. Tables 2-3 and 2-4 provide the average concentrations for Stage 2 radionuclides (historic and year 2000) at background locations for ESH-18 surface and storm water.

ESH-18 sampled surface water at three “background” locations (see Figure 2-9). These locations appear to likely represent true background concentrations:

- 98 (Jemez River)
- 174 (Rio Chama at Chamito)
- 177 (Rio Grande at Embudo).

We selected ESH-18 storm water locations positioned to the west of LANL to represent background conditions, which were different from the surface water background locations. Based on the location of PRSs within the burned area, it does not appear that these locations should be impacted by runoff across contaminated areas onsite. However, this does not imply that historical operations have not resulted in air deposition of contaminants at these locations. The background locations for ESH-18 storm water in 2000 were

- 50 (Canon del Valle above State Route [SR] 501)
- 115 (Los Alamos Canyon in Los Alamos)
- 119 (Los Alamos Reservoir)
- 155 (Pajarito Canyon above SR 501)
- 215 (Starmers Gulch above Highway 501)
- 228 (Twomile at Highway 501)
- 230 (Upper Los Alamos Reservoir)
- 234 (Water Canyon above SR 501).

In the *historic* storm water data from ESH-18 that we received, there were fewer background locations:

- Above LANL locations included 49 (Canon de Valle at SR 501) and 233 (Water Canyon at SR 501)
- Below LANL locations included 19 (Ancho Canyon at SR 4), 112 (LA Canyon at SR 4), 148 (Pajarito at SR 4), 186 (Sandia Canyon at SR 4), and 232 (Water Canyon at SR 4).

Since completing this monitoring data analysis, we have been told of additional locations that could be considered representative of background conditions that were not identified for this analysis because of inconsistencies in location nomenclature. In addition, LANL personnel have indicated that samples collected from both Guaje and Rendija Canyons could be considered to represent background. However, because of time and resource constraints, it was not possible to recreate the analyses presented here to incorporate this additional information. We do not believe this significantly impacts the general conclusions we reached in this chapter.

For some of the radionuclides in Tables 2-3 and 2-4, averages are given for both concentrations above and below the detection limit. In those cases, the average for nondetects was lower than for the detectable concentrations, as would generally be expected, except for ^3H and ^{238}U . We do not have an explanation for why the average for values reported as nondetects would be higher than the average for detectable concentrations, and a detailed investigation into this issue is beyond the scope of this work. Some contributing factors could be differences in the sample size or geometry or in the method of analysis.

These background locations were useful for providing some general perspective on the magnitude of surface water concentrations in locations that could be assumed to be removed from LANL impact. While it would have been very useful to have background water samples from fire-impacted areas distant from LANL, such samples were not collected by any agencies. In contrast, the sediment data analysis was enhanced because sediment samples were collected from locations quite distant from LANL in areas impacted and not impacted by the fire.

Table 2-3. ESH-18 Surface Water Data from Locations Designated as Background^a

Radionuclide ^b	Qualifier ^c	Average (pCi L ⁻¹)	Number of samples
Am-241		3.8	20
Cs-137		23	48
H-3		555	50
Pu-238		-0.006	53
Pu-239, 240		0.002	53
Sr-90		2.1	14
Sr-90	<	0.04	2
U-234		0.85	4
U-235		0.03	1
U-238		0.49	4

^a Locations 98, 174, 177; these are locations above or distant from LANL.

^b Stage 2 radionuclides (see Table 3-3).

^c The data qualifier, <, identifies average values for data reported as below detection limit for that radionuclide. The rows without the data qualifier, <, show average values for detectable data only; no results are presented for the mean of all samples.

2.2.3 Temporal Trends in Water Data

The ESH-18 surface water data sets enabled us to examine concentrations over time in surface water and provide a historic perspective of trends at similar locations, including some background locations. We focused on the human-made radionuclides listed in Table 3-3 that were expected to contribute most to potential risk to members of the public. ESH-18 surface water data covered the time from the early 1970s to the present. There were historic ESH-18 storm water data for a few onsite locations and some background locations.

Only year 2000 data were provided in the ER and NMED data sets we used for our analysis; therefore, we did not perform temporal data trend analyses on these data. We have also examined monitoring data for the chemicals listed in Table 3-6. However, there were either no post-fire monitoring data available for these chemicals, or the available post-fire results were reported as below the detection limit. Therefore, it was difficult to make any conclusive statements, based on available monitoring data, about the potential for movement of these contaminants and subsequent exposure to members of the public.

2.2.3.1 ESH-18 Surface Water. We examined the data for temporal trends of ¹³⁷Cs, ^{239,240}Pu, ²⁴¹Am, and ⁹⁰Sr to see if an additional impact from contaminated areas at LANL during the fire could be discerned. Figures 2-4 and 2-5 show concentrations of radionuclides measured at background locations to provide some perspective to the concentrations measured over time.

Cesium-137 measurements were made historically at the background location 98 beginning in August 1973. The data can be viewed in several ways to help understand the temporal trends. Figure 2-4 shows ¹³⁷Cs concentrations at several locations over time. Although increases in ¹³⁷Cs over average historic background levels were evident at several locations in the late 1980s and early 1990s, the concentrations were not different from concentrations at background locations. On the whole, these data do not indicate increases in ¹³⁷Cs concentrations at these river locations following the fire.

Table 2-4. ESH-18 Storm Water Data from Locations Designated by *RAC* as Background^a

Radionuclide ^b	Qualifier ^c	Average (pCi L ⁻¹)	Number of samples
Am-241		2.1	19
Am-241	<	0.59	41
Cs-137		69	13
Cs-137	<	0.44	23
Pu-239,240		1.2	18
Pu-239,240	<	0.01	12
Sr-90		11	29
Th-228		12	24
Th-228	<	0.06	5
Th-232		12	20
Th-232	<	0.01	9
U-238		6.6	31
U-238	<	42	28
Ba-140		60	2
Ba-140	<	16	15
Cd-109		27	2
Cd-109	<	8.0	27
H-3		-63	9
H-3	<	32	6
Pu-238		0.10	16
Pu-238	<	0.0032	14
Ru-106		4	2
Ru-106	<	0.64	34
U-234		6.5	30
U-234	<	0.08	2
U-235		22	4
U-235	<	5.9	32

^a Post-fire storm water locations (234, 50, 215, 155, 228, 119, 230, and 115); these are locations above or more distant from LANL.

^b Stage 2 radionuclides (see Table 3-3).

^c The data qualifier, <, identifies average values for data reported as below detection limit for that radionuclide. The rows without the data qualifier, <, show mean values for detectable data only; no results are presented for the mean of all samples.

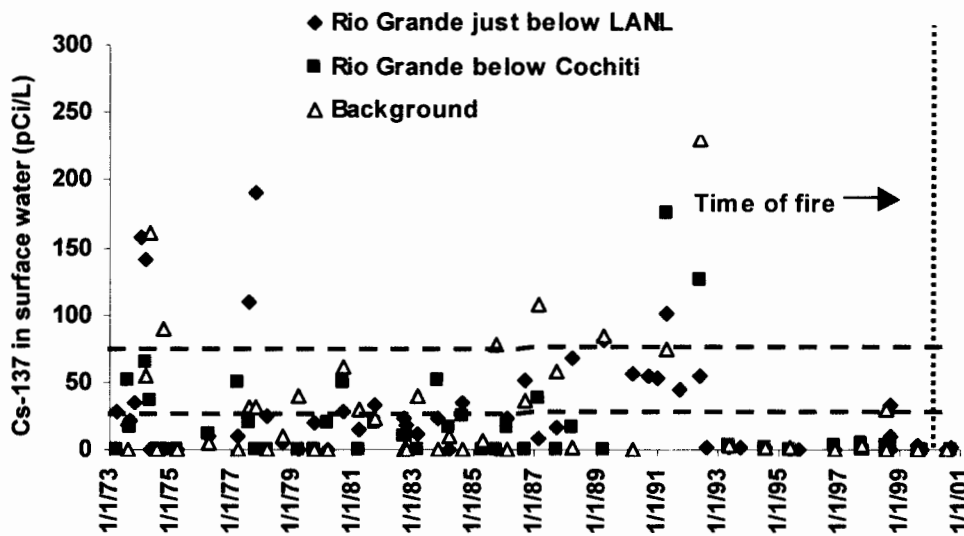


Figure 2-4. Concentrations of ^{137}Cs in surface water collected at a background location above LANL, at six locations just below LANL along the Rio Grande, and from the Rio Grande below Cochiti Reservoir. The lower green dotted line shows the average ^{137}Cs concentration from *surface water* locations designated as background, and the upper green dotted line shows average concentration of ^{137}Cs following the fire in *storm water* from locations designated as background. The vertical red dashed line shows the time of the fire.

Table 2-5 provides statistics on the ^{137}Cs data at the individual sampling locations along the Rio Grande just below LANL (grouped together in Figure 2-4 as Rio Grande just below LANL) that were collected historically and following the Cerro Grande Fire. These results do not suggest statistically significant (based on a general review of mean and standard deviation values) differences among ^{137}Cs concentrations when all data are grouped together by location.

When the $^{239,240}\text{Pu}$ monitoring data are graphed in a similar manner (Figure 2-5), there is a suggestion of higher $^{239,240}\text{Pu}$ concentrations after the fire in Rio Grande water collected from several locations just below LANL, compared to concentrations measured at the background location and below Cochiti Reservoir. However, the time trend also shows an elevated $^{239,240}\text{Pu}$ reading in water from the river just below LANL in September 1998, and elevated concentrations were also seen at the background location some distance from LANL. There were fluctuations in the data over time with indications of increased concentrations in 1994 and 1995.

Table 2-5. Statistics on ^{137}Cs Data Collected Historically through 2000

LANL location	Map ID #	Figure 2-4 designation	Number of samples (1973–2000)	Mean (pCi L ⁻¹)	Standard deviation (pCi L ⁻¹)	Maximum (pCi L ⁻¹)	Minimum (pCi L ⁻¹)
Jemez River	98	Background	46	28	47	231	-50
Ancho at Rio Grande	18	A ^a	30	37	72	350	-26
Frijoles at Rio Grande	69	B ^a	19	13	26	95	-45
Mortandad at Rio Grande	134	C ^a	34	22	36	114	-39
Pajarito at Rio Grande	147	D ^a	30	14	23	101	-58
Rio Grande at Frijoles (bank)	178	E ^a	11	19	50	178	-2
Rio Grande at Otowi	179	F ^a	46	30	49	190	-143
Rio Grande at Cochiti	176	Rio Grande below Cochiti Reservoir	49	18	34	175	-90

^a The *RioGrande* just below LANL data in Figure 2-4 includes this location.

The ^{241}Am data consisted of significantly fewer results than were available for ^{137}Cs and $^{239,240}\text{Pu}$. The pre-fire data showed measurable increases in concentration in 1998 and 1999 at locations just below LANL in the Rio Grande, and below Cochiti Reservoir, compared to ^{241}Am concentrations in water from the background location. The post-fire data showed no increases in ^{241}Am concentrations at any of these offsite locations.

Likewise, the ^{90}Sr data consisted of few results until the 1990s when more samples were collected in surface water at a greater number of locations. This monitoring pattern resembled that for ^{241}Am . There were few ^{90}Sr samples in the 1970s, none reported in the 1980s, and then the monitoring program was resumed in the 1990s. The pre-fire data showed some increases in measurable concentrations in the early and late 1990s at locations just below LANL in the Rio Grande, compared to ^{90}Sr concentrations in water from the background locations. The post-fire data showed no increases in ^{90}Sr concentrations at any of these offsite locations. As noted earlier, changes in analytical and/or sampling methods over time complicated drawing definitive conclusions based on these comparisons.

2.2.3.2 ESH-18 Storm Water Data. We compared concentrations of ^{137}Cs and $^{239,240}\text{Pu}$ in storm water samples collected by ESH-18 historically and in the year 2000 following the fire. Table 2-6 provides the average concentrations with standard deviations for ^{137}Cs , $^{239,240}\text{Pu}$, ^{241}Am , and ^{90}Sr . Historic storm water data for the locations we used from above LANL were limited, with fewer samples collected than for locations below LANL. Historic data from below LANL locations that we used in our analysis were more numerous for ^{137}Cs (21 samples) and for $^{239,240}\text{Pu}$ (94 samples), but it was limited for ^{241}Am (1 sample) and for ^{90}Sr (2 samples).

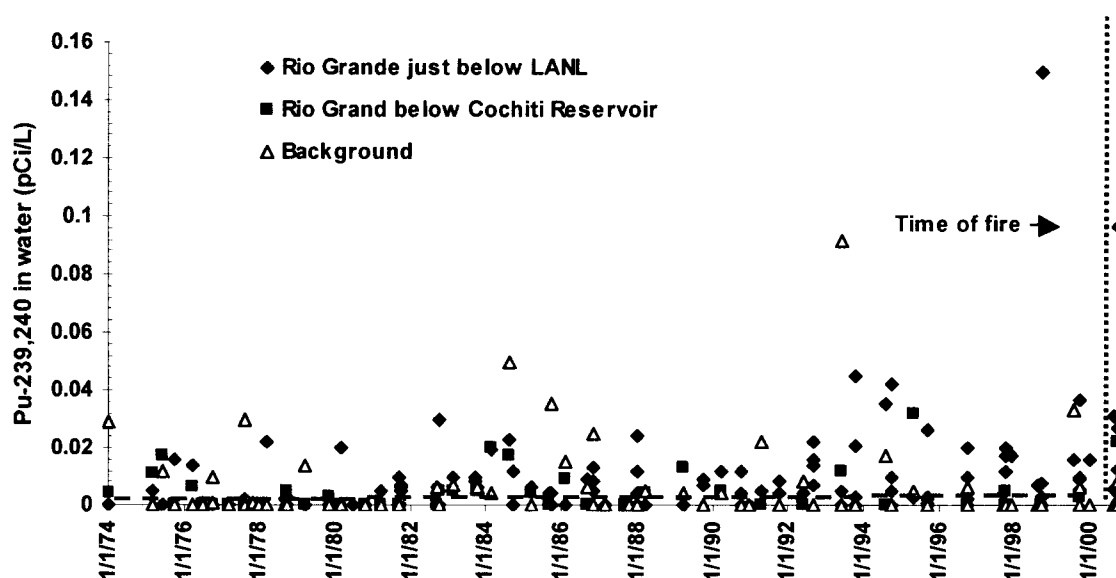


Figure 2-5. Concentrations of $^{239,240}\text{Pu}$ in surface water collected at a background location above LANL, at six locations just below LANL along the Rio Grande, and from the Rio Grande south of Cochiti Dam. The green dotted line shows the average $^{239,240}\text{Pu}$ concentration (0.002 pCi L^{-1}) from surface water locations designated as background (Table 2-5). Following the fire, the concentration of $^{239,240}\text{Pu}$ in *storm water* from locations designated as background is 1.2 pCi L^{-1} (Table 2-4). The red line shows the time of the fire.

Table 2-6. Average Concentrations of Radionuclides in Storm Water

Radionuclide	Data source ^a	Concentrations (pCi L^{-1}) ^b	
		Above LANL(n) ^c	Below LANL(n) ^c
Cs-137	Historic	93 ± 33 (2)	26 ± 62 (21)
	Post-fire	8.4 ± 6.4 (6)	22 ± 14 (7)
Pu-239,240	Historic	0.02 ± 0.01 (4)	0.07 ± 0.20 (94)
	Post-fire	0.88 ± 0.90 (6)	1.1 ± 1.6 (6)
$^{241}\text{Am-241}$	Historic	Not analyzed	0.03 (1)
	Post-fire	0.47 (15)	4.6 ± 15.7 (13)
$^{90}\text{Sr-90}$	Historic	Not analyzed	0.75 ± 0.64 (2)
	Post-fire	23 ± 19 (5)	10.5 ± 16.5 (6)

^a All data from ESH-18.

^b Values are averages ± 1 standard deviation.

^c Number of samples are in parentheses.

Table 2-6 shows similar levels of ^{137}Cs and $^{239,240}\text{Pu}$ concentrations in storm water below LANL historically and after the fire. The data for $^{239,240}\text{Pu}$, ^{241}Am , and ^{90}Sr at *below LANL* locations suggested possible increases in concentrations but are more difficult to interpret based on small sample size and large standard deviations. In addition, an increase in concentration of $^{239,240}\text{Pu}$ at *above LANL* locations was also suggested after the fire. While this trend may reflect additional materials mobilized by runoff over burned areas at locations both *above and below* LANL, these data should be viewed cautiously. Storm water events are quite unique and variable and the resulting level of contaminants in storm water depends upon the intensity of the event, the area where runoff occurred, and the timing of the grab sampling during or after the storm.

One of our questions posed in the Introduction was “*Are there differences in concentration seen before and after the fire in the Rio Grande?*” Our temporal trend analysis of the ESH-18 surface water data did not show increases in concentrations of ^{137}Cs , $^{239,240}\text{Pu}$, ^{241}Am , and ^{90}Sr above those concentrations measured historically in the Rio Grande. There are instances where increases of some radionuclides were measured at various times in the past, particularly in the 1990s. However, a more careful quantitative analysis would be needed to determine conclusively that there were no obvious increases following the fire. Concentration differences were seen, but the concentrations for some radionuclides measured after the fire tended to be less than concentrations measured in the years preceding the fire, in particular for ^{241}Am and $^{239,240}\text{Pu}$, and ^{90}Sr in the early 1990s. In storm water, increases of some radionuclides were measured in the Rio Grande, but similar increases were also measured at locations above LANL.

2.2.4 Spatial Trends in Surface and Storm Water Data

Spatial trend analysis examines how a material is distributed in the environment, and it may help to identify areas of surface water flow where higher concentrations of radionuclides were measured in the months following the Cerro Grande Fire. This type of analysis can show whether the areas of higher concentrations are onsite, near boundary areas, or offsite. The spatial trends for surface and storm water were limited to locations sampled, generally within LANL boundaries with a few locations away from the site. Figures 2-6 and 2-7 show the locations where increases in concentration of ^{137}Cs , measured by both ESH-18 and ER, occurred in surface water (Figure 2-6) and in storm water (Figure 2-7). Figure 2-6 shows two elevated areas of ^{137}Cs : at the bottom of Acid Canyon below the Weir for the ER data and in Mortandad Canyon at GS-1 for the ESH-18 location.

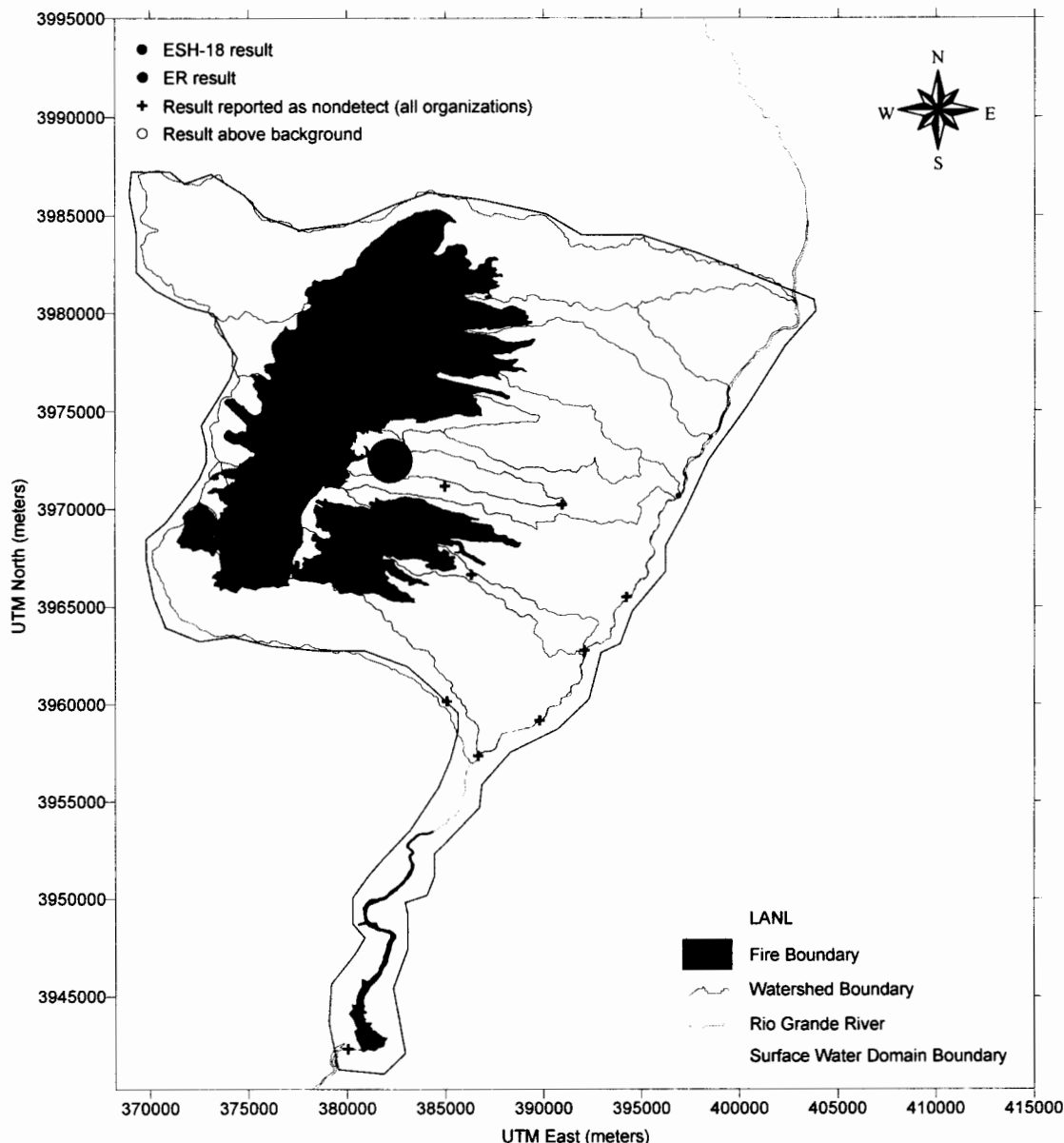


Figure 2-6. Relative magnitude of measured concentrations of ^{137}Cs in surface water collected following the Cerro Grande Fire. Concentrations reported as detectable range from 1.28–44 pCi L⁻¹. The size of the symbol is proportional to the reported concentration. Red-circled symbols indicate concentrations greater than the average surface water background concentration (22-7 pCi L⁻¹) (Table 2-3). Because of some symbol overlap, all reported concentrations are not visible on this map.

Relative levels of ^{137}Cs concentrations in storm water are shown in Figure 2-7, which shows elevated ^{137}Cs concentration in storm water samples from ESH-18, ER, and NMED. The locations of the elevated ^{137}Cs in ESH-18 storm water samples were from Los Alamos Canyon above SR 4, from Guaje Canyon at SR 502, and from Pajarito Canyon at SR 501. The ER storm water sample with the elevated ^{137}Cs concentration was collected in Pueblo Canyon upstream of Kwaje Canyon in connection with a flood on August 12, 2000.

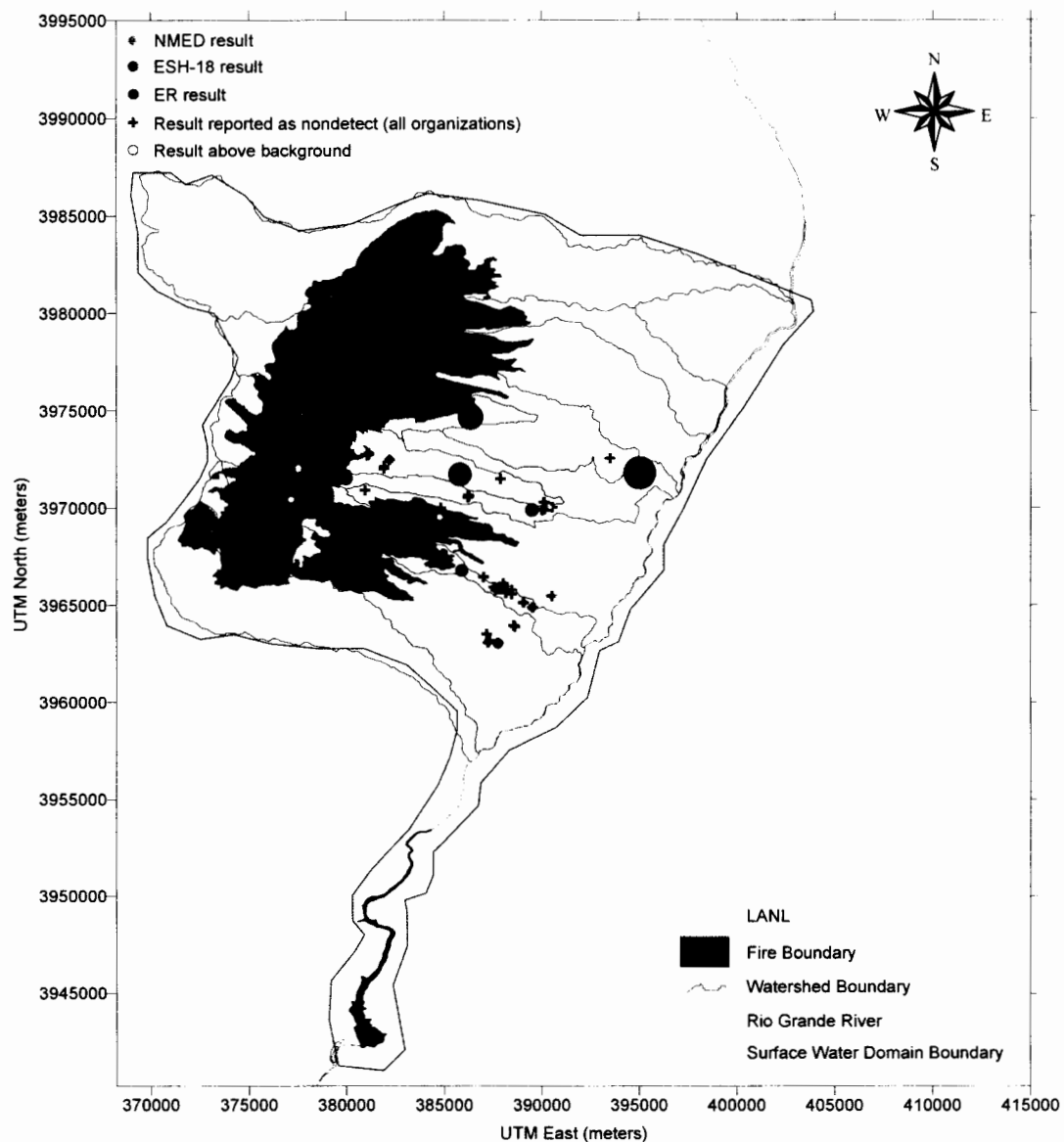


Figure 2-7. Relative magnitude of measured concentrations of ^{137}Cs in storm water collected following the fire. Concentrations reported as detectable range from 0.1–511 pCi L⁻¹. The size of the symbol is proportional to the reported concentration. Red-circled symbols indicate concentrations greater than the average surface water background concentration (22.7 pCi L⁻¹) (Table 2-3). Because of some symbol overlap, all reported concentrations are not visible on this map.

Data were available to do similar spatial analyses for the other important radionuclides. The spatial analyses of surface and storm water samples indicated no areas of high concentration offsite based on the sampled locations. We also compared concentrations of various radionuclides at locations upriver (locations 174 and 177) and downriver (location 176) for data collected in 2000 after the Cerro Grande Fire. Higher levels of radionuclides were readily apparent at onsite locations compared to offsite locations. However, interpreting spatial trends in offsite data must

be done with care because of the limited number of samples collected and analyzed at each location for each radionuclide. Although we could see certain patterns in the river data, it was difficult to draw definite conclusions about the relative differences in concentrations measured at offsite locations. It was also difficult to determine the source of these radionuclides and whether the Cerro Grande Fire impacted levels.

2.3 Sediment and Ash Monitoring Data

Sediment monitoring data can provide important information upon which to draw conclusions about the distribution and source of contaminants in the environment. In many cases, a greater understanding can be drawn from the sediment data than from the water data. For example, the sediment monitoring data we evaluated included several background locations for comparison. In addition, historical monitoring was performed at more of the year 2000 post-fire sampling locations, which allowed for more robust temporal comparisons for sediment than for water. Furthermore, sediment acts as an integrating medium, or sink, for many contaminants and can provide a more comprehensive understanding of contaminant distribution, particularly in a nonequilibrium system such as the canyons and drainages in the LANL area.

While the majority of sample results we analyzed were indicated to be sediment samples, we considered other media in the evaluation, including soil, sludge, muck, and ash. Soil samples were primarily used to understand regional background concentrations. Sediment, sludge, muck, and ash samples were generally considered to be the same for the purposes of this analysis because many post-fire samples consisted of some unknown fraction of ash and the distinction between these media was often subjective and differed between the various sampling agencies. Also, sampled media often were described as consisting of “sediment and sludge” or “sediment and ash,” making a clear distinction between media difficult.

2.3.1 Background Concentrations

To fully understand the impacts of the Cerro Grande Fire on contaminants in the environment resulting from LANL operations, it was helpful to examine concentrations of these contaminants in areas not affected by LANL operations (also referred to as background locations) that were impacted and not impacted by fire. Figures 2-8 and 2-9 show sediment sampling locations used by ESH-18 and ER, respectively, to monitor background concentrations. Figure 2-9 also shows several locations (116–120) useful for evaluating sediment concentrations in areas near the Rio Grande that could be impacted by migration of LANL-origin contamination, as well as sampling locations in Guaje (111–114) and Rendija (125–128) Canyons. Figure 2-10 shows NMED sediment and soil sampling locations that are not expected to be affected by LANL operations.

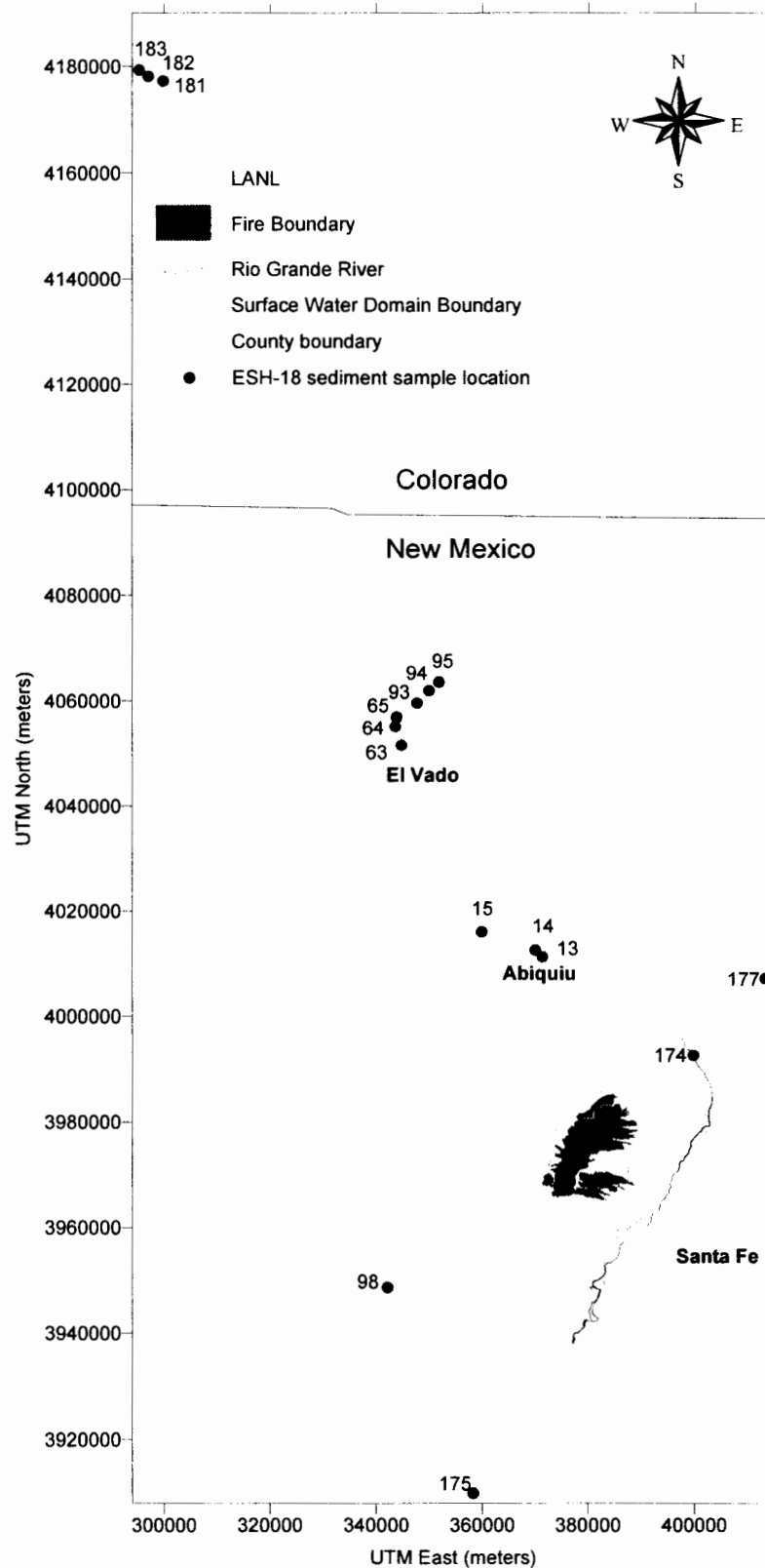


Figure 2-8. ESH-18 background sediment sampling locations. Locations 98, 174, and 177 are also background surface water sampling locations.

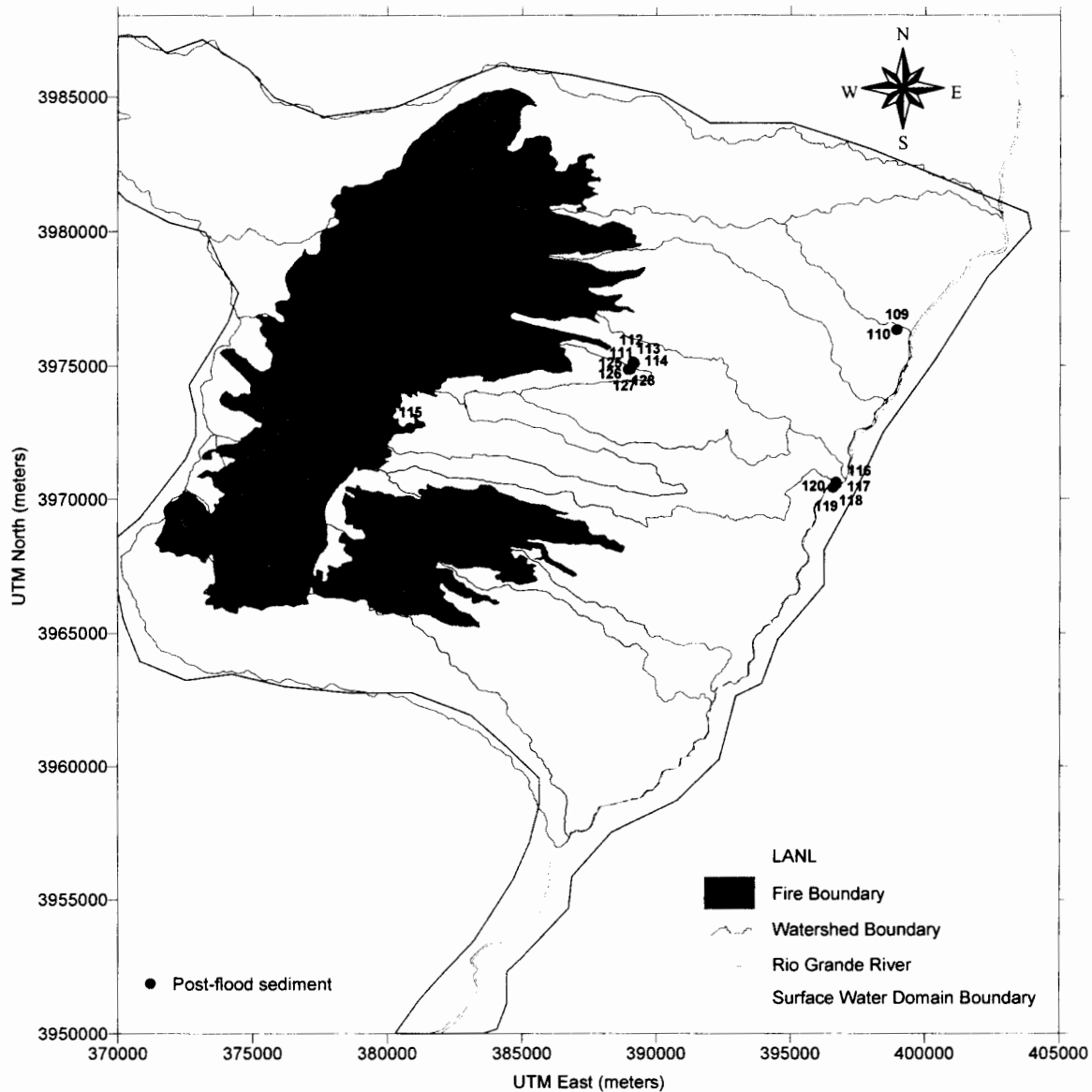


Figure 2-9. ER background sediment sampling locations (129, 115, 109, and 110). ER and RAC do not consider locations 116–120 to be background locations, but they are shown here as locations useful for evaluating sediment concentrations in areas near the Rio Grande that could be impacted by migration of LANL-origin contamination. Also shown are sampling locations in Guaje (111–114) and Rendija (125–128) Canyons.

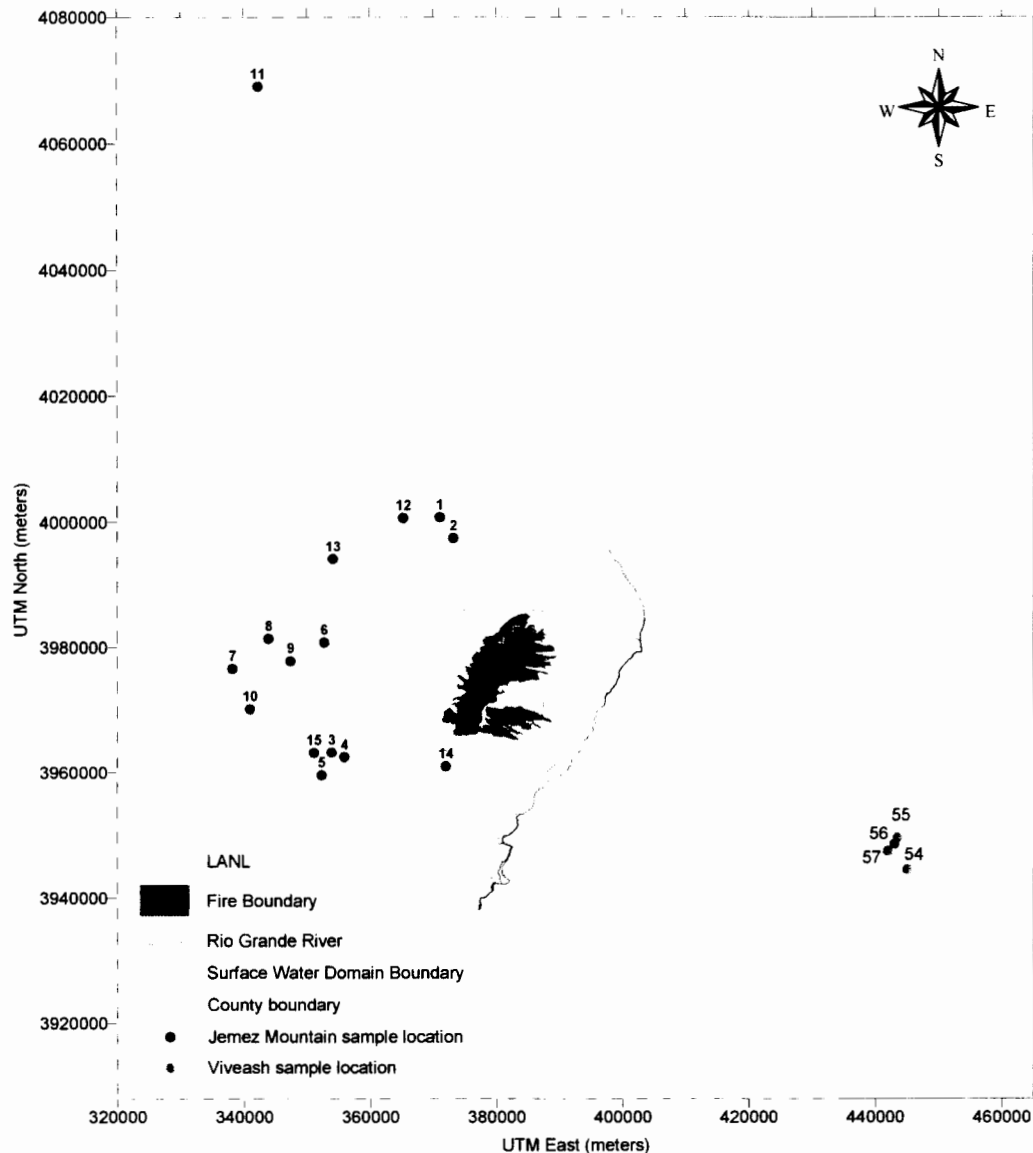


Figure 2-10. NMED background sediment/ash and soil sampling locations. Locations 1–15 represent Jemez Mountain background soil sample locations, and locations 54–57 represent sediment/ash sample locations indicated to be in the Viveash Fire area.

Table 2-7, compiled from several sources, lists concentrations of a number of primarily human-made radionuclides measured in sediment, muck, sludge, ash, and soil from areas not expected to be influenced by LANL operations or impacted by recent fires (see Table 3-3 for a list of priority radionuclides). It is important to note that the selection of locations considered representative of background locations was subjective in many instances, based on criteria established by the data-collecting agency. For example, the sources listed in Table 2-7 as Purtyman et al. (1987), ESH-18 (1), ESH-18 (2), and NMED included samples from locations far from the LANL site, and there was little question that they were appropriate indicators of regional background concentrations. The Ryti et al. (1998) source, on the other hand, consisted of locations within the LANL boundary, presumably in areas assumed to be uncontaminated. Similarly, the sources listed in Table 2-8 as ER Viveash and NMED Viveash included samples

from locations far from the LANL site. However, the ER (1) and ER (2) locations were from areas close to the LANL site. This is important because it is not known to what extent historical operations at LANL may have impacted regional chemical and radionuclide concentrations within and beyond the LANL boundary. For this reason, the designation of locations close to LANL as background was subjective and may or may not be appropriate. However, based on a comparison of values reported for areas far from the LANL site, it appeared that the locations designated as background and close to or within the LANL boundary were reasonable indicators of regional background concentrations.

Table 2-8 lists concentrations for the same radionuclides measured in areas not expected to be influenced by LANL operations but impacted by recent fires. Table 2-9 shows the range of concentrations reported in Tables 2-7 and 2-8 for areas impacted and not impacted by fire. The highlighted radionuclides show clearly higher measured concentrations in locations impacted by recent fires but not expected to be influenced by LANL operations. The existence of elevated chemical and radionuclide concentrations in ash collected from burned areas is examined again in Chapter 3, and that evaluation formed the basis for characterizing the burned area as a potential contributing source of chemicals and radionuclides for the surface water pathway transport calculations. We attempted to evaluate concentrations of priority chemicals (see Table 3-6) measured in sediment and soil from these areas, but no detectable concentrations were reported in any of the samples collected at these locations.

Table 2-7. Concentrations^a of Radionuclides in Areas Not Influenced by LANL Operations or Impacted by Recent Fires

Analyte	Source									
	Purtyman et al. (1987)		Ryti et al. (1998) ^b		ESH-18 (1) ^c		ESH-18 (2) ^d		NMED ^e	
	Soil	Sediment	Mean	# ^f	Mean	#	Mean	#	Mean	#
Am-241	NA ^g	NA	0.021	23/23	0.042	61/67	0.065	52/52	0.006	15/30
Cs-137	0.43	0.18	0.60	7/17	0.23	102/104	0.30	47/47	0.73	30/30
Pu-238	0.001	NA	0.002	22/24	0.007	81/84	0.0012	53/53	0.0012	15/15
Pu-239	0.007	0.005	0.018	23/23	0.014	109/109	0.007	55/55	0.021	15/15
Ru-106	NA	NA	NA		NA		NA		NA	
Sr-90	0.34	0.23	0.36	18/24	1.07	59/63	0.76	34/34	0.31	14/15
Th-228	NA	NA	1.44	24/24	1.43	4/4	NA		NA	
Th-232	NA	NA	1.43	24/24	1.3	4/4	NA		NA	
H-3	NA	NA	0.024	23/23	0.001	2/2	NA		NA	
U-234	NA	NA	1.4	24/24	0.77	9/9	NA		1.08	15/15
U-235	NA	NA	0.12	15/24	NA		NA		0.138	17/30
U-238	NA	NA	1.3	22/24	0.89	12/13	NA		1.07	15/15
Np-237	NA	NA	NA		NA		NA		NA	
Ba-140	NA	NA	NA		NA		NA		NA	
Cd-109	NA	NA	NA		NA		NA		NA	

^a Mean concentrations were calculated using only positive results reported as detected (pCi g⁻¹) and were for sediment samples only unless otherwise noted; NA indicates no results meeting these criteria.

^b Based on electronic compilation of tabular data supporting this report provided by ER (sediment samples).

^c Included sediment samples collected at ESH-18 locations 98, 174, 175, 177, 13, 14, and 15 (see Figure 2-8).

^d Included sediment samples collected at ESH-18 locations 63, 64, 65, 93, 94, and 95 (see Figure 2-8).

^e Included NMED Jemez Mountain soil sampling locations (see Figure 2-10).

^f # = the number of results reported as detected/the number of total results reported.

Table 2-8. Concentrations^a of Radionuclides in Areas not Influenced by LANL Operations but Impacted by Recent Fires

Analyte	Source							
	ER (1) ^b		ER (2) ^c		ER Viveash ^d		NMED Viveash ^e	
	Mean	# ^f	Mean	#	Mean	#	Mean	#
Am-241	0.13	6/7		0/5	0.81	1/8	0.046	5/5
Cs-137	4.39	7/7	4.48	4/5	5.08	6/8	3.94	5/5
Pu-238	0.037	3/7	0.049	1/4		0/8	0.014	5/5
Pu-239	0.37	7/7	0.225	3/5	0.134	6/8	0.084	5/5
Ru-106		0/7		0/5		0/8	NA	
	2.08							
Sr-90		7/7 ^g	1.74	2/5	1.41	6/8	0.48	5/5
Th-228	1.23	7/7	NA		NA		NA	
Th-232	1.07	7/7	NA		NA		NA	
H-3	NA		NA			0/8	NA	
U-234	1.38	7/7	1.48	5/5	1.56	8/8	0.97	5/5
U-235	0.13	7/7	0.089	1/5	0.17	6/8	0.032	5/5
U-238	1.85	7/7	1.66	5/5	1.31	8/8	0.93	5/5
Np-237	NA		NA		NA		NA	
Ba-140	NA		NA		NA		NA	
Cd-109	NA		NA		NA		NA	

^a Mean concentrations were calculated using only positive results reported as detected (pCi g⁻¹); NA indicates no results meeting these criteria.

^b ER Mountain Front sample locations 1–7 (see Figure 2-9) designated by ER as pre-flood (post-fire) and consisting of ash and muck according to the indicated sample type and soil according to the indicated sample matrix.

^c ER background sample locations 109, 110, 115, and 129 (see Figure 2-9) designated by ER as post-flood and consisting of sediment according to the indicated sample type and soil, sediment, and miscellaneous media according to the indicated sample matrix.

^d ER soil samples collected in the Viveash Fire area.

^e NMED sediment samples collected in the Viveash Fire area (see Figure 2-10).

^f # = the number of results reported as detected/the number of total results reported.

^g All detected results reported with qualifier (J+) indicating positive bias.

2.3.2 Data Trends

To examine the potential impacts of the Cerro Grande Fire on contaminant movement, we evaluated temporal and spatial trends in collected monitoring data. Evaluating changes in measured concentrations over time, or temporal trends, can assist in determining if the fire caused concentrations to increase, decrease, or had little noticeable impact. Likewise, examining concentrations by location, or spatially, can help identify those locations where the highest concentrations of a particular contaminant were measured.

The primary data sets that enable analyses of post-fire sediment concentrations in the LANL area included data collected by NMED, ER, and ESH-18. Figure 2-2 shows the sediment sampling locations maintained by ER during 2000. Figure 2-11 shows sediment sampling locations maintained by ESH-18 during 2000, and Figure 2-12 shows sediment sampling locations maintained by NMED. Of the 142 ESH-18 locations shown in Figure 2-11, 37 of those were sampled following the fire. Of those 37 locations, 35 were sampled at some point before the fire, enabling a comparison of post-fire and pre-fire data.

**Table 2-9. Range of Mean Background Radionuclide Concentrations in Areas not Impacted
by Fire and in Areas Impacted by Fire**

Analyte	Background concentration range ^a	
	Fire impacted (Table 2-8)	Not impacted by fire (Table 2-7)
Am-241	0.046–0.81	0.006–0.065
Cs-137	3.94–5.08	0.18–0.73
Pu-238	0.014–0.049	0.001–0.007
Pu-239,240	0.084–0.37	0.005–0.021
Ru-106	NA	NA
Sr-90	0.48–2.08	0.23–1.07
Th-228	1.23	1.43–1.44
Th-232	1.07	1.3–1.43
H-3	NA	0.001–0.024
U-234	0.97–1.56	0.77–1.4
U-235	0.032–0.17	0.12–0.14
U-238	0.93–1.85	0.89–1.3
Np-237	NA	NA
Ba-140	NA	NA
Cd-109	NA	NA

^a Based on mean concentrations (pCi g⁻¹) and data sources reported in Tables 2-7 and 2-8. The highlighted cells show radionuclides found in noticeably higher concentrations in areas impacted by fire.

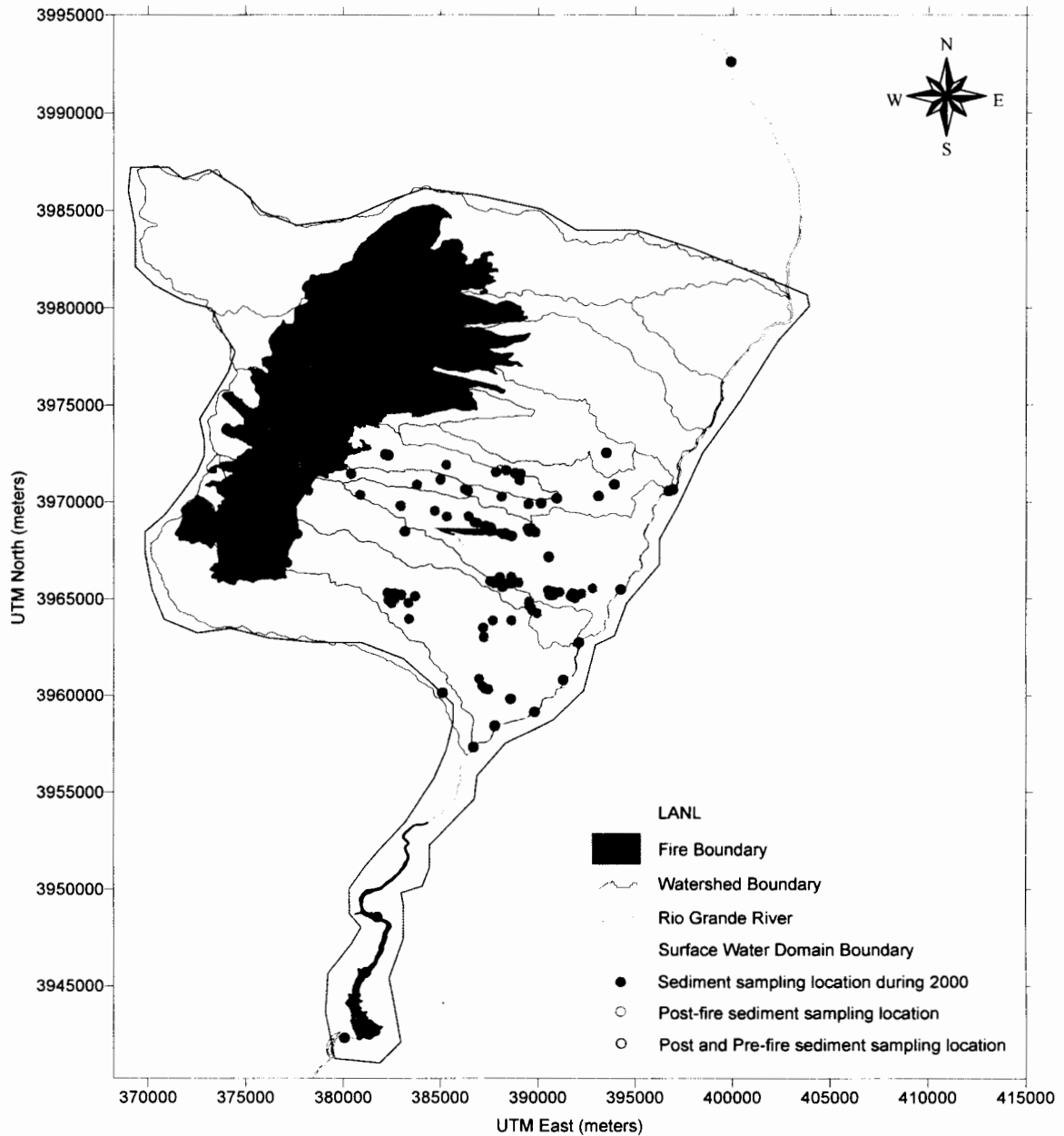


Figure 2-11. ESH-18 sediment sampling locations during 2000. The extent of the surface water domain is also shown. The two green-circled symbols represent locations that were sampled following the fire but not before the fire. The 35 black-circled symbols show those locations that were sampled both following and before the fire.

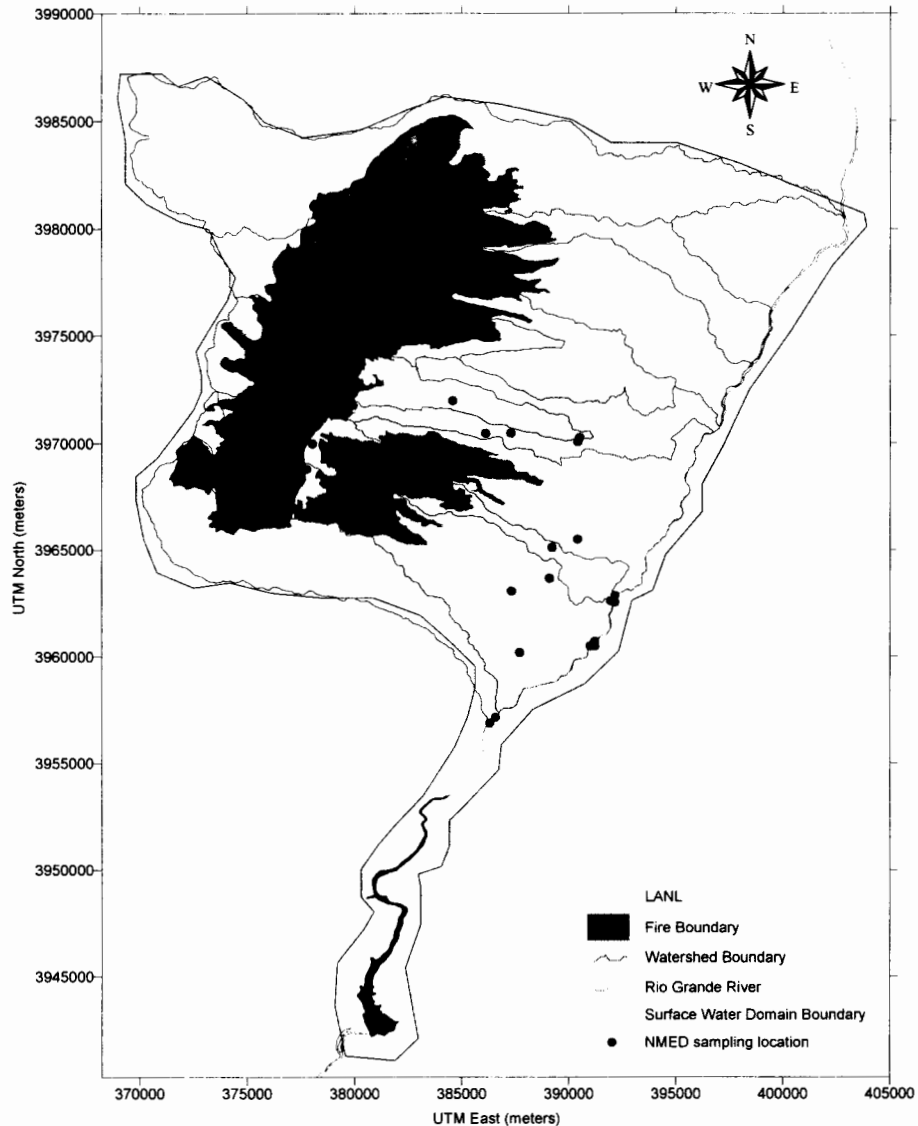


Figure 2-12. NMED sediment sampling locations during 2000. The extent of the surface water domain is also shown.

2.3.2.1 Temporal Trends. To assess potential impacts of the Cerro Grande Fire on contaminant movement, we examined trends in measured concentrations over time. The ESH-18 historical data set along with the ESH-18 year 2000 data set allowed us to compare concentrations measured in sediment at the same location over an extended period of time. For these analyses, we selected a number of sediment sampling locations maintained by ESH-18 that represented the following general areas (Figure 2-13):

- Above LANL (locations 233, 49, 229, 118, 90, and 107)
- Below LANL (locations 111, 179, 134, 147, 231, 18, 52, 178, and 69)
- Downriver (locations 53, 54, 55, and 176).

These locations were useful for examining temporal trends in measured concentrations in (1) areas not expected to be heavily influenced by runoff and erosion across contaminated sites at LANL (above LANL), (2) areas that could be influenced by runoff and erosion across contaminated sites at LANL (below LANL), and (3) areas farther downstream in the Rio Grande or in Cochiti Reservoir (downriver).

For these comparisons, we focused on the human-made radionuclides listed in Table 3-3 expected to contribute most to potential risk to members of the public. We also examined reported monitoring data for the chemicals listed in Table 3-6. However, there are either no post-fire monitoring data available for these chemicals or the post-fire results that were available are reported as below the detection limit. Therefore, it was difficult to make any conclusive statements, based on available monitoring data, about the potential for movement of these contaminants and subsequent exposure to members of the public.

Figures 2-14 through 2-18 show trends in ^{137}Cs , ^{241}Am , ^{90}Sr , ^{238}Pu , and $^{239,240}\text{Pu}$ concentrations measured in sediment collected from these three general areas. These radionuclides all appeared to show increases in average concentrations measured in samples collected from background areas impacted by fire (based on the data compiled in Table 2-9), so it was useful to examine trends for these radionuclides to discern any potential contribution by the LANL facility.

With the exception of ^{238}Pu , it was not apparent that post-fire concentrations of these radionuclides were elevated above levels that could be expected in sediments collected from background areas impacted by fire. The relatively high post-fire ^{238}Pu concentration shown in Figure 2-17 was measured at a location referred to as Cochiti Upper and is shown as location 55 in Figure 2-13. It is noted that a reanalysis of this sample and a duplicate sample analysis did not indicate the presence of ^{238}Pu , suggesting that this high value may be incorrect. Three below LANL locations (176, 231, and 18) also showed concentrations slightly elevated above the range of average concentrations measured in sediment collected from background areas impacted by fire. These data suggested the possibility of some amount of LANL impact on post-fire ^{238}Pu concentrations.

Concentrations for ^{137}Cs and $^{239,240}\text{Pu}$ appeared to have increased slightly following the fire, but not beyond levels seen at other background locations impacted by fire. Concentrations for ^{241}Am and ^{90}Sr did not appear elevated following the fire; in fact, concentrations appeared to have decreased from pre-fire levels. An explanation for the generally increasing trend in concentrations before the fire for these two radionuclides was not apparent, and it was not clear why post-fire concentrations would show such a dramatic decrease in concentration. However, the complicating factors discussed earlier, including changing methodologies and analytical procedures over time, likely contributed to the difficulty of interpreting these trends.

Post-fire concentrations for all of these radionuclides were not consistently above concentrations that could be expected in fire impacted areas. However, most of the radionuclides showed some pre-fire concentrations at locations below LANL and downriver that were above concentrations that could be expected in fire impacted areas and above concentrations that could be expected at background locations not impacted by fire (Table 2-7). This observation suggested the possibility of some degree of historical impact from contaminated areas at LANL at offsite locations unrelated to the Cerro Grande Fire during 2000.

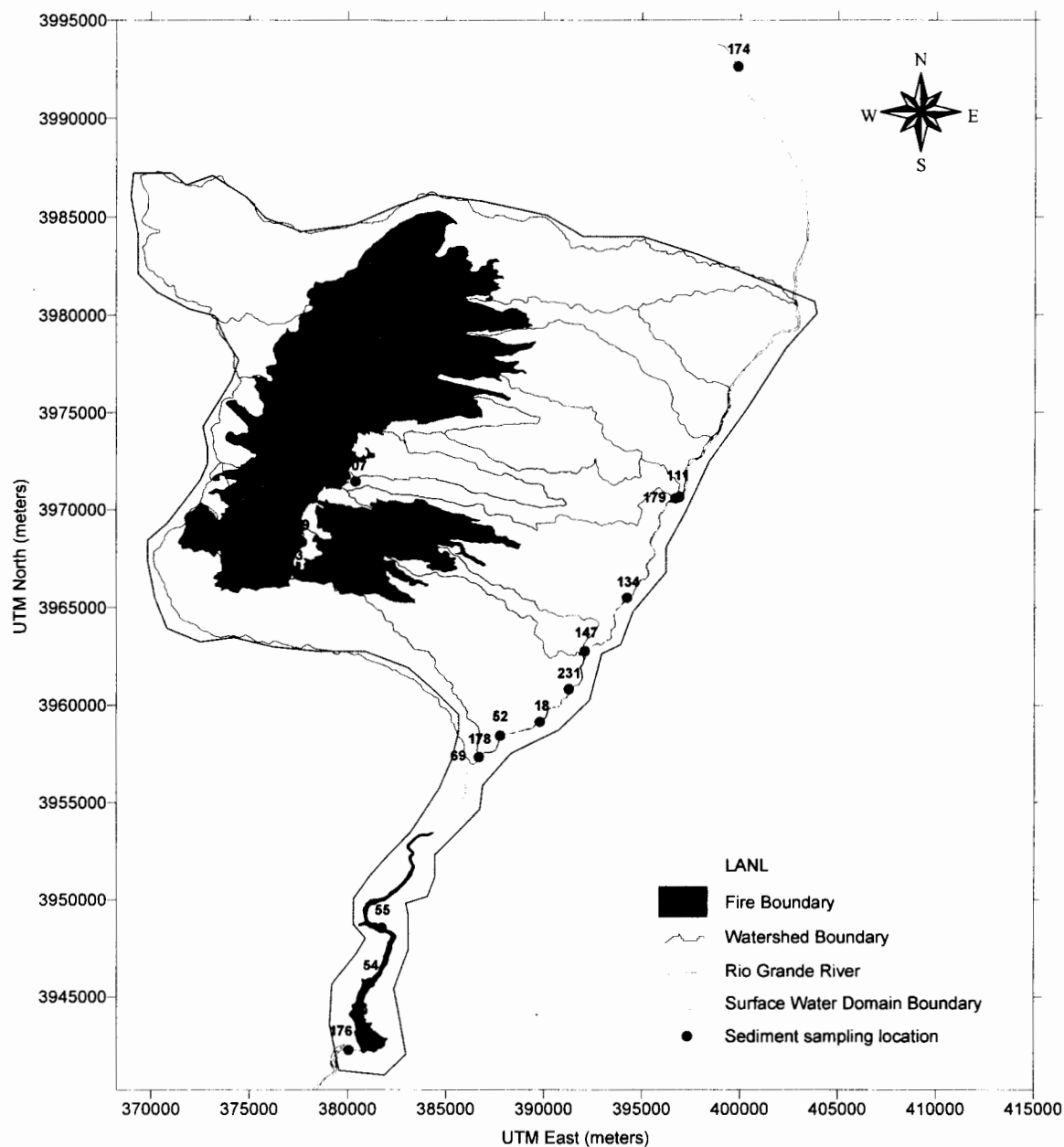


Figure 2-13. ESH-18 sediment sampling locations that *RAC* designated as above LANL, below LANL, and downriver. See the bulleted list at the beginning of this section for the location numbers associated with each location category.

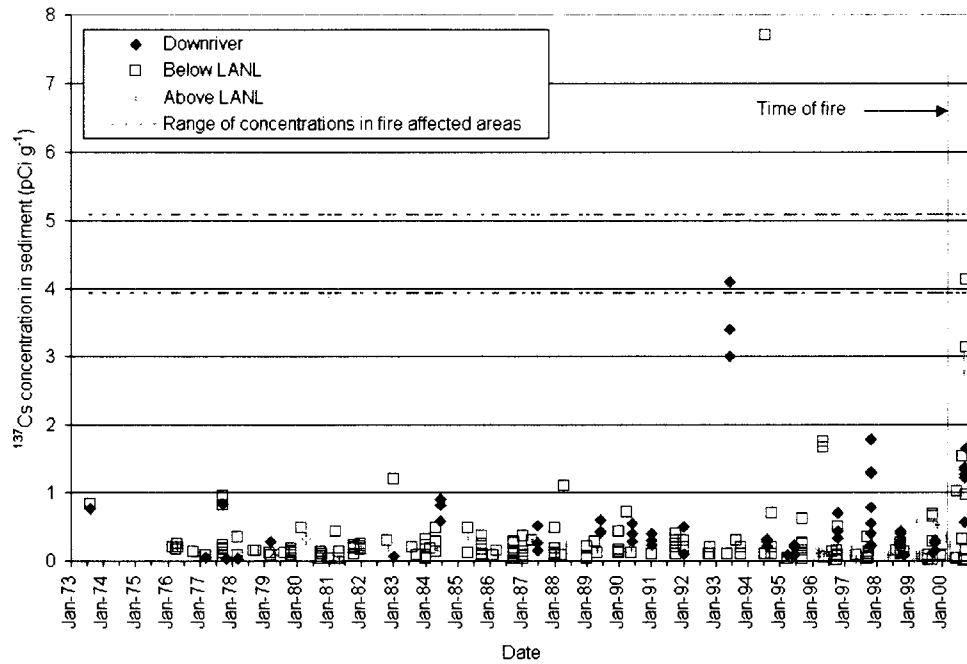


Figure 2-14. Cesium-137 concentrations measured in sediment collected from above LANL, below LANL, and downriver locations. The range of concentrations in fire-affected areas not influenced by LANL was based on the data presented in Table 2-9.

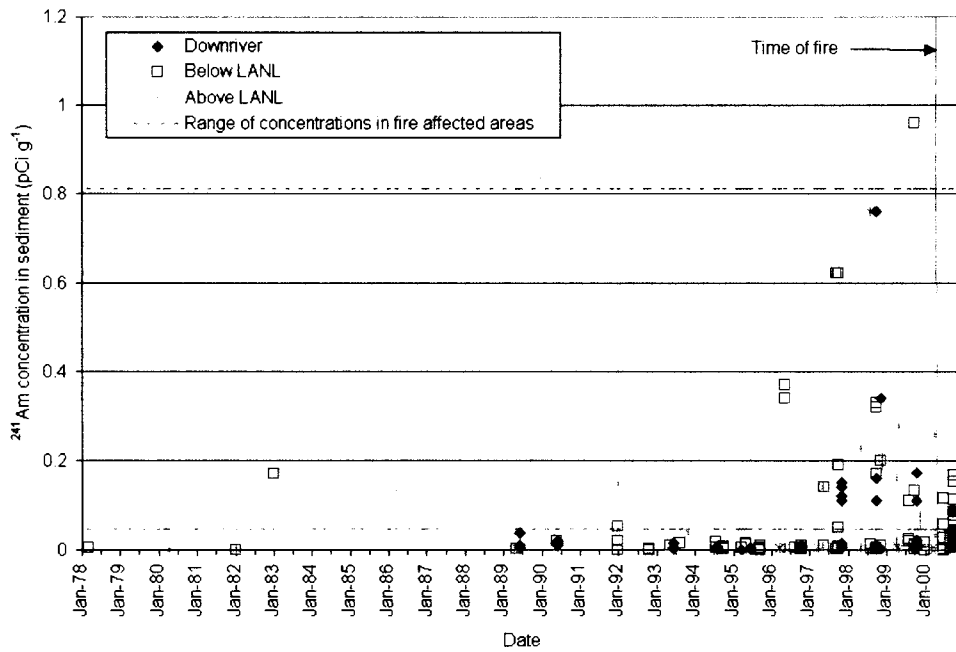


Figure 2-15. Americium-241 concentrations measured in sediment collected from above LANL, below LANL, and downriver locations. The range of concentrations in fire-affected areas not influenced by LANL was based on the data presented in Table 2-9.

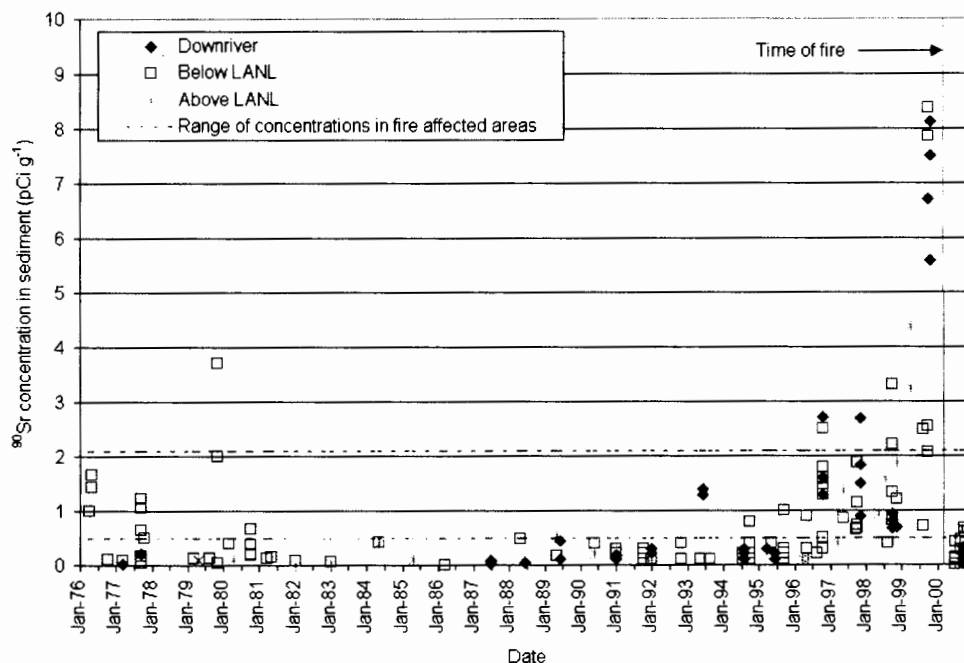


Figure 2-16. Strontium-90 concentrations measured in sediment collected from above LANL, below LANL, and downriver locations. The range of concentrations in fire-affected areas not influenced by LANL was based on the data presented in Table 2-9.

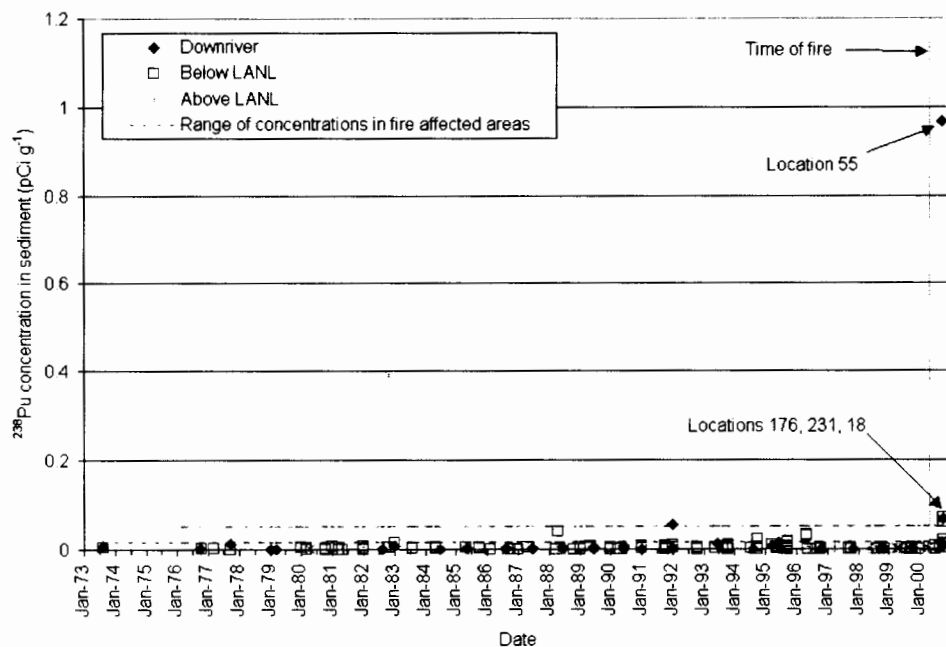


Figure 2-17. Plutonium-238 concentrations measured in sediment collected from above LANL, below LANL, and downriver locations. The range of concentrations in fire-affected areas not influenced by LANL was based on the data presented in Table 2-9.

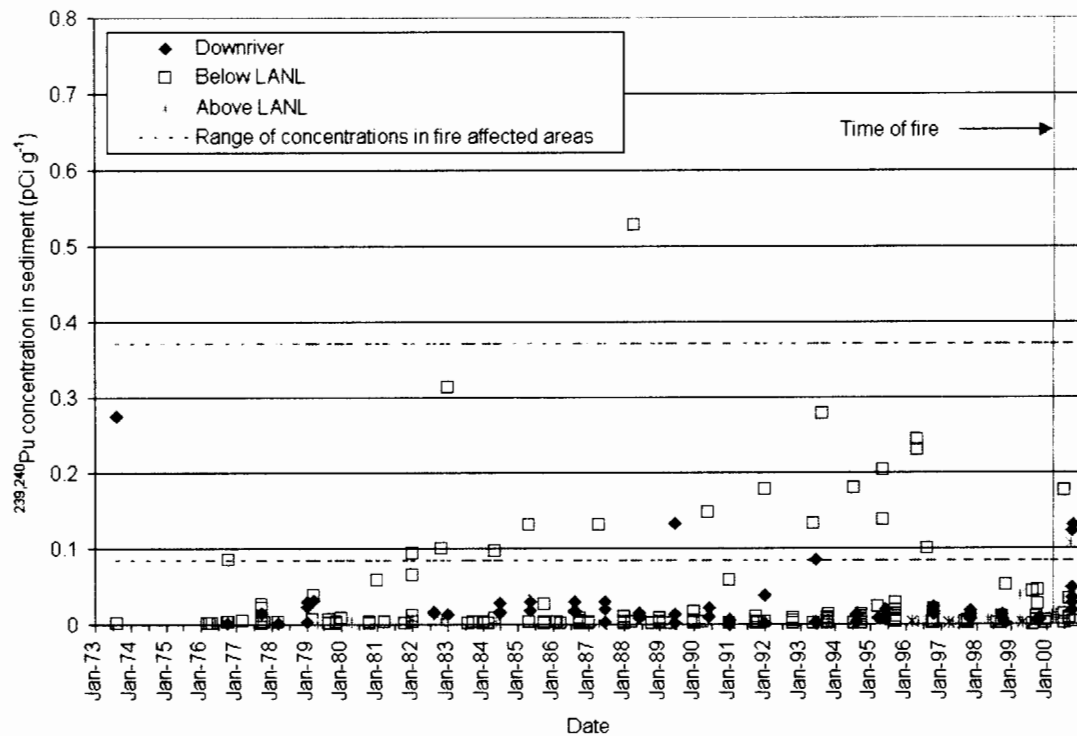


Figure 2-18. Plutonium-239,240 concentrations measured in sediment collected from above LANL, below LANL, and downriver locations. The range of concentrations in fire-affected areas not influenced by LANL was based on the data presented in Table 2-9.

2.3.2.2 Spatial Trends. The availability of historic sediment data at locations sampled during 2000 allowed us to assess temporal changes in concentration following the Cerro Grande Fire and identify where spatial increases in concentration occurred. The ESH-18 post-fire sediment monitoring data for ^{137}Cs and $^{239,240}\text{Pu}$ are shown in Figures 2-19 and 2-20, respectively. Red circles highlight locations where average^a post-fire measurements indicated an increase over average historic concentrations at the same location.

It is clear that concentrations measured following the fire increased over average historic concentrations at a number of locations for ^{137}Cs and $^{239,240}\text{Pu}$. However, the measured concentrations at offsite locations were generally within the range of those measured at other fire-affected locations, at areas removed from the influence of LANL; therefore, any impact related to LANL was not apparent. The one notable exception was the $^{239,240}\text{Pu}$ concentration of 1.15 pCi g^{-1} measured at a location along the northeastern part of the LANL boundary (Figure 2-20). For comparison, the pre-fire average for 32 samples collected at this location was 0.53 pCi g^{-1} , with a maximum concentration of 1.08 pCi g^{-1} measured in 1999.

^a Post-fire average concentrations generally consisted of one or two measurements, whereas pre-fire average concentrations were based on a significantly greater number of samples, often 20 to 30 or more.

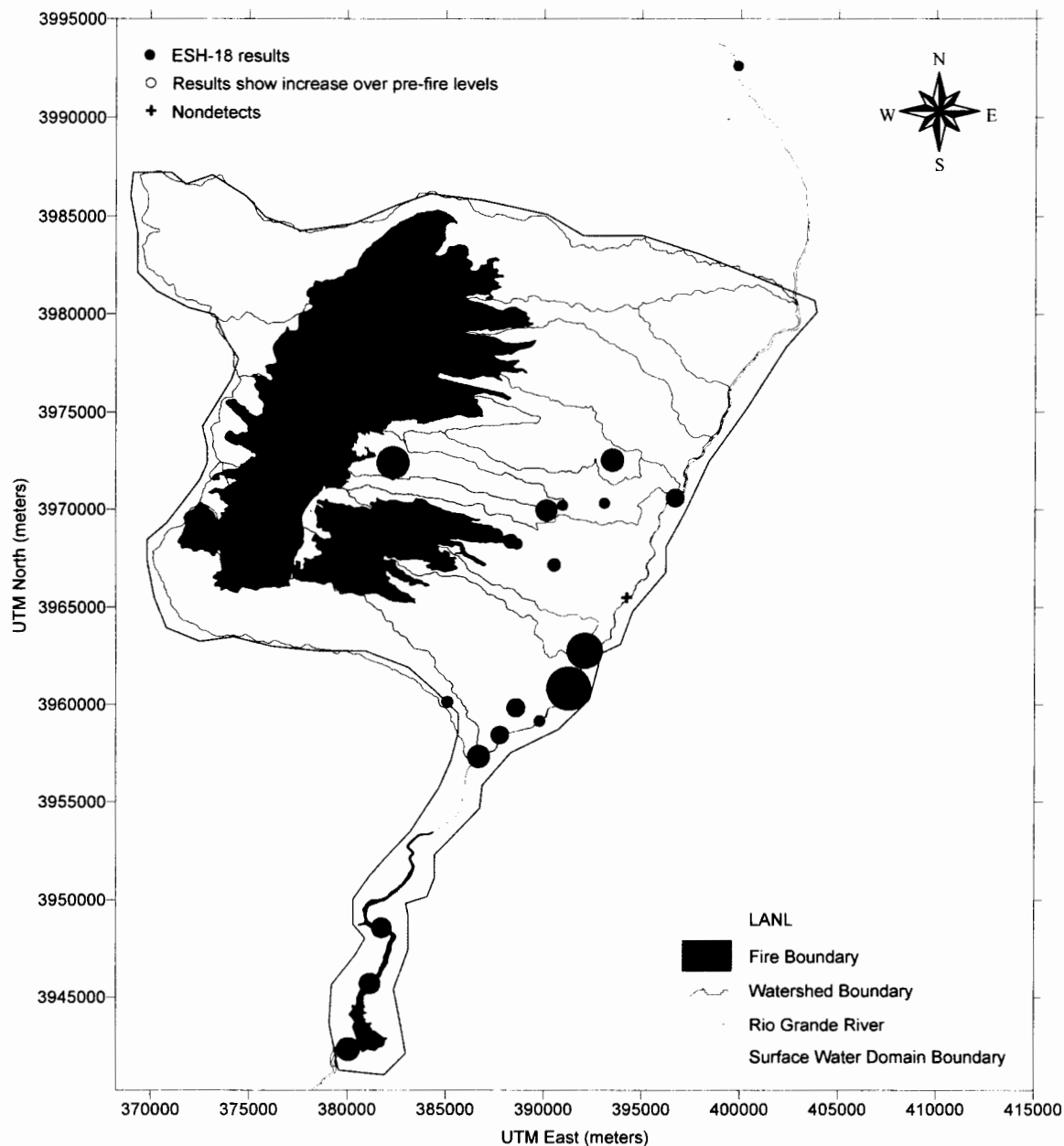


Figure 2-19. Relative magnitude of average measured concentrations of ^{137}Cs reported by ESH-18 for sediment at locations sampled historically and after the fire during 2000. Concentrations reported as detectable ranged from $0.006\text{--}4.13\text{ pCi g}^{-1}$. The diameter of the symbol is proportional to the reported concentration. Red-circled symbols indicate an increase over average pre-fire concentrations. Because of some symbol overlap, all reported concentrations are not visible on this map.

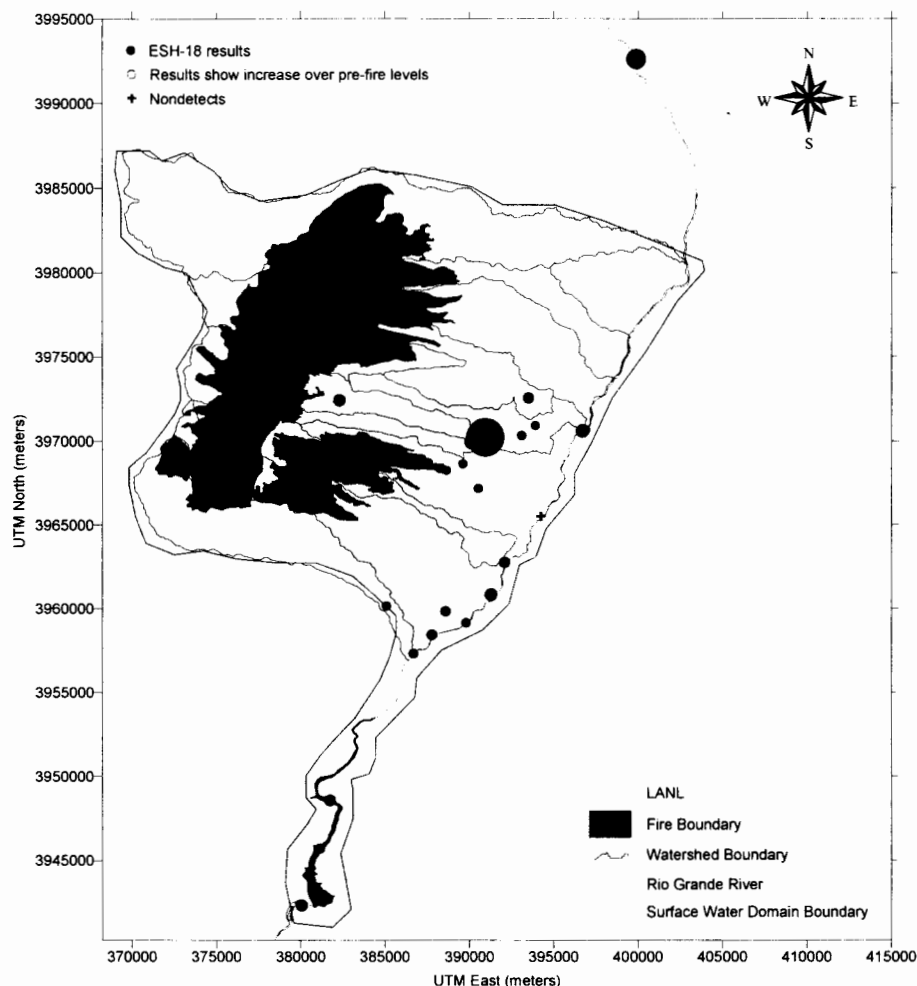


Figure 2-20. Relative magnitude of average measured concentrations of $^{239,240}\text{Pu}$ reported by ESH-18 for sediment at locations sampled historically and after the fire during 2000. Concentrations reported as detectable ranged from 0.002–1.15 pCi g⁻¹. Red-circled symbols indicate an increase over average pre-fire concentrations. Because of some symbol overlap, all reported concentrations are not visible on this map.

In addition to understanding where concentrations greater than historic *average* concentrations were evident, we examined contaminant concentrations in sediment spatially to understand the relative magnitude of concentrations measured by all organizations collecting data. Figures 2-21 and 2-22 show individual sample results for ^{137}Cs and $^{239,240}\text{Pu}$ concentrations reported by NMED, ESH-18, and ER in sediment collected following the fire.

Concentrations of ^{137}Cs in sediment higher than average ^{137}Cs concentrations measured in other areas impacted by fire (Table 2-8) were evident in locations along the Rio Grande (Figure 2-21). However, because these concentrations were below the maximum ^{137}Cs concentration measured by ER from the Viveash Fire area (maximum 6.8 pCi g⁻¹, mean 5.08 pCi g⁻¹), it is unlikely that they demonstrated an impact from LANL operations.

As was seen with ^{137}Cs concentrations, $^{239,240}\text{Pu}$ concentrations higher than average concentrations measured in other fire-impacted areas (Table 2-8) were evident in locations along

the Rio Grande (Figure 2-22). These concentrations were higher than the maximum measured $^{239,240}\text{Pu}$ concentration in an individual sediment sample collected by ER from the Mountain Front area to the west of LANL (maximum 0.7 pCi g^{-1} , mean 0.37 pCi g^{-1}). ER measured the highest concentration (1.59 pCi g^{-1}) for a location along the Rio Grande at its confluence with Los Alamos Canyon (see Figure 2-9, location 20). It is also important to note that the other concentration above 0.7 pCi g^{-1} (0.87 pCi g^{-1}) was measured by ESH-18 at a location that was not impacted by drainage across the LANL site (location 174 on Figure 2-8). However, the high concentration measured by ER following the fire near the Rio Grande provided evidence of levels significantly higher than those measured before the fire by ESH-18 at similar locations (179 and 111 in Figure 2-13).

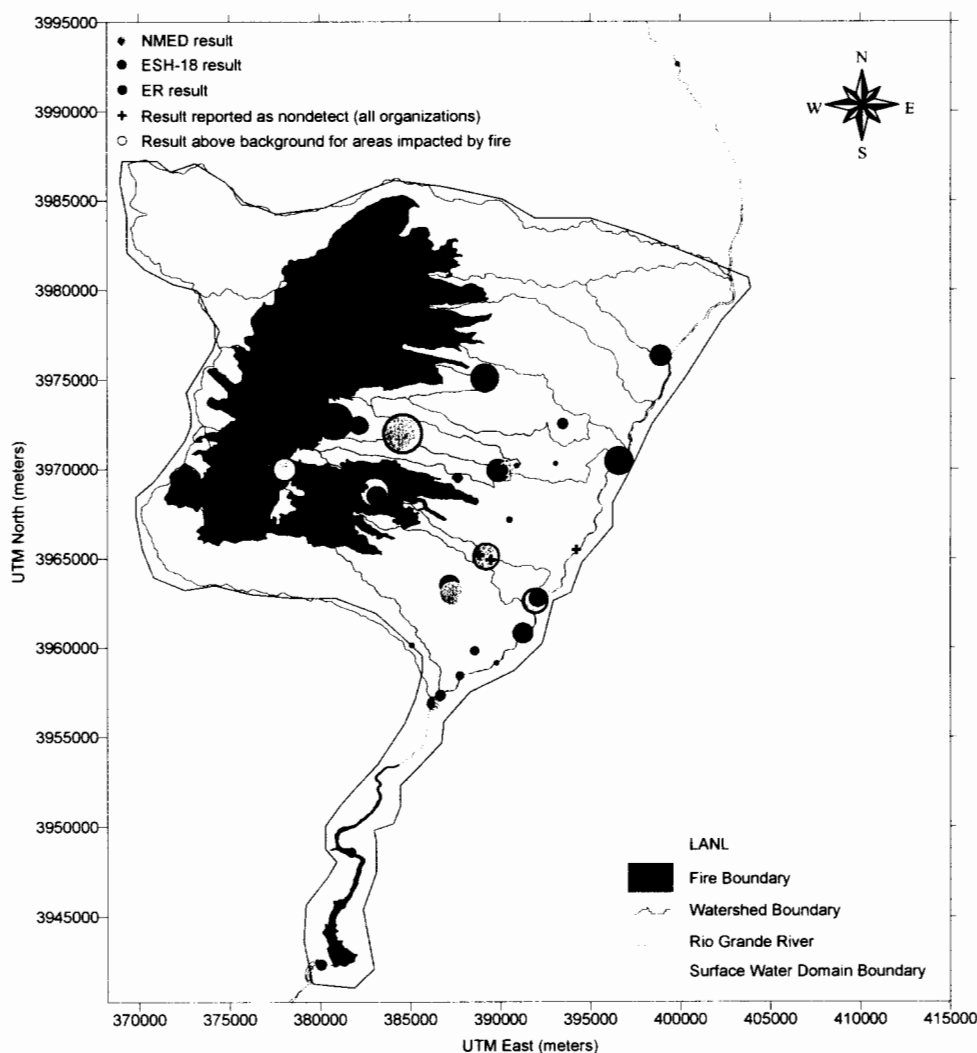


Figure 2-21. Relative magnitude of measured concentrations of ^{137}Cs in sediment collected following the fire. Concentrations reported as detectable range from $0.006\text{--}9.3 \text{ pCi g}^{-1}$. The diameter of the symbol is proportional to the reported concentration. Red-circled symbols indicate concentrations greater than the upper bound of average concentrations for fire-impacted areas (5.08 pCi g^{-1}) (Table 2-9). Because of some symbol overlap, all reported concentrations are not visible on this map.

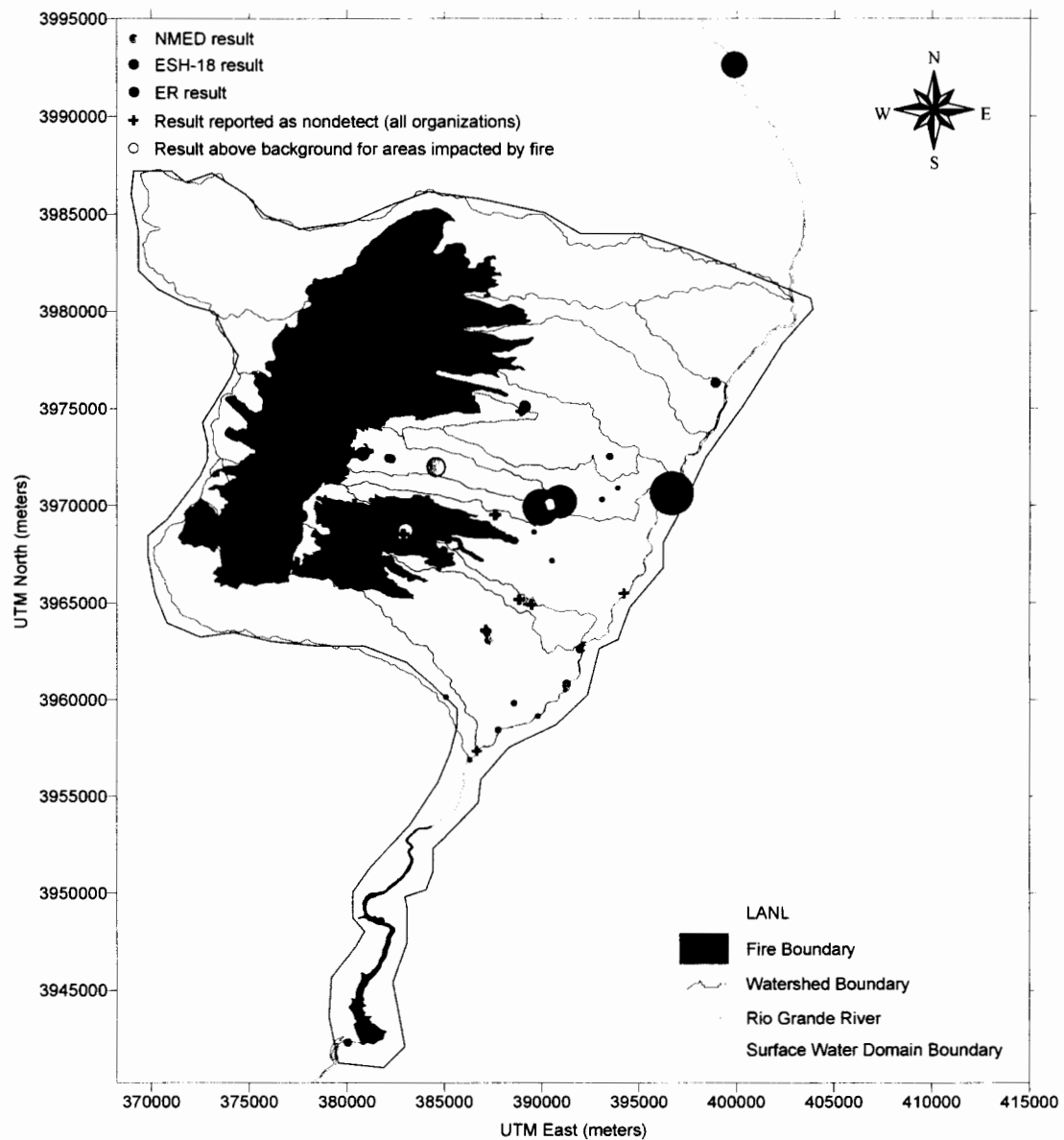


Figure 2-22. Relative magnitude of measured concentrations of $^{239,240}\text{Pu}$ in sediment collected following the fire. Concentrations reported as detectable ranged from $0.0009\text{--}1.59 \text{ pCi g}^{-1}$. The diameter of the symbol is proportional to the reported concentration. Red-circled symbols indicate concentrations greater than the upper bound of average concentrations for fire-impacted areas (0.37 pCi g^{-1}) (Table 2-9). Because of some symbol overlap, all reported concentrations are not visible on this map.

While our analyses of sediment is focused on human-made radionuclides, this same approach can be used to examine concentrations of some naturally occurring radionuclides and uranium isotopes that occur both naturally and also been introduced into the environment as a result of LANL operations. Figure 2-23 shows the ratio of ^{238}U to ^{234}U measured in the for samples collected following the fire by ESH-18, ER, and NMED. There are a few samples

collected from locations along the Rio Grande that showed ratios greater than 1.5. For the most part, however, the ratios indicated the presence of predominantly naturally occurring uranium in these samples.

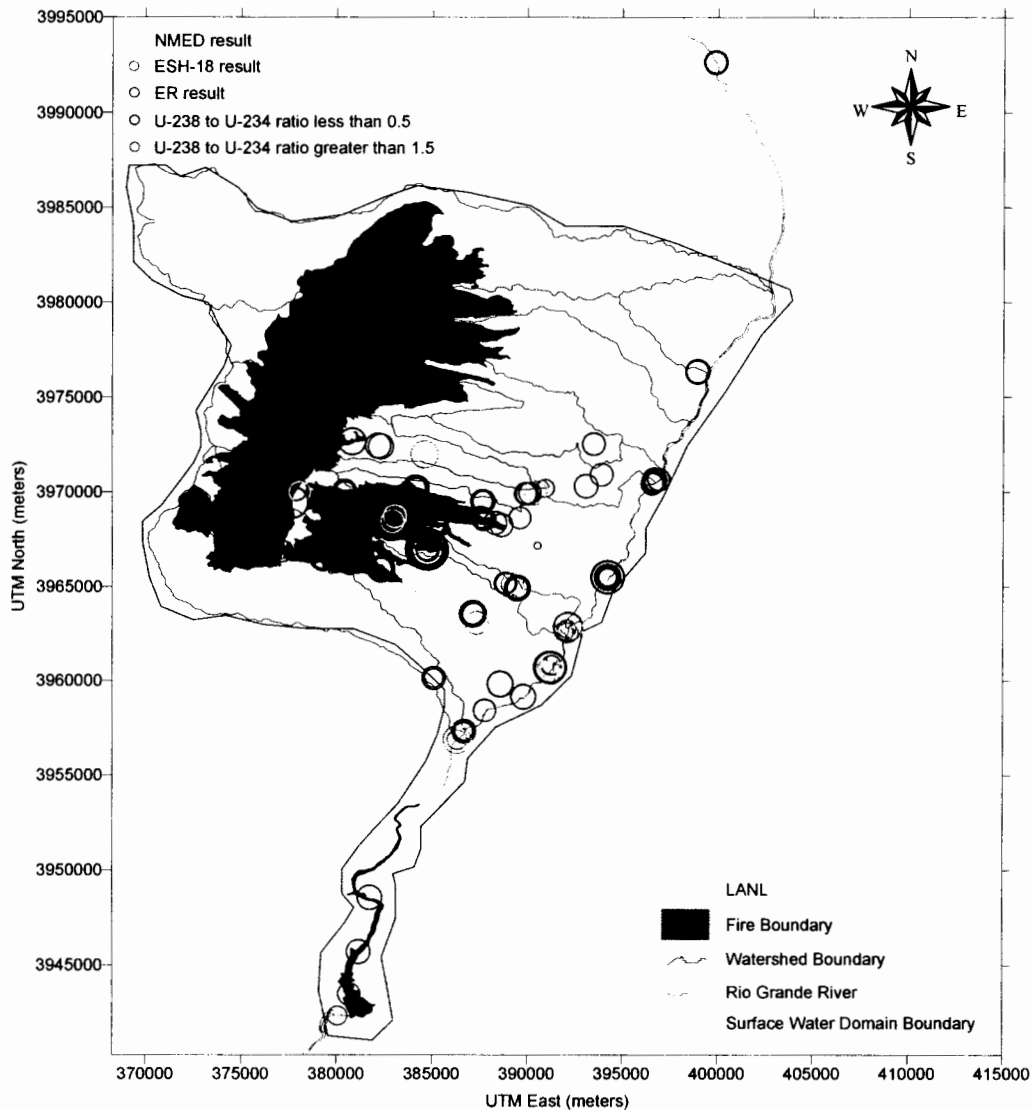


Figure 2-23. Relative ratio of ^{238}U to ^{234}U concentration measured in the same sample collected by ESH-18, ER, and NMED. Symbol diameter is proportional to the calculated ratios, which ranged from 0.22 to 2.05. Red-circled symbols show ratios greater than 1.5 and the single black circle shows a ratio less than 0.5.

Similar analyses of ^{226}Ra and ^{232}Th post-fire sediment concentrations reported by ESH-18, ER, and NMED do not appear to show patterns suggesting contamination related to LANL or increases related to the fire, and the range of concentrations was consistent with what would be expected for these radionuclides based on measured background concentrations (Tables 2-7 and 2-8); however, no results were available regarding concentrations of ^{226}Ra in background locations. Post-fire concentrations for other naturally occurring radionuclides (see Table 3-3 for a

list of priority radionuclides), including ^{210}Pb , ^{228}Ra , ^{224}Ra , ^{223}Ra , ^{234}Th , ^{228}Th , ^{230}Th , and ^{40}K , are similarly distributed and did not show any discernable trends suggesting LANL or fire-related impact. No data were available for ^{241}Pa .

2.4 Chemical Concentrations in Water and Sediments

We also examined monitoring data for the Stage 2 chemicals listed in Table 3-6. Evaluating chemicals either for temporal or spatial trends at LANL was not possible for a number of reasons. First, there were either no post-fire monitoring data available for these chemicals, or the available post-fire results were reported as below the detection limit. Second, historic monitoring data for chemicals were limited. This is a common observation at numerous facilities across the country. For the most part, monitoring chemicals in the environment was not a priority. At LANL, several water quality parameters were measured historically along with some inorganic chemicals, and a few organic compounds like xylene. Even so, much of the data were reported as below detectable limits. Therefore, it was difficult to make any conclusive statements, based on available monitoring data, about the potential for movement of these contaminants and subsequent exposure to members of the public. Table 2-10 summarizes the chemical monitoring data for sediment, surface, and storm water samples collected following the fire. Concentrations reported as nondetects are included in parentheses and were assumed to be the detection limit for the sample being analyzed. In some cases, several different nondetect values were provided for an analyte, so they may not all be shown in the table.

On the other hand, there were measurement data for two of the chemicals (aluminum and lead) emerging from the Stage 2 screening (see Table 3-6b) in surface water, storm water, and sediment. The patterns were quite similar for both chemicals, with storm water concentrations being much higher than surface water concentrations, as would be expected because of the higher levels of suspended solids in storm water. The monitoring data for aluminum and lead did not suggest the LANL facility as a specific source of elevated post-fire concentrations; however, concentrations of lead in burned area ash did appear to be elevated above expected background concentrations. This is discussed in greater detail in Chapter 3.

2.5 Surface Water Flow and Total Suspended Solids Data

In addition to identifying changes in chemical and radionuclide concentrations measured in water and sediments following the fire, we used additional monitoring data to develop the surface water modeling methodology. These additional data consisted primarily of total suspended solids (TSS) and surface water flow measurements and are discussed in greater detail in Chapter 4.

2.6 Recommendations for Monitoring

This section provides observations about monitoring that could improve evaluating releases to surface water from LANL following an event like the Cerro Grande fire. Ideally, the data would provide sufficient information to (a) verify predicted concentrations, (b) understand the impact of past contamination offsite, (c) provide information about representative background concentrations, and (d) identify potential health risks to members of the public based on the monitoring data.

Table 2-10. Chemical Data from LANL for Water and Sediment

Chemical	Sediment (mg kg ⁻¹)	Surface water (mg L ⁻¹)	Storm water (mg L ⁻¹)
Benzidine	No results	All U (9.28)	All U (9.28)
Dibenz(a,h)anthracene	All U (0.00466)	All U (12, 11, 0.18)	All U (960, 310....0.18)
Nitrosodimethylamine	No results	No results	No results
Tetrachlorodibenzodioxin [2,3,7,8-]	No results	No results	No results
Dibromoethane[1,2-]	No results	No results	No results
Bromobenzene	No results	No results	No results
Dibromo-3- chloropropane[1,2-]	No results	No results	No results
Butylbenzene	No results	No results	No results
Propylbenzene	No results	No results	No results
Benzo(a)pyrene	All U (0.00566)	All U (12, 11, 0.07)	All U (960, 310....0.07)
Benzene	No results	All U (5, 0.149)	7/12 detects (avg = 0.32), no pre-fire results
Hexachlorobenzene	All U (0.00466)	All U (12, 11, 0.16)	All U (960, 310....0.16)
Dibromo-3- chloropropane[1,2-]	No results	No results	No results
Tetryl	All U (0.0155, 0.65)	All U (0.091)	3 detects (18, 8.1, 3.7)
Aroclor-*	All U (79–0.00018)	All U (2.6–0.067)	All U (3–0.067)
Aroclor-* refers to Aroclor-1016, -1221, -1232, -1242, -1248, -1254, -1260, and -1262			

This evaluation would have benefited from changes in the methods used for data compilation, different sample locations, and increased numbers of samples at specific locations. From evaluating the surface water monitoring data, our key recommendation is that a range of expected concentrations should be established at several representative background locations in areas not impacted by LANL. Background locations should be situated at sites upriver from LANL. This step is critical to future surface water monitoring, especially in studying the effects of the Cerro Grande Fire. Some other suggestions for augmenting the current monitoring program are discussed below.

- Coordinate sampling and data compilation efforts among all organizations involved with environmental monitoring
- Carefully review the sampling methods and protocols and analytical procedures as they change over time. It is critical to understand how different sampling or analytical techniques may impact the comparability of results. Data compiled for the purpose of

understanding spatial or temporal trends should be confined to that determined suitable for the purpose (e.g., gamma scan results should not be included if there are alpha spectroscopy results for the same sample that are considered more reliable, and data known to be inaccurate for any reason should not be included).

- Focus effort on developing an overall monitoring plan for surface and storm water collection and analysis that will support spatial and temporal analyses of consistent offsite locations that are appropriate for understanding potential risk to members of the public. An onsite sampling plan should address runoff in all canyons to understand the movement of specific contaminants from those areas presenting the highest potential risk.
- Record the physical location of each sample (using multiple coordinate projections). It is also critical to identify clearly and consistently the same station used by multiple organizations. For all water samples, the flow measurement should be recorded concurrently with the sampling so that the concentration values can be correlated to the flow values.

2.7 Uses for the Environmental Monitoring Data

We used the water and sediment monitoring data in several ways to support the risk calculations for this project. As discussed in this chapter, we used these data to focus our evaluation here and in subsequent chapters on a more limited number of chemicals and radionuclides. The data are also useful for identifying apparent increases in concentration for some radionuclides and chemicals following the fire and for identifying the possibility of LANL impact on measured concentrations. However, the information available for the analyses presented in this chapter was limited to samples collected during the year 2000. As discussed in Chapter 4, we also used the post-fire environmental monitoring data to the extent possible to compare to the model-predicted concentrations.

Risk calculations can be based on actual monitoring data. LANL has completed such an evaluation (Kraig et al. 2001). In fact, if the goal is to understand possible risks based on current conditions and concentrations, environmental monitoring data are preferred because they are not impacted by the many uncertainties inherent in environmental transport modeling. Environmental monitoring data are always confined by the adequacy of the monitoring effort in terms of coverage (spatially, temporally, and for the right contaminants) and restricted to the intensity of the actual post-event environmental processes. For example, the environmental monitoring data related to surface water collected during 2000 following the Cerro Grande Fire can provide information about the consequences of contaminant movement during a relatively dry year; however, they provide little prospective information about the potential consequences of a significant rainfall. Analyses of data for several additional years after the fire are critical to strengthen the conclusions that can be drawn regarding impacts of the fire.

In the case of this project, public interest in the documentation and calculations that supported statements made about the risks related to flooding following the Cerro Grande Fire led to a need to better understand and evaluate the potential for risk. To accomplish this as part of the current project, predictive modeling was necessary. Many uncertainties are associated with environmental transport modeling, and the process of distinguishing between regional

background concentrations, concentrations expected in fire-impacted areas, and concentrations related to LANL operations complicated the calculations. However, the results of this type of predictive modeling can be used to identify specific areas or contaminants contributing most to potential risk. The modeling results are also useful for understanding the relative contribution of different potential sources of radionuclides and chemicals, something that cannot be learned from environmental monitoring data. The results of the surface water transport modeling calculations are presented in Chapter 4.

2.8 Conclusions

For this task, we compiled and reviewed water and sediment data from ESH-18 and ER at LANL and NMED. We developed and implemented a 2-stage screening procedure to focus on the radionuclides and chemicals most important for human health. Based on our Stage 2 screening assessment, 17 radionuclides ranked highest in terms of human health risk. We focused our evaluation of water and sediment monitoring data on the human-made radionuclides in this list.

Forty-five chemicals from our original list of almost 200 chemicals emerged from our Stage 2 screening process. However, there is a lack of post-fire monitoring data for many of the chemicals and, for other chemicals, the results were below detection limits. As a result, few definitive conclusions could be drawn from the chemical monitoring data for many of the Stage 2 chemicals. For other chemicals, such as aluminum and lead, measurement data allowed us to perform some spatial trend analysis of the post-fire data.

Our monitoring data evaluation focused on the analysis of the radionuclides ^{241}Am , ^{137}Cs , $^{239,240}\text{Pu}$, ^{238}Pu , and ^{90}Sr in surface water, storm water, and sediment. The sediment and water monitoring data were useful to evaluate spatial and temporal trends and identify the possibility of impact from either the fire or LANL operations. However, our interpretation of the data was complicated by a number of issues discussed in this chapter.

A number of observations can be made based on the sediment and water monitoring data we examined:

- The lack of pre-fire data and few post-fire detectable concentrations for chemicals in water or sediment prevented us from drawing conclusions regarding the distribution of chemicals in the environment and potential impact of the Cerro Grande Fire.
- Environmental media can be used to identify temporal changes in levels of contaminants, assuming the analytical methods are sound and consistent over time.
- Five radionuclides (^{137}Cs , $^{239,240}\text{Pu}$, ^{238}Pu , ^{90}Sr , and ^{241}Am) *suggest the possibility* of increases in sediment and soil concentrations in fire-impacted areas removed from the effect of LANL operations. Cesium-137, $^{239,240}\text{Pu}$, and ^{238}Pu showed consistent increases over pre-fire levels in the LANL area. Another possibility to be considered, however, is the post-fire additional water and sediment that may have increased the volumes of material transported down the canyons. Having had the opportunity for further data review since issuing the draft version of this report, concentrations of ^{235}U , barium, copper, and lead also appear to be increased in ash samples. Additional detail regarding

chemicals and radionuclides elevated in ash is provided in Chapter 3 in the section that discusses characterization of the burned area.

- Pre-fire concentrations for these five radionuclides *suggest the possibility* of LANL-related contamination existing before the Cerro Grande Fire at below LANL and downriver locations. Changes in analytical procedures over time limit the conclusions that can be drawn based on this observation.
- Of the five radionuclides (^{137}Cs , $^{239,240}\text{Pu}$, ^{238}Pu , ^{90}Sr , and ^{241}Am), there is evidence to *suggest the possibility* of LANL-influenced increases in both ^{238}Pu and $^{239,240}\text{Pu}$ post-fire sediment concentrations measured at locations below LANL along the Rio Grande and in Cochiti Reservoir.
- Strontium-90 and ^{241}Am show increasing trends in pre-fire concentrations throughout the 1990s for both water and sediment, followed by decreases after the fire for which an explanation was not immediately apparent. Our objective was not to examine pre-fire data in detail but instead to use average pre-fire concentrations for comparison purposes. Therefore, additional information is necessary to understand the reasons for elevated pre-fire concentrations of these contaminants. Again, changes in analytical techniques may be at least partly responsible for some of these trends.
- Because of evidence *suggesting the possibility* of fire-related and/or LANL impacts at publicly accessible locations for both $^{239,240}\text{Pu}$ and ^{238}Pu , additional monitoring to further quantify the levels of these radionuclides at these locations and augment the data available to assess post-fire conditions would enhance the ability to make more conclusive statements about the probability of a LANL contribution to health risks.

3. SURFACE WATER SOURCE TERM DEVELOPMENT

3.1 Ranking the Watersheds

To focus time and resources on those areas or sites with the greatest potential for creating a human health risk following the fire, we characterized and ranked the watersheds within the surface water domain (Figure 1-2) that drain into the Rio Grande at specific discharge points or outlets at the river (Figure 3-1).

We originally included the upper three watersheds (Chupaderos, Garcia, and Santa Clara Canyons) in our surface water domain in case air modeling revealed significant deposition of airborne contaminants in this area. However, the results of our atmospheric pathway assessment did not suggest significant deposition of airborne contaminants in these areas, and limited information was available to estimate surface water flow and concentrations of sediment in water for these watersheds (see Chapter 4). Furthermore, available data did not suggest LANL-related contamination in these watersheds. Based on the contamination location information we were provided, there were no contaminated areas (or PRSs) in these watersheds. As a result, we did not develop surface water flow values and ranking values for these watersheds.

In characterizing the remaining watersheds, we used three general categories of information to identify the watersheds that were the most likely to contribute to human health risk: (1) information on extent and severity of burned areas within the watersheds, (2) information on potential flow within the watersheds, and (3) information on existing contamination levels in the watersheds. Additional information related to the sources and adequacy of data available for source term development is discussed in a later section of this report.

For each of the three categories of information, we used several parameters to determine a final burn factor, flow factor, and contamination factor for each watershed that had an outlet point to the Rio Grande (Figure 3-1). We included the following parameters in the characterization and ranking:

- Burn factor (Tables B-1, B-2, and B-3; Appendix B)
 - Extent of burn within the watershed area
 - Severity of burned area (low, moderate, or severe) within each watershed
 - Extent of hydrophobic soils.
- Flow factor (Table B-4, Appendix B)
 - Flow rate at outlet of watershed to Rio Grande during 100-year flood event
 - Extent of watershed surface area.
- Contamination factor (Tables B-5 through B-8, Appendix B)
 - Extent of contamination in each watershed based on average ^{137}Cs and $^{239,240}\text{Pu}$ concentrations in sediment from both ER sediment data collected during 2000 and ESH-18 sediment data collected since 1995. For the ER sediment data, we assigned the locations to a watershed based on sampling coordinate information provided for the monitoring data files we received from ER early in the project. We assigned the ESH-18 data to a watershed based on the sampling location coordinates, using ArcInfo and the watershed GIS coverages we had obtained from LANL. The monitoring data files we received are discussed in greater detail in Chapter 1.
 - Erosion matrix score for PRSs within each watershed. These data were developed by LANL and transmitted to us by NMED. We used this list in combination with the list

of burned PRSs, which we received from LANL in September 2001 as an excel file transmitted via e-mail, to determine which PRSs fell into the burned/unburned categories, the number of PRSs within a given watershed, and the potential for erosion at those PRSs.

For some of the criteria, particularly the extent of contamination within each canyon or watershed, the amount of available information to quantitatively characterize each watershed was limited and varied substantially in completeness. Because of these data limitations, we requested documentation of the watershed and aggregate ranking done by both the ER (ER 2001) and NMED (Dinwiddie 1999) to try to better quantify watershed specific factors associated with existing contamination levels. We received some documentation of this ranking process, but details regarding the specific criteria that went into the final reported ranking designations were either not provided or we were unable to use the data to identify specific information about watershed contamination. However, the ER and NMED ranking information is referenced here and discussed later in this section to compare our independently derived ranking to other watershed ranking that had been previously completed.

Appendix B provides basic characteristics on the size, extent, and severity of burn in each watershed, and the tables provide details of the ranking process for determining the overall burn (Tables B-1 through B-3), flow (Table B-4), and contamination (Tables B-5 through B-8) factors. This characterization helped identify those watersheds that were most important in terms of the effects of the fire and on the potential for water flow to carry contaminants to locations where members of the public could be exposed. For surface water modeling purposes, we derived watersheds to include basins that have a discrete outlet into the Rio Grande (see Chapter 4). Therefore, in our analyses there are four sub-basins that compose the entire the Los Alamos watershed: Guaje, Los Alamos, Pueblo, and Rendija sub-basins (see Figure 3-1).

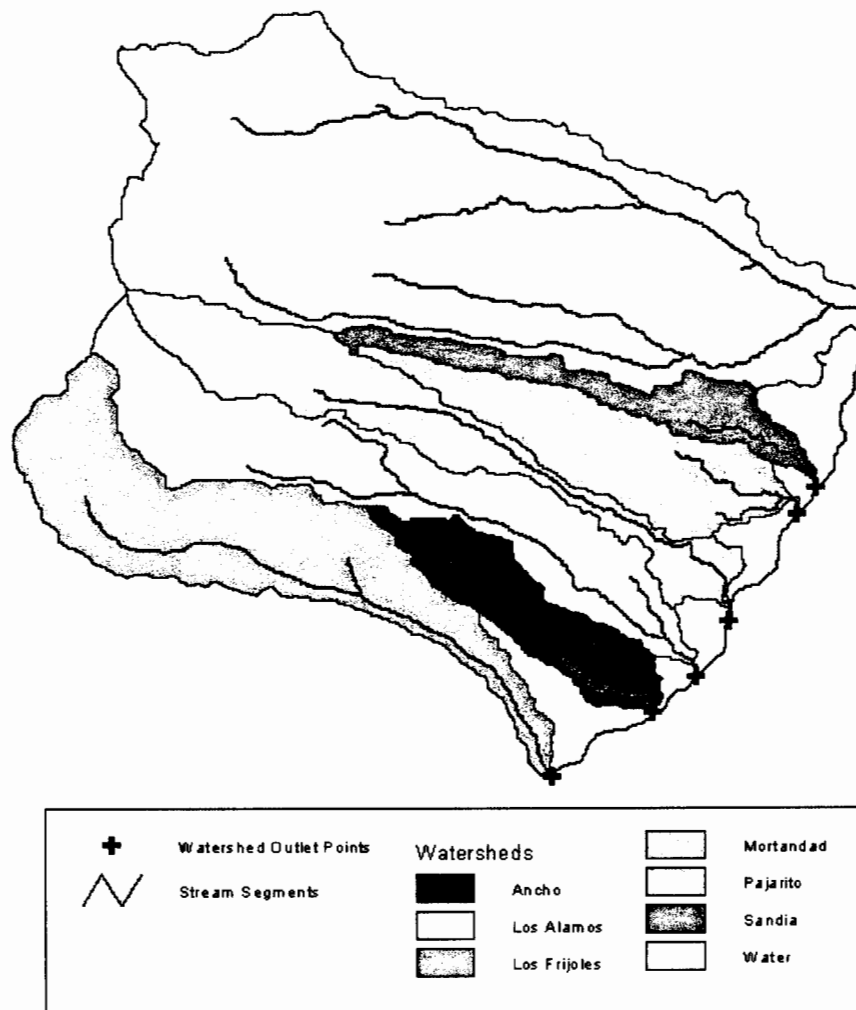


Figure 3-1. Outlet points on the Rio Grande for the LANL watersheds. Four sub-basins compose the entire the Los Alamos watershed: Guaje, Los Alamos, Pueblo, and Rendija sub-basins. We characterized and ranked the watersheds with outlet points to the Rio Grande.

Table 3-1 provides the final ranking values and identifies the Water, Los Alamos, and Mortandad watersheds as potentially the most important for the mobilization of contaminants of concern. When the combined ranking values for all sub-basins within the Los Alamos watershed are considered, the entire Los Alamos watershed (combined) ranked highest in terms of overall basin area and severity of burned area, the potential flow during flood events in the future, and extent of contaminants within the watershed areas. This ranking suggests that the Los Alamos watershed should be the focus of subsequent source term development and that other watersheds, like Los Frijoles and Pajarito, may not require the same level of effort. For the Water and Mortandad watersheds, which ranked high in the evaluation, methods to estimate source terms from contaminated areas will have to rely on less detailed information than is available for some

of the canyons within the Los Alamos watershed (see the following discussion regarding limitations and uncertainties related to information available to characterize source areas).

Our ranking is generally consistent with rankings developed by other organizations (Dinwiddie 1999; ER 2001), which identified these three watersheds as the most important. While the ER and NMED rankings considered human risk as an important criterion, they did not focus specifically on risk as it may relate to increased movement of contamination following the Cerro Grande Fire. For example, ER (2001a) ranks the Mortandad watershed as the second highest priority, and we ranked the Water watershed as the second highest priority. Our results were driven by the relatively high burn and flow potential factors for the Water watershed, and the Mortandad watershed results were driven primarily by the extent of contamination.

Table 3-1. Summary of Input Values to Total Ranking Factor

Watershed	Burn factor	Flow Factor	Contamination factor	Total ranking value ^a	% contribution to total ranking factor
Guaje	0.18	0.14	0.07	0.39	13%
Pueblo	0.13	0.05	0.23	0.42	14%
Rendija	0.19	0.07	0.03	0.30	10%
Los Alamos	0.13	0.11	0.18	0.42	14%
<i>Los Alamos (combined)^b</i>	<i>0.64</i>	<i>0.37</i>	<i>0.51</i>	<i>1.55</i>	<i>52%</i>
Los Frijoles	0.03	0.10	0.02	0.15	5%
Mortandad	0.03	0.08	0.24	0.36	12%
Pajarito	0.11	0.08	0.08	0.27	9%
Water	0.19	0.36	0.16	0.72	24%

^a Total value is the sum of the burn, flow, and contamination factors. See Appendix B for input data used for each factor.

^b Los Alamos (combined) includes all sub-basins or watersheds within the Los Alamos drainage basin watershed: Guaje, Los Alamos, Pueblo, and Rendija watersheds.

3.2 Identifying and Defining Source Areas

There are many areas in the LANL facility environs where chemicals and radionuclides were known or suspected to be present in soil or sediments. We identified four distinct categories of potential sources of chemicals and radionuclides that had the potential to be mobilized and distributed in storm water flow and consequent erosion. We refer to these areas collectively as source areas. The amount of data available to characterize these source areas was quite variable, and the following paragraphs describe each of the following four source area categories:

1. Potential Release Site soil characterized by available sampling data (PRSSs)
2. Canyon sediments characterized by available sampling data (Geomorphic Units)
3. Canyon sediments characterized by inventory estimates for ¹³⁷Cs and ^{239,240}Pu only (Unsampled Reaches)
4. Burned area ash characterized by available sampling data (Burned Areas).

We used available sampling data to identify the chemicals and radionuclides detected in each of the source areas and to estimate average, representative concentrations of chemicals and radionuclides in each source area. To accomplish this process, we completed three steps:

1. We first linked the sampling data to a specific source area.
2. Then we estimated an average concentration of chemicals and radionuclides using the sampling data.
3. Finally, we defined the surface area that could be characterized by those sampling data.

The only chemicals or radionuclides for which we were able to develop a generally complete characterization, based on all potential source areas (PRSS, Geomorphic Units, Unsampled Reaches, and Burned Areas) are ^{137}Cs and $^{239,240}\text{Pu}$. The only watershed for which generally complete characterization data were available was the greater Los Alamos watershed, including both Los Alamos and Pueblo Canyons.

3.2.1 Potential Release Site Source Areas

PRSS are potentially contaminated with hazardous or mixed wastes that are subject to the requirements of the Resource Conservation and Recovery Act (RCRA). The PRSS source areas evaluated for the surface water pathway included:

- PRSS within the infrared (IR)-defined burned area that were confirmed to be burned and were used for the atmospheric pathway assessment
- PRSS within the IR burn boundary that did not burn
- PRSS within defined floodplain areas
- PRSS identified by LANL as high priority for field verification immediately following the fire (faxed list of "Top 23 PRSS needing Field Verification").

We included all PRSS falling within the above-described categories in this assessment if surface soil sampling data were available to characterize them. Appendix W provides additional information regarding the specific PRSS included in our evaluation.

We initially based the areal extent of chemicals and radionuclides in surface soil within the PRSS on the areas defined by polygons as part of the GIS coverage files provided by LANL. However, we recognized that in some cases these polygon shapes, sizes, and locations did not correspond to either the locations of actual sampling data or to the extent of concentrations of chemicals and radionuclides in the soil. In those instances, ER personnel at LANL redefined the surface area extent of PRSS to more accurately reflect the available sampling data. In some cases, the surface extent of the chemicals and radionuclides could not be redefined if there were insufficient sampling data; therefore, we retained the original GIS polygon areas based on the initial coverage files provided by LANL.

A specific GIS coverage that represented the redefined PRS or included all of the identified PRSS was not available. Therefore, we developed a GIS polygon shapefile based on centroid coordinates for each PRS (based on the original PRS coverage files provided by LANL) and the redefined or original areas of each PRS. Because we did not know the precise boundary of each PRS, we represented the PRSS as circles with a radius calculated from the area of each PRS. When groups of PRS polygons partially or completely overlapped, we dissolved the PRS polygons that overlapped into a single polygon that represented the perimeter of the overlapped

PRS polygons. We developed a spreadsheet table to relate the original PRSs to the PRS polygons in the GIS shapefile. Figure 3-2 shows the PRS locations.

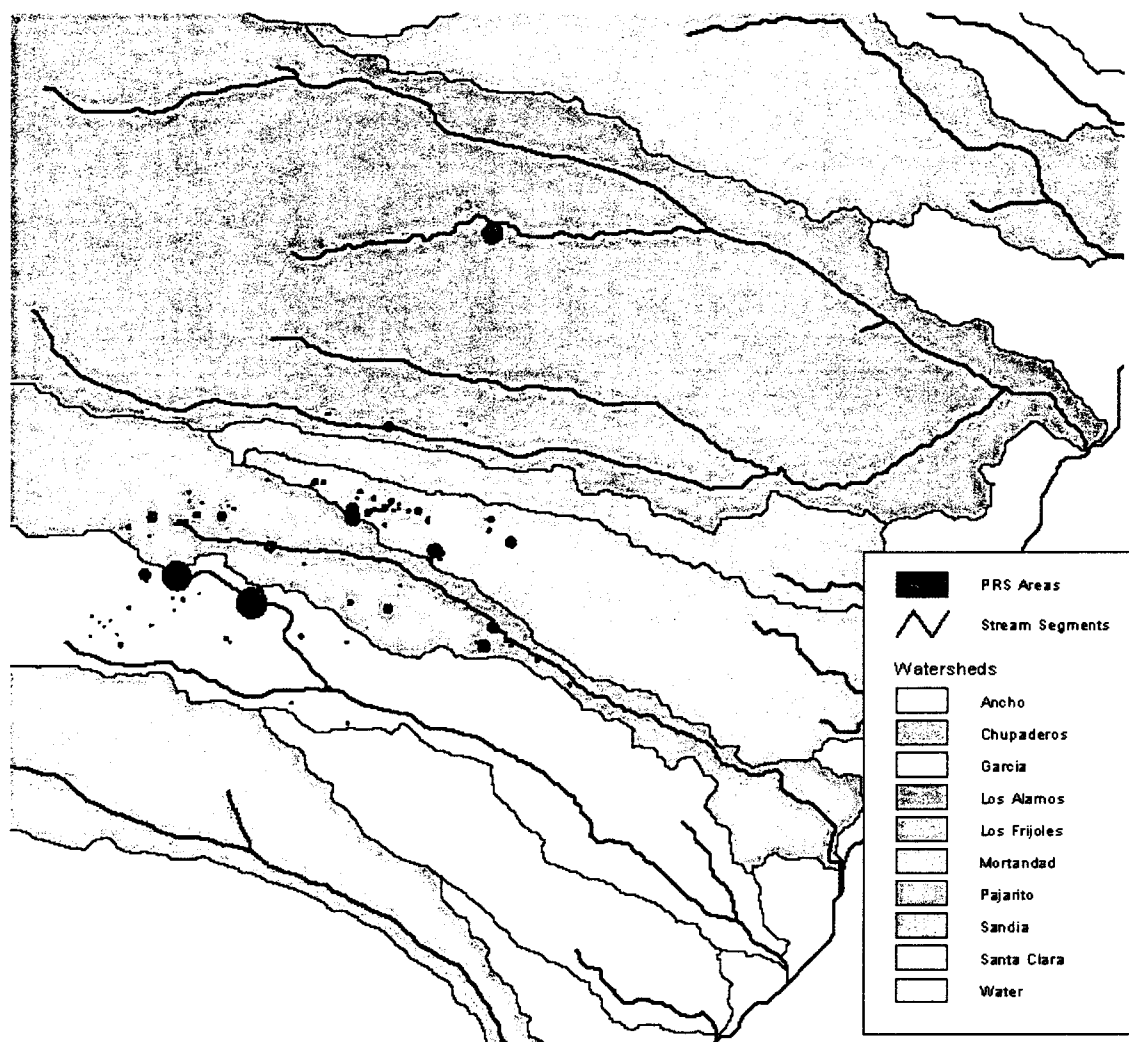


Figure 3-2. PRS source area locations.

3.2.2 Geomorphic Unit Source Areas

Geomorphic Unit source areas consist of previously defined areas of sediments potentially containing concentrations of chemicals and radionuclides within reaches of both Pueblo and Los Alamos Canyons. Each reach was long enough to capture local variations in concentrations of chemicals and radionuclides related to variations in the age, thickness, and particle size of young (post-1942) sediment deposits but short enough that the effects of downstream dilution of concentrations of chemicals and radionuclides were minimized. The geomorphic units within each reach defined the horizontal extent of chemicals and radionuclides in each reach and also provided grouping of areas with similar physical and/or radiological characteristics. Within each

geomorphic unit, we identified two general categories of sediment facies: overbank and channel facies.

Overbank facies refer to sediment generally transported as suspended load during floods, which are commonly deposited on floodplains from water that overtops stream banks. Channel facies refer to sediment generally transported as bed load and deposited along the main stream channel. Overbank facies sediment has a typical median particle size of silt to fine sand, and channel facies sediment has a typical median particle size of coarse or very coarse sand. Median sands could be assigned to either facies, depending on the stratigraphic context. These distinctions are somewhat arbitrary, with gradations commonly occurring. However, they form an important basis for differentiating sediment deposits of similar age that may have much different concentrations of chemicals and radionuclides (Reneau et al. 1998a, 1998b, and 1998c).

The surface area extent of the Geomorphic Unit source areas was based on information provided by Reneau et al. (1998a, 1998b, and 1998c). This information was provided for geomorphic units, which were defined in Pueblo and Los Alamos Canyon reaches only.

A specific GIS coverage that was representative of the Geomorphic Unit was not available. Therefore, similar to the procedure used to define the PRSs, we developed a GIS polygon shapefile represented as circles using estimated centroid coordinates (based on an average of the coordinates for all samples used to characterize each geomorphic unit) and a radius calculated from the area identified for each Geomorphic Unit. We dissolved overlapping groups of Geomorphic Unit polygons into a single polygon that was representative of the perimeter of the overlapped Geomorphic Unit polygons. We developed a spreadsheet table to relate the original Geomorphic Units to the Geomorphic Unit polygons in the GIS shapefile. Figure 3-3 shows the Geomorphic Unit locations.

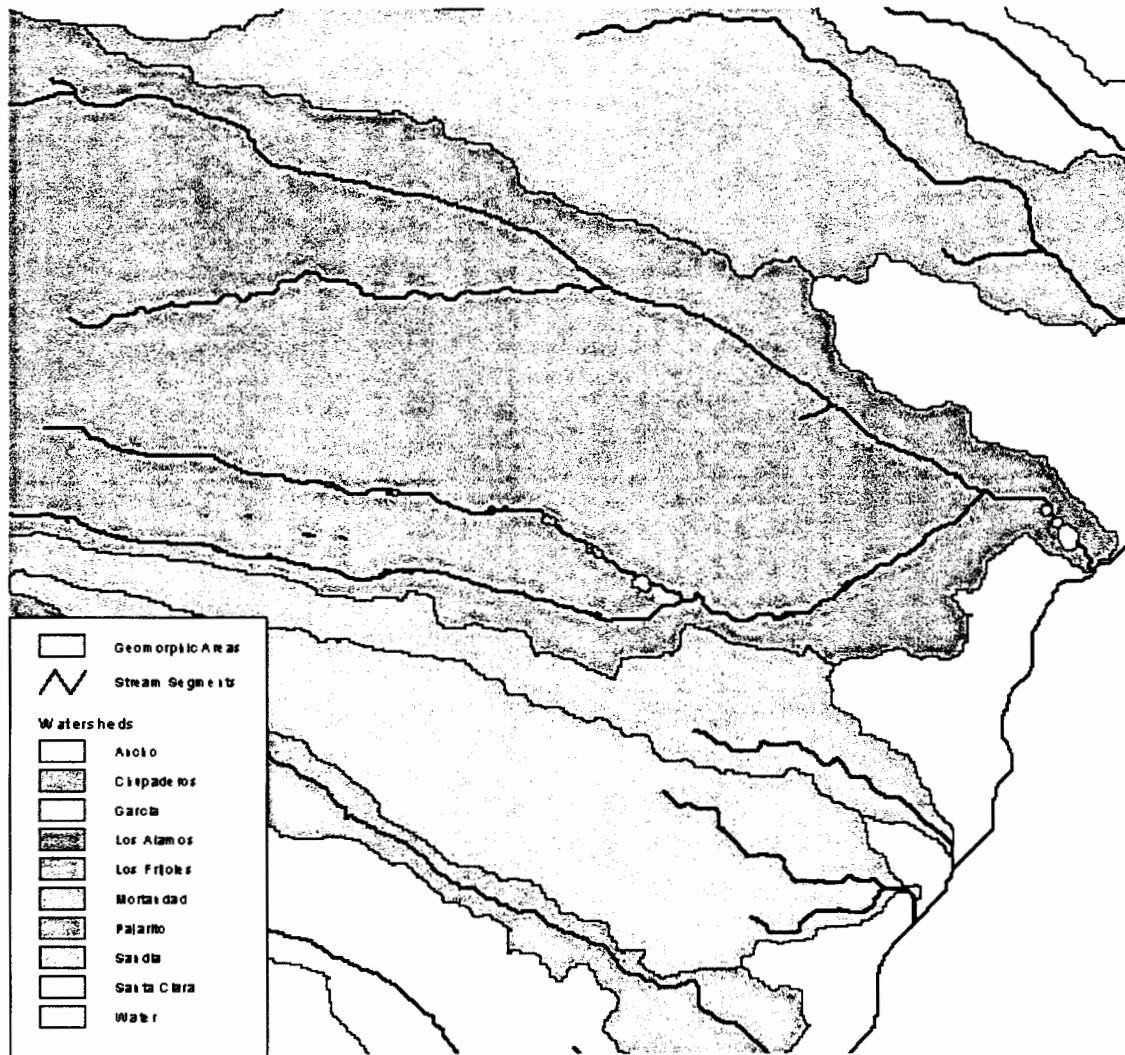


Figure 3-3. Geomorphic unit source area locations.

3.2.3 Unsourced Reach Source Areas

We included Unsourced Reach source areas to account for the fact that the majority of the ^{137}Cs and $^{239,240}\text{Pu}$ inventories in Los Alamos and Pueblo Canyons, as documented by Reneau et al. (1998a, 1998b, and 1998c), resides in stretches of canyon that are not characterized by actual sampling data. Instead, we were provided preliminary inventory estimates for ^{137}Cs and $^{239,240}\text{Pu}$ based on either average inventories of bounding sampled reaches or the same inventory found in an adjacent reach near tributary junctions. Because these canyon reaches account for the majority of the inventory for these two radionuclides, we considered it important to incorporate their potential impact on downstream concentrations.

Reneau et al. (1998a, 1998b, and 1998c) did not provide the surface area extent of the unsourced reach source area. Therefore, the areas for each Unsourced Reach are based on our approximations of the stream segment (reach) corresponding to the available inventory estimate and confined by immediately adjacent upstream and downstream sampled reaches.

We developed a GIS coverage for the Unsourced Reaches based on the GIS Reach coverage provided by LANL. We selected identified Unsourced Reaches that were included in the LANL GIS coverage and created a new GIS polygon shapefile that included only the selected Unsourced Reaches. We added identified Unsourced Reaches not included in the LANL GIS coverage to the new shapefile by drawing polygons. We estimated the size, shape, and location of the drawn polygons based on the stream segments developed during the storm water flow modeling (see Chapter 4) and known Unsourced Reach polygons. Figure 3-4 shows the Unsourced Reach locations.

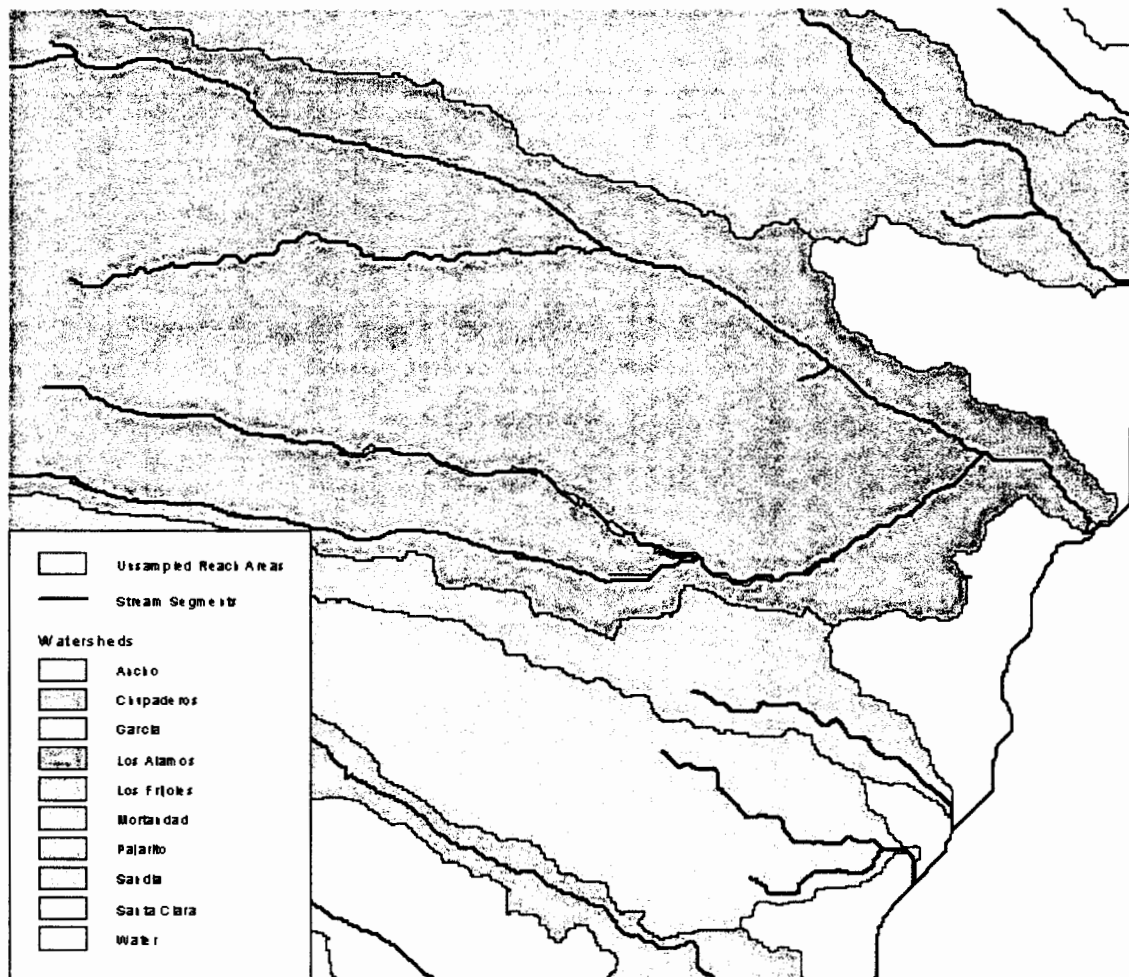


Figure 3-4. Unsourced reach source area locations.

3.2.4 Burned Area Source Areas

We included Burned Area source areas to account for the apparent increase in concentration of some chemicals and radionuclides in burned areas following the fire. Presumably, this increase was associated with a concentration in ash of burned trees, underbrush, forest litter, and other biomass. It is important to understand the impact burned areas made in elevated concentrations of chemicals and radionuclides that were measured in surface water following the fire.

The surface area of the Burned Area source area was based on the GIS coverage files that defined the burned areas within each watershed. Figure 3-5 shows the Burned Area locations.

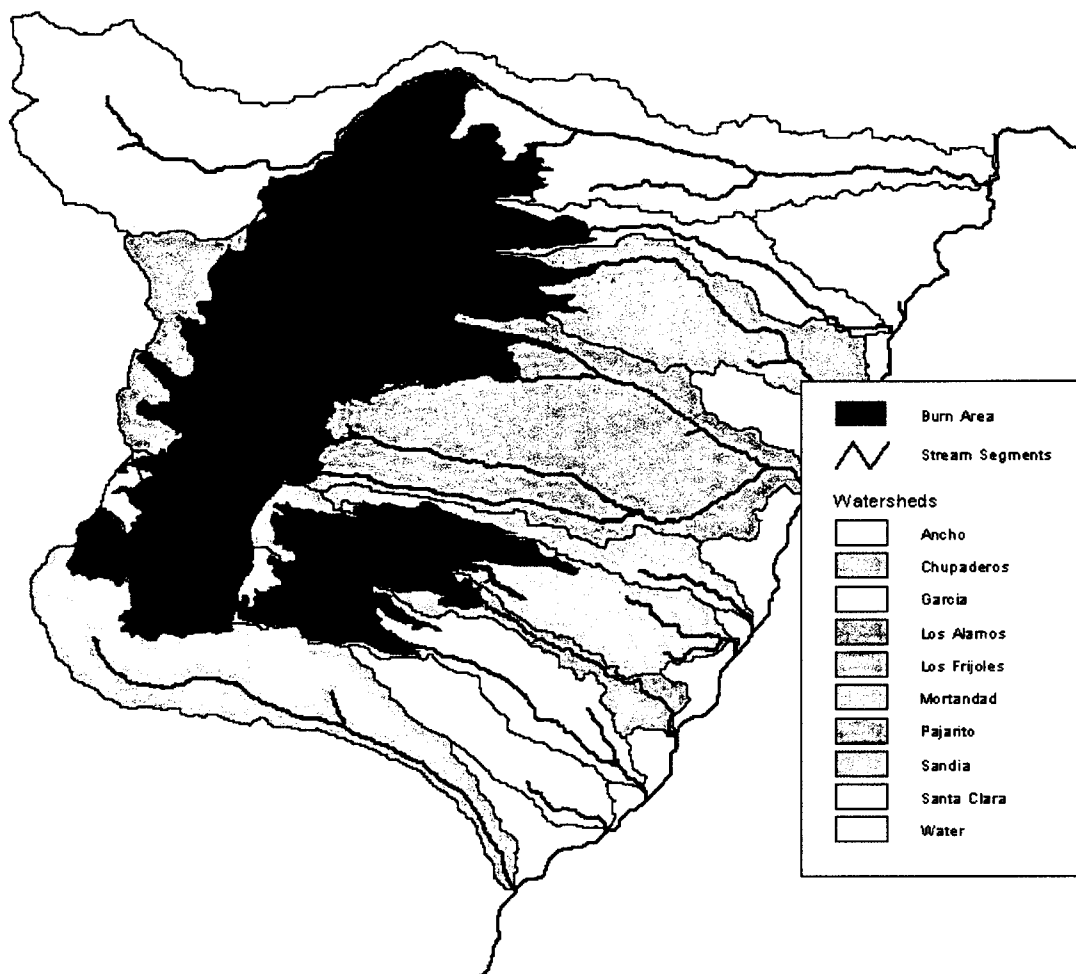


Figure 3-5. Burned area source area locations.

3.3 Screening Calculations to Prioritize Analysis of Radionuclides and Chemicals

Because of the great number of samples collected and analyzed for chemicals and radionuclides in a fairly short time period during and after the fire, we designed a screening procedure to focus our analysis on those analytes with the highest potential to contribute to the health risk. Our screening process used the available monitoring data for radionuclides and chemicals collected after the fire, along with readily available risk coefficients for radionuclides and slope factors and reference doses for chemicals, to calculate a screening index. We used measurement data from both ESH-18 and ER at LANL. The Stage 1 screening, described in more detail below, conservatively assumed the maximum measured value for each analyte as reported by either organization at both onsite and offsite locations. The Stage 2 screening process was more realistic and used the highest average of all reported values by each organization for each analyte.

To further ensure that no radionuclide or chemical that could be important to human health was excluded from our screening assessment, we made assumptions for our calculations that would maximize the exposure of a person to that radionuclide or chemical. For example, we assumed a person ingested the surface or storm water specifically at the location of the measured value. In addition, we included unfiltered water sample results in our analysis, even though routine ingestion of unfiltered water would be unlikely. With this cautious approach, we determined a screening index for each contaminant. By comparing this screening index to a predetermined criterion, we focused on and prioritized those chemicals and radionuclides that would be most important in terms of human health risk. The following sections describe our approach in detail.

3.3.1 Setting a Risk-based Decision Criterion

As previous studies have shown, before performing calculations to prioritize radionuclides or chemicals, it is important to determine the criteria that will be used to make risk-based decisions. In previous studies, radionuclides or chemicals that fell below some predetermined level of health risk, when risk was calculated conservatively, were removed from further consideration. Using this approach, we developed a list of chemicals of concern and radionuclides of concern, so the greatest effort was given to the analytes most important to human health risk. The first step in the process was selecting a risk-based decision criterion.

A risk-based decision criterion was used to identify those radionuclides and chemicals that were below a minimum level of concern. This section reviews risk-based decision criteria that have been used at other locations for similar projects and by other agencies. We recommended a risk-based decision criterion be used to identify the contaminants for which surface water and sediment monitoring data would be evaluated.

For radionuclides, the National Research Council (1995) has suggested a decision criterion of 0.07 Sv for a whole-body lifetime dose for identifying sites where a dose reconstruction may be warranted. This value is based on the Federal Register 10 CFR 20 maximum annual dose limit of 0.001 Sv to any individual at a nuclear site boundary, multiplied by 70 years to give a whole-body lifetime dose of 0.07 Sv. In terms of risk, this is roughly equivalent to a lifetime excess cancer incidence risk of 5×10^{-3} (or 1 chance in 200). For comparison, the average American has about a 1 in 5 chance of developing a fatal cancer

The Oak Ridge Health Agreement Steering Panel, of the Oak Ridge Dose Reconstruction study, established a decision criterion of 10^{-4} (1 chance in 10,000) lifetime excess cancer incidence risk for their study as a whole (Theissen et al. 1996). For screening releases of radionuclides to the aquatic pathways (i.e., those exposure pathways associated with the Clinch River), a lifetime excess cancer incidence risk criterion of 10^{-5} (1 chance in 100,000) was applied (Apostoei et al. 1999). The lower value was used because each radionuclide was compared to the decision guide independently for each exposure pathway rather than combining the exposure risk from all pathways. The calculated screening index was a conservatively biased estimate of excess lifetime risk to the most at-risk individual and was, therefore, expected to overestimate the risk to most or all real individuals (Apostoei et al. 1999, page 3-1).

In the Hanford Environmental Dose Reconstruction Project, one of the criteria used to define the physical area to be included in the study calculations was a thyroid dose of 1 rad (0.01 Gy) to a child or infant (Shleien 1992). This dose represents an increased lifetime risk for radiation-induced thyroid cancer on the order of 2×10^{-4} .

For continuous exposures to ionizing radiation, the National Council on Radiation Protection and Measurements (NCRP) recommends an annual limit for members of the public of 1 mSv effective dose (NCRP 1993). This is the same as the value recommended by the International Commission on Radiological Protection (ICRP) (ICRP 1991). This dose limit corresponds to a lifetime risk of about 4×10^{-3} , assuming the risk per sievert from fatal and nonfatal cancers is 6×10^{-2} (ICRP 1991, Table 3) and a 70-year lifetime exposure. The NCRP also defines an annual negligible individual dose (NID), which establishes a boundary below which the dose can be dismissed from consideration and sets the NID at 0.01 mSv effective dose. This corresponds to a lifetime risk of about 4×10^{-5} using the same assumptions as above.

The EPA has specified an upper bound individual lifetime cancer risk "target range" for carcinogens of 10^{-4} to 10^{-6} within which it strives to manage risks as a part of a Superfund cleanup. The risk estimates are determined using reasonable maximum exposure assumptions for either current or future land use (EPA 1991). Once a decision has been made to cleanup, EPA has expressed a preference for cleanups achieving the more protective end of the range of 10^{-6} . The upper boundary of the risk range is not a discrete line at 10^{-4} , although EPA generally uses 10^{-4} in making risk management decisions (e.g., deciding whether to implement remediation). EPA has stated that a specific risk estimate around 10^{-4} may be considered acceptable if justified based on site-specific conditions (EPA 1991). For example, in a Clean Air Act rulemaking establishing National Emissions Standards for Hazardous Air Pollutants (NESHAPs) for U.S. Nuclear Regulatory Commission (NRC) licensees, DOE facilities, and many other kinds of sites, EPA concluded that a risk level of 3×10^{-4} is essentially equivalent to the presumptively safe level of 1×10^{-4} . EPA explicitly rejected a risk level of 5.7×10^{-4} in the case of elemental phosphorus plants in this rulemaking. EPA has consistently concluded that levels of 15 mrem per year effective dose equivalent (EDE) (which EPA equates to approximately a 3×10^{-4} increased lifetime cancer risk) or less are protective and achievable (EPA 1997a). EPA has explicitly rejected levels above 15 mrem per year EDE as being not sufficiently protective. For example, the EPA has found the NRC dose limit of 25 mrem per year (equivalent to approximately 5.7×10^{-4} increased lifetime risk) specified in NRC's Radiological Criteria for License Termination (i.e., decommissioning rule) to be beyond the upper bound of the risk range generally considered protective under the Comprehensive Environmental Response, Compensation and Liability Act (EPA 1997a).

The EPA approach has been adapted to identify and prioritize potential remediation sites at the Idaho National Engineering and Environmental Laboratory using a target risk level of 10^{-6} . The scenarios evaluated are based on current residential or occupational exposure conditions with exposure durations of 30 and 25 years, respectively. The pathways evaluated are ingestion of drinking water, inhalation of contaminated particulates, ingestion of contaminated soil, and external exposure to soils. Each pathway is evaluated independently (Fromm 1996).

Based on the above information and the fact that we are assessing radionuclides and chemicals against the risk criterion on an individual basis, we adopted a protective risk criterion of 10^{-5} for this study. We conservatively calculated the screening risk indices based on the measured radionuclides and chemicals in surface water and sediments during and after the fire, using maximum concentrations and conservative exposure factors and compared those screening risk index values to the 10^{-5} level. Further analysis of monitoring data were not undertaken at this stage in the project for radionuclides and chemicals with screening risk indices below that level.

For chemicals, various values can be used to determine either the potential for a toxic effect when exposed to noncarcinogenic chemicals or the development of excess cancers when exposed to chemicals identified as carcinogens. For carcinogens, we used the oral slope factor (SF_o) with ingestion volumes to estimate the probability of increased cancer incidence over a lifetime. For noncarcinogens, we used the oral chronic reference dose (RfD_o) with ingestion intakes under chronic conditions (those lasting more than 7 years) to estimate the potential of systemic toxic effects. For our chemical screening process, we used two assessment criteria. For carcinogenic chemicals, we used the slope factor to calculate the screening risk index for comparison to the 1×10^{-5} level. For noncarcinogenic chemicals, we used the published RfD_o values and compared these to the actual water concentrations. We calculated a hazard quotient by dividing the measured concentration by the reference dose. When the hazard quotient was greater than 1, we prioritized noncarcinogens in the analysis for further consideration. Thus, two prioritized lists were necessary for chemicals: one list where contaminants were compared by hazard quotient and one list where contaminants were compared by the screening risk index. Contaminants that exceed either of the above criteria (hazard quotient > 1 or risk index $> 10^{-5}$) were analyzed further.

3.3.2 Screening of Contaminants Measured in Water Samples

The following sections describe the screening process calculations for both radionuclide and chemical concentrations reported for water samples collected following the fire. Figure 3-6 outlines the key steps in this process and highlights the two-stage screening process we used for both radionuclides and chemicals. The Stage 1 and 2 results of the screening calculations based on water concentrations are presented in Appendix C.

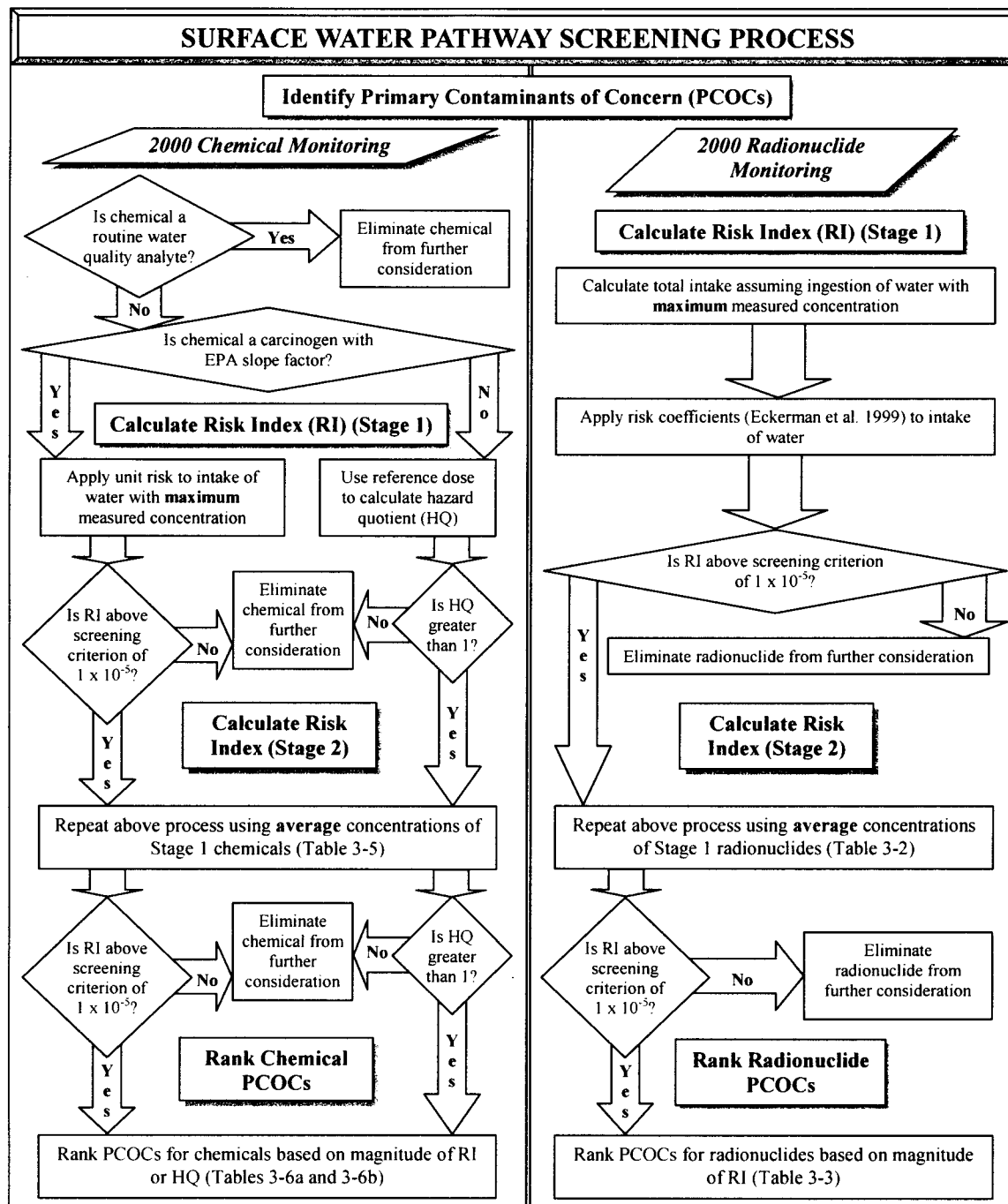


Figure 3-6. Surface water screening process for identifying primary radionuclides and chemicals of concern for further monitoring evaluation. Both procedures began with the water monitoring data collected after the Cerro Grande Fire in May 2000.

3.3.2.1 Radionuclides. Federal Guidance Report No. 13 reports risk coefficients for ingestion of radionuclides in tap water or food, expressed as the probability of radiogenic cancer mortality per unit intake (Eckerman et al. 1999). Except for tritium, the risk coefficient for

ingestion applies to all forms of the radionuclide. Separate risk coefficients are given for tritium as tritiated water and organically bound tritium. The risk, R_i , associated with the ingestion of a given radionuclide, i , involves multiplying the applicable risk coefficient, r_i , by the activity intake, I_i , as follows:

$$R = I_i \times r_i \quad (3-1)$$

where

$$I_i = C_i \times V \times CF_i \times CF_r$$

where

- I_i = intake of radionuclide over exposure period (Bq)
- C_i = measured concentration of radionuclide in surface water at LANL (pCi L⁻¹)
- V = volume of contaminated water ingested per day (L d⁻¹)
- CF_i = time of exposure (2.55×10^4 d)
- CF_r = radionuclide activity units conversion factor (0.037 Bq pCi⁻¹).

We based our assessment of radionuclides measured in surface water, storm water, and groundwater at LANL following the Cerro Grande Fire on intake of that water, where the intake is averaged over all ages and both genders. For radionuclides, we assumed the combined lifetime average intake of water of 1.11 L d⁻¹ (Eckerman et al. 1999) to estimate the total quantity of radionuclide ingested. We assumed an exposure period of 7 years. We completed the screening of radionuclides in two stages (Figure 3-6).

- In Stage 1, we used the *maximum* measured concentrations of the radionuclides combined with the risk coefficients to calculate the screening risk index. Those radionuclides that resulted in a risk index greater than 1×10^{-5} were identified as radionuclides of potential concern. These radionuclides are listed in Table 3-2. This first stage identified 35 of the original 76 radionuclides for further study. With our cautious assumptions, we are confident that the radionuclides with a risk index below the screening criterion of 1×10^{-5} are likely not important for future health risk, and resources available for this project should not be expended on a more detailed evaluation of them.
- In Stage 2, we used a less conservative calculation based on the average concentration of the 35 radionuclides identified in Stage 1 to calculate a second screening risk index (Table 3-3). After the Stage 2 screening, 17 radionuclides remained. The radionuclides that emerged from Stage 2 screening were grouped by their relative contribution to the total screening risk index.

Table 3-2. Radionuclides Emerging from Stage 1 Screening Evaluation ^a

Symbol	Radionuclide	Risk index	Symbol	Radionuclide	Risk index
Pb-210	Lead-210	2.6E-02	Sr-90	Strontium-90	1.4E-04
Po-210	Polonium-210	6.9E-03	U-235,236	Uranium-235/236	1.3E-04
Ra-226	Radium-226	5.6E-03	Pb-212	Lead-212	1.2E-04
Ra-228	Radium-228	4.8E-03	Ba-140	Barium-140	9.1E-05
K-40	Potassium-40	1.6E-03	H-3	Tritium	8.1E-05
Th-234	Thorium-234	8.8E-04	Cd-109	Cadmium-109	6.6E-05
Th-228	Thorium-228	7.3E-04	Pa-234m	Protactinium-234m	5.6E-05
Pa-231	Protactinium-231	7.0E-04	Th-227	Thorium-227	5.1E-05
Ra-223	Radium-223	5.2E-04	Ru-106	Ruthenium-106	4.2E-05
Ra-224	Radium-224	4.8E-04	Pu-238	Plutonium-238	3.1E-05
Cs-137	Cesium-137	4.7E-04	Ce-144	Cerium-144	2.2E-05
U-238	Uranium-238	4.3E-04	Cs-134	Cesium-134	1.4E-05
Th-230	Thorium-230	3.7E-04	Ac-228	Actinium-228	1.1E-05
Th-232	Thorium-232	3.5E-04	Nd-147	Neodymium-147	8.0E-06
Np-237	Neptunium-237	2.9E-04	Pa-233	Protactinium-233	8.0E-06
U-234	Uranium-234	2.9E-04	Na-22	Sodium-22	7.7E-06
Pu-239	Plutonium-239	2.36E-04	Eu-152	Europium-152	5.4E-06
Am-241	Americium-241	1.94E-04			

^a For the Stage 1 screening, we used the *maximum* measured concentrations of the radionuclides combined with the morbidity risk coefficients to calculate the screening risk index.

Table 3-3. Radionuclides Emerging from Stage 2 Screening ^a

Symbol	Radionuclide	Risk index
Pb-210	Lead-210 ^b	3.4E-03
Po-210	Polonium-210 ^b	4.2E-04
Ra-228	Radium-228 ^b	2.2E-04
Ra-226	Radium-226 ^b	5.6E-05
K-40	Potassium-40 ^b	5.1E-05
Th-234	Thorium-234 ^b	4.9E-05
U-238	Uranium-238 ^b	4.1E-05
Th-228	Thorium-228 ^b	3.5E-05
Ra-224	Radium-224 ^b	2.9E-05
Th-232	Thorium-232 ^b	2.6E-05
Th-230	Thorium-230 ^b	2.1E-05
U-234	Uranium-234 ^b	1.1E-05
Pa-234m	Protactinium-234m ^b	1.0E-05
Cs-137	Cesium-137	9.9E-06
Sr-90	Strontium-90	9.9E-06
Np-237	Neptunium-237	8.6E-06
H-3	Tritium	5.4E-06

^a In Stage 2, the *average* concentration for each radionuclide was used in the screening assessment. The screening level was 1×10^{-5} .

^b From natural decay series.

3.3.2.2 Chemicals. Figure 3-6 outlines the steps in our screening process for chemicals. As a first step in this process, we considered analytes that were monitored to meet federal and State water quality regulations. Data were routinely collected for a number of water quality parameters, including bromide; calcium; total and dissolved organic carbon; bicarbonates and carbonates (as CaCO_3); chlorides; iron; magnesium; nitrogen (as ammonia, nitrites and nitrates, and total Kjeldahl); phosphorus; potassium; sodium; and sulfate. Except for nitrogen (measured as nitrites and nitrates), none of these has an established drinking water standard. For this reason these water quality parameters were not considered further in our screening assessment.

As described previously, we used two different parameters to determine either the potential of a toxic effect (reference dose, or RfD) or the development of excess cancers (slope factors and unit risks) in a person from the chemicals. We calculated the incremental lifetime screening risk index or the hazard quotient for chemicals using the Oak Ridge National Laboratory Risk Assessment Information System Database (<http://risk/lrd.ornl.gov>). The Risk Assessment Information System (RAIS) contains risk assessment tools and information, is designed for use at all DOE sites, and can be customized for site-specific conditions. This database, where all information is referenced, contains information taken from the EPA's Integrated Risk Information System (IRIS), the Health Effects Assessment Summary Tables (HEAST), and other information sources.

For the carcinogens, we determined the risk index, RI_c , by multiplying the unit risk, U_c , for chemical, c , by the concentration (C_c) of the chemical in surface water at LANL.

$$RI_c = U_c \times C_c \quad (3-2)$$

where

U_c = lifetime mortality risk from ingesting chemical (per $\mu\text{g L}^{-1}$)

C_c = measured concentration of the chemical in surface water at LANL ($\mu\text{g L}^{-1}$).

The unit risk, U , is a lifetime risk from daily exposure to a chemical at a concentration that results in the specified cancer risk and is derived from the oral slope factor (Sf_o).

$$U_o = \frac{Sf_o \times V}{W \times CF_c} \quad (3-3)$$

where

Sf_o = slope factor (risk per mg kg^{-1} body weight d^{-1})

V = volume of contaminated water ingested per day (L d^{-1})

W = mean body weight (71.2 kg) (ORNL 2001)

CF_c = units conversion factor ($1 \times 10^3 \mu\text{g mg}^{-1}$).

For the noncarcinogens, we calculated the intake concentrations, below which adverse health effects would not be expected. We used the EPA's oral reference dose (RfD_o), which is based on the assumption that thresholds exist for certain toxic effects such as cellular necrosis. It is expressed in units of milligrams per kilogram per day. In general, the RfD_o is an estimate of a daily exposure to the human population (including sensitive subgroups) that is likely not to cause

an appreciable risk of harmful effects during a lifetime. We compared the RfD_0 with the dose level measured in surface water, storm water, or groundwater and calculated the hazard quotient, which is the ratio between the chemical intake based on the maximum measured concentration in water with the established RfD_0 . When the hazard quotient was >1 , we included the chemicals in the analysis. An RfD_0 has not been developed for some chemicals that present far more of an inhalation hazard than an ingestion hazard. For these, we derived an RfD_0 from an RfC , recognizing the great uncertainty associated with the conversion. An RfC is a reference concentration estimate (with uncertainty spanning perhaps an order of magnitude) of a continuous inhalation exposure to the human population (including sensitive subgroups) that is likely to be without an appreciable risk of deleterious noncancer effects during a lifetime.

We completed the screening of chemicals in two stages:

- In Stage 1, we used the *maximum* measured concentrations of the chemicals combined with the slope factors or the reference dose to calculate the screening risk index or hazard quotient. The carcinogenic chemicals selected in the Stage 1 screening are those with a risk index greater than our screening criterion of 1×10^{-5} . For noncarcinogenic chemicals, we included those chemicals with a calculated hazard quotient >1 in the list of chemicals emerging from the Stage 1 screening evaluation. In some cases, chemicals do not have either a reported slope factor or RfD . In those cases where applicable we used toxicity equivalency factors (TEF) in combination with the slope factor for a key carcinogen (ORNL 2001). For example, Tables 3-4a, 3-4b, and 3-4c list the TEFs for the carcinogenic polycyclic aromatic hydrocarbons (PAHs), the chlorinated dioxins, and the chlorinated furans that do not have a slope factor. The TEF is combined with the slope factor for benzo(a)pyrene to calculate a slope factor for other PAHs. Table 3-5 lists the chemicals that emerged as important from the Stage 1 screening, and lists 86 of almost 200 chemicals monitored in 2000 as potentially important for further evaluation.
- In Stage 2, we assumed a less conservative intake of each analyte that remained after Stage 1 by using the average measured concentration in water along with the unit risk or RfD to estimate the screening risk or hazard quotient, respectively. Two prioritized lists emerged from Stage 2 for chemicals: a list of 40 carcinogens where contaminants were compared by the risk index (Table 3-6a) and a list of 5 noncarcinogens where contaminants were compared by the hazard quotient (Table 3-6b). The 45 chemicals that emerged from the Stage 2 screening were grouped by their relative contribution to the total risk index or by the magnitude of the hazard quotient. The noncarcinogens are listed in Table 3-6b.

Table 3-4a. Toxicity Equivalency Factors for Carcinogenic Polycyclic Aromatic Hydrocarbons

Compound	Toxicity equivalency factors
Benzo(a)pyrene	1.0
Benz(a)anthracene	0.1
Benzo(b)fluoranthene	0.1
Benzo(k)fluoranthene	0.01
Chrysene	0.001
Dibenz(a,h)anthracene	1.0
Indeno(1,2,3-c,d)pyrene	0.1

Table 3-4b. Toxicity Equivalency Factors for Chlorinated Dioxins

Compound	Toxicity equivalency factors
2,3,7,8-TCDD	1.0
2,3,7,8-PeCDD (WHO)	0.5 (1)
2,3,7,8-HxCDD	0.1
2,3,7,8-HpCDD	0.01
OCDD	0.001 (0.0001)
Other CDDs	0

Table 3-4c. Toxicity Equivalency Factors for Chlorinated Furans^a

Compound	Toxicity equivalency factors
2,3,7,8-TCDF	0.1
1,2,3,7,8-PeCDF (WHO)	0.5 (0.05)
2,3,4,7,8-PeCDF (WHO)	0.05 (0.5)
2,3,7,8-HxCDF	0.1
2,3,7,8-HpCDF	0.01
OCDF	0.001 (0.0001)
Others	0

^a The TEF values from the World Health Organization are shown in parentheses

Table 3-5. Chemicals Emerging from Stage 1 Screening Evaluation ^a

Analyte code	Chemicals	Maximum concentration ($\mu\text{g L}^{-1}$)	Risk index	Hazard quotient
35822-46-9	1,2,3,4,6,7,8-HpCDD	2.4E-03	1.0E-04	
67562-39-4	1,2,3,4,6,7,8-HpCDF	2.3E-03	9.9E-05	
39227-28-6	1,2,3,4,7,8-HxCDD	7.1E-03	1.3E-03	
70648-26-9	1,2,3,4,7,8-HxCDF	6.6E-03	2.8E-04	
40321-76-4	1,2,3,7,8-PCDD	6.3E-03	1.4E-02	
57117-41-6	1,2,3,7,8-PCDF	5.8E-03	1.3E-02	
120-82-1	1,2,4-Trichlorobenzene	9.6E+02		1.5
106-46-7	1,4-Dichlorobenzene	9.6E+02	6.5E-04	
108-60-1	2,2'-oxybis[1-chloropropane]	9.6E+02	1.9E-03	
58-90-2	2,3,4,6-Tetrachlorophenol	4.8E+03		2.5
1746-01-6	2,3,7,8-TCDD	6.7E-04	3.0E-03	
51207-31-9	2,3,7,8-TCDF	4.9E-03	2.2E-03	
120-83-2	2,4-Dichlorophenol	9.6E+02		4.9
51-28-5	2,4-dinitrophenol	4.8E+03		37
121-14-2	2,4-Dinitrotoluene	9.6E+02		7.4
606-20-2	2,6-Dinitrotoluene	9.6E+02		7.4
95-57-8	2-Chlorophenol	9.6E+02		3
88-74-4	2-Nitroaniline	4.8E+03	7.7E-04	
88-75-5	2-Nitrophenol	9.6E+02		1.8
91-94-1	3,3'-Dichlorobenzidine	4.8E+03	6.2E-02	
534-52-1	4,6-Dinitro-2-Methylphenol	4.8E+03		37
59-50-7	4-Chloro-3-methylphenol	9.6E+02		3
106-47-8	4-chloroaniline	2.4E+03		9.3
7005-72-3	4-Chlorophenyl phenyl ether	9.6E+02	5.3E-05	
100-01-6	4-Nitroaniline	4.8E+03	7.7E-04	
100-02-7	4-Nitrophenol	4.8E+03		9.3
309-00-2	Aldrin	6.8E-02	3.3E-05	
Al	Aluminum	1.0E+06		38455
62-53-3	Aniline	2.4E+03	3.8E-04	
Sb	Antimony	2.8E+02		11
As	Arsenic	1.4E+02	6.9E-03	
103-33-3	Azobenzene	9.6E+02	3.0E-03	
Ba	Barium	2.1E+04		4.6
71-43-2	Benzene	5.0E+00	8.0E-03	
92-87-5	Benzidine	1.3E+01	8.7E-02	
56-55-3	Benzo(a)anthracene	9.6E+02	2.0E-02	
50-32-8	Benzo(a)pyrene	9.6E+02	2.0E-01	
205-99-2	Benzo(b)fluoranthene	9.6E+02	2.0E-02	
191-24-2	Benzo(g,h,i)perylene	9.6E+02	2.0E-04	
207-08-9	Benzo(k)fluoranthene	9.6E+02	2.0E-03	
B	Boron	3.2E+05		54

Table 3-5. (Continued).

Analyte code	Chemicals	Maximum concentration ($\mu\text{g L}^{-1}$)	Risk index	Hazard quotient
108-86-1	Bromobenzene	5.0E+00	8.0E-03	
74-97-5	Bromochloromethane	5.0E+00	9.0E-06	
75-27-4	Bromodichloromethane	1.2E+01	2.2E-05	
104-51-8	Butylbenzene[n-]	5.0E+00	8.0E-06	
135-98-8	Butylbenzene[sec-]	5.0E+00	8.0E-06	
98-06-6	Butylbenzene[tert-]	5.0E+00	8.0E-06	
56-23-5	Carbon tetrachloride	5.0E+00	1.9E-05	
Cr	Chromium	5.1E+02		2.6
CR	Chromium, Total	3.2E+02		1.6
218-01-9	Chrysene	9.6E+02	2.0E-04	
Cu	Copper	6.1E+02		1.8
53-70-3	Dibenz(a,h)anthracene	9.6E+02	2.0E-01	
132-64-9	Dibenzofuran	9.6E+02		3.7
96-12-8	Dibromo-3-Chloropropane[1,2-]	1.0E+01		2.7
107-06-2	Dichloroethane[1,2-]	5.0E+00	1.3E-05	
60-57-1	Dieldrin	1.4E-01	6.4E-05	
122-66-7	Diphenylhydrazine[1,2-]	2.0E+01	4.4E-04	
76-44-8	Heptachlor	6.8E-02	8.8E-06	
1024-57-3	Heptachlor Epoxide	6.8E-02	1.8E-05	
118-74-1	Hexachlorobenzene	9.6E+02	4.4E-02	
87-68-3	Hexachlorobutadiene	9.6E+02	2.1E-03	
77-47-4	Hexachlorocyclopentadiene	9.6E+02		2.1
67-72-1	Hexachloroethane	9.6E+02	3.8E-04	
193-39-5	Indeno(1,2,3-cd)pyrene	9.6E+02	2.0E-02	
78-59-1	Isophorone	9.6E+02	2.6E-05	
Pb	Lead	1.2E+03		7.9
Mn	Manganese	1.0E+05		34
99-09-2	Nitroaniline[3-]	4.8E+03	7.7E-04	
98-95-3	Nitrobenzene	9.6E+02		30
NO2-N/NO3-N	Nitrogen, Nitrate + Nitrite (As N)	1.8E+04		2.8
62-75-9	N-Nitrosodimethylamine	9.6E+02	1.3E+00	
86-30-6	N-Nitrosodiphenylamine	9.6E+02	1.3E-04	
621-64-7	N-nitrosodipropylamine	9.6E+02	1.9E-01	
3268-87-9	OCDD	1.5E-03	6.9E-06	
39001-02-0	OCDF	1.3E-03	5.6E-06	
36088-22-9	Pentachlorodibenzodioxins	2.3E-06	5.4E-06	
87-86-5	Pentachlorophenol	4.8E+03	1.4E-02	
103-65-1	Propylbenzene[1-]	5.0E+00	8.0E-06	
110-86-1	Pyridine	9.6E+02		15
41903-57-5	Tetrachlorodibenzodioxins	1.9E-06	8.4E-06	

Table 3-5. (Continued).

Analyte code	Chemicals	Maximum concentration ($\mu\text{g L}^{-1}$)	Risk index	Hazard quotient
Tl	Thallium	4.8E+01		9.2
8001-35-2	Toxaphene (Technical Grade)	6.8E+00	2.2E-04	
U	Uranium	1.5E+02		3.8
V	Vanadium	6.5E+02		1.1
75-01-4	Vinyl chloride	1.0E+01	4.2E-04	

^a For the Stage 1 screening,, we calculated the lifetime screening risk for chemicals for which a risk coefficient has been reported, using the maximum concentration of each radionuclide and the EPA slope factor (ORNL 2001). Those chemicals selected in the Stage 1 screening are those with a calculated screening risk value greater than our screening criteria of 1×10^{-5} . For chemicals that did not have an established slope factor or unit risk, the reference dose (RfD) value was used to calculate the hazard quotient, the ratio between the chemical intake based on the maximum measured concentration in water with the established RfD. Those chemicals with a calculated hazard quotient >1 were included in the list of chemicals emerging from the Stage 1 screening evaluation.

^b Chemicals are listed alphabetically.

Table 3-6a. Chemicals Identified in Stage 2 Screening Based on Risk Index^a

Analyte code	Chemical	Mean concentration ($\mu\text{g L}^{-1}$)	Risk index
92-87-5	Benzidine	1.1E+01	7.6E-02
62-75-9	N-Nitrosodimethylamine	4.6E+01	6.5E-02
40321-76-4	1,2,3,7,8-PCDD	6.0E-03	1.4E-02
57117-41-6	1,2,3,7,8-PCDF	5.5E-03	1.3E-02
108-86-1	Bromobenzene	5.0E+00	8.0E-03
71-43-2	Benzene	5.0E+00	8.0E-03
53-70-3	Dibenz(a,h)anthracene	3.7E+01	7.9E-03
50-32-8	Benzo(a)pyrene	3.7E+01	7.9E-03
621-64-7	N-nitrosodipropylamine	3.8E+01	7.5E-03
1746-01-6	2,3,7,8-TCDD	6.5E-04	2.9E-03
91-94-1	3,3'-Dichlorobenzidine	1.8E+02	2.3E-03
51207-31-9	2,3,7,8-TCDF	4.7E-03	2.1E-03
118-74-1	Hexachlorobenzene	3.8E+01	1.7E-03
39227-28-6	1,2,3,4,7,8-HxCDD	6.8E-03	1.2E-03
193-39-5	Indeno(1,2,3-cd)pyrene	3.7E+01	7.9E-04
205-99-2	Benzo(b)fluoranthene	3.7E+01	7.9E-04
56-55-3	Benzo(a)anthracene	3.7E+01	7.9E-04
87-86-5	Pentachlorophenol	1.9E+02	5.6E-04
As	Arsenic	1.0E+01	5.1E-04
103-33-3	Azobenzene	1.4E+02	4.3E-04
70648-26-9	1,2,3,4,7,8-HxCDF	6.4E-03	2.7E-04
75-01-4	Vinyl chloride	4.8E+00	2.0E-04
8001-35-2	Toxaphene (Technical Grade)	5.5E+00	1.7E-04
35822-46-9	1,2,3,4,6,7,8-HpCDD	2.3E-03	1.0E-04
67562-39-4	1,2,3,4,6,7,8-HpCDF	2.2E-03	9.6E-05
108-60-1	2,2'-oxybis[1-chloropropane]	4.3E+01	8.5E-05
207-08-9	Benzo(k)fluoranthene	3.7E+01	7.9E-05
60-57-1	Dieldrin	1.1E-01	4.9E-05
88-74-4	2-Nitroaniline	1.9E+02	3.0E-05
99-09-2	Nitroaniline[3-]	1.9E+02	3.0E-05
309-00-2	Aldrin	5.4E-02	2.6E-05
87-68-3	Hexachlorobutadiene	9.0E+00	2.0E-05
56-23-5	Carbon Tetrachloride	5.0E+00	1.9E-05
62-53-3	Aniline	1.1E+02	1.8E-05
106-46-7	1,4-Dichlorobenzene	2.3E+01	1.6E-05
67-72-1	Hexachloroethane	3.8E+01	1.5E-05
122-66-7	Diphenylhydrazine[1,2-]	6.8E-01	1.5E-05
1024-57-3	Heptachlor Epoxide	5.4E-02	1.4E-05
107-06-2	Dichloroethane[1,2-]	5.0E+00	1.3E-05
86-30-6	N-Nitrosodiphenylamine	7.6E+01	1.1E-05

^a For the Stage 2 screening, the average concentration of each chemical was used in the screening assessment with the reported unit risk (ORNL 2001).

Table 3-6b. Chemicals Emerging from Stage 2 Screening Based on Hazard Quotient^a

Analyte code	Chemical	Mean concentration	Hazard quotient ^b
		($\mu\text{g L}^{-1}$)	
Al	Aluminum	3.3E+04	1300
96-12-8	Dibromo-3-chloropropane[1,2-]		2.7
51-28-5	2,4-dinitrophenol	1.9E+02	1.4
534-52-1	4,6-Dinitro-2-Methylphenol	1.9E+02	1.4
Mn	Manganese	4.3E+03	1.4

^a For the Stage 2 screening, we used a ratio of the average concentration of each chemical to its RfD value (ORNL 2001) in the screening assessment.

^b The noncarcinogens that emerged from the Stage 2 screening were grouped by their relative hazard quotients. The chemicals with a hazard quotient >1 are included as potential contaminants of concern.

3.3.3 Screening of Contaminants Measured in Sediments

While the primary focus of this task was to evaluate surface water monitoring data, we also analyzed pre-fire and post-fire sediment data. We performed a similar screening procedure using maximum concentrations of chemicals and radionuclides measured in sediments by ER and ESH-18 during 2000. We took this step to determine if chemicals and radionuclides that were excluded from further analysis in our screening assessment for the water data might be important for human health risk if sediment were the medium of exposure, either through inadvertent ingestion or as a source of external exposure via radionuclides. For the inadvertent ingestion of chemicals or radionuclides in sediments, we assumed a person ingested 75 grams of soil per year (0.2 g d^{-1}) for an exposure period of 7 years. This soil ingestion rate was based on a review of various published soil ingestion studies. We fit a probability distribution to the data from these studies, and the resulting distribution was a lognormal distribution with a median value of 0.2 g d^{-1} (Till and Meyer 2001). Table D-1 in Appendix D presents the risk index for radionuclides in sediments, assuming sediment with the maximum activity of each radionuclide was ingested. It is important to note that the particle size distribution for these sediment samples impacts the partitioning of contaminants within the sample. However, since this level of detail is not available on a sample-specific basis, we obtained the risk index for each radionuclide by multiplying the 7-year ingestion rate and the risk coefficient for the radionuclide. Measured against our screening criteria of 1×10^{-5} , no radionuclide was present in sediment at a concentration that exceeded that screening level. Thus, no additional radionuclides were included in our final list of radionuclides of concern.

We followed a similar procedure for assessing chemicals in sediments, using the maximum measured concentrations. Table D-2 in Appendix D shows the results of that screening process. First, we compared the maximum measured concentration of the chemical for each chemical to the residential combined preliminary remediation goals (PRG) for soil (EPA 1999c), if available. The residential combined PRG for soil considers incidental ingestion, inhalation of particulates, inhalation of volatiles, and dermal contact. The PRGs are based on current EPA toxicity values using conservative exposure factors to estimate chemical concentrations in soil that are considered protective of humans, including sensitive groups, over a lifetime. If a chemical had a PRG value greater than the maximum concentration, we dropped it from further consideration.

Seventy-nine analytes had maximum average concentrations less than the PRG and were eliminated from further evaluation. For the remainder of the chemicals, we assumed ingestion of 0.2 gram per day and compared that value to the hazard quotient. If the hazard index was <1 , we dropped it from further consideration.

Measured against our screening criteria of 1×10^{-5} , no chemical was present in sediment at a concentration that exceeded that screening level. Thus, we did not include additional chemicals in our final list of radionuclides of concern.

For radionuclides, external exposure from standing on contaminated sediment might be a potential pathway of importance. For our screening assessment, we assumed a person was exposed for 7 years to each radionuclide. This assessment identified no additional radionuclides that had not already been identified as part of the water monitoring data evaluation.

3.4 Selecting Chemicals and Radionuclides for Surface Water Modeling Assessment

The surface soil characterization data that LANL provided included 198 analytes with detected concentrations of chemicals and radionuclides (Appendix E, Table E-1). Because of the extremely large number of potential chemicals and radionuclides, it was necessary to adopt procedures to help focus our transport calculations on those chemicals and radionuclides appearing to be most important in terms of potential risk.

To accomplish this, we calculated average concentrations of chemicals and radionuclides across each source area, described in the next section. We then compared the maximum average concentration for each chemical and radionuclide at any source area to the residential combined PRG for soil (EPA 1999c), if available. For these comparisons, we used the average concentrations before making any adjustments related to background, erosion matrix scores, or area differences associated with the polygons established for modeling purposes. The residential combined PRG for soil considers incidental ingestion, inhalation of particulates, inhalation of volatiles, and dermal contact. The PRGs are based on current EPA toxicity values using conservative exposure factors to estimate chemical concentrations in soil that are considered protective of humans, including sensitive groups, over a lifetime. Seventy-nine analytes had maximum average concentrations less than the PRG and were eliminated from further evaluation. Two analytes had average concentrations of 0 (^{129}I and friable asbestos). These were eliminated, which left a list of 117 analytes to consider for source term development.

Several of these 117 analytes included general water quality parameters, which were not considered for source term development. Others, such as total petroleum hydrocarbons and lubricant range organics, represented ranges of hydrocarbons for which risk values were not available, and these were also not considered for source term development.

We further refined the list of chemicals and radionuclides by selecting those chemicals and radionuclides that were identified following the above-described two-stage screening process used to evaluate the environmental monitoring data. If not already included in the list, we added any chemical or radionuclide identified as having significantly elevated concentrations in burned area ash, discussed below. Finally, we added chromium and mercury because of known public concern, and RDX and uranium because of the relatively high maximum average source area concentrations. This process resulted in a final list that includes a total of 37 chemicals and radionuclides for which we developed source term estimates (Table 3-7).

Table 3-7. Selected Chemicals and Radionuclides

Analyte code	Analyte name	Analyte code	Analyte name
309-00-2	Aldrin	Pu-238	Plutonium-238
Am-241	Americium-241	Pu-239,240	Plutonium-239
As	Arsenic	K-40	Potassium-40
Ba	Barium	Pa-234m	Protactinium-234M
56-55-3	Benzo(a)anthracene	Ra-224	Radium-224
50-32-8	Benzo(a)pyrene	Ra-226	Radium-226
205-99-2	Benzo(b)fluoranthene	Ra-228	Radium-228
207-08-9	Benzo(k)fluoranthene	121-84-4	RDX
Cs-137	Cesium-137	Sr-90	Strontium-90
Cu	Copper	Th-228	Thorium-228
Cr	Chromium	Th-230	Thorium-230
53-70-3	Dibenz(a,h)anthracene	Th-232	Thorium-232
1024-57-3	Heptachlor Epoxide	Th-234	Thorium-234
193-39-5	Indeno(1,2,3-cd)pyrene	H-3	Tritium
Pb	Lead	U	Uranium
Pb-210	Lead-210	U-234	Uranium-234
Hg	Mercury	U-235,236	Uranium-235
Np-237	Neptunium-237	U-238	Uranium-238
62-75-9	Nitrosodimethylamine[N-]		

3.5 Estimating Concentrations of Chemicals and Radionuclides in Source Areas

3.5.1 Soil and Sediment Concentrations

The modeling approach we selected used a representative concentration of chemicals and radionuclides in soil or sediment across defined source areas, in conjunction with water runoff and sediment erosion yields, to calculate downstream concentrations at points of exposure. Therefore, it was necessary to estimate a representative chemical and radionuclide concentrations across each source area. As with the PRS source terms developed for the air pathway assessment (Task 1), we calculated an average concentration to characterize each of the previously identified source areas.

Although measurements were collected for many analytes to help define and understand existing concentrations of chemicals and radionuclides at potential source areas, not all analytes had concentrations that were above detection limits. We eliminated all values reported as below the detection limit from further consideration and did not use them for calculating average concentrations across the source areas. Soil samples associated with sites that had been excavated and/or backfilled as part of a remediation project before the fire were identified in the database files with which we were provided. We eliminated these samples from consideration, as the corresponding data were not considered representative of site conditions existing at the time of the fire. These assumptions are consistent with those that were made for the air pathway assessment.

3.5.2 Potential Release Site Source Area Characterization

We obtained available soil characterization data from ER for each of the PRS source areas described above. Only those samples with a starting depth at the ground surface (i.e., depth equals zero) or with an end depth less than 2 ft were selected. We merged all PRS data into a single database table using Microsoft Access®, and modified analyte nomenclature where necessary to ensure consistency. We then wrote a totals query to calculate average concentrations for each analyte at each PRS.

Erosion matrix scores have been developed by the LANL for many PRSs and provide some measure of the susceptibility of each PRS to erosion, considering a number of factors assessed through site-specific field investigations, including the location of the PRS (e.g., on mesa top, canyon floor, or channel); site description; runoff contributors; runoff issues; topography; and ground cover. The erosion scores do not necessarily account for the effectiveness of best management practices (BMPs), except in some cases where permanent BMPs have been installed or the site has been stabilized (Veenis 2001). We considered it appropriate to include these scores in our calculations in cases where the impact of BMPs have been considered because the scores represented the only mechanism by which we could account for expected differences in erosion potential across different sites as a result of site-specific stabilization efforts. These site stabilization efforts, or BMPs, include such things as asphalt/concrete paving, check dams, asphalt run-on diversions, and sediment traps. Therefore, included only those erosion matrix scores where the erosion assessment was completed *after* the BMP installation. For all PRSs meeting the above described criterion, we used the erosion matrix scores (on a scale of 0–100; therefore, a score of 50 equals an adjustment factor of 0.5) as adjustment factors to modify the calculated average PRS soil concentrations to account for detailed factors influencing susceptibility to erosion that our modeling did not otherwise address. The erosion matrix score adjustment factors used for the PRS source areas are provided in Appendix F.

This method should be considered conservative in that it does not account for the many instances where BMPs have been installed at some time after the most current erosion assessment, which would be expected to provide at least some amount of erosion mitigation. To quantitatively assess the impact of using the erosion matrix scores to account for a decreased erosion potential at some sites, we also calculated point of exposure (POE) concentration estimates excluding all erosion matrix scores to show the resulting increase in POE concentrations (Appendix M).

3.5.3 Geomorphic Unit Source Area Characterization

Available sediment characterization data were obtained from ER for DP and Pueblo Canyons and upper and lower sections of Los Alamos Canyon. These canyons, composing the majority of the greater Los Alamos watershed, have been characterized most completely, a process described in detail by Reneau et al. (1998a, 1998b, and 1998c). We obtained the same set of data documented in these reports (hereafter referred to as the Reach Reports) and used it for our evaluation. Information to characterize concentrations of chemicals and radionuclides in other canyons, such as Water and Mortandad, was not available.

As described in the Reach Reports, characterization data were grouped, or binned, to calculate average concentrations of chemicals and radionuclides across defined areas for the

purpose of estimating inventory amounts in specific canyon reaches. This binning process is explained in the Reach Reports, and it is noted that "...data in each sub-reach were first examined after being binned by individual geomorphic units and sediment facies, and where appropriate these subsets of data were combined into larger bins to increase sample size and allow better statistical evaluation. In some cases additional subdivisions within a geomorphic unit were defined, particularly where concentrations of chemicals and radionuclides were highest."

Because of time and resource constraints, we were not able to duplicate this process of binning. However, because of the potentially important distinctions in both physical and radiological characteristics noted in the Reach Reports, particularly for different sediment facies, it was important to understand how different data binning procedures could affect the legitimacy of our calculations. Therefore, we examined the impact that different binning procedures would have on both ^{137}Cs and $^{239,240}\text{Pu}$ inventory calculations by binning on a geomorphic unit and sediment facies basis and by binning on simply a geomorphic unit basis. We used totals queries to calculate average concentrations according to both binning processes. We then calculated average thickness and density according to the values associated with each geomorphic unit and/or sediment facies type. To estimate inventories for each bin, we used this information in combination with the average concentrations and reported areas for each geomorphic unit. We then summed the binned inventories on a canyon basis for comparison to the inventories reported in the Reach Reports (Table 3-8).

Table 3-8. Comparison of Estimated Inventory Based on Different Binning Methods

Analyte	Canyon	Inventory (mCi) by binning method		
		1 ^a	2 ^b	3 ^c
Cs-137	Upper Los Alamos	62.5	60.7	53.5
Cs-137	Lower Los Alamos	15.4	21.8	20.7
Cs-137	Pueblo	9.4	10.3	nr ^d
Pu-239,240	Upper Los Alamos	21.5	21.7	22.0
Pu-239,240	Lower Los Alamos	31.5	41.9	27.6
Pu-239,240	Pueblo	317.6	311.0	408.1

^a Binned according to both geomorphic unit and sediment facies.
^b Binned according to geomorphic unit only.
^c Inventory reported in Reach Reports.
^d nr = not reported.

Comparing the calculated inventories shown in Table 3-8 suggests that the method of binning impacts the estimated inventory to some degree, but the values calculated using all three methods are generally consistent. This provided confidence that binning by geomorphic unit alone provided average concentration estimates that give reasonable approximations of the inventories reported in the Reach Reports. We selected geomorphic unit only method of binning (number 2 in Table 3-8) because it was the most readily achieved method considering the data organization and it was most compatible with the defined surface areas, which are reported on a geomorphic unit basis. As with the PRSs, we compiled all Geomorphic Unit source area characterization data in a database and wrote a totals query to calculate average concentrations for each analyte on a geomorphic unit basis.

3.5.4 Unsampled Reach Source Area Characterization

We compiled inventory estimates reported in the Reach Reports for both ^{137}Cs and $^{239,240}\text{Pu}$ along with the area estimates described above. We calculated average density and thickness values on a canyon basis (i.e., upper Los Alamos, lower Los Alamos, and Pueblo), based on the values associated with the sampled reaches in each canyon. We then used this information to estimate an average concentration across each Unsampled Reach source area.

3.5.5 Burned Area Source Area Characterization

We obtained available ash characterization data from three sources: sampling conducted by ER in 2000 and 2001 and samples collect by NMED in 2000. We used only concentrations reported as detects and calculated average concentrations for each analyte in each group of data. We compared the highest average concentration from all three groups of data for each analyte to background soil concentrations using information from LANL's ESH-20 Division and ER (Ryti et al. 1998). All analytes with an average concentration greater than 5 times the background concentration were retained for consideration in the surface water modeling assessment (Table 3-9). We selected this cutoff point as a reasonable indication that the Cerro Grande Fire resulted in significantly elevated concentrations. We then calculated weighted average concentrations, based on the number of samples used to calculate the average concentration for each source of data, using all three sources of data.

Table 3-9. Analytes with Average Concentrations in Ash at Least a Factor of Five Higher than Average Background Concentrations

Analyte	Units	ER ^a	ER ^b	NMED ^c	Weighted average	Background average ^d
Am-241	pCi g ⁻¹	0.14 ^e		0.07	0.08	0.01
Ba	mg kg ⁻¹	790	286	437	430	136
Cs-137	pCi g ⁻¹	4.6	10	3.9	5.6	0.33
Cu	mg kg ⁻¹	30	18	23	22	5.1
Pb	mg kg ⁻¹	58	40	68	57	11
Pu-238	pCi g ⁻¹	0.03		0.02	0.02	0.0032
Pu-239	pCi g ⁻¹	0.41	0.39	0.75	0.61	0.013
Sr-90	pCi g ⁻¹	2.4	2.0	1.4	1.7	0.28
U-235	pCi g ⁻¹	0.14	0.21	0.27	0.24	0.05

^a Samples collected by ER in 2000.

^b Samples collected by ER in 2001.

^c Samples collected by NMED in 2000.

^d Background concentrations based on data provided by ESH-20 and Ryti et al. (1998).

^e Highlighted cells show highest average concentration, which was at least 5 times greater than average background concentration.

3.5.6 Adjusting Concentrations for Polygons Established for Modeling

As discussed earlier, we developed GIS polygon shapefiles for the PRS source areas and the geomorphic unit sources areas. The area for each of these source areas was represented as a circle, using a calculated radius based on the surface area for each source area. In a number of

cases, this resulted in groups of source areas partially or completely overlapping. These groups of overlapping source areas were dissolved into a single polygon represented by the perimeter of the overlapping polygons. We calculated revised areas for each source area polygon and linked the original PRS or geomorphic unit identification to the new polygon in a spreadsheet table.

Because the surface area of the new polygon was less than the sum of the surface areas for the source areas dissolved into the new polygon and the total mass of chemicals and radionuclides is a function of the original source area surface area, we calculated an adjusted concentration for each chemical and radionuclide for the new polygon. This was necessary to ensure that the surface area of soil estimated from the polygons considered in the fate and transport estimates was not greater than the actual surface area.

To develop the adjusted concentrations of chemicals and radionuclides, we calculated an adjustment factor. This factor was based on the original area of each overlapping source area relative to the sum of the original surface area of the group of overlapping source areas. We used this ratio as an adjustment factor to modify the average concentrations associated with each original source area, which were then summed to derive a representative concentration for each chemical and radionuclide across the new combined source areas. The adjustment factors used for both the PRS and Geomorphic Unit source areas are provided in Appendix F.

3.5.7 Estimating Chemical and Radionuclide Levels Related to Either LANL Operations or the Cerro Grande Fire

Because the primary goal of this project was to predict risk from the Cerro Grande Fire resulting from LANL's contribution, it was important to determine background concentrations of chemicals and radionuclides in soil. Using information from LANL's ESH-20 Division and ER (Ryti et al. 1998), we determined average background concentrations of chemicals and radionuclides for both soils and sediments (Table 3-10). We subtracted these average background concentrations from the average concentrations of chemicals and radionuclides determined at each source area to calculate a net concentration of chemicals and radionuclides that could be attributed to either LANL operations (for the PRS, Geomorphic Unit, and Unsourced Reach source areas) or impacts of the fire (for the Burned Area source areas). We used background sediment concentrations for the Geomorphic Unit and Unsourced Reach source areas and background soil concentrations for the PRS and Burned Area source areas. These net concentrations provided the basis for defining average concentrations of chemicals and radionuclides at each source area for subsequent modeling of downstream concentrations of chemicals and radionuclides at selected points of exposure.

The assumed concentrations for each source area established for surface water modeling purposes are provided in Appendix G. An example calculation showing the methodology used for estimating the $^{239,240}\text{Pu}$ concentration at PRS-10, based on the characterization data for the original PRSs contributing to the PRS-10 source area, is provided in Appendix V-1.

Table 3-10. Assumed Soil and Sediment Background Concentrations for Chemicals and Radionuclides Included in the Surface Water Pathway Source Term

Source term analytes					
Chemicals	Units	Sediment	Source ^a	Soil	Source
Aldrin		NA ^b		NA	
Arsenic	mg kg ⁻¹	1.84	a	3.13	b
Barium	mg kg ⁻¹	60.4	a	136	b
Benzo(a)anthracene		NA		NA	
Benzo(a)pyrene		NA		NA	
Benzo(b)fluoranthene		NA		NA	
Benzo(k)fluoranthene		NA		NA	
Chromium (total)	mg kg ⁻¹	5.62	a	9.52	b
Copper	mg kg ⁻¹	4.57	a	5.08	b
Dibenz(a,h)anthracene		NA		NA	
Heptachlor Epoxide		NA		NA	
Indeno(1,2,3-cd)pyrene		NA		NA	
Lead	mg kg ⁻¹	9.25	a	10.9	b
Mercury	mg kg ⁻¹	0.012	a	0.032	b
N-Nitrosodimethylamine		NA		NA	
RDX		NA		NA	
Uranium	mg kg ⁻¹	0.685	a	0.985	a
Radionuclides					
Am-241	pCi g ⁻¹	0.026	a	0.0067	b
Cs-137	pCi g ⁻¹	0.211	a	0.326	b
Pb-210		NA		NA	
Np-237		NA		NA	
Pu-238	pCi g ⁻¹	0.0021	a	0.0032	b
Pu-239	pCi g ⁻¹	0.025	a	0.013	b
K-40	pCi g ⁻¹	29.8	a	29.8	a,c
Pa-234M		NA		NA	
Ra-224		NA		NA	
Ra-226		NA		NA	
Ra-228		NA		NA	
Sr-90	pCi g ⁻¹	0.229	a	0.275	b
Th-228	pCi g ⁻¹	1.44	a	1.44	a,c
Th-230	pCi g ⁻¹	1.37	a	1.37	a,c
Th-232	pCi g ⁻¹	1.43	a	1.43	a,c
Th-234		NA		NA	
Tritium	pCi g ⁻¹	0.024	a	0.133	b
U-234	pCi g ⁻¹	1.40	a	0.941	b
U-235	pCi g ⁻¹	0.087	a	0.0518	b
U-238	pCi g ⁻¹	1.22	a	0.852	b

^a Source: a = mean value reported by Ryti et al. (1998); b = average of the value reported by Ryti et al. (1998) and data provided by ESH-20; c = the sediment value was assumed for soil.

^b NA = no value available.

3.5.8 Limitations and Uncertainties Associated with Estimated Source Area Concentrations

Generally, a study involved with estimating potential releases and consequent exposures to individuals commits a large fraction of the resources available to understanding limitations and uncertainties of data sources and calculating the quantity of material available for release because the remainder of the study relies on the credibility of these values. The short time frame and limited resources available for this project required us to make several assumptions about the data.

Because this project involved predictive calculations of potential contaminant movement, it was necessary to use characterization data to calculate the quantity, or source term, of material available for potential release. The following sections discuss issues that relate to uncertainties and limitations associated with the different source areas we attempted to characterize for this project. An inherent uncertainty associated with each of the source areas is our inability, based on available data, to understand how radionuclide and chemical distribution at sites in the LANL environment may change over time and how this could impact our calculations. Much of the data used to characterize the source areas was collected from 1993 to 1997. Some changes in distribution and extent of contamination would be expected since that time, and it is not possible to quantify the degree to which this could impact our ability to characterize pre-fire conditions.

Additionally, we used generic background data on chemicals and radionuclides in LANL-area soils to determine net concentrations, and they do not reflect the spatial heterogeneity that would be expected at different PRSs. In other words, we assumed a single background value for each radionuclide or chemical and used that value to represent conditions at all source areas. It is not possible to quantify how this might contribute to the uncertainty, although it certainly would have some impact. However, the impact of background variability is likely less significant than the uncertainties associated with estimating the true areal extent of chemicals and radionuclides and with a value that appropriately characterizes the magnitude or level of chemicals and radionuclides across that areal extent. Both the areal extent and magnitude would be expected to vary by chemical or radionuclide. These sources of uncertainty are discussed in the following sections.

3.5.8.1 PRS Source Areas. Two primary issues contribute to uncertainties in the characterization information available for PRS source areas: the accuracy and representativeness of both the available sampling data and the estimated areal extent appropriately characterized by those data.

Uncertainties associated with the characterization data—ER collected the PRS characterization data for purposes of environmental restoration and remediation. These data were not collected with the intent of conducting risk analyses or developing an inventory, and the purposes for and manner in which the ER collected their data may not be consistent for different PRSs. Therefore, it was difficult to quantify the uncertainty and accuracy associated with the data. We used these data, compiled by LANL for us, to estimate potential source area inventories. These data represent point concentration information for surface soil samples collected from specific PRSs within the groups of PRSs described previously. ER is in the process of consolidating a number of these PRSs into a smaller number of combined units, but this process

is ongoing and it is unclear at this point how this reorganization would impact the process of site characterization. Because existing characterization data appear to be most appropriately organized on a PRS basis, we used and organized the data on the PRS basis as defined for us by ESH-17 and ER.

Although measurements were collected for many analytes to help define and understand existing concentrations of chemicals and radionuclides at potential source areas, not all analytes had concentrations that were above detection limits. As part of our conservative approach, we eliminated all values reported as below the detection limit from further consideration and did not use them for calculating average concentrations across the source areas. Soil samples associated with sites that had been excavated and/or backfilled as part of a remediation project before the fire were identified in the database files with which we were provided. We eliminated these samples from consideration, as the corresponding data were not considered representative of site conditions existing at the time of the fire.

Uncertainties are associated with the accuracy, completeness, and representativeness of the actual characterization data. LANL staff shifted from the concept of organizing the characterization data on a PRS basis to estimate potential atmospheric releases for a number of reasons. These reasons included uncertainties associated with the accuracy of PRS boundary data and the relationship of PRS boundaries to sample locations, concentration data outside established PRS boundaries, a lack of consistency in compiling the PRS field within the database, viable characterization data not included in the database, a lack of sufficient representative data for a given PRS, and uncertainties associated with the validity of certain analytical data (e.g., because there are no results for ^{241}Pu , the accuracy of the results for ^{241}Am and possibly ^{237}Np can be called into question).

Because of time and resource constraints, we had to rely on the characterization data that were provided to us and were not able to investigate in detail the rationale behind the collection of those data. However, we assumed that investigations into the nature and extent of contamination at each site were controlled to some extent by information about known or suspected radionuclides and chemicals likely to be present at that site. Such an approach would allow site characterizations and sample analyses to be guided by knowledge about historical operations, thereby limiting the compiled data to those contaminants suspected to be present at each site. Based on our limited review of the data in this regard, it appears that this issue could be complicated by the fact that full suite analyses for Resource Conservation and Recovery Act metals, for example, may have been requested regardless of the specific metals that were suspected at the site because the cost to do analyses for the entire suite of metals was the same as for an analyses for only one or two specific metals. A similar situation may exist for semi-volatile and volatile organic chemical analyses. An entire suite analyses may have been performed if any such chemical was suspected at a given site. For radionuclide analyses, different analytical techniques are considered more accurate than others (e.g., alpha spectroscopy is considered to provide a better indication of the true concentration of radionuclides such as ^{241}Am or ^{235}U than gamma spectrometry). It is not clear how population of the PRS databases accounted for these issues or how these issues may complicate the process of quantifying and identifying contamination at any given site.

The question of the legitimacy of the field that links the characterization data to a given PRS provides another example of how some of these uncertainties may have impacted our calculations. For PRSs characterized by multiple samples, we used the mean concentration to

calculate an inventory for the entire area. For areas with a single sample, we used that sample concentration to represent the concentration across the entire area. In some instances, individual samples were associated with more than one PRS; in these cases, results for a single sample were used to characterize more than one PRS. Although this may increase the uncertainty of the calculations, in the absence of any other information, it was the best available method. It is not possible to quantify this uncertainty, but there are some instances where additional sampling data would enable a more credible characterization of a given site.

We understand the limitations and uncertainties associated with the PRS data, and it is important to discuss these issues. Because of these uncertainties and limitations, we made conservative assumptions to avoid underestimating the quantity of contaminant available for potential release at each PRS (e.g., eliminating nondetect values likely biases the calculated inventory on the high side). Certainly, assuming a single value to be representative of potentially highly heterogeneous environmental conditions is problematic, but by eliminating nondetect values from our analyses, we believe our calculations were more likely to reflect the highest, or bounding, concentrations that could be expected at any given site. Once key contaminants and/or source areas are identified, it may be possible to further examine the impact of source area concentration heterogeneity. An appropriate place for LANL to focus additional efforts could be to better understand the variability and refine the assumed existence of contamination at certain sites.

Uncertainties associated with the extent and distribution of chemicals and radionuclides—Uncertainties are also related to the areal extent and distribution of chemicals and radionuclides. The areal extent of chemicals and radionuclides in surface soil within the PRSs was initially based on the areas defined by polygons as part of the GIS coverage files provided by LANL. However, we recognized that in some cases these polygon shapes, sizes, and locations did not correspond to either the locations of actual sampling data or to the extent of concentrations of chemicals and radionuclides in the soil. In those instances, ER personnel at LANL redefined the surface area extent of PRSs to more accurately reflect the available sampling data; however, different personnel did this on a subjective basis. Because information was not available to allow us to do otherwise, we have assumed the same surface area extent of contamination for each chemical or radionuclide detected at a given PRS; however, the true distribution in the environment would be expected to vary by contaminant.

It is not possible to quantify the uncertainty that may be involved with the different methods used to estimate these area values. However, we were provided with two different area estimates in two separate transmissions because two PRSs fell into both the IR-boundary and floodplain groupings (18-002a and 18-002b). The original areas based on the GIS coverage files were 0.15 and 0.36 m² for these two PRSs, respectively. The redefined areas for these two PRSs, based on the information provided for the *IR-boundary* group of PRSs, were 1733 and 1137 m², respectively. The redefined areas for these two PRSs, based on the information for the *floodplain* group of PRSs, were 33,098 and 39,807 m², respectively. Based on this information, the assumed PRS areas are dependent on the methods used for defining the areas, and in this case three different methodologies resulted in three significantly different areas.

In some cases, the surface extent of the chemicals and radionuclides could not be redefined if there were insufficient sampling data; therefore, we retained the original GIS polygon areas based on the initial coverage files provided by LANL. For sites where sufficient sample location did not exist to enable logical area estimation, it is also impossible to fully understand the impact

of retaining the original GIS-based area estimates. An examination of the ratios of the original GIS-based area to the redefined area (for all cases where areas were redefined) showed that in a number of cases, the redefined areas were substantially different, in some cases in excess of 5 orders of magnitude, than the GIS-based areas (Table 3-11). In most cases, the redefined areas were larger than the original GIS-based areas, but there were also a number of instances where the redefined areas were smaller than the original GIS-based areas. As noted, it was not possible to quantify the uncertainty associated with the process of providing updated area estimates, but an appropriate place for LANL to focus additional efforts could be to better understand and estimate the areal extent of key contaminants at certain sites.

**Table 3-11. Descriptive Statistics for the Ratio of
GIS-Based PRS Areas to PRS Areas that were
Redefined Based on Existing Sample Locations**

Parameter	Statistic
Maximum	7337
Minimum	1.34E-06
Median	0.29
Count	276
Number of ratios <0.1	108
Number of ratios >10	40

It is important for us to state that we share the discomfort noted by LANL staff in relying on PRS characterization data and boundaries about which considerable uncertainty appears to exist. Unfortunately, it is not possible to quantify these uncertainties. Nonetheless, the work plan and scope of this project required estimating potential release quantities, and an estimate of surface area extent in combination with the sampling data associated with each PRS represented the only available option for characterizing the PRS source areas.

3.5.8.2 Geomorphic Unit Source Areas. Characterization of the Geomorphic Unit source areas was impacted by some of the same uncertainties and limitations as the PRS source areas with regard to assuming a single representative concentration over a defined source area. However, the Geomorphic Unit characterization data were collected and the surface areas defined with the intent of developing inventory estimates for certain reaches within both the Los Alamos and Pueblo Canyons. Therefore, it could be expected that the uncertainties associated with the data used to characterize this group of source areas would generally be less than for the PRS source areas. However, no sampling data were available to characterize any of the canyons outside the greater Los Alamos watershed (e.g., Water and Mortandad Canyons).

3.5.8.3 Unsourced Reach Source Areas. Characterization of the Unsourced Reach source areas was impacted by a number of uncertainties and limitations. First, these stretches of canyon have been characterized by inventory estimates only that are not based on actual sampling data, as noted previously. Second, inventory estimates in unsourced reaches have been made for ^{137}Cs and $^{239,240}\text{Pu}$ in Los Alamos and Pueblo Canyons only. Finally, surface area estimates for these stretches of canyon were not available and we had to approximate them. It was not possible,

based on available data, to quantify the uncertainties associated with these issues and how they may have impacted our calculations.

3.5.8.4 Burned Area Source Areas. Characterization of the burned area source area was based on a relatively small number of samples collected from specific areas within the area that was burned. The coverage of these samples was insufficient to fully understand the spatial heterogeneity that would be expected to occur within the areas that were burned. Therefore, we approximated levels of certain chemicals and radionuclides that appear to have been concentrated to the greatest extent in ash deposited as a result of the fire and assumed these concentrations to be representative of and constant across the entire burned area. It was not possible, based on available data, to quantify the uncertainties associated with this assumption.

4 ESTIMATING CONCENTRATIONS OF CHEMICALS AND RADIONUCLIDES AT POINTS OF EXPOSURE

We developed concentration estimates for the selected chemicals and radionuclides (Section 3.4) for seven locations. These seven locations are identified as potential points of exposure within the surface water domain where an individual is likely to come in contact with environmental media (i.e., storm water, surface water, suspended sediments, or deposited sediments) containing concentrations of chemicals or radionuclides. We developed the concentration estimates for chemicals and radionuclides in storm water and surface water, in the dissolved phase of storm water and surface water, in suspended sediments, and in deposited sediments. We took a number of steps to develop the concentration estimates.

- We developed conservative estimates of the surface water flow within the watersheds and at outlets to the Rio Grande for 2-, 5-, 10-, 25-, 50-, 100-, and 500-year design storm events of 6-hour duration.
- We developed pre-fire and post-fire estimates of suspended sediment concentrations based on an analysis of pre-fire and post-fire empirical total suspended solids (TSS) data.
- We identified seven locations as points of exposure to address the exposure scenarios identified by the site conceptual model.
- We identified the watershed contributing storm water flow to each point of exposure and the source areas (i.e., PRS, geomorphic units, unsampled reaches, and burn area) that could potentially contribute chemical mass or radionuclide activity to each point of exposure.
- We estimated the maximum potential chemical mass and radionuclide activity that could result from storm water flow across a source area and estimated a total chemical mass and radionuclide activity that could be present at each point of exposure.
- We identified background storm water flow and suspended sediment concentration in the Rio Grande and surface water volume and suspended sediment in the Cochiti Lake to address points of exposure that were influenced by the Rio Grande or the Cochiti Lake.
- We distributed the chemical mass and radionuclide activity in environmental media to estimate the concentration of chemicals and radionuclides at each point of exposure.

Considering the complexities of developing hydrologic and transport models; the limited time available to complete the overall risk analysis project; and the variability in the empirical data concerning surface water flow, suspended sediment concentration (i.e., concentration of suspended sediments in surface water), and concentrations of chemical and radionuclides (e.g., chemical and radionuclide concentrations at points of exposure), this evaluation is not a comprehensive modeling effort. This evaluation is also limited by the availability of data to develop storm water flow, suspended sediment concentration estimates, source area chemical and radionuclide concentrations, and empirical data for comparison to these estimates. Because of time and other constraints, we used readily available and easily obtainable data from divisions within LANL and from publicly available sources such as the USGS. Information concerning the collection and compilation of the data is discussed in Chapters 1 and 2.

The approach employed does not yield a definitive calculation of the concentrations of chemicals and radionuclides in storm water, surface water, suspended sediments, and deposited sediments at the points of exposure. Rather, the calculations represent a methodology for

determining the relative relationship between pre-fire and post-fire concentrations of chemicals and radionuclides in a conservative way.

4.1 Storm Water Flow Estimates

We calculated storm water flow in several steps using the spatial and raster capabilities of ArcView 3.1 Geographic Information System (GIS) (ESRI 1998a) and existing spatial data collected from a number of sources (Chapter 3). First, we developed a hydrologic model to describe the watersheds associated with the LANL facility and within the surface water domain. Second, we established precipitation grids to describe rainfall for each of six design storm events. Third, to the extent data were available, we identified maximum storm water flow grids for pre-fire and post-fire conditions for each design storm. Finally, we ran hydrologic flow models using the U.S. Army Corps of Engineer's Hydrologic Modeling System (HEC-HMS) for two selected watersheds for comparison to the storm water flow grids (HEC 2001). These calculations were based on a number of assumptions and conditions:

1. The estimates of the storm water flow are limited by the data available.
2. A conservative approach to estimate storm water flow would tend to overestimate the actual flow within the watersheds.
3. The use of precipitation data based on various design storms would provide a range of precipitation estimates including a reasonable high-end estimate.
4. Given the size of the surface water domain and conservative nature of the calculation, the use of a 98-ft (30-m) grid cell size for the spatial data represents a manageable size at 1,317,500 cells and approximately 5 megabytes for each grid file and reasonable resolution.

4.1.1 Hydrologic Model

The hydrologic model was developed in ArcView 3.1 GIS using the Geo-HMS and ArcView spatial analyst extensions (HEC 2000c; ESRI 1998b). The spatial analyst extension provides the ability to work with raster-based grids. The Geo-HMS extension provides the capability to perform terrain preprocessing, basin processing, and HMS modeling support within a spatial environment using raster grids.

Figure 4-1 shows the basis for the development of the hydrologic model is the digital elevation model (DEM). The DEM provides data on the surface elevation and is generally available in varying resolutions. For the hydrologic model for the LANL facility, we selected 7.5-minute DEMs available from the USGS. These DEMs have 98×98 -ft (30×30 -m) grid spacing with a 3.3-ft (1-m) vertical resolution and are based on the Universal Transverse Mercator (UTM) geo-referencing system (USGS 1998). We merged 16-7.5-minute DEMs to create a composite DEM that was representative of the surface water and air model domains.

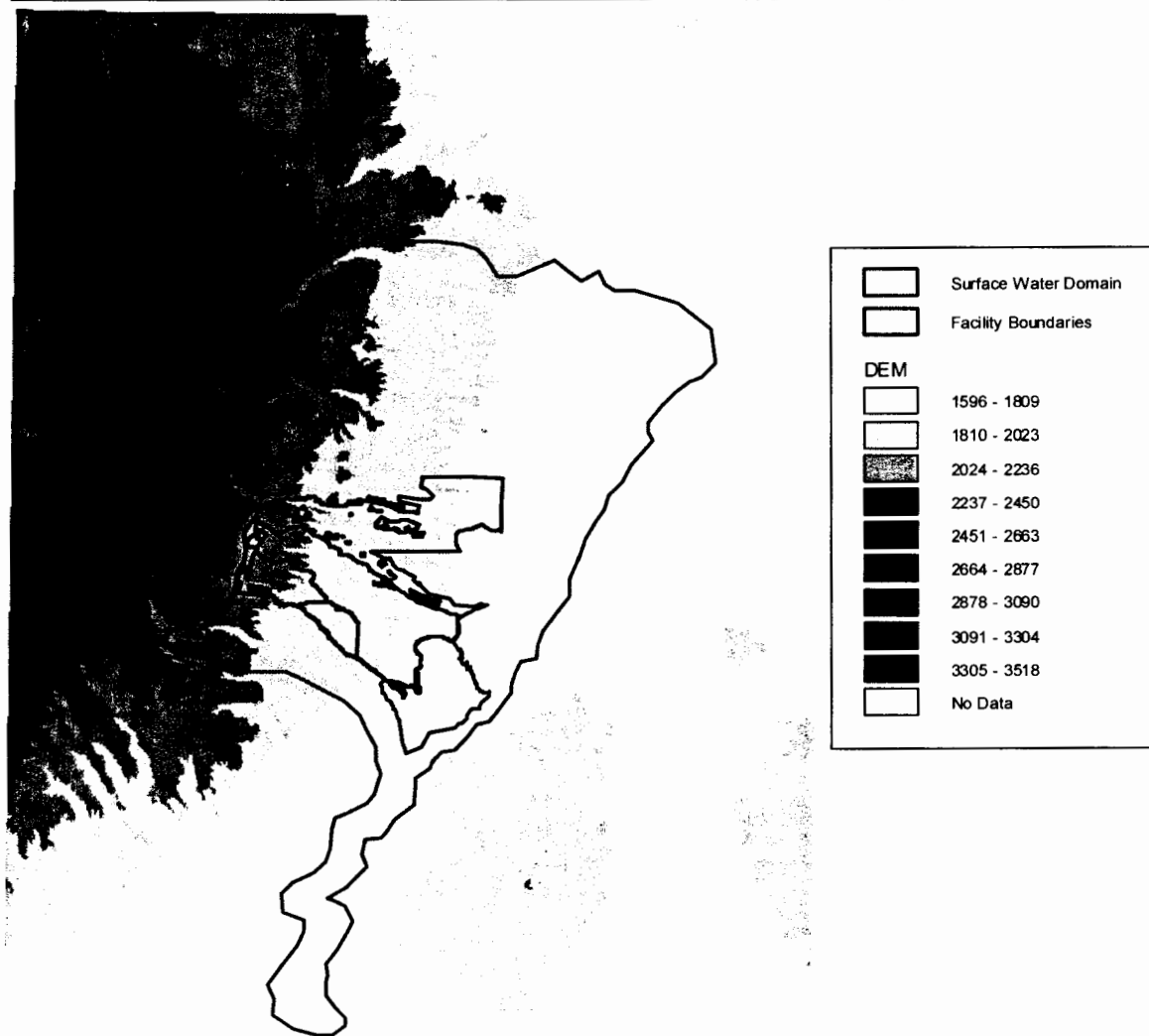


Figure 4-1. Composite digital elevation model.

The 33-yd (30-m) DEM provides a sufficient resolution, given the conservative nature of the storm water flow evaluation and the screening level approach for the risk evaluation for which the storm water flows are being derived. Further, the high relief, mountainous terrain within the study area provides adequate slope to support the use of 3.3-ft (1-m) vertical resolution (Maidment and Djokic 2000). In addition, a comparison of river segments generated using the composite DEM to the hydrology data contained on the Interagency Burned Area Emergency Rehabilitation (BAER) CD (LANL 2000) (i.e., cerro_hy.shp) and U.S. Census Bureau TIGER Hydrography line files (RGIS 2001) for the area, indicates that the river segments determined through Geo-HMS are consistent with those represented in these other data sources. Also, the 33-yd (30-m) resolution for the DEM was consistent with the resolution of the other available GIS data used in this evaluation. A higher resolution DEM may be needed if a more detailed analysis of surface water flow and potential risk is conducted subsequent to this analysis.

With the composite DEM as the basic element, we developed a hydrologic model using the ArcView Geo-HMS extension. The Geo-HMS extension provides a number of tools to extract topographic, topologic, and hydrologic information from digital spatial data such as the DEM.

This extension also provides several tools to develop input files for many parameters required by the HEC-HMS. Using this extension, we filled potential sinks in the DEM and created flow direction and flow accumulation grids. Once we determined the flow direction and flow accumulation, we identified a stream network based on a 3-mi² (8-km²) threshold for flow accumulation to define the initiation of a stream. We delineated watersheds for each stream segment and created ArcView shape files of the watersheds and the stream segments.

Others had previously conducted watershed delineation, and the GIS files for these delineations were provided on the BAER CD (LANL 2000). The watersheds delineated as a result of this evaluation using the Geo-HMS compared favorably to the watershed delineation provided on the BAER CD (i.e., bigsheds_sdl.shp and smallsheds.shp). As discussed earlier, the stream segment determination as a result of this evaluation using the Geo-HMS compared favorably to the hydrology data contained on the BAER CD (i.e., cerro_hy.shp) and U.S. Census Bureau TIGER Hydrography line files. Figure 4-2 shows the delineated watershed and the stream segments for the study area. Los Alamos, Guaje, Rendija, and Pueblo Canyons are incorporated into the Los Alamos watershed.

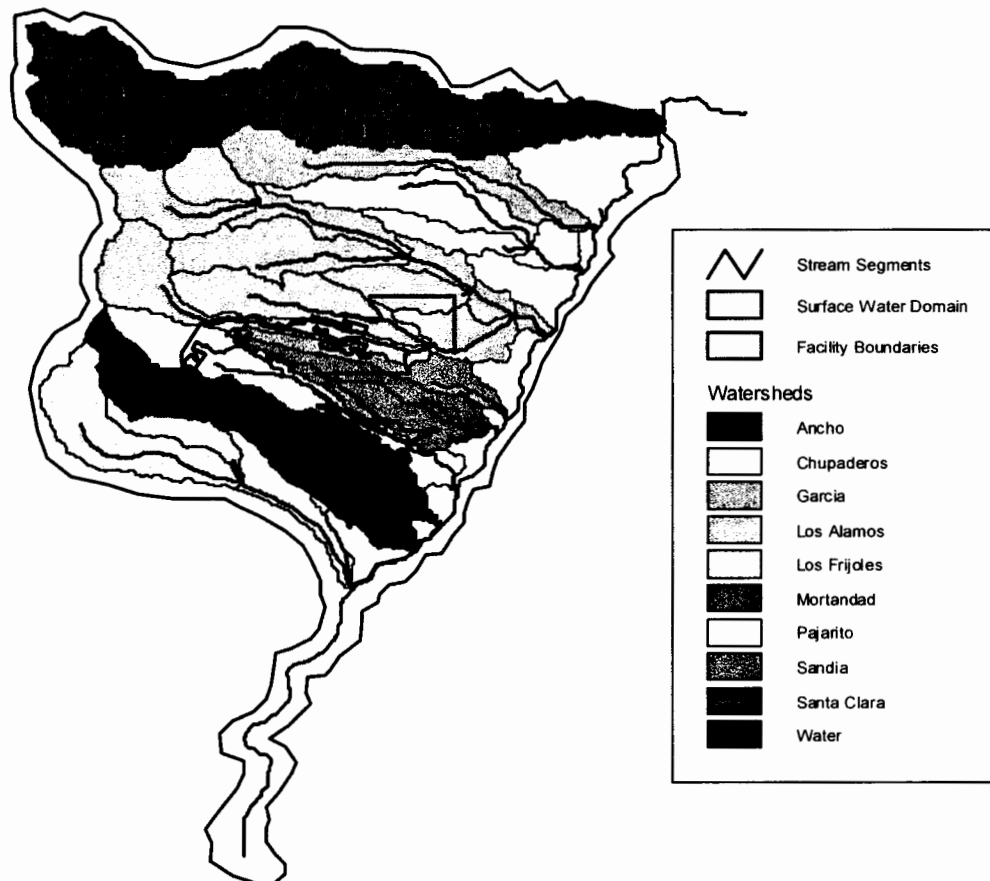


Figure 4-2. Delineated watersheds. The watersheds are identified by the presence of an outlet point to the Rio Grande.

Figure 4-3 includes the outlets for each of the watersheds that were used for the flow comparisons.

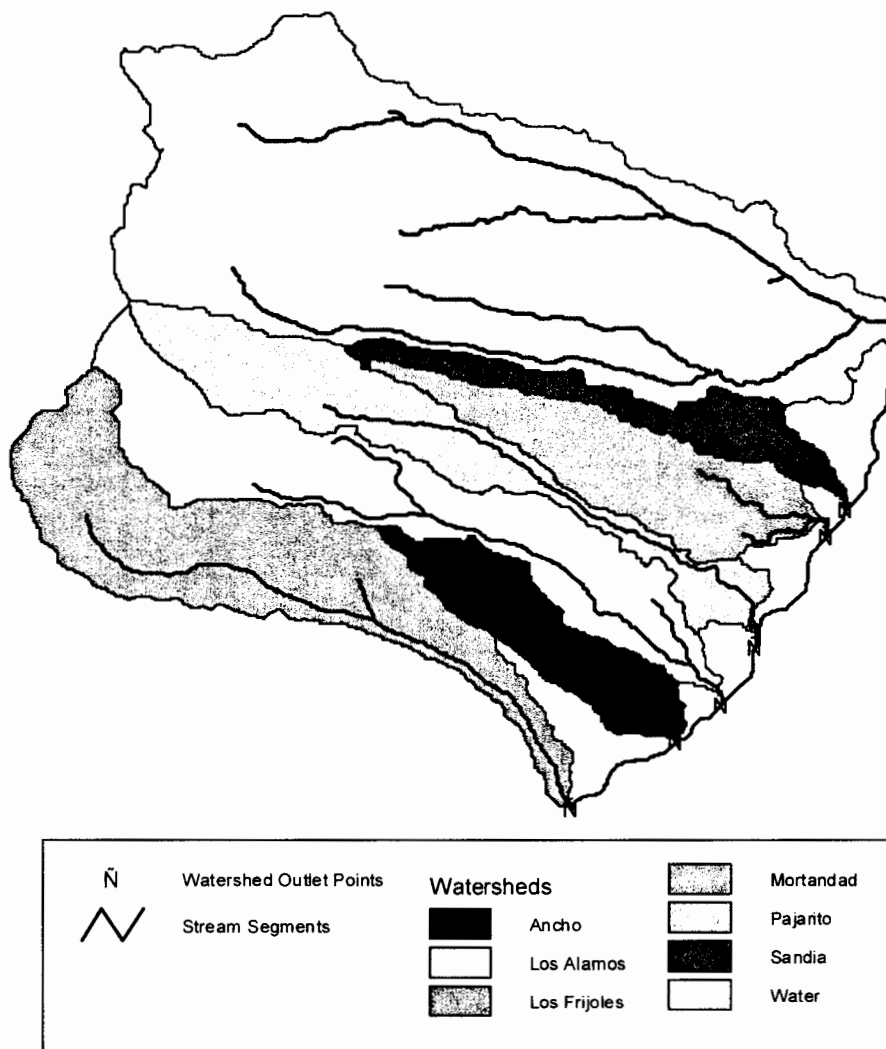


Figure 4-3. Watershed outlets.

4.1.2 Precipitation

Precipitation depth within the study area is related to elevation. We developed simple linear regression equations describing the relationship between precipitation depth and elevation for the 2-, 5-, 10-, 25-, 50-, 100-, and 500-year design storm events based on the 6-hour storm duration precipitation depths for gage locations TA-59 and TA-54 described in McLin (1992). Figure 4-4 shows the plot for the 100-year storm event and Table 4-1 provides the linear regression equations used to determine precipitation depth. Based on the linear regression equations and the composite DEM, we developed precipitation grids using the map calculator function in ArcView for each design storm event. These precipitation grids provide a total precipitation depth value for each 33-yd (30-m) grid cell within the study area based on each cell's elevation value. In Figure 4-4, elevations are reported in feet and precipitation depths are presented in inches per 6-hour

storm duration. Figure 4-5 shows precipitation grids for the 2-, 25-, 50-, and 100-year design storms, and the variation in shading illustrates the increasing levels of precipitation expected from more infrequent storm events. Wilson et al. (2001) and Nyhan et al. (2001) developed similar precipitation relationships for their studies.

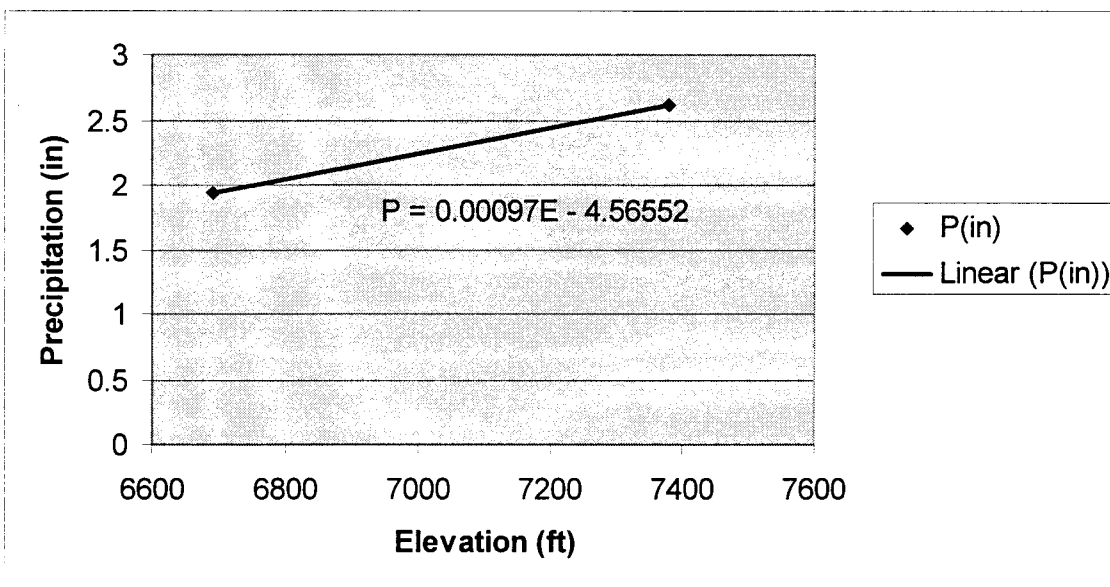


Figure 4-4. Linear regression equation development for the 100-year 6-hour design storm.

**Table 4-1. Linear Regression Equations Relating Elevation to
Precipitation Depths**

Design storm event (yr)	Linear regression algorithm ^a
2	$P = 0.00065E - 3.47938$
5	$P = 0.00078E - 4.07325$
10	$P = 0.00084E - 4.27164$
25	$P = 0.00090E - 4.43003$
50	$P = 0.00094E - 4.54132$
100	$P = 0.00097E - 4.56552$
500	$P = 0.00100E - 4.30971$

^a P = precipitation (in.) and E = elevation (ft).

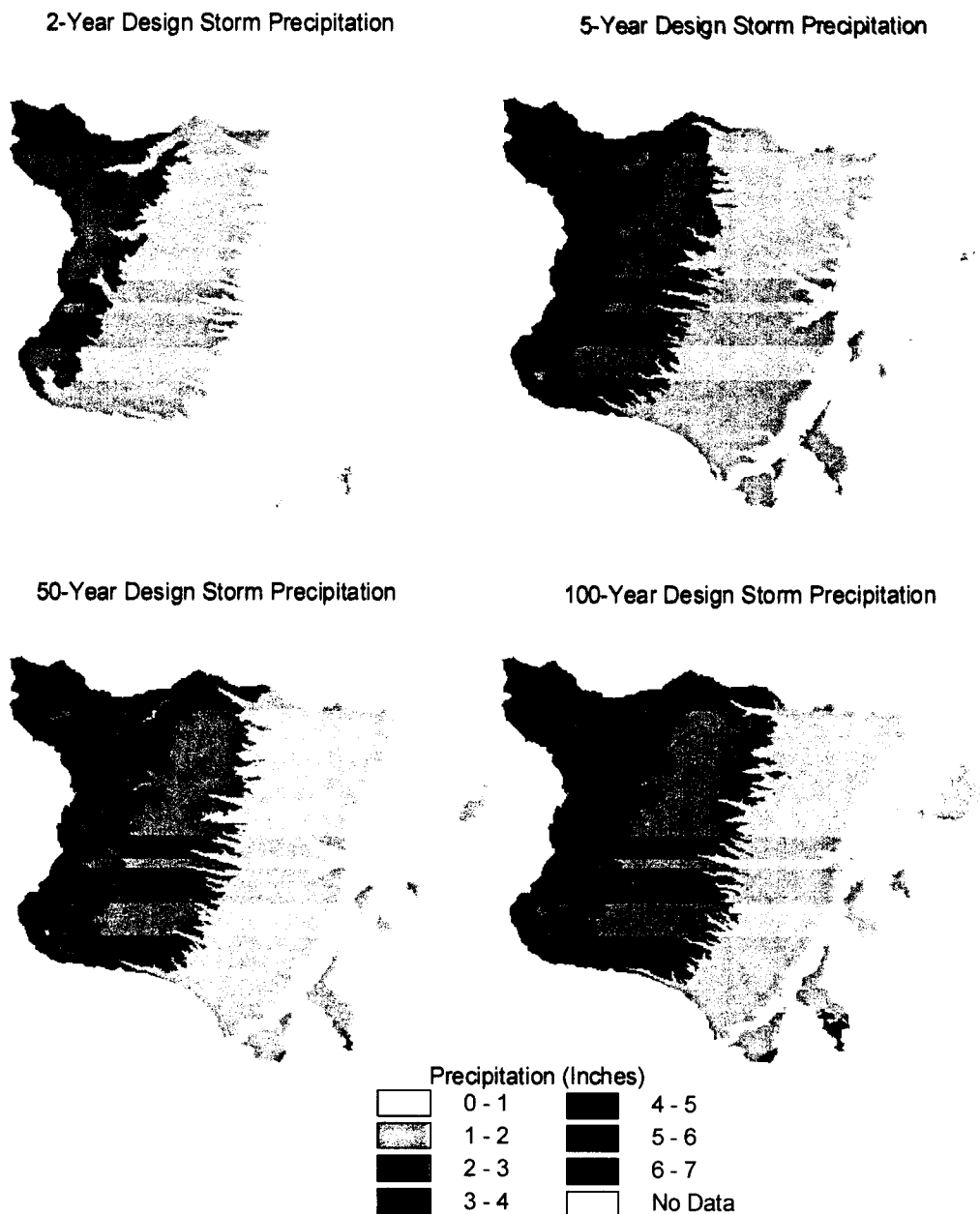


Figure 4-5. Two-, 25-, 50-, and 100-year precipitation depth grids. The levels of precipitation are represented by darker to lighter shading.

4.1.3 Storm Water Flow

For determining storm water flow, the grid-based calculation assumes that rainfall and the resulting storm water flow are uniformly distributed over the 6-hour duration of the storm event. This approach provides a conservative estimate of flow because the calculated flow is distributed over a shorter time frame (6-hours) than would be expected during an actual rainfall event and is

assumed to arrive at the outlet point instantaneously without any delays due to channel routing. This assumption simplifies the grid-based calculation considerably by eliminating the time variability of the flow over the spatial domain. On this basis, the estimated storm water flow is expected to be greater than the actual peak flow for a storm event. Figure 4-6 represents the potential peak flow for a uniformly distributed storm water flow following a 100-year storm event. We assumed that all flow at an outlet occurred during the duration of the storm versus storm water flow in a more realistic flow scenario where flow would continue for some period after the storm event.

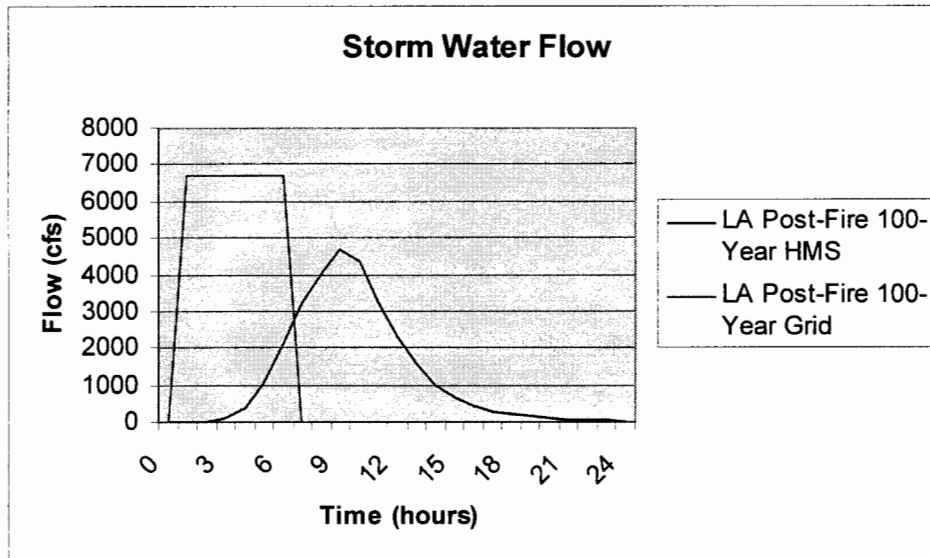


Figure 4-6. Comparison of uniformly distributed storm versus normally distributed storm. The Los Alamos (LA) post-fire 100-year grid simulation assumes all rainfall reaches the outlet to the Rio Grande within the 6-hour storm event time period. The Los Alamos (LA) post-fire 100-year HMS simulation assumes all rainfall reaches the outlet to the Rio Grande within 24 hours of the storm beginning.

To calculate the uniformly distributed flows, we performed grid calculations using the map calculator function in ArcView. First we calculated runoff for each design storm event for each grid cell within the study area. We then accumulated the runoff based on the contributing area for each grid cell. This represents the total maximum storm water flow for each grid cell within the study area, and the results of this evaluation are presented in grid format.

We calculated the runoff per unit area for each grid cell using the Soil Conservation Service (SCS) Curve Number model. This approach estimates excess precipitation or runoff (R) as a function of cumulative precipitation (P) and a curve number (CN), using Equation (4.1). The curve number represents the percent of runoff and is estimated as a function of land use, soil type, and antecedent moisture conditions of the soil (HEC 2000a).

$$R = \frac{(P - I_a)^2}{P - I_a + S} \quad (4.1)$$

where

I_a = the initial abstraction (initial loss). I_a is determined by Equation (4.2)
 S = potential maximum retention of a watershed

$$I_a = 0.2 \times S \quad (4.2)$$

S is determined by Equation (4.3)

$$S = \frac{1000 - 10 \times CN}{CN} \quad (4.3)$$

Therefore, by combining these equations, runoff is determined by Equation (4.4) (Chow et al. 1988)

$$R = \frac{(P - 0.2 \times S)^2}{P + 0.8 \times S} \quad (4.4)$$

The precipitation grids developed for each design storm event provide the cumulative precipitation for the runoff determination. Pre-fire and post-fire curve number grids, provided by the Earth and Environmental Sciences Group of the LANL facility were used for the runoff calculation. These curve numbers were based on values derived by the BAER estimates and existing pre-fire data (McLin 1992) that were modified to reflect observed runoff data in June 2000 (Wilson et al. 2001). These curve number grids were provided in a 100 × 100-ft (30.4 × 30.4-m) grid size and were resampled to correspond to a 33 × 33-yd (30 × 30-m) grid size. Figure 4-7 shows the pre-fire and post-fire grids used for this evaluation. Figure 4-8 shows the difference as a ratio between the post-fire and pre-fire curve number estimates.

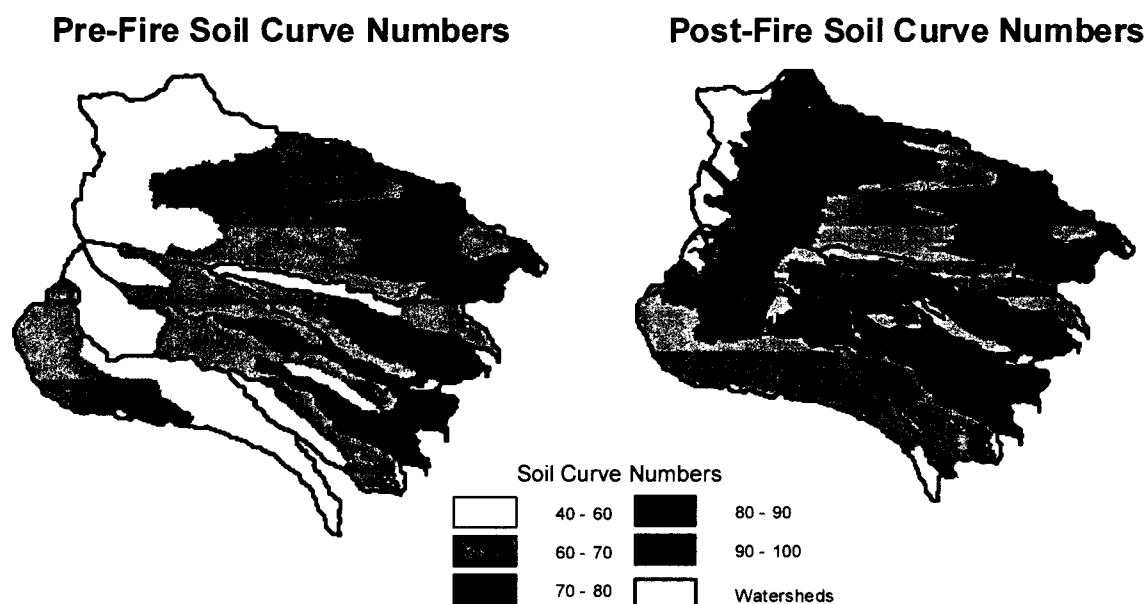


Figure 4-7. Pre-fire and post-fire soil curve number estimates. The curve number represents the percent of runoff and is estimated as a function of land use, soil type and antecedent moisture conditions in the soil. Higher curve numbers represent more impervious surfaces that will have higher runoff.

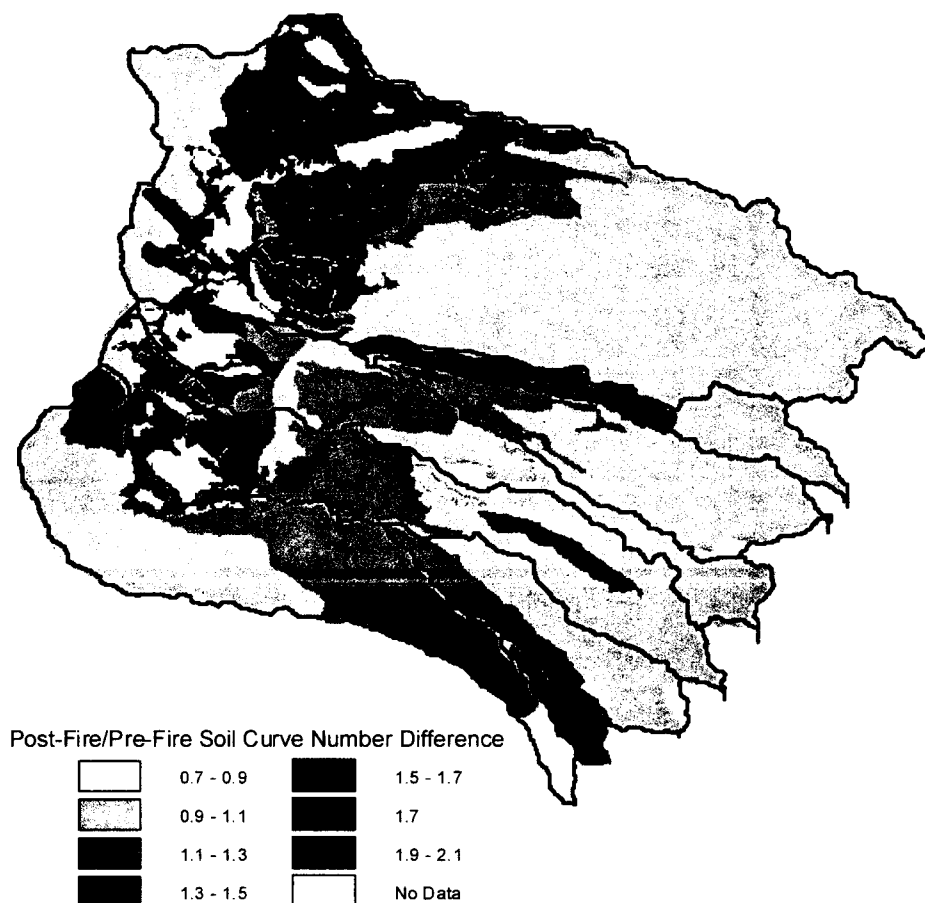


Figure 4-8. Ratio of post-fire to pre fire soil curve numbers. This ratio indicates the increased potential for storm water flow resulting from a rainfall event. As the ratio of post-fire to pre-fire curve numbers increases, the magnitude of the runoff increases.

We developed pre-fire and post-fire potential maximum retention (S) grids using Equation (4.3). We calculated pre-fire and post-fire runoff grids in units of inches per 6-hour for each design storm event using Equation (4.4) and the appropriate precipitation and maximum retention grids. In the calculations, if the $(P - 0.2S)$ value is negative, that is the initial abstraction is greater than the total precipitation, then the runoff for that grid cell is set to zero. We calculated pre-fire and post-fire surface water flow for each grid cell by multiplying the runoff by the area of the grid cell (i.e., 33×33 yd or 1089 yd² [30×30 m or 900 m²]) and converting to cubic feet per second (cfs) using Equation (4.5).

$$Q(cfs) = \frac{R \frac{\text{inch}}{6\text{-hours}} \times 900\text{m}^2 \times 0.000278 \frac{\text{hr}}{\text{sec}} \times 0.083 \frac{\text{ft}}{\text{inch}} \times 10.76 \frac{\text{ft}^2}{\text{m}^2}}{6\text{ - hours}} \quad (4.5)$$

4.1.4 Hydrologic Flow Model

We selected the U.S. Army Corps of Engineer's HEC-HMS model to calculate storm water flow estimates at basin and sub-basin outlets for the composite Los Alamos (includes Guaje, Los Alamos, Pueblo, and Rendija Canyons) and the Water watersheds. The HEC-HMS simulates precipitation and runoff processes in a watershed or basin, simulates infiltration losses, transforms excess precipitation into runoff, and simulates flow in open channels. We applied the HEC-HMS to two basins to verify that the grid-based storm water flow estimates were (1) conservative in estimating the storm water flow and (2) realistic in the relationship between pre-fire and post-fire storm water flow. As with the previous storm water flow estimates, we selected a relatively simple and conservative approach.

We selected Los Alamos and Water basins for a combination of reasons. First, these two basins generally have high storm water flow volumes based on the grid storm water estimates and the hydrograph peaks corresponding to the 6-hour design storms presented in McLin (1992). Second, a large number of potential release sites (PRSs) are located within these basins. Third, these basins, relative to the other basins, had a significant number of the sampling locations and available sampling data from pre-fire and post-fire sampling events.

We determined stream and watershed characteristics using Geo-HMS, including river lengths, slopes, centroids, longest flow lengths, and centroid flow lengths for each sub-basin within the Los Alamos and Water basins. We determined sub-basin centroids using the flow path method, which calculates the centroid based on the longest flow path for the sub-basin. Figure 4-9 and Figure 4-10 show the Los Alamos and Water basins, respectively, developed using Geo-HMS. The names for sub-basins, junctions, and reaches were assigned by Geo-HMS. Reaches are assigned a name that is a combination of an "R" with a number assigned for each reach from upstream to downstream (e.g., R670). Sub-basins are assigned a name that is a combination of the receiving reach name plus a "W" and a number assigned for each sub-basin (e.g., R670W940). Sub-basin junctions are assigned a name that is a combination of a "J" and the reach name (e.g., JR670) (HEC 2000b).

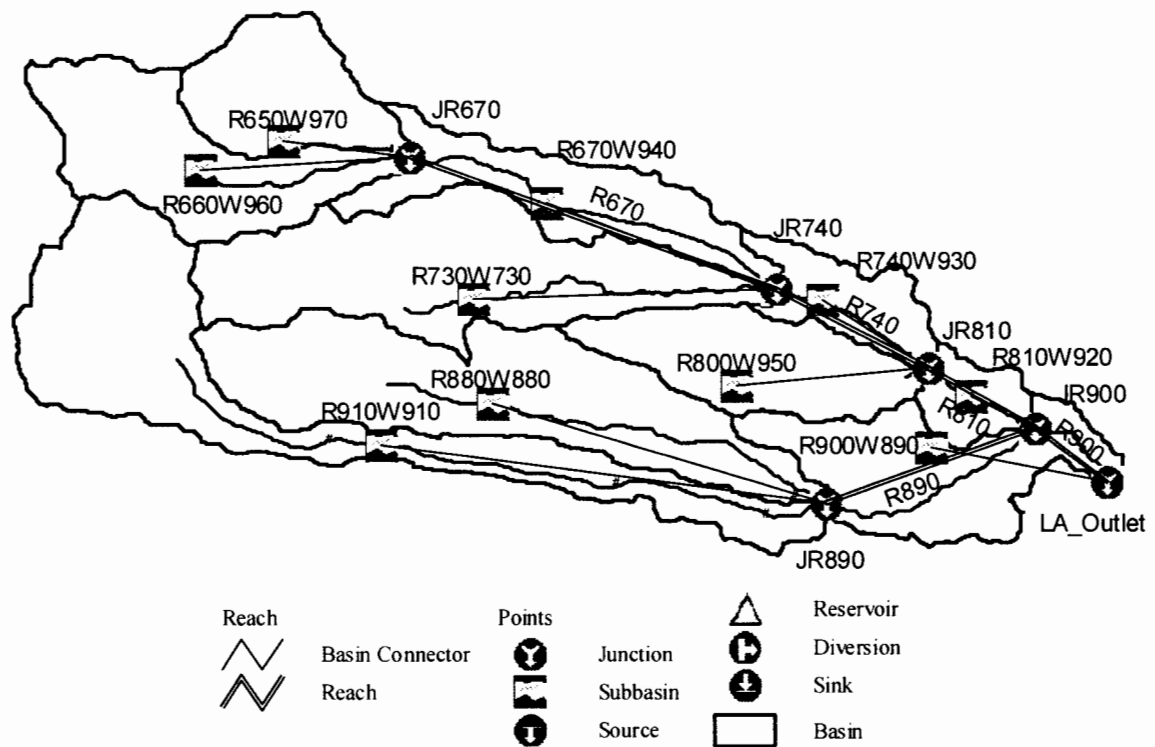


Figure 4-9. Results of the Geo-HMS stream and watershed characterization of the Los Alamos basin including sub-basins, junctions, reaches, river segments, longest flow path, and centroids for each sub-basin.

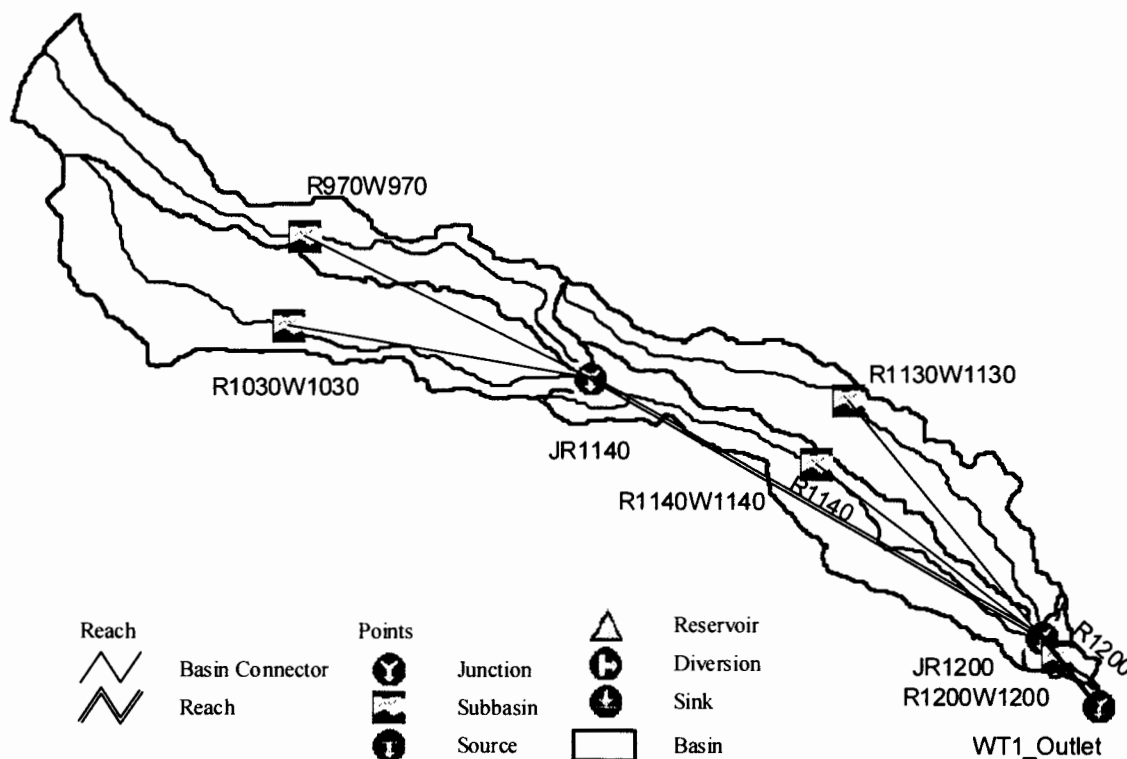


Figure 4-10. Results of the Geo-HMS stream and watershed characterization of the Water basin including sub-basins, junctions, reaches, river segments, longest flow paths, and centroids for each sub-basin.

We developed HEC-HMS model parameters including reach names, basin names, a background map file, and a basin model file for the Los Alamos and Water basins, all reported in English units (i.e., feet). We selected the lumped basin model because gridded values were not available for all input parameters. The lumped basin model defines the hydrologic elements, their connectivity, and related geographic information for use in a hydrologic model with single parameter values assigned to each sub-basin and reach (HEC 2000b). We determined methods and input parameters for the HEC-HMS for the sub-basin loss, transfer, base flow, channel routing, and precipitation. The following sections discuss these parameters in more detail.

4.1.4.1 Sub-basin Loss Method. As in the grid-based calculation, we used the SCS curve number method to calculate incremental excess precipitation (i.e., runoff) for each basin. Required parameters were initial loss and curve number. A percent impervious parameter was also optionally available. Weighted average pre-fire and post-fire curve numbers were estimated for each sub-basin using the curve number grids discussed above. We calculated the composite curve numbers using the average grid value on a polygon tool from the CRWR-Raster extension developed by the University of Texas at Austin (Olivera 1999). Because the grid cell size was the same for each grid, the CRWR-Raster function calculated the same weighted composite curve number as represented by Equation (4.6).

$$CN_{Composite} = \frac{\sum A_c \times CN_c}{A_t} \quad (4.6)$$

where

A_c (m²) = area of each cell (i.e., 900 m²)

CN_c = curve number for a individual cell

A_t (m²) = total drainage area or area of the sub-basin (HEC 2000a).

The initial loss was calculated for each sub-basin by Equation (4.2) using the composite curve number calculated by Equation (4.6). Given the substantial amount of undeveloped land in the study area and that the gridded curve numbers represented all of the land area within the basins, we assumed the additional percent of the area that was impervious was zero.

4.1.4.2 Sub-basin Transform Method. We used the SCS unit hydrograph method for the transform calculation. This method is commonly used and sufficient data were available for the Site to implement the method. The hydrograph (i.e., the flow as a function of time at the outlet) has a standard form and is defined for a basin by the peak flow and the lag time. The SCS lag time in minutes or hours is a required input to the model. The lag time (t_l) in hours was calculated for each sub-basin using Equation (4.7) (Chow et al. 1988)

$$t_l = t_c \times 0.6 \times 0.0167 \frac{\text{hours}}{\text{minute}} \quad (4.7)$$

where t_c (min) is the time of concentration to the outlet of each sub-basin calculated using Equation (4.8) (Chow et al. 1988)

$$t_c = \frac{100 \times L_w^{0.8} \times [(1000/CN) - 9]^{0.7}}{1900 \times S_l^{0.5}} \quad (4.8)$$

where L_w (ft) is the longest length of flow in the sub-basin and S_l (%) is the average watershed slope.

4.1.4.3 Sub-basin Base Flow Method. We assumed base flow to be zero. Available data from surface water and storm water gage stations indicate that flow is generally not present outside of rainfall events. This is consistent with the assumptions made in McLin (1992), indicating that all streams within the LANL facility are normally ephemeral.

4.1.4.4 Sub-basin Routing Method. We selected the Muskingum method, an accounting method to track the flow of water in the system and when it reaches the basin outlet, to calculate the storage volume of water within the stream channels as a function of the flow in the stream channels (Chow et al. 1988). This method is commonly used and the data available for the study area were sufficient to estimate the parameters for this method. Required parameters are Muskingum K (hour), which is a proportionality constant representing the time of travel of a flood wave through the reach, and Muskingum X (unitless), which is a weighting factor and the number of subreaches (unitless) (Chow et al. 1988). According to Chow et al. (1988), the

Muskingum X for natural streams has a range between 0 and 0.3, with an average value of 0.2. The Muskingum K is estimated using Equation (4.9) (HEC 2000a).

$$K = \frac{L_R}{1.667 \times V} \quad (4.9)$$

where L_R (ft) is the length of the reach or stream segment and V (ft s^{-1}) is the velocity of the flow in the stream segment estimated using Manning's equation for open channel flow given in Equation (4.10) (Chow et al. 1988).

$$V = \frac{1.49 \times R^{0.67} S_f^{0.5}}{n} \quad (4.10)$$

where R (ft) is the hydraulic radius, approximated to be 2 ft based on channel description (McLin 1992), S_f (unitless) is the slope of the channel, and n is the Manning roughness, approximated to be 0.1 (unitless) based on natural stream with heavy brush and timber (Chow et al. 1988).

The number of subreaches (N) was calculated by Equation (4.11) (HEC 2000a).

$$N = \frac{K}{\Delta t} \quad (4.11)$$

where Δt (min) is the time interval for the model run. For Δt , we used 15 minutes for the Los Alamos basin and 5 minutes for the Water canyon.

The various input parameters for the hydrologic flow modeling of the Los Alamos and Water basins are summarized in Table 4-2 and Table 4-3, respectively.

Table 4-2. HEC-HMS Model Input Parameters for Los Alamos Basin Precipitation

	Pre-fire CN (unitless)	Post-fire CN (unitless)	Pre-fire t_l (hr)	Post-fire t_l (hr)	Pre-fire t_c (min)	Post-fire t_c (min)	L_w (ft)	S_l (%)
R730W730	6.9E+01	8.3E+01	3.7E+00	2.4E+00	3.7E+02	2.4E+02	4.9E+04	7.0%
R880W880	6.5E+01	7.3E+01	5.2E+00	4.2E+00	5.2E+02	4.2E+02	5.4E+04	5.2%
R900W890	7.7E+01	7.7E+01	3.0E+00	3.0E+00	3.0E+02	3.0E+02	3.4E+04	4.0%
R910W910	5.8E+01	7.3E+01	7.8E+00	5.3E+00	7.8E+02	5.3E+02	6.9E+04	4.9%
R650W970	5.5E+01	8.0E+01	1.9E+00	9.7E-01	1.9E+02	9.7E+01	2.1E+04	14.4%
R660W960	5.5E+01	6.9E+01	3.4E+00	2.4E+00	3.4E+02	2.4E+02	3.3E+04	8.9%
R670W940	6.4E+01	8.2E+01	3.6E+00	2.2E+00	3.6E+02	2.2E+02	3.8E+04	6.2%
R740W930	7.5E+01	7.5E+01	1.6E+00	1.6E+00	1.6E+02	1.6E+02	1.9E+04	5.7%
R800W950	7.2E+01	7.2E+01	2.8E+00	2.8E+00	2.8E+02	2.8E+02	3.0E+04	4.7%
R810W920	7.0E+01	7.0E+01	1.3E+00	1.3E+00	1.3E+02	1.3E+02	1.1E+04	4.9%
	L_r (ft)	K (hr)	V (ft s ⁻¹)	R (ft)	n (unitless)	N (unitless)	Dt (hr)	
R670	3.1E+04	1.1E+00	4.7E+00	2.0E+00	1.0E-01	4.3E+00	2.5E-01	
R740	1.3E+04	5.5E-01	4.0E+00	2.0E+00	1.0E-01	2.2E+00	2.5E-01	
R810	9.6E+03	4.6E-01	3.5E+00	2.0E+00	1.0E-01	1.8E+00	2.5E-01	
R900	7.6E+03	3.6E-01	3.5E+00	2.0E+00	1.0E-01	1.4E+00	2.5E-01	
R890	1.9E+04	7.3E-01	4.4E+00	2.0E+00	1.0E-01	2.9E+00	2.5E-01	

Table 4-3. HEC-HMS Model Input Parameters for Water Basin Precipitation

	Pre-fire CN (unitless)	Post-fire CN (unitless)	Pre-fire T_l (hr)	Post-fire t_l (hr)	Pre-fire t_c (min)	Post-fire t_c (min)	L_w (ft)	S_l (%)
R970W970	5.8E+01	7.4E+01	4.3E+00	2.8E+00	4.3E+02	2.8E+02	4.4E+04	7.8%
R1030W1030	5.7E+01	8.1E+01	3.7E+00	2.0E+00	3.7E+02	2.0E+02	3.7E+04	8.1%
R1130W1130	6.7E+01	7.3E+01	4.5E+00	3.8E+00	4.5E+02	3.8E+02	3.9E+04	3.7%
R1140W1140	7.1E+01	7.2E+01	3.7E+00	3.6E+00	3.7E+02	3.6E+02	3.6E+04	3.8%
R1200W1200	7.6E+01	7.6E+01	5.4E-01	5.5E-01	5.4E+01	5.5E+01	8.1E+03	12.2%
	L_r (ft)	K (hr)	V (ft s ⁻¹)	R (ft)	n (unitless)	N (unitless)	Dt (hr)	
R1140	3.3E+04	1.2E+00	4.3E+00	2.0E+00	1.0E-01	1.4E+01	8.3E-02	
R1200	5.6E+03	5.3E-01	4.2E+00	2.0E+00	1.0E-01	6.3E+00	8.3E-02	

We selected the frequency storm method to provide the input for each precipitation event. Required input parameters are the exceedance probability (%), which represents the design storm event (e.g., 1% exceedance probability is representative of the 100-year design storm event); the desired output as either annual or partial duration; maximum intensity duration; storm duration; the percentage of the storm duration that occurs before the peak intensity; and the total drainage area or basin area. We developed meteorological models for each design storm event.

We set the exceedance probability based on the design storm event selected (i.e., 50% for 2-year, 4% for 25-year, and 1% for 100-year storm) and selected an annual desired output. We selected the maximum intensity as 15 minutes for the Los Alamos basin and 5 minutes for the Water basin. This difference was due to shorter lengths of the reaches in the Water basin. We

selected the storm duration as 6 hours, consistent with the 6-hour design storm events used for the evaluation. We selected the peak intensity as 50% assuming that the rainfall was evenly distributed. The basin area was obtained from the Geo-HMS attribute tables for the basins. The total basin area is 59.4 mi² (154 km²) for the Los Alamos basin and 18.53 mi² (48 km²) for the Water basin.

We calculated precipitation depths for 15 minutes and 1, 2, 3, and 6 hours for Los Alamos basin and 5 and 15 minutes and 1, 2, 3, and 6 hours for Water basin using the 6-hour storm distributions provided in McLin (1992). We estimated weighted average precipitation depths for each design storm event for each sub-basin using the precipitation grids discussed above. We calculated the composite precipitation depths using the average grid value on a polygon tool from the CRWR-Raster extension. Because the grid cell size is the same for each grid, this approach calculates a weighted composite precipitation depth similar to Equation (4.6) where CN is replaced by the precipitation depth. The precipitation distributions for Los Alamos and Water basins are presented in Table 4-4 and Table 4-5, respectively.

Table 4-4. Precipitation Depth Distributions for Los Alamos Basin

Time interval	Cumulative storm distribution (in.)					
	2-year	5-year	10-year	25-year	50-year	100-year
15 minutes	3.0E-03	6.0E-03	8.5E-03	1.1E-02	1.3E-02	1.4E-02
1 hour	1.7E-02	3.0E-02	4.1E-02	5.1E-02	6.0E-02	6.5E-02
2 hours	6.9E-02	9.8E-02	1.2E-01	1.4E-01	1.6E-01	1.7E-01
3 hours	9.6E-01	1.3E+00	1.5E+00	1.8E+00	2.0E+00	2.2E+00
6 hours	1.4E+00	1.8E+00	2.1E+00	2.4E+00	2.6E+00	2.8E+00
Total depth	1.4E+00	1.8E+00	2.1E+00	2.4E+00	2.6E+00	2.8E+00

Table 4-5. Precipitation Depth Distributions for Water Basin

Time interval	Cumulative storm distribution (in.)					
	2-year	5-year	10-year	25-year	50-year	100-year
5 minutes	9.6E-04	1.9E-03	2.7E-03	3.4E-03	4.2E-03	4.6E-03
15 minutes	2.9E-03	5.8E-03	8.2E-03	1.0E-02	1.3E-02	1.4E-02
1 hour	1.6E-02	2.9E-02	4.0E-02	4.9E-02	5.8E-02	6.3E-02
2 hour	6.6E-02	9.4E-02	1.2E-01	1.4E-01	1.6E-01	1.7E-01
3 hour	9.1E-01	1.2E+00	1.5E+00	1.7E+00	1.9E+00	2.2E+00
6 hour	1.4E+00	1.8E+00	2.0E+00	2.3E+00	2.5E+00	2.7E+00
Total depth	1.4E+00	1.8E+00	2.0E+00	2.3E+00	2.5E+00	2.7E+00

4.1.5 Grid-based Storm Water Flow Estimate Results

Using the procedures outlined in the "Methodology" section, we calculated pre-fire and post-fire cumulative storm water flow for each grid cell for each design storm event using the flow accumulation hydrologic function in ArcView. The flow accumulation function summarizes the storm water flow for each cell located upstream of a cell. Figure 4-11 shows storm water flow grids for pre-fire and post-fire 2- and 100-year design storm events.

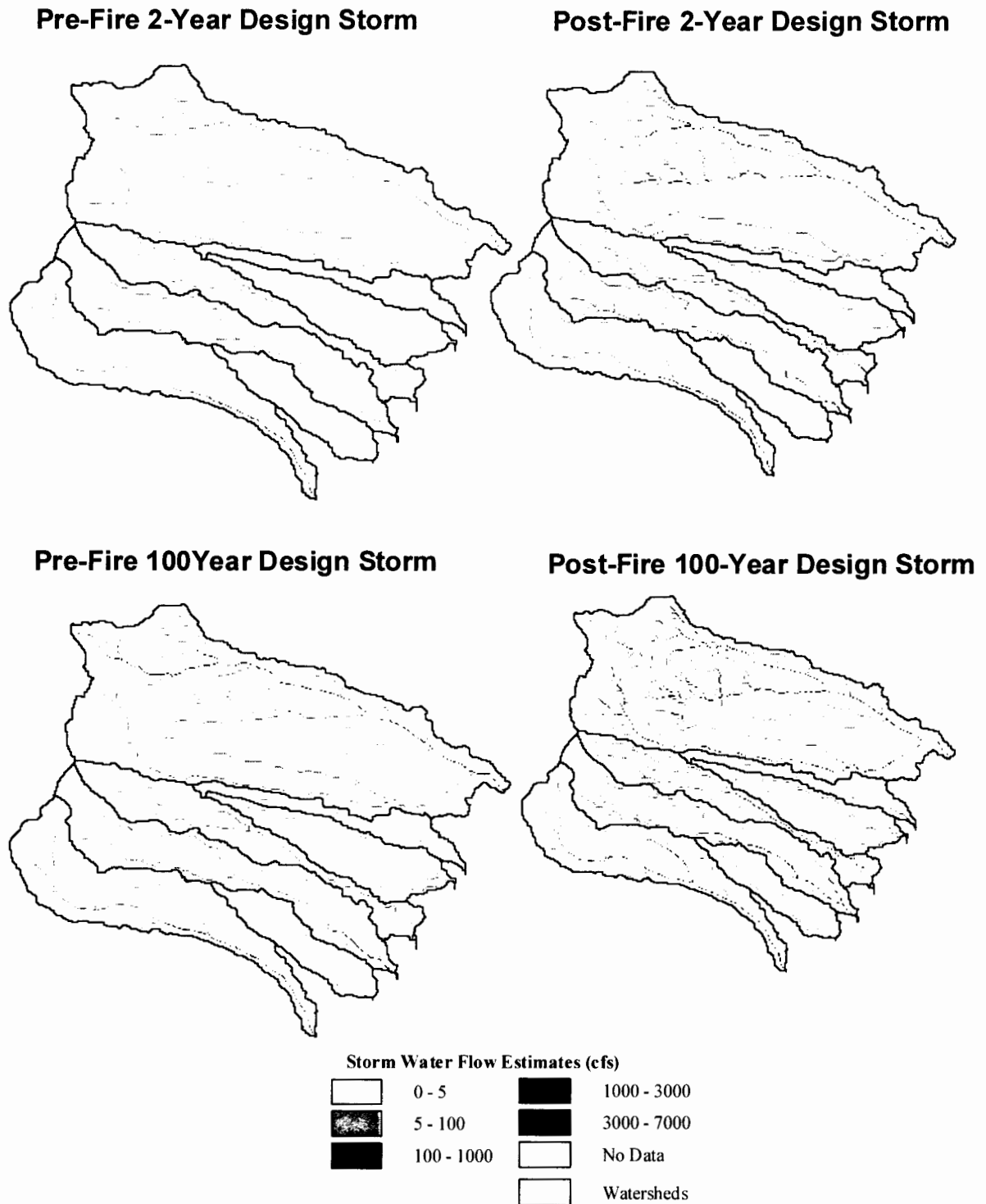


Figure 4-11. Storm water flow grids for pre-fire and post-fire 2- and 100-year design storm events.

Based on the stream segment determination and watershed delineation, we identified an outlet point immediately before the discharge to the Rio Grande from the individual watersheds. Figure 4-3 shows these outlet locations.

Pre-fire and post-fire surface water flow was identified for each outlet location and is provided in Table 4-6.

Table 4-6. Estimated Pre-fire and Post-fire Grid-based Storm Water Flow at Outlet Locations (cfs)

Point name	Watershed	Drainage area	2-year		5-year	
			Pre-fire	Post-fire	Pre-fire	Post-fire
LA_Outlet	Los Alamos	5.9E+01	2.3E+02	2.3E+03	6.5E+02	3.4E+03
LF_Outlet	Los Frijoles	2.0E+01	1.0E+02	2.9E+02	2.5E+02	5.1E+02
MT1_Outlet	Sandia	5.6E+00	1.9E-01	6.6E+00	1.0E+00	2.1E+01
MT2_Outlet	Mortandad	1.0E+01	3.0E+00	2.8E+01	2.8E+01	7.5E+01
PJ_Outlet	Pajarito	1.3E+01	3.7E+01	4.9E+02	1.2E+02	7.3E+02
WT1_Outlet	Water	1.9E+01	3.0E+01	5.7E+02	1.2E+02	9.0E+02
WT2_Outlet	Ancho	6.9E+00	7.0E-02	7.2E-02	9.2E-01	1.6E+00
			10-year		25-year	
			Pre-fire	Post-fire	Pre-fire	Post-fire
LA_Outlet	Los Alamos	5.9E+01	1.0E+03	4.2E+03	1.6E+03	5.2E+03
LF_Outlet	Los Frijoles	2.0E+01	3.6E+02	6.8E+02	5.2E+02	9.1E+02
MT1_Outlet	Sandia	5.6E+00	2.2E+00	3.6E+01	5.7E+00	6.0E+01
MT2_Outlet	Mortandad	1.0E+01	6.5E+01	1.3E+02	1.3E+02	2.1E+02
PJ_Outlet	Pajarito	1.3E+01	2.0E+02	9.0E+02	3.2E+02	1.1E+03
WT1_Outlet	Water	1.9E+01	2.1E+02	1.1E+03	3.6E+02	1.4E+03
WT2_Outlet	Ancho	6.9E+00	4.1E+00	7.2E+00	1.3E+01	2.2E+01
			50-year		100-year	
			Pre-fire	Post-fire	Pre-fire	Post-fire
LA_Outlet	Los Alamos	5.9E+01	2.0E+03	5.9E+03	2.5E+03	6.7E+03
LF_Outlet	Los Frijoles	2.0E+01	6.3E+02	1.1E+03	7.7E+02	1.3E+03
MT1_Outlet	Sandia	5.6E+00	1.1E+01	7.9E+01	2.0E+01	1.1E+02
MT2_Outlet	Mortandad	1.0E+01	1.8E+02	2.7E+02	2.5E+02	3.5E+02
PJ_Outlet	Pajarito	1.3E+01	4.1E+02	1.3E+03	5.1E+02	1.4E+03
WT1_Outlet	Water	1.9E+01	4.7E+02	1.7E+03	6.0E+02	1.9E+03
WT2_Outlet	Ancho	6.9E+00	2.3E+01	3.8E+01	3.8E+01	6.0E+01
			500-year			
			Pre-fire	Post-fire		
LA_Outlet	Los Alamos	5.9E+01	3.8E+03	8.6E+03		
LF_Outlet	Los Frijoles	2.0E+01	1.1E+03	1.7E+03		
MT1_Outlet	Sandia	5.6E+00	6.3E+01	1.9E+02		
MT2_Outlet	Mortandad	1.0E+01	4.6E+02	5.9E+02		
PJ_Outlet	Pajarito	1.3E+01	8.0E+02	1.9E+03		
WT1_Outlet	Water	1.9E+01	9.7E+02	2.5E+03		
WT2_Outlet	Ancho	6.9E+00	1.0E+02	1.4E+02		

A comparison of the estimated pre-fire storm water flow to the estimated post-fire storm water flow indicates that the post-fire storm water flow could, on average, range from 11 times higher than the pre-fire storm water flow for the 2-year design storm event to 3 times higher than the pre-fire storm water flow for the 100-year design storm event. This is consistent with information reported by Wilson et al. (2001), which indicates that the year 2000 measured peak storm water flow in “many canyons” was 10 times higher than the record peak flows and predicts post-fire runoff to increase 3 to 6 times over pre-fire runoff for the 100-year 6-hour design storm event. In addition, while storm water flow measurements were not available for the watershed outlets, Wilson et al. (2001) also indicates “significant storm flow to the Rio Grande” was measured during the storm season of 2000.

We also calculated the ratio of the estimated pre-fire storm water flow to the estimated post-fire storm water flow to evaluate the relationship between the design storm events. Table 4-7 shows the ratios of the pre-fire to post-fire storm water flow estimates.

Table 4-7. Ratio of Pre-fire to Post-fire for Grid Storm Water Flow Estimates

Point name	Watershed	2-year	5-year	10-year	25-year	50-year	100-year	500-year
LA_Outlet	Los Alamos	1.0E-01	1.9E-01	2.4E-01	3.0E-01	3.4E-01	3.7E-01	4.4E-01
LF_Outlet	Los Frijoles	3.6E-01	4.8E-01	5.3E-01	5.7E-01	5.9E-01	6.1E-01	6.4E-01
MT1_Outlet	Sandia	2.9E-02	5.0E-02	6.2E-02	9.6E-02	1.4E-01	1.9E-01	3.3E-01
MT2_Outlet	Mortandad	1.1E-01	3.7E-01	5.1E-01	6.2E-01	6.6E-01	7.0E-01	7.7E-01
PJ_Outlet	Pajarito	7.7E-02	1.6E-01	2.2E-01	2.8E-01	3.2E-01	3.6E-01	4.3E-01
WT1_Outlet	Water	5.2E-02	1.3E-01	1.9E-01	2.5E-01	2.8E-01	3.2E-01	3.9E-01
WT2_Outlet	Ancho	9.8E-01	5.8E-01	5.7E-01	5.9E-01	6.1E-01	6.4E-01	7.1E-01

The ratios generally indicate that as the design storm intensity increases, the difference between the pre-fire and post-fire storm flow estimates decrease or that the impacts of the Cerro Grande Fire on storm water flow is greater for the shorter return period design storm events. The pre-fire and post-fire storm water flow for the 2-year design storm for the Ancho outlet are essentially the same, resulting in a ratio of almost 1. This is because the rainfall in this canyon does not exceed the initial abstraction for a large portion of the canyon, resulting in very little runoff, and the soil curve numbers did not significantly change from pre-fire to post-fire, resulting in no change in the runoff. Figure 4-12 provides a comparison of the pre-fire/post-fire storm flow ratio for each storm event.

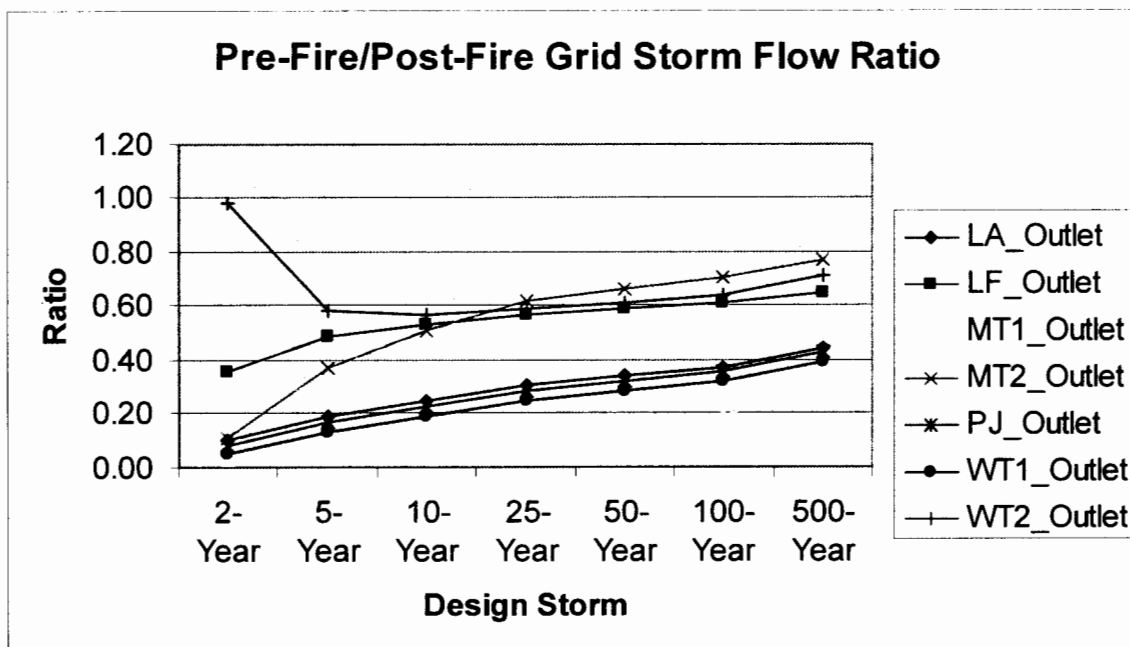


Figure 4-12. Comparison of grid pre-fire/post-fire storm flow ratio. The comparison indicates that the impacts of the Cerro Grande Fire on storm water flow are greater for the shorter return period design storm events.

4.1.6 HEC-HMS-based Storm Water Flow Results

Model runs were developed for the Los Alamos and Water basins for pre-fire storm water flow and post-fire storm water flow for the 2-, 25-, and 100-year design storm events. Table 4-8 presents results of the storm water flow estimates and the ratio of the estimated pre-fire storm water flow to the estimated post-fire storm water flow. Point locations are shown on Figure 4-9 and Figure 4-10.

Table 4-8. HEC-HMS Storm Water Flow Estimates for Los Alamos and Water Basins (cfs)

Storm water flow estimates by HMS (cfs)										
Point name	Watershed	2-year design storm			25-year design storm			100-year design storm		
		Pre-fire	Post-fire	Ratio	Pre-fire	Post-fire	Ratio	Pre-fire	Post-fire	Ratio
JR670	Los Alamos	0.0E+00	1.3E+02	0.0E+00	4.2E+01	7.1E+02	6.0E-02	1.2E+02	1.0E+03	1.2E-01
JR740	Los Alamos	1.3E+01	5.4E+02	2.5E-02	4.2E+02	2.2E+03	1.9E-01	7.1E+02	2.9E+03	2.4E-01
JR810	Los Alamos	5.2E+01	5.7E+02	9.1E-02	6.7E+02	2.5E+03	2.7E-01	1.1E+03	3.4E+03	3.1E-01
JR890	Los Alamos	6.1E-01	7.7E+01	7.9E-03	1.9E+02	7.3E+02	2.6E-01	3.3E+02	1.1E+03	3.1E-01
JR900	Los Alamos	5.6E+01	6.1E+02	9.2E-02	8.0E+02	3.0E+03	2.7E-01	1.3E+03	4.1E+03	3.1E-01
LA_Outlet	Los Alamos	1.2E+02	6.6E+02	1.8E-01	1.1E+03	3.3E+03	3.3E-01	1.7E+03	4.6E+03	3.7E-01
R650W970	Los Alamos	0.0E+00	1.3E+02	0.0E+00	2.4E+01	5.9E+02	4.1E-02	6.5E+01	7.9E+02	8.3E-02
R660W960	Los Alamos	0.0E+00	1.5E+01	0.0E+00	2.4E+01	2.7E+02	9.0E-02	6.6E+01	4.0E+02	1.6E-01
R670W940	Los Alamos	9.4E-02	1.2E+02	7.7E-04	9.1E+01	4.8E+02	1.9E-01	1.5E+02	6.3E+02	2.4E-01
R730W730	Los Alamos	1.3E+01	2.9E+02	4.5E-02	2.9E+02	1.0E+03	2.8E-01	4.4E+02	1.4E+03	3.3E-01
R740W930	Los Alamos	2.9E+01	2.9E+01	1.0E+00	2.0E+02	2.0E+02	1.0E+00	2.8E+02	2.8E+02	1.0E+00
R800W950	Los Alamos	2.5E+01	2.5E+01	1.0E+00	2.4E+02	2.4E+02	1.0E+00	3.5E+02	3.5E+02	1.0E+00
R810W920	Los Alamos	7.6E+00	7.6E+00	1.0E+00	1.0E+02	1.0E+02	1.0E+00	1.5E+02	1.5E+02	1.0E+00
R880W880	Los Alamos	6.1E-01	4.6E+01	1.3E-02	1.6E+02	4.1E+02	3.9E-01	2.6E+02	5.9E+02	4.5E-01
R900W890	Los Alamos	6.3E+01	6.3E+01	1.0E+00	3.6E+02	3.6E+02	1.0E+00	4.9E+02	4.9E+02	1.0E+00
R910W910	Los Alamos	0.0E+00	3.3E+01	0.0E+00	3.9E+01	3.3E+02	1.2E-01	8.6E+01	4.9E+02	1.8E-01
JR1140	Water	0.0E+00	2.1E+02	0.0E+00	8.0E+01	1.0E+03	7.9E-02	1.7E+02	1.4E+03	1.3E-01
JR1200	Water	1.4E+01	2.5E+02	5.7E-02	3.2E+02	1.4E+03	2.3E-01	5.3E+02	1.9E+03	2.8E-01
R1030W1030	Water	0.0E+00	1.9E+02	0.0E+00	4.8E+01	7.7E+02	6.2E-02	1.1E+02	1.0E+03	1.0E-01
R1130W1130	Water	3.7E+00	2.4E+01	1.5E-01	1.1E+02	2.1E+02	5.3E-01	1.8E+02	3.1E+02	5.8E-01
R1140W1140	Water	1.1E+01	1.6E+01	6.6E-01	1.4E+02	1.7E+02	8.7E-01	2.1E+02	2.4E+02	8.9E-01
R1200W1200	Water	1.2E+01	1.0E+01	1.1E+00	8.7E+01	8.2E+01	1.1E+00	1.3E+02	1.2E+02	1.1E+00
R970W970	Water	0.0E+00	3.6E+01	0.0E+00	3.3E+01	2.8E+02	1.2E-01	7.0E+01	3.9E+02	1.8E-01
WT1_Outlet	Water	1.4E+01	2.5E+02	5.7E-02	3.2E+02	1.4E+03	2.3E-01	5.3E+02	1.9E+03	2.8E-01
R890	Los Alamos	6.0E-01	7.6E+01	7.9E-03	1.9E+02	7.2E+02	2.6E-01	3.3E+02	1.0E+03	3.1E-01
R670	Los Alamos	0.0E+00	1.2E+02	0.0E+00	4.1E+01	6.6E+02	6.2E-02	1.1E+02	9.3E+02	1.2E-01
R740	Los Alamos	1.3E+01	5.3E+02	2.5E-02	4.2E+02	2.1E+03	2.0E-01	7.0E+02	2.9E+03	2.4E-01
R810	Los Alamos	5.2E+01	5.6E+02	9.2E-02	6.1E+02	2.5E+03	2.5E-01	1.1E+03	3.3E+03	3.2E-01
R900	Los Alamos	5.6E+01	6.0E+02	9.2E-02	8.0E+02	3.0E+03	2.7E-01	1.3E+03	4.1E+03	3.1E-01
R1140	Water	0.0E+00	2.1E+02	0.0E+00	7.9E+01	9.9E+02	8.0E-02	1.7E+02	1.3E+03	1.3E-01
R1200	Water	1.4E+01	2.5E+02	5.7E-02	3.2E+02	1.4E+03	2.3E-01	5.3E+02	1.9E+03	2.8E-01

Figure 4-13 provides a comparison of the estimated pre-fire to estimated post-fire storm water flow ratio for the Los Alamos and Water outlets for each storm event. Similar to the grid storm water flow estimates, the ratios generally indicate that as the design storm intensity increases, the difference between the pre-fire and post-fire storm water flow estimates decrease or that the impacts of the Cerro Grande fire on storm water flow is greater for the shorter return period design storm events.

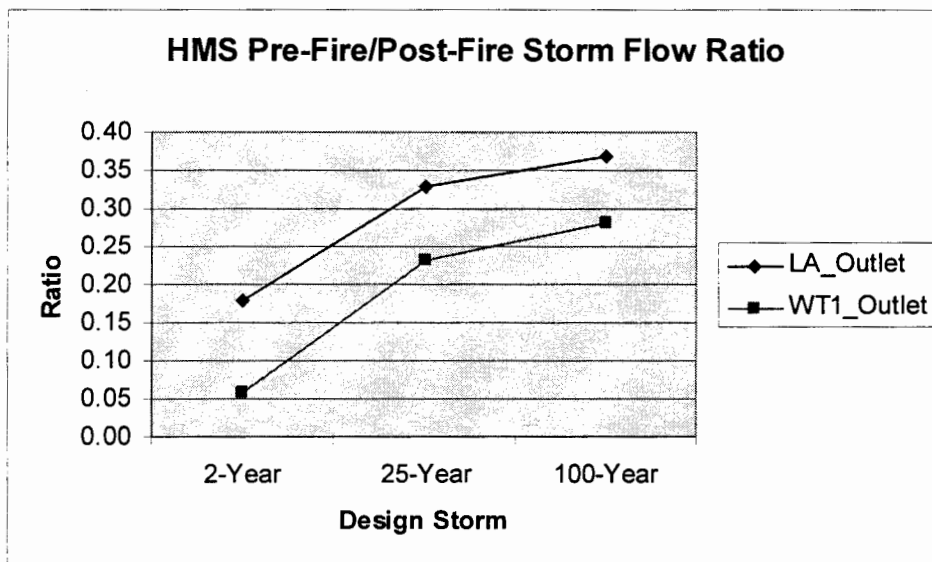


Figure 4-13. Comparison of HMS pre-fire/post-fire storm water flow ratio. The comparison indicates that the impacts of the Cerro Grande Fire on storm water flow are greater for the shorter return period design storm events.

The results of the HMS modeling indicate similar trends in the surface water flows as the grid model. Because the grid model is simpler to implement and allows the calculation of flow at any location on the defined stream networks without having to set up individual model runs, the grid model is preferred for the multiple calculations that were in the risk analysis. The grid model predicts higher peak flows than the HMS model, but within the uncertainty of the modeling and in an effort to provide conservative estimates; these higher values are likely to be reasonable for the risk analysis.

4.1.7 Storm Water Flow Estimate Results and Discussion

We obtained storm flow measurement data taken at 5-minute intervals for 23 gage stations from the ESH Division (Chapter 1) for the period of October 1, 1999, through April 15, 2001. Where coordinates were available for the gage stations, a GIS point coverage was developed for the gage stations. Coordinates were available for all gage locations except for E123, E218, and E263. In some cases, the gage station coordinates were located adjacent to, but not on, a stream segment defined as part of the hydrologic model. In these cases, it is likely that variability in the methodology used to identify the coordinates, variability due to the resolution of the DEM, and changes in the stream segment location due to flow and erosion over time contributed to the variance in the gage stations. Gage stations that were not located on a stream segment were assumed to be located on the closest adjacent stream segment for purposes of determining the estimated storm flow. There were no gage stations at the watershed outlets to the Rio Grande. Figure 4-14 shows the gage stations used for this evaluation.

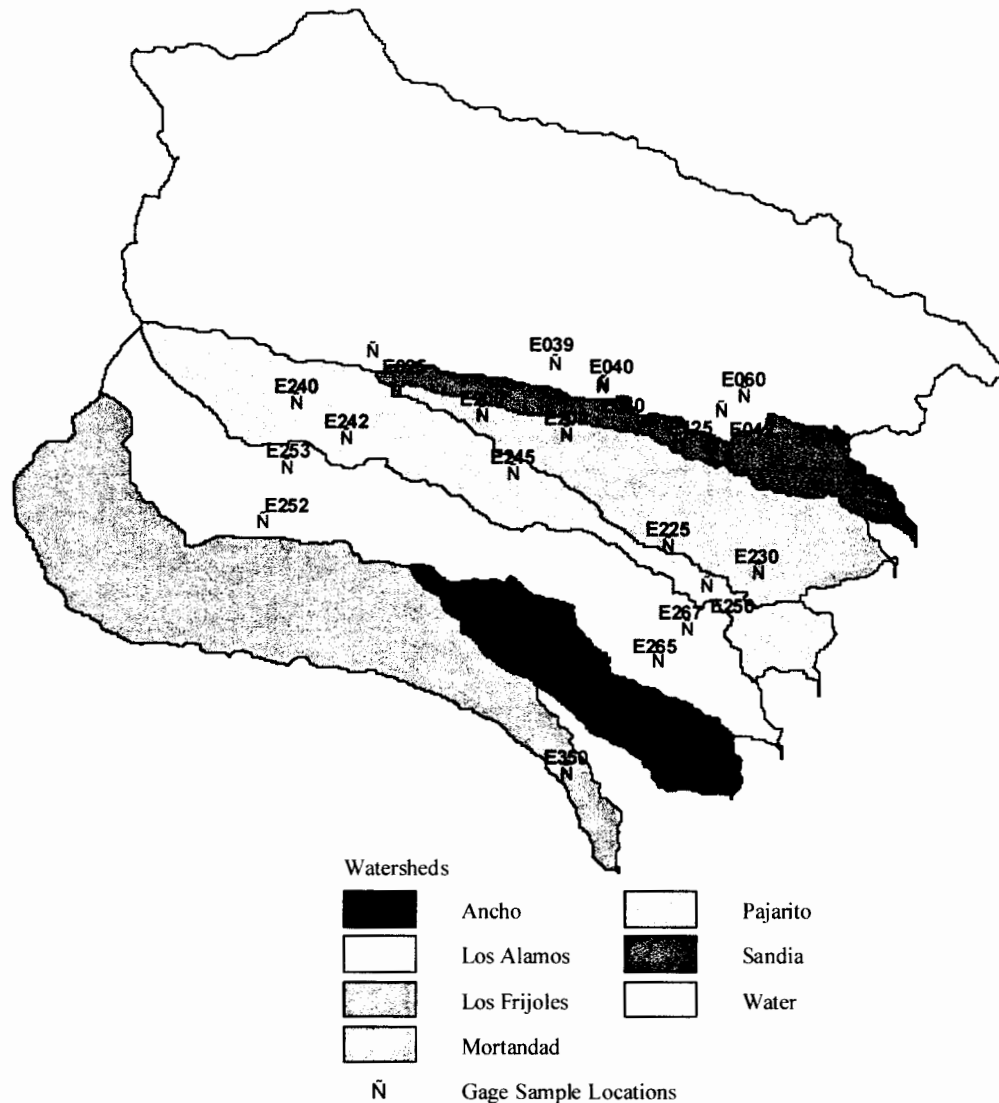


Figure 4-14. Storm flow gauging locations.

We reviewed the available daily precipitation data. These data were collected from 1/1/00 through 5/21/01 from six rain gage stations Figure 4-15 shows the rain gage locations. Based on this rainfall data, the maximum daily recorded rainfall ranged from 1.00 in. collected on 10/23/00 at TA-06 located in the Pajarito watershed to 1.71 in. collected on 8/18/00 at gage station TA-54 located along the divide between the Pajarito and Mortandad watersheds. The estimated precipitation depth for the 2-year design storm event ranged from 1.34 in. at gage station TA-06 to 3.20 in. at PJMTN. Table 4-9 summarizes the precipitation depths for the 2- and 5-year design storm events and the maximum measured daily rainfall. Based on these data, we selected the estimated storm water flow based on the 2- and 5-year design storm events for comparison to the measured storm water flow.

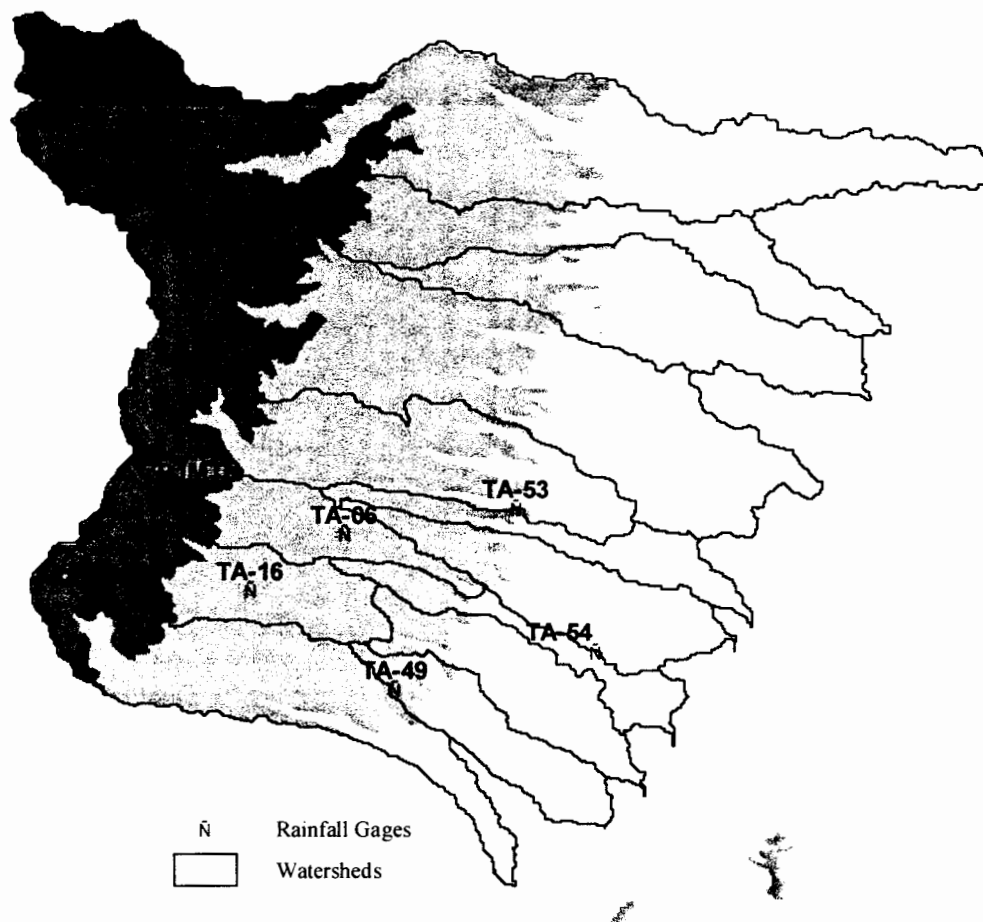


Figure 4-15. Gage station locations.

Table 4-9. Maximum Measured Precipitation Depth from 1/1/00 through 5/21/01 and Estimated Precipitation Depth for Gage Locations based on the 2-year and 5-year Design Storm Events

Gage	Rainfall depth (in.)		Maximum
	2-year design storm	5-year design storm	
TA-06	1.3E+00	1.7E+00	1.0E+00
TA-16	1.5E+00	1.9E+00	1.1E+00
TA-49	1.1E+00	1.4E+00	1.2E+00
TA-53	1.0E+00	1.4E+00	1.2E+00
TA-54	7.7E-01	1.0E+00	1.7E+00
PJMTN	3.2E+00	3.9E+00	1.3E+00

We obtained estimated storm water flows from the 2- and 5-year pre-fire and post-fire storm water flow grids for each sample locations. Table 4-10 provides a summary of the maximum-recorded storm water flow from the flow measurement data for each gage station before the Cerro Grande Fire (i.e., October 1999 through May 2000), and the 2- and 5-year pre-fire grid storm

water flow estimates. Table 4-11 provides a summary of the maximum-recorded storm flow from the flow measurement data for each gage station after the fire (i.e., June 2000 through April 15, 2001) and the 2- and 5-year post-fire grid storm water flow estimates.

Table 4-10. Summary of Maximum Measured and Estimated Pre-fire Storm Water Flow

Gage ID	Location description	Pre-fire storm water flow (cfs)			
		Grid estimate		Gage	
		2-year	5-year	Maximum	Date
E025	Los Alamos Canyon at Los Alamos	4.3E+01	1.3E+02	6.6E-02	10/01/99
E030	Los Alamos Canyon below Laboratory Technical Area (TA) 2 near Los Alamo	4.4E+01	1.3E+02	5.9E-01	02/16/00
E039	DP Canyon below Meadow at TA-21	4.7E-01	2.2E+00	1.8E-01	04/11/00
E040	DP Canyon at Mouth	7.2E-01	3.6E+00	5.9E+00	03/22/00
E042	Los Alamos Canyon near Los Alamos	4.5E+01	1.4E+02	2.4E-01	12/13/99
E060	Pueblo Canyon near Los Alamos	9.8E+00	5.2E+01	1.7E+01	01/10/00
E125	Sandia Canyon above Highway 4 near White Rock	1.5E-01	8.8E-01	0.0E+00	
E200	Mortandad Canyon at TA-50 near Los Alamos	2.7E-01	2.2E+00	3.4E+00	01/31/00
E202	Mortandad Canyon at Entrance to Sediment Traps	6.3E-01	5.3E+00	0.0E+00	
E225	Canada del Buey above White Rock	7.8E-01	6.0E+00	0.0E+00	
E230	Canada del Buey at White Rock	7.9E-01	6.5E+00	1.6E-01	11/24/99
E240	Pajarito Canyon above Highway 501 near Los Alamos	1.0E+01	3.0E+01	2.8E-01	11/20/99
E242	Starmers Gulch at TA-22	7.8E+00	2.1E+01	1.0E-01	05/02/00
E245	Pajarito Canyon above TA-18 near Los Alamos	3.1E+01	9.3E+01	0.0E+00	
E250	Pajarito Canyon above Highway 4 near White Rock	3.7E+01	1.2E+02	0.0E+00	
E252	Water Canyon above Highway 501 near Los Alamos	8.5E+00	3.1E+01	5.0E-02	04/26/00
E253	Canon del Valle above Highway 501 near Los Alamos	1.5E+01	4.2E+01	0.0E+00	
E265	Water Canyon below Highway 4 near White Rock	2.8E+01	1.1E+02	0.0E+00	
E267	Portillo Canyon near White Rock	1.8E+00	1.0E+01	0.0E+00	
E350	Rio de Los Frijoles at Bandelier	1.0E+02	2.5E+02	8.1E+00	02/02/00

A direct quantitative comparison of the estimated storm water flow to the maximum measured storm water flow is not entirely valid. However, a comparison of the estimated and measured storm water flow provides support to the assumption that the modeled storm water flow estimates are a conservative representation of the storm water flow in the identified canyons. A direct comparison is limited by a number of issues. First, the intensity of the rain event contributing to the measured maximum storm water flow cannot be associated with a specific design storm event. Second, as discussed previously, several of the gage station locations did not correspond to stream segments defined by the hydrologic model, so it is uncertain as to whether the estimated storm water flow determined for a gage station location is representative of that location. Third, the design storm events and the estimated storm water flow are high-end estimates that assume that rainfall and runoff are uniformly distributed. Fourth, rainfall may not occur uniformly throughout all of the canyons as indicated by the different dates when the maximum storm water flow was measured for each gage station. Fifth, the quantity of measured storm water flow data is limited to 19 months before the fire and 10 months after the fire.

Finally, the modeled storm water flow was not intended to accurately predict the storm water flow within the canyons. Rather, we intended to provide a conservative estimate of storm water flow to use in estimating incremental risks associated with exposure to radionuclides and

chemicals associated with the LANL facility. The critical issue in comparison of the estimated storm water flow to the maximum measured storm water flow data was whether the estimated storm water flow was consistent with our conservative assumption that these estimates were generally greater than actual storm water flow and that they played an important part in estimating risks.

Table 4-11. Summary of Maximum Measured and Estimated Post-fire Storm Water Flow

Gage ID	Location description	Post-fire storm water flow (cfs)			
		Grid estimate		Gage	
		2-year	5-year	Maximum	Date
E025	Los Alamos Canyon at Los Alamos	5.8E+02	8.4E+02	2.4E+01	07/18/00
E030	Los Alamos Canyon below Laboratory Technical Area (TA) 2 near Los Alamo	5.8E+02	8.6E+02	2.5E+01	10/23/00
E039	DP Canyon below Meadow at TA-21	4.7E-01	2.2E+00	NV	
E040	DP Canyon at Mouth	7.3E-01	3.6E+00	6.4E+01	10/27/00
E042	Los Alamos Canyon near Los Alamos	5.9E+02	8.6E+02	5.9E+01	10/27/00
E060	Pueblo Canyon near Los Alamos	2.8E+02	4.2E+02	1.5E+02	10/24/00
E125	Sandia Canyon above Highway 4 near White Rock	6.6E+00	2.0E+01	0.0E+00	
E200	Mortandad Canyon at TA-50 near Los Alamos	7.6E+00	1.5E+01	1.2E+01	08/19/00
E202	Mortandad Canyon at Entrance to Sediment Traps	1.4E+01	2.9E+01	1.6E+00	07/29/00
E225	Canada del Buey above White Rock	6.5E+00	1.7E+01	0.0E+00	
E230	Canada del Buey at White Rock	6.5E+00	1.7E+01	3.3E+01	08/09/00
E240	Pajarito Canyon above Highway 501 near Los Alamos	2.5E+02	3.4E+02	0.0E+00	
E242	Starmers Gulch at TA-22	8.4E+01	1.2E+02	1.8E+02	06/27/00
E245	Pajarito Canyon above TA-18 near Los Alamos	4.7E+02	6.9E+02	5.2E+02	06/08/00
E250	Pajarito Canyon above Highway 4 near White Rock	4.9E+02	7.2E+02	1.5E+01	06/28/00
E252	Water Canyon above Highway 501 near Los Alamos	3.0E+02	4.2E+02	2.5E-02	05/15/00
E253	Canon del Valle above Highway 501 near Los Alamos	1.7E+02	2.5E+02	9.2E-01	04/03/01
E265	Water Canyon below Highway 4 near White Rock	5.7E+02	8.7E+02	2.7E+02	06/28/00
E267	Portillo Canyon near White Rock	5.9E+00	2.0E+01	7.0E+00	08/09/00
E350	Rio de los Frijoles at Bandelier	2.9E+02	5.1E+02	4.0E+01	06/28/00

For the comparison of the measured pre-fire storm water flow to the estimated pre-fire storm water flow presented in Table 4-10, the estimated pre-fire storm water flows are generally higher than the measured pre-fire storm water flow. There are three gage stations (i.e., E040, E060, and E200) where this is not the case. For gage stations E040 and E200, the storm water flow estimates for the gage stations immediately downstream of these gage stations (i.e., E042 and E202, respectively) show 2-year design storm event storm water flow estimates higher (i.e., 45.29 cfs versus 0.24 cfs and 0.63 cfs versus 0.00 cfs, respectively) than the measured storm water flow. This could indicate retardants to flow (e.g., natural damming caused by debris and logs, ponding, and groundwater recharge) upstream from gage stations E040 and E200. These phenomena are not accounted for in the surface water models. For gage location E060, there are no downstream gage stations; however, the estimated storm water flow for the 5-year, 6-hour design storm is higher (i.e., 52.20 cfs versus 16.76 cfs) than the measured storm water flow. Given the

uncertainty in the rainfall events and their relationship to the design storm events, the measured storm water flows for these gage stations are consistent with the design storm events selected for this comparison.

For the comparison of the measured post-fire storm water flow to the estimated post-fire storm water flow presented in Table 4-11, the estimated post-fire storm water flows are also generally higher than the measured post-fire storm water flow. There are six gage stations (i.e., E040, E200, E230, E242, E245, and E267) where this is not the case. For gage stations E040, E200, and E245, the storm water flow estimates for the gage stations immediately down stream of these gage stations (i.e., E042, E202, and 250, respectively) show 2-year design storm event storm water flow estimates higher (i.e., 585.20 cfs versus 58.90 cfs, 13.60 cfs versus 1.64 cfs, and 485.203 cfs versus 14.96 cfs, respectively) than the measured storm water flow. This could indicate retardants to flow (e.g., natural damming caused by debris and logs, ponding, and groundwater recharge) upstream from gage stations E040, E200, and E245. An additional gage station (i.e., E242) is upstream from gage station E245. For gage stations E230 and E267, there are no downstream gage stations. For gage station E267, the estimated storm water flow for the 5-year, 6-hour design storm is higher (i.e., 19.52 cfs versus 7.04 cfs) than the measured storm water flow. Given the uncertainty in the rainfall events and their relationship to the design storm events, the measured storm water flows for these gage stations are consistent with the design storm events selected for this comparison.

For the gage station E230, the gage station immediately upstream of this gage station (i.e., E225) has a maximum measured storm water flow of 0.0 cfs, and the flow at gage station E230 is substantially higher (i.e., 33.38 cfs). The difference in the contributing area for the two storm water flow gage stations (i.e., 1.44 mi² for E225 versus 2.07 mi² for E230) does not seem to account for the large increase in storm water flow. Based on the measured storm water flow, this is a 42% increase in area with an increase in storm water flow from 0.0 cfs to 33.38 cfs. In addition, the characteristics of the contributing area do not appear to be significantly different based on the available information. This may indicate an additional water source upstream from gage station E230 or facility water discharge.

In summary, the grid storm water flow estimates conservatively estimate the storm water flow using the design storm events. These estimates are tempered by a number of contributing factors. The storm water flow estimates assume a uniformly distributed runoff and do not consider blockage or retardants to flow (e.g., natural damming, ponding, and groundwater recharge), which may affect the quantity or distribution of storm water flow. Similarly, the storm water flow estimates assume that the initial abstraction or infiltration is constant throughout the study area and fits a generally accepted estimate of 0.2S. We assumed precipitation varied by elevation, but otherwise to be uniformly distributed through the study area. Actual soil curve numbers, while estimated by sub-basin for pre-fire conditions and adjusted based on burn severity for post-fire conditions, varied within each sub-basin based on site-specific conditions.

4.2 Suspended Sediment Evaluation

The modeling of erosion can be a very complex task involving a large number of different physical processes. The physical process that must be accounted for and the factors that affect the amount of erosion in any particular land area are the topography, soil type, vegetative cover, land use, and climate (Maidment 1993). Changes in these factors necessarily affect the amount of

erosion from the land area. The significant changes brought about by the Cerro Grande Fire were, therefore, expected to affect the amount of erosion within the watersheds impacted by the fire. Our evaluation was based on a number of assumptions and conditions:

1. Because of the limited data for individual watersheds, we considered all watersheds to have a single set of homogeneous characteristics for purposes of estimating suspended sediment concentrations.
2. We analyzed the pre-fire and post-fire TSS measurements as two separate data sets.
3. We analyzed TSS measurements as a screening technique to develop representative concentrations of sediment in surface water.

4.2.1 Methodology

The area surrounding the LANL facility is characterized by significant topographic relief with the mesas and canyons of the Pajarito Plateau. Except for the cities of Los Alamos and White Rock and the developed areas of the LANL facility, the land use is generally forestland. The soils are characterized as sandy to silty loams with areas of bedrock outcrops (Nyhan 1978). For this risk analysis project, a conservative estimate of suspended sediment concentrations in storm water as a function of flow and estimates of sediment deposition at the points of exposure are needed. The suspended sediment acted as a carrier medium to transport chemicals and radionuclides from source areas at the LANL facility to exposure locations downstream.

Several groups at the LANL facility and other agencies have been studying the erosion processes and the potential for increases in erosion following the Cerro Grande Fire. The premise is that the fire-damaged areas are denuded of vegetation that would typically limit erosion of surface materials, and the soil in those areas has been impacted by the heat of the fire and have become hydrophobic, thereby decreasing storm water retention and infiltration. The BAER Team developed estimates of pre-fire and post-fire soil losses using the Universal Soil Loss Equation (USLE). The USLE methodology calculates long-term annual soil loss rates for land areas based on soil characteristics, rainfall, land slope, and the vegetation characteristics of the land area. Results are typically reported in tons of sediment per acre per year for a watershed (Maidment 1993). The results of the BAER Team's work are included in the BAER Team CD ROM (LANL 2000). Nyhan et al. (2001) used a similar methodology to the BAER Team. Their work involved refinements to the USLE method to account for further spatial resolution of the design precipitation events and the vegetative ground and canopy cover. The BAER Team estimated that there might be a 7-fold increase in soil erosion following the Cerro Grande Fire, while Nyhan et al. (2001) estimated up to a 70-fold increase in soil erosion (Nyhan et al. 2001). Table 4-12 provides a summary of the estimated annual soil erosion rates.

Table 4-12. Estimated Annual Soil Erosion Rates (from Nyhan et al. 2001)^a

	BAER Team (LANL 2000) (tons acre ⁻¹ yr ⁻¹)	Nyhan et al. (2001) (tons acre ⁻¹ yr ⁻¹)
Pre-fire	3.7E+05	3.0E+04
Post-fire	2.7E+06	2.1E+06
Increase	7 times	70 times

^a The reported values are total values for the entire modeling area that includes 16 defined watershed areas from Santa Clara Canyon in the north to Los Frijoles Canyon in the south.

The annual soil erosion rates calculated by these two methods give a perspective on the damage to the watershed and with the large predicted soil losses, the exacerbating difficulties inherent in vegetation regrowth within the burned areas. These conditions are an indicator of the potential for storm events to have a larger flow impact downstream in the watersheds and are important results for the overall risk analysis project. However, it is difficult to translate these annual soil erosion rates into stream loading values for transport calculations or to use these estimates to infer sediment deposition rates at receptor locations for the risk analysis.

Wilson et al. (2001) developed an innovative modeling methodology to estimate erosion using the Hillslope Erosion model (Lane et al. date unknown) integrated with GIS data to parameterize the Hillslope Erosion model. This Hillslope Erosion model addresses the translation of watershed erosion potential into actual stream channel delivery. The results of their study are estimates of sediment yield in tons within the stream channels. Additional stream channel modeling is required to develop resulting channel sedimentation and resuspension estimates. The runoff calculated for the 100-year, 6-hour storm in this modeling work indicates an increase of 3 to 6 times post-fire over pre-fire estimates. The sediment yields indicate a 10-fold increase in sediment with the 100-year, 6-hour storm. Wilson et al. (2001) estimated that the 100-year, 6-hour storm transported 30 to 100% of the hillslope-derived sediment to a given stream channel. The model is a significant improvement over existing methods for evaluating sedimentation; however, it is a research scale model for which field calibration is currently being developed.

We determined that a contribution to the understanding of erosion in the vicinity of the LANL facility might be made and estimates developed for use in the risk analysis if an empirical data analysis study were implemented. Data were gathered from the ESH storm water and surface water monitoring programs as well as from the studies performed by the ER Project. These were the sources of suspended sediment data identified in the earlier data collection tasks. The ESH Division conducts a surface water flow and water quality sampling program from a network of gage and sampling stations throughout the LANL facility area. Data are available for flow and water quality parameters for some of the locations back to 1974. The ER Project has performed a more limited evaluation of sediment concentrations from selected locations within the canyons that cross LANL. Data that were available from the ER Project were collected during 2000 following the Cerro Grande Fire.

Information was not available about the selection of sample locations for the ER Project data. The ESH Division data are from established surface water monitoring gage stations. Both data sets include surface water and storm water sample results. For the purpose of these analyses, the samples were not differentiated. It appears, based on the available information, that the storm water samples refer to samples collected during rainfall-runoff events and the surface water samples are from stream flow at other times. All of the samples are listed as unfiltered samples. For the ESH Division data, the results are identified as being from the general inorganic analysis suite. Some records note that the method used is EPA method 160.2, others indicate gravimetric analysis, still others indicate "EH-WET" and some records do not list a method. For the ER Project data, there are no analytical methods specified in the data tables. We assumed all of the results to represent equivalent quantities.

For this work, the important data are the measurements of TSS in surface water samples, the locations in stream channels from which the samples were taken, and the stream flow at the time the samples were collected. We designed our approach to develop relationships between pre-fire

and post-fire TSS concentrations, between TSS concentrations and flow, and TSS concentrations and drainage area. Availability of data was an important consideration in evaluating this approach. In the data set from the ER Project, there are approximately 40 results for TSS for surface water and storm water. These data were collected from June 17, 2000, through November 2, 2000, and were used in the evaluation of the post-fire TSS concentrations. In the historical and current data sets from the ESH Division there are over 400 individual measurements of TSS, including sample replicates and laboratory quality assurance samples, representing various flow conditions and spatial locations. These data were collected from April 15, 1974, through December 6, 2000. For the ESH data set, flow measurements were available for approximately 100 TSS concentration results. These include estimates of flows based on daily peak flows and sample replicates. All of the available flow and corresponding TSS data are from 2000; therefore, no values were available for the pre-fire conditions.

An initial evaluation of the combined data set revealed that there were insufficient data to characterize TSS concentrations based on individual watersheds (e.g., low number of sampling locations in the individual watersheds and less than 10 sample results for an individual sampling location pre- or post-fire). Therefore, we used the entire data set to evaluate the characteristics of the group of watersheds that cross the LANL facility.

In the evaluation of suspended sediment concentration as a function of drainage area, we used the calculated drainage patterns from the grid flow model discussed here to estimate the drainage area corresponding to each sampling location. The relationship between concentration and drainage area, based on studies conducted at the University of Texas (Melancon 1999), might be expected to be a linear relationship.

The relationship between suspended sediment concentration and flow is known as a sediment rating curve, and typically it is described by a power equation,

$$C_s = a \times Q^b \quad (4.12)$$

where the coefficients a and b are derived through regression analysis (Maidment 1993).

Event mean concentrations (EMC) can also be developed to represent suspended sediment concentrations under different flow conditions. These are derived from the flow and TSS concentration data for identified storm events. For the identified storm events, the TSS results are selected as a subset, and the statistics of these subsets are calculated and compared.

The empirical approach has the advantage of being site-based and relatively simple to implement, and it provides a comparison between the pre-fire and post-fire conditions. Because the risk analysis uses design storms for the risk calculations, the estimates of sediment concentrations at higher than normal surface water flows includes extrapolations from existing data and, therefore, includes potentially significant uncertainty.

4.2.2 Erosion Estimate Results and Discussion

The initial calculation is the comparison of TSS concentration before and after the fire. TSS data were divided into two groups: those collected before May 31, 2000, (pre-fire) and those after May 31, 2000, (post-fire). For simplicity in the analyses, we used only the primary sampling results, that is, we removed the sample replicates from the data sets before the data analyses were implemented. Based on a review of the replicate values, this approach was appropriate because

the variability in the replicate results was well within the overall variability of the data values. We calculated the descriptive statistics of each data set and the values for the base-10 logarithms of each data set. Table 4-13 gives the pre-fire results and Table 4-14 gives the post-fire results.

Table 4-13. Pre-fire TSS Concentration Descriptive Statistics

Measure	TSS (mg L ⁻¹)	Log(TSS) (mg L ⁻¹)
Number of results	1.9E+02	1.9E+02
Mean	9.9E+02	1.5E+00
Standard deviation	3.2E+03	1.2E+00
Coefficient of variation	2.4E+02	7.9E-01
Skewness	4.3E+00	5.3E-01
Standard error of the mean	2.4E+02	8.7E-02

Based on the results in Table 4-13, the logarithms of the pre-fire concentrations can be considered to be normally distributed, whereas the original data values cannot.

Table 4-14. Post-fire TSS Concentration Descriptive Statistics

Measure	TSS (mg L ⁻¹)	Log(TSS) (mg L ⁻¹)
Number of results	1.9E+02	1.9E+02
Mean	8.2E+03	3.0E+00
Standard deviation	1.5E+04	1.3E+00
Coefficient of variation	1.8E+00	4.2E-01
Skewness	3.8E+00	-6.7E-01
Standard error of the mean	1.1E+03	9.2E-02

The number of samples in the pre- and post-fire data sets coincidentally is equal. Based on the results in Table 4-14, as was seen with the pre-fire data, the logarithms of the post-fire concentrations can be considered to be normally distributed, whereas the original data values cannot. The values indicate a 10-fold increase in the average sediment concentration after the fire. These results are consistent with the model findings from Wilson et al. (2001) and Nyhan et al. (2001). We calculated the t-statistic to compare the means of the pre-and post-fire log (concentration) data. The t value is (-184), which indicates that the means are statistically different.

To evaluate the variation in the mean values based on the number of samples evaluated, we developed plots of cumulative mean compared to number of samples. These are shown in Figure 4-16 for the pre-fire data and in Figure 4-17 for the post-fire data.

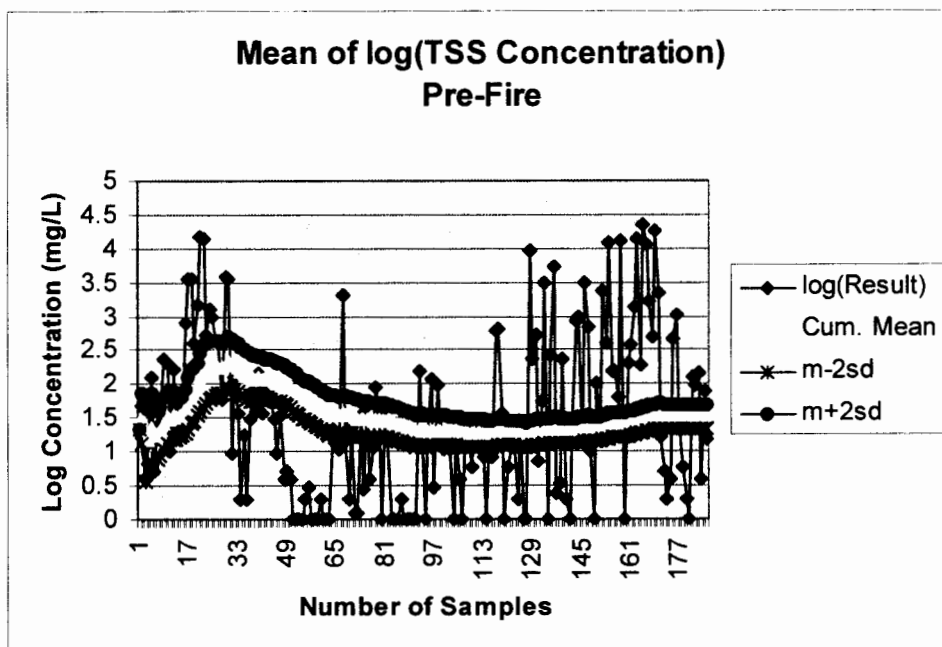


Figure 4-16. Pre-fire convergence of the sample mean. While there is a great deal of variability in the measured values, the data set is large enough to indicate the range of variation in the mean value. The variation in the mean value is represented by the mean plus and minus two standard deviations.

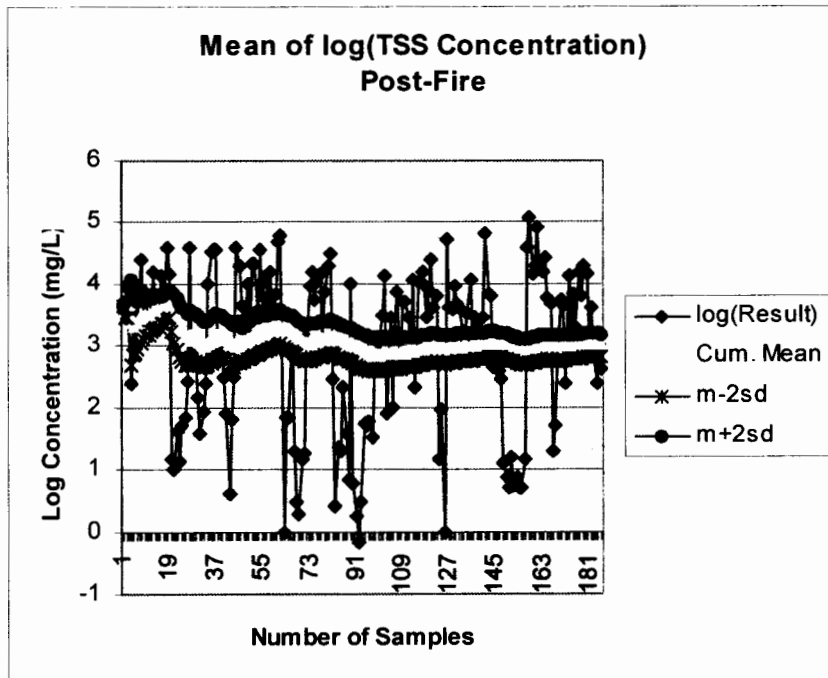


Figure 4-17. Post-fire convergence of the sample mean. While there is a great deal of variability in the measured values, the data set is large enough to indicate the range of variation in the mean value. The variation in the mean value is represented by the mean plus and minus two standard deviations.

The figures illustrate the variability of the measurements and the convergence of the uncertainties of the means of each of the data sets. While there is a great deal of variability in the measured values, the data sets are large enough to indicate the range of variation in the mean values. The variation in the mean value is represented by the mean plus and minus two standard deviations.

We explored the relationship between drainage area and TSS concentration using the data collected by the ESH Division. These data included specific monitoring locations where multiple samples have been collected. The locations of the ER Project samples were available as X and Y coordinates; however, for the most part, only individual samples were collected at each location. Due to sample variability, including temporal variability, we concluded that an average TSS concentration for each sample location would be a more appropriate measure to relate to drainage area. We used Geo-HMS data and the point coverage of sample locations for the ESH data to estimate the drainage area above each sample location. Because the stream networks and drainage areas were calculated locations, if the sample location was not directly on the stream channel, we moved it onto the stream channel so that the drainage area values were appropriate for the location.

Figure 4-18 shows the plot of the logarithms of the mean concentrations for each sampling location as a function of the estimated drainage area.

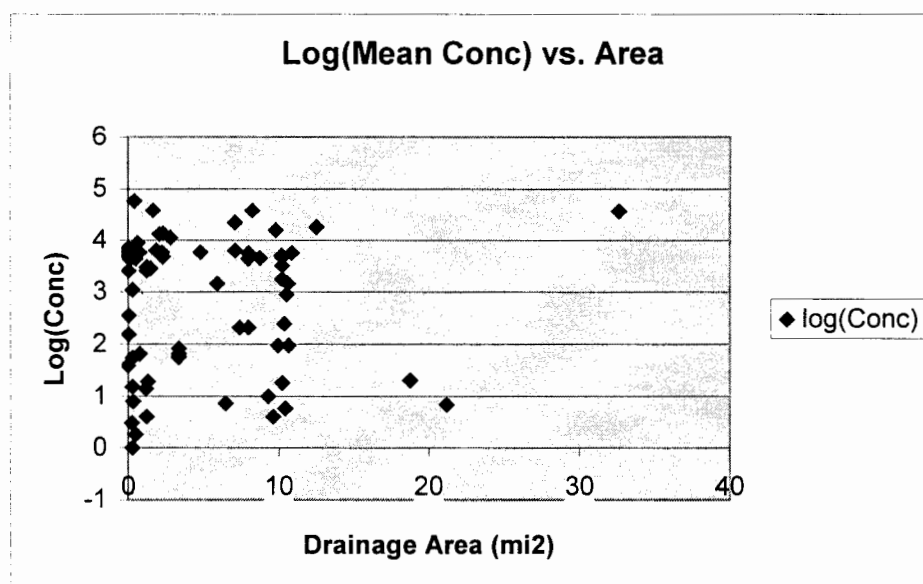


Figure 4-18. TSS concentration as a function of drainage area (in mi²).

The results do not indicate a functional relationship between the TSS concentrations and the drainage areas. Evaluating both quantities (i.e., concentration and drainage area) as logarithms also did not suggest a functional relationship. We conducted an additional analysis by selecting only the permanent monitoring stations with Gage ID "EXXX," for which drainage areas could be verified with the ESH Water year reports (e.g., LANL 1999b) and with 10 or more TSS results. Results for nine gage locations met these criteria. Figure 4-19 shows the results of this analysis.

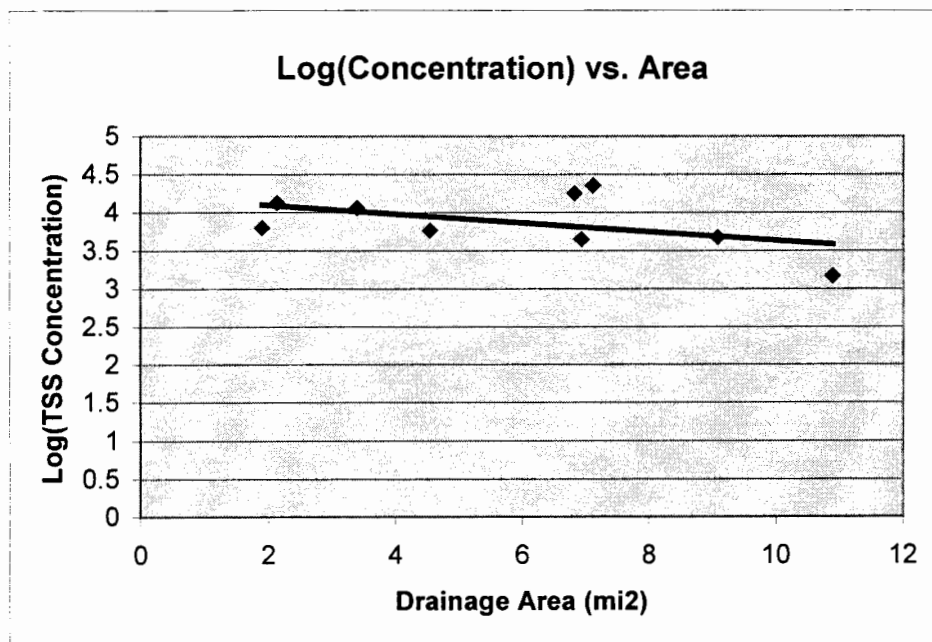


Figure 4-19. TSS concentration as a function of drainage area (mi²).

It is interesting to note based on the data plot that there appears to be something of an inverse relationship between drainage area and TSS concentration. It might be expected that the concentrations would increase with increasing drainage area. The trend is slight, which also might indicate that given the terrain, flow rates, and soil conditions that there is a maximum TSS concentration generated. The regression statistics for the linear relationship between drainage area and the logarithm of TSS concentrations are included in Table 4-15.

**Table 4-15. Regression Statistics for TSS
as a Function of Drainage Area**

Parameter	Value
Slope	-5.8E-02
Intercept	4.2E+00
t-statistic (slope)	-1.5E+00
t-statistic (intercept)	1.6E+01
F-ratio	2.2E+00
R-squared value	2.4E-01

The t-statistic for the intercept is the only test that is significant for the linear regression of the logarithm (concentration) and drainage area. A direct functional relationship cannot be developed from these data; however, the TSS values appear to fall within a range between 1000 and 40,000 mg L⁻¹ for the range of drainage areas evaluated. These data can be applied to the TSS estimating process for the risk analysis calculations.

We also analyzed the TSS data as a function of stream flow using TSS and flow data from 2000. These data represent post-fire conditions. The data analyses were implemented using the available flow data and the primary sampling results. The flow values were assigned from the

5-minute records from each surface water gage station. The flow values were assigned either using the exact start time from the flow record or the value from the next 5-minute interval (Alexander 2001). There are 38 flow and TSS records that met these criteria. Upon further inspection, there were eight TSS values assigned identical flow values, indicating that two samples appear to have been taken within the same 9-minute interval. For these values, the two measured concentrations were averaged. The final data set includes 34 flow and TSS records. These values were plotted to derive a sediment rating curve. The scatter plot of the data is shown in Figure 4-20.

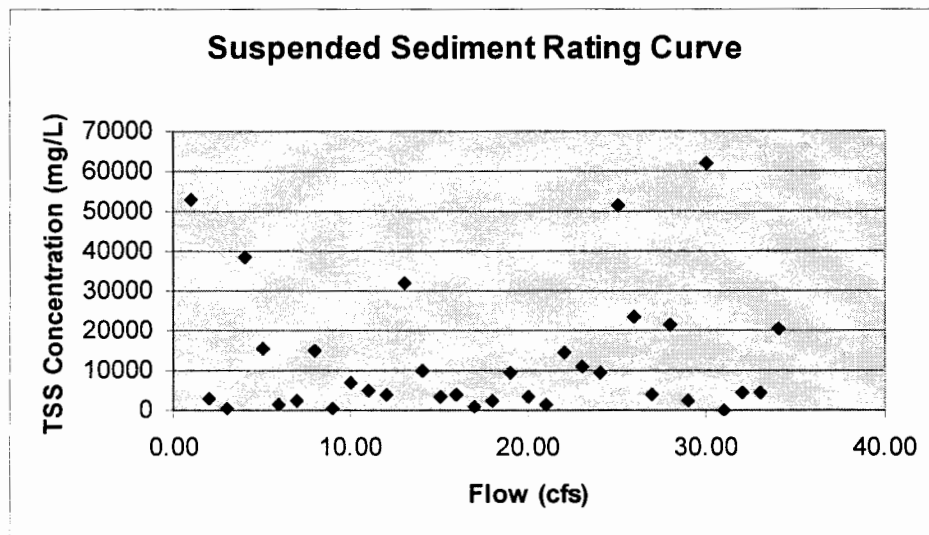


Figure 4-20. TSS concentration as a function of stream flow.

No functional relationship is evident from the scatter plot. It is possible that the variability in the flow measuring locations in the different channels and the range of flow regimes makes turbulence in the flow an important consideration in the TSS measurements. Therefore, the characteristics of each stream and each gage station would also factor into the relationship between flow and TSS concentration. However, the limited data set for TSS concentration with corresponding storm water low measurements precluded this further analysis.

4.3 Points of Exposure

We considered four scenarios for the risk calculations based on the results of the site conceptual model:

1. Local fisher and hunter from White Rock
2. Farm family living below Cochiti Lake
3. Resident living on the Rio Grande below the confluence of the Water Canyon outlet to the Rio Grande
4. Local fire cleanup worker and others on LANL site during and after the fire.

These scenarios are discussed in more detail in Chapter 5.

For each of these exposure scenarios, it was necessary to identify a likely point of exposure to represent a location where an individual, represented by a scenario, is likely to come in contact with storm water, surface water, suspended sediments, or deposited sediments containing concentrations of chemicals or radionuclides. However, the point of exposure can vary over a large area of the surface water domain. As a result, the concentration of chemicals and radionuclides to which an individual may be exposed can also vary depending on the location of the source areas, the storm water flow, and the suspended sediment at the point of exposure. Therefore, we selected points of exposure in areas where individuals represented by the scenarios were likely to be located that were immediately downgradient of source areas or at the outlet points of a watershed. In addition, to evaluate potential exposures to the highest potential concentration of chemicals and radionuclides, we conservatively assumed that the point of exposure for each scenario would be within a stream segment where the highest storm water flow and sediment concentration would be expected. These stream segments were identified as part of the delineation of the watersheds for the storm water flow estimates.

On this basis, we identified seven points of exposure (Figure 4-21) to represent the four exposure scenarios:

1. Point of exposure (POE) 1.1 is associated with the first scenario and represents a location where a local fisher and hunter from White Rock may hunt or fish on the east side of the Rio Grande just below LANL.
2. POE 1.2 is also associated with the first scenario and represents a location where a local fisher and hunter from White Rock that may hunt or fish in the lower Los Alamos Canyon.
3. POE 2.1BD is associated with the second scenario and represents a location where a farm family is living on land below the Cochiti Lake near the Rio Grande.
4. POE 2.1R is also associated with the second scenario and represents a location where a farm family living on land below the Cochiti Lake near the Rio Grande spends their leisure time boating and swimming in the Cochiti Lake.
5. POE 3.1 is associated with the third scenario and represents a location where a resident lives on the Rio Grande below the confluence of the Water Canyon outlet to the Rio Grande.
6. POE 4.1a is associated with the fourth scenario and represents a location where local fire cleanup workers and others on LANL site may have been present during and after the fire.
7. POE 4.1b is also associated with the fourth scenario and also represents a location where local fire cleanup workers and others on LANL site may have been present during and after the fire.

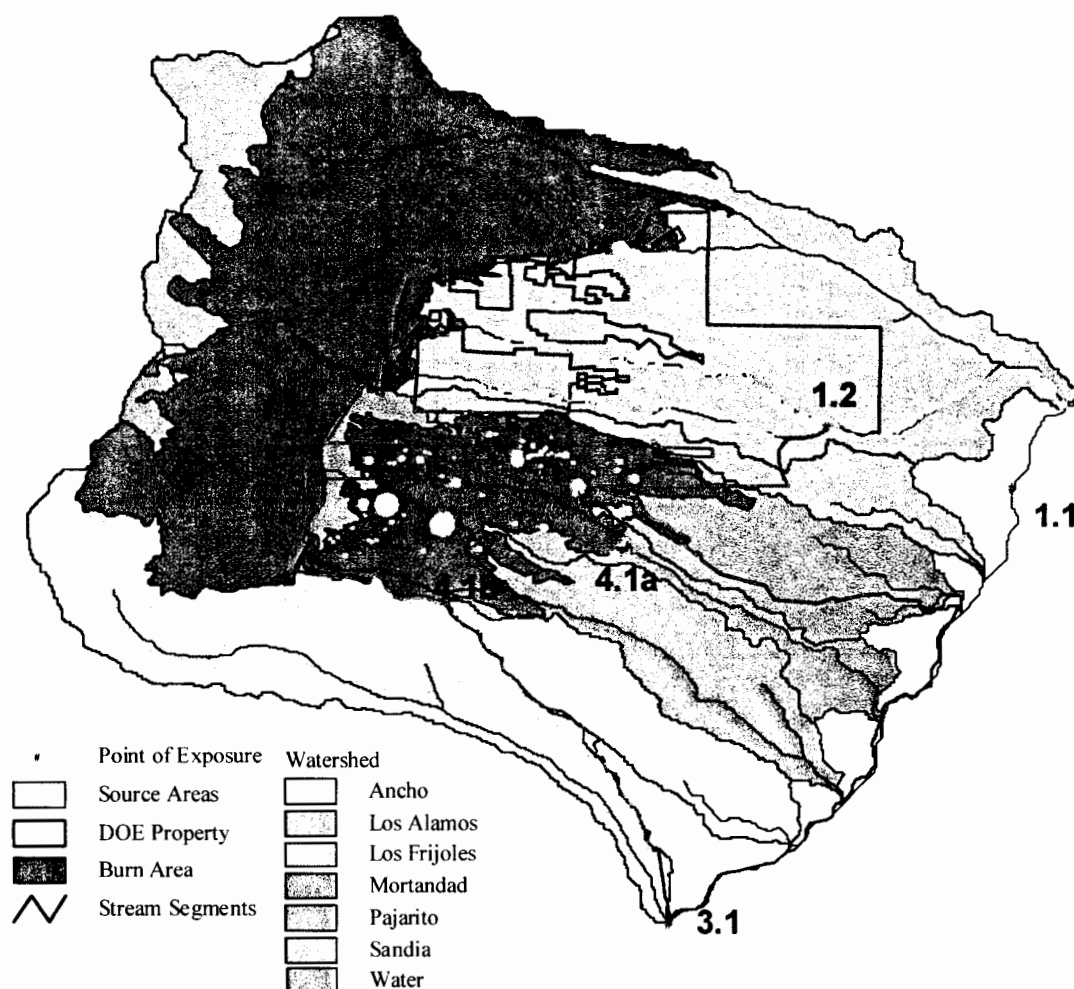


Figure 4-21. Point of exposure locations for POE 1.1, 1.2, 3.1, 4.1a, and 4.1b. The point of exposure locations for POE 2.1R and POE 2.1BD on and below Cochiti Lake are not shown.

We identified watersheds and stream segments that contributed storm water flow to each point of exposure using the methodology discussed previously and we created GIS polygon shape files. We obtained storm water flow at the point of exposure for each pre-fire and post-fire storm event from the storm water grids developed for the storm water modeling. Table 4-16 summarizes the storm water flow associated with each point of exposure. PRS, burn area, geomorphic units, and unsampled reaches (collectively referred to as source areas) associated with each watershed were identified by clipping the GIS polygon shapefiles for the burn area and source areas using the polygon shapefile for the watershed associated with each point of exposure.

Table 4-16. Storm Water Flow at the Points of Exposure

POE	2-year flow	5-year flow	10-year flow	25-year flow	50-year flow	100-year flow	500-year flow
Watershed pre-fire storm water flow (cfs)							
POE 1.1	2.3E+02	6.5E+02	1.0E+03	1.6E+03	2.0E+03	2.5E+03	3.8E+03
POE 1.2	5.5E+01	1.9E+02	3.2E+02	5.2E+02	6.6E+02	8.3E+02	1.3E+03
POE 2.1BD & 2.1R	4.1E+02	1.2E+03	1.9E+03	2.9E+03	3.7E+03	4.7E+03	7.3E+03
POE 3.1	4.1E+02	1.2E+03	1.9E+03	2.9E+03	3.7E+03	4.7E+03	7.3E+03
POE 4.1a	3.2E+01	9.6E+01	1.5E+02	2.4E+02	3.0E+02	3.7E+02	5.5E+02
POE 4.1b	2.6E+01	9.7E+01	1.6E+02	2.6E+02	3.3E+02	4.2E+02	6.3E+02
Watershed post-fire storm water flow (cfs)							
POE 1.1	2.3E+03	3.4E+03	4.2E+03	5.2E+03	5.9E+03	6.7E+03	8.6E+03
POE 1.2	8.7E+02	1.3E+03	1.6E+03	1.9E+03	2.2E+03	2.5E+03	3.1E+03
POE 2.1BD & 2.1R	3.7E+03	5.7E+03	7.1E+03	9.0E+03	1.0E+04	1.2E+04	1.6E+04
POE 3.1	3.7E+03	5.7E+03	7.1E+03	9.0E+03	1.0E+04	1.2E+04	1.6E+04
POE 4.1a	4.7E+02	6.9E+02	8.4E+02	1.0E+03	1.1E+03	1.3E+03	1.6E+03
POE 4.1b	5.6E+02	8.6E+02	1.1E+03	1.3E+03	1.5E+03	1.6E+03	2.0E+03

POE 1.1 is located along the Rio Grande below the outlet for the Los Alamos watershed as defined in the storm water flow modeling. Concentrations of chemicals and radionuclides in storm water, surface water, suspended sediments, and deposited sediments at this point of exposure result from source areas within the Los Alamos watershed. The volume of water at this point of exposure is a result of storm water flow within the Los Alamos watershed and surface water flow in the Rio Grande. The total volume of suspended sediments at this point of exposure is a result of erosion within the Los Alamos watershed and suspended sediments in the Rio Grande. Figure 4-22 shows the watershed, burn area, other source areas, and stream segments associated with POE 1.1. Table 4-17 summarizes the source areas that are included in the POE 1.1 watershed.



Figure 4-22. POE 1.1 watershed.

Table 4-17. Source Areas Included in POE 1.1

PRS-2	PRS-235	GEO-282	GEO-297	GEO-312	GEO-327	RCH-355
PRS-3	PRS-267	GEO-283	GEO-298	GEO-313	GEO-328	RCH-356
PRS-4	GEO-269	GEO-284	GEO-299	GEO-314	GEO-329	RCH-340
PRS-5	GEO-270	GEO-285	GEO-300	GEO-315	GEO-330	RCH-341
PRS-6	GEO-271	GEO-286	GEO-301	GEO-316	GEO-331	RCH-342
PRS-7	GEO-272	GEO-287	GEO-302	GEO-317	GEO-332	RCH-343
PRS-8	GEO-273	GEO-288	GEO-303	GEO-318	GEO-333	RCH-344
PRS-9	GEO-274	GEO-289	GEO-304	GEO-319	GEO-334	RCH-345
PRS-10	GEO-275	GEO-290	GEO-305	GEO-320	RCH-335	RCH-346
PRS-153	GEO-276	GEO-291	GEO-306	GEO-321	RCH-353	RCH-347
PRS-199	GEO-277	GEO-292	GEO-307	GEO-322	RCH-336	RCH-348
PRS-200	GEO-278	GEO-293	GEO-308	GEO-323	RCH-354	RCH-349
PRS-201	GEO-279	GEO-294	GEO-309	GEO-324	RCH-337	RCH-350
PRS-202	GEO-280	GEO-295	GEO-310	GEO-325	RCH-338	RCH-351
PRS-203	GEO-281	GEO-296	GEO-311	GEO-326	RCH-339	RCH-352

POE 1.2 is located on the stream segment immediately below the LANL property immediately below the confluence of the stream segments from the Pueblo and Los Alamos Canyons. Concentrations of chemicals and radionuclides in storm water, sediments, and deposited sediments at this point of exposure result from source areas within the Pueblo and Los Alamos Canyons. The total volume of suspended sediments at this point of exposure is a result of erosion

within the Pueblo and Los Alamos Canyons. The volume of water at this point of exposure is a result of storm water flow within the Pueblo and Los Alamos Canyons. Figure 4-23 shows the watershed, burn area, other source areas, and stream segments associated with POE 1.2. Table 4-18 summarizes the source areas that are in the POE 1.2 watershed.

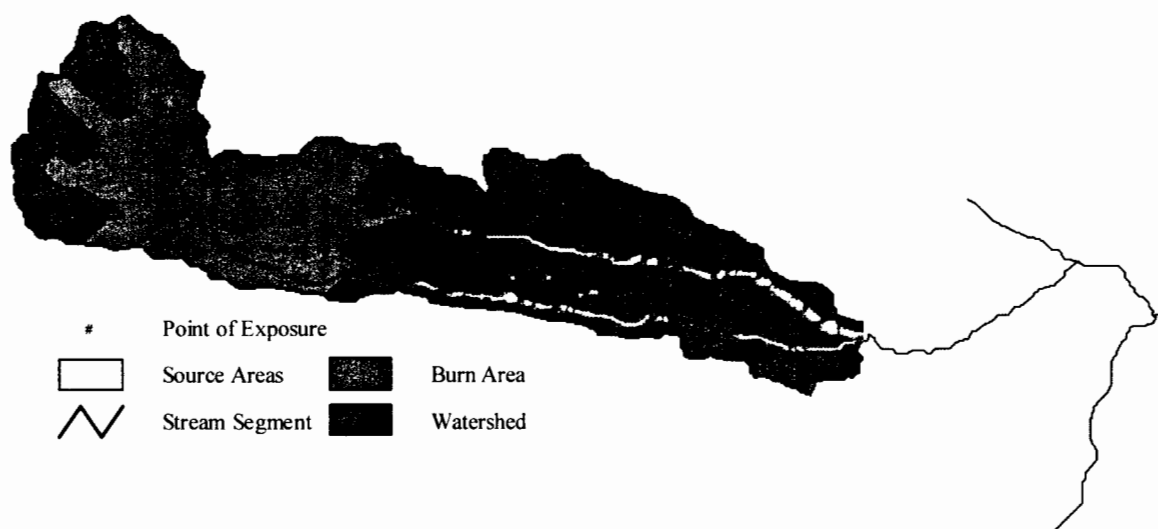


Figure 4-23. POE 1.2 watershed.

Table 4-18. Source Areas Included in POE 1.2

PRS-5	GEO-271	GEO-287	GEO-303	GEO-327	RCH-340
PRS-6	GEO-272	GEO-288	GEO-304	GEO-328	RCH-341
PRS-7	GEO-273	GEO-289	GEO-305	GEO-329	RCH-342
PRS-8	GEO-274	GEO-290	GEO-306	GEO-330	RCH-343
PRS-9	GEO-275	GEO-291	GEO-307	GEO-331	RCH-344
PRS-10	GEO-276	GEO-292	GEO-316	GEO-332	RCH-345
PRS-153	GEO-277	GEO-293	GEO-317	GEO-333	RCH-346
PRS-199	GEO-278	GEO-294	GEO-318	GEO-334	RCH-347
PRS-200	GEO-279	GEO-295	GEO-319	RCH-335	RCH-348
PRS-201	GEO-280	GEO-296	GEO-320	RCH-353	RCH-349
PRS-202	GEO-281	GEO-297	GEO-321	RCH-336	
PRS-203	GEO-282	GEO-298	GEO-322	RCH-354	
PRS-235	GEO-283	GEO-299	GEO-323	RCH-338	
PRS-267	GEO-284	GEO-300	GEO-324	RCH-339	
GEO-269	GEO-285	GEO-301	GEO-325	RCH-355	
GEO-270	GEO-286	GEO-302	GEO-326	RCH-356	

POE 2.1R is located on the Cochiti Lake and is not shown on Figure 4-21. Concentrations of chemicals and radionuclides in storm water, surface water, suspended sediments, and deposited sediments result from source areas within the Ancho, Los Alamos, Los Frijoles, Mortandad, Pajarito, Sandia, and Water watersheds. The total volume of suspended sediments at this point of exposure is a result of erosion within the Ancho, Los Alamos, Los Frijoles, Mortandad, Pajarito,

Sandia, and Water watersheds; suspended sediments in the Rio Grande; and suspended sediments in the Cochiti Lake. The volume of water at this point of exposure is a result of storm water flow within the Ancho, Los Alamos, Los Frijoles, Mortandad, Pajarito, Sandia, and Water watersheds; surface water flow in the Rio Grande; and the volume of water stored in the Cochiti Lake. Figure 4-24 shows the watershed, burn area, other source areas, and stream segments associated with POE 2.1R. All of the source areas contribute to this POE.

POE 2.1BD is located below the Cochiti Dam and is not shown on Figure 4-21. Concentrations of chemicals and radionuclides in storm water, surface water, suspended sediments, and deposited sediments result from source areas within the Ancho, Los Alamos, Los Frijoles, Mortandad, Pajarito, Sandia, and Water watersheds. Because the Cochiti Lake provides sediment control on the Rio Grande, the total volume of suspended sediments at this point of exposure is the suspended sediment in the Rio Grande after the Cochiti Dam. The volume of water at this point of exposure is a result of storm water flow within the Ancho, Los Alamos, Los Frijoles, Mortandad, Pajarito, Sandia, and Water watersheds; surface water flow in the Rio Grande; and the volume of water stored in the Cochiti Lake. Figure 4-24 shows the watershed, burn area, other source areas, and stream segments associated with POE 2.1BD. All of the source areas contribute to this POE.

POE 3.1 is located along the Rio Grande immediately below the confluence of the Los Frijoles watershed and the Rio Grande. Concentrations of chemicals and radionuclides in storm water, suspended sediments, and deposited sediments at this point of exposure result from source areas within the Ancho, Los Alamos, Los Frijoles, Mortandad, Pajarito, Sandia, and Water watersheds. The total volume of suspended sediments at this point of exposure is a result of erosion within the Ancho, Los Alamos, Los Frijoles, Mortandad, Pajarito, Sandia, and Water watershed and suspended sediments in the Rio Grande. The volume of water at this point of exposure is a result of storm water flow within the Ancho, Los Alamos, Los Frijoles, Mortandad, Pajarito, Sandia, and Water watersheds and surface water flow in the Rio Grande. Figure 4-24 shows the watershed, burn area, other source areas, and stream segments associated with POE 3.1. All of the source areas are in the POE 3.1 watershed.

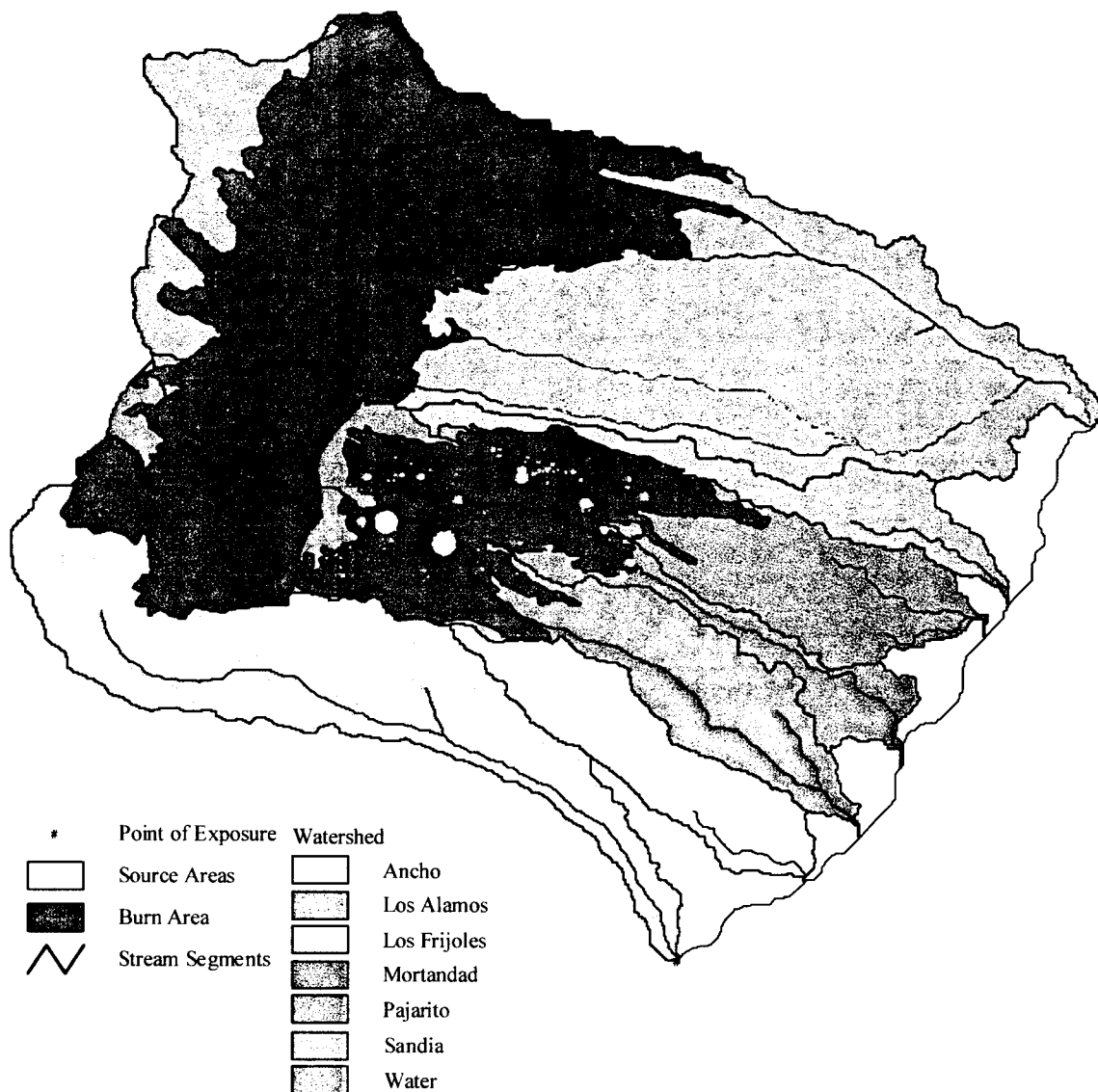


Figure 4-24. POE 2.1R, 2.1BD, and 3.1 watershed.

POE 4.1a is located on a stream segment immediately below the source areas in the Pajarito watershed. Concentrations of chemicals and radionuclides in storm water, suspended sediments, and deposited sediments at this point of exposure result from source areas within the portion of the Pajarito watershed contributing to this location on the stream segment. The total volume of suspended sediments at this point of exposure is a result of erosion within the portion of the Pajarito watershed contributing to this location on the stream segment. The volume of water at this point of exposure is a result of storm water flow within the portion of the Pajarito watershed contributing to this location on the stream segment. Figure 4-25 shows the watershed, burn area, other source areas, and stream segments associated with POE 4.1a. Table 4-19 summarizes the source areas that are in the POE 4.1a watershed.



Figure 4-25. POE 4.1a watershed.

Table 4-19. Source Areas Included in POE 4.1a

PRS-25	PRS-37	PRS-49	PRS-160	PRS-228	PRS-246
PRS-26	PRS-38	PRS-56	PRS-194	PRS-236	PRS-247
PRS-27	PRS-39	PRS-57	PRS-195	PRS-237	PRS-248
PRS-28	PRS-40	PRS-102	PRS-196	PRS-238	PRS-249
PRS-29	PRS-41	PRS-139	PRS-197	PRS-239	PRS-250
PRS-30	PRS-42	PRS-154	PRS-198	PRS-240	PRS-251
PRS-31	PRS-43	PRS-155	PRS-212	PRS-241	PRS-252
PRS-32	PRS-44	PRS-156	PRS-213	PRS-242	PRS-253
PRS-33	PRS-45	PRS-157	PRS-215	PRS-243	PRS-255
PRS-34	PRS-46	PRS-158	PRS-217	PRS-244	PRS-256
PRS-35	PRS-47	PRS-159	PRS-227	PRS-245	PRS-257
PRS-36	PRS-48				

POE 4.1b is located on a stream segment immediately below the source areas in the Water watershed. Concentrations of chemicals and radionuclides in storm water, suspended sediments, and deposited sediments at this point of exposure result from source areas within the portion of the Water watershed contributing to this location on the stream segment. The total volume of sediments at this point of exposure is a result of erosion within the portion of the Water watershed

contributing to this location on the stream segment. The volume of water at this point of exposure is a result of storm water flow within the portion of the Water watershed contributing to this location on the stream segment. Figure 4-26 shows the watershed, burn area, other source areas, and stream segments associated with POE 4.2b. Table 4-20 summarizes the source areas that are in the POE 4.1b watershed.

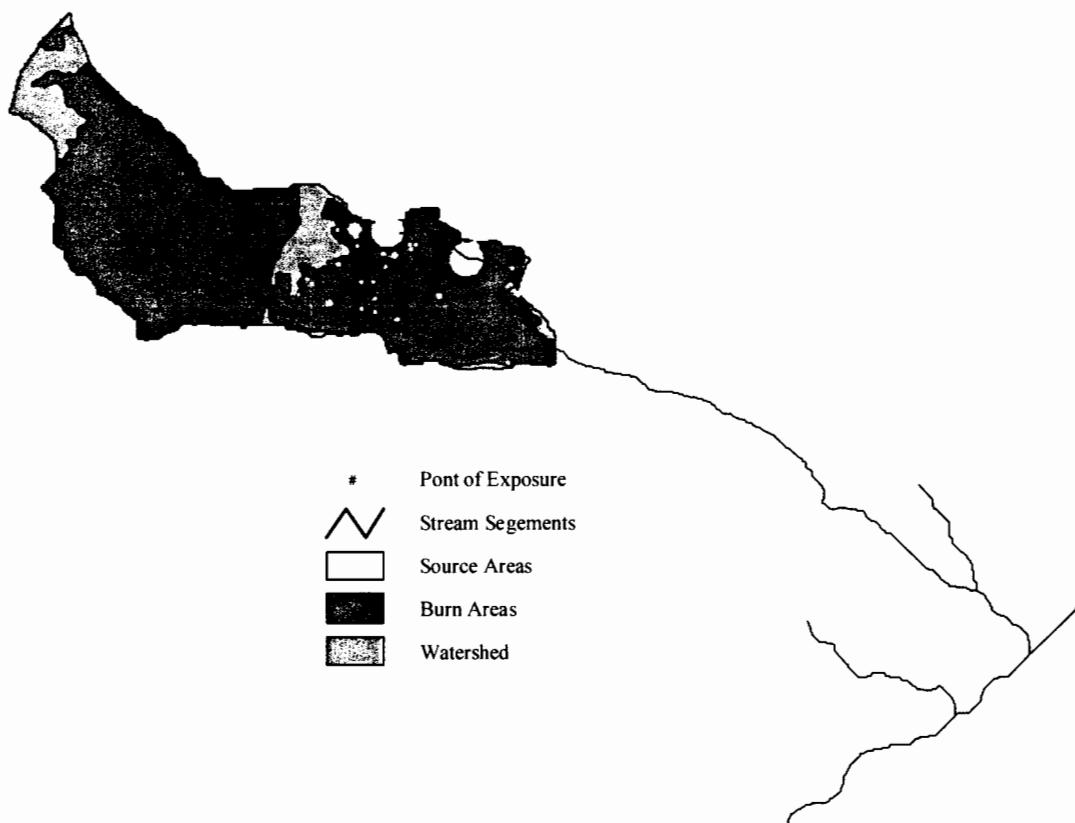


Figure 4-26. POE 4.1b watershed.

Table 4-20. Source Areas Included in POE 4.1b

PRS-50	PRS-77	PRS-92	PRS-106	PRS-120	PRS-134
PRS-51	PRS-78	PRS-93	PRS-107	PRS-121	PRS-135
PRS-52	PRS-79	PRS-94	PRS-108	PRS-122	PRS-136
PRS-53	PRS-81	PRS-95	PRS-109	PRS-123	PRS-224
PRS-54	PRS-82	PRS-96	PRS-110	PRS-124	PRS-260
PRS-55	PRS-83	PRS-97	PRS-111	PRS-125	PRS-261
PRS-60	PRS-84	PRS-98	PRS-112	PRS-126	PRS-262
PRS-61	PRS-85	PRS-99	PRS-113	PRS-127	PRS-263
PRS-62	PRS-86	PRS-100	PRS-114	PRS-128	PRS-264
PRS-63	PRS-87	PRS-101	PRS-115	PRS-129	PRS-265
PRS-64	PRS-88	PRS-102	PRS-116	PRS-130	
PRS-67	PRS-89	PRS-103	PRS-117	PRS-131	
PRS-75	PRS-90	PRS-104	PRS-118	PRS-132	
PRS-76	PRS-91	PRS-105	PRS-119	PRS-133	

4.4 Chemical and Radionuclide Concentration Estimates at Points of Exposure

To estimate the concentration of chemicals and radionuclides in suspended sediment, deposited sediment, storm water, and surface water at a point of exposure, we estimated the

- surface water flow and suspended sediment concentration in the Rio Grande
- volume of storm water that flowed across each source area
- volume of soil particles suspended in storm water as a result of soil erosion at each source area
- volume of suspended sediment and storm water transported to the point of exposure
- chemical mass or radionuclide activity transported to a point of exposure that was sorbed to suspended sediment in storm water and surface water
- chemical mass or radionuclide activity transported to the point of exposure that was dissolved in storm water and surface water.

The accumulated chemical mass and radionuclide activity in the volume of suspended sediment and storm water from a watershed contributing to a point of exposure provided the estimated concentrations of chemicals and radionuclides in suspended sediment, deposited sediment, storm water, and surface water at the point of exposure.

We developed estimated concentrations of chemicals and radionuclides for each point of exposure for pre-fire and post-fire 2-, 5-, 10-, 25-, 50-, 100-, and 500-year design storm events. To develop these estimates, we specified a number of assumptions and conditions:

1. The mass of suspended sediment movement from a source area to a point of exposure can be estimated from a TSS concentration.
2. The concentration of TSS is uniform throughout the surface water domain.
3. All TSS in storm water over a source area results from the source area for purposes of estimating the maximum chemical mass and radionuclide activity released from a source area during a storm event.
4. There is no loss of chemical mass or radionuclide activity through deposition or other attenuation mechanisms between the source area and the point of exposure.
5. The total chemical mass and radionuclide activity in suspended sediment at a point of exposure is equal to the sum of the chemical mass and radionuclide activity in the soil suspended during a storm event based on estimated average soil concentrations for each source area.
6. Concentrations of chemicals and radionuclides in storm water result from equilibrium partitioning between the soil particles and the water.
7. A simple mass balance of chemicals and radionuclides between storm water and soil particles is considered.
8. Dilution is the only attenuation mechanism considered for concentrations of chemicals and radionuclides in soil, sediments, and surface water at the points of exposure.

4.4.1 Chemical Mass and Radionuclide Activity at the Source Areas

The material that is transported by a storm event is a combination of the volume (V_w) of water that passes over a source area during a storm event and the volume (V_{ss}) of suspended sediment in the volume of water as a result of erosion of the surface soil in the source area. The total unit volume (V_T), a combination of the volume of water and suspended sediment is described in units of liters (L) by

$$V_T(L) = V_w(L) + V_{ss}(L) \quad (4.13)$$

In a similar fashion, the total chemical mass (M_T), a combination of the chemical mass (M_w) in water and sorbed to soil particles (M_{ss}), can be represented as follows, in units of milligrams (mg):

$$M_T(\text{mg}) = M_w(\text{mg}) + M_{ss}(\text{mg}) \quad (4.14)$$

The total activity of radionuclide (A_T), a combination of the activity of radionuclide (A_w) in water and sorbed to soil particles (A_{ss}), can be represented as follows, in unit of picocuries (pCi):

$$A_T(\text{pCi}) = A_w(\text{pCi}) + A_{ss}(\text{pCi}) \quad (4.15)$$

As discussed previously, concentrations of chemicals and radionuclides (C_{soil}) have been estimated for surface soils in source areas identified in the surface water domain based on analytical results from soil, sediment, and ash samples (Appendix G). For purposes of this evaluation, the sediment and ash were assumed to have similar properties to soil. Therefore, these concentrations are representative of chemical mass and radionuclide activity sorbed to the suspended sediment, dissolved in the soil pore water, and volatilized in the soil pore air, and they were assumed to be uniform throughout the depth of soil that would erode or be suspended in the volume of storm water that flows across a source area.

Once the soil has eroded and becomes suspended in the volume of storm water (V_w), the total chemical mass or radionuclide activity that was present in the soil then represents the total mass of chemical or radionuclide present in the total unit volume (V_T). This assumes that there were no losses of chemical mass or radionuclide activity as a result of the mixing or turbulence of storm water flow. We assumed the analytical results were reported on a dry weight basis, and that the total mass of soil was represented by the TSS measured in a unit volume. In addition, we assumed that all of the TSS concentration in storm water that passed over a source area resulted from that source area. We took this conservative approach to estimate the maximum potential chemical mass and radionuclide activity that could result from a storm event. Therefore, we calculated the total chemical mass at the source area that is present in the unit volume by:

$$M_T(\text{mg}) = C_{\text{soil}} \left(\frac{\text{mg}}{\text{kg}} \right) \times \text{TSS} \left(\frac{\text{mg}}{\text{L}} \right) \times \text{CF} \left(\frac{\text{kg}}{\text{mg}} \right) \times V_T(L) \quad (4.16)$$

where CF is used to represent a unit conversion factor.

The total radionuclide activity in a unit volume at the source area that is available to be distributed between the suspended sediment and the water phase is

$$A_T(\text{pCi}) = C_{\text{soil}} \left(\frac{\text{pCi}}{\text{g}} \right) \times \text{TSS} \left(\frac{\text{mg}}{\text{L}} \right) \times \text{CF} \left(\frac{\text{g}}{\text{mg}} \right) \times V_T(\text{L}) \quad (4.17)$$

The chemical mass in water (M_w) is related to the concentration of the chemical (C_w) in a volume of water (V_w) by

$$M_w(\text{mg}) = C_w \left(\frac{\text{mg}}{\text{L}} \right) \times V_w(\text{L}) \quad (4.18)$$

The radionuclide activity in water (A_w) is related to the concentration of the radionuclide (C_w) in a volume of water (V_w) by

$$A_w(\text{pCi}) = C_w \left(\frac{\text{pCi}}{\text{L}} \right) \times V_w(\text{L}) \quad (4.19)$$

The chemical mass sorbed to suspended sediment (M_{ss}) is related to the concentration of the chemical (C_{ss}) in a volume of suspended sediment (V_{ss}) by

$$M_{ss}(\text{mg}) = C_{ss} \left(\frac{\text{mg}}{\text{L}} \right) \times V_{ss}(\text{L}) \quad (4.20)$$

The radionuclide activity sorbed to suspended sediment (A_{ss}) is related to the concentration of the radionuclide (C_{ss}) in a volume of suspended sediment (V_{ss}) by

$$A_{ss}(\text{pCi}) = C_{ss} \left(\frac{\text{pCi}}{\text{L}} \right) \times V_{ss}(\text{L}) \quad (4.21)$$

If we assume equilibrium partitioning between the suspended sediment and the water using a soil to water partitioning coefficient (K_d) that is chemical or radionuclide specific, the concentration of a chemical in the suspended (C_{ss}) is

$$C_{ss} \left(\frac{\text{mg}}{\text{L}} \right) = C_w \left(\frac{\text{mg}}{\text{L}} \right) \times K_d \left(\frac{\text{L}}{\text{kg}} \right) \times \text{CF} \left(\frac{\text{kg}}{\text{g}} \right) \times \rho_s \left(\frac{\text{g}}{\text{cm}^3} \right) \times \text{CF} \left(\frac{\text{cm}^3}{\text{L}} \right) \quad (4.22)$$

The concentration of a radionuclide in suspended sediment is

$$C_{ss} \left(\frac{\text{pCi}}{\text{L}} \right) = C_w \left(\frac{\text{pCi}}{\text{L}} \right) \times K_d \left(\frac{\text{L}}{\text{kg}} \right) \times CF \left(\frac{\text{kg}}{\text{g}} \right) \times \rho_s \left(\frac{\text{g}}{\text{cm}^3} \right) \times CF \left(\frac{\text{cm}^3}{\text{L}} \right) \quad (4.23)$$

By substituting Equations (4.20) and (4.22) into Equation (4.14) and rearranging, the chemical mass in the water phase (M_w) is

$$M_w (\text{mg}) = \frac{M_T (\text{mg})}{\left(1 + \frac{K_d \left(\frac{\text{L}}{\text{kg}} \right) \times \rho_s \left(\frac{\text{g}}{\text{cm}^3} \right) \times V_{ss} (\text{L}) \times CF \left(\frac{\text{cm}^3}{\text{L}} \right) \times CF \left(\frac{\text{kg}}{\text{g}} \right)}{V_w (\text{L})} \right)} \quad (4.24)$$

By substituting Equations (4.21) and (4.23) into Equation (4.15) and rearranging, the radionuclide activity in the water phase (A_w) is

$$A_w (\text{pCi}) = \frac{A_T (\text{pCi})}{\left(1 + \frac{K_d \left(\frac{\text{L}}{\text{kg}} \right) \times \rho_s \left(\frac{\text{g}}{\text{cm}^3} \right) \times V_{ss} (\text{L}) \times CF \left(\frac{\text{cm}^3}{\text{L}} \right) \times CF \left(\frac{\text{kg}}{\text{g}} \right)}{V_w (\text{L})} \right)} \quad (4.25)$$

The chemical mass sorbed to suspended sediment in a unit volume at a source area (M_{ss}) is

$$M_{ss} (\text{mg}) = M_T (\text{mg}) - M_w (\text{mg}) \quad (4.26)$$

The radionuclide activity sorbed to suspended sediment in a unit volume at a source area (A_{ss}) is

$$A_{ss} (\text{pCi}) = A_T (\text{pCi}) - A_w (\text{pCi}) \quad (4.27)$$

4.4.2 Soil to Water Partition Coefficients (K_d)

We compiled distribution or partition coefficients for each chemical and radionuclide and used them to estimate concentrations of chemicals and radionuclides in storm water runoff at each source area, based on the soil or sediment concentrations calculated for each source area (Table 4-21). These coefficients are defined as the concentration of an analyte in the solid phase divided by the dissolved concentration of that analyte in the liquid phase of a solution containing both solids and liquids. Values for these coefficients are typically reported with units such as liters per kilogram or milliliter per gram. It follows then that a lower coefficient implies a higher liquid phase concentration.

Table 4-21. Soil-Water Distribution (K_d) and Organic Carbon Partition (K_{oc}) Coefficients for Surface Water Source Term Chemicals and Radionuclides ($L\ kg^{-1}$)

Analyte name	Analyte	ORNL K_{oc}	ORNL K_d	NCRP (1996)	Baes et al. (1984)	Sheppard and Thibault (1990) (values for sand)			ESH-18	NMED
						Sand	Min	Max		
Aldrin		2450000^a								
Americium-241	Am			1900	700	1900	8.2	300000	2799	1570
Arsenic	As		200	110	200				275	1979
Barium	Ba		41	52	60				3357 ^b	3011
Benzo(a)anthracene		398000								
Benzo(a)pyrene		1020000								
Benzo(b)fluoranthene		1230000								
Benzo(k)fluoranthene		1230000								
Cesium-137	Cs			270	1000	280	0.2	10000	1650	32087 ^c
Chromium (total)	Cr		19	30	850	70	1.7	1729	1821	12130
Copper	Cu		428	30	35				1939	5331
Dibenz(a,h)anthracene		3800000								
Heptachlor Epoxide		83200								
Indeno(1,2,3-cd)pyrene		3470000								
Lead	Pb		900	270	900	270	19	1405	23114	36334
Lead-210	Pb			270	900	270	19	1405	2480	
Mercury	Hg	52		19	10					
Neptunium-237	Np			5	30	5	0.5	390		
Nitrosodimethylamine[N-]		8.3								
Plutonium-238	Pu			550	4500	550	27	36000	1581	2545
Plutonium-239	Pu			550	4500	550	27	36000	8248	7694
Potassium-40	K			18	5.5	15	nr	nr	327	
Protactinium-234M	Pa			510	2500	550	nr	nr		
Radium-224	Ra			500	450	500	nr	nr		
Radium-226	Ra			500	450	500	nr	nr	1201	
Radium-228	Ra			500	450	500	nr	nr	618	
RDX		7.1695								
Strontium-90	Sr		35	15	35	15	0.05	190	555	802
Thorium-228	Th			3200	150000	3200	207	150000	22024	11786 ^d
Thorium-230	Th			3200	150000	3200	207	150000	17048	14625 ^d
Thorium-232	Th			3200	150000	3200	207	150000	35109	
Thorium-234	Th			3200	150000	3200	207	150000	157 ^d	
Tritium										
Uranium	U			15	450	35	0.03	2200	2383	4151
Uranium-234	U			15	450	35	0.03	2200	4475	5991
Uranium-235	U			15	450	35	0.03	2200	1205	20 ^d
Uranium-238	U			15	450	35	0.03	2200	5887	4529

^a Green highlighted values in bold type in the columns 3-7 are those that were selected for use in the soil/sediment to water partitioning calculations.

^b Site specific values determined using ESH-18 or NMED monitoring data that appear significantly higher than the range of values reported for sand by Sheppard and Thibault (1990) are highlighted yellow in the last two columns.

^c Based on only two samples.

^d Based on only one sample.

Selecting an appropriate and representative coefficient is an important part of this project because the estimated water concentrations of chemicals and radionuclides are driven entirely by this value, in combination with the source area soil and sediment concentrations. It is important to note that distribution coefficients can vary widely, often across several orders of magnitude, and they can be highly influenced by soil type (e.g., clay content) and various other environmental parameters, including pH (Whicker and Schultz 1982; Sheppard and Thibault 1990; EPA 1999d). In an effort to be conservative (i.e., to avoid underestimating water concentrations), we selected the lower of multiple possible values (Table 4-21). Tritium was treated as a special case because of its chemical and physical properties. A K_d value of zero was selected to maximize the partitioning of tritium into the dissolved phase.

We based our selected values on four primary sources: RAIS - Risk Assessment Information System (ORNL 2001), Sheppard and Thibault (1990), NCRP (1996), and Baes et al. 1984. The ORNL RAIS source provided information regarding organic carbon partition coefficients (K_{oc} s) for the organic chemicals in our final analyte list. These coefficients, in combination with an estimated fraction organic content (foc) were used to develop soil/sediment-water distribution coefficients (K_d s) for these analytes. An average fraction organic carbon value of 0.03 g-oc/g-soil was used and is considered representative of LANL area soils, based on data provided by NMED and email correspondence with LANL personnel (personal communication via e-mail regarding LANL-area representative soil organic carbon values, January 2002).

). The K_{oc} values were multiplied by the f_{oc} to obtain K_d values for the organic chemicals.

It is important to recognize the impact that the Cerro Grande Fire may have had on chemical and radionuclide mobility and solubility. In general, fires result in increased pH values in both soil and water, which correlates to a general decrease in solubility (i.e., higher K_d s) for many analytes (e.g., cesium, strontium, plutonium, thorium, and uranium), although in some cases significantly higher pH values are associated with lower K_d values (Bitner et al. 2001; EPA 1999d). However, Bitner et al. (2001) also notes that increases in pH may not be observed in the typically alkaline soils of the arid and semiarid Southwest. Some other materials (e.g., copper and zinc) have been reported to have increased mobility following a fire, although there is no mention of an associated increase in solubility (Auclair 1977, cited by Bitner et al. 2001). The cation exchange capacity (CEC) for soils is also reported to be decreased following a fire because the exchange site in organic matter were destroyed by the fire, which could suggest a decrease in solubility (i.e., chemicals and radionuclides already bound to soil may remain there because of fewer sites for exchange).

Although it is clear that the consequences of a fire may include changes in solubility and mobility for many materials, there is not sufficient quantifiable information to justify adjusting any K_d values to account for this effect. If the tendency following a fire is toward decreased solubility, assuming K_d values determined under normal (i.e., nonfire) conditions would be a conservative approach.

Because of the wide range of possible values and the generally unknown (i.e., not quantifiable) impacts of the fire on soil-water partitioning for each chemical and radionuclide, we attempted to use site-specific monitoring data to evaluate the potential consequences of relying on default values reported in the literature. The ESH-18 and NMED environmental monitoring data provide a valuable source for estimating site-specific K_d values for a number of analytes, for comparison to the values reported in the literature. We excluded all nondetect values from both data sets for the purpose of these calculations and used only post-fire monitoring data. It is

important to note that neither the NMED nor ESH-18 monitoring data were collected with this eventual use in mind; however, the NMED data were most readily used for this purpose because of reported analyte concentrations measured in suspended sediment. Also, in several instances (noted in Table 4-21), the number of samples available for the calculations was very small.

For the NMED data, we tied the unfiltered water concentration result to the suspended sediment concentration (SSC) result for each analyte, using date and location to identify matching samples. Next, we divided the SSC by the unfiltered water concentration to arrive at a K_d value for each sample pair. Finally, we calculated natural logs of the data and average values to arrive at a geometric mean value for each analyte.

The ESH-18 data required an additional step because they did not determine SSC values for chemicals and radionuclides as NMED did. Therefore, we used the filtered and unfiltered water results, along with the associated TSS measurements, again using date and location to identify matching samples for each analyte. Where multiple analyte or TSS results (i.e., because of duplicate analyses, reanalyses, etc.) were reported for a given sample, we calculated and used an average value. We first subtracted the filtered result from the unfiltered result and eliminated any negative values. Next, to arrive at a chemical or radionuclide concentration associated with the TSS, we divided this result by the TSS value. Finally, we calculated the K_d value by dividing this TSS chemical or radionuclide concentration by the filtered water result. As with the NMED data, we calculated natural logs of the data and geometric mean values.

The range of values reported by Sheppard and Thibault (1990) provided a measure of confidence in the validity of the values we calculated using the ESH-18 and NMED environmental monitoring data. Because we relied on post-fire monitoring data, the calculated values account for potential changes in soil/sediment-water partitioning that may have occurred as a result of the fire. In general, the K_d values we calculated based on site-specific monitoring data are significantly larger than the default values we used for our transport calculations. In many cases, however, these higher values are still within the range of values reported for sand by Shepard and Thibault (1990). It was not possible to examine in detail the causes of the higher values calculated using the site-specific data, but the higher values may be related to impacts on chemical or radionuclide solubility caused by the fire. In addition, because the samples were not originally collected with this use in mind, there may be factors (e.g., related to sample preparation) that complicate using the data in this way. Nevertheless, the site-specific values are consistently larger than those reported in the literature and this provided compelling evidence that the values we selected for our transport calculations provided conservative estimates of chemical and radionuclide concentrations in surface water. Because the majority of selected K_d s are relatively large (i.e., >10), assuming smaller K_d values than site-specific data suggest, did not significantly impact resulting soil and sediment concentrations. However, in cases where K_d values are relatively small, we examined the relative risks of exposures to both soil/sediment and water to determine if a higher K_d significantly increased the total risk.

4.4.3 Background Surface Water Flow in the Rio Grande

Background surface water flow and suspended sediment concentrations were needed to address the influence of the Rio Grande on point of exposure water and suspended sediment concentrations for the scenarios that include the Rio Grande. Surface water flow data in units of cubic feet per second (cfs) were obtained from the USGS National Water Information System for

the flow gage on the Rio Grande at Otowi Bridge (USGS 2001). This gage station is located immediately above the outlet point for the Los Alamos watershed providing a good source of background flow in the Rio Grande not influenced by the watersheds considered in this evaluation. The data obtained were for daily surface water flow measurements from January 1, 1900, through September 30, 1990. We calculated an average and a median flow for these flow data. We selected the median flow for use in the evaluation over the average flow because the average flow could be influenced by unusual high or low flow measurements. Table 4-22 summarizes the descriptive statistics for the flow data. We added this median surface water flow for the Rio Grande to the storm water flow estimates for POE 1.1, 2.1R, 2.1BD, and 3.1, which are summarized in Table 4-16.

Table 4-22. Descriptive Statistics for Rio Grande Flow Data

Descriptive statistics	Flow (cfs)	Log flow
Average	1.5E+03	3.0E+00
Standard error	1.0E+01	2.0E-03
Median	8.6E+02	2.9E+00
Standard deviation	1.9E+03	3.7E-01
Sample variance	3.7E+06	1.4E-01
Skewness	3.6E+00	6.3E-01
Range	2.2E+04	2.6E+00
Minimum	6.0E+01	1.8E+00
Maximum	2.2E+04	4.3E+00
Count	3.4E+04	3.4E+04

Because the Cochiti Lake and Dam influence the flow in the Rio Grande, surface water flow was needed for the Rio Grande below the Cochiti Dam. Surface water flow data in units of cubic feet per second (cfs) were obtained from the USGS National Water Information System for the flow gage on the Rio Grande below Cochiti Dam (USGS 2001). The data obtained were for daily surface water flow measurements from October 1, 1970, through September 30, 1999. We calculated an average and a median for these flow data. The median values were selected for use in the evaluation. Table 4-23 summarizes the descriptive statistics flow measurement data. This median surface water flow for the Rio Grande was included in the concentration estimates related to the Rio Grande below the Cochiti Lake for POE 2.1BD.

**Table 4-23. Descriptive Statistics for the Rio Grande Flow Data
below the Cochiti Dam**

Descriptive statistics	Flow (cfs)	Log flow
Mean	1.4E+03	3.0E+00
Standard error	1.4E+01	3.7E-03
Median	8.9E+02	2.9E+00
Standard deviation	1.4E+03	3.9E-01
Sample variance	2.1E+06	1.5E-01
Skewness	2.0E+00	-1.9E-01
Range	8.3E+03	4.2E+00
Minimum	5.1E-01	-2.9E-01
Maximum	8.3E+03	3.9E+00
Count	1.1E+04	1.1E+04

4.4.4 Background Suspended Sediment Concentration in the Rio Grande

Suspended sediment concentration data in units of milligrams per liter were obtained from the USGS Suspended Sediment Database for the station on the Rio Grande at Otowi Bridge (USGS 2002). This station is located immediately above the outlet point for the Los Alamos watershed, providing a good source of background suspended sediment in the Rio Grande not influenced by the watersheds considered in this evaluation. The data obtained were for daily suspended sediment measurements from October 1, 1955, through September 30, 1995. We calculated an average and a median suspended sediment concentration. We selected the median suspended sediment concentration for use in the evaluation. Table 4-24 summarizes the descriptive statistics for the suspended sediment concentration data. We used this suspended sediment concentration for the Rio Grande in the suspended sediment concentration estimates for POE 1.1, 2.1R, and 3.1.

**Table 4-24. Descriptive Statistics for Rio Grande Suspended Sediment
Concentrations Data**

Descriptive statistics	TSS (mg L ⁻¹)	Log TSS
Average	1.2E+03	2.7E+00
Standard error	1.8E+01	4.5E-03
Median	6.0E+02	2.8E+00
Standard deviation	2.1E+03	5.3E-01
Sample variance	4.3E+06	2.8E-01
Skewness	6.8E+00	-3.5E-02
Range	4.1E+04	3.6E+00
Minimum	1.1E+01	1.0E+00
Maximum	4.1E+04	4.6E+00
Count	1.4E+04	1.4E+04

Because the Cochiti dam provides flood and sediment control on the Rio Grande, a suspended sediment concentration for the Rio Grande below the dam was needed. Suspended

sediment concentration data in units of milligrams per liter were obtained from the USGS Suspended Sediment Database for the station on the Rio Grande below the Cochiti Dam (USGS 2002). The suspended sediment concentration data obtained were for daily suspended sediment measurements from July 1, 1974, through September 30, 1988. An average and a median suspended sediment concentration were calculated. The median suspended sediment concentration was selected for use in the evaluation. Table 4-25 summarizes the descriptive statistics for the suspended sediment concentration data. This suspended sediment concentration was used in concentration estimates related to the Rio Grande below the Cochiti Dam for POE 2.1BD.

**Table 4-25. Descriptive Statistics for Suspended Sediments in the
Rio Grande Below the Cochiti Dam**

Descriptive statistics	TSS (mg L ⁻¹)	Log TSS
Mean	2.6E+01	1.3E+00
Standard error	3.0E-01	5.0E-03
Median	2.0E+01	1.3E+00
Standard deviation	2.1E+01	3.5E-01
Sample variance	4.5E+02	1.2E-01
Skewness	3.0E+00	-3.5E-01
Range	3.4E+02	2.5E+00
Minimum	1.0E+00	0.0E+00
Maximum	3.4E+02	2.5E+00
Count	4.8E+03	4.8E+03

4.4.5 Water Volume and Suspended Sediment Concentration in the Cochiti Lake

We estimated the volume of water in Cochiti Lake to address the influence of the lake on the point of exposure concentrations at that location. We obtained volume information for the Cochiti Lake in units of acre-feet (ac-ft) from the United States Army Corps of Engineers Albuquerque District Reservoir Control Database (USACE 2002). The data were for daily reservoir water measurements from October 1, 1999, through September 29, 2001, with the average and median volumes provided. We selected the median value for use in the concentration estimates for POE 2.1R and 2.1BD. Table 4-26 summarizes the descriptive statistics for the volume.

Table 4-26. Descriptive Statistics for Volume in the Cochiti Lake

Descriptive statistics	Volume (L)	Log volume
Mean	5.0E+04	4.7E+00
Standard error	4.8E+01	3.9E-04
Median	5.0E+04	4.7E+00
Standard deviation	1.3E+03	1.1E-02
Sample variance	1.7E+06	1.1E-04
Skewness	5.4E-02	-6.7E-02
Range	6.2E+03	4.3E-02
Minimum	4.7E+04	4.7E+00
Maximum	5.3E+04	4.7E+00
Count	7.3E+02	7.3E+02

Specific suspended sediment concentration data for the lake were not identified; however, an average suspended sediment concentration was estimated using the median suspended sediment concentrations developed for the Rio Grande at the station at Otowi Bridge and the station below the Cochiti Dam. We assumed the suspended sediment concentrations for the Cochiti Lake to be uniform throughout the lake. We further assumed the Rio Grande median suspended sediment concentration for Otowi Bridge was the suspended sediment concentration entering the lake (TSS_{in}) and that the Rio Grande median concentration below the Cochiti Dam was the suspended sediment concentration at the outlet of the lake (TSS_{out}). On this basis, we estimated the average suspended sediment concentration for the lake as the average of the inlet concentration (600 mg L^{-1}) and the outlet concentration (20 mg L^{-1}) for a value of 310 mg L^{-1} .

4.4.6 Storm Water Flow across the Source Areas

Estimates of storm water flow across each source were obtained from the storm water flow grids developed for the pre-fire and post-fire 2-, 5-, 10-, 25-, 50-, 100-, and 500-year storm events. Storm water flow is based on the average flow across the polygon representing the source area using the neighborhood statistic function in ArcView. Where the source area was too small to allow an average storm water flow to be calculated, we used the storm water flow at the centroid of the source area polygon. The pre-fire and post-fire storm water flows are summarized in Table H-1 and Table H-2, respectively. These tables are provided in electronic format in the Excel file accompanying this report, called "AppH_Storm water flow.xls".

4.4.7 Suspended Sediment in Storm Water

Detailed erosion modeling was beyond the scope of this evaluation. However, the analysis of the TSS concentrations collected in the area of the LANL facility before and after the fire (Section 4.2) indicates an approximate 10-fold increase in the average suspended sediment concentration after the fire with a mean pre-fire TSS concentration of 1000 mg L^{-1} and a mean post fire TSS concentration of 8000 mg L^{-1} . This increase in average suspended sediment concentration is similar to the results of work done by Wilson et al. (2001), Nyhan et al. (2001), and the BAER Team (BAER 2000). There are questions about the reasonableness of the actual erosion loss estimates; however, an approximate 10-fold increase in the average suspended

sediment concentration after the fire as compared to the pre-fire conditions appears to be appropriate.

To estimate the maximum chemical mass and radionuclide activity that is transported from each source area during a storm event, a representative TSS concentration is needed. The empirical analysis (Section 4.2) was unable to identify a functional relationship between the surface water flow and the TSS concentration. In addition, no suspended sediment data were available for the overland flow. Further, no data was available to characterize particle size distribution of the suspended sediment. It was, therefore, determined that a reasonable estimate of the amount of soil particles leaving each source area would be a constant value throughout the watershed and should be based on the pre- and post-fire empirical data sets. Based on the data sets, the pre-fire TSS value was selected to be 1000 mg L^{-1} and the post-fire TSS value was selected to be $10,000 \text{ mg L}^{-1}$.

As discussed earlier, the concentration of TSS is assumed to be uniform throughout the study area, and estimates of the amount of soil particles leaving each source areas are based on this uniform TSS value and the estimated storm water flow across the source area. In a similar fashion, the estimates of suspended sediments at the point of exposure are also based on this uniform TSS value and the estimated storm water flow at the point of exposure. It is recognized that the method used to estimate the mass of suspended sediment for each source area may result in a sum of these estimates for all source areas that is greater than the mass of suspended sediment estimated at the point of exposure; however, we assumed that deposition occurred as storm water flow moved through the watershed to the outlet points resulting in the estimated suspended sediment at the point of exposure. Because no data were available on particle size distribution of suspended sediment, we could not develop a deposition attenuation factor for chemical mass and activity. In addition, we assumed that the total chemical mass and radionuclide activity moved through the watershed to the point of exposure and was not present in deposited sediments in the watershed prior to the point of exposure. This assumption provides a conservative estimate of concentration of chemicals and radionuclides at the point of exposure.

4.4.8 Suspended and Deposited Sediment Characteristics

For this evaluation, deposited sediment in the surface water study area is assumed to be a sandy material with total porosity (ϕ_T) estimated to be $0.4 \text{ cm}^3 \text{ cm}^{-3}$ (Charbeneau 2000). The particle density (ρ_s) for suspended sediments is estimated as 2.65 g cm^{-3} (Charbeneau 2000) and the bulk density (ρ_b) for deposited sediments is estimated as

$$\rho_b \left(\frac{\text{g}}{\text{cm}^3} \right) = \rho_s \left(\frac{\text{g}}{\text{cm}^3} \right) \times (1 - \phi_E) = 1.6 \left(\frac{\text{g}}{\text{cm}^3} \right) . \quad (4.28)$$

4.4.9 Total Volume of Storm Water

Because the volume of suspended sediment is much smaller than the water volume, the calculation may be simplified by assuming that the total volume (V_T) equals the water volume (V_w) which is based on the storm water flow (Q) at a specified point and the 6-hour storm duration (SD):

$$V_T(L) = V_w(L) = Q \left(\frac{\text{ft}^3}{\text{sec}} \right) \times SD(\text{sec}) \times CF \left(\frac{L}{\text{ft}^3} \right) \quad (4.29)$$

This can be demonstrated by comparing the volume of water in a unit volume to the volume of suspended sediment in a unit volume.

The volume of suspended sediment (V_{ss}) is

$$V_{ss}(L) = \frac{TSS \left(\frac{\text{mg}}{L} \right)}{\rho_s \left(\frac{\text{g}}{\text{cm}^3} \right) \times CF \left(\frac{\text{mg}}{\text{g}} \right) \times CF \left(\frac{\text{cm}^3}{L} \right)} \times V_T(L) \quad (4.30)$$

By rearranging Equation (4.13) and substituting Equation (4.30) for V_{ss} , the total water volume (V_w) is

$$V_w = V_T(L) \times \left(1 - \frac{TSS \left(\frac{\text{mg}}{L} \right)}{\rho_s \left(\frac{\text{g}}{\text{cm}^3} \right) \times CF \left(\frac{\text{cm}^3}{L} \right) \times \left(\frac{\text{mg}}{\text{g}} \right)} \right) \quad (4.31)$$

Based on the selected post-fire TSS value, the volume of suspended sediments was less than 1% of the total volume.

4.4.10 Concentrations of Chemicals and Radionuclides at the Point of Exposure

4.4.10.1 Total Concentrations of Chemicals or Radionuclides in Storm Water or Surface Water at the Point of Exposure. The total concentration of a chemical or radionuclide in the storm water or surface water and suspended sediment at the point of exposure (C_{poe-T}) would be the sum of the total chemical mass (M_T) or radionuclide activity (A_T) from all of the source areas contributing to the point of exposure divided by the total volume of water (V_{poe-T}) at the point of exposure:

For chemicals

$$C_{poe-T} \left(\frac{\text{mg}}{L} \right) = \frac{\sum M_T(\text{mg})}{V_{poe-T}(L)} \quad (4.32)$$

For radionuclides

$$C_{\text{poe-T}} \left(\frac{\text{pCi}}{\text{L}} \right) = \frac{\sum A_T (\text{pCi})}{V_{\text{poe-T}} (\text{L})} . \quad (4.33)$$

We calculated the total volume of water based on the estimated storm water flow at the point of exposure for each storm event and any contribution by the Rio Grande and the Cochiti Lake. Contribution to the volume of water at the point of exposure by the Rio Grande or the Cochiti Lake depended on the location of the point of exposure. The total volume of water ($V_{\text{poe-T}}$) at POE 1.2, 4.1a, and 4.1b was equal to the total volume of water at the outlet of the watershed contributing to the point of exposure, which is based on the storm water flow at the outlet of the watershed (Q_{wshd}) and the 6-hour storm duration (SD):

$$V_{\text{poe-T}} (\text{L}) = V_{\text{wshd}} (\text{L}) = Q_{\text{wshd}} \left(\frac{\text{ft}^3}{\text{sec}} \right) \times \text{SD} (\text{sec}) \times \text{CF} \left(\frac{\text{L}}{\text{ft}^3} \right) . \quad (4.34)$$

The total volume of water ($V_{\text{poe-T}}$) at the point of exposure for POE 1.1 and 3.1 is based on the storm water flow at the outlet of the watershed (Q_{wshd}) contributing to the point of exposure and surface water flow in the Rio Grande (Q_{RG}):

$$V_{\text{poe-T}} (\text{L}) = \left(Q_{\text{wshd}} \left(\frac{\text{ft}^3}{\text{sec}} \right) + Q_{\text{RG}} \left(\frac{\text{ft}^3}{\text{sec}} \right) \right) \times \text{SD} (\text{sec}) \times \text{CF} \left(\frac{\text{L}}{\text{ft}^3} \right) . \quad (4.35)$$

The total volume of water ($V_{\text{poe-T}}$) at the point of exposure for POE 2.1R and 2.1BD is based on the storm water flow at the outlet of the watershed (Q_{wshd}) contributing to the point of exposure, surface water flow in the Rio Grande (Q_{RG}), and the volume of water in the Cochiti Lake (V_{CR}):

$$V_{\text{poe-T}} (\text{L}) = \left(Q_{\text{wshd}} \left(\frac{\text{ft}^3}{\text{sec}} \right) + Q_{\text{RG}} \left(\frac{\text{ft}^3}{\text{sec}} \right) \right) \times \text{SD} (\text{sec}) \times \text{CF} \left(\frac{\text{L}}{\text{ft}^3} \right) + V_{\text{CR}} (\text{L}) . \quad (4.36)$$

The calculation of the total concentration of a chemical or radionuclide in the surface water and suspended sediment at the POE 2.1BD ($C_{\text{poe-T-RGD}}$) was modified to recognize the reduced concentration of suspended sediment after the Cochiti Dam (TSS_{RGD}). We assumed the concentration in the dissolved phase ($C_{\text{poe-w-RGD}}$) and the suspended sediment ($C_{\text{poe-ss-RGD}}$) was the same as the concentrations calculated for the lake. However, total concentration of a chemical or radionuclide would be reduced because of the reduced volume of sediments in the Rio Grande after the Cochiti Dam; therefore, the total concentration of chemicals and radionuclides in the Rio Grande below the Cochiti Dam is

For chemicals

$$C_{\text{poe-T-RGD}} \left(\frac{\text{mg}}{\text{L}} \right) = C_{\text{poe-w-RGD}} \left(\frac{\text{mg}}{\text{L}} \right) + \left(C_{\text{poe-ss-RGD}} \left(\frac{\text{mg}}{\text{kg}} \right) \times \text{TSS}_{\text{RGD}} \left(\frac{\text{mg}}{\text{L}} \right) \times \text{CF} \left(\frac{\text{kg}}{\text{mg}} \right) \right) . \quad (4.37)$$

For radionuclides

$$C_{\text{poe-T-RGD}} \left(\frac{\text{pCi}}{\text{L}} \right) = C_{\text{poe-w-RGD}} \left(\frac{\text{pCi}}{\text{L}} \right) + \left(C_{\text{poe-ss-RGD}} \left(\frac{\text{pCi}}{\text{g}} \right) \times \text{TSS}_{\text{RGD}} \left(\frac{\text{mg}}{\text{L}} \right) \times \text{CF} \left(\frac{\text{g}}{\text{mg}} \right) \right) \quad (4.38)$$

4.4.10.2 Dissolved Phase in Storm Water and Surface Water. The concentration of a chemical or radionuclide in the dissolved phase of storm water and surface water at the point of exposure ($C_{\text{poe-w}}$) would be the sum of the chemical mass (M_w) or activities of the radionuclide (A_w) in the dissolved phase from all of the source areas contributing to the point of exposure divided by the volume of water ($V_{\text{poe-w}}$) at the point of exposure:

For chemicals

$$C_{\text{poe-w}} \left(\frac{\text{mg}}{\text{L}} \right) = \frac{\sum M_w (\text{mg})}{V_{\text{poe-w}} (\text{L})} \quad (4.39)$$

For radionuclides

$$C_{\text{poe-w}} \left(\frac{\text{pCi}}{\text{L}} \right) = \frac{\sum A_w (\text{pCi})}{V_{\text{poe-w}} (\text{L})} \quad (4.40)$$

where the volume of water at the point of exposure ($V_{\text{poe-w}}$) is approximately equal to the total volume of water ($V_{\text{poe-T}}$) at the point of exposure (see discussion for Unit Volume (V_T) below). Therefore, for POE 1.2, 4.1a, and 4.1b, the volume of water ($V_{\text{poe-w}}$) is calculated using Equation (4.30), for POE 1.1 and 3.1 the volume of water ($V_{\text{poe-w}}$) is calculated using Equation (4.31), and for POE 2.1R and 2.1BD the volume of water ($V_{\text{poe-w}}$) is calculated using Equation (4.32).

4.4.10.3 Suspended Sediment. The concentrations of chemicals and radionuclides in suspended sediments was equal to the concentrations of chemicals and radionuclides sorbed to the soil particles. The concentration of a chemical or radionuclide in suspended sediment at the point of exposure ($C_{\text{poe-ss}}$) would be the sum of the chemical mass (M_{ss}) or radionuclide activity (A_{ss}) sorbed to suspended sediment divided by the total mass of suspended sediment at the point of exposure (M_{TSS}). Similar to the source areas, the total mass of suspended sediment at the point of exposure is represented by the TSS measured in a unit volume at the point of exposure. Therefore, the concentration of a chemical in suspended sediment at the point of exposure ($C_{\text{poe-ss}}$) is

$$C_{\text{poe-ss}} \left(\frac{\text{mg}}{\text{kg}} \right) = \frac{\sum M_{\text{ss}} (\text{mg})}{M_{\text{TSS}} (\text{mg})} \quad (4.41)$$

The concentration of a radionuclide in suspended sediment at the point of exposure ($C_{\text{poe-ss}}$) is

$$C_{\text{poe-ss}} \left(\frac{\text{pCi}}{\text{g}} \right) = \frac{\sum A_{\text{ss}} (\text{pCi})}{M_{\text{TSS}} (\text{g})} \quad (4.42)$$

The total mass of suspended sediment is calculated based on the mass of suspended sediment at the point of exposure for each storm event and any contribution by the Rio Grande and the Cochiti Lake. Contribution to the mass of sediment at the point of exposure by the Rio Grande or the Cochiti Lake depended on the location of the point of exposure. The total mass of suspended sediment (M_{TSS}) at POE 1.2, 4.1a, and 4.1b is based on the suspended sediment in storm water flow (TSS) at that location and the total volume of water ($V_{\text{poe-T}}$) at the point of exposure calculated by Equation (4.30):

For chemicals

$$M_{\text{TSS}} (\text{kg}) = \text{TSS} \left(\frac{\text{mg}}{\text{L}} \right) \times V_{\text{poe-T}} (\text{L}) \times \text{CF} \left(\frac{\text{kg}}{\text{mg}} \right) . \quad (4.43)$$

For radionuclides

$$M_{\text{TSS}} (\text{g}) = \text{TSS} \left(\frac{\text{mg}}{\text{L}} \right) \times V_{\text{poe-T}} (\text{L}) \times \text{CF} \left(\frac{\text{g}}{\text{mg}} \right) . \quad (4.44)$$

The total mass of suspended sediment (M_{TSS}) at POE 1.1 and 3.1 is based on the TSS concentration in storm water (TSS), the TSS concentration in Rio Grande (TSS_{RG}), the surface water flow in the Rio Grande (Q_{RG}), and the total volume of water (V_{wshd}) at the outlet of the watershed calculated by Equation (4.30):

For chemicals

$$M_{\text{TSS}} (\text{kg}) = \left[\left(\text{TSS} \left(\frac{\text{mg}}{\text{L}} \right) \times V_{\text{wshd}} (\text{L}) \right) + \left(\text{TSS}_{\text{RG}} \left(\frac{\text{mg}}{\text{L}} \right) \times Q_{\text{RG}} \left(\frac{\text{ft}^3}{\text{sec}} \right) \times \text{SD} (\text{sec}) \right) \right] \times \text{CF} \left(\frac{\text{kg}}{\text{mg}} \right) . \quad (4.45)$$

For radionuclides

$$M_{\text{TSS}} (\text{g}) = \left[\left(\text{TSS} \left(\frac{\text{mg}}{\text{L}} \right) \times V_{\text{wshd}} (\text{L}) \right) + \left(\text{TSS}_{\text{RG}} \left(\frac{\text{mg}}{\text{L}} \right) \times Q_{\text{RG}} \left(\frac{\text{ft}^3}{\text{sec}} \right) \times \text{SD} (\text{sec}) \right) \right] \times \text{CF} \left(\frac{\text{g}}{\text{mg}} \right) . \quad (4.46)$$

The total mass of suspended sediment (M_{TSS}) at the point of exposure for POE 2.1R is based on the TSS concentration in storm water (TSS), the TSS concentration in Rio Grande (TSS_{RG}), the TSS concentration in the Cochiti Lake (TSS_{CR}), the surface water flow in the Rio Grande

(Q_{RG}), the volume of water in the Cochiti Lake (V_{CR}), and the total volume of water (V_{wshd}) at the outlet of the watershed calculated by Equation (4.30):

For chemicals

$$M_{TSS}(kg) = \left[\left(TSS \left(\frac{mg}{L} \right) \times V_{wshd}(L) \right) + \left(TSS_{CR} \left(\frac{mg}{L} \right) \times V_{CR}(L) \right) + \left(TSS_{RG} \left(\frac{mg}{L} \right) \times Q_{RG} \left(\frac{ft^3}{sec} \right) \times SD(sec) \times CF \left(\frac{L}{ft^3} \right) \right) \right] \times CF \left(\frac{kg}{mg} \right) \quad (4.47)$$

For radionuclides

$$M_{TSS}(g) = \left[\left(TSS \left(\frac{mg}{L} \right) \times V_{wshd}(L) \right) + \left(TSS_{CR} \left(\frac{mg}{L} \right) \times V_{CR}(L) \right) + \left(TSS_{RG} \left(\frac{mg}{L} \right) \times Q_{RG} \left(\frac{ft^3}{sec} \right) \times SD(sec) \times CF \left(\frac{L}{ft^3} \right) \right) \right] \times CF \left(\frac{g}{mg} \right) \quad (4.48)$$

4.4.10.4 Deposited Sediments. Suspended sediments from storm water and surface water flow was deposited on the ground surface or the bed of the surface water at the point of exposure. We assumed that deposited sediments would have physical characteristics of a saturated soil. Therefore, the concentration of chemicals and radionuclides in deposited sediments was the combination of the concentrations of chemicals and radionuclides in the storm water or surface water and suspended sediments. We considered two options for addressing the concentrations of chemicals and radionuclides in deposited sediments. The first was to assume that the concentration in the deposited sediments would be equal to the concentration of chemicals and radionuclides in the suspended sediment. This assumption does not address any moisture content that may remain in the deposited sediment after the storm event and may understate the actual concentrations of chemicals and radionuclide with which a receptor may come in contact. This approach was not used for this evaluation.

The second option, which is the approach that was used for this evaluation, was to assume immediately after the storm water flow has ended, the deposited sediments would resemble a saturated sandy material with the water filled porosity (ϕ_w) equal to the total porosity (ϕ_T) and the concentration of chemicals and radionuclides in the pore water would be equal to the concentration of chemicals and radionuclides in the water at the point of exposure (C_{poe-w}). When saturated conditions exist, the effective porosity (ϕ_E) approximately equals the total porosity (ϕ_T), which equals the water filled porosity (ϕ_w) given a bulk density (ρ_b), the total concentration of chemicals in deposited sediments (C_{poe-ds}) at the point of exposure is

$$C_{poe-ds} \left(\frac{mg}{kg} \right) = \frac{C_{poe-w} \left(\frac{mg}{L} \right)}{\rho_b \left(\frac{g}{cm^3} \right) \times CF \left(\frac{cm^3}{L} \right) \times CF \left(\frac{mg}{g} \right)} \times \phi_E + C_{poe-ss} \left(\frac{mg}{kg} \right) \times (1 - \phi_E) \quad (4.49)$$

The total concentration of radionuclides in deposited sediments at the point of exposure is

$$C_{\text{poe-ds}} \left(\frac{\text{pCi}}{\text{g}} \right) = \frac{C_{\text{poe-w}} \left(\frac{\text{pCi}}{\text{L}} \right)}{\rho_b \left(\frac{\text{g}}{\text{cm}^3} \right) \times \text{CF} \left(\frac{\text{cm}^3}{\text{L}} \right)} \times \phi_E + C_{\text{poe-ss}} \left(\frac{\text{pCi}}{\text{g}} \right) \times (1 - \phi_E) \quad (4.50)$$

4.4.11 Point of Exposure Concentration Estimate Results and Discussion

The pre-fire and post-fire estimates for concentrations of chemicals and radionuclides in the environmental media at the point of exposure for each storm event evaluated are provided for POE 1.1 in Table I-1, for POE 1.2 in Table I-2, for POE 2.1R in Table I-3, for POE 2.1BD in Table I-4, POE 3.1 in Table I-5, for POE 4.1a in Table I-6 and for POE 4.1b in Table I-7. These tables are provided in electronic format in the Excel file accompanying this report, called "AppI_POE concentration.xls." An example calculation is provided in Appendix V for ^{239}Pu for POE 1.2. This example calculation is provided to help the reader review and evaluate the modeling approach.

Several findings are indicated by the results. First, the estimated concentrations of chemicals and radionuclides in total storm water or surface water (i.e., combined dissolved phase and suspended sediment) are generally higher after the fire than before the fire. However, the estimated concentrations of chemicals and radionuclides in the dissolved phase in storm water or surface water, suspended sediments, and deposited sediments are smaller after the fire than before the fire for at least one chemical or radionuclide at all points of exposure except for POE 2.1R and POE 2.1BD. The specific chemicals and radionuclides with smaller post-fire concentrations varied by point of exposure; however, they were limited to the poly-aromatics hydrocarbons, heptachlor epoxide, thorium 230 and thorium 234. These chemicals and radionuclides are ones with K_d values generally greater than 1000 l kg^{-1} . Table 4-27 provides the chemical and radionuclide K_d values and a summary of the difference in concentrations of chemicals and radionuclides from pre-fire to post-fire for 2-year storm event for POE 4.1b. For purposes of this and subsequent examples, POE 4.1b was selected because there are a substantial amount of PRS contributing to the concentrations at the point of exposure, the concentration estimates are not influenced by surface water flow or volume in the Rio Grande and Cochiti Lake and a substantial portion of the watershed is in the burn area providing a significant pre-fire to post-fire relationship. Chemicals and radionuclides with smaller concentrations after the fire than before the fire at POE 4.1b are highlighted in red.

In addition, the ratio of pre-fire to post-fire water volumes and suspended sediment volumes and the pre-fire to post-fire chemical mass (M_w , M_{ss}) and radionuclide activity (A_w , A_{ss}) in the dissolved phase and suspended sediment were calculated and a ratio of the chemical mass or radionuclide activity ratio to the water (V_T) and suspended sediment (V_{ss}) volume ratio was calculated. Chemicals and radionuclides that exhibited lower concentrations after the fire than before the fire also exhibited ratios for the chemical mass or radionuclide activity that were less than 3 times higher than the ratio of the water and suspended sediment volumes at the point of exposure. Table 4-28 provides a summary of the ratios for the 2-year storm event at POE 4.1b. Ratios for chemicals and radionuclides with smaller concentrations after the fire than before the fire are highlighted in red.

Second, there is not a consistent trend toward higher concentrations of chemicals and radionuclides with increased storm intensity. A general trend toward decreased concentrations of chemicals and radionuclides with increased storm intensity was observed in pre-fire concentration estimates for all environmental media at POE 1.2 and POE 4.1b and in post-fire concentration estimates for all environmental media at POE 1.2, POE 3.1, and POE 4.1b. Pre-fire and post-fire concentrations of chemicals and radionuclides from the 2-year storm event were compared to the 500-year storm event. Changes in pre-fire concentrations ranged from a decrease by a factor of 59 for ^{234}Th at POE 4.1a to an increase by a factor of 82 for ^{210}Pb at POE 2.1R and POE 2.1BD. Changes in post-fire concentrations ranged from a decrease by a factor of 10 for arsenic at POE 1.2 to an increase by a factor of 20 for heptachlor epoxide at POE 2.1R and POE 2.1BD.

Third, where concentrations of chemicals and radionuclides vary with storm intensity the variation is generally less than an order of magnitude and likely within the uncertainty in the concentration estimates.

Table 4-27. Difference in Predicted Concentrations from Pre-Fire to Post-Fire for POE 4.1b

Chemical and radionuclide ^a	K _d (L kg ⁻¹)	Total in surface water	Dissolved in surface water	Suspended sediment	Deposited sediment
Aldrin	7.4E+04		No source area concentrations		
Arsenic	1.1E+02	1.4E-03	5.3E-04	5.9E-02	3.5E-02
Barium	4.1E+01	1.7E+01	1.1E+01	4.5E+02	2.8E+02
Benzo(a)anthracene	1.2E+04	8.6E-03	-6.8E-05	-8.1E-01	-4.9E-01
Benzo(a)pyrene	3.1E+04	1.0E-02	-3.5E-05	-1.1E+00	-6.5E-01
Benzo(b)fluoranthene	3.7E+04	9.2E-03	-2.6E-05	-9.7E-01	-5.8E-01
Benzo(k) fluoranthene	3.7E+04	6.4E-03	-1.8E-05	-6.7E-01	-4.0E-01
Chromium	1.9E+01	1.2E-01	9.4E-02	1.8E+00	1.1E+00
Copper	3.0E+01	8.1E-02	5.8E-02	1.8E+00	1.1E+00
Dibenz(a,h)anthracene	1.1E+05	3.1E-03	-2.9E-06	-3.4E-01	-2.0E-01
Heptachlor Epoxide	2.5E+03		No source area concentrations		
Indeno(1,2,3-cd)pyrene	1.0E+05	7.6E-03	-7.9E-06	-8.3E-01	-5.0E-01
Lead	2.7E+02	7.0E-02	1.1E-02	3.0E+00	1.8E+00
Mercury	1.6E+00	5.0E-04	4.9E-04	7.6E-04	5.8E-04
Nitrosodimethylamine_N_	2.5E-01	8.8E-08	8.7E-08	2.2E-08	3.5E-08
RDX	2.2E-01	1.0E+01	1.0E+01	2.2E+00	3.8E+00
Uranium	1.5E+01	5.3E-03	4.5E-03	6.7E-02	4.1E-02
Americium-241	7.0E+02	7.5E-03	9.3E-04	6.5E-04	3.9E-04
Cesium-137	2.7E+02	6.0E-01	1.5E-01	4.1E-02	2.4E-02
Lead-210	2.7E+02		No source area concentrations		
Neptunium-237	5.0E+00	1.7E+00	1.6E+00	8.1E-03	5.2E-03
Plutonium-238	5.5E+02	1.3E-03	2.1E-04	1.1E-04	6.8E-05
Plutonium-239	5.5E+02	1.3E-03	1.2E-03	6.7E-06	4.3E-06
Potassium-40	5.5E+00	6.1E+01	5.7E+01	3.1E-01	2.0E-01
Protactinium-234M	5.1E+02	2.7E-01	1.3E-02	6.8E-03	4.1E-03
Radium-224	4.5E+02		No source area concentrations		
Radium-226	4.5E+02	8.3E+00	5.0E-01	2.3E-01	1.4E-01
Radium-228	4.5E+02		No source area concentrations		
Strontium-90	1.5E+01	1.4E-01	1.2E-01	1.8E-03	1.1E-03
Thorium-228	3.2E+03		No source area concentrations		
Thorium-230	3.2E+03	1.2E-06	1.4E-08	4.5E-08	2.7E-08
Thorium-232	3.2E+03		No source area concentrations		
Thorium-234	3.2E+03	1.7E-01	-3.3E-03	-1.1E-02	-6.3E-03
Tritium	0.0E+00		No source area concentrations		
Uranium-234	1.5E+01	3.9E-03	3.3E-03	5.0E-05	3.1E-05
Uranium-235	1.5E+01	2.2E-02	1.9E-02	2.9E-04	1.8E-04
Uranium-238	1.5E+01	1.8E-01	1.5E-01	2.3E-03	1.4E-03

^a Chemicals and radionuclides with smaller concentrations after the fire than before the fire at POE 4.1b are shaded.

Table 4-28. Comparison of Estimated Mass and Activity Ratios to Volume Ratios

Chemical and radionuclide ^a	Ratio M _w or A _w post-fire to M _w or A _w pre-fire	Ratio M _{ss} or A _{ss} post-fire to M _{ss} or A _{ss} pre- fire	Ratio M _w or A _w to ratio V _T	Ratio M _{ss} or A _{ss} to ratio V _{ss}
Ratio of V _T Post-Fire to V _T Pre-fire		21.4		
Ratio of V _{ss} Post-Fire to V _{ss} Pre-fire		213.9		
Aldrin		No source area concentrations		
Arsenic	59.6	595.9	2.8	2.8
Barium	82.1	820.9	3.8	3.8
Benzo(a)anthracene	12.1	120.9	0.6	0.6
Benzo(a)pyrene	11.6	115.7	0.5	0.5
Benzo(b)fluoranthene	11.5	115.2	0.5	0.5
Benzo(k) fluoranthene	11.5	115.3	0.5	0.5
Chromium	96.1	961.0	4.5	4.5
Copper	90.7	906.9	4.2	4.2
Dibenz(a,h)anthracene	11.3	113.3	0.5	0.5
Heptachlor Epoxide		No source area concentrations		
Indeno(1,2,3-cd)pyrene	11.3	113.4	0.5	0.5
Lead	40.6	406.3	1.9	1.9
Mercury	110.9	1109.3	5.2	5.2
Nitrosodimethylamine_N-	169.6	1696.2	7.9	7.9
RDX	110.7	1107.0	5.2	5.2
Uranium	97.8	978.0	4.6	4.6
Americium-241		No pre-fire concentrations		
Cesium-137	196.2	1961.6	9.2	9.2
Lead-210		No source area concentrations		
Neptunium-237	106.2	1061.6	5.0	5.0
Plutonium-238		No pre-fire concentrations		
Plutonium-239		No pre-fire concentrations		
Potassium-40	243.9	2438.7	11.4	11.4
Protactinium-234M	28.4	284.1	1.3	1.3
Radium-224		No source area concentrations		
Radium-226	29.2	292.4	1.4	1.4
Radium-228		No source area concentrations		
Strontium-90		No pre-fire concentrations		
Thorium-228		No source area concentrations		
Thorium-230	32.5	324.5	1.5	1.5
Thorium-232		No source area concentrations		
Thorium-234	14.2	141.9	0.7	0.7
Tritium		No source area concentrations		
Uranium-234	99.4	993.7	4.6	4.6
Uranium-235	454.5	4545.2	21.3	21.3
Uranium-238	98.4	984.5	4.6	4.6

^a Chemicals and radionuclides with smaller concentrations after the fire than before the fire at POE 4.1b are shaded.

Finally, the average soil loss across the PRS ranges from 1.2E-04 m to 3.0E-02 m for all POE and all pre-fire storm events and from 5.8E-03 m to 7.5E-01 m for all POE and all post-fire events. Average soil loss at a PRS (D_{PRS}) in meters was estimated by

$$D_{\text{PRS}}(\text{m}) = \frac{\text{TSS}\left(\frac{\text{mg}}{\text{L}}\right) * V_{\text{T}}(\text{L})}{\rho_{\text{b}}\left(\frac{\text{g}}{\text{cm}^3}\right) * \text{CF}\left(\frac{\text{cm}^3}{\text{m}^3}\right) * \text{CF}\left(\frac{\text{mg}}{\text{g}}\right) * A_{\text{PRS}}(\text{m}^2)} \quad (4.51)$$

where A_{PRS} is the area of the PRS in meters.

Table 4-29 provides a summary the average soil loss at the PRS. The average precipitation depth in a watershed contributing to each point of exposure for each storm event is also provided in Table 4-30 for reference.

Table 4-29. Average Soil Erosion for PRSs

POE	PRS area (m ²)	2-year storm (m)	5-year storm (m)	10-year storm (m)	25-year storm (m)	50-year storm (m)	100-year storm (m)	500-year storm (m)
Pre-fire								
POE 1.1	8,610	1.1E-03	3.3E-03	5.1E-03	7.6E-03	9.5E-03	1.1E-02	1.6E-02
POE 1.2	2,087	1.3E-03	4.0E-03	6.2E-03	9.2E-03	1.1E-02	1.4E-02	2.0E-02
POE 2.1	4,476	1.4E-03	4.7E-03	7.8E-03	1.2E-02	1.6E-02	2.0E-02	3.0E-02
POE 3.1	4,476	1.4E-03	4.7E-03	7.8E-03	1.2E-02	1.6E-02	2.0E-02	3.0E-02
POE 4.1a	6,749	1.2E-04	8.3E-04	1.6E-03	2.7E-03	3.6E-03	4.7E-03	7.5E-03
POE 4.1b	7,144	3.7E-04	1.6E-03	2.9E-03	4.8E-03	6.3E-03	8.0E-03	1.3E-02
Post-fire								
POE 1.1	8,610	1.4E-01	2.1E-01	2.5E-01	3.0E-01	3.4E-01	3.8E-01	4.6E-01
POE 1.2	2,087	1.7E-01	2.5E-01	3.1E-01	3.7E-01	4.1E-01	4.6E-01	5.6E-01
POE 2.1	4,476	1.8E-01	2.9E-01	3.6E-01	4.5E-01	5.1E-01	5.8E-01	7.5E-01
POE 3.1	4,476	1.8E-01	2.9E-01	3.6E-01	4.5E-01	5.1E-01	5.8E-01	7.5E-01
POE 4.1a	6,749	5.8E-03	1.6E-02	2.5E-02	3.9E-02	4.9E-02	6.0E-02	9.2E-02
POE 4.1b	7,144	5.2E-02	9.2E-02	1.2E-01	1.6E-01	1.9E-01	2.2E-01	2.9E-01

Table 4-30. Average Precipitation Depths in Inches by Storm Event and Point of Exposure

POE	2-year storm	5-year storm	10-year storm	25-year storm	50-year storm	100-year storm	500-year storm
POE 1.1	1.4	1.8	2.1	2.4	2.6	2.8	3.3
POE 1.2	1.6	2.0	2.3	2.6	2.8	3.0	3.5
POE 2.1	1.3	1.7	2.0	2.2	2.4	2.6	3.1
POE 3.1	1.3	1.7	2.0	2.2	2.4	2.6	3.1
POE 4.1a	1.7	2.2	2.4	2.8	3.0	3.2	3.7
POE 4.1b	1.8	2.3	2.6	2.9	3.1	3.3	3.8

The average soil loss across the geomorphic units and unsampled reaches ranged from 2.1E-03 m to 8.6E-02 m for all POE and all pre-fire storm events and from 3.1E-01 m to 2.5E-00 m for all POE and all post-fire events. Table 4-31 provides a summary the average soil loss at the geomorphic units and unsampled reaches.

Table 4-31. Average Soil Erosion for Geomorphic Units and Unsampled Reaches (in meters)

POE	Geomorphic units/reach area (m ²)	2-year storm	5-year storm	10-year storm	25-year storm	50-year storm	100-year storm	500-year storm
Pre-fire								
POE 1.1	7396	4.5E-03	1.4E-02	2.3E-02	3.5E-02	4.4E-02	5.4E-02	7.9E-02
POE 1.2	6063	5.0E-03	1.6E-02	2.5E-02	3.8E-02	4.8E-02	5.9E-02	8.6E-02
POE 2.1	7396	4.5E-03	1.4E-02	2.3E-02	3.5E-02	4.4E-02	5.4E-02	7.9E-02
POE 3.1	5200	2.1E-03	7.1E-03	1.2E-02	1.8E-02	2.3E-02	2.8E-02	4.3E-02
POE 4.1a	No geomorphic units or unsampled reaches							
POE 4.1b	No geomorphic units or unsampled reaches							
Post-fire								
POE 1.1	7396	6.9E-01	1.0E+00	1.2E+00	1.5E+00	1.6E+00	1.8E+00	2.2E+00
POE 1.2	6063	7.6E-01	1.1E+00	1.3E+00	1.6E+00	1.8E+00	2.0E+00	2.5E+00
POE 2.1	7396	6.9E-01	1.0E+00	1.2E+00	1.5E+00	1.6E+00	1.8E+00	2.2E+00
POE 3.1	5200	3.1E-01	4.6E-01	5.7E-01	7.0E-01	7.9E-01	8.9E-01	1.1E+00
POE 4.1a	No geomorphic units or unsampled reaches							
POE 4.1b	No geomorphic units or unsampled reaches							

4.5 Sensitivity of Point of Exposure Concentrations

Four major factors affect the concentration of chemicals and radionuclides at the points of exposure. These are the TSS concentrations, the storm water flow across the source areas and at the point of exposure, the K_d value, and the source areas contributing chemical mass or radionuclide activity to the point of exposure. A discussion of the sensitivity of these factors is presented below.

4.5.1 Source Areas

A number of uncertainties and limitations (discussed in Chapter 3) confound the identification of the source areas and their role in estimated concentrations of chemicals and radionuclides. As a result, understanding the impact of the various types of source areas (i.e., PRS, burn areas, geomorphic units, and unsampled reaches) and the key assumptions (i.e., average concentration and erosion matrix for PRS) is important for determining source area concentrations and for estimating concentration of chemicals and radionuclides at the point of exposure. To evaluate the impact of the various types of source areas, we recalculated the estimated concentrations of chemicals and radionuclides by excluding each type of source area, using maximum concentrations at PRS, and excluding the erosion matrix adjustment at the PRS and comparing the concentrations to the results presented in Section 4.4.11 (referred to here as

the base case concentrations). We provide the results of this evaluation electronically in the Excel file accompanying this report, called "AppJ_Burn Area effect.xls," "AppK_GeoUnits_Reaches.xls," "AppL_PRS Effect.xls," "AppM_Erosion matrix.xls," and "AppN_Max Conc Effect.xls." We presented the results for the TSS, erosion matrix, and maximum concentration comparison as multiplying factors of the base case concentrations. We presented the results of the PRS, burn area, geomorphic units, and unsampled reaches comparison as a percentage of the base case concentrations.

The impact of the burn area on the point of exposure concentrations was limited to the nine chemicals and radionuclides identified in the burn ash. The burn area has a significant impact on POE 4.1a and POE 4.1b, accounting for essentially all of the concentrations (>95%) of ^{235}U , ^{90}Sr , ^{238}Pu , ^{239}Pu , ^{137}Cs , and ^{241}Am at POE 4.1a and of ^{90}Sr , ^{238}Pu , ^{239}Pu , and ^{241}Am at POE 4.1b. In addition, the burn area accounted for a majority (>75%) of the concentrations of ^{235}U and ^{137}Cs at POE 4.1b. The burn area also had a significant impact on the concentrations of lead ($\approx 45\%$) and barium ($\approx 80\%$) at POE 4.1a, but had little to no effect on the remaining points of exposure with the exception of concentrations of barium at POE 1.1 ($\approx 20\%$) and POE 1.2 ($\approx 17\%$). The burn area in the watersheds contributing to POE 4.1a and 4.1b covered over 85% of the watershed area. We included the results of this evaluation in Appendix J, which is provided in electronic format in the Excel file ("AppJ_Burn Area effect.xls.") accompanying this report.

Concentrations of all chemicals and radionuclides were identified in the geomorphic units, but only ^{137}Cs and ^{239}Pu were identified in the unsampled reaches. Geomorphic units and unsampled reaches were not identified within the watershed area contributing to POE 4.1a and POE 4.1b. The geomorphic units and unsampled reaches had a significant impact on all other points of exposure. They accounted for essentially all of the concentrations (>90%) of all chemicals and radionuclides in both the pre-fire and post-fire estimates except barium (<11%), mercury (<31%), ^{234}U (<82%) and ^{238}U (<82%) at POE 1.1 and POE 1.2 and essentially all of the concentrations (>90%) in both the pre-fire and post-fire estimates of aldrin, ^{241}Am , ^{238}Pu , ^{239}Pu , ^{90}Sr , ^{228}Th , ^{230}Th , ^{232}Th , tritium, and ^{235}U at the other points of exposure. The geomorphic units and unsampled reaches are located along major stream segments within the Los Alamos watershed. These source areas generally have significantly higher flows than other source areas of the watershed resulting in greater volumes of suspended sediment and therefore greater contribution of chemical mass and radionuclide activity than other source areas. We included the results of this evaluation in Appendix K provided in electronic format in the Excel file ("AppK_GeoUnits_Reaches.xls.") accompanying this report.

Concentrations of all chemicals and radionuclides were identified in the PRS. The PRS are responsible for all of the concentrations of chemicals and radionuclides at POE 4.1a and POE 4.1b with the exception of the chemicals and radionuclides associated with the burn area discussed previously. For POE 1.1 and POE 1.2, the PRS contribute very little (<20%) to the concentrations of chemicals and radionuclides with the exception of barium and mercury. This is a result of the high contribution of chemical mass and radionuclide activity associated with the geomorphic units and unsampled reaches at these points of exposure. The PRS account for essentially all of the chemicals and radionuclides at POE 2.1R, POE 2.1BD, and POE 3.1 except for those chemicals and radionuclides associated with the burn area, geomorphic units, and unsampled reaches discussed previously. We included the results of this evaluation in Appendix L provided in electronic format in the Excel file ("AppL_PRS Effect.xls.") accompanying this report.

The erosion matrix was used to reduce the concentrations of chemicals and radionuclides to account for physical features at a PRS that would reduce the potential erosion and therefore the mass of chemical mass or radionuclide activity that would contribute to the concentration of chemicals and radionuclides at the points of exposure. This erosion matrix adjustment only applies to the PRS and does not impact the representative concentrations in the burn area or the geomorphic units and unsampled reaches. The elimination of the erosion matrix adjustment had no effect on POE 1.1 and POE 1.2; however, this is likely due to the very small number of PRS that are located within the watershed contributing to these points of exposure. Concentrations of chemicals and radionuclides without the erosion matrix adjustments increased for a number of chemicals and radionuclides by a factor ranging from 1.1 to 1.8 over the estimated concentrations with the erosion matrix adjustment. Increases were observed for arsenic (at POE 4.1b); RDX (at POE 4.1a); uranium (at POE 4.1b); ^{210}Pb (at POE 3.1, POE 2.1R, and POE 2.1BD); ^{237}Np (at POE 4.1a); ^{40}K (at POE 4.1a, POE 3.1, POE 2.1 BD, POE 2.1 R); ^{234}Pa (at POE 4.1b, POE 3.1, POE 2.1R, and POE 2.1BD); ^{234}Th (at POE 4.1b, POE 3.1, POE 2.1R, and POE 2.1BD); ^{234}U (at POE 4.1b); ^{235}U (at POE 4.1b), and ^{238}U (at POE 4.1b). Concentrations of ^{40}Pa exhibited the largest increase in concentration. However, the significance of the change associated with a particular chemical or radionuclide is a function of the number of PRS and the concentrations at the PRS contributing to a point of exposure as well as the magnitude of the contribution of a particular chemical or radionuclide from the burn area, geomorphic units, or unsampled reaches. A specific evaluation of the impact of one or more individual PRS was not conducted. We included the results of this evaluation in Appendix M provided in electronic format in the Excel file ("AppM_Erosion matrix.xls") accompanying this report.

We estimated representative concentrations for the PRS using the average of the concentration data available for each source area. The amount of concentration data and the distribution of that data varied for each PRS and for each chemical and radionuclide at each PRS. The use of the maximum concentration at a PRS rather than the average concentration results in an increase in concentrations at all points of exposure that range from no increase in concentrations of a number of chemicals and radionuclides to a factor of 8.1 increase for arsenic at POE 4.1b. Concentrations of chemicals and radionuclides at POE 4.1a and POE 4.1b exhibit the largest overall increases. The concentration of ^{230}Th at POE 4.1a exhibits an increase in concentration by a factor of 1420, however, ^{230}Th is only present in one PRS in the watershed contributing to this point of exposure and the maximum concentration for this PRS differs from the average concentration by the same factor. The pre-fire concentration of ^{137}Cs at POE 4.1b exhibits an increase in concentration by a factor of 18.8; however, ^{137}Cs is only present in three PRSs in the watershed contributing to this point of exposure and the maximum concentration for two of these PRSs differs from the average concentration by a similar factor. The magnitude of the increase is a function of the number of sample results and the distribution of the sample results used to calculate the average for each PRS for each chemical or radionuclide. The results of this evaluation are included in Appendix N provided in electronic format in the Excel file ("AppN_Max Conc Effect.xls") accompanying this report.

In summary, the PRSs are a significant contributor to the concentrations of chemicals and radionuclides at the points of exposure—particularly in cases where the burn area represents a small portion of the overall contributing watershed area and geomorphic units and reaches are not contributors. Concentrations of chemicals and radionuclides in soil and sediment in geomorphic units and reaches can play a dominant role on the concentrations at the points of exposure due to

the high storm water flow in these areas. In addition, where the burn area represents a substantial portion of the total area of the contributing watershed, the burn area can also play a dominant role on the concentrations of chemicals and radionuclides at the point of exposure. The elimination of the erosion matrix adjustment from the PRS representative concentrations estimates can result in larger concentrations at the points of exposure, however, not all chemicals and radionuclides are affected and the increase are less than a factor of 2. The use of maximum concentrations of chemicals and radionuclides at the PRS can result in larger concentrations at the points of exposure by up to a factor of 9.1 (except for the two outliers at POE 4.1b, ^{230}Th and pre-fire ^{137}Cs). However, neither the erosion matrix adjustment nor the use of the maximum concentrations results in a general order of magnitude change in the concentrations at the points of exposure.

4.5.2 TSS Concentration

The concentrations of chemicals and radionuclides in environmental media at the point of exposure were calculated based on a pre-fire TSS concentration of $1,000 \text{ mg L}^{-1}$ and a post-fire TSS concentration of $10,000 \text{ mg L}^{-1}$. Since there was significant variability in the available empirical data and specific relationships between storm water flow and TSS concentration could not be developed, pre-fire and post-fire TSS concentrations were selected based on the mean of historical data and an estimated 10-fold increase in post-fire concentration over pre-fire concentration. In addition, the chemical mass and radionuclide activity that would result from a source area was estimated assuming that the entire volume of TSS that would be in storm water flow over a source area resulted from that source area. Therefore, the total chemical mass and radionuclide activity is directly related to the TSS concentration.

As discussed previously, modeled estimates of the increase in soil erosion as a result of the fire ranged from 7-fold (BAER), 10-fold (Wilson et al 2001) to 70-fold (Nyhan et al 2001). To evaluate the impact of increased or decreased post-fire TSS concentrations on the concentrations of chemicals and radionuclides at the point of exposure, alternative concentrations for chemicals and radionuclides were calculated assuming TSS concentrations of $5,000 \text{ mg L}^{-1}$ (i.e., 5-fold increase over pre-fire), $15,000 \text{ mg L}^{-1}$ (i.e., 15-fold increase over pre-fire), and $20,000 \text{ mg L}^{-1}$ (i.e., 20-fold increase over pre-fire). We provided the results of this evaluation in electronic format in the Excel files ("AppO_TSS5000.xls," "AppP_TSS15000.xls," and "AppQ_TSS20000.xls.") accompanying this report.

Total concentrations of chemicals and radionuclides in storm water and surface water at the points of exposure for the alternative TSS concentrations changed at the same rate as the alternative TSS concentrations changed as compared to the study TSS concentration of $10,000 \text{ mg L}^{-1}$. For example, an increase in TSS concentration from $10,000 \text{ mg L}^{-1}$ to $20,000 \text{ mg L}^{-1}$ (2-fold increase) results in a 2-fold increase in the total concentration of chemical and radionuclide in storm water and surface water. This is expected since the source is assumed to be non-depleting and the total chemical mass and radionuclide activity is directly proportional to the TSS concentrations. However, the change in concentrations of chemicals and radionuclides in the dissolved phase, suspended sediments and deposited sediments varied based on the chemical or radionuclide K_d value. The chemicals and radionuclides with large K_d value (e.g., dibenz(a,h)anthracene = $1.1\text{E}+05 \text{ L kg}^{-1}$) exhibited little to no change in concentration as the TSS concentrations changed. While the chemicals and radionuclides with the small K_d values (e.g.

radionuclide K_d value. The chemicals and radionuclides with large K_d value (e.g., dibenz(a,h)anthracene = $1.1\text{E}+05 \text{ L kg}^{-1}$) exhibited little to no change in concentration as the TSS concentrations changed. While the chemicals and radionuclides with the small K_d values (e.g. RDX = $2.2\text{E}-01 \text{ L kg}^{-1}$) exhibited a change in concentration as the TSS concentrations proportional to the change in the TSS concentration.

4.5.3 Storm Water Flow across the Source Areas

Along with the TSS concentration, we used the volume of storm water that flows across a source area to estimate the chemical mass and radionuclide activity that would result from a source area. We estimated concentrations of chemicals and radionuclides at points of exposure for seven storm events representing increased precipitation intensities and storm water flows. However, as discussed previously, while there is some variation in the concentrations of chemicals and radionuclides with changes in storm intensity; the variation in concentration at the point of exposure is generally less than an order of magnitude. Therefore, given a non-depleting source, the intensity of the storm event does not significantly affect the concentration of chemicals and radionuclides in the environmental media. Table 4-32 provides a summary of the change in concentration from the 2-year to the 500-year storm event for all chemicals and radionuclides at each point of exposure.

4.5.4 Soil to Water Partitioning Coefficients (K_d)

As discussed in Section 4.4.2, the distribution coefficients can vary widely, often across several orders of magnitude, and can be highly influenced by soil characteristics and other environmental parameters. For inorganic chemicals and radionuclides, specific K_d values were selected from the lower-end of the range of possible values. For organic chemicals, and radionuclides, K_d values were derived based on the product of the chemical specific K_{oc} and an estimated f_{oc} assumed to be representative of soils throughout the watershed. Section 4.4.11 discusses the significance of the K_d values on the differences in concentrations of chemicals and radionuclides in the dissolved phase, suspended sediments and deposited sediments after the fire as compared to concentrations before the fire. Table 4-33 provides an example of the impact on environmental media concentrations of one and two orders of magnitude decrease in a higher K_d chemical (i.e., benzo(a)anthracene) and Table 4-34 provides an example of the impact on environmental media concentrations of one and two orders of magnitude increase in a lower K_d radionuclide (i.e., Cesium 137).

Table 4-32. Ratio of Concentrations for the 500-Year to 2-Year Storm Event for POE 4.1b

POE 4.1 B	Pre-fire				Post-fire			
	Total	Dissolved	Suspended	Deposited	Total	Dissolved	Suspended	Deposited
Aldrin	No source area concentrations							
Arsenic	1.8	1.8	1.8	1.8	1.1	1.1	1.1	1.1
Barium	1.5	1.5	1.5	1.5	1.0	1.0	1.0	1.0
Benzo(a)anthracene	1.8	1.8	1.8	1.8	1.1	1.1	1.1	1.1
Benzo(a)pyrene	1.8	1.8	1.8	1.8	1.1	1.1	1.1	1.1
Benzo(b)fluoranthene	1.8	1.8	1.8	1.8	1.1	1.1	1.1	1.1
Benzo(k) fluoranthene	1.8	1.8	1.8	1.8	1.1	1.1	1.1	1.1
Chromium	1.8	1.8	1.8	1.8	1.1	1.1	1.1	1.1
Copper	1.6	1.6	1.6	1.6	1.0	1.0	1.0	1.0
Dibenz(a,h)anthracene	1.8	1.8	1.8	1.8	1.1	1.1	1.1	1.1
Heptachlor Epoxide	No source area concentrations							
Indeno(1,2,3-cd)pyrene	1.8	1.8	1.8	1.8	1.1	1.1	1.1	1.1
Lead	1.6	1.6	1.6	1.6	1.0	1.0	1.0	1.0
Mercury	1.6	1.6	1.6	1.6	1.0	1.0	1.0	1.0
Nitrosodimethylamine_N-	2.5	2.5	2.5	2.5	2.1	2.1	2.1	2.1
RDX	1.5	1.5	1.5	1.5	1.0	1.0	1.0	1.0
Uranium	1.5	1.5	1.5	1.5	1.0	1.0	1.0	1.0
Americium-241	0.0	0.0	0.0	0.0	1.1	1.1	1.1	1.1
Cesium-137	1.5	1.5	1.5	1.5	1.1	1.1	1.1	1.1
Lead-210	No source area concentrations							
Neptunium-237	1.5	1.5	1.5	1.5	1.0	1.0	1.0	1.0
Plutonium-238	0.0	0.0	0.0	0.0	1.1	1.1	1.1	1.1
Plutonium-239	0.0	0.0	0.0	0.0	1.1	1.1	1.1	1.1
Potassium-40	3.3	3.3	3.3	3.3	2.0	2.0	2.0	2.0
Protactinium-234M	1.4	1.4	1.4	1.4	1.1	1.1	1.1	1.1
Radium-224	No source area concentrations							
Radium-226	1.5	1.5	1.5	1.5	1.0	1.0	1.0	1.0
Radium-228	No source area concentrations							
Strontium-90	0.0	0.0	0.0	0.0	1.1	1.1	1.1	1.1
Thorium-228	No source area concentrations							
Thorium-230	3.9	3.9	3.9	3.9	2.2	2.2	2.2	2.2
Thorium-232	No source area concentrations							
Thorium-234	1.5	1.5	1.5	1.5	1.0	1.0	1.0	1.0
Tritium	No source area concentrations							
Uranium-234	1.5	1.5	1.5	1.5	1.0	1.0	1.0	1.0
Uranium-235	1.4	1.4	1.4	1.4	1.1	1.1	1.1	1.1
Uranium-238	1.5	1.5	1.5	1.5	1.0	1.0	1.0	1.0

Table 4-33. The Effect of K_d Changes on Concentrations of Benzo(a)anthracene in Environmental Media at POE 4.1b

Kd (L kg ⁻¹)	Benzo(a)anthracene								
	Pre-fire			Post-fire			Difference (post-fire-pre-fire)		
	Original	One order	Two order	Original	One order	Two order	Original	One order	Two order
Total in surface water	1.2E+04	1.2E+03	1.2E+02	1.2E+04	1.2E+03	1.2E+02	1.2E+04	1.2E+03	1.2E+02
	mg L ⁻¹								
2 year	2.0E-03	2.0E-03	2.0E-03	1.1E-02	1.1E-02	1.1E-02	8.6E-03	8.6E-03	8.6E-03
5 year	1.6E-03	1.6E-03	1.6E-03	1.1E-02	1.1E-02	1.1E-02	8.9E-03	8.9E-03	8.9E-03
10 year	1.4E-03	1.4E-03	1.4E-03	1.0E-02	1.0E-02	1.0E-02	9.0E-03	9.0E-03	9.0E-03
25 year	1.3E-03	1.3E-03	1.3E-03	1.0E-02	1.0E-02	1.0E-02	8.9E-03	8.9E-03	8.9E-03
50 year	1.3E-03	1.3E-03	1.3E-03	1.0E-02	1.0E-02	1.0E-02	8.9E-03	8.9E-03	8.9E-03
100 year	1.2E-03	1.2E-03	1.2E-03	1.0E-02	1.0E-02	1.0E-02	8.8E-03	8.8E-03	8.8E-03
500 year	1.1E-03	1.1E-03	1.1E-03	9.8E-03	9.8E-03	9.8E-03	8.7E-03	8.7E-03	8.7E-03
Dissolved in surface water	mg L ⁻¹								
2 year	1.6E-04	9.2E-04	1.8E-03	8.8E-05	8.2E-04	4.9E-03	-6.8E-05	-1.0E-04	3.0E-03
5 year	1.2E-04	7.2E-04	1.4E-03	8.7E-05	8.1E-04	4.8E-03	-3.5E-05	8.9E-05	3.4E-03
10 year	1.1E-04	6.5E-04	1.3E-03	8.6E-05	8.0E-04	4.7E-03	-2.5E-05	1.5E-04	3.5E-03
25 year	1.0E-04	6.0E-04	1.2E-03	8.5E-05	7.9E-04	4.7E-03	-1.7E-05	1.9E-04	3.5E-03
50 year	9.8E-05	5.8E-04	1.1E-03	8.5E-05	7.9E-04	4.6E-03	-1.4E-05	2.1E-04	3.5E-03
100 year	9.5E-05	5.6E-04	1.1E-03	8.4E-05	7.8E-04	4.6E-03	-1.1E-05	2.2E-04	3.5E-03
500 year	8.7E-05	5.2E-04	1.0E-03	8.1E-05	7.6E-04	4.5E-03	-6.0E-06	2.4E-04	3.5E-03
Suspended sediment	mg L ⁻¹								
2 year	1.9E+00	1.1E+00	2.2E-01	1.1E+00	9.8E-01	5.8E-01	-8.1E-01	-1.2E-01	3.6E-01
5 year	1.5E+00	8.7E-01	1.7E-01	1.0E+00	9.7E-01	5.7E-01	-4.2E-01	1.1E-01	4.0E-01
10 year	1.3E+00	7.8E-01	1.5E-01	1.0E+00	9.6E-01	5.7E-01	-2.9E-01	1.8E-01	4.1E-01
25 year	1.2E+00	7.2E-01	1.4E-01	1.0E+00	9.5E-01	5.6E-01	-2.0E-01	2.3E-01	4.2E-01
50 year	1.2E+00	6.9E-01	1.4E-01	1.0E+00	9.4E-01	5.5E-01	-1.7E-01	2.5E-01	4.2E-01
100 year	1.1E+00	6.7E-01	1.3E-01	1.0E+00	9.3E-01	5.5E-01	-1.3E-01	2.6E-01	4.2E-01
500 year	1.0E+00	6.2E-01	1.2E-01	9.7E-01	9.0E-01	5.3E-01	-7.1E-02	2.9E-01	4.1E-01
Deposited sediment	mg kg ⁻¹								
2 year	1.1E+00	6.6E-01	1.3E-01	6.3E-01	5.9E-01	3.5E-01	-4.9E-01	-7.2E-02	2.2E-01
5 year	8.8E-01	5.2E-01	1.0E-01	6.3E-01	5.8E-01	3.5E-01	-2.5E-01	6.4E-02	2.4E-01
10 year	8.0E-01	4.7E-01	9.2E-02	6.2E-01	5.8E-01	3.4E-01	-1.8E-01	1.1E-01	2.5E-01
25 year	7.3E-01	4.3E-01	8.5E-02	6.1E-01	5.7E-01	3.4E-01	-1.2E-01	1.4E-01	2.5E-01
50 year	7.0E-01	4.2E-01	8.2E-02	6.1E-01	5.6E-01	3.3E-01	-9.9E-02	1.5E-01	2.5E-01
100 year	6.8E-01	4.0E-01	7.9E-02	6.0E-01	5.6E-01	3.3E-01	-7.9E-02	1.6E-01	2.5E-01
500 year	6.3E-01	3.7E-01	7.3E-02	5.8E-01	5.4E-01	3.2E-01	-4.3E-02	1.7E-01	2.5E-01

**Table 4-34. The Effect of K_d Changes on Concentrations of Cesium-137 in Environmental
Media at POE 4.1b**

	Pre-Fire			Post-Fire			Difference (post-fire-pre-fire)		
	Original	One order	Two order	Original	One order	Two order	Original	One order	Two order
K_d ($L\ kg^{-1}$)	2.7E+02	2.7E+03	2.7E+04	2.7E+02	2.7E+03	2.7E+04	2.7E+02	2.7E+03	2.7E+04
Total in surface water	pCi L^{-1}								
2 year	2.3E-02	2.3E-02	2.3E-02	6.2E-01	6.2E-01	6.2E-01	6.0E-01	6.0E-01	6.0E-01
5 year	1.9E-02	1.9E-02	1.9E-02	6.1E-01	6.1E-01	6.1E-01	5.9E-01	5.9E-01	5.9E-01
10 year	1.8E-02	1.8E-02	1.8E-02	6.1E-01	6.1E-01	6.1E-01	5.9E-01	5.9E-01	5.9E-01
25 year	1.7E-02	1.7E-02	1.7E-02	6.0E-01	6.0E-01	6.0E-01	5.8E-01	5.8E-01	5.8E-01
50 year	1.7E-02	1.7E-02	1.7E-02	5.9E-01	5.9E-01	5.9E-01	5.8E-01	5.8E-01	5.8E-01
100 year	1.6E-02	1.6E-02	1.6E-02	5.9E-01	5.9E-01	5.9E-01	5.7E-01	5.7E-01	5.7E-01
500 year	1.5E-02	1.5E-02	1.5E-02	5.8E-01	5.8E-01	5.8E-01	5.6E-01	5.6E-01	5.6E-01
Dissolved in surface water	pCi L^{-1}								
2 year	1.8E-02	6.3E-03	8.3E-04	1.7E-01	2.2E-02	2.3E-03	1.5E-01	1.6E-02	1.5E-03
5 year	1.5E-02	5.3E-03	7.0E-04	1.7E-01	2.2E-02	2.3E-03	1.5E-01	1.7E-02	1.6E-03
10 year	1.4E-02	4.9E-03	6.5E-04	1.6E-01	2.2E-02	2.2E-03	1.5E-01	1.7E-02	1.6E-03
25 year	1.3E-02	4.6E-03	6.1E-04	1.6E-01	2.1E-02	2.2E-03	1.5E-01	1.7E-02	1.6E-03
50 year	1.3E-02	4.5E-03	5.9E-04	1.6E-01	2.1E-02	2.2E-03	1.5E-01	1.7E-02	1.6E-03
100 year	1.3E-02	4.4E-03	5.8E-04	1.6E-01	2.1E-02	2.2E-03	1.5E-01	1.7E-02	1.6E-03
500 year	1.2E-02	4.1E-03	5.5E-04	1.6E-01	2.1E-02	2.1E-03	1.4E-01	1.7E-02	1.6E-03
Suspended sediment	pCi g^{-1}								
2 year	5.0E-03	1.7E-02	2.3E-02	4.6E-02	6.0E-02	6.2E-02	4.1E-02	4.3E-02	4.0E-02
5 year	4.1E-03	1.4E-02	1.9E-02	4.5E-02	5.9E-02	6.1E-02	4.1E-02	4.5E-02	4.2E-02
10 year	3.8E-03	1.3E-02	1.7E-02	4.4E-02	5.8E-02	6.0E-02	4.0E-02	4.5E-02	4.3E-02
25 year	3.6E-03	1.2E-02	1.6E-02	4.4E-02	5.8E-02	6.0E-02	4.0E-02	4.5E-02	4.3E-02
50 year	3.5E-03	1.2E-02	1.6E-02	4.3E-02	5.7E-02	5.9E-02	4.0E-02	4.5E-02	4.3E-02
100 year	3.4E-03	1.2E-02	1.6E-02	4.3E-02	5.7E-02	5.9E-02	4.0E-02	4.5E-02	4.3E-02
500 year	3.2E-03	1.1E-02	1.5E-02	4.2E-02	5.6E-02	5.8E-02	3.9E-02	4.5E-02	4.3E-02
Deposited sediment	pCi g^{-1}								
2 year	3.0E-03	1.0E-02	1.4E-02	2.7E-02	3.6E-02	3.7E-02	2.4E-02	2.6E-02	2.4E-02
5 year	2.5E-03	8.5E-03	1.1E-02	2.7E-02	3.5E-02	3.7E-02	2.4E-02	2.7E-02	2.5E-02
10 year	2.3E-03	7.9E-03	1.0E-02	2.7E-02	3.5E-02	3.6E-02	2.4E-02	2.7E-02	2.6E-02
25 year	2.2E-03	7.5E-03	9.8E-03	2.6E-02	3.5E-02	3.6E-02	2.4E-02	2.7E-02	2.6E-02
50 year	2.1E-03	7.2E-03	9.6E-03	2.6E-02	3.4E-02	3.5E-02	2.4E-02	2.7E-02	2.6E-02
100 year	2.1E-03	7.1E-03	9.3E-03	2.6E-02	3.4E-02	3.5E-02	2.4E-02	2.7E-02	2.6E-02
500 year	2.0E-03	6.7E-03	8.8E-03	2.5E-02	3.3E-02	3.5E-02	2.3E-02	2.7E-02	2.6E-02

4.6 Limitations and Uncertainties of Surface Water Pathway Calculations

There are a number of considerations that must be taken into account when reviewing the points of exposure concentration estimates. The goal of these modeling efforts was to develop conservative estimates of the relative concentrations between pre-fire and post-fire conditions for the surface water pathways. The estimation of concentrations at selected points of exposure was

central to these efforts. As a starting point for the calculations, simplifying assumptions were made. In addition, accommodations based on the limitations of the available data were made. Finally, it was beyond the scope of these screening calculations to complete a full, quantitative uncertainty analysis. However, as discussed in Section 4.5, sensitivity calculations were performed for the major input variables to understand their affect on the point of exposure concentration estimates.

When evaluating the point of exposure concentration estimates the following simplifying assumptions, which would tend to estimate higher concentrations at the points of exposure, should be considered:

- The volumes (for both clean water and sediments) used for the Rio Grande and the Cochiti Lake are median values, so they would tend to minimize the dilution of the concentrations.
- Storm events do not actually occur over the whole of the LANL watersheds at the same time, but the storm flows assume that it is raining all over LANL during the same 6-hour period.
- There is no time lag in the surface water model for travel time in the watersheds; all of the concentrations arrive at the point of exposure at the same time.
- No losses of chemical mass or radionuclide activity were attributed to the natural processes of deposition and resuspension as the storm water flows away from the source areas to the point of exposure.
- All TSS in storm water over a source area results from the source area, so that there are maximum chemical mass and radionuclide activity released from the source area during a storm event.
- The K_d values were chosen from the low-end of the possible range, which tends to predict higher water concentrations and lower suspended sediment concentrations. If suspended sediment-related exposure pathways are determined to have unacceptable risks, then the K_d values and the concentration calculations can be reevaluated.
- Dilution is the only attenuation mechanism considered for concentrations of chemicals and radionuclides in environmental media at the points of exposure.
- The source areas are assumed to be infinite. That is, there is sufficient chemical mass or radionuclide activity at the source areas to be in equilibrium with the storm water that flows over the source area for each design storm intensity.
- The effectiveness of best management practice was not included, except in cases where the erosion matrix score was assigned after the best management practice installation.
- There was a significant sediment removal operation that occurred in upper Los Alamos Canyon after the fire, which has not been included in the model.

In addition, there are a number of factors that lead to uncertainty in the calculated concentration values. A number of these issues were addressed in the sensitivity calculations; however, they remain sources of uncertainty:

- The K_d values used may not represent site conditions.
- The identified source areas may not include all of the actual source areas that exist at the LANL facility. For example, complete characterization exists for only ^{239}Pu and ^{137}Cs in Los Alamos/Pueblo Canyon sediments. There are no data available for other canyon sediments for these radionuclides.

- The mass of suspended sediment movement from a source area to a point of exposure was estimated from a TSS concentration. In reality, the movement from source areas to a point of exposure of suspended sediments containing chemicals and radionuclides is a very complex process that is not easily modeled. It depends on, among other things, the sediment particle size distribution, the specific chemical or radionuclide, the storm water flow rate and regime, and the soil properties at the source area. The sediment transport was also time-dependent during each storm event.
- The flow over each source area is independent. This was the only feasible way to implement the screening calculations. The implication is that there is clean water coming onto each source area and mobilizing the soil containing chemicals and radionuclides consistent with the TSS values.
- The concentration of TSS can be considered to be uniform throughout the surface water domain. Based on the empirical analyses conducted during this study, we know that this is not true; however, we chose values for TSS from the empirical data distributions for pre- and post-fire conditions. The empirical data distributions take into account the differences across all of the sampling locations.
- Concentrations of chemicals and radionuclides in storm water were the result of equilibrium partitioning between the soil particles and the water.
- A simple mass balance of chemicals and radionuclides between storm water and soil particles was considered.
- There were limited empirical data available to compare to the model estimates.
- Where PRS, geomorphic units, and unsampled reaches overlapped the burn area, no adjustments were made; that is, the contributing areas were treated as independent sources of chemicals or radionuclides.
- The source areas were characterized using a wide range of data sets, based on the availability of the data. Only the available soil concentration data for the top 2 ft of soil at each source area were used. For some areas the concentrations were estimated based on a fairly large number of samples, for others (e.g., the unsampled reaches) the concentrations were estimated based on similar source areas and no field samples for the actual source area. In addition, when the data sets were assembled for each source area the non-detect values were eliminated. The representativeness of the data for characterizing the defined source areas varied by chemical and radionuclide.
- PRS soil data analyses were not necessarily directed at only what was thought to be present (i.e., full-suite analyses) which complicates the understanding of which chemicals and radionuclides should be considered for source term development at each source area. By calculating net concentrations, we were able to overcome this issue to some degree.
- The applicability of the assumed aerial extent for a PRS is not known. In actuality the area for each source area was expected to vary by chemical and radionuclide.
- The effect of man-made barriers, flow diversions, and other best management practices on storm water flow and ultimately on the concentrations of chemicals and radionuclides at the point of exposure were not included in the calculations.
- Spatial heterogeneity applied to all of the input variables (e.g., TSS, f_{oc} , background values, ash concentrations); however, we chose single values. The storm water runoff was modeled as a spatially varying quantity with the grid-based model.

- The effect of suspended sediment particle size on sediment partitioning and transport properties was not included in the model.

4.7. Comparison of Predicted to Measured Concentrations

To understand how our predicted concentrations compare to measured concentrations, or empirical data, we compiled monitoring data that was appropriate for such comparisons at each point of exposure (POE). In the following sections, we discuss the criteria we used for selecting relevant monitoring data and compare the measured concentrations with the predicted concentrations.

4.7.1 Selecting Sampling Locations for Comparison

Because there are no monitoring locations that correspond exactly to the coordinates established for each POE, we compiled the available data for sampled locations in the general vicinity of each POE. We identified relevant locations using an iterative approach of increasing the maximum distance criteria between the x- and y-coordinates for each POE and any corresponding sampling locations, as noted in the environmental monitoring data sets provided by ESH-18, ER Project, and NMED, until sufficient sampling locations were selected to enable a meaningful comparison. We initially selected all sampling locations within 100 m of any POE location, but this yielded an insufficient number of sampling locations. Therefore, we increased the distance to 250 m, and used all sampling locations meeting that criterion for our comparisons. For each POE, all sampling locations within 250 m were selected, and all corresponding data were grouped to calculate average concentrations for comparison to the predicted POE concentrations. Table 4-35 provides the x- and y-coordinates for each POE.

Table 4-35. Point of Exposure Coordinates

POE	X Coordinate ^a	Y Coordinate ^a
1.1	395567	3968506
1.2	390769	3970116
2.1	380719	3942288
3.1	386690	3957214
4.1a	385457	3967250
4.1b	382423	3965945

^a Coordinates are Universal Transverse Mercator (UTM)
NAD 83, Zone 13, meters

In addition to sampling locations within 250 m of each POE, we identified additional data appropriate for comparison. Although the locations coordinates do not meet our 250 m criterion, there are three locations above the Cochiti Lake dam and one location below the dam that are sampled by ESH-18 and useful for comparison to concentrations predicted for POE 2.1. Additionally, the ER Project conducted sediment sampling in lower Los Alamos Canyon during March 2001 to assess the impacts of storm events on October 23-24, 2000 that reportedly corresponded to a one-year return period event. These data are included in our comparison of predicted and measured concentrations for POE 1.2. The ER Project also conducted sediment sampling during September 2001 at approximately the same area following a July 2, 2001 storm

event that reportedly corresponded to a ten-year return period event. These data are also included in our comparison of predicted and measured concentrations for POE 1.2. Table 4-36 provides the monitoring locations identified as relevant for comparison to each POE.

For the comparisons, we have selected all available results at each location corresponding to a particular POE, including nondetects. Average concentrations are then calculated by analyte for each location or group of locations corresponding to a given POE. Time and resource limitations prevented us from further segregating and examining the data to incorporate a discussion of the impact of including various different sampling or analytical techniques. As noted in Chapter 2, we have evaluated the data to the extent possible, based on the values that were provided to us. We do, however, identify those analytes where average concentrations are based entirely on nondetect values. We do not identify analytes where average concentrations are based on some detects and some nondetects.

4.7.2. Limitations of Comparing Predicted and Measured Concentrations

There are a number of issues that complicate the process of making comparisons of empirical data, or measured values, to the concentrations we have predicted at each POE. As discussed above, the comparisons we are able to make are limited to concentrations for samples collected in the general vicinity (i.e., within 250 m) of each POE. In some cases, this results in a very small number of samples with which to make comparisons. The concentrations measured in 1 or 2 samples may or may not be a reflection on the average concentration in the general area because of expected spatial heterogeneity. Also, in many instances, the only values to which we can make comparisons are reported as nondetects. This limits the usefulness of the comparison because nondetect values do not provide an indication of the true concentration, but rather an estimate of the upper bound value.

As discussed previously in this chapter, the concentrations we have predicted at each POE are likely conservative estimates of, or higher than, the true value that would be expected. This conservatism results from a number of different sources and assumptions that have been made throughout the calculations. Because of this, it would be anticipated that our predicted concentrations would consistently be higher than the observed or measured concentrations. This would be expected, all things being equal. However, our source area characterization is most complete for ^{137}Cs and $^{239,240}\text{Pu}$, with varying degrees of completeness for other chemicals and radionuclides (see Chapter 3). As a result of incomplete source terms for some chemicals and radionuclides, it is possible to predict concentrations that are lower than measured concentrations. For example, we have only included a certain set of radionuclides and chemicals that appear particularly elevated above background in ash for the burn area source term. Certainly, though, there would be contributions from the burn area for other chemicals and radionuclides, as well as from natural native soils that are eroded. In addition, characterization data for sediments in canyons other than Los Alamos and Pueblo Canyons are not available. Our primary goal was to provide a conservative estimate of the LANL contribution to POE concentrations of chemicals and radionuclides at known areas of contamination that we have been able to characterize, and we believe we have done that, considering the limitations and uncertainties discussed in Chapters 3 and 4.

Table 4-36. Environmental Monitoring Locations Identified as Relevant for Comparison to Predicted POE Concentrations

Organization	Sample Location	Monitoring data			Predicted data		
		X-UTM ^a	Y-UTM	Media	POE	Diff X ^b	Diff Y
ESH-18	Spring 2	395336	3968465	groundwater	1.1	231	41
				sediment, surface			
	Pueblo at SR-502	390960	3970210	water	1.2	191	94
				sediment, surface			
	Frijoles at Rio Grande	386645	3957344	water	3.1	45	130
	Rio Grande at Frijoles	386690	3957342	nd	3.1	0	127
	Rio Grande at Frijoles (bank)	386691	3957338	sediment, surface			
				water	3.1	1	123
	Rio Grande at Frijoles (wdth intgrt)	386718	3957328	nd	3.1	28	113
	Canon de Valle at Mouth	382234	3965987	storm water	4.1b	189	42
	Water Canyon at Beta	382491	3965931	surface water	4.1b	68	14
	Cochiti Lower ^c	380673	3943464	sediment	2.1 (above dam)	46	1176
	Cochiti Middle	381156	3945707	sediment	2.1 (above dam)	437	3419
	Cochiti Upper	381747	3948565	sediment	2.1 (above dam)	1028	6277
				sediment, surface			
NMED	Rio Grande at Cochiti	380061	3942321	water	2.1 (below dam)	658	33
	Pueblo Canyon (below Bayo treatment plant)	390528	3970263	sediment	1.2	241	148
	Pueblo Canyon @ SR 502	390550	3970255	nd	1.2	218	140
	Los Alamos Canyon near SR 4	390555	3970051	suspended sediment, water	1.2	214	64
	RG below Frijoles, top layer	386605	3957161	sediment/sludge	3.1	85	53
ER	WA-10024	382271	3965962	sediment	4.1b	152	17
	WA-10025	382288	3965957	sediment	4.1b	135	12
	WA-10026	382297	3965950	sediment	4.1b	126	5
	WA-10027	382309	3965949	sediment	4.1b	114	4
	WA-10028	382326	3965956	sediment	4.1b	97	11
	WA-10029	382337	3965948	sediment	4.1b	86	3
	Totavi	na	na	sediment	1.2	na	na

^a Coordinates are Universal Transverse Mercator (UTM) NAD 83, Zone 13, meters

^b Diff X and Diff Y are the absolute values of the difference (m) between the sampling and POE location x- and y-coordinates, respectively

^c The highlighted sampling locations may not be within 250 m of a POE or may be locations for which coordinates were not available; however, they are included for comparison as discussed in the report text preceding this table

Another complicating factor relates to the fact that background values were available for only certain radionuclides and chemicals in sediments and soil. Documented background values were not available for chemicals and radionuclides in water. The source term development (Chapter 3) and transport calculations discussed in this chapter resulted in net (i.e., in excess of background) concentrations for only those chemicals and radionuclides for which background values were available. For all other chemicals and radionuclides, total concentrations resulting from the considered source areas are calculated. As a result, comparisons of predicted and measured concentrations must be made with caution, and the conclusions that can be drawn vary by chemical or radionuclide and by media.

All of these complicating issues aside, we are still able to make some useful comparisons of predicted to measured concentrations that provide some measure of the performance of our transport calculations and predicted POE concentrations. These comparisons are presented in the following sections. All comparisons are made assuming the concentrations predicted for the two-year return period storm event.

4.7.3. Comparisons of Predicted and Measured Concentrations

To facilitate making comparisons of predicted and measured concentrations, we have divided the data into four categories, which are discussed in the following sections:

- 1) sediment concentrations with available background values
- 2) sediment concentrations without available background values
- 3) water concentrations for chemicals and radionuclides with available soil/sediment background values
- 4) water concentrations for chemicals and radionuclides without available soil/sediment background values.

4.7.3.1 Sediment Concentrations for Chemicals and Radionuclides with Available Background Values. For predicted suspended and deposited sediments with background values (see Table 3-10), we can add the assumed background concentration to our predicted concentration to derive a value that is appropriate for comparing to measured concentrations. This likely represents the most valid comparison we can make, although comparisons made for radionuclides or chemicals without available background values but that would not be expected to be present in the environment outside of LANL operational contributions should also be valid.

Tables 4-37, 4-38, and 4-39 show the predicted to observed ratios for sediments with background values at POEs 1.2, 3.1, and 2.1R, respectively. Predicted to observed ratios for POE 2.1BD are not shown, but they are similar to the ratios shown for POE 2.1R. Many of the radionuclides and chemicals show predicted concentrations within an order of magnitude or less of the observed concentrations. This results from adding background values to relatively small predicted concentrations and comparing to measured values likely representative of background conditions. There is a consistent trend of higher predicted concentrations by 1 to 2 orders of magnitude for radionuclides in deposited sediments where the predicted concentrations are much higher than background (i.e., ^{241}Am , ^{137}Cs , ^{238}Pu , and $^{239,240}\text{Pu}$; see Table 4-46). This trend suggests conservative, high-biased source term values for these radionuclides, along with

conservative transport calculations. This over-prediction appears less for suspended sediments at POE 1.2 (Table 4-37), though there are limited measurement results for comparison.

Comparing the predicted to observed ratios for the two sets of ER sampling data suggests generally lower observed concentrations corresponding to the ten-year return period event occurring in July 2001, although the ratios differ by less than a factor of two and are generally consistent with the range of ratios based on the other data sets included in Table 4-37. The lower observed concentrations for the ten-year event as compared to the one-year event are consistent with the slightly lower predicted concentrations as a function of increasing storm intensity. It is also possible that the quantity of ash containing elevated concentrations of materials available for release to runoff water had diminished between the October 2000 and July 2001 storm events. Appendix R-1 provides additional details regarding these comparisons.

Table 4-37. Predicted to Observed Ratios for Sediments with Background Values at POE 1.2

Analyte	Suspended sediment (NMED, post-fire)		Sediment (ESH-18, post-fire data)		Sediment (ER, post-fire data ^a)		Sediment (ER, post-fire data ^b)		Sediment (NMED, post-fire data)	
	P/O	n ^c	P/O	n	P/O	n	P/O	n	P/O	n
<i>Chemicals</i>										
Arsenic	6.5E-01	1			1.5E+00	8	2.9E+00	14	6.4E-01	1
Barium	4.6E-01	1			1.1E+00	8	1.8E+00	14	2.8E+00	1
Chromium	5.9E-01	1			1.6E+00	8			1.7E+00	1
Copper	4.8E-01	1			8.4E-01	8	1.6E+00	14	1.5E-01	1
Lead	1.8E+00	1			3.7E+00	8	6.1E+00	14	6.7E+00	1
Mercury	6.1E-01	1			2.3E+00	8	1.9E+00	14	3.7E-01	1
Uranium	4.2E-01	1								
<i>Radionuclides</i>										
Americium-241 ^d	7.5E+00	1	3.9E+01	2	-3.1E+02 ^e	9	2.0E+02	14	7.1E+01	1
Cesium-137 ^d	3.9E+00	1	5.3E+02	1	2.2E+01	9	3.1E+01	14		
Plutonium-238 ^d	9.1E+00 ^f	1	6.4E+01	1	4.7E+01	9	6.8E+01 ^f	14	3.6E+01	1
Plutonium-239 ^d	2.3E+01	1	1.6E+01	1	3.8E+01	9	5.1E+01	14	1.5E+01	1
Potassium-40			1.1E+00	1						
Strontium-90	2.6E-01	1	1.1E+00	3	1.9E+00	9	2.5E+00	14		
Uranium-234	5.8E-01	1	8.9E-01	1						
Uranium-235	1.1E+00	1	1.0E+00	1			5.5E-01	14		
Uranium-238	5.2E-01	1	1.1E+00	1						

^a March 2001 sampling after an October 2000 one-year return period event

^b September 2001 sampling after a July 2001 ten-year return period event

^c Number of environmental measurements or observations

^d Analytes with predicted concentrations much greater than background (see Table 4-46)

^e Analytes with negative average measured value

^f All available measurements or observations were recorded as nondetects

**Table 4-38. Predicted to Observed Ratios for Sediments
with Background Values at POE 3.1**

Analyte <i>Chemicals</i>	Sediment (ESH-18, post-fire data)		Sediment (NMED, post-fire data)	
	P/O	n ^a	P/O	n
Arsenic	1.3E+00	4		
Barium	1.2E+00	4		
Chromium	1.3E+00	4		
Copper	9.9E-01	4		
Lead	1.9E+00	4		
Mercury	2.1E+00	4		
<i>Radionuclides</i>				
Americium-241 ^b	-1.5E+03 ^c	11	6.1E+00	1
Cesium-137 ^b	1.3E+01	5	2.5E+00	1
Plutonium-238 ^b	7.1E+01	6		
Plutonium-239 ^b	3.6E+02	6		
Potassium-40	1.2E+00	5	8.6E-01	1
Strontium-90	2.1E+00	5		
Thorium-228	1.1E+00	7		
Thorium-230	1.1E+00	7		
Thorium-232	1.3E+00	7		
Uranium-234	8.2E-01	7		
Uranium-235	7.0E-01	8	1.1E-01	1
Uranium-238	8.8E-01	12		

^a Number of environmental measurements or observations^b Analytes with predicted concentrations much greater than
background (see Table 4-46)^c Analytes with negative average measured value

Table 4-39. Predicted to Observed Ratios for Sediments with Background Values at POE 2.1R

Analyte	Sediment (ESH-18, post-fire data)	
	P/O	n ^a
<i>Chemicals</i>		
Arsenic	8.1E-01	5
Barium	5.2E-01	5
Chromium	5.5E-01	5
Copper	3.9E-01	5
Lead	1.0E+00	5
Mercury	2.1E-01	5
<i>Radionuclides</i>		
Americium-241 ^b	1.2E+01	18
Cesium-137 ^b	3.5E+00	9
Plutonium-238 ^b	6.2E-01	11
Plutonium-239 ^b	6.3E+01	11
Potassium-40	1.5E+00	9
Strontium-90	2.6E+00	9
Thorium-228	9.3E-01	9
Thorium-230	9.8E-01	9
Thorium-232	1.3E+00	9
Uranium-234	8.7E-01	9
Uranium-235	6.1E-01	18
Uranium-238	6.6E-01	18

^a Number of environmental measurements or observations

^b Analytes with predicted concentrations much greater than background (see Table 4-46)

4.7.3.2 Sediment Concentrations for Chemicals and Radionuclides without Available Background Values. Comparisons for radionuclides or chemicals without available background values (see Table 3-10) but that would not be expected to be present in the environment outside of LANL operational contributions should also be valid. This does not imply that all radionuclides and chemicals presented in this section (e.g., radionuclides and PAHs) would not be expected to be present in the environment outside of LANL operational contributions. Tables 4-40 and 4-41 show the predicted to observed ratios for sediments without background values at POEs 3.1 and 2.1R, respectively. For the organic chemicals (e.g., PAHs), predicted values are generally 1 to 2 orders of magnitude greater than the observed values. It is important to note that nearly all of the comparisons are to nondetect values, suggesting an even greater over prediction of the true concentration. The significant under prediction for N-Nitrosodimethylamine is likely a result of a small source term and predicted concentrations well below the detection limit. The under prediction for radium and thorium isotopes is likely a result of not incorporating background values (i.e., no values were provided in available

documentation) into the calculations for these radionuclides combined with relatively low source area concentrations, as they would be expected to be naturally present in area soils. Appendix R-2 provides additional details regarding these comparisons.

**Table 4-40. Predicted to Observed Ratios for Sediments without
Background Values at POE 3.1**

POE 3.1 <i>Chemicals</i>	Sediment (ESH- 18, post-fire data)		Sediment (NMED, post- fire data)	
	P/O	n ^a	P/O	n
<i>Chemicals</i>				
Aldrin				
Benzo(a)anthracene	1.2E+02 ^b	3		
Benzo(a)pyrene	1.3E+02 ^b	3		
Benzo(b)fluor anthene	1.5E+02 ^b	3		
Benzo(k) fluoranthene	6.1E+01 ^b	3		
Dibenz(a,h)anthracene	6.3E+00 ^b	3		
Indeno(1,2,3-cd)pyrene	7.3E+01 ^b	3		
N-Nitrosodimethylamine	8.8E-09 ^b	3		
RDX	7.9E+00 ^b	3		
<i>Radionuclides</i>				
Protactinium-234M	1.5E-03 ^b	5	1.1E-03	1
Radium-224	6.1E-05	5		
Radium-226	7.1E-02	5		
Radium-228	2.8E-05	5		
Thorium-234	2.5E-03	5	7.3E-04	1

^a Number of environmental measurements or observations

^b All available measurements or observations were recorded as
nondetects

Table 4-41. Predicted to Observed Ratios for Sediments without Background Values at POE 2.1R

POE 2.1R	Sediment (ESH-18, post-fire data)	
<i>Chemicals</i>	P/O	n ^a
Aldrin		
Benzo(a)anthracene	3.8E+01 ^b	4
Benzo(a)pyrene	4.0E+01 ^b	4
Benzo(b)fluor anthene	4.6E+01 ^b	4
Benzo(k) fluoranthene	1.9E+01 ^b	4
Dibenz(a,h)anthracene	2.0E+00 ^b	4
Indeno(1,2,3-cd)pyrene	2.3E+01 ^b	4
N-Nitrosodimethylamine	1.3E-09 ^b	4
RDX	1.9E+00 ^b	4
<i>Radionuclides</i>		
Protactinium-234M	9.3E-04	9
Radium-224	2.3E-05	9
Radium-226	3.4E-02	9
Radium-228	1.3E-05	9
Thorium-234	8.1E-04	9

^a Number of environmental measurements or observations

^b All available measurements or observations were recorded as nondetects

4.7.3.3 Water Concentrations for Chemicals and Radionuclides with Available Soil/Sediment Background Values. We can also examine predicted to observed ratios in water concentrations for chemicals and radionuclides with available soil/sediment background values (see Table 3-10). Tables 4-42 and 4-43 show the predicted to observed ratios for water concentrations at POEs 1.2 and 3.1, respectively. Comparisons show predicted to observed ratios of 1 to 2 orders of magnitude for most analytes, with somewhat higher ratios (2 to 3 orders of magnitude) for those radionuclides with predicted sediment concentrations much higher than background. The relatively larger over prediction for water than for sediment (Tables 4-37, 4-38, and 4-39) provides support for our assertion that we have selected K_d values that likely provide conservative estimates of dissolved water concentrations. The over predictions would likely be even greater if background values were available for water to add to our predicted values for a more appropriate comparison to measured concentrations. The under prediction for arsenic likely results from the lack of a background water concentration to add to our predicted value for comparison to the measured values. Again, it is important to note that several of the comparisons are to nondetect values, suggesting an even greater over prediction of the true concentration in those cases. Appendix R-3 provides additional details regarding these comparisons.

**Table 4-42. Predicted to Observed Ratios for Water for Chemicals and Radionuclides
with Available Soil/Sediment Background Values at POE 1.2**

POE 1.2 <i>Chemicals</i>	Water, filtered (ESH-18, post-fire data)		Water, filtered (NMED, post-fire data)		Water, unfiltered (ESH-18, post-fire data)		Water, unfiltered (NMED, post-fire data)	
	P/O	n ^a	P/O	n	P/O	n	P/O	n
Arsenic	7.2E-04	3	2.3E-03	2	2.7E-03 ^b	1	1.1E-03	1
Barium	3.5E+00	3	6.2E-01	2	3.3E+00	1		1
Chromium	3.1E+01 ^b	2	5.7E+01	2	1.1E+02 ^b	1	5.6E+01 ^b	1
Copper	3.9E+01	3	1.7E+02	2	3.0E+01	1	1.3E+01	1
Lead	1.8E+02 ^b	3	2.7E+02	2			2.4E+01	1
Mercury			7.0E+01 ^b	2	1.9E+02 ^b	3	7.1E+01	1
Uranium	3.1E+01	1	1.7E+01	1				
<i>Radionuclides</i>								
Americium-241 ^d			-2.1E+00 ^c	1	-1.0E+02 ^c	5		
Cesium-137 ^d			1.5E+03	2	6.1E+02	3		
Plutonium-238 ^d			4.6E+00	1	2.2E+02	2		
Plutonium-239 ^d			1.8E+03	1	5.7E+03	2		
Strontium-90			1.5E+01	1	4.6E+01	2		
Tritium					-3.2E-02 ^c	2		
Uranium-234			3.7E+01	1	9.9E+01	2		
Uranium-235			4.7E-01	2	5.1E-01	4		
Uranium-238			7.2E+01	1	8.6E-01	4		

^a Number of environmental measurements or observations^b All available measurements or observations were recorded as nondetects^c Analytes with negative average measured value^d Analytes with predicted concentrations much greater than background for sediments (see Table 4-46)

Table 4-43. Predicted to Observed Ratios for Water for Chemicals and Radionuclides with Available Soil/Sediment Background Values at POE 3.1

Analyte	Water, filtered (ESH-18, post-fire data)	Water, unfiltered (ESH-18, post-fire data)		
<i>Chemicals</i>	P/O	n ^a	P/O	n
Arsenic	8.7E-01 ^b	6		
Barium	4.8E+01	6		
Chromium	2.9E+01 ^b	6		
Copper	1.2E+02 ^b	6		
Lead	5.8E+01 ^b	6		
Mercury	5.9E+01	4	6.4E+01	5
Uranium	3.0E+00	1		
<i>Radionuclides</i>				
Americium-241 ^d			-7.7E+00 ^c	11
Cesium-137 ^d			2.1E+02	5
Plutonium-238 ^d			3.5E+01	6
Plutonium-239 ^d			5.6E+03	6
Potassium-40			1.3E-04	5
Strontium-90			2.8E+01	6
Tritium			-1.8E-03 ^c	5
Uranium-234			8.6E+00	6
Uranium-235			4.5E-02	4
Uranium-238			2.0E-01	11

^a Number of environmental measurements or observations
^b All available measurements or observations were recorded as nondetects
^c Analytes with negative average measured value
^d Analytes with predicted concentrations much greater than background for sediments (see Table 4-46)

4.7.3.4 Water Concentrations for Chemicals and Radionuclides without Available Soil/Sediment Background Values. As noted for the sediment comparisons, comparisons for radionuclides or chemicals in water without available background values (see Table 3-10) but that would not be expected to be present in the environment outside of LANL operational contributions should also be valid. As noted above, this does not imply that all radionuclides and chemicals presented in this section (e.g., radionuclides and PAHs) would not be expected to be present in the environment outside of LANL operational contributions. Tables 4-44 and 4-45 show the predicted to observed ratios for water concentrations at POEs 1.2 and 3.1, respectively.

The comparisons suggest over predictions for the organic chemicals at POE 3.1 of 1 to 2 orders of magnitude, with an even greater over prediction of RDX at POE 3.1. The small under prediction for the organic chemicals at POE 2.1BD shows the impact of water dilution by the lake. As with the sediment, the significant under prediction for N-Nitrosodimethylamine is likely a result of a small source term and predicted concentrations well below the detection limit. As noted for the sediment comparisons, the under prediction for radium and thorium isotopes is likely a result of not incorporating background values (i.e., no values were provided in available documentation) into the calculations for these radionuclides, as they would be expected to be naturally present. Again, it is important to note that nearly all of the comparisons are to nondetect values, suggesting an even greater over prediction of the true concentration in those cases. Appendix R-4 provides additional details regarding these comparisons.

**Table 4-44. Predicted to Observed Ratios for Water for
Chemicals and Radionuclides without Available
Soil/Sediment Background Values at POE 3.1**

Analyte	Water, unfiltered (ESH-18, post-fire data)	
	P/O	n ^a
<i>Chemicals</i>		
Aldrin		
Benzo(a)anthracene	1.3E+02 ^b	4
Benzo(a)pyrene	1.4E+02 ^b	4
Benzo(b)fluor anthene	1.6E+02 ^b	4
Benzo(k) fluoranthene	6.2E+01 ^b	4
Dibenz(a,h)anthracene	6.7E+00 ^b	4
Indeno(1,2,3-cd)pyrene	7.5E+01 ^b	4
N-Nitrosodimethylamine	1.6E-06 ^b	4
RDX	1.9E+04 ^b	4
<i>Radionuclides</i>		
Lead-210		
Neptunium-237	7.1E-02 ^b	5
Protactinium-234M	4.2E-04 ^b	5
Radium-224	-6.7E-04 ^{b,c}	5
Radium-226	1.0E+00 ^b	5
Radium-228	8.2E-05 ^b	5
Thorium-234	6.9E-04	5

^a Number of environmental measurements or observations

^b All available measurements or observations were recorded as nondetects

^c Analytes with negative average measured value

Table 4-45. Predicted to Observed Ratios for Water for Chemicals and Radionuclides without Available Soil/Sediment Background Values at POE 2.1BD

Analyte	Water, unfiltered (ESH-18, post-fire data)	
	P/O	n ^a
<i>Chemicals</i>		
Aldrin		
Benzo(a)anthracene	1.7E-01 ^b	1
Benzo(a)pyrene	1.6E-01 ^b	1
Benzo(b)fluor anthene	1.8E-01 ^b	1
Benzo(k) fluoranthene	7.3E-02 ^b	1
Dibenz(a,h)anthracene	7.2E-03 ^b	1
Indeno(1,2,3-cd)pyrene	8.3E-02 ^b	1
N-Nitrosodimethylamine	5.3E-08 ^b	1
RDX	6.7E+02 ^b	1
<i>Radionuclides</i>		
Neptunium-237	-6.4E-03 ^{b,c}	2
Protactinium-234M	2.3E-06 ^b	2
Radium-224	6.6E-07 ^b	2
Radium-226	3.1E-03 ^b	2
Radium-228	7.9E-07 ^b	2

^a Number of environmental measurements or observations

^b All available measurements or observations were recorded as nondetects

^c Analytes with negative average measured value

4.7.4 Comparison of Predicted Sediment Concentrations with Background

It is also instructive to examine the predicted concentrations in deposited sediments as they related to assumed background values (Table 4-46) (assumed background values are presented in Table 3-10). As noted in the preceding tables, the predicted concentrations for ²⁴¹Am, ¹³⁷Cs, ²³⁸Pu, and ^{239,240}Pu are significantly greater than background concentrations because of the large contribution from modeled source areas, particularly the Los Alamos and Pueblo Canyon sediments (Geomorphic Unit and Unsampld Reach source areas). The relative contribution from these modeled source areas decreases with increasing distance from the source areas. These radionuclides do not show significant predicted concentrations at POE 4.1b because of the lack of contribution from modeled source areas (i.e., there are no canyon sediment source areas contributing to this POE).

**Table 4-46. Percent Contribution of Background When Background Concentrations are
Added to Predicted Deposited Sediment Concentrations**

Analyte	POE 1.2	POE 3.1	POE 2.1R	POE 2.1BD	POE 4.1b
<i>Chemicals</i>					
Arsenic	100.0%	94.3%	96.8%	96.8%	98.3%
Barium	98.6%	70.2%	81.3%	81.3%	26.8%
Chromium	89.6%	94.6%	97.0%	97.0%	87.2%
Copper	54.9%	52.4%	67.1%	67.1%	78.5%
Lead	16.3%	35.2%	49.9%	49.9%	74.2%
Mercury	65.3%	84.1%	92.1%	92.1%	97.8%
Uranium	94.5%	94.5%	97.0%	97.0%	94.9%
<i>Radionuclides</i>					
Americium-241	0.2%	0.8%	1.4%	1.4%	94.5%
Cesium-137	1.3%	5.4%	9.5%	9.5%	92.3%
Plutonium-238	0.8%	3.1%	5.6%	5.6%	97.9%
Plutonium-239	0.1%	0.3%	0.5%	0.5%	81.2%
Potassium-40	100.0%	100.0%	100.0%	100.0%	100.0%
Strontium-90	50.4%	81.4%	89.1%	89.1%	99.6%
Thorium-228	80.7%	94.7%	97.1%	97.1%	100.0%
Thorium-230	76.4%	93.3%	96.2%	96.2%	100.0%
Thorium-232	80.4%	94.6%	97.0%	97.0%	100.0%
Uranium-234	88.5%	97.1%	98.4%	98.4%	100.0%
Uranium-235	84.5%	95.9%	97.8%	97.8%	99.6%
Uranium-238	83.7%	95.7%	97.6%	97.6%	99.8%

4.7.5 Conclusions

The comparisons presented in this section suggest consistently over predicted concentrations by 1 to 2 orders of magnitude for ^{241}Am , ^{137}Cs , ^{238}Pu , and $^{239,240}\text{Pu}$, which all have predicted sediment concentrations much higher than background for POEs impacted by the Geomorphic Unit and Unsampled Reach source areas. Predicted concentrations for Hg, RDX, and PAHs are generally 1 to 3 orders of magnitude greater than measured concentrations. These comparisons are primarily to nondetect values, which suggests an even greater over prediction than noted. This over prediction supports the noted conservatism that has been incorporated into both the source term development and transport calculations. The over prediction is generally greater for water than for sediment, again supporting our use of likely low-biased K_d values, which translate into higher predicted water concentrations. Under predictions are likely the result of either incomplete source term information, or the fact that no background values are available to incorporate into the predictions. The relative contribution of background to predicted sediment concentrations is high for all analytes except ^{241}Am , ^{137}Cs , ^{238}Pu , and $^{239,240}\text{Pu}$. The Geomorphic Units and Unsampled Reaches in Los Alamos and Pueblo Canyons contribute significantly to the predicted concentrations for these radionuclides. As would be expected, the background contribution for these radionuclides increases with increasing distance from the Los Alamos watershed.

5 RISK ESTIMATES

5.1 Exposure Scenarios

An exposure scenario is a profile of a fictional but realistic person with lifestyle, diet, habits and residence, or work locations that are representative of individuals living in the area. Developing appropriate exposure scenarios is an effective approach to estimate a range of potential risks for different individuals in the area who may have been exposed to materials released during and following the Cerro Grande fire. It is not feasible or practical to develop an individual exposure assessment for every resident who lives or works in the LANL area and could be impacted by fire-related chemical and radionuclide transport. At the other extreme, it is not credible to evaluate only a single exposure situation that would apply to all potentially exposed residents.

Input from those directly impacted by the Cerro Grande Fire, including local residents, the NMED, LANL personnel, and other stakeholders, is important to establish as many site-specific parameters as possible for the scenarios. The surface water pathway exposure scenarios were designed for locations within the surface water model domain (see Figure 1-2). Surface water originating within or flowing across LANL travels through a series of discrete canyons eastward and drains into the Rio Grande. Land features of the general area and lifestyles of those living or visiting in the vicinity of LANL during and after the fire were considered in this assessment. While each scenario is designed to represent a single hypothetical individual, the combination of scenarios incorporates a number of typical lifestyle traits for residents in the area and takes into account variations in such things as location with respect to LANL and the fire, length of time in the area, work activity level, amount of time spent outdoors, age, and gender.

The scenarios were not designed to include all conceivable lifestyles of individuals who were in the area at the time of the fire and in the year(s) following. Rather, they provide a wide range of potential profiles of people in the area. It is also important to understand which parameters have the greatest impact on potential exposure and to develop credible scenarios that include the range of possible values for those parameters. We developed these exposure scenarios with caution so that a potentially exposed person or an exposure pathway would not be missed. It is important to emphasize that individuals represented by the exposure scenarios would have a risk greater than that of other individuals who might be in the area for less time or under less exposed conditions. For this reason, while some parameter values may be higher than average values used in other studies, they are not unrealistically high.

Four scenarios were considered for the risk calculations, based on the results of the site conceptual model (Chapter 4). One or more likely points of exposure (POE) were identified for each scenario (Section 4.3 and Figure 5-1) to represent locations at which an individual represented by a scenario is likely to come in contact with surface water, suspended sediments, or deposited sediment containing concentrations of chemicals or radionuclides. This section describes the exposure scenarios, and Table 5-1 lists the scenarios considered for evaluating surface water risks and provides the parameter values used as input to the exposure assessment and the risk calculations.

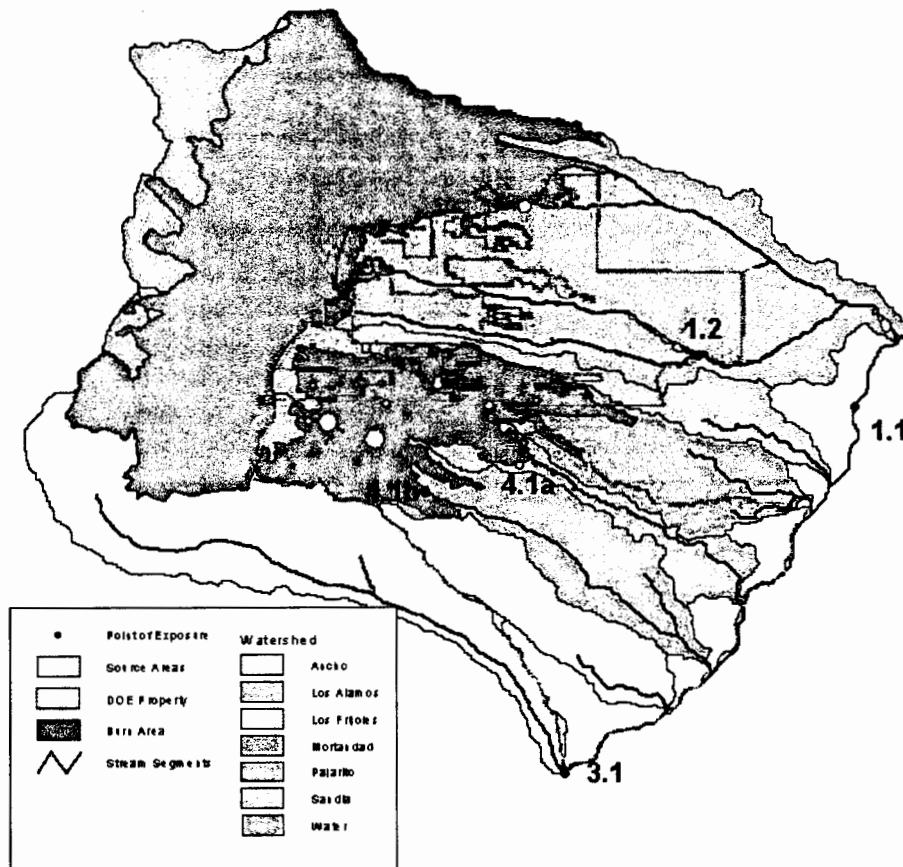


Figure 5-1. Point of exposure locations for POE 1.1, 1.2, 3.1, 4.1a, and 4.1b. The point of exposure locations for POE 2.1R and POE 2.1BD on the shore of and below Cochiti Lake are not shown.

1. Local hunter from White Rock:

- This person harvests, captures, and consumes wild game and fish from the LANL region.
- It is assumed that the individual uses Rio Grande water for 10% of drinking water needs.
- It is assumed this individual uses the fish or larger game animals as a food source.
- This person lives in White Rock and may hunt in at least two locations:
 - On the east side of the Rio Grande just below LANL; and in so doing, may inadvertently, ingest river water and sediments from just below LANL (POE 1.1).
 - On the lower Los Alamos Canyon; again may be exposed to water and sediments in the lower Los Alamos Canyon stream. (POE 1.2)
- This scenario uses parameter values that reflect a hunter lifestyle in terms of time at the designated POE. Because of a lack of data on transfer coefficients for chemicals and radionuclides in wild game animals like elk, we assume ingestion of beef cattle, which have used the water source at the designated POE locations.
- Potentially important pathways include ingestion of Rio Grande water, fish from the Rio Grande at POE 1.1, and beef cattle grazing near POE 1.1; external exposure from contaminated sediments/soils near the Rio Grande (POE 1.1) and near the lower Los Alamos Canyon stream (POE 1.2), and inadvertent ingestion of deposited sediments at those locations.

2. Farm family living below Cochiti Lake:

- This farm family scenario involves several exposed individuals who live on land below the reservoir near the river; they use water from the Rio Grande for irrigating their garden produce, which they use as a food source.
- This scenario includes an adult and a child who spend a majority of their time at the location on the Rio Grande below Cochiti Lake (POE 2.1BD), with recreational activities occurring in and near Cochiti Lake (POE 2.1R).
- These individuals spend their leisure time swimming in Cochiti Lake and during these activities inadvertently ingest water directly from the reservoir and sediments/soils from the shore. They also use fish caught in the reservoir for food.
- Potential pathways include ingestion of water from river and reservoir, inadvertent ingestion of deposited sediments from riverbank and shoreline, ingestion of fish from reservoir, ingestion of garden produce, and direct exposure from contaminated ground surface.

3. Resident living on the Rio Grande below the confluence of the Water Canyon outlet to the Rio Grande:

- This person spends much time outdoors, eats local garden produce, and uses Rio Grande water for 10% of drinking water needs.
- This individual spends a majority of time along the Rio Grande immediately below the confluence of the Los Frijoles watershed and the Rio Grande (POE 3.1).
- This individual is a hunter and fisherperson and uses these as an important part of this food sources along with garden produce, which is irrigated with water from the nearby river.
- Potential pathways include ingestion of water from river; inadvertent ingestion of deposited sediments from riverbank, ingestion of fish from river, ingestion of garden produce irrigated with river water, and direct exposure from contaminated ground.

4. Local fire cleanup worker and others using the LANL site during and after the fire:

- This person represents someone involved in local cleanup efforts onsite and offsite during and immediately following the fire.
- It is assumed that this person would be potentially exposed for a period of 4 months during and after the fire in the cleanup effort.
- Risks are calculated for two points of exposure on a stream segment immediately below the source areas in Pajarito watershed (POE 4.1a) and on a stream segment immediately below the source areas in the Water watershed (4.1b).
- Possible pathways include inadvertent ingestion of deposited sediments in watershed areas and external exposure from contaminated ground surface.

To determine the exposure duration (number of years of exposure due to the Cerro Grande Fire) for the surface water pathways, we estimated the length of time the post-fire conditions were expected to continue in the watersheds. The fire caused changes in the watershed that increased the potential for chemicals and radionuclides to be transported from the source areas into the

canyons, the Rio Grande, and Cochiti Lake. This condition will exist until the area revegetates and watersheds regain their pre-fire characteristics. A specific estimate of the time for the watershed to return to a pre-fire condition is not possible; however, some sources indicate that this condition could last for several years to decades in some locations (DOE 2000). For purposes of this risk analysis, we selected a period of 7 years.

Once the canyons return to a condition that is similar to the pre-fire conditions, the incremental risk associated with the fire will likely end or will, at least, be substantially reduced. For Scenarios 1, 2, and 3, we assumed a period of 7 years for the exposure duration. For Scenario 4, we assume that the firefighter and clean up personnel from offsite (who were not site employees) would have been onsite for 4 months (120 days) during and after the fire. However, we completed the risk calculations for a 1-year period for ease of comparison (see Appendix U). These risks can be used to approximate a multiple-year exposure risk by multiplying the annual values by an estimated number of years for the watersheds to regain their pre-fire characteristics (e.g., 7. years). This likely overstates the longer-term risks because we assumed that the concentrations of chemicals and radionuclides at the points of exposure would remain constant for the 7 year period even though the concentrations at those locations would likely decrease as the burned portions of the watersheds recovered from the impacts of the fire.

The exposure frequency (number of days per year of exposure) for storm water in the canyons is a function of the number of storm events per year and the duration of each storm event. Based on the Army Corp of Engineer's weather data for Cochiti Lake (USACE 2002) and the weather stations at LANL (LANL 2001b), there are an average of 88 days per year with recorded precipitation. We assumed it would be during this time that the water flow would contribute radionuclides and chemicals associated with fire down the canyons streams to the Rio Grande. For the risk calculations, we assumed an exposure frequency of 100 days per year for the individuals represented by Scenarios 1 and 4, representing those who are exposed while on or near LANL boundaries during hunting and outdoor activities, or who were fighting the fire or involved in cleanup activities. For the individuals living along the Rio Grande or on Cochiti Lake (represented by Scenarios 2 and 3), we assumed an exposure frequency of 365 days per year. Even with this time as the exposure frequency, the calculations were still conservative for at least three reasons:

- non-depleting sources are assumed,
- each rain event was assumed to occur throughout the watershed contributing to the point of exposure, and
- each rain event is assumed to result in the same concentrations of chemicals and radionuclides.

The exposure frequency for the surface water pathways depends on the exposed individual's activities and on the media being considered, including storm water in the canyons (which includes a dissolved water concentration and a suspended sediment concentration); surface water in the Rio Grande and Cochiti Lake (which includes a dissolved water concentration and a suspended sediment concentration); deposited sediments in the canyons; and deposited sediments in the river and reservoir beds. These media and assumed exposures to them are described in more detail below.

- **Storm Water in the Canyons**—The stream segments in the canyons are typically dry except during a rain event. The primary opportunity for an individual to contact storm water in the canyons is during a rain event. The concentration estimates were based on a

series of 6-hour storm events and assumed that the total volume of water and suspended sediment that can result from these storm events will arrive at the point of exposure at a single point in time. However, the actual flow through the canyons could take 24 hours or longer, based on the surface water modeling results (See Chapter 4). Therefore, we assumed the time for an individual to contact storm water in the canyons was 1 day per storm event.

The modeling results also indicated that, in general, there was not a significant difference in between storm events in the predicted concentrations (see Chapter 4). To be conservative, we assumed that rain events of lower intensity and duration than the 2-year, 6-hour storm will generate similar storm water and suspended sediment concentrations. A limitation for shorter rain events is that the volume of water may not be sufficient to cause flow from LANL at the POE; however, it is not unreasonable to assume that any rainfall event presents an opportunity for exposure to concentrations of chemicals or radionuclides in surface water. We also assumed that a given rain event created flow across all existing source areas located within each watershed, which in many situations would not be the case. Given an average of 88 days per year of recorded precipitation, we assumed an exposure frequency of 100 days per year for surface water in the canyons for individuals associated with POE 1.2, POE 3.1, POE 4.1a and POE 4.1b.

- **Surface Water in the Rio Grande**—For the Rio Grande, the surface water concentrations of chemicals and radionuclides associated with the fire would be discharged into the river only during the flow periods from the canyons that cross the LANL facility (an average of 88 days per year). However, to be conservative, we assumed an exposure frequency for surface water in the river was 100 days per year. This would apply to receptors associated with POE 1.1, POE 2.1, and POE 3.1
- **Surface Water in the Cochiti Lake**—For surface water in the Cochiti Lake, we based the exposure frequency on the number of precipitation events per year and the average retention time in the reservoir. The retention time would represent the length of time that the water from the Rio Grande was in the lake (reservoir). If Cochiti Lake was modeled as a completely mixed volume, then the residence time (t_r) would be calculated as a function of the reservoir volume (V_{res}) and the outlet flow at the dam (Q_{outlet}).

$$t_r = \frac{V_{res}}{Q_{outlet}} \quad (5.1)$$

Using median values for V_{res} (50,000 ac-ft discussed in Section 4.4.5) and Q_{outlet} (890 cfs based on Rio Grande flow below the dam discussed in Section 4.4.3), the t_r is 29 days. Given that there are on average 88 rain events per year, the surface water concentrations in the reservoir were assumed to be constant throughout the year. This would apply to receptors associated with POE 2.1R and POE 2.1BD.

- **Deposited Sediments in the Canyons, Rio Grande and Cochiti Lake** — The Rio Grande has cyclical fluctuation in water level, with the river and its tributaries draining land areas that encompass a widely varied landscape, including mountains, forested areas, and arid regions. In this mostly arid to semiarid region, the Rio Grande is characterized equally well by absence and presence of flow. Many of the river tributaries are intermittent streams. Much of the flow is controlled by numerous reservoirs in the basin. The potential for a receptor to contact sediments deposited in the stream segments within the canyons, in the river, and in the reservoir would, therefore, exist throughout the year. This would apply to receptors associated with POE 1.1, POE 1.2, POE 4.1a, and POE 4.1b.
- **Deposited Sediments in the River and Reservoir beds**—Based on the above discussion, the potential for an individual to contact sediments deposited in the river or in the reservoir would exist throughout the year. This assumption would apply to individuals associated with POE 1.1, POE 2.1, and POE 3.1.

The pathways considered to result in exposure to these media were:

1. Ingestion of drinking water (untreated) (*Scenario 1, POE 1.1 and 1.2; Scenario 2, POE 2.1R and POE 2.1BD; and Scenario 3, POE 3.1*).
2. Sediment exposure (ingestion, external exposure, and dermal contact) (*All scenarios and POEs*).
3. Swimming or contact with water in Cochiti Lake and Rio Grande (immersion and inadvertent ingestion) (*Scenario 2, POE 2.1R and POE 2.1BD*).
4. Consumption of fish (from Rio Grande and Cochiti Lake) (*Scenario 1, POE 1.1; Scenario 2, POE 2.1 R and POE 2.1BD; and Scenario 3, POE 3.1*).
5. Consumption of garden produce irrigated with river water (*Scenario 2, POE 2.1R and POE 2.1BD; and Scenario 3, POE 3.1*).
6. Consumption of meat from cattle using water from the river and Cochiti Lake (*Scenario 2, POE 2.1R and POE 2.1BD; and Scenario 3, POE 3.1*).

Table 5-1 summarizes the exposure parameter values used for the scenarios. In the following sections, we describe the equations and input parameters for each exposure pathway in detail.

Table 5-1. Scenarios and Selected Exposure Parameters for Surface Water Pathways^a

Scenario→	Hunter	Farmer	Child	Resident on Rio Grande	Fire cleanup personnel
Parameter↓				Below confluence of Water Canyon with Rio Grande	Burned areas of Water and Mortandad Canyons
General location	White Rock	Below Cochiti Lake			
Point of exposure (POE)	1.1, 1.2	2.1	2.1	3.1	4.1a, 4.1b
Time at location (h d ⁻¹)	12	24	24	24	12
Exposure frequency (d y ⁻¹) ^b	100	365	365	365	100
Exposure duration (y)	17	7	7	7	0.3
Body weight (kg)	70	70	30	70	70
Water ingestion pathway					
Water ingestion (L d ⁻¹)	2	2	1	2	2
Fraction of water from the Rio Grande	0.1	0.1	0.1	0.1	0
Sediment exposure pathways					
Sediment ingestion (g d ⁻¹)	0.1	0.1	0.1	0.1	0.2
External exposure to sediment (h d ⁻¹)	2	2	4	2	4
Dermal contact with sediment (h y ⁻¹)	15	50	50	50	15
Fraction of sediment that is impacted	0.5	0.5	0.5	0.5	1
Irrigation— garden produce consumption pathways					
Irrigation rate (L m ⁻² d ⁻¹)	na ^c	2	2	2	na
Produce ingested (kg d ⁻¹)	na	0.3	0.15	0.3	na
Fraction of homegrown produce impacted	na	0.2	0.2	0.2	na
Fish and meat consumption					
Freshwater fish consumption (kg d ⁻¹)	0.012 (POE 1.1)	0.012	0.005	0.012	na
Meat consumption (kg d ⁻¹)	0.04 (POE 1.1)	0.04	0.02	0.04	na
Fraction of meat that is impacted	0.1	0.1	0.1	0.1	
Immersion-dermal contact with water					
Swimming or dermal contact (h y ⁻¹)	na	50	50	na	na

- ^a These scenarios encompass the range of potential exposure scenarios for which risk calculations were estimated.
- ^b The exposure frequency for storm water is a function of the number of storm events per year and the duration of each storm event. There are only 88 days per year where it was assumed that water flowed in the canyons and contributed concentrations to the Rio Grande. This would impact only Scenario 1 (POE 1.2) and Scenario 4 (POE 4.1a and 4.1b). See text preceding this table for additional details.
- ^c Does not apply to this scenario.

5.2 Methods of Risk Calculation

5.2.1 Drinking Water Ingestion

The most direct pathway for exposure to water in the Rio Grande and Cochiti Lake was to as a source of drinking water. The EPA recommends drinking water intake rates of 2 L d⁻¹ for adults, and 1.5 L d⁻¹ for children for exposure assessments (EPA 1999a). These values represent upper percentile tap water intake rates, and they include drinking water consumed in the form of juices and other beverages containing tap water, such as coffee. We assumed a daily drinking water intake rate (U_w) for adults of 2 L d⁻¹ and for the child in Scenario 2 of 1.5 L d⁻¹. It was further assumed that 10% of the drinking water was obtained directly from the Rio Grande or Cochiti Lake without treatment or hold-up time and that drinking water was consumed at the same rate all year long (i.e., $F_{cw} = 0.1$; exposure frequency (EF) = depends on scenario). The ingestion of untreated drinking water is unlikely and contributed to the conservatism of the calculation.

The drinking water ingestion risk per year for radionuclides is given by

$$\frac{Risk}{y} = C_w \cdot U_w \cdot F_{cw} \cdot EF \cdot RF_{ing,w} \cdot CF_{activity} \quad (5.2)$$

where

- C_w = radionuclide concentration in river water (pCi L⁻¹)
- U_w = daily consumption rate of drinking water (L d⁻¹)
- F_{cw} = fraction of water containing radionuclide (unitless)
- EF = exposure frequency (d y⁻¹)
- $RF_{ing,w}$ = lifetime morbidity risk coefficient for ingestion of water (Risk Bq⁻¹)
- $CF_{activity}$ = conversion factor for activity (Bq pCi⁻¹).

Lifetime morbidity risk coefficient values for radionuclides for this and all pathways were taken from EPA Federal Guidance Report 13 (EPA 1999b) unless otherwise noted. Radionuclide risk coefficients used in the calculation of risk in this section are shown in Appendix S.

The drinking water ingestion risk per year for carcinogenic chemicals is given by

$$\frac{Risk}{y} = \frac{C_w \cdot U_w \cdot EF \cdot F_{cw} \cdot SF_o}{BW \cdot AT} \quad (5.3)$$

where

- C_w = chemical concentration in river water (mg L⁻¹)
- U_w = daily consumption rate of drinking water (L d⁻¹)
- F_{cw} = fraction of water containing chemical (unitless)
- EF = exposure frequency (d y⁻¹)
- SF_o = oral intake slope factor (kg d mg⁻¹)
- BW = body weight (kg)

AT = averaging time (d).

Slope factors for carcinogenic chemicals for this and all pathways were taken from EPA's Integrated Risk Information System (IRIS) (EPA 2001a), EPA's Preliminary Remedial Goal (PRG) tables (EPA 2000, 2001b), and the Oak Ridge National Laboratory Risk Assessment Information System Database (ORNL 2001). All chemical risk slope factors and reference doses used in the calculation of risk in this section are shown in Appendix P. Body weight was generally accepted to be 70 kg for a standard man, and an averaging time for carcinogenic chemical exposures was over a lifetime of 70 years, or 25,550 days.

The drinking water ingestion hazard quotient for noncarcinogenic chemicals is given by

$$HQ = \frac{C_w \cdot U_w \cdot EF \cdot ED \cdot F_{cw}}{BW \cdot AT} \div RfD_o \quad (5.4)$$

where

C_w = chemical concentration in river water (mg L^{-1})
 U_w = daily consumption rate of drinking water (L d^{-1})
 F_{cw} = fraction of water containing chemical (unitless)
 EF = exposure frequency (d y^{-1})
 ED = exposure duration (y)
 BW = body weight (kg)
 AT = averaging time (d)
 RfD_o = oral intake reference dose ($\text{mg kg}^{-1} \text{d}^{-1}$).

Reference doses for noncarcinogenic chemicals for this and all pathways were taken from EPA's IRIS (EPA 2001a), EPA's PRG tables (EPA 2000, 2001b), the Oak Ridge National Laboratory Risk Assessment Information System Database (ORNL 2001), and ATSDR Toxicological Profiles (ATSDR 1990–2000) and are detailed in Appendix T. Averaging time (d) for noncarcinogenic chemicals is equivalent to the exposure duration (y). For most of the scenarios, we used an exposure duration of 1 year. For cases where the exposure frequency is 365 d y^{-1} , the hazard quotient for 1 year would be equal to the hazard quotient for any exposure duration of interest.

5.2.2 Deposited Sediment Exposure Pathways

Several potential exposure pathways were associated with the accumulation of sediments containing chemicals and radionuclides along the shores or in shallower sections of the streams and river with slow moving waters. Potential exposure pathways associated with the accumulation of sediments along the stream and river banks and along the shores of Cochiti Lake were the inadvertent ingestion of sediments containing radionuclide and chemicals, external exposure to radionuclides in sediments, and dermal contact with chemical and radionuclides in the sediments. The individuals who may be exposed to sediment under these circumstances

included those represented by all the scenarios at all POE. We assumed that external exposure to sediments could occur throughout the year. However, it may not be reasonable to assume that a person would be exposed to sediment for 24 hours a day every day of the year. NCRP (1996) recommends an exposure time of 2000 h yr⁻¹ for screening calculations, which is roughly equivalent to 5.5 h d⁻¹ for 365 d y⁻¹. The EPA does not address this issue specifically but recommends a value of 1.5 h d⁻¹ for the time an adult spends outdoors as compared to 5 to 7 h d⁻¹ for children (3–11 years of age). We assumed an exposure frequency of 2 h d⁻¹ for adults in Scenarios 1, 2, and 3, and 4 h d⁻¹ for the child in Scenario 2 and the fire cleanup worker in Scenario 4. The sediment exposure pathways are discussed below.

5.2.2.1 Sediment Ingestion

Inadvertent ingestion of sediments and soils can occur where river sediments have accumulated and could occur during activities such as sitting, playing, digging, picking berries, or firefighting. While data on sediment ingestion rates are lacking, data regarding soil ingestion rates may be relevant. EPA recommends a central estimate value of 0.05 g d⁻¹ for daily soil ingestion by adults, and suggests a value of 0.1 g d⁻¹ as a conservative central estimate, with a value of 0.2 g d⁻¹ for children, 0–6 years (EPA 1999a). However, data on soil ingestion rates are limited, particularly in adults, and therefore uncertain. For the inadvertent ingestion of chemicals or radionuclides in sediments, we assumed an ingestion rate of 0.1 g d⁻¹ for adults in Scenarios 1, 2, and 3, and 0.2 g d⁻¹ for the child in Scenario 2 and the fire cleanup worker in Scenario 4. For Scenarios 1, 2, and 3, we further assumed that the fraction of sediment containing chemicals and radionuclides (F_{csed}) was 0.5. For Scenario 4, we assumed a F_{csed} of 1.

The equation that describes the risk per year from radionuclides from ingestion of sediments is

$$\frac{Risk}{y} = C_{sed} \cdot U_{sed} \cdot F_{csed} \cdot EF \cdot RF_{ing,d} \cdot CF_{activity} \quad (5.5)$$

where

C_{sed}	=	concentration of sediments (pCi g ⁻¹)
U_{sed}	=	ingestion rate of sediment (g d ⁻¹)
F_{csed}	=	fraction of sediment containing radionuclide (unitless)
EF	=	exposure frequency (d y ⁻¹)
$RF_{ing,d}$	=	lifetime morbidity risk coefficient for dietary ingestion (Risk Bq ⁻¹)
$CF_{activity}$	=	conversion factor (Bq pCi ⁻¹).

The equation that describes the risk per year from carcinogenic chemicals from ingestion of sediments is

$$\frac{Risk}{y} = \frac{C_{sed} \cdot U_{sed} \cdot F_{csed} \cdot EF \cdot SF_o \cdot CF_{mass}}{BW \cdot AT} \quad (5.6)$$

where

C_{sed}	=	concentration of sediments (mg kg ⁻¹)
U_{sed}	=	ingestion rate of sediment (g d ⁻¹)

F_{csed}	=	fraction of sediment containing chemical (unitless)
EF	=	exposure frequency (d y ⁻¹)
SF_o	=	oral intake slope factor (kg d mg ⁻¹)
CF_{mass}	=	conversion factor (kg g ⁻¹)
BW	=	body weight (kg)
AT	=	averaging time (d).

The equation that describes the hazard quotient for noncarcinogenic chemicals from ingestion of sediments is

$$HQ = \frac{C_{sed} \cdot U_{sed} \cdot F_{csed} \cdot EF \cdot ED \cdot CF_{mass}}{BW \cdot AT} \bigg/ RfD_o \quad (5.7)$$

where

C_{sed}	=	concentration of sediments (mg kg ⁻¹)
U_{sed}	=	ingestion rate of sediment (g d ⁻¹)
F_{csed}	=	fraction of sediment containing chemical (unitless)
EF	=	exposure frequency (d y ⁻¹)
ED	=	exposure duration (y)
CF_{mass}	=	conversion factor (kg g ⁻¹)
BW	=	body weight (kg)
AT	=	averaging time (d)
RfD_o	=	oral intake reference dose (mg kg ⁻¹ d ⁻¹).

5.2.2.2 External Exposure from Sediments.

External shoreline-type exposure to sediments applies only to the radionuclide pathway, because the effects of radioactivity are still measurable for some types of decay at some distance from the source. Dermal contact, when chemicals can be absorbed across the skin barrier, is the critical external sediment exposure pathway for chemicals. This pathway is discussed in the next section.

We assumed that external exposure to sediments could occur throughout the exposure period for radionuclides in sediments. We assumed an exposure period of 2 hours per day for the adults living below Cochiti Lake (Scenario 2) and on the Rio Grande (Scenario 3), and 4 hours per day for the hunter (Scenario 1), the child in Scenario 2, and the fire cleanup worker during and after the fire (Scenario 4).

Under some circumstances, a distinction can be made between low and high water levels which can uncover more or less of the sediment, and a unitless shielding factor may be applied. Based on the previous discussion of the surface water flow characteristics, for the external exposure to sediments pathway, we assumed no shielding factor for high water conditions.

The risk per year for external exposure to radionuclides in shoreline sediments is given by

$$\frac{Risk}{y} = C_{sed} \cdot ET \cdot F_{si} \cdot EF \cdot RF_{ext} \cdot CF_{time} \cdot CF_{activity} \cdot CF_{mass} \quad (5.8)$$

where

C_{sed}	=	sediment concentration (pCi g ⁻¹)
ET	=	exposure time (h d ⁻¹)
F_{si}	=	sorption adjustment factor (dimensionless) for radionuclide i
EF	=	exposure frequency (d y ⁻¹)
RF_{ext}	=	risk per unit dose for external exposure (Risk kg Bq ⁻¹ s ⁻¹)
CF_{time}	=	conversion factor (s h ⁻¹)
$CF_{activity}$	=	conversion factor (Bq pCi ⁻¹)
CF_{mass}	=	conversion factor (g kg ⁻¹).

Lifetime morbidity risk coefficient values for radionuclides for this and all pathways are taken from EPA Federal Guidance Report 13 (EPA 1999b) unless otherwise noted.

5.2.2.3 Dermal Contact/Absorption

Some activities could result in sediment containing chemicals and radionuclides adhering to the skin. Adsorption across the skin barrier is necessary for exposure to any hazardous chemicals. Similarly, for radionuclides the radiation must penetrate the skin barrier. This exposure pathway is referred to as dermal contact.

For radionuclides, electrons would probably not be energetic enough to be the cause of significant external exposure from standing on the shoreline (as calculated in the preceding section), but when sediment is applied directly to the skin, exposure becomes more likely. We consider dermal contact as a special case because no compilations of risk factors for radionuclides exist for these types of exposures. Our ability to assess this pathway was limited, but we used the information available on the dose delivered by dermal contact to assess the potential risk due to this pathway. Kocher and Eckerman (1987) estimated dose rate conversion factors for all of the radionuclides considered for this work. They assume that radioactivity is uniformly distributed over the entire body surface instead of just over some fraction of the body's surface area. In addition, gamma-emitting radionuclides in sediment on the skin surface would irradiate the entire body and not just the skin. This exposure was not included in the risk calculations for this pathway because it had a negligible effect on the dermal contact risk for radionuclides. The preceding section addresses external exposure to gamma radiation from sediments on the ground surface.

For chemicals, more information was available to assess the risk from dermal contact with sediments. Permeability constants have been defined for each chemical of concern that allow us to calculate risk from this pathway (Table 5-2). Generic factors for absorption were required, which make these calculations less quantitative. For exposure to sediments through dermal contact, we assumed exposure times would be similar to time spent swimming. In that case, a person might have actual physical contact with sediment if lying on the beach or playing on the shore (for the child in Scenario 2, for example). As a conservative estimate, we assumed dermal contact with sediments occurred 50 hours per year for individual in the Scenarios 2 and 3, and 15 hours per year for the hunter in Scenario 1 and the fire cleanup worker in Scenario 4. We also

assumed that all sediments contacted by an individual contained the predicted concentrations of chemicals and radionuclides.

On the whole, the risks calculated for the dermal contact pathway were considered to be more uncertain than other calculated risks because of unknowns associated with the calculations. We completed these calculations to check on the relative magnitude of the risks in comparison with other risks than as an absolute quantitative assessment of risk from dermal contact with sediments.

The risk per year for dermal contact with radionuclides in sediments is given by

$$\frac{Risk}{y} = C_{sed} \cdot \rho \cdot d \cdot ET \cdot EF \cdot DCF_{der} \cdot w_T \cdot RC \cdot CF_{time} \cdot CF_{activity} \cdot CF_{area} \quad (5.9)$$

where

C_{sed}	=	concentration of radionuclide in sediment (pCi g ⁻¹)
ρ	=	density of sediment (g m ⁻³)
d	=	depth of sediment for exposure (m)
ET	=	exposure time (h d ⁻¹)
EF	=	exposure frequency (d y ⁻¹)
DCF_{der}	=	dose conversion factor for dermal contact with radionuclides (Sv y ⁻¹ per Bq cm ⁻²)
w_T	=	tissue weighting factor (unitless)
RC	=	lifetime risk coefficient (Risk Sv ⁻¹)
CF_{time}	=	conversion factor (y h ⁻¹)
$CF_{activity}$	=	conversion factor (Bq pCi ⁻¹)
CF_{area}	=	conversion factor (m ² cm ⁻²).

Because the sediment concentrations emerging from the transport calculations are in units of pCi g⁻¹, we had to make assumptions about the density and depth of the sediment in order to arrive at a surface concentration. We assumed that the sediment density was 1.5 × 10⁶ g m⁻³ and that the top 1 cm (0.01 m) of sediment was available for the dermal contact pathway. Additionally, the dose conversion factors for dermal contact with sediments containing radionuclides assumed uniform distribution on the entire body surface, an exposure condition that is likely not very realistic.

We assumed a nominal lifetime cancer incidence risk coefficient of 6.0 × 10⁻² Sv⁻¹ based on ICRP Publication 60 (ICRP 1991, Table 3). This risk coefficient accounts for both fatal and non-fatal cancers. The ICRP tissue weighting factor of 0.01 for the skin (ICRP 1991, Table 2) was applied to convert the skin dose into an effective dose because the nominal cancer incidence risk coefficient relates to the effective (whole body) dose rather than the risk per unit dose to the skin.

The risk per year for dermal contact with carcinogenic chemicals in sediments is

$$\frac{Risk}{y} = \frac{C_{sed} \cdot AF \cdot ABS \cdot SA \cdot ET \cdot EF \cdot SF_{der} \cdot CF_{time} \cdot CF_{mass} \cdot CF_{area}}{AT \cdot BW} \quad (5.10)$$

where

C_{sed}	=	concentration of chemical in sediment (mg kg^{-1})
AF	=	adherence factor (mg cm^{-2})
ABS	=	absorption factor (unitless)
SA	=	surface area ($\text{m}^2 \text{d}^{-1}$)
ET	=	exposure time (h d^{-1})
EF	=	exposure frequency (d y^{-1})
SF_{der}	=	dermal contact slope factor (kg d mg^{-1})
CF_{time}	=	conversion factor (d h^{-1})
CF_{mass}	=	conversion factor (kg mg^{-1})
CF_{area}	=	conversion factor ($\text{cm}^2 \text{m}^{-2}$)
AT	=	averaging time (d)
BW	=	body weight (kg).

The hazard quotient for dermal contact with noncarcinogenic chemicals in sediments is given by:

$$HQ = \frac{C_{sed} \cdot AF \cdot ABS \cdot SA \cdot ET \cdot EF \cdot ED \cdot CF_{time} \cdot CF_{mass} \cdot CF_{area}}{AT \cdot BW} \div RfD_{der} \quad (5.11)$$

where

C_{sed}	=	concentration of chemical in sediment (mg kg^{-1})
AF	=	adherence factor (mg cm^{-2})
ABS	=	absorption factor (unitless)
SA	=	surface area ($\text{m}^2 \text{d}^{-1}$)
ET	=	exposure time (h d^{-1})
EF	=	exposure frequency (d y^{-1})
ED	=	exposure duration (y)
CF_{time}	=	conversion factor (d h^{-1})
CF_{mass}	=	conversion factor (kg mg^{-1})
CF_{area}	=	conversion factor ($\text{cm}^2 \text{m}^{-2}$)
AT	=	averaging time (d)
BW	=	body weight (kg)
RfD_{der}	=	dermal contact reference dose ($\text{mg kg}^{-1} \text{d}^{-1}$).

EPA (1990) derived the dermal chronic reference dose (RfD), dermal subchronic RfD, and dermal slope factors. The RfD is an estimate (with uncertainty spanning perhaps an order of magnitude) of a daily exposure to the human population (including sensitive subgroups) that is likely to be without an appreciable risk of deleterious effects. Uncertainties were introduced by the differences in routes of exposure and by the fact that the oral dose-response relationships were based on potential (i.e., administered) dose, whereas the dermal dose estimates were absorbed doses. Ideally, these differences in route and dose type would be resolved via pharmacokinetic modeling. Alternatively, if estimates of the gastrointestinal absorption fraction were available for the compound of interest in the appropriate vehicle, then the oral dose-response factor, unadjusted for absorption, could be converted to an absorbed dose basis (EPA 1992).

Available surface area is the average surface area for head, hands, forearms, and lower legs for an adult, and is estimated by EPA to be equal to $0.53 \text{ m}^2 \text{ d}^{-1}$ (EPA 1992). The adherence factor is a generic value for soil adherence to human skin of 1.0 mg cm^{-2} (EPA 1999b). Absorption factor varies with type of chemical, inorganic or organic, and it is equivalent to 0.1% for inorganic chemicals and 1.0% for organics (EPA 1992).

5.2.3 Fish Consumption

Fish consumption is an important primary exposure pathway identified for radionuclides and chemicals to the Rio Grande and Cochiti Lake. For freshwater fish consumption by the general population, EPA (1999a) recommended a value of 6.6 g d^{-1} (2.4 kg y^{-1}). The EPA recommends a higher mean fish consumption value for fish from recreational fishing of 0.18 g of fish per kg of body weight per day ($\text{g kg}^{-1} \text{ d}^{-1}$), or 5 kg y^{-1} for adults and 2 kg y^{-1} for children. For the surface water pathway risk, we assume a freshwater fish consumption rate of 12 g d^{-1} ($\sim 5 \text{ kg y}^{-1}$) for adults in Scenarios 1 (POE 1.1), 2 (POE 2.1), and 3 (POE 3.1), and 5 g d^{-1} ($\sim 2 \text{ kg y}^{-1}$) for a child in Scenario 2.1. The radionuclide-specific bioconcentration factors selected for these screening calculations for freshwater fish are shown in Table 5-3. We assumed no hold-up time between catch and consumption of the fish for the risk analysis.

The fish ingestion risk per year from radionuclides is given by

$$\frac{\text{Risk}}{y} = C_w \cdot BCF_{fw} \cdot U_{fw} \cdot EF \cdot RF_{ing,d} \cdot CF_{activity} \quad (5.12)$$

where

C_w	=	concentration of radionuclide in river water (pCi L^{-1})
BCF_{fw}	=	radionuclide specific bioaccumulation factor in freshwater fish (L kg^{-1})
U_{fw}	=	daily consumption rate of freshwater fish (kg d^{-1})
EF	=	exposure frequency (d y^{-1})
$RF_{ing,d}$	=	lifetime morbidity risk coefficient for dietary ingestion (Risk Bq^{-1})
$CF_{activity}$	=	conversion factor (Bq pCi^{-1}).

The fish ingestion risk per year from carcinogenic chemicals is given by the following equation:

$$\frac{\text{Risk}}{y} = \frac{C_w \cdot BCF_{fw} \cdot U_{fw} \cdot EF \cdot SF_o}{AT \cdot BW} \quad (5.13)$$

where

C_w	=	concentration of chemical in river water (mg L^{-1})
BCF_{fw}	=	chemical specific bioaccumulation factor in freshwater fish (L kg^{-1})
U_{fw}	=	daily consumption rate of freshwater fish (kg d^{-1})
EF	=	exposure frequency (d y^{-1})

SF_o = oral intake slope factor (kg d mg⁻¹)
 AT = averaging time (d)
 BW = body weight (kg).

The fish ingestion hazard quotient from noncarcinogenic chemicals is given by the following equation:

$$HQ = \frac{C_w \cdot BCF_{fw} \cdot U_{fw} \cdot EF \cdot ED}{AT \cdot BW} \div RfD_o \quad (5.14)$$

where

C_w = concentration of chemical in river water (mg L⁻¹)
 BCF_{fw} = chemical specific bioaccumulation factor in freshwater fish (L kg⁻¹)
 U_{fw} = daily consumption rate of freshwater fish (kg d⁻¹)
 EF = exposure frequency (d y⁻¹)
 ED = exposure duration (y)
 AT = averaging time (d)
 BW = body weight (kg)
 RfD_o = oral intake reference dose (mg kg⁻¹ d⁻¹).

5.2.4 Produce Consumption

Produce consumed by individuals could contain chemicals and radionuclides as a result of irrigation by both foliar interception of water containing chemicals and radionuclides and from uptake of radionuclides through roots growing in contaminated soil containing chemicals and radionuclides. Irrigation with Rio Grande water in northern New Mexico is known to occur in fields used for growing garden produce and crops south of Cochiti Lake. We assumed the individual in Scenario 2, which were the residents living on the Rio Grande below Cochiti Lake (POE 2.1), used water from the Rio Grande below Cochiti Lake for irrigation purposes. We used the NCRP screening models methodology (NCRP 1996) to calculate the concentration in fresh vegetables due to direct irrigation and buildup in soil over a 30-year time period. The irrigation rate recommended by NCRP for these calculations is 2 L m⁻² d⁻¹ (NCRP 1996) (see Table 5-1).

The EPA Exposure Factors Handbook (EPA 1999a) indicates that the median intake of vegetables for the U.S. population is 4.3 g kg⁻¹ d⁻¹. For the average 70 kg adult, this is approximately 0.30 kg d⁻¹ of vegetable consumption. The distribution of values for this parameter has a 95th percentile value of 0.72 kg d⁻¹. For these risk calculations, we assumed vegetable ingestion of 0.3 kg d⁻¹, with 20 % of vegetables consumed containing the predicted concentrations of chemicals and radionuclides. For the child in Scenario 2, we assumed a consumption rate of 0.15 kg d⁻¹ (55 kg y⁻¹) (NCRP 1996). Again, we were unable to complete this pathway for chemicals due to the unavailability of transfer coefficients from water to vegetation.

The equation for calculating risk per year for radionuclides from ingestion of food crops containing radionuclides is

$$\frac{Risk}{y} = C_{prod} \cdot U_{prod} \cdot F_{cp} \cdot EF \cdot RF_{ing,d} \cdot CF_{activity} \quad (5.15)$$

where

- U_{prod} = ingestion rate of produce containing radionuclide ($kg\ d^{-1}$)
- F_{cp} = fraction of consumed produce that contains radionuclide
- EF = exposure frequency ($d\ y^{-1}$)
- $RF_{ing,d}$ = lifetime morbidity risk coefficient for dietary ingestion ($Risk\ Bq^{-1}$)
- $CF_{activity}$ = conversion factor ($Bq\ pCi^{-1}$)

and

$$C_{prod} = C_{uw} \cdot F_{ir} \cdot CF_{veg} \quad (5.16)$$

where

- C_{prod} = concentration of radionuclide in produce ($pCi\ kg^{-1}$)
- C_{uw} = concentration of radionuclide in unfiltered river water ($pCi\ L^{-1}$)
- F_{ir} = irrigation rate ($L\ m^{-2}\ d^{-1}$)
- CF_{veg} = radionuclide specific transfer factor, including buildup in soil ($Bq\ kg^{-1}$ per $Bq\ m^{-2}\ d^{-1}$).

5.2.5 Meat Consumption

Beef cattle can ingest river water and forage containing chemicals and radionuclides. We used the NCRP screening model methodology (NCRP 1996) to calculate the concentration in forage due to direct irrigation and buildup in soil over a 30-year time period. We assumed beef ingestion occurred throughout the exposure period, with no holdup time between butchering the beef cattle and ingesting the meat. The EPA Exposure Factors Handbook (EPA 1999a) indicates that the median intake of beef for the U.S. population is $0.6g$ per $kg^{-1} \cdot d^{-1}$, or $0.04\ kg\ d^{-1}$ (adults) and $0.02\ kg\ d^{-1}$ (child). For these risk calculations, we assumed beef ingestion of $0.04\ kg\ d^{-1}$, for adults and $0.02\ kg\ d^{-1}$, for the child, with 10% of the meat consumed containing the predicted concentrations of chemicals and radionuclides. We also use values recommended by NCRP (1996) for beef cattle ingestion of water and forage of $50\ L\ d^{-1}$ and $12\ kg\ d^{-1}$, respectively. The irrigation rate recommended for these calculations is $2\ L\ m^{-2}\ d^{-1}$ (NCRP 1996).

The risk per year for radionuclides from meat consumption is given by

$$\frac{Risk}{y} = [C_{m,w} + C_{m,f}] \cdot U_m \cdot F_{ch} \cdot EF \cdot RF_{ing,d} \cdot CF_{activity} \quad (5.17)$$

where

- $C_{m,w}$ = concentration in meat from intake of river water containing radionuclide ($pCi\ kg^{-1}$)
- $C_{m,f}$ = concentration in meat due to intake of forage containing radionuclide ($pCi\ kg^{-1}$)
- U_m = daily meat ingestion ($kg\ d^{-1}$)

F_{cb}	=	fraction of consumed meat that contains radionuclide (unitless)
EF	=	exposure frequency (d y ⁻¹)
$RF_{ing,d}$	=	lifetime morbidity risk coefficient for dietary ingestion (Risk Bq ⁻¹)
$CF_{activity}$	=	conversion factor (Bq pCi ⁻¹)

and

$$C_{m,w} = C_{uw} \cdot Q_{wb} \cdot F_{cw} \cdot F_b \quad (5.18)$$

$$C_{m,f} = C_{for} \cdot Q_{fb} \cdot F_{cf} \cdot F_b \quad (5.19)$$

where

$C_{m,w}$	=	concentration of radionuclide in meat due to cattle ingestion of contaminated water (pCi kg ⁻¹)
C_{uw}	=	concentration of radionuclide in unfiltered water (pCi L ⁻¹)
Q_{wb}	=	ingestion rate of water by beef cattle (L d ⁻¹)
F_{cw}	=	fraction of consumed water that contains radionuclide (unitless)
F_b	=	transfer coefficient to beef (d kg ⁻¹)
$C_{m,f}$	=	radionuclide concentration in meat due to cattle ingestion of forage containing radionuclide (Bq kg ⁻¹)
C_{for}	=	radionuclide concentration in forage (Bq kg ⁻¹)
Q_{fb}	=	ingestion rate of forage by beef cattle (kg d ⁻¹)
F_{cf}	=	fraction of consumed forage that contains radionuclide (unitless)

and

$$C_{for} = C_{uw} \cdot F_{ir} \cdot CF_{for} \quad (5.20)$$

where

C_{for}	=	concentration of radionuclide in forage (pCi kg ⁻¹)
C_{uw}	=	concentration of radionuclide in unfiltered river water (pCi L ⁻¹)
F_{ir}	=	irrigation rate (L m ⁻² d ⁻¹)
CF_{for}	=	radionuclide specific transfer factor, including buildup in soil (Bq kg ⁻¹ per Bq m ⁻² d ⁻¹)

The risk per year for carcinogenic chemicals from meat consumption is given by

$$\frac{Risk}{y} = \frac{C_{m,w} \cdot U_m \cdot F_{cb} \cdot EF \cdot SF_o}{BW \cdot AT} \quad (5.21)$$

where

$C_{m,w}$	=	concentration in meat due to intake of river water containing chemical (mg kg ⁻¹)
U_m	=	daily meat ingestion (kg d ⁻¹)
F_{cb}	=	fraction of consumed meat that contains chemical

EF	=	exposure frequency (d y^{-1})
SF_o	=	oral intake slope factor (kg d mg^{-1})
BW	=	body weight (kg)
AT	=	averaging time (d)

and

$$C_{m,w} = C_{uw} \cdot Q_{wb} \cdot F_{cw} \cdot F_b \quad (5.22)$$

where

$C_{m,w}$	=	concentration of chemical in meat due to cattle ingestion of water that contains chemical (mg kg^{-1})
C_{uw}	=	concentration of chemical in unfiltered river water (mg L^{-1})
Q_{wb}	=	ingestion rate of water by beef cattle (L d^{-1})
F_{cw}	=	fraction of consumed water that contains chemical (unitless)
F_b	=	transfer coefficient to beef (d kg^{-1})

The hazard quotient for noncarcinogenic chemicals from meat consumption is given by

$$HQ = \frac{C_{m,w} \cdot U_m \cdot F_{cb} \cdot EF \cdot ED}{BW \cdot AT} \bigg/ RfD_o \quad (5.23)$$

where

$C_{m,w}$	=	concentration of chemical in meat due to intake of river water containing chemical (mg kg^{-1})
U_m	=	daily meat ingestion (kg d^{-1})
F_{cb}	=	fraction of consumed meat that contains chemical
EF	=	exposure frequency (d y^{-1})
ED	=	exposure duration (y)
BW	=	body weight (kg)
AT	=	averaging time (d)
RfD_o	=	oral intake reference dose ($\text{mg kg}^{-1} \text{d}^{-1}$)

and

$$C_{m,w} = C_{uw} \cdot Q_{wb} \cdot F_{cw} \cdot F_b \quad (5.24)$$

where

$C_{m,w}$	=	concentration of chemical in meat due to cattle ingestion of water containing chemical (mg kg^{-1})
C_{uw}	=	concentration of chemical in unfiltered river water (mg L^{-1})
Q_{wb}	=	ingestion rate of water by beef cattle (L d^{-1})

F_{cw} = fraction of consumed water that contains chemical (unitless)
 F_b = transfer coefficient to beef (d kg^{-1}).

We were unable to account for the chemical concentration in meat from beef cattle ingesting forage because transfer factors from water to forage or vegetation were unavailable for chemicals. A concentration in forage or vegetation would be required to complete such a pathway, and environmental data collected during and following the fire do not provide any useful information of this type.

5.2.6. Swimming

A swimmer in Cochiti Lake or in the Rio Grande is directly exposed to radionuclides and chemicals from immersion in or dermal contact with water containing chemicals and radionuclides, and as a result of inadvertent ingestion of water while swimming. This exposure pathway accounts for any activity where an individual is partly or totally immersed in the river water (bathing and washing of plant materials). Exposure from activities where someone is only partly immersed would therefore be overestimated. NCRP (1996) recommends a usage factor for immersion in water of 300 h yr^{-1} for screening calculations. For northern New Mexico, we assume swimming or wading may occur from May through September. For an individual represented by Scenario 2, we assumed swimming or immersion in water of 10 h mo^{-1} , over that 5 month time period, or 50 h yr^{-1} . For exposure to chemicals in water, chemical specific permeability constants were obtained from the EPA's Dermal Exposure Assessment (EPA 1992) and are listed in Table 5-2. The value for available surface area is an EPA total body average surface area for an adult of 1.94 m^2 (EPA 1992).

5.2.6.1. Immersion in water

The equation that describes the risk per year from radionuclides from immersion in river water is

$$\frac{\text{Risk}}{y} = C_w \cdot ET_s \cdot DCF_{imm} \cdot RC \cdot CF_{time} \cdot CF_{activity} \quad (5.25)$$

where

C_w = concentration of radionuclide in river water (pCi L^{-1})
 ET_s = exposure time for swimming (h yr^{-1})
 DCF_{imm} = dose conversion factor for immersion (Sv s^{-1} per Bq L^{-1})
 RC = lifetime risk coefficient (Risk Sv^{-1})
 CF_{time} = conversion factor (s h^{-1})
 $CF_{activity}$ = conversion factor (Bq pCi^{-1}).

We obtained dose conversion factors for swimming exposure from EPA Federal Guidance Report No. 12 (EPA 1993). EPA Federal Guidance Report 13 (EPA 1999a) does not provide morbidity risk coefficients for immersion therefore we assumed a nominal lifetime cancer incidence risk coefficient of $6.0 \times 10^{-2} \text{ Sv}^{-1}$ based on ICRP Publication 60 (ICRP 1991, Table 3).

This risk coefficient is an aggregated detriment that includes the probability of severe hereditary effects in addition to fatal and non-fatal cancers.

The risk per year from carcinogenic chemicals from dermal absorption of river water is:

$$\frac{Risk}{y} = \frac{C_w \cdot CF_{distance} \cdot CF_{volume} \cdot PC \cdot SA \cdot ET_s \cdot SF_{der}}{AT \cdot BW} \quad (5.26)$$

where

C_w	=	concentration of chemical in river water (mg L^{-1})
$CF_{distance}$	=	conversion factor (m cm^{-1})
CF_{volume}	=	conversion factor (L m^{-3})
PC	=	chemical specific permeability constant (cm h^{-1})
SA	=	total body surface area (m^2)
ET_s	=	exposure time for swimming (h y^{-1})
SF_{der}	=	dermal contact slope factor (kg d mg^{-1})
AT	=	averaging time (d)
BW	=	body weight (kg).

We obtained chemical-specific permeability constants from the EPA's Dermal Exposure Assessment (EPA 1992). Available surface area is an EPA total body average surface area for an adult of 1.94 m^2 (EPA 1992).

The hazard quotient for noncarcinogenic chemicals from dermal absorption of river water is:

$$HQ = \frac{C_w \cdot CF_{distance} \cdot CF_{volume} \cdot PC \cdot SA \cdot ET_s \cdot ED}{AT \cdot BW} \div RfD_{der} \quad (5.27)$$

where

C_w	=	concentration of chemical in river water (mg L^{-1})
$CF_{distance}$	=	conversion factor (m cm^{-1})
CF_{volume}	=	conversion factor (L m^{-3})
PC	=	chemical specific permeability constant (cm h^{-1})
SA	=	total body surface area (m^2)
ET_s	=	exposure time for swimming (h y^{-1})
ED	=	exposure duration (y)
AT	=	averaging time (d)
BW	=	body weight (kg)
RfD_{der}	=	dermal contact reference dose ($\text{mg kg}^{-1} \text{ d}^{-1}$).

5.2.6.2. Inadvertent Ingestion of River Water

Swimming exposure can also result in some inadvertent ingestion of river water. The quantity ingested would not be very large, certainly not as large as the amount of water ingested for dietary reasons each day. The EPA recommends an incidental ingestion rate of 0.05 L h^{-1} (EPA 1999b). The risk per year from radionuclides for ingestion of river water is shown below.

$$\frac{\text{Risk}}{y} = C_w \cdot U_{wi} \cdot F_{cw} \cdot ET_s \cdot RF_{\text{ing},w} \cdot CF_{\text{activity}} \quad (5.28)$$

where

- C_w = concentration of radionuclide in river water (pCi L^{-1})
- U_{wi} = inadvertent ingestion rate of river water while swimming (L h^{-1})
- F_{cw} = fraction of water ingested that contains radionuclide (unitless)
- ET_{sw} = exposure time for swimming (h y^{-1})
- $RF_{\text{ing},w}$ = lifetime morbidity risk coefficient for ingestion of water (Risk Bq^{-1})
- CF_{activity} = conversion factor (Bq pCi^{-1}).

The inadvertent ingestion risk per year for carcinogenic chemicals is given by

$$\frac{\text{Risk}}{y} = \frac{C_w \cdot U_{wi} \cdot ET_s \cdot F_{cw} \cdot SF_o}{BW \cdot AT} \quad (5.29)$$

where

- C_w = concentration of chemical in river water (mg L^{-1})
- U_{wi} = inadvertent ingestion rate of river water while swimming (L h^{-1})
- F_{cw} = fraction of water consumed that contains chemical (unitless)
- ET_s = exposure time for swimming (h y^{-1})
- SF_o = oral intake slope factor (kg d mg^{-1})
- BW = body weight (kg)
- AT = averaging time (d).

The inadvertent ingestion hazard quotient for noncarcinogenic chemicals is given by

$$HQ = \frac{C_w \cdot U_{wi} \cdot ET_s \cdot ED \cdot F_{cw}}{BW \cdot AT} \bigg/ RfD_o \quad (5.30)$$

where

- C_w = concentration of chemical in river water (mg L^{-1})
- U_{wi} = inadvertent ingestion rate of river water while swimming (L h^{-1})
- ET_s = exposure time for swimming (h y^{-1})
- ED = exposure duration (y)
- F_{cw} = fraction of water consumed contains chemical (unitless)
- BW = body weight (kg)
- AT = averaging time (d)

RfD_o = oral intake reference dose ($\text{mg kg}^{-1} \text{ d}^{-1}$).

Table 5-2. Transfer Coefficients for Chemicals of Concern

Chemical	CAS # ^a	Absorption factor, dermal	Beef transfer coefficient (d kg^{-1})	Fish bioaccumulation factor (L kg^{-1})	Permeability constant (cm h^{-1})
Aldrin	309002	0.01	2.5E-05	1.1E+02	1.6E-03
Arsenic, Inorganic	7440382	0.001	2.0E-03	2.8E+02	1.0E-03
Barium	7440393	0.001	2.0E-04	4.0E+00	1.0E-03
Benz[a]anthracene	56553	0.01	1.3E-02	2.0E+03	8.1E-01
Benzo[a]pyrene	50328	0.01	3.1E-02	2.0E+03	1.2
Benzo[b]fluoranthene	205992	0.01	3.1E-02	2.0E+03	1.2E+00
Benzo[k]fluoranthene	207089	0.01	1.6E-01	2.0E+03	6.0E-01
Chromium VI (particulates)	18540299	0.001	9.0E-03	2.0E+02	1.0E-03
Copper	7440508	0.001	9.0E-03	2.0E+02	1.0E-03
Dibenz[a,h]anthracene	53703	0.01	1.6E-01	8.0E+02	2.7
Heptachlor Epoxide	1024573	0.01	6.3E-03	7.5E+03	5.5E-02
Indeno[1,2,3-cd]pyrene	193395	0.01	1.0E-01	6.0E+03	1.9E+00
Lead And Compounds	7439921	0.001	4.0E-04	3.0E+02	1.0E-03
Mercury (elemental)	7439976	0.001	1.0E-02	1.0E+03	1.0E-03
Nitrosodimethylamine, N-	62759	0.01	6.7E-09	2.2E-01	2.7E-04
Hexahydro-1,3,5-trinitro- 1,3,5-triazine (RDX)	121824	0.01	5.0E-05	1.9E+02	1.9E-02
Uranium (Soluble Salts)	238	0.001	3.0E-04	1.0E+01	1.0E-03

^a CAS # = Chemical Abstract Service number.

Table 5-3. Transfer Coefficients for Radionuclides of Concern^a

Radionuclides	Half-life (d)	Decay rate (d ⁻¹)	B _{vs} (fresh veg)	B _{vas} dry forage	F _b beef (d kg ⁻¹)	BF _{fw} ^b fresh fish (L kg ⁻¹)	Cf _{veg} (Bq kg ⁻¹ per Bq m ⁻² d ⁻¹)	Cf _{forage} (Bq kg ⁻¹ per Bq m ⁻² d ⁻¹)
Am-241	1.58E+05	4.39E-06	1.00E-03	1.00E-01	5.00E-05	3.00E+01	2.34E+00	3.69E+01
Cs-137+D	1.10E+04	6.33E-05	2.00E-01	1.00E+00	5.00E-02	2.00E+03	8.50E+00	6.38E+01
Pb-210+D	8.14E+03	8.51E-05	4.00E-03	1.00E-01	8.00E-04	3.00E+02	2.41E+00	3.56E+01
Np-237+D	7.81E+08	8.87E-10	2.00E-02	1.00E-01	1.00E-03	3.00E+01	3.15E+00	3.70E+01
Pu-238	3.20E+04	2.16E-05	1.00E-03	1.00E-01	1.00E-04	3.00E+01	2.34E+00	3.66E+01
Pu-239	8.78E+06	7.89E-08	1.00E-03	1.00E-01	1.00E-04	3.00E+01	2.34E+00	3.70E+01
K-40	4.67E+11	1.48E-12	3.00E-01	3.00E+00	2.00E-02	1.00E+04	1.50E+01	1.60E+02
Pa-234m	2.79E-01	2.48E+00	1.00E-02	1.00E-01	5.00E-06	3.48E+01	4.74E-02	8.30E-01
Ra-224	1.53E-01	4.54E+00	4.00E-02	2.00E-01	1.00E-03	2.77E+02	2.62E-02	4.57E-01
Ra-226+D	5.84E+05	1.19E-06	4.00E-02	2.00E-01	1.00E-03	5.00E+01	3.98E+00	4.12E+01
Ra-228+D	2.10E+03	3.30E-04	4.00E-02	2.00E-01	1.00E-03	5.00E+01	2.77E+00	3.51E+01
Sr-90+D	1.06E+04	6.52E-05	3.00E-01	4.00E+00	1.00E-02	6.00E+01	1.15E+01	1.56E+02
Th-228+D	6.98E+02	9.92E-04	1.00E-03	1.00E-01	1.00E-04	1.00E+02	2.27E+00	3.29E+01
Th-230	2.81E+07	2.47E-08	1.00E-03	1.00E-01	1.00E-04	1.00E+02	2.34E+00	3.70E+01
Th-232	5.13E+12	1.35E-13	1.00E-03	1.00E-01	1.00E-04	1.00E+02	2.34E+00	3.70E+01
Th-234	2.41E+01	2.88E-02	1.00E-03	1.00E-01	1.00E-04	1.03E+02	1.52E+00	2.43E+01
H-3 (tritiated water)	4.51E+03	1.54E-04				1.00E+00	2.29E+00	3.28E+01
U-234	8.92E+07	7.77E-09	2.00E-03	1.00E-01	8.00E-04	1.00E+01	2.38E+00	3.70E+01
U-235+D	2.57E+11	2.70E-12	2.00E-03	1.00E-01	8.00E-04	1.00E+01	2.38E+00	3.70E+01
U-238+D	1.63E+12	4.25E-13	2.00E-03	1.00E-01	8.00E-04	1.00E+01	2.38E+00	3.70E+01

^a From ORNL Risk Assessment Information System Database (ORNL 2001).^b Decay corrected, assumed a 30-day biological half-life.

5.3 Risk Estimates

We estimated potential risks estimates for four scenarios and for eight different exposure pathways (see Table 5-1). Complete results of the risk calculations are available electronically as Excel[®] files (Appendix U). We developed conservative estimates of the surface water flow within the watersheds and at outlets to the Rio Grande for 2-, 5-, 10-, 25-, 50-, 100-, and 500-year design storm events of 6-hour duration (see Chapter 4). We completed and report risk calculations for the 2- and 500-year storm events. For these storm events, we present both *incremental* (pre-fire minus post-fire) and *post-fire* risks associated with concentrations of chemicals and radionuclides predicted for each exposure. Morbidity risks for carcinogens and hazard quotients for noncarcinogens, identified through the screening process (Chapter 3), were calculated annually as shown in Appendix U. We developed annual risk estimates for ease of comparisons among the fire cleanup worker and other exposure scenarios assumed to have longer exposure duration. For Scenarios 1, 2, and 3, we assumed a period of 7 years as the exposure duration. For Scenario 4, we assumed that the fire cleanup worker (who were not site employees) would have been onsite for 4 months (120 days) during and after the fire.

In the next sections, we present the results in sequence to answer the following key questions about the surface water pathway.

- Do any of the exposure pathways or scenarios result in risks higher than the risk criteria of 10⁻⁵ or HQ of 1?

- What exposure pathway results in the highest risk?
- What chemicals and radionuclides dominate the risks?
- What differences in risks are seen between the 2-year and 500-year storm events?
- Are there differences in risks to the child and adult in Scenario 2 living near Cochiti Lake?
- What differences are seen between the post-fire and incremental (post-fire minus pre-fire) risk estimates?

5.3.1 Annual Potential Risks by Individual Analyte

Risk estimates are presented in this section as annual morbidity risks for carcinogenic chemicals and radionuclides or as annual hazard quotients for noncarcinogens. Non-cancer health effects for noncarcinogens are expressed in terms of the fraction of the acceptable daily intake (or reference dose) of a given chemical (see Chapter 3). The acceptable daily intake is the amount of chemical that may be ingested over a period of time that will produce no adverse health effects.

We calculated annual risks on an annual basis for ease of comparison among the scenarios because the fire cleanup worker (Scenario 4) had a limited exposure period of less than a year. For a 7-year exposure duration (the time it may take to return to pre-fire vegetation conditions in the area), potential risks could be conservatively approximated to be proportionately higher. Table 5-4 gives an overview of the annual risk calculations and shows that no annual exposure pathway or scenario exceeded our risk criteria. Based on EPA guidelines and related studies and the fact that we assessed radionuclides and chemicals against the risk criterion on an individual basis, we adopted a protective risk criterion of 10^{-5} for this study for the carcinogenic chemicals and radionuclides (Chapter 3). These pathways included drinking water, sediment exposure through ingestion or dermal contact, swimming, and produce and meat ingestion. The following scenarios did not exceed our risk criteria for any of the pathways studied: the hunter (Scenario 1 with two points of exposure), the adult and child living near or below Cochiti Lake, the individual living at the confluence of the Rio Grande and Water Canyon, and the fire cleanup worker (Scenario 4 with two points of exposure).

Of these possible exposure pathways, the type of exposure contributing most to the potential risk was eating fish from the Rio Grande just below LANL or from Cochiti Lake. Figures 5-2, 5-3, and 5-4 examine the fish exposure pathway in more detail and show the range of annual risk values for exposure to carcinogenic chemicals and radionuclides for the adult in Scenario 3.1 (Figure 5.2) and for both the adult and child resident living below Cochiti Lake for exposure to carcinogenic chemicals (Figure 5-3) and to radionuclides (Figure 5-4). Risks for both the 2-yr and the 500-yr storm events are shown (see Chapter 4). An important observation from the figure is that the risks with the 500-yr storm event are generally less than an order of magnitude higher than the risks from the 2-yr storm event, and the differences between the two are likely within the uncertainties of the calculations (i.e., not statistically significant). We observed no significant differences in the estimated risks for any exposure pathway for concentrations after the 2-yr and 500-yr storm events. Risks to the child and adult were similar for exposure to carcinogenic chemicals and to radionuclides for all pathways.

Table 5-4. Identification of Scenario Pathways that Resulted in Annual Risks Greater than 1×10^{-5} or a Hazard Quotient Greater than 1 for at Least One Analyte^{a, b}

Scenario (POE) ^c	Exposure Pathways								
	Sediment exposure				Swimming		Ingestion		
	Drinking water	Ingestion	External	Dermal	Immersion	Inadvertent ingestion	Fish	Garden produce	Beef
1 (1.1)	No	No	No	No	na	na	No	na	na
1 (1.2)	No	No	No	No	na	na	na	na	na
2 (2.1) (adult) (below dam)	No	No	No	No	No	No	No	No	No
2 (2.1) (child) (below dam)	No	No	No	No	No	No	No	No	No
2 (2.1) (adult) (reservoir)	No	No	No	No	No	No	No	No	No
2 (2.1) (child) (reservoir)	No	No	No	No	No	No	No	No	No
3 (3.1)	No	No	No	No	na	na	No	No	No
4 (4.1a)	na	No	No	No	na	na	na	na	na
4 (4.1b)	na	No	No	No	na	na	na	na	na

^a The risk criteria set for this project for carcinogenic chemicals and radionuclides was 1×10^{-5} and for noncarcinogens was a hazard quotient greater than 1 (see Chapter 4).

^b na –this was not an exposure pathway for this scenario. No = a risk $< 1 \times 10^{-5}$ or HQ <1 .

^cPOE = point of exposure

For the adult in Scenario 3, the annual risks from exposure to carcinogenic chemicals from eating fish from the Rio Grande at the confluence of Water Canyon ranged from approximately 9×10^{-14} for nitrosodimethylamine[N-] up to about 3×10^{-6} for exposure to benzo(a)pyrene (Figure 5-2, top). For exposure to radionuclides through the fish ingestion pathway, the risks ranged from 3×10^{-14} for tritium up to 2×10^{-6} for exposure to ^{137}Cs (Figure 5-2, bottom).

For the adult and child living near Cochiti Lake (Scenario 2), the annual risks from exposure to carcinogenic chemicals (Figure 5.3) and to radionuclides (Figure 5.4) from eating fish from Cochiti Lake are slightly less than for the adult in Scenario 2. This result is not unexpected because of the increased dilution that would occur between the two locations.

When the exposure duration was increased to 7 years (the estimated time for revegetation to occur), the corresponding risks for exposure to any of the carcinogenic chemicals or radionuclides are proportionately higher, but they do not exceed our risk criteria. For all other exposure pathways, the risks for exposure to chemicals and radionuclides through the other pathways were lower than for the fish ingestion pathway shown in these figures. Appendix U provides complete results of the risk calculations electronically as Excel[®] files.

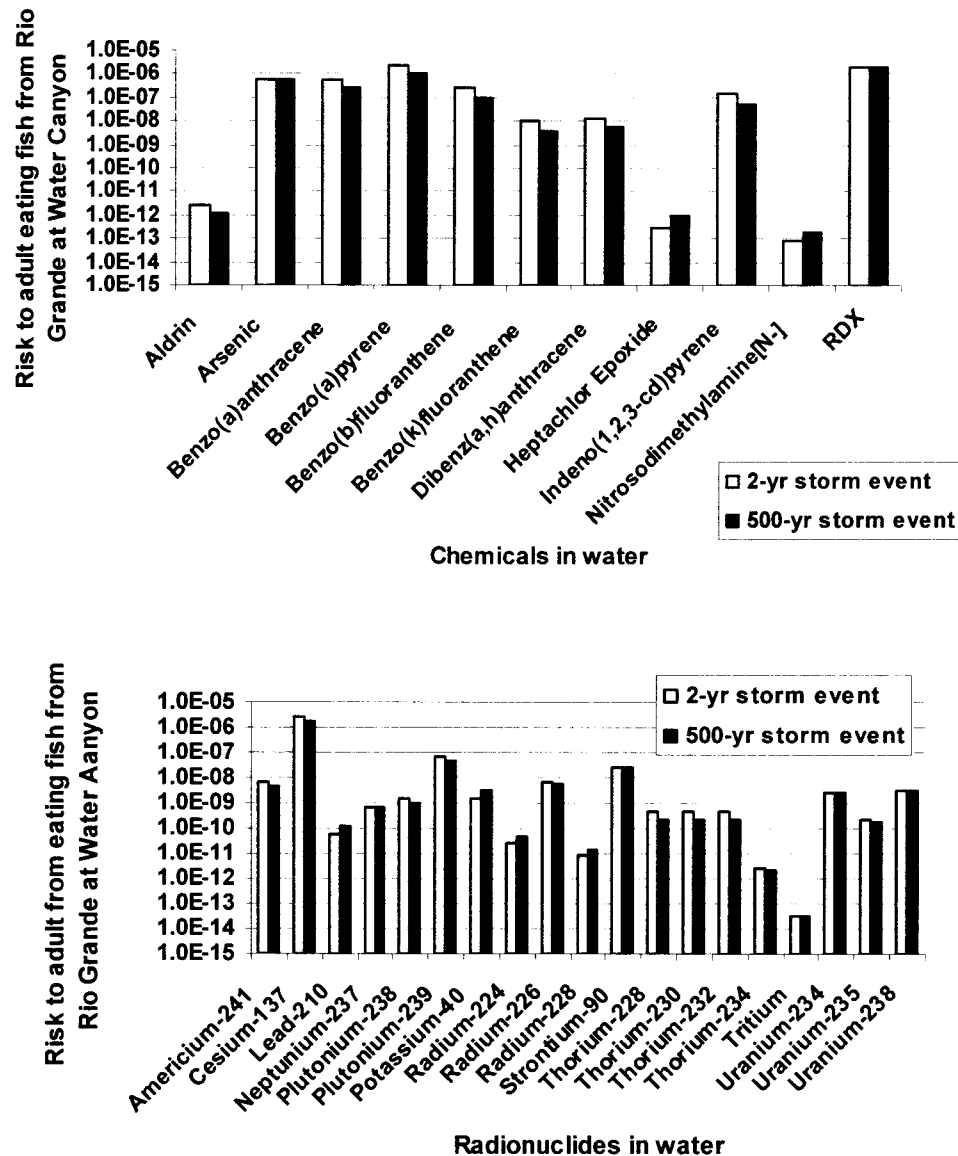


Figure 5-2. Comparison of annual risk values for exposure to carcinogenic chemicals (top) and radionuclides (bottom) for the adult in Scenario 3 eating fish from the Rio Grande at the confluence of Water Canyon. Risks are shown for a 2-yr and 500-yr storm event (see Chapter 4). The top figure shows that benzo(a)pyrene and RDX (hexahydro-1,3,5-trinitro-1,3,5-triazine) presented the highest risks (~3 in a million and 2 in a million, respectively) of any of the carcinogenic chemicals for this pathway. The bottom figure shows ¹³⁷Cs as the largest contributor to risk (~2 in a million) of any of the radionuclides for this pathway.

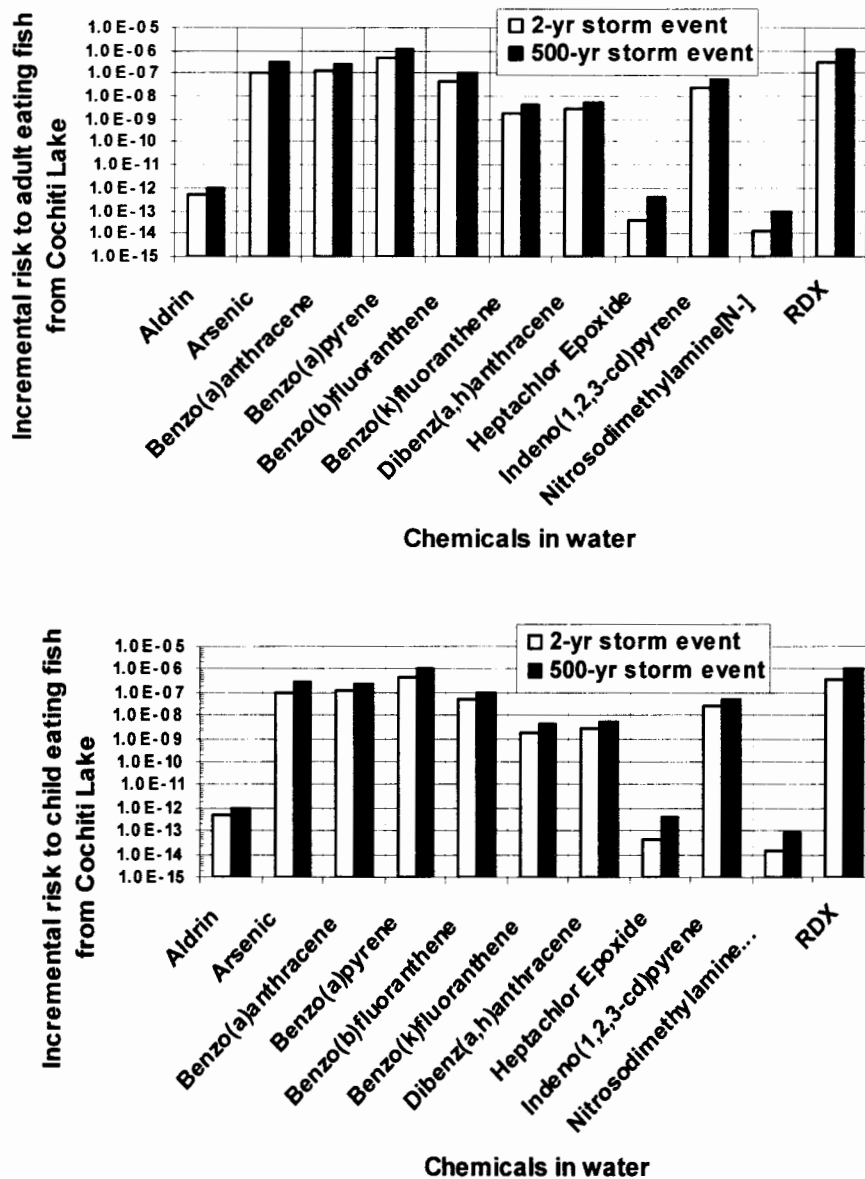


Figure 5-3. Comparison of annual risk values for exposure to carcinogenic chemicals through the fish ingestion pathway for the adult (top) and child (bottom) in Scenario 2 at Cochiti Lake. Risks are shown for a 2-yr and 500-yr storm event (see Chapter 4). The figure shows similar risks for the adult and child for exposure to chemicals from eating fish.

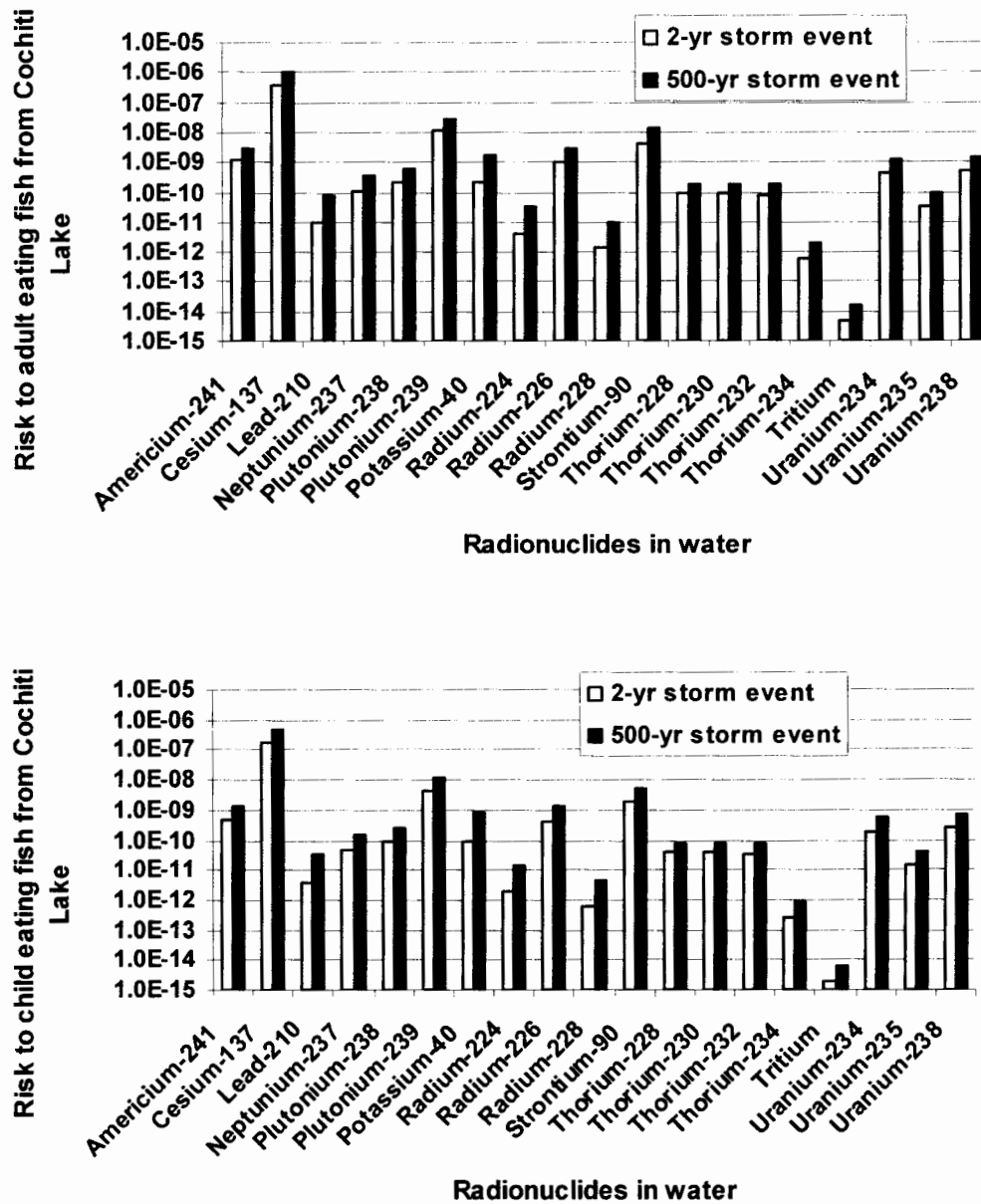


Figure 5-4. Comparison of annual risk values for exposure to radionuclides from eating fish for the adult (top) and child (bottom) in Scenario 2 at Cochiti Lake. Risks are shown for a 2-yr and 500-yr storm event (see Chapter 4). The figure shows similar risks for the adult and child for exposure to radionuclides from eating fish.

For the noncarcinogenic chemicals identified through the screening process, Figure 5-5 compares the hazard quotients for these chemicals for an adult ingesting fish from Cochiti Lake (Scenario 2) or from the Rio Grande at the confluence of Water Canyon (Scenario 3). Hazard quotients provide a way to express non-cancer health effects in terms of a comparison between the

concentration people might be exposed to and the acceptable daily intake (the amount of chemical that may be ingested over a period of time that will produce no adverse health effects) for a given chemical (see Chapter 3). Hazard quotients less than 1 indicate acceptable daily intakes. The hazard quotients for an annual or a 7-year exposure duration are equivalent. Figure 5-5 shows that the hazard quotients for all noncarcinogens were less than 1 for both scenarios, although they were higher for eating fish from the Rio Grande at the confluence of Water Canyon than from the Cochiti Lake.

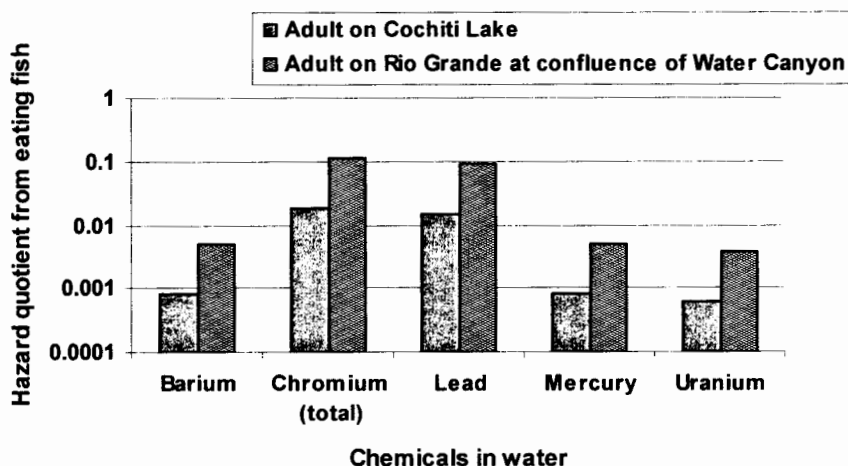


Figure 5-5. Comparison of hazard quotient values for exposure to noncarcinogens from eating fish from Cochiti Lake (Scenario 2) and from the Rio Grande at the confluence of the Water Canyon (Scenario 3).

Differences in risks from exposure to *post-fire* and *incremental* (post-fire minus pre-fire) concentrations of radionuclides and chemicals were relatively minor, as seen in Figure 5-6. This figure shows the range of risk values for carcinogenic chemicals and for radionuclides in water, assumed to be a source of drinking water for the hypothetical adult resident living below Cochiti Lake. Risks ranged from 9×10^{-17} for exposure to heptachlor epoxide up to 3×10^{-7} for exposure to RDX. This similarity in risk estimates for post-fire and incremental risk estimates was also seen for other exposure pathways and scenarios.

While none of these potential risks or hazard quotients exceeded our risk criteria, they should be viewed as upper bound values because of the conservatism we assumed in estimating concentrations of chemicals and radionuclides at these points of exposure and in selecting lifestyle activities and exposure parameter values for these hypothetical individuals.

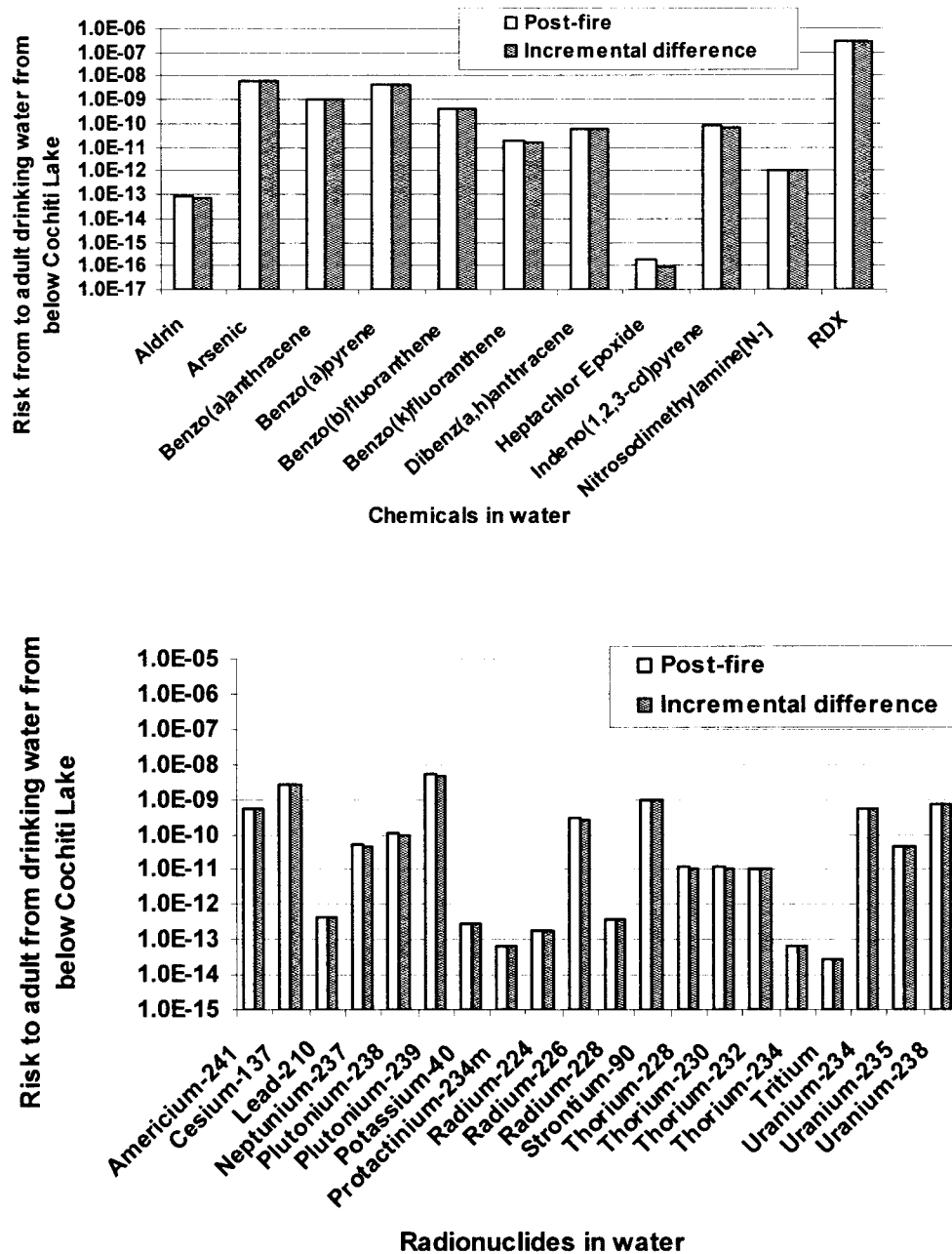


Figure 5-6. Comparison of potential annual risks to a hypothetical adult drinking water from the Rio Grande below Cochiti Reservoir with post-fire and incremental concentrations of carcinogenic chemicals (top) or radionuclides (bottom). For the chemicals, all risks fell below 1×10^{-6} , with RDX (hexahydro-1,3,5-trinitro-1,3,5-triazine) presenting the highest risk. For the radionuclides, all risks fell below 1×10^{-8} .

5.3.2 Potential Risks for 7-year Exposure Duration by Pathway

We summed the potential annual risks for individual carcinogenic chemicals or radionuclides to derive a total upper-bound risk by pathway and adjusted the total upper-bound risk for a 7-year exposure period, the time it may take to return to pre-fire vegetation conditions in the area. We show these total combined upper-bound risks by pathway for all radionuclides and for carcinogenic chemicals in Tables 5-5 and 5-6. For noncarcinogenic chemicals, we summed the potential hazard quotients of all of them to derive a total upper-bound hazard quotient by pathway and show these in Table 5-7. As discussed previously, the hazard quotient for 1 year would be equal to the hazard quotient for any exposure duration of interest. Therefore, it was not necessary to adjust the total upper-bound hazard for the 7-year exposure period. (It is not appropriate or meaningful to sum risks across the three categories of radionuclides, carcinogenic, and noncarcinogenic chemicals.)

For all three categories, these values are considered upper-bound potential risks or hazard quotients because we did not assume any changes in the environment over that 7-year period. In reality, we know that revegetation would gradually occur and that concentrations of materials in the Rio Grande near LANL and in Cochiti Lake from the Cerro Grande fire would decrease over that 7-year period.

These results indicate that, overall, the health impacts from exposure to the LANL-derived chemicals or radionuclides from the Cerro Grande Fire are below the criteria we established for this work for all exposure pathways, with the exception of the fish ingestion pathway for two scenarios. In each table, the pathway exceeding the risk criterion for that scenario is highlighted.

- For the total combined upper-bound risks from exposure to radionuclides in water for a 7-year period, the fish ingestion pathway just exceeded 1×10^{-5} , the risk criterion for the hypothetical individuals represented by Scenarios 1 (POE 1.1) and 3 (POE 3.1) in Table 5-5.
- For the total combined upper-bound risks from exposure to carcinogenic chemicals in water for a 7-year period, the fish ingestion pathway exceeded the risk criterion for the hypothetical resident near the Rio Grande at the confluence of Water Canyon (Scenario 3; POE 3.1) (Table 5-6).
- For the total combined upper-bound hazard quotient from exposure to noncarcinogens, none exceeded 1 (Table 5-7).

Examining the risk calculations in the accompanying Excel spreadsheet in Appendix U shows that the radionuclide that dominates the risks in the fish ingestion pathway shown in Table 5-5 was ^{137}Cs . For the carcinogenic chemicals, benzo(a)pyrene and RDX were the primary risk-drivers (Table 5-6), and chromium is the noncarcinogen that had the highest hazard quotient for the fish ingestion pathway (Table 5-7).

Table 5-5. Upper-bound Risk Estimates for 7-year Exposure by Pathway to All Radionuclides of Concern^a (Two-year Storm Event)

Scenario	POE	Ingestion	Sediment pathways		Ingestion pathways				Swimming	
			External exposure	Dermal contact	Drinking water	Fish	Produce	Meat	Inadvertent immersion	Ingestion
Hunter	1.1	6.2×10^{-8}	1.3×10^{-8}	4.7×10^{-8}	6.4×10^{-7}	2.5×10^{-5}	na ^b	na	na	na
Hunter	1.2	1.0×10^{-7}	1.8×10^{-8}	8.0×10^{-8}	1.6×10^{-6}	na	na	na	na	na
Adult on										
Cochiti (BD)	2.1	8.7×10^{-8}	9.9×10^{-9}	5.9×10^{-8}	7.1×10^{-8}	2.9×10^{-6}	3.0×10^{-7}	2.3×10^{-8}	8.5×10^{-12}	1.3×10^{-9}
Child on										
Cochiti (BD)	2.1	8.7×10^{-8}	2.0×10^{-8}	5.9×10^{-8}	3.8×10^{-8}	1.2×10^{-6}	1.7×10^{-7}	1.2×10^{-8}	8.5×10^{-12}	1.3×10^{-9}
Adult on										
Cochiti (R)	2.1	8.7×10^{-8}	9.9×10^{-9}	5.9×10^{-8}	7.1×10^{-8}	2.9×10^{-6}	1.1×10^{-6}	7.3×10^{-8}	8.5×10^{-12}	1.3×10^{-9}
Child on										
Cochiti (R)	2.1	8.7×10^{-8}	2.0×10^{-8}	5.9×10^{-8}	3.8×10^{-8}	1.2×10^{-6}	5.7×10^{-7}	3.7×10^{-8}	8.5×10^{-12}	1.3×10^{-9}
Resident on										
Rio Grande	3.1	3.9×10^{-8}	4.3×10^{-9}	3.8×10^{-7}	3.4×10^{-7}	1.7×10^{-5}	6.6×10^{-6}	4.6×10^{-7}	na	na
Fire cleanup worker	4.1a	4.9×10^{-11}	7.7×10^{-12}	5.6×10^{-9}	na	na	na	na	na	na
Fire cleanup worker	4.1b	1.4×10^{-9}	1.7×10^{-12}	7.4×10^{-10}	na	na	na	na	na	na

^a Risk for 7-year exposure period, except for the fire cleanup worker scenario (Scenario 4) who is assumed to be exposed only for a 4-month period during and after the fire. The highlighted cells indicate the exposure pathway with total radionuclide morbidity risk that exceeds the risk criterion of 10^{-5} .

^b This pathway was not applicable for this scenario.

While the fish ingestion pathway yielded risks and/or hazard quotients above the risk criteria established for this work for two scenarios, it is important to understand the conservatism associated with these calculations. The point of exposure concentration estimates are based on simplifying assumptions, which were designed to conservatively estimate concentrations at the points of exposure (Chapter 4). For example, there is no time-lag in the surface water model for travel time in the watersheds; all of the concentrations arrive at the point of exposure at the same time. Furthermore, no losses of chemical mass or radionuclide activity were attributed to the natural processes of deposition and resuspension as the storm water flows away from the source areas to the point of exposure. Other limitations of the characterization data and calculations of the concentrations are summarized in the next section.

**Table 5-6. Upper-bound Risk Estimates for 7-year Exposure by Pathway to All
Carcinogenic Chemicals of Concern^a (Two-year Storm Event)**

Scenario	POE	Sediment pathways		Ingestion pathways				Swimming	
		Ingestion	Dermal contact	Drinking water	Fish	Produce	Meat	Immersion	Inadvertent ingestion
Hunter	1.1	2.3×10^{-8}	5.0×10^{-10}	3.9×10^{-9}	4.7×10^{-7}	na ^b	na	na	na
Hunter	1.2	7.4×10^{-9}	1.5×10^{-10}	3.1×10^{-10}	na	na	na	na	na
Adult on									
Cochiti (BD)	2.1	2.9×10^{-6}	5.8×10^{-8}	2.2×10^{-6}	8.1×10^{-6}	c	8.1×10^{-9}	2.0×10^{-6}	3.7×10^{-8}
Child on									
Cochiti (DB)	2.1	6.9×10^{-6}	1.0×10^{-7}	2.5×10^{-6}	7.9×10^{-6}	c	9.5×10^{-9}	2.4×10^{-6}	6.5×10^{-8}
Adult on									
Cochiti [R]	2.1	2.9×10^{-6}	5.8×10^{-8}	2.2×10^{-6}	8.1×10^{-6}	c	2.4×10^{-7}	2.0×10^{-6}	3.7×10^{-8}
Child on									
Cochiti [R]	2.1	6.9×10^{-6}	1.0×10^{-7}	2.5×10^{-6}	7.9×10^{-6}	c	2.8×10^{-7}	2.4×10^{-6}	6.5×10^{-8}
Resident on									
Rio Grande	3.1	1.1×10^{-6}	3.1×10^{-7}	1.0×10^{-5}	4.5×10^{-5}	c	1.5×10^{-6}	na	na
Fire cleanup worker	4.1	3.3×10^{-12}	4.1×10^{-14}	na	na	na	na	na	na

^a Risk for 7-year exposure period, except for the fire cleanup worker scenario (Scenario 4) who is assumed to be exposed only for a 4-month period during and after the fire. The highlighted cell indicates the exposure pathway with total carcinogenic chemical morbidity risk that exceeds the risk criterion of 10^{-5} .

^b This pathway was not applicable for this scenario.

^c Because of the lack of availability of transfer coefficients from contaminated water to vegetation, we were unable to complete this pathway for chemicals.

The exposure parameters applied to the scenarios were developed to be somewhat conservative. For the fish ingestion pathway, for instance, the individuals described in Scenarios 1 and 3 (on the Rio Grande at points of exposure below LANL) were assumed to eat 12 g d^{-1} of fish from the Rio Grande for the entire exposure period (based on EPA recommended ingestion rates). Although this ingestion rate was plausible, it was still conservative, and lends to the overall conservatism of these risk calculations. It is important, therefore, to consider all of the factors contributing to these risk values to adequately understand their implications.

**Table 5-7. Upper-bound Health Impacts by Pathway For All Noncarcinogenic Chemicals^a
(Two-year Storm Event)**

Scenario	POE	Sediment pathways		Ingestion pathways				Swimming	
		Ingestion	Dermal contact	Drinking water	Fish	Produce	Meat	Immersion	Inadvertent ingestion
Hunter	1.1	0.0003	0.00000087	0.014	0.17	na ^b	na	na	na
Hunter	1.2	0.0006	0.000002	0.04	na	na	na	na	na
Adult on Cochiti (BD)	2.1	0.0009	0.000005	0.0068	0.036	c	0.0000078	0.019	0.00012
Child on Cochiti (BD)	2.1	0.0022	0.0000088	0.008	0.035	c	0.0000093	0.021	0.0002
Adult on Cochiti (R)	2.1	0.0009	0.000005	0.006	0.036	c	0.000098	0.019	0.00012
Child on Cochiti (R)	2.1	0.0022	0.000012	0.008	0.035	c	0.000011	0.0215	0.0002
Resident on Rio Grande	3.1	0.00045	0.000071	0.031	0.22	na	0.00006	na	na
Fire cleanup worker	4.1a	0.000037	0.00000057	na	na	na	na	na	na
Fire cleanup worker	4.1b	0.0035	0.00026	na	na	na	na	na	na

^a Hazard quotients for annual and 7-year exposure periods are the same.

^b This pathway was not applicable for this scenario.

^c Because of the lack of availability of transfer coefficients from contaminated water to vegetation, we were unable to complete this pathway for chemicals.

5.4 Limitations

We developed the process of estimating incremental risk associated with the Cerro Grande Fire to be a conservative analysis to estimate upper bound risks and identify potential areas and materials of concern to guide future actions. This approach was taken primarily because of uncertainties related to estimating the quantity of chemicals and radionuclides available for release (see Chapter 3). This approach used simple models along with conservative assumptions (Chapter 4) and conservative source term concentration estimates (Chapter 3) to predict concentrations of chemicals and radionuclides at points of exposure within the surface water domain. We estimated *post-fire risk* and *incremental* (pre-fire minus post-fire) risk using these predicted concentrations and exposure scenarios. The resulting risk estimates provide a conservative representation of potential impacts of the fire within the surface water domain. The limited monitoring data available for comparison to the model predictions supported the notion that the predicted values tend to be high (Section 4.7). We estimated that predicted concentrations may be as much as a factor of 10 to 1000 high, which would impact the risk values proportionately. There are a number of reasons that the predicted risks are conservative (i.e., likely biased high).

1. We eliminated all non-detectable concentrations from source area characterization and this likely biased the assumed average concentration across the source areas on the high side.
2. We assumed a nondepleting source.
3. We assumed no loss of chemical mass or radionuclide activity between the source area and point of exposure.
4. We assumed 50% of the sediments ingested would contain the predicted concentrations of chemicals and radionuclides.
5. We assumed that 100% of the sediments contacted by external exposure of radionuclides or dermal/absorption by chemicals and radionuclides would contain the predicted concentrations of chemicals and radionuclides.
6. We did not account for best management practice effectiveness beyond the limited use of the erosion matrix score.
7. We did not account for the sediment removal that occurred in upper Los Alamos Canyon as part of post-fire risk mitigation efforts.

Benzo(a)pyrene and RDX (hexahydro-1,3,5-trinitro-1,3,5-triazine) were identified as the main risk-drivers for the carcinogenic chemicals in fish. The specific contribution of a particular source area to the concentration of a chemical or radionuclide at a point of exposure is dependent on both the storm water flow across the source area and the concentrations of chemicals or radionuclides in that source area. As a result, the primary driver source area will vary by point of exposure. Table 5-8 provides a summary of the total mass of benzo(a)pyrene and RDX estimated for each point of exposure from the source areas that contributed the largest mass to the point of exposure.

Table 5-8 Summary of Source Area with Maximum Mass Contribution to POE

POE	Total Mass (mg)	Primary PRS Area	Source Area (m ²)	Primary PRS Mass (mg)	% of Total Mass
<i>Benzo(a)pyrene</i>					
POE 1.1	3.9E+06	GEO-277	1.5E+02	1.7E+06	43.6%
POE 1.2	3.9E+06	GEO-277	1.5E+02	1.7E+06	43.6%
POE 2.1R	3.0E+08	PRS-150	3.5E+02	2.9E+08	96.7%
POE 2.1BD	3.0E+08	PRS-150	3.5E+02	2.9E+08	96.7%
POE 3.1	3.0E+08	PRS-150	3.5E+02	2.9E+08	96.7%
POE 4.1a	4.6E+00	PRS-197	2.6E+02	3.3E+00	71.7%
POE 4.1b	4.4E+06	PRS-104	3.1E+02	4.4E+06	100.0%
<i>RDX</i>					
POE 1.1	0.0E+00	NV ^a	NV	0.0E+00	NV
POE 1.2	0.0E+00	NV	NV	0.0E+00	NV
POE 2.1R	4.3E+09	PRS-105	2.7E+05	4.3E+09	100.0%
POE 2.1BD	4.3E+09	PRS-105	2.7E+05	4.3E+09	100.0%
POE 3.1	4.3E+09	PRS-105	2.7E+05	4.3E+09	100.0%
POE 4.1a	1.1E+03	PRS-102	2.4E+05	7.2E+02	65.5%
POE 4.1b	4.3E+09	PRS-105	2.7E+05	4.3E+09	100.0%

^a NV = No value

For benzo(a)pyrene at POE 1.1 and POE 1.2, the major contributor of chemical mass was Geomorphic Unit GEO-277 ($2.2\text{E}+02\text{ m}^2$), contributing $1.7 \times 10^6\text{ mg}$ accounting for over 40% of the total mass. The ability to assess the impact of individual PRSs or other source areas for chemicals (like benzo(a)pyrene and RDX) is an important asset that can be derived from the models and information developed for this work (within the limitations of the conservative approach we used).

A key message from our surface water pathway risk results is that an individual PRS can have a significant impact on the concentrations at a point of exposure and that there is a need for continuing investigations into credibly establishing the magnitude and extent of chemicals and radionuclides at these PRSs. In addition, concentrations of chemicals and radionuclides in stream segments and reaches below the LANL facility can also have a significant impact at the point of exposure, and there is a need to further characterize additional stream segments and reaches. These results are not intended to alarm local communities about a potential for current or future harm. Rather the results suggest that additional sampling data is warranted, targeted at specific areas, materials, and media. Carefully evaluating the true effectiveness of the best management practices might be appropriate, and perhaps additional best management practices would be warranted at these sites. There may also be a need for some additional monitoring of fish for benzo(a)pyrene and other polycyclic aromatic hydrocarbons, as well as RDX.

LANL has sampled fish for strontium, cesium, and other radionuclides, and has seen no significant differences between locations upstream and downstream of the Laboratory (Fresquez et al. 1999). Uranium has been found in higher concentrations in fish from Cochiti Lake, especially bottom feeders, than in fish from Abiquiu Reservoir. However, isotopic ratios suggest that the uranium is natural. Cochiti Lake collects water from a larger watershed than Abiquiu Reservoir, which might explain why natural uranium levels are higher in fish from Cochiti (Fresquez 2002). However, uranium levels in all fish are below levels of health concern. In the same study, they identified levels of barium, copper, and mercury above detection limits in the muscle of fish collected from the confluence of canyons that cross LANL and the Rio Grande. However, none of the concentrations was significantly higher than in muscle of fish collected from background locations (Abiquiu Reservoir and Rio Grande at San Ildefonso) (Fresquez et al. 1999).

Both LANL and NMED have sampled fish in Cochiti Lake for polychlorinated biphenyls (PCBs) and other organic compounds (Gonzales et al. 1999). PCB levels greater than EPA fish consumption screening guidelines have been found in fish from Cochiti Lake. LANL (Fresquez 2002) and NMED (Ford-Schmid 2002) found that levels of PCBs in fish from the Abiquiu Reservoir had lower levels of PCBs than fish from Cochiti. It appears that monitoring for PAHs in the Rio Grande and Cochiti has not been done (Fresquez 2002; Ford-Schmid 2002).

Focusing additional efforts on sampling fish in a variety of locations for the chemicals and radionuclides contributing most to risk may be important. It should also be noted that current fish concentrations might not be a good indicator of current concentrations of chemicals in the river or reservoir because it takes time for materials to accumulate in fish.

6 CONCLUSIONS

We estimated the potential cancer risk from the Cerro Grande fire burning on the LANL site to be less than 3 in one million from exposure to any LANL-derived chemical or radionuclide that may have been carried in the surface water and sediments to the Rio Grande and Cochiti Lake. We presented risk estimates as morbidity risks for carcinogenic chemicals and radionuclides or as hazard quotients for noncarcinogens. Hazard quotients provide a way to express non-cancer health effects in terms of the fraction of the acceptable daily intake (the amount of chemical that may be ingested over a period of time that will produce no adverse health effects) of a given chemical. Table 6-1 summarizes the highest cancer risks or the hazard quotients for exposure to LANL-derived radionuclides and chemicals for three exposure pathways for our four scenarios.

We developed exposure scenarios and estimated risks of exposure to chemicals and radionuclides to hypothetical people drinking water from the Rio Grande or Cochiti Lake, contacting sediments near the edge of the water, eating fish from the Rio Grande or Cochiti Lake, eating produce irrigated with water from the lake, eating beef raised in the area, or participating in recreational activities like swimming. Of the different representative individuals considered in the exposure scenarios, the health risks to the hypothetical resident living year around near the Rio Grande at the confluence of Water Canyon were greatest when looking at single chemicals and radionuclides (Table 6-1). This hypothetical individual would be exposed to concentrations of chemicals and radionuclides in water and deposited sediments year round and had the highest potential risks for exposure to predicted benzo(a)pyrene (and other PAHs) and ^{137}Cs concentrations in fish. The hunter and firefighter, who were potentially exposed to higher concentrations in water and sediments, spent less time at those locations and were exposed through fewer exposure pathways. Exposure through other pathways was less important. For potential exposure to noncarcinogenic chemicals, intakes of all chemicals were less than acceptable intakes (a hazard quotient <1) established by the U.S. Environmental Protection Agency (EPA).

To estimate these potential risks, we estimated concentrations of radionuclides and chemicals released to storm water from source areas in the LANL facility environs during and after the Cerro Grande Fire at points of exposure locations selected to account for the different types of individuals, activities, and practices that may have resulted in exposure to these radionuclides and chemicals. We identified the chemicals and radionuclides through a screening process to focus the analysis on those with the highest potential to contribute to the health risk of those exposed. We estimated concentrations of chemicals and radionuclides at these points of exposure using a conservative modeling approach that accounted for storm water flow from design storm events across identified source areas associated with LANL, the suspension of soil from these source areas containing chemicals and radionuclides, and the transport of these chemicals and radionuclides to the point of exposure. We took this modeling approach because measured concentrations of radionuclides and chemicals in water and sediments did not have the temporal and spatial coverage necessary to comprehensively calculate exposure and risk throughout the model domain. Additionally, documented background concentrations were lacking for many of the radionuclides and chemicals of potential concern, particularly for water and suspended sediment. Also, one of the goals of this project was to estimate potential risks, based on possible storm events in the future, and the available environmental monitoring data collected following the fire are from relatively dry years. As a result, the conclusions that can be made about potential risks based on post-fire monitoring data were limited.

Table 6-1. Highest Estimated Impacts by Scenario, Individual Chemical or Radionuclide, and Selected Pathways^a

Eating fish from Rio Grande or Cochiti Lake	Lifetime cancer incidence risk (carcinogens)		Hazard quotient (noncarcinogens)
	Radionuclides	Chemicals	Chemicals
Scenario ^b			
Hunter	3.5×10^{-6}	5.5×10^{-9}	0.09
Residents near Cochiti Reservoir			
Adult	4.0×10^{-7}	5.1×10^{-7}	0.02
Child	1.7×10^{-7}	5.0×10^{-7}	0.02
Person near Rio Grande at Water Canyon	2.4×10^{-6}	2.7×10^{-6}	0.1
Fire cleanup person	na ^c	na	na
Important radionuclides and chemicals	^{137}Cs	B(a)P ^d	chromium, lead

Drinking water from Rio Grande or Cochiti Lake	Lifetime cancer incidence risk (carcinogens)		Hazard quotient (noncarcinogens)
	Radionuclides	Chemicals	Chemicals
Scenario ^b			
Hunter	4.3×10^{-8}	4.4×10^{-10}	0.0066
Residents near Cochiti Reservoir			
Adult	4.9×10^{-9}	3.0×10^{-7}	0.0033
Child	2.4×10^{-9}	3.5×10^{-7}	0.0039
Person near Rio Grande at Water Canyon	2.2×10^{-8}	1.4×10^{-6}	0.015
Fire cleanup person	na ^c	na	na
Important radionuclides and chemicals	^{137}Cs , ^{239}Pu	RDX ^d	barium, lead

Incidental sediment ingestion	Lifetime cancer incidence risk (carcinogens)		Hazard quotient (noncarcinogens)
	Radionuclides	Chemicals	Chemicals
Scenario ^b			
Hunter	6.1×10^{-9}	2.7×10^{-9}	0.00026
Residents near Cochiti Reservoir			
Adult	8.1×10^{-9}	3.2×10^{-7}	0.00052
Child	8.1×10^{-9}	7.4×10^{-7}	0.0012
Person near Rio Grande at Water Canyon	3.7×10^{-9}	1.2×10^{-7}	0.00024
Fire cleanup person	1.8×10^{-11}	4.7×10^{-9}	0.003
Important radionuclides and chemicals	^{239}Pu , ^{226}Ra	B(a)P, RDX ^d	lead, barium

^a For radionuclides and carcinogenic chemicals, the annual morbidity risks are presented for exposure to concentrations of radionuclides or chemicals after a two-year storm event (see Chapter 4); for noncarcinogens, the hazard quotient expresses the fraction of acceptable intake established by the EPA.

^b These scenarios represent hypothetical individuals; they do not represent known individuals with these characteristics at these locations.

^c This was not a realistic exposure pathway for this scenario.

^d B(a)P = benzo(a)pyrene; RDX = hexahydro-1,3,5-trinitro-1,3,5-triazine (an explosive material).

The goal of these modeling efforts was to develop conservative estimates of the relative concentrations for pre-fire and post-fire conditions for the surface water pathways. The estimation of chemical and radionuclide concentrations at selected points of exposure was central to these efforts. There are many uncertainties associated with environmental transport modeling, and the process of distinguishing between regional background concentrations, concentrations expected in fire-impacted areas, and concentrations related to LANL operations complicates the calculations. Because of the uncertainties inherent in modeling and estimating the source area concentration, we intended that the predicted concentrations and risk estimates be conservative or cautious. However, the results of this type of predictive modeling can be used to identify specific areas or chemicals and radionuclides contributing most to potential risk. The modeling results are also useful for understanding the relative contribution of different potential sources of chemicals and radionuclides, which is something that is difficult to do with the current environmental monitoring data.

An inherent uncertainty associated with each of the source areas we characterized is the inability, based on available data, to understand how chemical and radionuclide distribution at source areas in the LANL environment may change over time, which would be expected to vary by chemical or radionuclide, and how this could impact the calculations. Because much of the data used to characterize the source areas was collected from 1993 to 1997, some changes in distribution and extent of chemicals and radionuclides would be expected since that time.

Some general observations about the estimated concentrations at the points of exposure and the risk results can be made.

1. The modeled concentrations of chemicals and radionuclides are intended to be upper bound estimates to provide a conservative estimate of the potential concentrations and risks at the selected points of exposure. Available monitoring data from sampling points within 250 meters of the selected points of exposure indicate the estimated concentrations of chemicals and radionuclides contributing most to risk are within 1 to 3 orders of magnitude greater than the measurement results.
2. There was no consistent change in concentrations of chemicals and radionuclides from before the fire to after the fire. Both increases and decreases of concentrations of chemicals and radionuclides that were generally less than an order of magnitude occurred from pre-fire to post-fire. Estimated concentrations of chemicals and radionuclides in total storm water or surface water (i.e., combined dissolved phase and suspended sediment) are generally higher after the fire than before the fire, but estimated concentrations of chemicals and radionuclides in the dissolved phase in storm water or surface water, suspended sediments and deposited sediments are smaller after the fire in many cases. This suggests that while the fire did impact the potential transport of chemicals and radionuclides, the change in the resulting concentrations from pre-fire to post-fire can be either an increase or decrease, but generally the difference will not be greater than an order of magnitude and is likely within the uncertainty of the calculations. Overall, the effects of the fire on contaminant risks are not readily obvious and consistent in terms of direction and magnitude. However, the likely absolute total risks appear to be within EPA guidelines.
3. Concentrations of chemicals and radionuclides decrease as the point of exposure is moved further away from the source areas, resulting in higher concentrations within the canyons immediately below the LANL facility than along the Rio Grande and Cochiti Reservoir (e.g.,

POE 2.1 to POE 1.1) primarily due to dilution from portions of the contributing watershed that do not contain source areas.

4. The predicted concentrations of chemicals and radionuclides at a point of exposure are not significantly affected by storm intensity (less than an order of magnitude). It is therefore reasonable to assume that there is a potential for increased concentrations of chemicals and radionuclides at a point of exposure after the fire regardless of the magnitude of the storm event. The magnitude of the concentrations would be limited by a number of phenomena, including the volume of sediment and water generated by the storm event to transport chemicals and radionuclides to that point of exposure.
5. Deposited sediments in stream segments and reaches in portions of the canyons below the LANL facility can have a significant effect on concentrations of chemicals and radionuclides and the resulting risks. Chemical and radionuclide characterization data were available only for stream segments and reaches within Los Alamos and Pueblo Canyons. This circumstance limited our ability to evaluate the effects of chemicals and radionuclides that may be present in other canyons (i.e., Mortandad, Pajarito, Water Canyons). However, we did account for chemical and radionuclides from all PRSs that were located in these canyons.
6. Chemicals and radionuclides in the burn area ash significantly impact the concentrations of chemicals and radionuclides at a point of exposure where the area of the watershed contributing to that point of exposure is dominated by the burn area. This was seen at POE 4.1a and 4.1b where the burn area was greater than 85% of the contributing watershed area. In addition, the lack of sediment characterization data for canyons impacting these POEs (i.e., Water and Mortandad) likely contributed to the greater importance of the burn area. The burn area for the other points of exposure was less than 50% of the contributing watershed area.
7. This analysis has shown that both the concentration and areal extent assumed for each chemical and radionuclide in each source area and the potential flow of water across that area are important factors in understanding the relative importance on POE concentrations of one source area compared to another.
8. Risk estimates and hazard quotients for the child and the adult at Cochiti Reservoir (Scenario 2) are generally similar in magnitude for any pathway. The radionuclide risk coefficients represent population-averaged values and are not specific to either a child or an adult of a specific age. Therefore, the risks to the hypothetical individuals do not reflect age-specific differences in the dosimetry, but only age (and behavior) differences between the hypothetical individuals.
9. The post-fire and incremental cancer risk estimates for carcinogens, and hazard quotients (HQ) for noncarcinogens, potentially released to water from source areas associated with LANL, did not differ significantly from each other. There are a number of reasons for this observation.
10. Risks for all pathways associated with the 500-year storm event are generally higher by less than an order of magnitude than the risks from the 2-year storm event, and the differences between the two are likely within the uncertainties of the calculations.

Table 6-2 summarizes our qualitative estimate of the level uncertainty and conservatism for each aspect of the exposure risk calculation. The calculated inventories and resulting source term values and transport modeling probably contributed most to the overall uncertainty and conservatism of the risk estimates—probably overestimating them by 1 to 3 orders of magnitude.

Table 6-2. Summary of Conservatism and Uncertainty in Each Modeling Component of the Exposure and Risk Calculations for Surface Water Pathways

Modeling Component	Estimated Conservatism or Uncertainty	Comments
Selecting radionuclides or chemicals of potential concern	Moderate conservatism and uncertainty	Our screening process used available monitoring data for radionuclides and chemicals collected after the fire and readily available risk coefficients for radionuclides, and slope factors and reference doses for chemicals to calculate a screening index.
Identifying potential source areas	Unknown conservatism and uncertainty	We identified four distinct source areas with potential for release of chemicals and radionuclides and movement by erosion and storm water flow. These are: PRSs, geomorphic units, unsampled reaches; and burned area ash. Characterization data for canyon sediments outside of Los Alamos and Pueblo Canyons were not available. There are some areas that could not be considered because of a lack of available characterization data.
Estimating chemical and radionuclide concentration at the source areas and estimating the areal extent of those chemicals and radionuclides	Unknown conservatism and high uncertainty	Chemical and radionuclide characterization at each source area was based on the average of detected concentrations, excluding nondetect values. This likely biases our assumed characterization on the high side. We also showed that the use of maximum measured source area concentrations did not result in significantly larger POE concentrations (Appendix N).
Storm water flow estimates	Moderate conservatism and uncertainty	We assumed flow estimates based on design storm events occurring over the entire watershed and that all of the storm water arrived at the point of exposure at the same time.
Chemical and radionuclide transport	High conservatism and uncertainty	We assumed an infinite, nondepleting source, the movement of all chemical mass and radionuclide activity to the point of exposure, and dilution as the only attenuation mechanism. The chemical and radionuclide transport is a complex process that was modeled using an upper bound approach with combined parameters resulting in a number of sources of uncertainty.
Exposure scenario assumptions	Moderate conservatism and uncertainty	We developed scenarios with caution so that a potentially exposed person or an exposure pathway would not be missed and that risks estimated for the hypothetical individuals in the scenarios would be greater than risks of other individuals who might be in the area for less time or under less exposed conditions. The individuals described in the scenarios do not represent known individuals with these characteristics at these locations.
Exposure factors	Moderate conservatism and uncertainty	Parameter values may be above average values but they are not unrealistically high.
Radionuclide risk coefficients	Moderate conservatism and uncertainty	Radionuclide risk coefficients have been studied extensively for over 25 years.
Slope factors	High conservatism and uncertainty	Many confounding factors affect the level of conservatism and uncertainty in slope factors for a particular chemical including, the variation in sensitivity among the members of the human population and the uncertainty in extrapolating animal data to humans.
Hazard quotients	High conservatism for some chemicals	The use of chronic RfDs to express subchronic exposure may have resulted in large overestimates of noncarcinogenic health effects, in some cases.
Risk estimates	Overall, high conservatism and uncertainty	Our risk estimates may be overestimated by approximately 1-3 orders of magnitude as a result of the conservatism in our assumptions about source term, transport, and scenario parameters. This level of conservatism appears to be confirmed based on our comparisons of predicted to measured concentrations.

7 REFERENCES

- Alexander, M. 2001. LANL ESH-18. Email Communication. September 26, 2001.
- Apostolaei, A.I., B.G. Blaylock, B. Caldwell, S. Flack, J.S. Gouge, F.O. Hoffman, C.J. Lewis, S.K. Nair, E.W. Reed, K.M. Thiessen, B.A. Thomas, and T.E. Widner. 1999. *Radionuclides Released to the Clinch River from White Oak Creek on the Oak Ridge Reservation – An Assessment of Historical Quantities Released, Off-Site Radiation Doses, and Health Risks. Oak Ridge Dose Reconstruction, Volume 4*. ChemRisk, A Service of McLaren/Hart, Alameda, California. July.
- ATSDR (Agency for Toxic Substances and Disease Registry). 1990-2000. *Toxicological Profiles*. Atlanta, Georgia.
- Auclair, A.N.D. 1977. "Factors Affecting Tissue Nutrient Concentrations in a Carex Meadow." *Oecologia (Berl.)* 28: 233–246.
- BAER (Interagency Burned Area Emergency Rehabilitation Team). 2000. Cerro Grande Burned Area emergency Rehabilitation Plan, US Forest Service, Santa Fe, NM.
- Baes, C.F., R.D. Sharp, A.L. Sjoreen, and R.W. Shor. 1984. *A Review and Analysis of Parameters for Assessing Transport of Environmentally Released Radionuclides Through Agriculture*. ORNL-5786. Oak Ridge National Laboratory, Oak Ridge, Tennessee.
- Bitner, K., B. Gallaher, and K. Mullen. 2001. *Review of Wildfire Effects on Chemical Water Quality*. LA-13826-MS. May.
- Charbeneau, R.J. 2000. *Groundwater Hydraulics and Pollutant Transport*. Upper Saddle River, New Jersey: Prentice Hall, Inc.
- Chow, V.T., D.R. Maidment, and L.W. Mays. 1988. *Applied Hydrology*. New York, New York: McGraw Hill, Inc.
- Dinwiddie, R.S. 1999. *HRMB Recommendations Concerning the Proposed Watershed and Aggregate Prioritization*. Los Alamos National Laboratory, New Mexico 0890010515. New Mexico Environment Department, Hazardous and Radioactive Materials Bureau. March 23.
- DOE (U. S. Department of Energy). 2000. *Special Environmental Analysis for the Department of Energy, National Security Administration – Actions Taken in Response to the Cerro Grande Fire at Los Alamos National Laboratory, Los Alamos, New Mexico*. DOE/SEA-03, September.
- Eckerman, F.F., R.W. Leggett, C.B. Nelson, J.S. Puskin, and A.C.B. Richardson. 1999. *Cancer Risk Coefficients for Environmental Exposure for Radionuclides Federal guidance Report No. 13*. EPA 402-R-99-001. Office of Radiation and Indoor Air, U.S. Environmental Protection Agency, Washington, DC.

- EPA (U. S. Environmental Protection Agency). 1990. *Risk Assessment Guidance for Superfund: Volume 1, Human Health Evaluation Manual, Part A* (EPA/540/1-89/002). Environmental Protection Agency, Washington, D.C.
- EPA. 1991. Role of the Baseline Risk Assessment in Superfund Remedy Selection Decisions. Memorandum from Assistant Administrator Don R. Clay to the Regions. OSWER Directive 9355.0-30. Office of Solid Waste and Emergency Response, U.S. Environmental Protection Agency, Washington, DC. April 22.
- EPA. 1992. *Dermal Exposure Assessment: Principles and Applications*. EPA/600/8-91/011B, Interim Report. Office of Health and Environmental Assessment, Washington, D.C. January.
- EPA. 1993. *External Exposure to Radionuclides in Air, Water, and Soil*. Federal Guidance Report No. 12. EPA 402-R-93-081. EPA 402-R-99-001. Office of Radiation and Indoor Air, U.S. Environmental Protection Agency, Washington, D.C. September.
- EPA. 1997a. Establishment of Cleanup Levels for CERCLA Sites with Radioactive Contamination. Memorandum from Stephen D. Luftig, Director, Office of Emergency and Remedial Response and Larry Weinstock, Acting Director, Office of Radiation and Indoor Air. OSWER 9200.4-18. Office of Solid Waste and Emergency Response, U.S. Environmental Protection Agency, Washington, DC. August 22.
- EPA (Environmental Protection Agency). 1997b. *Health Effects Assessment Summary Tables*. EPA/540/R-95/036, Office of Solid Waste and Emergency Response, U.S. Environmental Protection Agency, Washington, D.C.
- EPA. 1999a. *Exposure Factors Handbook*. EPA/600/C-99/001. Office of Research and Development, U.S. Environmental Protection Agency, Washington, D.C. February.
- EPA. 1999b. *Cancer Risk Coefficients for Environmental Exposures to Radionuclides*. Federal Guidance Report No. 13. EPA 402-R-99-001. Office of Radiation and Indoor Air, U.S. Environmental Protection Agency, Washington, D.C. September.
- EPA. 1999c. Region 9 Preliminary Remediation Goals. www.epa.gov/region09/waste/sfund/prg. October.
- EPA. 1999d. *Understanding Variation in Partition Coefficient, K_d, Values. Volume II: Review of Geochemistry and Available K_d Values for Cadmium, Cesium, Chromium, Lead, Plutonium, Radon, Strontium, Thorium, Tritium (³H), and Uranium*. EPA402-R-99-004B. August.
- EPA. 2000. *Region IX Preliminary Remediation Goals*. Version 7. U.S. Environmental Protection Agency, Region IX. San Francisco, California. November.
- EPA. 2001a. *Integrated Risk Information System (IRIS)*. National Center for Environmental Assessment. Cincinnati, Ohio.

- EPA. 2001b. *Region III Risk-Based Concentration Table*. U.S. Environmental Protection Agency, Region III. Philadelphia, PA. September.
- ER (Environmental Restoration Project). 2001. *Environmental Restoration Project Life-Cycle Baseline Prioritization, Fiscal Year 2001 Revision, Programmatic Assumptions Document*. Los Alamos National Laboratory Report LA-CP-00-445, Los Alamos, New Mexico.
- ESRI (Environmental Systems Research Institute). 1998a. ArcView GIS. Version 3.1. Redlands, California.
- ESRI. 1998b. Spatial Analyst ArcView Extension Program. Version 1.1. Redlands, California.
- Ford-Schmid, R. 2002. Environmental Specialist, DOE Oversight Bureau, New Mexico Environment Department. Personal Communication with Patricia McGavran, RAC. March 25.
- Fresquez, P.R., D.H. Kraig, M.A. Mullen, and L. Naranjo. Jr. 1999. Radionuclides and Trace Elements in Fish Collected Upstream and Downstream of Los Alamos National Laboratory and the Doses to Humans from the Consumption of Muscle and Bone. *J. Environ. Sci. health*. B34(5): 885-899.
- Fresquez, P. 2002. Environmental Safety and Health, Los Alamos National Laboratory. Personal Communication with Patricia McGavran, RAC. March 26.
- Fromm, J. 1996. INEEL Environmental Toxicologist, Remediation Bureau. Memo to INEEL WAG Managers and Technical Support Staff. Subject: Radionuclide Risk-Based Concentration Tables. January 3.
- Gonzlaes, G.J., P.R. Fresquez, and J.W. Beveridge. 1999. Organic Contaminant Levels in Three Fish Species Downchannel from the Los Alamos National Laboratory. LA-13612-MS. Los Alamos National Laboratory. June.
- Hakonson, T.E., J.W. Nyhan, L.J. Johnson, and K.V. Bostick. 1973. *Ecological Investigation of Radioactive Materials in Waste discharge Areas at Los Alamos*. LA-5282-MS. Los Alamos National Scientific Laboratory, Los Alamos, New Mexico. May.
- HEC (Hydraulic Engineering Center). 2000a. "U.S. Army Corps of Engineers, Hydrologic Modeling System HEC-HMS, Technical Reference Manual." CPD-74B. Davis, California. March.
- HEC. 2000b. "U.S. Army Corps of Engineers, Geospatial Hydrologic Modeling Extension HEC-GeoHMS, User Manual." CPD-77. Davis, California. July.

- HEC. 2000c. Geo-HMS, HMS ArcView Extension Program. Version 1.0. Davis, California.
- HEC. 2001. HEC-HMS, Hydrologic Modeling System. Version 2.1.1. Davis, California.
- ICRP (International Commission on Radiological Protection). 1991. *Recommendations of the International Commission on Radiological Protection*. Oxford: Pergamon Press. ICRP Publication 60. Ann. ICRP 21, No. 1-3.
- Koch, R.J., D.A. Shaull, B.M. Gallaher, and M.R. Alexander. 2001. *Precipitation Events and Storm Water Runoff Events at Los Alamos National Laboratory after the Cerro Grande Fire*. Draft Report. Los Alamos National Laboratory, Los Alamos, New Mexico.
- Kocher, D.C. and K.F. Eckerman. 1987. "Electron Dose-Rate Conversion Factors for External Exposure of the Skin from Uniformly Deposited Activity on the Body Surface." *Health Physics* 53(2): 135-141. August.
- Kraig, D., R. Rytty, D. Katzman, T. Buhl, B. Gallaher, and P. Fresquez. 2001. *Radiological and Nonradiological Effects after the Cerro Grande Fire*. LA-UR-01-6868. Los Alamos National Laboratory, Los Alamos, New Mexico. December.
- Lambert, G., et al. 1991. Long-lived radon daughters signature of savanna fires. From Global Biomass Burning conference proceedings, pp 181-4. Joel S. Levine, ed. MIT Press.
- Lane, L.J., M.H. Nichols, and G.B. Paige. Unknown. "Modeling Erosion on Hillslopes: Concepts, Theory and Data." USDA-ARS.
- LANL (Los Alamos National Laboratory). 1999a. *Environmental Surveillance at Los Alamos during 1998*. LA-13633-ENV. Los Alamos National Laboratory, Los Alamos, New Mexico. September.
- LANL (Los Alamos National Laboratory). 1999b. *Surface Water Data at Los Alamos National Laboratory: 1998 Water Year*. LA-13551-PR. Los Alamos National Laboratory, Los Alamos, New Mexico.
- LANL. 2000. BAER Team Digital Geographic Data, Volume 2 CD-ROM. Cerro Grande Fire, Los Alamos, New Mexico.
- LANL. 2001a. *Los Alamos National Laboratory Groundwater Integration Team Action Plan for External Advisory Group: December 2000 Recommendations*. Los Alamos National Laboratory, Los Alamos, New Mexico. March 15.
- LANL. 2001b. The Weather Machine, www.weather.lanl.gov.
- leCloarec, M.F., et al. 1995. ^{210}Po in Savanna Burning Plumes. *Journal of Atmospheric Chemistry*. Vol. 22, pp 111-122.

- Maidment, D. R., ed. 1993. *Handbook of Hydrology*. New York, New York: McGraw-Hill.
- Maidment, D.R. and D. Djokic, eds. 2000. *Hydrologic and Hydraulic Modeling Support with Geographic Information Systems*. Redlands, California: ESRI Press.
- McLin, S.G. 1992. *Determination of the 100-Year Flood Elevations at the Los Alamos National Laboratory*. LA-12195-MS. Los Alamos National Laboratory. Los Alamos, New Mexico.
- Melancon, P.A. 1999. "A GIS Based Watershed Analysis System for Tillamook Oregon." Master's Thesis. Civil Engineering. The University of Texas at Austin. Austin, Texas.
- Mohler, H. J., K. R. Meyer, J. W. Aanenson, and H. A. Grogan. 2002. Analysis of Exposure and Risks to the Public from Radionuclides and Chemicals Released by the Cerro Grande Fire at Los Alamos. Task 3: Calculating and Communicating Risks: Observations and Recommendations. RAC Report No.15-NMED-2002-Final(Rev.1). Risk Assessment Corporation, Neeses, South Carolina. June 12.
- Nance, J.D., et al. 1993. Airborne measurements of gases and particles from an Alaskan wildfire. *Journal of Geophysical Research*. Vol. 98, No. D8, pp 14,873-14,882.
- National Research Council. 1995. *Radiation Dose Reconstruction for Epidemiologic Uses*. Washington DC: National Academy Press. ISBN 0-309-05099-5.
- NCRP (National Council on Radiation Protection and Measurements). 1993. *Limitation of Exposure to Ionizing Radiation*. NCRP Report No. 116.
- NCRP (National Council on Radiation Protection and Measurements). 1996. *Screening Models for Releases of Radionuclides to Atmosphere, Surface Water, and Ground*. NCRP Report No. 123. National Council on Radiation Protection and Measurements, Bethesda, Maryland. January.
- Nyhan, J.W. 1978. *Soil Survey of Los Alamos County*. LA-6779-MS. Los Alamos National Laboratory, Los Alamos, New Mexico.
- Nyhan, J.W., S. Koch, R. Balice, and S. Loftin. 2001. *Estimation of Soil Erosion in Burnt Forest Areas of the Cerro Grande Fire in Los Alamos, New Mexico*" LA-UR-01-4658. Los Alamos National Laboratory, Los Alamos, New Mexico.
- Olivera, F.R. 1999. CRWR Raster. ArcView Extension Program. Center for Research in Water Resources, University of Texas at Austin, Austin, Texas.
- ORNL (Oak Ridge National Laboratory). 2001. ORNL Risk Assessment Information System Database (RAIS®), Chemical Toxicity Values, at <http://risk/lsd.ornl.gov> , Oak Ridge, Tennessee. December.

- Purtyman, W.D., R.J. Peters, T.E. Buhl, M.N. Maes, and F.H. Brown. 1987. *Background Concentrations of Radionuclides in Soils and River Sediments in Northern New Mexico, 1974-1986*. LA-11134-MS. Los Alamos National Laboratory, Los Alamos, New Mexico. November.
- RAIS (Risk Assessment Information System Database (RAIS®)). 2002. (Oak Ridge National Laboratory. ORNL Risk Assessment Information System Database (RAIS®), Chemical Toxicity Values, at <http://risk/lsd.ornl.gov>, Oak Ridge, Tennessee.
- Reneau, S., R. Rytí, M. Tardiff, and J. Linn. 1998a. *Evaluation of Sediment Contamination in Upper Los Alamos Canyon: Reaches LA-1, LA-2, and LA-3*. LA-UR-98-3974. Los Alamos National Laboratory, Los Alamos, New Mexico. September.
- Reneau, S., R. Rytí, M. Tardiff, and J. Linn. 1998b. *Evaluation of Sediment Contamination in Lower Los Alamos Canyon: Reaches LA-4 and LA-5*. LA-UR-98-3975. Los Alamos National Laboratory, Los Alamos, New Mexico. September.
- Reneau, S., R. Rytí, M. Tardiff, and J. Linn. 1998c. *Evaluation of Sediment Contamination in Pueblo Canyon: Reaches P-1, P-2, and P-3*. LA-UR-98-3324. Los Alamos National Laboratory, Los Alamos, New Mexico. September.
- RGIS (New Mexico Resource Geographic Information System). 2001. U.S. Census Bureau Topologically Integrated Geographic Encoding and Referencing (TIGER) Hydrography, Earth Data Analysis Center, University of New Mexico, Albuquerque, New Mexico
- Rogers, M.A. 1977. *History and Environmental Setting of LASL Near-Surface Land Disposal Facilities for Radioactive Wastes (Areas A, B, C, D, E, F, G, and T) A Source Document*. LA-6848-MS, Volumes 1 and 2. Los Alamos National Scientific Laboratory, Los Alamos, New Mexico. June.
- Rood, A. S., J. W. Aanenson, S. S. Mohler, P. D. McGavran, J. J. Mohler, and H.A. Grogan. 2002. Analysis of Exposure and Risks to the Public from Radionuclides and Chemicals Released by the Cerro Grande Fire at Los Alamos. Task 1.7: Final Report on Estimated Risks from Releases to Air. RAC Report No. 3-NMED-2002-Final(Rev.1). June 12.
- Rytí, R.T., P.A. Longmire, D.E. Broxton, S.L. Reneau, and E.V. McDonald. 1998. *Inorganic and Radionuclide Background Data (sic) for Soils, Canyon Sediments, and Bandelier Tuff at Los Alamos National Laboratory*. LAUR-98-4847. Los Alamos National Laboratory, Los Alamos, New Mexico. September 22.
- Schiffmiller, G. 2002. Environmental Specialist, Surface Water Quality Bureau, New Mexico Environment Department. Personal Communication with Patricia McGavran, RAC. March 26.

- Sheppard, M. I. and D. H. Thibault. 1990. "Default Soil Solid/Liquid Partition Coefficients, K_{ds}, for Four Major Soil Types: A Compendium." *Health Physics* 59 (4): 471–482.
- Shleien, B. 1992. *Scoping Document for Determination of Temporal and Geographic Domains for the HEDR Study*. Hanford Technical Steering Panel. Summer.
- Theissen, K., J.S. Hammonds, C.J. Lewis, F.O. Hoffman, and E.I. White. 1996. *Screening Method for the Oak Ridge Dose Reconstruction. Appendix A in Screening-Level Evaluation of Additional Potential Materials of Concern. Reports of the Oak Ridge Dose Reconstruction, Vol. 6*. The Report of Project Task 4. July.
- Till, J.E. and K.R. Meyer. 2001. "Public Involvement in Science and Decision Making." *Health Physics* 80 (4): April.
- USACE (United States Army Corps of Engineers). 2002. Albuquerque District, Reservoir Information, Cochiti Lake, www.spa.usace.army.mil/
- USGS (United States Geological Survey). 1998. Digital Elevation Model CD, EROS Data Center Customer Services, Sioux Falls, South Dakota. May.
- USGS. 2001 National Water Information System, Surface Water Data for the Nation, www.water.usgs.gov/usa/nwis/sw/
- USGS. 2002. Suspended Sediment Database, webserver.cr.usgs.gov/sediment/.
- Veenis, S. 2001. Erosion Matrix Score and Best Management Practice (BMP) Installation Information. Database file obtained during October 2001 site visit.
- Whicker, F.W. and V. Schultz. 1982. *Radioecology: Nuclear Energy and the Environment, Volume I*. Boca Raton, Florida: CRC Press.
- Wilson, C.J., J.W. Carey, P.C. Beeson, M.O. Gard, and L. J. Lane. 2001. "Predicting Sediment Yield from the Cerro Grande Fire Using a Hillslope Erosion Model in a GIS Framework." *Hydrological Processes* 15 (15) (in press).

APPENDIX A

RADIONUCLIDES AND CHEMICALS MEASURED IN WATER SAMPLES AFTER THE FIRE BY LANL

Appendix A. Radionuclides and Chemicals Measured in Water

Table A-1a. Radionuclides Measured in Water Samples^a after the Fire by ESH-18

Radionuclide	Number of samples	Concentration (pCi L ⁻¹)		Radionuclide	Number of samples	Concentration (pCi L ⁻¹)	
		Mean	Maximum			Mean	Maximum
Ac-228	225	7.1E+00	1.9E+02	Nb-94	37	1.8E-01	1.6E+00
Am-241	437	1.5E-01	6.0E+01	Nb-95	138	8.1E-01	5.7E+00
Sb-124	138	7.5E-02	2.8E+00	Pu-238	225	1.7E-01	7.6E+00
Sb-125	138	2.1E-01	6.1E+00	Pu-239,240	226	1.0E+00	2.5E+01
Ba-133	138	-3.3E-01	2.9E+00	Po-210	55	3.7E+01	6.0E+02
Ba-140	80	9.2E+00	2.0E+02	K-40	224	6.7E+01	2.1E+03
Be-7	182	1.5E+01	2.6E+02	Pm-144	37	1.0E-01	2.1E+00
Bi-211	102	8.1E+00	3.1E+01	Pm-146	37	-1.2E-01	2.2E+00
Bi-212	225	3.3E-01	1.2E+02	Pa-231	145	-5.3E-01	1.3E+02
Bi-214	221	7.8E+00	1.3E+02	Pa-233	145	3.7E-01	4.7E+01
Cd-109	145	3.0E+00	4.5E+02	Pa-234m	145	1.3E+02	7.1E+02
Ce-139	181	-3.9E-01	2.9E+00	Ra-223	145	-3.5E+00	7.1E+01
Ce-141	138	8.4E-01	2.0E+01	Ra-224	102	5.6E+00	9.5E+01
Ce-144	181	2.2E-01	2.1E+01	Ra-226	203	4.8E+00	4.7E+02
Cs-134	226	-3.3E-01	3.5E+00	Ra-228	198	7.0E+00	1.5E+02
Cs-136	37	7.6E-01	6.7E+00	Rh-106	102	6.8E-02	2.6E+01
Cs-137	226	1.1E+01	5.1E+02	Ru-103	102	-5.9E-01	2.5E+00
Cr-51	138	1.3E+00	4.2E+01	Ru-106	183	6.4E-01	3.1E+01
Co-56	37	3.4E-02	2.1E+00	Se-75	145	-2.0E-01	4.0E+00
Co-57	224	3.8E-01	8.2E+00	Ag-110m	37	-1.8E-01	3.0E+00
Co-58	37	6.7E-02	1.4E+00	Na-22	226	4.6E-01	2.6E+01
Co-60	226	1.1E-01	5.7E+00	Sr-85	145	-7.3E+00	1.7E+01
Eu-152	183	7.9E-01	2.9E+01	Sr-90	315	5.8E+00	8.1E+01
Eu-154	138	5.7E-01	1.1E+01	Tl-208	224	2.1E+00	4.7E+01
Eu-155	37	1.9E+00	1.3E+01	Th-227	145	-1.6E+00	3.5E+01
I-133	101	-1.5E+10	0.0E+00	Th-228	124	1.1E+01	2.2E+02
Ir-192	37	-1.3E-02	1.6E+00	Th-230	161	7.7E+00	1.3E+02
Fe-59	138	2.0E-02	5.5E+00	Th-231	102	3.5E+00	1.7E+01
La-140	44	-2.1E-02	2.0E+00	Th-232	124	8.4E+00	1.2E+02
Pb-210	91	1.3E+02	9.6E+02	Th-234	181	7.0E+01	1.2E+03
Pb-211	145	-3.4E+00	1.3E+02	Sn-113	181	1.5E-01	4.1E+00
Pb-212	223	5.3E+00	1.6E+02	H-3	182	1.4E+03	7.6E+04
Pb-214	223	5.0E+00	1.4E+02	U-234	238	4.9E+00	1.4E+02
Mn-54	224	3.9E-02	6.0E+00	U-235,236	461	2.2E+00	6.0E+01
Hg-203	181	5.1E-01	5.2E+00	U-238	376	2.1E+01	2.2E+02
Nd-147	37	1.1E+00	3.8E+01	Y-88	181	4.7E-01	7.5E+00
Np-237	145	4.6E+00	1.6E+02	Zn-65	180	-3.5E-01	1.3E+01
Np-239	138	2.2E-01	1.2E+01	Zr-95	138	2.1E-01	7.4E+00

^a For our screening assessment, we used the highest measured concentration in surface water, storm water, and ground water samples to ensure a conservative approach. These data include both filtered and unfiltered samples. For our risk analysis, we used the surface water and storm water samples.

^b Environmental Safety and Health (ESH).

Table A-1b. Radionuclides Measured in Water Samples^a after the Fire by ER^b

Radionuclide-ER	Number of samples	Concentration (pCi L ⁻¹)	
		Mean	Maximum
Am-241	116	4.0E-01	6.1E+01
Cs-134	82	-1.3E-01	1.1E+01
Cs-137	82	3.8E+00	2.4E+02
Co-60	82	1.5E-01	3.2E+00
Eu-152	82	3.4E-01	7.9E+00
Pu-238	134	5.0E-02	2.7E+00
Pu-239	133	1.0E+00	5.7E+01
Ru-106	81	-2.7E-01	3.3E+01
Na-22	82	6.8E-01	2.6E+01
Sr-90	179	4.2E+00	6.0E+01
Th-228	7	1.6E+00	6.7E+00
Th-230	7	7.6E-01	3.2E+00
Th-232	7	1.2E+00	5.1E+00
H-3	30	3.5E+03	5.3E+04
U-234	85	6.2E-01	5.0E+00
U-235	145	1.6E+00	9.7E+01
U-238	85	4.3E-01	4.7E+00

^a For our screening assessment, we used the highest measured concentration in surface water, storm water, and ground water samples from both ESH-18 and ER to ensure a cautious or conservative approach. These data include both filtered and unfiltered samples. For our risk analysis, we used the surface and storm water samples only.

^b Environmental Restoration Project (ER).

Appendix A. Radionuclides and Chemicals Measured in Water

Table A-2a. Chemicals Measured in Water Samples^a After the Fire by ESH-18^b

Analyte code	Chemical	Number of samples	Concentration ($\mu\text{g L}^{-1}$)	
			Mean	Maximum
35822-46-9	1,2,3,4,6,7,8-HpCDD	27	2.3E-03	2.4E-03
67562-39-4	1,2,3,4,6,7,8-HpCDF	27	2.2E-03	2.3E-03
39227-28-6	1,2,3,4,7,8-HxCDD	27	6.8E-03	7.1E-03
70648-26-9	1,2,3,4,7,8-HxCDF	27	6.4E-03	6.6E-03
40321-76-4	1,2,3,7,8-PCDD	27	6.0E-03	6.3E-03
57117-41-6	1,2,3,7,8-PCDF	27	5.5E-03	5.8E-03
120-82-1	1,2,4-Trichlorobenzene	95	3.4E+01	9.6E+02
95-50-1	1,2-Dichlorobenzene	142	2.3E+01	9.6E+02
99-35-4	1,3,5-trinitrobenzene	78	3.0E-01	5.7E+00
541-73-1	1,3-dichlorobenzene	142	2.3E+01	9.6E+02
99-65-0	1,3-Dinitrobenzene	80	1.3E-01	1.9E+00
106-46-7	1,4-Dichlorobenzene	142	2.3E+01	9.6E+02
108-60-1	2,2'-oxybis[1-chloropropane]	72	4.3E+01	9.6E+02
58-90-2	2,3,4,6-Tetrachlorophenol	16	9.0E+02	4.8E+03
1746-01-6	2,3,7,8-TCDD	27	6.5E-04	6.7E-04
51207-31-9	2,3,7,8-TCDF	27	4.7E-03	4.9E-03
95-95-4	2,4,5-Trichlorophenol	85	5.1E+01	9.6E+02
88-06-2	2,4,6-trichlorophenol	85	3.8E+01	9.6E+02
118-96-7	2,4,6-Trinitrotoluene	80	1.1E-01	4.4E-01
120-83-2	2,4-Dichlorophenol	85	3.8E+01	9.6E+02
105-67-9	2,4-Dimethylphenol	85	3.8E+01	9.6E+02
51-28-5	2,4-dinitrophenol	85	1.9E+02	4.8E+03
121-14-2	2,4-Dinitrotoluene	165	1.9E+01	9.6E+02
606-20-2	2,6-Dinitrotoluene	165	1.9E+01	9.6E+02
35572-78-2	2-Amino-4,6-dinitrotoluene	80	1.7E-01	1.3E+00
91-58-7	2-Chloronaphthalene	85	3.7E+01	9.6E+02
95-57-8	2-Chlorophenol	85	3.8E+01	9.6E+02
91-57-6	2-Methylnaphthalene	86	3.7E+01	9.6E+02
95-48-7	2-Methylphenol	85	3.8E+01	9.6E+02
88-74-4	2-Nitroaniline	85	1.9E+02	4.8E+03
88-75-5	2-Nitrophenol	85	3.8E+01	9.6E+02
88-72-2	2-nitrotoluene	80	4.1E-01	1.4E+00
91-94-1	3,3'-Dichlorobenzidine	85	1.8E+02	4.8E+03
99-08-1	3-Nitrotoluene	80	4.6E-01	3.0E+00
534-52-1	4,6-Dinitro-2-Methylphenol	85	1.9E+02	4.8E+03
19406-51-0	4-Amino-2,6-dinitrotoluene	80	2.1E-01	2.8E+00
101-55-3	4-Bromophenyl phenyl ether	85	3.8E+01	9.6E+02
59-50-7	4-Chloro-3-methylphenol	85	4.1E+01	9.6E+02
106-47-8	4-chloroaniline	85	9.2E+01	2.4E+03
7005-72-3	4-Chlorophenyl phenyl ether	85	3.8E+01	9.6E+02
99-99-0	4-Methylnitrobenzene	80	4.1E-01	1.0E+00
106-44-5	4-Methylphenol	65	4.4E+01	9.6E+02
100-01-6	4-Nitroaniline	85	1.8E+02	4.8E+03
100-02-7	4-Nitrophenol	85	1.9E+02	4.8E+03
83-32-9	Acenaphthene	85	3.7E+01	9.6E+02
208-96-8	Acenaphthylene	85	3.7E+01	9.6E+02

Analysis of Exposure and Risks to the Public from Radionuclides and
Chemicals Released by the Cerro Grande Fire at Los Alamos

Analyte code	Chemical	Number of samples	Concentration ($\mu\text{g L}^{-1}$)	
			Mean	Maximum
67-64-1	Acetone	42	1.9E+01	2.3E+01
309-00-2	Aldrin	6	5.5E-02	6.8E-02
Al	Aluminum	236	3.3E+04	1.0E+06
62-53-3	Aniline	65	1.1E+02	2.4E+03
120-12-7	Anthracene	85	3.7E+01	9.6E+02
Sb	Antimony	271	3.5E+00	2.8E+02
12674-11-2	Aroclor-1016	102	5.8E-01	1.5E+00
11104-28-2	Aroclor-1221	102	1.3E+00	3.0E+00
11141-16-5	Aroclor-1232	102	6.3E-01	1.5E+00
53469-21-9	Aroclor-1242	102	6.4E-01	1.5E+00
12672-29-6	Aroclor-1248	102	6.0E-01	1.5E+00
11097-69-1	Aroclor-1254	102	6.0E-01	1.5E+00
11096-82-5	Aroclor-1260	102	5.8E-01	1.5E+00
37324-23-5	Aroclor-1262	17	9.4E-02	9.4E-02
As	Arsenic	248	1.0E+01	1.4E+02
103-33-3	Azobenzene	22	1.4E+02	9.6E+02
Ba	Barium	249	9.9E+02	2.1E+04
71-43-2	Benzene	89	2.5E+00	5.0E+00
92-87-5	Benzidine	45	9.2E+00	1.1E+01
56-55-3	Benzo(a)anthracene	85	3.7E+01	9.6E+02
50-32-8	Benzo(a)pyrene	85	3.7E+01	9.6E+02
205-99-2	Benzo(b)fluoranthene	85	3.7E+01	9.6E+02
191-24-2	Benzo(g,h,i)perylene	85	3.7E+01	9.6E+02
207-08-9	Benzo(k)fluoranthene	85	3.7E+01	9.6E+02
65-85-0	Benzoic Acid	87	1.6E+02	1.9E+03
100-51-6	Benzyl Alcohol	86	4.0E+01	9.6E+02
Be	Beryllium	401	3.9E+00	1.0E+02
319-84-6	BHC[alpha-]	6	5.5E-02	6.8E-02
319-85-7	BHC[beta-]	6	5.5E-02	6.8E-02
319-86-8	BHC[delta-]	6	5.5E-02	6.8E-02
58-89-9	BHC[gamma-]	6	5.5E-02	6.8E-02
111-44-4	Bis(2-chloroethyl)ether	85	3.8E+01	9.6E+02
117-81-7	Bis(2-ethylhexyl)phthalate	86	4.0E+01	9.6E+02
B	Boron	230	1.5E+03	3.2E+05
108-86-1	Bromobenzene	10	5.0E+00	5.0E+00
74-97-5	Bromochloromethane	10	5.0E+00	5.0E+00
75-27-4	Bromodichloromethane	89	2.1E+00	1.2E+01
75-25-2	Bromoform	89	2.4E+00	5.0E+00
74-83-9	Bromomethane	89	5.1E+00	1.0E+01
78-93-3	Butanone[2-]	42	2.0E+01	2.0E+01
104-51-8	Butylbenzene[n-]	10	5.0E+00	5.0E+00
135-98-8	Butylbenzene[sec-]	10	5.0E+00	5.0E+00
98-06-6	Butylbenzene[tert-]	10	5.0E+00	5.0E+00
85-68-7	Butylbenzylphthalate	85	3.8E+01	9.6E+02
Cd	Cadmium	275	1.9E+00	3.4E+01
75-15-0	Carbon Disulfide	42	4.8E+00	5.0E+00
86-74-8	Carbazole	26	1.2E+02	9.6E+02
56-23-5	Carbon tetrachloride	89	2.4E+00	5.0E+00

Appendix A. Radionuclides and Chemicals Measured in Water

Analyte code	Chemical	Number of samples	Concentration ($\mu\text{g L}^{-1}$)	
			Mean	Maximum
5103-71-9	Chlordane[alpha-]	6	5.5E-02	6.8E-02
5103-74-2	Chlordane[gamma-]	6	5.5E-02	6.8E-02
108-90-7	Chlorobenzene	89	2.7E+00	5.0E+00
75-00-3	Chloroethane	89	4.0E+00	1.0E+01
110-75-8	Chloroethylvinyl ether[2-]	47	8.5E-01	8.5E-01
67-66-3	Chloroform	89	2.8E+00	7.2E+00
74-87-3	Chloromethane	89	4.3E+00	1.0E+01
95-49-8	Chlorotoluene[2-]	10	5.0E+00	5.0E+00
106-43-4	Chlorotoluene[4-]	10	5.0E+00	5.0E+00
Cr	Chromium	248	2.0E+01	5.1E+02
218-01-9	Chrysene	85	3.7E+01	9.6E+02
Co	Cobalt	236	2.0E+01	4.8E+02
Cu	Copper	239	3.4E+01	6.1E+02
CN (amen)	Cyanide, Amenable	135	7.5E+00	6.2E-02
CN(Total)	Cyanide, Total	240	1.7E+01	1.8E-01
72-54-8	DDD[4,4'-]	6	1.1E-01	1.4E-01
72-55-9	DDE[4,4'-]	6	1.1E-01	1.4E-01
50-29-3	DDT[4,4'-]	6	1.1E-01	1.4E-01
53-70-3	Dibenz(a,h)anthracene	85	3.7E+01	9.6E+02
132-64-9	Dibenzofuran	85	3.8E+01	9.6E+02
96-12-8	Dibromo-3-Chloropropane[1,2-]	10	1.0E+01	1.0E+01
124-48-1	Dibromochloromethane	81	3.2E+00	1.2E+01
74-95-3	Dibromomethane	10	5.0E+00	5.0E+00
75-71-8	Dichlorodifluoromethane	42	1.0E+01	1.0E+01
75-34-3	Dichloroethane[1,1-]	89	2.4E+00	5.0E+00
107-06-2	Dichloroethane[1,2-]	89	2.4E+00	5.0E+00
540-59-0	Dichloroethene[cis/trans-1,2-]	21	5.0E+00	5.0E+00
156-59-2	Dichloroethene[cis-1,2-]	10	5.0E+00	5.0E+00
75-35-4	Dichloroethylene[1,1-]	89	2.4E+00	5.0E+00
156-60-5	Dichloroethylene[trans-1,2-]	57	9.6E-01	5.0E+00
78-87-5	Dichloropropane[1,2-]	89	2.4E+00	5.0E+00
142-28-9	Dichloropropane[1,3-]	10	5.0E+00	5.0E+00
594-20-7	Dichloropropane[2,2-]	10	5.0E+00	5.0E+00
563-58-6	Dichloropropene[1,1-]	10	5.0E+00	5.0E+00
10061-01-5	Dichloropropylene[cis-1,3-]	89	2.4E+00	5.0E+00
10061-02-6	Dichloropropylene[trans-1,3-]	89	2.4E+00	5.0E+00
60-57-1	Dieldrin	6	1.1E-01	1.4E-01
84-66-2	Diethylphthalate	85	3.8E+01	9.6E+02
131-11-3	Dimethyl Phthalate	72	4.3E+01	9.6E+02
84-74-2	Di-n-butylphthalate	85	3.8E+01	9.6E+02
117-84-0	Di-n-octylphthalate	85	3.8E+01	9.6E+02
122-39-4	Diphenyl amine	43	1.5E+00	1.5E+00
122-66-7	Diphenylhydrazine[1,2-]	43	6.8E-01	2.0E+01
959-98-8	Endosulfan I	6	5.5E-02	6.8E-02
33213-65-9	Endosulfan II	6	1.1E-01	1.4E-01
72-20-8	Endrin	6	1.1E-01	1.4E-01
1031-07-8	Endosulfan Sulfate	6	1.1E-01	1.4E-01

Analysis of Exposure and Risks to the Public from Radionuclides and
Chemicals Released by the Cerro Grande Fire at Los Alamos

Analyte code	Chemical	Number of samples	Concentration ($\mu\text{g L}^{-1}$)	
			Mean	Maximum
7421-93-4	Endrin Aldehyde	6	1.1E-01	1.4E-01
53494-70-5	Endrin Ketone	6	1.1E-01	1.4E-01
100-41-4	Ethylbenzene	89	2.4E+00	5.0E+00
206-44-0	Fluoranthene	85	3.7E+01	9.6E+02
86-73-7	Fluorene	85	3.7E+01	9.6E+02
F(-1)	Fluoride	152	4.5E+02	2.1E+00
76-44-8	Heptachlor	6	5.5E-02	6.8E-02
1024-57-3	Heptachlor Epoxide	6	5.5E-02	6.8E-02
37871-00-4	Heptachlorodibenzodioxins (Total)	1	4.0E-06	4.0E-06
55673-89-7	Heptachlorodibenzofuran[1,2,3,4,7,8,9-]	1	4.6E-06	4.6E-06
38998-75-3	Heptachlorodibenzofurans (Total)	1	3.7E-06	3.7E-06
118-74-1	Hexachlorobenzene	85	3.8E+01	9.6E+02
87-68-3	Hexachlorobutadiene	95	3.4E+01	9.6E+02
77-47-4	Hexachlorocyclopentadiene	85	3.8E+01	9.6E+02
57653-85-7	Hexachlorodibenzodioxin[1,2,3,6,7,8-]	1	2.2E-06	2.2E-06
19408-74-3	Hexachlorodibenzodioxin[1,2,3,7,8,9-]	1	2.0E-06	2.0E-06
34465-46-8	Hexachlorodibenzodioxins (Total)	1	2.1E-06	2.1E-06
57117-44-9	Hexachlorodibenzofuran[1,2,3,6,7,8-]	1	1.3E-06	1.3E-06
72918-21-9	Hexachlorodibenzofuran[1,2,3,7,8,9-]	1	2.3E-06	2.3E-06
60851-34-5	Hexachlorodibenzofuran[2,3,4,6,7,8-]	1	1.6E-06	1.6E-06
55684-94-1	Hexachlorodibenzofurans (Total)	1	1.6E-06	1.6E-06
67-72-1	Hexachloroethane	85	3.8E+01	9.6E+02
591-78-6	Hexanone[2-]	42	2.0E+01	2.0E+01
2691-41-0	HMX	80	4.4E-01	2.2E+00
193-39-5	Indeno(1,2,3-cd)pyrene	85	3.7E+01	9.6E+02
74-88-4	Iodomethane	10	5.0E+00	5.0E+00
78-59-1	Isophorone	85	3.8E+01	9.6E+02
98-82-8	Isopropylbenzene	10	5.0E+00	5.0E+00
99-87-6	Isopropyltoluene[4-]	10	5.0E+00	5.0E+00
Pb	Lead	265	5.9E+01	1.2E+03
Mn	Manganese	239	4.3E+03	1.0E+05
Hg	Mercury	171	1.8E-01	4.8E+00
72-43-5	Methoxychlor[4,4'-]	6	5.5E-01	6.8E-01
108-10-1	Methyl-2-pentanone[4-]	42	1.9E+01	2.0E+01
75-09-2	Methylene chloride	89	3.3E+00	1.6E+01
Mo	Molybdenum	225	4.3E+01	1.7E+03
91-20-3	Naphthalene	96	3.4E+01	9.6E+02
Ni	Nickel	246	2.8E+01	8.3E+02
NO3	Nitrate	39	1.1E+00	1.6E+01
NO3+NO2-N	Nitrate-Nitrite as N	194	1.4E+00	1.8E+01
99-09-2	Nitroaniline[3-]	85	1.9E+02	4.8E+03
98-95-3	Nitrobenzene	165	2.0E+01	9.6E+02
62-75-9	N-Nitrosodimethylamine	65	4.6E+01	9.6E+02
86-30-6	N-Nitrosodiphenylamine	42	7.6E+01	9.6E+02
621-64-7	N-nitrosodipropylamine	85	3.8E+01	9.6E+02
39001-02-0	OCDF	27	1.3E-03	1.3E-03
36088-22-9	Pentachlorodibenzodioxins (Total)	1	2.3E-06	2.3E-06
3268-87-9	OCDD	27	1.5E-03	1.5E-03

Appendix A. Radionuclides and Chemicals Measured in Water

Analyte code	Chemical	Number of samples	Concentration ($\mu\text{g L}^{-1}$)	
			Mean	Maximum
57117-31-4	Pentachlorodibenzofuran[2,3,4,7,8-]	1	1.8E-06	1.8E-06
30402-15-4	Pentachlorodibenzofurans (Totals)	1	1.9E-06	1.9E-06
87-86-5	Pentachlorophenol	85	1.9E+02	4.8E+03
ClO ₄	Perchlorate	132	2.3E+01	2.8E+02
85-01-8	Phenanthrene	86	3.7E+01	9.6E+02
108-95-2	Phenol	85	3.7E+01	9.6E+02
103-65-1	Propylbenzene[1-]	10	5.0E+00	5.0E+00
129-00-0	Pyrene	85	3.7E+01	9.6E+02
110-86-1	Pyridine	65	4.5E+01	9.6E+02
121-82-4	RDX (hexahydro-1,3,5-trinitro-1,3,5-triazine)	80	3.5E-01	8.4E-01
Se	Selenium	208	4.9E+00	5.7E+01
Ag	Silver	239	3.1E+00	1.7E+02
Sr	Strontium	225	4.8E+02	6.9E+03
100-42-5	Styrene	42	5.0E+00	5.0E+00
41903-57-5	Tetrachlorodibenzodioxins (Total)	1	1.0E-06	1.0E-06
55722-27-5	Tetrachlorodibenzofurans (Totals)	1	1.1E-06	1.1E-06
630-20-6	Tetrachloroethane[1,1,1,2-]	10	5.0E+00	5.0E+00
79-34-5	Tetrachloroethane[1,1,2,2-]	89	2.5E+00	5.0E+00
127-18-4	Tetrachloroethylene	89	2.6E+00	5.0E+00
479-45-8	Tetryl	80	7.8E-01	1.8E+01
Tl	Thallium	260	2.1E+00	4.8E+01
Sn	Tin	222	2.2E+01	5.6E+02
Ti	Titanium	214	3.3E+02	3.0E+03
108-88-3	Toluene	89	2.1E+00	5.0E+00
8001-35-2	Toxaphene (Technical Grade)	6	5.5E+00	6.8E+00
76-13-1	Trichloro-1,2,2-trifluoroethane[1,1,2-]	10	5.0E+00	5.0E+00
87-61-6	Trichlorobenzene[1,2,3-]	10	5.0E+00	5.0E+00
71-55-6	Trichloroethane[1,1,1-]	89	2.4E+00	5.0E+00
79-00-5	Trichloroethane[1,1,2-]	89	2.5E+00	5.0E+00
79-01-6	Trichloroethylene	89	2.4E+00	5.0E+00
75-69-4	Trichlorofluoromethane	89	2.4E+00	5.0E+00
96-18-4	Trichloropropane[1,2,3-]	10	5.0E+00	5.0E+00
95-63-6	Trimethylbenzene[1,2,4-]	10	5.0E+00	5.0E+00
108-67-8	Trimethylbenzene[1,3,5-]	10	5.0E+00	5.0E+00
U	Uranium	163	6.1E+00	1.5E+02
V	Vanadium	236	4.1E+01	6.5E+02
75-01-4	Vinyl chloride	89	4.8E+00	1.0E+01
1330-20-7	Xylene (Total)	42	5.0E+00	5.0E+00
95-47-6	Xylene[1,2-]	10	5.0E+00	5.0E+00
1330-20-7	Xylene[1,3-]+Xylene[1,4-]	10	5.0E+00	5.0E+00
Zn	Zinc	239	2.0E+02	3.6E+03

^a For our screening assessment, we used the highest measured concentration in surface water, storm water, and ground water samples to ensure a conservative approach. These data include both filtered and unfiltered samples. For our risk analysis, we used the surface water and storm water samples.

^b Environmental Safety and Health (ESH).

Table A-2b. Chemicals Measured in Water Samples^a After the Fire by ER^b

Analyte code	Chemical	Number of samples	Concentration ($\mu\text{g L}^{-1}$)	
			Mean	Maximum
83-32-9	Acenaphthene	15	1.1E+01	1.3E+01
208-96-8	Acenaphthylene	15	1.1E+01	1.3E+01
67-64-1	Acetone	7	2.3E+01	4.1E+01
309-00-2	Aldrin	20	5.4E-02	6.8E-02
AL	Aluminum	206	8.7E+03	6.1E+05
19406-51-0	Amino-2,6-dinitrotoluene[4-]	18	4.1E-01	5.0E-01
35572-78-2	Amino-4,6-dinitrotoluene[2-]	15	4.2E-01	5.0E-01
62-53-3	Aniline	15	1.7E+01	2.5E+01
120-12-7	Anthracene	15	1.1E+01	1.3E+01
SB	Antimony	206	2.1E+00	1.1E+01
12674-11-2	Aroclor-1016	20	1.1E+00	1.4E+00
11104-28-2	Aroclor-1221	20	2.1E+00	2.7E+00
11141-16-5	Aroclor-1232	20	1.1E+00	1.4E+00
53469-21-9	Aroclor-1242	20	1.1E+00	1.4E+00
12672-29-6	Aroclor-1248	20	1.1E+00	1.4E+00
11097-69-1	Aroclor-1254	20	1.1E+00	1.4E+00
11096-82-5	Aroclor-1260	20	1.1E+00	1.4E+00
AS	Arsenic	206	4.8E+00	1.0E+02
103-33-3	Azobenzene	15	1.7E+01	2.5E+01
BA	Barium	206	1.4E+02	3.7E+03
71-43-2	Benzene	7	5.0E+00	5.0E+00
92-87-5	Benzidine	7	1.1E+01	1.3E+01
56-55-3	Benzo(a)anthracene	15	1.1E+01	1.3E+01
50-32-8	Benzo(a)pyrene	15	1.1E+01	1.3E+01
205-99-2	Benzo(b)fluoranthene	15	1.1E+01	1.3E+01
191-24-2	Benzo(g,h,i)perylene	15	1.1E+01	1.3E+01
207-08-9	Benzo(k)fluoranthene	15	1.1E+01	1.3E+01
65-85-0	Benzoic Acid	14	4.3E+01	6.4E+01
100-51-6	Benzyl Alcohol	15	1.7E+01	2.5E+01
BE	Beryllium	206	6.4E-01	3.4E+01
319-84-6	BHC[alpha-]	20	5.4E-02	6.8E-02
319-85-7	BHC[beta-]	20	5.4E-02	6.8E-02
319-86-8	BHC[delta-]	20	5.4E-02	6.8E-02
58-89-9	BHC[gamma-]	20	5.4E-02	6.8E-02
111-44-4	Bis(2-chloroethyl)ether	15	1.1E+01	1.3E+01
117-81-7	Bis(2-ethylhexyl)phthalate	15	5.9E+00	1.3E+01
B	Boron	36	9.8E+01	4.0E+02
108-86-1	Bromobenzene	7	5.0E+00	5.0E+00
74-97-5	Bromochloromethane	7	5.0E+00	5.0E+00
75-27-4	Bromodichloromethane	7	5.0E+00	5.0E+00
75-25-2	Bromoform	7	5.0E+00	5.0E+00
74-83-9	Bromomethane	7	1.0E+01	1.0E+01
101-55-3	Bromophenyl-phenylether[4-]	15	1.1E+01	1.3E+01
78-93-3	Butanone[2-]	7	1.8E+01	2.0E+01
104-51-8	Butylbenzene[n-]	7	5.0E+00	5.0E+00
98-06-6	Butylbenzene[tert-]	7	5.0E+00	5.0E+00
135-98-8	Butylbenzene[sec-]	7	5.0E+00	5.0E+00

Appendix A. Radionuclides and Chemicals Measured in Water

Analyte code	Chemical	Number of samples	Concentration ($\mu\text{g L}^{-1}$)	
			Mean	Maximum
85-68-7	Butylbenzylphthalate	15	1.1E+01	1.3E+01
CD	Cadmium	206	2.1E-01	1.8E+00
86-74-8	Carbazole	8	1.1E+01	1.3E+01
75-15-0	Carbon Disulfide	7	4.4E+00	5.0E+00
56-23-5	Carbon Tetrachloride	7	5.0E+00	5.0E+00
5103-71-9	Chlordane[alpha-]	20	5.4E-02	6.8E-02
5103-74-2	Chlordane[gamma-]	20	5.4E-02	6.8E-02
59-50-7	Chloro-3-methylphenol[4-]	14	1.7E+01	2.5E+01
106-47-8	Chloroaniline[4-]	15	1.7E+01	2.5E+01
108-90-7	Chlorobenzene	7	5.0E+00	5.0E+00
124-48-1	Chlorodibromomethane	7	5.0E+00	5.0E+00
75-00-3	Chloroethane	7	1.0E+01	1.0E+01
67-66-3	Chloroform	7	5.0E+00	5.0E+00
74-87-3	Chloromethane	7	7.4E+00	1.0E+01
91-58-7	Chloronaphthalene[2-]	15	1.1E+01	1.3E+01
95-57-8	Chlorophenol[2-]	14	1.1E+01	1.3E+01
7005-72-3	Chlorophenyl-phenyl[4-] Ether	15	1.1E+01	1.3E+01
95-49-8	Chlorotoluene[2-]	7	5.0E+00	5.0E+00
106-43-4	Chlorotoluene[4-]	7	5.0E+00	5.0E+00
CR	Chromium, Total	206	6.1E+00	3.2E+02
218-01-9	Chrysene	15	1.1E+01	1.3E+01
CO	Cobalt	206	3.1E+00	1.1E+02
CU	Copper	206	6.6E+00	2.8E+02
CN(-1)A	Cyanide, Amenable to chlorination	6	1.0E+01	1.0E+01
CN(-1)	Cyanide, Total	31	5.1E+00	3.2E+01
72-54-8	DDD[4,4'-]	20	1.1E-01	1.4E-01
72-55-9	DDE[4,4'-]	20	1.1E-01	1.4E-01
50-29-3	DDT[4,4'-]	20	1.1E-01	1.4E-01
53-70-3	Dibenz(a,h)anthracene	15	1.1E+01	1.3E+01
132-64-9	Dibenzofuran	15	1.1E+01	1.3E+01
96-12-8	Dibromo-3-chloropropane[1,2-]	7	1.0E+01	1.0E+01
74-95-3	Dibromomethane	7	5.0E+00	5.0E+00
95-50-1	Dichlorobenzene[1,2-]	22	9.0E+00	1.3E+01
541-73-1	Dichlorobenzene[1,3-]	22	9.0E+00	1.3E+01
106-46-7	Dichlorobenzene[1,4-]	22	9.0E+00	1.3E+01
91-94-1	Dichlorobenzidine[3,3'-]	15	1.7E+01	2.5E+01
75-71-8	Dichlorodifluoromethane	7	1.0E+01	1.0E+01
75-34-3	Dichloroethane[1,1-]	7	5.0E+00	5.0E+00
107-06-2	Dichloroethane[1,2-]	7	5.0E+00	5.0E+00
75-35-4	Dichloroethene[1,1-]	7	5.0E+00	5.0E+00
156-59-2	Dichloroethene[cis-1,2-]	7	5.0E+00	5.0E+00
156-60-5	Dichloroethene[trans-1,2-]	7	5.0E+00	5.0E+00
120-83-2	Dichlorophenol[2,4-]	14	1.1E+01	1.3E+01
78-87-5	Dichloropropane[1,2-]	7	5.0E+00	5.0E+00
142-28-9	Dichloropropane[1,3-]	7	5.0E+00	5.0E+00
563-58-6	Dichloropropene[1,1-]	7	5.0E+00	5.0E+00
594-20-7	Dichloropropane[2,2-]	7	5.0E+00	5.0E+00

Analysis of Exposure and Risks to the Public from Radionuclides and
Chemicals Released by the Cerro Grande Fire at Los Alamos

Analyte code	Chemical	Number of samples	Concentration ($\mu\text{g L}^{-1}$)	
			Mean	Maximum
10061-01-5	Dichloropropene[cis-1,3-]	7	5.0E+00	5.0E+00
10061-02-6	Dichloropropene[trans-1,3-]	7	5.0E+00	5.0E+00
60-57-1	Dieldrin	20	1.1E-01	1.4E-01
84-66-2	Diethylphthalate	15	1.1E+01	1.3E+01
131-11-3	Dimethyl Phthalate	15	1.1E+01	1.3E+01
105-67-9	Dimethylphenol[2,4-]	14	1.1E+01	1.3E+01
84-74-2	Di-n-butylphthalate	15	7.7E+00	1.3E+01
534-52-1	Dinitro-2-methylphenol[4,6-]	14	4.3E+01	6.4E+01
99-65-0	Dinitrobenzene[1,3-]	18	3.8E-01	5.0E-01
51-28-5	Dinitrophenol[2,4-]	14	4.3E+01	6.4E+01
121-14-2	Dinitrotoluene[2,4-]	33	5.1E+00	1.3E+01
606-20-2	Dinitrotoluene[2,6-]	33	5.1E+00	1.3E+01
117-84-0	Di-n-octylphthalate	15	1.1E+01	1.3E+01
959-98-8	Endosulfan I	20	5.4E-02	6.8E-02
33213-65-9	Endosulfan II	20	1.1E-01	1.4E-01
1031-07-8	Endosulfan Sulfate	20	1.1E-01	1.4E-01
72-20-8	Endrin	20	1.1E-01	1.4E-01
7421-93-4	Endrin Aldehyde	20	1.1E-01	1.4E-01
53494-70-5	Endrin Ketone	20	1.1E-01	1.4E-01
100-41-4	Ethylbenzene	7	5.0E+00	5.0E+00
206-44-0	Fluoranthene	15	1.1E+01	1.3E+01
86-73-7	Fluorene	15	1.1E+01	1.3E+01
F(-1)	Fluoride	28	4.7E+02	1.4E+03
76-44-8	Heptachlor	20	5.4E-02	6.8E-02
1024-57-3	Heptachlor Epoxide	20	5.4E-02	6.8E-02
35822-46-9	Heptachlorodibenzodioxin[1,2,3,4,6,7,8-]	6	1.0E-05	2.4E-05
37871-00-4	Heptachlorodibenzodioxins (Total)	6	2.0E-05	5.2E-05
67562-39-4	Heptachlorodibenzofuran[1,2,3,4,6,7,8-]	6	3.0E-06	9.0E-06
55673-89-7	Heptachlorodibenzofuran[1,2,3,4,7,8,9-]	6	3.0E-06	4.8E-06
38998-75-3	Heptachlorodibenzofurans (Total)	6	5.0E-06	1.9E-05
118-74-1	Hexachlorobenzene	15	1.1E+01	1.3E+01
87-68-3	Hexachlorobutadiene	22	9.0E+00	1.3E+01
77-47-4	Hexachlorocyclopentadiene	15	1.1E+01	1.3E+01
39227-28-6	Hexachlorodibenzodioxin[1,2,3,4,7,8-]	6	3.0E-06	4.0E-06
57653-85-7	Hexachlorodibenzodioxin[1,2,3,6,7,8-]	6	3.0E-06	4.6E-06
19408-74-3	Hexachlorodibenzodioxin[1,2,3,7,8,9-]	6	3.0E-06	4.0E-06
34465-46-8	Hexachlorodibenzodioxins (Total)	6	3.0E-06	4.2E-06
70648-26-9	Hexachlorodibenzofuran[1,2,3,4,7,8-]	6	2.0E-06	2.8E-06
57117-44-9	Hexachlorodibenzofuran[1,2,3,6,7,8-]	6	2.0E-06	2.8E-06
72918-21-9	Hexachlorodibenzofuran[1,2,3,7,8,9-]	6	3.0E-06	5.1E-06
60851-34-5	Hexachlorodibenzofuran[2,3,4,6,7,8-]	6	2.0E-06	3.3E-06
55684-94-1	Hexachlorodibenzofurans (Total)	6	2.0E-06	5.2E-06
67-72-1	Hexachloroethane	15	1.1E+01	1.3E+01
591-78-6	Hexanone[2-]	7	2.0E+01	2.0E+01
74-88-4	Iodomethane	7	5.0E+00	5.0E+00
78-59-1	Isophorone	15	1.1E+01	1.3E+01
2691-41-0	HMX (octahydro-1,3,5,7-tetranitro-1,3,5,7-tetrazone)	18	5.1E+00	1.3E+01

Appendix A. Radionuclides and Chemicals Measured in Water

Analyte code	Chemical	Number of samples	Concentration ($\mu\text{g L}^{-1}$)	
			Mean	Maximum
193-39-5	Indeno(1,2,3-cd)pyrene	15	1.1E+01	1.3E+01
98-82-8	Isopropylbenzene	7	5.0E+00	5.0E+00
99-87-6	Isopropyltoluene[4-]	7	5.0E+00	5.0E+00
Pb	Lead	206	6.4E+00	3.1E+02
Mn	Manganese	206	6.2E+02	8.2E+03
Hg	Mercury	206	3.9E-02	7.2E-01
72-43-5	Methoxychlor[4,4'-]	20	5.4E-01	6.8E-01
108-10-1	Methyl-2-pentanone[4-]	7	2.0E+01	2.0E+01
75-09-2	Methylene Chloride	7	4.1E+00	5.0E+00
91-57-6	Methylnaphthalene[2-]	15	1.1E+01	1.3E+01
95-48-7	Methylphenol[2-]	14	1.1E+01	1.3E+01
106-44-5	Methylphenol[4-]	14	1.1E+01	1.3E+01
91-20-3	Naphthalene	22	9.0E+00	1.3E+01
Ni	Nickel	206	6.7E+00	2.1E+02
88-74-4	Nitroaniline[2-]	15	4.2E+01	6.4E+01
99-09-2	Nitroaniline[3-]	15	4.2E+01	6.4E+01
100-01-6	Nitroaniline[4-]	15	1.7E+01	2.5E+01
98-95-3	Nitrobenzene	33	8.1E+00	1.3E+01
NO ₂ -N/NO ₃ -N	Nitrogen, Nitrate + Nitrite (Expressed as N)	57	2.6E+03	1.8E+04
53-63-0	Nitroglycerin	14	1.2E+00	1.6E+00
88-75-5	Nitrophenol[2-]	14	1.1E+01	1.3E+01
100-02-7	Nitrophenol[4-]	14	4.3E+01	6.4E+01
62-75-9	Nitrosodimethylamine[N-]	15	1.1E+01	1.3E+01
621-64-7	Nitroso-di-n-propylamine[N-]	15	1.1E+01	1.3E+01
86-30-6	Nitrosodiphenylamine[N-]	15	1.1E+01	1.3E+01
88-72-2	Nitrotoluene[2-]	18	5.2E-01	1.0E+00
99-08-1	Nitrotoluene[3-]	18	6.0E+00	1.0E+01
99-99-0	Nitrotoluene[4-]	18	6.2E+00	1.0E+01
3268-87-9	Octachlorodibenzodioxin[1,2,3,4,6,7,8,9-]	6	6.0E-05	2.2E-04
39001-02-0	Octachlorodibenzofuran[1,2,3,4,6,7,8,9-]	6	1.0E-05	1.8E-05
108-60-1	Oxybis(1-chloropropane)[2,2'-]	15	1.1E+01	1.3E+01
40321-76-4	Pentachlorodibenzodioxin[1,2,3,7,8-]	6	2.0E-06	2.3E-06
36088-22-9	Pentachlorodibenzodioxins (Total)	6	2.0E-06	2.3E-06
57117-41-6	Pentachlorodibenzofuran[1,2,3,7,8-]	6	1.0E-06	2.3E-06
57117-31-4	Pentachlorodibenzofuran[2,3,4,7,8-]	6	1.0E-06	2.4E-06
30402-15-5	Pentachlorodibenzofurans (Totals)	6	2.0E-06	3.4E-06
87-86-5	Pentachlorophenol	14	4.3E+01	6.4E+01
ClO ₄ (-1)	Perchlorate	84	1.4E+01	2.8E+02
78-11-5	PETN	14	4.0E+00	5.0E+00
85-01-8	Phenanthrene	15	1.1E+01	1.3E+01
108-95-2	Phenol	14	1.1E+01	1.3E+01
103-65-1	Propylbenzene[1-]	7	5.0E+00	5.0E+00
129-00-0	Pyrene	15	1.1E+01	1.3E+01
110-86-1	Pyridine	15	1.1E+01	1.3E+01
121-82-4	RDX (hexahydro-1,3,5-trinitro-1,3,5-triazine)	18	9.1E-01	1.3E+00
Ag	Silver	206	6.1E-01	2.9E+00
Na	Sodium	206	3.5E+04	8.5E+04

Analysis of Exposure and Risks to the Public from Radionuclides and
Chemicals Released by the Cerro Grande Fire at Los Alamos

Analyte code	Chemical	Number of samples	Concentration ($\mu\text{g L}^{-1}$)	
			Mean	Maximum
Se	Selenium	206	2.3E+00	5.1E+00
100-42-5	Styrene	7	5.0E+00	5.0E+00
1746-01-6	Tetrachlorodibenzodioxin[2,3,7,8-]	6	1.0E-06	1.9E-06
41903-57-5	Tetrachlorodibenzodioxins (Total)	6	1.0E-06	1.9E-06
51207-31-9	Tetrachlorodibenzofuran[2,3,7,8-]	6	1.0E-06	1.6E-06
55722-27-5	Tetrachlorodibenzofurans (Totals)	6	1.0E-06	1.6E-06
630-20-6	Tetrachloroethane[1,1,1,2-]	7	5.0E+00	5.0E+00
79-34-5	Tetrachloroethane[1,1,2,2-]	7	5.0E+00	5.0E+00
127-18-4	Tetrachloroethene	7	5.0E+00	5.0E+00
479-45-8	Tetryl (N-methyl-N,2,4,6-tetranitroaniline)	18	2.6E+00	4.0E+00
TL	Thallium	206	2.3E+00	4.4E+00
108-88-3	Toluene	7	5.0E+00	5.0E+00
U	Total Uranium by ICPMS	55	1.1E+00	1.3E+01
8001-35-2	Toxaphene (Technical Grade)	20	5.4E+00	6.8E+00
76-13-1	Trichloro-1,2,2-trifluoroethane[1,1,2-]	7	5.0E+00	5.0E+00
87-61-6	Trichlorobenzene[1,2,3-]	7	5.0E+00	5.0E+00
120-82-1	Trichlorobenzene[1,2,4-]	22	9.0E+00	1.3E+01
71-55-6	Trichloroethane[1,1,1-]	7	5.0E+00	5.0E+00
79-00-5	Trichloroethane[1,1,2-]	7	5.0E+00	5.0E+00
79-01-6	Trichloroethene	7	5.0E+00	5.0E+00
75-69-4	Trichlorofluoromethane	7	5.0E+00	5.0E+00
95-95-4	Trichlorophenol[2,4,5-]	14	4.3E+01	6.4E+01
88-06-2	Trichlorophenol[2,4,6-]	14	1.1E+01	1.3E+01
96-18-4	Trichloropropane[1,2,3-]	7	5.0E+00	5.0E+00
95-63-6	Trimethylbenzene[1,2,4-]	7	5.0E+00	5.0E+00
108-67-8	Trimethylbenzene[1,3,5-]	7	5.0E+00	5.0E+00
99-35-4	Trinitrobenzene[1,3,5-]	18	3.8E-01	5.0E-01
118-96-7	Trinitrotoluene[2,4,6-]	18	3.8E-01	5.0E-01
V	Vanadium	206	1.2E+01	5.9E+02
75-01-4	Vinyl Chloride	7	1.0E+01	1.0E+01
1330-20-7	Xylene (Total)	7	5.0E+00	5.0E+00
95-47-6	Xylene[1,2-]	7	5.0E+00	5.0E+00

^a For our screening assessment, we used the measured concentration in surface water, storm water, and ground water samples from both ESH-18 and ER to ensure a cautious or conservative approach. These data include both filtered and unfiltered samples. For our risk analysis, we used the surface and storm water samples only.

^b Environmental Restoration Project (ER).

APPENDIX B

DATA FOR ESTIMATING BURN, FLOW, AND CONTAMINATION FACTORS FOR WATERSHED RANKING

The methods used for ranking the watersheds are in some cases based on subjective decisions made by *RAC*. It is recognized that some factors could be considered related, but we made best judgment decisions about what factors were important to consider and what could be evaluated independently, based on available information, which in many cases is very limited. We believed it important to average across a number of varied possible factors to reduce the amount of bias that could be introduced by relying too heavily on a single factor. We also believed it very important to fully document the calculations and assumptions that went into ranking the watersheds.

Appendix B. Data for Watershed Ranking

Table B-1. Extent of Hydrophobic Soils Following the Fire

LANL watershed	Watershed area (m ²)	Fraction of hydrophobic soil ^a	Hydrophobic area (m ²)	Total hydrophobic soil area factor ^b
Guaje	59,940,275	0.20	12,047,995	0.19
Los Alamos	46,511,555	0.23	10,511,612	0.16
Los Frijoles	50,700,471	0.05	2,332,222	0.04
Mortandad	52,434,967	0.00	0	0.00
Pajarito	33,752,864	0.18	6,143,021	0.10
Pueblo	21,798,112	0.52	11,291,422	0.17
Rendija	24,810,269	0.43	10,618,795	0.16
Water	77,315,836	0.15	11,597,375	0.18

^a From DOE (2000).^b Fraction of hydrophobic soil area within specified canyon; this value is carried over to Table B3.**Table B-2. Extent and Severity of Burn in the Canyons at LANL**

LANL watershed	% of watershed burned ^a	Fraction of total burn area burned	Fraction of watershed burned (high) ^a	Fraction of total burn area burned (high)	Fraction of watershed burned (medium) ^a	Fraction of total burn area burned (medium)	Fraction of watershed burned (low) ^a	Fraction of total burn area burned (low)	Total burn area factor	Fraction of total burn area factor ^b
Guaje	0.44	0.15	0.15	0.15	0.01	0.03	0.29	0.17	0.68	0.17
Los Alamos	0.26	0.07	0.12	0.10	0.01	0.03	0.12	0.06	0.42	0.10
Los Frijoles	0.10	0.03	0.01	0.01	0.01	0.02	0.09	0.05	0.11	0.03
Mortandad	0.17	0.05	0.00	0.00	0.03	0.10	0.14	0.08	0.27	0.07
Pajarito	0.61	0.12	0.15	0.09	0.03	0.06	0.43	0.15	0.53	0.13
Pueblo	0.31	0.04	0.22	0.08	0.04	0.06	0.05	0.01	0.37	0.09
Rendija	0.78	0.11	0.51	0.21	0.06	0.10	0.20	0.05	0.90	0.22
Water	0.34	0.15	0.07	0.09	0.03	0.17	0.24	0.18	0.79	0.20

^a From LANL (2001a, 2001b).^b Total burn area factor includes the % of the burned area that was burned severely, moderately or lightly. To recognize the impact that severely and moderately burned areas would have on the potential increased mobilization of contaminants, we multiplied the severely and moderately burned area percentages by 3 and 2, respectively. This factor is carried over to Table B-3.

Table B-3. Calculation of Final Burn Factor

LANL watershed	Watershed area (m ²)	Total hydrophobic soil area fraction ^a	Total burn area factor ^b	Total burn factor ^c
Guaje	59,940,275	0.19	0.17	0.18
Los Alamos	46,511,555	0.16	0.10	0.13
Los Frijoles	50,700,471	0.04	0.03	0.03
Mortandad	52,434,967	0.00	0.07	0.03
Pajarito	33,752,864	0.10	0.13	0.11
Pueblo	21,798,112	0.17	0.09	0.13
Rendija	24,810,269	0.16	0.22	0.19
Water	77,315,836	0.18	0.20	0.19

^a From Table B-1.^b From Table B-2.^c Total burn factor equals the average of the hydrophobic soils area fraction and the total burn area factor. This factor is reported in Table 3-1.**Table B-4. Flow Characteristics for the Watersheds at LANL**

LANL watersheds	Watershed area ^a (m ²)	Fractional extent of watershed	Flow (cfs) 100-yr storm event ^b	Flow potential ^c	Flow factor ^d
Guaje	59,940,275	0.16	2556	0.13	0.14
Los Alamos	46,511,555	0.13	1701	0.08	0.11
Los Frijoles	50,700,471	0.14	1253	0.06	0.10
Mortandad	52,434,967	0.14	459	0.02	0.08
Pajarito	33,752,864	0.09	1435	0.07	0.08
Pueblo	21,798,112	0.06	866	0.04	0.05
Rendija	24,810,269	0.07	1572	0.08	0.07
Water	77,315,836	0.21	10538	0.51	0.36

^a From DOE 2000.^b Projected flow for 100-yr storm event based on Army Corps of Engineer's Hydrologic Modeling System (HMS) implemented for surface water flow for this project (see Chapter 4).^c Flow potential is the fractional contribution of each watershed to the total projected flow from all watersheds.^d Flow factor is the average of the fractional extent of watershed and the flow potential; this factor is reported in Table 3-1.

Appendix B. Data for Watershed Ranking

Table B-5a. Ranking Based on Average ^{137}Cs and $^{239,240}\text{Pu}$ Concentrations Measured in Sediment Samples Collected by ESH-18 since January 1995 in LANL Watersheds^a

LANL watershed	Analyte	Average concentration in sediment (pCi g^{-1})	Fractional contribution to sum of averages	Number of samples	Beginning date	End date
Guaje	^{137}Cs	0.57	0.12	14	21-Mar-95	27-Jun-00
Los Alamos	^{137}Cs	0.51	0.11	109	21-Mar-95	31-Aug-00
Los Frijoles	^{137}Cs	0.27	0.06	15	13-Sep-95	22-Aug-00
Mortandad	^{137}Cs	1.60	0.35	217	21-Mar-95	25-Sep-00
Pajarito	^{137}Cs	0.28	0.06	66	21-Mar-95	11-Oct-00
Pueblo	^{137}Cs	1.03	0.23	33	02-May-95	25-Jul-00
Water	^{137}Cs	0.30	0.07	171	21-Mar-95	27-Sep-00
Guaje	$^{39,240}\text{Pu}$	0.02	0.00	12	21-Mar-95	27-Jun-00
Los Alamos	$^{39,240}\text{Pu}$	0.19	0.06	110	21-Mar-95	31-Aug-00
Los Frijoles	$^{39,240}\text{Pu}$	0.01	0.00	18	13-Sep-95	22-Aug-00
Mortandad	$^{39,240}\text{Pu}$	1.17	0.35	224	21-Mar-95	25-Sep-00
Pajarito	$^{39,240}\text{Pu}$	0.04	0.01	74	21-Mar-95	11-Oct-00
Pueblo	$^{39,240}\text{Pu}$	1.80	0.54	38	02-May-95	25-Jul-00
Water	$^{39,240}\text{Pu}$	0.08	0.02	174	21-Mar-95	27-Sep-00

^a See Chapter 1 for a discussion of data received.**Table B5b. Measure of Total Level of Contaminants Measured by ESH-18 in each Watershed**

LANL watershed	Average fractional contribution value from Table B-5a ^a
Guaje	0.06
Los Alamos	0.08
Los Frijoles	0.03
Mortandad	0.35
Pajarito	0.04
Pueblo	0.39
Water	0.04

^a Average fractional contribution is the average of the fractional contribution to sum of averages for the ^{137}Cs and $^{239,240}\text{Pu}$ sediment concentrations; these values are carried to Table B-8.

**Table B-6a. Average ^{137}Cs and $^{239,240}\text{Pu}$ Concentrations Measured in Post-flood Sediment
Samples Collected in LANL Watersheds By Environmental Restoration Project^a**

LANL watershed	Analyte	Average concentration in sediment (pCi g^{-1})	Number of samples	Fractional contribution to sum of averages
Guaje	^{137}Cs	3.13	4	0.16
Los Alamos	^{137}Cs	3.70	6	0.19
Pueblo	^{137}Cs	8.26	1	0.44
Mortandad	^{137}Cs	0.60	5	0.03
Pajarito	^{137}Cs	0.76	36	0.04
Rendija	^{137}Cs	1.61	5	0.08
Water	^{137}Cs	0.92	25	0.05
Guaje	$^{39,240}\text{Pu}$	0.23	2	0.12
Los Alamos	$^{39,240}\text{Pu}$	1.07	4	0.55
Pueblo	$^{39,240}\text{Pu}$	0.34	1	0.18
Mortandad	$^{39,240}\text{Pu}$	0.07	5	0.04
Pajarito	$^{39,240}\text{Pu}$	0.10	5	0.05
Rendija	$^{39,240}\text{Pu}$	0.08	3	0.04
Water	$^{39,240}\text{Pu}$	0.05	9	0.03

^a See Chapter 1 for a discussion of data received.**Table B-6b. Measure of Total Level of Contaminants Measured by
Environmental Restoration Project in each Watershed**

LANL watershed	Average fractional contribution from Table B6a ^a
Guaje	0.14
Los Alamos	0.37
Mortandad	0.03
Pajarito	0.04
Pueblo	0.31
Rendija	0.06
Water	0.04

^a Average fractional contribution is the average of the fractional contribution to sum of averages for the ^{137}Cs and $^{239,240}\text{Pu}$ sediment concentrations; these values are carried to Table B8.

Appendix B. Data for Watershed Ranking

Table B-7. Ranking Based on Potential Release Sites with Reported Erosion Matrix Scores^a

LANL watershed	Burned			Unburned			Combined ranking score ^b	Fractional contribution to sum of ranking scores ^c
	Average erosion matrix score	Number of PRSs with score	Ranking score	Average erosion matrix score	Number of PRSs with score	Ranking score		
Guaje	na	0	0.00	Na	0	0.00	0.00	0.00
Los Alamos	na	0	0.00	33.00	174	7.40	3.70	0.09
Los Frijoles	na	0	0.00	Na	0	0.00	0.00	0.00
Mortandad	43.84	67	10.42	30.23	202	7.87	14.35	0.34
Pajarito	21.42	70	5.32	25.17	75	2.43	6.53	0.15
Pueblo	na	0	0.00	27.87	21	0.75	0.38	0.01
Rendija	20.17	3	0.21	30.07	3	0.12	0.27	0.01
Water	26.49	142	13.34	19.40	301	7.53	17.10	0.40

^a LANL developed the data and transmitted them to us as an Excel file via NMED. We used this list in combination with the list of burned Potential Release Sites (PRSs) we received from LANL in September 2001 (as an Excel file transmitted via email) to determine which PRSs fell into the burned/unburned categories, the number of PRSs within a given watershed, and the potential for erosion at those PRSs.

^b We calculated the combined ranking score by averaging the ranking scores from the PRSs within the burned and unburned areas in each watershed, with the burned ranking score given double weight to account for assumed greater potential impact at burned PRSs.

^c We carried over the fractional contribution to Table B-8.

Table B-8. Summary of Input Values to Total Contamination Factor

LANL watershed	ESH-18 data contribution ^a	ER data contribution ^b	PRS data contribution ^c	Average input values ^d	Total contamination Factor ^e
Guaje	0.06	0.14	0.00	0.06	0.07
Los Alamos	0.08	0.37	0.09	0.17	0.18
Los Frijoles	0.03	nd	0.00	0.02	0.02
Mortandad	0.35	0.03	0.34	0.24	0.24
Pajarito	0.04	0.04	0.15	0.08	0.08
Pueblo	0.39	0.31	0.01	0.22	0.23
Rendija	nd	0.06	0.01	0.03	0.03
Water	0.04	0.04	0.40	0.16	0.16

^a From Table B-5b.

^b From Table B-6b.

^c From Table B-7.

^d This column represents the average value of the ESH-18 data, ER data, and PRS data contributions to the contamination factor.

^e Fractional contribution of each watershed to sum of averages; this factor is reported in Table 3-1.

APPENDIX C

SCREENING CALCULATIONS FOR RADIONUCLIDES AND CHEMICALS IN SURFACE WATERS AT LANL

Table C-1. Stage I Screening of Radionuclides Measured in Water at the LANL in 2000^a

Radionuclide	Number of samples	Maximum	Morbidity risk	Lifetime Intake		Risk Index
		activity (pCi/L)	coefficient (Bq-l)	(pCi)	(Bq)	
Ac-228	225	1.9E+02	5.38E-11	5.71E+06	2.11E+05	1.1E-05
Ag-110m	37	3.0E+00	2.67E-10	9.10E+04	3.37E+03	9.0E-07
Am-241	116	6.1E+01	2.81E-09	1.86E+06	6.89E+04	1.9E-04
Ba-133	138	2.9E+00	1.84E-10	8.97E+04	3.32E+03	6.1E-07
Ba-140	80	2.0E+02	4.03E-10	6.11E+06	2.26E+05	9.1E-05
Be-7	182	2.6E+02	2.34E-12	7.78E+06	2.88E+05	6.7E-07
Bi-211	102	3.1E+01	1.92E-11	9.55E+05	3.53E+04	6.8E-07
Bi-212	225	1.2E+02	1.92E-11	3.75E+06	1.39E+05	2.7E-06
Bi-214	221	1.3E+02	5.19E-12	3.90E+06	1.44E+05	7.5E-07
Cd-109	145	4.5E+02	1.30E-10	1.37E+07	5.08E+05	6.6E-05
Ce-139	181	2.9E+00	3.65E-11	8.97E+04	3.32E+03	1.2E-07
Ce-141	138	2.0E+01	1.25E-10	6.14E+05	2.27E+04	2.8E-06
Ce-144	181	2.1E+01	9.52E-10	6.35E+05	2.35E+04	2.2E-05
Co-56	37	2.1E+00	2.74E-10	6.41E+04	2.37E+03	6.5E-07
Co-57	224	8.2E+00	2.81E-11	2.50E+05	9.26E+03	2.6E-07
Co-58	37	1.4E+00	7.97E-11	4.18E+04	1.55E+03	1.2E-07
Co-60	226	5.7E+00	4.25E-10	1.72E+05	6.38E+03	2.7E-06
Cr-51	138	4.2E+01	5.01E-12	1.29E+06	4.78E+04	2.4E-07
Cs-134	82	1.1E+01	1.14E-09	3.24E+05	1.20E+04	1.4E-05
Cs-136	37	6.7E+00	2.34E-10	2.06E+05	7.61E+03	1.8E-06
Cs-137	226	5.1E+02	8.22E-10	1.56E+07	5.77E+05	4.7E-04
Eu-152	183	2.9E+01	1.64E-10	8.91E+05	3.30E+04	5.4E-06
Eu-154	138	1.1E+01	2.79E-10	3.39E+05	1.25E+04	3.5E-06
Eu-155	37	1.3E+01	5.13E-11	3.97E+05	1.47E+04	7.5E-07
H-3	30	5.3E+04	1.37E-12	1.61E+09	5.94E+07	8.1E-05
Hg-203	181	5.2E+00	1.54E-10	1.60E+05	5.90E+03	9.1E-07
Ir-192	37	1.6E+00	1.99E-10	4.76E+04	1.76E+03	3.5E-07
K-40	224	2.1E+03	6.68E-10	6.35E+07	2.35E+06	1.6E-03
La-140	44	2.0E+00	2.96E-10	6.00E+04	2.22E+03	6.6E-07
Mn-54	224	6.0E+00	6.16E-11	1.83E+05	6.78E+03	4.2E-07
Na-22	226	2.6E+01	2.60E-10	8.00E+05	2.96E+04	7.7E-06
Nb-94	37	1.6E+00	2.10E-10	5.01E+04	1.85E+03	3.9E-07
Nb-95	138	5.7E+00	6.60E-11	1.74E+05	6.45E+03	4.3E-07
Nd-147	37	3.8E+01	1.88E-10	1.16E+06	4.28E+04	8.0E-06
Np-237	145	1.6E+02	1.67E-09	4.77E+06	1.77E+05	2.9E-04
Np-239	138	1.2E+01	1.39E-10	3.57E+05	1.32E+04	1.8E-06
Pa-231	145	1.3E+02	4.67E-09	4.03E+06	1.49E+05	7.0E-04
Pa-233	145	4.7E+01	1.50E-10	1.44E+06	5.32E+04	8.0E-06
Pa-234m	145	7.1E+02	6.93E-11	2.17E+07	8.02E+05	5.6E-05
Pb-210	91	9.6E+02	2.38E-08	2.94E+07	1.09E+06	2.6E-02
Pb-211	145	1.3E+02	1.11E-11	4.06E+06	1.50E+05	1.7E-06
Pb-212	223	1.6E+02	6.76E-10	4.73E+06	1.75E+05	1.2E-04
Pb-214	223	1.4E+02	9.31E-12	4.27E+06	1.58E+05	1.5E-06
Pm-144	37	2.1E+00	9.02E-11	6.53E+04	2.42E+03	2.2E-07
Pm-146	37	2.2E+00	1.51E-11	6.56E+04	2.43E+03	3.7E-08
Po-210	55	6.0E+02	1.02E-08	1.83E+07	6.78E+05	6.9E-03
Pu-238	225	7.6E+00	3.55E-09	2.32E+05	8.59E+03	3.1E-05
Pu-239	133	5.7E+01	3.64E-09	1.75E+06	6.48E+04	2.4E-04

Analysis of Exposure and Risks to the Public from Radionuclides and
Chemicals Released by the Cerro Grande Fire at Los Alamos

Radionuclide	Number samples	Maximum activity (pCi/L)	Morbidity risk coefficient (Bq-1)	Lifetime Intake		Risk Index
				(pCi)	(Bq)	
Ra-223	145	7.1E+01	6.44E-09	2.16E+06	8.01E+04	5.2E-04
Ra-224	102	9.5E+01	4.50E-09	2.88E+06	1.07E+05	4.8E-04
Ra-226	203	4.7E+02	1.04E-08	1.44E+07	5.34E+05	5.6E-03
Ra-228	198	1.5E+02	2.81E-08	4.61E+06	1.71E+05	4.8E-03
Rh-106	102	2.6E+01	1.48E-11	7.84E+05	2.90E+04	4.3E-07
Ru-103	102	2.5E+00	1.04E-10	7.48E+04	2.77E+03	2.9E-07
Ru-106	81	3.3E+01	1.14E-09	9.92E+05	3.67E+04	4.2E-05
Sb-124	138	2.8E+00	3.48E-10	8.67E+04	3.21E+03	1.1E-06
Sb-125	138	6.1E+00	1.18E-10	1.86E+05	6.88E+03	8.1E-07
Se-75	145	4.0E+00	2.20E-10	1.22E+05	4.52E+03	9.9E-07
Sr-85	145	1.7E+01	6.12E-11	5.19E+05	1.92E+04	1.2E-06
Sr-90	315	8.1E+01	1.51E-09	2.47E+06	9.12E+04	1.4E-04
Th-227	145	3.5E+01	1.28E-09	1.08E+06	3.99E+04	5.1E-05
Th-228	124	2.2E+02	2.90E-09	6.81E+06	2.52E+05	7.3E-04
Th-230	161	1.3E+02	2.46E-09	4.06E+06	1.50E+05	3.7E-04
Th-231	102	1.7E+01	5.96E-11	5.25E+05	1.94E+04	1.2E-06
Th-232	124	1.2E+02	2.73E-09	3.51E+06	1.30E+05	3.5E-04
Th-234	181	1.2E+03	6.25E-10	3.79E+07	1.40E+06	8.8E-04
U-234	238	1.4E+02	1.91E-09	4.15E+06	1.54E+05	2.9E-04
U-235,236	461	6.0E+01	1.88E-09	1.83E+06	6.78E+04	1.3E-04
U-238	376	2.2E+02	1.73E-09	6.75E+06	2.50E+05	4.3E-04
Y-88	181	7.5E+00	1.13E-10	2.29E+05	8.46E+03	9.6E-07
Zn-65	180	1.3E+01	3.15E-10	3.93E+05	1.45E+04	4.6E-06
Zr-95	138	7.4E+00	1.24E-10	2.25E+05	8.32E+03	1.0E-06

^a The Stage 1 screening was based on the maximum concentration of each radionuclide measured in storm water, surface water, or groundwater in 2000 following the fire. Those radionuclides that are shaded met the screening criterion of 1×10^{-5}

Table C-2. Stage I Screening of Chemicals Measured in Water at the LANL in 2000

Analyte code	Analyte ^a	Maximum concentration (ug/L)	Unit risk (per ug/L)	Risk Index ^b	RfD (mg/kg/d)	Daily Intake (mg/kg)	Daily intake/body wt (mg/kg/d)	Hazard quotient ^c
35822-46-9	1,2,3,4,6,7,8-HpCDD	2.4E-03	4.3E-02	1.0E-04				
67562-39-4	1,2,3,4,6,7,8-HpCDF	2.3E-03	4.3E-02	9.9E-05				
39227-28-6	1,2,3,4,7,8-HxCDD	7.1E-03	1.8E-01	1.3E-03				
70648-26-9	1,2,3,4,7,8-HxCDF	6.6E-03	4.3E-02	2.8E-04				
40321-76-4	1,2,3,7,8-PCDD	6.3E-03	2.3E+00	1.4E-02				
57117-41-6	1,2,3,7,8-PCDF	5.8E-03	2.3E+00	1.3E-02				
120-82-1	1,2,4-Trichlorobenzene	9.6E+02			1.0E-02	1.1E+00	1.5E-02	1.5E+00
95-50-1	1,2-Dichlorobenzene	9.6E+02			9.0E-02	1.1E+00	1.5E-02	1.6E-01
99-35-4	1,3,5-trinitrobenzene	5.7E+00			3.0E-02	6.3E-03	8.8E-05	2.9E-03
541-73-1	1,3-dichlorobenzene	9.6E+02			9.0E-02	1.1E+00	1.5E-02	1.6E-01
99-65-0	1,3-Dinitrobenzene	1.9E+00			1.0E-04	2.1E-03	2.9E-05	2.9E-01
106-46-7	1,4-Dichlorobenzene	9.6E+02	6.8E-07	6.5E-04				
108-60-1	2,2'-oxybis[1-chloropropane]	9.6E+02	2.0E-06	1.9E-03				
58-90-2	2,3,4,6-Tetrachlorophenol	4.8E+03			3.0E-02	5.3E+00	7.4E-02	2.5E+00
1746-01-6	2,3,7,8-TCDD	6.7E-04	4.5E+00	3.0E-03				
51207-31-9	2,3,7,8-TCDF	4.9E-03	4.5E-01	2.2E-03				
95-95-4	2,4,5-Trichlorophenol	9.6E+02			1.0E-01	1.1E+00	1.5E-02	1.5E-01
88-06-2	2,4,6-trichlorophenol	9.6E+02			1.0E-01	1.1E+00	1.5E-02	1.5E-01
120-83-2	2,4-Dichlorophenol	9.6E+02			3.0E-03	1.1E+00	1.5E-02	4.9E+00
105-67-9	2,4-Dimethylphenol	9.6E+02			2.0E-02	1.1E+00	1.5E-02	7.4E-01
51-28-5	2,4-dinitrophenol	4.8E+03			2.0E-03	5.3E+00	7.4E-02	3.7E+01
121-14-2	2,4-Dinitrotoluene	9.6E+02			2.0E-03	1.1E+00	1.5E-02	7.4E+00
606-20-2	2,6-Dinitrotoluene	9.6E+02			2.0E-03	1.1E+00	1.5E-02	7.4E+00
35572-78-2	2-Amino-4,6-dinitrotoluene	1.3E+00	9.0E-07	1.2E-06				
91-58-7	2-Chloronaphthalene	9.6E+02			8.0E-02	1.1E+00	1.5E-02	1.9E-01
95-57-8	2-Chlorophenol	9.6E+02			5.0E-03	1.1E+00	1.5E-02	3.0E+00
91-57-6	2-Methylnaphthalene	9.6E+02			2.0E-02	1.1E+00	1.5E-02	7.4E-01
95-48-7	2-Methylphenol	9.6E+02			5.0E-02	1.1E+00	1.5E-02	3.0E-01
88-74-4	2-Nitroaniline	4.8E+03	1.6E-07	7.7E-04				
88-75-5	2-Nitrophenol	9.6E+02			8.0E-03	1.1E+00	1.5E-02	1.9E+00
88-72-2	2-nitrotoluene	1.4E+00			1.0E-02	1.6E-03	2.2E-05	2.2E-03
91-94-1	3,3'-Dichlorobenzidine	4.8E+03	1.3E-05	6.2E-02				
534-52-1	4,6-Dinitro-2-Methylphenol	4.8E+03			2.0E-03	5.3E+00	7.4E-02	3.7E+01
19406-51-0	4-Amino-2,6-dinitrotoluene	2.8E+00	9.0E-07	2.5E-06				
101-55-3	4-Bromophenyl phenyl ether	9.6E+02			1.0E-01	1.1E+00	1.5E-02	1.5E-01
59-50-7	4-Chloro-3-methylphenol	9.6E+02			5.0E-03	1.1E+00	1.5E-02	3.0E+00
106-47-8	4-chloroaniline	2.4E+03			4.0E-03	2.7E+00	3.7E-02	9.3E+00
7005-72-3	4-Chlorophenyl phenyl ether	9.6E+02	5.5E-08	5.3E-05				
106-44-5	4-Methylphenol	9.6E+02			5.0E-02	1.1E+00	1.5E-02	3.0E-01
100-01-6	4-Nitroaniline	4.8E+03	1.6E-07	7.7E-04				
100-02-7	4-Nitrophenol	4.8E+03			8.0E-03	5.3E+00	7.4E-02	9.3E+00
83-32-9	Acenaphthene	9.6E+02			6.0E-02	1.1E+00	1.5E-02	2.5E-01
208-96-8	Acenaphthylene	9.6E+02			2.0E-02	1.1E+00	1.5E-02	7.4E-01
67-64-1	Acetone	2.3E+01			1.0E-01	2.6E-02	3.6E-04	3.6E-03
309-00-2	Aldrin	6.8E-02	4.9E-04	3.3E-05				
Al	Aluminum	1.0E+06			4.0E-04	1.1E+03	1.5E+01	3.8E+04

Analysis of Exposure and Risks to the Public from Radionuclides and Chemicals Released by the Cerro Grande Fire at Los Alamos

Analyte code	Analyte ^a	Maximum concentration (ug/L)	Unit risk (per ug/L)	Risk Index ^b	RfD (mg/kg/d)	Daily Intake (mg/kg)	Daily intake/body wt (mg/kg/d)	Hazard quotient ^c
19406-51-0	Amino-2,6-dinitrotoluene[4-]	5.0E-01	9.0E-07	4.5E-07				
62-53-3	Aniline	2.4E+03	1.6E-07	3.8E-04				
120-12-7	Anthracene	9.6E+02			3.0E-01	1.1E+00	1.5E-02	4.9E-02
Sb	Antimony	2.8E+02			4.0E-04	3.1E-01	4.3E-03	1.1E+01
12674-11-2	Aroclor-1016	1.5E+00	1.0E-05	1.5E-05				
11104-28-2	Aroclor-1221	3.0E+00	1.0E-05	3.0E-05				
11141-16-5	Aroclor-1232	1.5E+00	1.0E-05	1.5E-05				
53469-21-9	Aroclor-1242	1.5E+00	1.0E-05	1.5E-05				
12672-29-6	Aroclor-1248	1.5E+00	1.0E-05	1.5E-05				
11097-69-1	Aroclor-1254	1.5E+00	1.0E-05	1.5E-05				
11096-82-5	Aroclor-1260	1.5E+00	1.0E-05	1.5E-05				
37324-23-5	Aroclor-1262	9.4E-02	1.0E-05	9.4E-07				
As	Arsenic	1.4E+02	5.0E-05	6.9E-03				
103-33-3	Azobenzene	9.6E+02	3.1E-06	3.0E-03				
Ba	Barium	2.1E+04			7.0E-02	2.3E+01	3.2E-01	4.6E+00
71-43-2	Benzene	5.0E+00	1.6E-03	8.0E-03				
92-87-5	Benzidine	1.3E+01	6.7E-03	8.7E-02				
56-55-3	Benzo(a)anthracene	9.6E+02	2.1E-05	2.0E-02				
50-32-8	Benzo(a)pyrene	9.6E+02	2.1E-04	2.0E-01				
205-99-2	Benzo(b)fluoranthene	1.3E+01	2.1E-05	2.7E-04				
191-24-2	Benzo(g,h,i)perylene	9.6E+02	2.1E-07	2.0E-04				
207-08-9	Benzo(k)fluoranthene	9.6E+02	2.1E-06	2.0E-03				
65-85-0	Benzoic Acid	1.9E+03			4.0E+00	2.1E+00	2.9E-02	7.3E-03
100-51-6	Benzyl Alcohol	9.6E+02			3.0E-01	1.1E+00	1.5E-02	4.9E-02
Be	Beryllium	1.0E+02			2.0E-03	1.1E-01	1.5E-03	7.7E-01
319-84-6	BHC[alpha-]	6.8E-02	5.1E-05	3.5E-06				
319-85-7	BHC[beta-]	6.8E-02	5.1E-05	3.5E-06				
319-86-8	BHC[delta-]	6.8E-02	5.1E-05	3.5E-06				
58-89-9	BHC[gamma-]	6.8E-02	5.1E-05	3.5E-06				
111-44-4	Bis(2-chloroethyl)ether	9.6E+02			2.2E+02	1.1E+00	1.5E-02	6.7E-05
117-81-7	Bis(2-ethylhexyl)phthalate	9.6E+02			2.2E+02	1.1E+00	1.5E-02	6.7E-05
B	Boron	3.2E+05			9.0E-02	3.5E+02	4.9E+00	5.4E+01
108-86-1	Bromobenzene	5.0E+00	1.6E-03	8.0E-03				
74-97-5	Bromochloromethane	5.0E+00	1.8E-06	9.0E-06				
75-27-4	Bromodichloromethane	1.2E+01	1.8E-06	2.2E-05				
75-25-2	Bromoform	5.0E+00	2.3E-07	1.2E-06				
74-83-9	Bromomethane	1.0E+01			1.4E-03	1.1E-02	1.5E-04	1.1E-01
78-93-3	Butanone[2-]	2.0E+01			1.0E-01	2.2E-02	3.1E-04	3.1E-03
104-51-8	Butylbenzene[n-]	5.0E+00	1.6E-06	8.0E-06				
135-98-8	Butylbenzene[sec-]	5.0E+00	1.6E-06	8.0E-06				
98-06-6	Butylbenzene[tert-]	5.0E+00	1.6E-06	8.0E-06				
85-68-7	Butylbenzylphthalate	9.6E+02			2.0E-01	1.1E+00	1.5E-02	7.4E-02
Cd	Cadmium	3.4E+01			5.0E-04	3.8E-02	5.2E-04	1.0E+00
86-74-8	Carbazole	9.6E+02			2.0E-02	1.1E+00	1.5E-02	7.4E-01
75-15-0	Carbon Disulfide	5.0E+00			1.0E-01	5.6E-03	7.7E-05	7.7E-04
56-23-5	Carbon tetrachloride	5.0E+00	3.7E-06	1.9E-05				
5103-71-9	Chlordane[alpha-]	6.8E-02	1.0E-05	6.8E-07				
5103-74-2	Chlordane[gamma-]	6.8E-02	1.0E-05	6.8E-07				

Estimated Risks from Releases to Surface Water
Appendix C. Screening Calculations for Water Monitoring Data

C-7

Analyte code	Analyte ^a	Maximum concentration (ug/L)	Unit risk (per ug/L)	Risk Index ^b	RfD (mg/kg/d)	Daily Intake (mg/kg)	Daily intake/body wt (mg/kg/d)	Hazard quotient ^c
106-47-8	Chloroaniline[4-]	2.5E+01			4.0E-03	2.8E-02	3.9E-04	9.7E-02
108-90-7	Chlorobenzene	5.0E+00			2.0E-02	5.6E-03	7.7E-05	3.9E-03
75-00-3	Chloroethane	1.0E+01			4.0E-01	1.1E-02	1.5E-04	3.9E-04
110-75-8	Chloroethylvinyl ether[2-]	8.5E-01	5.5E-08	4.7E-08				
67-66-3	Chloroform	7.2E+00	1.7E-07	1.2E-06				
74-87-3	Chloromethane	1.0E+01	3.7E-07	3.7E-06				
106-43-4	Chlorotoluene[4-]	5.0E+00			2.0E-02	5.6E-03	7.7E-05	3.9E-03
Cr	Chromium	5.1E+02			3.0E-03	5.7E-01	7.9E-03	2.6E+00
218-01-9	Chrysene	9.6E+02	2.1E-07	2.0E-04				
Co	Cobalt	4.8E+02			6.0E-02	5.3E-01	7.3E-03	1.2E-01
Cu	Copper	6.1E+02			5.0E-03	6.7E-01	9.4E-03	1.9E+00
CN (amen)	Cyanide, Amenable	6.2E-02			2.0E-02	6.9E-05	9.6E-07	4.8E-05
CN(-1)	Cyanide, Total	3.2E+01			2.0E-02	3.6E-02	4.9E-04	2.5E-02
72-54-8	DDD[4,4'-]	1.4E-01	6.9E-06	9.7E-07				
72-55-9	DDE[4,4'-]	1.4E-01	9.7E-06	1.4E-06				
50-29-3	DDT[4,4'-]	1.4E-01	9.7E-06	1.4E-06				
53-70-3	Dibenz(a,h)anthracene	9.6E+02	2.1E-04	2.0E-01				
132-64-9	Dibenzofuran	9.6E+02			4.0E-03	1.1E+00	1.5E-02	3.7E+00
96-12-8	Dibromo-3-Chloropropane[1,2-]	1.0E+01			5.7E-05	1.1E-02	1.5E-04	2.7E+00
124-48-1	Dibromochloromethane	1.2E+01			2.0E-01	1.3E-02	1.9E-04	9.3E-04
74-95-3	Dibromomethane	5.0E+00			1.0E-02	5.6E-03	7.7E-05	7.7E-03
91-94-1	Dichlorobenzidine[3,3'-]	2.5E+01	1.3E-05	3.3E-04				
75-71-8	Dichlorodifluoromethane	1.0E+01			2.0E-01	1.1E-02	1.5E-04	7.7E-04
75-34-3	Dichloroethane[1,1-]	5.0E+00			1.0E-01	5.6E-03	7.7E-05	7.7E-04
107-06-2	Dichloroethane[1,2-]	5.0E+00	2.6E-06	1.3E-05				
540-59-0	Dichloroethene[cis/trans-1,2-]	5.0E+00			9.0E-03	5.6E-03	7.7E-05	8.6E-03
156-59-2	Dichloroethene[cis-1,2-]	5.0E+00			9.0E-03	5.6E-03	7.7E-05	8.6E-03
75-35-4	Dichloroethylene[1,1-]	5.0E+00			9.0E-03	5.6E-03	7.7E-05	8.6E-03
156-60-5	Dichloroethylene[trans-1,2-]	5.0E+00			9.0E-03	5.6E-03	7.7E-05	8.6E-03
120-83-2	Dichlorophenol[2,4-]	1.3E+01			3.0E-03	1.4E-02	2.0E-04	6.7E-02
78-87-5	Dichloropropane[1,2-]	5.0E+00			1.1E-03	5.6E-03	7.7E-05	7.0E-02
142-28-9	Dichloropropane[1,3-]	5.0E+00			1.1E-03	5.6E-03	7.7E-05	7.0E-02
594-20-7	Dichloropropane[2,2-]	5.0E+00			1.1E-03	5.6E-03	7.7E-05	7.0E-02
563-58-6	Dichloropropene[1,1-]	5.0E+00			3.0E-02	5.6E-03	7.7E-05	2.6E-03
10061-01-5	Dichloropropylene[cis-1,3-]	5.0E+00	1.0E-06	5.0E-06				
10061-02-6	Dichloropropylene[trans-1,3-]	5.0E+00	1.0E-06	5.0E-06				
60-57-1	Dieldrin	1.4E-01	4.6E-04	6.4E-05				
84-66-2	Diethylphthalate	9.6E+02			8.0E-01	1.1E+00	1.5E-02	1.9E-02
131-11-3	Dimethyl Phthalate	9.6E+02			1.0E+01	1.1E+00	1.5E-02	1.5E-03
84-74-2	Di-n-butylphthalate	9.6E+02			1.0E-01	1.1E+00	1.5E-02	1.5E-01
117-84-0	Di-n-octylphthalate	9.6E+02			2.0E-02	1.1E+00	1.5E-02	7.4E-01
122-39-4	Diphenyl amine	1.5E+00			2.5E-02	1.7E-03	2.4E-05	9.5E-04
122-66-7	Diphenylhydrazine[1,2-]	2.0E+01	2.2E-05	4.4E-04				
959-98-8	Endosulfan I	6.8E-02			6.0E-03	7.5E-05	1.1E-06	1.8E-04
33213-65-9	Endosulfan II	1.4E-01			6.0E-03	1.6E-04	2.2E-06	3.6E-04
1031-07-8	Endosulfan Sulfate	1.4E-01			6.0E-03	1.6E-04	2.2E-06	3.6E-04
72-20-8	Endrin	1.4E-01			3.0E-04	1.6E-04	2.2E-06	7.2E-03
7421-93-4	Endrin Aldehyde	1.4E-01			3.0E-04	1.6E-04	2.2E-06	7.2E-03
53494-70-5	Endrin Ketone	1.4E-01			3.0E-04	1.6E-04	2.2E-06	7.2E-03
100-41-4	Ethylbenzene	5.0E+00			1.0E-01	5.6E-03	7.7E-05	7.7E-04
206-44-0	Fluoranthene	9.6E+02			4.0E-02	1.1E+00	1.5E-02	3.7E-01
86-73-7	Fluorene	9.6E+02			4.0E-02	1.1E+00	1.5E-02	3.7E-01
F(-1)	Fluoride	1.4E+03			6.0E-02	1.6E+00	2.2E-02	3.6E-01

Risk Assessment Corporation
"Setting the standard in environmental health"

Analysis of Exposure and Risks to the Public from Radionuclides and Chemicals Released by the Cerro Grande Fire at Los Alamos

Analyte code	Analyte ^a	Maximum concentration (ug/L)	Unit risk (per ug/L)	Risk Index ^b	RfD (mg/kg/d)	Daily Intake (mg/kg)	Daily intake/body wt (mg/kg/d)	Hazard quotient ^c
76-44-8	Heptachlor	6.8E-02	1.3E-04	8.8E-06				
1024-57-3	Heptachlor Epoxide	6.8E-02	2.6E-04	1.8E-05				
118-74-1	Hexachlorobenzene	9.6E+02	4.6E-05	4.4E-02				
87-68-3	Hexachlorobutadiene	9.6E+02	2.2E-06	2.1E-03				
77-47-4	Hexachlorocyclopentadiene	9.6E+02			7.0E-03	1.1E+00	1.5E-02	2.1E+00
67-72-1	Hexachloroethane	9.6E+02	4.0E-07	3.8E-04				
591-78-6	Hexanone[2-]	2.0E+01			5.0E+00	2.2E-02	3.1E-04	6.2E-05
2691-41-0	HMX	1.3E+01			5.0E-02	1.4E-02	2.0E-04	4.0E-03
193-39-5	Indeno(1,2,3-cd)pyrene	9.6E+02	2.1E-05	2.0E-02				
74-88-4	Iodomethane	5.0E+00			1.4E-03	5.6E-03	7.7E-05	5.5E-02
78-59-1	Isophorone	9.6E+02	2.7E-08	2.6E-05				
98-82-8	Isopropylbenzene	5.0E+00			1.0E-01	5.6E-03	7.7E-05	7.7E-04
99-87-6	Isopropyltoluene[4-]	5.0E+00			2.0E-01	5.6E-03	7.7E-05	3.9E-04
Pb	Lead	1.2E+03			1.5E+02	5.6E-03	7.7E-05	3.9E-04
Mn	Manganese	1.0E+05			4.6E-02	1.1E+02	1.6E+00	3.4E+01
Hg	Mercury	4.8E+00			3.0E-04	5.4E-03	7.5E-05	2.5E-01
72-43-5	Methoxychlor[4,4'-]	6.8E-01			5.0E-03	7.5E-04	1.1E-05	2.1E-03
108-10-1	Methyl-2-pentanone[4-]	2.0E+01			8.0E-02	2.2E-02	3.1E-04	3.9E-03
75-09-2	Methylene chloride	1.6E+01	2.1E-07	3.4E-06				
Mo	Molybdenum	1.7E+03			5.0E-03	5.6E-03	7.7E-05	3.9E-04
91-20-3	Naphthalene	1.3E+01			2.0E-02	1.4E-02	2.0E-04	1.0E-02
Ni	Nickel	8.3E+02			2.0E-02	5.6E-03	7.7E-05	3.9E-04
99-09-2	Nitroaniline[3-]	4.8E+03	1.6E-07	7.7E-04				
98-95-3	Nitrobenzene	9.6E+02			5.0E-04	1.1E+00	1.5E-02	3.0E+01
NO2-N/NO3-N	Nitrogen, Nitrate + Nitrite	1.8E+04			1.0E-01	2.0E+01	2.8E-01	2.8E+01
53-63-0	Nitroglycerin	1.6E+00			5.0E-02	1.8E-03	2.5E-05	4.9E-04
100-02-7	Nitrophenol[4-]	6.4E+01			8.0E-03	7.1E-02	9.9E-04	1.2E-01
99-08-1	Nitrotoluene[3-]	1.0E+01			1.0E-02	1.1E-02	1.5E-04	1.5E-02
99-99-0	Nitrotoluene[4-]	1.0E+01			1.0E-02	1.1E-02	1.5E-04	1.5E-02
62-75-9	N-Nitrosodimethylamine	9.6E+02	1.4E-03	1.3E+00				
621-64-7	N-nitrosodipropylamine	9.6E+02	2.0E-04	1.9E-01				
3268-87-9	OCDD	1.5E-03	4.5E-03	6.9E-06				
39001-02-0	OCDF	1.3E-03	4.3E-03	5.6E-06				
3268-87-9	Octachlorodibenzodioxin[1,2,3,4,6,7,8,9-]	2.2E-04	4.5E-03	9.8E-07				
87-86-5	Pentachlorophenol	4.8E+03	3.0E-06	1.4E-02				
ClO4	Perchlorate	2.8E+02			1.0E-02	3.1E-01	4.4E-03	4.4E-01
78-11-5	PETN	5.0E+00			5.0E-02	5.6E-03	7.7E-05	1.5E-03
85-01-8	Phenanthrene	9.6E+02			3.0E-01	1.1E+00	1.5E-02	4.9E-02
108-95-2	Phenol	9.6E+02			6.0E-01	1.1E+00	1.5E-02	2.5E-02
103-65-1	Propylbenzene[1-]	5.0E+00	1.6E-06	8.0E-06				
129-00-0	Pyrene	9.6E+02			3.0E-02	1.1E+00	1.5E-02	4.9E-01
110-86-1	Pyridine	9.6E+02			1.0E-03	1.1E+00	1.5E-02	1.5E+01
121-82-4	RDX	8.4E-01	3.1E-06	2.6E-06				
Se	Selenium	5.7E+01			5.0E-03	5.6E-03	7.7E-05	3.9E-04
Ag	Silver	1.7E+02			5.0E-03	1.9E-01	2.6E-03	5.3E-01
Sr	Strontium	6.9E+03			6.0E-01	7.7E+00	1.1E-01	1.8E-01
100-42-5	Styrene	5.0E+00			2.0E-01	5.6E-03	7.7E-05	3.9E-04
630-20-6	Tetrachloroethane[1,1,1,2-]	5.0E+00	7.4E-07	3.7E-06				
79-34-5	Tetrachloroethane[1,1,2,2-]	5.0E+00	7.4E-07	3.7E-06				
127-18-4	Tetrachloroethylene	5.0E+00	7.4E-07	3.7E-06				
479-45-8	Tetryl	1.8E+01			1.0E-02	2.0E-02	2.8E-04	2.8E-02
Tl	Thallium	4.8E+01			8.0E-05	5.3E-02	7.4E-04	9.2E+00
Sn	Tin	5.6E+02			6.0E-01	6.2E-01	8.7E-03	1.4E-02

Estimated Risks from Releases to Surface Water
Appendix C. Screening Calculations for Water Monitoring Data

C-9

Analyte code	Analyte ^a	Maximum concentration (ug/L)	Unit risk (per ug/L)	Risk Index ^b	RfD (mg/kg/d)	Daily Intake (mg/kg)	Daily intake/body wt (mg/kg/d)	Hazard quotient ^c
108-88-3	Toluene	5.0E+00			2.0E-01	5.6E-03	7.7E-05	3.9E-04
U	Total Uranium by ICPMS	1.3E+01			6.0E-04	1.5E-02	2.1E-04	3.4E-01
8001-35-2	Toxaphene (Technical Grade)	6.8E+00	3.2E-05	2.2E-04				
76-13-1	Trichloro-1,2,2-trifluoroethane[1,1,2-]	5.0E+00			3.0E+01	5.6E-03	7.7E-05	2.6E-06
87-61-6	Trichlorobenzene[1,2,3-]	5.0E+00			1.0E-02	5.6E-03	7.7E-05	7.7E-03
71-55-6	Trichloroethane[1,1,1-]	5.0E+00			2.0E-01	5.6E-03	7.7E-05	3.9E-04
79-00-5	Trichloroethane[1,1,2-]	5.0E+00			4.0E-03	5.6E-03	7.7E-05	1.9E-02
79-01-6	Trichloroethene	5.0E+00			6.0E-03	5.6E-03	7.7E-05	1.3E-02
79-01-6	Trichloroethylene	5.0E+00			6.0E-03	5.6E-03	7.7E-05	1.3E-02
75-69-4	Trichlorofluoromethane	5.0E+00			3.0E-01	5.6E-03	7.7E-05	2.6E-04
96-18-4	Trichloropropane[1,2,3-]	5.0E+00			5.0E-03	5.6E-03	7.7E-05	1.5E-02
95-63-6	Trimethylbenzene[1,2,4-]	5.0E+00			5.0E-02	5.6E-03	7.7E-05	1.5E-03
108-67-8	Trimethylbenzene[1,3,5-]	5.0E+00			5.0E-02	5.6E-03	7.7E-05	1.5E-03
118-96-7	Trinitrotoluene[2,4,6-]	5.0E-01	9.0E-07	4.5E-07				
U	Uranium	1.5E+02			6.0E-04	1.6E-01	2.3E-03	3.8E+00
V	Vanadium	6.5E+02			9.0E-03	7.3E-01	1.0E-02	1.1E+00
75-01-4	Vinyl chloride	1.0E+01	4.2E-05	4.2E-04				
1330-20-7	Xylene (Total)	5.0E+00			2.0E+00	5.6E-03	7.7E-05	3.9E-05
95-47-6	Xylene[1,2-]	5.0E+00			2.0E+00	5.6E-03	7.7E-05	3.9E-05
	Xylene[1,3-]+Xylene[1,4-]	5.0E+00			2.0E+00	5.6E-03	7.7E-05	3.9E-05
Zn	Zinc	3.6E+03			3.0E-01	4.0E+00	5.6E-02	1.9E-01

a Analytes in bold are those that emerged from the Stage 1 screening.

a For the Stage 1 screening, we calculated the lifetime screening risk for chemicals for which a risk coefficient had been reported, using the maximum concentration of each radionuclide and the EPA slope factor (ORNL 2001). Those chemicals selected in the first stage screening were those with a calculated screening risk value greater than our screening criteria of 1×10^{-5} .

c For chemicals that did not have an established slope factor or unit risk, we used the reference dose (RfD) value to calculate the hazard quotient, the ratio between the chemical intake based on the maximum measured concentration in water with the established RfD. Those chemicals with a calculated hazard quotient greater than 1 were included in the list of chemicals emerging from the first stage screening evaluation.

APPENDIX D

SCREENING CALCULATIONS FOR RADIONUCLIDES AND CHEMICALS IN SEDIMENTS AT LANL

Table D-1. Screening Calculations for Radionuclides in Sediment at the LANL

Radionuclide	Maximum activity (pCi/g)	Sediment ingestion			External exposure		
		Morbidity risk per Bq	Intake (Bq)	Risk Index	Morbidity risk (per kg/Bq-s)	External exposure (kg/Bq-s)	Risk index
Ac-228	2.4E+00	4.5E-11	4.5E+01	2.0E-09	1.3E-17	2.0E+10	2.6E-07
Sb-124	3.6E-02	5.0E-10	6.9E-01	3.4E-10	7.6E-15	3.0E+08	2.3E-06
Sb-125	7.9E-02	1.7E-10	1.5E+00	2.5E-10	1.6E-15	6.5E+08	1.0E-06
Ba-133	3.6E-02	2.6E-10	6.7E-01	1.7E-10	1.2E-15	2.9E+08	3.6E-07
Be-7	6.0E+00	3.3E-12	1.1E+02	3.7E-10	1.8E-16	4.9E+10	8.8E-06
Bi-211	0.0E+00	2.7E-11			1.6E-16		
Bi-212	1.7E+00	2.7E-11	3.2E+01	8.7E-10	7.6E-16	2.0E+09	1.5E-06
Bi-214	1.9E+00	7.2E-12	3.5E+01	2.5E-10	1.1E-16	1.5E+10	1.7E-06
Cd-109	0.0E+00	1.8E-10			7.5E-18		
Ce-139	2.4E-02	5.3E-11	4.6E-01	2.4E-11	3.9E-16	2.0E+08	7.7E-08
Ce-141	9.7E-02	1.8E-10	1.8E+00	3.4E-10	1.9E-16	7.9E+08	1.5E-07
Ce-144	1.2E-01	1.4E-09	2.3E+00	3.2E-09	4.3E-17	9.9E+08	4.2E-08
Cs-134	6.5E-02	1.4E-09	1.2E+00	1.7E-09	6.1E-15	5.3E+08	3.2E-06
Cr-51	5.9E-01	7.2E-12	1.1E+01	8.0E-11	1.1E-16	4.8E+09	5.2E-07
Co-57	7.4E-02	4.0E-11	1.4E+00	5.6E-11	3.0E-16	6.0E+08	1.8E-07
Co-60	3.2E-01	6.0E-10	6.0E+00	3.6E-09	1.1E-14	3.7E+08	3.9E-06
Eu-152	2.2E-02	2.4E-10	4.1E-01	9.6E-11	4.5E-15	1.8E+08	8.0E-07
Eu-154	1.2E-01	4.0E-10	2.3E+00	9.3E-10	5.0E-15	1.0E+09	5.0E-06
I-133	7.2E-06	5.6E-10	1.4E-04	7.6E-14	1.4E-15	5.9E+04	8.0E-11
Fe-59	7.3E-02	3.0E-10	1.4E+00	4.2E-10	5.0E-15	6.0E+08	3.0E-06
Pb-211	4.2E-01	1.6E-11	8.0E+00	1.3E-10	2.0E-16	4.9E+08	9.7E-08
Pb-212	2.4E+00	9.6E-10	4.6E+01	4.4E-08	4.4E-16	2.8E+09	1.2E-06
Pb-214	2.0E+00	1.3E-11	3.7E+01	4.9E-10	8.4E-16	2.3E+09	1.9E-06
Mn-54	5.8E-02	8.4E-11	1.1E+00	9.2E-11	3.3E-15	6.8E+07	2.3E-07
Hg-203	7.6E-02	1.6E-10	1.4E+00	2.2E-10	7.9E-16	8.8E+07	7.0E-08
Np-237	5.8E-01	2.2E-09	1.1E+01	2.5E-08	4.6E-17	4.8E+09	2.2E-07
Np-239	2.3E-01	2.0E-10	4.4E+00	9.0E-10	4.6E-16	1.9E+09	8.8E-07
Nb-95	1.1E-01	9.5E-11	2.1E+00	2.0E-10	3.0E-15	1.3E+08	3.9E-07
Pu-238	9.7E-01	4.6E-09	1.8E+01	8.4E-08	6.2E-20	1.1E+09	7.0E-11
Pu-239/240	1.2E+00	4.7E-09	2.2E+01	1.0E-07	1.7E-19	1.3E+09	2.3E-10
Pa-231	5.5E-01	6.1E-09	1.0E+01	6.3E-08	1.2E-16	4.5E+09	5.3E-07
Pa-233	7.0E-02	2.2E-10	1.3E+00	2.9E-10	6.4E-16	5.7E+08	3.7E-07
Ru-103	3.9E-02	1.5E-10	7.3E-01	1.1E-10	1.8E-15	3.2E+08	5.5E-07
Ru-106	1.7E-01	1.7E-09	3.3E+00	5.4E-09	0.0E+00	1.4E+09	0
Se-75	4.0E-02	2.9E-10	7.5E-01	2.2E-10	1.2E-15	3.3E+08	4.0E-07
Na-22	7.1E-02	3.4E-10	1.3E+00	4.6E-10	8.8E-15	5.8E+08	5.1E-06
Sr-85	5.1E-02	8.4E-11	9.7E-01	8.2E-11	1.9E-15	4.2E+08	7.9E-07
Th-227	2.2E-01	1.9E-09	4.1E+00	7.7E-09	3.2E-16	1.8E+09	5.8E-07
Th-231	2.6E-01	8.8E-11	4.8E+00	4.2E-10	2.1E-17	2.1E+09	4.4E-08
Sn-113	4.7E-02	1.7E-10	8.9E-01	1.5E-10	1.7E-17	3.8E+08	6.6E-09
U-235/236	5.5E-01	2.6E-09	1.0E+01	2.7E-08	4.4E-16	4.5E+09	2.0E-06
Y-88	4.5E-02	1.6E-10	8.5E-01	1.3E-10	1.2E-14	3.7E+08	4.3E-06
Zinc-65	1.0E-01	4.2E-10	1.9E+00	7.9E-10	2.4E-15	8.2E+08	2.0E-06
Zr-95	2.0E-01	1.8E-10	3.7E+00	6.6E-10	2.9E-15	1.6E+09	4.6E-06

^a Our screening criteria is 1×10^{-5} ; no radionuclide was present in sediment at a concentration that resulted in that limit from inadvertent sediment ingestion or external exposure.

Table D-2. Screening Calculations for Chemicals in Sediments^a

Analyte	Maximum concentration (mg kg ⁻¹)	PRG (mg/kg)	Intake ^a (mg d ⁻¹)	Daily intake ^b (mg d ⁻¹ kg ⁻¹)	RfD ^c (mg/kg/d)	Hazard quotient ^d	Slope factor (mg/kg-d) ⁻¹	Mortality risk ^e	Comment
Acenaphthylene	7.4E+00		1.5E-03	2.1E-05	2.0E-02	1.E-03			Below screening criterion
Amino-2,6-dinitrotoluene[4-]	8.6E-01		1.7E-04	2.4E-06	5.0E-04	5.E-03			Below screening criterion
Amino-4,6-dinitrotoluene[2-]	4.0E-01		8.0E-05	1.1E-06	5.0E-04	2.E-03			Below screening criterion
Aroclor-1016	1.4E-01		2.8E-05	3.9E-07	7.0E-05	6.E-03			Below screening criterion
Aroclor-1221	2.8E-01		5.6E-05	7.8E-07	7.0E-05	1.E-02			Below screening criterion
Aroclor-1232	1.4E-01		2.8E-05	3.9E-07	7.0E-05	6.E-03			Below screening criterion
Aroclor-1242	1.4E-01		2.8E-05	3.9E-07	7.0E-05	6.E-03			Below screening criterion
Aroclor-1248	1.4E-01		2.8E-05	3.9E-07	7.0E-05	6.E-03			Below screening criterion
Aroclor-1260	3.0E-01	2.2E-01	6.0E-05	8.4E-07	7.0E-05	1.E-02			Below screening criterion
Benzo(g,h,i)perylene	7.4E+00		1.5E-03	2.1E-05			7.30E-02	1.5E-06	Below screening criterion
BHC[alpha-] (hexachlorocyclohexane)	6.9E-03		1.4E-07	1.9E-09			6.30E+00	1.2E-08	Below screening criterion
BHC[beta-] (hexachlorocyclohexane)	6.9E-03		1.4E-06	1.9E-08			1.80E+00	3.5E-08	Below screening criterion
BHC[delta-] (hexachlorocyclohexane)	6.9E-03		1.4E-07	1.9E-09			1.80E+00	3.5E-09	Below screening criterion
BHC[gamma-] (hexachlorocyclohexane)	6.9E-03		1.4E-07	1.9E-09			1.80E+00	3.5E-09	Below screening criterion
Bis(2-chloroethoxy)methane	7.4E+00		1.5E-04	2.1E-06			1.30E-02	3.E-08	Below screening criterion
Bis(2-chloroethyl)ether	7.4E+00		1.5E-03	2.1E-05	5.0E-03	4.E-03			Below screening criterion
Bromide	1.4E+01		2.8E-03	3.9E-05	4.0E-03	1.E-02			Below screening criterion
Bromophenyl-phenylether[4-]	7.4E+00		1.5E-03	2.1E-05	2.0E-02	1.E-03			Below screening criterion
Chloro-3-methylphenol[4-]	1.5E+01		3.0E-03	4.2E-05	5.0E-03	8.E-03			Below screening criterion
Chlorophenyl-phenyl[4-] Ether	7.4E+00		1.5E-03	2.1E-05	1.94E-03	1.E-02			Below screening criterion
Cyanide, Total	4.3E+00		8.6E-04	1.2E-05	2.0E-02	6.E-04			Below screening criterion
Dichlorobenzene[1,4-]	7.4E+00	3.4E+00	1.5E-03	2.1E-05			2.40E-02	5.E-07	Below screening criterion
Endosulfan I	6.9E-03		1.4E-06	1.9E-08	6.0E-03	3.E-06			Below screening criterion
Endosulfan Sulfate	1.4E-02		2.8E-06	3.9E-08	6.0E-03	6.E-06			Below screening criterion
Endrin Aldehyde	1.4E-02		2.8E-06	3.9E-08	3.0E-04	1.E-04			Below screening criterion
Endrin Ketone	1.4E-02		2.8E-06	3.9E-08	3.0E-04	1.E-04			Below screening criterion
Heptachlorodibenzofuran[1,2,3,4,6,7,8-]	2.0E-05		4.0E-09	5.5E-11			1.50E+02	8.E-09	Below screening criterion
Heptachlorodibenzodioxins (Total)	1.3E-04		2.5E-08	3.5E-10			1.50E+03	5.E-07	Below screening criterion
Heptachlorodibenzofuran[1,2,3,4,7,8,9-]	1.7E-06		3.3E-10	4.6E-12			1.50E+02	7.E-10	Below screening criterion
Heptachlorodibenzofurans (Total)	5.1E-05		1.0E-08	1.4E-10			1.50E+02	2.E-08	Below screening criterion

Analyte	Maximum concentration (mg kg ⁻¹)	PRG (mg/kg)	Intake ^a (mg d ⁻¹)	Daily intake ^b (mg d ⁻¹ kg ⁻¹)	RfD ^c (mg/kg/d)	Hazard quotient ^d	Slope factor (mg/kg-d) ⁻¹	Mortality risk ^e	Comment
Hexachlorocyclopentadiene	7.4E+00		1.5E-03	2.1E-05	6.00E-03	3.E-03			Below screening criterion
Hexachlorodibenzodioxin[1,2,3,4,7,8-]	1.2E-06		2.5E-10	3.5E-12			1.50E+04	5.E-08	Below screening criterion
Hexachlorodibenzodioxin[1,2,3,6,7,8-]	3.0E-06		6.0E-10	8.4E-12			1.50E+04	1.E-07	Below screening criterion
Hexachlorodibenzodioxin[1,2,3,7,8,9-]	2.6E-06		5.2E-10	7.2E-12			1.50E+04	1.E-07	Below screening criterion
Hexachlorodibenzodioxins (Total)	2.3E-05		4.7E-09	6.5E-11			1.50E+04	1.E-06	Below screening criterion
Hexachlorodibenzofuran[1,2,3,4,7,8-]	1.6E-06		3.2E-10	4.5E-12			1.50E+03	7.E-09	Below screening criterion
Hexachlorodibenzofuran[1,2,3,6,7,8-]	1.3E-06		2.7E-10	3.7E-12			1.50E+03	6.E-09	Below screening criterion
Hexachlorodibenzofuran[1,2,3,7,8,9-]	3.1E-06		6.1E-10	8.5E-12			1.50E+03	1.E-08	Below screening criterion
Hexachlorodibenzofuran[2,3,4,6,7,8-]	1.5E-06		3.0E-10	4.2E-12			1.50E+03	6.E-09	Below screening criterion
Hexachlorodibenzofurans (Total)	2.6E-05		5.2E-09	7.3E-11			1.50E+03	1.E-07	Below screening criterion
Hexachloroethane	7.4E+00		1.5E-03	2.1E-05	1.00E-03	2.E-02			Below screening criterion
Isophorone	7.4E+00		1.5E-03	2.1E-05	0.2	1.E-04			Below screening criterion
Lead	7.5E+01	4.0E+02		0.0E+00					Retained -public concern
Methylnaphthalene[2-]	7.4E+00	no	1.5E-03	3.0E-05	2.00E-02	1.E-03			Below screening criterion
Nitrophenol[2-]	7.4E+00		1.5E-03	3.0E-05	6.00E-01	5.E-05			Below screening criterion
Nitrophenol[4-]	3.7E+01		7.4E-03	1.5E-04	6.00E-01	2.E-04			Below screening criterion
Nitrotoluene[2-]	4.4E-01		8.8E-05	1.8E-06	1.00E-02	2.E-04			Below screening criterion
Nitrotoluene[3-]	2.5E-01		5.0E-05	1.0E-06	1.00E-02	1.E-04			Below screening criterion
Nitrotoluene[4-]	2.5E-01		5.0E-05	1.0E-06	1.00E-02	1.E-04			Below screening criterion
Octachlorodibenzodioxin[1,2,3,4,6,7,8,9-]	6.8E-04		1.4E-07	2.7E-09			150	4.E-07	Below screening criterion
Octachlorodibenzofuran[1,2,3,4,6,7,8,9-]	5.3E-05		1.1E-08	2.1E-10			15	3.E-09	Below screening criterion
Oxybis(1-chloropropane)[2,2'-]	7.4E+00		1.5E-03	3.0E-05			7.00E-02	2.E-06	Below screening criterion
Pentachlorodibenzodioxin[1,2,3,7,8-]	4.9E-07		9.8E-11	2.0E-12			7.50E+04	1.E-07	Below screening criterion
Pentachlorodibenzodioxins (Total)	3.4E-06		6.7E-10	1.3E-11			7.50E+04	1.E-06	Below screening criterion
Pentachlorodibenzofuran[2,3,4,7,8-]	9.7E-07		1.9E-10	3.9E-12			7.50E+03	3.E-08	Below screening criterion
Pentachlorodibenzofurans (Totals)	1.4E-05		2.7E-09	5.5E-11			7.50E+04	4.E-06	Below screening criterion
Phenanthrene	8.8E+00		1.8E-03	3.5E-05			7.30E-02	3.E-06	Below screening criterion
Pentachlorodibenzofuran[1,2,3,7,8-]	4.1E-07		8.2E-11	1.6E-12			7.50E+04	1.E-07	Below screening criterion
Pyridine	7.4E+00		1.5E-03	3.0E-05	1.00E-03	3.E-02			Below screening criterion
Tetrachlorodibenzodioxins (Total)	8.7E-06		1.7E-09	3.5E-11			1.50E+05	5.E-06	Below screening criterion
Tetrachlorodibenzofurans (Totals)	1.0E-05		2.0E-09	4.1E-11			1.50E+04	6.E-07	Below screening criterion

Analyte	Maximum concentration (mg kg ⁻¹)	PRG (mg/kg)	Intake ^a (mg d ⁻¹)	Daily intake ^b (mg d ⁻¹ kg ⁻¹)	RfD ^c (mg/kg/d)	Hazard quotient ^d	Slope factor (mg/kg-d) ⁻¹	Mortality risk ^e	Comment
Tetryl	7.6E-01		1.5E-04	3.0E-06	1.00E-02	3.E-04			Below screening criterion
Thallium	4.1E+00		8.2E-04	1.6E-05	8.00E-05	2.E-01			Below screening criterion
Aldrin	6.9E-03								Identified in water screening
Aluminum	3.0E+04	7.6E+04							Identified in water screening
Aniline	1.5E+01	8.5E+01							Identified in water screening
Arsenic	6.6E+00								Identified in water screening
Azobenzene	1.5E+01								Identified in water screening
Benzidine	2.3E+00								Identified in water screening
Benzo(a)anthracene	7.4E+00								Identified in water screening
Benzo(a)pyrene	7.4E+00								Identified in water screening
Benzo(b)fluoranthene	7.4E+00								Identified in water screening
Benzo(k)fluoranthene	7.4E+00								Identified in water screening
Dibenz(a,h)anthracene	7.4E+00								Identified in water screening
Dichlorobenzidine[3,3'-]	1.5E+01	1.1E+00							Identified in water screening
Dieldrin	1.4E-02	3.0E-02							Identified in water screening
Dinitro-2-methylphenol[4,6-]	3.7E+01								Identified in water screening
Dinitrophenol[2,4-]	3.7E+01								Identified in water screening
Heptachlor	6.9E-03	5.3E-02							Identified in water screening
Heptachlor Epoxide	6.9E-03	5.3E-02							Identified in water screening
Hexachlorobenzene	7.4E+00	3.0E-01							Identified in water screening
Hexachlorobutadiene	7.4E+00								Identified in water screening
Indeno(1,2,3-cd)pyrene	7.4E+00	6.2E-01							Identified in water screening
Manganese	8.2E+03	1.8E+03							Identified in water screening
Nitroaniline[3-]	3.7E+01								Identified in water screening
Nitroaniline[4-]	1.5E+01	3.5E+00							Identified in water screening
Nitrosodimethylamine[N-]	7.4E+00	9.5E-03							Identified in water screening
Nitroso-di-n-propylamine[N-]	7.4E+00								Identified in water screening
Nitrosodiphenylamine[N-]	7.4E+00	9.9E+01							Identified in water screening
Pentachlorophenol	3.7E+01								Identified in water screening
Tetrachlorodibenzodioxin[2,3,7,8-]	2.1E-07	3.6E-06							Identified in water screening

Analyte	Maximum concentration (mg kg ⁻¹)	PRG (mg/kg)	Intake ^a (mg d ⁻¹)	Daily intake ^b (mg d ⁻¹ kg ⁻¹)	RfD ^c (mg/kg/d)	Hazard quotient ^d	Slope factor (mg/kg-d) ⁻¹	Mortality risk ^e	Comment
Tetrachlorodibenzofuran[2,3,7,8-]	9.8E-07								Identified in water screening
Toxaphene (Technical Grade)	6.9E-01								Identified in water screening
Acenaphthene	7.4E+00	3.7E+03							Discard-below PRG
Anthracene	7.4E+00	2.2E+04							Discard-below PRG
Antimony	2.1E+00	3.1E+01							Discard-below PRG
Aroclor-1254	1.4E-01	2.2E-01							Discard-below PRG
Barium	1.3E+03	5.4E+03							Discard-below PRG
Benzoic Acid	3.7E+01	1.0E+05							Discard-below PRG
Benzyl Alcohol	1.5E+01	1.8E+04							Discard-below PRG
Beryllium	1.7E+00	1.5E+02							Discard-below PRG
Bis(2-ethylhexyl)phthalate	7.4E+00	3.5E+01							Discard-below PRG
Butylbenzylphthalate	7.4E+00	1.2E+04							Discard-below PRG
Cadmium	3.9E+00	3.7E+01							Discard-below PRG
Carbazole	7.4E+00	2.4E+01							Discard-below PRG
Chlordane[alpha-]	6.9E-03	1.6E+00							Discard-below PRG
Chlordane[gamma-]	7.1E-03	1.6E+00							Discard-below PRG
Chloroaniline[4-]	1.5E+01	2.4E+02							Discard-below PRG
Chloronaphthalene[2-]	7.4E+00	3.9E+03							Discard-below PRG
Chlorophenol[2-]	7.4E+00	6.3E+01							Discard-below PRG
Chromium, Total	3.3E+02	2.1E+02							Discard-below PRG
Chrysene	7.4E+00	6.2E+01							Discard-below PRG
Cobalt	1.5E+01	4.7E+03							Discard-below PRG
Copper	1.3E+02	2.9E+03							Discard-below PRG
DDD[4,4'-]	1.4E-02	2.4E+00							Discard-below PRG
DDE[4,4'-]	2.3E-02	1.7E+00							Discard-below PRG
DDT[4,4'-]	6.1E-02	1.7E+00							Discard-below PRG
Dibenzofuran	7.4E+00	2.9E+02							Discard-below PRG
Dichlorobenzene[1,2-]	7.4E+00	3.7E+02							Discard-below PRG
Dichlorobenzene[1,3-]	7.4E+00	1.3E+01							Discard-below PRG

[illegible]

Analyte	Maximum concentration (mg kg ⁻¹)	PRG (mg/kg)	Intake ^a (mg d ⁻¹)	Daily intake ^b (mg d ⁻¹ kg ⁻¹)	RfD ^c (mg/kg/d)	Hazard quotient ^d	Slope factor (mg/kg-d) ⁻¹	Mortality risk ^e	Comment
Trinitrobenzene[1,3,5-]	2.5E-01	1.8E+03							Discard-below PRG
Trinitrotoluene[2,4,6-]	6.8E-01	1.6E+01							Discard-below PRG
Vanadium	4.4E+01	5.5E+02							Discard-below PRG
Zinc	1.8E+02	2.3E+04							Discard-below PRG

^a These analytes were measured in sediment at LANL and were divided into three groups: those identified as important through the water screening process (in bold); those with maximum sediment concentrations below the PRG; and those that were assumed to be ingested by an individual at the maximum concentration in sediment.

^b Assume daily intake of 0.2 g (75 g y⁻¹) (Till and Meyer 2001).

^c Assume 71.8 kg as average weight (EPA 1991).

^d Based on our screening criterion of an HQ > 1, we identified no additional analytes through the sediment screening process.

^e Based on our risk criterion of 10⁻⁵ for this study, we identified no additional analytes through the sediment screening process.

APPENDIX E

**SELECTION OF ANALYTES FOR SURFACE WATER MODELING
ASSESSMENT**

Table E-1. Analytes Considered for Surface Water Pathway Source Term Development

Status	Analyte	Maximum of means	Units	PRG (mg/kg)	Comment
Removed	2,4,6-Trichlorophenol	9.3E+00	MG/KG	4.4E+01	Highest average value < PRG
Removed	Acenaphthene	4.1E+01	MG/KG	3.7E+03	Highest average value < PRG
Removed	Acetone	7.1E-01	MG/KG	1.6E+03	Highest average value < PRG
Removed	Aluminum	1.7E+04	MG/KG	7.6E+04	Highest average value < PRG
Removed	Aniline	3.8E-01	MG/KG	8.5E+01	Highest average value < PRG
Removed	Anthracene	5.9E+01	MG/KG	2.2E+04	Highest average value < PRG
Removed	Benzene	2.0E-03	MG/KG	6.5E-01	Highest average value < PRG
Removed	Benzoic Acid	1.2E+00	MG/KG	1.0E+05	Highest average value < PRG
Removed	Benzyl Alcohol	2.5E-01	MG/KG	1.8E+04	Highest average value < PRG
Removed	Beryllium	3.2E+01	MG/KG	1.5E+02	Highest average value < PRG
Removed	Boron	5.7E+00	MG/KG	5.5E+03	Highest average value < PRG
Removed	Bromodichloromethane	4.0E-03	MG/KG	1.0E+00	Highest average value < PRG
Removed	Butylbenzylphthalate	1.3E+01	MG/KG	1.2E+04	Highest average value < PRG
Removed	Carbazole	1.8E+00	MG/KG	2.4E+01	Highest average value < PRG
Removed	Carbon Disulfide	1.2E-02	MG/KG	3.6E+02	Highest average value < PRG
Removed	Chlordane [alpha]	2.5E-01	MG/KG	1.6E+00	Highest average value < PRG
Removed	Chlordane [gamma]	1.8E-01	MG/KG	1.6E+00	Highest average value < PRG
Removed	Chloroaniline[4-]	1.4E-01	MG/KG	2.4E+02	Highest average value < PRG
Removed	Chloronaphthalene[2-]	2.7E-01	MG/KG	3.9E+03	Highest average value < PRG
Removed	Chlorophenol[2-]	3.7E-01	MG/KG	6.3E+01	Highest average value < PRG
Removed	Chromium (hexavalent)	3.1E+00	MG/KG	3.0E+01	Highest average value < PRG
Removed	Cobalt	4.6E+01	MG/KG	4.7E+03	Highest average value < PRG
Removed	Cyanide (total)	6.6E+00	MG/KG	1.1E+01	Highest average value < PRG
Removed	DDD[4,4'-]	2.1E-02	MG/KG	2.4E+00	Highest average value < PRG
Removed	DDE[4,4'-]	8.3E-02	MG/KG	1.7E+00	Highest average value < PRG
Removed	DDT[4,4'-]	1.2E-01	MG/KG	1.7E+00	Highest average value < PRG
Removed	Di-n-butylphthalate	1.0E+02	MG/KG	6.1E+03	Highest average value < PRG
Removed	Di-n-octylphthalate	4.5E+00	MG/KG	1.2E+03	Highest average value < PRG
Removed	Dibenzofuran	1.9E+01	MG/KG	2.9E+02	Highest average value < PRG
Removed	Dichlorobenzene[1,2-]	3.2E-01	MG/KG	3.7E+02	Highest average value < PRG
Removed	Dichlorobenzene[1,3-]	3.7E-01	MG/KG	1.3E+01	Highest average value < PRG
Removed	Dichlorobenzene[1,4-]	5.0E-02	MG/KG	3.4E+00	Highest average value < PRG
Removed	Dichlorobenzidine[3,3'-]	7.0E-01	MG/KG	1.1E+00	Highest average value < PRG
Removed	Dichlorodifluoromethane	5.0E-03	MG/KG	9.4E+01	Highest average value < PRG
Removed	Dieldrin	1.5E-02	MG/KG	3.0E-02	Highest average value < PRG
Removed	Diethylphthalate	3.7E-01	MG/KG	4.9E+04	Highest average value < PRG
Removed	Dimethyl Phthalate	7.6E-02	MG/KG	1.0E+05	Highest average value < PRG
Removed	Dimethylphenol[2,4-]	1.3E-01	MG/KG	1.2E+03	Highest average value < PRG
Removed	Dinitrotoluene[2,4-]	8.4E-01	MG/KG	1.2E+02	Highest average value < PRG
Removed	Dinitrotoluene[2,6-]	6.0E-01	MG/KG	6.1E+01	Highest average value < PRG
Removed	Endosulfan II	1.6E-02	MG/KG	3.7E+02	Highest average value < PRG
Removed	Endrin	1.1E-02	MG/KG	1.8E+01	Highest average value < PRG

Analysis of Exposure and Risks to the Public from Radionuclides and
Chemicals Released by the Cerro Grande Fire at Los Alamos

Status	Analyte	Maximum of means	Units	PRG (mg/kg)	Comment
Removed	Fluoranthene	2.1E+02	MG/KG	2.3E+03	Highest average value < PRG
Removed	Fluorene	3.7E+01	MG/KG	2.6E+03	Highest average value < PRG
Removed	Fluoride	6.0E+00	MG/KG	3.7E+03	Highest average value < PRG
Removed	Hexachlorobenzene	2.7E-01	MG/KG	3.0E-01	Highest average value < PRG
Removed	Lithium	1.1E+01	MG/KG	1.6E+03	Highest average value < PRG
Removed	Manganese	1.4E+03	MG/KG	1.8E+03	Highest average value < PRG
Removed	Methoxychlor[4,4'-]	2.4E-01	MG/KG	3.1E+02	Highest average value < PRG
Removed	Methylene Chloride	9.7E-02	MG/KG	8.9E+00	Highest average value < PRG
Removed	Methylphenol[2-]	1.7E+00	MG/KG	3.1E+03	Highest average value < PRG
Removed	Methylphenol[4-]	8.7E-01	MG/KG	3.1E+02	Highest average value < PRG
Removed	Molybdenum	4.9E+00	MG/KG	3.9E+02	Highest average value < PRG
Removed	Naphthalene	2.6E+01	MG/KG	5.6E+01	Highest average value < PRG
Removed	Nickel	7.0E+02	MG/KG	1.6E+03	Highest average value < PRG
Removed	Nitroaniline[4-]	6.8E-01	MG/KG	3.5E+00	Highest average value < PRG
Removed	Nitrobenzene	4.5E+00	MG/KG	2.0E+01	Highest average value < PRG
Removed	Nitroglycerin	3.0E+01	MG/KG	3.5E+01	Highest average value < PRG
Removed	Nitrosodiphenylamine[N-]	3.7E-01	MG/KG	9.9E+01	Highest average value < PRG
Removed	Pentachlorophenol	1.9E+00	MG/KG	3.0E+00	Highest average value < PRG
Removed	Phenol	1.9E+00	MG/KG	3.7E+04	Highest average value < PRG
Removed	Pyrene	1.8E+02	MG/KG	2.3E+03	Highest average value < PRG
Removed	Selenium	3.6E+02	MG/KG	3.9E+02	Highest average value < PRG
Removed	Silver	2.3E+02	MG/KG	3.9E+02	Highest average value < PRG
Removed	Strontium	7.2E+01	MG/KG	4.7E+04	Highest average value < PRG
Removed	Styrene	3.7E-02	MG/KG	1.7E+03	Highest average value < PRG
Removed	Toluene	2.0E-02	MG/KG	5.2E+02	Highest average value < PRG
Removed	Trichloro-1,2,2-trifluoroethane[1,1,2-]	3.0E+00	MG/KG	5.6E+03	Highest average value < PRG
Removed	Trichlorobenzene[1,2,4-]	3.7E-01	MG/KG	6.5E+02	Highest average value < PRG
Removed	Trichloroethane[1,1,1-]	2.1E+01	MG/KG	6.3E+02	Highest average value < PRG
Removed	Trichlorofluoromethane	1.9E-02	MG/KG	3.9E+02	Highest average value < PRG
Removed	Trimethylbenzene[1,2,4-]	2.6E-02	MG/KG	5.2E+01	Highest average value < PRG
Removed	Trimethylbenzene[1,3,5-]	8.2E-03	MG/KG	2.1E+01	Highest average value < PRG
Removed	Trinitrobenzene[1,3,5-]	3.4E+00	MG/KG	1.8E+03	Highest average value < PRG
Removed	Vanadium	9.6E+01	MG/KG	5.5E+02	Highest average value < PRG
Removed	Xylene (Total)	3.5E-02	MG/KG	2.1E+02	Highest average value < PRG
Removed	Xylene[1,2-]	1.5E-03	MG/KG	2.1E+02	Highest average value < PRG
Removed	Xylene[1,3-]	2.3E-03	MG/KG	2.1E+02	Highest average value < PRG
Removed	Zinc	7.5E+03	MG/KG	2.3E+04	Highest average value < PRG
Removed	Acenaphthylene	2.5E+00	MG/KG		Not identified by Task 2.1 screening
Removed	Actinium-228	2.4E+00	PCI/G		Not identified by Task 2.1 screening
Removed	Amino-2,6-dinitrotoluene[4-]	9.6E+00	MG/KG		Not identified by Task 2.1 screening
Removed	Amino-4,6-dinitrotoluene[2-]	2.0E+01	MG/KG		Not identified by Task 2.1 screening
Removed	Antimony	3.9E+01	MG/KG	3.1E+01	Not identified by Task 2.1 screening
Removed	Aroclor-1254	1.5E+01	MG/KG	2.2E-01	Not identified by Task 2.1 screening

Status	Analyte	Maximum of means	Units	PRG (mg/kg)	Comment
Removed	Aroclor-1260	2.3E+00	MG/KG	2.2E-01	Not identified by Task 2.1 screening
Removed	Asbestos (Friable)	0.0E+00	MG/KG		Zero concentration
Removed	Barium-140	2.1E-01	PCI/G		Not identified by Task 2.1 screening
Removed	Benzo(g,h,i)perylene	5.2E+01	MG/KG		Not identified by Task 2.1 screening
Removed	BHC[alpha-]	4.0E-03	MG/KG		Not identified by Task 2.1 screening
Removed	BHC[delta-]	1.6E-01	MG/KG		Not identified by Task 2.1 screening
Removed	BHC[gamma-]	3.1E-02	MG/KG		Not identified by Task 2.1 screening
Removed	Bis(2-ethylhexyl)phthalate	6.0E+01	MG/KG	3.5E+01	Not identified by Task 2.1 screening
Removed	Bismuth-211	4.2E+00	PCI/G		Not identified by Task 2.1 screening
Removed	Bismuth-212	3.8E+00	PCI/G		Not identified by Task 2.1 screening
Removed	Bismuth-214	4.6E+00	PCI/G		Not identified by Task 2.1 screening
Removed	Bromine	8.0E+00	MG/KG		Water quality parameter
Removed	Bromophenyl-phenylether[4-]	3.8E-01	MG/KG		Not identified by Task 2.1 screening
Removed	Butanone[2-]	2.7E-01	MG/KG		Not identified by Task 2.1 screening
Removed	Cadmium	7.3E+01	MG/KG	3.7E+01	Not identified by Task 2.1 screening
Removed	Cadmium-109	3.8E+00	PCI/G		Not identified by Task 2.1 screening
Removed	Calcium	6.4E+04	MG/KG		Water quality parameter
Removed	Carbon, Total	2.7E+04	MG/KG		Water quality parameter
Removed	Carbon, Total Organic	2.7E+04	MG/KG		Water quality parameter
Removed	Cesium	5.1E+00	MG/KG		Water quality parameter
Removed	Cesium-134	3.4E-01	PCI/G		Not identified by Task 2.1 screening
Removed	Chloro-3-methylphenol[4-]	5.3E+00	MG/KG		Not identified by Task 2.1 screening
Removed	Chromium (total)	4.0E+02	MG/KG	2.1E+02	Not identified by Task 2.1 screening
Removed	Chrysene	1.5E+02	MG/KG	6.2E+01	Not identified by Task 2.1 screening
Removed	Cobalt-57	1.6E-01	PCI/G		Not identified by Task 2.1 screening
Removed	Cobalt-60	2.0E+00	PCI/G		Not identified by Task 2.1 screening
Removed	Dichloroethene[cis-1,2-]	2.0E-03	MG/KG		Not identified by Task 2.1 screening
Removed	Dinitrobenzene[1,3-]	2.9E+01	MG/KG	6.1E+00	Not identified by Task 2.1 screening
Removed	Endosulfan Sulfate	1.8E-03	MG/KG		Not identified by Task 2.1 screening
Removed	Endrin Aldehyde	1.8E-01	MG/KG		Not identified by Task 2.1 screening
Removed	Europium-152	5.2E-01	PCI/G		Not identified by Task 2.1 screening
Removed	Gold	8.3E+02	MG/KG		Water quality parameter
Removed	Hexanone[2-]	3.5E-01	MG/KG		Not identified by Task 2.1 screening
Removed	HMX	1.7E+04	MG/KG	3.1E+03	Not identified by Task 2.1 screening
Removed	Hydrocarbons, Total Petroleum	6.8E+03	MG/KG		Range of hydrocarbons
Removed	Iodine-129	0.0E+00	PCI/G		Zero concentration
Removed	Iron	3.6E+04	MG/KG	2.3E+04	Water quality parameter
Removed	Isopropyltoluene[4-]	4.4E-02	MG/KG		Not identified by Task 2.1 screening
Removed	Lead-211	5.1E-01	PCI/G		Not identified by Task 2.1 screening
Removed	Lead-212	2.5E+00	PCI/G		Not identified by Task 2.1 screening
Removed	Lead-214	2.1E+00	PCI/G		Not identified by Task 2.1 screening
Removed	Lubricant Range Organics	2.1E+04	MG/KG		Range of hydrocarbons
Removed	Magnesium	2.4E+03	MG/KG		Water quality parameter

Analysis of Exposure and Risks to the Public from Radionuclides and Chemicals Released by the Cerro Grande Fire at Los Alamos

Status	Analyte	Maximum of means	Units	PRG (mg/kg)	Comment
Removed	Manganese-54	1.3E-01	PCI/G		Not identified by Task 2.1 screening
Removed	Mercury	6.3E+01	MG/KG	2.3E+01	Not identified by Task 2.1 screening
Removed	Methyl-2-pentanone[4-]	6.0E-02	MG/KG		Not identified by Task 2.1 screening
Removed	Methylnaphthalene[2-]	6.2E+00	MG/KG		Not identified by Task 2.1 screening
Removed	Nitrate (as NO3)	2.0E+01	MG/KG		Not identified by Task 2.1 screening
Removed	Nitrate + Nitrite (as N)	1.9E+00	MG/KG		Not identified by Task 2.1 screening
Removed	Nitrite (as NO2)	2.7E+00	MG/KG		Not identified by Task 2.1 screening
Removed	Nitrotoluene[2-]	1.6E+00	MG/KG		Not identified by Task 2.1 screening
Removed	Nitrotoluene[3-]	1.2E+00	MG/KG		Not identified by Task 2.1 screening
Removed	Nitrotoluene[4-]	6.7E+00	MG/KG		Not identified by Task 2.1 screening
Removed	Organics, Diesel Range	4.2E+03	MG/KG		Range of hydrocarbons
Removed	PETN	1.1E+02	MG/KG		Not identified by Task 2.1 screening
Removed	Phenanthrene	1.2E+02	MG/KG		Not identified by Task 2.1 screening
Removed	Platinum	4.2E+01	MG/KG		Water quality parameter
Removed	Potassium	3.1E+03	MG/KG		Water quality parameter
Removed	Protactinium-231	6.4E+00	PCI/G		Not identified by Task 2.1 screening
Removed	Protactinium-234	1.9E+00	PCI/G		Not identified by Task 2.1 screening
Removed	Radium-223	1.0E+00	PCI/G		Not identified by Task 2.1 screening
Removed	Radon-219	1.4E+00	PCI/G		Not identified by Task 2.1 screening
Removed	RDX	5.0E+03	MG/KG	4.4E+00	Not identified by Task 2.1 screening
Removed	Ruthenium-106	1.6E+00	PCI/G		Not identified by Task 2.1 screening
Removed	Silicon	1.6E+02	MG/KG		Water quality parameter
Removed	Silicon Dioxide	1.9E+04	MG/KG		Water quality parameter
Removed	Sodium	7.3E+03	MG/KG		Water quality parameter
Removed	Sodium-22	1.2E-01	PCI/G		Not identified by Task 2.1 screening
Removed	TATB	8.0E+00	MG/KG		Not identified by Task 2.1 screening
Removed	Technetium-99	4.2E-01	PCI/G		Not identified by Task 2.1 screening
Removed	Tetrachloroethene	3.3E-03	MG/KG		Not identified by Task 2.1 screening
Removed	Tetryl	9.5E+00	MG/KG		Not identified by Task 2.1 screening
Removed	Thallium	2.3E+02	MG/KG		Not identified by Task 2.1 screening
Removed	Thallium-208	1.4E+00	PCI/G		Not identified by Task 2.1 screening
Removed	Thorium-227	2.7E+01	PCI/G		Not identified by Task 2.1 screening
Removed	Thorium-231	5.4E-01	PCI/G		Not identified by Task 2.1 screening
Removed	Trichlorobenzene[1,2,3-]	2.0E-03	MG/KG		Not identified by Task 2.1 screening
Removed	Trichloroethene	1.3E+00	MG/KG		Not identified by Task 2.1 screening
Removed	Trinitrotoluene[2,4,6-]	3.6E+02	MG/KG	1.6E+01	Not identified by Task 2.1 screening
Removed	Uranium	1.1E+03	MG/KG	1.6E+01	Not identified by Task 2.1 screening
Retained	Aldrin	4.9E-02	MG/KG	2.9E-02	Identified by Task 2.1 screening
Retained	Americium-241	2.3E+01	PCI/G		Added (elevated in ash)
Retained	Arsenic	2.4E+01	MG/KG	3.9E-01	Identified by Task 2.1 screening
Retained	Barium	7.6E+04	MG/KG	5.4E+03	Added (elevated in ash)
Retained	Benzo(a)anthracene	1.2E+02	MG/KG	6.2E-01	Identified by Task 2.1 screening
Retained	Benzo(a)pyrene	1.0E+02	MG/KG	6.2E-02	Identified by Task 2.1 screening

Estimated Risks from Releases to Surface Water
Appendix E. Selection of Analytes for Transport Modeling

E-7

Status	Analyte	Maximum of means	Units	PRG (mg/kg)	Comment
Retained	Benzo(b)fluoranthene	1.2E+02	MG/KG	6.2E-01	Identified by Task 2.1 screening
Retained	Benzo(k)fluoranthene	7.2E+01	MG/KG	6.2E+00	Identified by Task 2.1 screening
Retained	Cesium-137	8.8E+01	PCI/G		Identified by Task 2.1 screening
Retained	Copper	1.4E+04	MG/KG	2.9E+03	Added (elevated in ash)
Retained	Chromium (total)	4.0E+02	MG/KG	2.1E+02	Added (public concern)
Retained	Dibenz(a,h)anthracene	5.4E+00	MG/KG	6.2E-02	Identified by Task 2.1 screening
Retained	Heptachlor Epoxide	1.1E-01	MG/KG	5.3E-02	Identified by Task 2.1 screening
Retained	Indeno(1,2,3-cd)pyrene	5.7E+01	MG/KG	6.2E-01	Identified by Task 2.1 screening
Retained	Lead	6.5E+03	MG/KG	4.0E+02	Added (elevated in ash)
Retained	Lead-210	8.8E+00	PCI/G		Identified by Task 2.1 screening
Retained	Neptunium-237	1.0E+00	PCI/G		Identified by Task 2.1 screening
Retained	Mercury	6.3E+01	MG/KG	2.3E+01	Added (public concern)
Retained	Nitrosodimethylamine[N-]	3.3E-01	MG/KG	9.5E-03	Identified by Task 2.1 screening
Retained	Plutonium-238	5.8E+00	PCI/G		Added (elevated in ash)
Retained	Plutonium-239	4.6E+02	PCI/G		Added (elevated in ash)
Retained	Potassium-40	6.1E+01	PCI/G		Identified by Task 2.1 screening
Retained	Protactinium-234M	8.2E+02	PCI/G		Identified by Task 2.1 screening
Retained	Radium-224	1.4E+01	PCI/G		Identified by Task 2.1 screening
Retained	Radium-226	6.7E+00	PCI/G		Identified by Task 2.1 screening
Retained	Radium-228	1.6E+00	PCI/G		Identified by Task 2.1 screening
Retained	RDX	5.0E+03	MG/KG	4.4E+00	Added because of high concentration
Retained	Strontium-90	2.4E+02	PCI/G		Identified by Task 2.1 screening
Retained	Thorium-228	2.5E+00	PCI/G		Identified by Task 2.1 screening
Retained	Thorium-230	2.3E+00	PCI/G		Identified by Task 2.1 screening
Retained	Thorium-232	4.0E+00	PCI/G		Identified by Task 2.1 screening
Retained	Thorium-234	4.4E+02	PCI/G		Identified by Task 2.1 screening
Retained	Tritium	3.3E+01	PCI/G		Identified by Task 2.1 screening
Retained	Uranium	1.1E+03	MG/KG	1.6E+01	Added because of high concentration
Retained	Uranium-234	1.6E+02	PCI/G		Identified by Task 2.1 screening
Retained	Uranium-235	2.1E+01	PCI/G		Added (elevated in ash)
Retained	Uranium-238	4.4E+02	PCI/G		Identified by Task 2.1 screening

APPENDIX F

PRS AND GEOMORPHIC UNIT SOURCE AREA CONCENTRATION ADJUSTMENT FACTORS AND PRS EROSION MATRIX ADJUSTMENT FACTORS

These adjustment factors, discussed in the text of the report, are provided in electronic format in the Excel file accompanying this report, called "AppF_Adjustment factors.xls."

APPENDIX G

ASSUMED SOURCE AREA CONCENTRATIONS

Assumed source area concentrations, referenced in Chapter 3, are provided in electronic format in the Excel file accompanying this report, called "AppG_Source Area Conc.xls."

APPENDIX H

PRE- AND POST-FIRE STORMWATER FLOW

Calculated pre- and post-fire stormwater flow values, referenced in Chapter 4, are provided in electronic format in the Excel file accompanying this report, called “AppH_Storm water flow.xls.”

APPENDIX I

ESTIMATED POE CONCENTRATIONS: BASE CASE

Calculated pre- and post-fire stormwater flow values, referenced in Chapter 4, are provided in electronic format in the Excel file accompanying this report, called "AppI_POE concentration.xls."

APPENDIX J

ESTIMATED POE CONCENTRATIONS EXCLUDING BURN AREA, COMPARED TO BASE CASE CONCENTRATIONS

The percent contribution of the burn area to POE concentrations, referenced in Chapter 4, are provided in electronic format in the Excel file accompanying this report, called “AppJ_Burn Area effect.xls.”

APPENDIX K

ESTIMATED POE CONCENTRATIONS EXCLUDING GEOMORPHIC UNIT AND UNSAMPLED REACH SOURCE AREAS, COMPARED TO BASE CASE CONCENTRATIONS

The percent contribution of the Geomorphic Unit and Unsourced Reach source areas to POE concentrations, referenced in Chapter 4, are provided in electronic format in the Excel file accompanying this report, called "AppK_GeoUnits_Reaches.xls."

APPENDIX L

ESTIMATED POE CONCENTRATIONS EXCLUDING PRS SOURCE AREAS, COMPARED TO BASE CASE CONCENTRATIONS

The percent contribution of the PRS source areas to POE concentrations, referenced in Chapter 4, are provided in electronic format in the Excel file accompanying this report, called "AppL_PRS Effect.xls."

APPENDIX M

ESTIMATED POE CONCENTRATIONS, EXCLUDING EROSION MATRIX SCORES

The impact of erosion matrix scores on POE concentrations, referenced in Chapter 4, is provided in electronic format in the Excel file accompanying this report, called "AppM_Erosion matrix.xls."

APPENDIX N

ESTIMATED POE CONCENTRATIONS, USING MAXIMUM PRS AND GEOMORPHIC UNIT SOURCE AREA CONCENTRATIONS

The impact of using maximum PRS and Geomorphic Unit source area concentrations on POE concentrations, referenced in Chapter 4, is provided in electronic format in the Excel file accompanying this report, called "AppN_Max Conc Effec.xls."

APPENDIX O

ESTIMATED POE CONCENTRATIONS, USING A POST-FIRE TSS VALUE OF 5000 INSTEAD OF 10000 mg L⁻¹

The impact of using a post-fire TSS value of 5000 instead of 10000 mg l⁻¹ on POE concentrations, referenced in Chapter 4, is provided in electronic format in the Excel file accompanying this report, called "AppO_TSS5000.xls."

APPENDIX P

ESTIMATED POE CONCENTRATIONS, USING A POST-FIRE TSS VALUE OF 15000 INSTEAD OF 10000 mg L⁻¹

The impact of using a post-fire TSS value of 15000 instead of 10000 mg l⁻¹ on POE concentrations, referenced in Chapter 4, is provided in electronic format in the Excel file accompanying this report, called "AppP_TSS15000.xls."

APPENDIX Q

ESTIMATED POE CONCENTRATIONS, USING A POST-FIRE TSS VALUE OF 20000 INSTEAD OF 10000 mg L⁻¹

The impact of using a post-fire TSS value of 20000 instead of 10000 mg l⁻¹ on POE concentrations, referenced in Chapter 4, is provided in electronic format in the Excel file accompanying this report, called "AppQ_TSS20000.xls."

APPENDIX R

COMPARISON OF BASE CASE CONCENTRATIONS TO RELEVANT EMPIRICAL DATA

Comparisons of predicted and measured concentrations are provided for the following categories of data, as discussed in Chapter 4:

- 1) sediment concentrations with available background values
 - file name: "AppR_1Sed_w_bkg.xls"
- 2) sediment concentrations without available background values
 - file name: "AppR_2Sed_wo_bkg.xls"
- 3) water concentrations for chemicals and radionuclides with available soil/sediment background values
 - file name: "AppR_3Water_w_bkg.xls"
- 4) water concentrations for chemicals and radionuclides without available soil/sediment background values
 - file name: "AppR_4Water_wo_bkg.xls"

APPENDIX S

RISK COEFFICIENTS AND DOSE CONVERSION FACTORS FOR RADIONUCLIDE CALCULATIONS

Table S-1. Radionuclide Risk Factors for Ingestion and External Exposure Pathways^a

Radionuclide	Water ingestion (Bq ⁻¹)	Dietary ingestion (Bq ⁻¹)	External exposure (kg Bq ⁻¹ s ⁻¹)
Americium-241	2.81×10^{-9}	3.63×10^{-9}	2.36×10^{-17}
Cesium-137	8.22×10^{-10}	1.01×10^{-9}	4.56×10^{-19}
Lead-210	2.38×10^{-8}	3.18×10^{-8}	1.21×10^{-18}
Neptunium-237	1.67×10^{-9}	2.24×10^{-9}	4.59×10^{-17}
Plutonium-238	3.55×10^{-9}	4.58×10^{-9}	6.18×10^{-20}
Plutonium-239	3.64×10^{-9}	4.7×10^{-9}	1.71×10^{-19}
Potassium-40	6.68×10^{-10}	9.26×10^{-10}	6.83×10^{-16}
Protactinium-234m	6.93×10^{-11}	0	5.88×10^{-17}
Radium-224	4.5×10^{-9}	6.42×10^{-9}	3.19×10^{-17}
Radium-226	1.04×10^{-8}	1.39×10^{-8}	1.96×10^{-17}
Radium-228	2.81×10^{-8}	3.86×10^{-8}	0
Strontium-90	1.51×10^{-9}	1.86×10^{-9}	4.30×10^{-19}
Thorium-228	2.9×10^{-9}	3.99×10^{-9}	4.79×10^{-18}
Thorium-230	2.46×10^{-9}	3.22×10^{-9}	7.01×10^{-19}
Thorium-232	2.73×10^{-9}	3.6×10^{-9}	2.93×10^{-19}
Thorium-234	6.25×10^{-10}	9.18×10^{-10}	1.40×10^{-17}
Tritium	1.37×10^{-12}	3.89×10^{-12}	0
Uranium-234	1.91×10^{-9}	2.58×10^{-9}	2.16×10^{-19}
Uranium-235	1.88×10^{-9}	2.55×10^{-9}	4.40×10^{-16}
Uranium-238	1.73×10^{-9}	2.34×10^{-9}	4.27×10^{-20}

^a From Federal Guidance Report No. 13 (EPA 1999).

Table S-2. Radionuclide Dose Conversion Factors for Immersion ^a and Dermal Contact Exposure Pathways

Radionuclide	Immersion (Sv s ⁻¹ per Bq L ⁻¹)	Dermal Contact (Sv y ⁻¹ per Bq cm ⁻²) ^b
Americium-241	2.03×10^{-15}	2.20×10^{-5}
Cesium-137	2.21×10^{-15}	1.40×10^{-2}
Lead-210	1.47×10^{-16}	0
Neptunium-237	2.33×10^{-15}	6.80×10^{-4}
Plutonium-238	1.03×10^{-17}	0
Plutonium-239	8.65×10^{-18}	0
Potassium-40	1.55×10^{-14}	1.80×10^{-2}
Protactinium-234m	1.70×10^{-15}	2.10×10^{-2}
Radium-224	9.66×10^{-16}	2.40×10^{-4}
Radium-226	6.62×10^{-16}	4.20×10^{-4}
Radium-228	7.70×10^{-24}	0
Strontium-90	1.00×10^{-16}	1.60×10^{-2}
Thorium-228	1.97×10^{-16}	4.00×10^{-4}
Thorium-230	4.05×10^{-17}	0
Thorium-232	1.99×10^{-17}	1.80×10^{-5}
Thorium-234	7.95×10^{-16}	3.10×10^{-3}
Tritium	0	0
Uranium-234	1.67×10^{-17}	2.10×10^{-5}
Uranium-235	1.49×10^{-14}	1.10×10^{-3}
Uranium-238	1.16×10^{-17}	1.60×10^{-5}

^a From Federal Guidance Report No. 12 (EPA 1993)

^b From Kocher and Eckerman (1987)

APPENDIX T

SLOPE FACTORS AND REFERENCE DOSES FOR CHEMICAL RISK CALCULATIONS

Table T-1. Slope Factors (kg d mg^{-1}) for Oral Intake and Dermal Contact^a		
Chemical	Oral intake	Dermal contact
Aldrin	17	34
Arsenic	1.50	3.66
Barium		
Benzo(a)anthracene	0.73	2.35
Benzo(a)pyrene	7.30	23.5
Benzo(b)fluoranthene	0.73	2.35
Benzo(k)fluoranthene	0.073	0.235
Chromium (total)		
Copper		
Dibenz(a,h)anthracene	7.30	23.5
Heptachlor Epoxide	9.10	12.6
Indeno(1,2,3-cd)pyrene	0.73	2.35
Lead		
Mercury		
Nitrosodimethylamine[N-]	51	102
RDX	0.11	
Uranium		

^a Compiled from ATSDR (2000), EPA (1997), EPA (2000), EPA (2001a), EPA (2001b), and ORNL (2001).

Table T-2. Reference Doses ($\text{mg kg}^{-1} \text{d}^{-1}$) for Oral Intake and Dermal Contact^a

Chemical	Oral Intake	Dermal Contact
Aldrin		1.50×10^{-5}
Arsenic		1.23×10^{-4}
Barium	0.07	4.90×10^{-3}
Benzo(a)anthracene		
Benzo(a)pyrene		
Benzo(b)fluoranthene		
Benzo(k)fluoranthene		
Chromium (total)	0.003	6.00×10^{-5}
Copper	b	
Dibenz(a,h)anthracene		
Heptachlor Epoxide		9.36×10^{-6}
Indeno(1,2,3-cd)pyrene		
Lead	0.015	
Mercury	0.04 ^c	2.10×10^{-5}
Nitrosodimethylamine[N-]		
RDX		3.00×10^{-3}
Uranium	0.0006	5.10×10^{-4}

^a Compiled from ATSDR (2000), EPA (1997a), EPA (2000), EPA (2001a), EPA (2001b), and ORNL (2001).

^b Health Effects Assessment Summary Tables (HEAST) concluded that toxicity data were inadequate for calculating an oral RfD for copper (RAIS 2002).

^c An EPA-approved oral chronic RfD for elemental mercury is currently not available; we chose to use the oral chronic RfD for mercuric sulfide as a surrogate because of the lack of knowledge about the specific form of mercury from LANL (ORNL 2001).

APPENDIX U

RISK CALCULATIONS FOR RADIONUCLIDES AND CHEMICALS FOR BASE CASE CONCENTRATIONS

All risk calculations, as discussed in Chapter 5, are provided electronically in the following files:

- 1) AppU_POE1.1 Risk.xls
- 2) AppU_POE1.2 Risk.xls
- 3) AppU_POE2.1BD-Adult Risk.xls
- 4) AppU_POE2.1BD-Child Risk.xls
- 5) AppU_POE2.1R-Adult Risk.xls
- 6) AppU_POE2.1R-Child Risk.xls
- 7) AppU_POE3.1 Risk.xls
- 8) AppU_POE4.1a Risk.xls
- 9) AppU_POE4.1b Risk.xls

APPENDIX V

EXAMPLE CALCULATIONS FOR CHAPTER 3, 4, AND 5

APPENDIX V1: ESTIMATING CONCENTRATIONS OF RADIONUCLIDES AND CHEMICALS IN SOURCE AREAS

GIS polygon shapefiles were developed for the PRS source areas and the Geomorphic Unit sources areas. The area for each of these source areas was represented as a circle, using a calculated radius based on the surface area for each source area. In a number of cases, this resulted in groups of source areas partially or completely overlapping. These groups of overlapping source areas were dissolved into a single polygon represented by the perimeter of the overlapping polygons. Revised areas were calculated for each source area polygon and the original PRS or Geomorphic Unit identification was linked to the new polygon in a spreadsheet table.

Since the surface area of the new polygon was less than the sum of the surface areas for the source areas dissolved into the new polygon and the total mass of chemicals and radionuclides is a function of the original source area surface area, an adjusted concentration for each chemical and radionuclide was calculated for the new polygon. This was necessary to ensure that the surface area of soil estimated from the polygons considered in the fate and transport estimates was not greater than the actual surface area.

To develop the adjusted concentrations of chemicals and radionuclides, we calculated an adjustment factor based on the original area of each overlapping source area relative to the sum of the original surface area of the group of overlapping source areas. This ratio was used as an adjustment factor to modify the average concentrations associated with each original source area, which were then summed to derive a representative concentration for each chemical and radionuclide across the new combined source areas.

This process, along with the subtraction of background and the adjustment for the erosion matrix score, is shown here in an example calculation for $^{239,240}\text{Pu}$ at PRS IDs 02-003(c), 02-007, and 02-009(c), combined to form PRS-10 for the transport calculations. Table V1-1 shows the original data available for the 3 PRSs as well as the ratio of the original area to the sum of the areas.

Table V1-1. Original PRS Data

Original PRS ID	Original area (m ²)	Mean $^{239,240}\text{Pu}$ Conc. (pCi g ⁻¹)	Ratio (area/sum)
02-003(c)	47.62	0.116	0.0509
02-007	96.52	0.014	0.1031
02-009(c)	791.73	0.775	0.8460
Total	935.87		

The new polygon formed by the merging of these three PRSs has an area of 928.59 m². Since the new total area is less than the sum of the original areas, we calculate a new area associated with each of the original PRSs by multiplying the area of the new polygon by the ratios calculated in Table V1-1. These new areas are shown in Table V1-2.

Table V1-2. New Areas Associated with PRSs based on New PRS Polygon

PRS ID	Ratio \times New total area =	New PRS area
02-003(c)	0.0509×928.59	47.25
02-007	0.1031×928.59	95.77
02-009(c)	0.8460×928.59	785.57

These new areas associated with each original PRS can be used to develop a ratio of this new area to the original PRS area. These ratios, multiplied by the ratios calculated in Table V1-1, form the concentration adjustment factor. These calculations are shown in Table V1-3.

Table V1-3. Concentration Adjustment Factor Calculations

PRS ID	Ratio (new area/original area)	Ratio \times Ratio =	Concentration Adjustment Factor
02-003(c)	1.008	1.008×0.0509	0.0513
02-007	1.008	1.008×0.1031	0.1039
02-009(c)	1.008	1.008×0.8460	0.8526

Erosion matrix scores are only included in these calculations if installation of a BMP precedes the date that the PRS was assessed. In the cases of these PRSs, either no erosion score was available or there was no BMP installed. Erosion scores and their use in these types of calculations are discussed more completely in Chapter 3.

The background concentration for $^{239,240}\text{Pu}$ was assumed to be $0.0125 \text{ pCi g}^{-1}$. This background concentration is subtracted from the mean concentration shown in Table V1-1 to obtain a net $^{239,240}\text{Pu}$ concentration, as shown in Table V1-4.

Table V1-4. Net $^{239,240}\text{Pu}$ Concentration Calculations

PRS ID	Mean $^{239,240}\text{Pu}$ Conc (pCi g^{-1})	Background $^{239,240}\text{Pu}$ Conc (pCi g^{-1})	Net $^{239,240}\text{Pu}$ Conc (pCi g^{-1})
02-003(c)	0.1162	0.0125	0.1037
02-007	0.014	0.0125	0.0015
02-009(c)	0.775465	0.0125	0.7629

Finally, the concentration adjustment factors calculated in Table V1-3 are multiplied by the net concentration to obtain an adjusted concentration for each PRS. Had there been a relevant erosion matrix adjustment factor, this factor would also be multiplied by this product. These adjusted concentrations are summed to obtain the total estimated concentration for the new PRS-10, as shown in Table V1-5.

Table V1-5. Adjusted Concentration Calculations

PRS ID	Concentration Adjustment Factor \times Net $^{239,240}\text{Pu}$ Conc =	Adjusted $^{239,240}\text{Pu}$ Conc (pCi g^{-1})
02-003(c)	0.0513×0.1037	0.005318
02-007	0.1039×0.0015	0.000156
02-009(c)	0.8526×0.7629	0.6505
TOTAL Conc for PRS-10		0.66

APPENDIX V2: CALCULATING CONCENTRATIONS OF RADIONUCLIDES AND CHEMICALS AT POE LOCATIONS

Concentrations were estimated at 6 points of exposure for 36 chemicals and radionuclides identified at one or more of 300 source areas for 7 storm events. Because of the magnitude of the calculations necessary to estimate the concentration, the following provides one example for the 2-year post fire storm event of the estimate of the activity of one radionuclide at two source areas and the estimate of the concentration of that radionuclide in surface water, suspended sediment and deposited sediment at a point of exposure. A discussion of the equations and their derivation is presented in Section 4.4.

Inputs

The following input values are used in the calculations. A discussion of the source of these values and a summary of the values for other source areas and points of exposure are presented in Section 4.4. Where the value is included in a table in Chapter 4.0, the table reference is also included.

Parameter	Variable	Units	Value	Source
Storm event			2-year post fire	
Storm Duration	SD	sec	2.2E+04	
Point of Exposure	POE		1.2	
Radionuclide	Pu-239		Plutonium-239	
Source Area	PRS		PRS-10	
Source Area	BA		Burn Area	
Partitioning Coefficient	k_d	l/kg	5.5E+02	Table 4-21
Concentration in PRS-10	C_{soil}	pCi/g	6.6E-01	Appendix G
Concentration in Burn Area	C_{soil}	pCi/g	5.9E-01	Appendix G
Average storm water flow at PRS-10	Q_{sa}	ft ³ /sec	5.8E+02	Table H2
Average storm water flow at Burn Area	Q_{sa}	ft ³ /sec	6.7E+00	Table H2
Storm water flow at POE	Q_{poe}	ft ³ /sec	8.7E+02	Table 4-16
Total activity in storm water at POE	$\sum A_T$	pCi	1.9E+11	Calculated
Total activity in water phase at POE	$\sum A_w$	pCi	2.9E+10	Calculated
Total activity in sediment POE	$\sum A_{ss}$	pCi	1.6E+11	Calculated
Total suspended sediment	TSS	mg/l	1.0E+04	Section 4.4.6
Soil total porosity	ϕ_T	cm ³ /cm ³	4.0E-01	Section 4.4.8.1
Soil particle density	ρ_s	g/cm ³	2.7E+00	Section 4.4.8.1
Soil bulk density	ρ_b	g/cm ³	1.6E+00	Section 4.4.8.1

Calculations

Pu-239 Activity at PRS-10 and the Burn Area

The total unit volume (V_T) of storm water and sediments that would pass over the source area is calculated by Equation 4-29:

$$V_T(L) = Q \left(\frac{\text{ft}^3}{\text{sec}} \right) \times SD(\text{sec}) \times CF \left(\frac{L}{\text{ft}^3} \right)$$

for PRS-10:

$$V_T(L) = 5.8E+02 \left(\frac{\text{ft}^3}{\text{sec}} \right) \times 2.2E+04(\text{sec}) \times 2.8E+01 \left(\frac{L}{\text{ft}^3} \right) = 3.6E+08(L)$$

for Burn Area:

$$V_T(L) = 6.7E+00 \left(\frac{\text{ft}^3}{\text{sec}} \right) \times 2.2E+04(\text{sec}) \times 2.8E+01 \left(\frac{L}{\text{ft}^3} \right) = 4.1E+06(L)$$

The total activity of a radionuclide in a unit volume at the source area that is available to be distributed between the soil particle phase and the water phase is calculated by Equation 4-17:

$$A_T(\text{pCi}) = C_{\text{soil}} \left(\frac{\text{pCi}}{\text{g}} \right) \times \text{TSS} \left(\frac{\text{mg}}{\text{L}} \right) \times CF \left(\frac{\text{g}}{\text{mg}} \right) \times V_T(L)$$

for PRS-10:

$$A_T(\text{pCi}) = 6.6E-01 \left(\frac{\text{pCi}}{\text{g}} \right) \times 1.0E+04 \left(\frac{\text{mg}}{\text{L}} \right) \times 1.0E-03 \left(\frac{\text{g}}{\text{mg}} \right) \times 3.6E+08(L) = 2.4E+09(\text{pCi})$$

for Burn Area:

$$A_T(\text{pCi}) = 5.9E-01 \left(\frac{\text{pCi}}{\text{g}} \right) \times 1.0E+04 \left(\frac{\text{mg}}{\text{L}} \right) \times 1.0E-03 \left(\frac{\text{g}}{\text{mg}} \right) \times 4.1E+06(L) = 2.4E+07(\text{pCi})$$

The maximum volume of suspended sediments (V_{ss}) that is present in the volume of water (V_T) is calculated by Equation 4-30:

$$V_{ss}(L) = \frac{TSS\left(\frac{mg}{L}\right)}{\rho_s\left(\frac{g}{cm^3}\right) \times CF\left(\frac{mg}{g}\right) \times CF\left(\frac{cm^3}{L}\right)} \times V_T(L)$$

for PRS-10:

$$V_{ss}(L) = \frac{1.0E+04\left(\frac{mg}{L}\right)}{2.65\left(\frac{g}{cm^3}\right) \times 1.0E+03\left(\frac{mg}{g}\right) \times 1.0E+03\left(\frac{cm^3}{L}\right)} \times 3.6E+08(L) = 1.4E+06(L)$$

for Burn Area:

$$V_{ss}(L) = \frac{1.0E+04\left(\frac{mg}{L}\right)}{2.65\left(\frac{g}{cm^3}\right) \times 1.0E+03\left(\frac{mg}{g}\right) \times 1.0E+03\left(\frac{cm^3}{L}\right)} \times 4.1E+06(L) = 1.5E+04(L)$$

The activity of radionuclide in the water phase (A_w) is calculated by Equation 4-25:

$$A_w(pCi) = \frac{A_T(pCi)}{\left(1 + \frac{K_d\left(\frac{L}{kg}\right) \times \rho_s\left(\frac{g}{cm^3}\right) \times V_{ss}(L) \times CF\left(\frac{cm^3}{L}\right) \times CF\left(\frac{kg}{g}\right)}{V_w(L)}\right)}$$

where the volume of water (V_w) is equal to the total volume of water and sediment (V_T) (Section 4.4.9).

for PRS-10

$$A_w(pCi) = \frac{2.4E+09(pCi)}{\left(1 + \frac{5.5E+02\left(\frac{L}{kg}\right) \times 2.7E+00\left(\frac{g}{cm^3}\right) \times 1.4E+06(L) \times 1.0E+03\left(\frac{cm^3}{L}\right) \times 1.0E-03\left(\frac{kg}{g}\right)}{3.6E+08(L)}\right)} = 3.5E+08(pCi)$$

for Burn Area:

$$A_w(\text{pCi}) = \frac{2.4\text{E} + 07(\text{pCi})}{1 + \frac{5.5\text{E} + 02\left(\frac{\text{L}}{\text{kg}}\right) \times 2.7\text{E} + 00\left(\frac{\text{g}}{\text{cm}^3}\right) \times 1.5\text{E} + 04(\text{L}) \times 1.0\text{E} + 03\left(\frac{\text{cm}^3}{\text{L}}\right) \times 1.0\text{E} - 03\left(\frac{\text{kg}}{\text{g}}\right)}{4.1\text{E} + 06(\text{L})} = 3.8\text{E} + 06(\text{pCi})$$

The activity of a radionuclide sorbed to suspended sediment in a unit volume at a source area (A_{ss}) is calculated by Equation 4-27:

$$A_{ss}(\text{pCi}) = A_T(\text{pCi}) - A_w(\text{pCi})$$

for PRS-10:

$$A_{ss}(\text{pCi}) = 2.4\text{E} + 09(\text{pCi}) - 3.5\text{E} + 08(\text{pCi}) = 2.1\text{E} + 09(\text{pCi})$$

for Burn Area:

$$A_{ss}(\text{pCi}) = 2.4\text{E} + 07(\text{pCi}) - 3.8\text{E} + 06(\text{pCi}) = 2.1\text{E} + 07(\text{pCi})$$

Pu-239 Concentration in Storm Water at POE 1.2

The total volume of water and sediment ($V_{\text{poe-T}}$) at the point of exposure is equal to the total volume of water and suspended sediment ($V_{\text{poe-w}}$) (Section 4.4.9) and is calculated Equation 4-34:

$$V_{\text{poe-T}} = V_{\text{poe-w}}(\text{L}) = Q_{\text{poe}}\left(\frac{\text{ft}^3}{\text{sec}}\right) \times \text{SD}(\text{sec}) \times \text{CF}\left(\frac{\text{L}}{\text{ft}^3}\right)$$

$$V_{\text{poe-T}}(\text{L}) = 8.7\text{E} + 02\left(\frac{\text{ft}^3}{\text{sec}}\right) \times 2.2\text{E} + 04(\text{sec}) \times 2.8\text{E} + 01\left(\frac{\text{L}}{\text{ft}^3}\right) = 5.3\text{E} + 08(\text{L})$$

The concentration of the radionuclide in the storm water at the point of exposure ($C_{\text{poe-T}}$) is calculated by Equation 4-33:

$$C_{\text{poe-T}}\left(\frac{\text{pCi}}{\text{L}}\right) = \frac{\sum A_T(\text{pCi})}{V_{\text{poe-T}}(\text{L})}$$

$$C_{\text{poe-T}}\left(\frac{\text{pCi}}{\text{L}}\right) = \frac{1.9\text{E} + 11(\text{pCi})}{5.3\text{E} + 08(\text{L})} = 3.6\text{E} + 02\left(\frac{\text{pCi}}{\text{L}}\right)$$

Pu-239 Concentration in Dissolved in Storm Water at POE 1.2

The concentration of the radionuclide in the dissolved phase at the point of exposure (C_{poe-w}) is calculated by Equation 4-40:

$$C_{poe-w} \left(\frac{pCi}{L} \right) = \frac{\sum A_w (pCi)}{V_{poe-w} (L)}$$

$$C_{poe-w} \left(\frac{pCi}{L} \right) = \frac{2.9E+10(pCi)}{5.3E+08(L)} = 5.5E+01 \left(\frac{pCi}{L} \right)$$

Pu-239 Concentration in Suspended Sediment at POE 1.2

The concentration of a radionuclide in suspended sediment at the point of exposure (C_{poe-ss}) is calculated by Equation 4-42:

$$C_{poe-ss} \left(\frac{pCi}{g} \right) = \frac{\sum A_{ss} (pCi)}{TSS \left(\frac{mg}{L} \right) \times V_T (L) \times CF \left(\frac{g}{mg} \right)}$$

$$C_{poe-ss} \left(\frac{pCi}{g} \right) = \frac{1.6E+11}{1.0E+04 \left(\frac{mg}{L} \right) \times 5.3E+08(L) \times 1.0E-03 \left(\frac{g}{mg} \right)} = 3.0E+01 \left(\frac{pCi}{g} \right)$$

Pu-239 Concentration in Deposited Sediment at POE 1.2

The total concentration of radionuclides in deposited sediment (C_{poe-ds}) at the point of exposure is calculated by Equation 4-50:

$$C_{poe-ds} \left(\frac{pCi}{g} \right) = \frac{C_{poe-w} \left(\frac{pCi}{L} \right)}{\rho_b \left(\frac{g}{cm^3} \right) \times CF \left(\frac{cm^3}{L} \right)} \times \varphi_E + C_{poe-ss} \left(\frac{pCi}{g} \right) \times (1 - \varphi_E)$$

$$C_{poe-ds} \left(\frac{pCi}{g} \right) = \frac{5.5E+01 \left(\frac{pCi}{L} \right)}{1.6E+00 \left(\frac{g}{cm^3} \right) \times 1.0E+03 \left(\frac{cm^3}{L} \right)} \times 4.0E-01 + 3.0E+01 \left(\frac{pCi}{g} \right) \times (1 - 4.0E-01) = 1.8E+01 \left(\frac{pCi}{g} \right)$$

APPENDIX V3: EXAMPLE CALCULATIONS FOR RISK FROM ^{239,240}Pu FROM ALL SOURCE AREAS AT POE 1.2

For this example, we show the calculation of risk for the sediment exposure pathways from all source areas contributing to the concentration of ^{239,240}Pu in sediments at POE 1.2 for the scenario defined for that location: the local fisher/hunter. The local fisher/hunter has the following exposure characteristics, with scenario parameters for sediment exposure shown in Table V3-1.

Local hunter from White Rock:

- This person captures, and consumes fish, deer, elk, and other wildlife from the LANL region.
- It is assumed that the individual uses Rio Grande water for 10% of drinking water needs.
- It is assumed this individual uses the fish or larger game animals as a food source.
 - This person lives in White Rock and may hunt in at least two locations:
 - On the west side of the Rio Grande just below LANL, and in so doing, may inadvertently ingest river water and sediments from just below LANL (POE 1.1).
 - On the lower Los Alamos Canyon; again may be exposed to water and sediments in the lower Los Alamos Canyon stream. (POE 1.2)
- This scenario uses parameter values that reflect a hunter lifestyle in terms of time at the designated POE location. Because of a lack of data on transfer coefficients for chemicals and radionuclides in wild game animals like elk, we assumed ingestion of beef cattle, which have used the water source at the designated POE locations.
- Potential important pathways include ingestion of Rio Grande water, fish from the Rio Grande at POE 1.1, and beef cattle grazing near POE 1.1; external exposure from contaminated sediments/soils near the Rio Grande (POE 1.1) and near the lower Los Alamos Canyon stream (POE 1.2), and inadvertent ingestion of sediments/soils at those locations.

Table V3-1. Scenarios and Selected Exposure Parameters for Example Calculation

Scenario→ Parameter↓	Hunter
General Location	White Rock
Point of exposure (POE)	1.2
Time at location (h d ⁻¹)	12
Exposure frequency (d y ⁻¹)	100
Exposure duration (y)	7
Body weight (kg)	70
Sediment exposure pathways	
Sediment ingestion (g d ⁻¹)	0.1
External exposure to sediment (h d ⁻¹)	4
Dermal contact with sediment (h d ⁻¹)	0.14
Fraction of sediment that is impacted	0.5

Sediment Exposure Pathways

Several potential exposure pathways are associated with the accumulation of contaminated sediments along the shores or in shallower sections of the streams and river with slow moving waters. Potential exposure pathways associated with the accumulation of contaminated sediments along the stream and river banks and along the shores of Cochiti Reservoir are the inadvertent ingestion of sediments, external exposure to radionuclides in sediments, and dermal contact with the sediments.

Sediment Ingestion

Inadvertent ingestion of sediments and soils can occur where river sediments have accumulated and could result from activities such as sitting, playing, digging, children playing, picking berries, or fire-fighting related activities. For the inadvertent ingestion of $^{239,240}\text{Pu}$ in sediments, we assumed an ingestion rate of 0.1 g d^{-1} for adults in the hunter scenario, and we further assume that the fraction of sediment contaminated at the POE (F_{csed}) is 0.5.

The equation that describes the risk per year from radionuclides from ingestion of contaminated sediments is shown below.

$$\frac{\text{Risk}}{y} = C_{sed} \cdot U_{sed} \cdot F_{csed} \cdot EF \cdot RF_{ing,d} \cdot CF_{activity} \quad (\text{V3-1})$$

where

C_{sed}	=	concentration of $^{239,240}\text{Pu}$ sediments (pCi g^{-1})
U_{sed}	=	ingestion rate of sediment (g d^{-1})
F_{csed}	=	fraction of sediment ingested that is contaminated (unitless)
EF	=	exposure frequency (d y^{-1})
$RF_{ing,d}$	=	lifetime morbidity risk coefficient for dietary ingestion (Risk Bq^{-1})
$CF_{activity}$	=	conversion factor (Bq pCi^{-1}).

For these example calculations, we use the incremental increase in concentration of $^{239,240}\text{Pu}$ in sediment at POE 1.2 from a 2-year storm event. Risk coefficients are taken from EPA (1999). Inserting the appropriate numerical values into the Equation R3-1 yields:

$$\frac{\text{Risk}}{y} = \left(12.23 \frac{\text{pCi}}{\text{g}}\right) \cdot \left(0.1 \frac{\text{g}}{\text{d}}\right) \cdot 0.5 \cdot \left(100 \frac{\text{d}}{\text{y}}\right) \cdot \left(4.7 \times 10^{-9} \text{ Bq}^{-1}\right) \cdot \left(0.03704 \frac{\text{Bq}}{\text{pCi}}\right) = 1.1 \times 10^{-8}$$

This value represents the increased incidence risk of cancer from one year of exposure to the contaminated sediments, using the exposure parameters consistent with a hunter at the given point of exposure. This is consistent with the calculations shown in Appendix U. To calculate risk for a seven-year exposure period, this number could simply be multiplied by 7.

External Exposure from Sediments

External shoreline-type exposure to sediments applies only to the radionuclide pathway, since radiation is still measurable for some types of decay at some distance from the source. It is assumed that external exposure to contaminated sediments could occur throughout the exposure period for radionuclides in sediments. We assume an exposure period of 4 hours per day for the hunter.

Under some circumstance, a distinction can be made between low and high water levels which uncover more or less of the sediment, respectively, and a unitless shielding factor may be applied. Based on the discussion of the surface water flow characteristics in Chapter 5, for the external exposure to sediments pathway, we assume no shielding factor for high water conditions.

The risk per year for external exposure to radionuclides in shoreline sediments is given by the following equation:

$$\frac{Risk}{y} = C_{sed} \cdot ET \cdot F_{si} \cdot EF \cdot RF_{ext} \cdot CF_{time} \cdot CF_{activity} \cdot CF_{mass} \quad (V3-2)$$

where

C_{sed}	=	sediment concentration (pCi g ⁻¹)
ET	=	exposure time (h d ⁻¹)
F_{si}	=	sorption adjustment factor (dimensionless) for radionuclide i
EF	=	exposure frequency (d y ⁻¹)
RF_{ext}	=	risk per unit dose for external exposure (Risk kg Bq ⁻¹ s ⁻¹)
CF_{time}	=	conversion factor (s h ⁻¹)
$CF_{activity}$	=	conversion factor (Bq pCi ⁻¹)
CF_{mass}	=	conversion factor (g kg ⁻¹).

Risk coefficients are taken from EPA (1999). Inserting the appropriate numerical values into Equation V3-2 yields:

$$\frac{Risk}{y} = \left(12.23 \frac{pCi}{g}\right) \cdot \left(4 \frac{h}{d}\right) \cdot 1 \cdot \left(100 \frac{d}{y}\right) \cdot \left(1.71 \times 10^{-19} \frac{kg}{Bq \cdot s}\right) \cdot \left(3600 \frac{s}{h}\right) \cdot \left(0.03704 \frac{Bq}{pCi}\right) \cdot \left(1000 \frac{g}{kg}\right)$$

$$\frac{Risk}{y} = 1.12 \times 10^{-10}$$

Dermal Contact/Absorption

Some activities could result in contaminated sediment adhering to the skin and allowing exposure of the skin to penetrating radiations (e.g., electrons). This exposure pathway is referred to as dermal contact.

For radionuclides, electrons would have insufficient energy to result in significant external exposure from standing on the shoreline (as calculated in the preceding section), but when sediment is applied directly to the skin, exposure becomes more likely. We consider dermal contact as a special case because no risk factors for radionuclides exist for these types of exposures. Our ability to assess this pathway is limited, but we use the information available on the dose delivered by dermal contact to assess the potential risk due to this pathway. Kocher and Eckerman (1987) estimated dose rate conversion factors for all of the radionuclides considered for this work. Kocher and Eckerman assume that radioactivity is uniformly distributed over the entire body surface instead of just over some fraction of the body's surface area.

The risk per year for dermal contact with radionuclides in sediments is given by the following equation:

$$\frac{\text{Risk}}{y} = C_{sed} \cdot \rho \cdot d \cdot ET \cdot EF \cdot DCF_{der} \cdot RC \cdot CF_{time} \cdot CF_{activity} \cdot CF_{area} \quad (\text{V3-3})$$

where

C_{sed}	=	sediment concentration (pCi g ⁻¹)
ρ	=	density of sediment (g m ⁻³)
d	=	depth of sediment for exposure (m)
ET	=	exposure time (h d ⁻¹)
EF	=	exposure frequency (d y ⁻¹)
DCF_{der}	=	dose conversion factor for dermal contact with radionuclides (Sv y ⁻¹ per Bq cm ⁻²)
RC	=	lifetime risk coefficient (Risk Sv ⁻¹)
CF_{time}	=	conversion factor (y h ⁻¹)
$CF_{activity}$	=	conversion factor (Bq pCi ⁻¹)
CF_{area}	=	conversion factor (m ² cm ⁻²).

Because the sediment concentrations emerging from our transport calculations are in units of pCi g⁻¹, we had to make assumptions about the density and depth of the sediment to arrive at a surface concentration. We assumed that the sediment density was 1.5×10^6 g m⁻³ and that the top 1 cm (0.01 m) of sediment was available for the dermal contact pathway. Additionally, the dose conversion factors for dermal contact with radionuclide-contaminated sediments assume uniform contamination of the entire body surface, an exposure condition that is likely not very realistic.

A lifetime risk coefficient of 7.3×10^{-2} Sv⁻¹ was assumed based on ICRP Publication 60 (1991). This risk coefficient is an aggregated detriment that includes the probability of severe hereditary effects in addition to fatal and non-fatal cancers.

Inserting the appropriate numerical values into Equations R3-3 yields:

$$\begin{aligned} \frac{\text{Risk}}{y} = & \left(12.23 \frac{\text{pCi}}{\text{g}} \right) \cdot \left(1.5 \times 10^6 \frac{\text{g}}{\text{m}^3} \right) \cdot 0.01 \text{ m} \cdot \left(0.14 \frac{\text{h}}{\text{d}} \right) \cdot \left(100 \frac{\text{d}}{\text{y}} \right) \cdot \left(0 \frac{\text{Sv} \cdot \text{y}^{-1}}{\text{Bq} \cdot \text{cm}^{-2}} \right) \cdot 0.073 \text{ Sv}^{-1} \\ & \cdot \left(1.14 \times 10^{-4} \frac{\text{y}}{\text{h}} \right) \cdot \left(0.03704 \frac{\text{Bq}}{\text{pCi}} \right) \cdot \left(1 \times 10^{-4} \frac{\text{m}^2}{\text{cm}^2} \right) = 0 \end{aligned}$$

Since the dose conversion factor for dermal contact with $^{239,240}\text{Pu}$ is zero, this exposure is also zero for this radionuclide.

APPENDIX W

INFORMATION RELATED TO PRS SOURCE AREAS

The potential release sites (PRSs) source areas evaluated for the surface water pathway included:

- PRSs within the infrared (IR)-defined burned area that were confirmed to be burned and were used for the atmospheric pathway assessment
- PRSs within the IR burn boundary that did not burn
- PRSs within defined floodplain areas
- PRSs identified by LANL as high priority for field verification immediately following the fire

We included all PRSs falling within the above-described categories in this assessment if surface soil sampling data were available to characterize them. Additional information regarding the specific PRSs included in our evaluation, referenced in Chapter 3, is provided in electronic format in the Excel file accompanying this report, called “AppW_PRS Info.xls.”

FINAL REPORT

Analysis of Exposure and Risks to the Public from Radionuclides and Chemicals Released by the Cerro Grande Fire at Los Alamos

Task 1.7: Estimated Risks from Releases to Air

**Revision 1
June 12, 2002**

***Submitted to the New Mexico Environment Department
in Partial Fulfillment of Contract No. 01 667 5500 0001***

"Setting the standard in environmental health"



Risk Assessment Corporation

417 Till Road, Neeses, SC 29107
Phone 803.536.4883 Fax 803.534.1995

FINAL REPORT

Analysis of Exposure and Risks to the Public from Radionuclides and Chemicals Released by the Cerro Grande Fire at Los Alamos

Task 1.7: Estimated Risks from Releases to Air

**Revision 1
June 12, 2002**

Contributing Authors

Arthur S. Rood, K-Spar, Inc.
Jill W. Aanenson, Scientific Consulting, Inc.
S. Shawn Mohler, Independent Consultant
Patricia D. McGavran, Environmental Risk Assessment, Inc.
H. Justin Mohler, Bridger Scientific, Inc.
Helen A. Grogan, Cascade Scientific, Inc.

Principal Investigator

John E. Till, Ph.D., *Risk Assessment Corporation*

***Submitted to the New Mexico Environment Department
in Partial Fulfillment of Contract No. 01 667 5500 0001***

EXECUTIVE SUMMARY

The Cerro Grande Fire, which burned about 45,000 acres (~180 km²) in northern New Mexico, originated in the Bandelier National Monument on the evening of May 4, 2000, and spread east-northeast over the next 16 days consuming residential structures within the County of Los Alamos and approximately 7500 acres (~30 km²) within the Los Alamos National Laboratory (LANL) boundary. Some of the areas that burned were known or suspected to be contaminated with radionuclides and chemicals. Concern was expressed by the public with regard to:

- Radionuclides and chemicals associated with soil and vegetation burned by the fire and subsequently suspended and transported via air
- Radionuclides and chemicals associated with soil, sediments, and ash mobilized and transported via surface water following the fire
- Potential exposures and health risks to people related to the transport of radionuclides and chemicals via both air and surface water.

In response to these concerns, the New Mexico Environment Department (NMED) contracted with *Risk Assessment Corporation (RAC)* to make an independent assessment of the potential incremental health risks to the communities of northern New Mexico from these radionuclides and chemicals. This report evaluates the risks to people exposed to radionuclides and chemicals in air from the Cerro Grande Fire.

Objectives of this Report

The original objective was to analyze the immediate consequences and the longer-term impacts of the Cerro Grande Fire in terms of increased public exposures and potential risks to those in the vicinity from radionuclides and chemicals associated with the LANL facility.

Specifically, this report focuses on the magnitude of incremental exposure and associated risks to the public, emergency response personnel, and firefighters from transport of radionuclides and chemicals associated with the LANL facility released as a result of the fire through the air transport pathway. The scope was subsequently changed to include an assessment of risks from naturally occurring radionuclides and metals released from burning of the forests around the LANL site. This report does not address the risks associated with the burning of buildings and home sites in Los Alamos.

Methodology and Approach

The risk analysis process for the air pathway included evaluating the available air monitoring data and procedures, identifying the sources and magnitude of airborne contaminant releases, modeling the release and transport of airborne contaminants entrained in the fire plume, identifying representative individuals for defining exposure scenarios, and estimating the associated health risks and the uncertainties. The process was divided into a number of steps that are described in the different chapters of this report.

Before proceeding with any numerical calculations, we first established a model domain. The total extent of the model domain was 37 × 35 mi (60 × 55 km) and encompassed an area of

815,430 acres (3300 km²). The domain encompassed the cities of Santa Fe and Española, and Cochiti Lake. The domain extended 9.3 mi (15 km) east and 4.5 mi (7.2 km) south of Santa Fe, 6.2 mi (10 km) north of Española, and 9.3 mi (15 km) west of the city of Los Alamos. The choice of the extent of the domain was in part dictated by the limitations of the computer model selected for atmospheric dispersion calculations and the ability of the model to resolve terrain features.

Available Monitoring Data

The data available to assess the concentrations of radionuclides and chemicals in the air during the Cerro Grande Fire included air and soil monitoring data collected before, during, and after the fire; soil characterization data for contaminated sites at LANL that burned during the fire; meteorological data; and data for airborne contaminants measured in other fires.

When we started the project, we anticipated that the environmental air monitoring data would be sufficiently comprehensive to allow source term estimates based on measured concentrations in air combined with atmospheric dispersion modeling and that this would provide the basis to calculate the risks from the fire. As we evaluated the available data, it became apparent that the air monitoring data could not be used directly because not enough different locations were monitored, analytical results were available for only a limited number of chemicals and radionuclides, and some of the data were insufficiently documented. Furthermore, the majority of the concentrations measured were below minimum detection limits because of the short sample times that were employed to avoid filter clogging. The available environmental data and the difficulties associated with them are described fully in Chapter 2.

Screening and Source Term Calculation

The environmental monitoring data were less useful than originally anticipated, therefore the soil characterization data for contaminated areas (potential release sites) that burned during the fire became the main source of information available on radionuclides and chemicals potentially released. Because we identified a large number of radionuclides and chemicals that were potentially released during the fire, a screening procedure was used to identify those that were most important in terms of health risk. We developed source term estimates for the radionuclides and chemicals that were identified as possible contaminants resulting from LANL operations. We removed contaminants from consideration that fell below a cancer incidence screening risk index of 10^{-5} or a screening hazard quotient of 1.0, when risk was calculated conservatively, as described in Chapter 3.

For this list of radionuclides and chemicals that were most important in terms of health risk, we calculated source terms using available information on inventory at the contaminated sites, volatility, maximum fire temperatures, boiling point of the chemicals and radionuclides, and particulate release rates measured during fires. We used these source terms in transport and dispersion calculations to calculate estimated air concentrations.

Atmospheric Transport and Air Concentration Calculation

Calculating dispersion of radionuclides and chemicals suspended into the air during burning of the potential release sites first required an understanding of the behavior of the fire itself. This understanding was gained by modeling the release and atmospheric transport of pollutants released by the fire. Fortunately, one of the pollutants released by the fire, (particulate matter less than 10 μm [PM10]), was also measured in air at a number of locations in the model domain. The model could then be calibrated to these measurements and, thereby, provide a measure of model uncertainty regarding the dispersion of material entrained in the smoke plume.

We then assumed the release and transport of radionuclides and chemicals derived from LANL sources to be proportional to the release and transport of PM10 from the fire. The dispersion of PM10, therefore, served as a “tracer” for particulate releases of radionuclides and chemicals. For volatile chemicals, carbon monoxide was used as a tracer.

The process of model calibration to PM10 measurements entailed (1) identifying the geographical area that was burned, (2) defining the temporal history of the fire, (3) estimating the quantity of PM10 released by the fire and the heat generated during burning, (4) modeling the atmospheric dispersion of pollutants released by the fire, and (5) calibrating predicted concentrations of PM10 with measured values. We estimated pollutant release rates and heat generation, and used the CALPUFF/CALMET model to calculate dispersion and deposition of these pollutants within the model domain. Contributions of PM10 from other sources besides the fire were accounted for in the calibration.

Overall, the distribution of the predicted-to-observed ratio of PM10 concentrations had a geometric mean of 0.87 and a geometric standard deviation of 1.7. Fifty percent of the predicted-to-observed ratios were greater than 1.0 and fifty percent were less than 1.0. Ninety percent of the predicted-to-observed ratios were between 0.32 and 1.8. Therefore, the model exhibited a slight negative bias and had an uncertainty of roughly a factor of 2. No spatially discernable trend was observed between model over and under prediction. Atmospheric transport is described in Chapter 4.

Using the methodology previously outlined, we calculated concentrations of radionuclides and chemicals identified as important through the screening process. In general, most air concentrations were below standard instrument detection limits. However, the explosive compounds, RDX, HMX, DNB and TNT exhibited relatively high air concentrations and deposition amounts. After the fire, however, explosive compounds were not detected in the limited soil sampling performed. Model deposition indicated that these compounds would have been easily detected in soil and suggested that the source terms for these compounds were overestimated.

Risk Estimates

We used four exposure scenarios to determine the risks to representative individuals from the LANL-derived radionuclides and chemicals released during the fire; a resident adult, a firefighter, an emergency response worker, and a resident child. The exposure parameters that define these scenarios are described in Chapter 5. Risks associated from radionuclides and chemicals on natural vegetation that burned during the Cerro Grande Fire were calculated for the

adult resident scenario only. These risks are not specific to LANL and would be incurred from any forest fire.

For each scenario we calculated cancer risk for radionuclides and carcinogenic chemicals, and hazard quotients for noncarcinogenic chemicals, at eight representative exposure locations, and the maximum value in the study area. The hazard quotient is the ratio of the average daily intake of a contaminant per unit body weight to an acceptable reference value or reference dose (RfD). For LANL-derived chemicals and radionuclides, the maximum risk occurred within the active burned area and on LANL property. The maximum total cancer incidence risk from LANL-derived radionuclides released during the fire was less than 1×10^{-13} (Table ES-1). In contrast, cancer incidence risks from radionuclides released from natural vegetation during the fire were estimated to be in the 10^{-7} range. Cancer incidence risks from LANL-derived chemicals released during the fire were generally less than 10^{-7} . The explosive compound RDX was a major contributor to this risk estimate and we believe the source term for this compound was overestimated. Cancer incidence risks from metals detected in natural vegetation and released during the fire were also in the 10^{-7} range.

The total hazard quotient used to assess noncancer health effects was generally less than or equal to 0.1 throughout the model domain for LANL derived chemicals. Near areas where the fire burned, however, hazard quotient values exceeded 1.0 and reached a maximum value of 2.0 for the resident adult scenario. The area of this excursion above the 1.0 level was limited to a small area within the LANL site near its western boundary. Most of the noncancer risk was associated with the explosive compounds RDX, HMX, DNB and TNT. As stated previously, we believe the sources terms for these compounds were overestimated.

Hazard quotients for metals released during the fire from natural vegetation were extremely high and were attributed to inhalation of manganese and, to a lesser extent, aluminum. The noncancer health effects from these two metals were based on a chronic RfDs that equated to an air concentration that was 1,000 to 10,000 times less than the occupational standards for these metals. We attributed the high hazard quotient calculated for these metals to the use of the chronic RfD. Using a reference dose based on occupational standards resulted in a maximum hazard quotient of less than 1.0. The calculated risks for all exposure scenarios at these eight locations are presented in Chapter 5.

Concentrations of PM10 in the model domain were sufficient to cause adverse health effects; however, these effects were not quantified. While researchers have published factors that estimate health effects such as the increase in daily mortality from exposure to PM10, application of these factors to environmental concentrations has not been fully explored, and for this reason, we excluded quantitative estimates of risk from exposure to PM10.

Table ES-1. Maximum Estimated Risks by Scenario, Contaminant Type and Source for the Air Pathway

Releases from potential release sites		Lifetime cancer incidence risk (carcinogens)		Hazard quotient (noncarcinogens)
Scenario		Radionuclides	Chemicals	Chemicals
Resident adult		6.7×10^{-14}	2.1×10^{-7}	2.0
Firefighter		1.0×10^{-13}	3.6×10^{-7}	3.4
Emergency response person		6.9×10^{-14}	2.2×10^{-7}	2.1
Resident child		2.6×10^{-14}	3.1×10^{-7}	2.9
Important radionuclides and chemicals		$^{238,239}\text{Pu}$, ^{231}Pa , ^{226}Ra	RDX	RDX, HMX, TNT, DNB
Releases from natural vegetation ^a		Lifetime cancer incidence risk (carcinogens)		Hazard quotient (noncarcinogens)
Scenario		Radionuclides	Chemicals	Chemicals
Resident adult		4.9×10^{-7}	4.4×10^{-7}	142 ^c
		4.1×10^{-7b}		0.78 ^d
Important radionuclides and chemicals		^{210}Pb , ^{210}Po , ^{226}Ra	Cr	Mn ^c , Al ^c , Ba ^d , Cr ^d , Fe ^d

^a See Appendix D for details.

^b Based on release of radionuclides inventories in litter and bark only.

^c Hazard quotient based on chronic reference dose for manganese and aluminum. Manganese and aluminum dominate the HQ.

^d Hazard quotient based on references doses derived from the 8-hour National Institute for Occupational Safety and Health standard for manganese and aluminum. Dominant metals are barium, chromium, and iron.

A summary of the conservatism and uncertainty associated with the different components of the exposure and risk calculations is provided in Table ES-2. A more complete discussion of the results is provided in Chapter 6 of this report.

**Table ES-2. Summary of Conservatism and Uncertainty in the Modeling Components of the
Exposure and Risk Calculations for the Air Pathway**

Modeling component	Estimated conservatism ^a	Estimated uncertainty ^b	Comments
Radionuclide or chemical inventories	Unknown (2–≥10)	≥10×	Radionuclide and chemical inventories at PRSs were based on average detected concentrations and are likely biased high because non-detect values were omitted.
Release of radionuclides and particulate chemicals	≤2	≥10×	Particulate releases were based on a resuspension rate constant reported in the literature. Releases were assumed to occur during the burning and smoldering phase of the fire.
Release of volatile chemicals	≥10	≥10×	One-hundred percent of the volatile chemical inventory was assumed to be released.
Atmospheric transport- particles	≤2	2×	Estimated conservatism and uncertainty is based on the assumption that particulate releases followed the same trend as PM10 emissions from the fire and behaved like PM10 in the atmosphere.
Atmospheric transport- volatiles	2–10	2×	Estimated conservatism and uncertainty is based on the assumption that volatile releases followed the same trend as CO emissions from the fire and behaved like a non-reactive tracer.
Exposure scenario assumptions	2–10	2–10×	
Radionuclide risk coefficients	2–10	2–10×	Population averaged risk coefficients were used to calculate risks for specific individuals.
Slope factors	≥10	≥10×	
Hazard quotients	≥10	≥10×	Use of chronic RfDs to express subchronic exposure may have resulted in large overestimates of noncancer health effects.
Overall cancer risk	2–10	≥10×	
Overall noncancer health effect	≥10	≥10×	Use of chronic RfDs to represent subchronic exposure biased the noncancer health effects high for some chemicals

^a The rating system is as follows: ≥10 equates to a factor of 10 or greater conservatism; 2–10 equates to a factor greater than 2 but less than 10 conservatism; ≤2 equates a factor of 2 or less conservatism.

^b The rating system is as follows: ≥10× equates to a factor of 10 (×+10) or greater uncertainty; 2–10× equates to a factor >2 but <10 uncertainty; 2× equates to factor of ≤2 (×+2) uncertainty.

Conclusions

Our analysis indicates that exposure to LANL-derived contaminants during the Cerro Grande Fire did not result in a significant increase in health risk over that incurred from the fire itself. The risk of cancer from exposure to radionuclides and metals in and on vegetation that burned was greater than that from radionuclides and chemicals released from contaminated sites at LANL. All cancer risks were below the U.S. Environmental Protection Agency range of acceptable risks of 10^{-6} to 10^{-4} . Hazard quotients from exposure to noncarcinogenic LANL-derived chemicals exceeded the 1.0 level at some locations on LANL property. However, the

estimated hazard quotients are conservative and likely overestimate the actual risks that occurred. It is likely that the risks from exposure to PM10 far outweigh the risks from LANL-derived radionuclides and chemicals and those released from natural vegetation during the fire.

CONTENTS

EXECUTIVE SUMMARY	iii
CONTENTS	xi
FIGURES	xiii
TABLES	xv
ACRONYMS	xvii
1 INTRODUCTION	1-1
1.1 Objectives	1-1
1.2 Approach	1-2
1.3 Air Model Domain.....	1-4
2 SUMMARY OF ENVIRONMENTAL MONITORING DATA	2-1
2.1 Air Monitoring Data	2-1
2.2 Biota and Soil Monitoring Data.....	2-6
2.3 Difficulties Related to Data Collection and Interpretation	2-8
2.4 Data Evaluation	2-10
2.5 Use of Environmental Monitoring Data to Evaluate Risk from the Cerro Grande Fire	2-24
3 SOURCE TERM DEVELOPMENT	3-1
3.1 Identifying and Defining Source Areas	3-1
3.2 Screening	3-2
3.3 Atmospheric Fate of Potential Contaminants of Concern	3-17
3.4 Source Term/Release Rate Calculations.....	3-28
4 ATMOSPHERIC TRANSPORT	4-1
4.1 Measured PM10 Concentrations	4-2
4.2 CALPUFF Modeling Protocol.....	4-10
4.3 Calculating Concentrations of Contaminants Released from PRSs	4-40
4.4 Air Concentration Estimates.....	4-48
4.5 Deposition Estimates	4-60
5 RISK ESTIMATES	5-1
5.1 Exposure Scenarios.....	5-1
5.2 Risk Calculation Methodology	5-6
5.3 Risk Estimates	5-7
6 SUMMARY AND CONCLUSIONS.....	6-1
6.1 Risk Estimates	6-1
6.2 Risks to Representative Individuals.....	6-3
6.3 Risks to Communities Outside the Model Domain	6-4
6.4 Conservatism and Uncertainty in the Risk Estimates	6-4
6.5 Conclusions	6-7
7 REFERENCES	7-1

APPENDICES

APPENDIX A.	Identifying Contaminants Released as a Direct Result of the Cerro Grande Fire Burning at Los Alamos National Laboratory.....	A-1
APPENDIX B.	Potential Contaminants of Concern Measured at Potential Release Site Locations.....	B-1
APPENDIX C.	Toxicity Values Used to Screen Nonradiological Potential Contaminants of Concern.....	C-1
APPENDIX D.	Methodology for Calculating Impacts From Contaminants on Standing Vegetation and Forest Litter Released During the Cerro Grande Fire.....	D-1
APPENDIX E.	Risk Factors for Contaminants Potentially Released to Air From Los Alamos National Laboratory During the Cerro Grande Fire and Identified as Important to Health Risk.....	E-1
APPENDIX F.	Health Effects Associated With Exposure to Particulate Matter and Wood Smoke.....	F-1

FIGURES

Figure 1-1. Overview of the air pathway risk analysis process.....	1-3
Figure 1-2. Regional model domain for analysis of the Cerro Grande Fire.....	1-5
Figure 2-1. Monitoring locations for air samples collected by LANL, NMED, and EPA. DOE RAP samples analyzed for this report were collected at 7 of the 20 EPA collection locations.....	2-2
Figure 2-2. Gross beta versus gross alpha concentrations in air collected during the Cerro Grande Fire.....	2-12
Figure 2-3. Americium-241 concentrations in air versus their analytical uncertainty for samples collected before and during the Cerro Grande Fire.	2-14
Figure 2-4. Concentrations of $^{239,240}\text{Pu}$ in air versus analytical uncertainty for samples collected before and during the Cerro Grande Fire.....	2-15
Figure 2-5. Air concentrations of ^{238}U versus ^{234}U collected during the Cerro Grande Fire.....	2-16
Figure 2-6. Strontium-90 concentrations in soil collected by LANL and NMED at various locations.....	2-17
Figure 2-7. Plutonium-239,240 concentrations in soil collected by LANL and NMED at various locations.....	2-18
Figure 2-8. Americium-241 concentrations in soil collected by LANL and NMED at various locations.....	2-18
Figure 2-9. Total uranium concentrations in soil collected by LANL and NMED at various locations.....	2-19
Figure 2-10. Uranium-238 versus ^{234}U concentrations in soil measured post-fire by NMED and LANL.	2-20
Figure 2-11. Particulate matter concentrations collected at TA-54 by LANL (LANL plot).....	2-23
Figure 3-1. Flow chart for air pathway screening analysis.....	3-4
Figure 3-2. Centerline area source χ/Q for a ground-level release as a function of the source area for Pasquill-Gifford stability class F and 2 m s^{-1} wind speed.....	3-9
Figure 3-3. Location of PRSs that burned during the Cerro Grande Fire.....	3-13
Figure 4-1. Twenty-four average PM10 concentrations as a function of time for monitoring stations located in or on the periphery of the model domain.....	4-4
Figure 4-2. Twenty-four hour averaged wind speed and 24-hour averaged PM10 concentration in Santa Fe.	4-6
Figure 4-3. Twenty-four hour average wind speed and 24-hour average PM10 concentration at TA-54 from March 14 to June 15, 2000.	4-7
Figure 4-4. Scatter plot with regression line of 24-hour average PM10 concentration as a function of natural log of the 24-hour average wind speed as measured in Santa Fe raised to the power of 3.....	4-9
Figure 4-5. Model domain for CALPUFF modeling of the Cerro Grande Fire.	4-13
Figure 4-6. Gridded terrain data as processed by the TERREL preprocessor representing a grid spacing of 1640 ft (500 m).....	4-15
Figure 4-7. Land use in the model domain as defined by the USGS CTG files.....	4-16

Figure 4-8. Wind roses for Los Alamos High School, Santa Fe Airport, San Ildefonso NEWNET, and TA-53 stations.....	4-18
Figure 4-9. Wind roses for Cochiti NEWNET, Española, Pajarito Mountain, and Santa Fe NMED stations.....	4-19
Figure 4-10. CALMET-generated wind vectors for layer 1 (0–20 m) on May 11, 2000, at 10:00 am.....	4-22
Figure 4-11. CALMET-generated wind vectors for layer 3 (60–100 m) on May 11, 2000, at 10:00 am.....	4-23
Figure 4-12. CALMET-generated wind vectors for layer 7 (1200–2000 m) on May 11, 2000, at 10:00 am.	4-24
Figure 4-13. Comparison of original EPM output for heat and PM10 emissions and the modified output for the fire that burned on May 6, 2000.....	4-29
Figure 4-14. Predicted and observed PM10 concentrations at TA-54, White Rock (EPA), Santa Clara (EPA), and San Ildefonso (EPA).	4-35
Figure 4-15. Predicted and observed PM10 concentrations at four stations.	4-36
Figure 4-16. Modeled hourly average PM10 concentrations at four locations.	4-38
Figure 4-17. Thirteen-day (May 6 to May 18) average PM10 concentration isopleths estimated by CALPUFF.....	4-39
Figure 4-18. Thirteen-day (May 6 to May 18) total deposition (mg m^{-2}) of PM10 in the model domain as a result of PM10 emissions from the fire.	4-40
Figure 4-19. One hundred and twenty seven-hour average PM10 concentration for releases from the fire identified as 11 North d that burned on May 11, 2000.....	4-44
Figure 4-20. Ten-hour average PM10 concentration for releases from the fire identified as 11 South Central that burned on May 11, 2000.....	4-45
Figure 4-21. Ten-hour average PM10 concentration for releases from the fire identified as 11 Southeast that burned on May 11, 2000.	4-46
Figure 4-22. Twelve-hour average PM10 concentration for releases from the fire identified as 11 Southwest that burned on May 11, 2000.	4-47
Figure 4-23. Ten-hour average PM10 concentration for releases from the fire identified as 13 South that burned on May 12 and 13, 2000.....	4-48
Figure 4-24. Location of LANL and EPA monitoring stations where ^{239}Pu was detected above the minimum detectable concentration and analytical uncertainty was less than the reported concentration value.....	4-54
Figure 4-25. Vertical profile of estimated PM10 concentration at the northeast corner of the model domain and 10 mi (16 km) south of the northeast corner	4-59
Figure 5-1. Isopleth map of the Hazard Quotient in the model domain from chemicals sources in burned PRS units for the adult resident scenario.....	5-10
Figure 5-2. Isopleth map of cancer risk in the model domain from chemicals sources in burned PRS units for the adult resident scenario.....	5-11
Figure 5-3. Isopleth map of cancer risk in the model domain from radionuclide sources in burned PRS units for the adult resident scenario.....	5-12

TABLES

Table 2-1. Averaging/Integration Times for Air Monitoring Data Collected During the Cerro Grande Fire	2-9
Table 2-2. PM10 Concentrations Measured at the Runnels Building	2-22
Table 3-1. List of Contaminants from the Potential Release Site Data with Screening Risk Index Values or Hazard Quotients Larger than the Decision Criteria	3-12
Table 3-2 Descriptive Statistics for the Ratio of GIS-Based PRS Areas to IR-boundary PRS Areas that were Redefined Based on Existing Sample Locations	3-17
Table 3-3. Physical Data for PCOCs Assumed to Have Fully Volatilized in the Cerro Grande Fire Based on Reported Boiling Point	3-24
Table 3-4. Physical Data for PCOCs Assumed Not to Have Volatilized in the Cerro Grande Fire Based on Reported Boiling Points	3-25
Table 3-5. Physical Data for PCOCs Assumed to Have Fully Volatilized in the Fire Based on Calculated Boiling Points	3-25
Table 3-6. Melting and Boiling Points of Primary Radionuclide Contaminants of Concern	3-28
Table 4-1. Measured 24-hour Average PM10 Concentrations Before, During, and After the Cerro Grande Fire ($\mu\text{g m}^{-3}$)	4-3
Table 4-2. Measured PM-10 Concentrations with High Volume Air Sampling by EPA	4-5
Table 4-3. Summary of Regression Statistics of PM10 and Average Wind Speed for Capshaw and Runnels	4-8
Table 4-4. Summary of Regression Statistics of PM10 and Average Wind Speed at TA-54	4-8
Table 4-5. U.S. Geological Survey Digital Elevation Model Data Used in the Terrain Model	4-14
Table 4-6. Surface Meteorological Surface Stations in the Model Domain	4-20
Table 4-7. Data for the EPM	4-30
Table 4-8. Fuel Loading Data for the EPM Model	4-31
Table 4-9. Pollutant Emissions Calculated with EPM	4-32
Table 4-10. Predicted-to-Observed Ratios of PM10 Concentrations Taken During the Fire	4-37
Table 4-11. Time-integrated PM10 and CO Concentration in the Vicinity of TA-54	4-42
Table 4-12. Time-Integrated Concentration of Radionuclides Released from PRSs as a Result of Cerro Grande Fire (aCi-d m^{-3})	4-49
Table 4-13. Time-Integrated Concentration of Carcinogens Released from PRSs as a Result of Cerro Grande Fire ($\mu\text{g-d m}^{-3}$)	4-50
Table 4-14. Time-Integrated Concentration of Noncarcinogens Released from PRSs as a Result of Cerro Grande Fire ($\mu\text{g-d m}^{-3}$)	4-52
Table 4-15. Plutonium-239 Concentrations Measured at Various Locations Before, During, and After the Cerro Grande Fire by LANL and EPA	4-53
Table 4-16. Concentrations of Pollutants Emitted from the Cerro Grande Fire ($\mu\text{g m}^{-3}$) Excluding Background	4-55
Table 4-17. Maximum Predicted Time-Integrated Concentration of Radionuclides Measured within the Model Domain	4-56
Table 4-18. Maximum Predicted Time-Integrated Concentration of Chemicals Within the Model Domain	4-57

Table 4-19. Estimated 24-Hour Average Ground-Level PM ₁₀ Concentrations Excluding Background at Selected Locations in the Model Domain for May 11, 2000.....	4-59
Table 4-20. Estimated Deposition of Radionuclides Released from PRSs as a Result of Cerro Grande Fire (pCi m ⁻²).....	4-60
Table 4-21. Estimated Deposition of Chemicals and Metals Released from PRSs as a Result of Cerro Grande Fire (mg m ⁻²).....	4-61
Table 5-1. Exposure Scenarios and Exposure Parameters for Atmospheric Releases	5-4
Table 5-2. Breathing Rates for Various Exercise Levels as Reported in Roy and Courtay (1991) and Layton (1993)	5-5
Table 5-3 Time Budgets and Breathing Rates for Representative Scenarios.....	5-5
Table 5-4 Incremental Lifetime Cancer Incidence Risks for Radionuclides.....	5-7
Table 5-5 Incremental Lifetime Cancer Incidence Risks for Chemical Carcinogens	5-8
Table 5-6 Hazard Quotient Estimates for Noncarcinogenic Chemicals	5-8
Table 5-7 Hypothetical Maximum Risks by Scenario and Contaminant Type	5-9
Table 6-1. Maximum Estimated Risks by Scenario, Contaminant Type, and Source.....	6-2
Table 6-2. Summary of Conservatism and Uncertainty in Each Modeling Component of the Exposure and Risk Calculation.....	6-5

ACRONYMS

ATSDR	Agency for Toxic Substances and Disease Registry
CERCLA	Comprehensive Environmental Response, Compensation and Liability Act
CTG	Composite Theme Grid
DEM	Digital Evaluation Model
DOE	U.S. Department of Energy
DOE RAP	U.S. Department of Energy Radiological Assistance Program
EDE	effective dose equivalent
EPA U.S.	Environmental Protection Agency
EPM	Emissions Production Model
ER	Environmental Restoration (Project)
ESH	Environmental Safety and Health (Group)
GIS	geographical information system
HE	high explosives
HQ	hazard quotient
ICRP	International Commission on Radiological Protection
IR	infrared
ISC	Industrial Source Complex
JAG	Joint Assessment Group
LANL	Los Alamos National Laboratory
NCDC	National Climatic Data Center
NCRP	National Council on Radiation Protection and Measurements
NESHAPs	National Emissions Standards for Hazardous Air Pollutants
NID	negligible individual dose
NMED	New Mexico Environment Department
NRC	U.S. Nuclear Regulatory Commission
PAH	polycyclic aromatic hydrocarbon
PCB	polychlorinated biphenyl
PCOC	potential contaminants of concern
PM	particulate matter
PRS	potential release site
PTLA	Protection Technology of Los Alamos

<i>RAC</i>	<i>Risk Assessment Corporation</i>
RCRA	Resource Conservation and Recovery Act
RfD	reference dose
STP	standard temperature and pressure
TA-54	Technical Area-54
TIC	time-integrated concentration
TSP	total suspended particulate
USGS	U.S. Geological Survey
UTM	Universal Transverse Mercator
VOC	volatile organic compounds

1 INTRODUCTION

The Cerro Grande Fire, which burned about 45,000 acres ($\sim 180 \text{ km}^2$) in northern New Mexico, originated in the Bandelier National Monument on the evening of May 4, 2000, and spread east-northeast over the next 16 days consuming residential structures within the County of Los Alamos and approximately 7500 acres ($\sim 30 \text{ km}^2$) within the Los Alamos National Laboratory (LANL) boundary (DOE 2000). LANL encompasses about 27,500 acres (110 km^2) and is situated on the Pajarito Plateau, described as a series of finger-like mesas separated by deep east-to-west oriented canyons cut by intermittent streams. The mesas range in elevation from approximately 7800 ft (2377 m) on the flanks of the Jemez Mountains to about 6200 ft (1890 m) above the Rio Grande Canyon. Some of the areas that burned were known or suspected to be contaminated with radionuclides and chemicals. Concern was expressed by the public with regard to:

- Radionuclides and chemicals associated with soil and vegetation burned by the fire and subsequently suspended and transported via air
- Radionuclides and chemicals associated with soil, sediments, and ash mobilized and transported via surface water following the fire
- Potential exposures and health risks to people related to the transport of radionuclides and chemicals via both air and surface water.

In response to these concerns, the New Mexico Environment Department (NMED) recognized the need for an independent assessment of exposures and risks to the public from radionuclides and chemicals associated with the LANL facility released as a result of the fire. NMED contracted with *Risk Assessment Corporation (RAC)* to evaluate the potential incremental health risks to the communities of northern New Mexico from these radionuclides and chemicals.

1.1 Objectives

The primary objective was to analyze the immediate consequences and the longer-term impacts of the Cerro Grande Fire in terms of increased public exposures and potential risks from radionuclides and chemicals associated with the LANL facility released as a result of the fire in the vicinity of the LANL. The study did not specifically address the impact the fire may have in the future on groundwater.

Specifically, the overall project focused on the

- Magnitude of incremental exposure and associated risks to the public, emergency response personnel, and firefighters from transport of radionuclides and chemicals associated with the LANL facility released as a result of the fire through the *air transport pathway*. The scope was subsequently changed to include a semi-quantitative assessment of risks from naturally occurring radionuclides and metals released from burning of the forests around the LANL site. This assessment is described in Appendix D.
- Magnitude of incremental exposure and associated risks to the public from transport of radionuclides and chemicals associated with the LANL facility released as a result of the fire through *surface water pathways*. The scope was also subsequently changed

to include risks from the fire from areas burned around the LANL site. This assessment is described in a companion report (Rocco et al. 2002).

- Conclusions of the study and recommendations for similar events in the future. An important goal of the study was to actively, openly, and accurately convey information about the risks from the fire to the public, including the lessons learned from the fire analysis and the effectiveness of communication with the public during and following the fire. These conclusions are presented in a companion report (Mohler et al. 2002).

1.2 Approach

The risk analysis process for the air pathway included evaluating the available air monitoring data and procedures, identifying the sources and magnitude of airborne contaminant releases, modeling the release and transport of airborne contaminants entrained in the fire plume, identifying representative individuals for defining exposure scenarios, and estimating the associated health risks and the uncertainties. The entire process was divided into a number of steps that are described in the different chapters of this report and summarized in Figure 1-1.

To characterize the risks from radionuclides and chemicals released into the atmosphere during the Cerro Grande Fire, we considered the following questions:

1. What environmental data related to the air pathway were available for periods during the fire and how could they be used to evaluate risk?
2. What was the primary exposure pathway for contaminants released to the air during the fire?
3. What types of individuals were located in the vicinity of the fire or in the path of the fire plume?
4. What activities were these individuals engaged in?
5. Where were these individuals located?
6. How many exposure scenarios are required to reasonably cover the range of exposure circumstances that occurred during the fire?
7. What are the uncertainties associated with this approach?
8. What potential sources of airborne contamination are not evaluated using this approach?

We compiled and evaluated the environmental data collected before, during, and after the fire pertaining to the air pathway as described in Chapter 2. Because a large number of radionuclides and chemicals were identified that were potentially released during the fire, we used a screening procedure to identify those that were potentially most important in terms of health risk. We removed contaminants from consideration that fell below some predetermined level of health risk, when risk was calculated conservatively, as described in Chapter 3. We developed source term estimates for the remaining radionuclides and chemicals that were identified as possible contaminants resulting from LANL operations (Chapter 3).

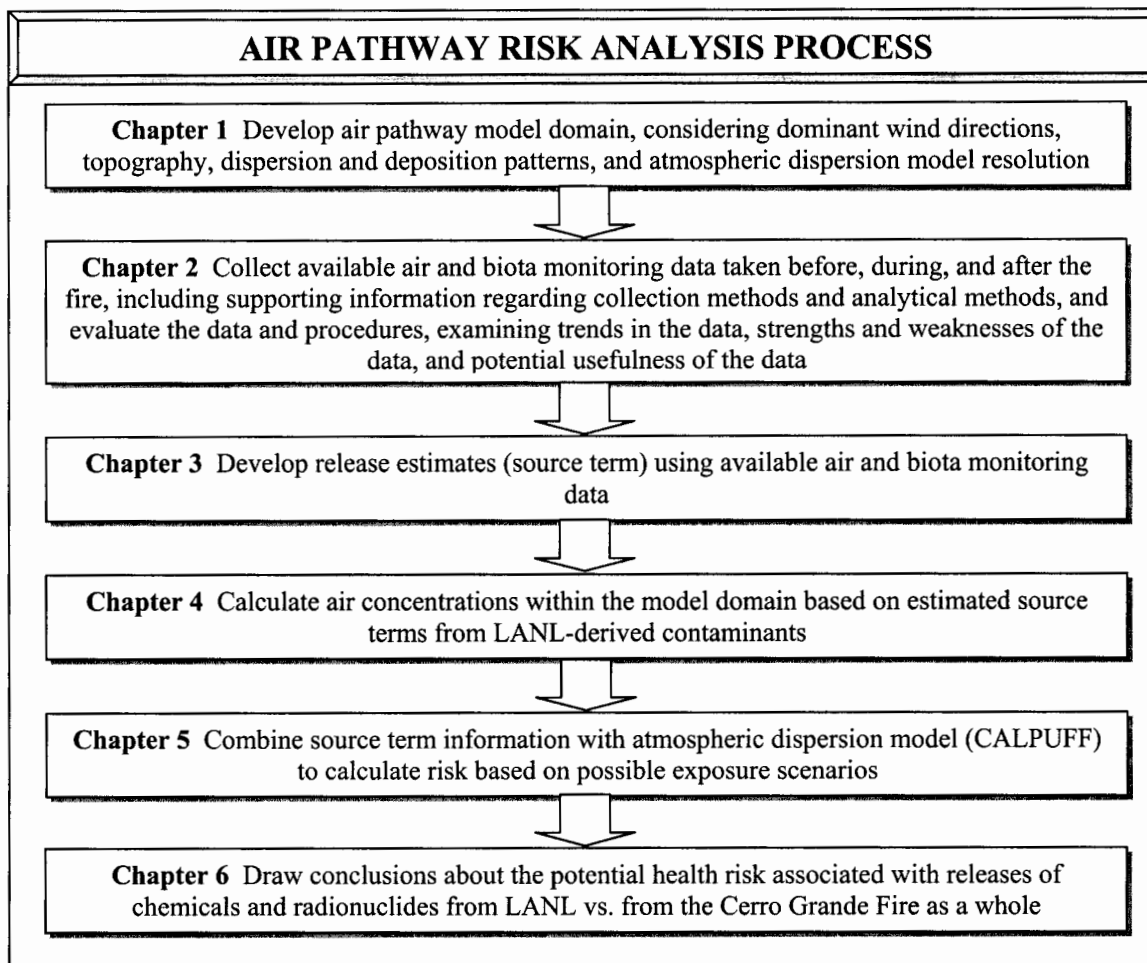


Figure 1-1. Overview of the air pathway risk analysis process.

Dispersion of the radionuclides and chemicals in the air required first an understanding of the behavior of pollutants released due to the fire itself. We estimated pollutant release rates and heat generated by the fire using the Emissions Production Model (Sandberg and Peterson 1984) and estimated dispersion and deposition of these pollutants with the CALPUFF computer code (Scire et al. 1999). We compared estimated 24-hour average concentrations of particulate matter less than 10 μm (PM10) released from the fire to measurement values in the model domain. This comparison formed the basis for model calibration. Using the estimated PM10 release rates and concentrations, we then calculated concentrations of radionuclides and chemicals in the model domain. Atmospheric transport is described in Chapter 4.

The exposure scenarios used to determine the risks to representative individuals from the radionuclides and chemicals released during the fire are described in Chapter 5. Chapter 5 also provides the method for risk calculations and the estimated risks.

1.3 Air Model Domain

An important first step of the study was to determine the extent of the air dispersion model domain. The air model domain is the geographic area over which the atmospheric dispersion, transport, and risk calculations were performed. To establish the atmospheric modeling domain, we considered many factors, including the dominant wind directions, topography, dispersion and deposition patterns, spatial resolution of the atmospheric transport model, data storage requirements, and computer runtimes. While it was desirable that the model domain cover as large an area as possible, its geographical extent was limited by the roughness of the topography and the resources needed to acquire and process spatial data.

The air model domain is shown in Figure 1-2. It includes the area impacted both directly and indirectly by the fire, key populations, and locations where environmental sampling was performed. We selected the CALPUFF model (Scire et al. 1999), a state-of-the-art complex terrain puff dispersion model, to perform the air dispersion calculations (see Chapter 4).

Features within the model domain were defined spatially according to a grid. The grid can be thought of as a series of points within the model domain, spaced equal-distance apart, upon which we defined domain features. For example, terrain was represented by assigning an elevation value to each of the grid nodes. Wider spacing between grid nodes results in coarser resolution of the feature. Because a finite number of grid nodes could be incorporated into any model simulation, there had to be a balance between the number of grid nodes, the size of the grid spacing, and the overall resolution required to represent the domain of interest.

Los Alamos is a challenging site to model because of its extremely variable terrain features. The steep canyons and mountainous terrain require that grid spacing be kept relatively small. While resolving the canyons that cut through the LANL site was important in terms of evaluating impacts within those features, we were more interested in evaluating impacts to offsite communities and the long-range transport of the plume. Additionally, because of their buoyant nature, the smoke plumes tended to rise to heights above the canyon features, and their transport was governed by air mass above the influence of the canyons. For this reason, we used a 1640-ft (500-m) grid spacing, which allowed a greater extent of the area surrounding the facility to be included in the domain.

In considering the extent of the domain (Figure 1-2), it was imperative that key population centers, such as Santa Fe and Española, were included in the domain. It was also important that the total area burned by the fire be included in the domain, along with as many air monitoring stations that were operating during the fire as possible. Most of the smoke plumes from the fire traveled east-northeast, which was consistent with the predominant wind direction during the fire. Therefore, the LANL site was situated in the western part of the model domain to capture the fullest extent of the smoke plume trajectory. Using these criteria, we established a regional domain that encompassed the cities of Santa Fe and Española, and Cochiti Lake. The domain extends 9.3 mi (15 km) east and 4.5 mi (7.2 km) south of Santa Fe, 6.2 mi (10 km) north of Española, and 9.3 mi (15 km) west of the city of Los Alamos. The domain contains 120 nodes in the east-west direction and 110 nodes in the north-south direction, with a grid spacing of 1640 ft (500 m). The total extent of the domain is 37×35 mi (60×55 km) and encompasses an area of 815,430 acres (3300 km²). The grid resolution of 1640 ft (500 m) allowed the major topographical features, including White Rock Canyon to be identified. Smaller canyons within the LANL boundary (Water, Los Alamos, Sandia, etc.) were not well resolved.

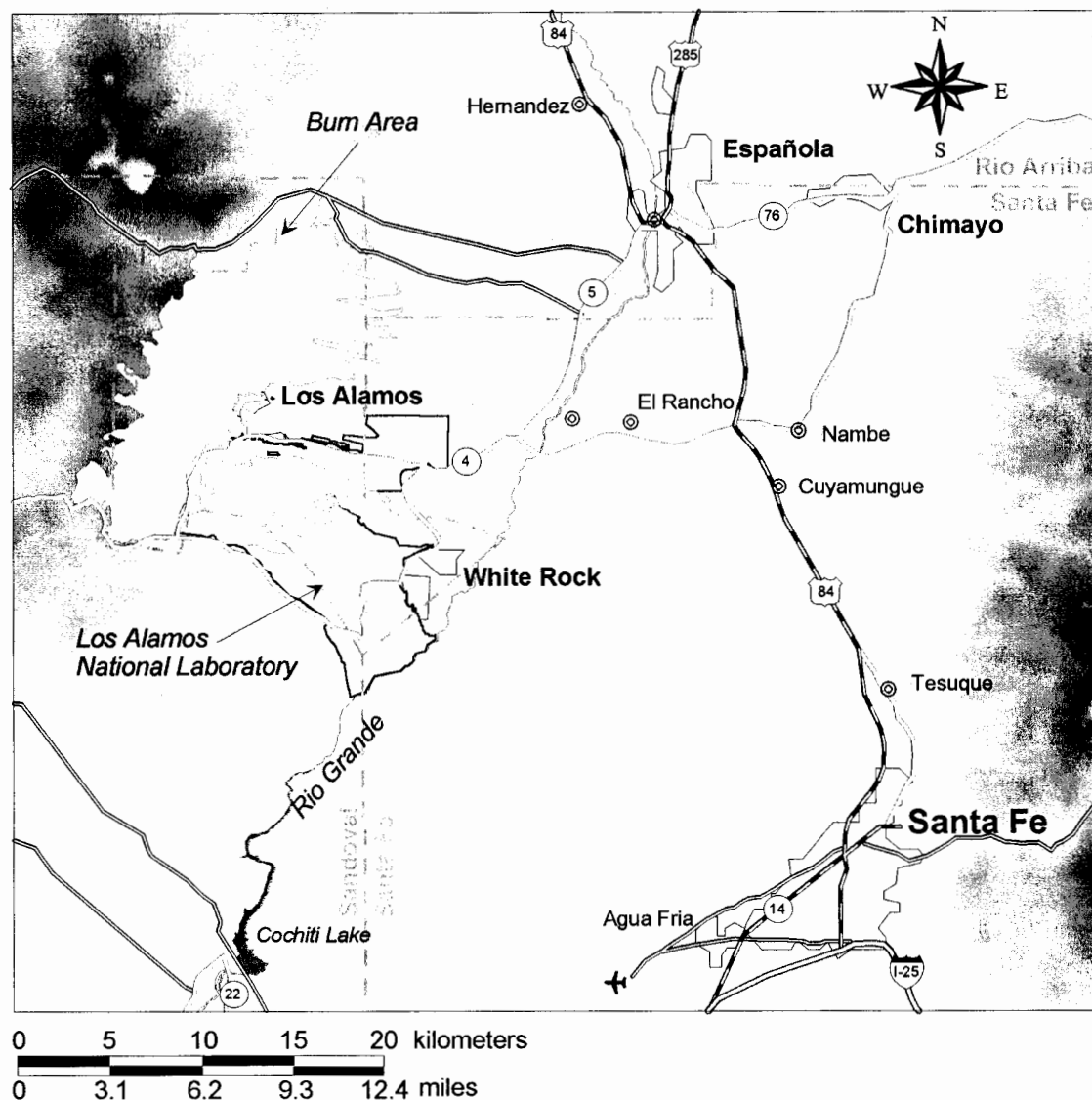


Figure 1-2. Regional model domain for analysis of the Cerro Grande Fire.

Communities outside the model domain also expressed concern. These communities, which are mostly northeast of the model domain and include Taos, were impacted from the smoke plume generated from the fire. Of particular concern was the possibility that contaminants entrained in the smoke plume lofted over most the nearby cities where monitoring stations were set up and, therefore, detected little contamination. This possibility would have impacted cities and towns located northeast of the model domain where the rise in elevation and general plume dispersion would have resulted in high ground-level concentrations. Indeed, higher than background concentrations of particulate matter were detected in Taos during the fire. The elevated concentrations were attributed to the smoke plume.

To evaluate concentrations outside the model domain, we provided a vertical cross section of the smoke plume at the boundary of the model domain (northeast corner) for those days when the fire burned across LANL. Because of the buoyant nature of forest fire emissions, the highest

concentrations are often times not at ground level, but they are at some height above the ground. The vertical concentration profile in the northeast corner of the model domain bounds any predicted concentrations outside of the model domain. In this way, our assessment included any potential impacts from contaminants that dispersed off the model domain that were potentially not detected at the ground surface.

2 SUMMARY OF ENVIRONMENTAL MONITORING DATA

At the outset of this project, we attempted to collect and compile all of the environmental monitoring data that were relevant to the air pathway. This primarily included air and soil monitoring data, although we also collected vegetation data. This chapter summarizes the available data, discusses gaps in the data, shows trends that were identified in the data, and discusses their usefulness for the analysis of risks for radionuclide and chemical releases to air.

2.1 Air Monitoring Data

During the Cerro Grande Fire, several agencies responded to the concern about possible releases of contaminants to air. There were many reports during the wildfire of dense smoke plumes, and these plumes presented an immediate concern to the individuals exposed to them. This concern increased after the wildfire began to burn on LANL property. The fire started as a prescribed burn in a forested area within the boundaries of Bandelier National Monument along a mountain slope of the Cerro Grande, and it escalated into a wildfire primarily because of the high winds at the time.

In addition to the routine air monitoring by LANL and NMED, which continued during the Cerro Grande Fire, the U.S. Environmental Protection Agency (EPA) and the U.S. Department of Energy Radiological Assistance Program (DOE RAP) responded to the emergency situation and collected air samples at various locations during the fire. Figure 2-1 shows the locations of LANL, NMED, and EPA air monitoring stations. This section summarizes the data collected by the different agencies and discusses the measurement and analytical techniques and locations monitored.

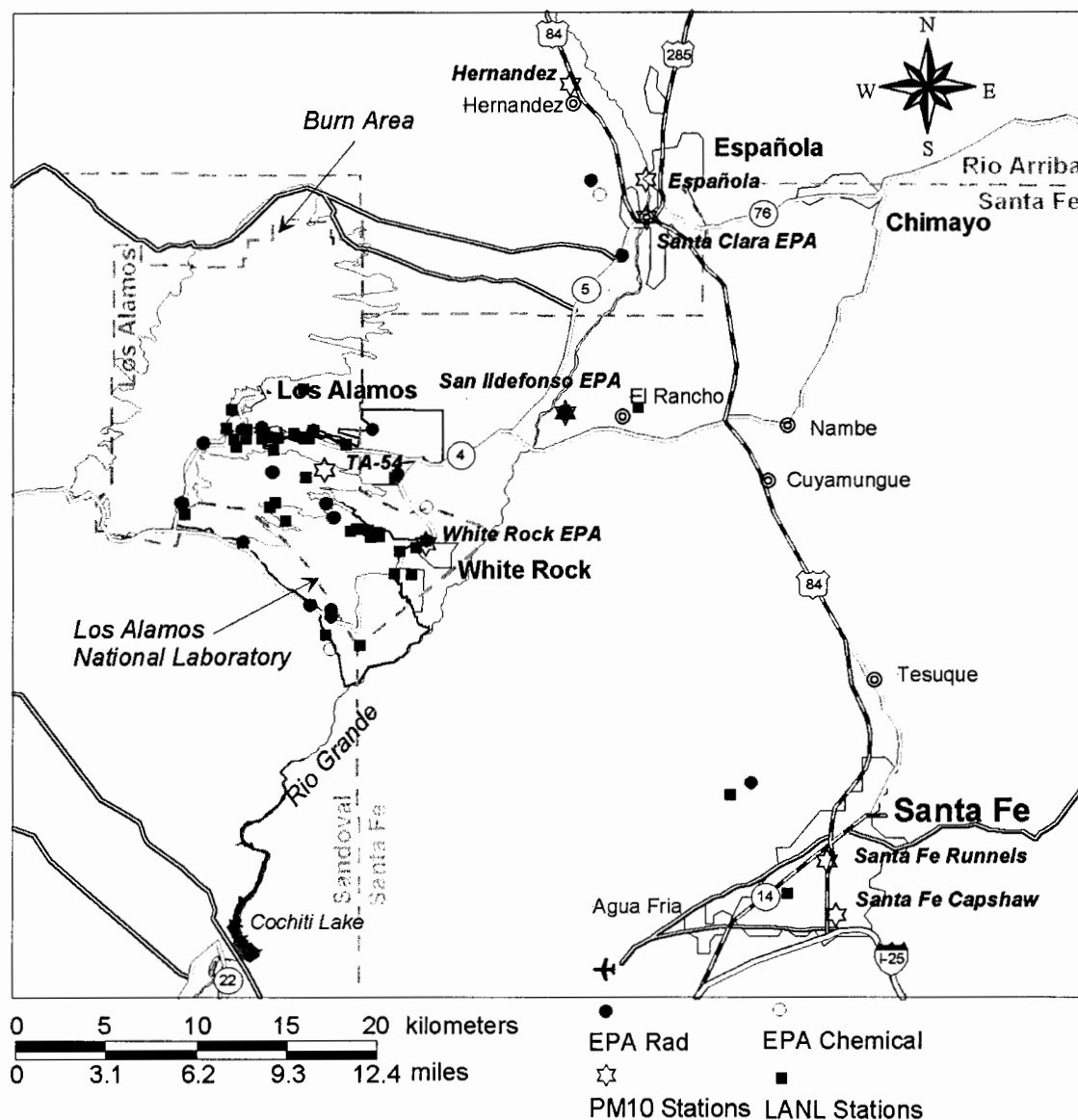


Figure 2-1. Monitoring locations for air samples collected by LANL, NMED, and EPA. DOE RAP samples analyzed for this report were collected at 7 of the 20 EPA collection locations. Not all sampling locations are shown, as some were outside the area of this map.

2.1.1 Los Alamos National Laboratory Monitoring

At LANL, the Air Quality Group of the Environmental Safety and Health Division (ESH-17) routinely collects air monitoring data using an onsite and LANL perimeter monitoring network known as AIRNET. AIRNET is a system of environmental air samplers located in and around the LANL property, which has been in operation for over 20 years. The samplers are located between

LANL facilities and potentially exposed members of the public or they encircle areas on the Laboratory property that have the potential to be major sources of diffuse emissions. There are also several regional stations at more remote locations that are regularly monitored for potential offsite releases. The AIRNET monitors provide important information about the releases during the fire.

Generally, AIRNET monitors collect samples of airborne particles for a 2-week period. The samples are collected using a sampler developed by LANL that has been studied for its particle collection properties, and it collects respirable particles efficiently, based on wind tunnel studies. The samplers are medium-flow samplers, using flow rates of about $4 \text{ ft}^3 \text{ min}^{-1}$ ($\sim 0.11 \text{ m}^3 \text{ min}^{-1}$), or about $81,223 \text{ ft}^3$ (2300 m^3) of air during a 2-week period. During the fire, however, the dust loading¹ on the filters was so great that samples were changed out more frequently. This dust loading significantly reduced the total volume of air sampled, reduced the sensitivity of the monitors (minimum detectable concentrations), and increased the uncertainty² in the measured concentrations by making sample result values fall below their associated analytical uncertainty values.

Under normal conditions, each 2-week sample is typically analyzed for alpha and beta particles using filter face-front counting, and regional samples are combined for gamma analysis to increase the sensitivity of the measurement. Composites of individual station samples are analyzed for gamma-emitting radionuclides quarterly. The 2-week samples from each station are cut in half and one-half is used to make a quarterly composite for analysis of radioactive isotopes using filter digestion and chemical separation. The purpose of this quarterly composite is to integrate the total air volume sampled and, thus, increase the chance of detecting any radionuclides.

During the fire, sampling periods ranged from 1 day to several days, with total air volume for each sample generally in the range from 5297 to $17,657 \text{ ft}^3$ (150 to 500 m^3). For the shorter duration fire samples, gross alpha and beta analysis using filter face-front counting was carried out on all the samples. In some cases, filter samples were divided in half, with one-half sent for immediate isotopic analysis. These samples were selected based on observation of elevated alpha and beta concentrations as well as a desire to maximize geographic coverage of the samples. It was also important to the ESH-17 staff not to analyze all samples in this manner, as they realized that the reduced volume of air would limit the information that could be obtained from these samples. The remaining halves of these samples were saved for the quarterly composite. The samples that were not halved for immediate analysis were retained for additional analyses or to maintain the ability to double-check any significant results.

LANL collected samples at all of their routine air monitoring locations during the fire. Because the fire burned onsite at some locations, power was shut down to areas of the Laboratory during the fire, resulting in the loss of some samples.

The NEWNET system operated by LANL measured environmental exposure rates (microrems per hour [$\mu\text{R h}^{-1}$]) and meteorological data at several locations in the vicinity of the Laboratory. A gross exposure rate monitor would not detect radionuclides released from LANL, so these data were not useful for this project.

¹ As a result of particles released from burned areas.

² Uncertainty is a general term used to describe the level of confidence in a given measurement, and its magnitude depends on the amount and quality of the evidence (data) available.

Although LANL does not regularly sample airborne dust concentrations, when the fire started, a PM10³ sampler was being tested at Technical Area-54 (TA-54), near the east boundary of the site (see Figure 2-1). This sampler collects particles suspended in air through a size-selective inlet. The airflow is then passed through a filter that collects the particles. A sensor continuously monitors changes in the mass of the filter and averages the changes in mass over time. Results can be averaged over any selected time period. We obtained 24-hour average PM10 concentrations for the period during the fire. These measurements were used in the air dispersion model calibration as discussed in Chapter 4. The air monitor at the ESH-17 laboratory location provided PM10 data during a time period when the fire passed close to the monitor (see also Figure 2-11). Although this location is onsite, it was an important dataset for examining the respirable mass of airborne particles. We obtained all of the data collected by LANL for periods before, during, and after the fire in electronic format.

2.1.2 New Mexico Environment Department Monitoring

Two different branches of the NMED conducted air monitoring during the fire: the Air Quality Bureau and the DOE Oversight Bureau. The DOE Oversight Bureau routinely collects samples of airborne particles at five locations that are collocated with LANL samplers (Figure 2-1). These five sampling locations are intended to serve as checks on the accuracy of LANL samples. The samples are collected with the same filter type, similar flow rates, and for the same duration as the LANL samples, but they are analyzed by a different organization. Quarterly composites are analyzed for isotopes of uranium, ²³⁸Pu, ^{239,240}Pu, and ²⁴¹Am. During the fire, two samples were collected and analyzed at shorter time increments than usual (2 days and 2 weeks). These samples were analyzed for radionuclide concentrations.

The Air Quality Bureau of NMED collects different types of air samples that serve a different purpose altogether. The Air Quality Bureau monitors total respirable particulate (PM10) concentrations at a number of sites across northern New Mexico. We obtained coordinates for these locations. These samples are collected solely for air quality purposes and not as a check on LANL. The PM10 samples were collected periodically, but not daily or on any defined schedule, during the fire. Samples collected were averaged over 24 hours.

The Air Quality Bureau uses commercially produced Wedging PM10 samplers for determining regional respirable particle concentrations. The Wedging sampler incorporates a critical flow device in which the desired flow is automatically maintained as long as there is a standing shock wave in the throat of the device. The shock wave is insensitive to changes in temperature, pressure, and blower motor speed.

Respirable particle concentrations using the Wedging samplers are 24-hour average concentrations. Filters are weighed and then placed in the sampler, removed after 24 hours and weighed again. The total particulate matter weight is obtained by difference. The airflow through the sampler is then calculated. The weight of the sample is divided by the volume to yield the

³ PM10 samplers selectively collect airborne particles with aerodynamic diameters less than or equal to 10 micrometers (μm). These samplers fractionate particulates by maintaining a constant critical velocity in the sampler such that particles greater than 10 μm in diameter are unable to follow the serpentine air stream in the sampler. Instead, they collide with oiled surfaces and are, thus, removed from the air stream. Particles smaller than 10 μm remain suspended in the air until they reach the filter. These particles are generally assumed to be within the respirable range.

concentration during that 24-hour period, generally expressed in units of micrograms per cubic meter ($\mu\text{g m}^{-3}$) for comparison to EPA standards. Flow is calculated at standard temperature and pressure as well as at ambient temperature and pressure, and PM10 concentrations are calculated both ways, but they are generally reported at standard conditions. This conversion to standard temperature and pressure is done at the request of the EPA for their use in comparison to PM10 conditions across the country. Reporting the data at standard temperature and pressure gives the highest average airborne particle concentration. Sampled air volume at standard temperature and pressure at these stations is generally about 45,908 ft^3 (1300 m^3) for a 24-hour sample (56,503 ft^3 [1600 m^3] at ambient conditions).

Airborne concentrations of particles having aerodynamic diameters $\leq 2.5 \mu\text{m}$ (PM2.5)⁴ are also measured by the Air Quality Bureau in a manner similar to the PM10 collection process. The PM2.5 data were too limited to be used in our analysis of the fire.

For PM10 and PM2.5 samples collected daily during the fire, NMED contracted with an analytical laboratory to analyze the filters for gross alpha, beta, and gamma, as well as specific radionuclides. Gross alpha and beta counting was done using filter face-front counting of a 2-in. (5 cm) diameter subsegment of the large 8 × 10-in. (20 × 25-cm) filter. This subsegment size was selected to conform to the detection equipment size and shape as well as the calibration source geometry. Gross gamma was counted using four 2-in. (5 cm) subsegments from the same sample. Chemical separation and analysis for radioisotopes was done on the entire filter for some samples. Other filters were retained for analysis of metals, dioxin, and asbestos. Ambient air volumes have been used in the evaluation of these data.

NMED also collected air samples during the fire near homes in the burned areas of the Los Alamos community and analyzed these for asbestos. We received these data in the form of a NMED press release.

2.1.3 U.S. Environmental Protection Agency Monitoring

The EPA collected air monitoring data during the Cerro Grande Fire as part of a Joint Assessment Group (JAG) effort. These data were collected using low volume air samplers placed at 20 locations across northern New Mexico. We obtained coordinates and data for 18 of these sampling locations (the remaining two samples were collected on Pueblo lands and were not publicly available). These samples were collected from May 15 to May 17, 2000. EPA staff indicated that flow rates were around 3 $\text{ft}^3 \text{min}^{-1}$ (0.09 $\text{m}^3 \text{min}^{-1}$) and samples were collected for about 24 hours, for a total collected volume of approximately 4238 ft^3 (120 m^3).

EPA data were evaluated at two different time periods after sample collection: between 10 and 24 hours, in an attempt to identify the short-lived decay products, and then at about 2 weeks. Samples were analyzed for gross alpha, beta, and gamma using counters in the EPA mobile laboratory. We requested more detailed information on the analysis techniques, but we did not receive it. The later analysis again evaluated alpha and beta concentrations and also looked at plutonium isotopes. All of the above data were obtained in text, not electronic, format from the NMED website and from the EPA.

⁴ Particulate matter with a diameter less than or equal to 2.5 μm . This particulate matter is now under EPA regulation in addition to PM10 concentrations. These particles are considered to be more hazardous than PM10 because they penetrate deeper into the lung when inhaled.

The EPA also collected data on chemical concentrations in air, including metals, polynuclear aromatic hydrocarbon (PAHs), pesticides, and volatile organic compounds (VOCs). Location information for these chemical data was very difficult to acquire, and some uncertainty remains about the location information.

Particulate data were collected by EPA, including PM₁₀ and total suspended particulate (TSP). Location information for these samples was inferred from a spreadsheet of the data provided by NMED. However, we were not able to obtain the integration time for individual samples. Data points were labeled with sample IDs that appeared to be related to the sampling location. Because these sampling locations filled in important gaps in the PM₁₀ data available to us, we used these data in our model calibration efforts, which are discussed in detail in Chapter 4.

2.1.4 U.S. Department of Energy Radiological Assistance Program

The DOE RAP monitoring involved three different sampling efforts. An emergency response phase was immediately undertaken. During this phase, RAP team members went to a large number of locations across northern New Mexico and made ground contamination measurements and took low volume, rapid air samples (about 35 ft³ [1 m³] of air per sample). This sampling effort was designed to immediately assess any public health risks posed by the fire. Air samples were evaluated for gross alpha, beta, and gamma at 24-hour, 72-hour, and later time increments from sample collection. This sampling effort lasted from May 11 through May 14, 2000.

The second phase of the sampling involved seven high volume air samplers that were placed in and around the White Rock and Los Alamos area. We obtained the location coordinates for these samplers, which collected approximately 10,594 ft³ (300 m³) of air per sample. These samples were also evaluated for gross alpha, beta, and gamma at 24 hours and at sometime between 72 and 168 hours following sample collection. This sampling effort covered the period from May 11 to May 17, 2000.

The final sampling effort was carried out in cooperation with the JAG sampling performed by the EPA. At seven of the sites monitored by the EPA, collocated samplers were placed by DOE. These low volume samplers operated at about 71 ft³ min⁻¹ (2 m³ min⁻¹), and each sample totaled about 3178 ft³ (90 m³) in sampled air volume, for a sample averaging time of less than 1 hour. These samples were again evaluated for gross alpha, beta, and gamma at 24 hours and about 72 hours after sample collection. These samples were collected between May 15 and May 17, 2000.

All of the DOE RAP data were received in text format. There was some indication that radionuclide identification studies were conducted, but we were unable to obtain these data.

2.2 Biota and Soil Monitoring Data

In response to the Cerro Grande Fire, LANL and NMED undertook several efforts to collect special sets of biota monitoring data. Both of these organizations have carried out some routine monitoring, providing some pre-fire concentrations with which to make comparisons.

2.2.1 Los Alamos National Laboratory Monitoring

Soil sampling by the LANL is done by the Ecology Group of Environmental Safety and Health in ESH-20. LANL operates a soil sampling network and has data dating back to the early 1970s. The network is composed of 25 locations including perimeter, regional background, and onsite locations. Onsite locations are not located at waste management units, but instead they are intended to evaluate deposition from stack releases and fugitive dust suspension. Soil samples are collected from the top 5 cm (2 in.) of soil. An analyzed area is typically a square, 33 ft (10 m) per side. Five samples are collected randomly within that area, and those samples are combined to form a composite sample for that area. Samples are typically analyzed for radionuclides as well as light metals, heavy metals, and nonmetal trace elements.

After the fire, samples were collected at the locations that compose the soil sampling network. These samples were collected in a manner consistent with that regularly used, but they were collected with greater frequency than normal in an effort to quantify effects of the fire. These samples were analyzed for the same constituents traditionally monitored. For radionuclides, this included ^3H , ^{90}Sr , ^{137}Cs , ^{238}U , ^{238}Pu , $^{239,240}\text{Pu}$, ^{241}Am , gross alpha, gross beta, and gross gamma. Chemical analyses were performed for silver, arsenic, barium, beryllium, cadmium, chromium, mercury, nickel, lead, tin, selenium, and tellurium. We obtained summaries of all of the pre- and post-fire data on soils from LANL in text format. We also obtained information about post-fire grab sampling for organic compounds in surface soils. These samples were collected at the 0 to 15-cm (0 to 6-in.) depth.

Produce data are also routinely monitored by LANL using onsite, perimeter, and regional background locations. Fruits, vegetables, and grains are collected annually during the growing season, ashed, and analyzed for most of the same radionuclides and chemicals mentioned above. We obtained pre-fire summary data on these foodstuffs, and we collected summary tables of post-fire information on radionuclides in produce in text form as well.

LANL collected six samples of garden soil from farms that were upwind and downwind of the fire. The soil samples were analyzed for 21 pesticides, 7 polychlorinated biphenyls (PCBs), 14 high explosives (HEs), 18 PAHs, and various radionuclides. A different laboratory analyzed the samples for seven dioxin compounds. The LANL data were transmitted to us in five letter reports (Fresquez 2000a, 2000b, 2000c, 2000d, 2000e).

2.2.2 New Mexico Environment Department Monitoring

Although NMED does not have a routine monitoring network for soils or produce, they conducted an analysis of background radionuclide and chemical concentrations in soil at locations in the Jemez Mountains in 1999. Soil samples were not collected at these locations again after the fire as they were mostly in areas that burned.

After the fire, NMED collected surface soil and produce samples at several northern New Mexico farms, including some organic farming locations. These data were analyzed for radionuclides and chemicals, including many of the metals for which LANL monitored, but they also included PAHs, pesticides, and PCBs. We obtained all of the NMED data in electronic format. NMED jointly collected samples at the same locations in garden farm soil as those collected by LANL. An independent laboratory from that used by LANL carried out the analyses. The NMED data were provided in spreadsheet format. NMED sampled produce from 12

locations for metals, PAHs, PCBs, and pesticides. The type of produce collected and sampling locations were provided with the data.

NMED also collected ash samples from burned areas on LANL property and from other forested burned areas. These samples were collected as both grab samples and composite samples collected in specific transects.

2.3 Difficulties Related to Data Collection and Interpretation

At the outset of the project, it was assumed that environmental monitoring data collected before, during, and following the fire would be readily available and in a format suitable for more or less immediate trend analysis. It was also assumed that sitewide contaminant inventory estimates would be available to serve as a starting point for developing estimates of contaminant releases to air from contaminated potential release site (PRS) areas during the fire. This was not the case, however, and the data collection process was much more complex than we anticipated.

Specifically, some of the key difficulties that we had collecting and understanding data related to the Cerro Grande Fire included the following:

- Knowing data were collected but being unable to locate the data
- Lack of consistent collection and analytical methods
- Receiving incomplete and repeatedly updated datasets
- Receiving hard copies of the data that required manual data input into electronic format
- Receiving data without location information.

2.3.1 Difficulty Locating Data

We were unable to obtain several sets of data. In some cases, the data are known to exist, but we have been unable to track them to their original source. For example, we had considerable trouble tracking the EPA chemical data to its source. In other cases, we obtained data summaries from organizations not responsible for the original collection of the data, but we were unable to contact anyone within the collecting organization to receive confirmation that the data were in their final form.

2.3.2 Lack of Consistent Collection and Analytical Methods

Because of the existing environmental monitoring programs in place at LANL and those conducted by other organizations, such as the NMED, *RAC* assumed that most of the key pieces of information would be readily available with some clear and consistent method of organization. This assumption was particularly important because of the massive amount of collected data and the additional sampling conducted by other organizations in response to the fire, such as the U. S. Geological Survey (USGS), EPA, and the Department of Energy (DOE). However, it quickly became evident that each organization had its own method for data compilation, and that there was limited communication or sharing of data between the various organizations. This was unfortunate because it substantially complicated the ability for anyone, including an independent evaluator who may not be familiar with the LANL site or various modes of data compilation, to draw conclusions quickly and efficiently about the meaning of spatial or temporal trends apparent in the data. It also diminished the effectiveness and utility of having multiple groups involved in

sampling and data collection efforts, which was clearly an important resource during an event like the Cerro Grande Fire. It seems reasonable that environmental monitoring data can be compiled by each organization using a common methodology, which would enable data to be contained and transferred, if necessary, as a single database file, for example. Agreeing on a common format would be far preferable to the current methodology, which resulted in the data being spread across a multitude of differently formatted files. We believe this is an objective that should be considered for the future.

In addition, data were collected using a variety of techniques, which were sometimes unknown to us, and, perhaps most importantly, using a range of collection times over which the sample concentrations in air were averaged. This disparity made it impossible to compare data effectively among the agencies collecting it. In a situation like the Cerro Grande Fire, where multiple agencies were collecting data specifically for the purposes of comparison and validation, the importance of such consistency in data collection is magnified.

Table 2-1 shows the different averaging/integration times for the sets of air monitoring data available for the Cerro Grande Fire.

Table 2-1. Averaging/Integration Times for Air Monitoring Data Collected During the Cerro Grande Fire

Data source	Alpha/beta	Radioactive isotopes	Chemicals	Particulate matter
LANL	Various	Various ^a	NA ^b	24 hours
NMED	24 hours	24 hours – 2 weeks	NA	24 hours
EPA	24 hours	24 hours	?	(probably 24 hours)
DOE	<1 hour	NA	NA	NA

^a These data were available for the quarterly composites that included the fire, but during the fire, averaging times ranged from 24 hours to 2 weeks.
^b NA = not applicable.

This wide range of averaging times made it difficult to show data trends, much less use the data quantitatively for screening, risk analysis, or validation. The PM10 data provided the most consistent set of data, and we used it to calibrate our atmospheric dispersion model, as described in Chapter 4. The remaining data were compiled in this chapter to show some data trends, but all data with varying averaging times that are compared must be interpreted with caution, and are best used only as a guide.

2.3.3 Incomplete Datasets

Analytical results for samples collected during 2000 were not complete for some datasets as of May 2001. Every effort was made to obtain all relevant datasets as soon as they became available, but because there was no centralized method for collecting the data, this effort required frequent and repeated communication with representatives from the various organizations that provided data. Further, some datasets have been updated and/or appended with new data and provided to RAC with no mechanism to know which values changed, so any manipulation or analysis begun with the initial datasets had to be repeated.

2.3.4 Format of Collected Data

Another difficulty we encountered was working with data in different forms. Some of the datasets were hard copies or in text format. In many instances, it was necessary to key data into an electronic spreadsheet format for analysis. The resources and time required for this process were not anticipated in the original schedule.

Also, data were often in formats that were difficult to decipher. Locations were often listed in files that were separate from the actual data values. Median concentrations were given with no indication as to how many samples made up the median. Some analytical data were transmitted with no guidance from the agency as to what the data represented. Where possible, we converted the data to formats that we could work with readily. In some cases, it was clear that the work involved was counterproductive.

2.3.5 Lack of Location Coordinates

One of the most time-consuming challenges of the data collection effort was obtaining location coordinates for collected samples. To determine important locations for radionuclide and chemical contamination, it was necessary to view the sampling locations relative to major geographic features, such as potential areas of contamination. In addition, it was critical to readily identify and select all sample results that corresponded to a given location. To accomplish this, all analytical results for a given sample needed to be linked to a specific location, identified by its coordinates. The ability to spatially visualize sampling locations was valuable for understanding where the highest concentrations of a given contaminant occurred geographically.

While organizations provided some maps with datasets, a map showing sampling locations was insufficient unless it specifically labeled each sampling location with a unique identifier that was linked to the analytical results. *RAC* received no datasets that met this requirement. Therefore, it was necessary to create additional requests for location coordinates, which were usually provided but were often subject to updates or revisions. In these cases, the coordinates were provided in separate files, which required some effort to link to the appropriate analytical results in a dataset containing thousands of records.

Furthermore, we received location coordinates in various projections (e.g., Universal Transverse Mercator, State Plane, and latitude-longitude). To facilitate comparison, all coordinates had to be in the same projection, and the necessary reprojection of many location coordinates required significant unanticipated effort. We carried out coordinate reprojection and map production efforts multiple times in some cases because of receiving updated coordinates.

2.4 Data Evaluation

Several types of information were critical for completing a thorough evaluation of the data from the Cerro Grande Fire. This information included:

- Thorough data documentation, including sample collection and analysis procedures
- Completed quality assurance of the data package
- Data collection location information
- Times at which data were collected

- Duration between sample collection and analysis—this was particularly important for the air data on gross activity
- Uncertainty
- Data consistency—we established some baseline to allow comparison of different datasets.

In many cases, all this information was not readily available, and it took some time to put the data into a form for comparative evaluation. In most cases, however, this comparison was of limited usefulness because different datasets had different averaging times. Our comparisons were useful primarily for evaluating trends and not for any detailed validation of results or calculation of risks.

2.4.1 Radionuclides

Of all the analytes measured in air during the Cerro Grande Fire, the most complete set of data were available for airborne radionuclides. All of the analyses done on air and biota data include some information about either gross activity or isotope-specific activity.

2.4.1.1 Gross Alpha, Beta, and Gamma Evaluation

Gross activity measurements are a popular analysis because they provide indications of trends relatively readily and inexpensively. Gross alpha, gross beta, and gross gamma data were all collected on the Cerro Grande Fire. Gross alpha and gross beta information can alert scientists to elevated radionuclide concentrations in the air, and because the properties of different nuclides are understood, alpha and beta trends over time provide an indication of the types of contamination that might be present.

LANL regularly evaluates gross alpha and beta concentrations at their AIRNET sites. The EPA and DOE have carried out nationwide sampling, so they are aware of typical ambient concentration levels from background.

Figure 2-2 shows gross beta versus gross alpha concentrations at most sampling locations collected during the fire. This graphic is an unrefined comparison—the samples collected are quite different in terms of variables such as collection capabilities, averaging times, and particle sizes. The graphic demonstrates some interesting trends, however, and should be viewed, along with all comparative graphics in this chapter, as an indicator of trends only and not as an absolute quantitative comparison.

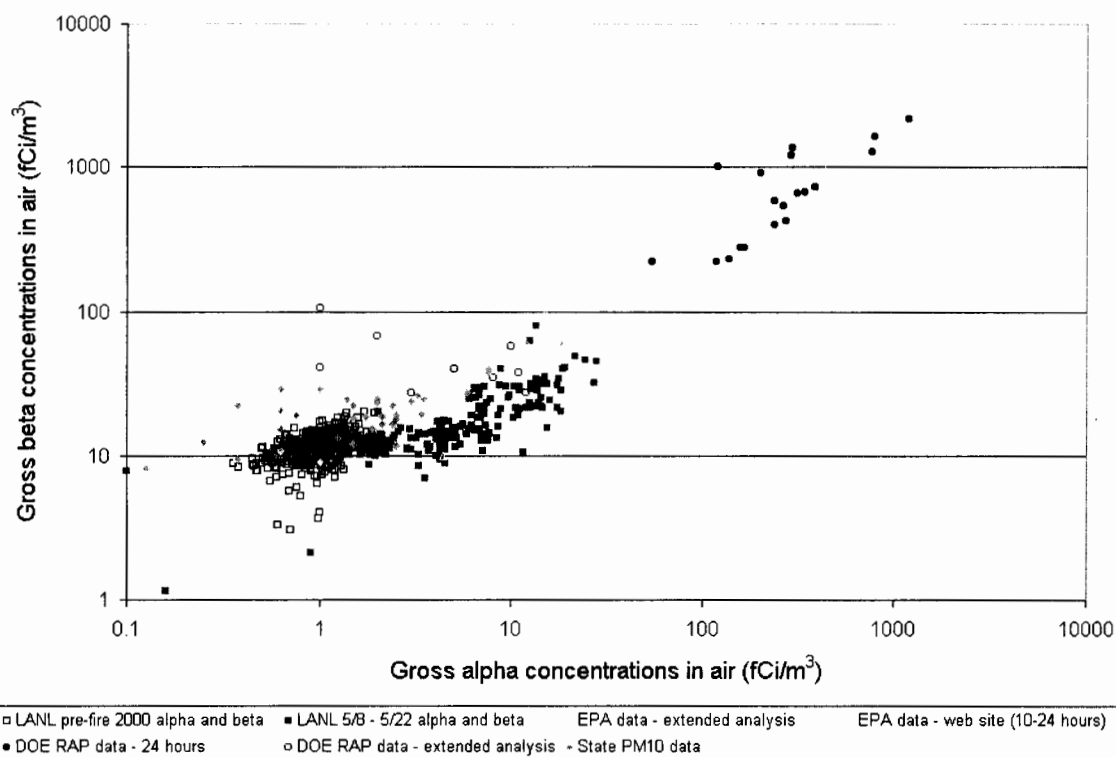


Figure 2-2. Gross beta versus gross alpha concentrations in air collected during the Cerro Grande Fire. Data from all agencies are plotted.

The data collected by LANL (pre-fire 2000 alpha and beta; May 8–May 22, 2000, alpha and beta) compose the largest subset of data. Typical alpha and beta concentrations measured by LANL are represented by open squares. The filled squares show alpha and beta concentrations measured by LANL during the fire. These data were analyzed about 1 week after sample collection. Clearly, concentrations of gross activity were elevated during the fire.

The DOE and EPA samples were collected and analyzed immediately for gross activity. The solid triangles and solid circles represent the low volume EPA and DOE data collected at the JAG sampler locations and analyzed within 24 hours of sample collection. The analysis was repeated on the same samples at least 72 hours later, and the open triangles and open circles show the 72-hour sample results. These data clearly demonstrate that there was a great deal of short-lived activity initially present in the samples that decayed away by the time the samples were reanalyzed. Although many more samples were collected by DOE, they are not shown here because they exhibit the same trends.

The final set of data shown in the figure are the NMED PM10 data analyzed for alpha and beta particle concentrations. While these data, on the whole, are not comparable to the data shown in the figure because they were collected in a manner that selectively collects particles that are <10 microns, they show good agreement with the alpha and beta trends. These data were analyzed approximately 1 week after sample collection.

Ample evidence exists to support the conclusion that gross activity in the air was elevated during the fire. Samples analyzed at various time increments after collection also support the

conclusion that a great deal of short-lived radioactivity was present during the fire, and it probably decayed away in as little as 3 days.

All samples were also analyzed for gross gamma concentrations. Gross gamma analysis showed elevated concentrations at specific energies, which identified the presence of certain nuclides in the sample because of their characteristic gamma energies. The EPA and DOE evaluations carried out within 24 hours displayed the characteristic energies of several short-lived radon decay products, including ^{214}Pb , ^{224}Ra , ^{212}Pb , ^{212}Bi , and ^{208}Tl . Some gamma evaluations also showed the gamma energy characteristic of ^7Be , a longer-lived, cosmogenically produced nuclide. The short-lived nuclides were not detected in any significant quantities in samples analyzed later than 1 day after collection.

Short-lived radionuclides, such as the ones present in the air samples, have their source in the naturally occurring decay series of uranium and thorium. These nuclides are present in soils and vegetation and decay over time, producing what we consider to be natural background radiation. The decay chains of ^{238}U and ^{232}Th contain short- and long-lived nuclides, which decay by alpha, beta, and gamma radiations. It is possible that the elevated alpha and beta activity concentrations in air during the fire resulted from increased levels of naturally occurring radionuclides associated with the burning of vegetation. This was the conclusion of LANL, EPA, and DOE. This possibility is discussed further in Chapter 4 and in Appendix D.

2.4.1.2 Radionuclide-specific Evaluation

Because the primary goal of this project was to identify health risk associated with any LANL-related impacts of the fire, we evaluated data collected for radionuclides that are most likely of LANL origin. The radionuclides that we evaluated were ^{90}Sr , ^{241}Am , ^{239}Pu , and isotopes of uranium.

ESH-17, NMED, and EPA analyzed data collected during the fire for radionuclides. NMED had two sources of radionuclide data: data they collected at samplers collocated with LANL AIRNET samplers and PM10 samples that they collected during the fire and selected for radionuclide analysis. Again, the data were collected with different averaging times and should only be evaluated in terms of trends.

Americium-241 is a decay product of ^{241}Pu and is the primary source of radiation dose at LANL from this plutonium isotope. Plutonium-241 can be released to the LANL environment via plutonium processing and the nuclear fuel cycle. LANL occasionally sees elevated airborne concentrations of ^{241}Am at the onsite waste disposal area sampler (Area G). An elevated concentration at offsite locations is rare.

The samples collected by LANL and analyzed for ^{241}Am contained a tracer contaminant. This contaminant came from the analytical laboratory's ^{241}Pu tracer, and it caused an increase in analytical measured concentration of ^{241}Am . It was possible to remove the analytical laboratory contribution to the LANL sample by subtracting out the results of a matrix blank prepared by the analytical laboratory.

Figure 2-3 shows the concentrations of ^{241}Am in the samples from the Cerro Grande Fire. Counting results, such as these, can be approximated by a normal distribution. If an estimated concentration is less than the 2-sigma analytical uncertainty of the measurement, then it is not considered highly reliable. The diagonal line represents the condition when the concentration is

equal to the 2-sigma sample uncertainty, so points below the line are not reliable. Similarly, points markedly above the line have much less uncertainty.

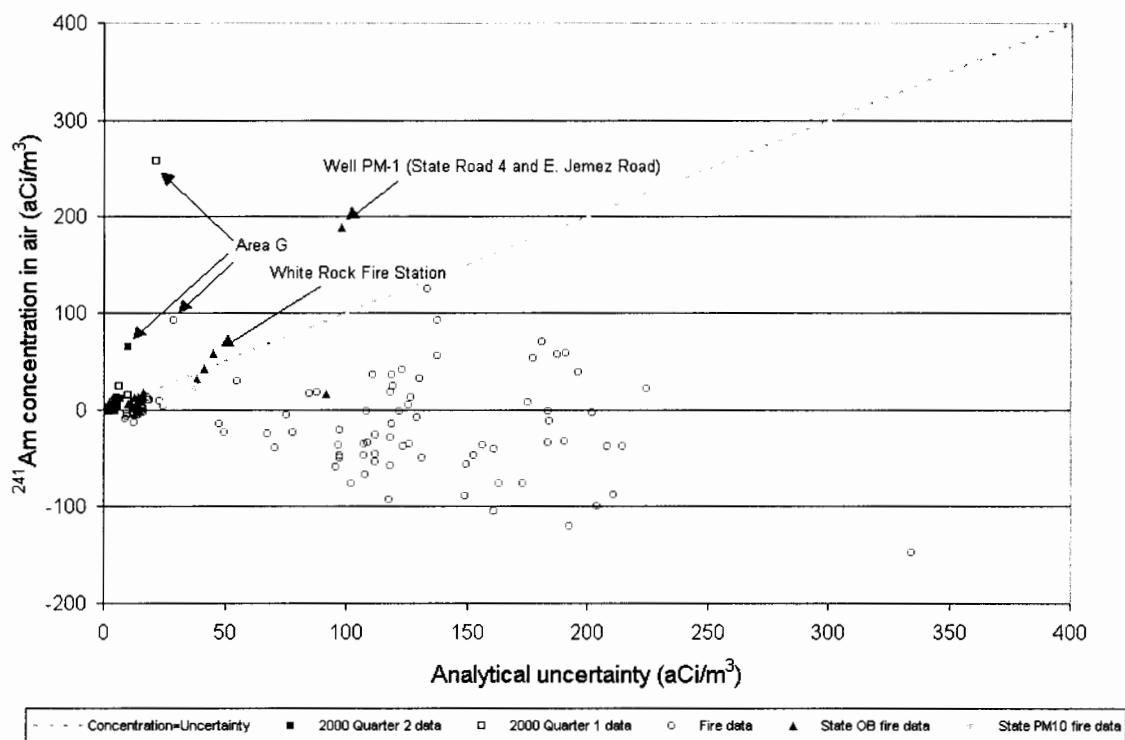


Figure 2-3. Americium-241 concentrations in air versus their analytical uncertainty for samples collected before and during the Cerro Grande Fire.

As measured by LANL, positive sample results existed only at Area G, where it is not unexpected to observe elevated ^{241}Am concentrations in air. The NMED Oversight Bureau data, however, showed elevated values for ^{241}Am at two unexpected offsite locations on the eastern boundary of LANL. The analytical laboratory used by the State used a ^{243}Am tracer in its chemical analysis; therefore, it is possible that this tracer was contaminated with ^{241}Am . During the course of our evaluation, we were unable to confirm or deny the presence of a tracer in the NMED samples. It is also possible that these values were caused by ^{241}Am released during the fire. Because of the high specific activity of ^{241}Am , these relatively elevated concentrations could be the result of only one or a few ^{241}Am particles on the filter.

Plutonium-239 is used in nuclear weapons activities. Contamination of soil with this nuclide is commonly seen near weapons production facilities and the associated waste disposal facilities. Plutonium-239 attaches to soil and can be resuspended on windy days. Elevated concentrations of ^{239}Pu are commonly seen at Area G waste disposal area samplers. Elevated offsite concentrations are not common, but in 1999, an elevated concentration was measured offsite in the Los Alamos town site. LANL personnel speculated that the elevated concentration resulted from soil disturbance in an old LANL technical site with soil contamination.

Concentrations of ^{240}Pu are not distinguishable from ^{239}Pu , so the measured values actually represent $^{239,240}\text{Pu}$ concentrations. Figure 2-4 shows the $^{239,240}\text{Pu}$ data collected during the fire.

Again, the diagonal line represents concentration equal to uncertainty. Values below this line are below their analytical uncertainty and do not represent statistically positive values.

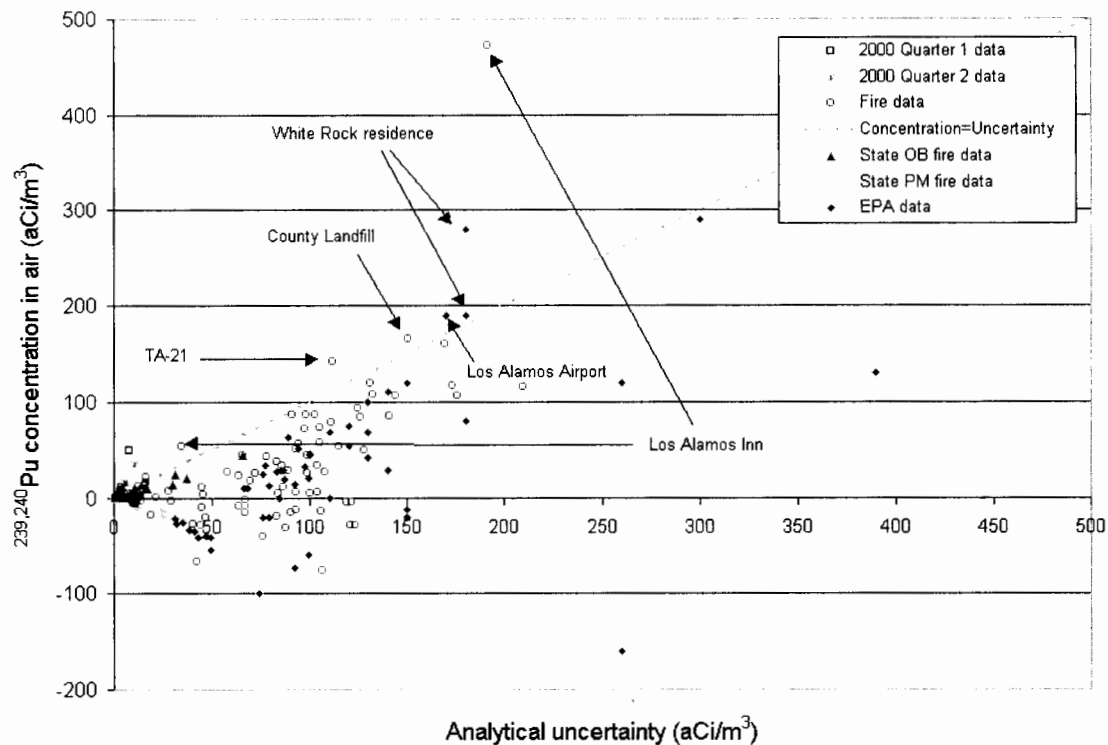


Figure 2-4. Concentrations of $^{239,240}\text{Pu}$ in air versus analytical uncertainty for samples collected before and during the Cerro Grande Fire.

The $^{239,240}\text{Pu}$ data are almost entirely below the analytical uncertainty values. The exceptions to this are two samples collected during the fire at the Los Alamos Inn, one collected at the County Landfill, and another collected at TA-21. There were also four EPA samples that had values above the analytical uncertainty. One of these values is large enough that it is beyond the scale of this graphic. At the Tsankawi National Monument, $^{239,240}\text{Pu}$ concentration in air measured $3.3 \times 10^{-4} \text{ Bq m}^{-3}$ (8800 aCi m^{-3}), three orders of magnitude higher than any $^{239,240}\text{Pu}$ concentration ever reported offsite.

Uranium isotopes are present naturally in the environment. It is relatively easy to discern natural uranium from facility-produced uranium because of the ratio of the uranium isotopes to each other. In natural concentrations, ^{234}U and ^{238}U are generally in a 1:1 activity ratio. At LANL, depleted uranium and enriched uranium are both potential contaminants. Depleted uranium would have a higher concentration of ^{238}U relative to ^{234}U , and enriched uranium would exhibit the opposite trend.

For data collected during the fire, we plotted the isotopic activity concentrations relative to each other to examine possible increased levels of uranium that did not come from the environment. Because concentration versus uncertainty is not plotted, it is important to be certain

that uranium concentrations are statistically positive before trying to infer anything about elevated uranium concentrations.

LANL occasionally measures elevated ^{238}U concentrations, particularly at sites where it has been used in explosives testing. Historically, elevated concentrations of ^{234}U have been seen at onsite samplers in enriched uranium processing areas. When offsite concentrations were measured, they were attributable to natural uranium, appearing in the expected ratio.

Figure 2-5 shows the isotopic concentrations relative to each other. The diagonal line shows the 1:1 ratio of ^{238}U to ^{234}U .

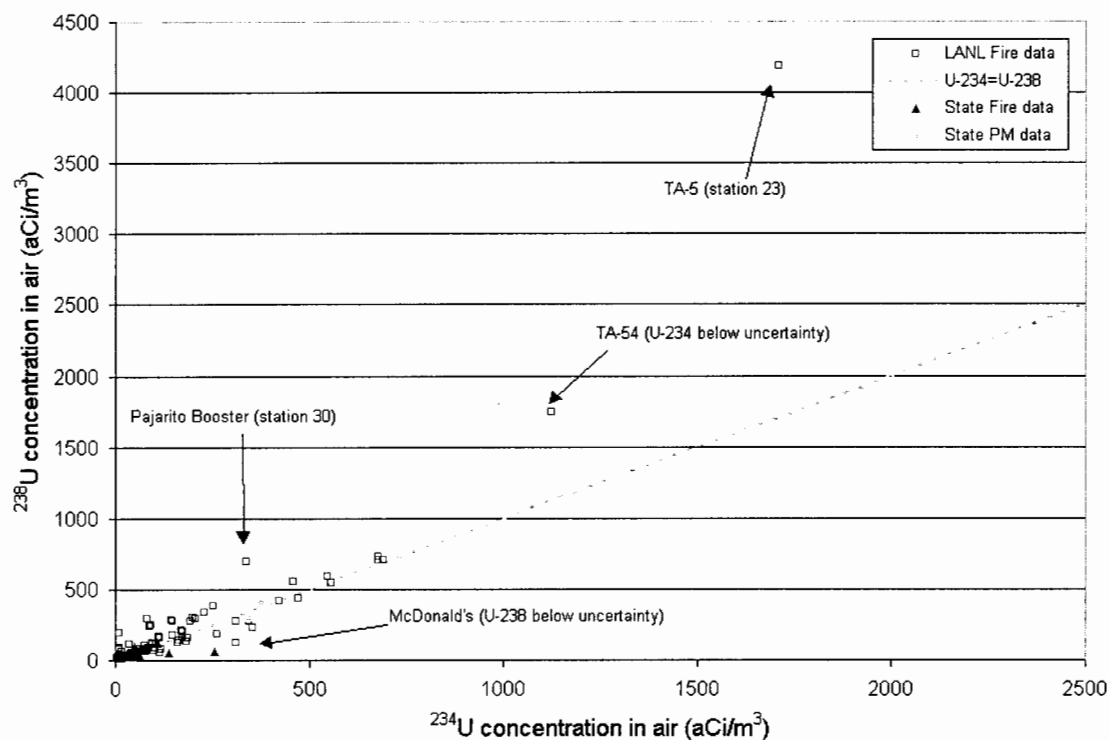


Figure 2-5. Air concentrations of ^{238}U versus ^{234}U collected during the Cerro Grande Fire.

Two of the four data points that exhibited ratios divergent from the expected 1:1 ratio had one of the two isotopic concentrations below the analytical uncertainty. This makes the ratios more difficult to interpret because one of the two values is not statistically valid. Neither of the ratios is so large as to imply that the uranium deviates from natural concentrations. The remaining two values appeared to show elevated levels of ^{238}U (that is, depleted uranium). These samplers are both onsite, but they do not traditionally exhibit elevated concentrations.

It was difficult to interpret the air monitoring data quantitatively because of the significant variations in averaging time, collection techniques, and analytical techniques. It appeared, however, that there were instances of increased isotopic concentrations measured offsite during the fire. There were not, however, enough of these instances to support the significant levels of gross alpha and beta measured during the fire, implying that there may have been a non-LANL source for these increased levels. This is discussed further later in this report.

The soil and produce data collected at locations where the fire plume passed over are another important source of isotopic data. The data received from LANL represented three different types of routine soil monitoring stations. In Figure 2-6 through Figure 2-8, the data for onsite stations (12 stations), perimeter stations (10 stations), and regional background stations (3 stations pre-fire, 4 stations post-fire) are all plotted as the same type of data point because distinctions between the types of stations were not important for this analysis. Another source of data received from LANL included soil samples collected at local farms downwind of the Cerro Grande Fire. These data are represented as a different type of data point. NMED data were collected at 21 farming locations in the path of the plume.

Figure 2-6 through Figure 2-8 show comparisons of pre- and post-fire concentrations of ^{90}Sr , $^{239,240}\text{Pu}$, and ^{241}Am . The analytical uncertainty represented on the x-axis is again the 2-sigma uncertainty.

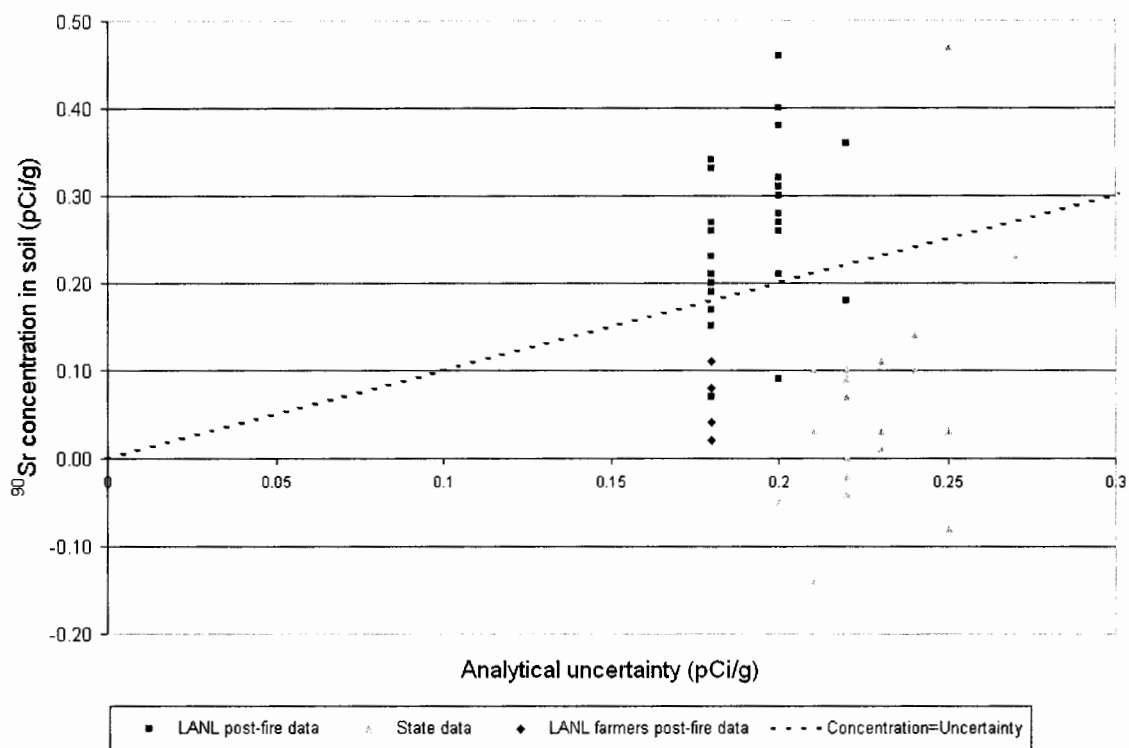


Figure 2-6. Strontium-90 concentrations in soil collected by LANL and NMED at various locations.

No pre-fire data are shown for ^{90}Sr . During 1999, LANL discovered a positive bias in the analytical laboratory's data. This resulted in the data reporting much larger values than were actually present in the soil. The 1999 data were reported by LANL, but they are much larger than the post-fire values shown here and do not provide a meaningful comparison. The mean of 1993–1996 data showed similar ^{90}Sr values to those shown here for post-fire conditions. The regional, perimeter, and onsite mean values for 1993–1996 were 1.1×10^{-2} , 1.3×10^{-2} , and 1.6×10^{-2} Bq g^{-1} ^{90}Sr (0.30, 0.34, and 0.42 pCi g^{-1}), respectively.

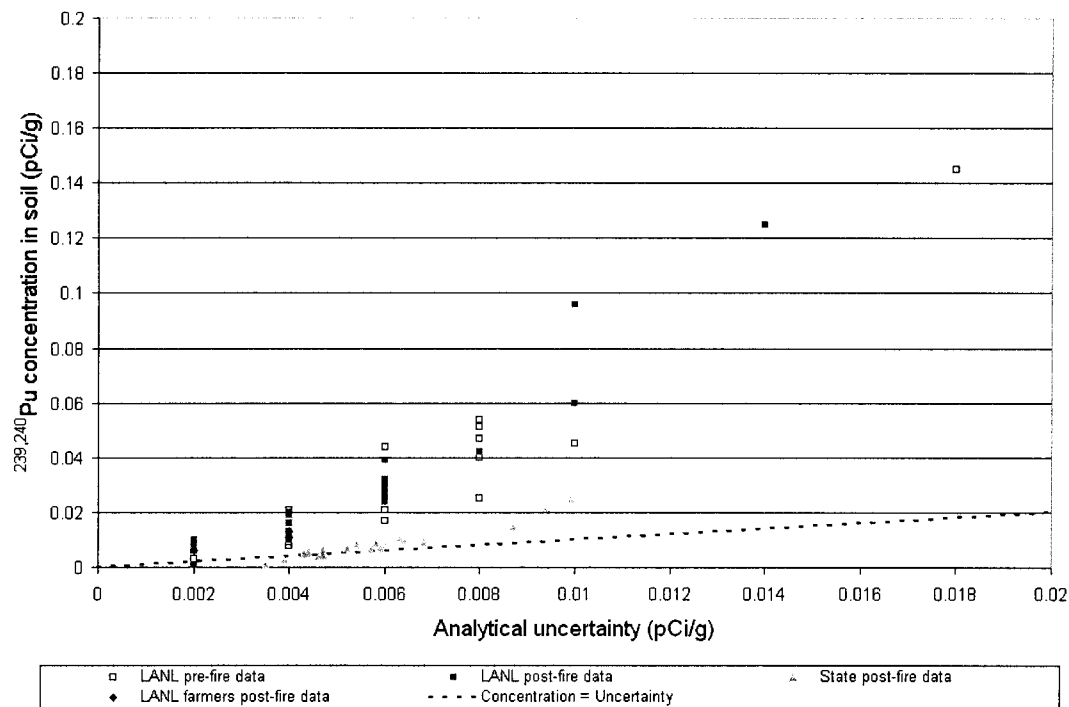


Figure 2-7. Plutonium-239,240 concentrations in soil collected by LANL and NMED at various locations.

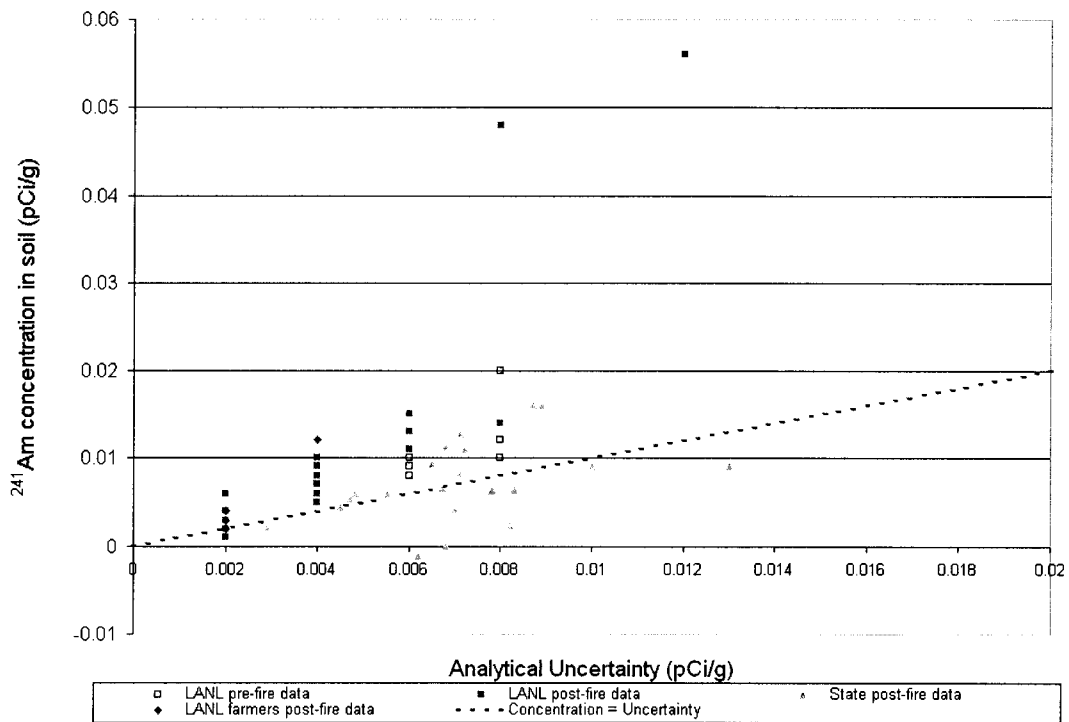


Figure 2-8. Americium-241 concentrations in soil collected by LANL and NMED at various locations.

The pre- and post-fire concentrations measured by LANL at their routine monitoring locations appeared to be relatively consistent, with values measured by both LANL and NMED at local farms generally exhibiting lower analytical values than the routine locations. This was not surprising since the samples collected at downwind farms were at a greater distance from the LANL than the routine monitoring locations. There appeared to be minimal impact on soil concentrations due to the fire.

Figure 2-9 shows total uranium concentrations measured pre- and post-fire by LANL and NMED.

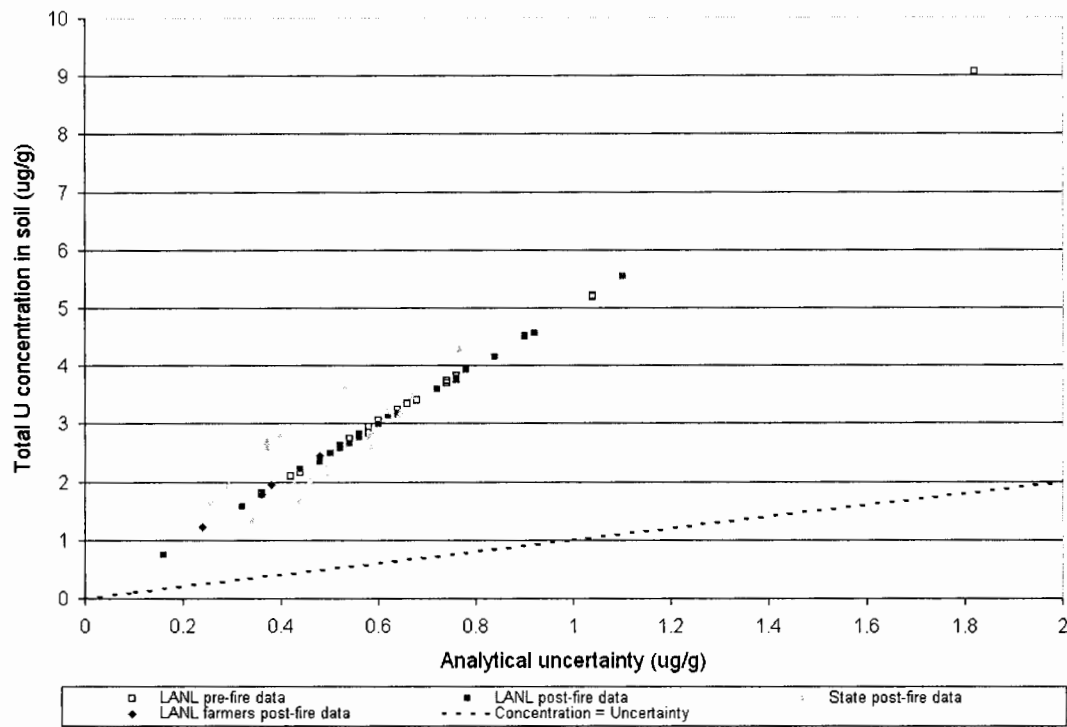


Figure 2-9. Total uranium concentrations in soil collected by LANL and NMED at various locations.

Pre- and post-fire concentrations appeared to be relatively consistent, and a comparison of the post-fire activity ratio of ^{238}U to ^{234}U seemed to support the conclusion that these uranium concentrations originated from natural sources. Figure 2-10 shows this comparison.

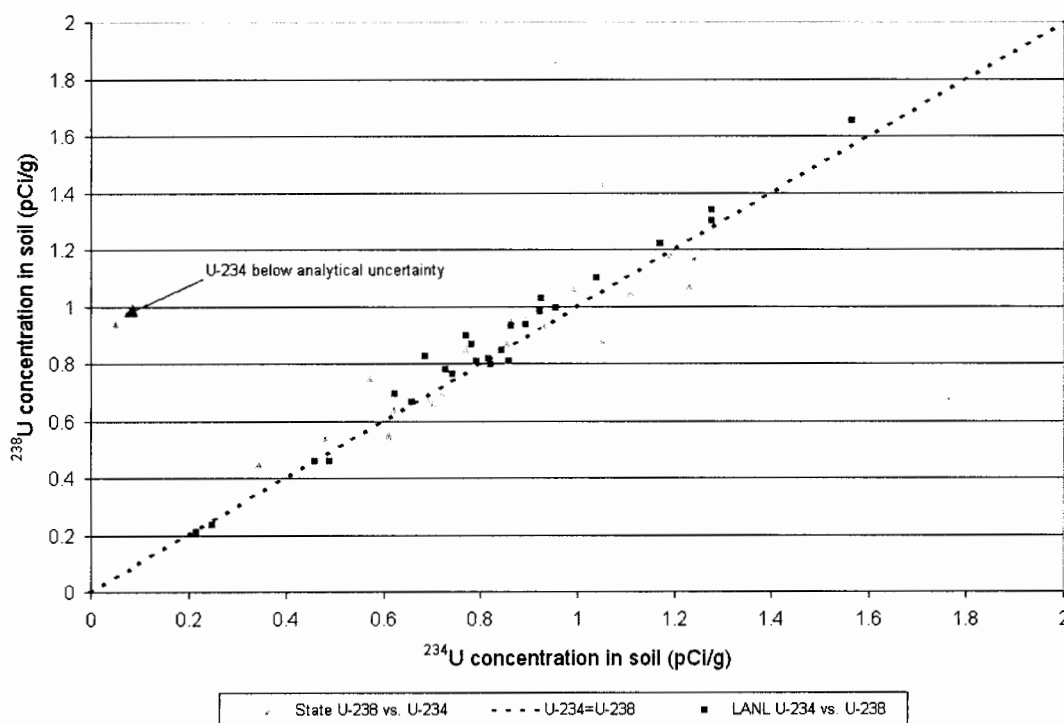


Figure 2-10. Uranium-238 versus ^{234}U concentrations in soil measured post-fire by NMED and LANL.

Two ratios deviated from the 1:1 line. The value to the extreme left side of the chart had a ^{234}U concentration that was less than the analytical uncertainty, making the ratio more difficult to interpret, as the concentration of ^{234}U is not known with certainty. The magnitude of the ratio implied that there may be an increased concentration of depleted uranium. The remaining value may also display an elevated concentration of depleted uranium.

Data on radionuclides measured in produce were also obtained from LANL and NMED. An initial review of the data indicated no discernible impact on produce radionuclide concentrations post-fire as compared to pre-fire. A detailed evaluation of produce data was not considered necessary or valuable for this project.

2.4.2 Chemicals

Air monitoring data on chemicals during the fire were available only from EPA. The EPA analyzed for 21 pesticides in the air samples and none were detected. The EPA analyzed their samples for 23 metals and published a summary on the NMED web site that reported all of the metal concentrations detected were below workplace standards. NMED, LANL, EPA, and the Agency for Toxic Substances and Disease Registry (ATSDR) thought that the metals detected appeared to be attributable to burning vegetation. They concluded that the concentration of metals seen would not be expected to cause adverse health effects. The EPA analyzed samples for 63 organic compounds, and 12 compounds were detected—all below workplace standards (NMED 2000).

Tables of summary data for May 12, 2000, sampling conducted by the EPA, available on the NMED web site, reported all of the concentrations measured that were above the detection limit. The tables also listed all of the pesticides, organic compounds, and metals that were included in the analysis. Benzene; chloroform; xylene; styrene; toluene; trimethylbenzene; PAHs (including acenaphthylene, acenaphthene, phenanthrene, anthracene, and chrysene); and metals (including aluminum, barium, calcium, chromium, copper, iron, magnesium, nickel, potassium, sodium, and zinc) were detected. The EPA concluded that all concentrations were less than standards established to protect health of workers or the public.

LANL soil sampling results indicate that no PCBs, HEs, or PAHs were detected above LANL reporting limits in any of the samples collected upwind or downwind from the fire. Dioxins were not detected in the six soil samples collected, with the exception of 1,2,3,4,6,7,8,9-octachlorodibenzo-p-dioxin (OCDD), which was detected in all the soil samples. DDE, a DDT breakdown product was detected in two of the six samples. Detailed individual data points were not received in a format conducive to further analysis.

Based on the farming soil and produce samples collected at upwind and downwind locations, in the summer following the fire, LANL concluded that there were no significant initial impacts to soil resources of downwind farmers from the air pathway (Fresquez 2000a, 2000d, 2000e). PCBs, HEs, PAHs, and all dioxins, except OCDD, were below detection limits. OCDD levels were less than 23 parts per trillion (ppt). All of the pesticides in farm soils were below detection limits except DDE, which was detected at a farm upwind and another downwind of the fire. DDE is a persistent breakdown product of DDT, which was banned for use in the U.S. in 1972. LANL did not detect DDT-related compounds in soil or ash samples collected after the fire at the soil sampling network locations. They speculated that the DDE detected in farm soil came from spraying operations on Forest Service land adjacent to LANL in the 1960s. If PAHs or HEs had been detected in notable quantities, the measurements could be used to characterize the effects of the fire occurring at LANL. It was not possible to extract any quantitative information on fire releases from the chemical samples collected.

NMED measured metals in farm soil in 21 samples taken from different locations from June 20 to July 21, 2000. NMED also conducted analyses of soil samples for PAHs from five locations on farms of nearby residents that were concerned about effects from the fire. Their results matched those reported by LANL.

NMED measured metals, cyanide, phosphorus, and total organic carbon in sediment, soils, ash, and sludge on LANL property. The ash samples included grab samples, transect, and duplicates or splits of LANL samples for ash.

For the NMED data collected at Los Alamos town site homes and analyzed for asbestos, the highest concentration was 0.013 fibers cm^{-3} from a sample collected near the intersection of Arizona and 36th Street. Surface wipe samples for asbestos were taken in 11 homes in the burned area and inside and outside the Mountain Elementary School and no asbestos was detected (NMED 2000).

Because there are little or no pre-fire data on chemical concentrations in the LANL soils, sediments, and air, it was difficult to evaluate post-fire concentrations. Appendix A to this report looks briefly at LANL operational history, air, soil, and sediment results obtained during the Cerro Grande Fire and results collected during other forest fires. We used this information to put the concentrations of chemicals measured during the Cerro Grande Fire into perspective, determine which may have resulted from LANL, and what chemicals not analyzed for in air

samples may have been present during the fire. This was primarily a qualitative analysis. Our approach to quantitatively evaluate chemical impacts of the Cerro Grande Fire at LANL rested primarily on contamination measured in areas onsite that burned, as described in the next chapter. Appendix F includes some discussion of the health risk implications of smoke inhalation.

2.4.3 Particulate Matter

NMED collected respirable particle (PM₁₀) data from air monitors sampling on various days at the Runnels Building, PERA Building, and Capshaw Middle School in Santa Fe. The data for these locations were obtained for all of 1999 and during the Cerro Grande Fire. NMED also provided data from air monitors they operated temporarily from April 30 to May 20, 2000, at Hernandez, Española, Bernalillo, Taos, and Questa.

Respirable particle levels measured weekly in 1999 and 2000 at the Capshaw Middle School in Santa Fe ranged from 3.7 to 42 $\mu\text{g m}^{-3}$ (ambient concentration not corrected to standard temperature and pressure [STP]). Levels were about 14 $\mu\text{g m}^{-3}$ on May 6, 2000, and about 20 $\mu\text{g m}^{-3}$ on May 12, 2000. The increased concentrations during the fire may have been due to natural sources. This and other aspects of the PM₁₀ measurements are discussed and analyzed further in Chapter 4. Samples were taken at the PERA Building on April 30, May 18, and May 24, 2000, but they were not taken during the time when smoke from the fire would have most influenced concentrations (May 6–17).

Table 2-2 presents respirable particle concentrations measured at the Runnels Buildings in Santa Fe at the time of the fire. They appear to reflect some increase from smoke, particularly during the period when the fire burned most intensely.

Table 2-2. PM₁₀ Concentrations Measured at the Runnels Building

Date measured	PM ₁₀ concentration ($\mu\text{g m}^{-3}$) ^a
May 4, 2000	12
May 6, 2000	13
May 8, 2000	20
May 10, 2000	13
May 14, 2000	21
May 15, 2000	53
May 16, 2000	15
May 17, 2000	21

^a Ambient concentration not corrected for STP.

Data collected at the Runnels Building before the fire showed similar fluctuations in concentration throughout the year, with a mean of 11 $\mu\text{g m}^{-3}$ and a standard deviation of 4.7 $\mu\text{g m}^{-3}$. The PM₁₀ variations during the fire may be due to many air quality conditions that influence PM₁₀ concentration; however, the May 15, 2000, sample may have been influenced by the fire.

Ambient PM₁₀ concentrations in Hernandez ranged from 12 to 18 $\mu\text{g m}^{-3}$ on May 12, 13, 16, and 17, then decreased to around 12 $\mu\text{g m}^{-3}$ in samples taken during the rest of May. Ambient PM₁₀ concentrations measured in four samples taken in Taos were 5.7 $\mu\text{g m}^{-3}$ on April 30, 18 $\mu\text{g m}^{-3}$ on May 1, 12 $\mu\text{g m}^{-3}$ on May 2, and 18 $\mu\text{g m}^{-3}$ on May 3, 2000.

m^{-3} on May 5, $37 \mu\text{g m}^{-3}$ on May 11, and $45 \mu\text{g m}^{-3}$ on May 17. These levels also appeared to represent a fire-related increase.

Ambient PM10 concentrations in Questa were $13 \mu\text{g m}^{-3}$ on May 12, $17 \mu\text{g m}^{-3}$ on May 16, and less than $9 \mu\text{g m}^{-3}$ on samples taken earlier in May. The earliest samples taken in Española were collected on May 15 and measured $41 \mu\text{g m}^{-3}$. The levels then decreased to $30 \mu\text{g m}^{-3}$ on May 16 and $20 \mu\text{g m}^{-3}$ on May 17. Although it appeared that levels in Española and Taos may have increased slightly during the fire, there are limited data from other time periods with which to compare the measurements, and apparent increases may not have been attributable to smoke from the fire.

The PM10 data alone cannot serve to differentiate the influence of LANL on air concentrations of particles because elevated PM10 levels following the fire would be expected from any smoke plume as well as other combustion sources, such as motor vehicles or dust. Some of the increases in PM10 around the time of the fire may be due to the smoke, but the contribution of smoke is difficult to determine. Only one of the measurements at the Runnels Building during the fire is outside the range of values (2.5 to $36 \mu\text{g m}^{-3}$) measured in 1999. This aspect of the PM10 measurements is explored in more detail in Chapter 4.

During the fire, PM data were also collected by LANL at TA-54, LANL's onsite AIRNET laboratory, and also in the vicinity of the hazardous waste facility. LANL was operating a particulate monitor that collected and analyzed PM10 quantities in air continuously, providing 30-minute and 24-hour averages. When the fire burned close to the area where the particulate monitor was located, distinct and dramatic increases in PM concentrations were measured. Figure 2-11 shows these data.

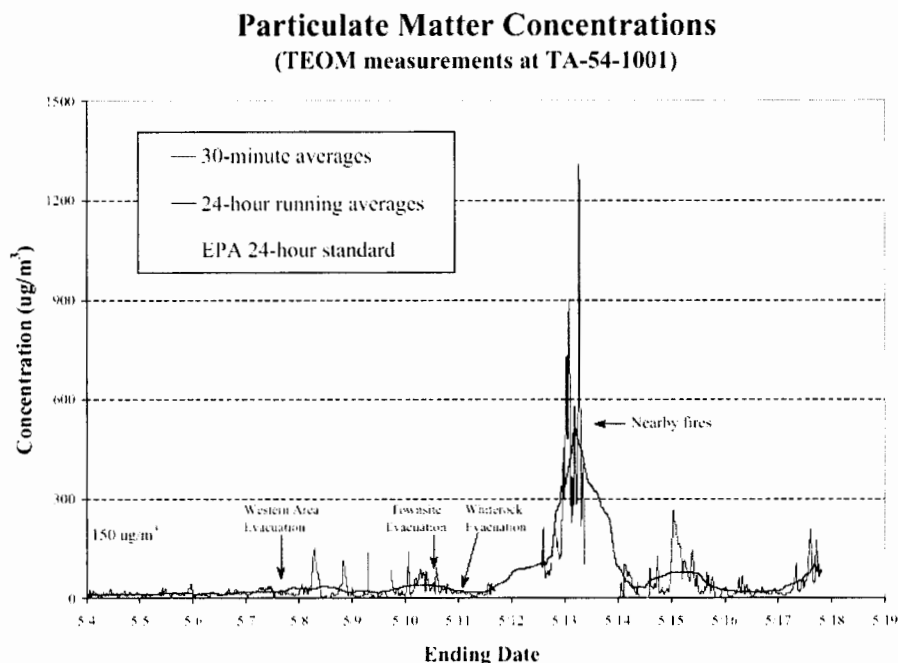


Figure 2-11. Particulate matter (PM10) concentrations measured at TA-54 by LANL (LANL plot).

These increases in concentration support the assumption that as the fire plume approached and passed over, PM10 concentrations probably increased dramatically, particularly at locations near the fire. Chapter 4 includes a full summary of how the PM10 data were used to calibrate our air dispersion model.

2.5 Use of Environmental Monitoring Data to Evaluate Risk from the Cerro Grande Fire

At the beginning of the project, our original intent was to use the environmental monitoring data to explicitly calculate health risk from the Cerro Grande Fire. However, there were too few statistically significant data values for such an analysis. Very few data points exhibited elevated concentrations of LANL-derived radionuclides and chemicals. Where radionuclide concentrations were elevated, we carried out screening-type calculations to examine the maximum measured radionuclide concentrations and determine the associated cancer incidence risk. Assuming the maximum concentrations were present throughout the fire and that exposure to these concentrations lasted for 24 hours a day for the 14-day duration of the fire, cancer risk levels remained below 10^{-7} for all LANL-derived radionuclides and below 10^{-6} for ^{210}Po , a naturally occurring radionuclide.

The environmental monitoring data offered some important insights into data trends. The gross alpha and beta data clearly showed increased concentrations of airborne radiation, especially in the short-term during and immediately after the fire. In addition there were isolated measurements of an increased concentration of LANL-derived radionuclides offsite during the fire; however, the increased alpha and beta activity concentrations did not correlate to these limited data. Chapters 4 and 5 describe the environmental transport modeling and the estimation of risk from materials released from PRS sites that burned. The particulate matter data (PM10) collected during the fire were fundamental for calibrating the model. We were unable to use the remaining environmental data to either quantitatively calculate risk from the Cerro Grande Fire or to validate the model predictions of chemical and radionuclide concentrations other than rough comparisons. Other possible sources contributing to the increased alpha and beta measurements during the fire and isolated measurements of chemicals and radionuclides in air are discussed in Appendix D.

Some key conclusions that we were able to draw from the available environmental monitoring data and their usefulness for evaluating risk were:

- Increased gross alpha and beta levels are clearly present, indicating some sort of radioactive release, whether from the naturally occurring radionuclides in vegetation or from contaminated LANL sites.
- Radionuclide data measured do not seem to support the increases in alpha and beta.
- Radionuclide data are extremely limited in terms of the locations and number of statistically significant increases in air concentration measured during the fire.
- Chemical data are very difficult to draw conclusions from because there are no pre-fire background data.
- Soil and biota monitoring data show no impact from the fire when compared to pre-fire measurements.
- We were unable to use the environmental monitoring data to make quantitative calculations of risk from the Cerro Grande Fire.

3 SOURCE TERM DEVELOPMENT

In this section, we develop the source term for airborne releases from LANL facilities and lands. The source term is defined as the release rate of radionuclides and chemicals from their point of origin (soil) to the transport medium (air). We used screening procedures to reduce the number of radionuclides and chemicals to those that posed the highest potential risk. This chapter discusses the methodology for estimating radionuclide and chemical inventories on burned LANL property and reviews atmospheric fate of chemicals identified as important. Finally, we make source term estimates for those radionuclides and chemicals that were identified as potentially important.

3.1 Identifying and Defining Source Areas

When we drafted the work plan for this project, we assumed that the air monitoring data would be sufficiently comprehensive to allow source term estimates based on measured concentrations in air combined with atmospheric dispersion modeling. As we evaluated the available data, it became apparent that the air monitoring data could not be used directly because not enough different locations were monitored, analytical results were available for only a limited number of chemicals and radionuclides, and some of the data were insufficiently documented. Furthermore, the majority of the concentrations measured were below minimum detection limits because of the short sample times that were employed to avoid filter clogging. As a secondary approach for estimating source terms, we considered the use of data that characterized known areas of contamination at LANL, referred to as potential release sites (PRSs), which burned during the fire. The PRSs are potentially contaminated with hazardous or mixed wastes that are subject to the requirements of the Resource Conservation and Recovery Act (RCRA).

Because of the inconclusive nature of much of the air monitoring data, we developed an alternative approach to estimate contaminants released during the Cerro Grande Fire that made use of both the air monitoring data and PRS data to the greatest extent possible. Although this alternative approach did not permit a detailed estimate of source terms and associated uncertainties, it provided a means for identifying a thorough list of possible contaminants at each PRS and for making some judgment about an upper bound for possible releases during the fire.

Our revised approach to estimating source terms during the fire took advantage of available PRS characterization data and measurements of particulate matter (PM), as well as radionuclides and chemicals in air. We used PRS characterization data provided by the Environmental Restoration (ER) Project at LANL and compiled by the ESH-17 Group to identify chemicals and radionuclides that could have been released during the fire, and used the environmental monitoring data collected by LANL, EPA, and NMED to identify those contaminants actually measured in air during the fire. We compiled information available in the open literature about other forest fires to determine radionuclide and chemical releases typically associated with such events in environments without a nuclear facility (see Appendix A). This approach yielded information about the most important contaminants that may have been released, provided us with a screening of contaminants based on their potential contribution to risk, and allowed us to make estimates of upper bound amounts that could have been released during the fire. These assessments allowed us to focus more carefully on the key radionuclides and chemicals in our analysis.

Excluded from our analysis were releases of radionuclides and chemicals from buildings on LANL property that were damaged or destroyed as a result of the Cerro Grande Fire. The buildings in question were primarily office trailers, and tool and supply sheds containing typical industrial cleaners, lubricants, compressed gases, and other common materials. LANL compiled inventories of the chemicals stored in the destroyed structures (McAtee 2001) and reported that none of the buildings affected were classified as a hazard and none had significant radiological or chemical inventories (LANL 2000). We reviewed the list of contents and inventories provided by McAtee (2001) and believe that quantities were too low to have been released into the air in sufficient amounts to present a health hazard. While burning buildings can expose firefighters to formaldehyde, asbestos, and products of burning plastic, the buildings burned were small and the contribution of these materials to hazardous components in smoke was likely negligible.

The PRS source areas evaluated for the atmospheric pathway include PRSs within the infrared (IR) defined burned area that were confirmed to be burned. We included all IR-boundary PRSs in this assessment, provided that surface soil sampling data were available to characterize them. We have used available sampling data to identify the chemicals and radionuclides detected at each of the source areas and to estimate average, representative concentrations of chemicals and radionuclides at each source area. To accomplish this, we completed three steps:

1. We first linked the sampling data to a specific source area.
2. Then we estimated an average concentration of chemicals and radionuclides using the sampling data.
3. Finally, we defined the surface area that could be characterized by those sampling data.

The areal extent of chemicals and radionuclides in surface soil within the PRSs was initially based on the areas defined by polygons as part of the geographical information system (GIS) coverage files provided by LANL. However, it was recognized that in some cases these polygon shapes, sizes, and locations did not correspond to either the locations of actual sampling data or to the extent of concentrations of chemicals and radionuclides in the soil. In those instances, LANL personnel redefined the surface area extent of PRSs to more accurately reflect the available sampling data. In some cases, the surface extent of the chemicals and radionuclides could not be redefined if there were insufficient sampling data; therefore, we retained the original GIS polygon areas based on the initial coverage files provided by LANL.

3.2 Screening

The primary focus of this project was to determine what contaminants were released from LANL as a result of the Cerro Grande Fire. Ideally, we had hoped to accomplish risk-based screening using (1) the environmental monitoring data collected by LANL, EPA, and NMED to identify those LANL-based contaminants actually measured in air during the fire and (2) the summaries of remedial investigation studies performed by ER at LANL and compiled by the ESH-17 Group to identify potential source areas of specific chemicals and radionuclides that might have been released during the fire.

Because of complications associated with using the air monitoring data to screen for contaminants and calculate risk, we used the data primarily for guidance about what contaminant quantities might be anticipated in the air and to alert us to trends in the data, as described in the preceding chapter. Air monitoring data from different agencies were collected for different and

sometimes unknown durations, resulting in different averaging times that made it extremely difficult to compare the data. The air monitoring data measurements are difficult to use for determining only the LANL contribution to the fire releases because these data reflect not only releases caused by contaminated areas at LANL burning but also (1) naturally occurring radionuclides, (2) anthropogenic (human-made) radionuclides that have deposited on vegetation and ground (such as $^{239/240}\text{Pu}$ and ^{137}Cs from global weapons testing fallout), (3) radionuclides originating from 50-years of LANL operations that have deposited on surrounding lands, (4) radionuclides and chemicals that may have been suspended from PRSs that were *not* burned during the Cerro Grande Fire, (5) radionuclides and chemicals released from PRSs to the air after the fire burned, and (6) combustion products from the burning of LANL structures. These other potential sources contributing to the total quantities measured in air required us to revise our methodology for screening for risk from the Cerro Grande Fire to focus on characterization data from contaminated areas at LANL that burned during the fire.

3.2.1 Screening Methodology

Because a large number of radionuclides and chemicals were identified that were potentially released during the fire, we used a screening procedure to identify those that were most important in terms of health risk. Contaminants that fell below some predetermined level of health risk, when risk was calculated conservatively, were removed from further consideration. We developed source term estimates for the radionuclides and chemicals that were identified as possible contaminants resulting from LANL operations.

The methodology used to obtain the screened list of potential contaminants of concern (PCOCs) is shown in Figure 3-1 and described in detail in the sections that follow. We used the contaminant quantities measured in soil at the PRS locations to estimate an inventory across the entire PRS area. We applied a dispersion coefficient to the inventory value to estimate a conservative⁵ air concentration, assuming the entire inventory was released during the fire. We used these air concentrations to calculate screening risk indices or compared them to reference concentrations to screen radionuclides and chemicals most important in terms of health risk.

⁵ In this context, the term conservative is used to mean an estimate that, in all likelihood, is larger than the actual estimate. When we make preliminary estimates in risk assessments, we want to be certain not to eliminate a contaminant by underestimating the potential effects.

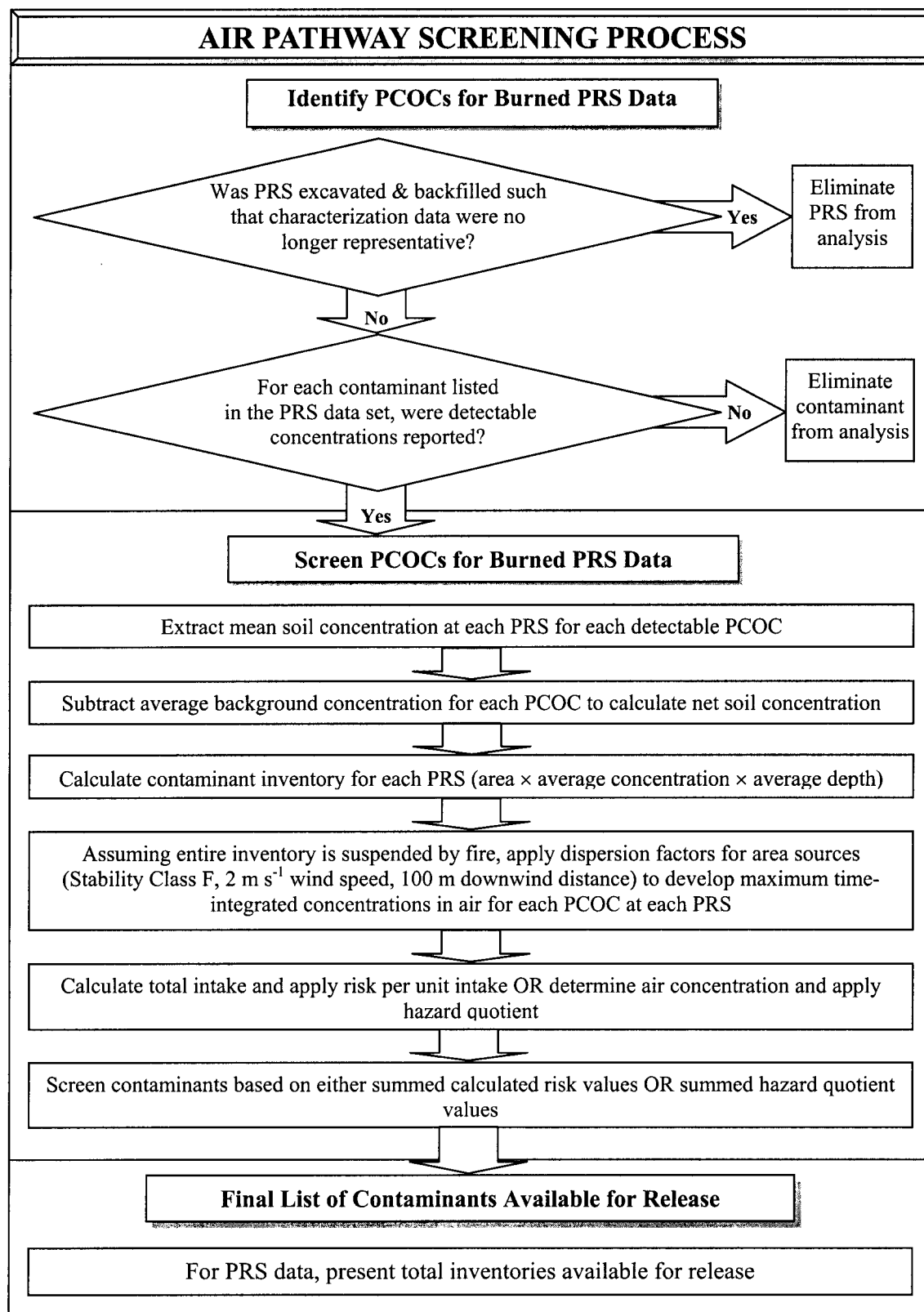


Figure 3-1. Flow chart for air pathway screening analysis.

3.2.2 Identification of Potential Contaminants of Concern

Data collected by the ER Project and compiled by the ESH-17 Group describing the PRSs that burned during the Cerro Grande Fire were available for determining PCOCs that may have been released because of the fire. LANL defines PRSs as sites contaminated with hazardous or mixed waste potentially available for release and subject to the requirements of RCRA. The data described sampling locations within different PRSs where concentrations of chemicals and radionuclides in soil were measured. One PRS may have had several point locations within which concentrations were measured.

Although measurements were collected for many analytes, not all analytes had concentrations that were above detection limits. For the purposes of this project, we did not use contaminant data for which concentrations were not known. We eliminated chemicals and radionuclides with concentrations below the detection limit from further consideration. If the analyte was detected in the PRS data, it was included at this stage of the evaluation.

Additionally, we eliminated PRS locations that were excavated as part of a remediation project before the outset of the fire from consideration because the data available to us for their evaluation were neither current nor reliable.

Appendix B lists the PCOCs identified as detected contaminants using PRS data.

3.2.3 Risk-based Decision Criteria

Before the calculations associated with screening the contaminants were undertaken, we determined the criteria to make the risk-based decisions. We used a risk-based decision criterion to identify those radionuclides that were below a minimum level of concern. This section reviews risk-based decision criteria that have been used at other locations for similar projects and by other agencies. Our methodology required developing different risk-based decision criteria for carcinogens and noncarcinogens to identify the contaminants that many have been released with the greatest impact on health risk.

3.2.3.1 Carcinogens

National Research Council (1995) suggested a decision criterion of 0.07 Sv for a whole-body lifetime dose for identifying sites where a dose reconstruction may be warranted. This value is based on the Federal Registry 10 CFR 20 maximum annual dose limit of 0.001 Sv to any individual at a nuclear site boundary, multiplied by 70 years. In terms of risk, this is roughly equivalent to a lifetime excess cancer incidence risk of 5×10^{-3} (1 chance in 200).

The Oak Ridge Health Agreement Steering Panel, of the Oak Ridge Dose Reconstruction study, established a decision criterion of 10^{-4} (1 chance in 10,000) lifetime excess cancer incidence risk for the study as a whole (Theissen et al. 1996). For screening releases of radionuclides to the aquatic pathways (Clinch River), a lifetime excess cancer incidence risk criterion of 10^{-5} (1 chance in 100,000) was applied (Apostoei et al. 1999). The lower value was used because each radionuclide was compared to the decision guide independently for each exposure pathway rather than combining the exposure risk from all pathways. The calculated screening index was a conservatively biased estimate of excess lifetime risk to the most at-risk

individual and was, therefore, expected to overestimate the risk to most or all real individuals (Apostoaie et al. 1999, page 3-1).

In the Hanford Environmental Dose Reconstruction Project, one of the criteria used to define the physical area to be included in the study calculations (study domain) was a thyroid dose of 1 rad (0.01 Gy) to a child or infant (Shleien 1992). This dose represents an increased lifetime risk for radiation-induced thyroid cancer in the order of 2×10^{-4} .

For continuous exposures to ionizing radiation, the National Council on Radiation Protection and Measurements (NCRP) recommends an annual limit for members of the public of 1 mSv effective dose (NCRP 1993). This is the same as the value recommended by the International Commission on Radiological Protection (ICRP) (ICRP 1991). This dose limit corresponds to a lifetime risk of about 4×10^{-3} , assuming the risk per sievert from fatal and nonfatal cancers is 6×10^{-2} (ICRP 1991, Table 3) and a 70-year lifetime exposure. The NCRP also defines an annual negligible individual dose (NID), which establishes a boundary below which the dose can be dismissed from consideration and sets the NID at 0.01 mSv effective dose. This corresponds to a lifetime risk of about 4×10^{-5} using the same assumptions as above.

EPA has specified an upper bound individual lifetime cancer risk "target range" for carcinogens of 10^{-4} to 10^{-6} within which it strives to manage risks as a part of a Superfund cleanup. The risk estimates are determined using reasonable maximum exposure assumptions for either current or future land use (EPA 1991). Once a decision has been made to cleanup, EPA has expressed a preference for cleanups achieving the more protective end of the range of 10^{-6} . The upper boundary of the risk range is not a discrete line at 10^{-4} , although EPA generally uses 10^{-4} in making risk management decisions. EPA has stated that a specific risk estimate around 10^{-4} may be considered acceptable if justified based on site-specific conditions (EPA 1991). For example, in a Clean Air Act rulemaking establishing National Emissions Standards for Hazardous Air Pollutants (NESHAPs) for U.S. Nuclear Regulatory Commission (NRC) licensees, DOE facilities, and many other kinds of sites, EPA concluded that a risk level of 3×10^{-4} is essentially equivalent to the presumptively safe level of 1×10^{-4} . EPA explicitly rejected a risk level of 5.7×10^{-4} in the case of elemental phosphorus plants in this rulemaking. EPA has consistently concluded that levels of 15 mrem yr⁻¹ effective dose equivalent (EDE) (which EPA equates to approximately a 3×10^{-4} increased lifetime cancer risk) or less are protective and achievable (EPA 1997). EPA has explicitly rejected levels above 15 mrem yr⁻¹ EDE as being not sufficiently protective. For example, EPA has found the NRC dose limit of 25 mrem yr⁻¹ (equivalent to approximately 5.7×10^{-4} increased lifetime risk) specified in NRC's Radiological Criteria for License Termination (decommissioning rule) to be beyond the upper bound of the risk range generally considered protective under the Comprehensive Environmental Response, Compensation and Liability Act (CERCLA) (EPA 1997).

The EPA approach has been adapted to identify and prioritize potential remediation sites at the Idaho National Engineering and Environmental Laboratory using a target risk level of 10^{-6} . The scenarios evaluated are based on current residential or occupational exposure conditions with exposure durations of 30 and 25 years, respectively. The pathways evaluated are ingestion of drinking water, inhalation of contaminated particulates, ingestion of contaminated soil, and external exposure to soils. Each pathway is evaluated independently (Fromm 1996).

Based on the above information and the fact that we were assessing carcinogenic contaminants against the risk criterion on an individual basis, we adopted the protective lifetime cancer risk criterion of 10^{-5} for this study. We conservatively assessed the screening risk index of

contaminants available for release during the fire and compared those indices to the 10^{-5} level. We eliminated contaminants with risk indices below that level from further analysis. Further research is warranted for contaminants that fell above the 10^{-5} level and that are probably LANL-produced.

3.2.3.2 Noncarcinogenic Chemicals

For noncarcinogenic chemicals, we used reference concentrations developed by EPA and other authoritative bodies (Appendix C) and compared these to the actual or predicted air concentration. Dividing the predicted concentration by the reference concentration developed a hazard quotient. A hazard quotient less than 1 suggested that exposures to that concentration would not have caused adverse health effects based on work done in the Oak Ridge Dose Reconstruction (Bruce et al. 1999). The reference concentrations are conservative and are designed to protect sensitive members of the public. Reference concentrations have not been derived for all of the chemicals considered. If a reference concentration was not available, then we used a workplace standard, divided by 10 (to account for the fact that such standards are designed for healthy workers exposed during a standard workweek rather than the public exposed 24-hours a day). We used the criterion that when the hazard quotient was greater than 1, noncarcinogens were maintained for further consideration.

Thus, two screened lists evolved: one where contaminants were compared by hazard quotient and one where contaminants were compared by risk index. We evaluated all contaminants that exceeded either of the above criteria (hazard quotient >1 or risk index $>10^{-5}$) further.

3.2.4 Screening of Potential Contaminants of Concern Identified with Potential Release Site Data

The data on PRSs that burned during the Cerro Grande Fire were delivered from LANL in the form of a database that listed, among other things, PRS ID number; sample location (UTM coordinates); analyte name; concentration (in picocuries per gram for radionuclides and milligrams per gram for chemicals); and depth of sample. We used this information to construct another database and calculate radionuclide or chemical inventory, a maximum potential air concentration, and screening risk index from inhalation of that concentration. We used the PRS database in this fashion because we recognized the potential for some contaminant releases that were not detected by the air monitoring system.

For each PRS ID number, several samples may have been analyzed for the same contaminant. In such situations, we calculated a mean concentration of the analyte at that PRS (picocuries per gram for radionuclides and milligrams per gram for chemicals). For PRS locations where only one sample was collected and analyzed for a given contaminant, we used that concentration as the concentration across the PRS. Because the primary goal of this project was to predict risk from the Cerro Grande Fire resulting from LANL's contribution, it was important to determine background concentrations in soil. Using both information from LANL's ESH-20 Group and ER Project, we determined average background concentrations of contaminants of concern at the PRSs. These average background levels were subtracted from the average

concentrations determined at each PRS to calculate a net concentration. These net concentrations were used to calculate inventory and screening risk for each contaminant.

For PRSs with more than one sample for a given contaminant, we averaged sample depths to obtain a mean sample depth. We obtained information about the area of each PRS from LANL. Using mean sampling depth (m), PRS area (m²), and a bulk soil density of 1.4 g cm⁻³, we calculated the mass of soil at each PRS (g) as shown below.

$$M = D_{mean} \cdot A \cdot \rho_b \cdot CF_a \quad (3.1)$$

where

- M = mass of soil in the PRS (g)
- D_{mean} = mean depth of samples collected at PRS (m)
- A = area of PRS (m²)
- ρ_b = bulk soil density (g cm⁻³)
- CF_a = area units conversion factor (10⁶ cm³ m⁻³).

The inventory of each radionuclide (pCi) or chemical (mg) was then calculated using the following equation:

$$I = M \cdot C_{net} \quad (3.2)$$

where

- I = inventory at PRS (pCi or mg)
- M = mass of soil at the PRS (g)
- C_{net} = net contaminant concentration at PRS (pCi g⁻¹ or mg g⁻¹).

This inventory was assumed to be the total inventory for that contaminant at each PRS location. We assumed that the entire inventory was released and used the dispersion estimates shown in Figure 3-2 and described here to obtain conservative estimates of the air concentrations and the amounts inhaled. We calculated area source χ/Q (concentration divided by source term s m⁻³) values using a straight-line Gaussian Plume model. Turner (1994) gives the standard dispersion equation for a ground-level point release along the plume centerline.

$$\frac{\chi}{Q} = \frac{1}{2\pi\sigma_y\sigma_z u} \quad (3.3)$$

where

- σ_y = standard deviation of the concentration distribution in the crosswind direction (m)
- σ_z = standard deviation of the concentration distribution in the vertical direction (m)
- u = wind speed (m s⁻¹).

For ground-level releases, the most conservative concentration estimate occurs under stability class F conditions, when σ_z is minimized. A wind speed of 2 m s⁻¹ is typically assumed

for such calculations. σ_y and σ_z for the Pasquill-Gifford stability class F are given by the following equations:

$$\sigma_y = \frac{1000 \cdot x \cdot \tan[4.1667 - 0.3691 \cdot \ln(x)]}{2.15} \quad (3.4)$$

$$\sigma_z = 15.209 \cdot x^{0.81558}$$

where x is the downwind distance in km and σ_z is applicable for distances that are less than 2 km. This equation defines χ/Q is for a point source. We estimated air concentrations from ground-level area sources by modifying σ_y in the point source solution to account for the initial dispersion induced by spreading the source over a larger area. For *square* area sources, this modification is approximated by

$$\sigma_y = \sigma_y + \frac{s}{4.3} \quad (3.5)$$

where s is the length of side of the square in meters. Figure 3-2 illustrates the area-adjusted χ/Q as a function of the area of the source.

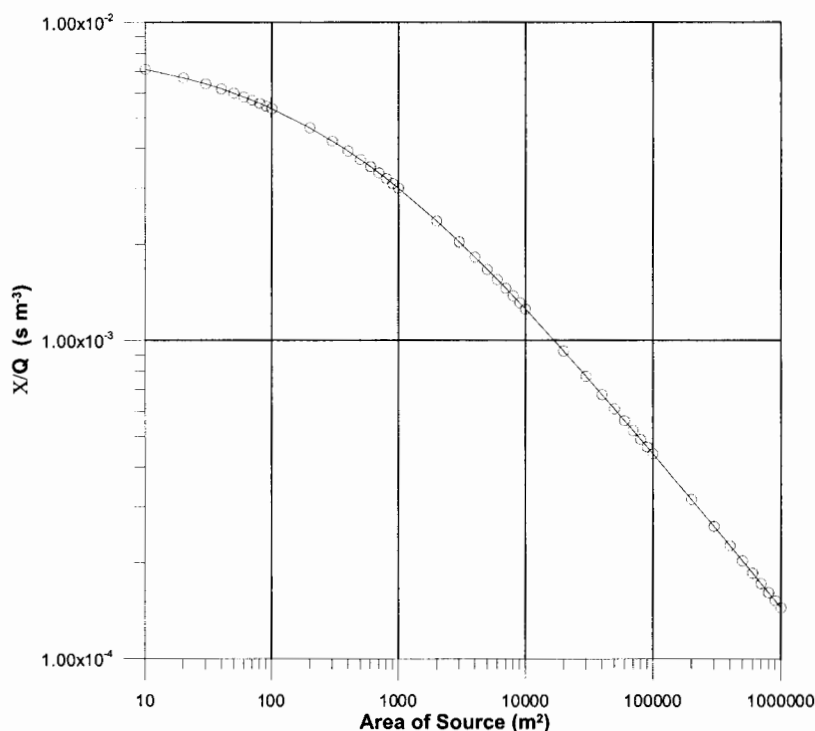


Figure 3-2. Centerline area source χ/Q for a ground-level release as a function of the source area for Pasquill-Gifford stability class F and 2 m s^{-1} wind speed. The χ/Q was calculated at 100 m from the center of the source. For source areas greater than $40,000 \text{ m}^2$, the receptor is within the source.

3.2.4.1 Radionuclide Screening Risk Index

These dispersion estimates, when applied to the radionuclide inventory, gave a conservative estimate of air concentration and, thus, total inhaled intake, assuming the entire inventory was released.

$$N_i = I \cdot \frac{\chi}{Q} \cdot BR \cdot CF_t \cdot CF_r \quad (3.6)$$

where

- N_i = total inhaled intake of contaminant (Bq)
- χ/Q = dispersion coefficient (s m^{-3})
- BR = breathing rate ($20 \text{ m}^3 \text{ d}^{-1}$)
- CF_t = time units conversion factor ($1.2 \times 10^{-5} \text{ d s}^{-1}$)
- CF_r = radionuclide activity units conversion factor ($0.037 \text{ Bq pCi}^{-1}$).

Once the total intake was calculated, we applied risk factors for radionuclides. Risk factors represent the risk per unit intake of a contaminant. For radionuclides, risk factors have been calculated for inhalation, ingestion, and external exposure (Eckerman et al. 1999). The risk is excess lifetime risk of cancer incidence, from the radionuclide of interest and all associated progeny that would be produced after intake of the parent. For inhalation, three different classes describe the biological clearance rate of most radionuclides within the respiratory tract: fast, medium, and slow. EPA recommends clearance classes for some radionuclides commonly found in the environment (Eckerman et al. 1999). In these cases, we used the morbidity (incidence) risk factor for the recommended clearance class. For radionuclides where no recommendation was made, we used the morbidity risk factors for the most conservative clearance class (slow). We summed the screening risk index value by nuclide across the PRSs to determine total screening risk index for exposure to each radionuclide.

$$RI = N_i \cdot RF \quad (3.7)$$

where

- RI = screening risk index
- N_i = total intake of contaminant (Bq)
- RF = risk factor (Bq^{-1}).

3.2.4.2 Noncarcinogenic Chemical Screening Hazard Quotient

For noncarcinogenic chemicals, we used total inventory and dispersion factor to calculate an average air concentration, assuming the entire contaminant inventory, calculated using Equation (3.2), was released over 2 weeks. This was calculated using the following equation:

$$C_{avg} = I \cdot \frac{\chi}{Q} \cdot \frac{1}{ED} \quad (3.8)$$

where

- C_{avg} = average air concentration during the period of the fire (mg m^{-3})
 I = inventory at PRS (mg)
 χ/Q = dispersion coefficient (s m^{-3})
 ED = exposure duration (s).

This estimated air concentration, based on the inventory data, was compared to a reference concentration below which adverse health effects are not expected to occur. We then calculated a screening hazard quotient, which is a simple ratio of the estimated air concentration to the reference concentration. A screening hazard quotient less than 1 suggested that exposures to that concentration would not have caused adverse health effects. The reference concentrations are conservative and are designed to protect sensitive members of the public. Reference concentrations have not been derived for all of the chemicals considered. If a reference concentration was not available, then we used a workplace standard, divided by 10 (to account for the fact that such standards are designed for healthy workers exposed during a standard workweek rather than the public exposed 24 hours per day). The reference concentrations are described in more detail in Appendix C.

For calculations of the predicted air concentration, we used an exposure duration of 2 weeks. The duration of the fire spanned a time period of approximately 2 weeks, so calculating a concentration assuming that exposure period would be a conservative assessment of potential air concentrations resulting from the fire. Also, many of the reference concentrations to which we compared the potential air concentrations were determined for subchronic exposures lasting from 2 weeks to 7 years. Although it is very conservative to compare reference concentrations likely developed for exposures of 7 years to exposures estimated to occur over 14 days, it may underestimate the screening hazard quotient to assume that the inventories at the PRSs were released over 7 years. This conservative approach toward screening produced conservative predicted concentrations and hazard quotients.

3.2.4.3 Carcinogenic Chemical Screening Risk Index

For carcinogenic chemicals, we used slope factors and estimated potential concentrations to calculate excess lifetime cancer incidence risk index. To apply the slope factor to an estimated concentration, we applied breathing rate, body weight, exposure time, and averaging time. The concentrations calculated using Equation (3.8) assumed that the total inventory was released over 14 days. Exposure time to the estimated concentration was assumed to be 14 days. We assumed the averaging time for a lifetime was 70 years and mean body weight was 158 lb (71.8 kg) (EPA 1999). We used this concentration in the equation below to calculate a risk index for carcinogenic chemicals.

$$RI = \frac{C_{max,p} \cdot SF \cdot BR \cdot ET}{W \cdot AT} \quad (3.9)$$

where

- RI = excess lifetime cancer incidence risk
 $C_{max,p}$ = maximum predicted potential concentration (mg m^{-3})

<i>SF</i>	=	cancer risk slope factor (kg d mg ⁻¹)
<i>BR</i>	=	breathing rate (m ³ d ⁻¹)
<i>ET</i>	=	exposure time (d)
<i>W</i>	=	weight (kg)
<i>AT</i>	=	averaging time (d).

Appendix C provides details of the methodology, including how reference concentrations, occupational standards or guidelines and slope factors were obtained or derived and how they were applied.

Applying risk factors, slope factors, and reference concentrations to these very conservative estimates of air concentration from contaminant inventory provided a screening-level estimate of risk index/hazard quotient. These values certainly do not represent the actual risk/hazard to this contaminant during the fire, but instead they provide a conservative evaluation of either screening risk index or screening hazard quotient by which to compare the impact of various contaminants. We compared these risk index values to the risk decision criterion of 10⁻⁵ and the hazard quotient of 1 established above and developed a screened list of contaminants from the PRS data (Table 3-1).

Table 3-1. List of Contaminants from the Potential Release Site Data with Screening Risk Index Values or Hazard Quotients Larger than the Decision Criteria

Acenaphthylene	Dinitrobenzene[1,3-]	Uranium
Aldrin	Dinitrotoluene[2,4-]	Vanadium
Aluminum	Fluoranthene	Zinc
Amino-2,6-dinitrotoluene[4-]	HMX	Protactinium-231
Amino-4,6-dinitrotoluene[2-]	Iron	Thorium-227
Antimony	Manganese	Uranium-234
Aroclor-1254	Mercury	Plutonium-239
Arsenic	Methylnaphthalene[2-]	Radium-226
Barium	Naphthalene	Thorium-232
Benzo(a)pyrene	Nickel	Uranium-238
Beryllium	Nitrobenzene	Americium-241
Cadmium	Nitrotoluene[4-]	Plutonium-238
Chromium (hexavalent)	Pyrene	Radium-224
Chromium (total)	RDX	Potassium-40
Cobalt	Selenium	Neptunium-237
Copper	Silver	Uranium-235
Cyanide (total)	TATB	Lead-210
Dibenz(a,h)anthracene	Thallium	Lead-212
Dibenzofuran	Trinitrotoluene[2,4,6-]	

For this screening analysis, we used a release fraction of 1 for all radionuclides and chemicals. This would certainly not be realistic for all contaminants. Many of the metals, such as aluminum, iron, nickel, silver, copper, and zinc, measured in soil samples taken from the PRSs may be present as solid materials. Iron structures, metal equipment, chunks of scrap metal, and building materials are examples of objects that would not be subject to dispersion and would not

readily be released from the soil or waste area into the air. Release fractions are discussed and applied in a later section of this chapter.

Figure 3-3 shows the locations of the PRSs contaminated with the above radionuclides and chemicals that burned. Because of the large number of locations, it was difficult to provide legible PRS ID numbers, so Figure 3-3 gives a general indication of where PRSs are located across the site.

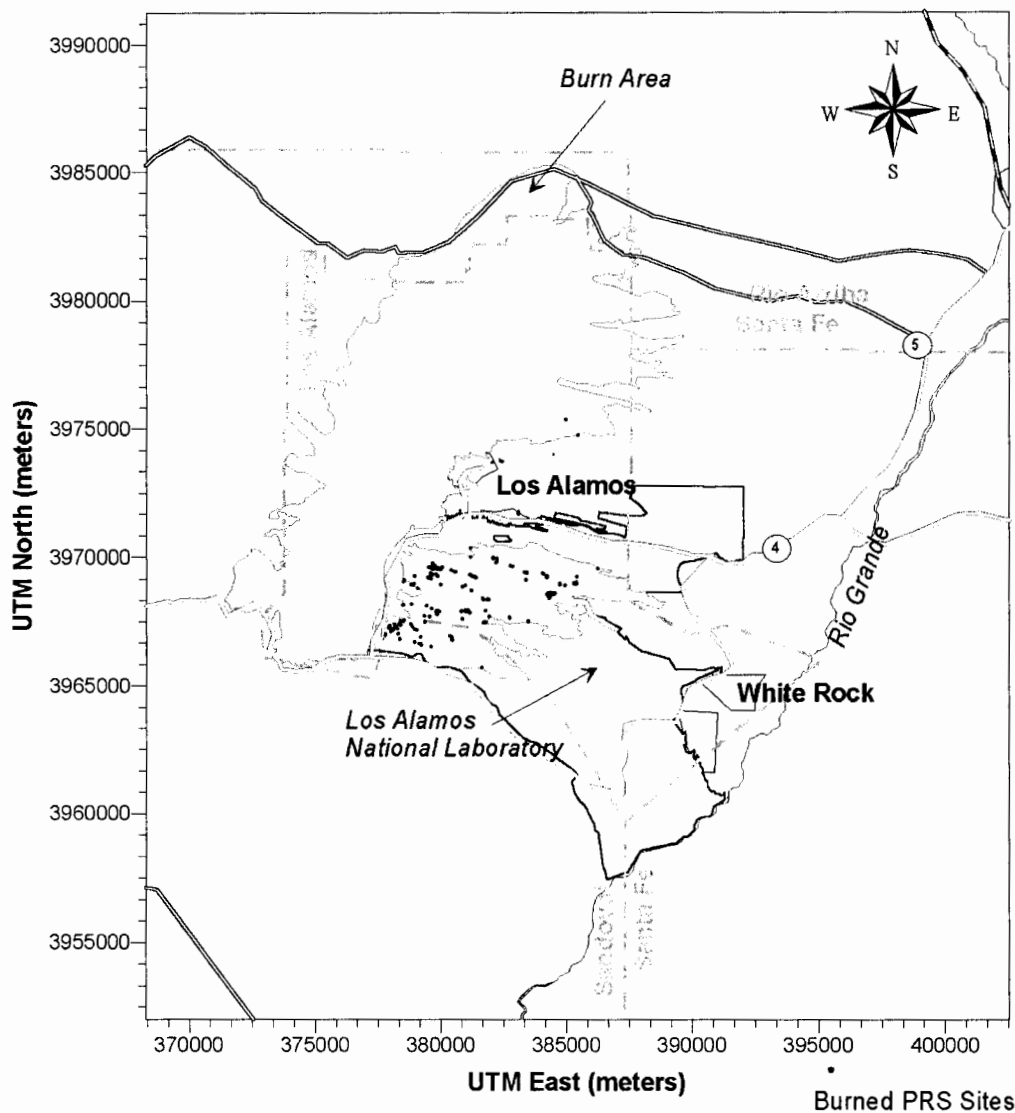


Figure 3-3. Location of PRSs that burned during the Cerro Grande Fire. Most of the sites burned on May 11, 2000. Several sites burned on May 12–13, 2000.

3.2.5 Limitations and Uncertainties Associated with Estimated Source Area Concentrations

Generally, a study involved with estimating potential releases and consequent exposures to individuals commits a large fraction of the resources available to identifying and characterizing data sources (i.e., understanding limitations and uncertainties) and calculating the quantity of material available for release (i.e., source terms) because the remainder of the study relies on the credibility of these values. The short time frame and limited resources available for this project required us to make several assumptions about the data. We used the data available to us in the most logical and reasonable manner, given these time and resource constraints.

The following sections provide a discussion of relevant issues as they relate to uncertainties and limitations associated with the source areas we characterized for this project. An inherent uncertainty associated with each of the source areas characterized was our inability, based on available data, to understand how chemical and radionuclide distribution at sites in the LANL environment has changed over time, which was expected to vary by analyte, and how this could have impacted our calculations. Much of the data used to characterize the source areas was collected from 1993 to 1997. Certainly, some changes in distribution and extent of contamination would be expected since that time, and it is not possible to quantify the degree to which this could impact our transport calculations.

Additionally, the background data used to determine net concentrations were generic background data on contaminants in LANL area soils and did not reflect the spatial heterogeneity that would be expected at different PRSs (i.e., we assumed a single background value for each radionuclide or chemical and used that value to represent conditions at all source areas). It is not possible to quantify how this might contribute to the uncertainty, although it certainly would have some impact. However, the impact of background variability is likely less significant than the uncertainties associated with estimating the true areal extent of contamination and a value that appropriately characterizes the magnitude or level of contamination across that areal extent, both of which would be expected to vary by contaminant. These sources of uncertainty are discussed in the following sections.

3.2.5.1 Uncertainties Associated with the PRS Characterization Data

The LANL ER Project collected the PRS characterization data for purposes of environmental restoration and remediation. These data were not collected with the intent of conducting risk analyses or contaminant inventory development, and the purposes for and manner in which the ER Project collected their data may not be consistent for different PRSs. Therefore, it was difficult to quantify the uncertainty and accuracy associated with the data. These data, compiled by LANL for *RAC*, were used to estimate potential source area inventories. These data represented point concentration information for surface soil samples collected from specific PRSs. The ER Project was in the process of consolidating a number of these PRSs into fewer but more comprehensive units, but that process was ongoing and it was unclear how it would impact the process of site characterization. Because the existing characterization data appeared to be most appropriately organized on a PRS basis, we used and organized the data on the PRS basis as defined for us by ESH-17 and ER.

Although measurements were collected for many analytes to help define and understand existing concentrations of chemicals and radionuclides at potential source areas, not all analytes had concentrations that were above detection limits. We eliminated all values reported as below the detection limit from further consideration and did not use them for calculating average concentrations across the source areas because our approach was designed to be conservative. Soil samples associated with sites that had been excavated and/or backfilled before the fire as part of a remediation project were identified in the database files that we were provided. We eliminated these samples from consideration, because they were not considered representative of site conditions existing at the time of the fire.

There are uncertainties associated with the accuracy, completeness, and representativeness of the actual characterization data. LANL staff shifted from the concept of organizing the characterization data on a PRS basis to estimate potential atmospheric releases for a number of reasons. These reasons included uncertainties associated with the accuracy of PRS boundary data and the relationship of PRS boundaries to sample locations, concentration data outside established PRS boundaries, a lack of consistency in the compilation of the PRS fields within the database, viable characterization data not included in the database, a lack of sufficient representative data for a given PRS, and uncertainties associated with the validity of certain analytical data (e.g., because there are no results for ^{241}Pu , the accuracy of the results for ^{241}Am and possibly ^{237}Np can be called into question).

Because of time and resource constraints, we had to rely on the characterization data that were provided to us, and we were not able to investigate in detail the rationale behind the collection of those data. However, we assumed that the nature and extent of contamination at each site were controlled to some extent by information about known or suspected radionuclides and chemicals likely to be present at that site. Such an approach would allow site characterizations and sample analyses to be guided by knowledge about historical operations, thereby limiting the compiled data to those contaminants suspected to be present at each site. Based on our limited review of the data in this regard, it appeared that this issue could be complicated by the fact that full suite analyses for RCRA metals, for example, may have been requested regardless of the specific metals that were suspected at the site because the cost to do analyses for the entire suite of metals was the same as for an analyses for only one or two specific metals. A similar situation may exist for semi-volatile and volatile organic chemical analyses in that entire suite analyses may have been performed if any such chemical was suspected at a given site. For radionuclide analyses, different analytical techniques are considered more accurate than others (e.g., alpha spectroscopy is considered to provide a better indication of the true concentration of radionuclides such as ^{241}Am or ^{235}U than gamma spectrometry). It was not clear how these issues were accounted for in the PRS databases, or how these issues may have complicated the process of quantifying and identifying contamination at any given site.

The question of the legitimacy of the field that links the characterization data to a given PRS provides another example of how some of these uncertainties may have impacted our calculations. For PRSs characterized by multiple samples, we used the mean concentration to calculate an inventory for the entire area. For areas with a single sample, we used that sample concentration to represent the concentration across the entire area. In some instances, individual samples were associated with more than one PRS; in these cases, we used results for a single sample to characterize more than one PRS. Although this may have increased the uncertainty of the calculations, in the absence of any other information, it was the best available method. It is

not possible to quantify this uncertainty, but certainly there are some instances where additional sampling data would enable a more credible characterization of a given site.

We understood the limitations and uncertainties associated with the PRS data, and considered it important to provide a discussion of these issues in this report. Because of these uncertainties and limitations, we made conservative assumptions to avoid underestimating the quantity of contaminant available for potential release at each PRS (e.g., eliminating nondetect values likely biased the calculated inventory on the high side). Certainly, assuming a single value to be representative of potentially highly heterogeneous environmental conditions was problematic, but by eliminating nondetect values from our analyses, we believed our calculations were more likely to reflect the highest, or bounding, concentrations that could be expected at any given site. Once key contaminants and/or source areas were identified, there was the option to further examine the impact of source area concentration heterogeneity. We concluded that LANL could usefully focus additional efforts to better understand the existence and variability of contamination at certain sites.

3.2.5.2 Uncertainties Related to the Areal Extent of Contamination

In addition to uncertainties associated with the accuracy, completeness, and representativeness of the actual characterization data, there were also uncertainties related to the areal extent of contamination. The areal extent of chemicals and radionuclides in surface soil within the PRSs was based initially on the areas defined by polygons as part of the GIS coverage files provided by LANL. However, it was recognized that in some cases these polygon shapes, sizes, and locations did not correspond to either the locations of actual sampling data or to the extent of concentrations of chemicals and radionuclides in the soil. In those instances, ER personnel at LANL redefined the surface area extent of PRSs to more accurately reflect the available sampling data. Because information was not available to allow us to do otherwise, we assumed the same surface area extent of contamination for each chemical or radionuclide detected at a given PRS; however, the true distribution in the environment was expected to vary by contaminant.

In some cases, the surface extent of the chemicals and radionuclides could not be redefined if there were insufficient sampling data; therefore, we retained the original GIS polygon areas based on the initial coverage files provided by LANL. For sites where sufficient sample location did not exist to enable logical area estimation, it was also impossible to fully understand the impact of retaining the original GIS-based area estimates. We examined the ratios of the original GIS-based area to the redefined area (for all IR-boundary PRSs where areas were redefined) and found that in a number of cases, the redefined areas were substantially different, in some cases in excess of five orders of magnitude, than the GIS-based areas (Table 3-2). In most cases, the redefined areas were larger than the original GIS-based areas, but there were also a number of instances where the redefined areas were smaller than the original GIS-based areas. As noted, it was not possible to quantify the uncertainty associated with the updated area estimates, but we concluded that LANL could usefully focus additional efforts to better understand and estimate the areal extent of key contaminants at certain sites.

It should be noted that we shared the discomfort expressed by LANL staff in relying on PRS characterization data and boundaries about which considerable uncertainty appeared to exist. Unfortunately, it was not possible to quantify these uncertainties. Nonetheless, we had to estimate

potential release quantities, and an estimate of surface area extent in combination with the sampling data associated with each PRS represented the only available option for characterizing the PRS source areas.

Table 3-2 Descriptive Statistics for the Ratio of GIS-Based PRS Areas to IR-boundary PRS Areas that were Redefined Based on Existing Sample Locations

Parameter	Statistic
Maximum	7337
Minimum	0.00000134
Median	0.52
Count	223
# <0.1	73
# >10	39

3.3 Atmospheric Fate of Potential Contaminants of Concern

This section provides an overview of the factors influencing the volatilization of chemicals from soil in forest fires, the most important being fire temperature and duration (and resulting soil temperatures), as well as physical data on the specific chemicals in question. Temperatures can vary significantly throughout a given burn area and from the soil surface to its interior. Therefore, we assumed a conservative mean soil temperature based on characteristics of the Cerro Grande Fire and temperature data reported in the literature. We then used the assumed temperature to evaluate volatilization of the PCOCs, the contaminants shown in Table 3-1, from the soil in the fire, in conjunction with physical data on the contaminants.

Degradation or removal of volatilized chemicals in the atmosphere may have occurred; however, we were not able to incorporate the effect into our calculations, except in the case of dry deposition, which was included in the atmospheric dispersion model. Gas-phase chemicals can be degraded in the atmosphere through processes such as photolysis and reactions with ozone, hydroxyl radicals, and nitrate radicals. Particles and gases may also be removed from the atmosphere through wet and dry deposition. Wet deposition was not a factor in the Cerro Grande Fire, however, because no precipitation was reported during the fire. Gas-phase chemicals may have decomposed upon exiting the flame zone; however, it was not possible to evaluate this possibility due to a lack of relevant information.

3.3.1 Chemical Volatility in Forest Fires

Elements may be transferred to the atmosphere during forest fires by either volatilization or by transport of particulates (Raison et al. 1985). The likelihood that a chemical will volatilize from soil in ambient conditions (60°F [~20°C]) is largely determined by characteristics of the chemical, including vapor pressure, water solubility, and soil sorption coefficient. In a forest fire, the temperature of the fire is an extremely important factor influencing chemical volatility because chemical vapor pressure, water solubility, and soil sorption are different at the temperatures found in a forest fire than at ambient temperatures.

3.3.1.1 Temperatures in Forest Fires

Although many factors influence the volatility of a chemical, the most important determinant of chemical volatility in a forest fire is the temperature of the fire in any given area. Potential temperatures during a fire must be evaluated to assess chemical volatilization. Descriptions of the Cerro Grande Fire were used to estimate potential soil temperatures by comparison with values reported in the literature. The following paragraphs present temperatures reported in other fires and discuss the variability of surface temperatures and thermal gradients in soil.

3.3.1.1.1 Characteristics of the Cerro Grande Fire. Because no direct measurements of temperatures at or below the soil surface during the Cerro Grande Fire were available, we used qualitative descriptions of the fire to determine approximate temperatures that would be expected in this type of fire. The Cerro Grande Fire began as a controlled burn, a low intensity surface fire intended to remove excess fuel from the ground. Primary vegetation types in the fire area included ponderosa pine, piñon pine, and juniper. Tree heights and diameters may have exceeded 50 ft (15 m) and 2 ft (0.6 m), respectively. However, fire crews lost control of the fire due to low humidity and wind speeds exceeding 60 mph (27 m s⁻¹). These conditions helped to convert the fire from a surface fire to a crown fire, a type of high intensity fire that can quickly spread through the dry needles at the tops of trees and burn deeply into the soil (DOE 2000).

The Cerro Grande Fire ultimately burned almost 50,000 acres (20,235 ha), including 7,500 acres (3035 ha) on LANL property. The burn was of high severity in 34% of the fire area, while 8% and 58% of the burn were considered to be of moderate and low severity, respectively (Interagency BAER Team 2000). The fire was reported to have caused significant soil heating, as well as the death of hundreds of thousands of trees (Fire Investigation Team 2000). To be conservative, it was assumed that surface temperatures during the Cerro Grande Fire throughout the model domain were consistent with maximum surface temperatures observed during other high intensity fires.

3.3.1.1.2 Maximum Surface Temperatures in Other Fires. Peak surface temperatures from 212°F (100°C) to over 932°F (500°C) have been reported in grassland and shrubland fires, while peak surface temperatures from 212°F (100°C) to over 1292°F (700°C) have been reported in forest fires (Whelan 1995; Wells et al. 1979). Intense chaparral fires leaving behind a “white ash” seedbed were found to produce surface temperatures greater than 950°F (510°C), while the peak surface temperature for a wildfire burning rapidly upslope in southern California was recorded as 1320°F (716°C) (Wells et al. 1979). Fire temperatures greater than 1832°F (1000°C) are uncommon, and generally occur when fuel is concentrated in large amounts, as in slash piles (Smith and Sparling 1966).

Subjective methods for burn classification using post-fire litter and soil appearance by Wells et al. (1979) and Chandler et al. (1983) were reported in Ulery and Graham (1993). Three classes of fire intensity were described, as follows:

- Low-intensity burning characterized by black ash, scorched litter, and maximum surface temperatures of 212 to 482°F (100 to 250°C)
- Moderate-intensity burning characterized by consumption of most vegetation, exposed but unaltered soil, and maximum surface temperatures of 572 to 752°F (300 to 400°C)
- High-intensity burning characterized by complete combustion of heavy fuel resulting in white ash and reddened soil and maximum surface temperatures exceeding 932°F (500°C).

Based on the temperatures reported in the literature for other fires, we concluded that surface temperatures during the Cerro Grande Fire could have approached 1832°F (1000°C) in some areas. However, it must be recognized that temperatures can vary significantly within a fire, as discussed below, and surface temperatures would also be expected to have been well below 1832°F (1000°C) in some areas. Therefore, this is a conservative estimate of average maximum surface temperatures during the Cerro Grande Fire.

3.3.1.1.3 Variability of Surface Temperatures. It is difficult to quantify the total amount of a given substance that is transferred to the atmosphere in a fire because of the temperature variability found within fires. Environmental conditions and fire characteristics influence the surface temperatures that occur during a fire. These factors include variability in available fuel and resulting fire intensity, slope, wind speed, type of fire, direction of fire front, and maximum height of fuel source.

Litter deposition patterns have been identified as a major cause of varying intensities in fires, and variability in the fuel complex is the major source of error in models of fire intensity and behavior (Williamson and Black 1981). Temperatures can also vary in fires due to changes in slope. A California wildfire reached a maximum surface temperature of 1320°F (716°C) while burning rapidly upslope, but the maximum surface temperature was only 600°F (316°C) when the same fire was burning slowly in a level area (Wells et al. 1979).

Wind speed may also have a marked effect on surface temperatures during fires. Whittaker (1961) reported an increase in the ground-level temperature as the wind speed increased from slight to moderate. However, a strong wind reduced the equivalent temperature as the rate of flame spread increased, in turn reducing the amount of heat transferred to the soil surface. Smith and Sparling (1966) also observed higher fire temperatures with increased vegetation density and decreased wind speed. The high wind speeds observed during the Cerro Grande Fire may have caused cooler temperatures at the soil surface.

Temperature and wind profiles in the tree canopy during crown fires have not been well described. However, flame observations have shown that “strong downdrafts of cooling air come in behind the flame front to feed the strong updrafts at the front” (Whelan 1995). A crown fire may, therefore, create intense heat of relatively short duration. It has also been suggested that the maximum temperature increase during a fire exists at some distance above the ground, possibly at the top of the fuel feeding the fire (Whelan 1995). Maximum temperatures of hotter fires were reported to occur at greater heights than those of cooler fires (Smith and Sparling 1966). Based on these observations, maximum surface temperatures were likely to be lower than overall maximum temperatures during the Cerro Grande Fire.

Furthermore, the range of surface temperatures, height of peak temperature, and fire duration vary between head fires and back fires. Head fires burn with the direction of the wind, while back fires burn into the wind. A greater range of temperatures may be observed at ground level during head fires than during back fires, with low peak temperatures at many locations but high peak temperatures at a few locations (Whelan 1995). Furthermore, hotter temperatures in head fires have been reported to occur at or over 18 in. (46 cm) above the surface, while hotter temperatures in back fires have been reported to occur below 18 in. (46 cm) above the surface. The ground surface is also exposed to high temperatures for a longer duration during back fires than during head fires, causing more damage to the soil (Stinson and Wright 1969). Conditions during the Cerro Grande Fire were probably consistent with those reported in head fires in many areas because the fire’s spread was strongly influenced by high winds.

3.3.1.1.4 Thermal Gradient in Soil. The thermal gradient in the soil is also important in terms of the volatilization of chemicals from the soil. Most of the heat energy produced by a wildfire travels upward and is lost to the atmosphere; however, some heat energy is also transferred downward into the soil. It was estimated that 8% of the heat energy generated from a burning chaparral canopy was "absorbed at the soil surface and transmitted downward in the soil" (Wells et al. 1979). Temperatures at varying depths in the soil are determined by fire intensity and duration, fuel type, nature of the litter layer, and soil properties, as well as by the efficiency of heat transfer from the fire to the soil surface (Wells et al. 1979; Steward et al. 1990). The transfer of heat through soil is a complex process involving conduction, convection, and radiation and also involves mass movement (primarily of moisture), evaporation, condensation, adsorption, and desorption, each having a heat effect (Steward et al. 1990).

The forest litter layer can act to insulate the soil and prevent significantly elevated soil temperatures, especially if it is moist or thick. In fact, even an ash layer can provide an insulating effect. Dry or thin litter layers may be partially or completely consumed in a fire, and significant heating in the underlying soil may occur (Wells et al. 1979). Soil water content can also alter soil temperature gradients during fires. Soil temperatures in a given layer will not exceed 212°F (100°C) until most water has evaporated or migrated to lower soil layers (DeBano et al. 1976).

Soil heating curves constructed from soil temperature data on California chaparral fires show maximum surface temperatures during intense, moderate and light burns to be about 1292°F (700°C), 797°F (425°C), and 482°F (250°C), respectively. Temperatures did not exceed 392°F (200°C) at a depth of 1 in. (2.5 cm) in the soil even during intense chaparral burns. Extreme soil heating may occur during burning of windrows of slash material. Soil temperatures under burning windrows of eucalyptus slash and logs ranged from 1230°F (666°C) just below the surface to 233°F (112°C) at a depth of 8.5 in. (21.6 cm) below the surface. A peak temperature of 527°F (275°C) was measured at a depth of 1 in. (2.5 cm) during an intense fire in a eucalyptus forest that had burned for 8 hours, while the maximum soil temperature at the same depth in a less intense eucalyptus fire was 347°F (175°C) (Wells et al. 1979). Studies have indicated that peak soil temperatures during forest fires at a depth of 1 in. (2.5 cm) rarely exceed 212°F (100°C) (Whelan 1995).

It was reported that the Cerro Grande Fire produced hydrophobic soils in some areas. A water-repellent layer can be formed in soil during a fire as organic compounds migrate downward into the soil from burning litter or duff. The thickness of the water-repellent layer is determined by fire intensity, soil water content, and soil physical properties. Over 90% of the decomposed organic matter is lost to the atmosphere as smoke or ash, but a small amount is distilled downward in the soil until it reaches cooler lower layers and condenses (Wells et al. 1979). More polar hydrophobic substances are "fixed" by heat pulses through the soil, creating a water-repellent layer, and less polar compounds are revolatilized, thereby expanding the water-repellent layer. Temperatures exceeding 482°F (250°C) are required for "fixing" and revolatilization; however, temperatures of 518 to 572°F (270 to 300°C) may degrade the organic compounds that cause water repellency. The water repellent layer may be found at greater depths in the soil when surface temperatures exceed these levels (DeBano et al. 1976). Although the depth and thickness of hydrophobic soils produced by the Cerro Grande Fire was not available, we can conclude that temperatures exceeded 482°F (250°C) at some point in the soil where a hydrophobic layer was formed.

3.3.1.2 Assumed Mean Soil Temperature for the Cerro Grande Fire

Many factors can cause variability in the surface temperatures observed within a fire, the fire duration, and the thermal gradient in the soil, as discussed above, and the severity of the Cerro Grande Fire varied significantly throughout the burn area. It was not feasible for us to determine maximum temperatures throughout the burn area, so it was necessary to assume a mean soil temperature. To be conservative, the assumed mean soil temperature was based on maximum surface temperatures reported during other high intensity fires, even though the Cerro Grande Fire was not of high intensity in all areas and the soil temperature below the surface would have been considerably lower than that at the surface. We investigated surface and soil temperatures during other high intensity fires and the range of these values helped us determine a conservative assumed mean soil temperature. We then referenced the assumed temperature to specific physical data on the chemicals and used them to assess chemical volatility.

We assumed a mean soil temperature of 1832°F (1000°C) throughout the burn area for the purposes of evaluating chemical volatilization from soil. This value is consistent with maximum surface temperatures reported in very intense fires. It is conservative because it is derived from observed maximum, not average, temperatures and because such maximum surface temperatures would not be expected in all areas. In fact, significantly lower surface temperatures would be expected in less severely burned areas. Of the approximately 211 acre (855,000 m²) area that comprises our burned source term area, only 3.4% of those areas were classified as moderately burned, with the remainder either unclassified or of low/unburned severity. Moreover, factors that may result in lower surface temperatures during forest fires, such as increased wind speed, maximum height of fuel source in excess of 50 ft (15 m), and movement of the fire with the wind, were present during the Cerro Grande Fire.

Furthermore, soil inventories for the PRSs were based on the mean soil depth of detectable sample results in each PRS, which ranged widely. The average depth of samples was 0.6 ft (0.18 m), with a minimum and maximum depth of 0 and 1.5 ft (0.45 m), respectively. Assuming a mean soil temperature of 1832°F (1000°C) introduces an additional level of conservatism when soil inventory depths are considered, since such temperatures would only be expected at the surface of the soil. Soil temperatures drop dramatically in the top few centimeters of soil (Whelan 1995). As stated previously, the soil temperature during a fire is unlikely to exceed 212°F (100°C) at a depth of 1 in. (2.5 cm), although it may approach 570°F (300°C) in very intense fires. The temperature at the soil surface certainly would be greater than the mean temperature in the top few centimeters of soil, which would in turn be significantly greater than the mean temperature in the top 8 in. (20 cm) of soil.

3.3.1.3 Other Factors Influencing Chemical Volatility

Once the assumed mean soil temperature of the fire was determined, we considered physical data for the PCOCs in assessing volatilization from the soil during the Cerro Grande Fire. These parameters are discussed in some detail below and include vapor pressure, boiling point, melting point, molecular weight, and water solubility and soil sorption.

3.3.1.3.1 Vapor Pressure. The volatilization of a given chemical from soil surfaces at ambient temperature (i.e., between 68 and 77°F [20 and 25°C]) and pressure is largely determined by the vapor pressure of the chemical. The vapor pressure of a chemical also helps determine

whether it will exist in the vapor or particulate phase in the atmosphere (Boethling and Mackay 2000).

In general, a liquid-phase vapor pressure less than 7.50×10^{-9} mmHg (9.87×10^{-12} atm) at ambient temperature indicates that the substance will exist primarily in the particle phase in the atmosphere, and a vapor pressure greater than 7.50×10^{-3} mmHg (9.87×10^{-6} atm) indicates that the substance will exist essentially totally in the gas-phase. Chemicals with vapor pressures between 7.50×10^{-9} and 7.50×10^{-3} mmHg (9.87×10^{-12} and 9.87×10^{-6} atm) will exist in both the gas and particle phase in the ambient atmosphere and are often referred to as semi-volatile compounds (Boethling and Mackay 2000).

However, volatility is also influenced by other factors including ambient temperature, soil sorption, and water solubility. The vapor pressure of a chemical increases rapidly as temperature increases and so does the portion of the chemical in the gas-phase. Vapor pressures at temperatures approaching those one would expect in an intense forest fire were not available for most of the primary PCOCs. Therefore, boiling points are a more relevant measure of chemical volatility in the fire.

3.3.1.3.2 Boiling Point. The boiling point for a given chemical is defined as the temperature at which the vapor pressure of a liquid is equal to the atmospheric pressure on the liquid, and it is generally reported at a pressure of exactly 1 atmosphere (760 mmHg). It is also a rough indicator of a chemical's volatility at ambient temperatures (Boethling and Mackay 2000). We used the boiling point as a benchmark for the temperature at which a given contaminant would be expected to rapidly volatilize and compared it to the assumed soil temperature during the fire.

We sorted the list of PCOCs in ascending order by the boiling point for each chemical, and assumed any chemical with a boiling point less than 1832°F (1000°C) fully volatilized in the fire. The physical data for these chemicals are reported in Table 3-3. Chemicals we assumed to volatilize completely, based on the reported boiling point, included high explosives, PAHs, PCBs, and other organic chemicals. We also included mercury, arsenic, selenium, cadmium, and zinc in this group based on their relatively low boiling points.

We assumed that chemicals with a boiling point greater than 1832°F (1000°C) did not volatilize from the soil in the fire; these chemicals and their physical data are listed in Table 3-4. This group included most of the metals from the list of PCOCs. No organic chemicals were included in this group.

Boiling points were not available for some of the PCOCs for the air pathway, including 4-amino-2,6-dinitrotoluene, 2-amino-4,6-dinitrotoluene, hexavalent chromium, RDX, TATB, and HMX. We used other methods to estimate the boiling points of these chemicals and to evaluate their volatility during a fire, as discussed in the following sections.

3.3.1.3.3 Melting Point. For organic chemicals, melting point is the most commonly reported physical property (Boethling and Mackay 2000), and melting points were available for six of the seven chemicals with no reported boiling points. In the absence of boiling point values for some chemicals, we used melting point to evaluate the volatility of the chemicals in a qualitative manner. The melting points for the six chemicals ranged from 340 to 529°F (171 to 276°C) (see Table 3-5), and, therefore, it is reasonable to assume that the boiling points for all of these chemicals are less than 1832°F (1000°C) based on boiling points for chemicals with similar melting points. Although it is possible to estimate the boiling point of a chemical from a known melting point and other structural information, we used a more straightforward formula

correlating molecular weight with boiling point to further evaluate the volatility of these chemicals, as described in the following section.

3.3.1.3.4 Molecular Weight. Molecular weight is the most important molecular property influencing boiling point, although other important factors include bonding strength and structure. The boiling point of a compound may be quickly estimated using Banks' Molecular Weight Correlation, as reported in Boethling and Mackay (2000), shown in Equation (3.10):

$$\log T_b = 2.98 - \frac{4}{\sqrt{M}} \quad (3.10)$$

where

T_b = boiling point (K)

M = molecular weight (g mol⁻¹).

We calculated boiling points for the six chemicals with no reported boiling point using the above equation; calculated boiling points ranged from 225 to 547.1°F (107.2 to 286.2°C), as reported in Table 3-5. These calculations support the assumption that these chemicals would have fully volatilized in the fire.

3.3.1.3.5 Soil Adsorption/Water Solubility. Chemicals that have high soil sorption coefficients are less likely to volatilize from dry soils. Chemicals that are relatively soluble are also less likely to volatilize from moist soils (Boethling and Mackay 2000). Some of the PCOCs have fairly high sorption coefficients and water solubilities at ambient temperatures. However, information regarding the effect of high temperatures on these parameters was not available, and we were unable to quantify the effect of soil sorption and water solubility on volatilization. Because sorption to soils and solubility in water tend to reduce chemical volatilization, it is conservative to ignore their effect.

Table 3-3. Physical Data for PCOCs Assumed to Have Fully Volatilized in the Cerro Grande Fire Based on Reported Boiling Point^a

Chemical	Molecular weight	Vapor pressure at 20–25°C (mmHg)	Boiling point (°C)	Melting point (°C)	Shortest reported atmospheric half-life (hr)	Atmospheric process with shortest reported half-life
Cyanide (total)						
Cyanogen ^b	52.00	3876	-21.1	NA ^c	NA	NA
Hydrogen Cyanide ^b	27.03	742	25.6	-13.4	12840	Hydroxyl radical reaction
Aldrin	364.91	1.2×10^{-3}	145	104	6	Hydroxyl radical reaction
Nitrobenzene	123.11	2.45×10^{-1}	210.8	5.7	5 ^d	Photolysis
Naphthalene	128.17	8×10^{-2}	217.8	78	8	Hydroxyl radical reaction
Nitrotoluene [4-]	137.14	1×10^{-1}	238.3	53-54	477	Hydroxyl radical reaction
Trinitrotoluene [2,4,6-]	227.13	2×10^{-3}	240	80	2640	Hydroxyl radical reaction
Methylnaphthalene [2-]	142.19	6.81×10^{-2}	241	-22	7.4	Hydroxyl radical reaction
Acenaphthylene	152.21	9.12×10^{-4}	265	92	1	Ozone reaction
Dibenzofuran	168.19	2.48×10^{-3}	287	86	98.4	Hydroxyl radical reaction
Dinitrotoluene [2,4-]	182.14	1.47×10^{-4}	300	71	1800	Hydroxyl radical reaction
Dinitrobenzene [1,3-]	168.12	3.89×10^{-3}	300	88.9	14.15	Hydroxyl radical reaction
Benzo(a)pyrene	252.32	5.50×10^{-9}	310	179	NA	NA
Mercury	200.59	1.2×10^{-3}	356.58	-38.87	At least a few days	NA
Aroclor-1254	327 (avg)	6×10^{-5}	365	NA	1896	Hydroxyl radical reaction
Fluoranthene	202.26	1×10^{-2}	384	111	8	Hydroxyl radical reaction
Pyrene	202.26	8.90×10^{-5}	393	151.2	8	Hydroxyl radical reaction
Dibenz(a,h)anthracene	278.33	1.00×10^{-10}	524	266	NA	NA
Arsenic	74.92	Approx. 0	613	613	NA	NA
Selenium	78.96	Approx. 0	684	217	NA	NA
Cadmium	112.41	Approx. 0	765	320.9	NA	NA
Zinc	65.38	Approx. 0	907	419.5	NA	NA

^a Source: ATSDR (2001), Burgess et al. (1998), HSDB (2001), Lide (1998), NIOSH (1994), and RAIS (2001).^b Supplemental information for cyanide.^c NA = not available.^d 38% degradation reported after 5 hours.

Table 3-4. Physical Data for PCOCs Assumed Not to Have Volatilized in the Cerro Grande Fire Based on Reported Boiling Points^a

Chemical	Molecular Weight	Vapor pressure		Melting point (°C)
		at 20–25°C (mmHg)	Boiling point (°C)	
Thallium	204.38	Approx. 0	1457	303.5
Antimony	121.75	Approx. 0	1635	630
Barium	137.33	Approx. 0	1640	725
Manganese	54.94	Approx. 0	1962	1243.9
Silver	107.87	Approx. 0	2000	960.5
Aluminum	26.98	Approx. 0	2327	660
Beryllium	9.01	Approx. 0	2472	1278
Copper	63.55	Approx. 0	2563	1082.8
Chromium (total)	52.00	Approx. 0	2642	1857
Nickel	58.69	Approx. 0	2730	1455
Iron	55.85	Approx. 0	2750	1535
Cobalt	58.93	Approx. 0	2870	1492.8
Vanadium	50.94	Approx. 0	3380	1890
Uranium	238.03	Approx. 0	3813	1132.3

^a Source: ATSDR (2001), HSDB (2001), Lide (1998), NIOSH (1994), and RAIS (2001).

Table 3-5. Physical Data for PCOCs Assumed to Have Fully Volatilized in the Cerro Grande Fire Based on Calculated Boiling Points^a

Chemical	Molecular weight	Vapor pressure at 20–25°C (mmHg)	Calculated boiling point (°C) (Equation 3.10)	Melting point (°C)	Shortest reported atmospheric half-life (hr)	Atmospheric process with shortest reported half-life
Amino-2,6-dinitrotoluene[4-]	197.15	NA ^b	222.6	171	NA	NA
Amino-4,6-dinitrotoluene[2-]	197.15	NA	222.6	NA	NA	NA
Chromium (hexavalent)	99.99	NA	107.2	NA	NA	NA
RDX	222.26	1.00E-06	241.9	205	1.5	Hydroxyl radical reaction
TATB	258.15	NA	265.3	250	NA	NA
HMX	296.20	3.30E-14	286.2	276	NA	NA

^a Source: ATSDR (2001a), Burgess et al. (1998), and HSDB (2001).

^b NA = not available.

3.3.2 Degradation of Chemicals in the Atmosphere

Chemicals can be transferred to the atmosphere through volatilization and other transport processes. In the atmosphere, degradation processes can serve to transform hazardous chemicals into harmless or less harmful substances or, conversely, more toxic substances can be formed. Potentially important removal and degradation processes in the atmosphere include atmospheric oxidation, photolysis, and wet and dry deposition (Boethling and Mackay 2000). Although multiple processes may act on some chemicals, producing an additive effect on the rate of chemical removal, we only tabulated the half-life of the most dominant (i.e., rapid) mechanism in Table 3-3 and Table 3-5. Additionally, during a fire, volatilized chemicals may be decomposed before exiting the flame zone. However, estimating removal and degradation rates and all of the byproducts of various degradation processes is beyond the scope of this project, and we did not consider the effect of removal and degradation processes in our calculations of air concentrations. Therefore, concentrations may be overestimated for some contaminants, while toxic degradation products that may be formed have not been addressed.

3.3.2.1 Atmospheric Reactions

Gas-phase organic compounds may be chemically changed in the atmosphere through reactions with ozone (O_3), hydroxyl (OH) radicals, and nitrate (NO_3) radicals. The ozone and hydroxyl radical reactions were most important for the PCOCs. Ozone is present in the troposphere because of downward transport from the stratosphere; it is also generated by in situ photochemical formation and destruction. Hydroxyl radicals are generated by photolysis of ozone, and significant concentrations exist only during daylight hours (Boethling and Mackay 2000). Eight chemicals had half-lives of less than 24 hours in the atmosphere due to degradation by reactions with ozone or hydroxyl radicals (see Table 3-3).

3.3.2.2 Photolysis

Photolysis may be defined as any chemical reaction that occurs only in the presence of light, and it can take place in the atmosphere, on soil, and in surface waters. Both direct and indirect photoreactions can occur; when a compound itself is transformed by a sunlight photon, it is termed a direct photoreaction. When a compound is transformed by a reaction with an oxidant generated by a photoreaction, it is termed an indirect photoreaction. The hydroxyl radical reaction, which is the primary loss mechanism for over 90% of organic compounds in the atmosphere, is an indirect photochemical reaction because the hydroxyl radical is generated by photolysis of ozone (Boethling and Mackay 2000). Direct photolysis was the dominant removal mechanism for one contaminant, nitrobenzene, for which 38% degradation in the atmosphere in 5 hours was reported.

3.3.2.3 Wet and Dry Deposition

Chemicals and particle-associated chemicals may be removed from the atmosphere by wet and dry deposition. Precipitation to the earth's surface in the form of rain, fog, or snow provides the mechanism for chemical removal through wet deposition. Wet deposition was not an

important removal process for the Cerro Grande Fire because no precipitation occurred during the period. Diffusion and sedimentation are the major processes involved in chemical removal through dry deposition. Particles with mean diameter between 0.3 and 0.5 μm have an estimated residence time in the atmosphere of 5 to 15 days considering removal by wet and dry deposition. The deposition velocity is a minimum for this particle size range and increases as particle size increases or decreases (Boethling and Mackay 2000). A bimodal particle size distribution has been reported for smoke particles with peaks at 0.5 μm and greater than 43 μm (Ward and Hardy 1991).

Dry deposition of particles and gases was accounted for in the atmospheric dispersion model. However, in both cases, deposition was only calculated for a “tracer substance” that represented either a particulate or gas contaminant. For particles, the tracer substance was particulate matter less than 10 μm . The size distribution was described by a geometric mean particle diameter of 0.48 μm and a geometric standard deviation of 2. This was the default size distribution for particulate matter less than 10 μm that is used in the CALPUFF (Scire et al. 1999) air dispersion model. The tracer substance for contaminants in the gas phase was carbon monoxide. Chapter 4 contains additional details concerning deposition.

3.3.2.4 Decomposition in the Flame Zone

Some chemicals may actually decompose before exiting the flame zone because of the extreme temperatures associated with forest fires. However, there is significant uncertainty surrounding the actual temperatures that may have existed during the Cerro Grande Fire and the variability of temperatures inherent in any fire, and it was not possible to evaluate chemical decomposition in our modeling approach. It is more conservative to assume that all volatilized contaminants actually reached the atmosphere.

3.3.3 Radionuclide Resuspension

Several studies have investigated the transport properties of radionuclides during a fire, particularly in the wake of the Chernobyl accident. In question for this work are the mechanisms by which radionuclides are released to the atmosphere and the rate with which the releases occurs.

Amiro et al. (1996) studied the mechanism for release of I, Cs, and Cl in biomass fires. While none of these nuclides are explicitly of concern for this work, we can make some assumptions about the release of K (analog of Cs). The remaining radionuclides in Table 3-1 are all classified as metals, with boiling points higher than 1832°F (1000°C) (see Table 3-6), which indicates that they would not volatilize and should be treated as particulate releases.

Table 3-6. Melting and Boiling Points of Primary Radionuclide Contaminants of Concern^a

Element	Melting point (°C)	Boiling point (°C)
Protactinium-231	1572	NA
Thorium-227, 232	1750	4788
Uranium-234, 235, 238	1135	4131
Plutonium-238, 239	640	3228
Radium-224, 226	700	NA
Americium-241	1176	2011
Neptunium-237	644	NA
Lead-210, 212	327.46	1749

^a Source: Lide (1998).

In a study of field and laboratory burns of straw, wood, peat, seaweed, and radish plants, Amiro et al. (1996) sampled smoke directly above the fire to give an indication of the relative gaseous and particulate emissions. In all burns, I and Cs were detected in the particulate matter present in the smoke. Gaseous species of I were also detected, but no gaseous Cs was detected. For I, the gas to particulate ratio was about 2:10, indicating that even with some gaseous phase release, the burning radionuclides release preferentially as particulate matter. Since K is a chemical analog of Cs, we can assume that it, too, would be released in a fire as particulate only. Additionally, the boiling point of K is 1398°F (759°C), indicating that it would be best represented as a particulate release. For this study, all radionuclides are treated as particulate releases.

3.4 Source Term/Release Rate Calculations

To calculate source term (or release rate) of the priority contaminants from the PRS locations, we used a different methodology for contaminants classified as volatiles than for contaminants classified as particulates.

3.4.1 Volatile Contaminant Release Rates

All chemicals classified as volatiles were assumed to completely volatilize during the Cerro Grande Fire. To calculate a release rate, we used the inventories calculated for each PRS as described previously in Section 3.2.4. Although it is unlikely that the ground was heated to depths such that the entire inventory was volatilized, there is enough unknown about the actual temperatures during the fire that it is reasonably conservative to assume that the entire inventory was released through volatilization.

As described in Chapter 4, the integrated release rate was used to develop a ratio of the concentration of a radionuclide or chemical to that of the trace substance. Because we assumed the total inventory of the volatile contaminant to be released, there was no need to calculate a release rate, and the total release represented the integrated amount over the burn time. The release rate of a volatile contaminant was assumed to follow the same trend as emissions from the fire. That is, emissions build up during ignition, build up to a maximum value, then decay off

over time after the flaming portion of the fire ceases. The average release rate over the burn time can be calculated as

$$RR_v = \frac{I_v}{T} \quad (3.11)$$

where

RR_v = release rate for volatiles (mg s^{-1})

I_v = inventory (mg)

T = burn duration (s).

3.4.2 Particulate Contaminant Release Rates

Because resuspension was assumed to be the primary mechanism by which particulate contaminants were released during the fire, a much different method for calculating release rate was required. Kashparov et al. (2000) studied forest fires in the Chernobyl area and investigated the processes of resuspension and redistribution of contaminants. These studies helped us predict a resuspension rate constant for particulate releases.

Kashparov et al. (2000) studied aerosol release properties during active experiments (controlled burning of prepared sites), a real-time fire, and laboratory experiments. The primary contaminant studied was ^{137}Cs , which Amiro et al. (1996) showed to release during a fire as particulate. Comparisons of the resuspension factor (m^{-1}) obtained during active experiments and the real-time forest fire showed good agreement, with observed differences explained by the increased intensity of the real fire. Kashparov et al. (2000) also looked at different phases of a fire (active burning, smoldering, and post-fire) and found that in different forest systems, values of the resuspension factor are the same for different phases of the fire. The resuspension factors observed in the study were very similar to resuspension factors obtained for Chernobyl radioactive aerosols measured in many countries in 1986–1987. The variation of the resuspension factor can, therefore, be explained by the properties of the radioactive aerosols.

Resuspension rate constants (s^{-1}) were also measured and showed consistency across different phases of the fire and at different distances from the fire. When compared with resuspension rate constants measured during agricultural works on areas contaminated by Chernobyl, the resuspension rates appeared higher than those during a fire. This is because the aerodynamic characteristics of particles resuspended during agricultural activities is very different than those resuspended by a fire.

Kashparov et al. (2000) reported resuspension rate constants of 10^{-10} s^{-1} for their experiments. This represents a rate constant that is consistent across different fire intensities and forest systems, and it is a reasonable value to use for these calculations.

To determine the particulate inventory available for resuspension, we must first determine the soil mass available for resuspension. We assumed that the depth of soil available for resuspension is 0.4 in. (1 cm). This is very conservative, as resuspension depths are generally ~0.04 in. (~1 mm). Because contaminant concentrations are represented in different quantities for chemicals (mg kg^{-1}) and radionuclides (pCi g^{-1}), we used two different calculations for soil mass. Equation (3.12) represents the soil mass calculation for chemicals, and Equation (3.13) is the soil mass calculation for radionuclides. We performed this calculation for each PRS.

$$M_c = A \cdot D_r \cdot \rho \cdot CF_v \cdot CF_m \quad (3.12)$$

where

- M_c = resuspendible soil mass for PRS with chemical contamination (kg)
 A = area (m²)
 D_r = resuspendible depth (m)
 ρ = soil density (1.4 g cm⁻³)
 CF_v = conversion factor for volume (10⁶ cm³ m⁻³)
 CF_m = conversion factor for soil mass (10⁻³ kg g⁻¹).

$$M_r = A \cdot D_r \cdot \rho \cdot CF_v \quad (3.13)$$

where

- M_r = resuspendible soil mass for PRS with radionuclide contamination (g).

Then, we calculated resuspendible inventory by multiplying the appropriate soil mass by the net concentration of the contaminant at the PRS, as shown in Equations (3.14) and (3.15).

$$I_c = C_c \cdot M_c \quad (3.14)$$

where

- I_c = inventory of chemical available for resuspension at PRS (mg)
 C_c = concentration of chemical at PRS (mg kg⁻¹)
 M_c = resuspendible soil mass for PRS with chemical contamination (kg).

$$I_r = C_r \cdot M_r \cdot CF_a \quad (3.15)$$

where

- I_r = inventory of radionuclide available for resuspension at PRS (Bq)
 C_r = concentration of radionuclide at PRS (pCi g⁻¹)
 M_r = resuspendible soil mass for PRS with radionuclide contamination (g)
 CF_a = conversion factor for activity (0.037 Bq pCi⁻¹).

Using the resuspension rate constant of 10⁻¹⁰ s⁻¹, we calculated release rates for each contaminant at each PRS using Equation (3.16).

$$RR_p = I_{r,c} \cdot RC \quad (3.16)$$

where

- RR_p = release rate for particulate release (Bq s⁻¹ or mg s⁻¹)
 $I_{r,c}$ = inventory of radionuclide or chemical available for release (Bq or mg)
 RC = resuspension rate constant (s⁻¹).

We then integrated the release rate over the burn time to obtain the total amount of radionuclide or chemical released during the fire. Similar to the treatment of volatile chemicals, we assumed the release rate of particulate matter to follow the same trend as emissions from the fire.

4 ATMOSPHERIC TRANSPORT

This chapter describes the models and methods we used to estimate the dispersion of radionuclides and chemicals in air that were released from PRSs. The time constraints of this project did not allow for a comprehensive model evaluation process. Therefore, we selected a model based on the assessment question, available resources and data, and physical constraints of the project. The assessment question is twofold: (1) what were the impacts to ambient air from contaminants released as a result of the Cerro Grande Fire to the communities surrounding LANL, and (2) what are the impacts of contaminants deposited from fire plumes on soil and the surrounding watersheds? The model must then have the capability to perform dispersion and deposition calculations for large area sources (as represented by the fire) consisting of particulate matter and gases. Furthermore, the model must be capable of addressing long-range transport (>31 mi [>50 km]) in complex terrain and plume rise for area source emissions.

Air dispersion models vary from the relatively simple straight-line Gaussian plume model represented by the Industrial Source Complex (ISC) model (EPA 1992) to the complex terrain puff dispersion model, CALPUFF (Scire et al. 1999). Gaussian plume models are simple to run and implement, and they are useful for short-range transport where concentrations are averaged over relatively long periods of time (~1 year). However, the assumptions inherent in the Gaussian plume model are violated when long-range transport and relatively short-term emissions are concerned.

The puff trajectory models, such as CALPUFF, are more suitable for the types of calculations necessary for this study. Puff trajectory models are capable of incorporating temporally and spatially varying meteorological conditions, along with terrain complexities and spatially variable surface features. The CALPUFF model represents the state-of-the art in puff dispersion models. It is well documented, has been verified and validated, and is designed to operate with meteorological and geophysical data that are readily available. For these reasons, RAC selected the CALPUFF model to perform these calculations.

The air pathway analysis of the Cerro Grande Fire estimated air concentrations of contaminants from burned PRSs and combustion products from burned vegetation that included particulate matter less than 10 μm and less than 2.5 μm (PM10 and PM 2.5, respectively), carbon monoxide (CO), carbon dioxide (CO₂), and methane (CH₄). Absent from this assessment are calculations of ambient air concentrations from (1) naturally occurring radionuclides, (2) man-made radionuclides that have deposited on vegetation and ground (such as ^{239/240}Pu and ¹³⁷Cs from global weapons testing fallout), (3) radionuclides originating from 50 years of LANL operations that have deposited on surrounding lands, (4) radionuclides and chemicals that may have been suspended from PRSs that were *not* burned during the Cerro Grande Fire, (5) radionuclides and chemicals released from PRSs to the air after the fire burned, and (6) combustion products from the burning of LANL structures. However, naturally occurring and man-made radionuclides and metals detected in vegetation that may have become airborne as a result of the Cerro Grande Fire are addressed in Appendix D of this report.

It was important to understand the behavior of the fire and the dispersion of pollutants released as a result of burning biomass before attempting to model the dispersion of radionuclides and chemicals suspended from PRSs. Wildfires emissions are typically accompanied by the release of large quantities of heat, resulting in lofted plumes that often attain significant heights above ground. Of particular interest was PM10 because this pollutant was also measured at

numerous monitoring stations within the model domain. Therefore, understanding the temporal and spatial distribution of modeled and measured PM₁₀ concentrations was important to understanding the behavior of the fire and dispersion of pollutants released during the fire.

In this section, we first examine the PM₁₀ measurements. Examination of the PM₁₀ measurements is warranted because this pollutant occurs from both fire emissions and from other sources, such as dust suspension. Next, we discuss the CALPUFF modeling protocol, including a description of the meteorological model CALMET that is used in conjunction with CALPUFF. This is followed by a description of the fire emissions model and the methodology for estimating air concentrations of radionuclides and chemicals released from PRSs. Finally, we present estimated atmospheric concentrations of each important radionuclide, chemical, and fuel combustion product at selected locations in the model domain.

4.1 Measured PM₁₀ Concentrations

Twenty-four hour average PM₁₀ concentrations taken before, during, and, after the fire are summarized in Table 4-1 and plotted in Figure 4-1. Except for TA-54, Española, and Hernandez, measurements cover the time period from about January 1999 to September 2000. Measurements at TA-54 cover the time period from March 2000 to December 2000, and measurements at Española and Hernandez cover times during and after the fire. Mean 24-hour average concentrations before the fire ranged from 8.6 $\mu\text{g m}^{-3}$ at Questa to as high as 15.6 $\mu\text{g m}^{-3}$ at Bernalillo. Maximum 24-hour average concentrations were as high as 41 $\mu\text{g m}^{-3}$ and minimums ranged from <2 to 4 $\mu\text{g m}^{-3}$. During the fire, most stations showed a slight, but significant, increase in the mean PM₁₀ concentration; however, the number of measurements was limited. The maximum 24-hour average concentration measured during the fire was at TA-54 on May 13 (181 $\mu\text{g m}^{-3}$). After the fire, mean concentration remained slightly higher than before the fire.

Table 4-1. Measured 24-hour Average PM10 Concentrations Before, During, and After the Cerro Grande Fire ($\mu\text{g m}^{-3}$)

	Pera ^a	Runnels	Capshaw	Taos ^a	Bernalillo ^a	Questa ^a	Española	Hernandez	TA-54
Before Cerro Grande Fire									
Dates	1/6/99– 4/30/00	1/2/99– 5/4/00	2/5/99– 4/30/00	1/12/99– 4/30/00	1/6/99– 4/30/00	1/13/99– 5/3/00	none	none	3/14/00– 5/5/00
Mean	9.8	11.1	14.2	14.4	15.6	8.6			12.2
Standard Error	0.4	0.3	0.9	0.7	0.8	0.4			1.1
<i>n</i>	79	242	70	63	80	110			53
Min	3.4	2.2	3.7	2.5	3.4	1.6			4.1
Median	8.8	10.4	12.6	13.5	14.3	7.7			9.6
Max	24.7	30.9	41.9	32.8	40.2	24.4			42.2
During Cerro Grande Fire (5/6/00–5/18/00)									
Mean	7.7	19.4	14.5	41.1	13.8	12.0	26.0	18.6	48.0
Standard Error		3.7	3.0	3.8	0.8	2.0	5.8	2.1	13.7
<i>n</i>	1	8	3	2	2	4	4	5	13
Min	7.7	9.4	9.7	37.2	13.0	8.1	14.4	11.6	12.8
Median	7.7	17.2	13.9	41.1	13.8	11.3	24.5	18.7	30.3
Max	7.7	43.3	20.0	44.9	14.6	17.2	40.5	24.6	181.5
After Cerro Grande Fire									
Dates	5/24/00– 9/27/00	5/22/00– 9/29/00	5/24/00– 9/27/00	5/23/00– 9/30/00	5/24/00– 9/27/00	5/24/00– 9/24/00	5/19/00– 5/21/00	5/19/00– 5/22/00	5/19/00– 12/31/00
Mean	12.1	12.3	14.7	17.3	16.0	12.6	15.2	12.9	14.9
Standard Error	1.0	0.4	1.6	2.7	1.1	1.0	2.6	0.7	1.3
<i>n</i>	19	66	16	12	22	31	3	4	13
Min	2.7	7.3	8.5	9.2	9.6	6.2	10.0	11.5	9.2
Median	11.3	11.4	12.4	14.7	15.2	11.6	17.0	12.8	14.6
Max	22.2	24.0	31.7	43.7	30.9	31.7	18.6	14.7	25.5
Sampler coordinates									
UTM E ^b		413400	413900				403300	399100	385462
UTM N ^b		3947800	3944800				3985500	3990800	3969471

^a These stations are outside the model domain.

^b Universal Transverse Mercator Coordinates in units of meters.

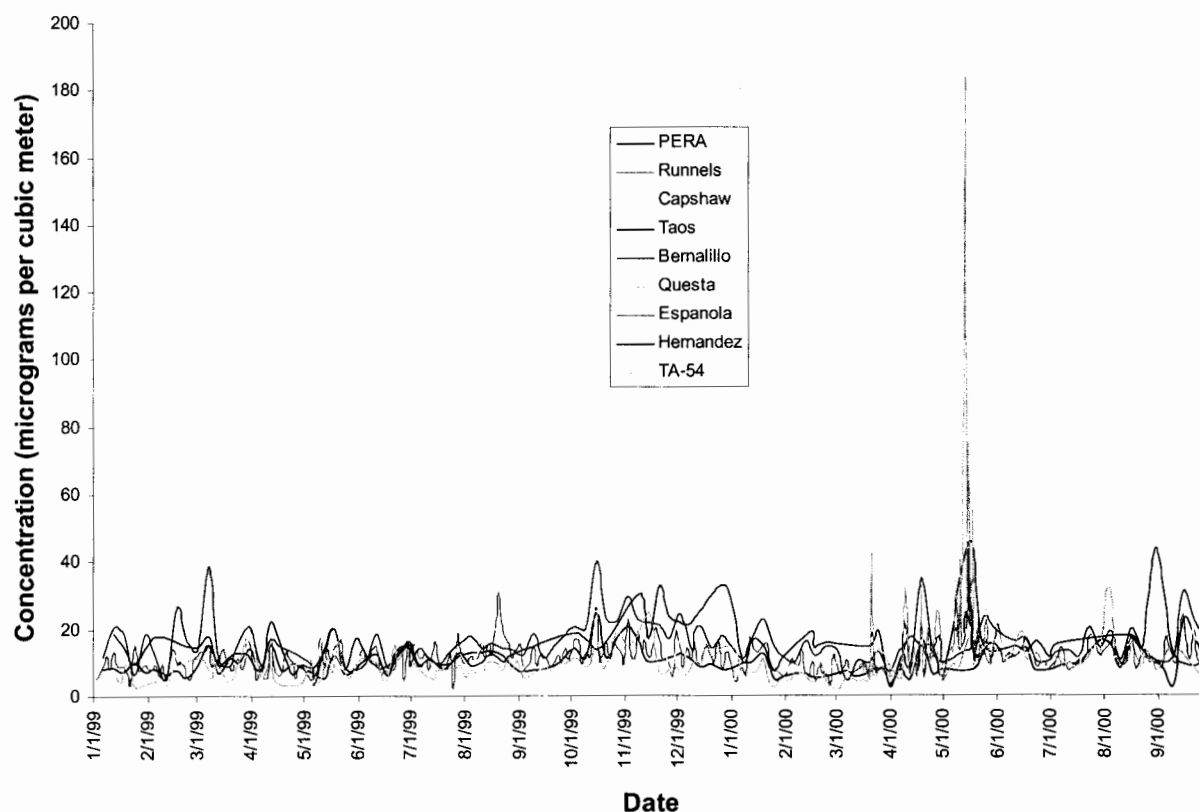


Figure 4-1. Twenty-four hour average PM10 concentrations as a function of time for monitoring stations located in or on the periphery of the model domain. For most stations, a continuous record does not exist and the line is interpolated between missing days. The signature of the Cerro Grande Fire is clearly seen at the TA-54 monitoring station.

Other measurements were also made by EPA Region 6 (Table 4-2) and results were posted on the NMED web site. No documentation accompanied these measurements, except for a spreadsheet containing all sampling locations that was provided by Erik Aaboe of NMED. Sampling locations were inferred from the data in this spreadsheet. However, the exact time the sampler was turned on was not specified, making it difficult to compare model predictions with these measurements precisely. Nevertheless, these data fill in important holes where data were lacking and provided some insight into the overall behavior of the fire. The measured concentrations are substantially above background and are likely due to the presence of smoke in the area.

Table 4-2. Measured PM-10 Concentrations with High Volume Air Sampling by EPA

Sample collection date ^a	Sample ID	Location ^b	Sampler run time (min)	PM10 concentration ($\mu\text{g m}^{-3}$)
May 14, 2000	SC-PM10-0513	Santa Clara	780	91.44
May 14, 2000	SI-PM10-0513	San Ildefonso	1550	74.34
May 15, 2000	WR-PM1-0514	White Rock	1398	117.11
May 15, 2000	SC-PM1-0514	Santa Clara	1161	63.16
May 15, 2000	SI-PM1-0514	San Ildefonso	1415	60.93
May 16, 2000	SC-PM01-0515	Santa Clara	1456	76.68
May 16, 2000	SI-PM01-0515	San Ildefonso	1262	69.26
May 16, 2000	WR-PM1-0515	White Rock	1556	48.45

^a The date is the day the sample was collected, not the day the sample was started as indicated by the sample ID number.

^b Sampling locations are inferred from spreadsheet provided by Erik Aaboe, NMED (UTM E UTM N); Santa Clara 403339, 3983402; San Ildefonso 398823, 3972580; White Rock 391073, 3965368

The PM10 measurements gave the clearest signal of the fire; however, measurements were limited and in some cases difficult to distinguish from background. Additionally, the source of the PM10 is not entirely clear. Popp et al. (2001) reports that PM10 measurements taken in Española showed a large contribution from crustal alkali and alkaline elements, suggesting convective dispersion of soil particles and incompletely burned biomass was the dominant mechanism for particle generation during the Cerro Grande Fire. This observation has implications concerning particulate releases from the Cerro Grande Fire because PM10 release estimates from the Emissions Production Model (EPM) do not include convective dispersion of soil particles. Particulate matter is also susceptible to suspension during high winds that occurred during the fire. However, the dust suspension process is often complicated by other factors that include (1) moisture content of the soil, (2) snow cover, (3) site-specific soil conditions, and (4) human activities (such as construction). These factors can either enhance or retard wind-driven suspension.

The question is, are the elevated PM10 concentrations observed during the fire a result of wind-driven suspension or is their origin from the burning of biomass? To address this question, we examined the PM10 concentration data and site-specific meteorological data. We chose the PM10 data at Capshaw and Runnels, located in downtown Santa Fe, coupled with meteorological data taken at the Santa Fe Airport and the NMED location for this analysis because the dataset was reasonably long and was coupled with site-specific meteorological data taken near the monitors. Data were obtained for the period beginning in January of 1999 and ending in September of 2000. The PM10 monitor at TA-54 coupled with TA-54 wind speed data were also analyzed; however, these data only went back to March of 2000. The PM10 data represent 24-hour average values, while meteorological conditions represent hourly observations. To bring these two datasets into the same time domain, we computed 24-hour average wind speeds for each day a PM10 measurement was available. We were interested in the correlation between the 24-hour average wind speed and the corresponding 24-hour average PM10 concentration and hypothesized that under certain conditions, days with high mean wind speeds are correlated to days with high PM10 concentrations.

Before performing the regression, it was useful to examine some of the raw data. Figure 4-2 shows a plot of the 24-hour average PM10 concentrations and the 24-hour average wind speed for the time period April to June 2000 in Santa Fe. Qualitatively, there appears to be a relationship between the wind speed and PM10 concentration, with one notable exception being the PM10 measurements made during the Cerro Grande Fire on May 15. A similar plot is shown for TA-54 in Figure 4-3.

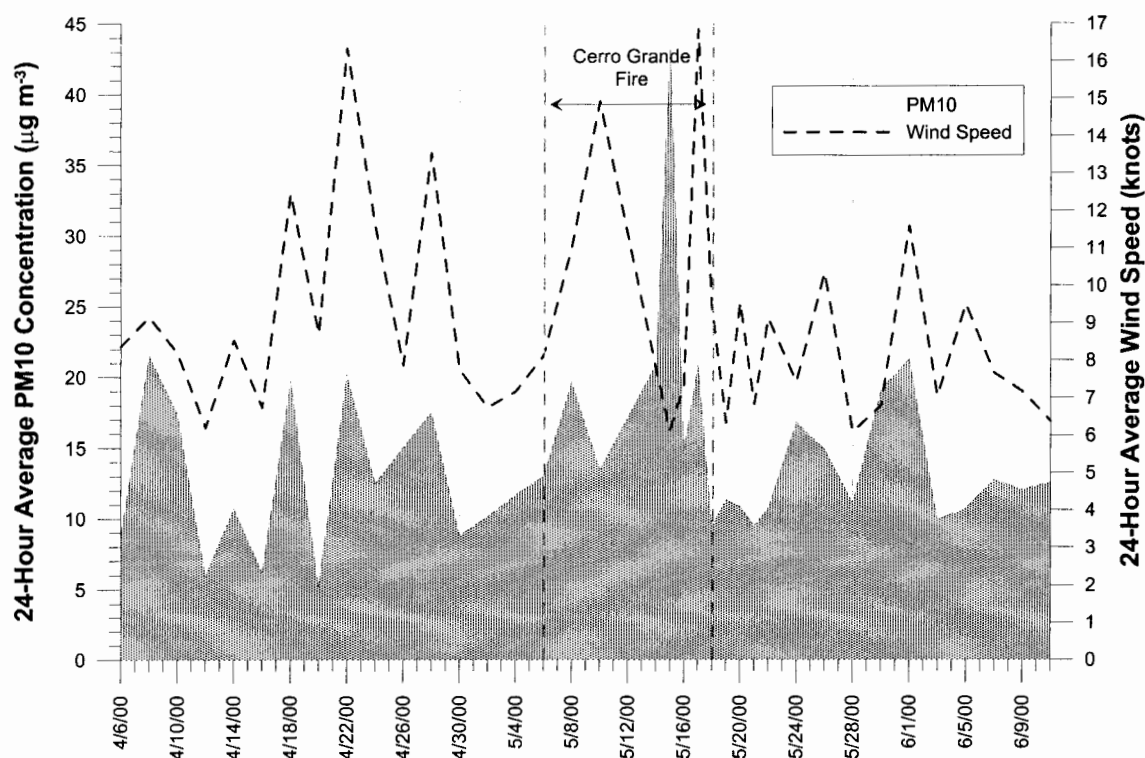


Figure 4-2. Twenty-four hour averaged wind speed and 24-hour averaged PM10 concentration in Santa Fe. PM10 concentrations represent an average of the Runnels and Capshaw measurements. Note that the highest reading on May 15 ($43 \mu\text{g m}^{-3}$) occurred during relatively calm conditions. Measurements were made about every 2 days except during the period from May 14–22 when daily measurements were made.

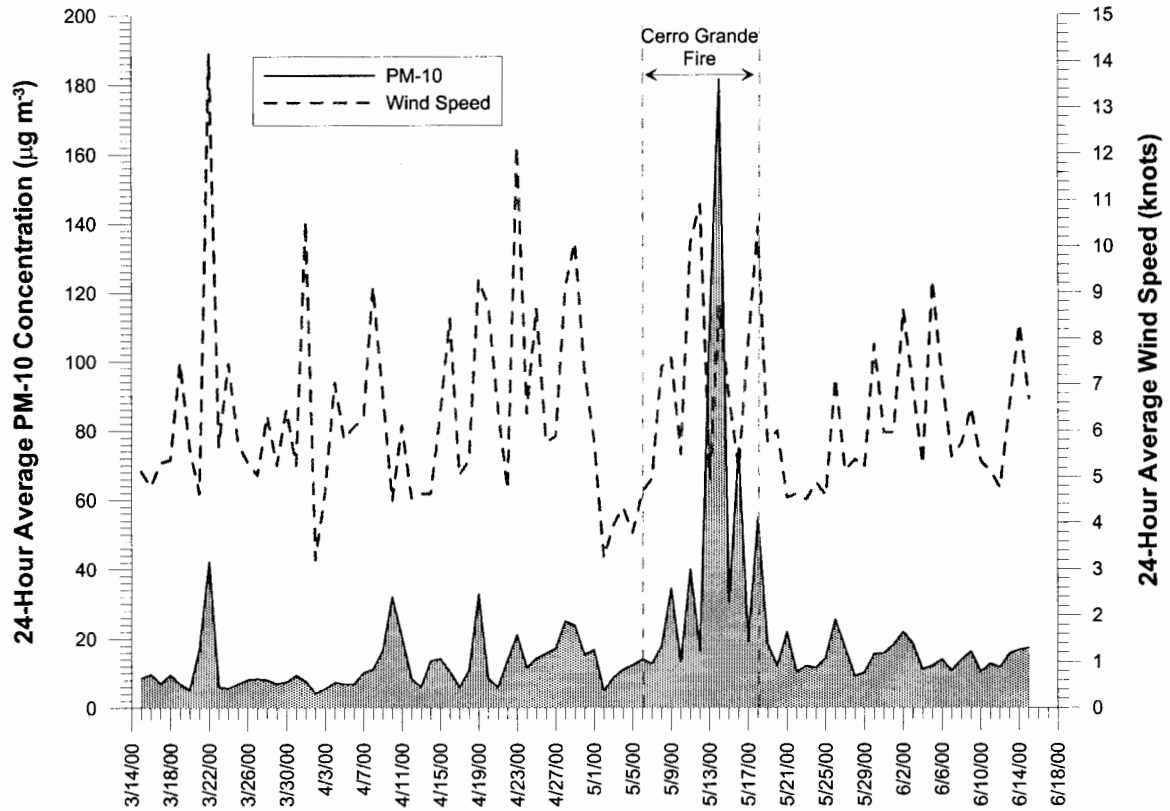


Figure 4-3. Twenty-four hour average wind speed and 24-hour average PM10 concentration at TA-54 from March 14 to June 15, 2000. Measurements were made daily during this period. The highest reading was observed on May 13.

We performed linear regression on the various subsets of the data. The linear correlation coefficient (r) was given by Bevington and Robinson (1992)

$$r = \frac{N \sum x_i y_i - \sum x_i \sum y_i}{\left[N \sum x_i^2 - (\sum x_i)^2 \right]^{1/2} \left[N \sum y_i^2 - (\sum y_i)^2 \right]^{1/2}} \quad (4.1)$$

where N = the number of x - y pairs. The probability of exceeding r in a random sample of observations taken from an uncorrelated parent population is given by

$$P_c = 2 \int_r^1 P_r dr \quad (4.2)$$

where, P_r is given by

$$P_r = \frac{1}{\sqrt{\pi}} \frac{\Gamma[(v+1)/2]}{\Gamma(v/2)} (1-r^2)^{(v-2)/2} \quad (4.3)$$

where $\nu = N-2$ and Γ is the gamma function approximated by Bevington and Robinson (1992)

$$\Gamma(n) = \sqrt{2} e^{-n} n^{(n-1/2)} (1 + 0.0833/n) . \quad (4.4)$$

Values for P_c were tabulated in Table C3 in Bevington and Robinson (1992) and intermediate values were interpolated.

The results for Capshaw and Runnels (Table 4-3) show a poor correlation between 24-hour averaged wind speed and PM10 when all data were considered. We obtained a somewhat better correlation by eliminating those days in which precipitation was measured. This regression yielded a r value of 0.222 and had a P value of 0.028. Limiting the regressions to snow-free months (March–October) yielded a slightly better regression ($r = 0.24$, $P_c = 0.016$). Limiting the regression to the months before and after the fire yielded a r value of 0.552 and corresponding P_c value of 0.0025 (Table 4-3). When the data from the fire (May 6–18) were regressed, a negative correlation was calculated, however the P value was >0.69 indicating probably no correlation at all. The results for TA-54 also showed similar results (Table 4-4).

Table 4-3. Summary of Regression Statistics of PM10 and Average Wind Speed for Capshaw and Runnels

Statistic	All data except fire ^a	All data except fire ^a & precipitation days	Snow-free months only ^b	Month before and after fire ^c	Cerro Grande Fire days ^d
n	213	163	111	28	10
r	0.109	0.222	0.24	0.552	-0.017
P_c	0.294	0.028	0.016	0.0025	>0.5

^a January 1999 through June 2000, excluding May 6–18, 2000.
^b March–October 1999–2000, excluding May 6–18, 2000, and days with precipitation.
^c April–June 2000, excluding May 6–18, 2000, and days with precipitation.
^d May 6–18, 2000.

Table 4-4. Summary of Regression Statistics of PM10 and Average Wind Speed at TA-54

Statistic	All data	All data except fire ^a & precipitation days	Cerro Grande Fire days ^b
n	93	56	13
r	0.247	0.385	0.036
P_c	0.014	0.0025	>0.5

^a April 2000–June 2000, excluding data from May 6–18, 2000.
^b May 6–18, 2000.

Other regression schemes were also considered. These included regressions of the 24-hour average PM10 concentration with the maximum wind speed and with the natural log of the wind speed raised to the power of 3. The latter regression was done because soil suspension is known to increase as a function of the wind speed raised to a power (Gillette 1974). None of these regressions yielded results any better than the results in Table 4-3 and Table 4-4, except when the

data were reduced to the period of time before and after the fire (column 5 on Table 4-3 and column 3 in Table 4-4). For these datasets, regression coefficients were markedly better. When fit to a power function, the r value for Santa Fe was 0.99 and the r value for TA-54 was 0.77. A plot of the regression for Santa Fe is shown in Figure 4-4.

These results show that for certain periods of the year when precipitation was lacking and soil moisture contents were presumably low, 24-hour average PM₁₀ concentrations are correlated with the 24-hour average mean wind speeds. The fact that wind speed and PM₁₀ concentrations during the fire were not correlated indicates an additional source of PM₁₀, which is presumably the fire.

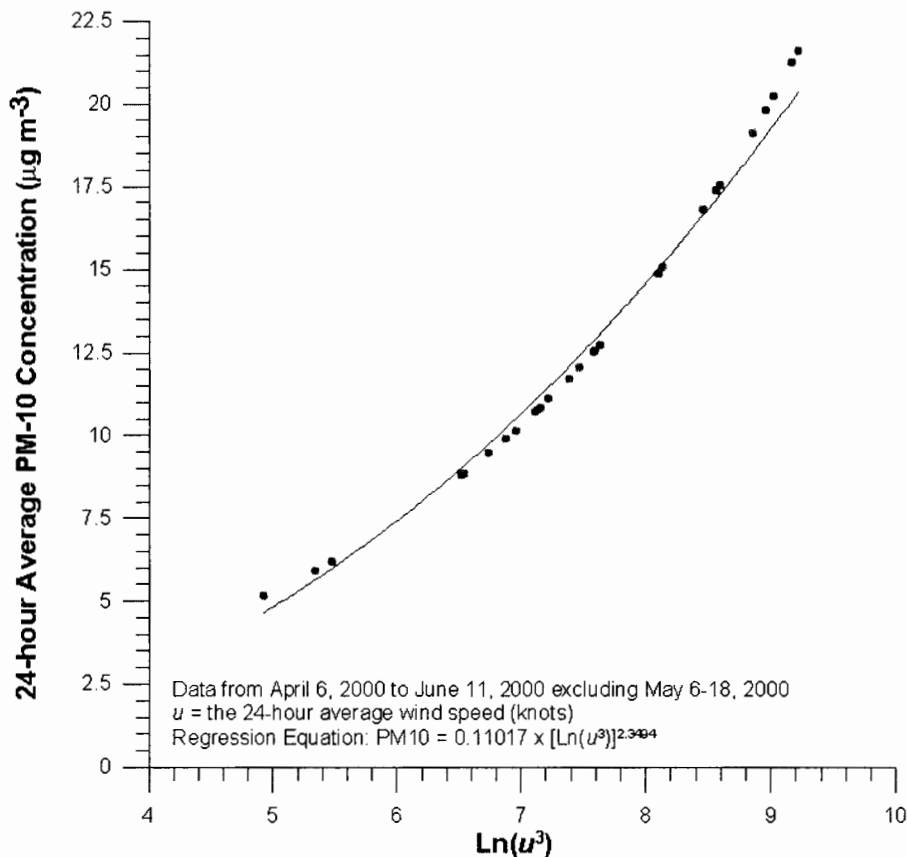


Figure 4-4. Scatter plot with regression line of 24-hour average PM₁₀ concentration as a function of natural log of the 24-hour average wind speed as measured in Santa Fe raised to the power of 3. PM₁₀ data were taken from the Runnels and Capshaw stations located in downtown Santa Fe. Measurements taken during the Cerro Grande Fire (May 6–18) and days with measurable precipitation were excluded.

Using the coefficients of the regression from the power fit, we now have a method to estimate the 24-hour PM₁₀ concentration from background sources based on the measured mean

wind speed. The regression equation for Santa Fe and other locations within the Rio Grande valley is

$$C_{PM10} = 0.11017 [\ln(u^3)]^{2.3494} \quad (4.5)$$

where C_{PM10} = the 24-hour average PM10 concentration ($\mu\text{g m}^{-3}$) and u = the 24-hour average wind speed (knots). The equation for locations in the vicinity of TA-54 is

$$C_{PM10} = 1.5144 [\ln(u^3)]^{1.26665} \quad (4.6)$$

These regression equations are by no means a mechanistic description of the process of soil and dust suspension. They only provide a means to estimate the amount of PM10 in air as a function of the 24-hour averaged wind speed for the period during the fire. The overall analysis provides evidence that the elevated PM10 observed at the monitoring stations during the fire were more than likely due to the presence of the smoke plume and not increased dust suspension. Increased dust suspension probably occurred on some of the windy days during the fire and the regression equations account for this increase.

These results are not surprising considering the other factors that affect soil suspension mentioned earlier. Precipitation appears to have a large impact on PM10 concentrations. Not only does it suppress soil suspension, it also removes particulates from the air through wet deposition. The regression analysis and examination of Figure 4-2 and Figure 4-3 also show that some of the highest PM10 concentrations during the fire occurred during relatively calm conditions. During calm conditions, the smoke plume from a smoldering fire will hold close to the ground and sink into valleys and other topographic lows during evening hours as a result of nocturnal drainage flow that is common in mountainous terrain.

4.2 CALPUFF Modeling Protocol

The CALPUFF model is actually a modeling system consisting of a meteorological model (CALMET), a dispersion and deposition model (CALPUFF), and a post processing program (CALPOST). The CALMET model uses surface and upper-air meteorological data and geophysical data (terrain and land use) to calculate hourly, three-dimensional wind fields and temperature on a three-dimensional gridded modeling domain. CALPUFF uses the hourly wind fields developed by CALMET to advect "puffs" of material emitted from modeled sources, simulating dispersion and transformation processes along the way. The primary output files from CALPUFF are gridded hourly concentrations and deposition fluxes. The CALPOST program is used to process the CALPUFF concentration and deposition files, computing time-averages and summary tabulations of results. In addition to the three main modules, numerous pre- and post-processing programs prepare the model input in the required format.

The procedure developed for estimating ambient air concentrations of contaminants suspended from burned PRSs as a result of the Cerro Grande Fire was to first model the fire itself. Modeling the fire involved estimating pollutant and heat emission rates from the fire. We then modeled these emission rates with CALPUFF. We compared estimated concentrations of PM10

(which is one of the pollutants emitted by the fire) with the measured values presented in the previous section. This process was iterative and involved many adjustments in the source term to bring the measured and predicted values within a reasonable range of agreement. The PM₁₀ emissions then served as a “tracer” for particulate contaminant emissions from burned PRS areas. We calculated concentrations of particulate contaminants by multiplying the PM₁₀ concentration by the ratio of the integrated contaminant release to the integrated PM₁₀ release. For volatile contaminants, we adopted a similar scaling procedure using the pollutant gas CO as the tracer.

We begin with a description of the CALMET modeling that was used to calculate wind fields in the model domain. Next, we describe how we calculated emission rates of pollutants from the fire. Next, we describe input parameters for the CALPUFF model and its calibration to PM₁₀ measurements. Finally, we present the methodology for calculating ambient air concentrations of contaminants from burned PRSs.

4.2.1 CALMET Modeling

We used the CALMET model to calculate gridded hourly three-dimensional wind fields within an established model domain. These wind fields are then used by CALPUFF to advect radionuclides, chemicals, and fire combustion products within the model domain. The first task in the modeling procedure is then to establish a modeling domain of interest.

4.2.1.1 Model Domain

The model domain is the geographic area of interest where dispersion and deposition calculations are performed (Figure 4-5). Ideally, we would want the model domain to cover as large of area as possible. However, for reasons discussed later, the spatial extent of the model domain was limited by the roughness of the topography, data storage requirements, and computer runtimes.

Features within the model domain are defined spatially according to a grid. The grid can be thought of as a series of points within the model domain, spaced equal-distance apart, upon which domain features are defined. For example, terrain is represented by assigning an elevation value to each of the grid nodes. The wider the spacing between grid nodes, the coarser the resolution of the feature. Because a finite number of grid nodes can be incorporated into any model simulation, there must be balance between the number of grid nodes, the size of the grid spacing, and the overall resolution required to represent the domain of interest.

Los Alamos is a challenging site to model because of its extremely variable terrain features. The steep canyons and mountainous terrain require that grid spacing be kept relatively small. Earlier efforts to grid the site required grid spacing of about 100 m to resolve the steep canyons that cut through the site. This spacing would not allow the domain to extend much beyond the LANL site boundary because large grids consume both disk space and computational time. Previous experience with CALMET showed that simulation run times for a problem involving a 167 node × 134 node grid running on a Linux-based 750 mHz Athlon system took about ~0.002 second per node per simulation hour to run. Assuming 13 simulation days (May 6–18), the runtime for the CALMET simulation alone would be about 4 hours. The corresponding CALPUFF simulation for multiple area sources took almost three times as long (0.0056 seconds per node per simulation hour). It was correctly anticipated that calibration of the model to

measured PM₁₀ concentrations would require many model simulations. Therefore, it was important to keep the number of nodes to a minimum while still adequately characterizing the major topographic features of the model domain.

While resolving the canyons that cut through the LANL site is important in terms of evaluating impacts within those features, we were more interested in evaluating impacts to offsite communities and the long-range transport of the plume. Additionally, because of their buoyant nature, smoke plumes tend to rise to heights above the canyon features and their transport is governed by air mass above the influence of the canyons. For this reason, we used a coarser grid spacing of 500 m, which allowed for a much larger domain around LANL to be modeled.

In considering the extent of the domain, it was imperative that key population centers, such as Santa Fe and Española, were included in the domain. It was also important that the total area burned by the fire be included in the domain, along with as many air monitoring stations that were operating during the fire as possible. Most of the fire smoke plumes traveled east–northeast, which is consistent with the predominant wind direction during the fire. Therefore, the LANL site was situated in the western part of the model domain to capture the fullest extent of the smoke plume trajectory. Using these criteria, we established a regional domain that encompasses the cities of Santa Fe and Española, and Cochiti Lake. The domain extends 9.3 mi (15 km) east and 4.5 mi (7.2 km) south of Santa Fe, 6.2 mi (10 km) north of Española, and 9.3 mi (15 km) west of the city of Los Alamos. The domain contains 120 nodes in the east–west direction and 110 nodes in the north–south direction, with a grid spacing of 1640 ft (500 m). The total extent of the domain is 37×34 mi (60×55 km) and encompasses an area of 1274 mi^2 (3300 km^2). The 1640 ft (500 m) grid allowed the major topographical features, including White Rock Canyon to be identified. Smaller canyons within the LANL boundary (Water, Los Alamos, Sandia, etc.) were not well resolved.

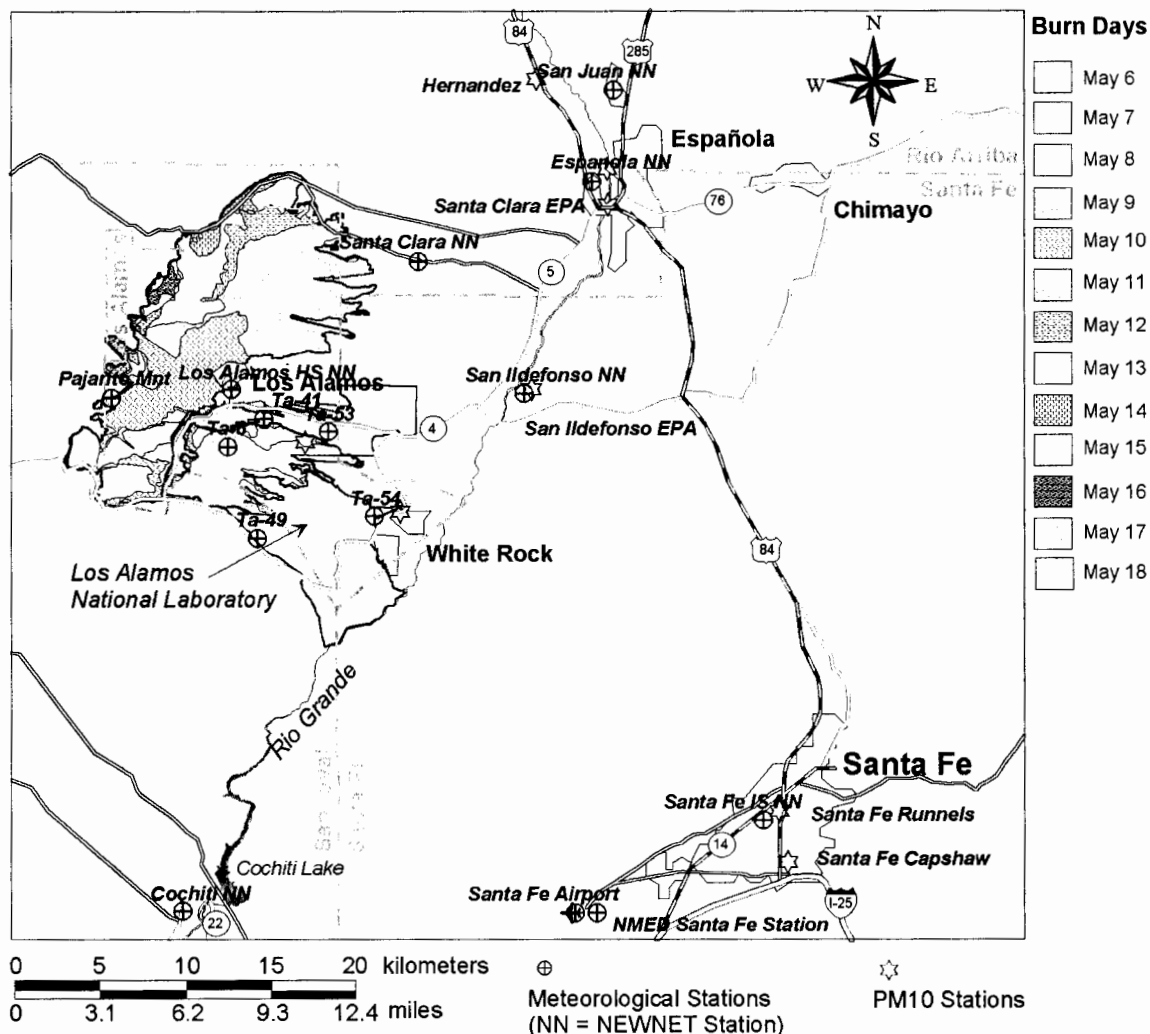


Figure 4-5. Model domain for CALPUFF modeling of the Cerro Grande Fire. Meteorological stations used in the CALMET modeling are shown; however, not all meteorological stations were used. The PM10 monitors listed in Table 4-1 and Table 4-2 are also shown. A digital representation of the daily progression of the fire was obtained from LANL. The shaded relief background was generated using the processed terrain data used in the CALPUFF/CALMET simulation.

4.2.1.2 Terrain and Land Use Modeling

The terrain model used USGS Digital Elevation Model (DEM) data (Table 4-5). These data are available as various resolutions and may be downloaded or ordered from the USGS internet site. For the area in the vicinity of the LANL site, we obtained 30-minute DEM data with a grid resolution of 30 m. For the surrounding area that bounds the model domain, we obtained 1-degree DEMs having a grid resolution of 90 m. The DEM data were processed through the CALPUFF utility, TERREL, which averages elevation data near each grid node and generates a gridded data

file for use in the MAKEGEO pre-processor and was suitable for import into the Surfer[®] program (Golden Software 1999). The gridded terrain elevations are contoured and plotted in Figure 4-6.

Digital elevation models use the Universal Transverse Mercator (UTM) coordinate system. This coordinate system is based on the distance (in meters) from a given reference point. The data for New Mexico are within UTM zone 13. All data in the CALPUFF model simulation were represented using the UTM coordinate system.

Table 4-5. U.S. Geological Survey Digital Elevation Model Data Used in the Terrain Model

DEM map name	Resolution	DEM map name	Resolution
Agua Fria NM	30 meter	Polvadera Peak NM	30 meter
Bland NM	30 meter	Puye NM	30 meter
Canada NM	30 meter	San Juan Pueblo NM	30 meter
Chili NM	30 meter	Valle Toledo NM	30 meter
Cochiti NM	30 meter	Vallecitos NM	30 meter
Española NM	30 meter	White Rock NM	30 meter
Frijoles NM	30 meter	Albuquerque East NM	90 meter
Guaje Mountain NM	30 meter	Aztec East NM	90 meter
Horcado Ranch NM	30 meter	Raton West NM	90 meter
Montoso Peak NM	30 meter	Santa Fe West NM	90 meter

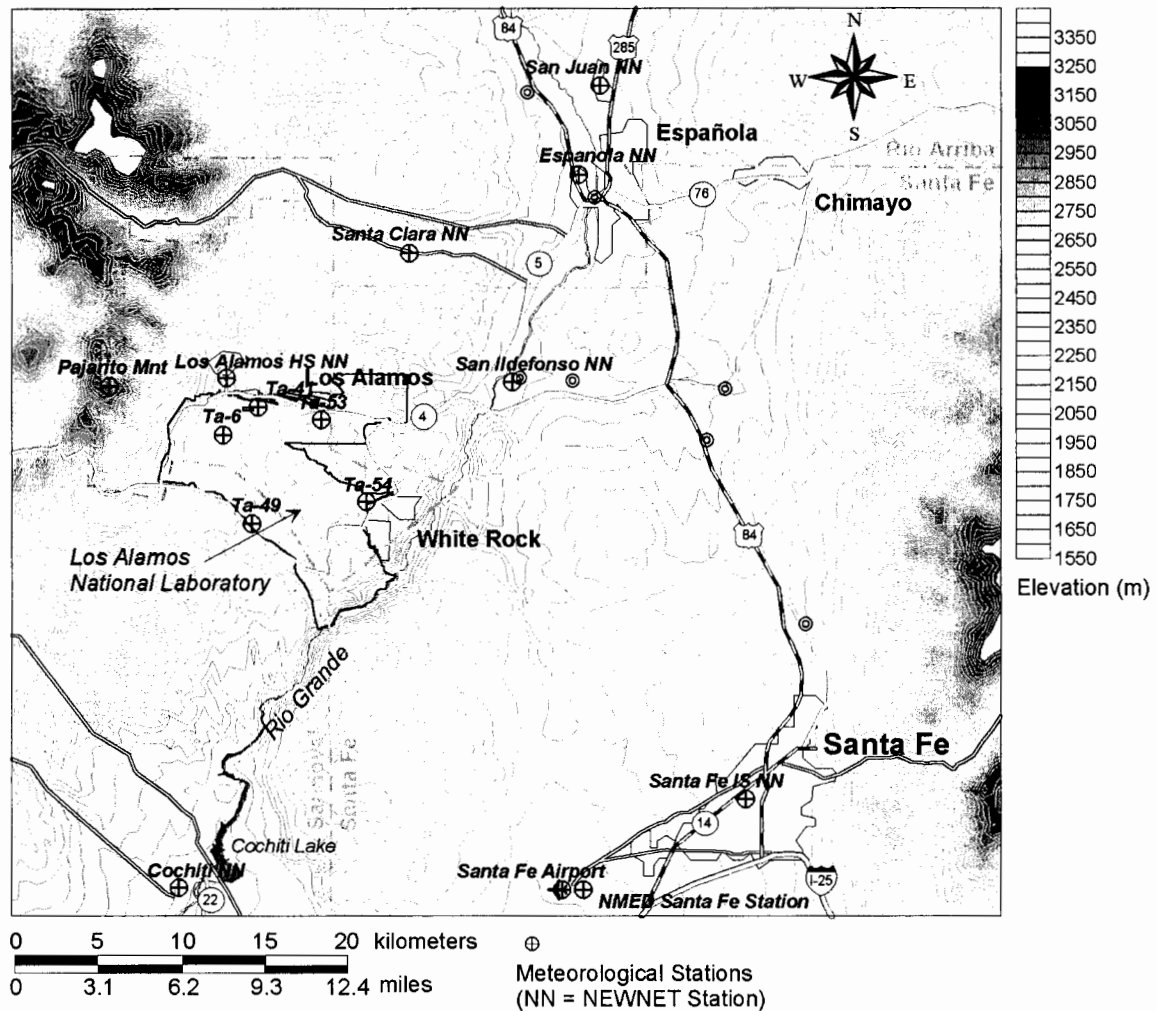


Figure 4-6. Gridded terrain data as processed by the TERREL preprocessor representing a grid spacing of 1640 ft (500 m).

We also obtained land use data from the USGS internet site in the Composite Theme Grid (CTG) format. Land use is important for defining the energy balance at each grid node and the surface roughness height. These data are available in the 1:250,000 scale with grid spacing of 200 m. Land use and land cover types are divided into 37 categories. The quadrants obtained included Albuquerque, Aztec, Raton, and Santa Fe. These data were processed through the CTGCOMP program, which compresses the data because the CTG format produces very large ASCII files. The compressed files are then processed through the CTGPROC program, which produces gridded fields of land use. Figure 4-7 presents the gridded land use data for the regional model domain.

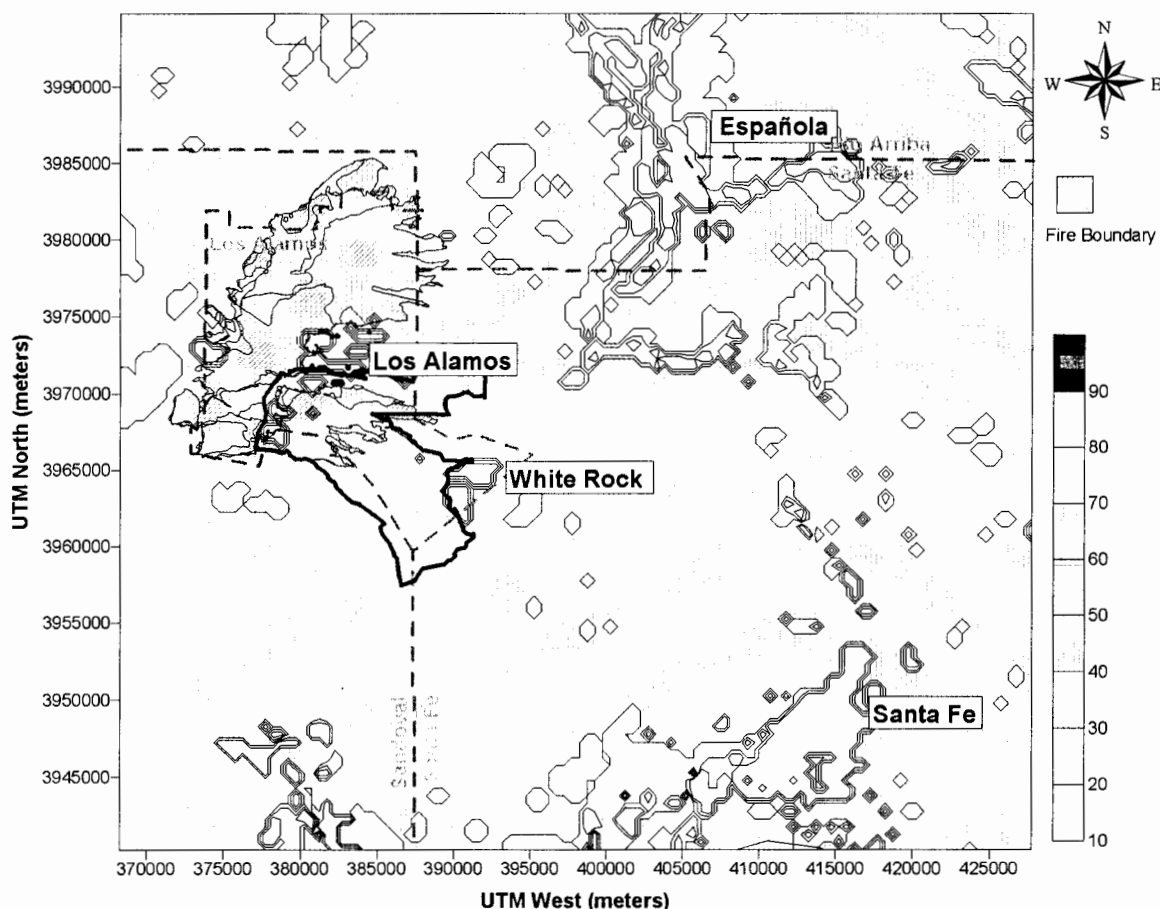


Figure 4-7. Land use in the model domain as defined by the USGS CTG files. Land use values are as follows: 10–17 urban or built-up; 20–24 agriculture; 30–33 rangeland; 40–43 forested land; 50–55 water; 60–62 wetland; 70–77 barren land; 80–85 tundra; and 90–92 perennial ice/snow.

4.2.1.3 Vertical Profile

The CALMET wind fields are generated on a three-dimensional grid. The horizontal grid spacing of 500 m is discussed in an earlier section. The vertical grid is specified by defining discrete layers in the atmosphere. For the Cerro Grande Fire simulation, we used nine layers. Face heights of each layer are 20, 60, 100, 300, 600, 1200, 2000, 3000, and 4000 m above ground level.

4.2.1.4 Meteorological Data

Meteorological data required by CALPUFF include both surface observations and upper-air observations. Surface observations include those taken routinely at airports and archived by the National Climatic Data Center (NCDC) and site-specific data. Site-specific data must be processed into the format required by the CALPUFF meteorological processors. Upper air data are somewhat more limited. These data are routinely taken at a limited number of airports around

the country. Albuquerque International Airport was the station nearest to the Cerro Grande model domain.

Surface meteorological data were obtained from LANL at six locations, the Santa Fe airport, the NMED meteorological station near Santa Fe, and the NEWNET air monitoring stations (Figure 4-5). The LANL data were taken every 15 minutes and consisted of wind speed, wind direction, temperature, and solar radiation. The station in Los Alamos Canyon (TA-41) was not included in the simulation because wind directions and speeds are highly influenced by its location within the canyon and do not reflect the regional flow across the mesas. We downloaded meteorological data obtained from the NEWNET air monitoring stations from the NEWNET web site (<http://newnet.lanl.gov>). These data included 15-minute observations of wind speed, wind direction, barometric pressure, precipitation, and temperature. Data from six stations were downloaded and processed. Data from the Los Alamos High School were omitted because the windrose for that station showed a substantially different pattern than the other stations (Figure 4-8). It is suspected that the wind directions may be off by 180 degrees. On the recommendation of Jean Dewart of LANL, we also removed the station at San Ildefonso Pueblo because the station is located between two buildings. Wind data from the Santa Fe Airport also exhibited irregularities when compared to corresponding data taken at the nearby NMED office. For this reason, we used only the cloud cover records from the Santa Fe Airport dataset. Wind roses for some of the other stations are presented in Figure 4-9. We used a total of 11 surface meteorological stations in the model simulation. Station locations and descriptions are found in Table 4-6.

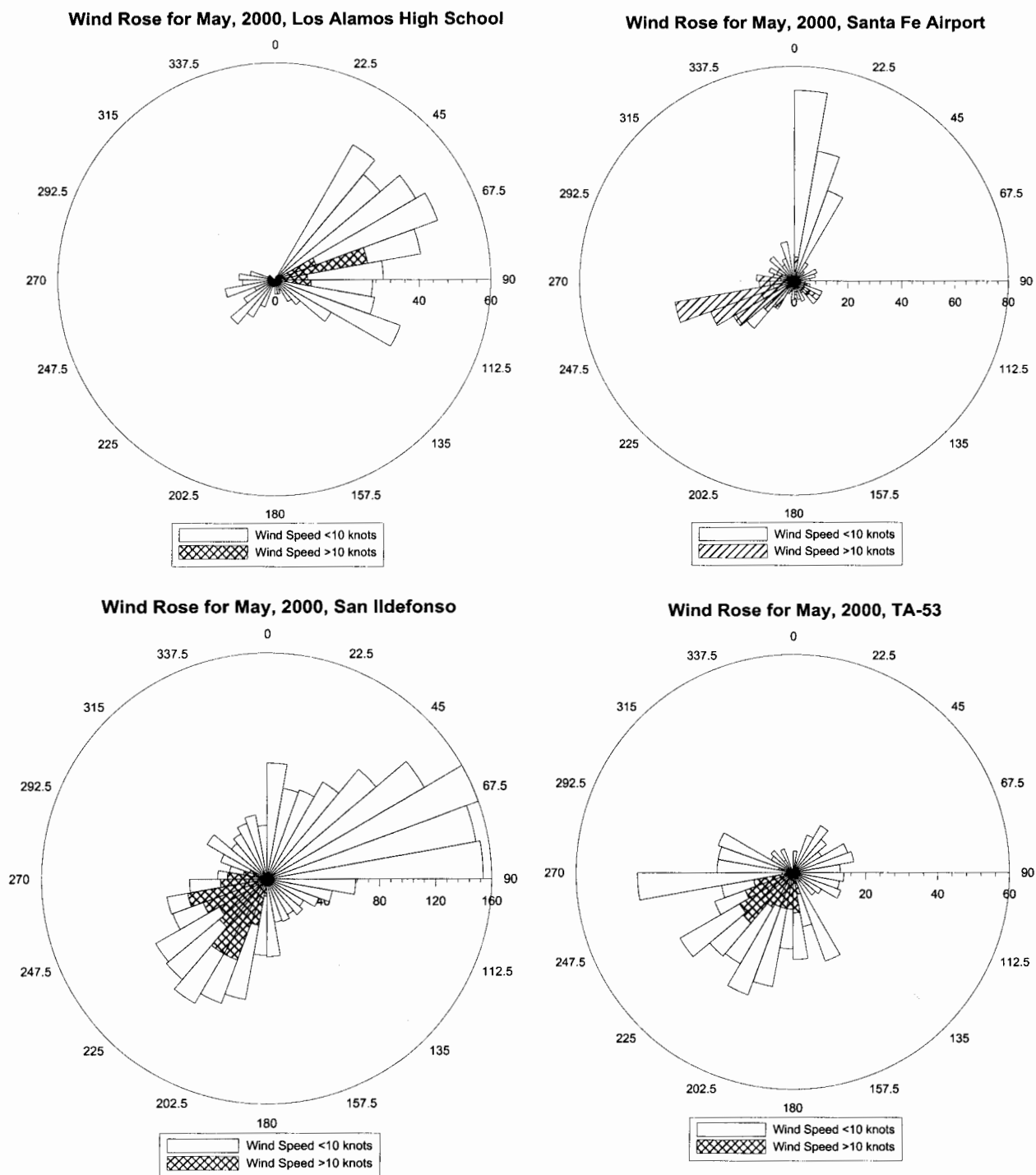


Figure 4-8. Wind roses for Los Alamos High School, Santa Fe Airport, San Ildefonso NEWNET, and TA-53 stations. Except for TA-53, these stations had potential problems because the predominant wind directions should have been from the southwest.

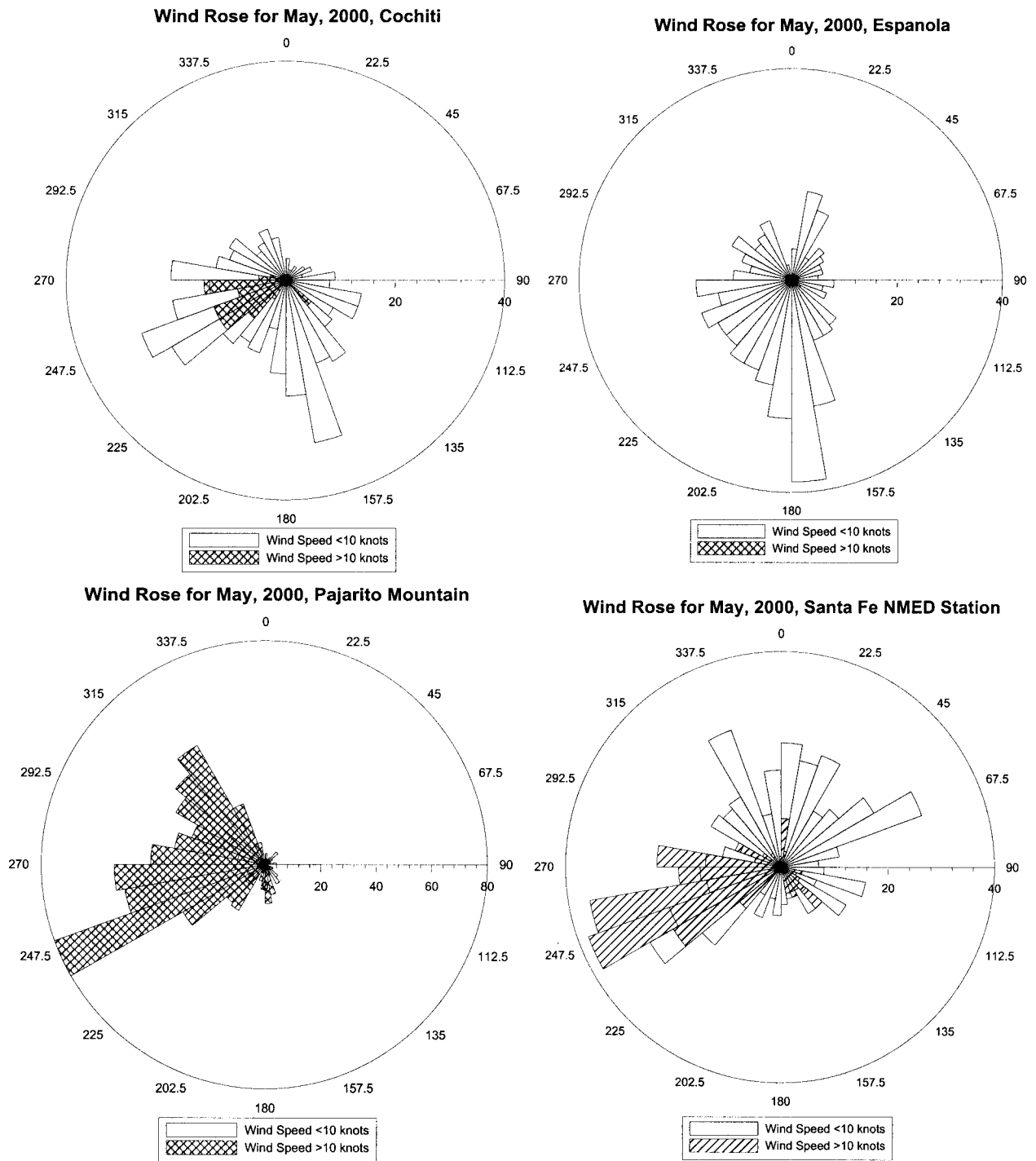


Figure 4-9. Wind roses for Cochiti NEWNET, Española, Pajarito Mountain, and Santa Fe NMED stations. The wind speeds at the top of Pajarito Mountain were significantly higher than the other stations.

Table 4-6. Surface Meteorological Surface Stations in the Model Domain

Station ID	UTM E (m)	UTM N (m)	Elev. (m)	Data description ^a
TA-6	380906	3969181	2263	LANL data. Observations taken at 4 levels. Station was disabled on May 11 due to the fire
TA-41	383018	3970813	2107	LANL data. Observations taken at 2 levels. Station situated in Los Alamos canyon and was not used in the simulation
TA-49	382664	3963816	2150	LANL data. Observations taken at 3 levels
TA-53	386814	3970067	2131	LANL data. Observations taken at 3 levels
TA-54	389545	3965113	1996	LANL data. Observations taken at 3 levels
Pajarito Mountain	374100	3972050	3158	LANL data. Observations taken at 1 level
Santa Fe Indian School	412440	3947241	2191	NEWNET station number 1720
San Juan	403641	3990143	1719	NEWNET station number 1701
Santa Clara	392130	3980077	1966	NEWNET station number 1721
Española	402380	3984764	1630	NEWNET station 1718
San Ildefonso	398355	3972329	1691	NEWNET station 1703. Station not used in simulation
Los Alamos	381130	3972575	1706	NEWNET station number 1706. Station not used in simulation
Cochiti	378278	3941950	1658	NEWNET station 1717
Santa Fe NMED	401376	3941819	2070	Station operated by New Mexico Environment Department
Santa Fe	401376	3941819	2075	Airport data. Only cloud cover data was used

^a Data used in CALMET were all taken from the 10-m level.

All LANL data had to be processed into a form compatible with input format required by the CALMET surface meteorological preprocessor, SMERGE. The SMERGE program uses the NCDC Card Deck 144 format (CD144). Because the time resolution of CALMET data is 1-hour, the 15-minute observations taken by LANL needed to be converted to hourly average observations. We performed time-averaging calculations using the EPA protocol (EPA 1987).

We obtained data from the Santa Fe airport from NCDC. These data consisted of hourly observations of wind speed, wind direction, cloud cover, temperature, and relative humidity. The cloud cover data are required by CALPUFF to calculate the amount of solar radiation that reaches the earth surface.

We obtained upper air data for the Albuquerque airport (Station Number 72365) from NCDC. These data were taken twice a day and include soundings from the surface up to the 500 mB level, which equates to an elevation of about 19,685 ft (6000 m) above ground level. Wind speed, direction, and temperature data are taken at each level.

4.2.1.5 CALMET Options

In general, we used the default model options in the CALMET simulation. Options that had no default value, or the default value was not selected, are discussed in this section.

The BIAS parameter determines the relative weight given to the vertically extrapolated surface observations versus the upper air soundings data in the computation of the initial guess

field. The default option is to give equal weight to the surface and upper air observations in each vertical layer. For this simulation, we gave the upper air observation no weight in the first two layers because the one upper air station that was used in the simulation was out of the model domain and we think the surface observations provide the best indication of surface conditions. For the third layer, a bias value of -0.5 was assigned, which results in slightly more weight given to the extrapolated surface observations compared to the upper air observation. We assigned a bias value of 0 for layer 4, which gives equal weight to the extrapolated surface observation and the upper air observation. The remaining layers are biased toward the upper air observations because surface influence of upper air winds diminish with height.

The radius of influence of terrain features (TERRAD) is a function of the dominant scale of the terrain. We chose a value of 2.5 km for this parameter based on the resolution of the terrain features at in the model domain. Choice of this parameter was difficult because terrain varies substantially across the model domain. In some parts of the domain (such as near Santa Fe or Española), the ground is relatively flat, and a larger TERRAD value may be more appropriate. However, in most of the model domain, especially in the burn areas, the terrain is quite rugged. Near some of the steep canyons that bisect the mesas, a smaller value on the order of a kilometer may be more appropriate. We chose the value of 2.5 km as a compromise between the relatively flat terrain near Santa Fe and Española and the more rugged terrain that characterizes the burn area.

The parameters R1 and R2 are distances from an observational station in which the observation and the first-guess wind field produced by the diagnostic wind field module are weighted equally. In this simulation, we assigned R1 a value of 5 km and R2 a value of 10 km. The value of R2 had little bearing on the simulation because the upper air station in Albuquerque was outside the model domain. Therefore, upper air wind fields produced by the diagnostic wind field model are given 100% of the weight when determining the final wind field.

4.2.1.6 Meteorological Wind Fields

The CALMET model was run for the regional model domain using the 11 surface meteorological data stations and the 1 upper air station. For illustration purposes, wind fields were output for the 1st, 3rd, and 7th atmospheric layers, which correspond to the heights above ground level of 0 – 20 m, 60 – 100 m, and 1200 – 2000 m, respectively, for May 11, 2000, at 10:00 am. May 11 was the most active day of the fire and the day LANL burned. At the first level (Figure 4-10), winds were generally out of the west-southwest. Terrain influences were most notable in White Rock Canyon (which is cut by the Rio Grande) where the wind appeared to be channeled up the canyon. Winds at the higher elevations (near Pajarito Mountain) were stronger and exhibited less directional variation. At the third level (Figure 4-11), winds tended to be stronger, but they still exhibited influences from the terrain. At the 7th level (Figure 4-12), winds were even stronger and generally unidirectional. Terrain influence was nonexistent at this level.

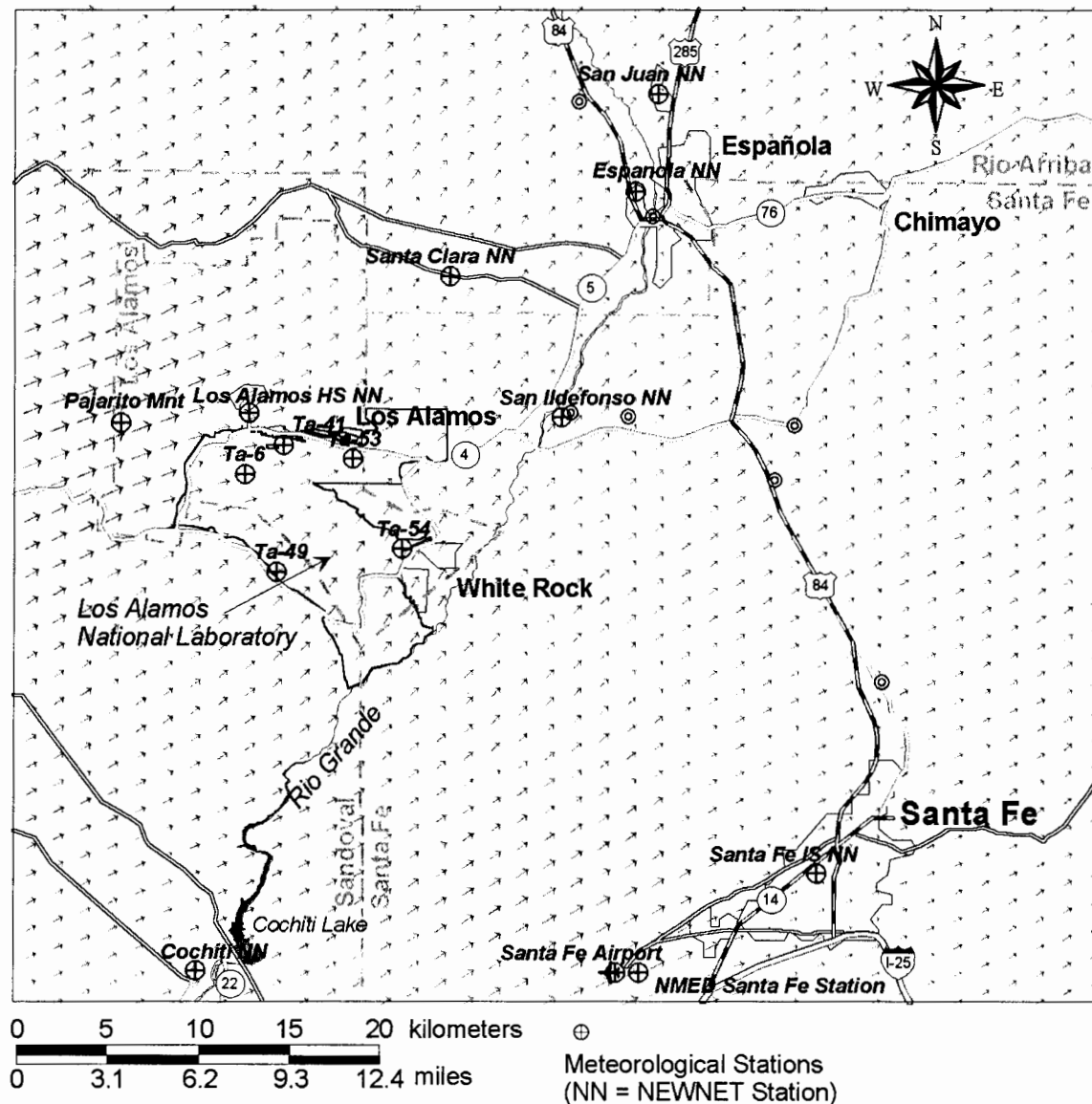


Figure 4-10. CALMET-generated wind vectors for layer 1 (0–20 m) on May 11, 2000, at 10:00 am. The length of the arrow is proportional to the wind speed. The NEWNET stations at Los Alamos HS, San Ildefonso, and the Santa Fe Airport data (excluding cloud cover data) were not used in the simulation.

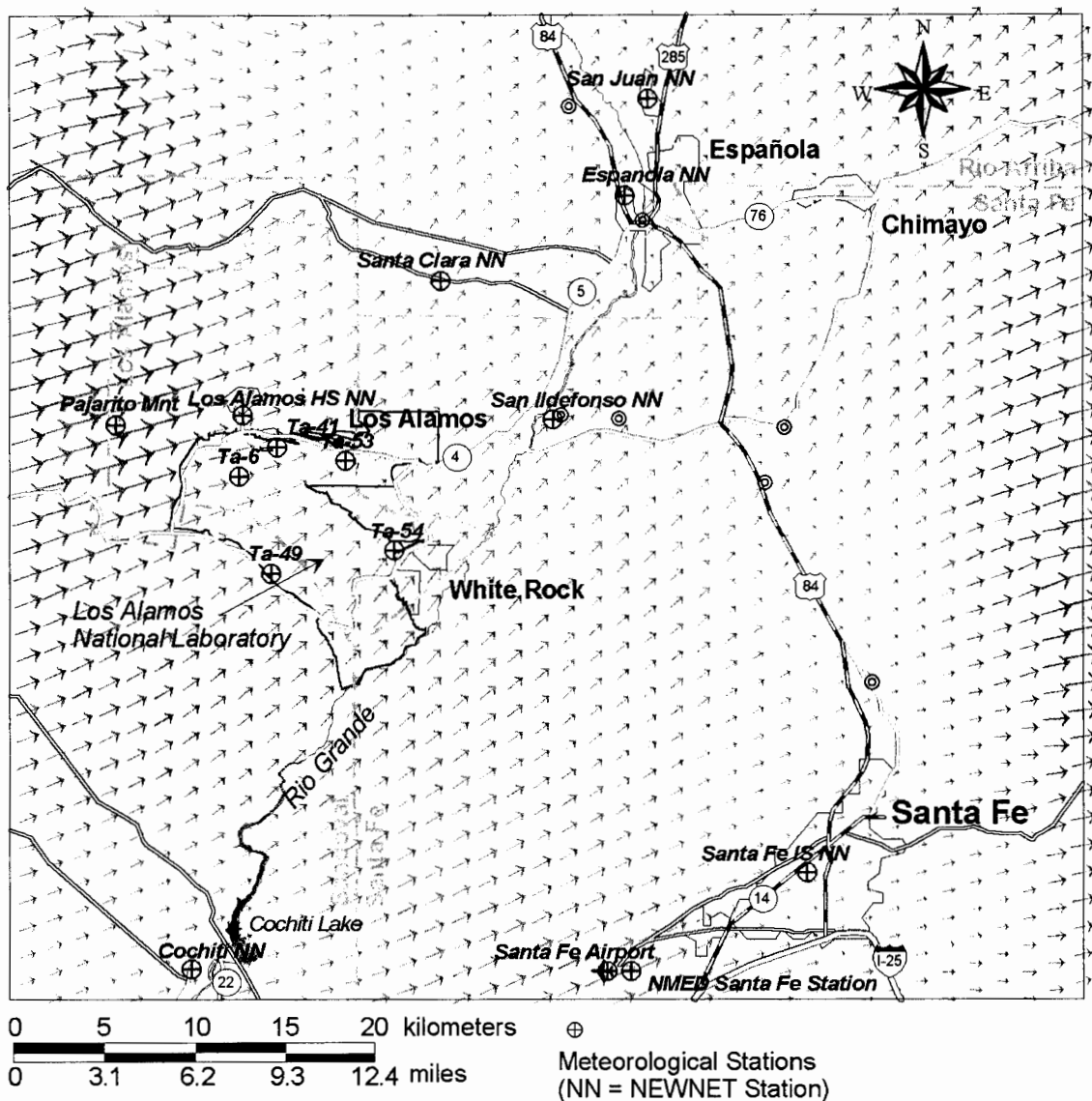


Figure 4-11. CALMET-generated wind vectors for layer 3 (60–100 m) on May 11, 2000, at 10:00 am. The length of the arrow is proportional to the wind speed. The NEWNET stations at Los Alamos HS, San Ildefonso, and the Santa Fe Airport data (excluding cloud cover data) were not used in the simulation.

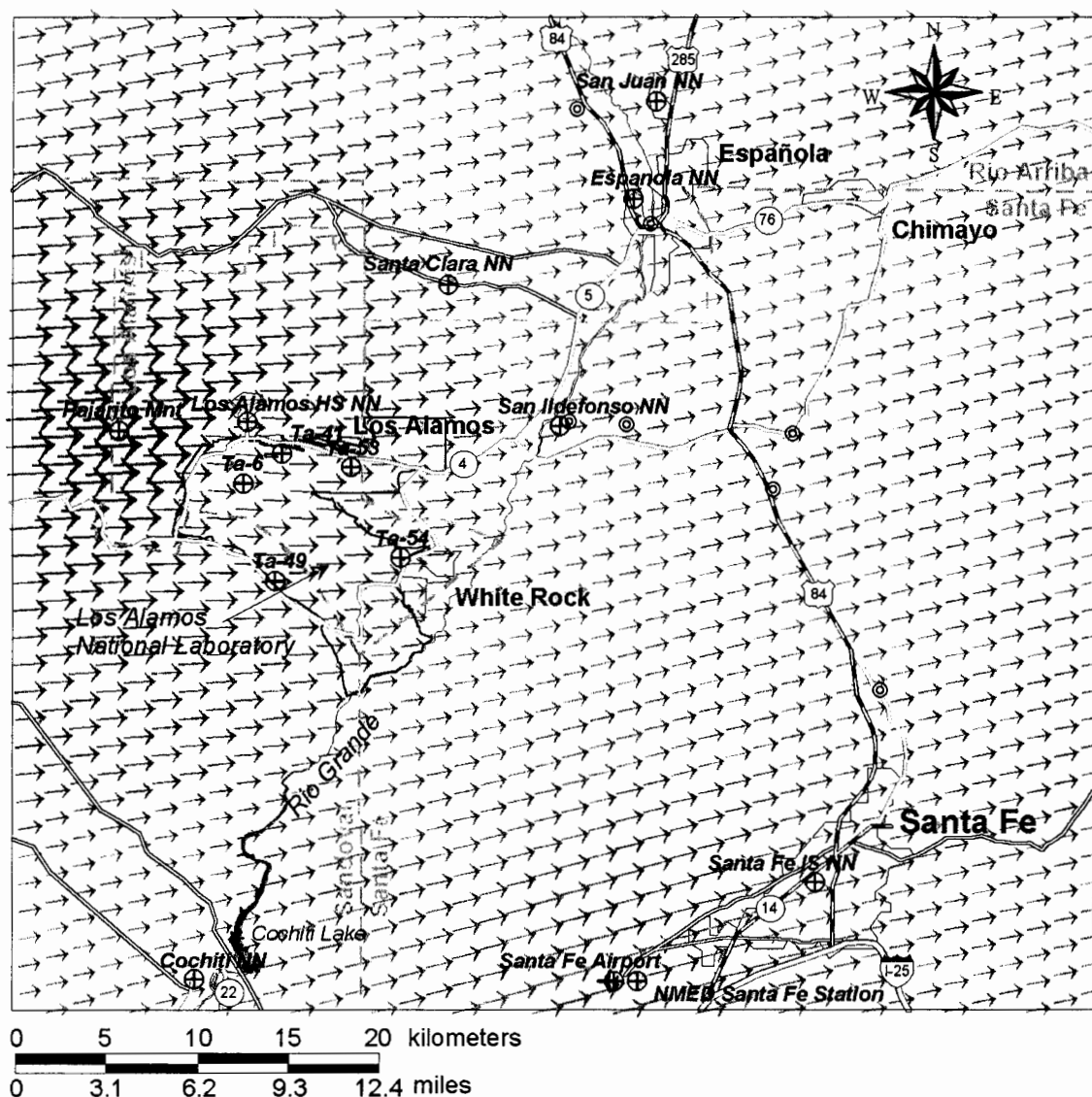


Figure 4-12. CALMET-generated wind vectors for layer 7 (1200–2000 m) on May 11, 2000, at 10:00 am. The length of the arrow is proportional to the wind speed. The NEWNET stations at Los Alamos HS, San Ildefonso, and the Santa Fe Airport data (excluding cloud cover data) were not used in the simulation.

4.2.2 Modeling the Cerro Grande Fire

The source term reported earlier in this report provides the release rates of various contaminants to the atmosphere. However, the dispersion of these contaminants once they are suspended depends on the physical characteristics of the fire because of the large amount of heat released during the burning. To account for the buoyant nature of the plume, the fire itself had to be modeled first. Modeling the Cerro Grande Fire involved first estimating the amounts of combustion products and heat emitted from the burning of biomass. We estimated combustion products and heat using the Emissions Production Model (EPM, Sandberg and Peterson 1984).

Emission rates as a function of time are estimated for five combustion products (PM10, PM2.5, CO, CO₂, and CH₄) and heat. The model takes as input, fuel loads of different sizes (in tons per acre), duff depth, and burn time. The code then computes the heat and combustion products produced and distributes their release over the burn time. Emissions and heat are assumed to build up and decay according to an exponential function. The decay and build up half-time is assumed to be proportional to the duff depth, however, no value or algorithm was provided for the half-time.

The EPM was designed for prescribed and slash burns—it was not designed for large wildfires. Despite these shortcomings, EPM is currently the only model available to estimate emission rates and heat from the burning of biomass. In addition, an interface has been written to integrate EPM derived emission rates into a CALPUFF simulation. For these reasons, we used EPM to calculate emission rates and heat released as a result of the fire. We made some modifications to the EPM output to better simulate the behavior of large wildfires. These modifications are discussed in a later section.

4.2.3 Description of Emissions Production Model

EPM was downloaded from the National Forest Service's Fire and Environmental Research Applications web site (<http://www.fs.fed.us/pnw/fera/sue/epm.html>). The source code was not available, but some limited documentation was included. A second code named CONSUME was also downloaded. The CONSUME code calculates total fire emissions of primary pollutants but does not report emission rates or heat generation as a function of time, which is what the source term model requires. However, CONSUME contained some default values of fuel loading and fuel moisture that were useful for deriving EPM input.

The EPM model first uses the predictive algorithm from Ottmar (1983) and Sandberg and Ottmar (1983) to compute fuel consumption (tons per acre) for each fuel bed component. Fuel bed components consist of biomass of different sizes and moisture content. The proportion burned in the two combustion phases, flaming and smoldering, is multiplied by the predicted fuel consumption. The total mass consumed is summed across all fuel bed components and combustion phases (tons per acre). These values are multiplied by the size of the fire (acres) and emission factors for flaming and smoldering to compute the emission yield in grams of each pollutant. A rate equation is then used to apportion emissions across the burning period. The rate equation for the flaming stage is simple. Ignition is assumed to proceed uniformly and source strength increases linearly for 10 or 20 minutes. Emissions during this period for a given fuel type are given by

$$E_f(t < T_f) = \frac{A EF_F WF}{T_f T_{ign}} t \quad (4.7)$$

where

E_f	=	emission rate of pollutants (g min ⁻¹)
A	=	area of burn (acres)
EF_F	=	emission factor for flaming stage (g of pollutant per ton consumed)
WF	=	consumption of fuel during flaming stage (tons per acre)
T_f	=	flaming period until smoldering begins (10-20 minutes)
T_{ign}	=	total ignition time over which the fire burns (minutes)

t = time from the start of the fire (minutes).

When $t > T_f$ and less than $T_f + T_{ign}$, the emission rate is given by

$$E_f = \frac{A EF_F WF}{T_{ign}} \quad (4.8)$$

The flaming phase then decreases linearly until $t = T_f + 2T_{ign}$. The emission rate for this period is given by

$$E_f(t > T_f + T_{ign}) = \frac{A EF_F WF}{T_{ign}} \left(1 - \frac{EF_F}{T_f} t \right) \quad (4.9)$$

Values for EF_F , WF , and T_f were not provided in the documentation. The parameter T_{ign} is provided by the user. The smoldering stage of the fire assumes an exponentially increasing and decreasing source strength. Smoldering begins when $t > T_f$ and increases exponentially reaching a steady state value until $t = T_{ign} + T_f$. Smoldering emissions for a given fuel type are given by

$$E_s(t) = A WS EF_s \left(1 - \exp\left(-\frac{t - T_f}{T_E}\right) \right) \quad (4.10)$$

where

- E_s = emission rate of pollutant during the smoldering stage (g min^{-1})
- EF_s = maximum emission rate of pollutant during the smoldering stage (g min^{-1})
- T_E = mean halftime of the smoldering time (minutes).

We noted an error in Equation (4.10) as it was reported in the original documentation (Sandberg and Perterson 1984), in that the units were not consistent in the exponential. Values for EF_s were not provided in the documentation. When $t > T_f + T_{ign}$, smoldering decreases exponentially and is given by

$$E_s(t) = A WS EF_s \left(\exp\left(-\frac{t - (T_f + T_{ign})}{T_E}\right) \right) \quad (4.11)$$

The EPM also calculates the heat released during the fire. The calculated heat values are used to compute plume rise, which is important in terms of ground-level concentrations. The heat released is assumed to follow the same buildup and decay curve as the emission rates of pollutants. In preliminary CALPUFF simulations, we observed that most of the pollutant emissions were lofted well above the ground surface, leaving minimal pollutant concentrations at ground level. This phenomenon has been documented during the active stages of a fire in

photographs that show the plume well above the ground surface. However, during the smoldering stage of the fire, the heat released is substantially lower, resulting in little plume rise and higher ground-level pollutant concentrations. This phenomenon has also been observed in photographs of the fire and reported in the literature. For example, Ward (1999) reports that smoldering combustion releases several times more particles than flaming combustion, and ~70% of the total particulate emissions from wild fires occur during the smoldering stage. He also states that "emissions released through the flaming stage are generally accompanied by the release of significant heat which lofts the emissions well above ground level." Most emissions having a ground-level signature are produced through smoldering combustion. Based on our initial modeling efforts, we concur with Ward's observations and conclude that the smoldering stage of the fire in EPM is poorly represented. That is, the smoldering stage of the fire is substantially longer than the EPM predicts, resulting in most of the pollutant emissions being emitted during the active fire stage when plume rise is greatest. This deficiency has been recognized by the Forest Service. According to Tim Reinhardt⁶ of the URS Corporation, a company contracted by the Forest Service to update EPM, the smoldering stage algorithms are currently being improved and updated. However, the computer code is not set for release until sometime in 2002.

4.2.4 Modifications to the EPM Output

To account for this apparent deficiency in EPM, we modified the EPM output so as to reapportion the heat and pollutant releases. This was done by decoupling the heat released from the pollutant releases and reapportioning them so more of the pollutant releases occur during the smoldering stage of the fire when heat release is minimal. The integrated heat and pollutant released was the same as estimated by EPM. The heat and pollutant release rates were envisioned to follow an exponentially increasing and decreasing curve over the burn and smolder time. The total emission of heat and pollutants can be described by

$$Q_T = Q \left(\int_0^{T_1} 1 - e^{-k_1 t} dt \right) + Q(T_2 - T_1) + Q \int_0^{T_3 - T_2} e^{-k_2 t} dt \quad (4.12)$$

where

- Q_T = total release of pollutants or heat (g or BTU)
- Q = steady-state release rate of pollutants and heat (g min^{-1} , BTU min^{-1})
- T_1 = buildup time of pollutant and heat emissions to its maximum value (min)
- k_1 = rate constant describing the buildup of the pollutant or heat (min^{-1})
- T_2 = time of active burning of fire (min)
- T_3 = total time of fire and smoldering (min)
- k_2 = rate constant describing the decay of pollutant emissions or heat (min^{-1}).

⁶ Personal communication with Tim Reinhardt, URS Corporation, Seattle Washington, August 24, 2001. A second call made on January 9, 2002 indicated that the revised EPM model is currently in the beta test stage and was sent to Dr. David Sandberg, National Forest Service for review. Dr. Sandberg did not want to release the code at this time.

The value of Q_T is obtained by integrating the EPM output over time for pollutant and heat releases. The value of Q is solved for in Equation (4.12) by assigning values for k_1 and k_2 . The release rates of pollutants and heat (Q) are then recalculated for the time periods $0 < t < T_1$, $T_1 < t < T_2$, and $t > T_2$. The values of k_1 and k_2 are calculated based on the following assumptions:

- 15% of the total time is allotted to buildup of heat and pollutant emissions to their maximum value
- 35% of the time is allotted to maximum heat generation
- 50% of the time is allotted to decay of heat generation from its maximum value
- 75% of the time is allotted to maximum pollutant releases
- 10% of the time is allotted to decay of the pollutant release rate from its maximum value.

The above assumptions essentially partition about 50% of the total emissions to occur during the smoldering stage of the fire when the heat release rate is decaying exponentially. Given the total time of emissions and assuming a ratio of Q/Q_{max} of 0.00001 at $t = 0$ and $t = \infty$, where Q_{max} is the maximum pollutant or heat release rate, values for $k_{1,2}$ are determined by

$$k = -\frac{\ln(0.00001)}{T_3 f} \quad (4.13)$$

where f is the fraction of time associated with decay or buildup of pollutants or heat.

Release rates of heat and PM10 are compared in Figure 4-13 for EPM and the modified EPM output. The net effect is to partition more of the emissions toward the smoldering stage of the fire when the heat of the fire is lower. As a consequence, the maximum heat released is larger in the modified EPM output while the maximum PM10 release rate is smaller. The total amount of heat and particulate emissions are the same. This method is by no means definitive and it is only a crude approximation that was arrived at from examining the measured PM10 concentrations coupled with the progression of the fire and our subsequent attempts to calibrate CALPUFF to measured PM10 concentrations.

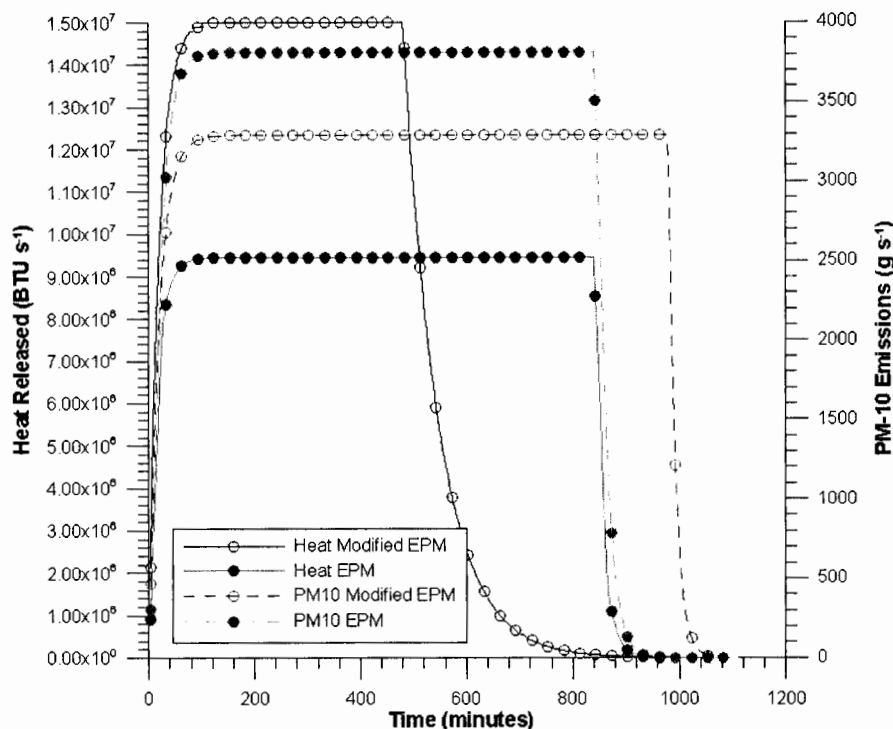


Figure 4-13. Comparison of original EPM output for heat and PM10 emissions and the modified output for the fire that burned on May 6, 2000.

4.2.5 EPM Inputs

The EPM requires estimates of the burn time, number of acres burned, mean wind speed, slope angle, and fuel loading (Table 4-7 and Table 4-8). A separate EPM run was performed for each day of the fire (May 6 through May 18). In cases when the fire burned in several locations on a given day, we made multiple EPM runs. A total of 42,623 acres were included in the fire simulation. Areas that burned each day were estimated from GIS shape files of the burned area. The burn time was estimated based on oral descriptions of the advance of the fire as described in an unpublished document provided by LANL in PDF format. For some of the large fires, we assumed a burn time that extended into the next few days and broke the fire up into several smaller areas (May 10 and 11). This was done because smoldering from these large areas continued for many days after the fire initially burned the area. We calculated the slope of the fire based on the average gradient across the fire area for the day the fire burned. We estimated mean wind speed from the meteorological data taken at the TA-54 station.

Table 4-7. Data for the EPM

Day of month	Subarea	Area (acres)	Coordinates of center of fire		Elevation (m)	Slope (%)	Mean windspeed (mph)	Ignition time	Burn time (hr)
			UTM E (m)	UTM N (m)					
6		805	372475	3969092	2861	10	6	7:00	14
7		1553	375783	3969389	2699	9	8	13:00	11
8		857	377392	3968688	2423	8	9	10:00	14
9		50	376451	3969678	2585	10	6	0:00	24
10	North a	1950	375841	3971814	2794	13	12	9:00	96
10	North b	1950	378208	3973275	2552	8	12	11:00	96
10	North c	1950	380452	3975510	2416	9	12	23:00	96
10	South	1625	376501	3967665	2470	5	12	10:00	96
11	North a	2909	383992	3977780	2299	4	13	6:00	96
11	North b	2909	384025	3980840	2275	4	13	12:00	96
11	North c	2909	386491	3977788	2157	4	13	23:00	96
11	North d	2909	384742	3975511	2249	5	13	23:00	96
11	South Central	2909	380131	3967220	2248	2	13	18:00	9
11	Southeast	2909	382465	3968919	2190	2	13	20:00	9
11 ^a	Southwest	2909	374892	3967170	2554	10	13	18:00	11
12	North	2069	382754	3982144	2462	11	6	9:00	15
12	South	517	383917	3969678	2169	2	6	b	3
13	North	3583	379966	3980015	2741	11	10	15:00	9
13	South	2389	385462	3969471	2112	2	10	b	9
14	North	1158	381013	3983027	2519	14	8	15:00	12
14	South	165	384338	3969315	2148	2	8	23:00	3
14	Central	331	374785	3973836	2838	12	8	23:00	6
15		397	376781	3977458	2681	12	6	12:00	12
16		539	377284	3978547	2951	10	9	9:00	15
17		378	376781	3978679	3008	14	13	13:00	11
18		711	385658	3983192	2166	4	7	12:00	6

^a Fire was ignited on the previous day^b These two fires were combined. Ignition began on the evening of May 12 at 9:00 pm. Total area burned was 2906 acres.

Fuel loading data (Table 4-8) were obtained from Balice et al. (2000) and were based on biomass surveys taken on LANL property and the surrounding National Forest. Fuel loading was segregated into three primary plant community types according to Balice et al. (2000). The ponderosa pine-type community was assigned to fires that burned at elevations between 6500–7200 ft (2000–2200 m). The ponderosa pine/mixed conifer-type community was assigned to fires that burned at elevations between 7200–8800 ft (2200–2700 m), and the mixed conifer/spruce-fir-type community was assigned to fires that burned at elevations greater than 8800 ft (2700 m). Fuel moisture was assigned a value of 11% for 1000-hour fuels and 2% for the 10-hours fuels based on the default data in CONSUME.

Fuel loads were based on the 97.5 percentile value of the *distribution* of measured fuel loads (Table 4-8). We used the 97.5 percentile value because preliminary model calibrations to PM10 data were consistently underpredicted. Part of the reason why we think PM10 concentrations were initially underestimated was because fuel load data apparently did not include live canopy cover, which in some locations was incinerated during the crown stage of the fire. The 97.5 percentile was calculated assuming a normal distribution and is given by

$$M_{97.5} = \bar{M} + Z s \quad (4.14)$$

where $M_{97.5}$ = the 97.5% fuel loading value (kg acre^{-1}), Z = the Z value for a normal distribution for $P=0.475$ (1.92), and s = the standard deviation (kg acre^{-1}). Minor adjustments to fuel loading were also made during model calibration. The data in Table 4-8 then represent the 97.5% values from Balice et al. (2000), with minor adjustments for model calibration.

Table 4-8. Fuel Loading Data for the EPM Model

Fuel type	Size class	Ponderosa pine	Ponderosa pine/mixed conifer	Mixed conifer/spruce -fir forest
1-hour	0.00–0.25-in. fuel (tons acre^{-1})	0.293	0.20	0.32
10-hour	0.25–1.00-in. fuel (tons acre^{-1})	2.885	2.90	4.71
100-hour	1–3-in. fuel (tons acre^{-1})	2.383	3.15	6.56
1000-hour	3–9-in. fuel (tons acre^{-1})	3.842	6.16	3.25
1000-hour	9–20-in. fuel (tons acre^{-1})	5.680	9.10	4.80
1000-hour	20+-in. fuel (tons acre^{-1})	7.517	12.04	6.35
	duff depth (in.) ^a	1.44	1.87	1.45
	litter depth (in.) ^b	0.530	0.50	0.70
	duff (tons acre^{-1})	17.473	22.58	17.50
	litter (tons acre^{-1})	1.591	1.49	2.09

^a Calculated based on a duff density of 0.107 g cm^{-3} .
^b Calculated based on a litter density of 0.0265 g cm^{-3} .

Balice et al. (2000) reports fuel loads for four types of fuel: 1-hour (0–0.25-in. diameter), 10-hour (0.25–1-in. diameter), 100-hour (1–3-in. diameter), and 1000-hour (1–20+-in. diameter). The sum of these four fuel types yielded the total fuel loads. Table 4-9 gives the total pollutant emissions calculated by EPM. We used the PM10 and CO pollutant emission estimates along with estimated PM10 and CO concentrations in air to calculate concentrations of radionuclides, metals, and volatile organic compounds in air.

Table 4-9. Pollutant Emissions Calculated with EPM

Burn day (day of month – subarea)	Acreage burned (acres)	PM-2.5 released (g)	PM10 released (g)	Total PM released (g)	Carbon monoxide released (g)	Carbon dioxide released (g)	Methane released (g)
6	805	1.65E+08	1.93E+08	3.30E+08	1.25E+09	4.64E+10	7.59E+07
7	1553	3.21E+08	3.72E+08	6.22E+08	2.57E+09	8.52E+10	1.57E+08
8	857	8.00E+08	8.68E+08	1.20E+09	6.74E+09	1.06E+11	3.23E+08
9	50	2.42E+07	2.62E+07	3.64E+07	2.04E+08	3.23E+09	9.75E+06
10-North a	1950	8.92E+08	9.68E+08	1.34E+09	7.52E+09	1.16E+11	3.62E+08
10-North b	1950	8.92E+08	9.68E+08	1.34E+09	7.52E+09	1.16E+11	3.62E+08
10-North c	1950	8.92E+08	9.68E+08	1.34E+09	7.52E+09	1.16E+11	3.62E+08
10-South	1625	7.51E+08	8.15E+08	1.13E+09	6.33E+09	9.79E+10	3.04E+08
11-North a	2909	1.09E+09	1.18E+09	1.63E+09	9.19E+09	1.39E+11	4.43E+08
11-North b	2909	1.09E+09	1.18E+09	1.63E+09	9.19E+09	1.39E+11	4.43E+08
11-North c	2909	1.09E+09	1.18E+09	1.63E+09	9.19E+09	1.39E+11	4.43E+08
11-North d	2909	1.09E+09	1.18E+09	1.63E+09	9.19E+09	1.39E+11	4.43E+08
11-South Central	2909	1.09E+09	1.18E+09	1.63E+09	9.18E+09	1.39E+11	4.43E+08
11-Southeast	2909	1.33E+09	1.45E+09	2.00E+09	1.12E+10	1.72E+11	5.41E+08
11-Southwest	1939	9.05E+08	9.81E+08	1.36E+09	7.63E+09	1.17E+11	3.67E+08
12-North	2069	4.83E+08	5.54E+08	9.03E+08	4.08E+09	1.20E+11	2.52E+08
12-South ^a	517	2.08E+08	2.26E+08	3.12E+08	1.75E+09	2.69E+10	8.44E+07
13-North	3583	8.53E+08	9.76E+08	1.58E+09	7.30E+09	2.08E+11	4.52E+08
13-South ^a	2389	1.42E+08	1.54E+08	2.12E+08	1.20E+09	1.79E+10	5.79E+07
14-North	1158	5.86E+08	6.35E+08	8.76E+08	4.93E+09	7.48E+10	2.38E+08
14-South	165	1.74E+08	1.89E+08	2.61E+08	1.47E+09	2.26E+10	7.07E+07
14-Central	331	1.64E+08	1.87E+08	3.03E+08	6.65E+08	4.05E+10	8.10E+07
15	397	8.12E+07	9.47E+07	1.61E+08	6.23E+08	2.25E+10	3.79E+07
16	539	1.10E+08	1.28E+08	2.17E+08	8.50E+08	3.03E+10	5.17E+07
17	378	1.00E+08	1.15E+08	1.86E+08	8.56E+08	2.44E+10	5.30E+07
18	711	3.93E+08	4.26E+08	5.86E+08	3.31E+09	4.94E+10	1.60E+08
TOTAL		1.59E+10	1.74E+10	2.47E+10	1.33E+11	2.33E+12	6.69E+09

^a These two fires were combined. Ignition began on the evening of May 12 at 9:00 pm. Total area burned was 2906 acres.

4.2.6 CALPUFF Inputs

In general, we used the default options recommended in CALPUFF. Those options where we did not choose the default, or for which no default value was available, include dispersion coefficients, puff splitting, and terrain adjustments.

Dispersion coefficient options include the Pasquill-Gifford scheme for urban and rural conditions and dispersion that is computed based on micrometeorological parameters. For this simulation, we chose dispersion coefficients that are computed based on micrometeorological conditions. This option calculates dispersion coefficients (σ_y and σ_z) based on an energy balance at the earth's surface. The energy balance is then related to turbulence using similarity theory. This method of dispersion coefficient estimation represents the current state-of-the-art in atmospheric dispersion.

Puff splitting allows for large puffs to be split into smaller puffs and tracked separately in the model domain. The splitting occurs in the horizontal direction when a puff is larger than a user-specified number of grid nodes, the rate of elongation of the puff exceeds a threshold value, and the peak concentration in the puff exceeds a user-specified value. We ran several test runs that used the puff splitting option and found run times were extremely long and the simulation was usually aborted because the number of puffs on the modeling grid exceeded the limits of the model. For this reason, we did not use the puff splitting option.

Terrain adjustment options include the simple ISC-type adjustment, the CALPUFF-type of terrain adjustment, and a partial plume path adjustment. For these simulations, we used the CALPUFF-type of terrain adjustment.

Dry deposition in the particle and gas phase was included in the PM10 and CO dispersion estimates, respectively. Because no measurable precipitation was recorded during the fire, we did not consider wet deposition. The model for dry deposition in CALPUFF is based on an approach which expresses the depositional velocity as the inverse of the sum of resistances. The resistances represent the opposition to transport of the material through the atmosphere. For particles, gravitational settling is also added. The deposition velocity for gases (v_d , m s^{-1}) at a reference height, z_s is expressed as the inverse sum of three resistances (Wesely and Hicks 1977; Hicks 1982).

$$v_d = (r_a + r_d + r_c)^{-1} \quad (4.15)$$

where r_a = atmospheric resistance (s m^{-1}), r_d = depositional layer resistance (s m^{-1}), and r_c = the canopy resistance (s m^{-1}). For particles, the depositional velocity is expressed as (Slinn and Slinn 1980; Pleim et al. 1984)

$$v_d = (r_a + r_d + r_d r_a v_g)^{-1} + v_g \quad (4.16)$$

where v_g = gravitational settling velocity (m s^{-1}). Gravitational settling is only significant for particles $>20 \mu\text{m}$. Atmospheric resistance is a function of the micrometeorological flux-gradient relationships described by Wesely and Hicks (1977) and is the same for gases and particles. Deposition layer resistance is a function of the molecular diffusion coefficient for gases and Brownian diffusivity for particles. Deposition layer resistance for both gases and particles are parameterized in terms of the Schmidt number, which is the kinematic viscosity of air divided by the molecular diffusivity of the pollutant. We used a value of $0.185 \text{ cm}^2 \text{ s}^{-1}$ for the molecular diffusivity of CO. For particles, the Schmidt number is computed internally within CALPUFF and is a function of the size of the particle. Canopy resistance depends on the reactivity of the pollutant. For these simulations, we assumed no reactivity. Additional details concerning the dry deposition model used in CALPUFF can be found in the CALPUFF user's manual.

As stated in an earlier section, gas-phase organic compounds may be chemically changed in the atmosphere through reactions with ozone (O_3), hydroxyl (OH) radicals, and nitrate (NO_3) radicals. The CALPUFF model includes models for chemical reactions of SO_2 , NO_x , and HNO_3 . While the model may be adapted to other chemicals, gathering the necessary data to model chemical transformations was beyond what could be accomplished in this exercise. Additionally,

the chemical transformation model in CALPUFF is specific to SO_2 , NO_x , and HNO_3 and may not be applicable to other compounds. For these reasons, we have not included chemical transformations in the CALPUFF simulation. Instead, we treated the dispersion of CO as a conservative tracer in the model domain.

4.2.7 Integration of Emission Estimates into CALPUFF

We entered emission estimates calculated with EPM into CALPUFF using the buoyant area source option. A preprocessor was used to format the EPM output into the format required by CALPUFF. This preprocessor also calculates the buoyancy flux from the heat release data. The preprocessor takes as input, the area of the fire, coordinates of the center of the fire, elevation of the fire center, the time the fire began, and the initial vertical spread. Twenty-six separate fires were modeled. The initial vertical spread was calculated using the slope data presented in Table 4-7. The fire in CALPUFF is approximated as a circular area source.

4.2.8 Comparison of Predicted and Observed PM10 Concentrations

We compared predicted PM10 concentrations to the concentrations observed (measured) at seven locations in Figure 4-14 and Figure 4-15. For each predicted value, we added a background value, which was the estimated PM10 concentration from background sources calculated using the regression equations described earlier (Equations [4.5] and [4.6]). Comparisons of PM10 concentrations at the EPA monitoring stations (White Rock, San Ildefonso, and Santa Clara) are tenuous because we are uncertain when the samplers were turned on.

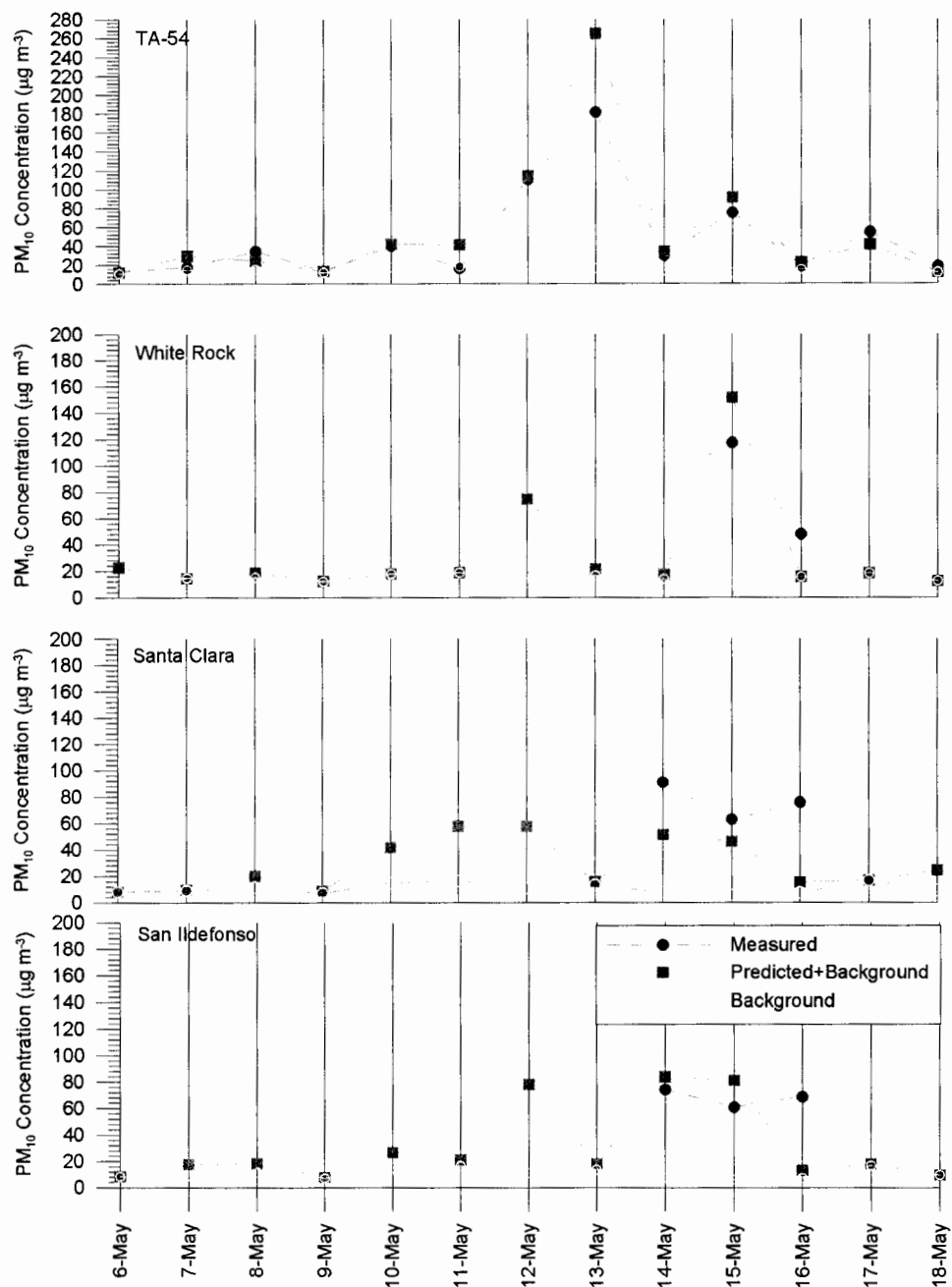


Figure 4-14. Predicted and observed PM10 concentrations at TA-54, White Rock (EPA), Santa Clara (EPA), and San Ildefonso (EPA). Model estimates and TA-54 measurements represent 24-hour averages. Measurements at San Ildefonso, Santa Clara and White Rock represent concentrations of varying averaging time.

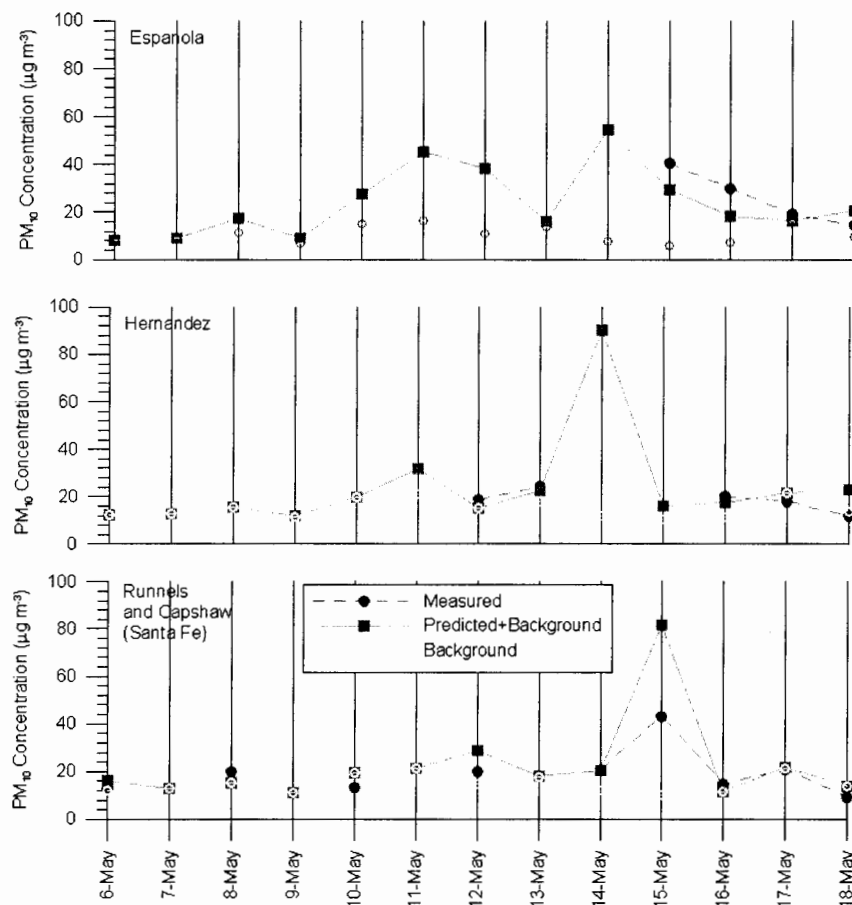


Figure 4-15. Predicted and observed PM10 concentrations at four stations. All data (including model estimates) represent 24-hour averages. Runnels and Capshaw were taken within the Santa Fe city limits and are plotted on the same graph.

Overall, the predicted-to-observed ratios of PM10 concentrations had a geometric mean of 0.87 and a geometric standard deviation of 1.7 (Table 4-10). Regression of the predicted to observed concentrations yielded a r^2 value 0.866 and a slope of 1.066 (when the regression was forced through the origin). However, for individual samplers, the model exhibited both underprediction and overprediction. Predicted-to-observed ratios for May 16 at the EPA stations are all less than 1.0, indicating model underprediction for this day. It does not seem plausible that smoke emissions from the relatively small acreage that burned on that day resulted in the high measured PM10 concentration. We suspect that continued smoldering from areas that had previously burned and from spot fires reported around LANL may have been the major contributors to the high PM10 concentration. Lacking any specific information about the time the sampling began, we have assumed the sample represents a 24-hour period (midnight-midnight) of the day the sample was collected. However, PM10 concentrations fluctuated (Figure 4-16) from hour-to-hour, and the 24-hour average PM10 concentration is highly dependent on which hours are included in the average.

Overall, the predicted-to-observed ratios provide a measure of the predictive capability of the model for PM₁₀ and are clearly within the limits of accuracy and precision of air dispersion models.

Table 4-10. Predicted-to-Observed Ratios of PM₁₀ Concentrations Taken During the Fire

Date	Runnels	Capshaw	Española	Hernandez	White Rock (EPA)	San Ildefonso (EPA)	Santa Clara (EPA)	Ta-54
5/6	0.92	0.76						0.97
5/7								1.64
5/8	0.58							0.70
5/9								1.02
5/10	1.12							1.05
5/11								2.51
5/12		1.06		0.60				1.03
5/13				0.75				1.46
5/14	0.78					1.13	0.60	1.15
5/15	1.79		0.73		1.29	1.33	0.47	1.22
5/16	0.50		0.62	0.80	0.32	0.19	0.24	1.16
5/17	0.82		0.87	0.93				0.75
5/18	1.03	1.00	1.41	2.01				0.67
GM	0.88	0.93	0.87	0.92	0.64	0.66	0.41	1.11
GSD	1.49	1.19	1.43	1.59	2.70	2.94	1.59	1.43
GM (all data)	0.87							
GSD (all data)	1.7							
50% (all data)	0.99							
2.5% (all data)	0.20							
97.5% (all data)	2.0							

The dispersion patterns of the 13-day average PM₁₀ concentration in the model domain are illustrated in Figure 4-17. As expected, most of the fire plume traveled east toward Española, although Santa Fe appears to show some impact from the fire. Concentrations do not include background concentrations of PM₁₀, which averaged about 13 $\mu\text{g m}^{-3}$ before the fire. Excluding points within the fire boundaries, the highest concentrations were observed at locations downwind where the elevated buoyant plume touched down near Española. Data taken in Española between May 12–17 by Popp et al. (2001) show that the average PM₁₀ concentration of 30 $\mu\text{g m}^{-3}$ agrees very well with the model estimate of 29 $\mu\text{g m}^{-3}$ (including background). These data are not reported in Table 4-1 and Table 4-2.

Deposition patterns of PM₁₀ are illustrated in Figure 4-18. The pattern differs from the concentration isopleths because deposition of fine particles increases as a function of surface roughness. The highest deposition outside the immediate area of the fire is east of Española where the terrain begins to rise and forest vegetation predominates.

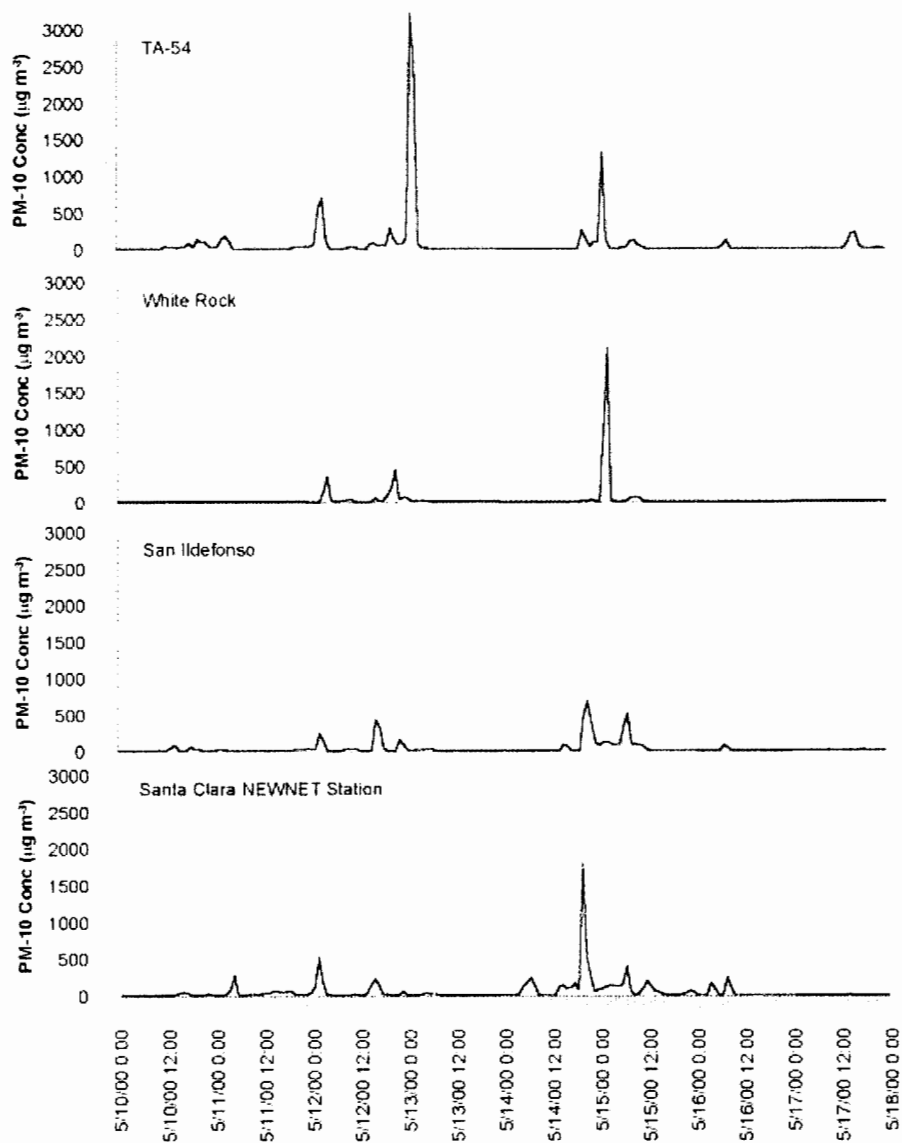


Figure 4-16. Modeled hourly average PM10 concentrations at four locations. Note that the Santa Clara location represents the NEWNET meteorological tower location and not the EPA PM10 sampler location. Concentrations do not include background.

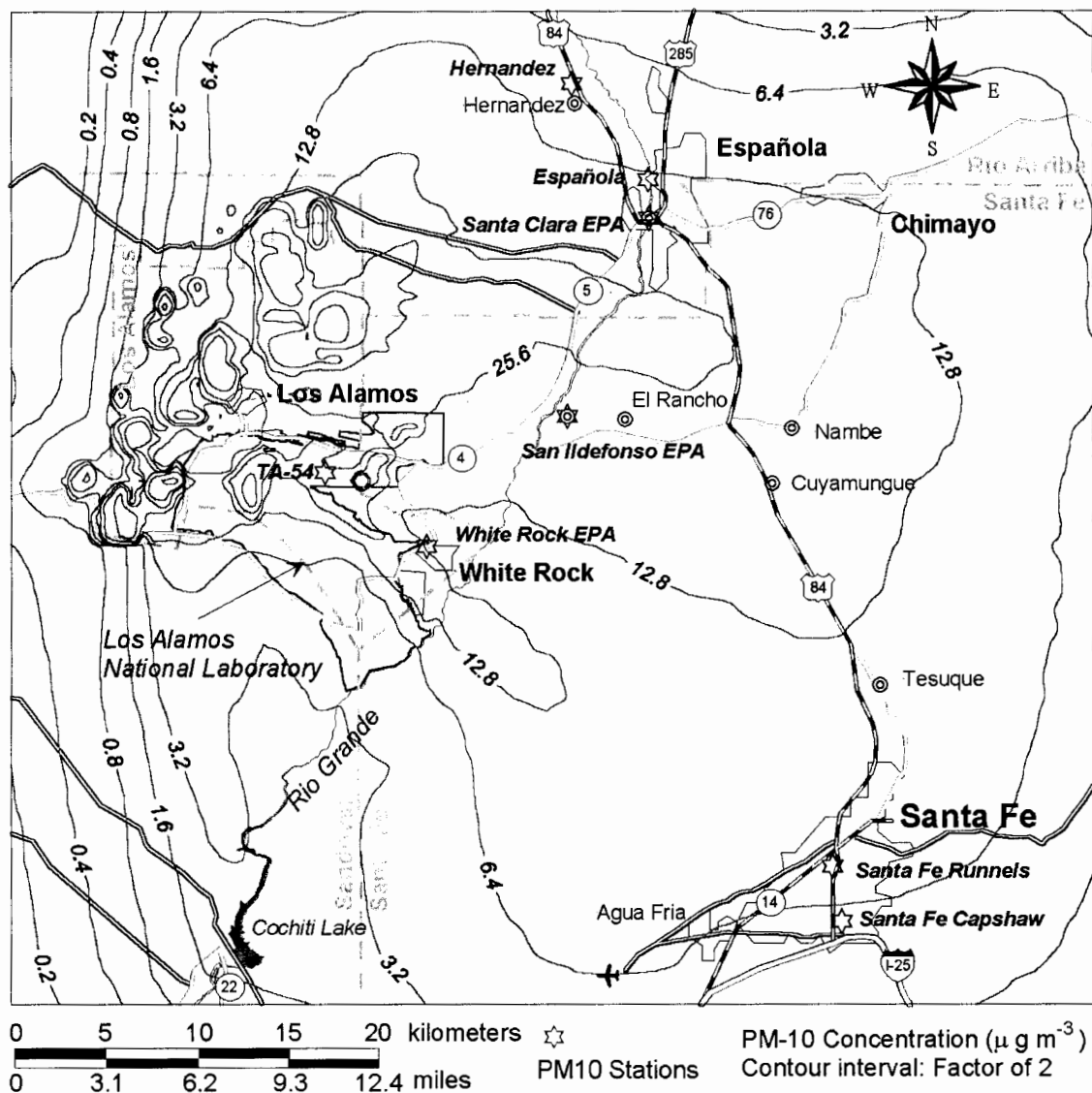


Figure 4-17. Thirteen-day (May 6 to May 18) average PM10 concentration isopleths estimated by CALPUFF. Concentrations do not include background contributions, which averaged about $13 \mu\text{g m}^{-3}$ in the model domain before the fire. The PM10 stations used for model calibration are also shown.

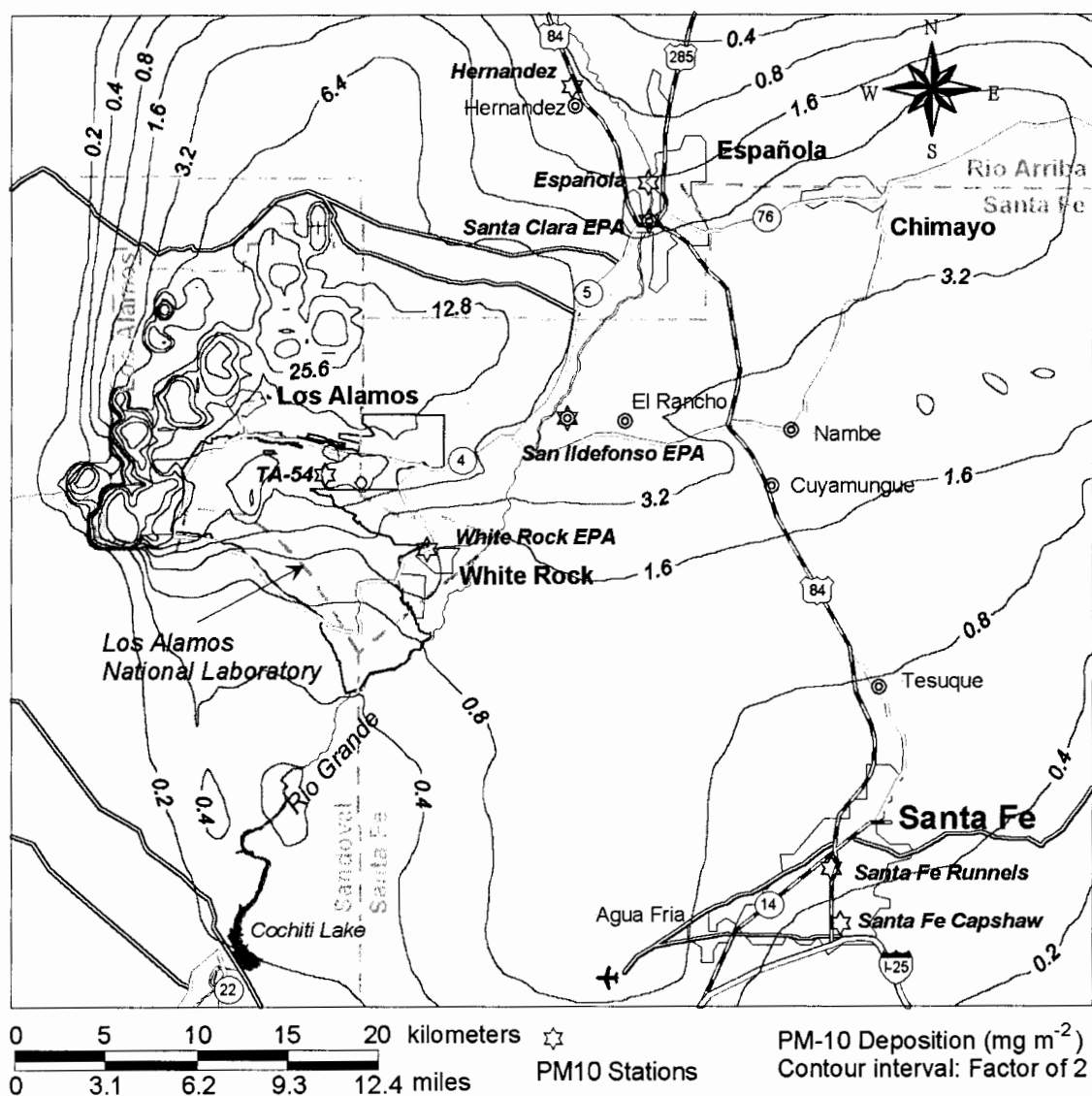


Figure 4-18. Thirteen-day (May 6 to May 18) total deposition (mg m^{-2}) of PM10 in the model domain as a result of PM10 emissions from the fire.

4.3 Calculating Concentrations of Contaminants Released from PRSs

The computer calculation runtimes for CALPUFF did not allow separate calculations (individual runs) to be performed for each PRS contaminant identified as potentially important through the screening process. Instead, concentrations of particulate and volatile contaminants were determined by scaling the time-integrated PM10 concentrations (or CO concentration for volatile components) by the integrated release of contaminants. Releases from PRSs were limited to 3 days from May 11 to 13. These 3 days involved five separate fire areas, mostly within the confines of LANL. It was assumed that particulate or volatile releases occurred when the PRS was burned. Each burned PRS was assigned to an individual fire by computing the distance from the center of the PRS to the center of each fire. This distance is given by

$$d = \sqrt{(X_1 - X_2)^2 + (Y_1 - Y_2)^2} \quad (4.17)$$

where

- d = distance from the center of the PRS to the center of the fire (m)
 $X_{1,2}$ = UTM east coordinates of the PRS and the center of a given fire respectively (m)
 $Y_{1,2}$ = UTM north coordinates of the PRS and the center of a given fire respectively (m).

For each PRS, a value of d is calculated for each of the five fires that burned PRSs. The PRS is then assigned to the fire that has the minimum d . Over 95% of the PRSs (151 sites) were assigned to the May 11 fires identified as Southeast and South Central. Two PRSs were assigned to the May 11 fire identified as North d and 35 PRSs were assigned to the May 13 fire identified as South (see Table 4-7).

Time-integrated concentrations (TICs) were computed individually for each fire area using an integration time that depended on the averaging time of the fire. The averaging time of the fire was typically the burn time plus a few extra hours to allow the plume to fully dissipate throughout the model domain. We used the TICs because they can be easily summed to compute contaminant intake. We calculated contaminant concentrations at each grid node in the model domain. The concentration of a contaminant for releases from the i th PRS, at the j th receptor node is given by

$$C_{i,j} = \int_0^t CPM10_{i,j} dt \frac{\int_0^{tb} Q_i dt}{\int_0^{tb} QPM10_i dt} \quad (4.18)$$

where

- $C_{i,j}$ = time-integrated contaminant concentration (mg or Bq h m⁻³) at the j th receptor node resulting from releases at the i th PRS
 $CPM10_{i,j}$ = PM10 concentration as a function of time (mg m⁻³) at the j th receptor node resulting from PM10 emitted during the fire that burned the i th PRS
 Q_i = contaminant release rate from the i th PRS (mg or Ci h⁻¹)
 $QPM10_i$ = PM10 release rate for the fire that burned the i th PRS (mg h⁻¹)
 tb = burn time of the fire (h)
 t = integration time of air concentrations (h).

For volatile compounds, we substituted the integrated CO concentration and release for the PM10 values. The total TIC of a contaminant is then the sum of the TICs from all burned PRS that emitted that contaminant. Values for $\int QPM10$ were readily obtained by numerically integrating the EPM output. These integrated PM10 and CO releases were reported in Table 4-9. Values for $\int CPM10$ were obtained from runtime averages reported in the CALPUFF output. Runtime averages were converted to TIC by multiplying the average concentration by the averaging time (Table 4-11). For volatile contaminants, integrated quantities of Q were already provided. For particulates, Q is a constant so the integral is simply $Q \times tb$.

Deposition is estimated in a similar manner using Equation (4.18). Instead of the PM₁₀ (or CO) concentration that is integrated over time, the hourly deposition rate ($\mu\text{g h}^{-1}$) is integrated over time. That is, the term *CPM10* is replaced with the hourly deposition rate.

Isopleth maps of the average PM₁₀ concentration for each of the five individual fires are presented in Figure 4-19 through Figure 4-23. The receptor locations where radionuclide and chemical concentrations and risk estimates were calculated and reported in subsequent tables are also shown in these figures.

Table 4-11. Time-integrated PM₁₀ and CO Concentration in the Vicinity of TA-54^a

Burn date	Subarea	Conc. averaging time (hours)	Average PM ₁₀ conc. ($\mu\text{g m}^{-3}$)	Time-integrated PM ₁₀ conc. ($\mu\text{g-h m}^{-3}$)	Average CO conc. ($\mu\text{g m}^{-3}$)	Time-integrated CO conc. ($\mu\text{g-h m}^{-3}$)
05/11	North d	127	3.5	444	26	3302
05/11	South Central	10	95	950	738	7380
05/11	Southeast	10	150	1500	1065	10650
05/11	Southwest	12	61	732	472	5664
05/13 ^b	South	10	310	3100	2420	24200

^a UTM Coordinates 385750 3969250.

^b Includes area burned on the evening of May 12.

This methodology has particular limitations related to volatile compounds. Namely, we have ignored the chemical-specific properties that govern deposition and atmospheric reactions that result in generation of secondary compounds or decay of the compound during transit. Ignoring decay and transformation will provide conservative estimates of the air concentration of the chemical in question. However, degradation products may also be a health concern and we have not addressed them here. Enhanced deposition of gases is a function of the chemical reactivity. Because we assumed no reactivity for CO, volatile chemicals will act as trace gases. This assumption will result in conservative estimates of air concentrations, but may underestimate deposition. For particulates, we have ignored decay during transit. For most radionuclides detected in PRSs, this is not a concern. However, in modeling short-lived radon progeny as was done in Appendix D, decay may be important at distant receptor locations and ignoring it will result in overestimation of air concentrations at these locations.

We have also assumed that the release history of particulates and volatile contaminants follows the same release history of PM₁₀ and CO respectively. The fire emissions model used in these calculations assumes about 50% of the total emissions occur during the smoldering stage of the fire, when plume rise is minimal and higher ground-level concentrations are observed. The assumption that 50% of the emissions occur during the smoldering stage of the fire was necessary for model calibration and is substantiated by observations of other researchers (Ward 1999). However, it is likely that the release of volatile compounds was substantially more pronounced during the active flaming stage of the fire, when soil temperatures were highest and plume rise was the greatest. The flaming stage of the fire is associated with significant heat generation and subsequent plume lofting, resulting in little ground-level representation of the plume. Particulate releases may also be enhanced during the flaming stage, especially when fire-generated wind storms are present. However, Kashparov et al. (2000) observed that values of the resuspension

factor were the same for different phases of the fire (see Chapter 3) so assuming the release history of particulates is the same as PM10 may not result in overly biased estimates of air concentrations.

The impact of these assumptions is illustrated by comparing the difference between ground-level concentrations calculated assuming 50% of the pollutant emissions occurred during the smoldering phase of the fire (as was done in this report) with ground-level concentrations assuming most of the emissions occurred during the flaming portion of the fire. The 12-hour average ground-level PM10 concentration at TA-54 for the May 11th fire described as Southwest was $61 \mu\text{g m}^{-3}$ (see Table 4-11, Figure 4-22). This concentration was based on the assumption that 50% of the emissions occurred during the smoldering phase of the fire (see Table 4-11). Assuming nearly all PM10 emissions occurred during the flaming portion of the fire yields a 12-hour average ground-level PM10 concentration at TA-54 of $10 \mu\text{g m}^{-3}$. Overall, the magnitude of the difference may be more or less depending on location and the particulars of the fire. Nevertheless, as shown here, the assumption that volatile releases follow the same release history as pollutants emitted by the fire may possibly result in overestimation of air concentrations in the model domain because the release of volatile compounds is dependent on soil temperature, which presumably would be highest during the flaming portion of the fire.

4.3.1 Sample Calculation

To illustrate the methodology, we calculated the ^{210}Pb concentration in air in the vicinity of TA-54 in this section. Lead-210 was detected at one PRS (04-001) and this site burned on May 11 in the fire described as Southeast. The estimated release rate from the PRS was $1.63 \times 10^{-3} \text{ Bq s}^{-1}$. The total release during the burn time was then $1.63 \times 10^{-3} \text{ Bq s}^{-1} \times 9 \text{ hours} \times 3600 \text{ s h}^{-1} = 52.812 \text{ Bq}$. The time-integrated PM10 concentration at TA-54 was $1500 \mu\text{g-h m}^{-3}$ ($62.5 \mu\text{g-d m}^{-3}$) (Table 4-11) and the PM10 released from that fire was $1.45 \times 10^9 \text{ g}$ ($1.45 \times 10^{15} \mu\text{g}$) (Table 4-9). The concentration of ^{210}Pb was then

$$62.5 \mu\text{g-d m}^{-3} / 1.45 \times 10^{15} \mu\text{g} \times 52.812 \text{ Bq} = 2.28 \times 10^{-12} \text{ Bq-d m}^{-3}.$$

The above quantity converted to units of aCi-d m^{-3} is 6.2×10^{-5} (Table 4-12)

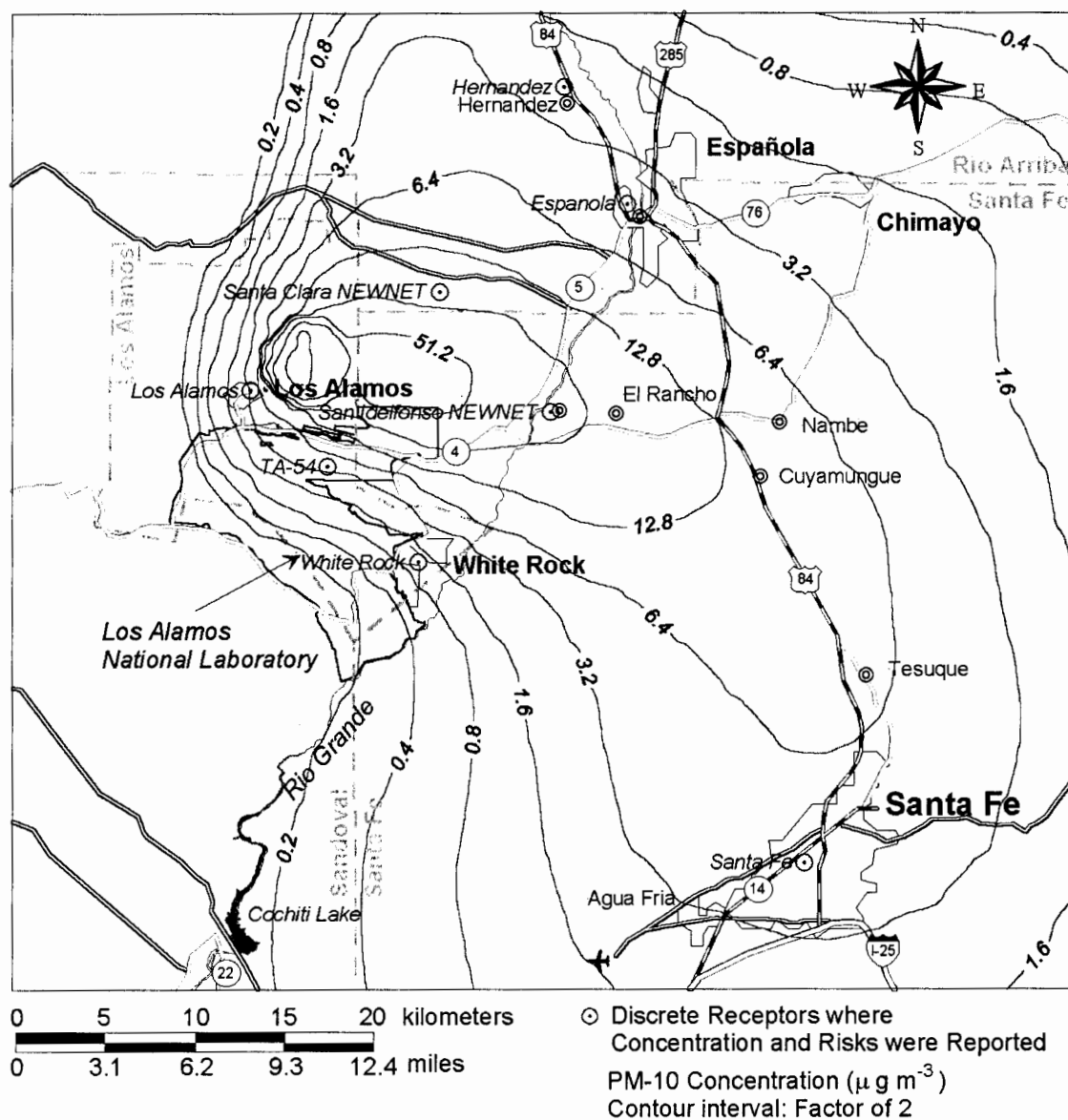


Figure 4-19. One hundred and twenty seven-hour average PM10 concentration for releases from the fire identified as 11 North d that burned on May 11, 2000.

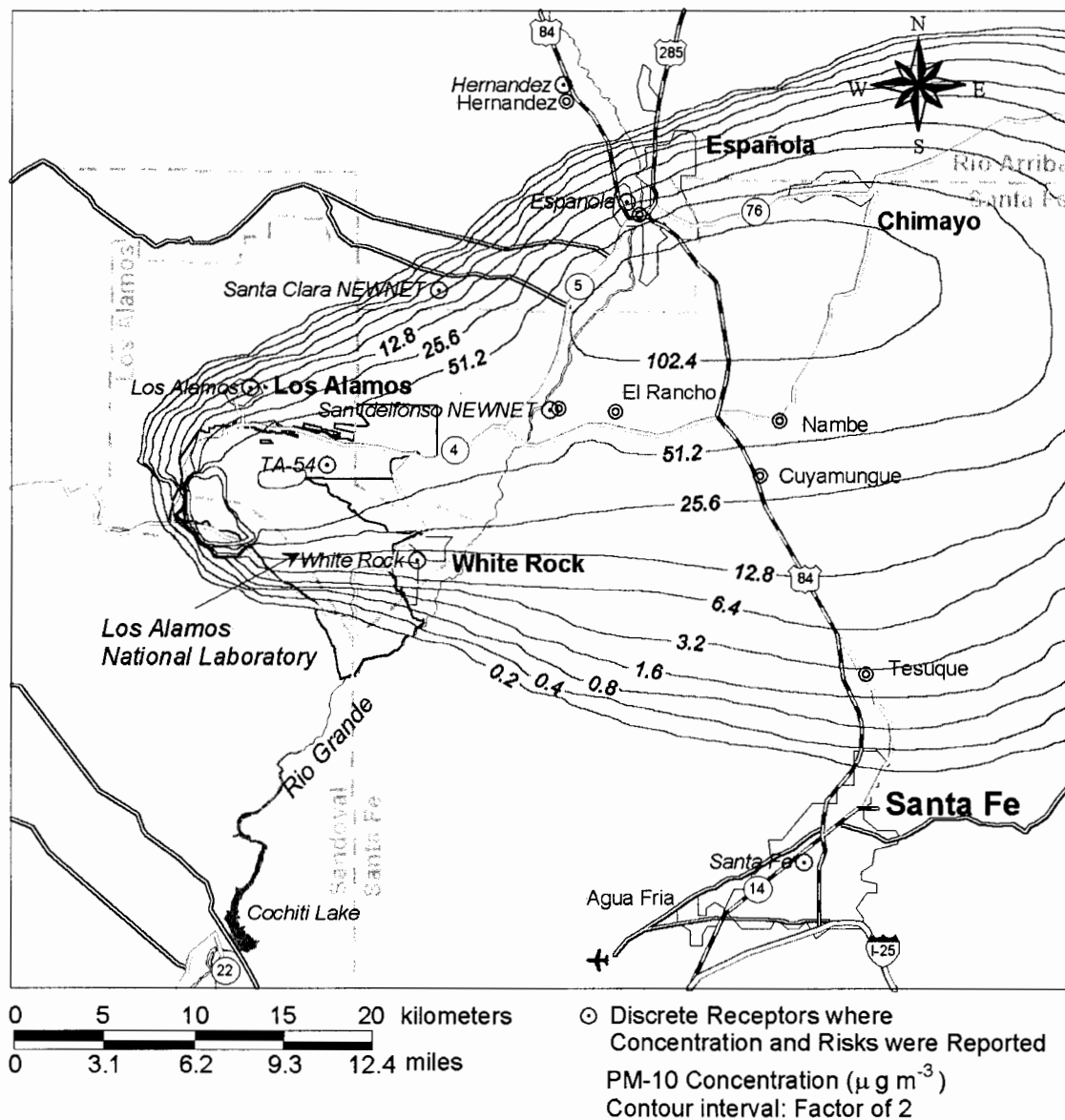


Figure 4-20. Ten-hour average PM10 concentration for releases from the fire identified as 11 South Central that burned on May 11, 2000.

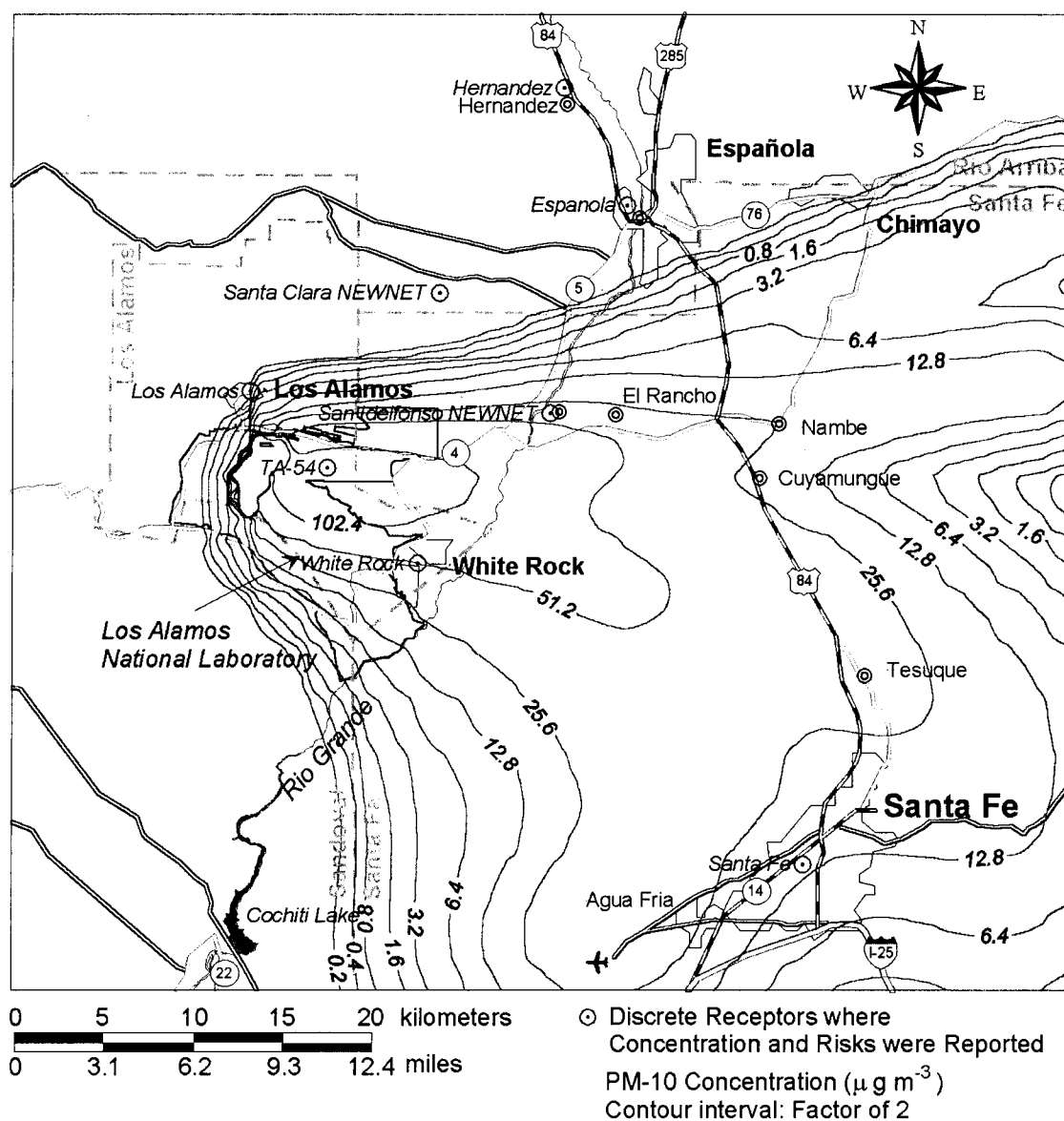


Figure 4-21. Ten-hour average PM₁₀ concentration for releases from the fire identified as 11 Southeast that burned on May 11, 2000.

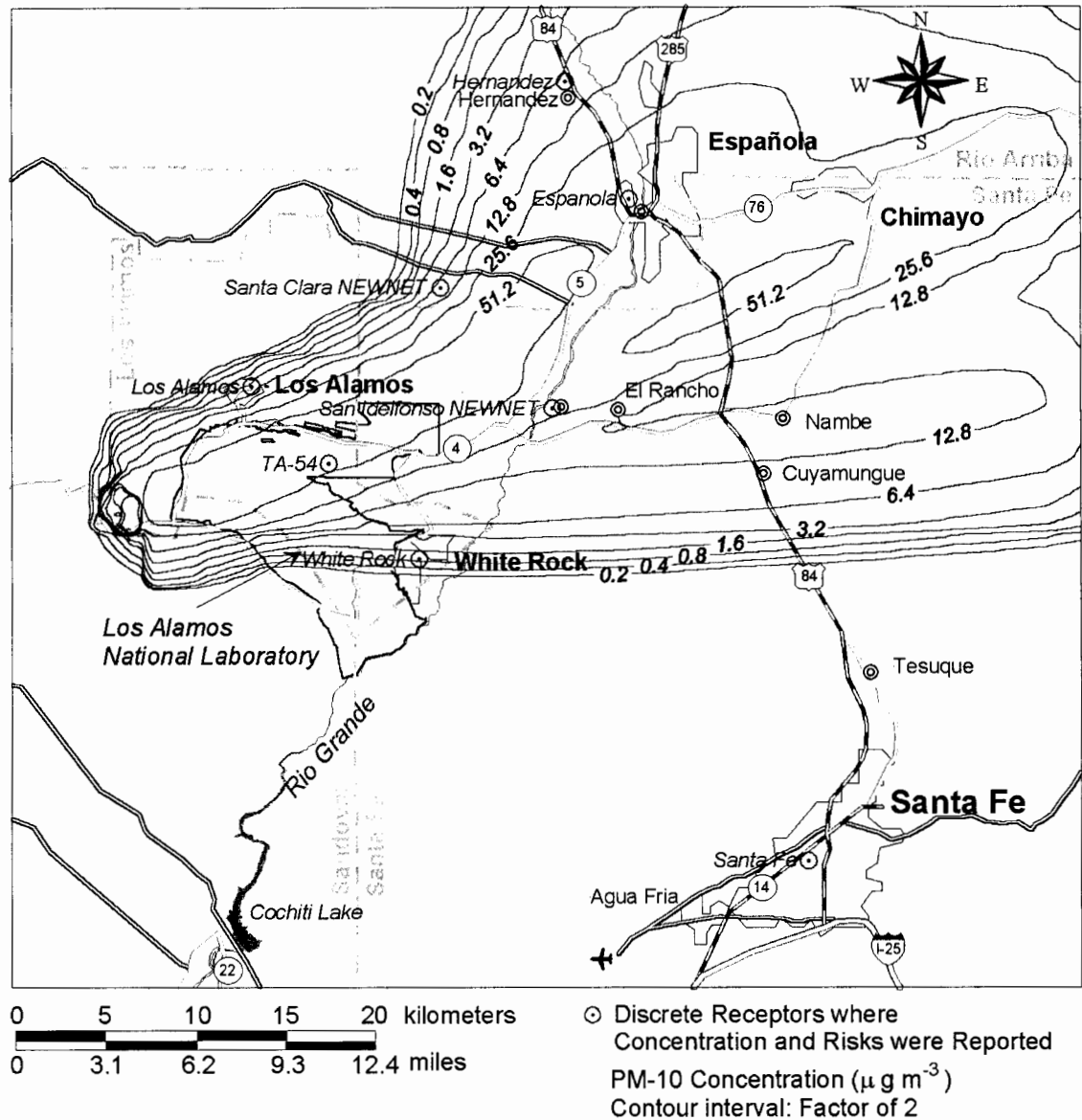


Figure 4-22. Twelve-hour average PM10 concentration for releases from the fire identified as 11 Southwest that burned on May 11, 2000.

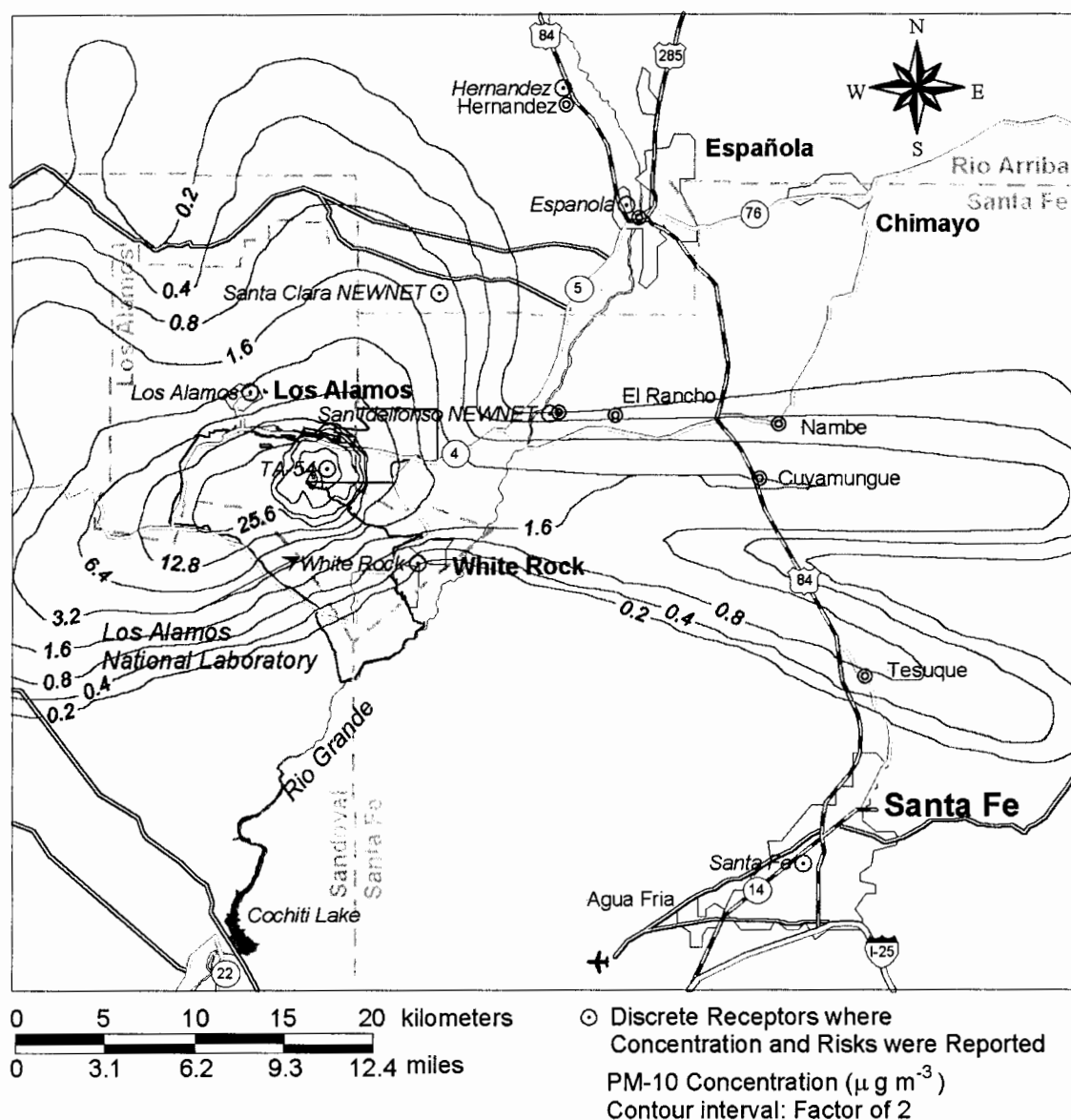


Figure 4-23. Ten-hour average PM10 concentration for releases from the fire identified as 13 South that burned on May 12 and 13, 2000.

4.4 Air Concentration Estimates

Estimates of the TIC at selected locations in the model domain are listed in Table 4-12 through Table 4-14 for radionuclides, carcinogenic chemicals, and noncarcinogenic chemicals, respectively. The values in these tables represent the sum of the TIC for all PRS sources that burned between May 11 and May 13. The average concentration during this period can be obtained by dividing the concentration by 3 days. The concentrations do not include contributions from (1) contaminants deposited on the surrounding lands from 50 years of LANL operations, (2) naturally occurring radionuclides on and in vegetation released as a result of the fire, (3) contaminants deposited on land due to worldwide fallout, and (4) releases from PRSs that were

not burned. We discuss natural and man-made sources of radionuclides and metals released to the air from burning vegetation in Appendix D.

Table 4-12. Time-Integrated Concentration of Radionuclides Released from PRSs as a Result of the Cerro Grande Fire (aCi-d m⁻³)

Nuclide	Española	Santa Clara ^a	Hernandez	San Ildefonso ^a	Santa Fe	White Rock	Los Alamos	TA-54
Am-241	5.8×10^{-8}	2.9×10^{-8}	1.3×10^{-10}	1.8×10^{-6}	5.9×10^{-7}	2.1×10^{-6}	1.2×10^{-7}	1.2×10^{-5}
Pb-210	0	0	0	1.6×10^{-5}	5.8×10^{-6}	2.0×10^{-5}	3.5×10^{-7}	6.2×10^{-5}
Pb-212	1.4×10^{-4}	2.8×10^{-5}	2.5×10^{-8}	5.1×10^{-4}	1.2×10^{-5}	1.2×10^{-4}	6.1×10^{-5}	2.0×10^{-3}
Np-237	9.5×10^{-5}	1.6×10^{-5}	0	3.2×10^{-4}	0	5.4×10^{-5}	3.1×10^{-5}	5.2×10^{-4}
Pu-238	1.9×10^{-8}	4.5×10^{-6}	3.2×10^{-8}	1.6×10^{-5}	5.2×10^{-6}	1.9×10^{-5}	1.7×10^{-5}	1.4×10^{-3}
Pu-239	5.4×10^{-8}	1.2×10^{-5}	8.3×10^{-8}	9.4×10^{-6}	2.2×10^{-6}	1.0×10^{-5}	4.4×10^{-5}	3.7×10^{-3}
K-40	3.4×10^{-3}	6.6×10^{-4}	6.1×10^{-7}	1.2×10^{-2}	2.9×10^{-4}	3.0×10^{-3}	1.5×10^{-3}	4.8×10^{-2}
Pa-231	4.5×10^{-4}	8.0×10^{-5}	3.3×10^{-8}	1.5×10^{-3}	4.3×10^{-6}	2.7×10^{-4}	1.6×10^{-4}	3.9×10^{-3}
Ra-226	4.6×10^{-4}	7.9×10^{-5}	2.7×10^{-9}	1.6×10^{-3}	8.4×10^{-6}	2.9×10^{-4}	1.5×10^{-4}	2.7×10^{-3}
Ra-224	2.6×10^{-8}	6.9×10^{-6}	4.9×10^{-8}	1.1×10^{-5}	3.3×10^{-6}	1.3×10^{-5}	2.6×10^{-5}	2.2×10^{-3}
Th-227	0	0	0	3.9×10^{-6}	1.4×10^{-6}	4.9×10^{-6}	8.5×10^{-8}	1.5×10^{-5}
U-234	3.4×10^{-7}	1.2×10^{-6}	8.1×10^{-9}	1.4×10^{-4}	4.8×10^{-5}	1.7×10^{-4}	7.3×10^{-6}	8.7×10^{-4}
U-235	2.9×10^{-7}	1.3×10^{-7}	5.4×10^{-10}	1.1×10^{-5}	3.6×10^{-6}	1.3×10^{-5}	6.0×10^{-7}	6.3×10^{-5}
U-238	6.6×10^{-6}	1.8×10^{-6}	4.9×10^{-9}	8.7×10^{-5}	2.3×10^{-5}	8.4×10^{-5}	6.2×10^{-6}	4.9×10^{-4}

^a These locations are the NEWNET meteorological stations.

Estimated radionuclide concentrations from the burned PRSs were relatively low and would probably be undetectable above background levels. For example, the estimated 3-day average ²³⁹Pu concentration at TA-54 from PRS releases was 1.2×10^{-3} aCi m⁻³. The *quarterly-averaged* pre-fire ²³⁹Pu air concentration measured on LANL property ranged from 2.1 to 50 aCi m⁻³ (Table 4-15 and Figure 4-24). Although it is not valid to compare a quarterly averaged concentration with a 3-day average concentration, short-term measurements often yield higher concentrations than long-term averages. The fact that the estimated 3-day average ²³⁹Pu concentration at TA-54 that resulted from the burning PRSs was considerably smaller than the quarterly-averaged pre-fire concentration measured onsite suggests that existing sources of ²³⁹Pu may have overwhelmed any contribution from the burned PRS units.

Many of the quarterly samples taken by LANL were below detection limits or the 2-sigma analytical uncertainty was greater than the reported value. Concentrations reported in Table 4-15 are only those where the reported concentration was greater than the 2-sigma analytical uncertainty. Valid measurements were mostly confined to samplers along the northern LANL boundary near State Highway 4. Comparisons with measured data were also complicated by inconsistent averaging times and averaging times that did not correspond to the time resolution of the model.

One to two-day average ²³⁹Pu concentrations taken during the Cerro Grande Fire were significantly higher than the quarterly averaged concentration for some monitoring stations, although many of the measurements were below detection limits. As discussed in Chapter 2, Section 2.1.1, sampling times were reduced to 1–2 days during the fire by LANL to capture any

fire-related releases. Personnel at LANL suspect⁷ that resuspension of plutonium-contaminated soil in unburned PRS units during the high wind events that occurred during the fire was responsible for these relatively high reading. Soil resuspension from unburned areas along with resuspension from already burned PRSs were potential sources of radionuclides and chemicals not included in this assessment.

The EPA measured high ²³⁹Pu concentrations at several locations including White Rock on May 17 (280 aCi m⁻³) and Tsankawi National Monument restrooms on May 15 (8800 aCi m⁻³). However, the sampling times for these measurements were not reported, making them difficult to evaluate. These measurements would represent sources from either (1) nonburned PRS units, (2) already burned PRS units, or (3) releases from burned vegetation. Releases would not have occurred during active burning of PRSs because the fire on LANL property essentially ceased after May 15. Thirteen-day average concentrations of ²³⁹Pu in air from the burning of natural vegetation at White Rock ranged between 0.02 to 9 aCi m⁻³ (see Appendix D). Without pre-fire measurements of the same time resolution, it is difficult to discern whether these relatively high ²³⁹Pu air concentrations observed by EPA and LANL during the fire were a direct result of the fire or the fluctuation of existing sources of plutonium.

Table 4-13. Time-Integrated Concentration of Chemical Carcinogens Released from PRSs as a Result of the Cerro Grande Fire (μg-d m⁻³)

Metal	Española	Santa Clara ^a	Hernandez	San Ildefonso ^a	Santa Fe	White Rock	Los Alamos	TA-54
Beryllium	6.6×10^{-12}	1.9×10^{-11}	1.3×10^{-13}	2.7×10^{-11}	8.7×10^{-14}	7.9×10^{-12}	7.0×10^{-11}	5.7×10^{-9}
Nickel	2.7×10^{-9}	3.3×10^{-9}	3.8×10^{-10}	1.2×10^{-8}	7.6×10^{-10}	1.6×10^{-9}	1.4×10^{-9}	1.6×10^{-8}
Arsenic	4.3×10^{-4}	7.7×10^{-5}	2.6×10^{-8}	1.5×10^{-3}	6.9×10^{-6}	2.7×10^{-4}	1.6×10^{-4}	3.6×10^{-3}
Cadmium	6.9×10^{-4}	2.2×10^{-4}	7.3×10^{-7}	2.5×10^{-3}	5.2×10^{-5}	6.0×10^{-4}	6.2×10^{-4}	3.7×10^{-2}
Chromium (hexavalent)	6.5×10^{-7}	1.0×10^{-6}	6.5×10^{-9}	2.4×10^{-6}	0	5.7×10^{-7}	3.7×10^{-6}	2.9×10^{-4}
Aldrin	0	0	0	1.1×10^{-7}	3.9×10^{-8}	1.4×10^{-7}	2.4×10^{-9}	4.1×10^{-7}
Amino-2,6-dinitrotolulene[4-]	3.3×10^{-3}	5.7×10^{-4}	0	1.1×10^{-2}	1.4×10^{-5}	2.0×10^{-3}	1.1×10^{-3}	1.9×10^{-2}
Amino-4,6-dinitrotolulene[2-]	7.0×10^{-3}	1.2×10^{-3}	0	2.4×10^{-2}	2.6×10^{-5}	4.1×10^{-3}	2.3×10^{-3}	3.9×10^{-2}
Aroclor-1254	0	0	0	1.0×10^{-6}	3.6×10^{-7}	1.3×10^{-6}	2.2×10^{-8}	3.8×10^{-6}
Benzo(a)pyrene	5.1×10^{-5}	1.1×10^{-5}	1.7×10^{-8}	2.0×10^{-4}	8.8×10^{-6}	6.1×10^{-5}	2.7×10^{-5}	1.1×10^{-3}
RDX	1.4×10^0	2.3×10^{-1}	0	4.5×10^0	4.7×10^{-5}	7.8×10^{-1}	4.5×10^{-1}	7.5×10^0
Trinitrotolulene[2,4,6-]	1.0×10^{-1}	0	8.4×10^{-10}	3.5×10^{-1}	0	5.9×10^{-2}	3.4×10^{-2}	5.7×10^{-1}
Dibenz(a,h)anthracene	1.1×10^{-5}	2.2×10^{-6}	2.9×10^{-9}	4.7×10^{-5}	3.9×10^{-6}	2.0×10^{-5}	5.3×10^{-6}	2.3×10^{-4}
Dinitrotolulene[2,4-]	2.5×10^{-4}	4.2×10^{-5}	0	8.3×10^{-4}	0	1.4×10^{-4}	8.3×10^{-5}	1.4×10^{-3}

^a These locations are the NEWNET meteorological stations.

Estimated concentrations of metals and volatiles also appeared to be very low compared to measured values taken during the fire. However, it is difficult to evaluate the impact of the fire on ambient concentrations without a clear understanding of background concentrations. The explosive compounds RDX and HMX were noted to have relatively high estimated

⁷ Email correspondence from Jean Dewart, LANL to John Till and Helen Grogan, RAC, August 28, 2001

concentrations. These compounds were used extensively at LANL for ordinance experiments and the high airborne concentrations appear to be a result of the high inventories calculated for these compounds.

For some of the locations listed in Table 4-12 through Table 4-14, the estimated concentration was zero. Zero concentrations occur when the contaminant was limited to a few PRSs that when burned, the resulting contaminant plume did not impact specific locations. Take, for example, the calculation of ^{210}Pb air concentration described in the previous section. Lead-210 was only reported in one PRS (04-001), and this site burned on May 11 in the fire described as Southeast. Figure 4-21 shows a plot of the PM10 plume for that fire. Note that PM10 concentrations are less than $1\text{ }\mu\text{g m}^{-3}$ for Española, Hernandez, and Santa Clara NEWNET. (The actual value listed in the CALPUFF output is $0\text{ }\mu\text{g m}^{-3}$ for all three locations). Therefore, the time-integrated contaminant concentration would also be zero. To address the possibility that we may have missed a maximum concentration because the selected locations were not in the plume path, we calculated the maximum TIC observed in the entire model domain. These concentrations are presented later in this section.

The results of this exercise indicate that unless we have grossly underestimated the source term, releases from PRSs during the active burning stage of the fire appear to have minimum impact on airborne contaminant concentrations. Predicted and observed PM10 concentrations were generally within a factor of two of one another. This factor of two uncertainty alone would not account for the large discrepancy between the predicted and observed contaminant concentrations, as noted for ^{239}Pu . Particulate resuspension rates would have to be five to seven orders of magnitude higher than our estimates to bring measured values in line with predicted values. Based on measured values reported in the literature, this increase is not reasonable.

Resuspension releases from PRSs that were unburned, along with naturally occurring radionuclides and anthropogenic sources (such as global fallout of chemicals and radionuclides) present on biomass, may also have been significant contributors to airborne contamination. The issue of contamination in burned biomass is addressed in Appendix D. Measurements of ^{239}Pu taken by the EPA following the active burning of LANL lands on May 15, 16, and 17, indicate higher than expected concentrations were present. These releases may be due to enhanced resuspension from PRSs as a result of the high winds during the fire, but further investigation and additional field monitoring under similar conditions may be needed to confirm this. Sources such as these would have greater impacts on ground-level concentrations because most of the contaminants would be released at ground level and not in a buoyant plume. These sources were not accounted for in the assessment but may be important in terms of overall exposure. This analysis does indicate that contaminant releases from PRSs *while* they were actively burning probably resulted in minimal ground-level concentrations of contaminants.

**Table 4-14. Time-Integrated Concentration of Noncarcinogens Released from PRSs as a
Result of the Cerro Grande Fire ($\mu\text{g-d m}^{-3}$)**

Volatile	San							
	Española	Santa Clara ^a	Hernandez	Ildefonso ^a	Santa Fe	White Rock	Los Alamos	TA-54
Acenaphthylene	1.2×10^{-6}	2.0×10^{-7}	0	5.5×10^{-6}	5.7×10^{-7}	2.7×10^{-6}	4.2×10^{-7}	1.2×10^{-5}
Aldrin	0	0	0	1.1×10^{-7}	3.9×10^{-8}	1.4×10^{-7}	2.4×10^{-9}	4.1×10^{-7}
Amino-2,6-dinitrotoluene 4-	3.3×10^{-3}	5.7×10^{-4}	0	1.1×10^{-2}	1.4×10^{-5}	2.0×10^{-3}	1.1×10^{-3}	1.9×10^{-2}
Amino-4,6-dinitrotoluene 2-	7.0×10^{-3}	1.2×10^{-3}	0	2.4×10^{-2}	2.6×10^{-5}	2.3×10^{-3}	2.3×10^{-3}	3.9×10^{-2}
Aroclor-1254	0	0	0	1.0×10^{-6}	3.6×10^{-7}	1.3×10^{-6}	2.2×10^{-8}	3.8×10^{-6}
Cyanide (total)	4.0×10^{-4}	6.8×10^{-5}	0	1.3×10^{-3}	8.9×10^{-8}	2.3×10^{-4}	1.3×10^{-4}	2.2×10^{-3}
Dibenzofuran	2.1×10^{-5}	3.7×10^{-6}	1.2×10^{-9}	8.7×10^{-5}	6.0×10^{-6}	2.5×10^{-5}	8.0×10^{-6}	2.3×10^{-4}
Dinitrobenzene 1,3	9.8×10^{-3}	1.7×10^{-3}	0	3.3×10^{-2}	0	5.6×10^{-3}	3.3×10^{-3}	5.4×10^{-2}
Dinitrotoluene 2,4	2.5×10^{-4}	4.2×10^{-5}	0	8.3×10^{-4}	0	1.4×10^{-4}	8.3×10^{-5}	1.4×10^{-3}
Fluoranthene	8.9×10^{-5}	1.9×10^{-5}	2.8×10^{-8}	3.7×10^{-4}	2.4×10^{-5}	1.4×10^{-4}	4.6×10^{-5}	2.0×10^{-3}
HMX	5.8×10^0	9.9×10^{-1}	0	$1.9 \times 10^{+1}$	1.7×10^{-4}	3.3	1.9×10^0	$3.2 \times 10^{+1}$
Mercury	7.7×10^{-5}	1.5×10^{-5}	1.2×10^{-8}	4.7×10^{-4}	7.6×10^{-5}	3.1×10^{-4}	3.7×10^{-5}	1.8×10^{-3}
Methylnaphthalene	2.0×10^{-5}	3.6×10^{-6}	1.4×10^{-9}	7.3×10^{-5}	2.5×10^{-6}	2.0×10^{-5}	7.6×10^{-6}	2.0×10^{-4}
Naphthalene	3.8×10^{-5}	6.8×10^{-6}	1.4×10^{-9}	1.6×10^{-4}	1.2×10^{-5}	6.5×10^{-5}	1.4×10^{-5}	4.1×10^{-4}
Nitrobenzene	1.5×10^{-4}	2.5×10^{-5}	0	5.0×10^{-4}	0	8.5×10^{-5}	5.0×10^{-5}	8.3×10^{-4}
Nitrotoluene	2.3×10^{-3}	3.9×10^{-4}	0	7.6×10^{-3}	0	1.3×10^{-3}	7.5×10^{-4}	1.3×10^{-2}
Pyrene	1.1×10^{-4}	2.2×10^{-5}	2.8×10^{-8}	4.1×10^{-4}	1.7×10^{-5}	1.2×10^{-4}	5.2×10^{-5}	2.0×10^{-3}
RDX	1.4×10^0	2.3×10^{-1}	0	4.5×10^0	4.7×10^{-5}	7.8×10^{-1}	4.5×10^{-1}	7.5×10^0
Selenium	6.2×10^{-4}	6.5×10^{-4}	7.2×10^{-5}	2.9×10^{-3}	1.8×10^{-4}	6.9×10^{-4}	3.1×10^{-4}	4.2×10^{-3}
TATB	1.9×10^{-6}	3.7×10^{-6}	2.4×10^{-8}	7.2×10^{-6}	0	6.4×10^{-7}	1.3×10^{-5}	1.1×10^{-3}
Trinitrotoluene-2,4,6	1.0×10^{-1}	1.8×10^{-2}	0	3.5×10^{-1}	0	5.9×10^{-2}	3.4×10^{-2}	5.7×10^{-1}
Zinc	2.0×10^{-7}	6.0×10^{-8}	3.1×10^{-10}	7.1×10^{-7}	1.7×10^{-8}	1.8×10^{-7}	1.6×10^{-7}	9.3×10^{-6}
Aluminum	1.2×10^{-8}	2.1×10^{-9}	0	4.3×10^{-8}	8.1×10^{-10}	9.7×10^{-9}	4.0×10^{-9}	7.5×10^{-8}
Antimony	2.1×10^{-11}	4.5×10^{-12}	6.3×10^{-15}	7.9×10^{-11}	2.9×10^{-12}	2.2×10^{-11}	1.0×10^{-11}	4.1×10^{-10}
Barium	1.1×10^{-6}	1.8×10^{-7}	2.3×10^{-13}	3.5×10^{-6}	1.2×10^{-10}	6.0×10^{-7}	3.5×10^{-7}	5.8×10^{-6}
Beryllium	6.6×10^{-12}	1.9×10^{-11}	1.3×10^{-13}	2.7×10^{-11}	8.7×10^{-14}	7.9×10^{-12}	7.0×10^{-11}	5.7×10^{-9}
Cobalt	1.5×10^{-10}	5.9×10^{-11}	2.3×10^{-13}	5.2×10^{-10}	1.5×10^{-13}	9.5×10^{-11}	1.7×10^{-10}	1.1×10^{-8}
Copper	1.3×10^{-8}	2.9×10^{-9}	5.3×10^{-12}	5.2×10^{-8}	3.6×10^{-9}	2.0×10^{-8}	7.2×10^{-9}	3.4×10^{-7}
Iron	4.0×10^{-8}	6.9×10^{-9}	9.8×10^{-13}	1.3×10^{-7}	5.5×10^{-11}	2.3×10^{-8}	1.4×10^{-8}	2.6×10^{-7}
Manganese	5.5×10^{-9}	1.9×10^{-9}	6.8×10^{-12}	1.9×10^{-8}	3.8×10^{-11}	3.5×10^{-9}	5.5×10^{-9}	3.3×10^{-7}
Nickel	2.7×10^{-9}	3.3×10^{-9}	3.8×10^{-10}	1.2×10^{-8}	7.6×10^{-10}	1.6×10^{-9}	1.4×10^{-9}	1.6×10^{-8}
Silver	3.0×10^{-10}	6.5×10^{-11}	9.3×10^{-14}	1.2×10^{-9}	5.5×10^{-11}	3.7×10^{-10}	1.5×10^{-10}	6.3×10^{-9}
Thallium	2.9×10^{-10}	4.9×10^{-11}	1.9×10^{-16}	9.6×10^{-10}	5.3×10^{-13}	1.7×10^{-10}	8.5×10^{-11}	1.6×10^{-9}
Uranium	2.5×10^{-10}	4.3×10^{-10}	2.7×10^{-12}	9.9×10^{-10}	2.5×10^{-11}	3.1×10^{-10}	1.5×10^{-9}	1.2×10^{-7}
Vanadium	1.4×10^{-10}	2.6×10^{-11}	9.3×10^{-15}	4.9×10^{-10}	3.2×10^{-12}	9.3×10^{-11}	5.3×10^{-11}	1.2×10^{-9}

^a These locations are the NEWNET meteorological stations.

Table 4-15. Plutonium-239 Concentrations Measured at Various Locations Before, During, and After the Cerro Grande Fire by LANL and EPA

Sampling Location (ID Number)	Start Date	End Date	Duration (d)	Concentration ^a (aCi m ⁻³)	Uncertainty ^b (aCi m ⁻³)
Pre-fire quarterly measurements made by LANL					
Gulf/Exxon/Shell Station (7)	20-Dec-99	27-Mar-00	98	6.0	3.6
Los Alamos Airport (9)	20-Dec-99	27-Mar-00	98	3.6	2.4
White Rock Fire Station (15)	20-Dec-99	27-Mar-00	98	2.1	2.1
TA-21 Area B (20)	20-Dec-99	27-Mar-00	98	12	3.6
TA-54 Area G by QA (27)	20-Dec-99	27-Mar-00	98	6.5	3.2
County Landfill TA-48 (32)	20-Dec-99	27-Mar-00	98	5.5	3.4
TA-54 Area G-1 (34)	20-Dec-99	27-Mar-00	98	50	7.9
TA-54 Area G-QA (38)	20-Dec-99	27-Mar-00	98	9.0	3.6
TA-54 - Area G/ N Perimeter (47)	20-Dec-99	27-Mar-00	98	7.6	3.2
County Landfill - Experimental (65)	20-Dec-99	27-Mar-00	98	5.2	5.1
TA-21.03 NE Bldg 344 (73)	20-Dec-99	27-Mar-00	98	3.1	2.4
TA-21.04 SE Bldg 344 (74)	20-Dec-99	27-Mar-00	98	7.4	3.4
Average (standard deviation)				9.8 (13)	
Quarterly measurements including Cerro Grande Fire made by LANL					
Gulf/Exxon/Shell Station (7)	27-Mar-00	19-Jun-00	84	11	5.31
McDonalds (8)	27-Mar-00	19-Jun-00	84	4.8	2.85
White Rock Fire Station (15)	27-Mar-00	19-Jun-00	84	2.4	2.28
TA-21 Area B (20)	27-Mar-00	19-Jun-00	84	5.5	2.92
TA-5 (23)	27-Mar-00	19-Jun-00	84	7.1	3.67
TA-54 Area G by QA (27)	27-Mar-00	19-Jun-00	84	16	5.06
County Landfill TA-48 (32)	27-Mar-00	19-Jun-00	84	7.2	4.6
TA-54 Area G-1 (34)	27-Mar-00	19-Jun-00	84	13	4.3
TA-54 Area G-QA (38)	27-Mar-00	19-Jun-00	84	15	6.44
TA-54 - Area G/ SE (45)	27-Mar-00	19-Jun-00	84	3.2	2.87
Los Alamos Inn - South (66)	27-Mar-00	19-Jun-00	84	31	9.1
TA-21.01 NW Bldg 344 (71)	27-Mar-00	19-Jun-00	84	3.5	2.8
Average (standard deviation)				10 (8)	
Cerro Grande Fire measurements made by LANL					
TA-54 Area G-1 (34)	25-Apr 8:47	12-May 8:31	17.0	21	16
Crossroads Bible Church (62)	24-Apr 11:22	09-May 10:47	15.0	13	13
Los Alamos Inn - South (66)	24-Apr 16:15	10-May 8:15	15.7	30	19
TA-21.01 NW Bldg 344 (71)	09-May 10:39	11-May 14:05	2.1	140	130
Los Alamos Inn - South (66)	10-May 8:15	13-May 14:42	3.3	470	200
Cerro Grande Fire measurements made by EPA					
Los Alamos Airport (4)	16-May-00	?	?	190	170
Tsanakawi National Monument (6)	15-May-00	?	?	8800	1900
415 Estante Way, White Rock (8)	16-May-00	?	?	190	180
415 Estante Way, White Rock (8)	17-May-00	?	?	280	180
Post-fire quarterly measurements made by LANL					
Gulf/Exxon/Shell Station (7)	19-Jun-00	25-Sep-00	98	3.2	2.9

Sampling Location (ID Number)	Start Date	End Date	Duration (d)	Concentration ^a (aCi m ⁻³)	Uncertainty ^b (aCi m ⁻³)
TA-21 Area B (20)	19-Jun-00	25-Sep-00	98	3.5	3.0
TA-54 Area G by QA (27)	19-Jun-00	25-Sep-00	98	8.7	3.9
County Landfill TA-48 (32)	19-Jun-00	25-Sep-00	98	5.5	3.9
TA-54 Area G-1 (34)	19-Jun-00	25-Sep-00	98	7.1	3.5
TA-54 Area G-QA (38)	19-Jun-00	25-Sep-00	98	13	4.5
TA-54 - Area G/ SE Perimeter (45)	19-Jun-00	25-Sep-00	98	11	4.1
TA-54 - Area G/ N Perimeter (47)	19-Jun-00	25-Sep-00	98	3.6	3.0
TA-54 - Area G - expansion (50)	19-Jun-00	25-Sep-00	98	2.5	2.4
Average (standard deviation)				6.4 (3.8)	

a. Concentrations >MDC and greater than the 2-sigma analytical uncertainty are reported

b. Two sigma analytical uncertainty

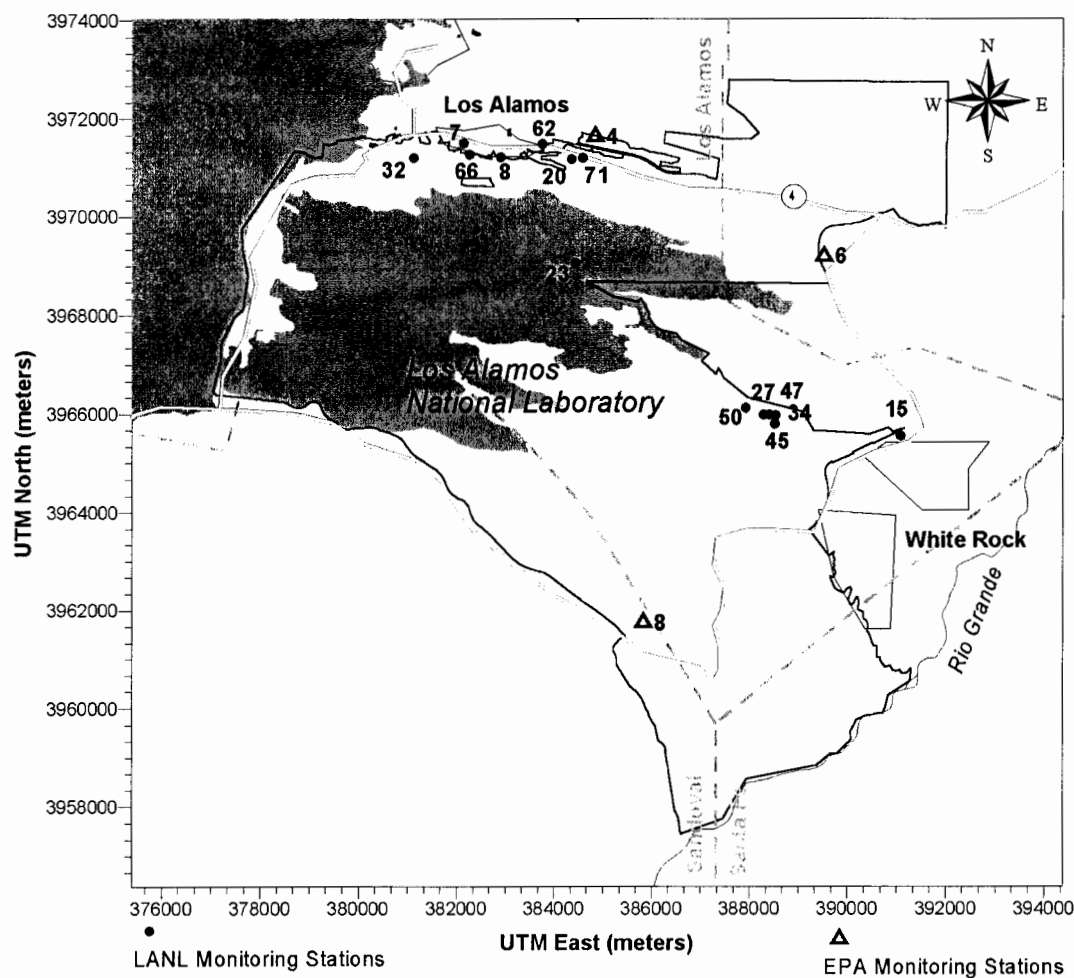


Figure 4-24. Location of LANL and EPA monitoring stations where ²³⁹Pu was detected above the minimum detectable concentration and analytical uncertainty was less than the reported concentration value.

Table 4-16 contains average concentrations of pollutants emitted by the fire for various locations within the model domain and various averaging times. Except for the location identified in Table 4-16 as Santa Clara, these locations are the same as the PM10 monitoring locations. Release rates for these pollutants were calculated using the EPM code and represent the major combustion products produced during a wild fire. Concentrations are reported for several different averaging times that include 13-day, 24-hour, and 3-hour. The 24-hour and 3-hour values are the maximum of a rolling average for the given location. Concentrations do not include background contributions.

Maximum time-integrated concentrations of radionuclides and chemicals are presented in Table 4-17 and Table 4-18, respectively. The maximum concentration generally occurred within the burn areas of the fire. Exposure to these concentrations was possible for firefighters and other emergency personnel; however this assumes the persons were present at the location 24-hours per day for 3 consecutive days.

**Table 4-16. Concentrations of Pollutants Emitted from the Cerro Grande Fire ($\mu\text{g m}^{-3}$)
Excluding Background^a**

	Santa Clara ^b	San Ildefonso ^b	White Rock	Santa Fe-Runnels	Santa Fe-Capshaw	Española	Hernandez	TA-54	Total release (Mg)
PM10									17,377
3-hour average ^c	850	394	1,039	313	256	188	276	1,930	
24-hour average ^c	197	115	134	77	59	39	42	288	
13-day average	31	21	18	8	6	14	10	44	
PM 2.5									15,884
3-hour average ^c	777	360	949	286	234	172	252	1,764	
24-hour average ^c	180	105	123	70	54	36	38	264	
13-day average	29	19	16	7	5	12	9	40	
CO									132,864
3-hour average ^c	6,498	3,009	7,941	2,395	1,961	1,436	2,108	14,757	
24-hour average ^c	1,505	879	1,025	585	454	299	319	2,205	
13-day average	238	158	135	58	45	103	74	335	
CO ₂									2,327,661
3-hour average ^c	113,842	52,710	139,117	41,966	34,348	25,154	36,928	258,531	
24-hour average ^c	26,373	15,395	17,964	10,249	7,948	5,234	5,588	38,630	
13-day average	4,177	2,771	2,366	1,020	785	1,810	1,291	5,861	
CH ₄									6,685
3-hour average ^c	327	151	400	121	99	72	106	743	
24-hour average ^c	76	44	52	29	23	15	16	111	
13-day average	12	8	7	3	2	5	4	17	

^a These concentrations represented intermediate values in the overall calculation of risk. The number of significant digits are included for numerical accuracy in any subsequent hand calculations and do not represent the true accuracy of the values.

^b These locations are the NEWNET meteorological stations.

^c These values are the maximum of a 3 hour and 24- hour rolling average across the 13-day period.

**Table 4-17. Maximum Predicted Time-Integrated Concentration of
Radionuclides Measured within the Model Domain**

Contaminant	Maximum time-integrated concentration (aCi-d m ⁻³)	Location of maximum	
		UTM E	UTM N
Am-241	1.2×10^{-4}	381750	3968750
Pb-210	1.2×10^{-3}	381750	3968750
Pb-212	1.0×10^{-2}	379750	3967250
Np-237	6.5×10^{-3}	379750	3967250
Pu-238	2.1×10^{-3}	385462	3969471
Pu-239	5.4×10^{-3}	385462	3969471
K-40	2.3×10^{-1}	379750	3967250
Pa-231	3.0×10^{-2}	379750	3967250
Ra-226	3.0×10^{-2}	379750	3967250
Ra-224	3.2×10^{-3}	385462	3969471
Th-227	3.0×10^{-4}	381750	3968750
U-234	1.0×10^{-2}	381750	3968750
U-235	7.6×10^{-4}	381750	3968750
U-238	4.9×10^{-3}	381750	3968750

Table 4-18. Maximum Predicted Time-Integrated Concentration of Chemicals Within the Model Domain

Contaminant	Maximum time-integrated concentration (mg-d m ⁻³)	Location of maximum	
		UTM East	UTM North
Acenaphthylene	1.2×10^{-7}	381750	3968750
Aldrin	8.0×10^{-9}	381750	3968750
Amino-2,6-dinitrotolulene[4-]	2.3×10^{-4}	379750	3967250
Amino-4,6-dinitrotolulene[2-]	4.8×10^{-4}	379750	3967250
Aroclor-1254	7.4×10^{-8}	381750	3968750
Benzo(a)pyrene	3.6×10^{-6}	379750	3967250
Cyanide (total)	2.7×10^{-5}	379750	3967250
Dibenz(a,h)anthracene	8.8×10^{-7}	381750	3968750
Dibenzofuran	1.4×10^{-6}	379750	3967250
Dinitrobenzene 1,3	6.7×10^{-4}	379750	3967250
Dinitrotoluene 2,4	1.7×10^{-5}	379750	3967250
Dinitrotolulene[2,4-]	1.7×10^{-5}	379750	3967250
Fluoranthene	6.2×10^{-6}	379750	3967250
HMX	3.9×10^{-1}	379750	3967250
Methylnaphthalene	1.4×10^{-6}	379750	3967250
Naphthalene	2.7×10^{-6}	381750	3968750
Nitrobenzene	1.0×10^{-5}	379750	3967250
Nitrotoluene	1.5×10^{-4}	379750	3967250
Pyrene	7.4×10^{-6}	379750	3967250
RDX	9.2×10^{-2}	379750	3967250
TATB	1.6×10^{-6}	385462	3969471
Trinitrotolulene[2,4,6-]	7.0×10^{-3}	379750	3967250
Aluminum	8.2×10^{-10}	379750	3967250
Antimony	1.5×10^{-12}	379750	3967250
Arsenic	3.0×10^{-5}	379750	3967250
Barium	7.2×10^{-8}	379750	3967250
Beryllium	8.3×10^{-12}	385462	3969471
Cadmium	5.2×10^{-5}	385462	3969471
Chromium (hexavalent)	4.3×10^{-7}	385462	3969471
Cobalt	1.6×10^{-11}	385462	3969471
Copper	8.7×10^{-10}	379750	3967250
Iron	2.7×10^{-9}	379750	3967250
Manganese	4.7×10^{-10}	385462	3969471
Mercury	1.6×10^{-5}	381750	3968750
Nickel	1.4×10^{-10}	379750	3967250
Selenium	3.4×10^{-5}	379750	3967250
Silver	2.1×10^{-11}	379750	3967250
Thallium	1.9×10^{-11}	379750	3967250
Uranium	1.8×10^{-10}	385462	3969471
Vanadium	9.8×10^{-12}	379750	3967250
Zinc	1.4×10^{-8}	379750	3967250

4.4.1 Concentrations Outside the Model Domain

Concern was expressed about transport of chemicals and radionuclides entrained in the smoke plume to locations northeast of the model domain. In particular, the residents of the city of Taos (located about 60 km northeast of the model domain and at an elevation of about 7000 ft) expressed concern over possible exposure to LANL-derived chemicals and radionuclides. Measured PM₁₀ concentrations in Taos on May 11 and May 17, 2000, had values of 37 and 44 $\mu\text{g m}^{-3}$ respectively. The concentrations observed on May 11 included emissions from LANL lands that were burned. Therefore, this day is of particular interest.

Dispersion of material in the form of a non-buoyant ground-level release typically results in decreasing concentrations with distance from the source and in such cases, concentrations decrease with increasing distance from the source. However, in the case of buoyant plumes, concentrations at distant locations may actually be higher than concentrations close to the source because the plume is lofted over the nearby receptors. In such cases, the maximum concentration downwind is not at ground level, but at points above the ground. The concern expressed by residents outside the model domain was that they were exposed to the elevated plume and therefore, higher concentrations of radionuclides and chemicals.

To evaluate potential exposure to the elevated plume at locations outside the model domain, we constructed a cross section of the PM₁₀ plume in the northeast corner of the model domain for May 11 (Figure 4-25). A second cross section was also constructed about 10 mi. (16 km) south of the northeast corner of the model domain where the main portion of the plume was predicted to have exited the model domain. We included 12-hour and 24-hour averaging times in each cross section. Concentrations do not include background contributions, which in Taos averaged about 14 $\mu\text{g m}^{-3}$ before the fire and could have been as high as 33 $\mu\text{g m}^{-3}$. The height above ground level of the maximum concentration in the plume varied between 3280 and 4921 ft (1000 and 1500 m). The *peak* concentration in the plume cross sections provides a means of *bounding* possible exposures at other locations outside the model domain because concentrations will decrease (due to dispersion and dilution) with increased travel time. Risk estimates at locations outside the model domain may then be scaled from risk estimates at locations within the model domain by computing the ratio of the 24-hour average PM₁₀ concentration calculated at locations in the model domain for May 11, 2000 to the peak 24-hour average PM₁₀ concentration in the plume cross section (Table 4-19). For example, the 24-hour average PM₁₀ concentration in Española for May 11, 2000 was 29 $\mu\text{g m}^{-3}$ (excluding background). The 24-hour average PM₁₀ concentration 1500 m above ground level in the northeast corner of the model domain was 28 $\mu\text{g m}^{-3}$. Because the ratio of these two concentration is approximately equal to 1.0, the estimated radionuclide and chemical concentrations at locations outside the model domain (such as Taos) can be roughly approximated by radionuclide and chemical concentrations estimated for Española.

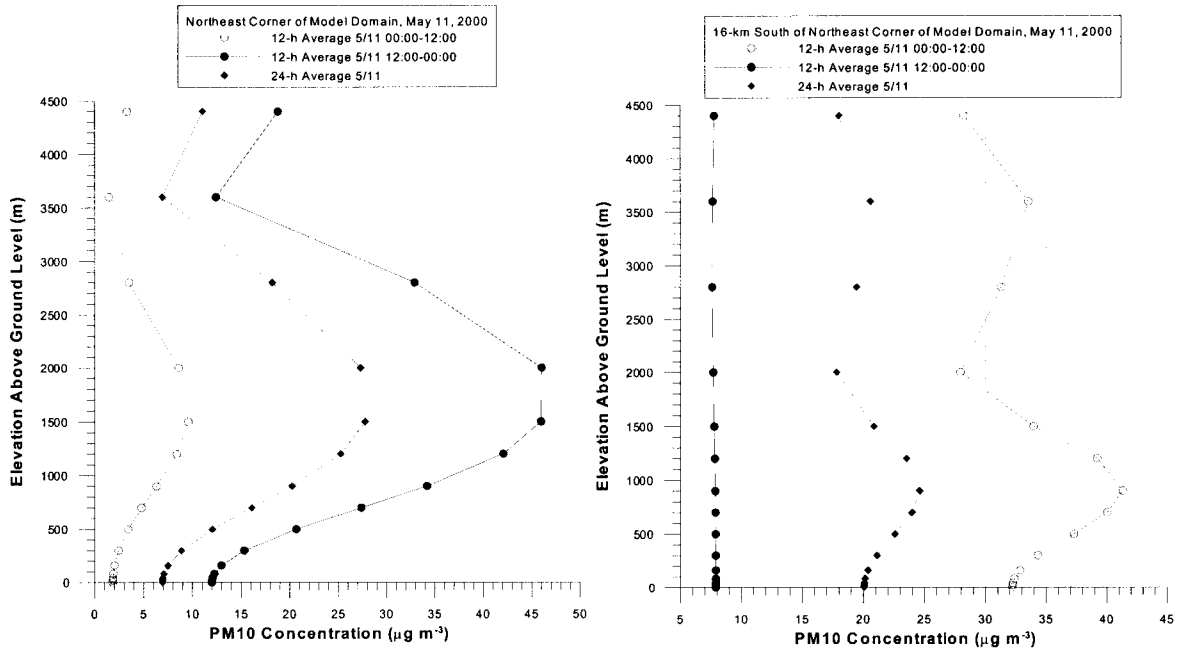


Figure 4-25. Vertical profile of estimated PM10 concentration at the northeast corner of the model domain (left graph) and 10 mi (16 km) south of the northeast corner (right graph). Concentrations do not include background contributions.

Table 4-19. Estimated 24-Hour Average Ground-Level PM10 Concentrations Excluding Background at Selected Locations in the Model Domain for May 11, 2000

Location	24-hour average PM10 concentration for May 11 ($\mu\text{g m}^{-3}$)
Santa Clara (EPA PM10 monitor)	41
San Ildefonso NEWNET station	5
White Rock	0
Santa Fe- Runnels	0
Santa Fe- Capshaw	0
Española	29
Hernandez	10
Ta-54	23
Northeast corner of model domain at 1500 m above ground level	28
16 km south of the northeast corner at 1000 m above ground level	25

4.5 Deposition Estimates

We calculated estimates of deposition in the model domain using a variation of Equation (4.18) as explained in Section 4.3.1. Surface deposition may be converted to a soil concentration by assuming a minimum mixing depth and soil bulk density. For illustration, assume a mixing depth of 1 in. (2.54 cm) and a soil bulk density of 1.5 g cm⁻³. The conversion is then

$$C_{soil} = \frac{C_{surf} \frac{1 \text{ m}^2}{10,000 \text{ cm}^2} \frac{1}{2.54 \text{ cm}}}{1.5 \text{ g cm}^{-3}} = 2.62 \times 10^{-5} C_{surf} \quad (4.19)$$

where

C_{soil} = concentration of a chemical or radionuclide in soil (mg or pCi g⁻¹)

C_{surf} = soil surface concentration of a chemical or radionuclide (mg or pCi m⁻²).

Estimated deposition of radionuclides from burned PRSs would generally not be detectable in soil (Table 4-20). The same can be said for most of the chemicals and metals (Table 4-21), with the exception of the explosive compounds RDX and HMX. At the receptor locations listed in Table 4-21, the maximum RDX surface soil concentration was 2.3 mg m⁻², which equates to a soil concentration of 60 µg g⁻¹ or 60 ppm. This concentration would easily be detectable in soil. However, LANL soil sampling results indicated that no high explosive compounds were detected above LANL reporting limits in any of the samples collected upwind or downwind from the fire (see Chapter 2, Section 2.4.2). Therefore, we suspect that the source term for these compounds was grossly overestimated.

Table 4-20. Estimated Deposition of Radionuclides Released from PRSs as a Result of the Cerro Grande Fire (pCi m⁻²)

Nuclide	Española	Santa Clara ^a	Hernandez	San Ildefonso ^a	Santa Fe	White Rock	Los Alamos	TA-54
Am-241	2.9E-13	2.3E-13	7.4E-16	2.9E-11	3.5E-12	2.4E-11	1.5E-12	1.8E-10
Pb-210	0.0E+00	0.0E+00	0.0E+00	2.5E-10	3.5E-11	2.3E-10	6.3E-12	1.1E-09
Pb-212	7.3E-10	3.5E-10	1.4E-13	9.3E-09	7.0E-11	9.2E-10	1.3E-09	4.7E-08
Np-237	4.8E-10	2.2E-10	0.0E+00	5.8E-09	0.0E+00	3.0E-10	8.1E-10	2.2E-08
Pu-238	1.1E-13	2.4E-11	1.8E-13	2.4E-10	3.1E-11	2.1E-10	1.0E-10	1.6E-08
Pu-239	2.9E-13	6.2E-11	4.6E-13	1.4E-10	1.3E-11	9.0E-11	2.6E-10	3.9E-08
K-40	1.7E-08	8.1E-09	3.4E-12	2.2E-07	1.7E-09	2.2E-08	3.1E-08	1.1E-06
Pa-231	2.3E-09	1.0E-09	1.8E-13	2.8E-08	2.5E-11	1.6E-09	3.9E-09	1.2E-07
Ra-226	2.3E-09	1.0E-09	1.5E-14	2.9E-08	5.0E-11	1.8E-09	3.9E-09	1.1E-07
Ra-224	1.4E-13	3.6E-11	2.7E-13	1.7E-10	2.0E-11	1.3E-10	1.5E-10	2.3E-08
Th-227	0.0E+00	0.0E+00	0.0E+00	6.0E-11	8.4E-12	5.6E-11	1.5E-12	2.6E-10
U-234	1.7E-12	6.8E-12	4.5E-14	2.1E-09	2.9E-10	1.9E-09	8.0E-11	1.3E-08
U-235	1.5E-12	1.1E-12	3.0E-15	1.7E-10	2.2E-11	1.5E-10	8.1E-12	9.9E-10
U-238	3.3E-11	1.9E-11	2.7E-14	1.4E-09	1.4E-10	9.4E-10	9.6E-11	8.0E-09

^a. These locations are the NEWNET meteorological stations.

Table 4-21. Estimated Deposition of Chemicals and Metals Released from PRSs as a Result of the Cerro Grande Fire (mg m⁻²)

Chemical	Española	Santa Clara ^a	Hernandez	San Ildefonso ^a	Santa Fe	White Rock	Los Alamos	TA-54
Acenaphthylene	2.0E-07	5.8E-08	0.0E+00	1.5E-06	9.6E-08	5.4E-07	1.3E-07	3.8E-06
Aldrin	0.0E+00	0.0E+00	0.0E+00	3.0E-08	6.5E-09	3.1E-08	7.3E-10	1.2E-07
Aluminum	6.1E-11	2.7E-11	0.0E+00	7.7E-10	4.8E-12	7.1E-11	1.0E-10	2.9E-09
Amino-2,6-dinitrotoluene[4-]	5.7E-04	1.7E-04	0.0E+00	3.0E-03	2.4E-06	2.6E-04	3.3E-04	5.8E-03
Amino-4,6-dinitrotoluene[2-]	1.2E-03	3.5E-04	0.0E+00	6.3E-03	4.3E-06	5.4E-04	6.9E-04	1.2E-02
Antimony	1.1E-13	5.2E-14	3.5E-17	1.4E-12	1.7E-14	1.8E-13	2.0E-13	8.3E-12
Aroclor-1254	0.0E+00	0.0E+00	0.0E+00	2.8E-07	6.1E-08	2.9E-07	6.8E-09	1.1E-06
Arsenic	7.4E-05	2.2E-05	5.8E-09	3.9E-04	1.2E-06	3.8E-05	4.5E-05	1.1E-03
Barium	5.4E-09	2.4E-09	1.3E-15	6.5E-08	7.4E-13	3.4E-09	9.0E-09	2.5E-07
Benzo(a)pyrene	8.8E-06	3.1E-06	3.7E-09	5.4E-05	1.5E-06	1.1E-05	6.9E-06	3.1E-04
Beryllium	3.3E-14	1.1E-13	7.2E-16	4.7E-13	5.2E-16	2.5E-14	4.5E-13	6.1E-11
Cadmium	1.2E-04	5.6E-05	1.6E-07	6.7E-04	8.8E-06	9.3E-05	1.4E-04	9.9E-03
Chromium(hexavalent)	1.1E-07	2.2E-07	1.4E-09	7.0E-07	0.0E+00	5.0E-08	7.1E-07	7.8E-05
Cobalt	7.8E-13	5.2E-13	1.3E-15	9.6E-12	8.8E-16	5.0E-13	2.0E-12	1.4E-10
Copper	6.3E-11	3.2E-11	3.0E-14	9.2E-10	2.1E-11	1.8E-10	1.3E-10	6.0E-09
Cyanide (total)	6.8E-05	2.0E-05	0.0E+00	3.6E-04	1.5E-08	3.0E-05	3.9E-05	6.9E-04
Dibenz(a,h)anthracene	1.8E-06	6.1E-07	6.3E-10	1.3E-05	6.6E-07	3.9E-06	1.4E-06	6.4E-05
Dibenzofuran	3.6E-06	1.1E-06	2.7E-10	2.4E-05	1.0E-06	6.3E-06	2.3E-06	6.9E-05
Dinitrobenzene[1,3-]	1.7E-03	4.9E-04	0.0E+00	8.9E-03	0.0E+00	7.3E-04	9.7E-04	1.7E-02
Dinitrotoluene[2,4-]	4.3E-05	1.2E-05	0.0E+00	2.2E-04	0.0E+00	1.8E-05	2.4E-05	4.3E-04
Fluoranthene	1.5E-05	5.3E-06	6.3E-09	1.0E-04	4.1E-06	2.6E-05	1.2E-05	5.6E-04
HMX	9.9E-01	2.9E-01	0.0E+00	5.2E+00	2.8E-05	4.3E-01	5.7E-01	9.9E+00
Iron	2.0E-10	9.1E-11	5.4E-15	2.4E-09	3.3E-13	1.3E-10	3.4E-10	9.6E-09
Manganese	2.8E-11	1.8E-11	3.8E-14	3.4E-10	2.2E-13	1.9E-11	6.8E-11	4.5E-09
Mercury	1.3E-05	4.2E-06	2.8E-09	1.3E-04	1.3E-05	6.6E-05	1.0E-05	5.2E-04
Methylnaphthalene[2-]	3.4E-06	1.0E-06	3.1E-10	2.0E-05	4.2E-07	3.5E-06	2.1E-06	5.8E-05
Naphthalene	6.6E-06	1.9E-06	3.2E-10	4.4E-05	2.1E-06	1.3E-05	4.1E-06	1.2E-04
Nickel	1.5E-11	4.2E-11	2.7E-12	1.6E-10	3.5E-12	1.2E-11	2.3E-11	5.2E-10
Nitrobenzene	2.6E-05	7.4E-06	0.0E+00	1.3E-04	0.0E+00	1.1E-05	1.5E-05	2.6E-04
Nitrotoluene[4-]	3.9E-04	1.1E-04	0.0E+00	2.0E-03	0.0E+00	1.7E-04	2.2E-04	3.9E-03
Pyrene	1.8E-05	6.1E-06	6.2E-09	1.1E-04	2.9E-06	2.2E-05	1.4E-05	5.7E-04
RDX	2.3E-01	6.7E-02	0.0E+00	1.2E+00	7.9E-06	1.0E-01	1.3E-01	2.3E+00
Selenium	1.4E-04	2.6E-04	3.7E-05	7.7E-04	3.5E-05	1.4E-04	1.1E-04	1.3E-03
Silver	1.5E-12	7.6E-13	5.2E-16	2.1E-11	3.3E-13	3.2E-12	2.9E-12	1.2E-10
TATB	3.3E-07	8.0E-07	5.3E-09	2.1E-06	0.0E+00	1.5E-07	2.6E-06	2.8E-04
Thallium	1.5E-12	6.5E-13	1.1E-18	1.8E-11	3.1E-15	9.3E-13	2.4E-12	6.7E-11
Trinitrotoluene[2,4,6-]	1.8E-02	5.1E-03	0.0E+00	9.3E-02	0.0E+00	7.7E-03	1.0E-02	1.8E-01
Uranium	1.2E-12	2.6E-12	1.5E-14	1.8E-11	1.5E-13	1.8E-12	1.0E-11	1.3E-09
Vanadium	7.3E-13	3.3E-13	5.2E-17	8.9E-12	1.9E-14	5.8E-13	1.3E-12	3.8E-11
Zinc	3.4E-08	1.5E-08	1.0E-10	1.9E-07	2.9E-09	2.8E-08	3.8E-08	2.5E-06

^a These locations are the NEWNET meteorological stations.

5 RISK ESTIMATES

Risk is a general term applied to adverse health effects resulting from exposure to radionuclides or chemicals. To quantify risk, a health endpoint is first identified. Then, values for the risk per unit exposure are obtained and multiplied by the estimated exposure to the radionuclide or chemical. Estimated exposure is calculated using the estimated air concentration for each radionuclide or chemical at a given location and an assumed exposure scenario. The exposure scenario is a quantitative description of the physical attributes and behavior characteristics of a hypothetical individual that affects the amount of radionuclide or chemical taken in via the exposure pathway. Inhalation is the only exposure pathway considered in this assessment.

We calculated two health endpoints for this assessment: incremental lifetime cancer incidence risk and subchronic noncancer health effects. Incremental lifetime cancer incidence risk applies to radionuclides and carcinogenic chemicals. Subchronic noncancer health effects apply to chemicals only. We compute and report cancer risks associated with radionuclides separately from the cancer risks associated with carcinogenic chemicals.

Risk estimates are restricted to radionuclides and chemicals released from PRSs during the Cerro Grande Fire. Absent from this assessment are calculations of risk from (1) naturally occurring radionuclides, (2) man-made radionuclides that have deposited on vegetation and ground (such as $^{239/240}\text{Pu}$ and ^{137}Cs from global weapons testing fallout), (3) radionuclides originating from 50 years of LANL operations that have deposited on surrounding lands, (4) radionuclides and chemicals that may have been suspended from PRSs that were *not* burned during the Cerro Grande Fire, (5) radionuclides and chemicals released from PRSs to the air after the fire burned, and (6) combustion products from the burning of LANL structures. Radionuclides and chemicals present on the natural vegetation that burned during the Cerro Grande Fire are assessed in Appendix D. Risks associated with exposure to particulate matter and pollutants found in wood smoke are addressed in Appendix F.

5.1 Exposure Scenarios

The risk to a person from exposure during and after the Cerro Grande Fire depended on a number of factors, including

- Their location
- Their general level of activity (i.e., were they doing strenuous physical activity or something more sedentary)
- Their length of time in a particular area
- Their age and gender.

Each exposure scenario represents an individual with unique physical and behavioral characteristics. These characteristics include variables correlated to risk, which for contaminant releases to air during the Cerro Grande Fire primarily relate to breathing rate. The scenarios are defined in such a way that they are independent of location and length of time in a particular area. This allows risk to be calculated for each representative individual throughout the model domain. In this way, the spatial-dependency of risk throughout the model domain for each scenario can be observed.

We defined exposure scenarios for four hypothetical, but representative individuals. The physical activity level of an individual is a key parameter that determines exposure and, therefore, risk because the greater the physical exertion, the greater the breathing rate and the greater the volume of air that is drawn into the lungs in any given time period. We defined exposure scenarios for a firefighter, an emergency response person (other than a firefighter), a resident adult, and a resident child. The scenarios are organized according to time spent during each day at different levels of activity, ranging from sleeping to heavy manual labor. Firefighters and emergency response personnel were active outside for extended periods of time each day and had relatively short rest and sleep periods. The firefighters were involved in physically strenuous work that ranged from fireline operations, including backfires, fighting spot fires, and building firebreaks. Emergency response personnel, such as security guards, were also situated in close proximity to the fire for extended periods of time, but they generally had lower physical activity levels than the firefighters. These emergency response personnel may also include LANL, NMED, EPA, and DOE personnel who were responding to concerns about health impacts of the fire by placing and removing air samples from various locations across the site.

Local residents from Los Alamos and White Rock did not perform their typical daily routines during the time of the fire because local businesses and LANL were shut down, and the area was evacuated. Many residents from the town of Los Alamos were initially evacuated to White Rock only to be reevacuated to more distant locations after their arrival in White Rock. Evacuation procedures for portions of the Los Alamos town site were initiated at 1:00 pm Sunday, May 7. LANL announced an emergency closure effective Monday, May 8, and all businesses were closed in the Los Alamos town site on Monday, May 8, together with Los Alamos schools and county offices (except for emergency services). A mandatory evacuation for the remainder of the Los Alamos town site was ordered around 1:00 pm Wednesday, May 10, when the fire crossed Camp May Road north into the upper watershed of Los Alamos Canyon, directly threatening the town site. The town site of White Rock was evacuated at 1:00 am, Thursday, May 11. The fire burned across LANL property primarily on May 11, 12, and 13, 2000. While residents at locations more distant from the fire experienced a more typical daily routine during this time, they were also in a state of heightened anxiety and stress.

For these calculations, the resident adult and resident child were assumed to be more active than might normally be the case. Evacuation of residents from Los Alamos and White Rock was not considered explicitly in the scenarios. The scenarios assumed the adult, child, firefighter, and emergency personnel remained at the same location in the model domain throughout the entire period of exposure. Although contaminant concentrations tend to be lower indoors than outdoors for outdoor contaminant sources, this is very dependent on the type of building structure and individual preferences; therefore, for all scenarios in this assessment, outdoor air concentrations were assumed for all situations.

Input from those directly impacted by the Cerro Grande Fire, including local residents, the NMED, LANL personnel, and other stakeholders, was important to establish as many individual-specific parameters as possible for the scenarios. These exposure scenarios were developed with caution so that a potentially exposed person would not be missed and individuals represented by the exposure scenarios would have a risk greater than that of other individuals who might have been in the area for less time or under less exposed conditions. For this reason, while some parameter values may be above the average values used in other studies, they are not

unrealistically high. General characteristics considered for the different exposure scenarios are given below.

1. Firefighter

- Los Alamos County Fire Department firefighters from the five local fire stations were involved from the outset of the fire. Firefighters were brought in from many locations all over the U.S. to fight the Cerro Grande Fire.
- It is assumed the firefighter was exposed during the entire duration of the fire and that this represents a maximal period of exposure.
- Activity levels: very strenuous work fighting the fire, extremely long hours, and minimal rest and sleep periods. Local firemen report that during the peak of the fire, they slept for only 2 to 3 hours per night before resuming activity. Local volunteer groups provided food.
- It is assumed that no respiratory apparatus was used by the firefighters. Based on discussions with firefighters of the Cerro Grande Fire, there was minimal use of respiratory apparatus for firefighting activities because of the weight of the apparatus and the magnitude and extent of the fire. Respiratory apparatus would reduce the amount of contaminants inhaled. It was reported that dust masks were worn by some firefighters, but because they were not used by all firefighters and their efficiency in reducing contaminant intake is uncertain, we have not taken them into account in the assessment.
- Inhalation of airborne contaminants released from the fire is the primary exposure route.
- Parameters have been chosen to reflect a realistic upper estimate of exposure.
- An estimated 600 personnel were deployed on the fire lines.

2. Emergency response person

- This scenario encompasses a wide range of individuals who may have been close to the fire for significant periods of time. Security officers from Protection Technology Los Alamos (PTLA) were evacuated as a precaution on Sunday, May 7, but they resumed patrols of the controlled area later that evening when conditions warranted.
- It is assumed this person was active for long hours with short sleep periods. The physical activity level was assumed to be less than that of a firefighter, but it was still above normal daily levels.
- Inhalation of airborne contaminants released from the fire is the primary exposure route.

3. Resident adult

- This scenario represents an adult who resides in the local community.
- This scenario accounts for both active and more sedentary activities during the course of a day; appropriate parameter values were chosen to reflect these levels of activity.
- Inhalation of airborne contaminants released from the fire is the primary exposure route.

4. Resident child

- This scenario represents a child who resides in the local community.
- This scenario accounts for a range of different activity levels during the course of a day; appropriate parameter values were chosen to reflect these levels of activity.
- Inhalation of airborne contaminants released from the fire is the primary exposure route.

Table 5-1 provides a summary of the exposure parameters for the four scenarios. The parameter values were based on published information on breathing rates for active and sedentary adults, children, and infants that *RAC* compiled for a previous study (Rood and Grogan 1999). These methods and assumptions are described in the next section.

Table 5-1. Exposure Scenarios and Exposure Parameters for Atmospheric Releases^a

Parameter	Firefighter	Emergency response person	Resident adult	Resident child
Weighted daily average breathing rate ($\text{m}^3 \text{h}^{-1}$)	2.19	1.49	1.44	0.56
Body weight (kg)	67	74	74	20
Exposure duration ^a (h d ⁻¹)	24	24	24	24
Exposure location	Entire domain	Entire domain	Entire domain	Entire domain

^a Exposure throughout the entire release period is assumed for all scenarios.

5.1.1 Breathing Rates, Time Budgets, and Body Weights

Each exposure scenario was divided into three types of activities: sleeping, light activities, and heavy activities. Some examples of light exercise are laboratory work, woodworking, housecleaning, and painting. Heavy exercise corresponds to occupations such as mining, construction, farming, and ranching. For each exercise level, an age-specific breathing rate was assigned. Breathing rates (Table 5-2) for persons age 8 and higher were obtained from Roy and Courtay (1991) and for children age 0–7 from Layton (1993). Although we present gender-specific breathing rates in the following table, risk factors that are specific to gender were not available. For this reason, for any given age, we used the larger of the two breathing rates for each activity level as a conservative representation of total air inhaled.

Time budgets for the representative individuals in each scenario (Table 5-3) were based on discussions with different groups of individuals who experienced the fire, combined with data presented in Roy and Courtay (1991). The maximum breathing rates in Table 5-2 are for a male 18 year old, and these were assumed for the firefighter scenario. The breathing rates reported for the adult male age 30–60 were assumed for the emergency response person and adult resident scenarios, and the breathing rates reported for a male age 3–7 were assumed for the child scenario. We then applied a weighted-average breathing rate to each activity based on the number of hours spent at each exercise level. Although contaminant concentrations tend to be lower indoors than outdoors, this is very dependent on the type of building structure and individual preferences. Therefore, for this assessment, we assumed outdoor air concentrations for all situations.

Table 5-2. Breathing Rates for Various Exercise Levels as Reported in Roy and Courtay (1991) and Layton (1993)

Gender	Age	Exercise level		
		Resting (m ³ h ⁻¹)	Light (m ³ h ⁻¹)	Heavy (m ³ h ⁻¹)
Male	30-60	0.45	1.50	3.00
Female	30-60	0.32	1.26	2.70
Male	18	0.50	1.58	3.06
Female	18	0.35	1.32	2.70
Male	16	0.43	1.52	3.02
Female	16	0.35	1.30	2.70
Male	15	0.42	1.38	2.92
Female	15	0.35	1.30	2.57
Male	14	0.41	1.40	2.71
Female	14	0.33	1.20	2.52
Male	12	0.38	1.23	2.42
Female	12	0.33	1.13	2.17
Male	10	0.31	1.12	2.22
Female	10	0.31	1.12	1.84
Male	8	0.29	1.02	1.68
Female	8	0.29	1.02	1.68
Male	3-7	0.24	0.72	1.68
Female	3-7	0.23	0.68	1.59
Male	0-3	0.19	0.58	1.35
Female	0-3	0.14	0.45	1.02

Table 5-3 Time Budgets and Breathing Rates for Representative Scenarios

Scenario	Hours per day at an activity level			Weighted daily average breathing rate (m ³ h ⁻¹)
	Sleeping	Light	Heavy	
Firefighter	3.0	9.0	12.0	2.12
Emergency response person	6.0	14.0	4.0	1.49
Resident adult	7.0	13.0	4.0	1.44
Resident child	12.0	10.0	2.0	0.56

We calculated time-weighted average breathing rates for the three activities for which each representative individual was engaged. The time-weighted average breathing rate is given by

$$WBR = \sum_{i=1}^3 BR_i f_i \quad (5.1)$$

where

WBR = time-weighted average daily breathing rate (m³ h⁻¹)

BR_i = breathing rate for the i^{th} activity level (m³ h⁻¹)

f_i = fraction of time (hours per day divided by 24) spent at the i^{th} activity level (unitless).

To summarize, three activities were defined for each exposure scenario: sleeping, light activities, and heavy activities. The location of exposure for light and heavy activities was assumed to be the same for all individuals represented by the scenarios. The breathing rate for the entire day was calculated as a time-weighted average of the breathing rates at the three activity levels during the day.

5.2 Risk Calculation Methodology

The following general procedure was used to estimate risk for each scenario.

- Time-integrated contaminant concentrations in air (Bq-d m^{-3} for radionuclides or mg-d m^{-3} for chemicals) at each grid node in the model domain were calculated.
- The time-integrated air concentration was multiplied by the average breathing rate for the representative individual over the exposure period (e.g., $\text{mg-d m}^{-3} \times \text{m}^3 \text{d}^{-1} = \text{mg}$ of contaminant intake) to determine the total contaminant intake.
- The total contaminant intake was averaged over the representative individual's body weight (for nonradionuclides only) and multiplied by the appropriate risk factor to estimate the increased lifetime cancer incidence risk or subchronic health effects. For chemical carcinogens and radionuclides, slope factors and risk coefficients were used, respectively. For the noncarcinogenic contaminants, toxicity values based on subchronic reference doses (if available), reference concentrations, or occupational standards were used to estimate noncancer health effects.
- For radionuclides the incremental lifetime cancer risk is given by

$$R = TIC \times BR \times RC \quad (5.2)$$

where

TIC = time integrated concentration (Bq-d m^{-3})

BR = breathing rate ($\text{m}^3 \text{d}^{-1}$)

RC = lifetime cancer incidence risk coefficient (Bq^{-1}).

The calculations for radionuclides were performed in units of curies and were converted to becquerels ($1 \text{ Ci} = 3.7 \times 10^{10} \text{ Bq}$) for the risk calculation.

- For carcinogenic chemicals the incremental lifetime cancer risk is given by

$$R = \frac{TIC \times BR \times SF}{BW \times AT} \quad (5.3)$$

where

TIC = time integrated concentration (mg-d m^{-3})

BW = body weight (kg)

SF = slope factor (kg-d mg^{-1})

AT = averaging time (d), typically assigned a value of 25,550 d (70 yr).

- For noncarcinogenic chemicals, the hazard quotient (HQ) is given by

$$HQ = \frac{\left(\frac{TIC \times BR}{BW \times AT} \right)}{RfD} \quad (5.4)$$

where

RfD = reference dose (mg kg-d^{-1})

AT = averaging time (d).

The HQ is essentially the ratio of the average daily intake of a chemical per unit body mass to a corresponding acceptable value. Acceptable daily intake per unit body mass is reported by EPA as the RfD and is the daily intake of a chemical per unit body mass that results in no adverse health effects. For subchronic health effects, averaging time values can range from 14 days to 7 years; we assumed an averaging time of 14 days for these risk calculations. A summary of the risk factors and HQs for contaminants addressed in this report is provided in Appendix E. Appendix E also contains information on how the risk factor or HQ was developed for chemicals with limited toxicity data.

5.3 Risk Estimates

We developed risk estimates and HQs for the representative individuals as represented by the 4 exposure scenarios. The concentrations, risks, and HQs can be calculated at any grid node within the model domain, but we selected the eight locations given in Chapter 4 as representative of the model domain to present the data. Complete results of the calculations are available electronically.

Cancer risk to each representative individual at each location was separated into risk from radionuclides, and risk from carcinogenic chemicals (Tables 5-4 and 5-5). Hazard Quotients are shown in Table 5-6.

Table 5-4 Incremental Lifetime Cancer Incidence Risks for Radionuclides

Scenario	Total cancer risk to representative individuals at each location							
	Espanola	Santa Clara ^a	Herandez	San Ildefonso ^a	Santa Fe	White Rock	Los Alamos	TA-54
Resident adult	9.7×10^{-16}	2.0×10^{-16}	2.1×10^{-19}	3.4×10^{-15}	5.8×10^{-17}	7.6×10^{-16}	4.4×10^{-16}	1.5×10^{-14}
Firefighter	1.5×10^{-15}	3.0×10^{-16}	3.2×10^{-19}	5.2×10^{-15}	8.7×10^{-17}	1.1×10^{-15}	6.7×10^{-16}	2.3×10^{-14}
Emergency worker	1.0×10^{-15}	2.0×10^{-16}	2.2×10^{-19}	3.5×10^{-15}	6.0×10^{-17}	7.9×10^{-16}	4.5×10^{-16}	1.6×10^{-14}
Resident child	3.8×10^{-16}	7.6×10^{-17}	8.2×10^{-20}	1.3×10^{-15}	2.2×10^{-17}	3.0×10^{-16}	1.7×10^{-16}	5.9×10^{-15}

^a These are at the NEWNET meteorological station locations (Figure 5-3).

Table 5-5 Incremental Lifetime Cancer Incidence Risks for Chemical Carcinogens

Scenario	Total cancer risk to representative individuals at each location							
	Espanola	Santa Clara ^a	Her-nandez	San Ildefonso ^a	Santa Fe	White Rock	Los Alamos	TA-54
Resident Adult	3.1×10^{-9}	5.5×10^{-10}	1.2×10^{-13}	1.0×10^{-8}	9.0×10^{-12}	1.8×10^{-9}	1.1×10^{-9}	2.3×10^{-8}
Firefighter	5.2×10^{-9}	9.2×10^{-10}	2.1×10^{-13}	1.8×10^{-8}	1.5×10^{-11}	3.1×10^{-9}	1.9×10^{-9}	3.8×10^{-8}
Emergency worker	3.2×10^{-9}	5.7×10^{-10}	1.3×10^{-13}	1.1×10^{-8}	9.4×10^{-12}	2.0×10^{-9}	1.1×10^{-9}	2.4×10^{-8}
Resident child	4.5×10^{-9}	7.9×10^{-10}	1.8×10^{-13}	1.5×10^{-8}	1.3×10^{-11}	2.7×10^{-9}	1.6×10^{-9}	3.3×10^{-8}

^a These are at the NEWNET meteorological station locations (Figure 5-2).

Table 5-6 Hazard Quotient Estimates for Noncarcinogenic Chemicals

Scenario	Total noncancer hazard quotient for representative individuals at each location							
	Espanola	Santa Clara ^a	Her-nandez	San Ildefonso ^a	Santa Fe	White Rock	Los Alamos	TA-54
Resident adult	2.9×10^{-2}	5.0×10^{-3}	1.3×10^{-6}	9.8×10^{-2}	3.5×10^{-5}	1.7×10^{-2}	9.8×10^{-3}	1.6×10^{-1}
Firefighter	4.9×10^{-2}	8.4×10^{-3}	2.1×10^{-6}	1.7×10^{-1}	5.8×10^{-5}	2.9×10^{-2}	1.6×10^{-2}	2.7×10^{-1}
Emergency worker	3.0×10^{-2}	5.2×10^{-3}	1.3×10^{-6}	1.0×10^{-1}	3.6×10^{-5}	1.8×10^{-2}	1.0×10^{-2}	1.7×10^{-1}
Resident child	4.2×10^{-2}	7.2×10^{-3}	1.8×10^{-6}	1.4×10^{-1}	5.0×10^{-5}	2.5×10^{-2}	1.4×10^{-2}	2.3×10^{-1}

^a These are at the NEWNET meteorological station locations (Figure 5-1).

Using the maximum air concentrations given in Chapter 4, we calculated the maximum cancer risk for each scenario from radionuclides, carcinogenic chemicals, and the maximum HQ from noncarcinogenic chemicals. These risk estimates are shown in Table 5-7. These maximum risks assume that the representative individual remained in one place for the entire duration of the fire. For radionuclides and carcinogenic chemicals, the risk is minimal. However, noncancer HQs exceed the acceptable value of 1.0 in all cases. HQs were dominated by four chemicals; Dinitrobenzene [1,3] (11.2% of total HQ), HMX (13.1% of total), RDX (51% of total), and Trinitrotoluene[2,4,6] (23.4%). Figure 5-1 shows the distribution of HQ values across the model domain for the resident adult scenario. HQ values greater than 1 are restricted to a small area within the LANL site near its western boundary.

These higher than expected HQs for the high explosive compounds appear to be an artifact of the either high source terms estimated for these compounds or that significant degradation of these compounds occurred during atmospheric transport. Estimates of deposition in the model domain (see Chapter 4) indicated concentrations of RDX and HMX would be easily detectable. However, sampling by LANL after the fire both up and down wind of the smoke plume showed no concentrations of high explosive compounds above their reporting limits. Although these specific compounds were not mentioned in the summary of the data received by RAC from LANL (Fresquez 2000a, 2000b, 2000c), we have assumed that these compounds were included in their assessment of high explosives in soil.

Isopleth maps of cancer risk from chemicals (Figure 5-2) and radionuclides (Figure 5-3) show slightly different patterns of exposure compared to the HQ isopleth map. Radionuclide cancer risk was considerably lower compared to cancer risk for chemicals. The high explosive, RDX, which is also a suspected carcinogen and has a published slope factor, was the dominant

chemical, followed by chromium. The radionuclides, ^{226}Ra , ^{231}Pa , and ^{239}Pu were the dominant radionuclides; however, risks from these nuclides were less than 10^{-14} . Ra-226 is also naturally occurring and as shown in Appendix D, the inhalation risk from this nuclide is substantially greater from natural sources compared to those in the burned PRS units.

Table 5-7 Hypothetical Maximum Risks by Scenario and Contaminant Type

Scenario	Maximum hypothetical risk or hazard quotient (for noncarcinogens)		
	Radionuclides	Carcinogenic chemicals	Noncarcinogenic chemicals
Resident adult	6.7×10^{-14}	2.1×10^{-7}	2.0
Firefighter	1.0×10^{-13}	3.6×10^{-7}	3.4
Emergency worker	6.9×10^{-14}	2.2×10^{-7}	2.1
Resident child	2.6×10^{-14}	3.1×10^{-7}	2.9

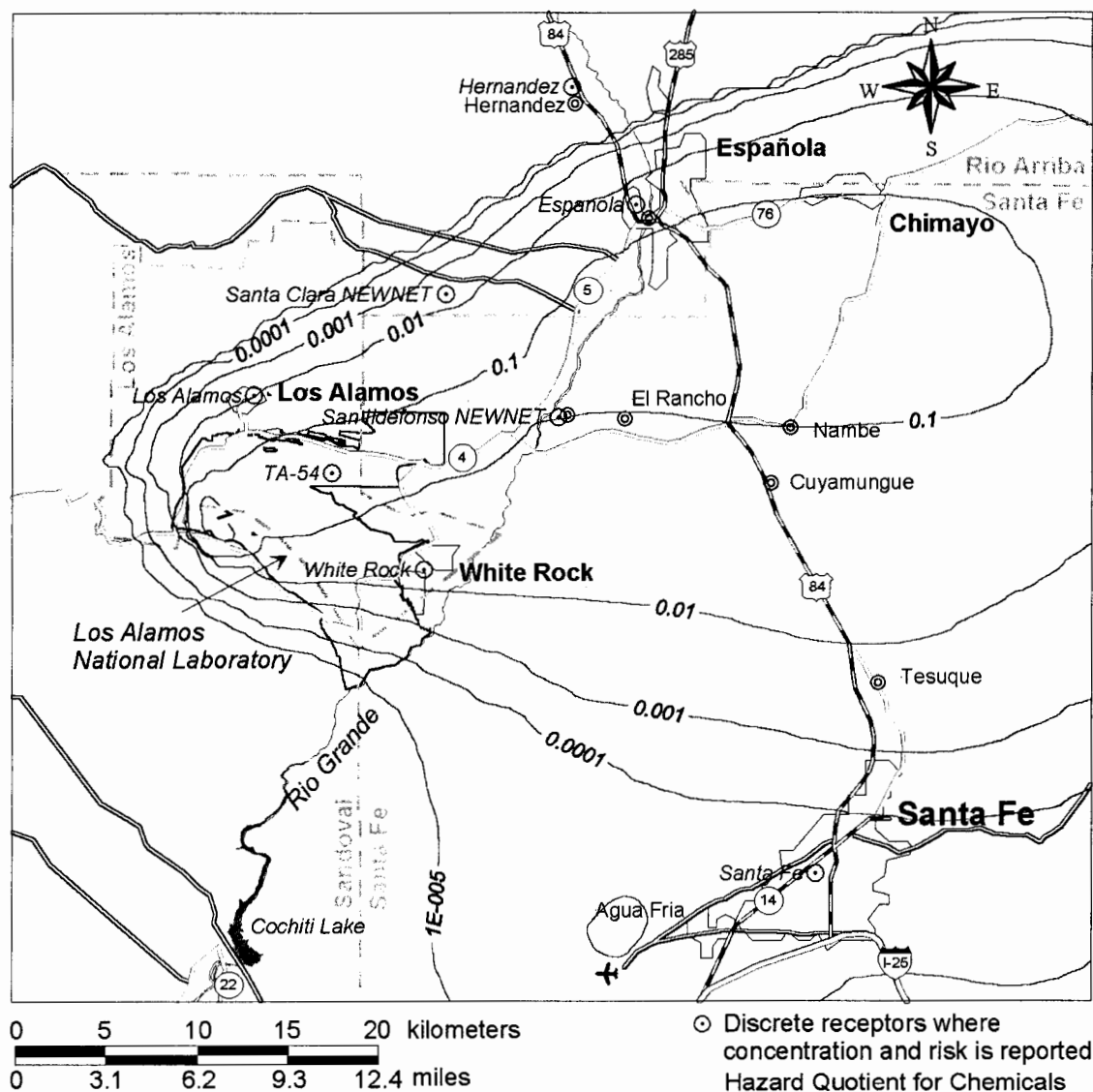


Figure 5-1. Isopleth map of the Hazard Quotient in the model domain from chemical sources in burned PRS units for the adult resident scenario. Risks include both particulate and volatile releases.

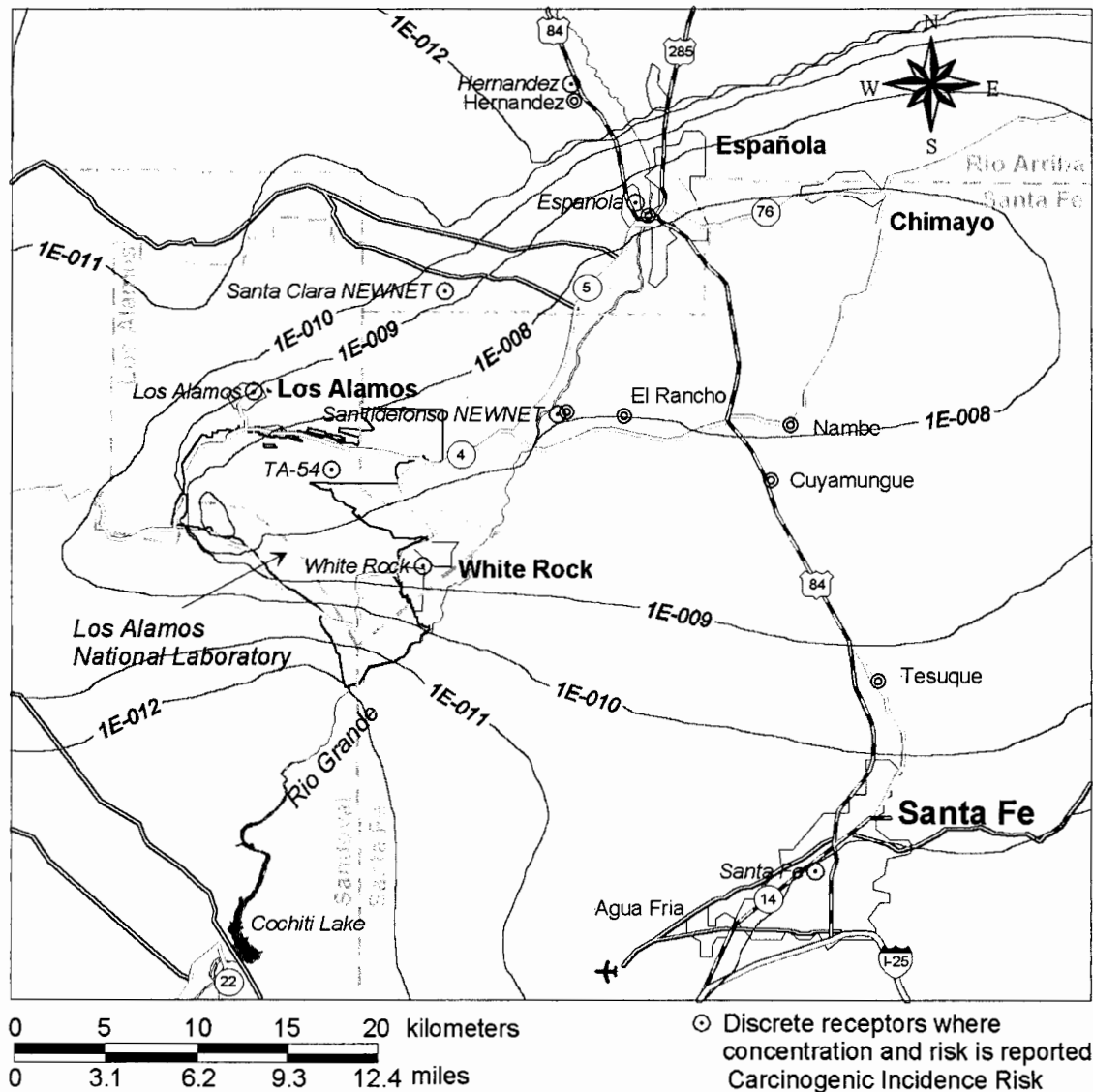


Figure 5-2. Isopleth map of incremental cancer risk in the model domain from chemical sources in burned PRS units for the adult resident scenario. Risks include both particulate and volatile releases.

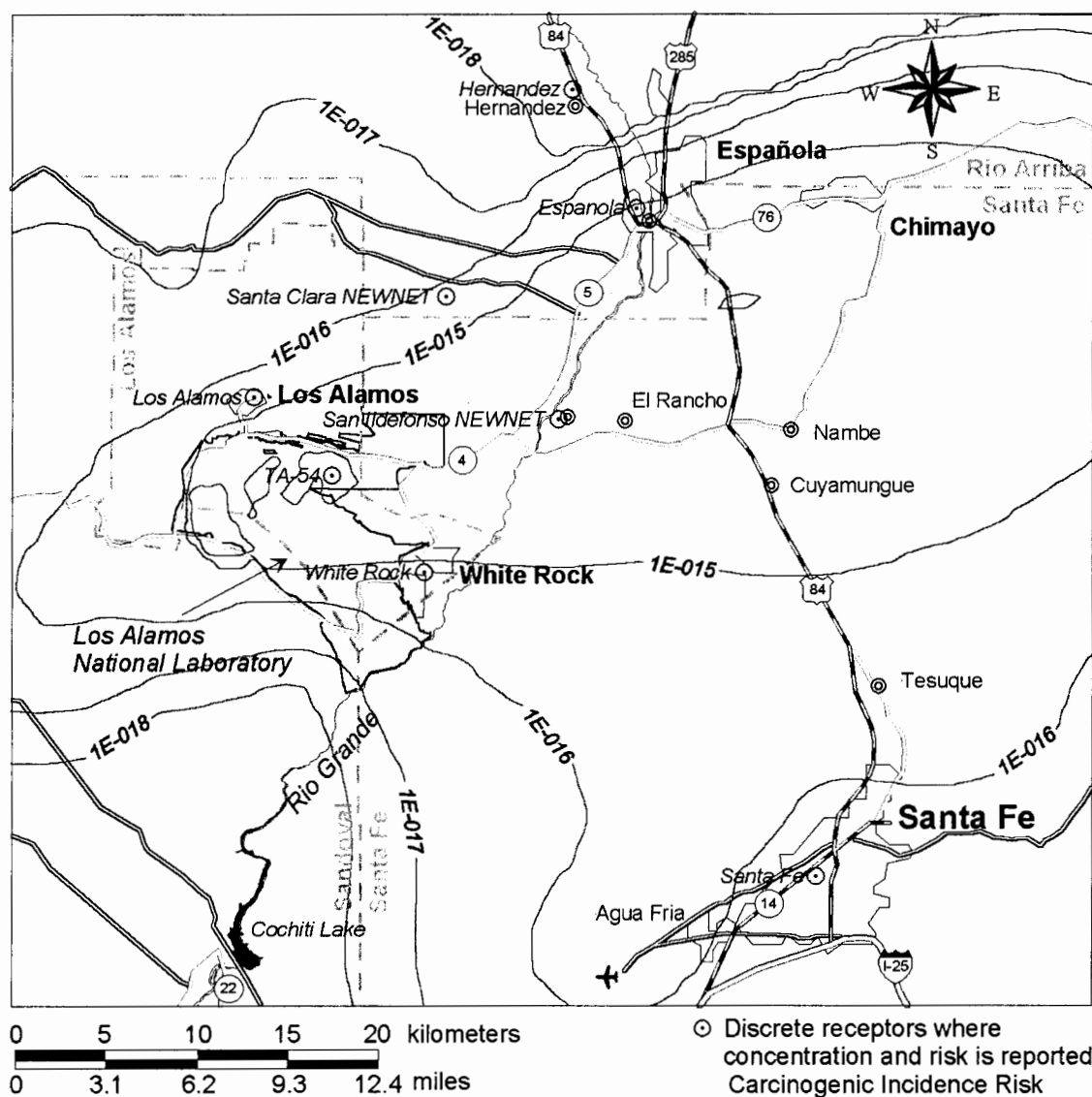


Figure 5-3. Isopleth map of incremental cancer risk in the model domain from radionuclide sources in burned PRS units for the adult resident scenario.

6 SUMMARY AND CONCLUSIONS

We used modeled air concentrations instead of measurement data to estimate exposure and risk from radionuclides and chemicals released from PRSs during the Cerro Grande Fire. We took this approach because measured concentrations of radionuclides and chemicals did not have the temporal and spatial coverage necessary to calculate exposure and risk throughout the model domain. Additionally, ambient air concentrations were lacking for many of the radionuclides and chemicals of potential concern. Because of the uncertainties inherent in modeling, the concentration and risk estimates were intended to error on the side of conservatism.

6.1 Risk Estimates

The cancer risk estimates for carcinogens and HQs for noncarcinogens potentially released from contaminated areas of LANL (PRSs) and from natural vegetation (analyzed in Appendix D) that burned during the Cerro Grande Fire are summarized in Table 6-1. The cancer risks from inhaled radionuclides and chemicals that were potentially released to air from PRSs that burned during the Cerro Grande Fire were all below the range of acceptable risks defined by EPA (10^{-6} to 10^{-4}). For radionuclides, the maximum cancer risk from PRS sources was 6.7×10^{-14} . For chemical carcinogens, the maximum cancer risk from PRS sources was 2.1×10^{-7} and was dominated by the explosive RDX. We believe the source term for RDX was overestimated because direct data were lacking. The locations of maximum cancer risk were restricted to the active burn area.

In comparison, the cancer risks from inhaled radionuclides and chemicals that were present in and on the forest vegetation that burned in the Cerro Grande Fire were greater (see Appendix D) than the cancer risks from contaminated PRSs that burned. The maximum lifetime cancer incidence risk for radionuclides from burning forest vegetation was 4.9×10^{-7} for the adult resident scenario, which was orders of magnitude larger than the risk of 6.7×10^{-14} from burned PRSs. For carcinogenic chemicals, the maximum lifetime cancer incidence risk from burning vegetation was 4.4×10^{-7} , about a factor of 2 greater than the risk of 2.1×10^{-7} calculated for the PRS-derived chemicals. Some radionuclides and chemicals on vegetation in the burn area may be of LANL origin, but for the most part, they were naturally occurring or the result of worldwide fallout from weapons testing or industrial practices (see Appendix D).

The total maximum HQ values for both the PRS-derived contaminants and natural vegetation were greater than the generally acceptable value of 1.0 (Table 6-1). However, calculation of the HQ was complicated by the application of chronic reference doses (RfDs) to subchronic exposures because subchronic RfDs were not available for many of the assessed chemicals. The chronic RfDs are derived for a 30-year exposure period, whereas subchronic values are derived for a 2-week to 7-year exposure duration. The Cerro Grande Fire lasted for 2 weeks. Based on the use of chronic RfDs to express subchronic exposure, HQ values exceeded the acceptable value of 1.0 for both the PRS-derived chemicals and those in and on natural vegetation.

Table 6-1. Maximum Estimated Risks by Scenario, Contaminant Type, and Source

Releases from PRSs		Lifetime cancer incidence risk (carcinogens)		Hazard quotient (noncarcinogens)
Scenario		Radionuclides	Chemicals	Chemicals
Resident adult		6.7×10^{-14}	2.1×10^{-7}	2.0
Firefighter		1.0×10^{-13}	3.6×10^{-7}	3.4
Emergency response person		6.9×10^{-14}	2.2×10^{-7}	2.1
Resident child		2.6×10^{-14}	3.1×10^{-7}	2.9
Important radionuclides and chemicals		$^{238,239}\text{Pu}$, ^{231}Pa , ^{226}Ra	RDX	RDX, HMX, TNT, DNB
Releases from natural vegetation^a		Lifetime cancer incidence risk (carcinogens)		Hazard quotient (noncarcinogens)
Scenario		Radionuclides	Chemicals	Chemicals
Resident adult		4.9×10^{-7}	4.4×10^{-7}	142 ^c
		4.1×10^{-7b}		0.78 ^d
Important radionuclides and chemicals		^{210}Pb , ^{210}Po , ^{226}Ra	Cr	Mn ^c , Al ^c , Ba ^d , Cr ^d , Fe ^d

^a See Appendix D for details.^b Based on release of radionuclides inventories in litter and bark only.^c HQ based on chronic RfD for manganese and aluminum. Manganese and aluminum dominate the HQ.^d HQ based on RfDs derived from the 8-hour National Institute for Occupational Safety and Health standard for manganese and aluminum. Dominant metals are barium, chromium, and iron.

The maximum HQ for PRS-derived noncarcinogenic metals and chemicals was 2.0 for the resident adult scenario (Table 6-1). This HQ was driven primarily by the explosive compounds 1,3-dinitrobenzene (DNB) (11.2% of total HQ), HMX (13.1% of total), RDX (51% of total), and 2,4,6-trinitrotoluene (TNT) (23.4%). These are man-made compounds that do not occur naturally. The spatial extent of excursions above the 1.0 HQ level was limited to the active burn areas on LANL property. The estimated concentrations of these explosives in air during the fire were high relative to the other noncarcinogenic chemicals, which were mostly metals and other organic chemicals, primarily because of the large soil inventories calculated for these compounds. Data from soil sampling performed after the fire did not support the model-estimated deposition of the explosive compounds in the model domain, which suggested that the relatively high concentrations calculated in both air and soil could be attributed to either gross overestimation of the source term, significant degradation of these compounds during transit, or some combination of these factors. Conservative assumptions included maximizing the potential soil inventory, maximizing the soil temperatures during the burn, ignoring potential degradation processes in air, and the use of chronic oral RfD values to assess subchronic inhalation exposures. All of these factors contributed to what we think are an overestimation of risk in the model domain for these compounds. Excluding these four compounds from the risk estimate resulted in a maximum HQ value of 0.017.

The HQ for metals released from the burning of natural vegetation was 142 for the adult resident scenario (Table 6-1). Excursion above a HQ of 1.0 was widespread and included most of the major population centers. However, we are certain this is a significant overestimate of

noncancer health effects because the RfD values for the chemicals most responsible for the high HQ values (manganese and aluminum) were based on chronic exposure. Additionally, there appears to be some controversy within available literature regarding the toxicity of these metals. The RfD values given in Appendix E, converted to reference concentrations, are about 4 orders of magnitude less than the occupational exposure limits. Using RfD values derived from occupational exposure limits results in no excursions above the HQ limit of 1.

The risks calculated for the radionuclides and metals on vegetation are characteristic of all forest fires and would not be expected to be appreciably different at a location far removed from LANL.

Impacts from the pollutants emitted by the fire (PM₁₀, PM_{2.5}, CO, CO₂, and CH₄) were also likely to be greater than the risks posed by the release of radionuclides and chemicals from PRSs that burned during the fire. Both measured and modeled particulate matter concentrations (PM₁₀ and PM_{2.5}) showed that, at various times and in various locations in the model domain during the Cerro Grande Fire, PM₁₀ and PM_{2.5} concentrations were above ambient air quality standards and were sufficient to cause adverse health effects; however, these effects were not quantified. While researchers have published factors that estimate health effects such as the increase in daily mortality from exposure to PM₁₀ (Delfino et al. 1997; Zanobetti et al. 2000; Gauderman et al. 2000; Costa 2001; WHO 2000), application of these factors to environmental concentrations has not been fully explored. In contrast, risk factors for radionuclides and chemicals that have been published by the EPA include specific methodology on how to apply them to environmental exposures. The EPA has been reviewing PM₁₀ standards but so far has not revised its current 24-hour standard of 150 $\mu\text{g m}^{-3}$. Health impacts of PM₁₀ and PM_{2.5} and other pollutants released during a forest fire are discussed further in Appendix F. Particulate matter emissions are a problem for all forest fires, especially smoldering fires. Therefore, increases in PM emissions during the Cerro Grande Fire were not due to the presence of the LANL site, rather they were created primarily by the large amount of materials that burned during the entire progression of the fire.

6.2 Risks to Representative Individuals

Of the different representative individuals considered, the health risks to the firefighter from all sources were greatest. This is not surprising because the firefighter inhaled the largest volumes of air. For this assessment, we calculated the risks to representative individuals throughout the entire model domain assuming the individual remained at that location throughout the entire 2-week period of the fire. Evacuation of residents and civilians was not accounted for in the assessment; therefore, the risks for those locations will be overestimated.

For carcinogenic and noncarcinogenic chemicals, the resident child exposure scenario had the second highest risk and HQ, respectively. For radionuclides, the emergency response person scenario had the second highest risk. This difference between radionuclides and chemicals is due to the inclusion of body weight in the chemical risk calculation. Although the child breathes less air (therefore, has a lower overall intake), their average daily intake per unit body weight is actually higher because the child weighs less than the adult.

We should note that the radionuclide risk coefficients represent population-averaged values and are not specific to either a child or an adult of a specific age. Therefore, the risks to the

hypothetical individuals do not reflect age-specific differences in the dosimetry but only age (and behavior) differences between hypothetical individuals.

6.3 Risks to Communities Outside the Model Domain

Risks to communities outside the model domain may be extrapolated from the ground-level PM10 concentrations in communities within the model domain and PM10 concentrations at heights above the ground surface estimated in the northeast corner of the model domain. Twenty-four hour average PM10 concentrations were approximately equal in Española and 4921 ft (1500 m) above ground level in the northwest corner of the model domain for May 11, the day the largest acreage of forest burned and the fire spread across LANL. This was also the day a high PM10 concentration was measured in air at Taos ($37 \mu\text{g m}^{-3}$ averaged over 24-hours). Therefore, the risks calculated at Española were roughly equivalent to the risks incurred in communities northeast of the model domain, which includes Taos. For communities west of the model domain, risks were expected to be significantly lower because the prevailing winds during the fire drove the smoke plume to the east.

6.4 Conservatism and Uncertainty in the Risk Estimates

Modeling radionuclide and chemical releases from the Cerro Grande Fire was not straightforward because there was scant information readily available about the materials present at LANL that might be suspended into the atmosphere during the fire. Therefore, the modeling had to encompass the uncertainties associated with estimating the inventories of radionuclides and chemicals present before the fire, the amounts that were released during the fire, and their subsequent dispersion and deposition in the environment.

Table 6-2 summarizes our qualitative estimate of the level uncertainty and conservatism for each aspect of the exposure risk calculation from PRS releases. Conservatism is analogous to a positive bias (overestimation) in the estimated quantity. Uncertainty addresses the precision of the estimated quantity.

The calculated inventories and resulting source term values probably contributed most to the overall uncertainty and conservatism of the risk estimates—probably overestimating them in the range of a factor of 10 or 100. Conversely, if the radionuclides and chemicals released during the fire behaved similarly to the PM10 emissions, then we would expect only about a factor of 2 uncertainty in the dispersion estimate based on the model calibration to measured PM10 values. Our use of the PRS characterization data probably resulted in an estimate of the highest, or bounding, concentrations that could be expected at any PRS. We assumed a high soil temperature and severe or moderate burn over the PRS area. We estimated source terms for volatile chemicals assuming that the entire inventory calculated for each PRS was completely volatilized and released into the air during the fire. Our estimate of air concentrations did not consider removal or degradation of chemicals. Although not factoring in the degradation rate may contribute to the high risk estimates for some chemicals, this approach did not address toxic byproducts of degradation that may be formed. Estimating degradation rates and formation of byproducts was beyond the scope of this project.

We chose exposure parameters (like physical activity levels) for the representative individuals to represent a realistic but maximum upper bound estimate. While the choice of

exposure parameters was intentionally biased high, their overall impact on the estimated risks was probably minimal because of the high uncertainties related to the release and transport of radionuclides and chemicals overwhelm their influence.

The HQs for the noncarcinogenic chemicals were calculated using RfDs, many of which were derived from studies of chronic exposure. Although it depends greatly on the mechanism of action, using chronic RfDs to assess the health effects from subchronic exposures generally results in higher HQ estimates.

Table 6-2. Summary of Conservatism and Uncertainty in Each Modeling Component of the Exposure and Risk Calculation

Modeling component	Estimated conservatism ^a	Estimated uncertainty ^b	Comments
Radionuclide or chemical inventories	Unknown (2–≥10)	≥10×	Radionuclide and chemical inventories at PRSs were based on maximum detected concentrations.
Release of radionuclides and particulate chemicals	≤2	≥10×	Particulate releases were based on a resuspension rate constant reported in the literature. Releases were assumed to occur during the burning and smoldering phase of the fire.
Release of volatile chemicals	≥10	≥10×	One-hundred percent of the volatile chemical inventory was assumed to be released.
Atmospheric transport- particles	≤2	2×	Estimated conservatism and uncertainty is based on the assumption that particulate releases followed the same trend as PM10 emissions from the fire and behaved like PM10 in the atmosphere.
Atmospheric transport- volatiles	2–10	2×	Estimated conservatism and uncertainty is based on the assumption that volatile releases followed the same trend as CO emissions from the fire and behaved like a non-reactive tracer.
Exposure scenario assumptions	2–10	2–10×	
Radionuclide risk coefficients	2–10	2–10×	Population averaged risk coefficients were used to calculate risks for specific individuals.
Slope factors	≥10	≥10×	
Hazard quotients	≥10	≥10×	Use of chronic RfDs to express subchronic exposure may have resulted in large overestimates of noncancer health effects.
Overall cancer risk	2–10	≥10×	
Overall noncancer health effect	≥10	≥10×	Use of chronic RfDs to represent subchronic exposure biased the noncancer health effects high for some chemicals.

^a The rating system is as follows: ≥10 equates to a factor of 10 or greater conservatism; 2–10 equates to a factor greater than 2 but less than 10 conservatism; ≤2 equates a factor of 2 or less conservatism.

^b The rating system is as follows: ≥10× equates to a factor of 10 (×÷10) or greater uncertainty; 2–10× equates to a factor >2 but <10 uncertainty; 2× equates to factor of ≤2 (×÷2) uncertainty.

For the explosive compounds described earlier, we used oral RfDs because inhalation RfDs were not reported or have not been derived. EPA Regional Preliminary Remedial Goals Tables

(EPA 2001) list the oral RfD value as both the oral and inhalation value for all four of these chemicals, as well as several other chemicals identified as potential contributors to noncancer health effects. In the supporting documentation for the Preliminary Remedial Goals, the EPA explains that the values are intended to be screening values and that oral RfD values were used for both oral and inhaled exposures for compounds lacking inhalation values. They acknowledge that the appropriateness of this assumption for specific contaminants has not been verified (EPA 1997). There is neither a simple nor direct relationship between inhalation RfDs and oral RfDs, and deriving one from the other is complex. It involves an understanding of the comparative inhaled dose, physical characteristics of the toxicant, behavior in the respiratory tract, mechanisms of action, absorption, excretion, and metabolism (EPA 2002). Converting the oral RfDs for the purposes of this project was beyond the scope of the work. Federal facilities, like LANL, have had much experience in handling these compounds over the years, and may have more information about the inhalation toxicology of these compounds than we found in EPA and ATSDR sources. Using chronic oral RfD values to assess exposures best reflected by subchronic inhalation RfD values contributed greatly to the conservatism of this approach to estimating health risk (EPA 2001).

We rated the overall conservatism of the risk estimates as moderate and the uncertainty as high. We chose a moderate conservatism rating because it is difficult to judge the level of conservatism of the assumption that the release of radionuclides and chemicals from PRSs followed the same general trend of pollutants released from fire. Depending on the circumstances, this assumption could lead either to an underestimation or overestimation of air concentration. Additionally, we have not included in our assessment airborne releases of radionuclides and chemicals that could have occurred after the area burned. We think the uncertainty in our risk estimates is high, and they should be interpreted as order-of-magnitude estimates. If we consider only radionuclides and carcinogenic chemicals, the upper bound risk estimates from PRSs (assuming a factor of 100 uncertainty) are still relatively low. Noncarcinogenic chemicals showed potential health effects and the circumstances regarding the high risk estimates were discussed earlier.

Other potential contaminant sources in air included suspension from contaminated areas that did not burn, suspension of contaminants from PRSs following burning, and suspension from previously deposited materials. These sources were not evaluated as part of this study. One contaminant of concern, ^{239}Pu , was measured by the EPA at Tsankawi National Monument on May 15 (after the fire burned across LANL) at a concentration of 8800 aCi m^{-3} , a concentration that far exceeded any value ever measured in air historically at LANL. Although that concentration was measured only on 1 day and presumably represents a 24-hour average (the exact sampling time was not provided), when we assumed that a person stood in that location and inhaled that concentration in air for the entire 2-week duration of the fire, the estimated cancer risk was 8.2×10^{-8} , a low level of risk. Such evaluations, however, could only be made for contaminants actually measured in air, and many of the contaminants analyzed in the air samples collected during the fire were at levels below detection limits.

6.5 Conclusions

The release of radionuclides and chemicals into the air from contaminated sites at LANL that burned during the Cerro Grande Fire resulted in minimal increases in cancer risk to exposed individuals. It was not possible to draw firm conclusions regarding the health risks associated with releases of noncarcinogenic chemicals from these sites. Hazard quotients for these exposures exceeded 1.0. We believe the estimated noncancer HQs are overly conservative and do not reflect the actual health effect impacts that occurred, largely because risk factors derived for chronic exposure circumstances had to be used to assess the subchronic exposure.

The amounts of LANL-derived radionuclides and chemicals deposited on the ground during the fire were estimated to be too small to be detected, with the exception of 3 chemical explosives. Post-fire sampling by LANL indicated no detectable presence of these explosive compounds in soil, which suggests the source term estimates for these compounds are overestimates.

In contrast, the risk of cancer from exposure to radionuclides and metals in and on vegetation that burned was greater than that from radionuclides and chemicals released from contaminated sites at LANL. In the case of radionuclides, cancer risks from radionuclides on vegetation were several orders of magnitude higher compared to cancer risks from PRS-derived radionuclides. All cancer risks were below the EPA range of acceptable risks of 10^{-6} to 10^{-4} .

Particulate matter emissions are a problem for all forest fires, especially smoldering fires, and were not unique to the Cerro Grande Fire. The impact of particulate matter emissions and other pollutants emitted by all fires (eg. CO, CO₂, and CH₄) was likely greater than the health risks posed by the release of radionuclides and chemicals from PRSs that burned during the fire. Both measured and modeled particulate matter concentrations (PM₁₀ and PM_{2.5}) showed that, at various times and in various locations during the Cerro Grande Fire, PM₁₀ and PM_{2.5} concentrations were above ambient air quality standards and were sufficient to cause adverse health effects; however, these effects were not quantified. While researchers have published factors that estimate health effects, such as the increase in daily mortality from exposure to PM₁₀, application of these factors to environmental concentrations has not been fully explored. The reader is referred to Appendix F for a more in-depth discussion of these matters.

7 REFERENCES

- Amiro, B.D., S.C. Sheppard, F.L. Johnston, W.G. Evenden, and D.R. Harris. 1996. "Burning Radionuclide Question: What Happens to Iodine, Cesium, and Chlorine in Biomass Fires?" *The Science of the Total Environment*. 187: 93–103. March.
- Apostoaeci, A.I., B.G. Blaylock, B. Caldwell, S. Flack, J.S. Gouge, F.O. Hoffman, C.J. Lewis, S.K. Nair, E.W. Reed, K.M. Thiessen, B.A. Thomas, and T.E. Widner. 1999. *Radionuclides Released to the Clinch River from White Oak Creek on the Oak Ridge Reservation—An Assessment of Historical Quantities Released, Off-Site Radiation Doses, and Health Risks*. Oak Ridge Dose Reconstruction, Volume 4. ChemRisk, A Service of McLaren/Hart, Alameda, California. July.
- ATSDR (Agency for Toxic Substances and Disease Registry) 2001a. *Toxicological Profiles*. List updated March 8, 2001. <http://www.atsdr.cdc.gov/toxpro2.html> (August 28, 2001).
- Balice R.G., J.D. Miller, B.P. Oswald, C. Edminster, and S.R. Yool. 2000. *Forest Surveys and Wildfire Assessment in the Los Alamos Region; 1998–1999*. LA-13714-MS. Los Alamos National Laboratory, Los Alamos, New Mexico.
- Bevington, P.R. and D.K. Robinson. 1992. *Data Reduction and Error Analysis for the Physical Sciences, Second Edition*. New York: McGraw-Hill Inc.
- Boethling, R. and D. Mackay (eds.) 2000. *Handbook of Property Estimation Methods for Chemicals: Environmental and Health Sciences*. Boca Raton: CRC Press LLC.
- Bruce, G.M., J.E. Buddenbaum, J.K. Cockroft, S.M. Flack, R.E. Burmeister, T. Ijaz, and T.E. Widner. 1999. *Screening Level Evaluation of Additional Potential Materials of Concern*. Oak Ridge Dose Reconstruction, Volume 6. ChemRisk, A Service of McLaren/Hart, Alameda, California. July.
- Burgess, C.E., J.D. Woodyard, K.A. Rainwater, J.M. Lightfoot, B.R. Richardson, and A.L. Woods. 1998. *Literature Review of the Lifetime of DOE Materials: Aging of Plastic Bonded Explosives and the Explosives and Polymers Contained Therein*. ANCRP-1998-12. Amarillo National Resource Center for Plutonium.
- Chandler, C., P. Cheney, P. Thomas, L. Traub, and D. Williams. 1983. *Fire in Forestry. Vol. 1: Forest Fire Behavior and Effects*. New York: John Wiley & Sons.
- Costa, D. 2001 "Air Pollution". In: *Casarett and Doull's Toxicology*. 6th edition. Edited by C.D. Klaassen. McGraw-Hill, New York. 979-1012.
- DeBano, L.F., S.M. Savage, and D.A. Hamilton. 1976. "The Transfer of Heat and Hydrophobic Substances during Burning." *Soil Science Society of America Journal* 40: 779–782.

- Delfino, R.J., A.M. Murphy-Moulton, R.T. Burnett, J.R. Brook, and M.R. Becklake. 1997. "Effects of Air Pollution on Emergency Room Visits for Respiratory Illnesses in Montreal, Quebec." *American Journal of Respiratory and Critical Care Medicine*, Vol. 155:568-576.
- DOE (U.S. Department of Energy). 2000. *Special Environmental Analysis: Actions Taken in Response to the Cerro Grande Fire at Los Alamos National Laboratory, Los Alamos, New Mexico*. DOE/SEA-03. U.S. Department of Energy, Los Alamos Area Office, Los Alamos, New Mexico.
- Eckerman, K.F., R.W. Leggett, C.B. Nelson, J.S. Puskin, and A.C.B. Richardson. 1999. *Cancer Risk Coefficients for Environmental Exposures to Radionuclides*. Federal Guidance Report No. 13. EPA 402-R-99-001. Office of Radiation and Indoor Air, U.S. Environmental Protection Agency, Washington, DC. September.
- EPA (U.S. Environmental Protection Agency). 1987. *On-Site Meteorological Program Guidance for Regulatory Modeling Applications*. EPA-450/4-87-013. Research Triangle Park, North Carolina.
- EPA. 1991. *Role of the Baseline Risk Assessment in Superfund Remedy Selection Decisions*. Memorandum from Assistant Administrator Don R. Clay to the Regions. OSWER Directive 9355.0-30. Office of Solid Waste and Emergency Response, Washington, DC. April 22.
- EPA. 1992. *User's Guide for the Industrial Source Complex (ISC) Dispersion Models, Vol 1, User's Instructions*. EPA-450/4-92-008a. Research Triangle Park, North Carolina.
- EPA. 1997. *EPA Region IX Preliminary Remedial Goal Tables*. U.S. Environmental Protection Agency, Region IX. San Francisco, California. January.
- EPA. 1997. *Establishment of Cleanup Levels for CERCLA Sites with Radioactive Contamination*. Memorandum from Stephen D. Luftig, Director, Office of Emergency and Remedial Response and Larry Weinstock, Acting Director, Office of Radiation and Indoor Air. OSWER 9200.4-18. Office of Solid Waste and Emergency Response, Washington, DC. August 22.
- EPA. 1999. *Exposure Factors Handbook*. EPA/600/C-99/001. Office of Research and Development, Washington, DC. February.
- EPA. 2001. *Region III Risk-Based Concentration Table*. U.S. Environmental Protection Agency, Region III. Philadelphia, Pennsylvania. September.
- EPA. 2002. IRIS Hotline. ARSC Aerospace Corporation. Contractor for the EPA, National Center for Environmental Assessment. Cincinnati, Ohio.
- Fire Investigation Team. 2000. *Cerro Grande prescribed fire May 4-8, 2000: Investigation report May 18, 2000*. US Department of the Interior, National Park Service; US Department of the

- Interior, Bureau of Land Management; US Department of Agriculture, Forest Service; US Department of Energy; and New Mexico Energy, Minerals & Natural Resources Department, Forestry Division. National Interagency Fire Center. Boise, Idaho.
- Fresquez, P.R. 2000a. LANL Ecology Group, ESH-20, Letter to the Santa Fe Farmers Market Task Force. Subject: Results of Trace Elements in Soils from Gardens Downwind of the Cerro Grande Fire. July 28.
- Fresquez, P.R. 2000b. LANL Ecology Group, ESH-20, Letter to the Santa Fe Farmers Market Task Force. Subject: Preliminary Results of Radionuclides and Radioactivity in Soils from Local Farms Downwind of the Cerro Grande Fire: Data to Date. August 10.
- Fresquez, P.R. 2000c. LANL Ecology Group, ESH-20, Letter to the Santa Fe Farmers Market Task Force. Subject: Results of Radionuclides and Radioactivity in Soils from Local Farms Downwind of the Cerro Grande Fire (Raw Data). August 24.
- Fresquez, P.R. 2000d. LANL Ecology Group, ESH-20, Letter to the Santa Fe Farmers Market Task Force. Subject: Results of Trace Elements in Soils from Gardens Downwind of the Cerro Grande Fire (Raw Data). August 24.
- Fresquez, P.R. 2000e. LANL Ecology Group, ESH-20, Letter to the Santa Fe Farmers Market Task Force. Subject: Results of Organic Constituents in Soils from Local Farms Downwind of the Cerro Grande Fire. September 7.
- Fromm, J. 1996. INEEL Environmental Toxicologist, Remediation Bureau. Memo to INEEL WAG Managers and Technical Support Staff. Subject: Radionuclide Risk-Based Concentration Tables. January 3.
- Gauderman, J.W., R. McConnell, F. Gilliland, S. London, D. Thomas, E. Avol, H. Vora, K. Berhane, E.B. Rappaport, F. Lurmann, H.G. Margolis, and J. Peters. 2000. "Association between Air Pollution and Lung Function Growth in Southern California Children". *American Journal of Respiratory and Critical Care Medicine*, Vol. 162:1383-1390.
- Gillette, D.A. 1974. "On the Production of Soil Wind Erosion of Soil: Effect of Wind and Soil Texture" *Atmospheric and Gaseous Pollutants* ERDA Symposium Series 38. Oak Ridge, Tennessee. 591-609.
- Golden Software Inc. 1999. Surfer Version 7. Golden Software Inc, Golden Colorado.
- Hicks, B.B. 1982. *Critical Assessment Document on Acid Deposition*. ATDL Contribution File No. 81/24. Atmospheric Turbulence and Diffusion Laboratory, NOAA, Oak Ridge Tennessee.

- HSDB® (Hazardous Substances Data Bank). TOXNET® (Toxicology Data Network), National Library of Medicine. Last updated April 18, 2001. <http://toxnet.nlm.nih.gov/cgi-bin/sis/htmlgen?HSDB> (August 24, 2001).
- Interagency BAER Team. 2000. Bureau of Indian Affairs, Pueblo of Santa Clara, Pueblo of San Ildefonso, Department of Energy, Los Alamos National Laboratory, City and County of Los Alamos, NM, National Park Service, Bandelier National Monument, U.S. Forest Service, Santa Fe National Forest. *Cerro Grande Fire Burned Area Emergency Rehabilitation (BAER) Plan*. Los Alamos, New Mexico.
- ICRP (International Commission on Radiological Protection). 1991. *Recommendations of the International Commission on Radiological Protection*. Oxford: Pergamon Press. ICRP Publication 60. Ann. ICRP 21, No. 1–3.
- Kashparov, V.A., S.M. Lundin, A.M. Kadygrib, V.P. Protsak, S.E. Levchuk, V.I. Yoschenko, V.A. Kashpur, and N.M. Talerko. 2000. "Forest Fires in the Territory Contaminated as a Result of the Chernobyl Accident: Radioactive Aerosol Resuspension and Exposure of Fire-Fighters." *Journal of Environmental Radioactivity* 51: 281–298.
- LANL (Los Alamos National Laboratory). 2000. A Special Edition of the SWEIS Yearbook Wildfire. LA-UR-00-3471. Los Alamos National Laboratory, Los Alamos, New Mexico. August.
- Layton, D.W. 1993. "Metabolically Consistent Breathing Rates for Use in Dose Assessments." *Health Physics* 64 (1): 23–36.
- Lide, D.R. (ed.). 1998. *CRC Handbook of Chemistry and Physics, 79th Edition*. Boca Raton: CRC Press, Inc.
- McAtee, J.L. 2001. *Response to Request for Information on Structures Impacted by the Cerro Grande Fire at Los Alamos National Laboratory*. ESH-DO:01-138. Los Alamos National Laboratory, Los Alamos, New Mexico. October 30.
- Mohler, H.J., K.R. Meyer, J.W. Aanenson, and H.A. Grogan. 2002. *Analysis of Exposure and Risks to the Public from Radionuclides and Chemicals Released by the Cerro Grande Fire at Los Alamos. Task 3: Calculating and Communicating Risks: Observations and Recommendations*. RAC Report No.15-NMED-2001-FINAL(Rev.1). Risk Assessment Corporation, Neeses, South Carolina. June 12.
- National Research Council. 1995. *Radiation Dose Reconstruction for Epidemiologic Uses*. Washington D.C.: National Academy Press. ISBN 0-309-05099-5.
- NCRP (National Council on Radiation Protection and Measurements). 1993. *Limitation of Exposure to Ionizing Radiation*. NCRP Report No. 116.

- NIOSH (National Institute for Occupational Safety and Health). 1994. *Pocket Guide to Chemical Hazards*. U.S. Department of Health and Human Services, Public Health Service, Centers for Disease Control and Prevention. Washington, DC. U.S. Government Printing Office.
- NMED (New Mexico Environment Department). 2000. Press release dated May 19, 2000.
- Ottmar, R.D. 1983. "Predicting Fuel Consumption by Fire Stages for Developing Prescribed-Fire Strategies to Reduce Smoke." *Proceedings of the Northwest Fire Council Annual Meeting*; 1983 November 21–22, Olympia, Washington. 87–106.
- Pleim, J., A. Venkatram, and R.J. Yamartino. 1984. *ADOMT/TADAP model development program. Volume 4; the Dry Deposition Model*. Ontario Ministry of the Environment, Rexdale, Ontario, Canada.
- Popp, C.J., R.S. Martin, and R. Arimoto. 2001. "Atmospheric Effects of Large Fires: Spring 2000 Cerro Grande, NM (Los Alamos) Fire." A Millennium Symposium on Atmospheric Chemistry: Past, Present, and Future, Sponsored by the American Meteorological Society. January 14–18, 2001, Albuquerque New Mexico.
- RAIS[®] (Risk Assessment Information System). "Chemical-Specific Factors." Oak Ridge National Laboratory. http://risk.lsd.ornl.gov/cgi-bin/tox/TOX_select?select=csf (August 22, 2001).
- Raison, R.J., P.K. Khanna, and P.V. Woods. 1985. "Transfer of Elements to the Atmosphere during Low-intensity Prescribed Fires in Three Australian Subalpine Eucalypt Forests." *Canadian Journal of Forest Research* 15: 657–664.
- Rocco, J.R., K.R. Meyer, H.J. Mohler, J.W. Aanenson, L. Hay Wilson, A.S. Rood, and P.D. McGavran. 2002. *Analysis of Exposure and Risks to the Public from Radionuclides and Chemicals Released by the Cerro Grande Fire at Los Alamos. Task 2.7: Estimated Risks from Releases to Surface Water*. Final Report, RAC Report No.4-NMED-2002-FINAL(Rev.1). Risk Assessment Corporation, Neeses, South Carolina. June 12.
- Rood, A.S. and H.A. Grogan. 1999. *Estimated Exposure and Lifetime Cancer Incidence Risk from 903 Area Plutonium Releases at the Rocky Flats Plant*. RAC Report No. 1-CDPHE-RFP-1999-FINAL. Prepared by Radiological Assessments Corporation, Neeses, SC, for Colorado Department of Public Health and Environment (www.cdphe.state.co.us/rf). August.
- Roy, M. and C. Courtay. 1991. "Daily Activities and Breathing Parameters for Use in Respiratory Tract Dosimetry." *Radiation Protection Dosimetry* 35 (3): 179–186.
- Lide, D.R. (ed.). 1991. *CRC Handbook of Chemistry and Physics, 72nd Edition*. Boca Raton: CRC Press, Inc.
- Sandberg, D.V. and R.D. Ottmar. 1983. "Slash Burning and Fuel Consumption in the Douglas-fir Subregion." *Proceedings of the 7th American Meteorological Society Conference in Fire and Forest Meteorology*, April 25–29, 1983, Fort Collins Colorado. American Meteorological Society, Boston Massachusetts. 90–93.

- Sandberg, D.V. and Peterson, J. 1984. "A Source Strength Model for Prescribed Fires in Coniferous Logging Slash." Annual Meeting of the Air Pollution Control Association, Pacific Northwest Section, November 12–14, Portland, Oregon.
- Scire, J.S., D.G. Strimaitis, and R.J. Yamartino. 1999. *A User's Guide for the CALPUFF Dispersion Model (Version 5.0)*. Earth Tech, Inc., Concord, Massachusetts.
- Shleien, B. 1992. *Scoping Document for Determination of Temporal and Geographic Domains for the HEDR Study*. Hanford Technical Steering Panel. Summer.
- Slinn, S.A. and W.G.N. Slinn. 1980. "Predictions for Particle Deposition on Natural Waters." *Atmospheric Environment* 14, 1013–1016.
- Smith, D.W. and J.H. Sparling. 1966. "The Temperatures of Surface Fires in Jack Pine Barren." *Canadian Journal of Botany* 44: 1285–1298.
- Steward, F.R., S. Peter, and J.B. Richon. 1990. "A Method for Predicting the Depth of Lethal Heat Penetration into Mineral Soils Exposed to Fires of Various Intensities." *Canadian Journal of Forest Research* 20: 919–926.
- Stinson, K.J. and H.A. Wright. 1969. "Temperatures of Headfires in the Southern Mixed Prairie of Texas." *Journal of Rangeland Management* 22: 169–174.
- Theissen, K., J.S. Hammonds, C.J. Lewis, F.O. Hoffman, and E.I. White. 1996. *Screening Method for the Oak Ridge Dose Reconstruction. Appendix A in Screening-Level Evaluation of Additional Potential Materials of Concern*. Reports of the Oak Ridge Dose Reconstruction, Vol. 6. The Report of Project Task 4. July.
- Turner, D.B. 1994. *Workbook of Atmospheric Dispersion Estimates: An Introduction to Dispersion Modeling*. Boca Raton, Florida: CRC Press Inc., Lewis Publishers.
- Ulery, A.L. and R.C. Graham. 1993. "Forest Fire Effects on Soil Color and Texture." *Soil Science Society of America Journal* 57: 135–140.
- Ward, D.E. 1999. "Smoke from Wildland Fires." USDA Forest Service Fire Chemistry Project, Missoula, Montana. In: *Health Guidelines for Vegetation Fire Events*. World Health Organization, Lima, Peru, October 6–9.
- Ward, D.E. and C.C. Hardy. 1991. "Smoke Emissions from Wildland Fires." *Environment International* 17: 117–134.
- Wells, C.G., R.E. Campbell, L.F. DeBano, C.E. Lewis, R.L. Fredriksen, E.C. Franklin, R.C. Froelich, and P.H. Dunn. 1979. *Effects of Fire On Soil*. U.S. Forest Service General Technical Report WO-7. U.S. Forest Service, Washington, D.C.

- Wesely, M.L., and B.B. Hicks. 1977. "Some Factors that Affect the Deposition Rates of Sulfur Dioxide and Similar Gases on Vegetation." *J. Air Pollution Control Association*, 27, 1110–1116.
- Whelan, R.J. 1995. *The Ecology of Fire*. Cambridge: Cambridge University Press.
- Whittaker, E. 1961. "Temperatures in Heath Fires." *Journal of Ecology* 49: 709–715.
- WHO (World Health Organization) 2000. "Health-based Guidelines." Chapter 3 in *Guidelines for Air Quality*. World Health Organization, Geneva, Switzerland.
- Williamson, G.B. and E.M. Black. 1981. "High Temperatures of Forest Fires under Pines: A Selective Advantage over Oaks." *Nature* 293: 643–644.
- Zanobetti, A., J. Schwartz, and D. Gold. 2000. "Are there Sensitive Subgroups for the Effects of Airborne Particles?" *Environ. Health Perspectives*, Vol. 108(9):841-845.

APPENDIX A

IDENTIFYING CONTAMINANTS RELEASED AS A DIRECT RESULT OF THE CERRO GRANDE FIRE BURNING AT LOS ALAMOS NATIONAL LABORATORY

APPENDIX A

IDENTIFYING CONTAMINANTS RELEASED AS A DIRECT RESULT OF THE CERRO GRANDE FIRE BURNING AT LOS ALAMOS NATIONAL LABORATORY

To determine the chemicals and radionuclides released during the Cerro Grande Fire that were a direct consequence of the Los Alamos National Laboratory (LANL) site operations requires an understanding of releases that occur during any wildfire and ambient air and soil concentrations routinely measured in the LANL vicinity. The air and soil monitoring data collected before, during, and after the fire are evaluated in Chapter 2 of this document. These data identified a small number of radionuclides that may have been released during the fire; however, the large analytical uncertainties associated with much of the data precluded a detailed evaluation of release estimates. Air monitoring also suggested that the fire released particulate matter (PM), trace elements, polyaromatic hydrocarbons (PAHs), and other organic compounds, but the data were limited and all forest fires release many of the compounds measured.

This appendix summarizes applicable air and soil monitoring data taken before, during, and after the fire. We searched for trends in the monitoring data that might reflect soil deposition of a contaminant from the smoke. We used higher contaminant concentrations in the predominant downwind direction of the smoke to help define where the plume traveled and identify contaminants deposited from the smoke. We also evaluated information in the literature about other forest fires and looked for contaminants that might not be found in the smoke from typical forest fires. We reviewed LANL reports and studies to help us understand the site's contribution to contaminants in smoke and soil. This is particularly appropriate for chemicals, for which no background air monitoring data exist, and for which little data were collected during the fire. In many cases, a qualitative analysis such as this remains the only means of evaluating chemical constituents present in the air because of the fire.

AIR MONITORING DATA

Chemical Air Monitoring Data Collected by the U.S. Environmental Protection Agency and Reviewed by the Agency for Toxic Substances and Disease Registry

The U.S. Environmental Protection Agency (EPA) placed air monitors around LANL and in surrounding towns from May 11–15, 2000. They detected metals, organic compounds, and PAHs below levels that the EPA and Agency for Toxic Substances and Disease Registry (ATSDR) consider to be of health concern (EPA 2001; ATSDR 2001). The EPA reported that all concentrations measured were less than workplace (Occupational Health and Safety Administration [OSHA]) standards (EPA 2001). These standards are designed to protect healthy workers exposed 8 hours each day, 5 days each week. They are less restrictive than standards to protect the public, which is assumed to be exposed 24 hours a day and may be more sensitive because of age, illness, and other considerations. The EPA used the OSHA standards because the time period over which the fire occurred presented shorter exposure duration than the long-term or lifetime exposures for which public standards are designed (ATSDR 2001).

ATSDR reviewed the available monitoring data collected by the various agencies for their health consultation (ATSDR 2001). They concluded that there was “not a specific health hazard

to the general public from releases of hazardous materials, either chemicals or radioactive materials, in the fire.” ATSDR compared the EPA monitoring data they received to health comparison values designed to protect the public. Some of the air concentrations ATSDR summarized in their Health Consultation are considerably higher than concentrations reported in the EPA data that *Risk Assessment Corporation (RAC)* obtained. On July 25, 2001, *RAC* received copies of the EPA data sent to ATSDR in the summer of 2000. It appears that some of the concentrations reported by EPA and ATSDR were the net weight of the sample, rather than the mass concentration measured in micrograms per cubic meter. We used concentrations in micrograms per cubic meter for our analysis.

Air Monitoring Data Collected by LANL

LANL summarized their interpretation of the air monitoring results from the Cerro Grande Fire in the *Special Edition of the SWEIS Yearbook, Wildfire 2000* (LANL 2000). LANL concluded that the increased radionuclide, PM, and chemical concentrations were typical of other wildfires and did not reflect an impact of the LANL facility.

Chapter 2 included a review of the particulate matter <10 microns (PM10) monitoring carried out by LANL, EPA, and New Mexico Environment Department (NMED). LANL and NMED do not routinely monitor oxides of nitrogen (NOx) or carbon monoxide (CO) around the LANL site. For the *Draft Year 2000 Environmental Surveillance Report*, LANL calculated NOx, CO, and PM emissions using the acreage burned, estimated fuel loading, and EPA emission factors for wildfires and prescribed burning. They did atmospheric dispersion calculations, using the EPA Industrial Source Complex model, to calculate air concentrations. Using meteorological data collected during the fire, they estimated downwind air concentrations from May 10–15, 2000. The modeled concentrations of PM compared well to measurements taken during the fire. Estimated concentrations of PM, NOx, and CO exceeded National Ambient Air Quality Standards by factors of 2 to 20 in areas close to the fire. LANL published the following table reporting area, fuel load, PM, CO, and NOx in tons (Dewart 2001).

Table A-1. Release Estimates for Particulate Matter (PM), Carbon Monoxide (CO) and Nitrogen Oxides (NOx) from LANL and non-LANL Sources during the Cerro Grande Fire

Source	PM (tons)	CO (tons)	NOx (tons)
LANL	748	6160	176
Non-LANL	6715	55300	1580
Total	7463	61460	1756

^a Source: Dewart (2001).

LANL conducted air monitoring for volatile organic compounds (VOCs), PM10, metals, and radionuclides in response to concern about emissions from Material Disposal Area-R (MDA-R), in Technical Area (TA)-16, which burned in the fire and smoldered for several weeks. MDA-R is a World War II high explosives burning area that contains elevated levels of metals and high explosives. Air sampling was done at MDA-R from June 2–16, 2000, when the area was still smoldering. No VOCs were detected above background concentrations. VOCs measured upwind and downwind of the area and at a background location were not significantly different. All of the

measurements for VOCs were more than 1000 times less than occupational standards (Eklund 2001). The sample results for the metal analysis have not yet been interpreted by LANL. All of the metals measured appeared to be at much lower concentrations than those measured in the smoke by the EPA, except for chromium, which was $0.016 \mu\text{g m}^{-3}$ in the smoke from the smoldering fire at MDA-R (Dewart 2001) and $0.02 \mu\text{g m}^{-3}$ in the highest EPA sample onsite (EPA 2001).

Beryllium in LANL air samples has been attributed to natural beryllium in resuspended dust (Dewart 2001). Quarterly composited samples from 27 sites, located near potential sources of beryllium or in communities, were analyzed for beryllium in 2000. All values measured were 2% or less of the community standard. Beryllium concentrations were highest at TA-54, Area G (0.2 ng m^{-3}), the County Landfill offsite (0.18 ng m^{-3}), and Site 7. These sites are not associated with any beryllium handling operations, so LANL hypothesized that the beryllium was probably from resuspended construction dust or road dust. Beryllium concentrations were directly correlated to concentrations of cerium, which occurs naturally in soils and is not released by LANL, further supporting the idea that beryllium was from naturally occurring beryllium in soil. Samples taken at the TA-15-36 site, where beryllium has been used in high explosives testing, were not elevated (Dewart 2001).

In January 1991, a short-term air-monitoring program was conducted at ground level over 7 consecutive days. Concentrations of 20 VOCs; six metals (beryllium, cadmium, chromium, lead, silver, and uranium) in PM; and five inorganic acid vapors were measured. Measurements were made at four locations downwind of several technical areas (TA-3A, TA-3B, TA-55, and TA-59) and at one upwind, remote location, near Bandelier National Monument, intended to represent background. Measurements taken during the week were compared to those taken over the weekend. Lead was the only metal detected, with a range of 0.01 to $0.04 \mu\text{g m}^{-3}$, well below OSHA's permissible exposure limit of $50 \mu\text{g m}^{-3}$. Although low, the detected concentrations of lead, toluene, benzene, and PM correlated with LANL operating times. LANL attributed these pollutant emissions to vehicular traffic on the public roads around LANL, but they acknowledged that the number of sampling sites was not sufficient to allow LANL operations in the TAs to be distinguished from emissions from public roads. All of the concentrations measured were far less than occupational standards and were less than levels of concern for community health effects (Williams and Eberhart 1991). Lead concentrations in air measured by the EPA during the Cerro Grande Fire ranged from 0.002 – $0.02 \mu\text{g m}^{-3}$, similar to those measured in 1991 (EPA 2001).

Air Monitoring Data Collected in Española by University Researchers

Researchers at New Mexico Tech, Utah State University, and New Mexico State University, working together, monitored air in the community of Española from May 12–17, 2000, for organic compounds, PM, radionuclides, NO_x, ozone, and trace elements (Popp et al. 2001). Ozone measured at Española was similar to that measured in Socorro, which is about 97 mi (156 km) south-southwest of Española and should not have been affected by the smoke plume. After analyzing the NO_x and ozone measurements for an indication of plume transport and impact, they concluded that the “commonality indicates that the larger-scale phenomena were controlling the regional and local photochemical pollutant mixing levels.” Carboxylic acid and carbonyl compounds (like formaldehyde, acetone, methyl ethyl ketone, and acetaldehyde) are produced by combustion of biomass. These were only slightly elevated in the Cerro Grande

samples compared to rural and mountain area clean air monitored in 1997 and 1998. Measurements of PM and hydrocarbons (like benzene and toluene) seem to correspond to periods of high and low pressure, more so than with any particular fire plume event. Concentrations of pollutants were generally lower than those measured for savanna fires (Popp et al. 2001).

They compared their sampling data to air sampling data from fires in the Amazon Basin and in South Africa and to measurements of pollutants in ambient air under nonfire conditions in Carlsbad, New Mexico. The concentrations of most elements in the Cerro Grande smoke at Española were lower, by a factor of 3 to 20, than concentrations measured in Carlsbad. The authors reasoned that this was because Carlsbad has more air pollution in general. Zinc, chromium, nickel, arsenic, silver, and vanadium were notably lower for both the PM₁₀ and the PM_{2.5} samples. Levels of these elements are considered indicators of the amount of biomass burning. Lead levels in the Cerro Grande smoke were lower than those seen in Africa. Strontium and rubidium concentrations were lower and chromium, cobalt, and antimony concentrations were higher than those measured in South Africa. The authors supposed that this might be because of the phase out of leaded gasoline in the U.S., differences in materials burned, and the overall higher level of these pollutants in the air in New Mexico (Popp et al. 2001).

Crustal (coarse-particle) elements (like alkaline and alkaline earth metals) were measured in the PM₁₀ samples at concentrations higher than samples from Carlsbad. This indicated that the fire suspended large amounts of crustal particles to the air. The authors theorized that since earth elements comprise the coarse particles (PM₁₀) and pollution-derived elements comprise the fine particles (PM_{2.5}), their data suggest that the dominant mechanism for particle generation during the Cerro Grande Fire was convection dispersion of soil material and incompletely burned biomass rather than gas-to-particle conversion. They thought that crustal elements suspended into the air by the fire could have masked the signatures of burning biomass (Popp et al. 2001).

We contacted the authors and requested copies of the data and/or summary information; graphs, tables, or spreadsheets; and maximum concentrations measured so that we could use this for the ranking, but never received the data. We do not believe Popp et al. supplied their data to NMED or LANL. Unfortunately, the graphs that were published in the Proceedings of the American Meteorological Society meeting in Albuquerque are very small and unreadable.

SOIL MONITORING DATA

Because air monitoring data were very limited, soil monitoring data were evaluated for the air pathway analysis. LANL and NMED reported the results of soil and produce sampling from farms, communities, and other locations onsite and offsite.

Soil Monitoring Data Collected by LANL

LANL has collected soil surface samples annually since the early 1970s for radionuclide and trace metal analysis from 12 onsite, 10 perimeter, and 3 background locations. After the fire, the analysis was expanded to include VOCs, pesticides, polychlorinated biphenyls (PCBs), high explosives, and dioxin-like compounds. Soil samples were collected on June 1–19, 2000, at locations that were not waste disposal areas, firing sites, outfalls, etc. The areas were chosen because they were flat and open and downwind from major facilities or operations. The background sites were 20 mi (32 km) to 60 mi (96 km) from the site boundary. The predominant direction of the fire plume was toward the northeast. One of the background sites, Embudo, was

predominantly downwind of the fire, so results for that location were compared to pre-fire soil sample results. Results of the analysis for radionuclides, radioactivity, and all mean trace element concentrations from the sampling were “statistically similar to soils collected in 1999, before the fire.” (Fresquez et al. 2000). Samples were not analyzed for cyanide before the fire, but cyanide concentrations in soils after the fire were similar in all locations. Radionuclides, radioactivity, and trace element concentrations in soil samples from TA-06, TA-15, and TA-16 (the TAs most affected by the fire) and samples collected from locations at the site perimeter that were in the predominant downwind direction (the Airport, North Mesa, Sportsman Club, and Tsankawi Areas) were similar to concentrations in soil samples collected in 1999 (Fresquez et al. 2000).

Soil Monitoring Data Collected by NMED

NMED collected produce and soil samples from farms and communities after the fire. Many of the metals measured were higher in predominantly upwind communities or communities out of the main smoke plume, such as Santa Fe, Pena Blanca, and Abiquiu, than in downwind communities like Embudo, Española, and Dixon. Levels measured in soil from the Jemez Mountains were similar or greater than those measured in locations downwind of the fire (NMED 2001).

Metals that have been used and disposed of at the site, such as barium, copper, beryllium, mercury, and silver, were either not increased or below detection limits. The influence of fallout from the smoke plume was not discernible in the soil samples taken. Air pollution, background soil levels, and fertilizer application could have affected the levels measured. NMED detected several PAHs in soil samples from communities (NMED 2001). PAH concentrations in soils from downwind communities were not higher than those from upwind locations, and they could be influenced by other fires, incinerators, and other sources of air pollution.

Pre-fire sediment and sludge samples from the LANL site did have lower concentrations of many metals than post-fire samples. Sediment samples taken from the Viveash Fire¹ contain higher concentrations of metals than the LANL pre-fire samples. Concentrations of barium, manganese, lead, selenium, and antimony were generally higher in LANL post-fire sediment samples than in the Viveash fire samples. The Viveash samples had higher cobalt and nickel concentrations than the LANL samples. Post-fire manganese and barium samples at various locations around LANL are about twice as high as concentrations seen in Viveash sediments. This suggests that LANL may be contributing to the concentrations of manganese and barium in sediments. All of the sediment and sludge samples are primarily influenced by surface water runoff and soil erosion and may not reflect air deposition (NMED 2001).

Asbestos Monitoring

Asbestos was used as a construction material in many of the homes and probably some of the buildings that burned. NMED conducted air sampling and stated in a press release that they found “relatively low” asbestos concentrations, below levels of health concern. No asbestos was detected in the small number of ash and swipe samples taken from the burned houses in Los Alamos (Benchmark Environmental 2000).

¹ The Viveash Fire happened shortly after the Cerro Grande Fire at another location in New Mexico.

QUALITATIVE COMPARISON OF COMPONENTS IN CERRO GRANDE SMOKE AND IN SOIL OF THE PRSs TO SUBSTANCES IN SMOKE FROM OTHER FIRES

Many of the contaminants measured in the Cerro Grande smoke or in the soil of the PRSs could have come from burning vegetation, forest litter, and soil that was not influenced by LANL activities. However, LANL may have been the primary or the only source for some of the contaminants measured. We reviewed the literature to determine if the trace elements, PAHs, and other compounds identified by our screening as high priority contaminants have been identified in smoke from other forest fires or wood smoke in general. We also reviewed the literature for information on whether the course of chemicals in smoke was from burning biomass, suspended soil, or from deposited air pollutants from industrial activities or vehicles.

Most of the information in the literature on pyrogenic aerosols and particles comes from studies of fires of tropical rainforest, savanna burning, or burning of agricultural residues. Because of concerns about health effects in urban areas, components of smoke from wood-fueled stoves have been well studied.

Many chemicals, including carbon monoxide, carbon dioxide, methane, oxides of nitrogen, ammonia, and many different hydrocarbons (like benzene), have been measured in smoke plumes and in wood smoke. The metals and many of the other compounds in smoke are components of the PM that is measured. In general, coarse particles (larger than 2.5 micrometers [μm]) come from windblown dust or soil. Fine particles (less than 2.5 μm) come from burning fuel.

Metals in Smoke

We included the metals listed below in our list of potential contaminants of concern (PCOCs).

Aluminum	Cobalt	Silver
Antimony	Copper	Thallium
Arsenic	Iron	Uranium
Barium	Manganese	Vanadium
Beryllium	Mercury	Zinc
Cadmium	Nickel	
Chromium	Selenium	

The Smoke Cloud and Radiation (SCAR) Project measured parameters for smoke particles from prescribed biomass (primarily western red cedar debris left over from logging) burning in the western United States in 1994. The project involved measurements of particulates and gases in the smoke using aircraft. Manganese, iron, nickel, copper, zinc, chromium, and lead were detected in the smoke (Martins et al. 1996; Hobbs et al. 1996).

Shum and Loveland (1974) detected aluminum, antimony, arsenic, chromium, cobalt, copper, iron, mercury, manganese, and vanadium in smoke from field burning in the Willamette Valley of Oregon. Barium levels were at or below the detection limit of 30 ng m⁻³. They did not sample for zinc, uranium, silver, or thallium.

Aircraft sampling above fires in the Amazon Basin found aluminum, iron, manganese, zinc, copper, nickel, lead, vanadium, chromium, and strontium in smoke (Artaxo et al. 1993). Maenhaut et al. (1996) analyzed aerosol in smoke from savannas in Amazonia for 47 chemical elements and attempted to identify the source of the elements. They identified aluminum, antimony, arsenic, barium, cadmium, chromium, cobalt, copper, iron, manganese, mercury, nickel, silver, selenium, thallium, uranium, vanadium, and zinc in the smoke plume.

Cahill et al. (1996) studied particle emissions measured using aircraft flown through the smoke from the 1991 Kuwait Oil fires. They found aluminum, chromium, copper, cobalt, nickel, lead, vanadium, manganese, and zinc.

Turn et al. (1997) looked at components of PM using wind tunnel simulations of biomass burning for five herbaceous and four wood fuel sources. They detected aluminum, antimony, arsenic, barium, cadmium, chromium, cobalt, copper, iron, lead, manganese, mercury, nickel, selenium, silver, uranium, vanadium, and zinc in fuels and smoke. Chromium, cobalt, nickel, and vanadium were at lower concentrations in wood smoke than in smoke from various straws and agricultural residue.

Popp et al. (2001) sampled air in the community of Española from May 12–17, 2000, for organic compounds, PM, radionuclides, NO_x, ozone, and trace elements. They compared their sampling data to data from air sampling from fires in the Amazon Basin and in South Africa and to measurements of pollutants in ambient air of Carlsbad, New Mexico, under nonfire conditions. The amount of trace elements in air in the Cerro Grande Fire was comparable to or smaller than amounts measured in the African Savanna fires or Amazon Basin fires. The concentrations of most elements in the Cerro Grande smoke at Española were lower, by a factor of 3 to 20, than concentrations measured in Carlsbad under non-fire conditions. The authors speculated that this was because Carlsbad has more air pollution in general than the area around Española. Zinc, chromium, nickel, arsenic, silver, and vanadium were notably lower in both PM₁₀ and the PM_{2.5} samples from Española. Lead levels in the Cerro Grande Fire smoke were lower than those seen in Africa. Strontium concentrations were lower, and chromium, cobalt, and antimony concentrations were higher than those measured in South Africa. The authors supposed that this might be due to the phase out of leaded gasoline in the U.S., differences in materials burned, and the overall higher level of these pollutants in the air in New Mexico. Differences in the amount of biomass burned may be the reason that the amount of trace elements in air in the Cerro Grande Fire were comparable to or smaller than amounts measured in the African Savanna fires or Amazon Basin fires (Popp et al. 2001).

Popp et al. (2001) speculated that copper concentrations in air might have been elevated because of LANL. However, they were unsure if concentrations might be increased as a result of Laboratory weapons testing or biomass burning because of a lack of monitoring data from other fires to which to compare their data (Arimoto 2001). Because the concentrations of trace elements are relatively low and are similar to or less than those from other fires, the LANL contribution to the pollutants cannot be determined from their data. Their data do not clearly demonstrate that any of the pollutants were due to LANL operations rather than the fire alone.

Mercury has been measured in the smoke plumes from many different types of fires (Maenhaut et al. 1996). Mercury deposited on the ground and in forest litter and trees is liberated in forest fires. Friedli and Radke, at the University of Washington, have studied smoke from wood burning in a controlled laboratory setting and from overflights of wildfires in Canada and

the Pacific Northwest. Emissions from wildfires were generally higher, probably because the smoke also contained mercury from soil and ground litter (NCAR 2001).

Most of the metals that were identified as PCOCs are present in the earth's crust and are released to the air in windborne dust from forest fires. In addition, many of the metals are contained in wood and forest litter and are released when these burn. With the possible exception of beryllium, all of the metals on the list of contaminants to be considered further have been identified in smoke from other fires.

Maenhaut et al. (1996) identified antimony, arsenic, barium, cadmium, cobalt, iron, nickel, selenium, silver, thallium, uranium, vanadium, and zinc in smoke from savanna fires in South America. Aluminum, chromium, copper, manganese, nickel, vanadium, and zinc were components of smoke plumes from oil fires in Kuwait and fires in Brazil (Cahill et al. 1996; Maenhaut et al. 1996). Chromium, copper, iron, manganese, nickel, and zinc were also detected in SCAR Project samples of smoke from forest fires in the western U.S. (Martins et al. 1996; Hobbs et al. 1996). Vanadium has also been identified in smoke produced in a laboratory setting from burning fuel oil (Maenhaut et al. 1996). Aerosols from biomass burning are consistently enriched in zinc; therefore, zinc can be used as an indicator of burning biomass, as opposed to windborne dust or other sources of particulates (Cachier et al. 1996).

Measurements of beryllium were not included in the analyses of smoke in the papers we reviewed. The background levels of beryllium in the soil at LANL are high relative to soil in other parts of the U.S. In some areas of the site, naturally occurring beryllium concentrations in soil have exceeded screening levels used by the EPA for assessment of waste disposal areas (Dory 2001). Beryllium in LANL air samples has been attributed to naturally occurring beryllium in soil suspended as dust (Dewart 2001).

Sources of Metals in Smoke

Sources of many of these compounds can be industrial pollution, pollution from motor vehicles, or biomass burning. Not much is known about how pollutants that settle onto vegetation, forest litter, and soil are mobilized by fire.

We compiled information in the literature about the potential sources of the elements and whether they are thought to be from burning vegetation or from soil. Source profiles for various types of savanna and tropical forest burnings have been developed. However, the elements measured and the methods used to differentiate biogenic versus crustal sources vary among the various studies, which makes comparing the results of the studies to one another or to measurements taken during the Cerro Grande Fire difficult. Smoke components vary according to fuel type and the composition of PM released during flaming and smoldering phases of the fire. For example, smoldering combustion releases many more fine particles than flaming combustion (Ward 1999).

Popp et al. (2001) attempted to develop ratios to see what elements are from vegetation versus some other source, like background pollution, for the Cerro Grande, Amazon, and savanna fires. They used aluminum as a crustal indicator and potassium as a biomass burning indicator. For all of the fires, strontium, manganese, zinc, copper, and lead levels correlated with potassium, indicating a vegetation source. The correlations for manganese, zinc, copper, and lead were very weak, which suggested to the authors that background pollution, rather than vegetation, may be a source for these elements. Iron varied with aluminum, suggesting a crustal source. The sources of

chromium, vanadium, and cobalt could not be determined because they did not correlate with aluminum or potassium.

Areas in the Amazon where the savanna smoke has been studied have very little industrial activity, suggesting the elements found in smoke from these fires are mostly from natural sources. Nearly 100% of the measured aluminum, vanadium, iron, cobalt, nickel, arsenic, barium, and thallium in savanna smoke was attributed to mineral dust. Aluminum was used as a marker for mineral dust. About 93% of the manganese was attributed to mineral dust and 7% was thought to be from biomass burning. Fine PM, generally attributed to noncrustal sources, contained antimony, arsenic, lead, vanadium, and zinc. About 70% of the copper was attributed to biomass burning. More than 90% of the zinc, antimony, and lead was attributed to biomass burning. Maenhaut et al. (1996) believed that zinc, antimony, arsenic, and lead have a pyrogenic source for some fires but may also be due to deposition of air pollution from other sources. These studies suggest that the source of antimony, lead, and zinc in smoke is from burning vegetation, and aluminum, iron, cobalt, nickel, and thallium may come, primarily, from suspension of soil. Arsenic, copper, manganese, and vanadium seem to come from both soil and vegetation (Maenhaut et al. 1996).

Polyaromatic Hydrocarbons in Smoke

Burning organic matter at high temperature creates PAHs. PAHs are produced from a variety of combustion processes, including forest fires (Ward 1999). In fact, PAHs can serve as tracers or pyrogenic markers for the transport of biomass burning products. PAH concentrations in sediments have been used as indicators of historical vegetation fires (Ballantine et al. 1996). The PAHs measured in smoke during the Cerro Grande Fire are slightly elevated at some locations, but concentrations upwind were equal to or greater than concentrations downwind and concentrations could not be used to trace the smoke plume (EPA 2001).

The PAHs in the list below were measured in smoke from the fire.

Benzo(a)anthracene	Anthracene
Benzo(a)pyrene	Dibenz(a,h)anthracene
Benzo(b)fluoranthene	Fluoranthene
Benzo(g,h,i)perylene	Indeno(1,2,3-cd)pyrene
Benzo(k)fluoranthene	Pyrene

Benz(a)anthracene, pyrene, fluoranthene, benzo(b&k) fluoranthene, benzo(a)pyrene, indeno(1,2,3-cd) pyrene, and benzo(ghi) perylene are all ubiquitous in many different kinds of smoke (HSDB 2001).² Benz(a)anthracene exposure to wildfire fighters in Northern California from 1986–1989 and emissions from combustion of different types of wood have been studied (HSDB 2001). Indeno(1,2,3-cd)pyrene has been identified in the leaves of tobacco, beech trees, and oak trees. Benzo(ghi)perylene and indeno(1,2,3-cd)pyrene have been identified in smoke from forest fires in Amazonia (HSDB 2001).

Many PAHs have been identified in both laboratory and sugar cane field burning, including fluoranthene, benzo(k)fluoranthene, benzo(a&e)pyrene, pyrene, and benzo(a)anthracene (Ballantine et

² This database compiles information from peer-reviewed journals, EPA reports, International Agency for Research on Cancer (IARC) monographs, and other sources.

al. 1996; Simoneit et al. 1996; HSDB 2001). Ballantine et al. (1996) measured PAHs in smoke from sugar cane fires in South Africa. The cane fields were in remote areas and thought not to be affected by air pollution from industrial or vehicular sources. Simoneit et al. (1996) studied PAHs in Amazon biomass smoke. Using gas chromatography-mass spectrometric analysis, they identified benzo(a)fluoranthene, benzo(a,e)pyrene, indeno(1,2,3-cd)pyrene, fluoranthene, and benzo(ghi)perylene (Simoneit et al. 1996). Fluoranthene has been found in smoke from controlled burns of forest litter in Brazil, industrial combustion sources, and wood burning stoves (HSDB 2001). Pyrene is a product of incomplete combustion and has been found in motor vehicle exhaust; cigarette smoke; and smoke from coal, oil, and wood fires (HSDB 2001).

Anthracene was found in the personal air samples of all 20 of the wildfire fighters studied in California in 1988 (HSDB 2001). Anthracene may have been produced as a product of combustion, but it is also used for high explosives testing (HSDB 2001). The anthracene measured in air may have come from either source, but anthracene in soil after explosives testing would be expected to have broken down. Half-lives in soil of 20–135 days have been reported. Anthracene also breaks down in air, with an estimated half-life of about 4 hours.

All typical forest fires are sources of the same PAHs that were measured in the Cerro Grande Fire smoke.

Organic Chemicals, Explosives, and Other Chemicals in Smoke

Other organic chemicals on the list of PCOCs are listed below.

Acenaphthylene	Bis(2-ethylhexyl)phthalate	Naphthalene
Aldrin	Cyanide	Nitrosodimethylamine (N-)
Amino-2,6-dinitrotoluene (4-)	Dibenzofuran	Pentachlorophenol
Amino-4,6-dinitrotoluene (2-)	Dichlorobenzidine[3,3'-]	PETN
Aniline	Dinitrobenzene (1,3-)	RDX
Arochlor-1254	HMX	TATB
Arochlor-1260	Methylnaphthalene (2-)	Trinitrotoluene (2,4,6-)

Koppmann et al. (1996) examined organic compounds in smoke from savanna fires and sugar cane fields in South Africa. They detected furans, including benzofuran. Many of the organic compounds on our list that may be derived from fires were not included in the Koppmann et al. (1996) analysis. Andreae et al. (1996) also detected furans, including methylfurans, dimethylfuran, and furfural, in African savanna fires. Dibenzofuran has been measured in smoke from the combustion of coal, refuse, diesel oil, biomass, and tobacco (HSDB 2001).

Cyanide occurs naturally in fruits, seeds, roots, and leaves of many plants. Vehicle exhaust and biomass burning are considered significant sources of cyanide released into the atmosphere.

We did not find any information about the occurrence of bis(2-ethylhexyl)phthalate, dichlorobenzidine[3,3'-], and aniline in smoke from typical forest fires. An International Agency for Research on Cancer (IARC) publication about industrial chemicals reported that bis(2-ethylhexyl)phthalate is a natural product in animals and plants (HSDB 2001). Aniline has been found in cigarette smoke and emissions from oil refineries and coal conversion plants. Nitrosoamines are components of smoke and are some of the carcinogens contained in cigarette smoke, but we have not found a reference for smoke containing nitrosodimethylamine[N-], specifically. Naphthalene, methylnaphthalene, and acenaphthylene are natural components of

crude oil and coal and are released from forest fires (HSDB 2001). Naphthalenes have been identified in smoke from wood burned in a laboratory setting and in smoke from burning sugar cane fields (Ballantine et al. 1996; Simoneit et al. 1996).

As far as we know, 4-amino-2,6-dinitrotoluene and 2-amino-4,6-dinitrotoluene (breakdown products of TNT); 3,3-dichlorobenzidine; RDX; HMX; trinitrotoluene; dinitrobenzene; pentaerythritol tetranitrate (PETN); and TATB do not occur naturally. Dinitrobenzene[1,3-], amino-2,6-dinitrotoluene[4-], amino-4,6-dinitrotoluene[2-], HMX, PETN, RDX, TATB, and trinitrotoluene[2,4,6-] were identified as soil contaminants of the PRSs. These compounds are probably in the soil as a result of explosives testing and development at LANL. We have no information as to whether they might be found in smoke from wood or forest fires. PCBs (Aroclor-1254 and Aroclor-1260) are often a contaminant of soil at federal facilities like LANL because of historical disposal of transformer fluid, capacitors, and other materials. Aldrin is a pesticide that is no longer in use. It may have been used historically by LANL, the National Park Service, the U.S. Forest Service, and on farms or in communities. Pentachlorophenol is a manmade wood preservative. We would not expect to find PCBs, pentachlorophenol, or aldrin in smoke from rural forest fires.

LANL STUDIES AND REPORTS THAT MAY HELP US UNDERSTAND THE SITE'S CONTRIBUTION TO CONTAMINANTS IN SMOKE AND SOIL

Several monitoring studies that may help determine LANL's contribution to chemicals in air and soil are described in the first section of this appendix. Results of soil analysis for radionuclides, radioactivity, and trace element concentrations from the sampling were "statistically similar to soils collected in 1999, before the fire" (Fresquez et al. 2000). The influence of fallout from the fire was not discernible in the soil samples taken by NMED (NMED 2001). Metals that have been used and disposed of at the site and might be elevated in a smoke plume, such as barium, copper, beryllium, mercury, and silver, were either not increased or were below detection limits. NMED detected several PAHs in soil samples from communities, but concentrations from downwind communities were not higher than those from upwind locations. LANL conducted an air monitoring program for VOCs and metals over 7 consecutive days in January 1991. They detected lead, toluene, and benzene in the air and attributed these to vehicular traffic on the public roads around LANL, but they acknowledged that the number of sampling sites was not sufficient to allow LANL operations in the technical areas to be distinguished from emissions from public roads (Williams and Eberhart 1991).

To help assess whether the chemicals of potential concern were used onsite or were components of waste areas, we reviewed chemical release inventory reports and inventories compiled for the Emergency Planning and Community Right-to-Know Act of 1986, Title III, Section 313 requirements, commonly called Superfund Amendments and Reauthorization Act of 1986 (SARA) reports (LANL 1994, 1995, 1997; McBride 1997). These inventories do not include materials used at the site historically that are no longer used.

Table A-2 shows the maximum amount reported for any 1 year, in the reports for 1993, 1994, and 1996. Metals and metal compounds were combined. Compounds not listed were not reported or the amount reported for them was zero.

**Table A-2. Maximum Inventory Reported by LANL for the SARA Reports
for 1993, 1994 and 1996**

Chemical	Maximum reported inventory or purchased amount in pounds	Chemical	Maximum reported inventory or purchased amount in pounds
Aldrin	0.12	Dinitrobenzene	0.05
Aluminum	736	Lead	10081
Aniline	47	Manganese	1205
Anthracene	4	Mercury	490
Antimony	37	Naphthalene	38
Arsenic	85	Nickel	1313
Barium	24	Nitrobenzene	39
Cadmium	69	Pentachlorophenol	0.2
Chromium	1406	Silver	56
Cobalt	736	Selenium	59
Copper	6432	Thallium	70
Cyanide	1240	Vanadium	96
2,4-dinitrotoluene	5	Zinc	2702

The site has used notable quantities of chromium, cyanide, lead, manganese, mercury, nickel, and zinc in recent years. Although occurrence in the inventory does not mean that components of the smoke were LANL-derived, it does give some idea of whether the contaminant was used or stored at LANL.

Ten explosives were reviewed in the 1997 SARA report, including barium nitrate and nitrobenzenes. In 1997, LANL processed about 6000 pounds of beryllium. In 1996, LANL decontaminated about 40,000 pounds of radioactive lead shielding using a wet process. In 1997, 5000 pounds of lead in ammunition was shot at the firing range and 5100 pounds of lead was melted and shaped into shielding and storage containers.

Emissions inventories done by LANL in the late 1980s identified more than 600 potential air contaminants in LANL emissions. These reports are large and in the interest of time, we did not review them for this analysis.

Another source of information about whether a contaminant of smoke or soil has been used or disposed of onsite are the Solid Waste Management Unit (SWMU) descriptions in the SWMU report. The numbers given to the PRSs correspond to the numbers given to SWMUs. An example of the kind of information that can be derived from the SWMU report is a list of materials at SWMU 36-004c used in the test shots conducted at firing sites. The materials include aluminum, barium, beryllium, lead, copper, iron, depleted uranium, nitrobenzene, and high explosives. Lead, iron, and uranium have been found in waste storage areas. Barium, beryllium, copper, chromium, lead, silver, zinc, thallium, and uranium have been detected in soil near waste areas. Background levels of some of the metals in soil are quite high, so the contribution to contamination from the waste is unclear. The SWMU report is currently being updated. The latest finalized version was published in 1990 in four volumes. This report is not available electronically. The time constraints of this project prohibited us from exploring this source of information more thoroughly.

REFERENCES

- Andreae, M.O., E. Atlas, H. Cachier, W.R. Cofer III, G.W. Harris, G. Helas, R. Koppmann, J. Lacaux, and D.E. Ward. 1996. "Trace Gas and Aerosol Emissions from Savanna Fires." Chapter 27 in *Biomass Burning and Global Change*. Edited by J.S. Levine. Cambridge, Massachusetts: MIT Press. 278–295.
- Arimoto, R. 2001. New Mexico State University, Carlsbad, New Mexico. Personal communication with Patricia McGavran, *Risk Assessment Corporation*. Subject: His publication in the Proceedings of a Conference on Planned and Inadvertent Weather Modification. American Meteorological Society. May.
- Artaxo, P., M.A. Yamasoe, J.V. Martins, S. Kocinas, S. Carvalho, and W. Maenhaut. 1993. "Case Study of Atmospheric Measurements in Brazil: Aerosol Emissions from Amazon Basin Fires." Chapter 9 in *Fire in the Environment: The Ecological, Atmospheric and Climatic Importance of Vegetation Fires*. Edited by P.J. Crutzen and J.G. Golammer. John Wiley & Sons. 139–158.
- ATSDR (Agency for Toxic Substances and Disease Registry). 2001. *Health Consultation: Potential Public Health Impacts from the Cerro Grande Fire Airborne Emissions: LANL*. Draft for Public Comment. June 28.
- Ballantine, D.C., S.A. Macko, V.C. Turekian, W.P. Gilhooly, and B. Martincigh. 1996. "Chemical and Isotopic Characterization of Aerosols Collected during Sugar Cane Burning in South Africa." Chapter 43 in *Biomass Burning and Global Change*. Edited by J.S. Levine. Cambridge, Massachusetts: MIT Press. 460–465.
- Benchmark Environmental. 2000. *Wipe Sample and Debris Analytical Results: Analysis Reports Albuquerque, NM. May 17*. Report to New Mexico Environment Department.
- Cachier, H., C. Lioussé, M. Pertuisot, A. Gaudichet, E. Francisci, and J.P. Lacaux. 1996. "African Fire Particulate Emissions and Atmospheric Influence." Chapter 41 in *Biomass Burning and Global Change*. Edited by J.S. Levine. Cambridge, Massachusetts: MIT Press. 428–440.
- Cahill, C.F., J.A. Herring, R.J. Ferek, and P. V. Hobbs. 1996. "Composition and Evolution of Aerosols in the Smoke Plumes from the 1991 Kuwait Oil Fires." Chapter 82 in *Biomass Burning and Global Change*. Edited by J.S. Levine. Cambridge, Massachusetts: MIT Press. 877–888.
- Dewart, J. 2001. ESH-17, Los Alamos National Laboratory. Personal Communication with Patricia McGavran and Jill W. Aanenson, *Risk Assessment Corporation*. Subject: MDA-R PM and TSP Air Monitoring Data, Beryllium Monitoring Data, and Draft Material for the Year 2000 Environmental Surveillance Report. June 16.

- Dory, A. 2001. EH-18, Los Alamos National Laboratory. Personal communication with Pat McGavran, *Risk Assessment Corporation*. Subject: PRS Characterization. May 2001.
- Eklund, B. 2001. Memo to J. Dewart, ESH-17, Los Alamos National Laboratory and M. Stockton, URS/Radian. Subject: Results of Ambient Air Monitoring for VOCs at MDA-R. July 28.
- EPA (U.S. Environmental Protection Agency). 2001. L. Biasco, G. Brozowski, and J. Benetti, EPA Regional Office in Dallas, Texas and EPA Laboratory in Las Vegas, Nevada. Personal communication with L. Biasco, G. Brozowski, and J. Benetti. *Risk Assessment Corporation*. Subject: Data Tables and Data Summaries. June.
- Fresquez, P.R., W.R. Velasquez, and L. Naranjo, Jr. 2000. *Effects of the Cerro Grande Fire (Smoke and Fallout Ash) on Soil Chemical Properties Within and Around Los Alamos National Laboratory*. LA-13769-MS. November.
- HSDB (*Hazardous Substances Database*). 2001. HSDB[®], National Library of Medicine (NLM) Toxicology Data Network (TOXNET[®]). Bethesda, Maryland. <<http://toxnet.nlm.nih.gov/cgi-bin/sis/htmlgen?HSDB>>.
- Hobbs, P.V., J.S. Reid, J.A. Herring, J.D. Nance, R.E. Weiss, J.L. Ross, D.A. Hegg, R.D. Ottmar, and C. Liousse. 1996. "Particle and Trace-Gas Measurements in the Smoke from Prescribed Burns of Forest Products in the Pacific Northwest." Chapter 66 in *Biomass Burning and Global Change*. Edited by J.S. Levine. Cambridge, Massachusetts: MIT Press. 716–725.
- Koppmann, R., A. Khedim, J. Rudolph, G. Helas, M. Welling, and T. Zenker. 1996. "Airborne Measurements of Organic Trace Gases from Savanna Fires in South Africa during SAFARI-92." Chapter 29 in *Biomass Burning and Global Change*. Edited by J.S. Levine. Cambridge, Massachusetts: MIT Press. 309–319.
- LANL (Los Alamos National Laboratory). 1994. *Emergency Planning and Community Right-to-Know Act—Section 313 Release Estimates*. Los Alamos, New Mexico. June.
- LANL. 1995. *Emergency Planning and Community Right-to-Know Act—Section 313 1994 Release Estimates*. Los Alamos, New Mexico. June.
- LANL. 1997. *Emergency Planning and Community Right-to-Know Act—Section 313 1996 Release Estimates*. Los Alamos, New Mexico. August.
- LANL. 2000. *Special Edition of the SWEIS Yearbook, Wildfire 2000*. LA-UR-00-3471. August.
- Maenhaut, W., G. Koppen, and P. Artaxo. 1996. "Long-term Atmospheric Aerosol Study in Cuiaba, Brazil: Multielemental Composition, Sources and Impact of Biomass Burning." Chapter 61 in *Biomass Burning and Global Change*. Edited by J.S. Levine. Cambridge, Massachusetts: MIT Press. 637–652.

- Martins, J.V., P. Artaxo, P.V. Hobbs, C. Lioussé, H. Cachier, Y. Kaufman, and A. Plana-Fattori. 1996. "Particle Size Distributions, Elemental Composition, Carbon Measurements and Optical Properties of Smoke from Biomass Burning in the Pacific Northwest of the United States." Chapter 67 in *Biomass Burning and Global Change*. Edited by J.S. Levine. Cambridge, Massachusetts: MIT Press. 726–738.
- McBride, H. 1997. *1997 Chemical Release Inventory Report for the Emergency Planning and Community Right-to-Know Act of 1986, Title III, Section 313*. LA-13560-MS. Los Alamos, New Mexico. July.
- NCAR (National Interagency Fire Center). 2001. Mercury in Smoke: News Bulletin. August 2001. <www.EnvironmentalNewsService.com>.
- NMED (New Mexico Environment Department) 2001. Oversight Bureau. Personal communication with Dave Englert. Subject: Soil and Produce monitoring Data. May.
- Popp, C.J., S. Huang, R.S. Martin, and R. Arimoto. 2001. "Atmospheric Effects of Large Fires: Spring 2000 Cerro Grande, NM (Los Alamos) Fire." *Proceedings of a Conference on Planned and Inadvertent Weather Modification*. American Meteorological Society. Albuquerque, New Mexico. January.
- Shum, Y.S. and W.D. Loveland. 1974. "Atmospheric Trace Element Concentrations Associated with Agricultural Field Burning in the Willamette Valley of Oregon." *Atmospheric Environment* 8: 645–655.
- Simoneit, B.R.T., M.R. bin Abas, G.R. Cass, W.F. Rogge, M. Mazurek, L.J. Standley, and L.M. Hildemann. 1996. "Natural Organic Compounds as Tracers for Biomass Combustion in Aerosols. Chapter 48 in *Biomass Burning and Global Change*." Edited by J.S. Levine. Cambridge, Massachusetts: MIT Press. 496–509.
- Turn, S.Q., B.M. Jenkins, J.C. Chow, L.C. Pickett, D. Campbell, T. Cahill, and S.A. Whalen. 1997. "Elemental Characterization of PM Emitted from Biomass Burning: Wind Tunnel derived Source Profiles for Herbaceous and Wood Fuels." *J. Geophysical Res.* 102 (D3): 3683–3699.
- Ward, D.E. 1999. *Smoke from Wildland Fires. World Health Organization (WHO) Health Guidelines for Vegetation Fire Events, Lima, Peru 6-9 October*. USDA Forest Service, Fire Chemistry Project, Missoula, Montana.
- Williams, C.H. and C.F. Eberhart. 1991. *Ambient Air Monitoring for Organic Compounds, Acids and Metals at Los Alamos National Laboratory*. LA-UR-92-3170. January.

APPENDIX B

POTENTIAL CONTAMINANTS OF CONCERN MEASURED AT POTENTIAL RELEASE SITE LOCATIONS

APPENDIX B

POTENTIAL CONTAMINANTS OF CONCERN MEASURED AT POTENTIAL RELEASE SITE LOCATIONS

**Table B-1. Potential Contaminants of Concern Identified
at Potential Release Site Locations**

Aluminum	Antimony
Arsenic	Asbestos (friable)
Barium	Beryllium
Cadmium	Calcium
Cesium	Chromium (hexavalent)
Chromium (total)	Cobalt
Copper	Cyanide (total)
Fluoride	Gold
Gravel	Iron
Lead	Lithium
Magnesium	Manganese
Mercury	Molybdenum
Nickel	Nitrate (as NO ₃)
Nitrate + Nitrite (as N)	Nitrite (as NO ₂)
Platinum	Potassium
Selenium	Silver
Sodium	Strontium
Thallium	Uranium
Vanadium	Water (unbound)
Zinc	Acenaphthene
Acenaphthylene	Acetone
Aldrin	Amino-2,6-dinitrotoluene[4-]
Amino-4,6-dinitrotoluene[2-]	Aniline
Anthracene	Aroclor-1254
Aroclor-1260	Benzene
Benzo(a)anthracene	Benzo(a)pyrene
Benzo(b)fluoranthene	Benzo(g,h,i)perylene
Benzo(k)fluoranthene	Benzoic Acid
Benzyl Alcohol	BHC[alpha-]
BHC[delta-]	BHC[gamma-]
Bis(2-ethylhexyl)phthalate	Bromodichloromethane
Bromophenyl-phenylether[4-]	Butanone[2-]
Butylbenzylphthalate	Carbazole
Carbon Disulfide	Carbon, Total Organic
Chloro-3-methylphenol[4-]	Chloroaniline[4-]
Chloronaphthalene[2-]	Chlorophenol[2-]
Chrysene	DDD[4,4'-]

Table B-1. (Continued)

DDE[4,4'-]	DDT[4,4'-]
Di-n-butylphthalate	Di-n-octylphthalate
Dibenz(a,h)anthracene	Dibenzofuran
Dichlorobenzene[1,2-]	Dichlorobenzene[1,3-]
Dichlorobenzene[1,4-]	Dichlorobenzidine[3,3'-]
Dichlorodifluoromethane	Dichloroethene[cis-1,2-]
Dieldrin	Diethylphthalate
Dimethyl Phthalate	Dimethylphenol[2,4-]
Dinitrobenzene[1,3-]	Dinitrotoluene[2,4-]
Dinitrotoluene[2,6-]	Endosulfan II
Endosulfan Sulfate	Endrin
Endrin Aldehyde	Fluoranthene
Fluorene	Heptachlor Epoxide
Hexachlorobenzene	Hexanone[2-]
HMX	Hydrocarbons, Total Petroleum
Indeno(1,2,3-cd)pyrene	Isopropyltoluene[4-]
Lubricant Range Organics	Methoxychlor[4,4'-]
Methyl-2-pentanone[4-]	Methylene Chloride
Methylnaphthalene[2-]	Methylphenol[2-]
Methylphenol[4-]	Naphthalene
Nitroaniline[4-]	Nitrobenzene
Nitroglycerin	Nitrosodimethylamine[N-]
Nitrosodiphenylamine[N-]	Nitrotoluene[2-]
Nitrotoluene[3-]	Nitrotoluene[4-]
Organics, Diesel Range	Pentachlorophenol
PETN	Phenanthrene
Phenol	Pyrene
RDX	TATB
Tetrachloroethene	Tetryl
Toluene	Trichloro-1,2,2-trifluoroethane[1,1,2-]
Trichlorobenzene[1,2,3-]	Trichlorobenzene[1,2,4-]
Trichloroethane[1,1,1-]	Trichloroethene
Trichlorofluoromethane	Trimethylbenzene[1,2,4-]
Trimethylbenzene[1,3,5-]	Trinitrobenzene[1,3,5-]
Trinitrotoluene[2,4,6-]	Xylene (Total)
Xylene[1,2-]	Xylene[1,3-]
Actinium-228	Americium-241
Barium-140	Bismuth-211
Bismuth-212	Bismuth-214
Cadmium-109	Cesium-134
Cesium-137	Cobalt-57
Cobalt-60	Europium-152
Iodine-129	Lead-210
Lead-211	Lead-212

Table B-1. (Continued)

Lead-214	Manganese-54
Neptunium-237	Plutonium-238
Plutonium-239	Potassium-40
Protactinium-231	Protactinium-234
Protactinium-234m	Radium-223
Radium-224	Radium-226
Radium-228	Radon-219
Ruthenium-106	Sodium-22
Strontium-90	Thallium-208
Thorium-227	Thorium-228
Thorium-230	Thorium-231
Thorium-232	Thorium-234
Tritium	Uranium-234
Uranium-235	Uranium-238

APPENDIX C

TOXICITY VALUES USED TO SCREEN NONRADIOLOGICAL POTENTIAL CONTAMINANTS OF CONCERN

APPENDIX C

TOXICITY VALUES USED TO SCREEN NONRADIOLOGICAL POTENTIAL CONTAMINANTS OF CONCERN

To focus on developing source terms for the most important contaminants that could have presented a health risk if released to the air in sufficient quantities, we ranked contaminants based on measured concentrations in soil at the potential release sites (PRs) and toxicity or carcinogenicity. We used the toxicity values shown in this appendix to screen and prioritize contaminants for further study.

The toxicity values for noncarcinogens were intakes, or concentrations, below which adverse health effects would not be expected. For most of the chemicals, we used the U.S. Environmental Protection Agency's (EPA's) reference concentration (RfC). For values that were published as a reference dose for inhalation (RfD_i), we converted an RfD to an RfC using the relationship:

$$RfC_i = \frac{RfD_i \cdot W}{BR} \quad (C-1)$$

where

- RfC_i = reference concentration for inhalation (mg m⁻³)
- RfD_i = reference dose for inhalation (mg d⁻¹ kg⁻¹)
- W = body weight (kg)
- BR = breathing rate (m³ d⁻¹).

RfC and RfD are defined by the EPA as provisional estimates (with uncertainty spanning perhaps an order of magnitude) of the daily exposure to the human population (including sensitive subgroups) that are likely to be without an appreciable risk of deleterious effects during a portion of the lifetime (subchronic values) or the entire lifetime (chronic values).

For most chemicals, the subchronic RfD and RfC correspond to exposures that last from 2 weeks to 7 years. Chronic RfDs are for exposures lasting longer than 7 years. In many cases, the chronic values were derived from studies of animals exposed for a lifetime or a portion of a lifetime, often approximated by time periods of 70 or 30 years for humans. We used the subchronic RfD or RfC, whenever one was available, because the shorter time frame is more applicable to the very short-term exposure from the Cerro Grande Fire.

No RfD or RfC could be derived for some chemicals, so we used an occupational standard or guideline. The standards or guidelines we used are given different names by the different agencies that develop them. The National Institute for Occupational Safety and Health (NIOSH) publishes recommended exposure limits (RELs), which are time-weighted average concentrations for up to a 10-hour workday during a 40-hour week. The Occupational Safety and Health Administration (OSHA) develops regulatory standards called permissible exposure limits (PELs). PELs are time-weighted average concentrations that must not be exceeded during any 8-hour work shift of a 40-hour work week. The American Conference of Industrial Hygienists publishes threshold limit values (TLVs), which are recommended maximum time-weighted average concentrations for an 8-hour workday during a 40-hour week. For our ranking, all of these values were called TLVs. We used the TLVs to rank contaminants for which RfCs, RfDs, inhalation slope factors (SF_i), or other toxicity comparison values (such as those developed by Agency for

Toxic Substances and Disease Registry [ATSDR]) for exposures to the public have not been developed. The occupational exposure guidelines are intended to protect healthy workers exposed 8 hours each day, 5 days each week. They are higher than standards designed to protect the public, who are exposed 24 hours a day and may be more sensitive due to age, illness, pregnancy, and other considerations. To help account for the variation in sensitivity among people and the longer exposure duration, we divided the TLVs by a factor of 10.

Inhalation RfDs and TLVs have not been developed for acenaphthene or lithium, so we used an RfD_o (oral reference dose). Lithium can be toxic by ingestion but generally does not pose an inhalation hazard. We have found no information on the inhalation toxicity of acenaphthene. The difference in oral and inhalation RfDs depends greatly on the chemical, how readily it is absorbed via different intake routes, and its mechanism of action. Ideally, differences in the route of administration or intake should be resolved using toxicokinetic modeling, but this information is rarely available. We recognize that this is a simplistic conversion that does not take into account differences in absorption between the respiratory and gastrointestinal system, in the physicochemical properties of contaminants, deposition, clearance mechanisms, and other factors that are important for assessing the toxicity of inhaled contaminants.

We used SF_i for carcinogens to rank contaminants that are known or potential carcinogens. Slope factors (also called potency factors) have been estimated by the EPA and others using mathematical extrapolation models (most commonly the linearized multistage model) to estimate the largest possible linear slope (within the 95% confidence limit) at low, extrapolated doses that are consistent with the experimental data. The slope factor is considered an upper-bound estimate and the actual risk is not likely to exceed the estimate. The slope factor is in units of risk per milligram per kilogram per day. There is considerable amount of uncertainty in these values, but they are generally very conservative. In developing them, the EPA used safety factors, modifying factors, and uncertainty factors. These factors accounted for variability in sensitivity among different people, uncertainties in using the results of animal studies to predict health effects in humans, extrapolating from exposures of different durations, and other uncertainties.

Some carcinogens also cause chronic noncancer health effects. In general, the concentrations that can cause cancer are lower than those that cause noncancer effects, so we used the SF_i for the ranking. For chemicals that seem to be an exception to this assumption (such as beryllium, which is weakly carcinogenic but causes a chronic immune-related disease associated with relatively low exposures), ranking was done using both the SF_i and the RfC. For some chemicals, for which RfCs seemed very uncertain, we used both the TLV/10 and the RfC for the screening. Table C-1 shows the values we used for the screening.

Table C-1. Toxicity Values used to Screen Potential Contaminants of Concern

Chemical	RfC ^a (mg m ⁻³)	(TLV ^b /10) (mg m ⁻³)	SF _i ^c (1/(mg/kg/d))
Acenaphthylene		0.0049	
Aluminum	0.0049		
Antimony	0.0004		
Arsenic			15
Asbestos (Friable)		0.1 (fibers/cc)	
Barium	0.005		
Beryllium	0.00002		8.4
Cadmium			6.1
Chromium (hexavalent)			290
Chromium (total) ^d			42
Cobalt		0.01	
Copper		0.1	
Cyanide (total)	0.00301		
Iron		0.1	
Lead		10	
Lithium	0.07		
Magnesium		1.5	
Manganese	0.000049		
Mercury	0.000301		
Molybdenum		0.5	
Nickel		0.1	
Nitrate (as NO ₃)		1.6	
Nitrite (as NO ₂)		0.1	
Selenium		0.02	
Silver		0.001	
Thallium		0.15	
Uranium		0.008	
Vanadium		0.005	
Zinc		1.5	
Acenaphthene	0.21		
Acenaphthylene	0.003		
Acetone	0.35		
Aldrin	0.00003		
Amino-2,6-dinitrotoluene[4-]	0.0001		
Amino-4,6-dinitrotoluene[2-]	0.0001		
Aniline			0.0073
Anthracene	1.05		
Aroclor-1254			2
Aroclor-1260			2
Benzene			0.027
Benzo(a)anthracene			0.31
Benzo(a)pyrene			3.1
Benzo(b)fluoranthene			0.31

Table C-1. (Continued)

Chemical	RfC ^a (mg m ⁻³)	(TLV ^b /10) (mg m ⁻³)	SF _i ^c (1/(mg/kg/d))
Benzo(g,h,i)perylene			0.031
Benzo(k)fluoranthene			0.031
Benzoic Acid	14		
Benzyl Alcohol	1.05		
BHC[alpha-]			6.3
BHC[delta-]			1.8
BHC[gamma-]			1.3
Bis(2-ethylhexyl)phthalate			0.014
Bromodichloromethane			0.062
Bromophenyl-phenylether[4-]			0.12
Butanone[2-]	1		
Butylbenzylphthalate	0.7		
Carbazole			0.02
Carbon Disulfide	0.7		
Chloro-3-methylphenol[4-]			0.12
Chloroaniline[4-]	0.014		
Chloronaphthalene[2-]	0.28		
Chlorophenol[2-]	0.0175		
Chrysene			0.0031
DDD[4,4'-]			0.24
DDE[4,4'-]			0.34
DDT[4,4'-]			0.34
Di-n-butylphthalate	0.35		
Di-n-octylphthalate	0.077		
Dibenz(a,h)anthracene			3.1
Dibenzofuran	0.014		
Dichlorobenzene[1,2-]	0.2		
Dichlorobenzene[1,3-]	0.00315		
Dichlorobenzene[1,4-]			0.022
Dichlorobenzidine[3,3'-]			0.45
Dichlorodifluoromethane	0.2		
Dichloroethene[cis-1,2-]	0.035		
Dieldrin			0.45
Diethylphthalate	2.8		
Dimethyl Phthalate	35		
Dimethylphenol[2,4-]	0.07		
Dinitrobenzene[1,3-]	0.00035		
Dimethylphenol[2,4-]	0.007		
Dinitrotoluene[2,6-]	0.0035		
Dinitrotoluene[2,4-]	0.007		
Endosulfan II	0.021		
Endosulfan Sulfate	0.021		

Table C-1. (Continued)

Chemical	RfC ^a (mg m ⁻³)	(TLV ^b /10) (mg m ⁻³)	SF _i ^c (1/(mg/kg/d))
Endrin	0.00105		
Endrin Aldehyde	0.00105		
Fluoranthene	0.14		
Fluorene	0.14		
Heptachlor Epoxide			9.1
Hexachlorobenzene			1.6
Hexanone[2-]		0.1	
HMX	0.175		
Indeno(1,2,3-cd)pyrene			0.31
Isopropyltoluene[4-]	0.035		
Methoxychlor[4,4'-]	0.0175		
Methyl-2-pentanone[4-]	0.0805		
Methylene Chloride			0.0016
Methylnaphthalene[2-]	0.003		
Methylphenol[2-]	0.175		
Methylphenol[4-]	0.0175		
Naphthalene	0.003		
Nitroaniline[4-]	0.0002		
Nitrobenzene	0.002		
Nitroglycerin			0.014
Nitrosodimethylamine[N-]			49
Nitrosodiphenylamine[N-]			0.0049
Nitrotoluene[2-]	0.035		
Nitrotoluene[3-]	0.035		
Nitrotoluene[4-]	0.035		
Organics, Diesel Range		90	
Pentachlorophenol			0.12
PETN			0.014
Phenanthrene	1.05		
Phenol	2.1		
Pyrene	0.105		
RDX			0.11
TATB	0.0001		
Tetrachloroethene			0.006
Tetryl		0.15	
Toluene	0.90		
Trichlorotrifluoroethane	30		
Trichlorobenzene[1,2,3-]	2		
Trichlorobenzene[1,2,4-]	2		
Trichloroethane[1,1,1-]	22.1		
Trichloroethene	0.014		
Trichlorofluoromethane	7		
Trimethylbenzene[1,2,4-]	0.00595		

Table C-1. (Continued)

Chemical	RfC ^a (mg m ⁻³)	(TLV ^b /10) (mg m ⁻³)	SF _i ^c (1/(mg/kg/d))
Trimethylbenzene[1,3,5-]	0.00595		
Trinitrobenzene[1,3,5-]	0.105		
Trinitrotoluene[2,4,6-]			0.03
Xylene (Total)	0.7		
Xylene[1,2-]	0.7		
Xylene[1,3-]	0.7		

^a Reference concentration.^b Threshold limit value divided by 10.^c Inhalation slope factor.^d Total chromium assumes a ratio of 1:6 Cr(VI):Cr(III).

Compounds for which no toxicity values have been derived can often be compared to a similar compound that has been studied and for which toxicity values have been derived. We obtained equivalency information relating the toxicity of compounds from several sources, primarily EPA (2001), ORNL (2001), Gosselin et al. (1984), and ATSDR (1990–2000). We did not find toxicity values for aminodinitrotoluene, bromophenyl-phenylether, chloro-3-methylphenol, isopropyltoluene, methylnaphthalene, or PETN, so we used values for dinitrotoluene, pentachlorophenol, pentachlorophenol, nitrotoluene, naphthalene, and nitroglycerin, which are similar compounds but probably more toxic or carcinogenic and expected to cause health effects at lower concentrations.

Toxicity values were used for metals in the form of dust. We did not use toxicity values for more toxic metal salts and compounds with toxic anions, or toxicity much greater than the metal alone, such as cyanide compounds, selenium hexafluoride, and metal oxide fumes. BHC (hexachlorocyclohexane) was once a widely used insecticide and was a mixture of the three isomers. Most of the insecticidal activity comes from the gamma isomer, known as lindane.

We included nitrates and nitrites, although they may be far more important for surface water contamination and do not generally present an inhalation hazard. Carbon, calcium, gold, sodium, platinum and potassium were detected in soil samples at the PRSs but were not included in the ranking because they are relatively nontoxic by inhalation.

Slope factors are intended to estimate the probability of increased cancer risk over a lifetime. We recognize that exposures to smoke would have occurred over a short time period, perhaps 10 days. In contrast, toxicity values like RfCs and slope factors are generally derived for daily exposure over a lifetime or over a time period of 30 years. These values are derived from chronic or subchronic toxicity studies in animals or from epidemiological studies conducted over various time periods. Toxicity values for long-term exposures are almost always more conservative (more cautious) than those derived for acute exposure. The concentrations that cause chronic health effects are generally lower than concentrations that cause short-term effects. Therefore, using the values derived from chronic exposure data is conservative and works well for the ranking. Using toxicity values derived for comparison to exposures lasting for years contributes to the conservatism of the methods and leads to estimates of risk that are greater than risks that would be estimated over a more realistic exposure duration.

REFERENCES

- ATSDR (Agency for Toxic Substances and Disease Registry). 1990–2000. Toxicological Profiles. Atlanta, Georgia.
- EPA (U.S. Environmental Protection Agency). 2001. Integrated Risk Information System (IRIS) Database. <EPA.gov>.
- Gosselin, R.E., R.P. Smith, and H. C. Hodge. 1984. *Clinical Toxicity of Commercial Products*. Baltimore, Maryland: Williams and Wilkins.
- ORNL (Oak Ridge National Laboratory). 2001. ORNL Risk Assessment Information System Database. <<http://risk/lrd.ornl.gov>>.

APPENDIX D

METHODOLOGY FOR CALCULATING IMPACTS FROM CONTAMINANTS ON STANDING VEGETATION AND FOREST LITTER RELEASED DURING THE CERRO GRANDE FIRE

APPENDIX D

METHODOLOGY FOR CALCULATING IMPACTS FROM CONTAMINANTS ON STANDING VEGETATION AND FOREST LITTER RELEASED DURING THE CERRO GRANDE FIRE

INTRODUCTION

When initially conceived, the analysis of the air pathway for the Cerro Grande Fire was intended to address airborne suspension and subsequent transport of contaminants present in the soil and related to Los Alamos National Laboratory (LANL) operations. During the course of the work, concern has been expressed not only about contaminants present in soil, but also about those present in the standing vegetation and forest litter in the areas that were burned. The contaminants may be present as a result of (1) naturally occurring radionuclides, (2) worldwide fallout from nuclear weapons tests and industrial processes, and (3) over 50 years of LANL operations. Contamination from naturally occurring radionuclides and worldwide fallout is not LANL-specific and is present not only on LANL lands but also in the surrounding National Forest.

This appendix describes the methodology used to assess the potential airborne release and dispersion of contaminants from burned vegetation during the Cerro Grande Fire.

METHODOLOGY

Calculating releases of radionuclides and metals from standing vegetation and forest litter during the Cerro Grande Fire requires an estimate of the contaminant inventories in these media. Measurements of regional radionuclide and metal concentrations in standing biomass and forest litter have been made by LANL, the New Mexico Environmental Department (NMED), and the U.S. Environmental Protection Agency (EPA). The methodology described here is only intended to provide an estimate of potential releases related to the burning of standing vegetation and forest litter. It is not intended to be definitive.

We used seven steps to calculate the releases:

1. Estimate radionuclide and metal concentrations in standing vegetation and forest litter (pCi g^{-1} or mg kg^{-1}).
2. Estimate the mass of standing vegetation and forest litter (kg acre^{-1}) using the fuel loading data.
3. Calculate total mass of standing vegetation and forest litter consumed during the fire (kg) by multiplying the fuel loading data by the number of acres burned.
4. Calculate the total radionuclide and metal activity in burned vegetation (pCi or mg) by multiplying the mass of standing vegetation and forest litter by the activity concentration.
5. Assume 100% release fraction of metals and radionuclides and releases are proportional to the PM10 releases during the fire.
6. Calculate the total PM10 emitted from the fire.

7. Calculate air concentrations of metals and radionuclides in the model domain by multiplying the 13-day average PM10 concentration by the ratio of the total activity (or metal mass) in biomass (standing vegetation and litter) to the total PM10 emitted.

Assumption 5 may seem unrealistic since there are obviously charred trees left standing in the burned areas. Therefore, we also calculated air concentrations resulting from the burning of bark and litter only, omitting the contribution from pulp. Each of the steps is explained in the following sections

Contaminant Concentrations in Vegetation

We obtained data regarding concentrations of radionuclides and metals in and on vegetation from a number of different sources. NMED provided raw data for both radionuclides and metals in individual samples collected by NMED and EPA. Two LANL documents provided additional information related to average radionuclide concentrations measured in and on vegetation (Gonzales et al. 2000 and 2001). Finally, because of the importance of radon decay products with regard to measured air concentrations, we obtained average concentrations in vegetation samples for ^{226}Ra , ^{210}Pb , and ^{210}Po (Thomas 2000). Each of these sources of data is discussed further in the following sections.

NMED and EPA Data

Concentrations of contaminants in and on vegetation were provided by NMED on two Microsoft Excel[®] spreadsheets named “2000_OB_Forest_Component_Data” for NMED data and “2000TechLawForestComponentData” for EPA data. These data provided radionuclide and metal mass concentrations in wood pulp, bark, and forest litter. Estimates of contaminant inventories and air concentrations are limited to the constituents measured. Mass concentrations represent the concentration in the muffed/ashed sample and were reported in pCi g⁻¹ for radionuclides and mg kg⁻¹ for metals. The total weight reduction from the fresh-weight to the muffed/ashed sample was also reported for each sample allowing conversion to the concentration in fresh-weight sample of the vegetation. The fresh-weight concentration is given by

$$C_{fw} = \frac{C_a}{WRR} \quad (\text{D-1})$$

where

C_{fw}	=	contaminant concentration in fresh-weight (pCi g ⁻¹ or mg kg ⁻¹)
C_a	=	contaminant concentration in the ashed/muffed sample (pCi g ⁻¹ or mg kg ⁻¹)
WRR	=	weight reduction ratio, reported on a sample-specific basis (unitless).

For radionuclides, a distinction was made in the samples between Douglas Fir and Ponderosa Pine. We did not make that distinction in our analysis and instead grouped the samples into three vegetation media: wood pulp, bark, or forest litter.

Average concentrations of radionuclides and metals were computed from the raw concentration data in wood pulp, bark, and forest litter. Where laboratory duplicates were

reported, the average concentration between the laboratory duplicate and the original sample was used. Additionally, sample results were omitted if the sample was reported as a "less than" value or the concentration was negative. One exception was made for mercury because all the samples were reported as "less than" values and mercury is typically a chemical of concern. In this case, the less than value was used to compute average concentrations.

Some contaminants had no concentration values reported for bark or forest litter but measurable concentrations in wood pulp. In these cases, we estimated the average concentration in bark or forest litter by multiplying the average wood pulp concentration of the contaminant by the average bark/pulp concentration ratio to obtain the bark concentration or the average litter/pulp concentration ratio to obtain forest litter concentrations. The average bark/pulp (14 for radionuclides and 10 for metals) or litter/pulp (38 for radionuclides and 32 for metals) concentration ratio was determined from contaminants that had measurable quantities in all three vegetation media. Average concentrations for radionuclides and metals based on NMED and EPA data are reported in Tables D-1 and D-2, respectively.

Table D-1. Average Radionuclide Concentrations (pCi g⁻¹ fresh weight) Reported by NMED and EPA for Three Vegetation Types

Radionuclide	Vegetation type		
	Litter	Pulp	Bark
⁹⁰ Sr	1.7×10^{-1}	9.7×10^{-3}	1.1×10^{-1}
²³⁸ Pu	2.1×10^{-4}	2.5×10^{-5}	1.6×10^{-4}
^{239,240} Pu	2.9×10^{-3}	5.0×10^{-5}	1.4×10^{-3}
²⁴¹ Am	1.0×10^{-3}	6.4×10^{-5}	8.3×10^{-4}
¹³⁷ Cs	9.7×10^{-2}	2.8×10^{-3}	5.0×10^{-2}
²²⁸ Ac ^a	8.0×10^{-2}	3.6×10^{-3}	4.8×10^{-2}
⁷ Be ^a	2.4×10^0	2.1×10^0	2.9×10^1
²¹⁴ Bi ^a	7.4×10^{-2}	5.0×10^{-3}	6.7×10^{-2}
⁴⁰ K ^a	1.6×10^0	3.8×10^{-1}	1.7×10^0
²¹² Pb ^a	9.5×10^{-2}	1.4×10^{-3}	2.0×10^{-2}
²¹⁴ Pb ^a	7.1×10^{-2}	5.8×10^{-4}	7.9×10^{-3}
²³⁴ Th ^a	4.3×10^{-1}	5.0×10^{-3}	6.7×10^{-2}
²⁰⁸ Tl ^a	2.9×10^{-2}	6.0×10^{-4}	8.2×10^{-3}

^a Concentrations in bark were computed from pulp concentration and the average bark/pulp concentration ratio of 14.

Table D-2. Average Metal Concentrations (mg kg⁻¹ fresh weight) Reported by NMED and EPA for Three Vegetation Types

Metal	Vegetation type			Metal	Vegetation type		
	Litter	Pulp	Bark		Litter	Pulp	Bark
Cyanide ^a	5.1×10^{-2}	6.2×10^{-3}	2.4×10^{-2}	Pb	2.7×10^0	4.0×10^{-2}	1.8×10^0
Al	1.1×10^3	1.0×10^1	2.3×10^2	Mg	7.8×10^2	8.3×10^1	2.5×10^2
Sb ^{b,c}	3.0×10^{-2}	9.4×10^{-4}	9.6×10^{-3}	Mn	2.0×10^2	2.1×10^1	2.1×10^2
As	2.1×10^{-1}	6.6×10^{-3}	9.0×10^{-2}	Mo	1.3×10^{-1}	3.4×10^{-3}	1.2×10^{-2}
B	8.1×10^0	9.6×10^{-1}	6.8×10^0	Ni	9.7×10^{-1}	4.6×10^{-2}	6.4×10^{-1}
Ba	2.0×10^1	7.3×10^0	4.0×10^1	K	7.0×10^2	4.6×10^2	1.3×10^3
Bi ^{b,c}	3.9×10^0	1.3×10^{-1}	1.3×10^0	Se	1.4×10^{-1}	5.8×10^{-3}	4.5×10^{-2}
Be	5.3×10^{-2}	6.6×10^{-4}	7.4×10^{-3}	Si	1.5×10^2	1.1×10^1	6.5×10^1
Cd	6.1×10^{-2}	1.8×10^{-3}	4.5×10^{-2}	Sn ^b	2.1×10^{-1}	6.8×10^{-3}	8.2×10^{-2}
Ca	4.9×10^3	6.8×10^2	5.9×10^3	Sr	1.5×10^1	3.1×10^0	1.6×10^1
Cr	7.4×10^{-1}	2.7×10^{-2}	2.1×10^{-1}	Ag ^{b,c}	6.4×10^{-1}	2.0×10^{-2}	2.1×10^{-1}
Co	6.1×10^{-1}	2.9×10^{-2}	1.8×10^{-1}	Na	1.9×10^2	1.3×10^1	5.9×10^1
Cu	3.9×10^0	4.6×10^{-1}	3.4×10^0	Tl ^b	1.6×10^{-1}	5.0×10^{-3}	3.6×10^{-2}
Fe	1.1×10^3	1.8×10^1	1.4×10^2	V	1.8×10^0	1.1×10^{-2}	2.5×10^{-1}
Hg	6.7×10^{-3}	2.5×10^{-4}	1.6×10^{-3}	Zn	2.2×10^1	1.5×10^0	8.8×10^0
Li	1.1×10^0	5.7×10^{-2}	2.8×10^{-1}				

^a Cyanide is not considered a metallic element.^b Concentrations in litter were computed from the pulp concentration and the average litter/pulp concentration ratio of 32.^c Concentrations in bark were computed from the pulp concentration and the average bark/pulp concentration ratio of 10.

LANL Data

Additional data regarding measured concentrations of radionuclides were obtained from Gonzales et al. (2000, 2001). Gonzales et al. (2000) reported concentrations for both understory and overstory plants sampled from within and around LANL. Overstory plants are described as shrubs and trees and are comprised of samples collected from the 1- to 2-inch portion of the shoot tip of the plant containing needles, leaves, and some live wood. For the purpose of these calculations, we considered overstory plants to be in the same category as the NMED and EPA bark samples. Understory plants are described as grasses and forbs and are considered to be in the same category as the forest litter samples. As with the NMED and EPA data, LANL reported concentrations for ashed samples; however, a weight reduction factor is not provided. To calculate fresh-weight concentrations, we obtained moisture conversion ratios for both understory and overstory native vegetation from Fresquez and Ferenbaugh (1999). The fresh-weight concentration is calculated by

$$C_{fw} = C_a \times MCR_{ad} \times MCR_{dw} \quad (D-2)$$

where

C_{fw}	=	contaminant concentration in fresh-weight (pCi g ⁻¹)
C_a	=	contaminant concentration in the ashed sample (pCi g ⁻¹)
MCR_{ad}	=	ash to dry moisture conversion ratio (unitless)
MCR_{dw}	=	dry to wet moisture conversion ratio (unitless).

Table D-3 gives average concentrations for both types of samples after conversion from ash-to wet-weight for regional background, perimeter, and onsite stations. No clearly discernable trends are evident as a function of either vegetation type or location, although the data suggest the possibility of higher ¹³⁷Cs, ^{239,240}Pu, and ²⁴¹Am concentrations in onsite samples.

Table D-3. Average Radionuclide Concentrations (pCi g⁻¹ fresh weight) in Vegetation Samples Based on Data Reported by Gonzales et al. (2000)

Type	Location	⁹⁰ Sr	²³⁸ Pu	^{239,240} Pu	²⁴¹ Am	¹³⁷ Cs
Overstory ^a	Background	4.7×10^{-2}	1.8×10^{-5}	5.4×10^{-5}	1.1×10^{-4}	8.8×10^{-3}
	Perimeter	5.9×10^{-2}	4.3×10^{-5}	1.8×10^{-4}	1.5×10^{-4}	1.2×10^{-2}
	Onsite	4.4×10^{-2}	9.0×10^{-6}	1.9×10^{-4}	3.2×10^{-4}	3.4×10^{-2}
Understory ^b	Background	6.7×10^{-2}	3.2×10^{-5}	8.6×10^{-5}	1.3×10^{-4}	7.5×10^{-3}
	Perimeter	1.3×10^{-1}	1.1×10^{-4}	5.0×10^{-4}	1.6×10^{-4}	7.3×10^{-3}
	Onsite	4.7×10^{-2}	1.9×10^{-5}	2.6×10^{-4}	2.3×10^{-4}	1.9×10^{-2}

^a Assumed analogous to bark.

^b Assumed analogous to litter.

Gonzales et al. (2001) reported radionuclide concentrations for both bark and wood samples collected from Ponderosa Pines from three sections along Mortandad Canyon and one reference or background location northwest of LANL off of New Mexico State Road 4. Again, concentrations are reported for ashed samples. Sample-specific ash-to-wet weight ratios are also reported, and we multiplied these values by the reported ashed concentrations to convert the values to fresh-weight concentrations. Because Gonzales et al. (2001) was the only source of uranium isotopic data, we estimated litter concentrations based on the litter-to-pulp radionuclide concentration ratio determined from the NMED and EPA data.

Table D-4 shows average concentrations for the three onsite samples along with the concentrations reported for the background sample. These data suggest generally higher concentrations in bark compared to wood, and they also suggest higher concentrations in the onsite samples collected from Mortandad Canyon compared to the data in the background location.

The data presented in Tables D-3 and D-4 suggest the possibility of higher concentrations for some radionuclides in vegetation samples collected from onsite locations. However, more detailed analyses to identify any statistically significant trends, either spatially or by vegetation type were precluded in this study. Furthermore, it is not apparent that the available data would enable such analyses. Additional data could help determine the fraction of burned vegetation potentially impacted by LANL operations and help better understand the variability in concentrations, both as a function of location and vegetation type.

**Table D-4. Average Radionuclide Concentrations (pCi g⁻¹ fresh weight) in Conifer Tree
Samples Based on Data Reported by Gonzales et al. (2001)**

Type	Location (n)	⁹⁰ Sr	²³⁸ Pu	^{239,240} Pu	²⁴¹ Am	¹³⁷ Cs	²³⁴ U	²³⁵ U	²³⁸ U
Wood ^a	Onsite (3)	1.8E-01	-6.6E-07	4.9E-05	1.2E-04	3.5E-03	1.6E-04	5.2E-05	1.1E-04
	Background (1)	8.3E-03	0.0E+00	5.8E-06	4.3E-05	1.5E-03	1.4E-04	3.3E-05	1.0E-04
Bark	Onsite (3)	1.8E-01	1.0E-02	2.8E-02	3.9E-02	3.3E-02	1.1E-02	1.2E-03	1.7E-02
	Background (1)	4.9E-03	1.8E-05	1.8E-05	4.0E-05	9.6E-04	9.3E-04	5.8E-06	9.6E-04
Litter ^b	Onsite (3)						5.9E-03	2.0E-03	4.2E-03
	Background (1)						5.5E-03	1.2E-03	3.8E-03

^a Assumed analogous to pulp.^b Calculated using litter/pulp radionuclide concentration ratio of 38 determined using NMED and EPA data.

n = Number of samples.

Radon Decay Product Data

Based on measured air concentrations, the primary contributors to potential dose from radionuclides suspended in Cerro Grande Fire smoke appear to be radon decay products, including ²¹⁰Pb, ²¹⁰Po, and ²¹⁰Bi. Because the information sources discussed above did not provide any information regarding concentrations of radon decay products on or in vegetation, we estimated concentrations based on data reported by Thomas (2000). Concentrations of ²²⁶Ra, ²¹⁰Pb, and ²¹⁰Po are given for Black Spruce and Jackpine needles and twigs (assumed analogous to bark) as well as litter samples from a control site (i.e., presumably not impacted by mill operations) near a uranium mill in Saskatchewan, Canada. Thomas (2000) reported concentrations on a dry-weight basis; therefore, we used the dry to wet moisture conversion ratios for both understory (assumed analogous to litter) and overstory (assumed analogous to bark) vegetation reported by Fresquez and Ferenbaugh (1999) to estimate fresh-weight concentrations. Because Thomas (2000) represents the only source we have been able to locate regarding radon decay product concentrations in or on vegetation, we estimated concentrations in pulp based on the bark-to-pulp concentration ratio determined from the NMED and EPA data. To calculate air concentrations for ²¹⁰Bi, we assumed vegetation concentrations to be the same as those reported for ²¹⁰Pb. Table D-5 shows the range of average values reported by Thomas (2000) for samples consisting of either needles and twigs or litter.

To estimate a range of potential contaminant inventories in forest components, we used the lowest and highest values reported (Tables D-1, D-3, D-4, and D-5) wherever multiple values were available for a given contaminant. This applies only to radionuclides because the NMED and EPA data set represents the only source of metal concentrations in vegetation. We used the average concentrations shown in Table D-2 to calculate metal inventories in the three classes of forest components, and we did not calculate a range of inventories. Similarly, the NMED and EPA data represent the only source of measurements for certain radionuclides (²²⁸Ac, ⁷Be, ²¹⁴Bi, ⁴⁰K, ²¹²Pb, ²¹⁴Pb, ²³⁴Th, and ²⁰⁸Tl), so we did not calculate a range of inventories. Table D-6 shows the lowest and highest average values for all radionuclides where we compiled multiple values from different sources. The values in Table D-6 for the radionuclides listed were used to estimate radionuclides inventories and subsequent air concentrations and risks.

Table D-5. Average Radionuclide Concentrations (pCi g⁻¹ fresh weight) in Vegetation Samples Based on Data Reported by Thomas (2000)

Sample type	Value	²¹⁰ Pb	²¹⁰ Po	²¹⁰ Bi ^a	²²⁶ Ra
Needles and twigs ^b	Max average	3.2E+00	2.2E+00	3.2E+00	9.8E-01
	Min average	6.4E-01	2.1E-01	6.4E-01	2.4E-02
Litter	Max average	4.0E+00	2.0E+00	4.0E+00	5.2E-01
	Min average	1.7E+00	1.6E+00	1.7E+00	4.5E-01
Pulp ^c	Max average	2.3E-01	1.6E-01	2.3E-01	7.0E-02
	Min average	4.6E-02	1.5E-02	4.6E-02	1.7E-03

^a Not reported by Thomas (2000), but assumed equal to ²¹⁰Pb concentrations.

^b Assumed analogous to bark.

^c Calculated based on needle and twig concentrations and bark/pulp radionuclide concentration ratio of 14 determined from NMED and EPA data.

Table D-6. Range of Average Concentrations (pC g⁻¹ fresh-weight) Compiled in Tables D-1, D-3, D-4, and D-5 for Vegetation Samples

Radionuclide	Bark		Pulp		Litter	
	Maximum	Minimum	Maximum	Minimum	Maximum	Minimum
⁹⁰ Sr	1.8E-01	4.9E-03	1.8E-01	8.3E-03	1.7E-01	4.7E-02
²³⁸ Pu	1.0E-02	9.0E-06	2.5E-05	0.0E+00	2.1E-04	1.9E-05
^{239,240} Pu	2.8E-02	1.8E-05	5.0E-05	5.8E-06	2.9E-03	8.6E-05
²⁴¹ Am	3.9E-02	4.0E-05	1.2E-04	4.3E-05	1.0E-03	1.3E-04
¹³⁷ Cs	5.0E-02	9.6E-04	3.5E-03	1.5E-03	9.7E-02	7.3E-03
²¹⁰ Pb	3.2E+00	6.4E-01	2.3E-01	4.6E-02	4.0E+00	1.7E+00
²¹⁰ Po	2.2E+00	2.1E-01	1.6E-01	1.5E-02	2.0E+00	1.6E+00
²¹⁰ Bi	3.2E+00	6.4E-01	2.3E-01	4.6E-02	4.0E+00	1.7E+00
²²⁶ Ra	9.8E-01	2.4E-02	7.0E-02	1.7E-03	5.2E-01	4.5E-01
²³⁴ U	1.1E-02	9.3E-04	1.6E-04	1.4E-04	5.9E-03	5.5E-03
²³⁵ U	1.2E-03	5.8E-06	5.2E-05	3.3E-05	2.0E-03	1.2E-03
²³⁸ U	1.7E-02	9.6E-04	1.1E-04	1.0E-04	4.2E-03	3.8E-03

Radionuclide and Metal Inventories in the Burned Areas

Contaminant inventories in the burned areas were calculated by multiplying the fresh-weight concentration in vegetation by the mass of vegetation in the burned area for each of the three vegetation types: bark, pulp, and litter. We took the mass of standing vegetation and forest litter in the burned areas from the fuel loading data used in the Emissions Production Model (Sandberg and Peterson 1984) (Table D-7). Fuel loading values were taken from Balice et al. (2000), and they represent the 97.5 percentile value of the *distribution* of measured fuel load values. We used the 97.5 percentile value because dispersion model calibrations with PM10 concentration data required higher fuel loading to bring model estimates in line with measurements. Assuming normal statistics apply, the 97.5 percentile is given by

$$M_{97.5} = \bar{M} + Z s \quad (\text{D-3})$$

where

- $M_{97.5}$ = the 97.5% fuel loading value (kg acre^{-1}),
 Z = the Z value for a normal distribution for $P=0.475$ (1.92), and
 s = the standard deviation (kg acre^{-1}).

Minor adjustments to fuel loading were also made during model calibration and the values given in Table D-7 represent the values used in the calibrated fire simulation. Balice et al. (2000) reports fuel loads for four types of fuel; 1 hour (0–0.25-inch diameter), 10 hours (0.25–1-inch diameter), 100 hours (1–3-inch diameter), and 1000 hours (1–20+-inch diameter). The sum of these four fuel types yielded the total standing vegetation mass. Table D-7 also includes pollutant emission estimates calculated by the Emissions Production Model (EPM), which we used along with estimated PM10 concentrations in air to calculate concentrations of radionuclides and metals in air.

Table D-7. Burn Area, Vegetation Mass, and Pollutant Release Estimates

Burn day ^a	Vegetation type	Acreage burned (acres)	Mass of standing vegetation (kg) ^b	Mass of forest litter (kg)	Emissions Production Model release estimates					
					PM-2.5 released (g)	PM10 released (g)	Total PM released (g)	Carbon monoxide released (g)	Carbon dioxide released (g)	Methane released (g)
6	Conifer/Spruce	805	2.2E+07	1.3E+06	1.7E+08	1.9E+08	3.3E+08	1.3E+09	4.6E+10	7.6E+07
7	Ponderosa/Mixed Conifer	1553	6.9E+07	2.1E+06	3.2E+08	3.7E+08	6.2E+08	2.6E+09	8.5E+10	1.6E+08
8	Ponderosa/Mixed Conifer	857	3.8E+07	1.2E+06	8.0E+08	8.7E+08	1.2E+09	6.7E+09	1.1E+11	3.2E+08
9	Ponderosa/Mixed Conifer	50	2.2E+06	6.7E+04	2.4E+07	2.6E+07	3.6E+07	2.0E+08	3.2E+09	9.7E+06
10	Conifer/Spruce	1950	5.4E+07	3.1E+06	8.9E+08	9.7E+08	1.3E+09	7.5E+09	1.2E+11	3.6E+08
10	Ponderosa/Mixed Conifer	1950	8.6E+07	2.6E+06	8.9E+08	9.7E+08	1.3E+09	7.5E+09	1.2E+11	3.6E+08
10	Ponderosa/Mixed Conifer	1950	8.6E+07	2.6E+06	8.9E+08	9.7E+08	1.3E+09	7.5E+09	1.2E+11	3.6E+08
10	Ponderosa/Mixed Conifer	1625	7.2E+07	2.2E+06	7.5E+08	8.1E+08	1.1E+09	6.3E+09	9.8E+10	3.0E+08
11	Ponderosa/Mixed Conifer	2909	1.3E+08	3.9E+06	1.1E+09	1.2E+09	1.6E+09	9.2E+09	1.4E+11	4.4E+08
11	Ponderosa/Mixed Conifer	2909	1.3E+08	3.9E+06	1.1E+09	1.2E+09	1.6E+09	9.2E+09	1.4E+11	4.4E+08
11	Ponderosa	2909	6.0E+07	4.2E+06	1.1E+09	1.2E+09	1.6E+09	9.2E+09	1.4E+11	4.4E+08
11	Ponderosa/Mixed Conifer	2909	1.3E+08	3.9E+06	1.1E+09	1.2E+09	1.6E+09	9.2E+09	1.4E+11	4.4E+08
11	Ponderosa/Mixed Conifer	2909	1.3E+08	3.9E+06	1.1E+09	1.2E+09	1.6E+09	9.2E+09	1.4E+11	4.4E+08
11	Ponderosa	2909	6.0E+07	4.2E+06	1.3E+09	1.4E+09	2.0E+09	1.1E+10	1.7E+11	5.4E+08
11	Ponderosa/Mixed Conifer	1939	8.6E+07	2.6E+06	9.0E+08	9.8E+08	1.4E+09	7.6E+09	1.2E+11	3.7E+08
12	Ponderosa/Mixed Conifer	2069	9.1E+07	2.8E+06	4.8E+08	5.5E+08	9.0E+08	4.1E+09	1.2E+11	2.5E+08
12	Ponderosa	517	1.1E+07	7.5E+05	2.1E+08	2.3E+08	3.1E+08	1.8E+09	2.7E+10	8.4E+07
13	Conifer/Spruce	3583	9.9E+07	5.8E+06	8.5E+08	9.8E+08	1.6E+09	7.3E+09	2.1E+11	4.5E+08
13	Ponderosa	2389	4.9E+07	3.4E+06	1.4E+08	1.5E+08	2.1E+08	1.2E+09	1.8E+10	5.8E+07
14	Ponderosa/Mixed Conifer	1158	5.1E+07	1.6E+06	5.9E+08	6.3E+08	8.8E+08	4.9E+09	7.5E+10	2.4E+08
14	Ponderosa	165	3.4E+06	2.4E+05	1.7E+08	1.9E+08	2.6E+08	1.5E+09	2.3E+10	7.1E+07
14	Conifer/Spruce	331	9.2E+06	5.3E+05	1.6E+08	1.9E+08	3.0E+08	6.7E+08	4.0E+10	8.1E+07
15	Ponderosa/Mixed Conifer	397	1.8E+07	5.4E+05	8.1E+07	9.5E+07	1.6E+08	6.2E+08	2.3E+10	3.8E+07
16	Conifer/Spruce	539	1.5E+07	8.7E+05	1.1E+08	1.3E+08	2.2E+08	8.5E+08	3.0E+10	5.2E+07
17	Conifer/Spruce	378	1.0E+07	6.1E+05	1.0E+08	1.1E+08	1.9E+08	8.6E+08	2.4E+10	5.3E+07
18	Ponderosa	711	1.5E+07	1.0E+06	3.9E+08	4.3E+08	5.9E+08	3.3E+09	4.9E+10	1.6E+08
TOTAL		42370	1.5E+09	6.0E+07	1.6E+10	1.7E+10	2.5E+10	1.3E+11	2.3E+12	6.7E+09

^a See also Table 4-7 in Chapter 4 to identify subareas that burned on a given day.

^b Includes both bark and pulp.

The inventory of activity or contaminant mass in the burned areas is calculated by multiplying the average concentration in the vegetation by the fuel loads in the burned area and summing across all vegetation types.

$$Q = \sum_{j=1}^m C_j M_j \quad (D-4)$$

where

- Q = contaminant inventory in pulp, bark, or forest litter (pCi or mg)
 C_j = average fresh-weight concentration in the j^{th} vegetation type (pCi kg⁻¹, mg kg⁻¹)
 M_j = mass of j^{th} vegetation type that was burned (kg)
 m = number of vegetation types (three).

For radionuclides, we converted concentrations to pCi kg⁻¹ to obtain consistent units of measure. The mass of standing vegetation presumably includes both the mass of the bark and wood pulp. The bark-to-pulp weight ratio is dependent on the type of vegetation, the diameter of the trunk and branches, and the moisture content of the vegetation just to name a few parameters. While the contaminant concentrations in bark are in most cases substantially higher relative to that of the pulp, the total mass of bark is presumably smaller. Therefore, it is necessary to estimate the total mass of both bark and pulp, based on an assumed bark-to-pulp weight ratio. The mass of bark is given by

$$M_{bark} = M_t \phi \quad (D-5)$$

where

- M_{bark} = the mass of bark (kg),
 M_t = the total mass of standing vegetation (kg),
 ϕ = the bark-to-pulp weight ratio.

The mass of pulp (M_{pulp}) is given by

$$M_{pulp} = M_t (1 - \phi) \quad (D-6)$$

The mass of individual pulp and bark samples was recorded in the spreadsheets provided by NMED; however, this information is inadequate to determine a bark-to-pulp weight ratio because the sampled volume was not representative of the proportions of bark and pulp found in natural vegetation. The *relative* mass of bark and pulp was also not reported in Balice et al. (2000). Gonzales et al. (2001) did report bark and wood percent composition by weight for three samples. The average bark-to-pulp weight ratio for these three samples ranged from 0.12 to 0.20. We assumed a ratio of 0.2 for our calculations.

Radionuclide inventories in the burned areas are tabulated in Table D-8, and metal inventories are tabulated in Table D-9. These values represent the total calculated contaminant inventories in the bark, pulp, and forest litter. For those radionuclides with a range of average concentration values, maximum and minimum inventory values are tabulated. The entire inventory was assumed to be released as a result of the fire (100% release fraction).

Table D-8. Range of Radionuclide Inventories (Ci) in Vegetation at the Areas Burned during the Cerro Grande Fire

Radionuclide	Litter ^a		Pulp ^b		Bark ^c	
	Maximum	Minimum	Maximum	Minimum	Maximum	Minimum
⁹⁰ Sr	1.0E-02	2.8E-03	2.2E-01	1.0E-02	5.5E-02	1.5E-03
²³⁸ Pu	1.3E-05	1.2E-06	3.1E-05	0.0E+00	3.1E-03	2.7E-06
^{239,240} Pu	1.7E-04	5.2E-06	6.0E-05	7.1E-06	8.5E-03	5.4E-06
²⁴¹ Am	6.1E-05	7.9E-06	1.5E-04	5.2E-05	1.2E-02	1.2E-05
¹³⁷ Cs	5.8E-03	4.4E-04	4.2E-03	1.8E-03	1.5E-02	2.9E-04
²¹⁰ Pb	2.4E-01	1.0E-01	2.7E-01	5.6E-02	9.6E-01	2.0E-01
²¹⁰ Po	1.2E-01	9.9E-02	1.9E-01	1.8E-02	6.6E-01	6.3E-02
²¹⁰ Bi	2.4E-01	1.0E-01	2.7E-01	5.6E-02	9.6E-01	2.0E-01
²²⁶ Ra	3.1E-02	2.7E-02	8.5E-02	2.1E-03	3.0E-01	7.4E-03
²²⁸ Ac	4.8E-03		4.4E-03		1.5E-02	
⁷ Be	1.4E-01		2.6E+00		8.7E+00	
²¹⁴ Bi	4.4E-03		6.0E-03		2.0E-02	
⁴⁰ K	9.9E-02		4.6E-01		5.1E-01	
²¹² Pb	5.7E-03		1.8E-03		5.9E-03	
²¹⁴ Pb	4.3E-03		7.1E-04		2.4E-03	
²³⁴ Th	2.6E-02		6.0E-03		2.0E-02	
²⁰⁸ Tl	1.7E-03		7.3E-04		2.5E-03	
²³⁴ U	3.6E-04	3.3E-04	1.9E-04	1.7E-04	3.3E-03	2.8E-04
²³⁵ U	1.2E-04	7.5E-05	6.3E-05	4.0E-05	3.6E-04	1.8E-06
²³⁸ U	2.5E-04	2.3E-04	1.4E-04	1.2E-04	5.1E-03	2.9E-04

^a Mass of litter in the burned areas was estimated to be 6.0×10^7 kg.

^b Mass of pulp in the burned areas was estimated to be 1.2×10^9 kg.

^c Mass of bark in the burned areas was estimated to be 3.0×10^8 kg.

**Table D-9. Metal Inventories (mg) in Vegetation at the Areas
Burned during the Cerro Grande Fire**

Metal	Litter ^a	Pulp ^b	Bark ^c
Cyanide	5.1E-02	6.2E-03	2.4E-02
Al	1.1E+03	1.0E+01	2.3E+02
Sb	3.0E-02	9.4E-04	9.6E-03
As	2.1E-01	6.6E-03	9.0E-02
B	8.1E+00	9.6E-01	6.8E+00
Ba	2.0E+01	7.3E+00	4.0E+01
Bi	3.9E+00	1.3E-01	1.3E+00
Be	5.3E-02	6.6E-04	7.4E-03
Cd	6.1E-02	1.8E-03	4.5E-02
Ca	4.9E+03	6.8E+02	5.9E+03
Cr	7.4E-01	2.7E-02	2.1E-01
Co	6.1E-01	2.9E-02	1.8E-01
Cu	3.9E+00	4.6E-01	3.4E+00
Fe	1.1E+03	1.8E+01	1.4E+02
Hg	6.7E-03	2.5E-04	1.6E-03
Li	1.1E+00	5.7E-02	2.8E-01
Pb	2.7E+00	4.0E-02	1.8E+00
Mg	7.8E+02	8.3E+01	2.5E+02
Mn	2.0E+02	2.1E+01	2.1E+02
Mo	1.3E-01	3.4E-03	1.2E-02
Ni	9.7E-01	4.6E-02	6.4E-01
K	7.0E+02	4.6E+02	1.3E+03
Se	1.4E-01	5.8E-03	4.5E-02
Si	1.5E+02	1.1E+01	6.5E+01
Sn	2.1E-01	6.8E-03	8.2E-02
Sr	1.5E+01	3.1E+00	1.6E+01
Ag	6.4E-01	2.0E-02	2.1E-01
Na	1.9E+02	1.3E+01	5.9E+01
Tl	1.6E-01	5.0E-03	3.6E-02
V	1.8E+00	1.1E-02	2.5E-01
Zn	2.2E+01	1.5E+00	8.8E+00

^a Mass of litter in the burned areas was estimated to be 6.0×10^7 kg.^b Mass of pulp in the burned areas was estimated to be 1.2×10^9 kg.^c Mass of bark in the burned areas was estimated to be 3.0×10^8 kg.

Estimating Air Concentrations

Air concentrations resulting from the release of contaminants in vegetation that burned during the fire were calculated based on the assumption that (1) 100% of the contaminant inventory was released during the fire and (2) the release and dispersion of contaminants was proportional to the release and dispersion of PM10 emitted from the fire. These are essentially the same assumptions made for computing air concentrations from contaminants released from potential release sites (PRSs). For this exercise, we computed the 13-day average concentration at selected receptor locations (May 6–18). The 13-day average contaminant concentration (C_{air}) is given by

$$C_{air} = \frac{X_{PM10}}{Q_{PM10}} Q \quad (D-7)$$

where

X_{PM10} = 13-day average PM10 concentration (g m^{-3})

Q_{PM10} = total PM10 released during the fire (g)

Q = inventory of contaminant in areas burned during the Cerro Grande Fire (mg or Ci).

Values for X were calculated using the CALPUFF model (Scire et al. 1999) coupled with PM10 emission estimates made using the EPM model. These calculations are detailed in the main body of this report in Chapter 4. Total PM10 emissions are reported in Table D-7 column 7 of this Appendix. Values for Q are the sum of the bark, pulp, and litter contaminant inventories reported in Tables D-8 and D-9. We calculated contaminant concentrations in air at several locations in the model domain. These locations roughly correspond to PM10 monitor locations and are illustrated in Figure D-1 along with the 13-day average PM10 concentrations. Radionuclide decay during atmospheric transport was not considered.

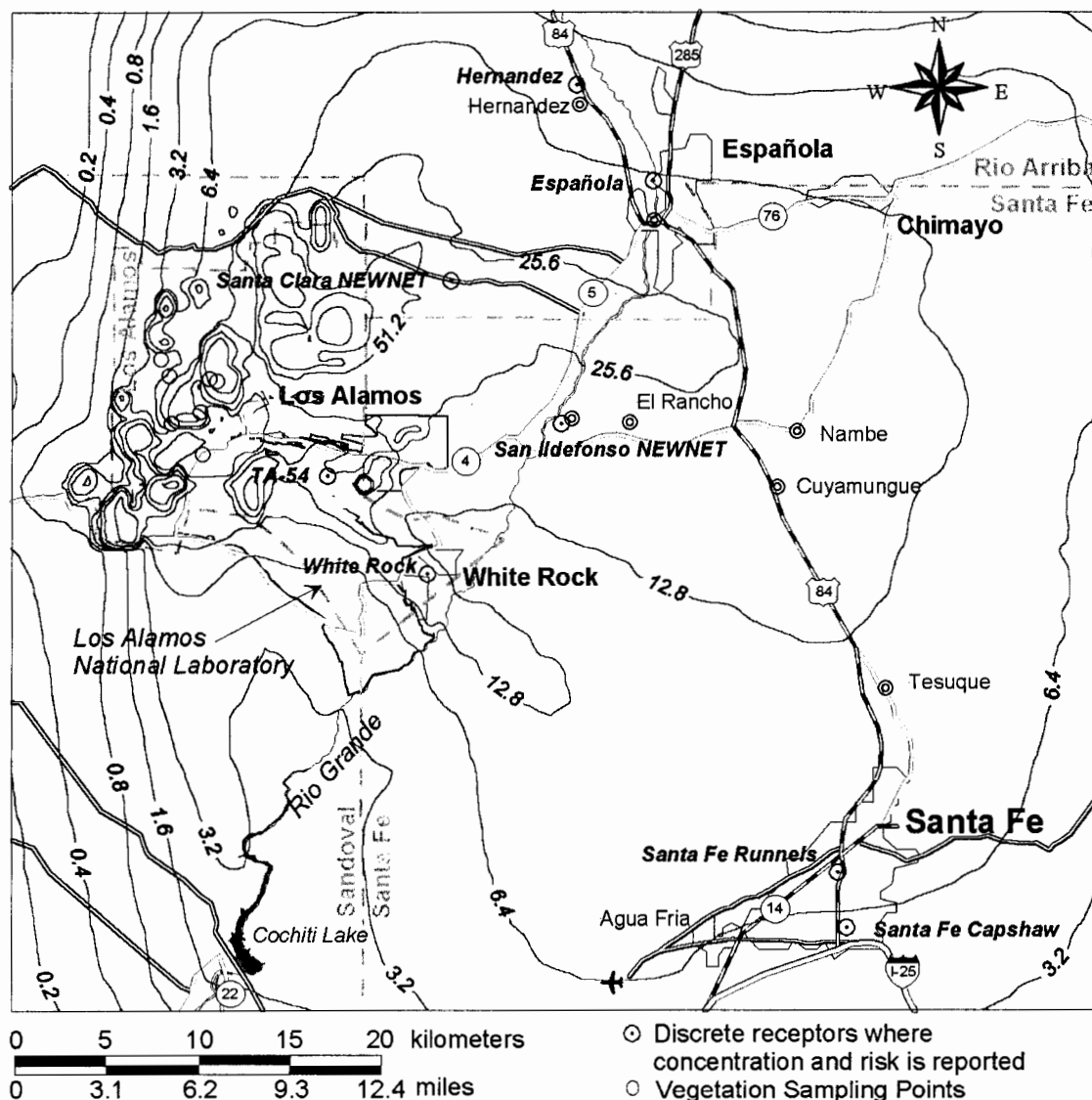


Figure D-1. Thirteen-day average PM₁₀ concentration in the model domain. Concentrations represent contributions from the fire only. Background contributions are not included. Vegetation sampling points are also indicated (except for those in the Viveash area)

ESTIMATED AIR CONCENTRATIONS

Concentrations of radionuclides in air (Table D-10) were generally within the $\mu\text{Ci m}^{-3}$ range with the exception of ^7Be , ^{40}K , ^{210}Pb , ^{210}Po , and ^{210}Bi . These radionuclides had concentrations in the fCi m^{-3} range. Potassium-40 is a primordial natural radionuclide that typically has concentrations in soil ranging from 10–40 pCi g^{-1} . Beryllium-7 is also a naturally occurring radionuclide produced in the atmosphere from interaction of air molecules with cosmic rays. Polonium-210 and ^{210}Bi are all short-lived decay products of ^{222}Rn , which is a gas and a decay product of ^{226}Ra (which is a decay product of ^{238}U). Lead-210 is a relatively long-lived decay product (half-life = ~22 years) from ^{222}Rn . They occur naturally in soils containing ^{238}U , and they

can be deposited as particles on the surfaces of both vegetation and soil following the decay of the gas ^{222}Rn . Similar concentrations of ^{234}U and ^{238}U suggest the primary source is naturally occurring uranium as opposed to a LANL source of depleted or enriched uranium.

The choice of isotopes measured in some of the vegetation samples is somewhat puzzling. For example, ^{234}Th (half-life = 24 days) is the daughter of ^{238}U and generally does not occur in nature alone. We might make the implied assumption that ^{238}U is in secular equilibrium with ^{234}Th and, therefore, the concentrations of ^{234}Th should also represent concentrations of ^{238}U . This is difficult to determine conclusively because the ^{234}Th data are from a different source than the ^{238}U data, and the reported concentrations of the two isotopes differ by 1 to 2 orders of magnitude (Tables D-1 and D-6).

The short-lived isotopes ^{214}Pb (half-life = 27 minutes) and ^{214}Bi (half-life = 20 minutes) also do not exist in nature without a source of their parent ^{222}Rn (half-life = 3.82 days), which is a daughter of ^{226}Ra (half-life = 1600 years). These nuclides provide an indication of the presence of ^{226}Ra ; however, without knowledge of the specific measurement techniques used in the analysis, it is difficult to draw any specific conclusions about ^{226}Ra . The fact that ^{214}Pb and ^{214}Bi activities do not exhibit equilibrium is an indication that the sample was analyzed shortly after collection and that the concentrations probably represent deposited ^{222}Rn daughters rather than a substantial ^{226}Ra source in the vegetation. Again, it is difficult to make explicit comparisons of the ^{214}Pb and ^{214}Bi data with the ^{210}Pb , ^{210}Po , and ^{226}Ra data because they are from different sources and the latter data are not site-specific.

Table D-10. Thirteen-day Average Radionuclide Concentrations in Air ($\mu\text{Ci m}^{-3}$) at Selected Locations in the Model Domain Resulting from Releases Associated with Burned Vegetation

Station	Santa Clara NEWNET Station		San Ildefonso NEWNET Station		White Rock		Santa Fe (Runnels Office Building)		Espanola		TA-54	
X/Q value (m^{-1})	1.8E-15		1.2E-15		1.0E-15		4.4E-16		7.8E-16		2.5E-15	
Nuclide	Max	Min	Max	Min	Max	Min	Max	Min	Max	Min	Max	Min
^{90}Sr	5.2E+02	2.6E+01	3.4E+02	1.7E+01	2.9E+02	1.5E+01	1.3E+02	6.3E+00	2.2E+02	1.1E+01	7.2E+02	3.6E+01
^{238}Pu	5.7E+00	7.0E-03	3.8E+00	4.6E-03	3.2E+00	3.9E-03	1.4E+00	1.7E-03	2.5E+00	3.0E-03	8.0E+00	9.8E-03
$^{239,240}\text{Pu}$	1.6E+01	3.2E-02	1.0E+01	2.1E-02	8.9E+00	1.8E-02	3.8E+00	7.7E-03	6.8E+00	1.4E-02	2.2E+01	4.4E-02
^{241}Am	2.2E+01	1.3E-01	1.4E+01	8.6E-02	1.2E+01	7.3E-02	5.3E+00	3.2E-02	9.4E+00	5.6E-02	3.1E+01	1.8E-01
^{137}Cs	4.5E+01	4.6E+00	3.0E+01	3.0E+00	2.6E+01	2.6E+00	1.1E+01	1.1E+00	2.0E+01	2.0E+00	6.3E+01	6.4E+00
^{210}Pb	2.6E+03	6.4E+02	1.8E+03	4.2E+02	1.5E+03	3.6E+02	6.5E+02	1.6E+02	1.1E+03	2.8E+02	3.7E+03	8.9E+02
^{210}Po	1.7E+03	3.2E+02	1.2E+03	2.1E+02	9.9E+02	1.8E+02	4.3E+02	7.9E+01	7.6E+02	1.4E+02	2.4E+03	4.5E+02
^{210}Bi	2.6E+03	6.4E+02	1.8E+03	4.2E+02	1.5E+03	3.6E+02	6.5E+02	1.6E+02	1.1E+03	2.8E+02	3.7E+03	8.9E+02
^{226}Ra	7.5E+02	6.5E+01	4.9E+02	4.3E+01	4.2E+02	3.7E+01	1.8E+02	1.6E+01	3.2E+02	2.8E+01	1.0E+03	9.2E+01
^{228}Ac	4.3E+01		2.8E+01		2.4E+01		1.0E+01		1.9E+01		6.0E+01	
^7Be	2.0E+04		1.4E+04		1.2E+04		5.0E+03		8.8E+03		2.9E+04	
^{214}Bi	5.5E+01		3.7E+01		3.1E+01		1.4E+01		2.4E+01		7.8E+01	
^{40}K	1.9E+03		1.3E+03		1.1E+03		4.7E+02		8.3E+02		2.7E+03	
^{212}Pb	2.4E+01		1.6E+01		1.4E+01		5.9E+00		1.0E+01		3.4E+01	
^{214}Pb	1.3E+01		8.8E+00		7.5E+00		3.2E+00		5.7E+00		1.9E+01	
^{234}Th	9.4E+01		6.2E+01		5.3E+01		2.3E+01		4.1E+01		1.3E+02	
^{208}Tl	8.9E+00		5.9E+00		5.0E+00		2.2E+00		3.9E+00		1.2E+01	
^{234}U	6.9E+00	1.4E+00	4.6E+00	9.4E-01	3.9E+00	8.0E-01	1.7E+00	3.4E-01	3.0E+00	6.1E-01	9.7E+00	2.0E+00
^{235}U	9.7E-01	2.1E-01	6.5E-01	1.4E-01	5.5E-01	1.2E-01	2.4E-01	5.1E-02	4.2E-01	9.1E-02	1.4E+00	2.9E-01
^{238}U	9.8E+00	1.2E+00	6.5E+00	7.7E-01	5.5E+00	6.6E-01	2.4E+00	2.8E-01	4.2E+00	5.0E-01	1.4E+01	1.6E+00

To examine the relative contribution to predicted air concentrations from burned vegetation and from burned PRSs, we compared the air concentrations calculated at TA-54 from both sources of releases (Table D-11). To avoid overestimating the concentrations resulting from burned vegetation and thereby understating the relative contribution of the PRSs, we have used the minimum concentration values to calculate the percent contribution from vegetation. Concentrations from PRS sources were reported as time-integrated concentration ($\mu\text{Ci-d m}^{-3}$). The 13-day average concentration was obtained by dividing the time-integrated concentration by 13 days. Based on these comparisons, it appears that releases and consequent air concentrations associated with burned vegetation are significantly higher than releases and consequent air concentrations associated with burned PRSs. If the maximum air concentration resulting from vegetation releases is assumed, the contribution from vegetation is even greater.

Table D-11. Comparison of Predicted 13-Day Average Air Concentrations (aCi m⁻³) at TA-54 Based on Releases of Radionuclides from Both Vegetation and PRSs

Radionuclide	Source of release		PRS	% contribution of vegetation ^a
	Vegetation			
	Maximum	Minimum		
²³⁸ Pu	8.0E+00	9.8E-03	1.1E-04	98.9%
^{239,240} Pu	2.2E+01	4.4E-02	2.8E-04	99.4%
²⁴¹ Am	3.1E+01	1.8E-01	9.4E-07	100.0%
²¹⁰ Pb	3.7E+03	8.9E+02	4.7E-06	100.0%
²²⁶ Ra	1.0E+03	9.2E+01	2.1E-04	100.0%
⁴⁰ K	2.7E+03		3.7E-03	100.0%
²³⁴ U	9.7E+00	2.0E+00	6.7E-05	100.0%
²³⁵ U	1.4E+00	2.9E-01	4.9E-06	100.0%
²³⁸ U	1.4E+01	1.6E+00	3.8E-05	100.0%

^a Assuming minimum predicted concentration resulting from releases related to burned vegetation, except for ⁴⁰K, which did not have a range of average concentrations (i.e., vegetation concentrations from more than one source).

Because it may be unrealistic to assume total consumption of all forest components during a fire, particularly the pulp component, we examine the % contribution from vegetation assuming release of the inventories associated with bark and litter only (Table D-12). Based on these comparisons, which assume concentrations resulting from burned bark and litter only and may be more realistic than the comparisons shown in Table D-11, the burning of forest components still appears to dominate predicted air concentrations.

Table D-12. Comparison of Predicted 13-Day Average Air Concentrations (aCi m⁻³) at TA-54 Based on Releases of Radionuclides from Both Vegetation (Bark and Litter Only) and PRSs

Radionuclide	Source of release		PRS	% contribution of vegetation ^a
	Vegetation			
	Maximum	Minimum		
²³⁸ Pu	7.9E+00	9.8E-03	1.1E-04	98.9%
^{239,240} Pu	2.2E+01	2.7E-02	2.8E-04	99.0%
²⁴¹ Am	3.0E+01	5.1E-02	9.4E-07	100.0%
²¹⁰ Pb	3.0E+03	7.5E+02	4.7E-06	100.0%
²²⁶ Ra	8.3E+02	8.6E+01	2.1E-04	100.0%
⁴⁰ K	1.5E+03		3.7E-03	100.0%
²³⁴ U	9.2E+00	1.5E+00	6.7E-05	100.0%
²³⁵ U	1.2E+00	1.9E-01	4.9E-06	100.0%
²³⁸ U	1.3E+01	1.3E+00	3.8E-05	100.0%

^a Assuming minimum predicted concentration resulting from releases related to burned bark and litter, except for ⁴⁰K, which did not have a range of average concentrations (i.e., bark and litter concentrations from more than one source).

Predicted concentrations of metals in air (Table D-13) were generally in the ng m^{-3} range with the exception of alkali earth and transition elements such as Ca, K, Al, and Fe. These elements are abundant in soil and were noted by Popp et al. (2001) to be present in PM10 samples taken between May 12 and 17 in Española.

Table D-13. Thirteen-day Average Metal Concentrations in Air ($\mu\text{g m}^{-3}$) at Selected Locations in the Model Domain Resulting from Releases Associated with Burned Vegetation

	Santa Clara NEWNET Station	San Ildefonso NEWNET	White Rock	Santa Fe (Runnels Building)	Santa Fe (Capshaw)	Espanola	Hernandez	TA-54
X/Q value (m^{-1})	1.8E-15	1.2E-15	1.0E-15	4.4E-16	3.4E-16	7.8E-16	5.5E-16	2.5E-15
Metal								
Cyanide	3.2E-05	2.1E-05	1.8E-05	7.8E-06	6.0E-06	1.4E-05	9.9E-06	4.5E-05
Al	2.6E-01	1.7E-01	1.5E-01	6.3E-02	4.9E-02	1.1E-01	8.0E-02	3.6E-01
Sb	1.0E-05	6.9E-06	5.9E-06	2.5E-06	2.0E-06	4.5E-06	3.2E-06	1.5E-05
As	8.6E-05	5.7E-05	4.9E-05	2.1E-05	1.6E-05	3.7E-05	2.7E-05	1.2E-04
B	6.6E-03	4.4E-03	3.8E-03	1.6E-03	1.2E-03	2.9E-03	2.1E-03	9.3E-03
Ba	4.0E-02	2.6E-02	2.3E-02	9.7E-03	7.5E-03	1.7E-02	1.2E-02	5.6E-02
Bi	1.4E-03	9.3E-04	7.9E-04	3.4E-04	2.6E-04	6.0E-04	4.3E-04	2.0E-03
Be	1.1E-05	7.4E-06	6.3E-06	2.7E-06	2.1E-06	4.8E-06	3.5E-06	1.6E-05
Cd	3.5E-05	2.3E-05	2.0E-05	8.6E-06	6.6E-06	1.5E-05	1.1E-05	4.9E-05
Ca	5.2E+00	3.5E+00	3.0E+00	1.3E+00	9.8E-01	2.3E+00	1.6E+00	7.3E+00
Cr	2.5E-04	1.7E-04	1.4E-04	6.2E-05	4.8E-05	1.1E-04	7.8E-05	3.5E-04
Co	2.2E-04	1.5E-04	1.3E-04	5.5E-05	4.2E-05	9.7E-05	6.9E-05	3.1E-04
Cu	3.2E-03	2.2E-03	1.8E-03	7.9E-04	6.1E-04	1.4E-03	1.0E-03	4.5E-03
Fe	2.4E-01	1.6E-01	1.3E-01	5.8E-02	4.4E-02	1.0E-01	7.3E-02	3.3E-01
Hg	2.1E-06	1.4E-06	1.2E-06	5.2E-07	4.0E-07	9.2E-07	6.6E-07	3.0E-06
Li	3.9E-04	2.6E-04	2.2E-04	9.6E-05	7.4E-05	1.7E-04	1.2E-04	5.5E-04
Pb	1.4E-03	9.0E-04	7.7E-04	3.3E-04	2.6E-04	5.9E-04	4.2E-04	1.9E-03
Mg	4.0E-01	2.7E-01	2.3E-01	9.8E-02	7.5E-02	1.7E-01	1.2E-01	5.6E-01
Mn	1.8E-01	1.2E-01	1.0E-01	4.4E-02	3.4E-02	7.9E-02	5.6E-02	2.6E-01
Mo	2.8E-05	1.8E-05	1.6E-05	6.8E-06	5.2E-06	1.2E-05	8.6E-06	3.9E-05
Ni	5.6E-04	3.7E-04	3.2E-04	1.4E-04	1.0E-04	2.4E-04	1.7E-04	7.8E-04
K	1.8E+00	1.2E+00	1.0E+00	4.4E-01	3.4E-01	7.9E-01	5.6E-01	2.5E+00
Se	5.2E-05	3.4E-05	2.9E-05	1.3E-05	9.8E-06	2.3E-05	1.6E-05	7.3E-05
Si	7.5E-02	5.0E-02	4.3E-02	1.8E-02	1.4E-02	3.3E-02	2.3E-02	1.1E-01
Sn	8.3E-05	5.5E-05	4.7E-05	2.0E-05	1.6E-05	3.6E-05	2.6E-05	1.2E-04
Sr	1.7E-02	1.1E-02	9.7E-03	4.2E-03	3.2E-03	7.4E-03	5.3E-03	2.4E-02
Ag	2.2E-04	1.5E-04	1.3E-04	5.5E-05	4.2E-05	9.7E-05	7.0E-05	3.2E-04
Na	8.1E-02	5.4E-02	4.6E-02	2.0E-02	1.5E-02	3.5E-02	2.5E-02	1.1E-01
Tl	4.8E-05	3.2E-05	2.7E-05	1.2E-05	9.0E-06	2.1E-05	1.5E-05	6.7E-05
V	3.6E-04	2.4E-04	2.0E-04	8.7E-05	6.7E-05	1.5E-04	1.1E-04	5.0E-04
Zn	1.1E-02	7.0E-03	6.0E-03	2.6E-03	2.0E-03	4.6E-03	3.3E-03	1.5E-02

Again, to examine the relative contribution to predicted air concentrations from burned vegetation and from burned PRSs, we compared the air concentrations calculated at TA-54 from both sources of releases (Table D-14). Concentrations from PRS sources were reported as time-integrated concentration ($\mu\text{g-d m}^{-3}$). The 13-day average concentration was obtained by dividing the time-integrated concentration by 13 days. Based on these comparisons, it appears that releases and consequent air concentrations associated with burned vegetation are significantly higher than releases and consequent air concentrations associated with burned PRSs, with the exception of cadmium and to a lesser extent, chromium.

Again, because it may be unrealistic to assume total consumption of all forest components during a fire, particularly the pulp component, we examine the percent contribution from vegetation assuming release of the inventories associated with bark and litter only (Table D-15). Based on these comparisons, which assume concentrations resulting from burned bark and litter only and may be more realistic than the comparisons shown in Table D-14, the burning of forest components still appears to dominate predicted air concentrations, with the exception of cadmium and to a lesser extent, chromium.

Table D-14. Comparison of Predicted 13-Day Average Air Concentrations ($\mu\text{g m}^{-3}$) at TA-54 Based on Releases of Metals from Both Vegetation and PRSs

Metal	Source of release		% contribution of vegetation
	Vegetation	PRS	
Aluminum	3.6E-01	5.8E-09	100.0%
Antimony	1.5E-05	3.2E-11	100.0%
Barium	5.6E-02	4.5E-07	100.0%
Beryllium	1.6E-05	4.4E-10	100.0%
Cadmium	4.9E-05	2.8E-03	1.7%
Chromium	3.5E-04	1.8E-05	95.1%
Cobalt	3.1E-04	8.4E-10	100.0%
Copper	4.5E-03	2.6E-08	100.0%
Iron	3.3E-01	2.0E-08	100.0%
Manganese	2.6E-01	2.5E-08	100.0%
Nickel	7.8E-04	1.2E-09	100.0%
Silver	3.2E-04	4.9E-10	100.0%
Thallium	6.7E-05	1.2E-10	100.0%
Vanadium	5.0E-04	9.5E-11	100.0%

Table D-15. Comparison of Predicted 13-Day Average Air Concentrations ($\mu\text{g m}^{-3}$) at TA-54 Based on Releases of Metals from Both Vegetation (Bark and Litter Only) and PRSs

Metal	Source of release		% contribution of vegetation
	Vegetation	PRS	
Aluminum	3.3E-01	5.8E-09	100.0%
Antimony	1.2E-05	3.2E-11	100.0%
Barium	3.4E-02	4.5E-07	100.0%
Beryllium	1.4E-05	4.4E-10	100.0%
Cadmium	4.4E-05	2.8E-03	1.5%
Chromium	2.7E-04	1.8E-05	93.8%
Cobalt	2.3E-04	8.4E-10	100.0%
Copper	3.2E-03	2.6E-08	100.0%
Iron	2.8E-01	2.0E-08	100.0%
Manganese	1.9E-01	2.5E-08	100.0%
Nickel	6.4E-04	1.2E-09	100.0%
Silver	2.5E-04	4.9E-10	100.0%
Thallium	5.2E-05	1.2E-10	100.0%
Vanadium	4.7E-04	9.5E-11	100.0%

It should be noted that these calculations do not consider the potential contribution related to releases of background levels of contaminants in soil from burned areas. This source, in combination with releases related to burned vegetation, appear to be the primary contributors to measured concentrations of contaminants in air.

ESTIMATED RISKS

Using the concentration data listed in the previous section, estimated risks from radionuclides, carcinogenic metals, and non-carcinogenic metals were calculated at the selected locations in the model domain for the resident adult scenario described in Chapter 5 of the main report. The representative resident adult had a breathing rate of $34 \text{ m}^3 \text{ d}^{-1}$ and a body weight of 74 kg. Risks were calculated for the case where 100 percent of the radionuclide or metal inventory in bark, litter, and pulp was assumed to be released. Risks were calculated for radionuclides and metals that had either risk coefficients, slope factors or reference doses as given in Appendix E. Risks were calculated according to the methodology described in Chapter 5. For radionuclides and carcinogenic metals, the lifetime cancer incidence risk was calculated. Cancer risks were averaged over a person's lifetime (70 years). For non-carcinogens, the hazard quotient was calculated, which is the ratio of the average daily intake of the metal divided by the acceptable average daily intake or reference dose. The noncancer hazard quotient was intended to represent sub-chronic exposure and was averaged over 14 days. However, subchronic reference doses were unavailable for all metals, and in these cases, the chronic reference dose was substituted. The use of chronic reference doses to represent subchronic effects may result in overly conservative estimates of non-cancer subchronic health effects because 1) chronic exposure reference doses are typically lower than subchronic values, and 2) chronic exposure is typically averaged over a persons lifetime while subchronic exposure is averaged over a period of 2 weeks to seven years.

Radionuclide and metal cancer risks were less than 10^{-6} at all selected locations (Tables D-16 and D-17). The 10^{-6} value is lower than the EPA range of acceptable risks of 10^{-4} to 10^{-6} . Noncancer risks for metals (Table D-18) were also lower than the acceptable hazard quotient of 1.0 for all metals except manganese. The hazard quotient for this metal ranged from 1.0 (in Santa Fe) to 7.6 (at TA-54). The high hazard quotient for this metal is mostly attributed to the use of a chronic reference dose to represent subchronic exposure. For example, a comparison of the 13-day average concentration of manganese at TA-54 ($0.26 \mu\text{g m}^{-3}$, see Table D-13) to the 8-hour NIOSH limit of 1 mg m^{-3} (NIOSH 1994) adjusted for 24-hour exposure ($1 \text{ mg m}^{-3} \times 8 \text{ h} \div 24 \text{ h} = 0.33 \text{ mg m}^{-3}$) indicates that the estimated manganese air concentration was substantially below the NIOSH limit by about three orders of magnitude. Differences between the chronic reference doses and exposure limits are discussed further in Appendix E.

Table D-16. Lifetime Cancer Incidence Risk at Selected Locations in the Model Domain Resulting from Radionuclide Releases Associated with Burned Vegetation based on Maximum Concentrations in Litter, Bark, and Wood Pulp

	Santa Clara NEWNET Station	San Ildefonso NEWNET	White Rock	Santa Fe (Runnels Building)	Santa Fe (Capshaw)	Espanola	Hernandez	TA-54
⁹⁰ Sr	9.69E-11	6.43E-11	5.49E-11	2.37E-11	1.82E-11	4.20E-11	3.00E-11	1.36E-10
²³⁸ Pu	8.40E-11	5.58E-11	4.76E-11	2.05E-11	1.58E-11	3.64E-11	2.60E-11	1.18E-10
^{239,240} Pu	2.30E-10	1.53E-10	1.30E-10	5.63E-11	4.33E-11	9.98E-11	7.12E-11	3.23E-10
²⁴¹ Am	2.70E-10	1.79E-10	1.53E-10	6.60E-11	5.08E-11	1.17E-10	8.35E-11	3.79E-10
¹³⁷ Cs	2.24E-12	1.49E-12	1.27E-12	5.48E-13	4.21E-13	9.71E-13	6.93E-13	3.15E-12
²¹⁰ Pb	3.23E-09	2.14E-09	1.83E-09	7.89E-10	6.07E-10	1.40E-09	9.99E-10	4.53E-09
²¹⁰ Po	1.12E-08	7.41E-09	6.32E-09	2.73E-09	2.10E-09	4.84E-09	3.45E-09	1.57E-08
²¹⁰ Bi	5.31E-10	3.52E-10	3.01E-10	1.30E-10	9.98E-11	2.30E-10	1.64E-10	7.45E-10
²²⁶ Ra	3.78E-09	2.51E-09	2.14E-09	9.23E-10	7.10E-10	1.64E-09	1.17E-09	5.30E-09
²²⁸ Ac	9.33E-13	6.19E-13	5.28E-13	2.28E-13	1.75E-13	4.04E-13	2.88E-13	1.31E-12
⁷ Be	1.93E-12	1.28E-12	1.09E-12	4.71E-13	3.62E-13	8.35E-13	5.95E-13	2.70E-12
²¹⁴ Bi	7.59E-13	5.04E-13	4.30E-13	1.85E-13	1.43E-13	3.29E-13	2.35E-13	1.07E-12
⁴⁰ K	1.89E-10	1.25E-10	1.07E-10	4.62E-11	3.55E-11	8.19E-11	5.84E-11	2.65E-10
²¹² Pb	6.14E-12	4.07E-12	3.48E-12	1.50E-12	1.15E-12	2.66E-12	1.90E-12	8.61E-12
²¹⁴ Pb	2.34E-13	1.55E-13	1.32E-13	5.71E-14	4.39E-14	1.01E-13	7.23E-14	3.28E-13
²³⁴ Th	1.28E-12	8.47E-13	7.23E-13	3.12E-13	2.40E-13	5.53E-13	3.95E-13	1.79E-12
²⁰⁸ Tl	1.45E-24	9.64E-25	8.23E-25	3.55E-25	2.73E-25	6.30E-25	4.49E-25	2.04E-24
²³⁴ U	3.49E-11	2.31E-11	1.98E-11	8.52E-12	6.56E-12	1.51E-11	1.08E-11	4.90E-11
²³⁵ U	4.34E-12	2.88E-12	2.46E-12	1.06E-12	8.16E-13	1.88E-12	1.34E-12	6.09E-12
²³⁸ U	4.04E-11	2.68E-11	2.29E-11	9.86E-12	7.58E-12	1.75E-11	1.25E-11	5.66E-11

Table D-17. Lifetime Cancer Incidence Risk at Selected Locations in the Model Domain Resulting from Metal Releases Associated with Burned Vegetation based on Concentrations in Litter, Bark, and Wood Pulp

	Santa Clara NEWNET Station	San Ildefonso NEWNET	White Rock	Santa Fe (Runnels Building)	Santa Fe (Capshaw)	Espanola	Hernandez	TA-54
As	3.02E-10	2.00E-10	1.71E-10	7.38E-11	5.67E-11	1.31E-10	9.34E-11	4.24E-10
Be	2.19E-11	1.46E-11	1.24E-11	5.36E-12	4.12E-12	9.51E-12	6.78E-12	3.08E-11
Cd	5.02E-11	3.33E-11	2.84E-11	1.23E-11	9.43E-12	2.18E-11	1.55E-11	7.04E-11
Cr	1.71E-08	1.14E-08	9.71E-09	4.19E-09	3.22E-09	7.43E-09	5.30E-09	2.41E-08

Table D-18. Hazard Quotients at Selected Locations in the Model Domain Resulting from Metal Releases Associated with Burned Vegetation based on Concentrations in Litter, Bark, and Wood Pulp

	Santa Clara NEWNET Station	San Ildefonso NEWNET	White Rock	Santa Fe (Runnels Building)	Santa Fe (Capshaw)	Espanola	Hernandez	TA-54
Cyanide	1.6E-05	1.1E-05	9.0E-06	3.9E-06	3.0E-06	6.9E-06	4.9E-06	2.2E-05
Al	7.9E-02	5.2E-02	4.5E-02	1.9E-02	1.5E-02	3.4E-02	2.4E-02	1.1E-01
Sb	4.0E-05	2.7E-05	2.3E-05	9.9E-06	7.6E-06	1.8E-05	1.3E-05	5.7E-05
B	5.0E-04	3.3E-04	2.8E-04	1.2E-04	9.3E-05	2.2E-04	1.5E-04	7.0E-04
Ba	1.2E-02	8.0E-03	6.9E-03	3.0E-03	2.3E-03	5.2E-03	3.7E-03	1.7E-02
Be	8.3E-04	5.5E-04	4.7E-04	2.0E-04	1.6E-04	3.6E-04	2.6E-04	1.2E-03
Cd	5.8E-05	3.8E-05	3.3E-05	1.4E-05	1.1E-05	2.5E-05	1.8E-05	8.1E-05
Cr	3.8E-03	2.5E-03	2.1E-03	9.2E-04	7.1E-04	1.6E-03	1.2E-03	5.3E-03
Co	2.0E-04	1.3E-04	1.1E-04	4.9E-05	3.8E-05	8.7E-05	6.2E-05	2.8E-04
Cu	1.5E-04	9.6E-05	8.2E-05	3.5E-05	2.7E-05	6.3E-05	4.5E-05	2.0E-04
Fe	1.1E-02	7.0E-03	6.0E-03	2.6E-03	2.0E-03	4.6E-03	3.3E-03	1.5E-02
Hg	1.1E-05	7.0E-06	6.0E-06	2.6E-06	2.0E-06	4.6E-06	3.3E-06	1.5E-05
Mn	5.4E+00	3.6E+00	3.1E+00	1.3E+00	1.0E+00	2.4E+00	1.7E+00	7.6E+00
Ni	1.7E-03	1.1E-03	9.4E-04	4.1E-04	3.1E-04	7.2E-04	5.1E-04	2.3E-03
V	3.2E-04	2.1E-04	1.8E-04	7.8E-05	6.0E-05	1.4E-04	9.9E-05	4.5E-04
Zn	9.5E-05	6.3E-05	5.4E-05	2.3E-05	1.8E-05	4.1E-05	2.9E-05	1.3E-04

Maximum concentrations and risks in the model domain (Table D-19) indicates that for both radionuclides and carcinogenic chemicals, the maximum risk is below the EPA range of acceptable risks of 10^{-4} to 10^{-6} . Maximum risks exhibited the same pattern as maximum PM10 concentration (Figure D-1); that is, maximum values were restricted to areas within active burning of the fire.

The maximum hazard quotient was significantly greater than unity and was dominated by manganese and to a lesser extent, aluminum. Again, we reiterate that the relatively high hazard quotients are thought to be primarily due to the use of chronic reference doses for a subchronic exposure. For example, suppose we were to define the subchronic reference dose (RfD) in terms

of the NIOSH occupational exposure limit adjusted for 24-hour exposure. The corresponding RfD for manganese would be

$$RfD = \frac{1 \frac{\text{mg}}{\text{m}^3} \times \frac{8 \text{ h}}{24 \text{ h}} \times 20 \frac{\text{m}^3}{\text{d}}}{70 \text{ kg}} = 0.0952 \frac{\text{mg}}{\text{kg} \cdot \text{d}} \quad (\text{D-8})$$

The aluminum subchronic RfD for a NIOSH 8-hour limit of 10 mg m^{-3} would be $0.95 \text{ mg kg}^{-1} \text{ d}^{-1}$. The corresponding RfD values used in the calculation were $0.001 \text{ mg kg}^{-1} \text{ d}^{-1}$ and $1.4 \times 10^{-5} \text{ mg kg}^{-1} \text{ d}^{-1}$ for aluminum and manganese respectively. These values are about 4 orders of magnitude lower than corresponding RfD values derived from occupational exposure. Using RfDs derived from the NIOSH occupational exposure limits for aluminum and manganese results in hazard quotients that are all less than 1.0. The spatial extent of excursion above the HQ of 1.0 is illustrated in Figure D-2. Excursion above a HQ of 1.0 includes most of the major population centers.

Table D-19 Maximum Radionuclide and Metal Lifetime Cancer Incidence Risk and Maximum Hazard Quotient from Burning Vegetation

Lifetime cancer incidence risk, radionuclides	Lifetime cancer incidence risk, metals	Hazard Quotient- metals	Hazard Quotient- metals with NIOSH derived RfDs
4.9×10^{-7}	4.4×10^{-7}	142	0.78

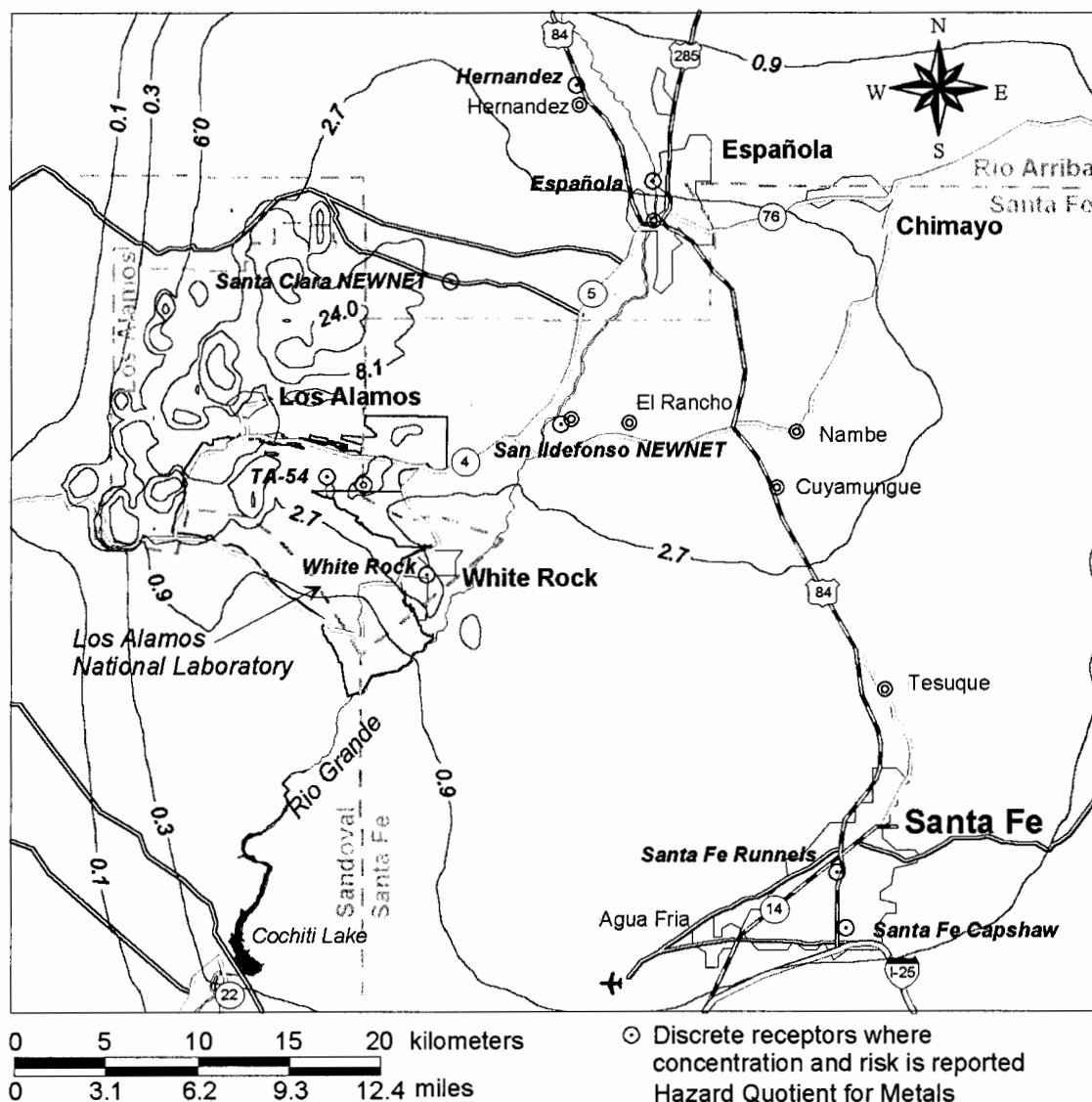


Figure D-2. Hazard quotient for metals released from burning vegetation for the adult resident scenario. Reference doses for manganese and aluminum were based on chronic RfDs as reported in Appendix E.

REFERENCES

- Balice R.G., J.D. Miller, B.P. Oswald, C. Edminster, and S.R. Yool. 2000. *Forest Surveys and Wildfire Assessment in the Los Alamos Region; 1998–1999*. LA-13714-MS Los Alamos National Laboratory, Los Alamos, NM.
- Fresquez, P.R. and J.K. Ferenbaugh. 1999. *Moisture Conversion Ratios for the Foodstuffs and Biota Environmental Surveillance Programs at Los Alamos National Laboratory (Revision 1)*. LA-UR-99-253.

- Gonzales, G.J., P.R. Fresquez, M.A. Mullen, and L. Naranjo, Jr. 2000. *Radionuclide Concentrations in Vegetation at the Los Alamos National Laboratory in 1998*. LA-13704-PR (Progress Report). March.
- Gonzales, G.J., P.R. Fresquez, and C.M. Bare. 2001. *Contaminant Concentrations in Conifer Tree Bark and Wood Following the Cerro Grande Fire*. LA-UR-01-6157. November.
- NIOSH (National Institute for Occupational Health and Safety) 1994. *NIOSH Pocket Guide to Chemical Hazards*. U.S. Department of Health and Human Services, National Institute for Occupational Health and Safety.
- Popp, C.J., R.S. Martin, and R. Arimoto. 2001. "Atmospheric Effects of Large Fires: Spring 2000 Cerro Grande, NM (Los Alamos) Fire." A Millennium Symposium on Atmospheric Chemistry: Past, Present, and Future, Sponsored by the American Meteorological Society. January 14–18, Albuquerque, New Mexico.
- Sandberg, D.V. and J. Peterson. 1984. "A Source Strength Model for Prescribed Fires in Coniferous Logging Slash." Annual Meeting of the Air Pollution Control Association, Pacific Northwest Section, November 12–14, Portland Oregon.
- Scire, J.S., D.G. Strimaitis, and R.J. Yamartino. 1999. *A User's Guide for the CALPUFF Dispersion Model (Version 5.0)*. Earth Tech, Inc., Concord, Massachusetts.
- Thomas, P.A. 2000. "Radionuclides in the Terrestrial Ecosystem Near a Canadian Uranium Mill." *Health Physics* 10: 614–624.

APPENDIX E

RISK FACTORS FOR CONTAMINANTS POTENTIALLY RELEASED TO AIR FROM LOS ALAMOS NATIONAL LABORATORY DURING THE CERRO GRANDE FIRE AND IDENTIFIED AS IMPORTANT TO HEALTH RISK

APPENDIX E

RISK FACTORS FOR CONTAMINANTS POTENTIALLY RELEASED TO AIR FROM LOS ALAMOS NATIONAL LABORATORY DURING THE CERRO GRANDE FIRE AND IDENTIFIED AS IMPORTANT TO HEALTH RISK

The risk factors presented in this appendix were used to calculate risk and hazard quotient from contaminants determined to be most important in terms of risk in this study.

For radionuclides, we used lifetime cancer morbidity (incidence) risk to calculate health risk for exposure to representative individual scenarios from the Cerro Grande Fire. These values are published in U.S. Environmental Protection Agency's (EPA's) Federal Guidance Report 13 (Eckerman et al. 1999). The values used for our calculations are shown in Table E-1.

**Table E-1. Radionuclide Lifetime Cancer Risk Coefficients
for Inhalation (Bq^{-1}) Taken from EPA Federal Guidance Report No. 13^a**

Radionuclide	Morbidity	Mortality
Americium-241	7.60E-07	6.59E-07
Lead-210	7.48E-08	6.84E-08
Lead-212	1.56E-08	1.46E-08
Lead-214	9.81E-10	9.31E-10
Neptunium-237	4.79E-07	4.18E-07
Plutonium-238	9.07E-07	8.04E-07
Plutonium-239	8.99E-07	7.94E-07
Potassium-40	6.01E-09	5.61E-09
Protactinium-231	1.23E-06	1.15E-06
Radium-224	2.70E-07	2.56E-07
Radium-226	3.10E-07	2.93E-07
Thorium-227	9.48E-07	9.00E-07
Thorium-232	1.17E-06	1.10E-06
Uranium-234	3.08E-07	2.90E-07
Uranium-235	2.73E-07	2.57E-07
Uranium-238	2.52E-07	2.38E-07

^a Source: Eckerman et al. (1999), Table 2.1.

We used three types of toxicity values to estimate risk from exposure to chemicals: the inhalation slope factor (SF_i) to estimate cancer risk, the inhalation reference dose (RfD_i), and the threshold limit value (TLV) that is defined for occupational exposure to estimate noncancer risks. Table E-2 shows the toxicity values, the source of the values, and the Chemical Abstracts Service and Registry (CAS) number for the potential contaminants of concern (PCOCs). The toxicity values are described in more detail below.

Table E-2. Chemical Risk Factors^a

Chemical name	CAS Number	RfD _i ^b (mg/kg-day)	Chronic or subchronic RfD _i ^b	TLV ^c /10 (mg m ⁻³)	Sf _i ^d (mg/kg-day) ⁻¹
Inorganics					
Aluminum	7429-90-5	0.001 ¹	Chronic		
Antimony	7440-36-0	0.00011 ²	Subchronic		
Arsenic	7440-38-2				15.1 ¹
Barium	7440-39-3	0.0014 ³	Subchronic		
Beryllium	7440-41-7	0.00000571 ¹	Chronic		8.4 ¹
Cadmium	7440-43-9	0.00026 ³	Subchronic		6.1 ³
Chromium (hexavalent)	18540-29-9				290 ¹
Chromium (total) ^e	7440-47-3				42 ²
Cobalt	7440-48-4	0.000476 ^h		0.005 ⁴	
Copper	7440-50-8	0.00952 ^h		0.1 ⁴	
Cyanide (total)	57-12-5	0.00086 ²	Chronic		
Iron	7439-89-6	0.00952 ^h		0.1 ⁴	
Manganese	7439-96-5	0.000014 ¹	Chronic		
Mercury	7439-97-6	0.000086 ²	Subchronic		
Nickel	7440-02-0	0.000143 ^h		0.0015 ⁴	
Selenium	7782-49-2	0.0019 ^h		0.02 ⁵	
Silver	7740-22-4	0.0000952 ^h		0.001 ⁴	
Thallium	7440-28-0	0.000952 ^h		0.01 ⁴	
Uranium	7440-61-1	0.000476 ^h		0.005 ⁴	
Vanadium	7440-62-2	0.000476 ^h		0.005 ⁴	
Zinc	7440-66-6	0.0476 ^h		0.5 ⁵	
Organics					
Acenaphthylene ^f	208-96-8	0.000857 ³	Chronic		
Aldrin	309-00-2	0.00000876 ⁶	Subchronic		1.72 ³
Amino-2,6-dinitrotoluene[4-] ^g	19406-51-0	0.002 ²	Chronic		0.68 ²
Amino-4,6-dinitrotoluene[2-] ^g	35572-78-2	0.002 ²	Chronic		0.68 ²
Aroclor-1254	11097-69-1				2 ³
Benzo(a)pyrene	50-32-8				3.1 ²
Dibenz(a,h)anthracene	53-70-3				3.1 ²
Dibenzofuran	132-64-9	0.004 ²	Chronic		
Dinitrobenzene[1,3-]	99-65-0	0.0001 ²	Chronic		
Dinitrotoluene[2,4-]	121-14-2	0.002 ²	Chronic		0.68 ²
Fluoranthene	206-44-0	0.04 ²	Chronic		
HMX	2691-41-0	0.05 ²	Chronic		
Methylnaphthalene[2-] ^f	91-57-6	0.000857 ³	Chronic		
Naphthalene	91-20-3	0.000857 ³	Chronic		
Nitrobenzene	98-95-3	0.000571 ³	Chronic		
Nitrotoluene[4-]	99-99-0	0.01 ²	Chronic		

Table E-2. (Continued).

Pyrene	129-00-0	0.03 ²	Chronic	
RDX	121-82-4	0.003 ²	Chronic	0.11 ²
TATB ^g	3058-38-6	0.002 ²	Chronic	
Trinitrotoluene[2,4,6-]	118-96-7	0.0005 ²	Chronic	0.03 ¹

^a Sources of data are indicated with superscript numbers: ¹ EPA (2001); ² EPA (2000); ³ ORNL (2001); ⁴ NIOSH (1994); ⁵ ACGIH (1996); ⁶ EPA (1997).
^b Reference dose for inhalation.
^c Threshold limit value.
^d Inhalation cancer slope factor.
^e A ratio of 1:6 Cr(VI):Cr(III) was assumed.
^f Naphthalene value was substituted.
^g Dinitrotoluene[2,4-] values were substituted.
^h RfD_i calculated from TLV.

We used inhalation slope factors for carcinogens to estimate risk for known or potential carcinogens. Slope factors (also called potency factors) have been estimated by the EPA and others using mathematical extrapolation models (most commonly the linearized multistage model) to estimate the largest possible linear slope (within the 95% confidence limit) at low, extrapolated doses that is consistent with the experimental data. The SF_i is considered an upper-bound estimate, and the actual risk is not likely to exceed the estimate. The slope factor is in units of risk per mg kg⁻¹ d⁻¹. There is considerable amount of uncertainty associated with these values, but they are generally very conservative. In developing them, the EPA used safety factors, modifying factors, and uncertainty factors to account for variability in sensitivity among different people, uncertainties in using the results of animal studies to predict health effects in humans, extrapolating from exposures of different durations, and other uncertainties.

Risk of noncancer health effects was assessed using an RfD_i. The RfD is expressed in units of mg d⁻¹ kg⁻¹ and is defined as an estimate (with uncertainty spanning perhaps an order of magnitude) of daily exposure to the human population (including sensitive groups) that is likely to be without appreciable risk of deleterious effects during a portion of the lifetime (subchronic values) or the entire lifetime (chronic values). The reference concentration (RfC), in units of mg m⁻³, is related to the RfD_i by the relationship

$$RfC_i = \frac{RfD_i \cdot W}{BR} \quad (E-1)$$

where

RfC_i = reference concentration for inhalation (mg m⁻³)

RfD_i = reference dose for inhalation (mg d⁻¹ kg⁻¹)

W = body weight (kg)

BR = breathing rate (m³ d⁻¹).

A breathing rate of 20 m³ d⁻¹ and a body weight of 70 kg was used for converting values found in the literature to RfD_i. Other breathing rates and body weights will be used in the intake

calculations to account for activity level and age relevant to the exposure scenario being considered.

The toxicity values we used were obtained from the EPA Region III Risk-Based Concentration Table, the EPA Region IX Risk Preliminary Remediation Goal Table, and from the Oak Ridge National Laboratory (ORNL) Risk Assessment Information System Database (ORNL 2001). These sources were used because they are relatively complete, well reviewed, and available online through the EPA Region's homepages and ORNL. Most of the values in the tables were obtained or derived by the Regions and ORNL from values in EPA's Integrated Risk Information System (IRIS) Database or EPA's Health Effects Assessment Summary Tables (HEAST).

The EPA has derived RfD_i values for chemicals that are widespread environmental pollutants or common contaminants at hazardous waste sites. RfD_i or RfC values have not been derived for some chemicals, many of which are considered more of an ingestion, rather than inhalation, hazard to the general public. For chemicals with no RfD_i or RfC, we used an occupational standard or guideline developed by the National Institute for Occupational Safety and Health (NIOSH) or the American Conference of Industrial Hygienists (ACGIH). NIOSH's recommended exposure limits (RELs) are time-weighted average concentrations for up to a 10-hour workday during a 40-hour week (NIOSH 1994). ACGIH's threshold limit values (TLVs), which are recommended maximum time-weighted average concentrations for an 8-hour workday during a 40-hour week (ACGIH 1996). In Table E-2, all of the occupational guidelines are under the column heading "TLV". The occupational exposure guidelines are intended to protect healthy workers exposed 8–10 hours each day, 5 days each week, and they are more liberal than standards designed to protect the public, who are exposed 24 hours a day and may be more sensitive due to age, illness, pregnancy, and other considerations. To help account for the variation in sensitivity among people and the longer exposure duration, we divided the TLVs by a safety factor of 10.

Like RfC values, TLV/10 values are in units of mg m^{-3} . TLV/10 values were converted to RfD_i values by the same relationship given in Equation (E-1), using a breathing rate of $20 \text{ m}^3 \text{ d}^{-1}$, a body weight of 70 kg, and an additional conversion factor of 0.33 days because TLV values are derived for 8-hour exposures rather than exposures of 1 day. We believe this is a simple and conservative application of the TLVs.

We did not find toxicity values for aminodinitrotoluene or acenaphthylene so we used values for dinitrotoluene and naphthalene, which are similar compounds (Gosselin et al. 1984; ATSDR 1990–2000).

We recognize that exposures to smoke from the Cerro Grande Fire would have occurred over a relatively short time period, probably less than 14 days. Slope factors are intended to estimate the probability of increased cancer risk over a lifetime. For most chemicals, the subchronic RfD_i or RfC correspond to exposures that last from 2 weeks to 7 years. Chronic RfD_is are applied to exposures lasting longer than 7 years. In many cases, the chronic values were derived from studies of animals exposed for a lifetime or a portion of a lifetime, often approximated by time periods of 70 or 30 years for humans. Occupational standards and guidelines apply to 8–10 hour exposures during a 40-hour week. Because the exposures to smoke from the Cerro Grande Fire were on the order of days to 2 weeks, we used a subchronic RfD_i whenever one was available. However, for many of the compounds, a chronic value was the only value published. Converting a chronic value to a subchronic value is not straightforward because the dose-effect relationship depends on the mechanism of action of the toxicant.

Toxicity values for long-term exposures are almost always more conservative and more cautious than those derived for acute exposures. The concentrations that cause chronic health effects are generally lower than concentrations that cause subchronic effects. Therefore, using the values derived from long-term exposure data to assess exposures of shorter durations is a cautious approach. Using toxicity values derived for comparison to chronic exposures contributes to the conservatism of the methods and leads to estimates of risk that are greater than risks that would be estimated over a more realistic exposure duration.

Other Details Concerning Explosive Compounds

RDX (Royal Demolition Explosive) is 1,3,5-trinitro-1,3,5-triazine. State air quality guidelines for RDX range from about 2 to 30 $\mu\text{g m}^{-3}$ for 8 hours (ATSDR 1995a). Hathaway and Buck (1977) found no adverse health effects following chronic exposure of workers to levels of RDX in dust in air that averaged 280 $\mu\text{g m}^{-3}$. The occupational standard is 1500 $\mu\text{g m}^{-3}$ (ATSDR 1995a). The greatest time-integrated concentrations calculated for RDX during the Cerro Grande Fire were 7.5 $\mu\text{g-d m}^{-3}$ at Technical Area (TA)-54, 4.5 $\mu\text{g-d m}^{-3}$ at San Ildefonso, and 1.4 $\mu\text{g-d m}^{-3}$ at Española. EPA's RfD for chronic oral exposure to RDX is 3.0×10^{-3} mg/kg-d. This value was derived from a 2-year study of rats fed RDX in their diet, using a critical effect of inflammation of the prostate and an uncertainty factor of 100 (EPA 2002). The EPA has not derived an inhalation value for RDX. The vapor pressure of RDX is 1.0×10^{-9} mm Hg at 20°C, indicating that it is not particularly volatile. RDX degrades in air because of reactions with radicals formed by photochemical reactions. The half-life of RDX in the atmosphere is approximately 1.5 hours.

HMX (High Melting Explosive) is 1,3,5,7-tetranitro-1,3,5,7-tetrazocine. Animal studies suggest that oral or dermal exposure to HMX can cause liver and central nervous system effects (U.S. Army 1985). EPA derived an RfD for chronic oral exposure of 0.05 mg kg⁻¹ d⁻¹, based on liver damage in rats exposed to HMX in their diet for 13 weeks, using an uncertainty factor of 1000 (EPA 2002). The EPA has not derived an inhalation value for HMX. The highest time-integrated concentrations calculated for HMX during the Cerro Grande Fire were 32.0 $\mu\text{g-d m}^{-3}$ at TA-54, 19 $\mu\text{g-d m}^{-3}$ at San Ildefonso, 1.9 $\mu\text{g-d m}^{-3}$ at Los Alamos, and 1.8 $\mu\text{g-d m}^{-3}$ at Española. The vapor pressure of HMX is 3.3×10^{-14} mm Hg at 25°C, which suggests it is not particularly volatile. The fate of HMX in air is unclear (ATSDR 1997).

The time-integrated concentrations calculated for 1,3-Dinitrobenzene (1,3-DNB) and 2,4,6-TNT are shown in Chapter 4, Table 4-14. 1,3-DNB can cause anemia and affects the nervous system. Workers inhaling unknown amounts of 1,3-DNB have experienced difficulty breathing, heart palpitations, low blood pressure, cyanosis (altered hemoglobin), headache, and dizziness (ATSDR 1995b; Okubo and Shigeta 1982). No inhalation studies on animals have been done. The EPA derived a chronic oral RfD EPA of 1.0×10^{-4} mg kg⁻¹ d⁻¹ for 1,3-DNB, based on increased splenic weight in rats after oral exposure using an uncertainty factor of 3000 (EPA 2002). The EPA has not derived an inhalation value for 1,3-DNB because of a lack of data. The vapor pressure of 1,3-DNB suggests that almost all or most of the 1,3-DNB in air would exist in vapor phase. 1,3-DNB would be expected to undergo photolysis in sunlight, but the half-life for the reaction is probably on the order of years (ATSDR 1995b). The half-life of 1,3-DNB in the atmosphere is approximately 14 hours for reactions with hydroxyl radicals (HSDB 2001).

Hematological effects, liver damage and cataracts have occurred in workers making 2,4,6-TNT (ATSDR 1995c). The EPA derived an RfD for chronic oral exposure of $5 \times 10^{-4} \text{ mg kg}^{-1} \text{ d}^{-1}$ based on liver effects observed in dogs after a 6-month exposure, using a uncertainty factor of 1000 (EPA 2002). No inhalation values have been derived because of a lack of human and animal data. The vapor pressure of 2,4,6-TNT is about $2 \times 10^{-4} \text{ mmHg}$, suggesting it would exist in both the vapor and particulate phase in the atmosphere. 2,4,6-TNT in air is subject to photolysis, with an estimated half-life of 4–12 hours (ATSDR 1995c).

REFERENCES

- ACGIH (American Conference of Governmental Industrial Hygienists). 1996. *Threshold Limit Values for Chemical Substances and Physical Agents*. American Conference of Governmental Industrial Hygienists, Cincinnati, Ohio.
- ATSDR (Agency for Toxic Substances and Disease Registry). 1990–2000. *Toxicological Profiles*. Atlanta, Georgia.
- ATSDR. 1995a. *Toxicology Profile for RDX*. U.S. Department of Health and Human Services, Public Health Service. June.
- ATSDR. 1995b. *Toxicology Profile for 1,3-dinitrobenzene and 1,3,5-trinitrobenzene*. U.S. Department of Health and Human Services, Public Health Service. June.
- ATSDR. 1995c. *Toxicology Profile for 2,4,6-trinitrotoluene*. U.S. Department of Health and Human Services, Public Health Service. June.
- ATSDR. 1997. *Toxicology Profile for HMX*. U.S. Department of Health and Human Services, Public Health Service. September.
- Eckerman, K.F., R.W. Leggett, C.B. Nelson, J.S. Puskin, and A.C.B. Richardson. 1999. *Cancer Risk Coefficients for Environmental Exposures to Radionuclides*. Federal Guidance Report No. 13. EPA 402-R-99-001. Office of Radiation and Indoor Air, U.S. Environmental Protection Agency, Washington, DC. September.
- EPA (U.S. Environmental Protection Agency). 1997. *Health Effects Assessment Summary Tables*. EPA/540/R-95/036. Office of Solid Waste and Emergency Response, U.S. Environmental Protection Agency, Washington, DC.
- EPA. 2000. *Region IX Preliminary Remediation Goals*. Version 7. U.S. Environmental Protection Agency, Region IX, San Francisco, California. November.
- EPA. 2001. *Region III Risk-Based Concentration Table*. U.S. Environmental Protection Agency, Region III, Philadelphia, Pennsylvania. September.

- EPA. 2002. *Integrated Risk Information System (IRIS)*. National Center for Environmental Assessment, Cincinnati, Ohio.
- Gosselin, R.E., R.P. Smith, and H. C. Hodge. 1984. *Clinical Toxicity of Commercial Products*. Baltimore, Maryland: Williams and Wilkins.
- Hathaway, J.A. and C.R. Buck. 1977. "Absence of Health Hazards Associated with RDX Manufacture and Use." *J. Occup. Med.* 19: 269-272.
- HSDB® (Hazardous Substances Data Bank). 2001. TOXNET® (Toxicology Data Network), National Library of Medicine. Last updated April 18, 2001. <<http://toxnet.nlm.nih.gov/cgi-bin/sis/htmlgen?HSDB>> (August 24, 2001).
- NIOSH (National Institute for Occupational Safety and Health). 1994. *Pocket Guide to Chemical Hazards*. U.S. Department of Health and Human Services, Public Health Service, Centers for Disease Control and Prevention, Cincinnati, Ohio.
- Oak Ridge National Laboratory (ORNL). 2001. ORNL Risk Assessment Information System Database (RAIS®), Chemical Toxicity Values, <<http://risk/lsd.ornl.gov>> Oak Ridge, Tennessee. December.
- Okubo T. and S. Shigeta. 1982. "Anemia Cases after Acute m-dinitrobenzene Intoxication due to an Occupational Exposure." *Industrial Health* 20: 297-304.
- U.S. Army. 1985. *HMX: 14-day Toxicity Study in Rats by Dietary Administration*. Ft. Detrick, MD, Research and Development Command, U.S. Army Medical Bioengineering Research and Development Laboratory. AD-A171 597. Summarized in ATSDR (1997).

APPENDIX F

HEALTH EFFECTS ASSOCIATED WITH EXPOSURE TO PARTICULATE MATTER AND WOOD SMOKE

APPENDIX F

HEALTH EFFECTS ASSOCIATED WITH EXPOSURE TO PARTICULATE MATTER AND WOOD SMOKE

Reviewing and summarizing the large amount of literature on particulate matter (PM) and other toxicants in smoke was beyond the scope of this project. In this appendix we present some information taken from literature compiled by the American Lung Association and the U.S. Environmental Protection Agency (EPA). The 1996 EPA review of PM standards provides summaries of relevant epidemiological studies. The results of some of the key epidemiological studies are reviewed by Samet et al. (2000).

Information on the overall toxicity of smoke from wildland fires or how this toxicity varies from fire to fire is limited. However, we can draw parallels from studies on wood smoke from household fireplaces and woodstoves and from studies of smoke from other combustion processes. It is clear that smoke exposure contributes to cardiovascular disease, lung diseases like asthma, pneumonia, emphysema, and bronchitis, and irritation of the eyes and respiratory system (WDOE 1999).

Smoke from wildfires contains thousands of chemicals in particulate and gaseous forms, but the best smoke indicator is probably particulate matter <2.5 microns (μm) in diameter (PM_{2.5}) and less than 10 μm in diameter (PM₁₀). Particulate matter is the most visible manifestation of a fire. Particulates from forest fires may be mostly condensed organic compounds (Dost 1991). Particulate matter also includes elemental material and minerals from fine soil suspended in updrafts. Particles are known to carry adsorbed and condensed toxic gases and free radicals (Ward 1999).

PM₁₀ can be inhaled, but much of it will be deposited in the upper respiratory tract. PM_{2.5} is of more concern because it is deposited deep in the lungs where it can remain and cause structural and chemical changes. Studies on the size distribution of forest fire smoke suggest that a large percentage of smoke particles are respirable (Ward 1999). More than 70% of the PM in wood smoke is probably less than 2.5 μm in diameter (WDOE 1999; Breyse 1983).

Many studies have correlated exposure to fine particles to respiratory related emergency room visits and hospital admissions, work and school absences, premature death, aggravation of asthma, emphysema, heart disease, chronic bronchitis and acute respiratory symptoms, including cough, and difficulty breathing. Elderly people and people with heart or lung disease or respiratory infections are more sensitive to PM. Because they breathe in more air for their size than adults, children seem to be more sensitive than adults to pulmonary toxicants. The relationship between PM and asthma and lung development in children has been well established by numerous epidemiological studies (Zanobetti et al. 2000; Gauderman et al. 2000). A panel of asthmatics in Southern California exhibited asthma symptoms after 1-hour exposures to PM concentrations ranging from 30 to 108 $\mu\text{g m}^{-3}$ (Peters et al. 1999).

Death rates in several U.S. cities have been shown to increase with higher concentrations of fine PM in the air (WDOE 1999). Hospital admissions in Australia for elderly patients have been correlated with a 90th percentile exposure concentration of 44 $\mu\text{g m}^{-3}$. A series of studies on smoke pollution in Indonesia suggests hospital admissions increase as exposure is prolonged into days or weeks. A nationwide study on the short-term effects of air pollution, jointly funded by the EPA and industry, called the National Morbidity, Mortality and Air Pollution Study (NMMAPS) studied 90 cities in the US and found that overall mortality increased 0.5% for every 10 $\mu\text{g m}^{-3}$

increase in PM₁₀ (presumably averaged over 24 hours) measured the day before death. NMMAPS found PM exposure was strongly and consistently associated with hospital admissions in the elderly. For each 10 $\mu\text{g m}^{-3}$ increase in PM₁₀ there was an increase in hospital admissions for pneumonia and chronic obstructive lung disease of about 2%. Cardiovascular and respiratory mortality increases have generally been associated with levels greater than 30 $\mu\text{g m}^{-3}$ (Delfino et al. 1997). The overall relationship between mortality and PM₁₀ concentration developed by NMMAPS agrees reasonably well with the World Health Organization (WHO 2000) estimate of the increase in daily mortality from exposure to PM₁₀. The WHO estimates an increase in daily mortality of $0.07\% \pm 0.012\%$ per $\mu\text{g m}^{-3}$ of PM₁₀. Although it is not entirely clear what averaging time is associated with the PM₁₀ concentration, WHO (2000) states the dose response relationship is for short-term exposures, and refers to mean 24-hour concentrations.

EPA and University Medical Center researchers have found an association between heart disease and exposure to particulate pollution. Inhalation of PM has also been linked to heart pattern changes in laboratory animals (Cone 2000; Samet et al. 2000). Smoke also contains carbon monoxide (CO), which has adverse effects on the heart (WDOE 1999). Changes in cardiovascular function have been associated with 1- and 4-hour exposures to levels less than 50 $\mu\text{g m}^{-3}$. Increases in hospital admissions for cardiovascular symptoms have been associated with PM exposures less than 50 $\mu\text{g m}^{-3}$ (Gold et al. 2000).

Different epidemiological studies have used different assumptions about the number of days following exposure to air pollution that adverse effects will occur. Many studies assume symptoms occur one day after exposure but some evidence suggests that symptoms may occur for several days after a single exposure.

Taken together, the literature suggests that PM concentrations as low as 30 $\mu\text{g m}^{-3}$ cause significant pulmonary function changes in sensitive populations and PM concentrations greater than 50 $\mu\text{g m}^{-3}$ can cause adverse health effects in the general population. A threshold for increased mortality has not been noted. Associations appear to be linear down to the lowest levels utilized in the studies.

The EPA has been reviewing its PM₁₀ standard and defending new standards for PM_{2.5}. Current Standards are shown in Table F-1.

Table F-1. Current Standards for Particulate Matter (PM)

	Averaging time	PM ₁₀ ($\mu\text{g m}^{-3}$)	PM _{2.5} ($\mu\text{g m}^{-3}$)
EPA	24-h	150	65
	Annual	50	15
California	24-h	50	—
	Annual	30	—

A Smoke, Fire and Health Workshop held in June of 2000 convened a workgroup on health advisories for smoke emissions. Air Pollution Control Agencies would like to develop short-term standards so that they can implement burning bans for grass field, wheat stubble, and prescribed burns of forests as PM concentrations rise near populated areas. The workshop participants acknowledged that "there were no directly relevant epidemiological or controlled human exposure studies that offer guidance in the selection of [1 hour] health advisory levels, useful in limiting exposure to smoke from wildfires, slash and agricultural burning (University of

Washington 2001). Their recommendations, and the categories and breakpoints used by the EPA for Air Quality Guidelines are summarized in Table F-2.

Exposure guidelines and standards for PM are based on annual average or 24-hour exposures. The Cerro Grande Fire created exposures lasting from <1 to 14 days. A standard corresponding to this timeframe has not been developed; however, estimated PM₁₀ levels did exceed the EPA and California 24-hour standard for several days of the fire at some locations.

Table F-2. EPA Air Quality Guidelines and Smoke, Fire, and Health Workshop, Health Advisory Workgroup Recommendations for PM₁₀ and PM_{2.5}.

EPA ^a PM ₁₀ 24-h exp. ($\mu\text{g m}^{-3}$)	EPA ^a PM _{2.5} 24-h exp. ($\mu\text{g m}^{-3}$)	Category	Pollution Cautionary Statements ^c	Workgroup ^b 1-h exp. ($\mu\text{g m}^{-3}$)
0 – 54	0 – 15.4	Good	None	0 – 40
55 – 154	15.5 – 40.4	Moderate	None	41 – 80
155 – 254	40.5 – 65.4	Unhealthy for sensitive groups	People with respiratory and heart disease, the elderly and children should limit exertion	81 – 175
255 – 354	65.5 – 150.4	Unhealthy	Everyone should limit prolonged exertion	176 – 300
355 – 424	150.5 – 250.4	Very unhealthy	Significant aggravation of heart and lung disease	301 – 500
425 – 504	250.5 – 350.4	Hazardous	Serious risk of aggravation of heart and lung disease, respiratory effects likely in everyone, premature mortality in people with heart and lung disease, and the elderly	>500
505 – 604	350.5 – 500.4	Hazardous		

^aFrom EPA (1999)

^bFrom University of Washington (2001), Health Advisory Workgroup recommendations.

^cDescriptions given in EPA (1999) are lengthy and have been summarized and paraphrased here.

The measured and estimated PM₁₀ and PM_{2.5} concentrations show that PM concentrations at various times and in various locations during the Cerro Grande Fire were sufficient to cause adverse health effects. The EPA's PM₁₀ standards are 150 $\mu\text{g m}^{-3}$ for 24 h average and 50 $\mu\text{g m}^{-3}$ (expected annual arithmetic mean) averaged over 3 years (EPA 2002). Although epidemiological studies of regional PM₁₀ air monitoring data in many U.S. cities demonstrate increases in daily mortality and morbidity trends at levels less than the current NAAQS, the EPA has not developed toxicity values or risk factors that can be used for risk assessment.

Epidemiological studies consistently show a positive and significant correlation for exposure to ambient PM with mortality and morbidity. Mortality rates and air pollution data have been compiled and compared for many US cities. The collective data for U.S. cities suggest that daily fluctuations in the mass concentration of PM₁₀ above 10 $\mu\text{g m}^{-3}$ results in an increase of about 0.6 to 1% excess mortality (Costa 2001). The EPA summarized many studies on increased mortality and morbidity associated with long-term exposure to PM. The EPA also reviewed 18 studies on short-term exposure. The EPA reported that estimates for the increase in mortality per 10 $\mu\text{g m}^{-3}$ 24-h increment in PM₁₀ or PM_{2.5} ranged from about 0.4 to 13%. The EPA concluded the excess risk estimates for hospital admissions and respiratory-related doctors visits range from 5 – 25% per 50 $\mu\text{g m}^{-3}$ 24-h PM₁₀ increment. Hospital admissions for asthma increase the most.

Many confounding factors like smoking, diabetes, respiratory illness, and other conditions that can affect cardiovascular and respiratory disease were not considered in these studies. Calculations using the 1969-1971 life tables suggested that a chronic exposure increase of $10 \mu\text{g m}^{-3}$ of PM was associated with a reduction of 1.3 years for the entire population life expectancy at age 25.

Although many studies on the effects of PM exposure on humans and animals have been done in recent years, the basic understanding of the dose-response is not sufficient for quantitative risk assessment. We believe that the uncertainty associated with quantifying the detrimental effects of PM₁₀ is too great, for a number of reasons, to allow meaningful estimates of risk to be calculated. Nevertheless, one may apply the risk estimates described earlier to the estimated PM₁₀ concentrations if a quantitative risk estimate is desired. For example, using the increase in daily mortality from exposure to PM₁₀ of $0.07\% \pm 0.012\%$ per $\mu\text{g m}^{-3}$ of PM₁₀ (presumably average over 24-hours) estimated by the WHO (2000) and the maximum estimated 24-hour average PM₁₀ concentration during the Cerro Grande Fire (see Table 4-16), a provisional estimate of the increase in daily mortality at the time of the Cerro Grande Fire would range from 3% ($0.07\% \text{ m}^3 \mu\text{g}^{-1} \times 39 \mu\text{g m}^{-3} \approx 3\%$) at Española to 20% at TA-54 ($0.07\% \text{ m}^3 \mu\text{g}^{-1} \times 288 \mu\text{g m}^{-3} \approx 20\%$) assuming a person was exposed to this concentration. We show this calculation to illustrate the possible application of PM₁₀ risk data; however, such calculations should be interpreted with extreme caution.

Assessing exposure to PM, determining the toxicity of different particles under different conditions for many different endpoints is very complex and a good understanding of both exposure and toxicity assessment is needed to estimate risk. Therefore, any quantitative estimates of risk need to be approached with extreme caution. Some of the sources of uncertainty associated with developing risk factors from morbidity and mortality data are summarized below.

The toxicity of PM is complex and depends on many characteristics of the PM, including: particle size, physical and chemical properties, solubility in the lung, reactivity and particle composition. The latter is particularly important because PM can consist of many different types of inorganic and organic compounds, including toxic and carcinogenic metals, irritants, and biogenic compounds like endotoxin. Particles with different compositions will exhibit different dose-response relationships. Different kinds of particles cause different kinds of health effects with different times between exposure and disease or exposure and deaths.

Pollution containing PM may also contain carbon monoxide and oxides of sulfur and nitrogen and other pollutants that also adversely affect the cardiovascular and respiratory systems. Estimating community wide exposure concentrations for use in epidemiological studies from monitoring data is uncertain because annual PM concentrations in urban areas can differ over time more than $100 \mu\text{g m}^{-3}$. Illustrative of this, the PM₁₀ concentration measurements taken at the Capshaw School in Santa Fe in 1999 and 2000 range from 5 to $50 \mu\text{g m}^{-3}$. Different sources produce different types of PM. Much of the studies have been on urban air pollution, road dust suspension from vehicular traffic, diesel exhaust or other engine emissions. The PM from the Cerro Grande Fire was from burning vegetation and suspended soil.

It is probable that the calculated risk from PM₁₀ is greater than the risk from all chemicals and radionuclides combined. It should be noted that PM emissions are a problem for all forest fires, especially smoldering fires, and PM emissions would not be increased because of current or past activities at LANL.

Other Common Components of Smoke

Smoke close to forest fires contains hundreds of organic and inorganic combustion products. Many are irritants, toxic or carcinogenic. Carbon monoxide, formaldehyde, acrolein, furfural, and benzene have been identified as potential health threats to firefighters doing prescribed burning in the Pacific Northwest (Reinhardt 1991). Polyaromatic hydrocarbons are found in smoke and many of these are carcinogenic. Respiratory irritants found in smoke include acrolein, nitrogen oxide, sulfur dioxide, ammonia and aldehydes, although emissions of nitrogen oxides are not thought to be "toxicologically significant" (Dost 1991). Phosgene and cyanide have been included in studies of smoke inhalation injury in burn patients and occupational lesions observed in firefighters. Cyanide is produced from the combustion of nitrogen containing materials, especially plastics and polyurethanes (Ferreira et al. 1998). Cyanide production in forest fires is not well understood.

Personal monitoring of firefighters in Montana, California, and the Pacific Northwest and measurements taken near firefighters tending prescribed burns have found that carbon monoxide, formaldehyde, and sulfur dioxide can exceed occupational exposure limits under some conditions (NIOSH 1992, Materna et al. 2000). Carbon monoxide impairs oxygen delivery by several mechanisms and causes damage to the neurological system and heart (Teofilo and Lee-Chiong 1998). Exposure to concentrations greater than 35 ppm for three hours will result in symptoms of disorientation and fatigue. Although carbon monoxide is probably responsible for 50% of house and building fire related health-effects, Dost (1991) asserts, "CO is a hazard in forest burning only in rare instances."

Formaldehyde causes nose cancer in rodents and it may cause cancer in humans. Eye, nose and throat irritation will occur in most people exposed to aldehyde concentrations greater than 0.1 ppm, and concentrations of 0.4–3 ppm may occur near a fire (Dost 1991). Formaldehyde was included in the LANL Site-Wide Environmental Impact Statement, which analyzed hypothetical accident scenarios including a wildfire that consumed several buildings, but it did not appear to be a major component of Cerro Grande smoke. Formaldehyde degrades through photolysis, 80–90% per day in sunlight. It also oxidizes to formic acid in air. Even though it is reactive and much of it must degrade, degradation in smoke has not been studied.

Acrolein is another respiratory tract and eye irritant, and many of the irritant effects described by firefighters are probably primarily due to acrolein in smoke (Reinhardt 1991). Concentrations of acrolein can range from 0.1 to 10 ppm near forest fires (Ward 1999). Much more acrolein is produced in the early flaming phases than in the smoldering phase of a fire (Dost 1991). Acrolein also degrades readily in sunlight.

Ozone, a pulmonary toxicant, is not a product of combustion but forms in dispersing smoke plumes from reactions involving oxygen, oxides of nitrogen, and hydrocarbons. It would not be a concern near the fire line but Dost (1991) suggested that levels as high as 100 ppb could be produced several kilometers downwind and high above the ground.

Concentrations of these chemicals in smoke are extremely variable and depend on the type of fuel, weather conditions, efficiency of combustion, and other factors. Appendix A includes a discussion of the organic chemicals and metals that have been measured in smoke from forest and grass fires. The EPA chemical monitoring taken during and after the fire and LANL monitoring for volatile organic chemicals at MDA-R which smoldered after the fire, suggest that these

chemicals were probably not present in high enough concentrations to pose a health threat to most people.

Because our assessment has been based on contaminants measured in air, on smoke particles, and in soil from the potential release sites (PRSSs), our analysis has not addressed the formation of toxic compounds. Hypothetically, reactive compounds, metal fumes and other chemicals could have been formed in the fire. It is likely that the monitoring network would have detected any that were monitored for, but it is possible that not all of the chemicals in smoke would have been monitored. Such an analysis of the theoretical and complex formation of secondary compounds is beyond the scope of this project, and toxicological interactions between components of smoke were not addressed in our analysis. A review of some of what is known about potential interactions was published by Dost (1991). He predicted that formation of "remarkable" or "exotic" toxic substances would not occur. The science of determining additive, synergistic or antagonistic interactions among chemicals is very uncertain, and there was no simple way to address this issue within the scope of this project.

REFERENCES

- American Lung Association. 1996-2001. Literature on the Health Effects of Particulate Matter. Web site and Printed Materials.
- Breysse, P.A. 1983. "Smoke Inhalation is Hazardous to Your Health." In: *New forests for a Changing World*; Proceedings of the Convention of the Society of American Foresters. Portland, Oregon. October 16-20. pp. 170-172.
- Cone, M. 2000. Los Angeles Times, Environmental Column. Studies Link Heart Attacks to Moderate Air Pollution Health: Particles apparently can alter rhythms in weak or diseased hearts, even at levels common in L.A., other cities.
- Costa, D. 2001 "Air Pollution". In: *Casarett and Doull's Toxicology*. 6th edition. Edited by C.D. Klaassen. McGraw-Hill, New York. 979-1012.
- Delfino, R.J., A.M. Murphy-Moulton, R.T. Burnett, J.R. Brook, and M.R. Becklake. 1997. "Effects of Air Pollution on Emergency Room Visits for Respiratory Illnesses in Montreal, Quebec." *American Journal of Respiratory and Critical Care Medicine*, Vol. 155:568-576.
- Dost, F.N. 1991. Acute Toxicology of Vegetation Smoke. Reviews of Environmental Contamination and Toxicology. Vol. 119:1-46. Springer-Verlag, New York.
- EPA (U.S. Environmental Protection Agency). 1999. Office of Research and Development. Air Quality Criteria for Particulate Matter. EPA/600/P99/002b. October.
- EPA. 2002. *Third External Review Draft of Air Quality Criteria for Particulate Matter* EPA/600/P-99/002aC. April.

- Ferreira, A.J., L. Cabral, C. Cruzeiro, and L.C. Oliveira. 1998. *Smoke Inhalation Injury in Burn Patients*. III International Conference on Forest Fire Research, 14th Conference on Fire and Forest Meteorology, Proceedings. Vol. I:153-160, Luso 16/20. November.
- Gauderman, J.W., R. McConnell, F. Gilliland, S. London, D. Thomas, E. Avol, H. Vora, K. Berhane, E.B. Rappaport, F. Lurmann, H.G. Margolis, and J. Peters. 2000. "Association between Air Pollution and Lung Function Growth in Southern California Children". *American Journal of Respiratory and Critical Care Medicine*, Vol. 162:1383-1390.
- Gold, D.R., A. Litonjua, J. Schwartz, E. Lovett, A. Larson, B. Nearing, G. Allen, M. Verrier, R. Cherry, and R. Verrier. 2000. "Ambient Pollution and Heart Rate Variability". *Circulation*. Vol.101:1267.
- Materna, B.L., J.R. Jones, P.M. Sutton, N. Rothman, and R.J. Harrison. 2000. "Occupational Exposure in California Wildland Fire Fighting." *Abstract. AIHAJ*: Vol. 53(1):69-76.
- NIOSH. 1991. Health Haz. Eval. Report HETA 91-152-2140 for the U.S. Dept. of Interior, NPS, California. September 1991.
- NIOSH. 1992. Health Haz. Eval. Report HETA 91-312-2185. PB92-193945 for the U.S. Dept. of Interior, NPS, Gallatin National Forest, Montana. March.
- Peters, J.M., E. Evol, W. Navidi, S.J. London, W.J. Gauderman, F. Lurmann, W.S. Linn, H. Margolis, E. Rappaport, J. Hong Jr., and D.C. Thomas. 1999. "A Study of Twelve Southern California Communities with Differing Levels and Types of Air Pollution; I. Prevalence of Respiratory Morbidity." *American Journal of Respiratory and Critical Care Medicine*, Vol. 159:760-767.
- Reinhardt, T.E. 1991. *Monitoring Firefighter Exposure to Air Toxins at Prescribed Burns of Forest and Range Biomass*. US Forest Service, Department of Agriculture, Pacific Northwest Research Station. PNW-RP-441. October.
- Samet, J.M., F. Domnici, F.C. Curriero, I. Coursac, and S.L. Zeger. 2000. "Fine Particulate Air Pollution and Mortality in 20 U.S. Cities. 1987-1994." *New England Journal of Medicine*. 343(24):1742-1749.
- Teofilo, L., and Lee-Chiong Jr. 1998. *Clinical Pulmonary Medicine*. Vol. 5(4):260-266. July.
- University of Washington. 2001. Summary of Health Advisory Workgroup Report, Smoke, Fire and Health Workshop. June 5-6, 2001. Seattle Washington.
- Ward, D.E. 1999. Smoke from Wildland Fires. World Health Organization (WHO) Health Guidelines for Vegetation Fire Events, Lima, Peru 6-9 October. USDA Forest Service, Fire Chemistry Project, Missoula, Montana.

WDOE (Washington State Department of Ecology). 1999. Educational Materials on Wood Smoke Pollution. Health Effects of Wood Smoke. Wood Smoke and Your Health. Controlling Wood Smoke Pollution.

WHO (World Health Organization) 2000. "Health-based Guidelines." Chapter 3 in *Guidelines for Air Quality*. World Health Organization, Geneva, Switzerland.

Zanobetti, A., J. Schwartz, and D. Gold. 2000. "Are there Sensitive Subgroups for the Effects of Airborne Particles?" *Environ. Health Perspectives*, Vol. 108(9):841-845.

FINAL REPORT

Analysis of Exposure and Risks to the Public from Radionuclides and Chemicals Released by the Cerro Grande Fire at Los Alamos

Task 3: Calculating and Communicating Risks: Observations and Recommendations

Revision 1
June 12, 2002

*Submitted to New Mexico Environment Department
in partial fulfillment of contract No. 01 667 5500 0001*

"Setting the standard in environmental health"



Risk Assessment Corporation

417 Till Road, Neeses, SC 29107
Phone 803.536.4883 Fax 803.534.1995

FINAL REPORT

Analysis of Exposure and Risks to the Public from Radionuclides and Chemicals Released by the Cerro Grande Fire at Los Alamos

Task 3: Calculating and Communicating Risks: Observations and Recommendations

**Revision 1
June 12, 2002**

Contributing Authors

**H. Justin Mohler, Bridger Scientific, Inc.
Kathleen R. Meyer, Ph.D., Keystone Scientific, Inc.
Jill W. Aanenson, Scientific Consulting, Inc.
Helen Grogan, Ph.D., Cascade Scientific, Inc.
James R. Rocco, Sage Risk Solutions LLC**

Principal Investigator

John E. Till, Ph.D., Risk Assessment Corporation

***Submitted to New Mexico Environment Department
in partial fulfillment of contract No. 01 667 5500 0001***

EXECUTIVE SUMMARY

This report was written to assist agencies involved in the activities during and after the Cerro Grande Fire with improving their ability to efficiently and credibly calculate and communicate risks in the future. The recommendations and observations in this report are provided from the perspective of an independent organization (*Risk Assessment Corporation*) and are based on our experiences with using available data to estimate potential risks as well as a thorough review of information reported to the public. This report focuses on general issues that impacted our ability to estimate potential risks or that affected the credibility of statements made during and following the fire about health risks to the public. We provide specific recommendations, in this and companion reports, about estimating the risks from the air and surface water pathways. In cases where specific solutions or recommendations are beyond the scope of this project, we provide general recommendations to guide future efforts.

Our primary recommendation related to *calculating risk* is to ensure that objectives for data collection are identified and met and that data collection efforts are guided by a thorough information needs analysis. Other important recommendations are to characterize all contaminated sites in a comprehensive and systematic way to provide the fundamental basis for a defensible risk assessment, thoroughly document background concentrations of materials in the environment, and develop an integrated and consistent method for data compilation. The key recommendations related to *communicating risk* are to develop a protocol to manage and coordinate the dissemination of information with a clear understanding of the capabilities and responsibilities of all organizations, link all statements about risk to available data and acknowledging the associated uncertainties and limitations, and encourage constructive critical interaction and input from all stakeholders.

In all instances, the fundamental purpose behind the recommendations presented in this report is to understand and communicate potential risks to the public in the most effective, efficient, and defensible manner possible—a goal that is common to all stakeholders. Successfully achieving this goal hinges on collecting and compiling data to optimize their use for meeting identified objectives, only one of which is understanding the impact of extreme events. To be effective, particularly in an emergency situation, the data collection and compilation procedures must be in place before the emergency occurs.

We wrote this report understanding and recognizing the extraordinary effort undertaken by all personnel who responded to the Cerro Grande Fire. It was a catastrophic event of immense personal, financial, cultural, and ecological loss. During the fire, many decisions were made using the best information and resources available to save lives and property. Obviously, our task of looking back at how the fire itself and risks from the fire were dealt with was a simpler task than that of individuals making decisions in the midst of the crisis. We have great respect for all organizations and individuals involved in managing the Cerro Grande Fire. We hope that our independent and retrospective analysis will improve the process of estimating and communicating risks in the future.

CONTENTS

EXECUTIVE SUMMARY	iii
CONTENTS	iv
ACRONYMS	v
INTRODUCTION	1
Objectives	1
Approach	2
CALCULATING HEALTH RISKS	3
Understanding the Goals and Limitations of Data Collection	5
Characterizing Contaminated Areas to Support Risk Assessment: Developing Source Terms ...	8
Coordinating Data Collection	9
Specific Observations and Recommendations Related to Calculating Risks: Information Needed to Refine Risk Estimates and Reduce and Quantify Uncertainty	11
COMMUNICATING HEALTH RISKS	13
Establishing Effective and Coordinated Communication	14
Emergency Response Background: Existing Capabilities and Plans	15
Managing the Risk Communication Response	16
Involving All Stakeholders in Risk Communication	17
Linking Preliminary Statements about Risk to Available Data	19
Continuing Post-Fire Communication and Risk Assessment	20
RECOMMENDATIONS	21
Calculating Health Risks	22
Communicating Health Risks	23
REFERENCES	24

ACRONYMS

BAER	Burned Area Emergency Rehabilitation (team)
BMP	best management practice
CCNS	Concerned Citizens for Nuclear Safety
DOE	U.S. Department of Energy
EPA	U.S. Environmental Protection Agency
ER	Environmental Restoration (Project)
ERT	Emergency Rehabilitation Team
ESF	Emergency Support Function
ESH	Environment, Safety, and Health Division
FCO	Federal Coordinating Officer
FEMA	Federal Emergency Management Agency
FRMAC	Federal Radiation Monitoring and Assessment Center
FRERP	Federal Radiological Emergency Response Plan
FRP	Federal Response Plan
ICS	Incident Command System
IFRAT	Interagency Flood Risk Assessment Team
JOC	Joint Operations Center
JIC	Joint Information Center
LANL	Los Alamos National Laboratory
LFA	Lead Federal Agency
MAC	Multi-Agency Coordination (team)
NMED	New Mexico Environment Department
PAG	Public Advisory Group
PM	particulate matter
POE	point of exposure
PRS	potential release site
RAC	<i>Risk Assessment Corporation</i>
RRES	Risk Reduction and Environmental Stewardship
SSC	Suspended Sediment Concentration (of radionuclides or chemicals)
TSS	Total Suspended Solids

CALCULATING AND COMMUNICATING RISKS: OBSERVATIONS AND RECOMMENDATIONS

INTRODUCTION

The Cerro Grande Fire, which burned about 45,000 acres ($\sim 180 \text{ km}^2$) in northern New Mexico, originated in the Bandelier National Monument on the evening of May 4, 2000, and spread east-northeast over the next 16 days consuming residential structures within the County of Los Alamos and approximately 7500 acres ($\sim 30 \text{ km}^2$) within the Los Alamos National Laboratory (LANL) boundary (DOE 2000a). LANL encompasses about 27,500 acres (110 km^2) and is situated on the Pajarito Plateau, described as a series of finger-like mesas separated by deep east-to-west oriented canyons cut by intermittent streams. The mesas range in elevation from approximately 7800 ft (2377 m) on the flanks of the Jemez Mountains to about 6200 ft (1890 m) above the Rio Grande Canyon.

The fire caused significant damage to structures and property on LANL land. Some of the areas that burned were known or suspected to be contaminated with radionuclides and chemicals. Concern was expressed by the public with regard to

- Radionuclides and chemicals associated with soil and vegetation burned by the fire and subsequently suspended and transported via air
- Radionuclides and chemicals associated with soil, sediments, and ash mobilized and transported via surface water following the fire
- Potential exposures and health risks to people related to the transport of radionuclides and chemicals via both air and surface water.

In response to these concerns, the New Mexico Environment Department (NMED) recognized the need for an independent assessment of exposures and risks to the public from radionuclides and chemicals associated with the LANL facility released as a result of the fire. NMED contracted with *Risk Assessment Corporation (RAC)* to evaluate the potential incremental health risks to the communities of northern New Mexico from these radionuclides and chemicals.

Objectives

The primary objective of this project was to analyze the immediate consequences and the longer-term impacts of the Cerro Grande Fire in terms of increased public exposures and potential risks from radionuclides and chemicals associated with the LANL facility released as a result of the fire in the vicinity of the LANL. The study did not specifically address the impact the fire may have in the future on groundwater.

Specifically, the overall project focused on the

- Magnitude of incremental exposure and associated risks to the public, emergency response personnel, and firefighters from transport of radionuclides and chemicals associated with the LANL facility released as a result of the fire through the *air transport pathway*. The scope was subsequently changed to include a semi-

quantitative assessment of risks from naturally occurring radionuclides and metals released from burning of the forests around the LANL site. The assessment of the *air transport pathway* is described in a companion report (Rood et al. 2002).

- Magnitude of incremental exposure and associated risks to the public from transport of radionuclides and chemicals associated with the LANL facility released as a result of the fire through *surface water pathways*. The scope was also subsequently changed to include risks related to ash from areas burned around the LANL site. This assessment is described in a companion report (Rocco et al. 2002).
- Conclusions of the study and recommendations for similar events in the future. An important goal of the study was to actively, openly, and accurately convey information about the risks from the fire to the public, including the lessons learned from the fire analysis and the effectiveness of communication with the public during and following the fire. These conclusions are presented in this report.

Approach

Following the Cerro Grande Fire, it was essential to study how available technical information was used to make rapid decisions and communicate information about the potential risks to local residents and emergency response personnel. In this report, we make specific recommendations for calculating and communicating LANL-related health risks from impacted areas contaminated with radionuclides and chemicals, as well as a number of general recommendations that may be applicable to LANL and other sites.

Several agencies and organizations have documented particular experiences they had in responding to emergency technical issues and in communicating with the public during and after the fire (LANL 2001a; DOE 2000b; Pergler 2000, Alvarez and Arends 2000). The primary observation from many of these reports was the critical need to have an emergency response plan in place and operational before a crisis situation occurs, along with an efficient system to interpret the many pieces of information required to understand potential risks. A number of other important recommendations from these sources coincide with the issues discussed in this report.

This report examines two broad areas regarding lessons that can be learned to prepare for and be responsive to future emergencies. The two areas are

1. *Calculating Health Risks*—Identifying health risk issues and answering technical questions about risk with defensible and efficient calculations. Defensible calculations must be based on a comprehensive and systematic assessment of the potential contributors to risk, and efficiency is achieved by integrating the data from all agencies involved in a consistent format. The limitations and uncertainties of the calculations must also be made clear. These issues relate to calculating risk during the fire, immediately following the fire, and subsequent to the fire— future and potential risk studies. Three specific topics are examined:
 - Understanding the goals and limitations of data collection
 - Characterizing contaminated source areas to support risk assessment
 - Coordinating data collection.

2. *Communicating Health Risks*—Conveying the magnitude and impact of potential risks to the public and other stakeholders both during and after the fire (or other emergency) in a technically defensible, coordinated fashion by all agencies involved. Stakeholders can include individuals in the community, people involved in monitoring on and around the LANL site, and those associated with government or private organizations who may be potentially at risk from materials released from the site to air and water. Three issues important to open public communication and interaction are examined:
 - Establishing effective and coordinated communication
 - Linking preliminary statements about risk to available data
 - Continuing post-fire communication and risk assessment.

This report focuses on identifying areas where changes to methods in place at the time of the Cerro Grande Fire could result in a more efficient, credible, transparent, or defensible calculation and communication of risks from a future emergency. This report does not seek to criticize specific groups and individuals. In fact, we recognize and commend the hard work of many individuals under difficult circumstances.

Reviewing data from different organizations allowed us, as an independent organization, to evaluate the utility and adequacy of the various data for assessing potential risks. This process incorporated information from all organizations involved, and did not focus on any single individual or organization. It was equally important for us to assess information reported by the press as it reflected the public perception of how events were handled and how information was disclosed. This information formed the basis for a number of the observations made in this report. It is important also to understand that public perception may include the opinions and observations of many different groups of individuals often with widely varying opinions and attitudes toward LANL.

CALCULATING HEALTH RISKS

In emergency planning, all potential sources of risk or areas contributing to risk need to be considered, and those areas or sources with the greatest potential to contribute to risk should be identified. For the Cerro Grande Fire, contaminated land was the primary potential source of risk from LANL, not the buildings that were damaged or destroyed (Rood et al. 2002). Other emergency scenarios may involve other sources of risk.

To calculate potential risk from contaminated areas at LANL, we needed data to answer the following questions:

1. What media (e.g., soil, sediment, storm water) were likely sources of chemicals and radionuclides onsite and offsite and what chemicals and radionuclides were present in these media?
2. Where were the contaminated areas located and what was the distribution of chemicals and radionuclides in each of these areas (defined source areas)?
3. What was the average concentration or inventory of chemicals and radionuclides across each defined source area?
4. What were the potential release and transport mechanisms for the chemicals and radionuclides? The objective is to understand how these materials could move and what are the processes that would control that movement. For example, for the Cerro Grande

Fire, both direct releases to the atmosphere at the time of the fire as well as the potential longer-term releases to water through runoff needed to be evaluated.

5. Where were the likely points of exposure, and what were the predicted potential concentrations at each point of exposure? What were the pathways through which individuals could be exposed to these concentrations of radionuclides or chemicals at the points of exposure?
6. How did the predicted concentrations compare to measured concentrations?
7. What were typical background concentrations for these radionuclides and chemicals?
8. What were the uncertainties and limitations associated with answering these questions?

In general, data collected to answer the first five questions provide the information needed to (a) estimate a source term, which is the amount of chemicals and radionuclides available at a site for release by some mechanism, (b) model and estimate movement of that source term, and (c) predict potential human exposure to that source term. Data collected to address question 6 can generally be categorized as monitoring or surveillance data, which help identify, or monitor, the actual impact of contaminated sites on the ambient environment. Question 7 addresses the need to understand and have available for ready comparison regional background concentrations of chemicals and radionuclides normally present (e.g., anthropogenic and naturally occurring chemicals and radionuclides not associated with the LANL facility) in the environment before an emergency so that increases in concentrations can be readily identified. Question 8 is answered through an ongoing process of understanding the entire set of components needed to estimate potential risk and identifying specific areas where additional information could help refine or improve risk calculations. All of these components are subject to uncertainty, validation, communication, public participation, and management (Till 1996).

As an organization independent from LANL, NMED, the U.S. Environmental Protection Agency (EPA), and U.S. Department of Energy (DOE), we identified three main issues that influenced the ease with which available data were able to be used to calculate health risks. The issues are summarized below. This project focused on evaluating and using *readily available data*, and we did not investigate all issues that may impact interpretation of the data.

First, the goals and limitations of the data collection system in place before an emergency must be understood. The purpose of the original data collection effort may not be ideally suited to achieve the goals of assessing risk following an emergency situation. Data can be collected for various reasons, including the desire to research and understand systems and processes in the environment, the need to evaluate potential risk from routine operations and from accidents to assist with decision making, and the need to address various regulatory compliance requirements. Compliance is, in general terms, the legal requirement to show that chemicals and radionuclides released to the environment are below some predetermined regulatory level. The data required to meet compliance goals and to calculate risk from a fire or other emergency may not be the same. While we reviewed large volumes of data collected at the site by various organizations, the data collection protocol and locations were not always suited for the risk evaluation that we were conducting.

A second issue is the ability to quantitatively characterize the important sources of chemicals and radionuclides sufficiently to support a predictive exposure risk assessment for the air or surface water pathways. We found data characterizing contaminated sites at LANL difficult to use in our analysis despite the large volumes of characterization data that existed. Although it is

likely that there is additional institutional knowledge about the areas that contribute most to risk, as an independent evaluator, the current organization of these data did not allow us to discern this readily.

Third, there is a need for increased coordination and communication among all groups collecting environmental monitoring data related to LANL. At the present time, it is difficult to compare data collected by different agencies (e.g., NMED and LANL), and even different groups within LANL (e.g., ESH and ER). This is due primarily to the use of different collection, analysis, and data management procedures. In some instances, it appears that sampling efforts could be coordinated and refined to avoid unnecessary duplication or even tripling of effort and resources.

Understanding the Goals and Limitations of Data Collection

A systematic and comprehensive process is required for developing a sampling or surveillance system that results in collecting data suitable for meeting identified objectives and goals. Data can be collected for a variety of reasons and with a number of goals in mind. In addition, it may be necessary to use an individual data value to address several different goals. Identifying the goals for the data at the outset is important to ensure that data are collected and compiled so those goals can be achieved.

During the course of the Cerro Grande Fire, rapid decisions had to be made about environmental monitoring and data collection. Data collected during the fire were necessarily focused on the decisions that needed to be made to address the emergency and were valuable for understanding the relative magnitude of the immediate potential risks posed by the fire. Data collected following the fire were used as the basis for statements about potential risks to members of the public resulting from erosion and transport of chemicals and radionuclides from the fire (e.g., IFRA 2001; Kraig et al. 2001). However, the strength and scope of the conclusions and results of these studies were limited by the adequacy and representativeness of the environmental monitoring and other data upon which they were based. It is important to identify and communicate these limitations.

As noted above, the purpose of the current data collection for monitoring or compliance may not be ideally suited to evaluating the fate and transport of chemicals and radionuclides beyond the boundaries of the LANL facility or to assessing the potential short- and long-term risks following an emergency. The goals associated with data acquired for compliance, and consequently the utility of those data for other purposes, may not correspond to what is needed for risk analysis and model validation. For example, AIRNET (which is a system of environmental air samplers located in and around the LANL site that uses fabric filters to collect samples for gross alpha, beta, or specific isotopic analyses) has not been traditionally identified as an emergency response asset for LANL. Reliance on the AIRNET system during the fire played an important role in tracking some radionuclide and chemical movement in air, but certain data collection shortcomings resulted that the system was not designed to address, many of which are noted in LANL (2001a). Air monitoring data are collected at site boundary locations for compliance purposes. While these data may be sufficient for demonstrating compliance with the Clean Air Act, they may provide limited comprehensive information about contaminant movement from onsite areas to offsite locations during emergency situations, depending on the nature of the release. Rather, they provide only a history of contamination at previously defined

locations, which may or may not be appropriate for understanding the consequences of an emergency. As another example, existing historical air monitoring data and data collected during the Cerro Grande Fire do not have comparable averaging times in most cases. As a result, it was difficult to understand how the short-term (i.e., over 24 hours) fluctuations in concentration seen during the Cerro Grande Fire related to typical historical short-term fluctuations, which can vary significantly depending on the time of year or season.

This issue also applies to data collected to characterize existing areas of contamination. For example, it was very difficult to use existing site characterization data, which are intended to meet regulatory requirements, to develop the comprehensive quantitative source term information necessary for a predictive assessment of the fate and transport of chemicals and radionuclides through the surface water pathway. The significance of these data is discussed in more detail in the following section.

Although the current environmental data collection and monitoring programs at LANL have been designed around a significant knowledge base of historical operations and known areas of contamination, the primary purpose of these programs is to comply with regulatory requirements. To this extent, the existing data appear to meet these objectives. However, data collection for purposes of evaluating the potential release, fate, and transport of chemicals and radionuclides from source areas to potential points of exposure and associated risk needs to be focused on the specific requirements of the model or evaluation approach to be employed and the decision making process used to address the potential risks. Current data collection objectives do not appear to include these needs. As a result, the existing compliance-driven data collection and environmental monitoring programs may not be ideally suited to specifically monitor the immediate impact of emergency situations or extreme events, such as fires, floods, or terrorism, or to understand and estimate potential future risk.

The purpose and goals of the data collected by other organizations are also important. For example, one objective of NMED data collection is to validate results reported by LANL. In many cases, this is a difficult task because of differences in the timing and location of sampling and because there is no system to assist in comparing NMED data with LANL data. Developing a protocol to achieve this and other identified goals would help ensure that data collection efforts are adequate to meet these goals. Establishing a mechanism to allow environmental monitoring by (or splitting samples with) other groups independent from LANL can also provide confidence in results obtained by LANL and regulatory agencies normally involved in data collection. The independent groups must be completely open to public scrutiny. The EPA and U.S. Geological Survey performed some independent monitoring during the Cerro Grande Fire to confirm LANL measurements or to identify data gaps and areas not covered by the existing sampling network. However, the credibility of this independent monitoring was questioned when there were delays in providing the data and closed meetings to discuss the data, as described in the section titled "Communicating Health Risks."

Collecting environmental data before and following an emergency provides information about what is actually happening in response to environmental events (e.g., rain, snowmelt, and consequent flooding and contaminant dispersal) and how these events impact the concentrations of contaminants in environmental media at specific locations. In fact, it is generally preferable to use measurement data rather than modeled or predicted concentrations to reduce the significant uncertainty often associated with predicted concentrations. However, monitoring data can be limited by the adequacy of the data collection effort in terms of coverage (spatially [location],

temporally [time], and for the contaminants of concern) and by the intensity and duration of the actual post-emergency environmental events. For example, surface water monitoring during 2000 following the Cerro Grande Fire provided information about the consequences of contaminant movement during a relatively dry year; however, it provided limited information about the potential consequences of a significant rainfall in the future.

On the other hand, predictive modeling is useful for understanding and quantifying potential future risks. Because of the considerable complexity related to evaluating and understanding potential risks, attempting to answer questions and derive numbers related to risk through separate and independent methods can lead to improved confidence in the results. As a result, the combination of both model predictions and environmental measurements can provide a very effective method for assessing risks in the most comprehensive and defensible manner possible.

In addition to real-time estimates of chemical and radionuclide concentrations in the environment, measured data also provide important input to predictive transport models and, as a result, the limitations of measured data can also impact the modeling effort. For example, storm water flow monitoring and TSS concentration data provided information on flow and TSS both before and after the fire, but the timing of the data collection limited its usefulness in determining a relationship between storm water flow and TSS concentration.

Implementing a system that meets as many identified goals and objectives as possible requires a long-term perspective and input from people with diverse skills. However, we believe it is possible to not only meet regulatory requirements but also better detect changes directly related to LANL operations that are not caused by natural fluctuations in environmental processes or constituents (such as wind speed, rain intensity, drought, or particle size). This would require developing good statistical relationships between identified appropriate variables and consequent responses in the levels of materials measured in the environment. Then, as was done for wind speed and particulate matter less than 10 microns in diameter (PM-10) concentrations for the *air pathway analysis* (Rood et al. 2002), it will be possible to begin to identify and better understand causal factors.

In conclusion, it is imperative that the goals of monitoring data collection be defined at the outset and modified as necessary so that the appropriate data for understanding risks or refining risk estimates and reducing uncertainty are collected. Considering the Cerro Grande Fire, we recommend that new and more refined monitoring efforts and capabilities be explored for usefulness in the event of another emergency without compromising the current goals of the monitoring program. Consideration should be given to augmenting the program to provide adequate sensitivity for sampling periods and locations that are consistent with the needs for information about environmental levels at important public exposure locations during emergency situations. Efforts aimed at collecting data to refine environmental transport calculations and reduce uncertainty in risk estimates should also consider the importance of using as much site-specific data as possible (e.g., soil-water partition coefficients, soil organic carbon content, spatial characterization of total suspended solids [TSS] in runoff, and bioaccumulation factors). More available data to specifically characterize the environment around a facility such as LANL will lead to a more defensible risk assessment (Till 1996).

Characterizing Contaminated Areas to Support Risk Assessment: Developing Source Terms

The source term, or type and quantity of contamination, is the most fundamental category of data needed to understand the potential health impacts of an event like the Cerro Grande Fire. However, establishing a credible source term, including the quantification of associated uncertainties, is often the most time and resource intensive component of estimating risk. As a result, adequate source term development is often not achieved, and yet this step of risk assessment is where the greatest potential lies for losing scientific and public credibility (Till 1996). A well-characterized source term provides the foundation for making defensible statements about risk and requires that an inventory or average concentration be established across a defined area. Also, when there are as many contaminated sites to consider as there are at LANL, it is critical to be able to readily establish those sites of most concern in the evaluation of potential risk. This ranking may differ depending on the exposure pathway (e.g., releases to atmosphere versus releases to surface water).

Credible source term information is needed to support a defensible predictive transport modeling effort, which can in turn be used to understand potential future risks and guide risk-based decision making. Therefore, it is important to strike a balance between the level of effort placed on developing credible source terms and that directed toward designing functional predictive models. While environmental transport modeling may be limited by inherent uncertainties, it allows for a conservative approach that can lead to bounding estimates of risk, which identify the largest potential risk values. Results from the conservative or bounding approach are particularly important for identifying the need for and focusing further, more detailed evaluations. A systematic process of characterizing sites and modeling potential transport can also lead to a defensible method for prioritizing sites for cleanup. Further, with careful planning, the relative potential impact of the fire (or other emergency) on runoff and contaminant dispersion can be quantified efficiently so that defensible statements about potential risk can be made. The results of the companion *surface water pathway* risk report (Rocco et al. 2002) support these statements about the utility of the source term and transport modeling process developed as part of this project.

The data available for this project did not allow us to efficiently calculate average concentrations and/or inventories for contaminated source areas at LANL or achieve a quantifiable understanding of the uncertainties associated with the source term estimates we were able to make. A systematic and comprehensive process is needed to improve the ability to quantify contamination at defined areas and to identify the most important areas in terms of potential exposure and risk. Various efforts have been undertaken by LANL to prioritize and guide work at defined areas (LANL 2001b; ER 2000), but the prioritization criteria encompass aspects other than human health risk and are not readily tied to the measurement data available to quantify contamination at specific areas.

Characterizing a site such as LANL is an extremely complex process because LANL is not a static environment. There are ongoing disposal and remediation activities, and the nature of the watersheds results in contaminated areas and contaminant transport processes that can change from year to year. Because of this complexity, it is reasonable for LANL to focus on establishing a program of sufficient coverage to monitor actual conditions in the environment rather than on establishing a detailed source term for all contaminated areas, which may not be feasible or

necessary. Defensible characterization data are critical, though, for those sites identified as most important in terms of potential risk to human health, and monitoring should be focused on evaluating the impact of those sites.

In conclusion, additional work is needed to establish a systematic process for quantitatively characterizing the contaminated sites most important in terms of risk to human health. This type of targeted characterization should consider the key factors influencing potential radionuclide and chemical dispersal, including potential flow over and erosion potential at source areas, as well as the magnitude and spatial extent of radionuclide and chemical levels at these areas.

Coordinating Data Collection

One of the greatest obstacles to completing this project was the lack of a preexisting robust and well-planned design for compiling, organizing, and interpreting the large amount of data that is currently collected. A comprehensive design that spans the various divisions within LANL as well as different outside organizations (e.g., NMED, LANL, and EPA) is not currently in place, and yet it is critical for efficient data retrieval and dissemination and rapid data interpretation. A summary of some important considerations surrounding this issue is provided in Chapter 2 of Rocco et al. (2002).

Following the fire, DOE recognized the need for a data collection and compilation team consisting of organizations currently involved in data collection and reporting (DOE 2000b). DOE also noted the need for a risk evaluation team, which would be responsible for producing the overall health risk results and making preliminary bounding risk estimates based on the available data during the emergency. The data collection and compilation team would be responsible for providing data to the risk evaluation team for source term compilation. While the DOE concept is good, it cannot be implemented in a short period of time. Its success requires establishing a robust data compilation system with meaningful input from all stakeholders and thorough testing *before* the next emergency situation. However, DOE (2000b) provides little guidance in terms of the many specific issues that must be addressed to actually implement this concept.

A number of current procedures and activities can be incorporated into the overall design of a more efficient system. An essential prerequisite is to *first* identify the potential uses of environmental monitoring, site characterization, and other data and *then* to develop a design that readily accommodates those uses. Once a framework and design for data compilation has been developed and tested, previously existing data can be compiled. The existing protocols (i.e., resources or tools already in place at LANL, NMED, or EPA) that complement such a design should be used wherever possible and modified where necessary. This will require input and assistance from many different organizations and a willingness to adopt new procedures and methods. However, we believe the long-term benefits of increased credibility and efficiency will far outweigh these initial efforts and costs.

To rapidly assess risk from an event such as the Cerro Grande Fire, it must be easy to compare all measurements related to a set of samples collected at a given time and location. It is also important to be able to clearly understand and be aware of potential biases that may result from sample collection, preparation, or analytical techniques and that may impact interpretation of the results. These biases include identified laboratory problems, different analytical procedures for the same analyte, different collection methods used by various organizations, or data known to

be inaccurate. To have effective interaction among agencies and for independent assessment efforts, it is important for agencies to provide *all* collected data, rather than a subset of the data collected, in a format that facilitates interpretation. Efficient access to all available data is important for meaningful technical data evaluation and, more importantly, to establish a transparent process that is credible in the eyes of the public.

In some instances, sampling efforts could be coordinated to avoid unnecessary duplication of effort. For example, both ESH-18 and the Environmental Restoration (ER) Project at LANL^a monitor for contaminants in sediment and water, yet there is no indication of any sharing or integration of the resulting analytical data and consequent benefit from this apparent duplication of effort. It is not clear why data collected through the extensive water monitoring network maintained by ESH-18 would not meet the needs of ER to understand contaminant movement. Likewise, it is not clear why the significant amount of onsite sediment monitoring data collected by ESH-18 could not be used to augment the ER database to expedite and strengthen the process of characterizing canyon contamination, which has been completed for Los Alamos, Pueblo, and DP Canyons to date. This type of integrated approach could be extended to include monitoring data collected by other agencies or groups, such as NMED. We believe a more integrated approach would increase the credibility and efficiency of the various programs as perceived by the public. Further, the integrated approach of adopting consistent design concepts should include both environmental and site characterization data and encompass all monitored media.

An integrated and consistent design for compiling data would also support the interest to make data publicly available as rapidly as possible. Long delays in the release of data jeopardize the credibility of that data and the organization presenting the data, as well as reduce the usefulness of the data in identifying problems or supporting decisions. Delays in obtaining data were encountered during this project where monitoring data that were collected early enough in the evaluation process to be helpful but were not released until after much of the analysis was already complete.

It is essential that an integrated and well-planned design, guided by the potential uses for the data, be developed for compiling all monitoring data. Following the fire, a statement was made that, "In response to the fire and its impacts, we have increased our air, water and soil sampling to monitor environmental safety" (LANL 2000). While this increase in sampling is important, it is equally important that additional data be collected with careful planning so they can be readily used. The currently inconsistent and disconnected methods maintained by the various data collecting organizations prevent an efficient and effective interpretation of the data, particularly by an independent organization.

An independent assessment creates trust by the public. However, a successful assessment relies heavily on guidance from involved parties and requires prompt data input from all organizations to help guide the risk calculations. Our experience with the current independent assessment shows the need for an integrated (i.e., consistent across all organizations collecting data) data compilation and organization system that does not rely on numerous reports and documents generated by the different organizations for data interpretation.

^a Since the start of this project, LANL has undergone restructuring that places both the ER and ESH groups within a single division now referred to as Risk Reduction and Environmental Stewardship (RRES).

Specific Observations and Recommendations Related to Calculating Risks: Information Needed to Refine Risk Estimates and Reduce and Quantify Uncertainty

The following discussion provides some ideas on additional information and data that could help refine the process of estimating risk, as well as reduce and quantify the associated uncertainties. These issues all contribute to the extremely complex process of understanding and estimating risk. It was beyond the scope of this project to develop an overall plan designed to meet and prioritize needs for additional data; however, the models, concepts, and information developed as part of this project can serve as a starting point and provide a framework for focusing future efforts. We believe it is possible, with careful planning and within available resources, to develop a program that both meets regulatory requirements and improves the ability to estimate risk.

It is important that future efforts be guided by a thorough analysis of what will contribute most to refining risk calculations, reducing and quantifying uncertainties, and meeting established goals (including regulatory requirements), so that minimizing and understanding risk to the public proceeds in the most efficient, practical, and effective way possible. This value of information analysis should consider input from all stakeholders and must incorporate a wide array of disciplines (e.g., improved timber and watershed management requires communication between and input from both waste site engineers and ecologists). It cannot be overstated that decisions about the steps that are needed and most important to mitigate and understand risk must be based on and guided by good science if they are to be defensible in the long run. The key to efficiently utilizing data collected to meet specific goals and objectives revolves around an integrated and consistent design for compiling those data.

As discussed previously, a credible source term provides the foundation of a defensible risk assessment. There are many issues related to improving the ability to estimate a source term, some of which include

- Identifying and prioritizing the key contributors to potential risk, including both the most important sites and the most important radionuclides and chemicals. This provides the basis for targeting additional efforts, such as those noted below.
- Improving the spatial coverage (location) of characterization data, both at the ground surface and as a function of depth. This may require different approaches for different radionuclides and chemicals or different source areas, and the process should be guided by a systematic and comprehensive identification of the key contributors to potential risk, as noted above.
- Developing a better understanding related to the partitioning of different chemicals and radionuclides among various soil and sediment particle sizes. Some of this information is available for Los Alamos and Pueblo Canyon sediments.
- Improving the ability to quantify uncertainties related to understanding the magnitude of important radionuclide and chemical levels at key source areas.
- Continuing the effort to quantify the fraction of standing vegetation that may be carrying increased radionuclide or chemical burdens as a result of LANL operations, with a focus

on understanding trends in concentrations as a function of both location and vegetation type.

- Continuing the effort to characterize source areas with regard to erosion susceptibility, considering the impact of such things as plant cover, slope, and soil composition. The erosion matrix scores developed for many of the potential release site (PRS) source areas provide a good foundation for this, but in many cases they are not representative of current conditions and do not reflect the impact of existing best management practices (BMPs).

In addition to improving the ability to estimate source terms, there are many parameters and variables controlling movement and partitioning of materials in the environment and ultimately risk to humans that could be better understood and contribute to refinements in risk estimates. A number of efforts to this end may be appropriate to consider, some of which include

- Establishing monitoring protocols targeted at quantifying the impact of specific potential emergencies. Such protocols could include placement of additional air samplers at areas both onsite and offsite likely to be impacted by resuspension or deposition, as well as sampling points in areas likely to be impacted by surface water flow and sediment transport and utilized by members of the public.
- Continuing efforts to collect samples from consistent onsite and offsite locations over time to better understand temporal (time) trends. These locations should be positioned to provide adequate sensitivity for sampling periods and locations that correspond to the needs for information about environmental levels at public exposure locations identified as potentially important before, during, and following emergency situations.
- Establishing a list of potential chemicals and radionuclides for future targeted analysis, to include both those required for regulatory compliance and those identified as important contributors to potential risk.
- Establishing site-specific distributions and central tendencies (at identified important points of exposure [POEs] and source areas) for parameters that impact chemical and radionuclide movement, including soil-water distribution coefficients, fraction organic carbon, and fish concentration ratios or bioaccumulation factors.
- Improving the current understanding of the relationship between parameters such as TSS and flow, watershed area, or location.
- Collecting additional monitoring data to quantify suspended sediment concentrations (SSC) of chemicals and radionuclides.
- Augmenting available data to quantify and characterize background concentrations of radionuclides and chemicals, particularly in water and suspended sediments, using locations appropriate and suited for that purpose.

- Acquiring data to better understand typical short-term fluctuations in air concentration for different chemicals and radionuclides, as well as PM, to enable relevant comparisons to the short-term average concentrations measured during an emergency.
- Collocating PM-10 and PM-2.5 monitors since recent studies show that, in general, PM-2.5 is a better predictor of health effects than PM-10 (WHO 2000). Conducting chemical composition analyses of PM because evidence is emerging that constituents of PM, such as sulfates and strongly acidic particles, may be more closely correlated to health effects than the PM (WHO 2000). Advancing the development of methods appropriate for applying PM health risk factors to environmental concentrations.
- Improving the understanding of burn temperature on the mobility of chemicals and radionuclides in soil and the erodibility of soil particles over time. Continuing to assess the rate of recovery following a fire as a function of location, soil type, slope, and other factors.
- Improving the understanding of the impact of fire on the destruction and creation of organic chemicals.
- Continuing to compile the most recent data available to assess risks associated with exposure to chemicals.

The data needs discussed in this section should neither be considered an exhaustive list of all potentially useful data, nor should these lists be construed to be in any prioritized order of importance. However, it is likely that the greatest reduction in uncertainty related to estimating potential risks would be through targeted refinement of source term information.

COMMUNICATING HEALTH RISKS

The second part of this report addresses the experiences from the Cerro Grande Fire that can provide guidance for communicating potential health risks to the public and providing perspective for those risks during future emergencies. Local citizens, employees at LANL, and emergency personnel are the populations at potential risk from an emergency such as the Cerro Grande Fire, and they must all be considered in the process of communicating information about risk. This section examines the public communication tools used during and after the fire by LANL, DOE, State and local officials, other government agencies, and the news media. It also provides some ideas for interacting with concerned citizens and other stakeholders in the future in an emotionally charged environment.

Since May 4, 2000, there have been many statements, press releases, and announcements about the potential for immediate and future health risks as a result of the Cerro Grande Fire burning across LANL property. This deluge of written material may not have been expected for a fire in another situation. Thus, this fire and associated events provide an opportunity to review and learn from the actions taken, or not taken, in the public communication arena when an emergency event involves the potential release of chemicals and radionuclides from areas of contamination.

While there are numerous issues related to public communication about health risks during and following an emergency, most can be grouped into three main categories, which are discussed in the following sections:

1. Establishing effective and coordinated communication
2. Linking preliminary risk estimates to available data
3. Continuing the post-fire communication and risk assessment.

Establishing Effective and Coordinated Communication

Coordinating public communication during and immediately following an emergency requires extraordinary effort and diligence by all involved. First, the proper foundation to enable the necessary coordination must be established and in place before the emergency situation occurs. One concern voiced by many within various agencies was that there was not a well defined coordinated emergency response plan for collecting and disseminated information in place at LANL before the Cerro Grande Fire occurred. A coordinated process promotes an efficient, immediate response and allows information to be disseminated about the crisis through a technically and publicly credible mechanism. If implemented effectively, it enables a timely and professional response when decisions must be made without delay.

Clearly, some loss of coordination resulted from different missions and goals of participating agencies. Nevertheless, the fire emphasized that when responding to an emergency, a viable goal should be for all agencies with ties to LANL to coordinate public communication so information about risks can be consistent, swift, technically defensible, and supported by everyone. Community interaction is not a part-time activity that only occurs when problems arise. Rather, it must be based on a history of ongoing and meaningful public interaction.

During an emergency, especially during the early stages, it is important to identify all the potential sources of risk and concern. From the DOE and LANL perspective, the most immediate concern was the security of buildings containing nuclear materials. For many residents and business owners impacted by the Cerro Grande Fire, the most immediate concern related to physical safety and to loss of homes, possessions, pets, and other less tangible items. These immediate concerns understandably took precedence over potential health risks related to the possible release of contaminants from outdoor locations at LANL and are reflected by the relative scarcity of articles about these risks in the local Los Alamos newspaper by comparison to other regional newspapers. Developing a comprehensive overview of the situation and being cognizant of all concerns during the fire, or any emergency, is essential.

Understanding what can be conclusively drawn from available information and the coordination of a consistent message is critical to risk communication. The message must be timely, truthful, and without bias. All conclusive statements about risk should be based on available data only. Statements that are not supported by factual data, even if the intent is to allay fear among the public and the assumptions appear sound, can be harmful in the long run. Finally, many members of the public place more trust in individuals other than that of government officials when the source of risk is a government facility. Thus, government agencies need to recognize the value of involving an independent source for review and observation during a crisis and adopting a system that supports such a review.

Emergency Response Background: Existing Capabilities and Plans

This section provides some background information on federal and State agencies that were in place at the time of the fire. Much of this discussion highlights existing plans and capabilities (but not necessarily used during the Cerro Grande Fire) to deal with emergencies in general and extends beyond the topic of communicating health risks. However, it is important to understand the functions and responsibilities of the various organizations and plans that are or have been designed to assist with responding to emergency events, particularly as they relate to calculating and communicating risk. This section is not intended to advocate one plan over another or to identify which plan(s) were most appropriate to deal with the Cerro Grande Fire. It is also not intended to provide a comprehensive description of the capabilities and responsibilities of the various organizations that could be involved during an emergency. It is not entirely clear that the Cerro Grande Fire constituted a radiological emergency, which is what some of these plans are designed to address. However, the definitions set forth in the various plans established to deal with such emergencies suggest that any disaster or emergency with the potential to release radioactive (or other hazardous) materials to the environment could be classified as a "radiological emergency." In that sense, the Cerro Grande Fire could be considered a radiological emergency. The following paragraphs summarize the various organizations and plans that could be used in an emergency situation.

In a radiological emergency, DOE and EPA would establish a Federal Radiological Monitoring and Assessment Center (FRMAC) to help organize the response and monitor the impact. The FRMAC is established under the umbrella of the Federal Radiological Emergency Response Plan (FRERP), which is designed to help coordinate efforts in the event of a major radiological emergency by providing an operational plan for federal agencies to discharge their responsibilities during peacetime radiological emergencies (DOE 2000c). The FRERP establishes an organized, integrated capability for participating federal agencies to respond to a wide range of peacetime radiological emergencies. DOE leads the development of the FRMAC during initial response to an emergency, with support from EPA and other agencies. EPA would assume the long-term leadership of the center after the emergency phase of an accident. Information gathered and interpreted by the FRMAC would be used by the Lead Federal Agency (LFA) (in this case, DOE) along with federal guidelines to recommend actions to the State for protecting public health and the environment. While this organization is prepared for such situations and may be designed to ensure uniformity of measurement techniques, FRMAC was not involved in the Cerro Grande Fire emergency.

A second federal emergency support is the Federal Response Plan (FRP), which describes the structure for organizing, coordinating, and mobilizing federal resources to augment state and local response efforts (FEMA 1999). The EPA is responsible for the overall management of preparedness and response coordination activities for the Emergency Support Function (ESF) defined under the FRP. DOE (2000c) notes that, "In particular, the FRP may be implemented concurrently with the FRERP. Except for the coordination between the Federal Coordinating Officer (FCO) and the LFA, the functions and responsibilities of the FRERP do not change."

Under federal emergency measures, the LFA is directed to coordinate the overall activities (both onsite and offsite) of all federal agencies during all phases of a radiological emergency response and to establish on scene response centers. Examples of the response centers established during the Cerro Grande Fire were the Joint Operations Center (JOC), which was the

coordination center for the overall federal response, and the Joint Information Center (JIC), which coordinated dissemination of information to the public and media (DOE 2000c). The JIC was comprised of individuals from the New Mexico Office of Emergency Management, the Federal Emergency Management Agency (FEMA), the U.S. Department of Agriculture Forest Service, the DOE and LANL, the National Park Service, the Bureau of Indian Affairs, the New Mexico National Guard, the EPA, the Small Business Administration, the Santa Clara Pueblo, the New Mexico County Agencies, the American Red Cross, and the Bureau of Land Management.

Disasters of this type may also fall under the Incident Command System (ICS), which was developed to coordinate interagency responses and information releases in the wake of the 1970 California wildfires that burned into residential areas in several fire districts. The ICS is now widely used throughout the United States by fire agencies, and it is increasingly used for law enforcement, other public safety applications, and for emergency and event management.

Another group organized under federal authority to respond to the emergency caused by the Cerro Grande Fire was the Burned Area Emergency Rehabilitation (BAER) team. The BAER team is formed after major fires to assess damage caused by the fire and to implement a rehabilitation plan that will prevent loss of life and property and reduce further natural resource damage. The Cerro Grande Fire BAER team was comprised of personnel from the U.S. Department of Agriculture, Forest Service, Bureau of Land Management, National Park Service, U. S. Geological Survey, and LANL. A Multi-Agency Coordination (MAC) team was also formed during the fire, and it included representatives from all the landowner agencies to act as the umbrella organization during the assessment and rehabilitation. The goal of the MAC team was to provide interagency communications and minimize red tape.

All of these plans and groups are developed to help organize and manage a coordinated interagency response and release of information to the public in the event of an emergency. The FRERP, FRMAC, and FRP focus on emergencies involving radiological or hazardous materials and provide guidance where the release or spread of radioactivity is possible. For example, the FRMAC's description of support capabilities includes gathering radiological information and data, providing results of data collection and sample analysis, and compiling a complete database containing all offsite radiological monitoring and sampling data. These issues relevant to the Cerro Grande Fire may not be covered by other plans. Regardless, the effectiveness of these groups or any emergency plan hinges on preparedness before the event actually happens, coupled with familiarity and understanding by all involved of the capabilities and responsibilities of each source of assistance.

Managing the Risk Communication Response

Statements about health risk are best issued from a central point, which reflects consensus and avoids confusion and contradictory messages. Joint press releases are exceptionally effective mechanisms to provide technical information to the public. While all members of the public may not fully understand some of the technical information, knowing that different regulatory agencies are in agreement with the statements generates confidence that the reported information is credible. However, it is essential that the contributing organizations have an equal voice in the development of the consensus statement. In the event that it is not possible to reach agreement on certain issues, there must be a viable and recognized mechanism to allow those responsible for contributing to consensus statements to provide alternate interpretations or opinions.

Additional guidance for managing and coordinating the communication efforts may help prevent some of the miscommunication and misunderstandings that occurred after the Cerro Grande Fire. There was an attempt to provide joint press releases following the fire, but the process of reaching a consensus among different groups about key pieces of information was difficult to achieve. NMED broke away from this attempt to collaboratively issue public information when it seemed impossible to reach consensus with the DOE, LANL, and the EPA (*Albuquerque Tribune* 2000a). Others noted that there appeared to be inconsistent guidance for approvals required in developing the joint press releases with EPA, NMED, and FEMA (LANL 2001a). This eventually led to closed meetings, which generated a great deal of public mistrust and miscommunication (*Albuquerque Tribune* 2000b, 2000c). Closed meetings may be important for developing consensus in a crisis, but the meetings must be brief and they must be followed by prompt, clear-cut announcements that are based only on information available at the time.

Managing the risk communication response also involves placing health risk, which must be based on sound technical data, in a context that provides the public with a meaningful and appropriate perspective of the magnitude of the risk. For example, some press releases and other documents compared levels of chemicals (metals, organics, and asbestos) in air samples collected during the fire to workplace standards (JIC 2000; LANL 2000b; DOE 2000a). At a minimum, such comparisons require further explanation because workplace standards are designed to control exposures to healthy adult workers exposed for 8 hours per day, not to control 24-hour exposures to members of the public including elderly, infants, and sensitive subgroups. Integrating additional information (such as current protective standards, specific health risks associated with different chemicals and radionuclides, representative background values, historical trends, and factors such as risk coefficients) into the data collection design would further support timely dissemination of meaningful information to the public.

In an emergency where the public is placed at risk or there is potential for risk, the agency perceived by the public as responsible for the risk should not be the initial or primary source for communicating information about that risk. To avoid this situation, the primary responsibility of *risk communication* should be delegated to an independent agency that is working closely with the many individuals and organizations involved in the emergency. By engaging an independent agency for this task, the difficulties associated with achieving credibility in the eyes of the public are greatly reduced.

Involving All Stakeholders in Risk Communication

The importance of effective, open, and honest communication cannot be overstated. It is the foundation of developing a trusting relationship between all stakeholders. Whether the communication is directed at informing the public of potential health risks or providing some perspective on measured concentrations of contaminants in the environment, it is critical that information be relayed in an understandable manner. Further, it can only be effective in the long term if it is based on sound facts and the current state of knowledge. Involving stakeholders in the efforts to provide information about the emergency reduces confusion and disagreement and results in fewer misleading statements.

When a facility such as LANL is met with the daunting task of responding to an event like the Cerro Grande Fire, it is critical that mechanisms to guide the involvement of stakeholders be in place before the event happens. Early in the response period during the Cerro Grande Fire,

access to the site was denied for safety reasons. However, the process for identifying those individuals who may need access for monitoring or other purposes left some local officials frustrated (*Albuquerque Tribune* 2000d). As a result of the strong negative impact closing the LANL site had, an unprecedented tour of LANL facilities was arranged for reporters in an attempt to allay fears.

There is little question that the resources and time available to those actively managing and monitoring an emergency can be stretched significantly. Nonetheless, the public views delays in analyzing and providing data with skepticism and suspicion (*Albuquerque Tribune* 2000b, 2000c). Both San Ildefonso and Santa Clara Pueblos expressed frustration at being excluded from the decision making process in the early days of the disaster and not being informed of or invited to meetings despite being in the direct path of the fire (*Albuquerque Journal* 2000e). Other groups, including the Pueblos and NMED, expressed concerns about receiving insufficient information regarding air quality during the fire (LANL 2001a).

When data are limited and preliminary, it is important to avoid statements to the public that are too strong or inappropriately conclusive. There are many examples during the Cerro Grande Fire of officials reporting no risks or describing impacts as none or insignificant (*Albuquerque Journal* 2000f, 2000g, 2000h, 2000i; *Santa Fe New Mexican* 2000a, 2000b; *Los Alamos Monitor* 2000; ERT 2000a). In some cases, there may not have been sufficient information upon which to base such assertive statements. Any statement about potential health impacts should be backed by quantitative and substantive facts. Furthermore, uncertainties, limitations, and data gaps must be discussed along with any conclusive statements that are made. Other statements were less assertive and acknowledged the difficulty and uncertainty of knowing for certain the potential risks and impacts related to the fire (*Albuquerque Journal* 2000j, 2000k; *Santa Fe New Mexican* 2000c).

In addition to basing statements about risk on factual information, it is also important to be sure that the type or source of risk is identified. In some cases, the statements about risk did not fully convey the source of the risk (e.g., whether it was from a building storing nuclear materials or a contaminated land area that burned) or the nature of the risk endpoint (e.g., cancer development or the toxic effect of a chemical). When there are remarks about risk being insignificant or nonexistent, the source and nature of the risk must be clearly stated. For example, in the early stages of the fire, there was a great deal of concern about the possible impact on buildings storing nuclear and other materials, and statements were made to indicate these facilities were safe and did not present a risk. However, some members of the public expressed concern that other sources of risk, such as contaminated land areas, were not given adequate attention (*Albuquerque Journal* 2000f, 2000g, 2000j; *Santa Fe New Mexican* 2000d, 2000e).

Pergler (2000) suggests that fear and distrust in an emergency are not caused by the event itself but emerge from past issues and, in this case, the historical lack of communication from DOE and LANL to surrounding communities. He further states that while Los Alamos citizens tend to be more educated with regard to scientific topics and have a working knowledge of LANL operations, this may not be true of citizens in the surrounding communities. As a result, conclusions drawn from press releases and other publicly available information may be based on different interpretations of the information. These different perspectives are particularly important to consider during the process of communicating information about potential risks.

In conclusion, guidelines for disseminating information to the public should be developed based on input from all stakeholders. Constructive critical interaction among all stakeholders

should be encouraged, but it must be focused on understanding and communicating potential risks to the public in the most effective and efficient ways possible. For this approach to be effective, the interaction must be sensitive to the issues of all stakeholders but not driven by individual or unrelated agendas.

Linking Preliminary Statements about Risk to Available Data

The second issue related to public communication about health risks surrounds the ability to rapidly access and interpret technical data to provide a defensible basis for calculating and communicating preliminary risks to the public (see the section titled “Coordinating Data Collection”). While many facets of an organized response were operating during the Cerro Grande Fire, certain aspects of the response could have been implemented more effectively if data issues were more clearly defined at the outset. As outlined in the section “Coordinating Data Collection,” difficulties related to making preliminary statements about risk, in some cases, were compounded by the lack of coordination and agreement by the various organizations and agencies in

- Locating and collecting environmental samples in a consistent and comparable manner
- Compiling and analyzing data
- Releasing timely monitoring data.

There is a clear need to coordinate the data analyses so that preliminary risk results are timely, accurate, and respond to public concerns. It is equally important to understand what can be learned very rapidly from monitoring data and what may take more time to fully understand. During the Cerro Grande Fire, initial statements suggested no increase in natural radioactivity. Later statements acknowledged some increases in gross radioactivity levels but attributed them entirely to naturally occurring radionuclides, apparently before the detailed isotopic analyses were available to support such statements (*Albuquerque Tribune* 2000b, 2000c).

The time sequence of reporting risks is very important, and it is critical that statements about risk be couched within the limitations of the available data. The Cerro Grande Fire provides a good example of an event that fortunately did not result in extremely high levels of airborne radionuclide contaminants. This was something that could be stated very quickly based on rapid gross activity measurements. There is a clear need for these immediate order-of-magnitude risk results (DOE 2000b). However, discerning the degree to which contaminated areas at LANL may have contributed to the slightly higher levels of gross activity took more time. The desire to make rapid statements, even if they were based only on preliminary assumptions and data that suggested a minimal contribution from LANL, appears to have contributed to the difficulty of reaching consensus agreement by all organizations, as well as the general distrust by the public and criticism from other scientists.

Making raw data available to all (e.g., via web postings) may help address some public concerns; however, organizations involved in the emergencies also have legitimate concerns that the public will misunderstand or misinterpret raw data. These organizations must be prepared to assist the public with data interpretation, and stress that early data are provisional. There may also be some lack of understanding of current monitoring capabilities (e.g., NEWNET, a system for real-time telemetry of meteorological data and gamma exposure rates from locations on and around LANL, which does not provide the same type of data that AIRNET provides). Therefore,

misunderstandings and confusion can be lessened and trust built when a plan is in place before the emergency occurs to provide rapid access to understandable data and identify monitoring capabilities and limitations.

As discussed earlier in this report, the key to providing timely access to technical data (regardless of whether it is for a member of the public or an independent risk assessor) hinges on developing a coordinated protocol for data compilation. A coordinated design for data compilation would increase the ability of data collecting organizations to rapidly present raw data to the public in a meaningful and understandable manner with comparisons to relevant protective standards or regional background levels. Members of the public appreciate timely access to the actual data being collected, and a system that allows this would greatly enhance and foster public trust. Many issues must be addressed to develop this type of system. Some of these issues include developing a protocol for disseminating preliminary or provisional data, adopting appropriate procedures for providing data that are understandable and meaningful to the public, and maintaining Pueblo sovereignty over data related to samples collected from their land.

Continuing Post-Fire Communication and Risk Assessment

The third issue concerning public communication about health risks relates to continued communication and risk assessment following the emergency, when additional time and resources typically become available to allow the health risks to be assessed in more detail. This was the case with the Cerro Grande Fire and resulted in our independent analysis of the exposure and risks. There were also notable efforts in fostering more communication between the public and various agencies since the fire, including LANL's efforts to communicate with and include the views of outside consultants, including NMED and some Pueblos, in their post-fire rehabilitation plans (ERT 2000b). After the fire, interagency groups were created, like the Interagency Flood Response Assessment Team (IFRAT), and public action organizations, like the Emergency Rehabilitation Team (ERT) and the Public Advisory Group (PAG). The IFRAT was a consortium of government organizations established to integrate communications and deliver information on the flood and contamination risks related to the aftermath of the Cerro Grande Fire. The ERT was put into place to identify and implement corrective measures following the fire. The PAG was organized to focus specifically on communications issues as they relate to potential runoff and flood mitigation. Concerned Citizens for Nuclear Safety (CCNS) also organized meetings and issued a report related to the fire and its aftermath (Alvarez and Arends 2000).

Many of these efforts and meetings were described and announced through the LANL website and open to the public. A measure of the dedication of these efforts for more open communication will rely heavily on how long and to what extent these efforts (and others) continue into the future. As a practical note, involvement by some of these groups was intentionally reduced as a result of this project and the perceived greater independence of RAC to assess LANL-related risks.

As with preliminary statements, it is equally important to coordinate health risk statements in the weeks and months following an emergency to ensure those statements are based on sound and defensible studies. After the Cerro Grande Fire, some stakeholder concern arose from the perceived lack of information about existing contamination at LANL upon which to base statements about potential risk (*Santa Fe New Mexican* 2000f). We were also not able to find comprehensive reports about contamination onsite that could be used to make definitive

statements about the potential long-term risks related to releases associated with increased post-fire surface water runoff. It is important that such statements about risks be supported by an assessment of the risks.

Other assessments based on actual monitoring data, such as the one completed by IFRAT (2001) and the assessment by Kraig et al. (2001), are useful, but their limitations for assessing potential future health risks must be recognized. This is particularly true because the assessment was based on data collected during a relatively dry monsoon season that did not produce the heavy rains that could result in significantly more chemical and radionuclide movement.

Cooperation by all involved organizations in the time following an emergency can leave behind a legacy of trust and allow constructive and consequential input by the public. While some agencies may view members of the public as individuals who can never be convinced of “no additional risk,” this focus is misplaced. The useful and more productive attitude should be to provide information based on available data and assist with interpreting the risk. The process of fostering trust must begin with receiving, understanding, and addressing input from the public.

RECOMMENDATIONS

The following recommendations are based on our experiences and efforts during this project of independently assessing potential risks to members of the public as a result of the Cerro Grande Fire. Although these recommendations are directed at identifying areas where improvements or changes could result in a more efficient, or defensible end result, certain considerations may complicate their implementation. For example, consensus statements are important and effective, but in some cases such statements may not be possible, and all stakeholders should be afforded a viable option for presenting alternative interpretations. Likewise, while improved site characterization would greatly enhance the ability to understand potential risks, public interests to “stop characterizing and start clean up” create conflicting pressures. As another example, a key to building trust and credibility involves ensuring that statements about risk are tied to valid and thoroughly analyzed data, but there is a competing desire by the public to have information provided immediately.

Recognizing these potentially conflicting issues by State and federal officials and members of the public is critical to developing and adopting procedures that meet stakeholders’ needs. There will always be limitations related to collecting, compiling, interpreting, and disseminating information. At the same time, identifying areas where changes could result in more efficient, timely, or comprehensive availability of data is important. Similarly, there is a certain level of site characterization that is required to direct and focus cleanup efforts, and the dynamic environment at LANL in combination with a long history of operational impact complicates site characterization. A comprehensive and systematic approach for using those characterization data in combination with other relevant information must be in place to understand potential risks and defensibly guide cleanup efforts that minimize the potential for human exposure to chemicals and radionuclides. It is important to strike a balance between responding to public wishes, working efficiently to calculate and communicate potential risks, and realizing practical limitations on what is possible to achieve. The key to successfully implementing these recommendations will be involving all stakeholders in developing and adopting new procedures. Incorporating this input into decision making may alleviate the impact of these potential conflicts and assist with meeting

the varied wishes of the public while at the same time moving effectively toward the common goal of understanding, communicating, and minimizing risks to the public.

The following general recommendations are grouped into the two broad categories: calculating health risks and communicating health risks.

Calculating Health Risks

- Review the existing routine and emergency monitoring programs and their goals. Refine these to design and establish a comprehensive monitoring program that addresses current and potential needs for data collection. Because of the stress on monitoring and analytical capabilities during an emergency, these efforts must be focused to provide timely information for the appropriate locations, with adequate sensitivity to provide the basis for early assessments and decisions.
- Establish a systematic and comprehensive effort to quantitatively characterize the chemicals and radionuclides that may be available for release from contaminated areas and rank the relative importance of those areas and the chemicals and radionuclides with respect to offsite human health risk. The bounding approach developed for this project can serve as a starting point and model to guide future efforts to improve estimates of potential risk, identify areas and materials onsite that contribute most to the health risk for offsite individuals, guide cleanup or stabilization efforts, and target areas where additional information could lead to reduced and quantifiable uncertainty or where additional refinement of sensitive parameters is warranted.
- Design and implement an integrated and consistent method for monitoring and data compilation that is based on identified uses and needs for the data that are collected. All such efforts should be guided by a thorough analysis of what additional information will contribute most to refining risk calculations, reducing and quantifying uncertainties, and meeting established goals (including regulatory requirements) so that minimizing and understanding risk to the public proceeds in the most efficient, practical, and effective way possible.
- Comprehensively define “background” conditions for the site and surrounding area so any increases in contaminant concentrations in the future can be statistically verified.
- Acquire data to represent typical short-term (e.g., hourly or daily) fluctuations in air concentration, which can vary significantly depending on the time of year or season. To understand the potential impact of an emergency like the Cerro Grande Fire, it is imperative that appropriate comparisons be made. Averaging times must be reported along with measured air concentrations, and comparisons of hourly or daily average concentrations with biweekly or quarterly averages may have little validity and impart limited information about the impact of an emergency event.

- Maintain data collection and storage in a consistent and easily retrievable format so that preliminary risk results are timely, respond to public concerns, and can be readily interpreted by independent organizations.
- Employ a mechanism to link issues impacting data interpretation (e.g., known biases) to the actual data. Design data collection to enable rapid comparison of monitoring data to appropriate background values, protective standards, risk coefficients, or other relevant values.

Communicating Health Risks

- Delegate the primary responsibility of *risk communication* to an independent agency that works closely with the agencies involved in the emergency. In an emergency where the public is placed at risk or there is potential for risk, the agency perceived by the public as responsible for the risk should not be the initial or primary source for communicating that risk to the public.
- Maintain a central point for issuing statements about health risk to avoid contradictory messages. Establish a protocol for reaching consensus agreement about statements that are issued. A viable and recognized mechanism must be developed to allow alternate interpretations or opinions in the event that complete agreement is not possible.
- Implement a well-coordinated and practiced emergency response plan that clearly identifies the responsibilities and capabilities of LANL, State and federal agencies, local communities, Pueblos, and other stakeholders with regard to understanding and communicating risks.
- Involve members of the local community in the coordination efforts for disseminating information about the emergency. Adopt a consistent mechanism for providing appropriate perspective on the magnitude of measured concentrations. Such measures will lead to less confusion and disagreement and fewer misleading statements.
- Base statements about immediate risks and potential future risks on available data only, and identify limitations associated with data gaps or uncertainties. Clearly identify the origin of the risk and the nature of the risk endpoint.
- Establish a mechanism to allow environmental monitoring by groups, independent of State and federal agencies, to provide additional confidence in the results obtained by the site and regulatory agencies normally involved in data collection. Encourage constructively critical interaction by all stakeholders.
- Maintain a concerted effort to actively and effectively involve the local citizens in emergency and other planning. The process of fostering trust among all stakeholders must not wane as the memory of an emergency, fades away.

REFERENCES

- Albuquerque Tribune*. 2000a. "Radioactive Smoke Reports Lack Facts, Officials Say." May 20.
- Albuquerque Tribune*. 2000b. "Two Scientists Dispute No-Radiation Reports." May 17.
- Albuquerque Tribune*. 2000c. "Los Alamos Fire-radiation Findings Are Based On Inadequate Data, Critics Say." May 18.
- Albuquerque Tribune*. 2000d. "Plutonium Waste-storage Area at Lab Worries Some." May 12.
- Albuquerque Journal*. 2000e. "Pueblos Angry at Being Ignored." May 18.
- Albuquerque Journal*. 2000f. "Lab Says Nuclear Materials Protected." May 11.
- Albuquerque Journal*. 2000g. "Materials Safe, DOE Boss Says." May 12.
- Albuquerque Journal*. 2000h. "Officials Expect Some Radioactivity." May 14.
- Albuquerque Journal*. 2000i. "Closer Scrutiny of Fire's Effect Sought." July 9.
- Albuquerque Journal*. 2000j. "No LANL Hazards in Smoke, Officials Say." May 13.
- Albuquerque Journal*. 2000k. "Post-Fire Runoff Studied." July 19.
- Alvarez, R. and J. Arends. 2000. *Fire, Earth and Water: An Assessment of the Environmental, Safety and Health Impacts of the Cerro Grande Fire on Los Alamos National Laboratory, a Department of Energy Facility*. Concerned Citizens for Nuclear Safety. Santa Fe, New Mexico. December. Executive Summary and conference transcripts available at <http://www.nuclearactive.org>.
- DOE (U.S. Department of Energy). 2000a. *Special Environmental Analysis: Actions Taken in Response to the Cerro Grande Fire at Los Alamos National Laboratory, Los Alamos, New Mexico*. DOE/SEA-03. Los Alamos Area Office, Los Alamos, New Mexico.
- DOE. 2000b. Risk Needs Analysis: Cerro Grande Fire. July 27.
- DOE. 2000c. *Overview of FRMAC Operations, Federal Radiological Monitoring and Assessment Center, a U.S. Department of Energy Emergency Response Asset*. DOE/NV/11718—146-Rev 5. April.
- DOE. 2001. DOE Wildland Fire Lessons. <http://www.hanford.gov/lessons/sitell/1101/wildlandfires.pdf>. March 19.

- ERT (Emergency Rehabilitation Team). 2000a. Emergency Rehabilitation Team provides update No. 10. <<http://www.lanl.gov/orgs/pa/News/062000.html#anchor9>>. June 20.
- ERT. 2000b. Overall Plan/Summary of Efforts. Los Alamos National Laboratory. <<http://www.lanl.gov/worldview/news/fire/ert/ERTSummFINAL0630.doc>>. June 30.
- ER (Environmental Restoration Project). 2000. *Site and Watershed Aggregation and Prioritization, Draft G*. ER2000-xxxx. Los Alamos National Laboratory. September.
- FEMA (Federal Emergency Management Agency). 1999. *Federal Response Plan: Emergency Support Function #10, Hazardous Materials Annex*. 9230.1-PL. April.
- IFRAT (Interagency Flood Risk Assessment Team). 2001. *IFRAT Risk Model: Purpose, Construction, and Results*. NMED-01-001. New Mexico Environment Department, Hazardous Waste Bureau, Santa Fe, NM. July 25.
- JIC (Joint Information Center). 2000. *Cerro Grande Fire Chemical Contaminant Air Sampling around Los Alamos National Laboratory First Data Set*. FEMA-DR-1329-NM-PR54. May 19.
- Kraig, D., R. Rytz, D. Katzman, T. Buhl, B. Gallaher, and P. Fresquez. 2001. *Radiological and Nonradiological Effects after the Cerro Grande Fire*. LA-UR-01-6868. Los Alamos National Laboratory, Los Alamos, New Mexico. December.
- LANL (Los Alamos National Laboratory). 2000a. Daily News Bulletin. June 5.
- LANL. 2000b. *A Special Edition of the SWEIS Yearbook: Wildfire 2000*. LA-UR-00-3471. Los Alamos National Laboratory, Los Alamos, New Mexico. August.
- LANL. 2001a. *Lessons Learned in ESH-17 from Cerro Grande Fire*. Los Alamos National Laboratory, Los Alamos, New Mexico. July 20.
- LANL. 2001b. *FY-02 ER Prioritization Database, Filemaker Pro Version 5.0*. LA-UR-01-4110. Los Alamos National Laboratory, Los Alamos, New Mexico. September 17.
- Los Alamos Monitor*. 2000. "Lab Runoff Consistent with Prior Tests." July 23.
- Pergler, C. 2000. *Meeting Observations, Impressions, and Recommendations Resulting from the Concerned Citizens for Nuclear Safety Public Forum—Fire, Water and the Aftermath: The Cerro Grande Fire and its Effect on the Rio Grande/Bravo Watershed*. July 11.
- Rocco, J.R., K.R. Meyer, H.J. Mohler, J.W. Aanenson, L. Hay Wilson, A.S. Rood, and P.D. McGavran. 2002. *Analysis of Exposure and Risks to the Public from Radionuclides and Chemicals Released by the Cerro Grande Fire at Los Alamos. Task 2.7: Estimated Risks*

from Releases to Surface Water. RAC Report No.4-NMED-2002-FINAL(Rev.1). Risk Assessment Corporation, Neeses, South Carolina. June 12.

Rood, A.S., J.W. Aanenson, S.S. Mohler, P.D. McGavran, H.J. Mohler, and H.A. Grogan. 2002. *Analysis of Exposure and Risks to the Public from Radionuclides and Chemicals Released by the Cerro Grande Fire at Los Alamos. Task 1.7: Final Report on Estimated Risks from Releases to Air. RAC Report No. 3-NMED-2002-FINAL(Rev.1). Risk Assessment Corporation, Neeses, South Carolina. June 12.*

Santa Fe New Mexican. 2000a. "Contamination Concerns." June 12.

Santa Fe New Mexican. 2000b. "Lab Moves Contaminated Dirt from Canyon." June 24.

Santa Fe New Mexican. 2000c. "Work to Start on Capturing Contaminated Runoff." May 20.

Santa Fe New Mexican. 2000d. "LANL Officials Deny Fire's Proximity Poses Risk." May 9.

Santa Fe New Mexican. 2000e. "Los Alamos: A 'Time Bomb in the Forest.' " May 10.

Santa Fe New Mexican. 2000f. "Madrid Demands Proof that LANL Runoff is Safe." June 21.

Till, J.E. 1996. "Methodology of Environmental Dose Assessment." Proceedings of the 1996 International Congress on Radiation Protection, IRPA 9, Vienna, Austria, April 14–19.

WHO (World Health Organization). 2000. Health Based Guidelines. Chapter 3 in *Guidelines for Air Quality*. World Health Organization, Geneva, Switzerland.

SUMMARY REPORT

Analysis of Exposure and Risks to the Public from Radionuclides and Chemicals Released by the Cerro Grande Fire at Los Alamos

June 12, 2002

*Submitted to the New Mexico Environment Department
in Partial Fulfillment of Contract No. 01 667 5500 0001*

"Setting the standard in environmental health"



Risk Assessment Corporation

417 Till Road, Neeses, SC 29107
Phone 803.536.4883 Fax 803.534.1995

CONTENTS

INTRODUCTION	1
Overview of Study Results	1
Estimated Risks from Releases to Air	1
Estimated Risks from Releases to Surface Water	2
Calculating and Communicating Risks: Observations and Recommendations	2
STUDY OBJECTIVES	3
STUDY AREAS	3
ESTIMATED RISKS FROM RELEASES TO AIR	5
Available Monitoring Data	5
Screening and Source Term Calculation	5
Atmospheric Transport and Air Concentration Calculation	6
Risk Estimates	7
ESTIMATED RISKS FROM RELEASES TO SURFACE WATER	9
Monitoring Data Evaluation	9
Source Term Development	9
Development of Scenarios and Points of Exposure	10
Transport Modeling	12
Comparison to Measured Values	12
Risk Estimates	13
CALCULATING AND COMMUNICATING RISKS: OBSERVATIONS AND RECOMMENDATIONS	14
Recommendations for Calculating Health Risks	14
Recommendations for Communicating Health Risks	15
REFERENCES	16

FIGURES

Figure 1. Study areas for analysis of releases to air and surface water from the Cerro Grande Fire..	4
Figure 2. Points of exposure for the exposure scenarios used in the surface water pathway risk analysis of the Cerro Grande Fire	11

TABLES

Table 1: Exposure Scenarios for the Surface Water Pathway Risk Analysis	11
---	----

INTRODUCTION

The Cerro Grande Fire burned about 45,000 acres (~180 km²) in northern New Mexico in May 2000. It originated in the Bandelier National Monument on the evening of May 4, 2000, and spread east-northeast over the next 16 days consuming residential structures within the County of Los Alamos. The fire burned approximately 7500 acres (~30 km²) within the Los Alamos National Laboratory (LANL) boundary, causing significant damage to structures and property on LANL land. Some of the areas that burned were known or suspected to be contaminated with radionuclides and chemicals.

At the request of the New Mexico Environment Department (NMED), the U.S. Department of Energy (DOE) provided funds for an independent study of public health risks from radionuclides and chemicals associated with the LANL facility released as a result of the fire. The NMED contracted with *Risk Assessment Corporation (RAC)* to estimate the potential increased health risk to people in the communities of northern New Mexico from these radionuclides and chemicals.

A team of national and international scientists, led by scientists from Colorado State University, conducted technical peer review of the work. The NMED provided opportunities for public input throughout the 18-month study period. In addition, *Risk Assessment Corporation* held three public meetings during the project to answer questions and talk about study findings.

This report summarizes information provided in more detail in the following final reports. For additional information regarding the study or the final reports, contact the NMED DOE Oversight Bureau in Santa Fe, New Mexico. The final reports, listed here, can be obtained from the NMED website (www.nmenv.state.nm.us/DOE_Oversight/RAC.htm).

- *Task 1.7: Estimated Risks from Releases to Air* (Rood et al. 2002)
- *Task 2.7: Estimated Risks from Releases to Surface Water* (Rocco et al. 2002)
- *Task 3: Calculating and Communicating Risks: Observations and Recommendations* (Mohler et al. 2002)

Overview of Study Results

The following sections provide a brief overview of the key results from each of the three tasks involved in the study.

Estimated Risks from Releases to Air

Our analysis indicated that exposure to LANL-derived chemicals and radionuclides released to the air during the Cerro Grande Fire did not result in a significant increase in health risk over the risk from the fire itself. The risk of cancer from exposure to radionuclides and carcinogenic (cancer-causing) metals in and on vegetation that burned was greater than that from radionuclides and chemicals released from contaminated sites at LANL. All cancer risks were below the U.S. Environmental Protection Agency (EPA) range of acceptable risks of 10^{-6} to 10^{-4} (1 to 100 chances in 1 million) (EPA 1991). Potential intakes of noncarcinogenic LANL-derived chemicals exceeded acceptable intakes established by the U.S.

The cancer incidence risk from breathing any LANL-derived chemical or radionuclide released to the air during the fire was less than 1 chance in 1 million.

Risk Assessment Corporation
"Setting the standard in environmental health"

EPA at some locations on LANL property. However, the estimated intakes are conservative and likely overestimate the actual risks that occurred. It is likely that the risks from exposure to particulate matter far outweigh the risks from LANL-derived radionuclides and chemicals and those released from natural vegetation during the fire.

While the modeling we developed is quite reliable, the estimates of the quantities of materials available for release to the air, the rate at which these materials were released to the air, and the risk associated with short-term exposure to some chemicals are less certain. Therefore, we made conservative (or cautious) assumptions to ensure we did not underestimate the risks.

Estimated Risks from Releases to Surface Water

Cancer risks from exposure to LANL-derived radionuclides and carcinogenic chemicals released to surface water as a result of the Cerro Grande Fire were within acceptable limits established by the U.S. EPA. Estimated intakes of noncarcinogenic LANL-derived chemicals were also less than acceptable limits established by the U.S. EPA. Of the *exposure scenarios* we considered, the estimated health risks were highest for the hypothetical resident living year round on the bank of the Rio Grande near the confluence of Water Canyon. The most important type of exposure in terms of risk was eating fish.

Exposure scenarios describe the lifestyle and activities of hypothetical people to estimate likely ranges of exposure and risks to them from radionuclides and chemicals.

Aside from an understanding of maximum potential risks, an important contribution from this work is the ability to look at the impact of individual contaminated areas of LANL, known as potential release sites, or other source areas on potential exposures. An individual potential release site can have a significant impact on the concentrations at a point of exposure, and there is a need for further and continuing investigations into the magnitude and extent of chemicals and radionuclides at the potential release sites. In addition, concentrations of chemicals and radionuclides in stream segments and reaches below the LANL facility can have a significant impact at the point of exposure, and thus there is also a need to characterize additional stream segments and reaches.

Calculating and Communicating Risks: Observations and Recommendations

We provided specific recommendations and observations to help agencies involved in the activities during and after the Cerro Grande Fire to improve the ability to calculate and communicate risks in the future. The recommendations were based in large part on our experiences during this project, focusing on general issues that impacted our ability to estimate potential risks or that appear to have affected the credibility of information provided to the public about risks during and following the fire. Our recommendations were intended to help understand and communicate potential risks to the public in the most effective, efficient, and defensible manner possible. The key to successfully implementing these recommendations will be to involve all stakeholders in developing and adopting new procedures for the future.

STUDY OBJECTIVES

The primary goal of the study was to analyze the immediate and longer-term impacts of the Cerro Grande Fire in terms of increased public exposures and potential risks from radionuclides and chemicals associated with the LANL facility that were released to air and surface water as a result of the fire. The study did not specifically address the risks associated with the burning of buildings and home sites in Los Alamos or the impact of the fire on groundwater in the future.

Our three major objectives were to

1. Estimate the increased exposure and associated risks to the public, emergency response personnel, and firefighters from transport of LANL-derived radionuclides and chemicals released as a result of the fire through the *air pathway*. We also performed a preliminary evaluation of risks from naturally occurring radionuclides and metals released from burning of the forests around the LANL site.
2. Estimate the increased exposure and associated risks to the public from transport of LANL-derived radionuclides and chemicals released as a result of the fire through *surface water pathways*. We also evaluated risks related to ash from burned areas around the LANL site.
3. Recommend steps that could be taken to improve communication of risks to the public for future emergency situations, based on the conclusions of our study, and recommendations for similar events in the future. An important goal of the study was to openly and accurately convey information about risks from the fire to the public, including the lessons learned regarding calculating and communicating risk.

Pathways are routes that radionuclides and chemicals can travel from the location of a release to human populations, such as through air or water.

STUDY AREAS

Before making any calculations, we first established the geographical areas of study for the air and surface water pathways (See Figure 1). The total extent of the study area for the air pathway was 37×35 mi (60×55 km). It encompassed approximately 815,000 acres (3300 km²), and it included the cities of Santa Fe and Española, as well as Cochiti Lake. We also investigated potential exposures through the air pathway at locations outside the study area (such as Taos). Exposures at locations outside the study area were less than the maximum exposures calculated within the study area.

The surface water pathway study area encompassed approximately 182,000 acres (738 km²). In relation to the LANL facility, the study area extended to the west to include the upper Pajarito Plateau watersheds for the canyons that cross the LANL facility, to the north to include the extent of the burned area in Santa Clara Canyon, to the east to include the Rio Grande, and to the south along the Rio Grande and downstream of Cochiti Dam.

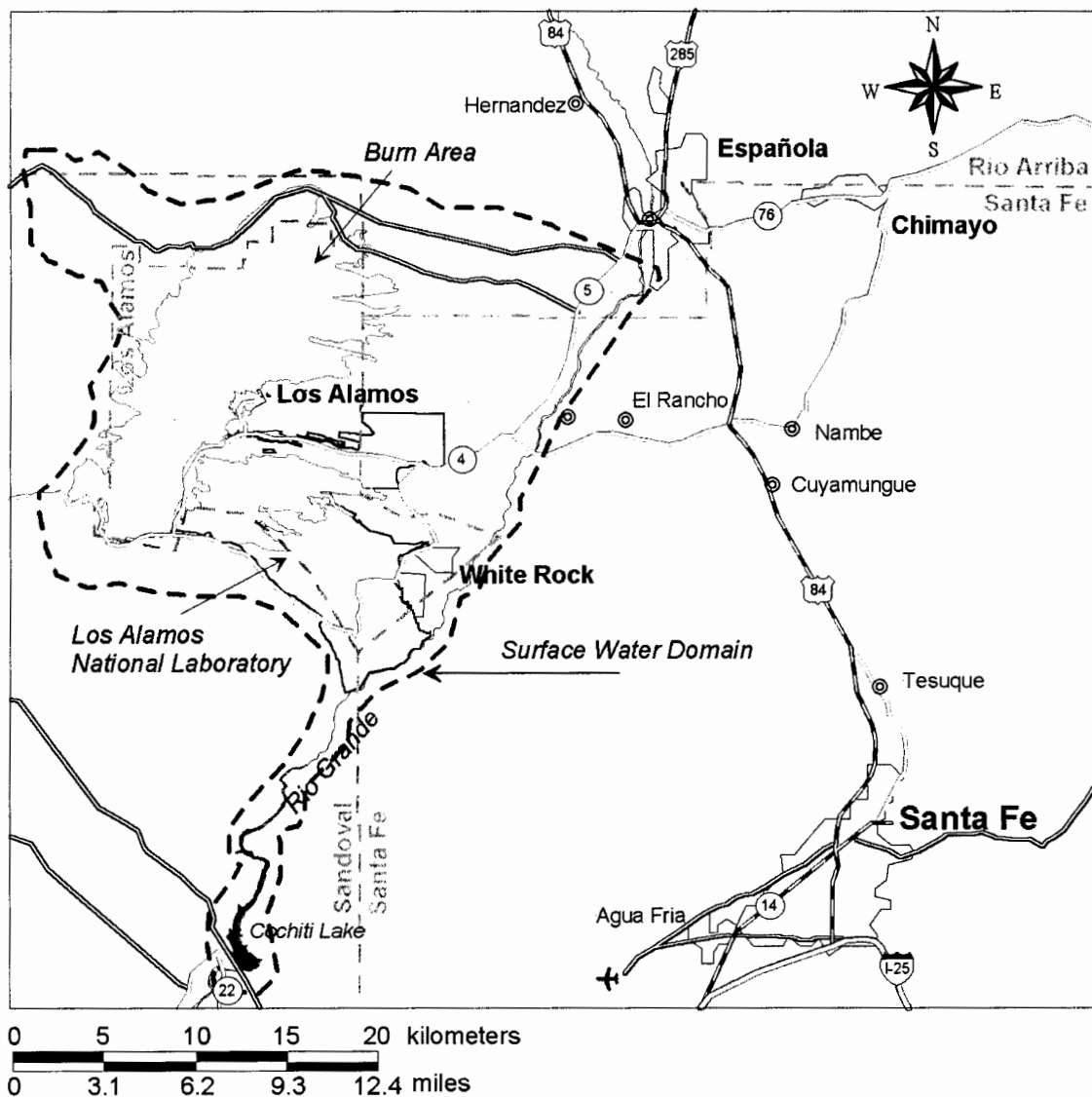


Figure 1. Study areas for analysis of releases to air and surface water from the Cerro Grande Fire. The total area shown was studied for the air pathway. The surface water study area (outlined in blue) was smaller and was restricted to watersheds that were impacted by the fire and the Rio Grande downstream to Cochiti Lake.

ESTIMATED RISKS FROM RELEASES TO AIR

Our primary focus for the air pathway was the analysis of radionuclides and chemicals derived from LANL operations that may have been released during the Cerro Grande Fire while the fire actively burned on LANL property. A secondary objective was to estimate the release of radionuclides and chemicals from the burning of natural vegetation both on and off LANL property. The sources of radionuclides and chemicals on natural vegetation included naturally occurring radionuclides and metals and worldwide fallout of radionuclides from atmospheric testing of nuclear weapons. Some radionuclides on natural vegetation are also attributed to the presence of LANL. To calculate the potential risks associated with these releases, we

- Evaluated the available air monitoring data and procedures
- Identified the sources and amounts of LANL-derived chemical and radionuclide on LANL lands that burned during the fire
- Estimated amounts of radionuclides and chemicals on all vegetation that burned during the Cerro Grande Fire
- Used computer modeling to estimate the release and transport of chemicals and radionuclides carried in the fire plume
- Identified representative individuals for defining exposure scenarios
- Estimated the resulting health risks and the associated uncertainties.

Available Monitoring Data

The data available to assess the concentrations of radionuclides and chemicals in the air during the Cerro Grande Fire included air and soil samples collected before, during, and after the fire; soil characterization data for contaminated sites at LANL that burned during the fire; meteorological data; and data for airborne contaminants measured in other fires.

When we started the project, we anticipated that the environmental air monitoring data would be complete enough to allow us to estimate *source terms* based on the measured concentrations in air combined with computer models that estimate how contaminants move in air. We believed these source terms would provide the basis to calculate the risks

A source term is the quantity of a chemical or radionuclide released from an area or event to an environmental media (air, water, or soil) over a certain period of time.

from the fire. However, the air monitoring data could not be used directly because not enough different locations were monitored, only a limited number of chemicals and radionuclides were measured, and the documentation for some of the data was incomplete. In addition, most of the concentrations measured were below the detection limits of the laboratory equipment used to analyze the samples.

Screening and Source Term Calculation

Because the environmental monitoring data were less useful than originally anticipated, we used soil characterization data for potential release sites at LANL that burned during the fire as our main source of information available on radionuclides and chemicals that may have been released. We identified a large number of radionuclides and chemicals that were potentially

Risk estimates describe the probability that individuals exposed to a chemical or radionuclide will develop an adverse reaction, such as cancer.

The range of acceptable risks defined by the U.S. Environmental Protection Agency is from 1 to 100 chances in 1 million.

released during the fire, so we used a screening procedure to identify those that were most important in terms of health risk.

We developed conservative release estimates for the radionuclides and chemicals that were possibly released from LANL operations by using cautious assumptions to ensure that we did not

underestimate risks. We then calculated cancer incidence *risk estimates* for radionuclides and carcinogenic chemicals and *hazard quotients* for noncarcinogenic chemicals. We removed contaminants from consideration that had a cancer incidence screening risk estimate of less than 1 chance in 100,000 or a screening hazard quotient of less than 1.

Then, for these most important radionuclides and chemicals, we calculated source terms using available information on the quantities present at the contaminated sites and how they may have been released to the air during the Cerro Grande Fire. We used these source terms to estimate air concentrations.

A hazard quotient is the ratio of the average daily intake of a contaminant per unit body weight to an acceptable reference value, established by the EPA. A hazard quotient less than 1 indicates no adverse health effects.

Atmospheric Transport and Air Concentration Calculation

Calculating transport of radionuclides and chemicals released into the air during burning of the potential release sites first required an understanding of the behavior of the fire itself. During forest fires, combustion products in the form of particulate matter are emitted in large quantities. We used computer models to estimate the movement of combustion products common

PM10 is particulate matter less than 10 microns in diameter (roughly 1/2500th of an inch), and it is produced by all wildfires.

to all wildfires in the study area. Particulate matter less than 10 micrometers (*PM10*) was measured in air at a number of locations in the model domain. PM10 concentrations in air are commonly monitored, as this small particulate matter can be inhaled and cause adverse health effects. We compared the computer

model-estimated concentrations of PM10 with the measured concentrations to confirm the computer model estimates and to better understand the uncertainty associated with the results.

The process of calibrating the model to PM10 measurements involved (1) identifying the geographical area that was burned, (2) defining the time history of the fire, (3) estimating the amount of vegetation that burned, (4) estimating the amount of PM10 released by the burning vegetation and the heat generated during burning, and (5) modeling the transport in air of PM10 released by the fire. We accounted for contributions of PM10 from sources other than the fire in the calibration.

We then assumed the release and transport of radionuclides and chemicals from LANL sources to be proportional to the release and transport of PM10. The dispersion of PM10, therefore, served to trace or track particulate releases of radionuclides and chemicals. For volatile

chemicals (chemicals that vaporize easily), carbon monoxide, which is also a forest fire combustion product, was used as a tracer.

We then calculated concentrations of radionuclides and chemicals identified as important through the screening process. In general, most predicted air concentrations were low. However, the predicted air concentrations and deposition amounts for the explosive compounds RDX, HMX, DNB, and TNT were relatively high. After the fire, however, explosive compounds were not detected in the limited soil sampling performed. The predicted deposition of these compounds would have been easily detected in soil, and this suggested that we overestimated the source terms for these compounds because of the cautious assumptions we made in our calculations.

Risk Estimates

We used four exposure scenarios to determine the risks to representative individuals from the LANL-derived radionuclides and chemicals released to the air during the fire; a resident adult, a firefighter, an emergency response worker, and a resident child. For each scenario we calculated cancer risk for radionuclides and carcinogenic chemicals, and hazard quotients for noncarcinogenic chemicals. We used the model-estimated concentrations at eight representative exposure locations, as well as the maximum predicted concentration in the study area. We calculated risks from naturally occurring radionuclides and chemicals on vegetation that burned during the Cerro Grande Fire for the adult resident scenario only. These risks would be associated with any forest fire and are not specific to LANL.

For LANL-derived chemicals and radionuclides, the maximum risk occurred within the active burned area and on LANL property. The maximum total *cancer incidence risk* from breathing any LANL-derived radionuclide released to the air during the fire was less than 1 chance in 10 million. In comparison, cancer incidence risks from breathing radionuclides released to the air from natural vegetation during the fire were estimated to be approximately 1 chance in 1 million. Cancer incidence risks from LANL-derived chemicals released during the fire were generally less than 1 chance in 1 million. The explosive compound RDX was a major contributor to this risk estimate, and we believe we overestimated the source term and risk for this compound. Cancer incidence risks from metals detected in natural vegetation and released during the fire were also approximately 1 chance in 1 million.

The total hazard quotient used to assess non-cancer health effects was generally less than or equal to 0.1 throughout the model domain for LANL-derived chemicals. Near areas where the fire burned, however, hazard quotients exceeded 1.0 and reached a maximum value of 2.0 for the resident adult scenario. This excursion above the acceptable level of 1 was limited to a small area within the LANL site near its western boundary. Most of the non-cancer risk was associated with the explosive compounds RDX, HMX, DNB, and TNT. As stated previously, we believe we overestimated the source terms for these compounds.

Hazard quotients indicated that intakes of LANL-derived noncarcinogenic chemicals released during the fire exceeding acceptable levels were limited to a small area of the LANL site.

Hazard quotients for metals released during the fire from natural vegetation were less than

A reference dose is an estimate of a daily exposure to the human population (including sensitive groups such as children) that is likely to be without a significant risk of negative health effects.

1.0 except for the metal manganese and, to a lesser extent, aluminum. However, the *reference doses* available to calculate the non-cancer health effects from these two metals were developed to evaluate chronic, or long-term, exposures, not short-term exposures such as those during the Cerro Grande Fire. They equated to air concentrations that were much lower than the

occupational standards for these metals. We believe the use of these chronic reference doses resulted in the unrealistically high hazard quotients for these metals. Using a reference dose based on occupational standards resulted in a maximum hazard quotient of less than 1.

Concentrations of PM₁₀ in the model domain exceeded U.S. EPA air quality standards for PM₁₀ averaged over 24 hours at some locations in the study area and were sufficient to cause adverse health effects; however, we did not quantify the number or type of health effects resulting from PM₁₀ exposure. We estimated that the deposition of radionuclides and chemicals from burned potential release sites would not be detectable in soil, with the exception of the explosive compounds RDX and HMX. We believe we overestimated the amount of these explosives released during the fire because soil sampling analyses did not detect these compounds in the soil even though the predicted concentrations were well above the detection limits of standard laboratory equipment. Exposure from the subsequent resuspension of the deposited radionuclides and chemicals was not calculated explicitly.

ESTIMATED RISKS FROM RELEASES TO SURFACE WATER

The Cerro Grande Fire destroyed vegetation and changed the surface soil, allowing greater quantities of storm water to flow through the canyons. This increased storm water flow can carry greater amounts of soil, sediment, and ash from the entire burned watershed, including some areas at LANL where chemicals and radioactive materials have been detected in soils. To estimate the potential increased exposure through the surface water pathway that occurred as a result of the fire and the associated risks, we

- Evaluated the available surface and storm water monitoring data
- Identified the sources and amounts of chemical and radionuclide releases
- Modeled the release and transport of radionuclides and chemicals in surface and storm water
- Identified representative individuals for defining exposure scenarios
- Estimated the associated health risks.

Monitoring Data Evaluation

We reviewed data on the concentrations of chemicals and radionuclides in water and sediments collected by LANL and the NMED before and after the fire. Because of the large number of measured chemicals and radionuclides, we developed a screening procedure to focus on those chemicals and radionuclides that were most likely to contribute to the health risk of those exposed directly or indirectly to surface water runoff from LANL.

Of the more than 250 chemicals and 75 radionuclides evaluated during this screening process, we identified 45 chemicals and radionuclides as most important in terms of the potential human health risk. We focused our evaluation of trends in the monitoring data on the human-made radionuclides in this list because there was a lack of post-fire monitoring data for many of the chemicals. Furthermore, for other chemicals, the results were below detection limits of the laboratory equipment used to analyze the samples so few conclusions could be drawn. As a result, we focused primarily on the radionuclides americium-241, cesium-137, strontium-90, plutonium-238, and plutonium-239,240 in surface water, storm water, and sediment. The monitoring data were useful for identifying apparent increases in concentration for some radionuclides and chemicals following the fire and also for identifying the possibility of LANL impact on measured concentrations.

Source Term Development

The most critical step in the risk estimation process is calculating the source term, or the amounts of chemicals and radionuclides in source areas available for movement into surface water. Our modeling approach for this step used measured concentrations of chemicals and radionuclides in soil or sediment, along with water runoff and sediment erosion yields. We then calculated downstream

Points of exposure are locations where an individual would likely come in contact with surface water, suspended sediments, or deposited sediments containing chemicals or radionuclides.

concentrations of chemicals and radionuclides at defined *points of exposure*, focusing on those that were most important in terms of potential health risk.

To identify the most important radionuclides and chemicals, we

- Calculated the average concentrations of chemicals and radionuclides across each source area and compared the highest average concentration to the U.S. EPA residential combined preliminary remediation goals for soil. Preliminary remediation goals are concentrations developed by the U.S. EPA for use as guidelines for evaluating and cleaning up contaminated sites, and they are calculated based on toxicity data and assumptions about exposure.
- Eliminated general water quality sampling results for which associated risks are not expected, and some other general categories of materials (like total petroleum hydrocarbons and lubricant range organics) for which information needed to calculate risk was not available in current regulatory guides
- Selected the chemicals and radionuclides that were also identified through the screening process used to evaluate the environmental monitoring data (described above), and if not already included, added chemicals or radionuclides that had significantly elevated concentrations in burned area ash
- Added chromium, mercury, RDX (a high explosive compound), and uranium because of either known public concern or high source area concentrations.

This process resulted in a final list of 37 chemicals and radionuclides for which we developed source term estimates.

Development of Scenarios and Points of Exposure

We designed four exposure scenarios to represent the different ways that individuals may be exposed to radionuclides and chemicals released to surface water. We developed the scenarios with caution so that a broad range of potential exposures would be represented. However, the hypothetical individuals described in the scenarios do not represent known individuals with these characteristics at these locations. Risks estimated for the hypothetical individuals in the scenarios would be greater than risks of other individuals who might be in the area for less time or under less exposed conditions.

The hypothetical individuals included (1) a local hunter, (2) a resident family (adult and child) living below Cochiti Lake, (3) a resident living below Water Canyon, and (4) a local fire cleanup worker at the LANL Site. The points of exposure for these individuals are shown in Figure 2, and the exposure pathways for the hypothetical individuals in each exposure scenario are shown in Table 1.

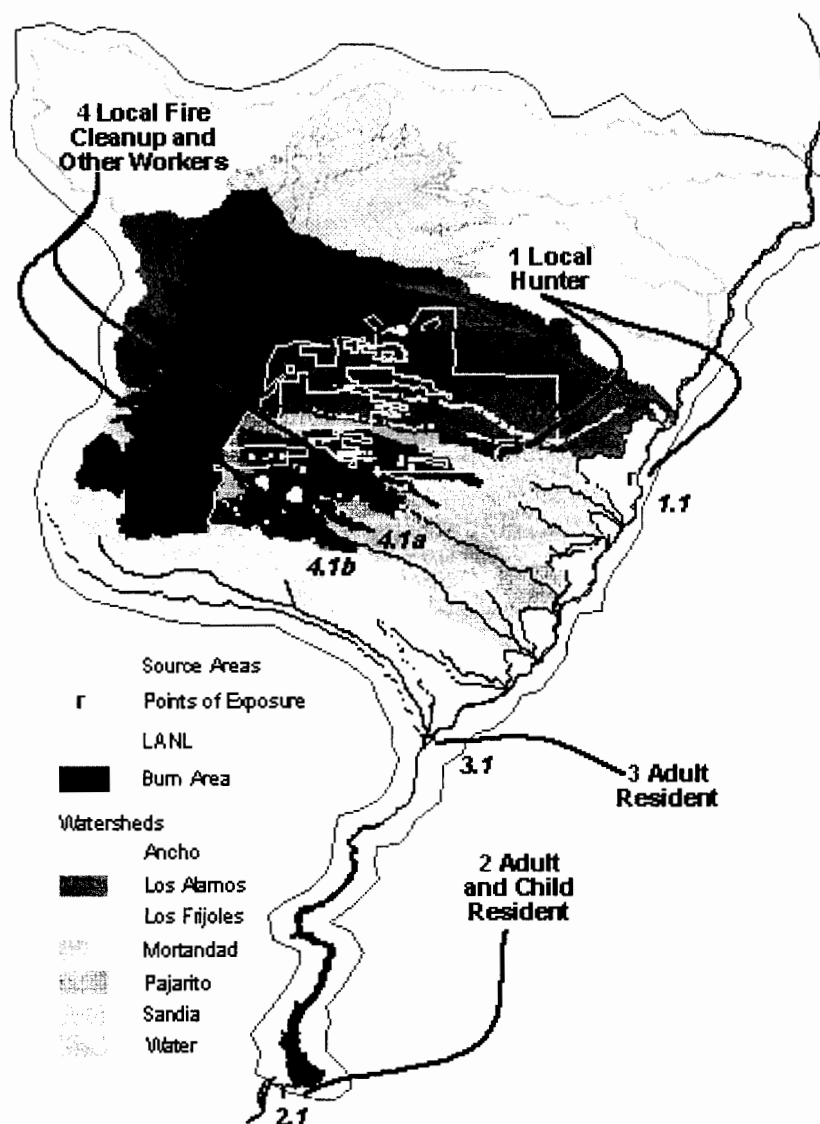


Figure 2. Points of exposure for the exposure scenarios used in the surface water pathway risk analysis of the Cerro Grande Fire.

Table 1: Exposure Scenarios for the Surface Water Pathway Risk Analysis

Surface water pathways	Individuals in scenarios			
	1	2	3	4
Drinking untreated water from the Rio Grande or Cochiti Lake	▶	▶	▶	
Sediment exposure (ingestion, external exposure, and dermal contact)	▶	▶	▶	▶
Swimming or contact with water in Cochiti Lake and the Rio Grande (immersion and accidental ingestion)		▶		
Eating fish from the Rio Grande and Cochiti Lake	▶	▶	▶	
Eating garden produce irrigated with river water		▶	▶	
Eating beef from cattle using water from the river and Cochiti Lake		▶	▶	

Transport Modeling

Next, we estimated the concentration at the points of exposure for the 37 chemicals and radionuclides in storm water, surface water, and suspended and deposited sediments. To accomplish this, we

- Estimated the surface water flow within the watersheds and at outlets to the Rio Grande for storm events of various severities, all 6 hours in length (ranging from a 2-year to a 500-year design storm event).
- Developed estimates of suspended sediment concentrations before and after the fire based on an analysis of pre-fire and post-fire total suspended solids sampling data from the U.S. Geological Survey and LANL.
- Identified the watersheds contributing storm water flow to each point of exposure and the important source areas in the watershed.
- Estimated the maximum potential chemical mass and radionuclide activity that could be present at each point of exposure as a result of storm water flow across a source area.
- Identified background, or typical, storm water flow and suspended sediment concentration in the Rio Grande and in Cochiti Lake.
- Estimated distribution of the chemical mass and radionuclide activity in environmental media to estimate concentrations at each point of exposure.

The results of the transport modeling suggest that while the fire did impact the potential transport of chemicals and radionuclides, there was no consistent change in the resulting concentrations from pre-fire to post-fire. In other words, concentrations of chemicals and radionuclides measured in water after the fire differed by less than a factor of ten from concentrations measured before the fire. Concentrations of chemicals and radionuclides decreased as the point of exposure was moved further away from the source areas, resulting in higher concentrations within the canyons immediately below the LANL facility than in the Rio Grande and in Cochiti Lake.

Comparison to Measured Values

We compared predicted and measured concentrations of selected chemicals and radionuclides in surface water and sediment at each point of exposure. These comparisons

Comparisons between available measured concentrations and predicted concentrations suggest that our predictions were likely overestimated.

suggest that our predicted concentrations are consistently greater than measured values (10 to 100 times greater) for americium-241, cesium-137, plutonium-238, and plutonium-239,240 in sediments. Predicted concentrations for the explosive RDX and polycyclic aromatic hydrocarbons are generally 10 to 1,000 times greater than measured concentrations. This over

prediction supports the noted conservatism of both our source term development and transport calculations. The over prediction is generally greater for water than for sediment.

Risk Estimates

We presented risk estimates as cancer incidence risks for carcinogenic chemicals and radionuclides or as hazard quotients for noncarcinogens. We estimated the potential annual cancer risk from the Cerro Grande Fire burning on the LANL site to be less than 3 in one million from exposure to any LANL-derived chemical or radionuclide that may have been carried in the surface water and sediments to the Rio Grande and Cochiti Lake. If exposure to the same concentrations of LANL-derived chemicals or radioactive materials was assumed to continue for 7 years (the time it may take to return to pre-fire vegetation conditions in the area), then the potential cancer risk was greater at about 20 in 1 million. Estimated intakes of noncarcinogenic LANL-derived chemicals were less than acceptable intakes (a hazard quotient less than 1) established by the U.S. Environmental Protection Agency.

Cancer risks for LANL-derived radionuclides and chemicals were within the range of acceptable risks defined by the U.S. EPA.

Estimated intakes of noncarcinogenic LANL-derived chemicals were less than the U.S. EPA's acceptable intakes.

Of the different individuals considered in the hypothetical exposure scenarios, the health risks were highest for the hypothetical resident living year round on the bank of the Rio Grande near the confluence of Water Canyon. The type of exposure contributing most to the potential risk was eating fish. For this type of exposure, we assumed that the hypothetical individuals in the exposure scenarios consumed approximately 10 pounds of fish per year, all from the river or Cochiti Lake. However, the risks should be viewed as upper bound, or maximum, values because of the conservatism we assumed in estimating concentrations and in selecting lifestyle activities and values for the hypothetical individuals. The risks for all other types of exposure are lower than those for eating fish.

The hunter and firefighter, who were potentially exposed to higher concentrations in water and sediments, spent less time at those locations and had fewer types of exposures. Risk estimates and hazard quotients for the child and the adult at Cochiti Lake were generally similar. In general, risks for all pathways associated with the 500-year storm event were less than 10 times higher than the risks from the 2-year storm event, and the differences are likely to be within the range of uncertainty calculated.

CALCULATING AND COMMUNICATING RISKS: OBSERVATIONS AND RECOMMENDATIONS

A key element following the Cerro Grande Fire was to learn how available technical data was used to make rapid decisions and to communicate information about the potential risks to local residents and emergency response personnel. We made specific recommendations to improve the calculation and communication of risk from future emergency events that may be applicable to LANL and other sites. We examined two broad areas regarding lessons that can be learned to prepare for and be responsive to future emergencies: 1) calculating health risks and 2) communicating those risks to the public.

The following recommendations were based on our experiences and efforts during this project of independently assessing potential risks to the public as a result of the Cerro Grande Fire. Although these recommendations are directed at identifying areas where improvements or changes could be made, certain considerations may complicate their implementation. For example, while improved site characterization would greatly enhance our understanding of potential risks, public interests to “stop characterizing and start clean up” create conflicting pressures. As another example, a key to building trust and credibility involves ensuring that statements about risk are tied to valid and thoroughly analyzed data, but there is a competing desire by the public to have information provided immediately.

Recognizing these potentially conflicting concerns of State and federal officials and members of the public is critical to developing and adopting procedures that meet stakeholders’ needs as effectively as possible. There will always be limitations related to collecting, compiling, interpreting, and disseminating information. At the same time, identifying areas where changes could result in more efficient, timely, or comprehensive availability of data should be an ongoing process. It is important to strike a balance between responding to public wishes, working efficiently to calculate and communicate potential risks, and realizing practical limitations on what is possible to achieve. The key to successfully implementing these recommendations will be to involve all stakeholders in developing and adopting new procedures.

Recommendations for Calculating Health Risks

- Expand existing monitoring programs to establish a comprehensive program that addresses current and potential needs for both routine and emergency monitoring data collection.
- Characterize contaminated areas to determine the amount of chemicals and radionuclides that may be available for release, and rank the relative importance of those areas and the chemicals and radionuclides in terms of public health risk.
- Design and implement methods for monitoring and data compilation that are based on uses for the data that are collected. Determine the additional information needs to refine risk calculations, reduce and quantify uncertainties, and meet established goals (including regulatory requirements) so that an understanding of public risk, as well as minimization of the risk, is achieved efficiently and effectively.
- Define “background”, or typical, concentrations of chemicals and radionuclides throughout the site and surrounding area so that increases in contaminant concentrations in the future can be quickly identified.

- Collect data to understand typical short-term (e.g., hourly or daily) changes in air concentration, which can vary significantly with time of year or season. Collection times must be reported along with measured air concentrations.
- Maintain data collection and storage in a consistent and easily retrievable format so that preliminary risk results are timely, respond to public concerns, and can be easily understood by independent organizations.
- Link issues affecting the interpretation of data to the actual data. Design data collection to allow for rapid comparison of monitoring data to appropriate background values, protective standards, risk coefficients, or other relevant values.

Recommendations for Communicating Health Risks

- Give the primary responsibility of risk communication to an independent agency that works closely with the agencies involved in the emergency. When there is potential for public risk, the agency that the public views as responsible for the risk should not be the initial or primary source for communicating that risk to the public.
- Maintain a central point for issuing statements about health risk to avoid conflicting messages. Establish a way to reach agreement between agencies about statements that are issued. Develop a method to allow communication of other interpretations or opinions if complete agreement is not possible.
- Implement a well-coordinated and practiced emergency response plan that clearly identifies the responsibilities and capabilities of LANL, State and federal agencies, local communities, Pueblos, and other stakeholders with regard to understanding and communicating risks.
- Involve members of the local community in efforts to provide information about the emergency. Adopt a consistent method to provide appropriate perspective on the magnitude of measured concentrations.
- Base statements about immediate risks and potential future risks on available data only, and identify limitations, such as data gaps or uncertainties. Clearly identify the origin of the risk and the nature of the risk.
- Establish a method to allow environmental monitoring by groups, independent of State and federal agencies, to provide additional confidence in the results obtained by the site and regulatory agencies normally involved in data collection. Encourage constructive criticism by all stakeholders.
- Maintain a concerted effort to actively and effectively involve the local citizens in emergency and other planning. Continue to foster trust among all stakeholders.

REFERENCES

- EPA (U.S. Environmental Protection Agency). 1991. *Role of the Baseline Risk Assessment in Superfund Remedy Selection Decisions*. Memorandum from Assistant Administrator Don R. Clay to the Regions. OSWER Directive 9355.0-30. Office of Solid Waste and Emergency Response, Washington, D.C. April 22.
- Mohler, H.J., K.R. Meyer, J.W. Aanenson, and H.A. Grogan. 2002. *Analysis of Exposure and Risks to the Public from Radionuclides and Chemicals Released by the Cerro Grande Fire at Los Alamos. Task 3: Calculating and Communicating Risks: Observations and Recommendations*. RAC Report No.15-NMED-2001-FINAL(Rev.1). Risk Assessment Corporation, Neeses, South Carolina. June 12.
- Rocco, J.R., K.R. Meyer, H.J. Mohler, J.W. Aanenson, L. Hay Wilson, A.S. Rood, and P.D. McGavran. 2002. *Analysis of Exposure and Risks to the Public from Radionuclides and Chemicals Released by the Cerro Grande Fire at Los Alamos. Task 2.7: Estimated Risks from Releases to Surface Water*. RAC Report No.4-NMED-2002-FINAL(Rev.1). Risk Assessment Corporation, Neeses, South Carolina. June 12.
- Rood, A.S., J.W. Aanenson, S.S. Mohler, P.D. McGavran, H.J. Mohler, and H.A. Grogan. 2002. *Analysis of Exposure and Risks to the Public from Radionuclides and Chemicals Released by the Cerro Grande Fire at Los Alamos. Task 1.7: Final Report on Estimated Risks from Releases to Air*. RAC Report No. 3-NMED-2002-FINAL(Rev.1). Risk Assessment Corporation, Neeses, South Carolina. June 12.